

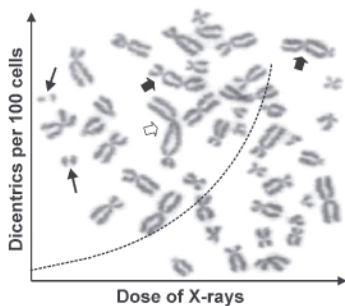
# Chromosome Aberrations

XXY/XXX/XXXY/XXXXY/XX/XXX/XXY/XXX/XXXY/XXXXY/XX/XXX/XXY/XXX/XXXXY/XXY/XXXXY/XX/XXX/XXY/XX

Editors

**Günter Obe**

**Adyapalam T. Natarajan**



**KARGER**

---

Single topic volume

# Chromosome Aberrations

---

Editors

*Günter Obe*, Essen

*Adyapalam T. Natarajan*, Leiden

164 figures, 26 in color, and 84 tables, 2004

**KARGER**

Basel · Freiburg · Paris · London · New York ·  
Bangalore · Bangkok · Singapore · Tokyo · Sydney

# Contents

## 5 Introduction

### Basic Aspects

- 7 Pathways of DNA double-strand break repair and their impact on the prevention and formation of chromosomal aberrations**  
Pfeiffer P, Goedecke W, Kuhfittig-Kulle S, Obe G
- 14 Mechanisms of DNA double strand break repair and chromosome aberration formation**  
Iliakis G, Wang H, Perrault AR, Boecker W, Rosidi B, Windhofer F, Wu W, Guan J, Terzoudi G, Pantelias G
- 21 The role of homologous recombination repair in the formation of chromosome aberrations**  
Griffin CS, Thacker J
- 28 Recombination repair pathway in the maintenance of chromosomal integrity against DNA interstrand crosslinks**  
Sasaki MS, Takata M, Sonoda E, Tachibana A, Takeda S
- 35 Repair rates of R-band, G-band and C-band DNA in murine and human cultured cells**  
Sanders MH, Bates SE, Wilbur BS, Holmquist GP
- 46 On the nature of visible chromosomal gaps and breaks**  
Savage JRK
- 56 Molecular targets and mechanisms in formation of chromosomal aberrations: contributions of Soviet scientists**  
Belyaev I
- 65 Progress towards understanding the nature of chromatid breakage**  
Bryant PE, Gray LJ, Peresse N
- 72 Human-hamster hybrid cells used as models to investigate species-specific factors modulating the efficiency of repair of UV-induced DNA damage**  
Marcon F, Boei JJWA, Natarajan AT
- 77 Mechanisms and consequences of methylating agent-induced SCEs and chromosomal aberrations: a long road traveled and still a far way to go**  
Kaina B
- 87 Human fibroblasts expressing hTERT show remarkable karyotype stability even after exposure to ionizing radiation**  
Pirzio LM, Freulet-Marrière M-A, Bai Y, Fouladi B, Murnane JP, Sabatier L, Desmaze C
- 95 Mechanisms of formation of chromosomal aberrations: insights from studies with DNA repair-deficient cells**  
Palitti F
- 100 In situ DNase I sensitivity assay indicates DNA conformation differences between CHO cells and the radiation-sensitive CHO mutant IRS-20**  
Marañon DG, Laudicina AO, Muhlmann M
- 104 DNA damage processing and aberration formation in plants**  
Schubert I, Pecinka A, Meister A, Schubert V, Klatte M, Jovtchev G

### Telomeres

- 109 DNA and telomeres: beginnings and endings**  
Bailey SM, Goodwin EH
- 116 DNA repair factors and telomere-chromosome integrity in mammalian cells**  
Hande MP
- 123 Interstitial telomeric repeats are not preferentially involved in radiation-induced chromosome aberrations in human cells**  
Desmaze C, Pirzio LM, Blaise R, Mondello C, Giulotto E, Murnane JP, Sabatier L
- 131 Lack of spontaneous and radiation-induced chromosome breakage at interstitial telomeric sites in murine *scid* cells**  
Wong H-P, Mozdarani H, Finnegan C, McIlrath J, Bryant PE, Slijepcevic P
- 137 Cytological indications of the complex subtelomeric structure**  
Drets ME

## Modelling

---

- 142 Quantitative analysis of radiation-induced chromosome aberrations**  
Sachs RK, Levy D, Hahnfeldt P, Hlatky L
- 149 Models of chromosome aberration induction: an example based on radiation track structure**  
Ballarini F, Ottolenghi A
- 157 Virtual radiation biophysics: implications of nuclear structure**  
Kreth G, Finsterle J, Cremer C

## Low-LET Radiation

---

- 162 Dose dependency of FISH-detected translocations in stable and unstable cells after  $^{137}\text{Cs}$   $\gamma$  irradiation of human lymphocytes in vitro**  
Romm H, Stephan G
- 168 Effect of DMSO on radiation-induced chromosome aberrations analysed by FISH**  
Cigarrán S, Barrios L, Caballín MR, Barquiner JF
- 173 DNA damage in Chinese hamster cells repeatedly exposed to low doses of X-rays**  
Güerci AM, Dulout FN, Seoane AI
- 178 Potassium bromate but not X-rays cause unexpectedly elevated levels of DNA breakage similar to those induced by ultraviolet light in Cockayne syndrome (CS-B) fibroblasts**  
Mosesso P, Penna S, Pepe G, Lorenti-Garcia C, Palitti F
- 182 Distribution of breakpoints induced by etoposide and X-rays along the CHO X chromosome**  
Martínez-López W, Folle GA, Cassina G, Méndez-Acuña L, Di-Tomaso MV, Obe G, Palitti F
- 188 The repair of  $\gamma$ -ray-induced chromosomal damage in human lymphocytes after exposure to extremely low frequency electromagnetic fields**  
Lloyd D, Hone P, Edwards A, Cox R, Halls J
- 193 Ionizing radiation-induced instant pairing of heterochromatin of homologous chromosomes in human cells**  
Abdel-Halim HI, Imam SA, Badr FM, Natarajan AT, Mullenders LHF, Boei JJWA
- 200 Cytogenetic damage in lymphocytes for the purpose of dose reconstruction: a review of three recent radiation accidents**  
Wojcik A, Gregoire E, Hayata I, Roy L, Sommer S, Stephan G, Voisin P

## High-LET Radiation

---

- 206 Complex chromatid-isochromatid exchanges following irradiation with heavy ions?**  
Loucas BD, Eberle RL, Durante M, Cornforth MN
- 211 G2 chromatid damage and repair kinetics in normal human fibroblast cells exposed to low- or high-LET radiation**  
Kawata T, Ito H, Uno T, Saito M, Yamamoto S, Furusawa Y, Durante M, George K, Wu H, Cucinotta FA

- 216 Cytogenetic effects of densely ionising radiation in human lymphocytes: impact of cell cycle delays**  
Nasonova E, Ritter S
- 221 Chromosome aberrations induced by high-LET carbon ions in radiosensitive and radioresistant tumour cells**  
Virsik-Köpp P, Hofman-Huether H
- 227 Induction of homologous recombination in the *hprt* gene of V79 Chinese hamster cells in response to low- and high-LET irradiation**  
Olsson G, Czene S, Jenssen D, Harms-Ringdahl M
- 232 Cytogenetic analyses in peripheral lymphocytes of persons living in houses with increased levels of indoor radon concentrations**  
Oestreicher U, Braselmann H, Stephan G
- 237 Effect of high-level natural radiation on chromosomes of residents in southern China**  
Hayata I, Wang C, Zhang W, Chen D, Minamihisamatsu M, Morishima H, Wei L, Sugahara T
- 240 Complex chromosomal rearrangements induced in vivo by heavy ions**  
Durante M, Ando K, Furusawa Y, Obe G, George K, Cucinotta FA
- 245 Chromosome aberrations of clonal origin are present in astronauts' blood lymphocytes**  
George K, Durante M, Willingham V, Cucinotta FA

## Heritable Effects

---

- 252 Transgenerational transmission of radiation- and chemically induced tumors and congenital anomalies in mice: studies of their possible relationship to induced chromosomal and molecular changes**  
Nomura T, Nakajima H, Ryo H, Li LY, Fukudome Y, Adachi S, Gotoh H, Tanaka H
- 261 Contribution of chromosomal imbalance to sperm selection and pre-implantation loss in translocation-heterozygous Chinese hamsters**  
Sonta S
- 271 Heritable translocations induced by dermal exposure of male mice to acrylamide**  
Adler I-D, Gonda H, Hrabé de Angelis M, Jentsch I, Otten IS, Speicher MR
- 277 Chromosome banding in Amphibia.**  
XXX. Karyotype aberrations in cultured fibroblast cells  
Schmid M, Steinlein C, Haaf T

## Aneuploidy and Micronuclei

---

- 283 Investigations into the biological relevance of in vitro clastogenic and aneugenic activity**  
Parry JM, Fowler P, Quick E, Parry EM
- 289 Region-specific chromatin decondensation and micronucleus formation induced by 5-azacytidine in human TIG-7 cells**  
Satoh T, Yamamoto K, Miura KF, Sofuni T
- 295 Micronuclei in lymphocytes of uranium miners of the former Wismut SDAG**  
Müller W-U, Kryscio A, Streffer C

**299 A liver micronucleus assay using young rats exposed to diethylnitrosamine: methodological establishment and evaluation**

Suzuki H, Shirotori T, Hayashi M

Sister Chromatid Exchanges

**304 Insights into the mechanisms of sister chromatid exchange formation**

Wojcik A, Bruckmann E, Obe G

**310 Frequent occurrence of UVB-induced sister chromatid exchanges in telomere regions and its implication to telomere maintenance**

Jin G, Ikushima T

**315 SCE analysis in G2 lymphocyte prematurely condensed chromosomes after exposure to atrazine: the non-dose-dependent increase in homologous recombinational events does not support its genotoxic mode of action**

Malik SI, Terzoudi GI, Pantelias GE

Applied Aspects/Cancer

**320 X chromosome inactivation-mediated cellular mosaicism for the study of the monoclonal origin and recurrence of mouse tumors: a review**

Tanooka H

**325 Chromosomal mutagen sensitivity associated with mutations in BRCA genes**

Speit G, Trenz K

**333 Possible causes of chromosome instability: comparison of chromosomal abnormalities in cancer cell lines with mutations in BRCA1, BRCA2, CHK2 and BUB1**

Grigorova M, Staines JM, Ozdag H, Caldas C, Edwards PAW

**341 Quantitative PCR analysis reveals a high incidence of large intragenic deletions in the FANCA gene in Spanish Fanconi anemia patients**

Callén E, Tischkowitz MD, Creus A, Marcos R, Bueren JA, Casado JA, Mathew CG, Surrallés J

**346 Analysis of ETV6/RUNX1 fusions for evaluating the late effects of cancer therapy in ALL (acute lymphoblastic leukemia) cured patients**

Brassesso MS, Camparoto ML, Tone LG, Sakamoto-Hojo ET

**352 Comparative genomic hybridization (CGH): ten years of substantial progress in human solid tumor molecular cytogenetics**

Gebhart E

**359 Chromosomal aberrations in arsenic-exposed human populations: a review with special reference to a comprehensive study in West Bengal, India**

Mahata J, Chaki M, Ghosh P, Das JK, Baidya K, Ray K, Natarajan AT, Giri AK

**365 Chromosomal radiosensitivity and low penetrance predisposition to cancer**

Scott D

**371 Cytogenetic studies in mice treated with the jet fuels, Jet-A and JP-8**

Vijayalaxmi, Kligerman AD, Prihoda TJ, Ullrich SE

**376 Chromosomal aberrations and risk of cancer in humans: an epidemiologic perspective**

Bonassi S, Znaor A, Norppa H, Hagmar L

**383 New developments in automated cytogenetic imaging: unattended scoring of dicentric chromosomes, micronuclei, single cell gel electrophoresis, and fluorescence signals**

Schunck C, Johannes T, Varga D, Lörch T, Plesch A

**390 mBAND: a high resolution multicolor banding technique for the detection of complex intrachromosomal aberrations**

Chudoba I, Hickmann G, Friedrich T, Jauch A, Kozłowski P, Senger G

**394 Author Index Vol. 104, 2004**

after **394 Contents Vol. 104, 2004**

S. Karger  
Medical and Scientific Publishers  
Basel · Freiburg · Paris · London  
New York · Bangalore · Bangkok  
Singapore · Tokyo · Sydney

Drug Dosage

The authors and the publisher have exerted every effort to ensure that drug selection and dosage set forth in this text are in accord with current recommendations and practice at the time of publication. However, in view of ongoing research, changes in government regulations, and the constant flow of information relating to drug therapy and drug reactions, the reader is urged to check the package insert for each drug for any change in indications and dosage and for added warnings and precautions. This is particularly important when the recommended agent is a new and/or infrequently employed drug.

All rights reserved.

No part of this publication may be translated into other languages, reproduced or utilized in any form or by any means, electronic or mechanical, including photocopying, recording, microcopying, or by any information storage and retrieval system, without permission in writing from the publisher or, in the case of photocopying, direct payment of a specified fee to the Copyright Clearance Center (see 'General Information').

© Copyright 2004 by S. Karger AG,  
P.O. Box, CH-4009 Basel (Switzerland)  
Printed in Switzerland on acid-free paper by  
Reinhardt Druck, Basel

## Introduction

The importance of chromosome aberrations for evolution and their association with human health have been recognized for almost a century. However, the mechanisms involved in the formation of chromosome aberrations are still not well understood. Ionizing radiation is most efficient in inducing chromosome aberrations and the basic principles of aberration formation were laid out in the early 1930's, even though the molecular structure of the eukaryotic chromosome was not known at that time. Techniques to prepare and stain chromosomes have improved gradually in the last decades, parallel with increased ability to identify and quantify chromosome aberrations, thus leading to a better understanding of their origin. Use of colchicine, squash technique for plant chromosomes, hypotonic shock for mammalian chromosomes, various banding techniques in the 1960's, sister chromatid differentiation in the early 1970's and fluorescence in situ hybridization (FISH) in the late 1980's have been main break-throughs enabling us to study chromosome aberrations in great detail. Especially the increasing availability of whole chromosome-specific, arm-specific, region-specific, centromere- and telomere-specific DNA probes has revolutionized the ways to look at chromosomes and their aberrations.

The articles in this volume deal with chromosome structure, mechanisms of aberration formation and applied aspects of aberration analyses. Papers which were presented at the 6th International Symposium on Chromosome Aberrations held at the University of Duisburg-Essen, Germany (10th to 13th September, 2003) and a collection of invited papers in this field are included.

The first group of 14 papers deal with **Basic Aspects** of chromosome aberrations, such as DNA damage processing in relation to aberration formation, the importance of non-homologous end joining, homologous recombination and the nature of aberrations.

The role of telomeres and telomerase in maintaining the integrity of chromosomes is an important area of research and five papers under **Telomeres** deal with this area.

Chromosome aberrations induced by ionizing radiation have been studied in great detail over the years and data generated in the 1930's and 1940's were used as a quantitative basis for formulating theories to explain the biological action of radiation. Knowledge of types and frequencies of lesions induced by ionizing radiation, especially DNA double strand breaks, as well as the quantification of aberrations have increased in the last decade and it has been possible to generate biophysical models for the origin of radiation-induced chromosome aberrations. Three papers are presented under **Modelling**.

Papers dealing with ionizing radiation-induced chromosome aberrations are presented in two groups, namely **Low-LET-Radiation** (eight papers) and **High-LET-Radiation** (nine papers). There are qualitative and quantitative differences between chromosome aberrations induced by low LET (such as X-rays and  $\gamma$ -rays) and high LET radiation (such as neutrons, heavy ions and radon). High LET radiation induces high frequencies of complex chromosome exchanges and FISH studies have shed light on the origin of these types of aberrations.

A fraction of chromosome aberrations induced in germ cells are transmitted to the next generation and this is of great concern from the point of view of genetic risk. Four papers included under **Heritable Effects** deal with this aspect.

Numerical and structural aberrations are important both in congenital abnormalities and tumors. Studying micronuclei using centromere-specific probes can easily make assessment of aneuploidy as well as chromosome breaks. Four papers are presented in the section **Aneuploidy and Micronuclei**.

Sister chromatid exchanges (SCEs) are intrachromosomal exchanges probably reflecting a homologous recombination process. Three papers dealing with mechanisms of formation of SCEs are presented under **Sister Chromatid Exchanges**.

Cells derived from patients suffering from recessive diseases (such as ataxia telangiectasia, Fanconi anemia, Bloom's syndrome) are chromosomally unstable. The genetic basis of these diseases is understood now, thanks to the molecular biological techniques, which have become available. Specific chromosome translocations or deletions characterize many human cancers. Chromosome aberrations in lymphocytes of individuals can be used as a biomarker of cancer risk. Twelve papers in this area of research are presented under the heading **Applied Aspects/Cancer**.

The papers in this special issue show the importance of basic and applied aspects of studying chromosome aberrations. It becomes clear that this field of research is of great interest and by far not out of the scope of modern science. Molecular cytogenetics is an especially rapidly expanding field and has contributed to our knowledge of chromosome structure and interphase nuclei, as well as the formation of chromosome aberrations. In the area of clinical genetics and oncology, these techniques have been of great value in diagnosis and prevention of outcome of diseases. We strongly believe that the future for this area is very bright.

We would like to thank Mrs. Rita Nadorf for her unfailing and devoted assistance in organizing the symposium as well as in editing of this volume.

*G. Obe*

*A.T. Natarajan*

# Pathways of DNA double-strand break repair and their impact on the prevention and formation of chromosomal aberrations

P. Pfeiffer, W. Goedecke, S. Kuhfittig-Kulle and G. Obe

Universität Duisburg-Essen, Essen (Germany)

**Abstract.** DNA double-strand breaks (DSB) are considered the critical primary lesion in the formation of chromosomal aberrations (CA). DSB occur spontaneously during the cell cycle and are induced by a variety of exogenous agents such as ionising radiation. To combat this potentially lethal damage, two related repair pathways, namely homologous recombination (HR) and non-homologous DNA end joining (NHEJ), have evolved, both of which are well conserved from bacteria to humans. Depending on the pathway used, the underlying

mechanisms are capable of eliminating DSB without alterations to the original genomic sequence (error-free) but also may induce small scale mutations (base pair substitutions, deletions and/or insertions) and gross CA (error-prone). In this paper, we review the major pathways of DSB-repair, the proteins involved therein and their impact on the prevention of CA formation and carcinogenesis.

Copyright © 2003 S. Karger AG, Basel

Faithful maintenance and replication of the genetic material is central to all living organisms. The integrity of the extremely long and fragile DNA molecules is constantly challenged by attack from agents arising from normal cell metabolism (e.g. oxygen free radicals) and from environmental agents (e.g. radiation and chemicals). The manifestation of such DNA damage in the form of mutations may lead to altered or severely impaired cell functions that may cause carcinogenesis or cell death.

To counteract this potentially lethal damage, complex and tightly regulated networks of repair mechanisms exist in all organisms. These mechanisms are highly specialized for different subsets of DNA lesions and are well conserved throughout evolution. Lesions that affect only one DNA strand, such as

base modifications and mismatches, are excised and repaired by using the intact complementary strand as a template to restore the original sequence (base excision repair: BER; nucleotide excision repair: NER; mismatch repair: MMR). Defects in these pathways (especially MMR) lead to a mutator phenotype that is characterized by elevated levels of point mutations and small deletions and/or insertions (Lengauer et al., 1998). In contrast, double-strand breaks (DSB) and inter-strand cross-links (ICL) affect both DNA strands so that no intact template remains available for repair. These lesions are especially genotoxic and, therefore, potent inducers of chromosomal aberrations (CA). Two major pathways, homologous recombination (HR) and nonhomologous end joining (NHEJ) are involved in the elimination of DSB (Pfeiffer et al., 2000). Genetic defects in either of these pathways lead to a chromosomal instability phenotype which is characterized by elevated levels of CA (Jasin, 2000; Ferguson and Alt, 2001; van Gent et al., 2001).

Common CA, often observed in tumour cells, include, for instance, the loss (deletion) or gain (insertion) of chromosome fragments as well as reciprocal translocations in which chromosome arms are exchanged (Obe et al., 2002). While larger deletions may lead to the inactivation of tumour suppressor genes (e.g. by loss of heterozygosity; LOH), insertions and transloca-

Supported by three grants to P.P. and G.O. (Deutsche Forschungsgemeinschaft: Pf 229/11-2; Wilhelm Sander-Stiftung für Krebsforschung: 1996.053.3 and 2002.108.1)

Received 8 September 2003; manuscript accepted 27 November 2003.

Request reprints from PD Dr. Petra Pfeiffer, Universität Duisburg-Essen  
Campus Essen, Fachbereich 9 Genetik, Universitätsstrasse 5  
DE-45117 Essen (Germany); telephone: +49-201-2281  
fax: +49-201-4397; e-mail: petra.pfeiffer@uni-essen.de



tions may be associated with deregulation of gene expression or gene fusion, which may cause the activation of proto-oncogenes (Lengauer et al., 1998). The biological significance of the different DNA repair pathways for the prevention of carcinogenesis is underscored by the pre-disposition to cancer at a young age of patients carrying inherited mutations in DNA repair genes (e.g. defects in MMR are associated with hereditary non-polyposis colon cancer: HNPCC; deregulation of HR is associated with familial breast cancer; defects in NHEJ are associated with a variety of lymphomas) (Lengauer et al., 1998; Venkitaraman, 2000; Duker, 2002). Because of their importance for the maintenance of genome integrity and thus the prevention of tumorigenesis, DNA repair genes have also been designated as “caretakers” (Levitt and Hickson, 2002) in contrast to the so-called “gate-keepers” (oncogenes and tumour suppressor genes), which are involved in the regulation of cell cycle and growth (Levine, 1997). In this review, we focus on the repair of DSB by HR and NHEJ and their importance for the prevention and formation of CA in mammalian cells.

### Sources of DSB

The first evidence that DSB are potent inducers of CA came from studies in which cells or animals were exposed to ionizing radiation (IR), an agent that generates many different lesions of which DSB are the most genotoxic (Ward, 2000). At relatively low doses, IR does not cause cell death but markedly contributes to the formation of CA (Sachs et al., 2000). Later, treatment of cells with restriction endonucleases (RE; enzymes that induce only DSB), gave direct evidence that DSB are indeed the primary lesion responsible for the formation of CA (Bryant, 1984; Natarajan and Obe, 1984). However, DSB are not only induced by exogenous factors but also by a variety of endogenous factors produced during the normal cellular metabolism (e.g. oxygen free radicals) (Barnes, 2002). An estimated ten DSB arise spontaneously in each S-phase because each single-strand break (SSB) in a parental strand which is passed by the replication fork may be converted to a DSB in the corresponding sister chromatid (Haber, 1999). Finally, DSB are intermediates in such important processes as meiotic recombination, which is essential for germ cell development (Dresser, 2000), NHEJ-mediated V(D)J recombination of immunoglobulin (Ig) or T-cell receptor (Tcr) genes in B- and T-lymphocytes, respectively (Bassing et al., 2002), Ig heavy class switching (Honjo et al., 2002), and somatic hypermutation (Reynaud et al., 2003).

Mechanisms capable of eliminating DSB are subdivided in homology-dependent and -independent processes. The former are based on HR which requires extensive sequence homologies of several hundred base pairs to restore the original sequence at the break site (error-free DSB repair). In contrast, homology-independent processes are based on NHEJ, which can completely dispense with sequence homology and is able to rejoin any two DSB ends end-to-end. Thereby, it often creates small sequence alterations at the break site (error-prone DSB repair). Mammalian cells harboring defects in NHEJ or HR display increased sensitivity to IR (and other clastogenic agents) and elevated frequencies of spontaneous CA which

indicates that both mechanisms are involved in DSB repair and counteract the formation of CA (Thacker and Zdzienicka, 2003). The relative contribution of these pathways to DSB repair and the prevention of CA depend on the organism, cell type and cell cycle stage. In yeast, DSB are primarily repaired via HR while in higher eukaryotes, both NHEJ and HR are important. However, marked differences in the preference of pathway usage exist between different model systems (e.g. DT40 chicken cells vs. mammalian cells) (van Gent et al., 2001). In mammals, defects in both HR and NHEJ lead to a predisposition to cancer and at the cellular level the frequency of CA is increased.

### Homology-dependent mechanisms

Homologous recombination is a universal process that is highly conserved from bacteria to mammals. The best paradigm for HR is found in meiosis where it serves to create genetic diversity in germ cells (Keeney, 2001). However, HR also plays important roles in the error-free repair of DSB in mitotic cells (Richardson et al., 1998), in the restarting of stalled replication forks (Alberts, 2003), and in telomere length maintenance in cells lacking telomerase (Neumann and Reddel, 2002). Accordingly, defects in HR result in sensitivity to genotoxic agents, mitotic and meiotic CA, and genome instability.

HR comprises conservative (error-free) DSB repair, which is also called “gene conversion” (GC; this term is originally derived from meiotic recombination but is nowadays also used as a synonym for conservative HR occurring in mitotic cells) and non-conservative (error-prone) single-strand annealing (SSA) (Paques and Haber, 1999). In its core reaction, conservative HR utilizes a long DNA 3'-single-strand, generated exonucleolytically from a DSB or a stalled replication fork, to invade an intact DNA duplex at a site of sequence homology (d-loop formation). There, homologous pairing is initiated followed by formation of a Holliday junction (HJ) intermediate, branch migration, and HJ resolution. This reaction finally results in strand exchange in which the sequence information of the intact donor is transferred to the broken recipient to yield two intact DNA copies (= conservative). In meiotically dividing germ cells, HR occurs between the two homologues resulting in GC with associated cross-over (exchange between two alleles of the same gene) and thus genetic diversity. In mitotic cells, HR occurs with high preference (factor 100–1,000) between the identical sister chromatids so that the original sequence is restored at the break site (GC without associated cross-over) (Johnson and Jasin, 2001). In this way, exchange between different alleles is suppressed, which otherwise could lead to LOH by loss of the wild-type allele and the concomitant expression of the recessive mutant allele. The high abundance of repetitive sequences in the mammalian genome poses another problem to conservative HR because erroneous strand exchange between homologous sequences (such as repeat units) on heterologous chromosomes (= ectopic or homeologous recombination) can cause CA in the form of reciprocal translocations (Richardson et al., 1998).

In contrast to the conservative HR, the non-conservative SSA process utilizes two regions of sequence homology (e.g. repeat units) within the same or two different chromosomes, which results in the loss of one repeat unit and the intervening sequence (= non-conservative) (Paques and Haber, 1999). Intra-chromosomal SSA leads to interstitial deletions, inter-chromosomal SSA to translocations that are associated with deletions. Therefore, SSA may be regarded as an error-prone sub-pathway of HR (Venkitaraman, 2002). Like HR, SSA is also initiated by long DNA single strands that originate from a DSB. These, however, do not invade an intact DNA duplex (and thus do not result in strand exchange) but interact with each other directly via their shared regions of sequence homology (as little as ~30 bp but typically several hundred bp).

In the yeast *Saccharomyces cerevisiae*, conservative HR requires (among several accessory proteins like RPA, DNA polymerases, ligases, and nucleases) nine specialized recombination proteins of the Rad52 epistasis group (Rad51p, Rad52p, Rad54p, Rad55p, Rad57p, Rad59p) as well as Rad50p, Mre11p and Xrs2p (Haber, 2000). All these proteins are highly conserved and some of them possess several homologues in vertebrate cells. Homozygous loss of the recA-like strand exchange protein Rad51p is lethal in mammalian cells (Sonoda et al., 1998). The catalytic activity of Rad51p is fundamental for HR: many Rad51p monomers bind the long DSB-derived 3'-single strand to form a nucleoprotein filament which invades a homologous duplex (Eggleter et al., 2002). Thereafter, Rad51p catalyses the strand exchange reaction. The importance of this reaction is reflected by the existence of five RAD51 paralogues in mammalian cells (RAD51B/RAD51L1; RAD51C/RAD51L2; RAD51D/RAD51L3; XRCC2; XRCC3) some of which interact with each other and with Rad51p and probably modulate its activity in dependence of the corresponding task. Interestingly, homozygous loss of most of the RAD51 paralogues leads to embryonic lethality, and strong reduction of HR accompanied by simultaneous increase of CA frequency on the cellular level which indicates the important role of these genes in HR (Thacker and Zdzienicka, 2003). While Rad52p plays a central role in *S. cerevisiae*, its loss does not cause a visible phenotype in mammalian cells indicating that there might be backup proteins for Rad52p (e.g. Rad59p) (Rijkers et al., 1998). Rad52p forms heptameric rings that bind to the ends of long DNA single-strands and probably help to promote the formation and/or stabilization of the Rad51p nucleoprotein filament (Benson et al., 1998; Stasiak et al., 2000). DNA-bound Rad52p furthermore promotes the annealing of homologous DNA single strands, the basic reaction of the error-prone SSA-pathway for which Rad51p is not required (Reddy et al., 1997; Kagawa et al., 2001). Rad55p and Rad57p form a heterodimer that also assists the formation of the Rad51p nucleoprotein filament (Sung, 1997). Rad54p is a chromatin remodeling ATPase that interacts with Rad51p and stabilises the nucleoprotein filament (Jaskelioff et al., 2003; Mazin et al., 2003). In mammalian cells, Rad54p plays a key role in sister chromatid recombination while its homologue Rad54Bp appears to participate in inter-chromosomal transactions (Miyagawa et al., 2002). Rad59p apparently interacts with Rad52p and augments its SSA-activity (Davis and Symington, 2001). In yeast, Rad59p plays a role

in ectopic HR that depends on the presence of Rad52p but is independent of the function of Rad51p (SSA) (Jablonovich et al., 1999). Therefore, Rad59p may act in a salvage mechanism that operates when the Rad51p nucleoprotein filament is not functional.

The Rad50p-Mre11p-Nbs1p protein complex is essential for several different processes such as HR, SSA, NHEJ, telomere maintenance, induction of meiotic DSB, regulation of the G<sub>2</sub>/M cell cycle checkpoint, and chromatin structure (Haber, 1998). The components of the protein complex are conserved between yeast and mammalian cells and the bacterial homologues of RAD50 and MRE11 are the SbcC and SbcD genes, respectively (Connelly and Leach, 2002). Mre11p is a nuclease that is involved in generation of the long DNA single-strands from DSB termini which are required for HR and SSA. Complete inactivation of MRE11 or RAD50 is lethal in mammalian cells (Xiao and Weaver, 1997; Luo et al., 1999). Mutations in the NBS1 gene, the human orthologue of the yeast XRS2 gene, cause Nijmegen Breakage Syndrome (NBS), a recessive hereditary disorder that is similar to Ataxia telangiectasia (AT) (Varon et al., 1998; Carney et al., 1998). Non-null mutations in the human MRE11 gene (hMRE11), which result in partial loss of function (hypomorphic), also cause an AT-like disorder (ATLD) (Stewart et al., 1999). Cells from patients with NBS, AT, or ATLD are extremely sensitive to DSB-inducing agents and display radiation-resistant DNA synthesis (RDS) after irradiation with IR, and NBS1-deficient cells show reduced levels of HR (Tauchi et al., 2002). The finding that the ATM kinase (the protein defective in AT cells) phosphorylates Nbs1p after damage induction indicates a further role of the Rad50p-Mre11p-Nbs1p complex in damage-dependent cell cycle regulation (S-phase check point) (Petrini, 1999).

Because of the high content of repetitive DNA in the mammalian genome, tight regulation of HR is essential to prevent ectopic recombination and thus the formation of CA. Here, the products of the breast cancer tumour suppressor genes BRCA1 and BRCA2 play a fundamental role (Venkitaraman, 2002). Both genes encode very large proteins (1,833 aa and 3,418 aa), which are expressed in the nucleus during S- and G<sub>2</sub>-phase. They share little similarity with each other, and no orthologues have yet been identified in invertebrates. Complete inactivation of BRCA1 or BRCA2 leads to cellular lethality and hypomorphic mutations cause high frequencies of CA indicating that both proteins are involved in the maintenance of chromatin structure (Ludwig et al., 1997). Furthermore, both proteins appear to function in DNA repair, recombination, cell cycle control, and regulation of transcription. By binding of several Rad51p monomers via its eight central BRC-repeat motifs (each ~30–40 aa), Brca2p inhibits formation of the Rad51p nucleoprotein filament and thus regulates the availability and activity of Rad51p to prevent undesired HR reactions during normal cell metabolism (Davies et al., 2001). This model is supported by the observation that cells with BRCA2 deficiency perform less accurate HR but instead more error-prone SSA that does not require Rad51p (Tutt and Ashworth, 2002). If this model was correct, the Rad51p-Brca2p complex would have to be activated by DNA damage or replication arrest (e.g. by an ATM-mediated phosphorylation cascade). This activa-

tion could lead to a steric alteration of the Rad51p-Brc1p complex and thus to a controlled loading of a DNA single-strand with Rad51p (Davies et al., 2001).

The role of Brc1p in the HR reaction is less well defined. One of many different interactors of Brc1p is the Rad50p-Mre11p-Nbs1p complex (Zhong et al., 1999; Wang et al., 2000). Since Brc1p binds directly to DNA and inhibits the nuclease activity of Mre11p *in vitro*, it is possible that Brc1p regulates the length of the DNA single strands generated by Mre11p at the DSB (Paull et al., 2001). This is also supported by the finding that HR and SSA (both need long single strands) but not NHEJ are impaired in BRCA1 deficient cells. Brc1p probably also plays a more general role in signaling of DSB and the following regulation cascades because it is phosphorylated by the ATM and CHK2 kinase after IR-irradiation (Wang et al., 2000). Furthermore, Brc1p appears to be involved in chromatin remodelling after damage induction because Brc1p foci appear very early at sites of induced DSB (Celeste et al., 2003). Together with Bard1p, Brc1p forms a heterodimer exhibiting E3 ubiquitin ligase activity, which is possibly involved in the degradation of proteins responsible for RNA stability by polyadenylation (Ruffner et al., 2001; Hashizume et al., 2001). Such an enzymatic function of Brc1p would have profound consequences for the stability and activity of the corresponding substrate proteins and could help to explain the diverse biological functions of Brc1p.

A further connection to HR and the two BRCA genes emerges from the investigation of the FANC genes which are defective in the hereditary disease Faconi anaemia (FA) (Stewart and Elledge, 2002; D'Andrea and Grompe, 2003). Cells derived from FA patients display increased sensitivity towards DSB- and ICL-inducing agents and highly elevated frequencies of CA. ICL completely block transcription and replication and are probably converted to a DSB intermediate, which is subsequently repaired by HR. This thesis is supported by the observation that cells with defects in BRCA1 and BRCA2 or RAD51C display extremely increased sensitivity towards ICL-inducing agents and strongly elevated frequencies of spontaneous CA. With the exception of FANC-B, all other known FANC genes (-A, C, D1, D2, E, F, G) have been cloned. Interestingly, the corresponding proteins neither share homology with each other nor with other known proteins, and no homologues have yet been identified in invertebrates. At least five proteins (FancAp, Cp, Ep, Fp, Gp) form a larger stable complex that regulates the (possibly Brc1p-mediated) ubiquitination of FancD2p after ICL induction, which then is recruited to Rad51p containing repair foci. Furthermore, FancD2p interacts with Nbs1p and is phosphorylated by the ATM kinase after IR irradiation (Nakanishi et al., 2002). The fact that patients belonging to the FANC-D1 complementation group harbour hypomorphic mutations within the BRCA2 gene, lead to the surprising finding that FANC-D1 (and probably also FANC-B) is identical with BRCA2 (Howlett et al., 2002). This and the fact that FancAp interacts directly with Brc1p and FancGp interacts with Brc2p/FancD1p implies a role of the FANC gene products in the HR mediated repair of DSB and ICL (Folias et al., 2002; Hussain et al., 2003).

## Homology-independent mechanisms

In contrast to HR which is most active through late S/G<sub>2</sub>-phase of the cell cycle, the homology-independent NHEJ pathway is active during all cell cycle phases and appears to play a major role in eliminating spontaneous and IR-induced DSB during G<sub>1</sub> and G<sub>0</sub> phases (Rothkamm et al., 2003). Furthermore, it is essential for the repair of DSB occurring during V(D)J recombination and Ig class switch (Jackson and Jeggo, 1995). NHEJ is able to join DNA ends directly in the absence of sequence homology and thus to restore an intact DNA duplex. However, the original sequence is only precisely restored if two complementary ends are re-ligated. In contrast, two non-complementary ends first have to be processed by DNA polymerases and/or nucleases to yield a ligatable structure. These modifications lead to small scale alterations in the range of a few base pairs or kilobases, which are only detectable by restriction mapping or sequence analysis. If ends that originate from different chromosomes are erroneously rejoined, CA (e.g. translocations and dicentric) may arise (Pfeiffer, 1998).

Obviously, NHEJ is – in contrast to conservative HR – inaccurate and can cause mutations. Considering this mutagenic potential, it is surprising that mammalian cells preferentially use the NHEJ pathway for DSB repair (Wang et al., 2001). This could be related to the independence of NHEJ of sequence homology, which facilitates repair in G<sub>0</sub> and G<sub>1</sub>. Independence of sequence homology and the fact that the majority of cells are in G<sub>1</sub> might also be responsible for the remarkably high efficiency of this pathway (in an HR-deficient background, the majority of IR-induced DSB is repaired by NHEJ after only one hour) (Wang et al., 2001). The consequences of NHEJ-mediated DSB repair should be tolerable if the number of initial DSB remains small so that originally connected ends are rejoined with high preference. The probability that small sequence alterations at break points affect a critical region of an essential expressed gene is expected to be low because of the low proportion of coding sequences in the mammalian genome (~ 1%). If, still, an essential gene was affected in diploid cells, the intact allele could compensate for the defective one, and irreversibly damaged cells could be eliminated by apoptosis. Thus, NHEJ-mediated DSB repair is expected to cause disadvantageous mutations and CA only in a few cases.

The investigation of different hamster cell lines displaying extreme sensitivity to IR and defects in DSB repair led to the identification of the genes XRCC4 to XRCC7 and LIG4 (Jeggo, 1998; Thacker and Zdzienicka, 2003). All five genes are essential for NHEJ-mediated DSB repair and V(D)J recombination, and XRCC4 and LIG4 also perform essential functions in early embryonic development (Barnes et al., 1998; Gao et al., 1998). The corresponding gene products are Xrcc4p, which forms a protein complex with DNA ligase IV (Lig4p) and greatly stimulates ligation activity (Grawunder et al., 1997). XRCC5, 6, and 7 encode the three components of the DNA dependent protein kinase (DNA-PK), which consists of the Ku70/Ku80 heterodimer and the catalytic sub-unit of the kinase (DNA-PK<sub>CS</sub>) (Featherstone and Jackson, 1999a, b). Loss of any of the three components causes the SCID (severe combined immuno deficiency) phenotype in mice (Jackson and

Jeggo, 1995). Because of its ability to bind with high preference to DNA ends in a sequence-independent manner, the Ku70/80 heterodimer probably functions as an alignment factor that binds to DSB ends and subsequently stimulates their alignment and ligation by Lig4p (Thode et al., 1990; Feldmann et al., 2000). The latter two steps require the interaction of Ku with DNA-PK<sub>CS</sub>. DNA-PK<sub>CS</sub> also participates in signal transduction after DNA damage and the recruitment of further repair enzymes to the DSB site (Jackson, 2002).

Before Lig4p can catalyse the final NHEJ reaction step of DNA backbone ligation, most DSB ends have to be converted into ligatable structures by DNA nucleases and/or polymerases. The enzymes involved in these steps are not yet well defined, but Polμ is implicated in the filling of small single-stranded (ss) gaps (Cooper et al., 2000; Mahajan et al., 2002). Mutations in the recently cloned Artemis gene cause the human radiosensitive SCID (RS-SCID) phenotype (Moshous et al., 2001). The gene encodes a member of the metallo-β-lactamase superfamily, a nuclease that is essential for the opening of the hairpin intermediates that occur during V(D)J recombination (Ma et al., 2002). Its endonucleolytic activity on ss overhangs suggests an additional role in the trimming of complex IR-induced DSB ends during NHEJ (Jeggo and O'Neill, 2002). Finally, the Rad50p-Mre11p-Nbs1p complex also participates in NHEJ. This is supported by the fact that Mre11p interacts with Ku70 in mammalian cells and that mutations in the three yeast homologues lead to a 50- to 100-fold decrease of NHEJ in a RAD52 background (Critchlow and Jackson, 1998; Goedecke et al., 1999). Although the precise role of the Rad50p-Mre11p-Nbs1p complex in NHEJ is yet unclear it is possible that the nucleolytic activities of Rad50p and Mre11p are involved in the removal of unpaired bases. Furthermore, Rad50p possesses long flexible hooks (Cys-X-X-Cys motif), which – together with Mre11p – can form complexes supposed to function as bridges between two sister chromatids or two DSB ends (de Jager et al., 2001). How and in which order the Ku70/80 heterodimer and the Rad50p-Mre11p-Nbs1 complex interact with each other in the NHEJ reaction is not yet clarified.

Apart from the “classical” Ku-dependent NHEJ pathway, there exists at least one more, Ku-independent NHEJ pathway that is error-prone because it generates mostly small deletions carrying microhomologies (small homology patches of 1–7 bp) at their break points, which are reminiscent of the SSA pathway (Göttlich et al., 1998; Feldmann et al., 2000). This slower backup NHEJ pathway appears to take over in cells in which the more efficient (20–30 fold faster) Ku-dependent NHEJ pathway is inactivated due to mutations in XRCC4 to XRCC7, or LIG4, respectively (Wang et al., 2001, 2003). Because of its error-proneness, the Ku-independent pathway could be responsible for the formation of certain complex translocations found in some aggressive B-cell lymphomas that arise in NHEJ-deficient mice as a result of incorrectly re-joined V(D)J intermediates (Roth, 2002). The factors participating in this NHEJ mechanism are presently unknown. Due to the high frequency of deletions with characteristic sequence homologies at their break points, it cannot be excluded, however, that the backup NHEJ pathway recruits components of the SSA pathway (e.g. Rad50p-Mre11p-Nbs1p; Rad52p).

## Conclusions

The recent research on DSB repair pathways has not only provided insights in the functioning of these mechanisms but has also shown that the number of proteins and the complexity of their interactions is much larger than previously anticipated. Surprisingly, many proteins do not only function in one single but several different pathways (e.g. Rad50p-Mre11p-Nbs1p). This may, in part, explain the pleiotropic phenotypes of cells carrying mutations in the corresponding genes. Such complex interactions between proteins within different pathways requires tight regulation within the cell cycle which is achieved by post-translational modifications such as phosphorylation, ubiquitination, or sumoylation.

Another, most interesting question concerns the regulation of pathway selection. NHEJ appears to be most active when HR is not possible due to the absence of a homologous donor sequence. Thus, HR is most active and important during late S/G<sub>2</sub>-phase, where it is coupled to replication and participates in the repair of replication-induced DSB and the restarting of stalled replication forks. On the other hand, the Ku-dependent NHEJ pathway is probably responsible for the repair of DSB during G<sub>0</sub> and G<sub>1</sub>. This view is supported by recent reports showing that not only eukaryotes but also some bacteria (e.g. *B. subtilis*) and archaea possess operons that encode functional NHEJ components (YKoV = Ku70/80; YKoU = Lig4 plus associated nuclease and primase) (Aravind and Koonin, 2001; Doherty et al., 2001; Weller and Doherty, 2001). This unexpected finding not only provides new evolutionary insights into the core biochemistry of NHEJ but also suggests that selection of NHEJ in bacteria, and perhaps eukaryotes, might be driven by prolonged periods of mitotic exit. Many microorganisms, including NHEJ-containing prokaryotes, initiate a defined cellular state of prolonged cell cycle exit (stationary phase) in response to environmental stress. Therefore, NHEJ might be especially efficient in stationary phase to counteract DSB induced by heat, desiccation and other factors. NHEJ might also participate in “adaptive mutagenesis” postulated as a mechanism for genome diversification under stress during stationary phase which is independent of RecA in *B. subtilis*. Thus it is possible that NHEJ is activated in preference to HR during prolonged periods of mitotic exit (Wilson et al., 2003).

In summary, the data reviewed here show that mammalian cells possess different highly efficient mechanisms to deal with DSB in different situations. Of these DSB repair pathways, only HR is usually highly accurate while SSA and NHEJ are error-prone because they generate small scale mutations in the form of deletions and/or insertions. When malfunctioning, all three pathways have the potential to generate CA which may be regarded as the light microscopically visible part of a much larger spectrum of mutations induced by these mechanisms. This becomes especially obvious in cells carrying mutations in the corresponding HR and NHEJ repair genes because these cells exhibit highly elevated frequencies of spontaneous CA. This shows that the same mechanisms that usually prevent the formation of deleterious CA are also responsible for the formation of CA when DSB induced in different chromosomes are erroneously re-joined or recombined.

## References

- Alberts B: DNA replication and recombination. *Nature* 421:431–435 (2003).
- Aravind L, Koonin EV: Prokaryotic homologs of the eukaryotic DNA-end-binding protein Ku, novel domains in the Ku protein and prediction of a prokaryotic double-strand break repair system. *Genome Res* 11:1365–1374 (2001).
- Barnes DE: DNA damage: air-breaks? *Curr Biol* 12: R262–R264 (2002).
- Barnes DE, Stamp G, Rosewell I, Denzel A, Lindahl T: Targeted disruption of the gene encoding DNA ligase IV leads to lethality in embryonic mice. *Curr Biol* 8:1395–1398 (1998).
- Bassing CH, Swat W, Alt FW: The mechanism and regulation of chromosomal V(D)J recombination. *Cell* 109 Suppl:S45–S55 (2002).
- Benson FE, Baumann P, West SC: Synergistic actions of Rad51 and Rad52 in recombination and DNA repair. *Nature* 391:401–404 (1998).
- Bryant PE: Enzymatic restriction of mammalian cell DNA using *PvuIII* and *BamHI*: evidence for the double-strand break origin of chromosomal aberrations. *Int J Radiat Biol Relat Stud Phys Chem Med* 46:57–65 (1984).
- Carny JP, Maser RS, Olivares H, Davis EM, Le Beau M, Yates JR, III, Hays L, Morgan WF, Petrini JH: The hMre11/hRad50 protein complex and Nijmegen breakage syndrome: linkage of double-strand break repair to the cellular DNA damage response. *Cell* 93:477–486 (1998).
- Celeste A, Fernandez-Capetillo O, Kruhlik MJ, Pilch DR, Staudt DW, Lee A, Bonner RF, Bonner WM, Nussenzweig A: Histone H2AX phosphorylation is dispensable for the initial recognition of DNA breaks. *Nature Cell Biol* 5:675–679 (2003).
- Connelly JC, Leach DR: Tethering on the brink: the evolutionarily conserved Mre11-Rad50 complex. *Trends Biochem Sci* 27:410–418 (2002).
- Cooper MP, Machwe A, Orren DK, Brosh RM, Ramsden D, Bohr VA: Ku complex interacts with and stimulates the Werner protein. *Genes Dev* 14:907–912 (2000).
- Critchlow SE, Jackson SP: DNA end-joining: from yeast to man. *Trends Biochem Sci* 23:394–398 (1998).
- D'Andrea AD, Grompe M: The Fanconi anaemia/BRCA pathway. *Nature Rev Cancer* 3:23–34 (2003).
- Davies AA, Masson JY, McIlwraith MJ, Stasiak AZ, Stasiak A, Venkitaraman AR, West SC: Role of BRCA2 in control of the RAD51 recombination and DNA repair protein. *Mol Cell* 7:273–282 (2001).
- Davis AP, Symington LS: The yeast recombinational repair protein Rad59 interacts with Rad52 and stimulates single-strand annealing. *Genetics* 159: 515–525 (2001).
- Doherty AJ, Jackson SP, Weller GR: Identification of bacterial homologues of the Ku DNA repair proteins. *FEBS Lett* 500:186–188 (2001).
- Dresser ME: Meiotic chromosome behavior in *Saccharomyces cerevisiae* and (mostly) mammals. *Mutat Res* 451:107–127 (2000).
- Duker NJ: Chromosome breakage syndromes and cancer. *Am J Med Genet* 115:125–129 (2002).
- Eggle AL, Inman RB, Cox MM: The Rad51-dependent pairing of long DNA substrates is stabilized by replication protein A. *J Biol Chem* 277:39280–39288 (2002).
- Featherstone C, Jackson SP: DNA-dependent protein kinase gets a break: its role in repairing DNA and maintaining genomic integrity. *Br J Cancer* 80 Suppl 1:14–19 (1999a).
- Featherstone C, Jackson SP: Ku, a DNA repair protein with multiple cellular functions? *Mutat Res* 434:3–15 (1999b).
- Feldmann E, Schmiemann V, Goedecke W, Reichenberger S, Pfeiffer P: DNA double-strand break repair in cell-free extracts from Ku80-deficient cells: implications for Ku serving as an alignment factor in non-homologous DNA end joining. *Nucl Acids Res* 28:2585–2596 (2000).
- Ferguson DO, Alt FW: DNA double strand break repair and chromosomal translocation: lessons from animal models. *Oncogene* 20:5572–5579 (2001).
- Folias A, Matkovic M, Bruun D, Reid S, Hejna J, Grompe M, D'Andrea A, Moses R: BRCA1 interacts directly with the Fanconi anemia protein FANCA. *Hum Mol Genet* 11:2591–2597 (2002).
- Gao Y, Sun Y, Frank KM, Dikkes P, Fujiwara Y, Seidl KJ, Sekiguchi JM, Rathbun GA, Swat W, Wang J, Bronson RT, Malynn BA, Bryans M, Zhu C, Chaudhuri J, Davidson L, Ferrini R, Stamato T, Orkin SH, Greenberg ME, Alt FW: A critical role for DNA end-joining proteins in both lymphogenesis and neurogenesis. *Cell* 95:891–902 (1998).
- van Gent DC, Hoeijmakers JH, Kanaar R: Chromosomal stability and the DNA double-stranded break connection. *Nature Rev Genet* 2:196–206 (2001).
- Goedecke W, Eijpe M, Offenberg HH, van Aalderen M, Heyting C: Mre11 and Ku70 interact in somatic cells, but are differentially expressed in early meiosis. *Nature Genet* 23:194–198 (1999).
- Göttlich B, Reichenberger S, Feldmann E, Pfeiffer P: Rejoining of DNA double-strand breaks in vitro by single-strand annealing. *Eur J Biochem* 258:387–395 (1998).
- Grawunder U, Wilm M, Wu X, Kulesza P, Wilson TE, Mann M, Lieber MR: Activity of DNA ligase IV stimulated by complex formation with XRCC4 protein in mammalian cells. *Nature* 388:492–495 (1997).
- Haber JE: The many interfaces of Mre11. *Cell* 95:583–586 (1998).
- Haber JE: DNA recombination: the replication connection. *Trends Biochem Sci* 24:271–275 (1999).
- Haber JE: Recombination: a frank view of exchanges and vice versa. *Curr Opin Cell Biol* 12:286–292 (2000).
- Hashizume R, Fukuda M, Maeda I, Nishikawa H, Oyake D, Yabuki Y, Ogata H, Ohta T: The RING heterodimer BRCA1-BARD1 is a ubiquitin ligase inactivated by a breast cancer-derived mutation. *J Biol Chem* 276:14537–14540 (2001).
- Honjo T, Kinoshita K, Muramatsu M: Molecular mechanism of class switch recombination: linkage with somatic hypermutation. *A Rev Immunol* 20:165–196 (2002).
- Howlett NG, Taniguchi T, Olson S, Cox B, Waisfisz Q, Die-Smulders C, Persky N, Grompe M, Joenje H, Pals G, Ikeda H, Fox EA, D'Andrea AD: Biallelic inactivation of BRCA2 in Fanconi anemia. *Science* 297:606–609 (2002).
- Hussain S, Witt E, Huber PA, Medhurst AL, Ashworth A, Mathew CG: Direct interaction of the Fanconi anaemia protein FANCG with BRCA2/FANCD1. *Hum molec Genet* 12:2503–2510 (2003).
- Jablonovich Z, Liefshitz B, Steinlauf R, Kupiec M: Characterization of the role played by the RAD59 gene of *Saccharomyces cerevisiae* in ectopic recombination. *Curr Genet* 36:13–20 (1999).
- Jackson SP: Sensing and repairing DNA double-strand breaks. *Carcinogenesis* 23:687–696 (2002).
- Jackson SP, Jeggo PA: DNA double-strand break repair and V(D)J recombination: involvement of DNA-PK. *Trends Biochem Sci* 20:412–415 (1995).
- de Jager M, van Noort J, van Gent DC, Dekker C, Kanaar R, Wyman C: Human Rad50/Mre11 is a flexible complex that can tether DNA ends. *Mol Cell* 8:1129–1135 (2001).
- Janin M: Chromosome breaks and genomic instability. *Cancer Invest* 18:78–86 (2000).
- Jaskelioff M, Van Komen S, Krebs JE, Sung P, Peterson CL: Rad54p is a chromatin remodeling enzyme required for heteroduplex DNA joint formation with chromatin. *J Biol Chem* 278:9212–9218 (2003).
- Jeggo PA: Identification of genes involved in repair of DNA double-strand breaks in mammalian cells. *Radiat Res* 150:S80–S91 (1998).
- Jeggo P, O'Neill P: The Greek Goddess, Artemis, reveals the secrets of her cleavage. *DNA Repair (Amst)* 1:771–777 (2002).
- Johnson RD, Janin M: Double-strand-break-induced homologous recombination in mammalian cells. *Biochem Soc Trans* 29:196–201 (2001).
- Kagawa W, Kurumizaka H, Ikawa S, Yokoyama S, Shibata T: Homologous pairing promoted by the human Rad52 protein. *J Biol Chem* 276:35201–35208 (2001).
- Keeney S: Mechanism and control of meiotic recombination initiation. *Curr Top Dev Biol* 52:1–53 (2001).
- Lengauer C, Kinzler KW, Vogelstein B: Genetic instabilities in human cancers. *Nature* 396:643–649 (1998).
- Levine AJ: p53, the cellular gatekeeper for growth and division. *Cell* 88:323–331 (1997).
- Levitt NC, Hickson ID: Caretaker tumour suppressor genes that defend genome integrity. *Trends Mol Med* 8:179–186 (2002).
- Ludwig T, Chapman DL, Papaioannou VE, Efstratiadis A: Targeted mutations of breast cancer susceptibility gene homologs in mice: lethal phenotypes of *Brcal*, *Brcal2*, *Brcal1/Brcal2*, *Brcal1/p53*, and *Brcal2/p53* nullizygous embryos. *Genes Dev* 11:1226–1241 (1997).
- Luo G, Yao MS, Bender CF, Mills M, Bladl AR, Bradley A, Petrini JH: Disruption of mRad50 causes embryonic stem cell lethality, abnormal embryonic development, and sensitivity to ionizing radiation. *Proc Natl Acad Sci USA* 96:7376–7381 (1999).
- Ma Y, Pannicke U, Schwarz K, Lieber MR: Hairpin opening and overhang processing by an Artemis/DNA-dependent protein kinase complex in nonhomologous end joining and V(D)J recombination. *Cell* 108:781–794 (2002).
- Mahajan KN, Nick McElhinny SA, Mitchell BS, Ramsden DA: Association of DNA polymerase mu (pol mu) with Ku and ligase IV: role for pol mu in end-joining double-strand break repair. *Mol Cell Biol* 22:5194–5202 (2002).
- Mazin AV, Alexeev AA, Kowalczykowski SC: A novel function of Rad54 protein. Stabilization of the Rad51 nucleoprotein filament. *J Biol Chem* 278: 14029–14036 (2003).
- Miyagawa K, Tsuruga T, Kinomura A, Usui K, Katsura M, Tashiro S, Mishima H, Tanaka K: A role for RAD54B in homologous recombination in human cells. *EMBO J* 21:175–180 (2002).
- Moshous D, Callebaut I, de Chasseval R, Corneo B, Cavazzana-Calvo M, Le Deist F, Tezcan I, Sanal O, Bertrand Y, Philippe N, Fischer A, de Villartay JP: Artemis, a novel DNA double-strand break repair/V(D)J recombination protein, is mutated in human severe combined immune deficiency. *Cell* 105:177–186 (2001).
- Nakanishi K, Taniguchi T, Ranganathan V, New HV, Moreau LA, Stotsky M, Mathew CG, Kastan MB, Weaver DT, D'Andrea AD: Interaction of FANCD2 and NBS1 in the DNA damage response. *Nature Cell Biol* 4:913–920 (2002).
- Natarajan AT, Obe G: Molecular mechanisms involved in the production of chromosomal aberrations. III. Restriction endonucleases. *Chromosoma* 90:120–127 (1984).

- Neumann AA, Reddel RR: Telomere maintenance and cancer – look, no telomerase. *Nature Rev Cancer* 2:879–884 (2002).
- Obe G, Pfeiffer P, Savage JR, Johannes C, Goedecke W, Jeppesen P, Natarajan AT, Martinez-Lopez W, Folle GA, Drets ME: Chromosomal aberrations: formation, identification and distribution. *Mutat Res* 504:17–36 (2002).
- Paques F, Haber JE: Multiple pathways of recombination induced by double-strand breaks in *Saccharomyces cerevisiae*. *Microbiol Mol Biol Rev* 63:349–404 (1999).
- Paull TT, Cortez D, Bowers B, Elledge SJ, Gellert M: Direct DNA binding by Brca1. *Proc natl Acad Sci, USA* 98:6086–6091 (2001).
- Petrini JH: The mammalian Mre11-Rad50-nbs1 protein complex: integration of functions in the cellular DNA-damage response. *Am J hum Genet* 64:1264–1269 (1999).
- Pfeiffer P: The mutagenic potential of DNA double-strand break repair. *Toxicol Lett* 96–97:119–129 (1998).
- Pfeiffer P, Goedecke W, Obe G: Mechanisms of DNA double-strand break repair and their potential to induce chromosomal aberrations. *Mutagenesis* 15: 289–302 (2000).
- Reddy G, Golub EI, Radding CM: Human Rad52 protein promotes single-strand DNA annealing followed by branch migration. *Mutat Res* 377:53–59 (1997).
- Reynaud CA, Aoufouchi S, Faili A, Weill JC: What role for AID: mutator, or assembler of the immunoglobulin mutasome? *Nature Immunol* 4:631–638 (2003).
- Richardson C, Moynahan ME, Jasin M: Double-strand break repair by interchromosomal recombination: suppression of chromosomal translocations. *Genes Dev* 12:3831–3842 (1998).
- Rijkers T, Van Den OJ, Morolli B, Rolink AG, Baarends WM, Van Sloun PP, Lohman PH, Pastink A: Targeted inactivation of mouse RAD52 reduces homologous recombination but not resistance to ionizing radiation. *Mol Cell Biol* 18:6423–6429 (1998).
- Roth DB: Amplifying mechanisms of lymphomagenesis. *Mol Cell* 10:1–2 (2002).
- Rothkamm K, Kruger I, Thompson LH, Lobrich M: Pathways of DNA double-strand break repair during the mammalian cell cycle. *Mol Cell Biol* 23:5706–5715 (2003).
- Ruffner H, Joazeiro CA, Hemmati D, Hunter T, Verma IM: Cancer-predisposing mutations within the RING domain of BRCA1: loss of ubiquitin protein ligase activity and protection from radiation hypersensitivity. *Proc natl Acad Sci, USA* 98:5134–5139 (2001).
- Sachs RK, Hlatky LR, Trask BJ: Radiation-produced chromosome aberrations: colourful clues. *Trends Genet* 16:143–146 (2000).
- Sonoda E, Sasaki MS, Buerstedde JM, Bezzubova O, Shinohara A, Ogawa H, Takata M, Yamaguchi-Iwai Y, Takeda S: Rad51-deficient vertebrate cells accumulate chromosomal breaks prior to cell death. *EMBO J* 17:598–608 (1998).
- Stasiak AZ, Larquet E, Stasiak A, Muller S, Engel A, Van Dyck E, West SC, Egelman EH: The human Rad52 protein exists as a heptameric ring. *Curr Biol* 10:337–340 (2000).
- Stewart G, Elledge SJ: The two faces of BRCA2, a FANCTastic discovery. *Mol Cell* 10:2–4 (2002).
- Stewart GS, Maser RS, Stankovic T, Bressan DA, Kaplan MI, Jaspers NG, Raams A, Byrd PJ, Petrini JH, Taylor AM: The DNA double-strand break repair gene hMRE11 is mutated in individuals with an ataxia-telangiectasia-like disorder. *Cell* 99:577–587 (1999).
- Sung P: Yeast Rad55 and Rad57 proteins form a heterodimer that functions with replication protein A to promote DNA strand exchange by Rad51 recombinase. *Genes Dev* 11:1111–1121 (1997).
- Tauchi H, Kobayashi J, Morishima K, van Gent DC, Shiraishi T, Verkaik NS, vanHeems D, Ito E, Nakamura A, Sonoda E, Takata M, Takeda S, Matsuura S, Komatsu K: Nbs1 is essential for DNA repair by homologous recombination in higher vertebrate cells. *Nature* 420:93–98 (2002).
- Thacker J, Zdzienicka MZ: The mammalian XRCC genes: their roles in DNA repair and genetic stability. *DNA Repair (Amst)* 2:655–672 (2003).
- Thode S, Schäfer A, Pfeiffer P, Vielmetter W: A novel pathway of DNA end-to-end joining. *Cell* 60:921–928 (1990).
- Tutt A, Ashworth A: The relationship between the roles of BRCA genes in DNA repair and cancer predisposition. *Trends Mol Med* 8:571–576 (2002).
- Varon R, Vissinga C, Platzer M, Cersaletti KM, Chrzanowska KH, Saar K, Beckmann G, Seemanova E, Cooper PR, Nowak NJ, Stumm M, Weemaes CM, Gatti RA, Wilson RK, Digweed M, Rosenthal A, Sperling K, Concannon P, Reis A: Nibrin, a novel DNA double-strand break repair protein, is mutated in Nijmegen breakage syndrome. *Cell* 93:467–476 (1998).
- Venkitaraman AR: Chromosomal instability and cancer predisposition: insights from studies on the breast cancer susceptibility gene, BRCA2. *Cold Spring Harb Symp Quant Biol* 65:567–572 (2000).
- Venkitaraman AR: Cancer susceptibility and the functions of BRCA1 and BRCA2. *Cell* 108:171–182 (2002).
- Wang H, Zeng ZC, Bui TA, Sonoda E, Takata M, Takeda S, Iliakis G: Efficient rejoining of radiation-induced DNA double-strand breaks in vertebrate cells deficient in genes of the RAD52 epistasis group. *Oncogene* 20:2212–2224 (2001).
- Wang H, Perrault AR, Takeda Y, Qin W, Wang H, Iliakis G: Biochemical evidence for Ku-independent backup pathways of NHEJ. *Nucl Acids Res* 31: 5377–5388 (2003).
- Wang Y, Cortez D, Yazdi P, Neff N, Elledge SJ, Qin J: BASC, a super complex of BRCA1-associated proteins involved in the recognition and repair of aberrant DNA structures. *Genes Dev* 14:927–939 (2000).
- Ward JF: Complexity of damage produced by ionizing radiation. *Cold Spring Harb Symp Quant Biol* 65:377–382 (2000).
- Weller GR, Doherty AJ: A family of DNA repair ligases in bacteria? *FEBS Lett* 505:340–342 (2001).
- Wilson TE, Topper LM, Palmbois PL: Non-homologous end-joining: bacteria join the chromosome breakdance. *Trends Biochem Sci* 28:62–66 (2003).
- Xiao Y, Weaver DT: Conditional gene targeted deletion by Cre recombinase demonstrates the requirement for the double-strand break repair Mre11 protein in murine embryonic stem cells. *Nucl Acids Res* 25:2985–2991 (1997).
- Zhong Q, Chen CF, Li S, Chen Y, Wang CC, Xiao J, Chen PL, Sharp ZD, Lee WH: Association of BRCA1 with the hRad50-hMre11-p95 complex and the DNA damage response. *Science* 285:747–750 (1999).

# Mechanisms of DNA double strand break repair and chromosome aberration formation

G. Iliakis,<sup>a,b</sup> H. Wang,<sup>b</sup> A.R. Perrault,<sup>b</sup> W. Boecker,<sup>a</sup> B. Rosidi,<sup>a</sup> F. Windhofer,<sup>a</sup> W. Wu,<sup>a</sup> J. Guan,<sup>b</sup> G. Terzoudi,<sup>c</sup> and G. Pantelias<sup>c</sup>

<sup>a</sup>Institute of Medical Radiation Biology, University of Duisburg-Essen Medical School, Essen (Germany);

<sup>b</sup>Department of Radiation Oncology, Division of Experimental Radiation Oncology, Kimmel Cancer Center, Jefferson Medical College, Philadelphia PA (USA);

<sup>c</sup>Laboratory of Health Physics and Environmental Hygiene, MCSR Demokritos, Athens (Greece)

**Abstract.** It is widely accepted that unrepaired or misrepaired DNA double strand breaks (DSBs) lead to the formation of chromosome aberrations. DSBs induced in the DNA of higher eukaryotes by endogenous processes or exogenous agents can in principle be repaired either by non-homologous endjoining (NHEJ), or homology directed repair (HDR). The basis on which the selection of the DSB repair pathway is made remains unknown but may depend on the inducing agent, or process. Evaluation of the relative contribution of NHEJ and HDR specifically to the repair of ionizing radiation (IR) induced DSBs is important for our understanding of the mechanisms leading to chromosome aberration formation. Here, we review recent work from our laboratories contributing to this line of inquiry. Analysis of DSB rejoining in irradiated cells using pulsed-field gel electrophoresis reveals a fast component operating with half times of 10–30 min. This component of DSB rejoining is severely compromised in cells with mutations in DNA-PKcs, Ku, DNA ligase IV, or XRCC4, as well as after chemical inhibition of DNA-PK, indicating that it reflects classical NHEJ; we termed this form of DSB rejoining D-NHEJ to signify its dependence on DNA-PK. Although chemical inhibition, or mutation, in any of these factors delays processing, cells ultimately remove the majority of DSBs using an alternative pathway operating with slower kinetics (half time 2–10 h). This alternative, slow pathway of DSB rejoining remains unaffected in mutants deficient in several genes of the RAD52 epistasis group, suggesting that it may not reflect HDR. We proposed that it reflects an alternative form of NHEJ that operates as a

backup (B-NHEJ) to the DNA-PK-dependent (D-NHEJ) pathway. Biochemical studies confirm the presence in cell extracts of DNA end joining activities operating in the absence of DNA-PK and indicate the dominant role for D-NHEJ, when active. These observations in aggregate suggest that NHEJ, operating via two complementary pathways, B-NHEJ and D-NHEJ, is the main mechanism through which IR-induced DSBs are removed from the DNA of higher eukaryotes. HDR is considered to either act on a small fraction of IR induced DSBs, or to engage in the repair process at a step after the initial end joining. We propose that high speed D-NHEJ is an evolutionary development in higher eukaryotes orchestrated around the newly evolved DNA-PKcs and pre-existing factors. It achieves within a few minutes restoration of chromosome integrity through an optimized synapsis mechanism operating by a sequence of protein-protein interactions in the context of chromatin and the nuclear matrix. As a consequence D-NHEJ mostly joins the correct DNA ends and suppresses the formation of chromosome aberrations, albeit, without ensuring restoration of DNA sequence around the break. B-NHEJ is likely to be an evolutionarily older pathway with less optimized synapsis mechanisms that rejoins DNA ends with kinetics of several hours. The slow kinetics and suboptimal synapsis mechanisms of B-NHEJ allow more time for exchanges through the joining of incorrect ends and cause the formation of chromosome aberrations in wild type and D-NHEJ mutant cells.

Copyright © 2003 S. Karger AG, Basel

This work was supported by grants RO1 CA42026, RO1 CA56706 awarded from NIH, DHHS, a grant from the IFORES program of the University of Duisburg-Essen and a grant from the Volkswagenstiftung.

Received 31 October 2003; accepted 22 November 2003.

Request reprints from: Dr. George Iliakis, Institute of Medical Radiation Biology  
University of Duisburg-Essen Medical School  
Hufelandstrasse 55, DE-45122 Essen (Germany); telephone: +49-201-723 4152  
fax: +49-201-723 5966; e-mail: Georg.Iliakis@uni-essen.de.

DNA double strand breaks (DSBs) can be induced in the genome of eukaryotic cells by endogenous processes associated with oxidative metabolism, errors during DNA replication and various forms of site-specific DNA recombination, as well as by exogenous agents such as ionizing radiation (IR) and chemicals. DSBs disrupt the integrity of the genome and are therefore severe lesions, which, if unrepaired or if misre-

paired, can cause genomic instability and cancer, mutations, or cell death.

Three enzymatically distinct processes, homology directed repair (HDR), single strand annealing (SSA), and non-homologous end joining (NHEJ) can, in principle, repair DSBs with a different degree of fidelity (Jackson, 2002; Khanna and Jackson, 2001; Thompson and Limoli, 2003). HDR removes DSBs by utilizing homologous DNA segments, on the same or different DNA molecules, and restores faithfully the original DNA sequence around the break. SSA removes DSBs by annealing the DNA segment containing the break with a homologous segment on the same DNA molecule while excising intervening non-homologous segments. The process restores the DNA sequence around the break, but is associated with a loss of genetic material; it is therefore a mutagenic process. Finally, NHEJ removes DSBs from the genome by simply joining the DNA ends without homology requirements and without ensuring sequence restoration around the break.

While single strand annealing, predominantly documented in yeast (Paques and Haber, 1999), makes an uncertain contribution in higher eukaryotes, NHEJ and HDR are documented processes with well developed enzymatic machineries that have been implicated in DSB repair in higher eukaryotes (Jackson, 2002; Khanna and Jackson, 2001; Thompson and Limoli, 2003). Model systems developed for studying the role of HDR in DSB repair have provided estimates that this process accounts for the removal of approximately 50% of the DSBs induced by a rare cutting restriction endonuclease, *I-Sce I* (Jasin, 2000; Pierce et al., 2001). The remaining breaks are thought to be repaired by NHEJ.

It is not immediately clear whether similar estimates regarding the involvement of HDR and NHEJ also hold for IR-induced DSBs. Notably, estimates from DSB repair kinetics in mutants with defects in homologous recombination (see below) suggest a much lower HDR contribution and implicate NHEJ in the removal of the majority of IR-induced DSBs. Discrepancies regarding the contribution of different repair mechanisms between results obtained with restriction endonuclease-induced DSBs and IR-induced DSBs raise the possibility that the type of ends presented to the repair machineries contributes to pathway selection as it has been suggested for yeast (Lewis and Resnick, 2000; Lewis et al., 1999). We focus therefore here on IR-induced DSBs.

There is evidence that most common chromosome aberrations observed in cells exposed to IR derive either from unrepaired or misrepaired DSBs (Bryant, 1984, 1988; Natarajan, 2002; Natarajan et al., 1986; Obe et al., 2002; Pfeiffer et al., 1996). It is likely that pathway selection for the removal of these lesions from the genome will also determine the probability that a particular DSB will remain unrepaired, or how it will be misrepaired to a chromosomal aberration. Therefore, information on the pathways involved in the repair of DSBs, will have profound consequences for our understanding of the mechanisms of chromosome aberration formation. Key questions remain regarding the identity of the pathways involved and the characterization of their relative contribution. To address this question we have undertaken systematic genetic and biochemical studies focusing on the mechanisms of rejoin-

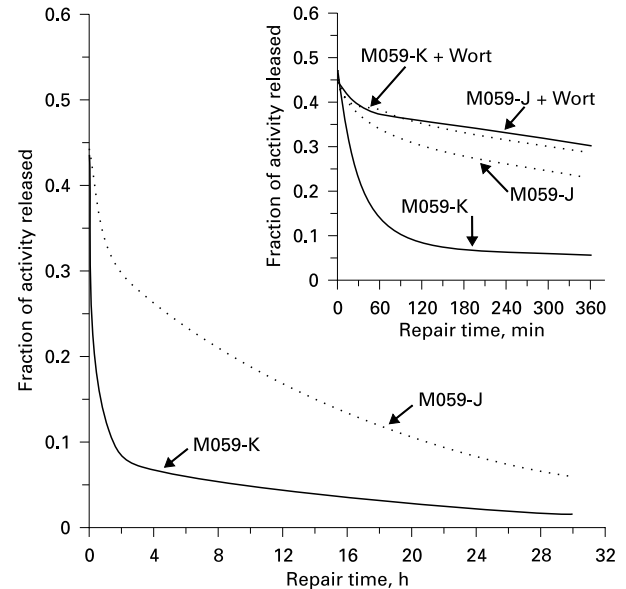


**Fig. 1.** Rejoining of DSB as measured by pulsed-field gel electrophoresis in M059J and M059K cells exposed to IR. Note the difference in the kinetics between wild type (M059K) and DNA-PKcs deficient M059J cells. The insert shows similar results obtained with cells treated with wortmannin.

ing of IR-induced DSBs. Below we summarize key findings from these studies and discuss them from the perspective of chromosome aberration formation.

#### *Fast rejoining of DSBs through DNA-PK-dependent NHEJ (D-NHEJ)*

We evaluated DSB rejoining in irradiated cells of different genetic backgrounds using pulsed-field gel electrophoresis. The rationale was to combine a methodology allowing quantitative analysis of the rejoining kinetics, with mutants defective in a specific repair pathway to delineate the contribution of NHEJ and HDR in the processing of IR-induced DSBs. As a possible outcome we anticipated a relatively fast removal of DSBs by NHEJ and a slower removal, following kinetics similar to those observed in yeast, for DSBs repaired by HDR.

The contribution of DNA-PK dependent NHEJ in the processing of IR-induced DSBs can be analyzed by evaluating the kinetics of rejoining in cells defective in components of the DNA-PK complex. Initial studies were carried out using as a biological system M059J and M059K cells. M059J cells are radiosensitive compared to their isogenic counterpart, M059K, and the increased radiosensitivity is caused by a defect in DNA-PK activity resulting from a mutation in DNA-PKcs (Alalunis-Turner et al., 1993; Anderson et al., 2001; Lees-Miller et al., 1995). Figure 1 depicts previously described kinetics of DSB rejoining in these cell lines (DiBiase et al., 2000). The data indicates that in M059K cells, approximately 80% of the breaks are rejoined in less than 2 h; rejoining is practically complete within 6 h. The kinetics is biphasic and dominated by a fast component operating with half-times of approximately 20 min removing over 80% of the induced DSBs. It is followed



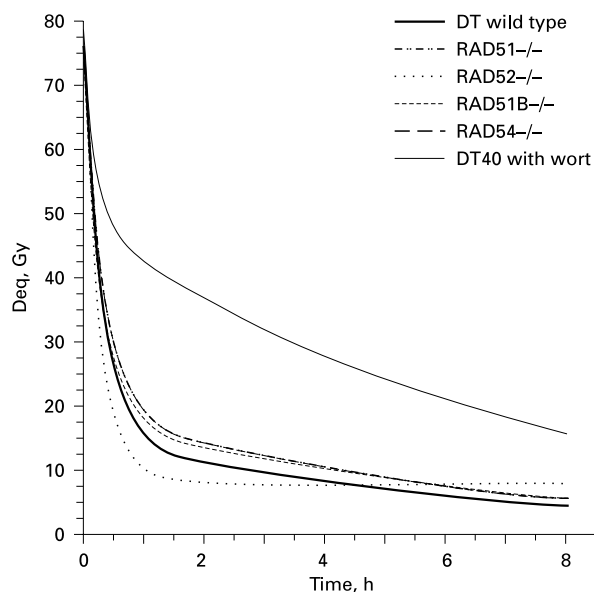


**Fig. 2.** Results similar to those described in Fig. 1 but for DT40 cells and various mutants obtained by targeted gene disruption. The lines drawn for *RAD51*<sup>-/-</sup> and *Rad54*<sup>-/-</sup> cells are practically identical and cannot be discriminated from each other.

by a slow component that rejoins remaining DSBs with a half time of 10–12 h (DiBiase et al., 2000).

In M059J cells rejoining is impaired with fewer breaks rejoined at any given time as compared to M059K cells (Fig. 1). Despite this deficiency, biphasic kinetics is observed with half times for the fast and slow components similar to those of M059K cells. Yet, in M059J cells less than 30% of DSBs are removed with fast kinetics. At 24 h, the DSB repair signal reaches values only slightly higher than those measured in M059K cells, suggesting nearly complete rejoining of DSBs. Thus, in M059J cells, DNA-PK deficiency reduces the fraction of DSBs removed with fast kinetics, but does not gravely reduce the overall fraction of DSBs rejoined, as compared to wild type cells; this is in agreement with results obtained with *scid* cells (Nevaldine et al., 1997). Because longer repair times are required to evaluate the fate of IR-induced DSBs in mutants with defects in components of DNA-PK, earlier studies including measurements for only up to 4–6 h gave the incorrect impression that nearly 50% of IR-induced DSBs remained unrepaired. A crucial conclusion from the observation that M059J cells ultimately rejoin the majority of IR induced DSBs is that human cells, and probably cells of higher eukaryotes in general, are equipped with a DSB rejoining apparatus that remains active in the absence of DNA-PK, and which can remove nearly all DSBs from the genome (DiBiase et al., 2000).

Similar results were obtained in experiments using mutants deficient in Ku (Wang et al., 2001a) and DNA ligase IV (Wang et al., 2001b), as well as wild type cells exposed to wortmannin to chemically inactivate DNA-PK (Wang et al., 2001b), indicating the generality of the observations. In addition, recent experiments using premature chromosome condensation to visualize interphase chromosomes in human lymphocytes have

provided results similar to those described above at much lower doses of radiation (to be described in detail elsewhere). In aggregate these findings allow the following conclusions. First, the fast component of DSB rejoining is DNA-PK- and DNA ligase IV-dependent as it becomes significantly compromised when these factors are inactivated, chemically or genetically. An estimated 20–30% of DSBs that rejoined in M059J cells and other mutants with similar defects, with fast kinetics may be due to residual activity, as treatment of M059J cells with wortmannin reduces this fraction to less than 10% (insert in Fig. 1). We proposed to term this component of DSB rejoining D-NHEJ to indicate that it reflects DNA-PK-dependent NHEJ. Second, the slow component of DSB rejoining is a DNA-PK-independent process, as it remains active in DNA-PK and DNA ligase IV deficient cells. This component of DSB rejoining was a good candidate for HDR based on its slow kinetics, and characterization of its nature, the goal of a subsequent series of investigations.

#### *Slow rejoining of DSBs may not be attributed to HDR*

We carried out genetic studies to systematically evaluate the role of genes implicated in homologous recombination in the rejoining of IR-induced DSBs with particular emphasis on the slow component. We employed as a model DT40 cells, a chicken B cell line which relies on gene conversion to generate immunoglobulin diversity (Bezzubova and Buerstedde, 1994) and which has as a result 1000-fold upregulated levels of homologous recombination compared to mammalian cells (Buerstedde and Takeda, 1991). This increase in homologous recombination greatly facilitates the generation of mutants by gene targeting and enables an evaluation of the role of HDR in DNA DSB rejoining.

Figure 2 shows a summary of previously published results of pulsed field gel electrophoresis experiments carried out using DT40 cells (Wang et al., 2001a). When fitted to the sum of two exponential functions repair half-times of approximately 13 min and 4.5 h are calculated for the fast and the slow components of rejoining, respectively. It is estimated that 78% of the DSBs are removed by the fast component and 22% by the slow component of rejoining. These values are similar to those discussed above and indicate that despite the 1000-fold increase in homologous recombination, DT40 cells remove DSBs from their genome with a similar relative distribution between the fast and the slow component as mammalian cells. Similar to the results with M059K cells treatment with 20  $\mu$ M wortmannin inhibited rejoining, and fitting estimated that 37% and 63% of the DSBs were processed with fast and slow kinetics, respectively (Fig. 2).

To further evaluate the role of HDR in DSB rejoining we studied DT40 mutants generated by targeted disruption of genes involved in HDR. Figure 2 includes results obtained with a conditional *Rad51* mutant tested under conditions suppressing expression of *RAD51* (Sonoda et al., 1998). It is evident that this deficiency is not accompanied by a measurable defect in DSB rejoining. Analysis of *RAD51B*<sup>-/-</sup> DT40 cells indicates mild radiosensitivity to IR and suggests roles in homologous recombination for this protein distinct from those of *Rad51* and other proteins of the *RAD52* epistasis group (Takata et al.,

2000). Yet, *RAD51B*<sup>-/-</sup> cells rejoin DSBs as efficiently as wild type cells. *RAD52*<sup>-/-</sup> DT40 mutants show no hypersensitivity to killing by IR (Yamaguchi-Iwai et al., 1998) and, not surprisingly, DSB rejoining kinetics indistinguishable from those of wild type cells. Deletion of *RAD54* in DT40 renders cells radiosensitive to killing (Bezzubova et al., 1997; Takata et al., 1998). Figure 2 shows that despite these defects, DSB rejoining proceeds in *RAD54*<sup>-/-</sup> rapidly and with kinetics similar to those of wild type cells.

The above results failed to demonstrate a detectable role of HDR in DSB rejoining. However, it could be argued that actual defects in HDR deficient cells are masked by an overly active and extremely fast NHEJ apparatus that is capable of efficiently removing DSBs from the genome, thus limiting the possible consequences of HDR defects. We tested this by comparing rejoining of DSBs between a *KU70*<sup>-/-</sup> and *KU70*<sup>-/-</sup>/*RAD54*<sup>-/-</sup> double knockout (Takata et al., 1998). The double mutant showed kinetics similar to that of *KU70*<sup>-/-</sup> cells (Wang et al., 2001a) suggesting that even disruption of *RAD54* on a *KU70*<sup>-/-</sup> background does not significantly affect the kinetics of DSB rejoining.

Thus, a 1000-fold increase in the potential for homologous recombination in DT40 cells, targeted disruption of genes critical for homologous recombination such as *RAD51*, *RAD51B*, *RAD52* and *RAD54*, and even double mutations in *KU70*<sup>-/-</sup>/*RAD54*<sup>-/-</sup> produce no measurable alterations in the rejoining kinetics. In aggregate these observations are not compatible with a role of HDR in the slow component of DSB rejoining. But if no HDR then which process underlies the slow form of DSB rejoining? Based on the above observations and on reports that the slow component of DSB rejoining is error-prone (Evans et al., 1996; Loeblich et al., 1995) we proposed that it represents a second form of NHEJ distinct from the DNA-PK dependent D-NHEJ (Wang et al., 2001a). Under normal circumstances, D-NHEJ dominates rejoining and quickly removes DSBs from the genome. However, when D-NHEJ is compromised, DSB rejoining is not halted but is brought to near completion by this alternative pathway that acts as a backup – thus the term B-NHEJ. Extensive literature addressing DNA end joining from a different angle also points to the operation of alternative, DNA-PK independent, pathways of NHEJ in cells of higher eukaryotes preferentially utilizing terminal homologies of a few nucleotides which may be equivalent to B-NHEJ (Chang et al., 1993; Harrington et al., 1992; Kabotyanski et al., 1998; Roth et al., 1985; Verkaik et al., 2002).

#### *Biochemical evidence for backup repair pathways in cells of higher eukaryotes*

Biochemical studies are extensively used to study DSB repair (Labhart, 1999), and conditions developed that reproduce a DNA-PK dependent form of NHEJ (Baumann and West, 1998; Huang and Dynan, 2002). We inquired therefore whether similar studies can also provide supporting evidence for the operation of alternative pathways of NHEJ, such as B-NHEJ. We employed an assay utilizing restriction endonuclease linearized plasmid as a substrate and cellular extracts as a source of enzymes to evaluate DNA end joining activity in vitro. Recently reported results showed high DNA end joining

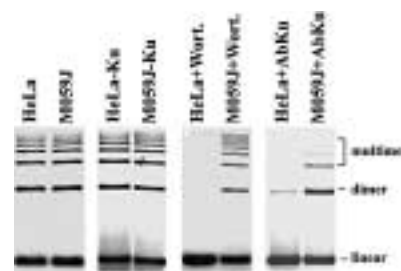


**Fig. 3.** End joining in vitro of linearized plasmid DNA by activities present in extracts of HeLa and M059J cells. End joining leads to the formation of dimers and multimers. Shown are results obtained with normal cell extracts, extracts in which Ku was removed by immunodepletion (HeLa-Ku, M059J-Ku), extracts treated with 2  $\mu$ M wortmannin (HeLa+Wort, M059J+Wort), as well as extracts treated with a serum containing anti-Ku antibodies (HeLa+AbKu, M059J+AbKu).

activity in HeLa cell extracts leading to the formation of dimers, trimers and other higher order multimers; more than 70% of the input plasmid is ligated after 1 h at 25 °C (Wang et al., 2003) (see also Fig. 3). However, efficient DNA end joining is also observed under the conditions employed in reactions assembled with extracts of M059J cells (Fig. 3). Thus, despite the absence of DNA-PKcs, DNA end joining activity can be high. We also evaluated the role of Ku in DNA end joining by depleting this protein through immunoprecipitation from extracts of HeLa and M059J cells. Despite Ku depletion, DNA end joining was not diminished in reactions assembled with either HeLa or M059J cell extracts (Fig. 3). These observations confirm the presence in HeLa cell extracts of activities efficiently catalyzing DNA end joining in the absence of Ku or DNA-PKcs, probably via an alternative DNA end joining pathway that may be operationally equivalent to the genetically defined B-NHEJ.

Although end joining is taking place in the absence of DNA-PKcs or Ku, these factors are engaged in a dominant fashion in the reaction when present in the extracts. This is suggested by the observation that treatment with wortmannin to inactivate DNA-PK completely inhibits DNA end joining in HeLa cells but not in M059J cells that lack DNA-PKcs (Fig. 3). Similarly, sera from individuals with polymyositis-scleroderma overlap syndrome that contain antibodies against Ku, inhibit DNA end joining in reactions assembled with HeLa cell extracts and to a lesser degree with M059J cell extracts (Fig. 3). These results are in line with a priority engagement of Ku and DNA-PKcs in DNA end joining and suggest that further processing of the break becomes impaired when these factors are inhibited.

Overall, biochemical observations provide supporting evidence for the operation of alternative, DNA-PK-independent pathways of NHEJ and reproduce the dominant character in the engagement of DNA-PKcs and Ku in the reaction.

#### *How is HDR contributing to DSB repair?*

The lack of a detectable role for HDR in the repair of IR-induced DSBs is in apparent contradiction with genetic studies indicating a contribution for HDR to cell radiosensitivity to killing. Combination of these observations to those presented

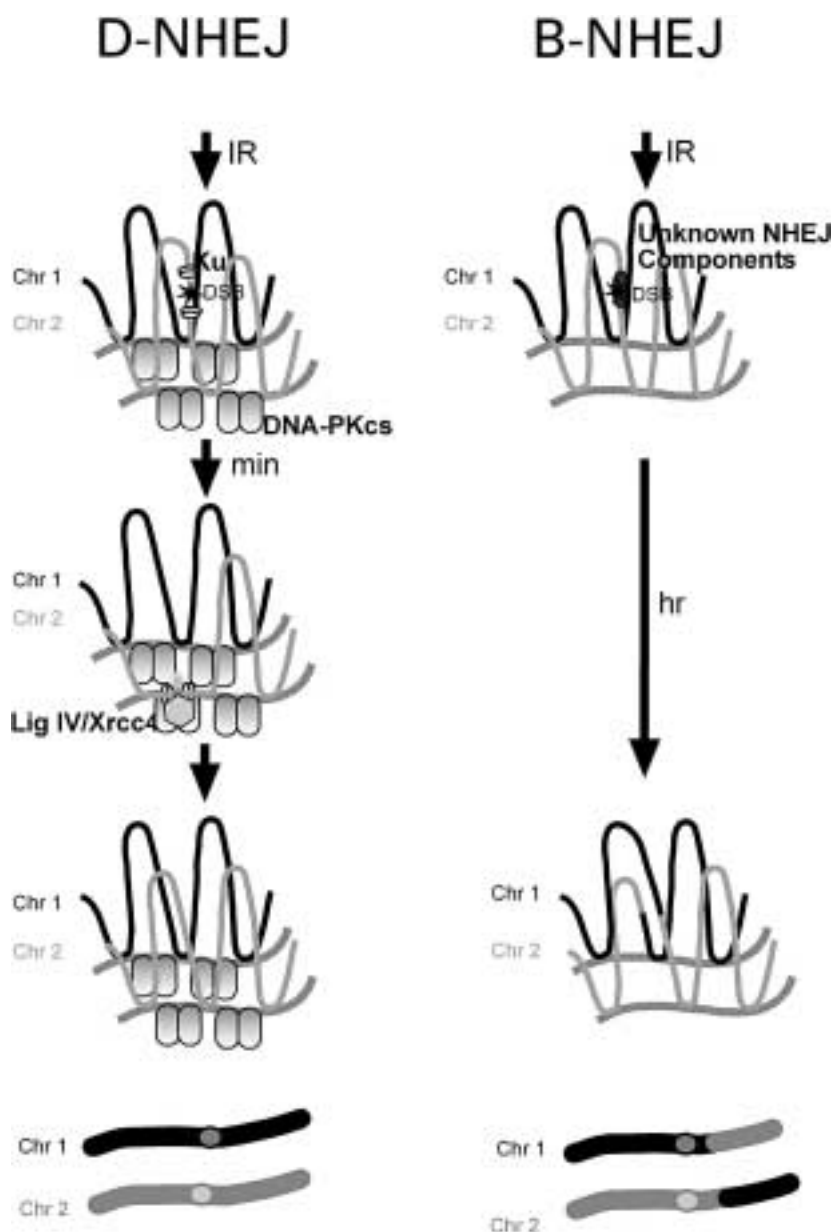


**Fig. 4.** Model for DSB rejoining in human cells (see text for details).

here leads us to propose that HDR either handles a very small subset of highly lethal DSBs, or, more likely, is recruited after the initial stage of rejoining. We have proposed (Asaad et al., 2000; DiBiase et al., 2000; Wang et al., 2001a, 2003; Xia et al., 2001) that in vertebrate cells, the closure of the initial DSB is carried out by D-NHEJ or B-NHEJ to generate a hypothetical transitional state of the original lesion designated T\*, marked as such by, as of yet, unidentified proteins. T\* is then recognized by the HDR system which is recruited on T\* with the purpose of restoring the sequence around the original break – a task that cannot be reliably accomplished by NHEJ. By introducing NHEJ, cells of higher eukaryotes rapidly restore integrity in their large genome, relying on HDR only to restore critical DNA sequences at a later time. This controlled approach to HDR may reduce illegitimate recombination events that could

be initiated by repeat sequences (Bennett et al., 1996) and may explain the suppression observed in the utilization of HDR for the initial rejoining event. Thus, although mammalian cells can freely shift between fast (D-NHEJ) and slow (B-NHEJ) forms of NHEJ, they appear genetically, or otherwise, constrained from shifting to HDR. This is equivalent to a genetic programming or a “hard-wiring” towards the use of NHEJ for the removal of DNA DSBs from their genome and is opposite to what is seen in yeast, where nearly all repair of IR-induced breaks is carried out by HDR.

*A kinetic model of DSB rejoining in higher eukaryotes: consequences for the formation of chromosome aberrations*

D-NHEJ may be an evolutionarily young pathway of DSB processing that evolved around DNA-PKcs but which also uti-

lized pre-existing components such as for example Ku and DNA ligase IV. These pre-existing proteins may have operated as part of a NHEJ pathway similar to B-NHEJ. Speed appears as the main feature of this new development, and is probably mediated by improved interactions, through DNA-PKcs, between the participating proteins. DNA-PKcs in turn may act as a platform and activator of the different participants (Smith and Jackson, 1999). It is as if DNA-PKcs evolved to accelerate the function of B-NHEJ. Judging from the difference in the half times between the fast and the slow components of rejoining, this acceleration is impressive and amounts to 32-fold in mammalian cells such as M059K and about 20-fold in the avian DT40 cells. By stimulating the function of a pre-existing B-NHEJ apparatus, DNA-PKcs may have allowed higher eukaryotes to shift effectively and parsimoniously the task of DSB rejoining from homologous recombination to D-NHEJ. However, the mechanisms by which HDR is suppressed in higher eukaryotes at the open break status remain obscure.

The model in Fig. 4 recapitulates the interpretation of the results presented here. In the presence of Ku and DNA-PKcs, DNA ends are quickly captured and chromatin structure is locally altered (not shown) to facilitate synapsis. This is the rate-limiting step of the reaction and is considered to occur close to the nuclear matrix mediated by a complex set of protein-protein interactions between DNA-PKcs, Ku, DNA ligase IV, XRCC4, histones and other unidentified factors. End joining is catalyzed by DNA ligase IV. The high speed of the process and local changes in chromatin structure facilitate joining of correct ends and suppress the formation of chromosome aberrations. In the absence of Ku or DNA-PKcs, DNA ends are not captured and local changes in chromatin structure fail to occur. Ends remain open and are processed by components of B-NHEJ with slow kinetics (hours) because of inefficient synapsis at random locations in the nucleus. The long-lived DNA ends may interact with other DNA ends in the vicinity, generated by IR or other processes, causing the formation of chromosome aberrations. In this model quick capture and local processing of the DNA ends through optimized protein-protein

interactions and chromatin conformation changes is the central mechanism by which joining errors are prevented during D-NHEJ. The fast and slow components in the kinetics of DSB rejoining in normal cells may reflect DNA-PK-dependent and DNA-PK-independent rejoining as a consequence of the local availability of DNA-PKcs rather than of the nature of the lesion. We proposed the term "DNA-PK surveillance domains" to describe regions in the nucleus benefiting from the presence of DNA-PKcs.

## Summary

The observations reviewed above provide an alternative model of DSB repair in cells of higher eukaryotes exposed to IR. According to this model, there is no provision for pathway selection in the repair of DSBs but rather a tandem operation of NHEJ and HDR, which together constitute the overall repair process. As first step, NHEJ removes DSBs by joining DNA ends without restoring DNA sequence. Subsequently, HDR is initiated in a cell cycle dependent manner in a significant fraction of the original DSB sites to restore DNA sequence. DSBs are removed predominantly by the extremely fast D-NHEJ. If D-NHEJ is not available in the vicinity of the DSB, or in the particular cell, B-NHEJ removes remaining breaks with slow kinetics. Both D-NHEJ and B-NHEJ are promiscuous in their choice of ends and have no developed mechanisms for ensuring that the correct ends are put back together. Rejoining of incorrect ends leads to the formation of chromosome aberrations. Correct rejoining is enhanced by spatial confinement of the DNA ends that may be provided in part by the organization of DNA in chromatin. Diffusion of ends apart is also limited in D-NHEJ by its high speed of operation. B-NHEJ is error-prone mainly due to its slow kinetics. Chromosome aberrations are likely to be formed by B-NHEJ and less likely by D-NHEJ. In this model, HDR is unlikely to contribute to the formation of chromosome aberrations.

## References

- Allalunis-Turner MJ, Barron GM, Day RS, Dobler K, Mirzayans R: Isolation of two cell lines from a human malignant glioma specimen differing in sensitivity to radiation and chemotherapeutic drugs. *Radiat Res* 134:349–354 (1993).
- Anderson CW, Dunn JJ, Freimuth PI, Galloway AM, Allalunis-Turner MJ: Frameshift mutation in PRKDC, the gene for DNA-PKcs, in the DNA repair-defective, human, glioma-derived cell line M059J. *Radiat Res* 156:2–9 (2001).
- Asaad NA, Zeng Z-C, Guan J, Thacker J, Iliakis G: Homologous recombination as a potential target for caffeine radiosensitization in mammalian cells: Reduced caffeine radiosensitization in *XRCC2* and *XRCC3* mutants. *Oncogene* 19:5788–5800 (2000).
- Baumann P, West SC: DNA end-joining catalyzed by human cell-free extracts. *Proc natl Acad Sci, USA* 95:14066–14070 (1998).
- Bennett RA, Gu X-Y, Povirk LF: Construction of a vector containing a site-specific DNA double-strand break with 3'-phosphoglycolate termini and analysis of the products of end-joining in CV-1 cells. *Int J Radiat Biol* 70:623–636 (1996).
- Bezzubova OY, Buerstedde JM: Gene conversion in the chicken immunoglobulin locus: A paradigm of homologous recombination in higher eukaryotes. *Experientia* 50:270–276 (1994).
- Bezzubova O, Silbergleit A, Yamaguchi-Iwai Y, Takeda S, Buerstedde J-M: Reduced X-ray resistance and homologous recombination frequencies in a *RAD54*<sup>-/-</sup> mutant of the chicken DT40 cell line. *Cell* 89:185–193 (1997).
- Bryant PE: Enzymatic restriction of mammalian cell DNA using Pvu II and Bam HI: evidence for the double-strand break origin of chromosomal aberrations. *Int J Radiat Biol* 46:57–65 (1984).
- Bryant PE: Use of restriction endonucleases to study relationships between DNA double-strand breaks, chromosomal aberrations and other end-points in mammalian cells. *Int J Radiat Biol* 54:869–890 (1988).
- Buerstedde J-M, Takeda S: Increased ratio of targeted to random integration after transfection of chicken B cell lines. *Cell* 67:179–188 (1991).
- Chang C, Biedermann KA, Mezzina M, Brown JM: Characterization of the DNA double strand break repair defect in scid mice. *Cancer Res* 53:1244–1248 (1993).
- DiBiase SJ, Zeng Z-C, Chen R, Hyslop T, Curran WJ Jr, Iliakis G: DNA-dependent protein kinase stimulates an independently active, nonhomologous, end-joining apparatus. *Cancer Res* 60:1245–1253 (2000).
- Evans JW, Liu XF, Kirchgessner CU, Brown JM: Induction and repair of chromosome aberrations in scid cells measured by premature chromosome condensation. *Radiat Res* 145:39–46 (1996).

- Harrington J, Hsieh CL, Gerton J, Bosma G, Lieber MR: Analysis of the defect in DNA end joining in the murine scid mutation. *Mol Cell Biol* 12:4758–4768 (1992).
- Huang J, Dynan WS: Reconstruction of the mammalian DNA double-strand break end-joining reaction reveals a requirement for an Mre11/Rad50/NBS1-containing fraction. *Nucleic Acids Res* 30:1–8 (2002).
- Jackson SP: Sensing and repairing DNA double-strand breaks. *Carcinogenesis* 23:687–696 (2002).
- Jasin M: Chromosome breaks and genomic instability. *Cancer Invest* 18:78–86 (2000).
- Kabotyanski EB, Gomelsky L, Han J-O, Stamato TD, Roth DB: Double-strand break repair in Ku86- and XRCC4-deficient cells. *Nucleic Acids Res* 26:5333–5342 (1998).
- Khanna KK, Jackson SP: DNA double-strand breaks: signaling, repair and the cancer connection. *Nature Genet* 27:247–254 (2001).
- Labhart P: Nonhomologous DNA end joining in cell-free systems. *Eur J Biochem* 265:849–861 (1999).
- Lees-Miller SP, Godbout R, Chan DW, Weinfeld M, Day RS III, Barron GM, Allalunis-Turner J: Absence of p350 subunit of DNA-activated protein kinase from a radiosensitive human cell line. *Science* 267:1183–1185 (1995).
- Lewis LK, Resnick MA: Tying up loose ends: nonhomologous end-joining in *Saccharomyces cerevisiae*. *Mutat Res* 451:71–89 (2000).
- Lewis LK, Westmoreland JW, Resnick MA: Repair of endonuclease-induced double-strand breaks in *Saccharomyces cerevisiae*: Essential role for genes associated with nonhomologous end-joining. *Genetics* 152:1513–1529 (1999).
- Loeblich M, Rydberg B, Cooper PK: Repair of x-ray-induced DNA double-strand breaks in specific *NotI* restriction fragments in human fibroblasts: Joining of correct and incorrect ends. *Proc natl Acad Sci, USA* 92:12050–12054 (1995).
- Natarajan AT: Chromosome aberrations: past, present and future. *Mutat Res* 504:3–16 (2002).
- Natarajan AT, Darroudi F, Mullenders LHF, Meijers M: The nature and repair of DNA lesions that lead to chromosomal aberrations induced by ionizing radiations. *Mutat Res* 160:231–236 (1986).
- Nevaldine B, Longo JA, Hahn PJ: The *scid* defect results in much slower repair of DNA double-strand breaks but not high levels of residual breaks. *Radiat Res* 147:535–540 (1997).
- Obe G, Pfeiffer P, Savage JRK, Johannes C, Goedecke W, Jeppesen P, Natarajan AT, Martinez-Lopez W, Folle GA, Drets ME: Chromosomal aberrations: formation, identification and distribution. *Mutat Res* 504:17–36 (2002).
- Paques F, Haber JE: Multiple pathways of recombination induced by double-strand breaks in *Saccharomyces cerevisiae*. *Microbiol Mol Biol Rev* 63:349–404 (1999).
- Pfeiffer P, Göttlich B, Reichenberger S, Feldmann E, Daza P, Ward JF, Milligan JR, Mullenders LHF, Natarajan AT: DNA lesions and repair. *Mutat Res* 366:69–80 (1996).
- Pierce AJ, Stark JM, Araujo FD, Moynahan ME, Berwick M, Jasin M: Double-strand breaks and tumorigenesis. *Trends Cell Biol* 11:S52–S59 (2001).
- Roth DB, Porter TM, Wilson JH: Mechanisms of nonhomologous recombination in mammalian cells. *Mol Cell Biol* 5:2599–2607 (1985).
- Smith GCM, Jackson SP: The DNA-dependent protein kinase. *Genes Develop* 13:916–934 (1999).
- Sonoda E, Sasaki MS, Buerstedde J-M, Bezzubova O, Shinohara A, Ogawa H, Takata M, Yamaguchi-Iwai Y, Takeda S: Rad51-deficient vertebrate cells accumulate chromosomal breaks prior to cell death. *EMBO J* 17:598–608 (1998).
- Takata M, Sasaki M S, Sonoda E, Morrison C, Hashimoto M, Utsumi H, Yamaguchi-Iwai Y, Shinohara A, Takeda S: Homologous recombination and nonhomologous end-joining pathways of DNA double-strand breaks. *EMBO J* 17:5497–5508 (1998).
- Takata M, Sasaki MS, Sonoda E, Fukushima T, Morrison C, Albala JS, Swagemakers SM, Kanaar R, Thompson LH, Takeda S: The Rad51 paralogue Rad51B promotes homologous recombinational repair. *Mol Cell Biol* 20:6476–6482 (2000).
- Thompson LH, Limoli CL: Origin, recognition, signaling, and repair of DNA double-strand breaks in mammalian cells (Eurekah.com and Kluwer Academic/Plenum Publishers, 2003).
- Verkaik NS, Esveldt-van Lange REE, van Heemst D, Brüggewirth HT, Hoeijmakers JHJ, Zdzienicka MZ, van Gent DC: Different types of V(D)J recombination and end-joining defects in DNA double-strand break repair mutant mammalian cells. *Eur J Immunol* 32:701–709 (2002).
- Wang H, Zeng Z-C, Bui T-A, Sonoda E, Takata M, Takeda S, Iliakis G: Efficient rejoining of radiation-induced DNA double-strand breaks in vertebrate cells deficient in genes of the RAD52 epistasis group. *Oncogene* 20:2212–2224 (2001a).
- Wang H, Zhao-Chong Z, Perrault AR, Cheng X, Qin W, Iliakis G: Genetic evidence for the involvement of DNA ligase IV in the DNA-PK-dependent pathway of non-homologous end joining in mammalian cells. *Nucleic Acids Res* 29:1653–1660 (2001b).
- Wang H, Perrault AR, Takeda Y, Qin W, Wang H, Iliakis G: Biochemical evidence for Ku-independent backup pathways of NHEJ. *Nucleic Acids Res* 31:5377–5388 (2003).
- Xia F, Taghian DG, DeFrank JS, Zeng Z-C, Willers H, Iliakis G: Deficiency of human BRCA2 leads to impaired homologous recombination but maintains normal nonhomologous end joining. *Proc natl Acad Sci, USA* 98:8644–8649 (2001).
- Yamaguchi-Iwai Y, Sonoda E, Buerstedde J-M, Bezzubova O, Morrison C, Takata M, Shinohara A, Takeda S: Homologous recombination, but not DNA repair, is reduced in vertebrate cells deficient in *RAD52*. *Mol Cell Biol* 18:6430–6435 (1998).

# The role of homologous recombination repair in the formation of chromosome aberrations

C.S. Griffin and J. Thacker

Medical Research Council, Radiation and Genome Stability Unit, Harwell, Oxfordshire (UK)

**Abstract.** The repair of DNA double strand breaks by homologous recombination can occur by at least two pathways: a Rad51-dependent pathway that is predominantly error free, and a Rad51-independent pathway (single strand annealing, SSA) that is error prone. In theory, chromosome exchanges can result from (mis)repair by either pathway. Both repair pathways will involve a search for homologous sequence, leading to

co-localization of chromatin. Genes involved in homologous recombination repair (HRR) have now been successfully knocked out in mice and the role of HRR in the formation of chromosome exchanges, particularly after ionising radiation, is discussed in the light of new evidence.

Copyright © 2003 S. Karger AG, Basel

## Pathways of homologous recombination repair

Homologous recombination repair (HRR) is the predominant mechanism for the repair of severe DNA damage in yeast, but in mammalian cells was thought to be less important in the repair of double strand breaks (dsb) than non-homologous end joining (NHEJ). In particular the large number of sequence repeats in mammalian cells, compared to yeast, could potentially lead to high numbers of undesirable inter-chromosome interactions through HRR. However in recent years HRR has been shown to have an important role in the maintenance of genome integrity, particularly during DNA replication (Johnson and Jasin, 2000). Although it has long been known that dsb are the main inducers of chromosome aberrations, mechanisms of chromosome aberration formation are still unresolved. The production of mice with disruption (“knocking out”) of specific repair genes has made available considerable information on the role of repair genes in chromosome aberration formation,

especially for non-homologous end joining mechanisms (Ferguson and Alt, 2001; Blasco, 2002). Since there is a high degree of homology between man and mouse, and chromosome aberrations can result in malignant transformation, understanding the role played by repair genes in the formation of chromosome aberrations in knockout mice will potentially aid our understanding of the mechanism of cancer progression in humans.

Homologous recombination repair has at least two distinct pathways; a conservative error-free RAD51-dependent pathway and a non-conservative error-prone RAD51-independent pathway. The RAD51-dependent pathway, known also as gene conversion, involves a homology search and strand invasion to allow dsb repair by copying (resynthesis) of an undamaged homologous sequence. The majority of these events involve the resynthesis of only a small amount of homologous sequence without any lasting exchange of material. However, a unique feature of this pathway is the formation of cross-stranded intermediates (Holliday junctions, HJ) that may be resolved by cutting either where they intersect, or in the outer strands (Fig. 1). If cutting is purely at random, then the outcome should be equal numbers of crossovers and non-crossovers, with the former having the potential to form a chromosome exchange. In yeast the repair of dsb by gene conversion yields crossovers between chromosomes at widely variable frequencies depending on the genetic locus, with an average of 10–20% (Paques and Haber, 1999), while in mammalian cells the use of reporter gene constructs has found crossing-over frequencies to be negligible (Richardson et al., 1998; Johnson and Jasin, 2000). In

We are grateful to the Medical Research Council and the European Commission (contract FIGH-CT1999-00010) for the support of our studies.

Received 10 September 2003; manuscript accepted 11 December 2003.

Request reprints from Dr Carol S. Griffin  
MRC Radiation and Genome Stability Unit, Harwell  
Oxfordshire OX11 0RD (UK); telephone: 44 1235 841000  
fax: 44 1235 841200; e-mail: c.griffin@har.mrc.ac.uk

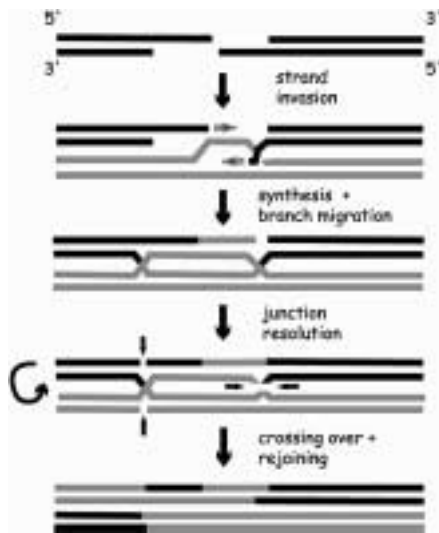
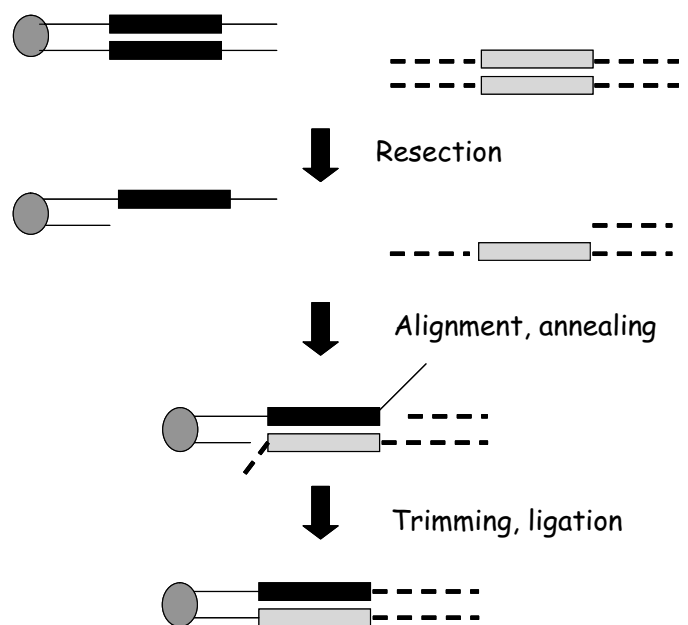


**Fig. 1.** Model of repair of a DNA double-strand break by homologous recombination, showing junction resolution leading to crossing over. At the site of a double-strand break in one DNA molecule (black), where the ends have been resected to give long 3' single-stranded tails, strand invasion can occur into a homologous undamaged molecule (grey). The undamaged molecule acts as a template for resynthesis of the broken region (grey arrowheads). Crossing over occurs when certain strands are cut and rejoined: in this instance, the lefthand junction is cut on the outer DNA strands (small vertical arrows) while the righthand junction is cut on the inner strands (small horizontal arrows). If the grey molecule is rejoined to the black molecule at the lefthand junction, as shown by curved arrow, then crossing over is achieved.

yeast, a minimum of 68 bp is needed to allow for homologous invasion although the system works better with around 200 bp (Paques and Haber, 1999; Richardson and Jasin, 2000a). A length of homology of >1.7 kb resulting in the formation of a long heteroduplex intermediate appears to promote crossing over in yeast (Inbar et al., 2000).

A non-conservative HRR pathway, known as single-strand annealing (SSA), has been identified in both mammalian cells (Lin et al., 1984) and yeast (Sugawara et al., 2000). SSA relies on the annealing of repeat sequences positioned adjacent to the dsb. DNA strand ends provide an entry site for an exonuclease to expose single strands that are then available for reannealing at the repeats (Fig. 2). SSA requires a homology search, but not a strand invasion step, and the efficiency of repair is directly related to the length of homology with around 200 bp being optimum (Sugawara et al., 2000). In yeast SSA competes with the error-free HRR pathway, but repair by SSA always results in small chromosome deletions. When a dsb occurs in each of two chromosomes an exchange may be formed by SSA between the chromosomal repeats (Fig. 2). Haber and Leung (1996) showed that the SSA pathway in yeast could repair a dsb with equal efficiency by inter-chromosomal events as by intra-chromosomal events, showing that homology searches are not restricted by proximity requirements.

A further recombination process known as break-induced replication (BIR) appears to require the same proteins as SSA, but involves one ended strand invasion followed by DNA syn-



### Chromosome exchange with microdeletion

**Fig. 2.** Chromosome exchange arising from single-strand annealing: double-strand breaks occur near to repeat sequences (black or grey rectangles) in heterologous chromosomes (solid line or dashed line), and following resection these are annealed and ligated.

thesis. BIR can either proceed to the end of the chromosome or to a second dsb if available (Kraus et al., 2001). Simplistically, BIR appears to be a special case of gene conversion over long chromosomal distances; it is therefore a useful mechanism for repairing the broken end of a chromosome.

### The involvement of specific chromosomal regions in aberration formation

The HRR pathway is active predominantly during S and G<sub>2</sub> phase when the sister chromatid is available as a template; during DNA replication HRR plays a particularly important role in resolving stalled replication forks (Cox, 2001). In G<sub>1</sub> phase when the sister chromatid is not available, the homologous chromosome or sequence repeats in heterologous chromosomes can be utilized for HRR. More than 50% of the human genome consists of repeat sequences of which >45% are transposable elements such as Alu repeats. Alu repeat sequences have been found associated with chromosomal breakpoints and this association is greater than would be expected on a purely random basis (Jeffs et al., 1998, 2001). Breakpoints have also been shown to coincide with fragile sites, many of which contain CCG trinucleotide repeat sequences and are common viral integration sites (Glover, 1998). Herpes simplex type 1 virus has been found to alter the proteins bound to centromeric protein CENP-C disrupting chromosome segregation as well as in-

ducing chromosome breakage (Everett et al., 1999). The p and q arms of chromosome 5 are frequently involved in rearrangements in many tumours, breakage occurring near the centromere which contains LINE 1 retrotransposons bounding alpha satellite sequences which may render the region unstable (Puechberty et al., 1999).

The transfer of chromosome segments to several different chromosomes has been reported in individual cells in tumour cell populations and called "jumping translocations" (Lejeune et al., 1979). These events are nonrandom and nonreciprocal involving only a few recipient and donor chromosomes and the breakpoints appear to be associated predominantly with centromeric regions or close to viral integration sites (Padilla-Nash et al., 2001). It has been postulated that jumping translocations originate from recombination between chromosome regions containing homologous viral DNA sequences that have integrated into the genome followed by clonal selection.

Increased recombination at the centromeric regions of chromosome arms 1q, 9q, 16q and 19q has also been reported, and hypomethylation and decondensation of the heterochromatin has been proposed as a mechanism for the formation of exchanges in the centromeric region (Hoffshir et al., 1992; Sawyer et al., 1998). The pericentromeric region has long been known to be a highly recombinogenic region containing large blocks of DNA with a high degree of sequence similarity between non-homologous chromosomes leading to integration of DNA and chromosome exchange (Sumner et al., 1998; Horvath et al., 2000; Yonggang et al., 2000). Centromeric DNA is AT rich, heterochromatic and late replicating, and cells deficient in HRR may be unable to resolve stalled replication forks in late replicating DNA before the cell enters mitosis. This may result in cells entering mitosis with unresolved dsb in centromeric DNA leading to chromosome breakage. Delayed replication has been shown to prevent mitotic chromosome condensation at mitosis resulting in chromosome instability (Smith et al., 2001).

### Chromosome aberrations in HRR-deficient knockout mice

Live offspring are not obtained when members of the *Rad51* gene family, including *Rad51* (Lim and Hasty, 1996; Tsuzuki et al., 1996) and the *Rad51*-like genes *Xrcc2* (Deans et al., 2000), *Rad51l1* (Shu et al., 1999) and *Rad51l3* (Pittman and Schimenti, 2000), are knocked out in mice. These data show that these genes are not functionally redundant and are required to repair endogenous DNA damage, particularly in the developing embryo when cells are undergoing rapid cell division. Rad51 is a key protein for strand invasion in the gene conversion pathway: even fibroblasts derived from *Rad51<sup>-/-</sup>p53<sup>-/-</sup>* mice fail to thrive (Tsuzuki et al., 1996). However, embryonic fibroblasts (MEFs) have been successfully isolated from 14-day-old *Xrcc2<sup>-/-</sup>* embryos and detailed chromosome analysis has been undertaken of passage 1 MEFs using multicolour spectral karyotyping (SKY) (Deans et al., 2003).

In the *Xrcc2<sup>-/-</sup>* MEFs chromosomal interchanges were the main aberration type, with a high frequency of spontaneous exchanges involving complex multiple rearrangements. Chromosomal fragments or intrachanges were less frequently observed with a ratio of interchanges to fragments of 4:1. However a significant number of chromosomal breaks were found to occur at or near the centromere (detached centromeres). This is in marked contrast with published data from NHEJ-deficient mouse cells where the main aberration type was a chromosome fragment and the ratio of interchanges to fragments was 1:4 (Ferguson et al., 2000). Interchanges involving homologues occurred at a frequency of 17 % in primary MEFs, significantly more than expected from random interactions (<3%). The majority of homologue rearrangements were dicentric and these could have arisen as a result of an interchange between sister chromatids (sister unions, SU) leading to the formation of an isodicentric. However the frequency of SU, measured directly in both primary *Xrcc2<sup>-/-</sup>* MEFs and the *Xrcc2*-deficient hamster cell line *irs1* was found to be very low (Griffin et al., 2000; Deans et al., 2003).

Primary *Xrcc2<sup>-/-</sup>* MEFs exposed to 3 Gy X-rays in G<sub>1</sub> phase fail to enter mitosis presumably due to unrepaired damage triggering cell cycle checkpoints. However when spontaneously immortalised *Xrcc2<sup>-/-</sup>* MEFs with inactive checkpoint controls were exposed to 3 Gy X-rays in G<sub>1</sub> phase, metaphases could be collected for analysis. The aberration spectrum in immortalized MEFs was found to be similar to that observed in unirradiated primary MEFs, with interchanges and detached centromeres being the predominant aberration types (Deans et al., 2003). Detached centromeres were the result of either breakage within the centromere or in the pericentromeric region, presumably following failed exchanges (see above).

### Chromosome aberrations are not the main cause of cell death in embryos deficient in HRR?

It has been suggested that high frequencies of chromosomal breaks are the cause of death in chick Rad51 knockout cells (Sonoda et al., 1998). Chromosome aberrations were also observed at a high frequency in 14 day *Xrcc2<sup>-/-</sup>* mouse embryonic fibroblasts (MEFs) after 24 h in culture (Deans et al., 2000). However, experiments designed to detect chromosome aberrations directly in 8–10 day embryonic tissue failed to show an increase after 1 h incubation in colcemid. This suggests that the high frequency of chromosome aberrations observed in *Xrcc2<sup>-/-</sup>* MEFs in vitro may have arisen due to an inability to cope with in vitro culturing conditions (e.g., higher oxygen levels than in vivo) and/or that DNA damage in earlier embryonic stages is not converted into aberrations. In particular, it was found that *Xrcc2<sup>-/-</sup>* embryos have increased levels of apoptosis, with a marked increase throughout embryonic tissues by 9.5 days, and extensive cell death particularly in the nervous system at later stages (Deans et al., 2000). These data suggest that damage triggers apoptosis in vivo, while fibroblast cultures (which may apoptose less readily) show genetic instability.

However, cells from 8–10 day *Xrcc2<sup>-/-</sup>* embryos do show a significant level of aneuploidy (10% in *Xrcc2<sup>-/-</sup>* compared to 0% in controls) which may be predominantly caused by chromosome fragmentation at mitosis (Griffin et al., 2000; Deans et



al., 2003). DNA double-strand breaks and replication defects have been shown to be one of the primary causes of centrosome disruption at mitosis, and in *Drosophila* embryos, nuclei with defective centrosomes are eliminated from the cell pool by apoptosis (Takada et al., 2003). The lack of chromosome aberrations in cells taken from *Xrcc2*<sup>-/-</sup> embryos at 8–10 days suggests that aneuploidy in *Xrcc2*<sup>-/-</sup> mouse cells arises without the presence of chromosome aberrations and may be the result of centrosome breakup caused by unrepaired DNA damage.

### **The role of single-strand annealing (SSA) and homologue interactions**

The SSA pathway has been shown to be active in both yeast and mammalian cells, but many of these studies have involved the introduction of reporter (direct repeat) sequences into their respective genomes. It is therefore not clear whether SSA represents a major pathway for repair in genomic DNA, especially in mammalian cells. The relative lack of evidence for recurrent breakpoint locations in translocations, given the requirement for significant homology (see above) may suggest that SSA is uncommon. Of relevance to this review, evidence has been found for the use of SSA to repair endonuclease-induced dsb in heterologous mammalian chromosomes, causing translocations (Richardson and Jasin, 2000b; see below). Data consistent with the use of SSA has also been found in cells defective in the breast cancer gene *Brca2*, which has been shown to have a role in the regulation of RAD51-dependent HRR. Endonuclease-induced dsb in hypomorphic *Brca2* mutant mouse ES cells showed a decrease in repair by gene conversion, and by inference a substantial elevation in repair by SSA (Tutt et al., 2001). The *Brca2* mutant mouse ES cells and embryonic fibroblasts also show high levels of chromosome interchanges. The high frequency of chromatid interchanges observed in primary *Xrcc2* and *Brca2* knockout MEFs may suggest the activity of SSA. Additionally the higher than expected frequency of interactions between homologous chromosomes in *Xrcc2*<sup>-/-</sup> MEFs (Deans et al., 2003) is an indication of the possible involvement of SSA.

However, direct studies on cells deficient in SSA in mammalian cell systems are limited. The ERCC1 gene product is an endonuclease suggested to be involved in cutting the single-stranded flaps generated during SSA, and has been successfully knocked out in mice (Melton et al., 1998). Studies on the effects of UV irradiation on chromosome aberration formation in *Ercc1*<sup>-/-</sup> cells show a 10-fold increase in the frequency of breaks relative to exchanges, compared to wild type cells (Chipchase and Melton, 2002), suggesting that SSA is a major pathway for UV-induced chromosome exchange formation.

In order for homologue interactions to take place either they must be closely situated in the nucleus or significant strand movement must occur. Somatic pairing of homologues has been observed in budding yeast (Burgess et al., 1999) and in *Drosophila* (Wu, 1993). As noted above, interactions between chromosomes in yeast have been found to be as frequent as those within chromosomes, and primarily governed by the size of the sequence homology rather than the location of the

sequences (Haber and Leung, 1996). Site-specific recombination investigated using the Cre/loxP system in diploid yeast show that collisions between loci are more frequent between sequences on homologues than on heterologues (Burgess and Kleckner, 1999). In mammalian cells there is evidence for non-random positioning of chromosomes (Parada and Misteli, 2002; Tanabe et al., 2002; Williams and Fisher, 2003), but evidence of homologue interactions is rare (LaSalle and Lalande, 1996). However, where structure-function parameters such as gene density or transcription help determine chromosome positioning, it may be expected that homologues will be closer together than heterologues.

Studies on the complexity of chromosome interchanges detected using M-FISH demonstrates that overlap in chromosome “territories” must be greater than previously supposed (Savage, 2002). Live studies on mammalian cells show chromosome movement to be limited suggesting that interactions are restricted to neighbouring transcriptionally active loci (Buchenau et al., 1997). Fluorescence in situ hybridisation (FISH) was used to investigate positioning of centromeric heterochromatin and the TP53 gene in human leukaemia cell lines after ionising radiation. Some movement of homologous centromeres and the TP53 genes was observed 0.5–5 h after radiation but this movement was related to changes occurring in chromatin condensation after exposure to 5 Gy  $\gamma$ -rays (Jirsova et al., 2001). Studies tracking the movement of specific chromosomes do show a directed movement of homologous chromosomes after ionizing radiation (Dolling et al., 1997). However, wild-type mammalian cells after ionising radiation show a random interaction of chromosomes with no preference for homologue interactions (Cornforth et al., 2002). Recently it has been shown that recombination between direct repeats (SSA) in yeast requires functional microtubules, suggesting that microtubule-dependent chromosomal movement may be required (Thrower et al., 2003). However, in mammalian systems it is possible that interactions between repeat sequences on heterologous chromosomes will occur predominantly between neighbouring loci and the sufficiently large number of repeats in the mammalian genome may prevent the need for a large scale movement to search for a homologue sequence.

The high frequency of homologous chromosome interactions in unirradiated primary *Xrcc2*<sup>-/-</sup> MEFs was not observed in immortalised MEFs after ionising radiation. This suggests that following irradiation, repair occurs predominantly by NHEJ in the immortalised MEFs. Conversely, primary *Xrcc2*<sup>-/-</sup> MEFs exposed to endogenous oxidative damage in vitro are delayed from entering S phase by a G<sub>1</sub> checkpoint control when the cell may have time to undertake a homology search resulting in the observed elevation of interactions between homologues.

### **The one-hit exchange and the role of HRR**

Studies with ultrasoft X-rays, where a single track cannot span more than one chromosome, led to the proposal that chromosome interchanges could be formed from a single “hit”

(Thacker et al., 1980; Goodhead et al., 1993; Griffin et al., 1998). If two ultrasoft X-ray tracks (i.e., a track through each of two chromosomes) were required for exchange formation then the response should be purely dose-squared, but it was found that there was a substantial linear component to the exchange induction curve. However the question of whether chromosome exchanges can be generated by one dsb remains controversial. One issue is whether pseudo-linearity of the dose-response can occur. Dose-response data were initially obtained from the scoring of dicentric chromosomes from solid-stained preparations (Thacker et al., 1980); with the advent of FISH a considerable amount of additional dose-response data has been generated (Griffin et al., 1998). While the painting of only a few chromosomes for determining dose response may result in an apparent linear response (Sachs et al., 2000; Savage, 2000), data obtained using M-FISH, where all interactions should be visible, show a significant linear component to the dose-response curve for simple exchanges (Loucas and Cornforth, 2001).

More recently studies to determine the number of dsb needed to form an exchange have involved the use of the rare cutting *I-SceI* endonuclease in mouse ES cells (Richardson and Jasin, 2000b). Recombination substrates carrying homologous mutant genes incorporating *I-SceI* cut sites were introduced into chromosomes 14 and 17 and, following expression of the endonuclease, interchanges between chromosomes were determined by two-colour FISH. Chromosome interchanges were only detected in cells where both chromosomes carried *I-SceI* cut sites, and not when only one of the chromosomes had a cut site. Sequence analysis of the breakpoints revealed that none of the recombinants could have arisen by gene conversion accompanied by crossing over, and the authors proposed that they were the result of SSA between homologous sequences of the mutant genes. However, breaks induced by enzymes will be simple compared to the clustered damage sites containing radiation-induced breaks. The repair of clustered damage sites may involve additional repair proteins, compared to endonuclease-induced dsb, including the use of HRR with an enhanced possibility of crossing over.

A number of studies have looked for further evidence of the one-hit exchange following ionising radiation. However, these experiments, which involve the fusion of irradiated with unirradiated cells to examine interaction between damaged and undamaged chromosomes, have yielded conflicting results (Cornforth, 1990; F. Darroudi, pers. comm.). More recently it was found that when the radioactive isotope  $^{125}\text{I}$  was incorporated into early-replicating chromosomal regions of synchronized hamster cells, a significant level of exchanges occurred in the late replicating Xq chromosome arm that had not incorporated the isotope (Ludwikow et al., 2002). This result suggests that radiation-induced damage can lead to untargeted effects, perhaps through the initiation of a homology search in order to repair clustered lesions.

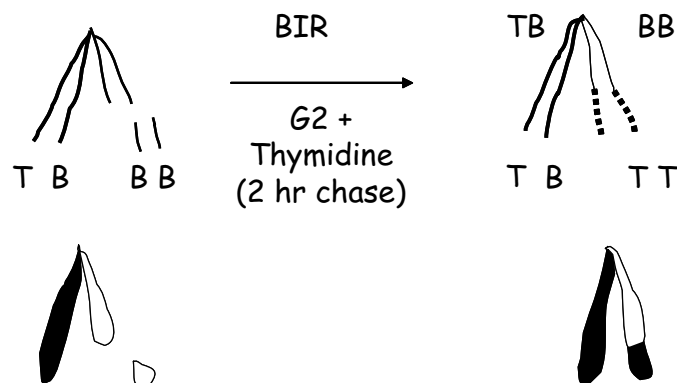


**Fig. 3.** Scheme for identification of break-induced replication (BIR) in harlequin stained chromosomes after exposure of mammalian cells to BrdU (B) for two cell cycles followed by a two-hour thymidine (T) chase. The completely BrdU-substituted strand (BB) is broken and replaced by BIR in the presence of thymidine (TT).

### Is there a role for HRR in the formation of complex exchanges?

Complex chromosome rearrangements involving three or more breaks in two or more chromosomes have been shown to be a common occurrence especially after high LET radiation (Griffin et al., 1995; Simpson and Savage, 1996). One of the questions that remains to be answered is how multiple chromosomes can be involved in interactions when they occupy discrete domains in interphase and movement is limited (see above). Calculations using Monte Carlo computer software simulating chromosome aberrations from FISH data found that complex exchanges were underpredicted by a random recombinational repair mechanism and therefore favoured their formation by random breakage and reunion (Sachs et al., 2000).

Using the premature chromosome condensation technique it has been shown that there is a delay in the appearance of complex exchanges after ionising radiation (Darroudi et al., 1998). *Xrcc2*<sup>-/-</sup> MEFs show a very high background frequency of complex exchanges which increases after both low and high LET radiation indicating that HRR protects against complex exchange formation. *Brca2*<sup>-/-</sup> ES cells also show a high frequency of complex exchanges in culture (Tutt et al., 2001). However the relatively low frequency of complex exchanges in *Ercc1*<sup>-/-</sup> mouse cells indicates that SSA may be involved in their formation and the time needed to undertake a homology search would account for the delay in the appearance of complex exchanges at mitosis after ionizing radiation. The sequencing of breakpoints induced in the HPRT gene after alpha particle irradiation of primary human fibroblasts has revealed short sequence repeats commonly found at the breakpoints (Singleton et al., 2002). This indicates that small 2–5 bp repeats may assist the repair of complex clustered damage produced by high LET radiation and that simple end joining by non-homologous mechanisms is not sufficient.

## Is break-induced replication (BIR) utilized by mammalian cell systems?

Evidence for BIR in hamster cell lines V79 (wild type) and *irs1* (*Xrcc2*<sup>-/-</sup>) after ionizing radiation was determined by incubating cells in BrdU for two cell cycles. Immediately after irradiation cells were washed and exposed to thymidine to mark the location of new DNA synthesis (Fig. 3). Cells were stained with Giemsa/Hoechst in order to obtain harlequin chromosomes (pale strand BT/dark strand TT) (Perry and Wolff, 1974). DNA repair synthesis occurring after irradiation could then be identified by dark patches on a pale-stained chromatid. A small number of chromosomes with dark patches were identified, however their frequency was extremely low and there was no difference in frequency between wild type and HRR-deficient mutant hamster cell lines suggesting that BIR is not a common method of repair of radiation-induced breaks in mammalian cell systems.

## References

Blasco MA: Mouse models to study the role of telomeres in cancer, aging and DNA repair. *Eur J Cancer* 38:2222–2228 (2002).

Buchenau P, Saumweber H, Ardt-Jovin D: The dynamic nuclear redistribution of an hnRNP K-homologous protein during *Drosophila* embryo development and heat shock. Flexibility of transcription sites in vivo. *J Cell Biol* 137:291–303 (1997).

Burgess SM, Kleckner N: Collisions between yeast chromosomal loci in vivo are governed by three layers of organisation. *Genes Dev* 13:1871–1883 (1999).

Burgess SM, Kleckner N, Weiner BM: Somatic pairing of homologs in budding yeast: existence and modulation. *Genes Dev* 13:1627–1641 (1999).

Chipchase MD, Melton DW: The formation of UV-induced chromosome aberrations involves *ERCC1* and *XPF* but not other nucleotide excision repair genes. *DNA Repair* 1:335–340 (2002).

Cornforth MN: Testing the notion of the one-hit exchange. *Int J Radiat Biol* 121:21–27 (1990).

Cornforth MN, Greulich-Bode KM, Loucas BD, Arsuaiga J, Vazquez M, Sachs RK, Bruckner M, Molls M, Hahnfeldt P, Hlatky L, Brenner DJ: Chromosomes are predominantly located randomly with respect to each other in interphase human cells. *J Cell Biol* 159:237–244 (2002).

Cox MM: Historical overview: searching for replication help in all of the rec places. *Proc natl Acad Sci, USA* 98:8173–8180 (2001).

Darroudi F, Fomina J, Meijers M, Natarajan AT: Kinetics of the formation of chromosome aberrations in X-irradiated human lymphocytes, using PCC and FISH. *Mut Res* 404:55–65 (1998).

Deans B, Griffin CS, Maconochie M, Thacker J: *Xrcc2* is required for genetic stability, embryonic neurogenesis and viability in mice. *EMBO J* 19:6675–6685 (2000).

Deans B, Griffin CS, O'Regan P, Jasin M, Thacker J: Homologous recombination deficiency leads to profound genetic instability in cells derived from *Xrcc2* knockout mice. *Cancer Res* 63:8181–8187 (2003).

Dolling JA, Boreham DR, Brown DL, Raaphorst GP, Mitchel REJ: Rearrangement of human cell homologous chromosome domains in response to ionizing radiation. *Int J Radiat Biol* 72:303–311 (1997).

## Conclusions

The conservative HRR pathway ensures precise and correct rejoining of DNA damage by gene conversion during S and G<sub>2</sub> phase with the predominant use of the sister chromatid as a repair template. However the error-prone SSA repair pathway in competition with conservative HRR may lead to the formation of chromosome interchanges particularly after ionizing radiation damage, if the many repeat sequences act as substrates for repair. Evidence of nonrandom breakage occurring at pericentromeric regions suggests the possible involvement of repeat sequences, and SSA is one mechanism that could result in exchanges occurring in these regions. The interaction between homologous chromosomes could be the consequence of SSA and account for the high frequency of homologue interactions in *Xrcc2*<sup>-/-</sup> MEFs. Cells lacking checkpoint controls in addition to repair deficiency will accumulate high levels of exchanges, contributing to genetic instability and potentially to malignant transformation.

Everett RD, Earnshaw WC, Findlay J, Lomonte P: Specific destruction of kinetochore protein CENP-C and disruption of cell division by herpes simplex virus immediate-early protein NnW110. *EMBO J* 18:1526–1538 (1999).

Ferguson DO, Alt FW: DNA double strand break repair and chromosomal translocation: lessons from animal models. *Oncogene* 20:5572–5579 (2001).

Ferguson DO, Sekiguchi JM, Chang S, Frank KM, Gao Y, DePinho RA, Alt FW: The nonhomologous end-joining pathway of DNA repair is required for genomic stability and the suppression of translocations. *Proc natl Acad Sci, USA* 97:6630–6633 (2000).

Glover TW: Instability at chromosomal fragile sites. *Recent Results Cancer Res* 154:185–199 (1998).

Goodhead DT, Thacker J, Cox R: Effects of radiations of different qualities on cells: molecular mechanisms of damage and repair. *Int J Radiat Biol* 63:543–556 (1993).

Griffin CS, Marsden SJ, Stevens DL, Simpson P, Savage JRK: Frequencies of complex chromosome exchanges aberrations induced by <sup>235</sup>Pu  $\alpha$ -particles and detected using fluorescence *in situ* hybridisation using single chromosome specific probes. *Int J Radiat Biol* 67:431–439 (1995).

Griffin CS, Hill MA, Papworth DG, Townsend KMS, Savage JRK, Goodhead DT: Effectiveness of 0.28 keV carbon K ultrasoft X-rays at producing simple and complex chromosome exchanges in human fibroblasts *in vitro* detected using FISH. *Int J Radiat Biol* 73:591–598 (1998).

Griffin CS, Simpson P, Wilson CR, Thacker J: Mammalian recombination-repair genes *XRCC2* and *XRCC3* promote correct chromosome segregation. *Nature Cell Biol* 2:757–761 (2000).

Haber JE, Leung W-Y: Lack of chromosome territoriality in yeast: Promiscuous rejoining of broken chromosome ends. *Proc natl Acad Sci, USA* 93:13949–13954 (1996).

Hoffshir F, Ricoul M, Lemieux N, Estrade S, Cassingena R, Dutrillaux B: Jumping translocations originate clonal rearrangements in SV40-transformed human fibroblasts. *Int J Cancer* 52:130–136 (1992).

Horvath JE, Viggiano L, Loftus BJ, Adams MD, Archidiacono N, Rocchi M, Eichler EE: Molecular structure and evolution of an alpha satellite/non-alpha satellite junction at 16p11. *Hum molec Genet* 9:113–123 (2000).

Inbar O, Liefshitz B, Bitan G, Kupiec M: The relationship between homology, length and crossing over during the repair of a broken chromosome. *J Biol Chem* 275:30833–30838 (2000).

Jeffs AR, Benjes SM, Smith TL, Sowerby SJ, Morris CM: The *BCR* gene recombines preferentially with Alu elements in complex *BCR-ABL* translocations of chronic myeloid leukaemia. *Hum molec Genet* 7:767–776 (1998).

Jeffs AR, Wells E, Morris CM: Nonrandom distribution of interspersed repeat elements in the *BCR* and *ABL1* genes and its relation to breakpoint cluster regions. *Genes Chrom Cancer* 32:144–154 (2001).

Ji Y, Eichler EE, Schwartz S, Nicholls RD: Structure of chromosomal duplicons and their role in mediating human genomic disorders. *Genome Res* 10:597–610 (2000).

Jirsova P, Kozubek S, Bártová E, Kozubek M, Lukášová E, Cafourková A, Koutná I, Skalniková M: Spatial distribution of selected genetic loci in nuclei of human leukemia cells after irradiation. *Radiat Res* 155:311–319 (2001).

Johnson RD, Jasin M: Sister chromatid gene conversion is a prominent double-strand break repair pathway in mammalian cells. *EMBO J* 19:3398–3407 (2000).

Kozubek S, Bartova E, Kozubek M, Lukasova E, Cafourkova A, Koutna I, Skalnikova M: Spatial distribution of selected genetic loci in nuclei of human leukemia cells after irradiation. *Radiat Res* 155:311–319 (2001).

Kraus E, Leung W-Y, Haber JE: Break-induced replication: A review and an example in budding yeast. *Proc natl Acad Sci, USA* 98:8255–8262 (2001).

Kuppers R, Dall-Favera R: Mechanism of chromosomal translocations in B cell lymphomas. *Oncogene* 20:5580–5594 (2001).

LaSalle JM, Lalande M: Homologous association of oppositely imprinted chromosomal domains. *Science* 272:725–728 (1996).

- Lejeune J, Maunoury C, Prieur M, Van den Akker J: Translocation sauteuse (5p;15q),8q;15q),(12q;15q). *Ann Génét* 22:210–213 (1979).
- Lim DS, Hasty P: A mutation in mouse rad51 results in an early embryonic lethal that is suppressed by a mutation in p53. *Mol Cell Biol* 16:7133–7143 (1996).
- Lin F-L, Sperle K, Sternberg N: Model for homologous recombination during transfer of DNA into mouse L cells: Role for DNA ends in the recombination process. *Mol Cell Biol* 4:1020–1034 (1984).
- Loucas BD, Cornforth MN: Complex chromosome exchanges induced by gamma rays in human lymphocytes: an M-FISH study. *Radiat Res* 155:660–671 (2001).
- Ludwikow G, Xiao Y, Hoebe RA, Franken NAP, Darroudi F, Stap J, Van Oven CH, Van Nororden CJF, Aten JA: Induction of chromosome aberrations in unirradiated chromatin after partial irradiation of a cell nucleus. *Int J Radiat Biol* 78:239–247 (2002).
- Melton DW, Ketchen A-M, Nunez F, Bonatti-Abbondandolo S, Abbondandolo A, Squires S, Johnson RT: Cells from *ERCC1*-deficient mice show genome instability and a reduced frequency of S-phase-dependent illegitimate chromosome exchange but a normal frequency of homologous recombination. *J Cell Sci* 111:395–404 (1998).
- Padilla-Nash HM, Heselmeier-Haddad K, Wangsa D, Zhang H, Ghadimi BM, Macville M, Augustus M, Schrock E, Hilgenfeld E, Reid T: Jumping translocations are common in solid tumor cell lines and result in recurrent fusions of whole chromosome arms. *Genes Chrom Cancer* 30:349–363 (2001).
- Paques F, Haber JE: Multiple pathways of recombination induced double strand breaks in *Saccharomyces cerevisiae*. *Micro Mol Biol Rev* 63:349–404 (1999).
- Parada L, Misteli T: Chromosome positioning in the interphase nucleus. *Trends Cell Biol* 12:425–432 (2002).
- Perry P, Wolff S: New Giemsa method for the differential staining of sister chromatids. *Nature* 251:156–158 (1974).
- Pittman DL, Schimenti JC: Midgestation lethality in mice deficient for the RecA-related gene, Rad51/ Rad51l3. *Genesis* 26:167–173 (2000).
- Puechberty J, Laurent A-M, Gimenez S, Billult A, Brun-Laurent M-E, Calenda A, Marçais B, Prades C, Ioannou P, Yurov Y, Roizes G: Genetic and physical analyses of the centromeric and pericentromeric regions of the human chromosome 5: recombination across 5cen. *Genomics* 56:274–287 (1999).
- Richardson C, Jasin M: Coupled homologous and non-homologous repair of a double-strand break preserves genomic integrity in mammalian cells. *Mol Cell Biol* 20:9068–9075 (2000a).
- Richardson C, Jasin M: Frequent chromosomal translocations induced by DNA double-strand breaks. *Nature* 405:697–700 (2000b).
- Richardson C, Moynahan ME, Jasin M: Double-strand break repair by interchromosomal recombination: suppression of chromosomal translocations. *Genes Dev* 12:3831–3842 (1998).
- Sachs RK, Rogoff A, Chen AM, Simpson P, Savage JRK, Hahnfeldt P, Hlatky LR: Underprediction of visibly complex chromosome aberrations by a recombinational-repair (“one-hit”) model. *Int J Radiat Biol* 76:129–148 (2000).
- Savage JRK: Comment on Reply to letter from Chadwick and Leenhouts: On the dose-effect relationship of the simple chromosomal rearrangements. *Int J Radiat Biol* 76:1428–1429 (2000).
- Savage JR: Reflections and meditations upon complex chromosomal exchanges. *Mut Res* 512:93–109 (2002).
- Sawyer JR, Tricot G, Mattox S, Jagannath S, Barlogie B: Jumping translocations of chromosome 1q in multiple myeloma: evidence for a mechanism involving decondensation of pericentromeric heterochromatin. *Blood* 91:1732–1741 (1998).
- Shu Z, Smith S, Wang L, Rice MC, Kmiec EB: Disruption of muREC2/RAD51L1 in mice results in early embryonic lethality which can be partially rescued in a *p53(-/-)* background. *Mol Cell Biol* 19:8686–8693 (1999).
- Simpson P, Savage JRK: Dose-response curves for simple and complex chromosome aberrations induced by x-rays and detected using fluorescence in situ hybridisation. *Int J Radiat Biol* 69:429–436 (1996).
- Singleton BK, Griffin CS, Thacker J: Clustered DNA damage leads to complex genetic changes in irradiated human cells. *Cancer Res* 62:6263–6269 (2002).
- Smith L, Plug A, Thayer M: Delayed replication timing leads to delayed mitotic chromosome condensation and chromosomal instability of chromosome translocations. *Proc natl Acad Sci, USA* 98:13300–13305 (2001).
- Sonoda E, Sasaki MS, Buerstedde JM, Bezzubova O, Shinohara A, Ogawa H, Takata M, Yamaguchi-Iwai Y, Takeda S: Rad51-deficient vertebrate cells accumulate chromosomal breaks prior to cell death. *EMBO J* 17:598–608 (1998).
- Sugawara N, Grzegorz I, Haber JE: DNA length dependence of the single-strand annealing pathway and the role of *Saccharomyces cerevisiae* *RAD59* in double-strand break repair. *Mol Cell Biol* 20:5300–5309 (2000).
- Sumner AT, Mitchell AR, Ellis PM: A FISH study of chromosome fusion in the ICF syndrome: involvement of paracentric heterochromatin but not of the centromeres themselves. *J med Genet* 35:833–835 (1998).
- Takada S, Kelkar A, Theurkauf WE: *Drosophila* checkpoint kinase 2 couples centrosome function and spindle assembly to genomic integrity. *Cell* 113:87–99 (2003).
- Tanabe H, Muller S, Neusser M, von Hase J, Calcagno E, Cremer M, Solovei I, Cremer C, Cremer T: Evolutionary conservation of chromosome territory arrangements in cell nuclei from higher primates. *Proc natl Acad Sci, USA* 99:4424–4429 (2002).
- Thacker J, Cox R, Goodhead DT: Do carbon ultrasoft x-rays induce exchange aberrations in cultured mammalian cells? *Int J Radiat Biol* 38:469–472 (1980).
- Thrower DA, Stemple J, Yeh E, Bloom K: Nuclear oscillations and nuclear filament formation accompany single-strand annealing repair of a dicentric chromosome in *Saccharomyces cerevisiae*. *J Cell Sci* 116:561–569 (2003).
- Tsuzuki T, Fujii Y, Sakumi K, Tominaga Y, Nakao K, Sekiguchi M, Matsushiro A, Yoshimura Y, Morita T: Targeted disruption of the *Rad51* gene leads to lethality in embryonic mice. *Proc natl Acad Sci, USA* 93:6236–6240 (1996).
- Tutt A, Bertwistle D, Valentine J, Gabriel A, Swift S, Ross G, Griffin CS, Thacker J, Ashworth A: Mutation of *Brca2* stimulates error-prone homology-directed repair of DNA double-strand breaks occurring between repeated sequences. *EMBO J* 20:4704–4716 (2001).
- Williams RR, Fisher AG: Chromosomes, positions please! *Nature Cell Biol* 5:388–390 (2003).
- Wu C: Transvection, nuclear structure, and chromatin proteins. *J Cell Biol* 120:587–590 (1993).
- Yonggang J, Eichler EE, Scheartz S, Nicholls RD: Structure of chromosomal duplicons and their role in mediating human genomic disorders. *Genome Res* 10:597–610 (2000).

# Recombination repair pathway in the maintenance of chromosomal integrity against DNA interstrand crosslinks

M.S. Sasaki,<sup>a</sup> M. Takata,<sup>b</sup> E. Sonoda,<sup>c</sup> A. Tachibana,<sup>a</sup> and S. Takeda<sup>c</sup><sup>a</sup>Radiation Biology Center, Kyoto University, Kyoto;<sup>b</sup>Department of Immunology and Molecular Genetics, Kawasaki Medical University, Kurashiki;<sup>c</sup>Department of Radiation Genetics, Faculty of Medicine, Kyoto University, Kyoto (Japan)

**Abstract.** DNA interstrand crosslinks (ICL) present a major threat to cell viability and genome integrity. In eukaryotic cells, the ICLs have been suggested to be repaired by a complex process involving Xpf/Ercc1-mediated endonucleolytic incision and homologous recombination (HR). However, the entire feature of the ICL tolerating mechanism is still poorly understood. Here we studied chromosome aberrations (CA) and sister chromatid exchanges (SCE) by the use of the crosslinking agent mitomycin C (MMC), in chicken DT40 cells with the HR genes disrupted by targeted replacement. The disruption of the Rad54, Rad51B, Rad51C, Rad51D, Xrcc2 and Xrcc3 genes resulted in a dramatic reduction of spontaneous and MMC-induced SCEs. Interestingly, while HR-deficient cells were hypersensitive to cell killing by MMC, MMC-induced CAs

were also suppressed in the HR-deficient cells except for Rad51D-, Xrcc2- and Xrcc3-deficient cells. These observations indicate that DNA double strand breaks (DSB) at stalled replication forks and those arising as repair intermediates present strong signals to cell death but can be tolerated by the HR repair pathway, where Rad54, Rad51B and Rad51C have an initiative role and repair can be completed by their paralogs Rad51D, Xrcc2 and Xrcc3. The impairment of the HR pathway, which otherwise leads to cell death, may be somewhat substituted by an alternative mechanism such as the Mre11/Rad50/Nbs1 pathway, resulting in reduced frequencies of SCEs and CAs.

Copyright © 2003 S. Karger AG, Basel

DNA interstrand crosslinks (ICL) are introduced by covalent binding of intercalating bifunctional alkylating agents. With their *trans* bridging nature in DNA duplexes the ICLs effectively cause cell death and chromosome aberrations (CA) by preventing efficient DNA replication, and also make their repair a special problem. The repair of ICLs also presents a spe-

cial concern in the human genetic disease Fanconi anemia (FA), whose cells are characterized by hypersensitivity to crosslinking agents such as mitomycin C (MMC) and have been suggested to be defective in the repair of ICLs (Sasaki and Tonomura, 1973; Sasaki, 1975). Although ICL repair has been envisaged to be mediated by sequential nucleotide excision repair (NER) and homologous recombination (HR) in bacteria such as *Escherichia coli* (Cole, 1973), little is known about the mechanisms of ICL repair in mammalian cells. Recently, however, an analogous repair pathway was identified in mammalian cells, where the heterodimeric endonuclease of Xpf (xeroderma pigmentosum complementation group F) and Ercc1 (excision repair cross complementation group 1) plays a role in the 5' → 3' incision/recombination process (Kuraoka et al., 2000; De Silva et al., 2000). An involvement of Rad1/Rad10, the yeast homologs of Xpf/Ercc1, in HR was suggested in *Saccharomyces*

This work was supported in part by Grants-in-Aid for scientific research from the Ministry of Education, Science, Culture, Sports and Technology, and research grant from the Ministry of Health, Labor and Welfare of Japan.

Received 10 September 2003; accepted 8 December 2003.

Request reprints from: Dr. M. S. Sasaki  
17-12 Shironosato, Nagaokakyo-shi  
Kyoto 617-0835 (Japan); telephone: +81-75-955-8943; fax: +81-75-955-8943  
e-mail: msasaki@emp.mbox.media.kyoto-u.ac.jp.

**Table 1.** The frequencies of CAs and SCEs in untreated and MMC-treated DT40 cells with different genetic backgrounds

Cell lines	Chromosome aberrations (CAs/cell)			Sister chromatid exchanges (SCEs/cell)		
	Untreated	MMC-treated	Net induced	Untreated	MMC-treated	Net induced
DT40 (wild type)	0.013±0.009	1.393±0.096	1.380±0.096	2.74±1.74	6.17±2.98	3.43±3.45
Ku70 <sup>-/-</sup>	0 ±0.050	1.127±0.087	1.127±0.100	2.69±1.73	6.52±3.34	3.83±3.76
Rad54 <sup>-/-</sup>	0.100±0.031	0.633±0.065	0.533±0.072	1.66±1.34	3.38±2.26	1.72±2.63
Ku70 <sup>-/-</sup> /Rad54 <sup>-/-</sup>	0.113±0.028	0.607±0.064	0.494±0.070	1.50±1.25	2.75±1.70	1.25±2.11
Rad51B <sup>-/-</sup>	0.147±0.031	0.487±0.057	0.340±0.065	0.93±1.02	1.82±1.53	0.89±1.84
Rad51C <sup>-/-</sup>	0.160±0.033	0.313±0.046	0.153±0.057	1.05±1.13	1.67±1.40	0.62±1.80
Rad51D <sup>-/-</sup>	0.580±0.076	1.940±0.139	1.360±0.158	1.38±1.15	2.05±1.49	0.67±1.88
Xrcc2 <sup>-/-</sup>	0.213±0.038	1.633±0.105	1.420±0.112	1.91±1.26	1.87±1.43	-0.04±1.91
Xrcc3 <sup>-/-</sup>	0.195±0.031	1.320±0.115	1.125±0.119	0.90±0.98	1.27±1.11	0.37±1.48

*cerevisiae* (Fishman-Lobell and Haber, 1992; Bardwell et al., 1994), and moreover, the role of Ercc1 in HR was also demonstrated in mammalian cells (Sargent et al., 2000; Niedernhofer et al., 2001). HR plays a critical role in the repair of DNA double strand breaks (DSB). Indeed, a DSB is generated as an intermediate of the ICL repair process (Magana-Schwenke et al., 1982; Dardalhon and Averbeck, 1995; McHugh et al., 2000) and by processing of a replication fork stalled at ICL site (De Silva et al., 2000). The studies of radiosensitive mutants of yeast and mammalian cells have revealed a series of Rad52 epistasis group genes relevant to HR including Rad51, which is a structural and functional homolog of bacterial RecA (review by Shinohara and Ogawa, 1995; Baumann and West, 1998; Kanaar et al., 1998).

Sister chromatid exchange (SCE) is an isolocus switch of a newly replicated chromatid with its sister and has been thought to be a chromosomal manifestation of recombination repair. Recently, Reiss et al. (2000) reported that the ectopic overexpression of RecA in tobacco plants stimulated SCEs. Previously, we also reported that spontaneous and MMC-induced SCEs were modulated in the chicken DT40 cells which were defective in some genes of the Rad52 epistasis group (Sonoda et al., 1999; Takata et al., 2001). These observations are consistent with the involvement of the HR pathway in the cellular response to ICLs. Here, we have extended the analysis to the CAs with their relevance to SCEs and cell killing in HR-deficient DT40 cells in response to the ICL-inducing agent MMC. The effect of non-homologous end-joining (NHEJ) was also studied in Ku70-deficient cells.

The results show that the disruption of Rad54, Rad51B, Rad51C, Rad51D, Xrcc2 and Xrcc3 decreases the frequencies of spontaneous and MMC-induced SCEs. A decrease in the frequencies of MMC-induced CAs was also observed in Rad54, Rad51B and Rad51C mutants but not in Rad51D, Xrcc2 and Xrcc3 mutants although all HR mutants showed hypersensitivity to MMC. These paradoxical observations have been interpreted by invoking apoptotic cell elimination under conditions of an impaired HR pathway, leaving an alternative repair pathway utilizing Mre11, which does not generate SCEs and gross CAs.

## Materials and methods

### Cells and cell culture

DT40 chicken B-lymphocyte cells were cultured in RPMI-1640 culture medium supplemented with 1 mM β-mercaptoethanol, 10% fetal calf serum and 1% chicken serum, and were maintained at 39.5 °C in 5% CO<sub>2</sub>-95% air. The generation of Ku70<sup>-/-</sup>, Rad54<sup>-/-</sup>, Rad51B(Rad51L1)<sup>-/-</sup>, Rad51C(Rad51L2)<sup>-/-</sup>, Rad51D(Rad51L3)<sup>-/-</sup>, Xrcc2<sup>-/-</sup> and Xrcc3<sup>-/-</sup> knock-out mutant cells have been described previously (Bezzubova et al., 1997; Sonoda et al., 1998; Takata et al., 1998, 2000, 2001). The culture conditions for the mutant cells were essentially the same as those for parental DT40 cells.

### Analysis of CAs and SCEs

The cells were incubated for 18–21 h in the presence of 10 μM BrdU. To see the response to ICLs, the cells were treated with MMC (Kyowa Hakkō Kogyo, Tokyo) for the last 8–12 h at a concentration of 0.05 μg/ml. The time of treatment with BrdU was adjusted to cover approximately two cell cycle periods, and MMC treatment to cover the last cell cycle, depending on the cell lines. With this experimental condition, approximately 30% of cells are in their first mitoses, 70% were in the second mitoses and a negligible fraction is in the third mitoses after addition of BrdU. The cells were then harvested for making air-drying chromosome preparations after treatment with 0.1 μg/ml Colcemid for the final 1.5–2 h. The chromosome preparations prepared were then stained with the modified fluorescent-plus-Giemsa (FPG) method of Perry and Wolff (1974) for SCE analysis or stained with conventional Giemsa staining method for CA analysis. A minimum of 150 cells were scored for SCEs and 200 cells for CAs. The frequencies were analyzed only in the 12 macrochromosomes including one Z chromosome, 2A(1-5),+A2,+Z.

## Results

The results of analysis of CAs and SCEs in untreated and MMC-treated cells with different genetic backgrounds are presented in Table 1 and their frequencies are depicted in Figure 1. CAs were exclusively chromatid-type aberrations, including single- or iso-chromatid breaks and chromatid exchanges. In the parental DT40 cells, the MMC treatment at this dose (0.05 μg/ml) showed approximately a two-fold and 100-fold increase of SCEs and CAs, respectively, as compared to the spontaneous frequency. The frequencies in the Ku70-deficient cells were not significantly different from those of the isogenic parental DT40 cells, indicating that the NHEJ pathway was not a significant determinant of the spontaneous and MMC-induced SCEs and CAs. The frequencies of the spontaneous CAs were significantly elevated in all cell lines deficient in

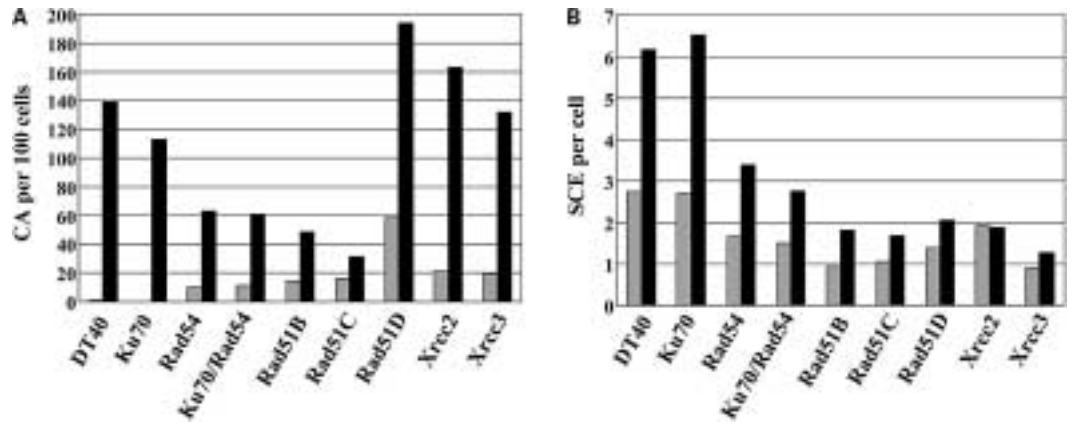


**Fig. 1.** The frequencies of CAs and SCEs in untreated and MMC-treated DT40 cells with different genetic background. (A) CAs. (B) SCEs. Shaded bars: untreated cells. Black bars: MMC-treated cells.

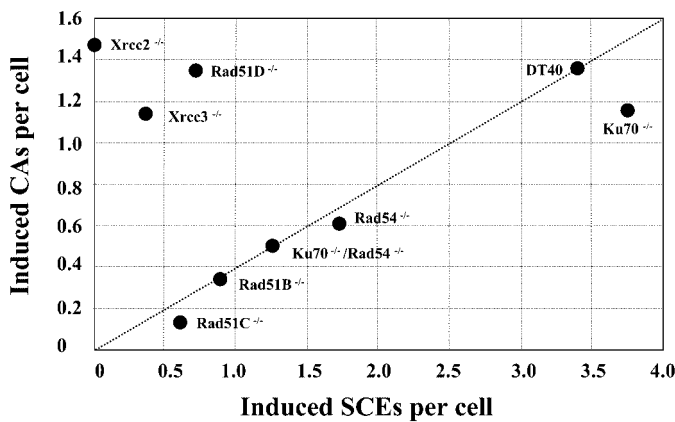


**Fig. 2.** Relationship between MMC-induced SCEs and CAs. The net-induced frequency of CAs is plotted against the net-induced frequency of SCEs. The dotted line shows a 1:1 correlation or equivalent reduction.

the HR genes, namely, Rad54<sup>-/-</sup>, Rad51B<sup>-/-</sup>, Rad51C<sup>-/-</sup>, Rad51D<sup>-/-</sup>, Xrcc2<sup>-/-</sup> and Xrcc3<sup>-/-</sup> cells. Thus, impaired HR constitutes the genetic basis of the chromosomal instability.

However, the effects of HR deficiency on MMC-induced CAs, and spontaneous and MMC-induced SCEs were different among the mutants. Disruption of the HR genes suppressed the frequencies of both spontaneous and MMC-induced SCEs. The suppressive effect on the MMC-induced SCEs differed among mutants, ~ 50% for Rad54<sup>-/-</sup>, ~ 80% for Rad51B<sup>-/-</sup>, Rad51C<sup>-/-</sup> and Rad51D<sup>-/-</sup>, and 90% or more for Xrcc2<sup>-/-</sup> and Xrcc3<sup>-/-</sup> cells. Surprisingly, the frequencies of MMC-induced CAs were also suppressed in Rad54<sup>-/-</sup>, Rad51B<sup>-/-</sup> and Rad51C<sup>-/-</sup> cells. The Rad54<sup>-/-</sup>/Ku70<sup>-/-</sup> double knockout mutant responded similarly to the Rad54<sup>-/-</sup> cells, again indicating no relevance of the NHEJ process in the induction of CAs and SCEs by MMC. It was noteworthy that Rad51D<sup>-/-</sup>, Xrcc2<sup>-/-</sup> and Xrcc3<sup>-/-</sup> were exceptional, in that the

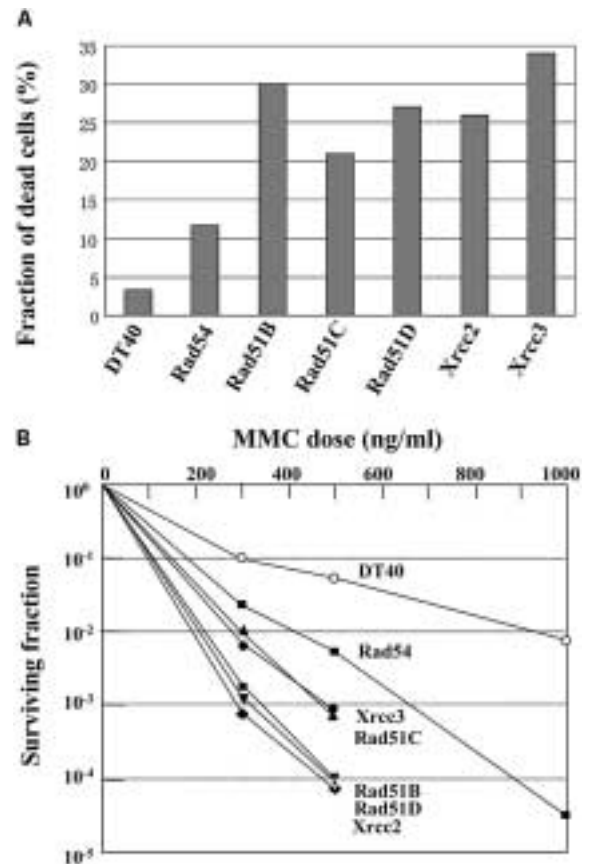


**Fig. 3.** Spontaneous and MMC-induced lethality of mutant cells (reconstructed from Takata et al., 2000, 2001). (A) Level of spontaneous cell death measured by flow cytometry of propidium iodide uptake. (B) Clonogenic survival after treatment with MMC. The cells were treated for 1 h with MMC, washed three times and grown in medium containing methylcellulose.

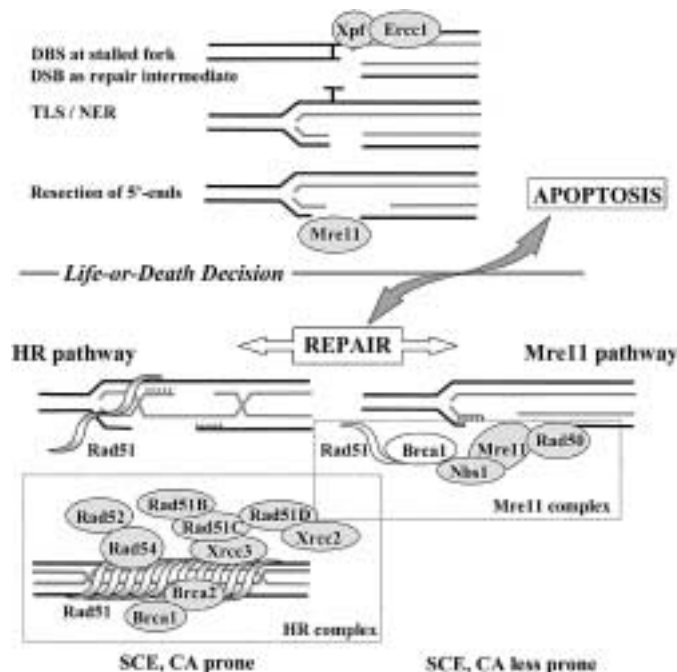
frequencies of MMC-induced CAs were not reduced at all whereas the SCE frequencies were strongly suppressed. The effect of MMC was evaluated by subtracting the spontaneous frequencies. Figure 2 shows the relationship between net-induced SCEs and CAs; there was a clear 1:1 relationship in the reduction rates except for *Rad51D*<sup>-/-</sup>, *Xrcc2*<sup>-/-</sup> and *Xrcc3*<sup>-/-</sup> cells, which were totally refractory to the reduction of MMC-induced CAs.

Figure 3 shows the spontaneous frequencies of dead cells as determined by flow cytometric analysis and clonogenic cell survival after MMC treatment. The spontaneous death rate as measured by the intake of propidium iodide is elevated in the HR-deficient cells, which is consistent with the elevated frequency of spontaneous CAs, or chromosomal instability of these cells. However, such parallelism does not hold for the sensitivity to cell killing and CAs by MMC, particularly in the *Rad54*<sup>-/-</sup>, *Rad51B*<sup>-/-</sup> and *Rad51C*<sup>-/-</sup> cells, where the cells are highly sensitive to cell killing whereas CA frequencies are reduced. This discordance suggests that CA formation is not a major pathway to cell killing.

To see any effects of the recombination processes on the formation of chromosome aberrations, the ratio of SCE to non-SCE at the junction of iso-chromatid breaks was studied in differentially stained chromatids of cells treated with MMC. These were 9/37 (24.3%) for the parental DT40 cells, 15/28 (53.6%) for *Rad51D*<sup>-/-</sup> cells, 26/57 (45.6%) for *Xrcc2*<sup>-/-</sup> cells and 11/35 (31.4%) for *Xrcc3*<sup>-/-</sup> cells. Although statistically non-significant, the breaks associated with SCE tended to be higher in the mutant cells, indicating that in these mutants of Rad51 paralogs strand exchanges took place, but the HR process could not be completed and hence resulted in chromatid discontinuity.

## Discussion

We have studied chromosomal effects of the impaired NHEJ and HR repair pathways in DT40 cells in response to ICL-inducing agent, MMC. The results presented here together with those of our previous observations (Sonoda et al., 1999; Takata et al., 2000, 2001) clearly show that the HR pathway presents a critical determinant of the level of spontaneous and MMC-induced CAs and SCEs. However, a striking difference in chromosomal effects among mutants indicates that the consequences are different depending on the components of the HR repair pathway that are impaired. Our particular interest is the discordance among the endpoints, CAs, SCEs and cell killing, in response to MMC in HR-deficient cells. Although all of the HR-deficient cells showed MMC hypersensitivity to cell killing, both the frequencies of SCEs and CAs were reduced at a comparable level in *Rad54*<sup>-/-</sup>, *Rad51B*<sup>-/-</sup> and *Rad51C*<sup>-/-</sup> cells but not in *Rad51D*<sup>-/-</sup>, *Xrcc2*<sup>-/-</sup> and *Xrcc3*<sup>-/-</sup> cells, where SCEs were reduced while CAs were not. The discordance between the CA level and cell killing suggests that CA formation is not a major pathway of cell killing by ICLs, at least in the present experimental system, but that the unsuccessful repair of ICLs may lead to immediate cell death. The surviving cells might be those rescued from cell death by other yet unidentified mechanisms that are not linked to SCE and CA, and hence represent a



**Fig. 4.** Proposed model for the ICL repair pathway in relation to the chromosomal manifestations. ICLs are highly cytotoxic and may lead to cell death by preventing efficient DNA replication, but are tolerated by a sequence of repair pathways involving Xpf/Erc1 structure-specific endonucleolytic unhooking followed by HR repair, which is prone to SCE and CA formation. HR-deficient cells are either killed or rescued by an alternative repair pathway, for instance, the Mre11-mediated homologous end-joining pathway, which is less prone to SCE and CA formation. Mre11 pathway: repair pathway by Mre11/Rad50/Nbs1 complex. TLS: trans-lesion synthesis. NER: nucleotide excision repair.

reduced number of SCEs and CAs. The back-up pathway through Ku-mediated NHEJ is less likely because the levels of SCEs and CAs were not different between *Rad54*<sup>-/-</sup> cells and *Ku70*<sup>-/-</sup>/*Rad54*<sup>-/-</sup> double mutants.

ICL is a unique damage in that it involves both strands of DNA, presenting a disturbance of DNA replication and hence strong cytotoxicity. It is thus tempting to speculate on the presence of an efficient life-or-death decision system in response to ICLs, where the HR repair pathway plays a key role in tolerating ICL lesions to survive. Indeed, small or fragmented cells accumulate in HR-deficient cells, suggesting an increased level of apoptotic cell death (Takata et al., 2000, 2001). In Chinese hamster ovary (CHO) cells, the enhanced cytotoxicity by ICLs has been demonstrated to be associated with apoptotic cell killing and reduced mutagenicity (Cai et al., 2001). Furthermore, Becker et al. (2002) studied death pathways in Chinese hamster V79 cells with different sensitivities to crosslinking agents and reported that apoptosis was a predominant mechanism of the cell death, which was accompanied by the accumulation of DSBs in a dose-dependent manner. DSBs are probably common intermediates following treatment with crosslinking agents and provide lesions to be repaired by HR. Recently, De Silva et al. (2000) reported that DSBs accumulate in CHO and



V79 cells after treatment with the crosslinking agent nitrogen mustard. The accumulation of DSBs was independent of the dysfunction of Xpf, Ercc1, Xrcc2 and Xrcc3 genes, in which the level of DSBs was comparable to that in the wild type cells.

A putative life-or-death decision pathway in tolerating ICLs is proposed in Figure 4. DSBs generated at the stalled DNA replication forks or those introduced as intermediates of Xpf/Ercc1-mediated incision process, may activate a complex HR pathway, where DNA ends are first resected in the 5'→3' direction and the resulting 3' single-strand tails being stabilized by RPA, and Rad51 catalyzing the invasion of single-strand tails into the DNA double helix with sequence homology followed by resynthesis of gaps, and then the resultant Holiday junctions being resolved to yield two intact DNA molecules. This Rad51-dependent exchange reaction is facilitated by Rad54 DNA-dependent ATPase and coordinated by other members of Rad52 epistasis group including Rad51B, Rad51C, Rad51D, Xrcc2, Xrcc3, and Brca1 and Brca2 (review by Khanna and Jackson, 2001). The involvement of the Rad51-mediated HR pathway in the ICL repair was suggested by subnuclear assembly of the Rad51 protein in cells treated with MMC (Takata et al., 2000). Unsuccessful HR repair, depending on the role of the components therein, could lead to cell death. The physical interaction between Rad51 and Xrcc3, between Xrcc3 and Rad51C, between Rad51B and Rad51C, between Rad51C and Rad51D, and between Rad 51D and Xrcc2 (Braybrooke et al., 2000; Liu et al., 1998; Schild et al., 2000; Thompson and Schild, 1999) suggests, that these Rad51 paralogs constitute functional complexes to cooperate with Rad51. Although the role of each component in the HR repair process is still poorly defined, it is likely that the impairment of the early steps in HR could lead to immediate cell death, whereas the defective operation in the later steps could lead to abortive exchanges, which may again present a signal for cell death or appear as chromosomal discontinuity when surviving and would be visualized as a CA at the junction of a SCE. Recently, Xrcc3 has been reported to function not only in the initial stages of HR but also in the later stages in the formation and resolution of HR intermediates, possibly by stabilizing heteroduplex DNA (Brenneman et al., 2002). The high level of CAs in Rad51D<sup>-/-</sup>, Xrcc2<sup>-/-</sup> and Xrcc3<sup>-/-</sup> cells is consistent with this expectation.

It is paradoxical that induction of CAs and SCEs by MMC is apparently suppressed in Rad54<sup>-/-</sup>, Rad51B<sup>-/-</sup> and Rad51C<sup>-/-</sup> cells while these HR mutants are all highly sensitive to cell killing by MMC. However, it may be speculated that the deficiency in the HR repair pathway evokes an alternative pathway to cope with the ICL damage. A potential role of NHEJ in ICL repair has been suggested in yeast (McHugh et al., 2000). However, as mentioned above, the back-up operation of NHEJ is less likely in our cell system because the response to MMC in Rad54<sup>-/-</sup> cells was not different from that in the Ku70<sup>-/-</sup>/Rad54<sup>-/-</sup> cells. In this respect, it is of particular interest that MMC treatment also activates the subnuclear assembly of the Mre11/Rad50/Nbs1 complex (Mre11 complex) (Nakanishi et al., 2002; Pichierri et al., 2002) which catalyzes the homology-directed end-joining or single strand annealing of the extended single strand tails at DSBs resulting in end-joining of broken ends (review by D'Amours and Jackson, 2002). The yeast

Mre11 mutant shows ICL sensitivity (McHugh et al., 2000), and Nbs1-mutated human genetic disease Nijmegen breakage syndrome is at least moderately sensitive to MMC (Kraakman-van der Zwet et al., 1999; Nakanishi et al., 2002). Unlike the HR pathway, the Mre11 pathway does not result in SCE unless both sister chromatids contain DSBs. The molecular mechanism of the interplay between HR- and Mre11-pathway is not known, but the impaired Mre11 pathway has been reported to enhance HR (Ivanov et al., 1992; Rattray and Symington, 1995; Tsubouchi and Ogawa, 1998). HR requires processing of DSB into a resected DNA duplex with protruding 3' single stranded DNA tail. However, Mre11 exhibits 3'→5' exonuclease activity producing a 5' single strand tail, which may not provide a substrate for Rad51 to initiate strand invasion toward HR (Haber, 1998; Sung et al., 2000; Symington, 2002). Given the role of the strict preference of the sequence polarity, the Mre11 complex could assist in making a choice for one of the two pathways. The deficiency in HR pathway may stimulate the Mre11 pathway, and hence presents the reduction of SCEs and CAs in HR-deficient mutants when they survive to mitosis. However, the proposed model is highly speculative and should be further validated experimentally.

The human genetic disease Fanconi anemia is known to be hypersensitive to the ICL-inducing agents (Sasaki and Tonomura, 1973). To date, eight responsible genes have been identified, including FancA, FancC, FancD1 (Brca2), FancD2, FancE, FancF, FancG (Xrcc9) and FancL (Joenje and Patel, 2001; Bagby, 2003; Meetei et al., 2003). The encoded proteins form a multisubunit nuclear complex and appear to cooperate in a common cellular pathway because a mutation in each gene causes similar clinical phenotypes. Furthermore, recent two-hybrid and immunoprecipitation experiments indicate a direct interaction with the HR pathways, e.g. the physical association of FancA with Rad51, FancD2 with Nbs1, FancD1 (Brca2) with Rad51, FancA with Brca1 and FancG with Brca2 (Joenje and Patel, 2001; Nakanishi et al., 2002; Folias et al., 2002; Husain et al., 2003). More direct evidence for the involvement in HR was demonstrated by Takata and his colleagues (Yamamoto et al., 2003). They showed that the repair by HR of I-SceI-induced DSBs was severely suppressed in FancG-knockout DT40 cells. The SCE response to MMC in FA cells is controversial; a nearly normal response (Novotná et al., 1979), reduced response (Latt et al., 1975) and variable among patients (Kano and Fujiwara, 1981; Sasaki, 1982). In our earlier studies, a patient FA17JTO showed a somewhat elevated SCE response to MMC, but another patient FA20JTO showed a below normal response (Kano and Fujiwara, 1981; Sasaki, 1982). FA17JTO was assigned as group G and FA20JTO as group A by mutation analysis (Tachibana et al., 1999, and their unpublished data). In the FancG knockout DT40 cells, the frequencies of spontaneous SCEs are higher than that in wild type cells but those after MMC treatment are equivalent to that in the wild type cells (Yamamoto et al., 2003), indicating that the net-induced frequencies are rather reduced in the MMC-treated mutant cells. However, because of the limited data available at this stage, the SCE response in FA cells must await further studies.

Clearly, the HR repair pathway is of central importance for the maintenance of chromosomal integrity towards ICLs. The HR repair pathway is regulated by multiple genes and the chromosomal manifestations of the ICL response are largely dependent on the impaired subunits of the pathway. Moreover, emerging evidence suggests the interplay with other repair complexes; and these may be corporative, substitutive, or discriminative depending on the cell cycle stages, and this further complicates the ICL tolerating mechanism and its chromosomal

consequences. Inappropriate repair is a hallmark of clastogenicity, mutagenesis and carcinogenicity, but living cells have an alternative pathway, here referred to as death pathway, to escape from the effects of genotoxic insult. The death pathway seems to have considerable weight in tolerating ICL damage. The life-or-death decision with its signaling mechanism may vary among types of damage and cell types, and should constitute a significant determinant of the chromosomal manifestation of the response to DNA damage, in particular to ICLs.

## References

- Bagby GC: Genetic basis of Fanconi anemia. *Curr Opin Hematol* 10:68–76 (2003).
- Bardwell AJ, Bardwell L, Tomkinson AE, Friedberg EC: Specific cleavage of model recombination and repair intermediates by the yeast Rad1-Rad10 DNA endonuclease. *Science* 265:2082–2085 (1994).
- Baumann P, West SC: Role of the human RAD51 protein in homologous recombination and double-strand-break repair. *Trends Biochem Sci* 23:247–251 (1998).
- Becker R, Ritter A, Eichhorn U, Lips J, Bertram B, Wiessler M, Zdzienicka MZ, Kaina B: Induction of DNA breaks and apoptosis in crosslink-hypersensitive V79 cells by the cytostatic drug beta-D-glucosyl-ifosfamide mustard. *Br J Cancer* 7:130–135 (2002).
- Bezzubova OY, Sibergleit A, Yamaguchi-Iwai Y, Take-da S, Buerstedde JM: Reduced X-ray resistance homologous recombination frequencies in *RAD54*<sup>-/-</sup> mutant of the chicken DT40 cell line. *Cell* 89:185–193 (1997).
- Braybrooke JP, Spink KG, Thacker J, Hickson ID: The RAD51 family member, RAD51L3, is a DNA-stimulated ATPase that forms a complex with XRCC2. *J Biol Chem* 274:29100–29106 (2000).
- Brenneman MA, Wagener BM, Miller CA, Allen C, Nickoloff JA: XRCC3 controls the fidelity of homologous recombination: roles for XRCC3 in late stages of recombination. *Mol Cell* 10:387–395 (2002).
- Cai Y, Ludeman SM, Wilson LR, Chung AB, Dolan ME: Effect of O6-benzylguanine on nitrogen mustard-induced toxicity, apoptosis, and mutagenicity in Chinese hamster ovary cells. *Mol Cancer Ther* 1:21–28 (2001).
- Cole RS: Repair of DNA containing interstrand crosslinks in *Escherichia coli*: sequential excision and recombination. *Proc natl Acad Sci USA* 70:1064–1068 (1973).
- Cupido M, Bridges BA: *Uvr*-independent repair of 8-methoxypsoralen crosslinks in *Escherichia coli*: evidence for a recombinational process. *Mutat Res* 146:135–141 (1985).
- D'Amours D, Jackson SP: The MRE11 complex: at the crossroads of DNA repair and checkpoint signaling. *Nature Rev Mol Cell Biol* 3:317–327 (2002).
- Dardalhon M, Averbeck D: Pulse-field gel electrophoresis analysis of the repair of psoralen plus UVA induced DNA photoproducts in *Saccharomyces cerevisiae*. *Mutat Res* 336:49–60 (1995).
- De Silva IU, McHugh PJ, Clingen PH, Hartley JA: Defining the role of nucleotide excision repair and recombination in the repair of DNA interstrand crosslinks in mammalian cells. *Mol Cell Biol* 20:7980–7990 (2000).
- Fishman-Lobell J, Haber JE: Removal of nonhomologous DNA ends in double-strand break recombination: the role of the yeast ultraviolet repair gene RAD1. *Science* 258:480–484 (1992).
- Folias A, Matkovic M, Bruun D, Reid S, Hejna J, Grompe M, D'Andrea A, Moses R: BRCA1 interacts directly with Fanconi anemia protein FANCA. *Hum Mol Genet* 11:2591–2597 (2002).
- Haber JE: The many interfaces of Mre11. *Cell* 95:583–586 (1998).
- Hussain S, Witt E, Huber PAJ, Medhurst AL, Ashworth A, Mathew CG: Direct interaction of the Fanconi anaemia protein FANCG with BRCA2/FANCD1. *Hum Mol Genet* 12:2503–2510 (2003).
- Ivanov EL, Korolev VG, Fabre F: *XRS2*, a DNA repair gene of *Saccharomyces cerevisiae*, is needed for meiotic recombination. *Genetics* 132:651–664 (1992).
- Joenje H, Patel KJ: The emerging genetic and molecular basis of Fanconi anaemia. *Nature Rev Genet* 2:446–457 (2001).
- Kanaar R, Hoeijmakers JH, Van Gent DC: Molecular mechanisms of DNA double strand break repair. *Trends Cell Biol* 8:483–489 (1998).
- Kano Y, Fujiwara Y: Role of DNA interstrand crosslinking and its repair in the induction of sister-chromatid exchange and a higher induction in Fanconi's anemia cells. *Mutat Res* 81:365–375 (1981).
- Khanna KK, Jackson SP: DNA double-strand breaks: signaling, repair and the cancer connection. *Nature Genet* 27:247–254 (2001).
- Kraakman-van der Zwet M, Overkamp WJ, Friedl AA, Klein B, Verhaegh GW, Jaspers NG, Nidro AT, Eckardt-Schupp F, Lohm PH, Zdzienicka MZ: Im-mortalization and characterization of Nijmegen breakage syndrome fibroblasts. *Mutat Res* 434:17–27 (1999).
- Kuraoka I, Kobertz WR, Ariza RR, Biggerstaff M, Essigmann JM, Wood RD: Repair of an inter-strand DNA crosslink initiated by ERCC1-XPF repair/recombination nuclease. *J Biol Chem* 275:26632–26636 (2000).
- Latt SA, Stetten G, Juergens LA, Buchanan GR, Gerald PS: Induction by alkylating agents of sister chromatid exchanges and chromatid breaks in Fanconi's anemia. *Proc natl Acad Sci USA* 72:4066–4070 (1975).
- Liu N, Lamerdin JE, Tebbs RS, Schild D, Tucker JD, Shen MR, Brookman KW, Siciliano MJ, Walter CA, Fan W, Narayama LS, Zhou Z-Q, Adamson AW, Sorensen KJ, Chen DJ, Jones NJ, Thompson LH: XRCC2 and XRCC3, new human Rad51-family members, promote chromosome stability and protect against DNA crosslinks and other damages. *Mol Cell* 1:783–793 (1998).
- Magana-Schwencke N, Henriques JA, Chanet R, Moustacchi E: The fate of 8-methoxypsoralen photoinduced crosslinks in nuclear and mitochondrial yeast DNA: comparison of wild type and repair deficient strains. *Proc natl Acad Sci USA* 79:1722–1726 (1982).
- McHugh PJ, Sones WR, Hartley JA: Repair of intermediate structures produced at DNA interstrand cross-links in *Saccharomyces cerevisiae*. *Mol Cell Biol* 20:3425–3433 (2000).
- Meetei AR, de Winter JP, Medhurst AL, Wallisch M, Waisfisz Q, van de Vrugt HJ, Oostra AB, Yan Z, Ling C, Bishop CE, Hoatlin ME, Joenje H, Wang W: A novel ubiquitin ligase is deficient in Fanconi anemia. *Nature Genet* 35:165–170 (2003).
- Nakanishi K, Taniguchi T, Ranganathan V, New HV, Moreau LA, Stotsky M, Mathew CG, Kastan MB, Weaver DT, D'Andrea AD: Interaction of FANCD2 and NBS1 in the DNA damage response. *Nature Cell Biol* 4:913–920 (2002).
- Niedernhofer LJ, Essers J, Weeda G, Beverloo B, De Wit J, Muijters M, Obijk H, Hoeijmakers JH, Kanaar R: The structure-specific endonuclease ERCC1/XPF is required for targeted gene replacement in embryonic stem cells. *EMBO J* 20:6540–6549 (2001).
- Novotná B, Goetz P, Surkova NI: Effects of alkylating agents on lymphocytes from control and from patients with Fanconi's anemia. Studies of sister chromatid exchanges, chromosome aberrations, and kinetics of cell division. *Hum Genet* 49:41–50 (1979).
- Perry P, Wolff S: Giemsa technique for the differential staining of sister chromatids. *Nature* 251:156–158 (1974).
- Pichiéri P, Averbeck D, Rosselli F: DNA cross-link-dependent RAD50/MRE11/NBS1 subnuclear assembly requires the Fanconi anemia C protein. *Hum Mol Genet* 11:2531–2546 (2002).
- Rattray AJ, Symington LS: Multiple pathways for homologous recombination in *Saccharomyces cerevisiae*. *Genetics* 139:45–56 (1995).
- Reiss B, Schubert IS, Köpchen K, Wendeler E, Schell J, Puchta H: RecA stimulates sister chromatid exchange and the fidelity of double-strand break repair, but not gene targeting, in plants transformed by *Agrobacterium*. *Proc natl Acad Sci USA* 97:3358–3363 (2000).
- Sargent RG, Meservy JL, Perkins BD, Kilburn AE, Intody Z, Adair GM, Nairn RS, Wilson JH: Role of the nucleotide excision repair gene ERCC1 in formation of recombination-dependent rearrangements in mammalian cells. *Nucleic Acids Res* 28:3771–3778 (2000).
- Sasaki MS: Is Fanconi's anemia defective in a process essential to the repair of DNA cross-links? *Nature* 257:501–503 (1975).
- Sasaki MS: Sister chromatid exchange as a reflection of cellular DNA repair, in Sandberg AA (ed): *Sister Chromatid Exchange*, pp 135–161 (Alan R Liss, New York 1982).
- Sasaki MS, Tomomura A: A high susceptibility of Fanconi's anemia to chromosome breakage by DNA cross-linking agents. *Cancer Res* 33:1829–1836 (1973).

- Schild D, Lio Y-C, Collins DW, Tsomondo T, Chen DJ: Evidence for simultaneous protein interactions between human Rad51 paralogs. *J Biol Chem* 275:16443–16444 (2000).
- Shinohara A, Ogawa T: Homologous recombination and the roles of double-strand breaks. *Trends Biochem Sci* 20:387–391 (1995).
- Sonoda E, Sasaki MS, Buerstedde JM, Bezzubova O, Shinohara A, Ogawa H, Takata M, Yamaguchi-Iwai Y, Takeda S: Rad51 deficient vertebrate cells accumulate chromosomal breaks prior to cell death. *EMBO J* 17:598–608 (1998).
- Sonoda E, Sasaki MS, Morrison C, Yamaguchi-Iwai Y, Takata M, Takeda S: Sister chromatid exchanges are mediated by homologous recombination in vertebrate cells. *Mol Cell Biol* 19:5166–5169 (1999).
- Sung P, Trujillo KM, Van Komen S: Recombination factors of *Saccharomyces cerevisiae*. *Mutat Res* 451:257–275 (2000).
- Symington LS: Role of RAD52 epistasis group genes in homologous recombination and double-strand break repair. *Microbiol Mol Biol Rev* 66:630–670 (2002).
- Tachibana A, Kato T, Ejima Y, Yamada T, Shimizu T, Yang L, Tsunematsu Y, Sasaki MS: The FANCA gene in Japanese Fanconi anemia: reports of eight novel mutations and analysis of sequence variability. *Hum Mutation* 13:237–244 (1999).
- Takata M, Sasaki MS, Sonoda E, Morrison C, Hashimoto M, Utsumi H, Yamaguchi-Iwai Y, Shinohara A, Takeda S: Homologous recombination and non-homologous end-joining pathways of DNA double-strand break repair have overlapping roles in the maintenance of chromosomal integrity in vertebrate cells. *EMBO J* 17:5497–5508 (1998).
- Takata M, Sasaki MS, Sonoda E, Fukushima T, Morrison C, Albala JS, Swagemakers SMA, Kanaar R, Thompson LH, Takeda S: The Rad51 paralog Rad51B promotes homologous recombinational repair. *Mol Cell Biol* 20:6476–6482 (2000).
- Takata M, Sasaki MS, Tachiiri S, Fukushima T, Sonoda E, Schild D, Thompson LH, Takeda S: Chromosome instability and defective recombinational repair in knockout mutants of the five Rad51 paralogs. *Mol Cell Biol* 21:2858–2866 (2001).
- Thompson LH, Schild D: The contribution of homologous recombination in preserving genome integrity in mammalian cells. *Biochimie* 81:87–105 (1999).
- Tsubouchi H, Ogawa H: A novel mre11 mutation impairs processing of double-strand breaks of DNA during both mitosis and meiosis. *Mol Cell Biol* 18:260–268 (1998).
- Yamamoto K, Ishida M, Matsushita N, Arakawa H, Lamerdin JE, Buerstedde J-M, Tanimoto M, Harada M, Thompson LH, Takata M: Fanconi anemia FANCG protein in mitigating radiation- and enzyme-induced DNA double-strand breaks by homologous recombination in vertebrate cells. *Mol Cell Biol* 23:5421–5430 (2003).

# Repair rates of R-band, G-band and C-band DNA in murine and human cultured cells

M.H. Sanders,<sup>a</sup> S.E. Bates,<sup>a</sup> B.S. Wilbur<sup>b</sup> and G.P. Holmquist<sup>a</sup><sup>a</sup>Beckman Research Institute, Department of Biology, City of Hope Medical Center, Duarte, CA;<sup>b</sup>Department of Bioengineering, University of Utah, Salt Lake City, Utah (USA)

**Abstract.** Repair of cyclobutane pyrimidine dimers (CPDs) in cultured neonatal human fibroblasts and in *Mus spretus* × *M. castaneus* F<sub>1</sub> neonatal skin fibroblasts was analyzed after UVC-irradiation by cleavage with T4 endonuclease V cyclopyrimidine dimer glycosylase, alkaline-agarose gel electrophoresis, and Southern blotting. The blots were sequentially probed with <sup>32</sup>P-labeled Alu, or B2, to preferentially illuminate R-band DNA, by L1 to preferentially illuminate G-band DNA, and by satellite DNA to illuminate C-band DNA. These three different DNA populations showed slightly different global nucleotide excision repair rates that are in the order of speed, R-band DNA > G-band DNA > C-band DNA. Fibroblasts from outbred neonatal mice and humans showed similar band-specific repair rate ratios and the global repair rate of murine fibroblasts was almost as rapid as that of the human fibroblasts. The mass distribution of the human Alu-probed signal was further

analyzed. Gel mobility data was fitted to a logistic equation to include all M<sub>r</sub> values. Hypothetical distributions of DNA randomly cleaved to a particular number-average molecular weight were fit to the logistic gel mobility function to determine how such a randomly cleaved distribution of a particular cleavage frequency would be displayed along the experimental gel. This revealed a rapidly repaired kinetic fraction that represented 17% of the Alu-probed signal (R-band DNA), almost none of the L1 probed signal (G-band DNA), and reflects transcription coupled repair of active genes. The remaining Alu-probed DNA showed a random distribution of UVC-induced CPDs throughout all stages of global nucleotide excision repair. The Alu-probed CPDs disappeared with an excellent fit to first order kinetics and with a half-life of seven hours.

Copyright © 2003 S. Karger AG, Basel

Nucleotide excision repair (NER) shows DNA domain-specific repair rates. The first reported domain rate difference was a relatively slow nucleotide excision repair rate for furocoumarin adducts and N-acetoxy-2-acetylaminofluorene but not for cyclobutane pyrimidine dimers (CPDs) in African green monkey  $\alpha$ -satellite DNA compared with that of the remaining, euchromatic, DNA (Zolan et al., 1982). If the satellite DNA of C-bands shows slow NER relative to the euchromatic portion

(R-bands and G-bands) of the genome, then what is the relative repair rate of the R-bands, G-bands, and C-bands?

Global NER acts slowly on all DNA. Transcription-coupled repair (TCR) is a very rapid repair of the transcribed strand of active (Mellon et al., 1987) or transcriptionally poised (Mullenders et al., 1991) genes. In hamster cell lines where global NER is virtually absent, one report shows that CPD repair by TCR in the DHFR gene is limited to the transcribed region of the transcribed strand (Spivak and Hanawalt, 1996). While human cells show efficient global NER, TCR is so rapid that 24 h after UVC irradiation, large regions exist which are CPD free. These CPD-free regions are especially apparent in Xeroderma pigmentosum type C (XPC) fibroblasts (Kantor and Deiss-Tolbert, 1995). XPC cells lack global NER activity (Venema et al., 1991) and some 15% of the XPC genome receives 50% of the repair activity (Kantor et al., 1990). CPD-free domains do not form in Cockayne syndrome fibroblasts (Shanower and Kantor, 1997), cells that lack TCR activity and retain only global

Supported by NIH grant 1P01CA69449.

Received 5 September 2003; revision accepted 6 November 2003.

Request reprints from Gerald P. Holmquist  
Department of Biology, City of Hope Medical Center  
1450 E. Duarte rd., Duarte, CA 91010 (USA)  
telephone: +1-626-301-8350; fax: +1-626-358-7703  
e-mail: gholm@coh.org

NER activity (van Hoffen et al., 1993). The CPD-free domains are observed in GC-rich DNA (Kantor and Deiss-Tolbert, 1995) in which active genes are concentrated. CPD-free domains are large, 50 kb, and extend far from the boundaries of the 3.5-kb  $\beta$ -actin gene (Barsalou et al., 1994) or the 20-kb p53 gene (Tolbert and Kantor, 1996).

R-bands differ from G-bands in behavior and sequence with R-band DNA constitutively replicating early while G-band DNA usually replicates late (Goldman et al., 1984; Holmquist, 1987). About 79% of cytologically mapped genes map to R-bands (Musio et al., 2002). The R-bands are GC rich and the G-bands are AT rich (Bernardi, 2001). Humans have a subset of very AT-rich R-bands called T-bands (Dutrillaux, 1973). These bands are extremely enriched in genes (Holmquist, 1992; Saccone et al., 1999; Bernardi, 2001). Surralles et al. (2002) made probes from TCR-mediated repair sites of UVC-irradiated Xeroderma pigmentosum group C cells, cells that can only repair the transcribed strand of active genes. These probes illuminated a general R-band pattern with the strongest signal over T-bands. Thus, TCR occurs in bands with active genes, R-bands, and predominantly in the gene-richest of these R-bands, T-bands.

Almost half of the human genome is composed of families of interspersed repeats (Smit, 1999). The short interspersed repeats are called SINEs and the long ones are called LINEs (Singer, 1982). Most SINE families are concentrated in early replicating, GC-rich, R-band DNA while most LINE families are found concentrated in the late replicating, G-band DNA (Goldman et al., 1984; Holmquist and Caston, 1986). This band-related distribution for the SINE family Alu and for the LINE family L1 was first reported by Laura Manuelidis who used in situ hybridization to localize the human L1 family to G-bands (Manuelidis, 1982) and the Alu SINE family to R-bands (Manuelidis and Ward, 1984), by Soriano et al. (1983) who found L1 concentrated in AT-rich isochores (G-band DNA) and Alu concentrated in GC-rich isochores (R-band DNA), and by Korenberg and Rykowski (1988) who used FISH to produce a G-banding pattern with an L1 probe and an R-banding pattern with an Alu probe. The band-specific enrichments have been quantified. Holmquist and Caston (1986) showed that 77% of the signal from the L1 probe A36Fc was in late replicating HeLa DNA while 23% of its signal was in early replicating DNA. Smit (1999), using the sequenced human genome, reported that the two light (AT-rich) isochores in autosomes are comprised of 7.9% Alu and 17.6% L1 while the three heavy (GC-rich) isochores are comprised of 17.1% Alu and 7.3% L1. Some human R-bands, T-bands, have higher concentrations of Alu than do other R-bands. This extreme Alu-richness is correlated with extreme gene richness (Holmquist, 1992). Thus, using an L1 probe and an Alu probe to distinguish G-band DNA from R-band DNA is not ideal but should well reflect any trends of different damage or repair for these two band classes of DNA.

FISH to mouse chromosomes using the murine SINE family, B2, and the murine LINE family, L1, showed the same band specificity (Boyle et al., 1990) as that previously reported for human chromosomes using Alu and L1 (Korenberg and Rykowski, 1988).

A replication banding pattern along chromosomes is common to all vertebrates (Holmquist, 1988). Superimposed upon this replication time pattern, GC richness of the early replicating bands arose independently with homeothermia in birds and mammals less than 350 million years ago (Holmquist, 1988). Alu arose about 65 million years ago (Deininger and Daniels, 1986) eventually concentrating in R-bands. The mutational load or substitutional cost was calculated for these patterns of base composition or Alu concentration to have been generated by random mutagenesis followed by selection against the "inappropriate" or selection for the "appropriate" regional base composition or regional Alu concentration and found to be impossibly large (Holmquist, 1989). Consequently, the genomic patterns of base composition differences and Alu concentration differences must be due to some pattern-organized mutational pressure (Holmquist, 1989; Holmquist and Filipinski, 1994). One possible cause of pattern-organized mutational pressure is mediated by chromatin domains that exhibit differing levels of vulnerability to damage or accessibility to repair.

Primary human fibroblasts are ideal for cyclobutane pyrimidine dimer (CPD) repair experiments because, after a high dose of UV, they cease to enter S-phase while maintaining a normal active CPD repair capacity. In contrast, the CPD repair capacity of murine cells is problematic. Established rodent cell lines only repair about 20% of induced CPDs (Bohr et al., 1986) and this is predominantly due to transcription coupled repair of transcribed strands (Mellon et al., 1987; Hanawalt, 1990). The repair capacity of *Mus musculus* primary embryonic cells decreases with both the age of the donor embryo and the passage number of the culture. These data suggest that the genetic information for global excision repair in culture is turned off after 17–19 days of development (Peleg et al., 1977). In mouse skin, one study showed that the epidermal cells removed CPDs only from active genes (Ruven et al., 1993); global CPD repair appeared to be absent. Another study (Mitchell et al., 1999) showed that while some murine epidermal cells do show slow global repair, others in the same tissue appear incapable of global CPD repair. These mouse and hamster cells usually have very low levels of DNA damage binding protein 2 (DDB2-protein or p48-protein). p53 activity is required to upregulate this DDB-2 protein and DDB-2 is required for global CPD repair along the non-transcribed strand but not for transcription-coupled repair (Tang et al., 2000; Zhu et al., 2000). We searched for and found a murine cell line from a cross of *Mus spretus*  $\times$  *M. castaneus* that shows levels of global NER almost equivalent to that of humans.

Mutagen-induced lesions often appear to be randomly distributed along the genome. When randomly distributed DNA lesions are converted into DNA breaks, the resulting frequency distribution of fragment sizes is given by the Eq. 1 (Kuhn, 1930).

$$W_b \Big|_0^b = \int_0^b W \omega^b = 1 - (1 + Pb) e^{-Pb} \quad (1)$$

The number average molecular weight of a population of polymers,  $M_n$ , is obtained by adding the number of molecules in each fraction, each multiplied by its molecular weight, and dividing the sum for all fractions by the total number of mole-

cules. The weight average molecular weight,  $M_w$ , is obtained by adding mass of molecules in each fraction, each multiplied by its molecular weight, and dividing the sum for all fractions by the total weight (see Tanford, 1961, pp. 146).

For randomly cleaved DNA,  $M_w = 2M_n$ . If one determines Eq. 1 for all sizes and plots the log of  $b$  on the X axis and  $W_x$ , along the Y axis, then a sigmoidal curve is obtained with Y values that vary from 0 to 1. Such a plot describes the cumulative weight fraction of DNA less than size "b" bases. This equation was used along with gel electrophoresis by Hamer and Thomas (1975) and by Peterson (2000) to show that restriction endonucleases cleave genomic DNA in a random fashion. With modern computers, one can create small polymer-length intervals and determine the weight fraction expected in each small interval. The result is shown in Fig. 1A.

The plot in Fig. 1A describes the mass of randomly cleaved DNA as a function of  $M_r$ . When the X-axis is changed to  $\log_{10}$  of  $M_r$ , then the plot accurately describes the DNA mass as it is size-fractionated in the log-linear mobility range of agarose gel electrophoresis. In such a plot, the peak DNA concentration occurs at an  $M_r$  which equals weight average molecular weight,  $M_w$  (Drouin et al., 1996; Rodriguez et al., 1999). Using gel electrophoresis of radiolabeled DNA, one can slice the gel and, after scintillation counting, obtain a linear response to the  $^3\text{H}$ -DNA content of each gel slice. Cleavage of tritiated V79 hamster cell DNA with *EcoRI* or *HhaI* produced mobility distributions that fit a Kuhn distribution (Holmquist, 1988). In contrast, *MspI*-cleaved DNA showed a low  $M_r$  shoulder outside the expected Kuhn distribution (Holmquist, 1988). This we now know is due to the presence of CpG islands and their high concentrations of *MspI* cleavage sites at CCGG sequences and shows how data deviating from the random cleavage assumption indicates patterns of genome organization. Using fluorochrome-stained denaturing agarose gels, we showed that peroxyl radical-induced oxidized guanines produced a random distribution of FAPY + Endonuclease III-sensitive sites similar to the distribution produced by restriction endonucleases (Rodriguez et al., 1999). Thus, Kuhn's equation and modern linear detection systems allow one to both determine an average cleavage frequency and also test the randomness of the cleavage pattern. But these determinations and tests require that the DNA fragments fall within the log-linear range of the gel electrophoresis system.

For standard alkaline agarose gels that utilize a constant voltage gradient, the log-linear mobility range extends about ten fold, for example, from 2.5 to 20 kb in Fig. 1B. To determine the behavior of randomly cleaved DNA outside this range, one must fit the Kuhn distribution to the entire mobility function of the gel and not to just within the log-linear range. The mobility function in gels run with a constant voltage (Fig. 1B) is known (Willis et al., 1988) and is a logistic function. In the gel, infinitely long DNA does migrate into the gel with a mobility  $\mu_{\min}$  and very short DNA molecules migrate with a mobility  $\mu_{\max}$ . Between these extremes,  $M_r$  fractionation follows a logistic function reflecting the same Pascal sampling phenomenon as that experienced by a protein which partitions between the stationary phase and the mobile phase during column chromatography. Equations relating mobility  $\mu$  and  $M_r$  are  $\mu = \mu_0 + a/$

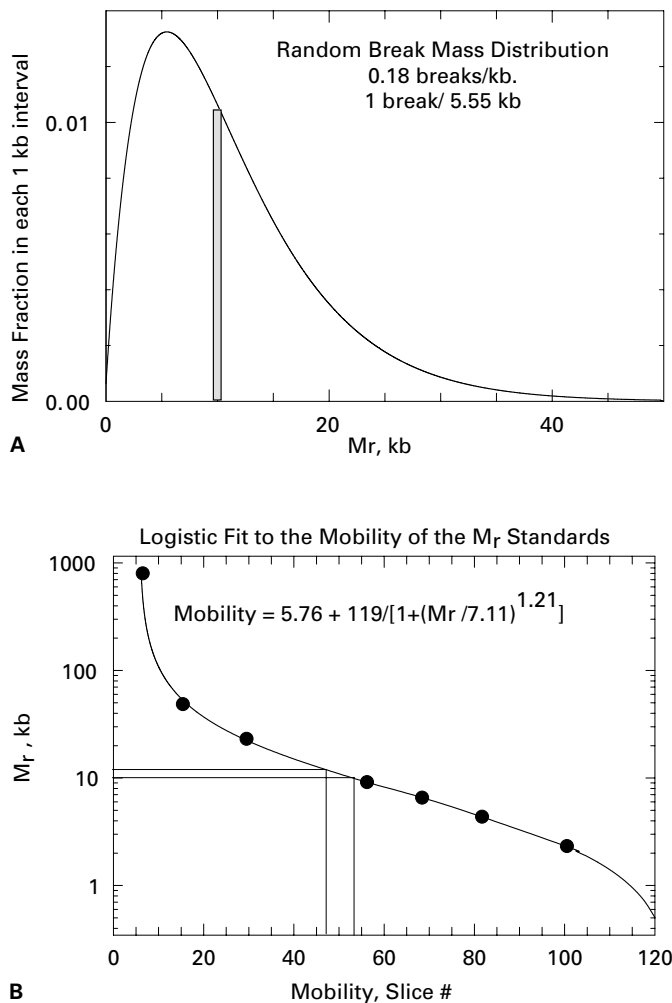


**Fig. 1. (A)** The mass fraction  $W_m$  of molecules "b" bases long was generated for a randomly cleaved infinitely long polymer. The probability of a bond being cleaved is  $P = 0.00018$ .  $W_m = P^2 b(1 - P)^{b-1}$  where  $W_m$  is the mass fraction of DNA molecules of length  $b$  in bp. Kuhn showed that the mass fraction  $< b$  is  $W_b \leq b = \text{integral from 0 to } b \text{ of } W_b \text{ db} = 1 - (1 + Pb)e^{-Pb}$  (Kuhn, 1930). This integral equation and Microsoft Excel were used, for example, to calculate the mass fraction between 18,100 and 18,200 bp as mass fraction =  $(1 - (1 + 18,200P)e^{-(18,200P)}) - (1 - (1 + 18,100P)e^{-(18,100P)})$ . Repeating this for a continuum of intervals generated the curve shown. An interval corresponding to the mobility of molecules from 10 to 11 kb is shown hatched. **(B)** A four-parameter logistic mobility function for electrophoretic mobility  $\mu = \mu_0 + a/(1 + (M_r/x_0)^b)$  was fit to the mobility of the leftmost  $M_r$  standards from Fig. 2 using SigmaPlot's Regression Wizard program. The 800-kb marker in Fig. 2 was estimated as the mobility attained when undamaged DNA reached 30% of its maximum signal. Since the autoradiogram's lane scan was divided into 120 slices, mobility is expressed as slice number instead of mm. Lines from the axes to the curve show how one would determine that molecules in slices 47–53 include a  $M_r$  range of 10–11 kb. The shaded rectangle in panel A shows the expected mass fraction in slices 47–53.

$(1 + (M_r/x_0)^b)$  and  $M_r = x_0[(a/(\mu - \mu_0)) - 1]^{1/b}$  where the parameters  $\mu_0 = \mu_{\min}$ ,  $a = \mu_{\max} - \mu_0$ ,  $x_0$ , and  $b$ , are, for a given electrophoresis buffer, well defined functions of agarose concentration and voltage gradient (Willis et al., 1988). For a particular gel run where the time and voltage gradient are the same for all samples,

mobility  $\mu$  can be measured in distance migrated. If each lane of DNA is divided into many slices, mobility can be expressed as slice number as in Fig. 1B. The parameters as determined by best fit regression to the mobility of the  $M_r$  markers yielded the equation  $\mu = 5.76 + [119/(1 + (M_r/7.11))]^{1.21}$ . In Fig. 1B,  $\mu_{\min} = 5.76$  slices and  $\mu_{\max} = 119$  slices while the parameters 7.11 and 1.21 describe the shape of the sigmoidal curve between the maximum and minimum mobility limits.

We fit the Kuhn distribution to the entire electrophoretic mobility function to accurately predict the shape of the gel mobility profile of randomly cleaved genomic DNA. Using T4-pdg-cleaved DNA from UV-irradiated cells, we show that the analysis method yields accurate estimates of global CPD repair rates (T4-pdg-dependent  $M_n$  increases) and that deviations from random CPD distributions during repair are due to the rapidly repaired domains associated with TCR.

## Materials and methods

Primary neonatal human foreskin fibroblasts were obtained by collagenase digestion and grown to confluence in 150-mm petri dishes in DMEM medium + 10% fetal calf serum. Medium was replaced two days before irradiation. The cells were washed once in isotonic saline. To prevent desiccation of the cells during irradiation, 2 ml of isotonic saline was added to each plate. Cells were then irradiated with 20 J/m<sup>2</sup> of UVC. UVC fluence was monitored with a Blak Ray UV meter (Ultraviolet Products Inc., Upland, CA, USA). After irradiation, the isotonic salt solution was replaced with fresh medium. Cells were periodically harvested over a two-day repair period.

*Mus spretus* × *M. castaneus* F<sub>1</sub> neonatal skin fibroblasts were obtained by collagenase digestion and cultured in DMEM medium + 10% fetal calf serum. Using a cytogenetic analysis of metaphase spreads, cell population showed 10% aneuploid cells after 5 days in culture and 100% aneuploid cells after 14 days in culture. After 20 days, the "post-crisis" fibroblasts were replated. Plates of 95% confluent cells were UVC (10 J/m<sup>2</sup>) irradiated as described for the human cells and murine cells that adhered tightly to the culture plate were harvested over a three-day repair period. In a separate experiment to determine the response of the attached cells to UVC, a log-phase culture of these murine fibroblasts was irradiated, 10 J/m<sup>2</sup> of UVC, and examined periodically by phase microscopy. At t = 0 h and 3 h, cells were rapidly dividing and many telophase cells were present. At 18 and 28 h, telophase cells were absent and there was a noticeable increase in rounded, refractile, and floating cells. At 48 h, 35% of the cells were floating or loosely attached.

After repair and harvesting of cells by trypsinization, DNA was phenol-extracted from isolated nuclei (Ye et al., 1998), quantified by A<sub>260</sub>, digested to completion with T4-pdg (a gift from Steven Lloyd) as previously described by Pfeifer et al. (1992), phenol extracted, and re-quantified by A<sub>260</sub>. 5 µg of DNA in 3 µl was mixed with 3 µl of 100 mM NaOH, 4 mM EDTA. To this, 4 µl of 1 M NaOH, 50% glycerol, and 0.05% bromocresol green was added. 10 µl/lane were loaded into the gel wells for alkaline 0.7% agarose gel electrophoresis (running buffer; 30 mM NaOH, 2 mM EDTA) as previously described by Drouin et al. (1996).

Analysis tools: After neutralization, fluorescent ethidium bromide-stained gels were scanned with a FluorImager, S1. Southern blots were imaged using a Molecular Dynamics, Inc. Storm 850 PhosphorImager. Images were cropped, rotated, and saved as 16 bits/pixel TIFF files using ImageQuant Tools v. 2.0. Lanes in the images were outlined by a rectangle that included signal from the entire lane. Signal in each lane's rectangle was quantified as 120 different slices per lane using the grid option in an ImageQuant 5.0 software package and saved as Excel files. To determine the parameters for fitting logistic curves to the mobility of  $M_r$  standards, logistic regression was done using the Regression Wizard option of SigmaPlot version 4, SPSS, Inc.

<sup>32</sup>P-labeled probes were made as follows. End-labeled probes against lambda DNA were made by extending *Hind*III-digested lambda with Klenow DNA polymerase in the presence of <sup>32</sup>[P]-α-dCTP. Plasmids pSP6-4-B2

and KS13A containing the murine B2 and L1 sequences (Boyle et al., 1990) were obtained from Terry Ashley. Probes were made from plasmids by random priming using randomly synthesized octamers, a Boehringer Mannheim Random-Primed-DNA-labeling kit, and <sup>32</sup>[P]-α-dCTP. The remaining probes were made after PCR amplification of 1–2 µg of genomic DNA. The appropriate sized bands were eluted from the ethidium bromide-stained neutral agarose gels using the extraction procedure recommended by QUIAEX (Quiagen, Inc.). A second round of PCR amplification and gel purification completed the preparation of DNA template for labeling. <sup>32</sup>[P]-dCTP-labeled probes were synthesized from PCR-amplified DNA sequences either by random priming or by several rounds of linear PCR extension using only one primer. The sequences amplified, primers used, and probe labeling methods respectively are summarized as follows:

Human satellite probe: the 171-bp *Eco*RI satellite DNA fragment described as fragment II in Fig. 9 of Wu and Manuelidis (1980): 5'ATATTTCCTATTCTACCATGACCTCAAAG and 5'TTCTCAGTAACTTCCTGTGTTGTGTG, Randomly primed.

Human L1: GenBank HUMALUL1A, #M93406: 5'AGTGCTATCCCTGCCCTGC and 5'GGACATAGGCATGGGCAAGG Linear PCR amplification using the upper primer.

Human Alu: Blur8 GenBank HUMRSAB8, #J00091: 5'CTCGCTCTGTCACCAGGCTGG and 5'AATCCGAGCACTTTGGGAGGC, Randomly primed.

*Mus musculus* major satellite probe: GenBank MMSDNA1: 5'CTGAAATCACGGAAAATGAG and 5'GCCTTCAGTGTGCATTCTCA.

2 µg of *Mus musculus* DNA was PCR amplified for 25 cycles using Taq polymerase to produce ethidium bands at 240 and 480 bp. These bands were excised from the neutral agarose gel and PCR amplified again. The product was randomly primed to generate a <sup>32</sup>P-labeled probe.

Alkaline gels were neutralized, the DNA partially depurinated (10 min 24°C, 0.25 N HCl), the gels were reneutralized, and the DNA was transferred to membranes (Qiagen Inc.) by capillary blotting (Holmquist and Caston, 1986) and fixed to the membranes by UVB irradiation. Hybridization was carried out as described by Tornaletti and Pfeifer (1996) excepting that the pre-hybridization solution was modified so that 200 ml contained 0.4 g of powdered non-fat milk and 2.5 ml of 15 mg/ml sonicated herring sperm DNA. Another modification was that the hybridization solution was made 1× in Denhart's solution (Holmquist and Caston, 1986). Before rehybridization using a different probe, stripping of probes from membranes was accomplished in boiling 0.1–1% SDS (Ausubel et al., 1997; Current Protocols 2.10.7). All Southern blotting results were repeated three times over a period of three years.

## Results

DNA in the two chromosomal compartments, Alu- or B2-probed "R-band" DNA, and L1-probed "G-band" DNA, is damaged similarly (Figs. 3 and 8; 0 h repair). Satellite DNA is tandemly repetitious and non-random in sequence. Its CPD distribution was not amenable to the Kuhn equation and to this comparison.

The repair of CPDs in the human fibroblasts is, except for the C-band DNA, almost complete by 48 h. Between these temporal extremes, all three chromosome compartments (Fig. 3) show repair rates in the order, R-band DNA is faster than G-band DNA, which is faster than C-band DNA. These rate differences are most apparent in the partially repaired DNA profiles from the 8 h and 16 h samples. A visual inspection of the 8 h repair profiles suggests that the Alu-probed DNA has a rapidly repaired kinetic component that is almost completely repaired by 8 h. A similar kinetic component is slightly noticeable in the L1-probed signal. Excluding this rapid component from consideration, the repair rates observed in DNA from the three chromosomal compartments are in the relation Alu-probed >

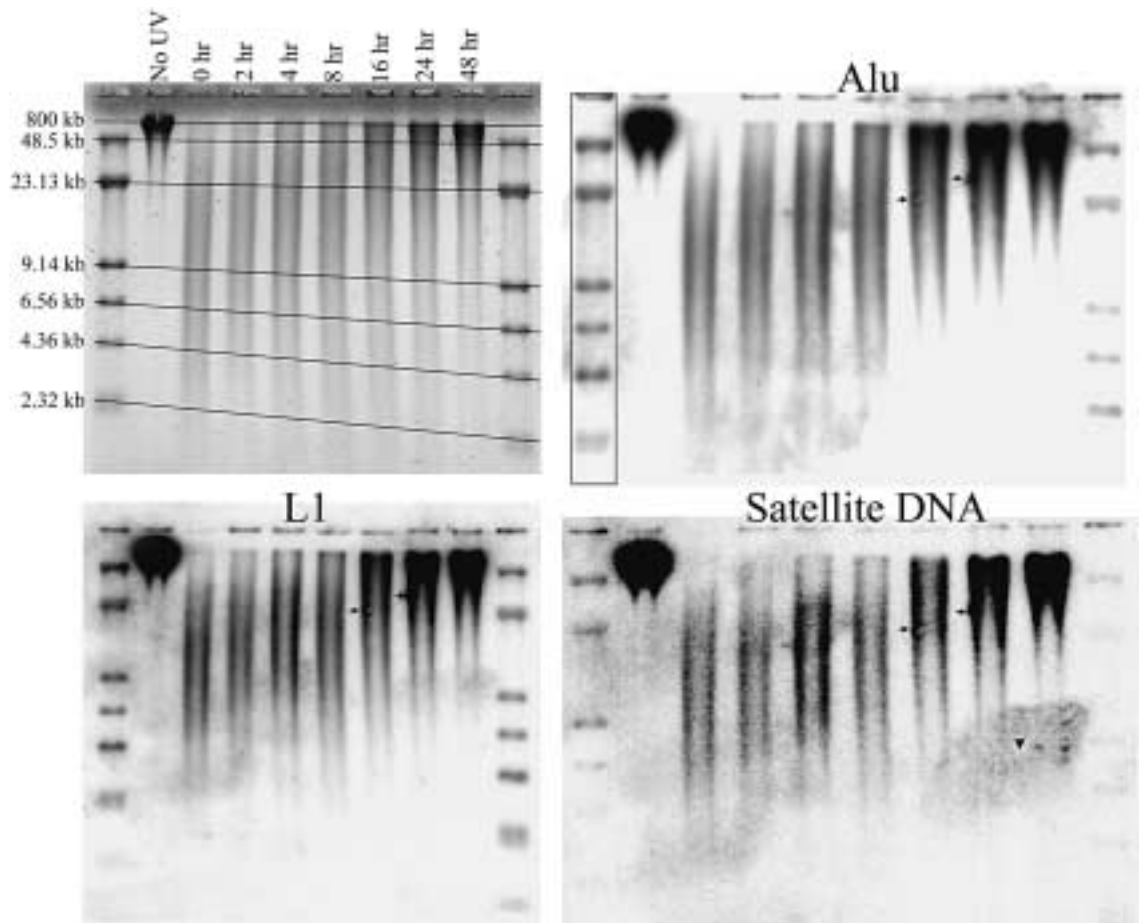


**Fig. 2.** A CPD repair panel from 20 J/m<sup>2</sup> UVC-irradiated human fibroblasts. DNA was size fractionated in alkaline 0.7% agarose and stained with ethidium bromide. Southern blots from this gel were sequentially probed with <sup>32</sup>[P]-Alu, <sup>32</sup>[P]-L1, and <sup>32</sup>[P]-Satellite DNA. The M<sub>r</sub> of full length λ phage DNA and *Hind*III-digested λ phage DNA are shown at the left. The mobility of 800-kb DNA was estimated as the mobility of uncut DNA when the signal on the well-proximal side of the peak of undigested DNA was 30% of maximum. The right side of the gel migrated faster than the left side. Assuming a linear dependence of dVoltage/dx along the horizontal axis, the M<sub>r</sub> mobility of intermediate lanes was estimated from the straight-line segments connecting M<sub>r</sub> markers. Repair times are indicated at the top. Small arrows indicate spots and smudges that appear as aberrant peaks in Fig. 3.

L1-probed > Satellite probed (R-band > G-band > C-band). The differences are quite apparent in Fig. 3 because the same Southern transfer was probed several times and the resulting autoradiograms could be exactly aligned before analysis. These global nucleotide excision repair rate differences seem too small to account for evolution of the base compositional differences between R- and G-band DNA.

Fitting a Kuhn random break distribution to the mobility function and comparing this to the Alu-probed signal (Fig. 4) yields two kinds of information, 1) a test of the shape of the Alu-weighted mass distribution, and 2) a number average Alu-weighted molecular weight (breaks/kb in Fig.4). The realized mobility distributions of the Alu signal and the calculated random cleavage distributions were similar except after 8 h of repair when a shoulder of high M<sub>r</sub> DNA falls outside the fitted curve. Figure 5 shows that the 8-hour Alu-probed data can be approximated by the sum of two randomly cleaved weight dis-

tributions. The higher M<sub>r</sub> distribution is 22.5% of the Alu-probed signal, has 0.029 breaks/kb, and represents a rapidly repaired R-band component. The lower M<sub>r</sub> distribution of the Alu-probed DNA is 77.5% of the signal, has 0.12 breaks/kb, and represents the more slowly repaired component.

The unirradiated signal in Fig. 4 reflects possible DNA breakage during preparation. This was estimated in Fig. 4 as 0.018 breaks/kb. When this frequency of breakage is subtracted from that of UV-irradiated, T4 Endo V cut DNA samples, the result is an estimate of CPD density. This CPD density is plotted in Fig. 6 as a function of repair time. Here, the CPD density closely follows first order kinetics and half of the CPDs are removed every 7 h. A lag of up to several hours has been noted between the time of UVC irradiation and the time when CPD repair initiates (reviewed in Holmquist and Gao, 1997). Such a lag was not detected in Fig. 6.



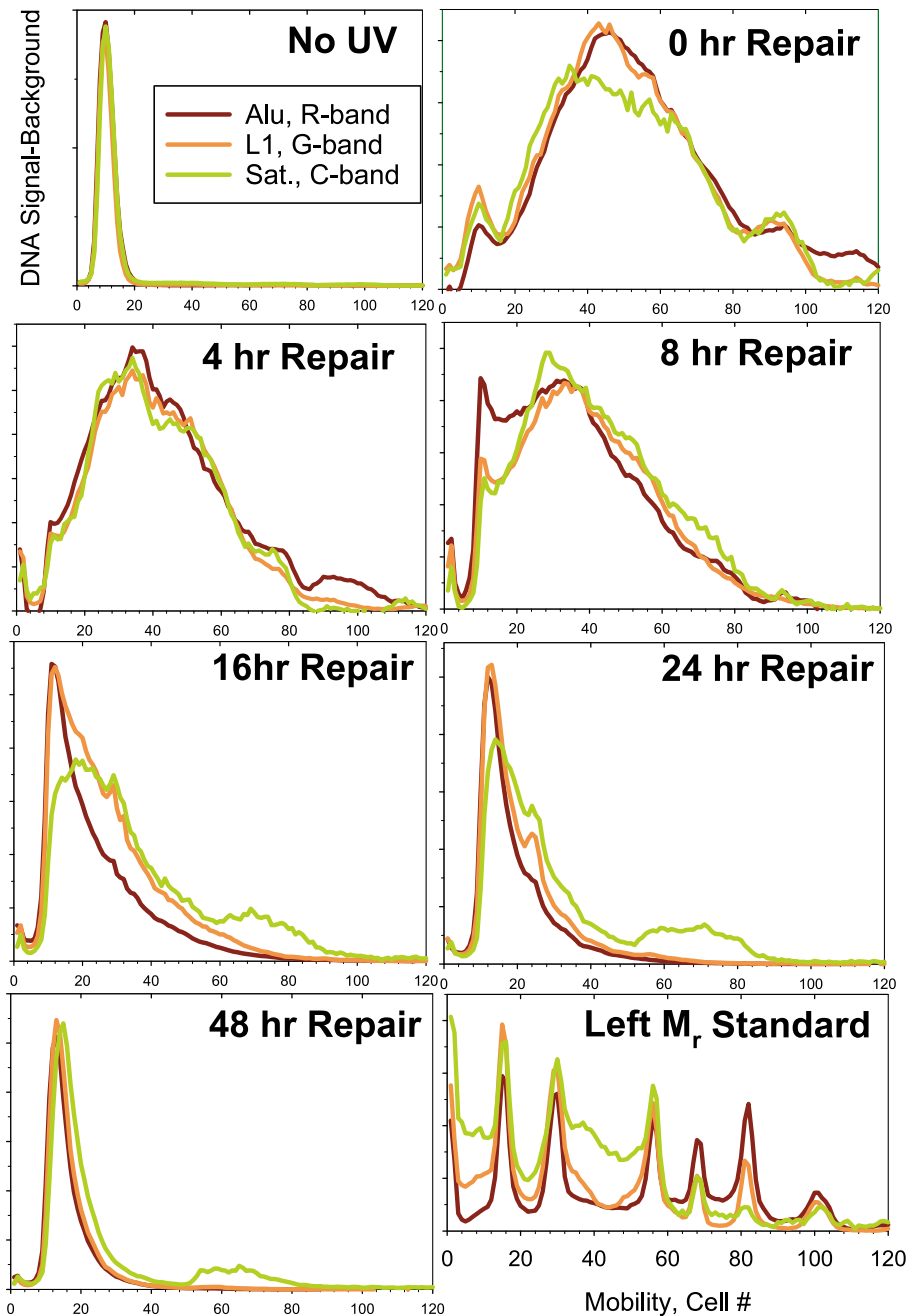


**Fig. 3.** Quantified “lane scans” from the three human autoradiograms in Fig. 2. In the Alu autoradiogram of Fig. 2, a rectangle is shown enclosing the left  $M_r$  marker lane. This rectangle was partitioned into 120 slices. The sliced rectangle was copied onto each lane. The CPM in each slice was determined using ImageQuant software and transferred to an Excel file to generate the “lane scans”. The ten partitioned rectangles for the ten lanes were selected, grouped, and copied onto the TIFF images of the L1 and satellite DNA probed autoradiograms. At 8 h and 24 h of repair, it is apparent that the relative repair rates are Alu-probed signal > L1-probed signal > Satellite-probed signal.

Southern blots of the mouse cells’ repair (Fig. 7) and scans of these blots (Fig. 8) revealed the same repair rate trends as were demonstrated by human fibroblasts but with a murine global repair rate about half that of the human fibroblasts. The B2-probed “R-band” DNA repaired faster than did the L1-probed “G-band” DNA. The B2-probed DNA but not the L1-probed DNA had a rapidly repaired component that was noticeable in the 16 and 24 h mobility profiles (Fig. 7). Before repair, the mouse major satellite-probed DNA mobility profile showed a higher  $M_r$  than did the B2- or L1-probed profiles (Fig. 7), and did not fit a Kuhn distribution (data not shown). There are few-

er (52) dipyrimidines than expected by chance (116) along the 234-bp subunit of the *Mus musculus* major satellite and these are asymmetrically disposed, 31 along one strand and 21 along the other. Consequently, we expected a low density of induced CPDs and a non-random mass distribution for the satellite-probed signal.

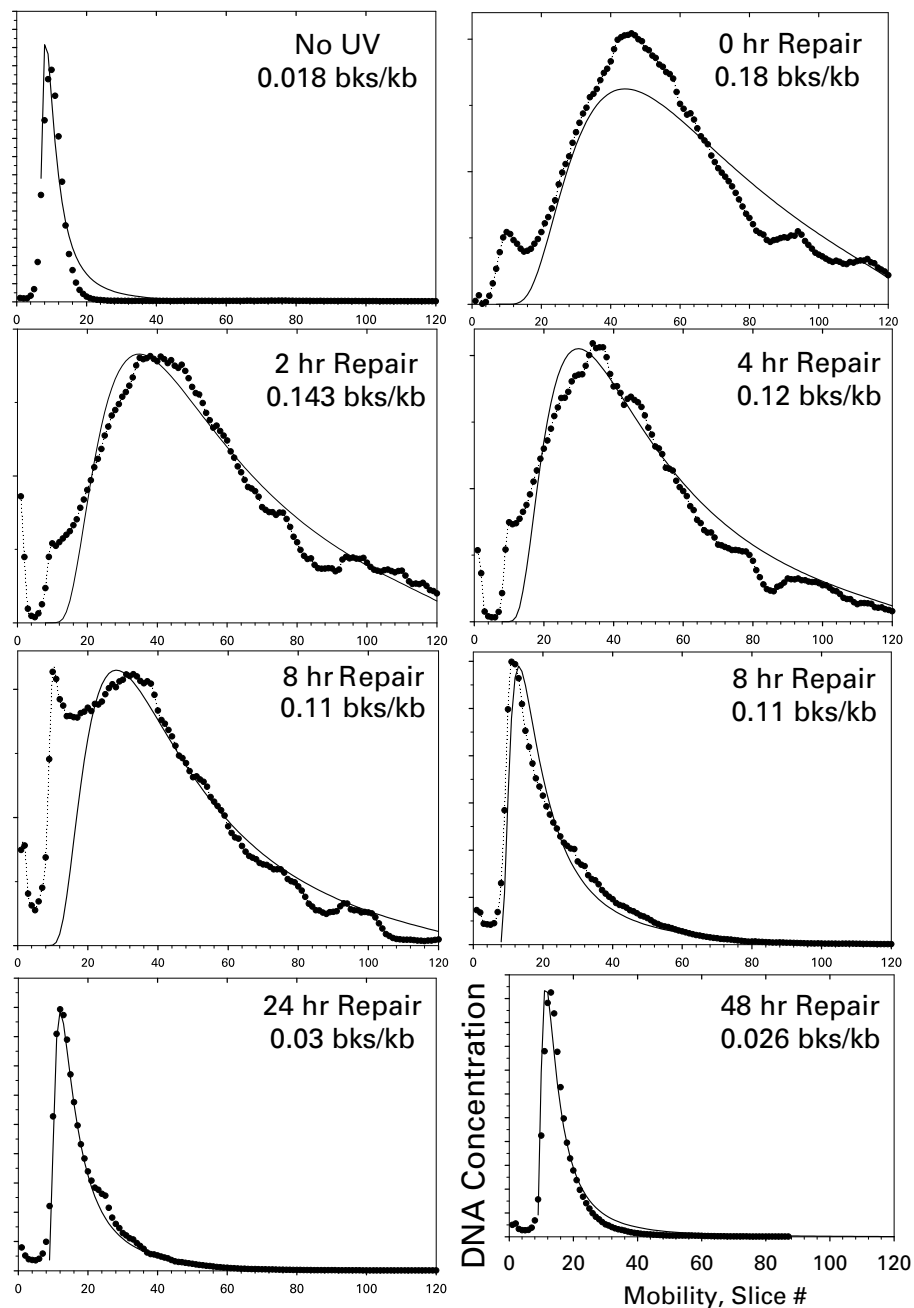


**Fig. 4.** Random cleavage weight distributions (solid lines) fitted to the mobility of experimentally determined Alu-probed signal (filled circles). The mobility (slice #) of the  $M_r$  standards (horizontal lines connecting  $M_r$  bands of the left and right  $M_r$  standard lanes in Fig. 2) were determined for each lane. Parameters for a logistic mobility function as in Fig. 1B were fitted by non-linear regression for each lane using Sigma Plot regression wizard software. From each lane's mobility function, the  $M_r$  of the upper and lower boundaries of each slice was determined. From these  $M_r$  values, the mass fraction of DNA expected in the slice was calculated as in Fig. 1A.  $P$  (breaks/kb) was varied manually until a best fit was obtained between data and the mass fraction calculations.

## Discussion

The three major chromosome compartments, R-bands, G-bands, and C-bands, respectively, show CPD repair rates which vary from faster to slower in that stated order for all three compartments (Fig. 3) and for R- and G-band murine compartments (Fig. 8). The Alu-probed human R-band DNA has two distinct repair rate components, with the slower repaired component of R-band DNA being repaired slightly faster than G-band DNA (Fig. 3).

In the human and murine cells, the distribution of UVC-induced CPDs showed no noticeable difference between R-band DNA and G-band DNA (Figs. 3 and 8; 0 h repair). Although R-band DNA is located in the interior of nuclei and G-band DNA is usually near the nuclear membrane (Cremer et al., 2000) where it could act as a bodyguard (Hsu, 1975) against UV damage, a differential CPD induction response was not seen. Kantor and Deiss-Tolbert (1995) showed that several 50- to 80-kb regions have quite different CPD densities immediately after UV irradiation and this is not inconsistent with our data. Their small sampling suggested that GC-rich isochores

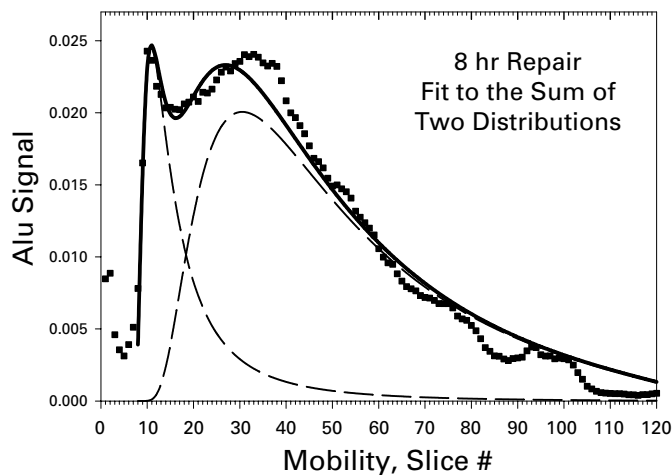


**Fig. 5.** The Alu-probed 8 h repair data (filled squares) from Fig. 4 were fitted to the sum (thick line) of two random cleavage weight distributions (dashed lines). These two component distributions had P values of 0.12 breaks/kb and of 0.029 breaks/kb, respectively, and correspond to the slowly repaired (77.5% of total) and rapidly repaired (22.5% of total) kinetic components, respectively.

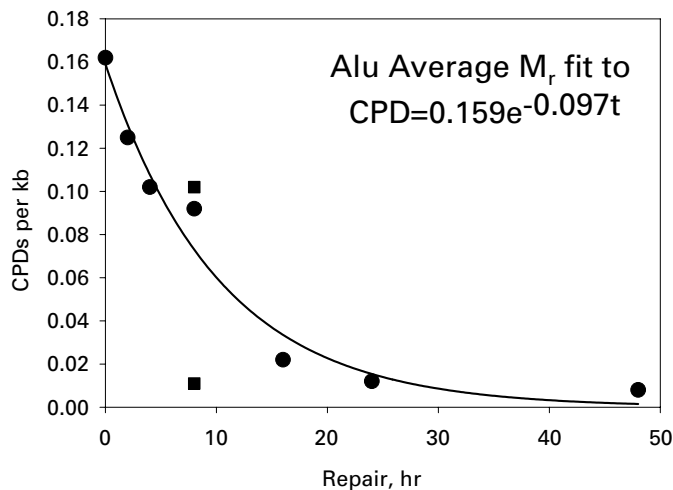


**Fig. 6.** Global repair rate of R-band DNA. P values in breaks/kb from Fig. 4 (filled circles) and Fig. 5 (filled squares) in the 8 h data) were used. The P value of DNA from non-irradiated cells, 0.018 breaks/kb, was subtracted from each P value from irradiated cells to determine the additional breaks attributable to UV irradiation followed by T4-pdg digestion. Global repair follows the first-order kinetics shown wherein CPDs in R-bands disappear with a half-life of about 7 h.

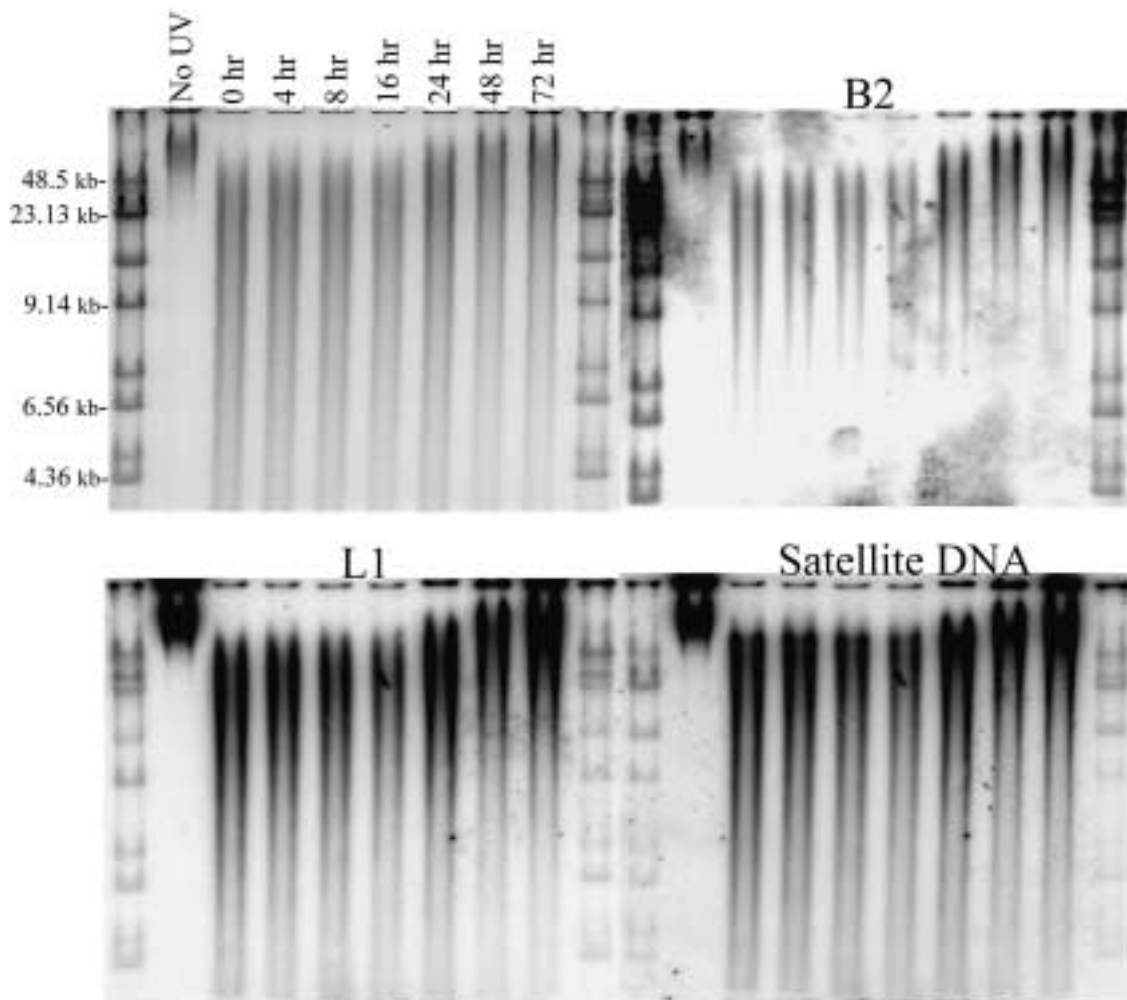


**Fig. 7.** A CPD repair panel from 10 J/m<sup>2</sup> UVC-irradiated murine fibroblasts was prepared as in Fig. 2. A murine B2 repeat was used to probe R-band DNA. The blots were reprobbed with murine L1 and *M. musculus* major satellite DNA.

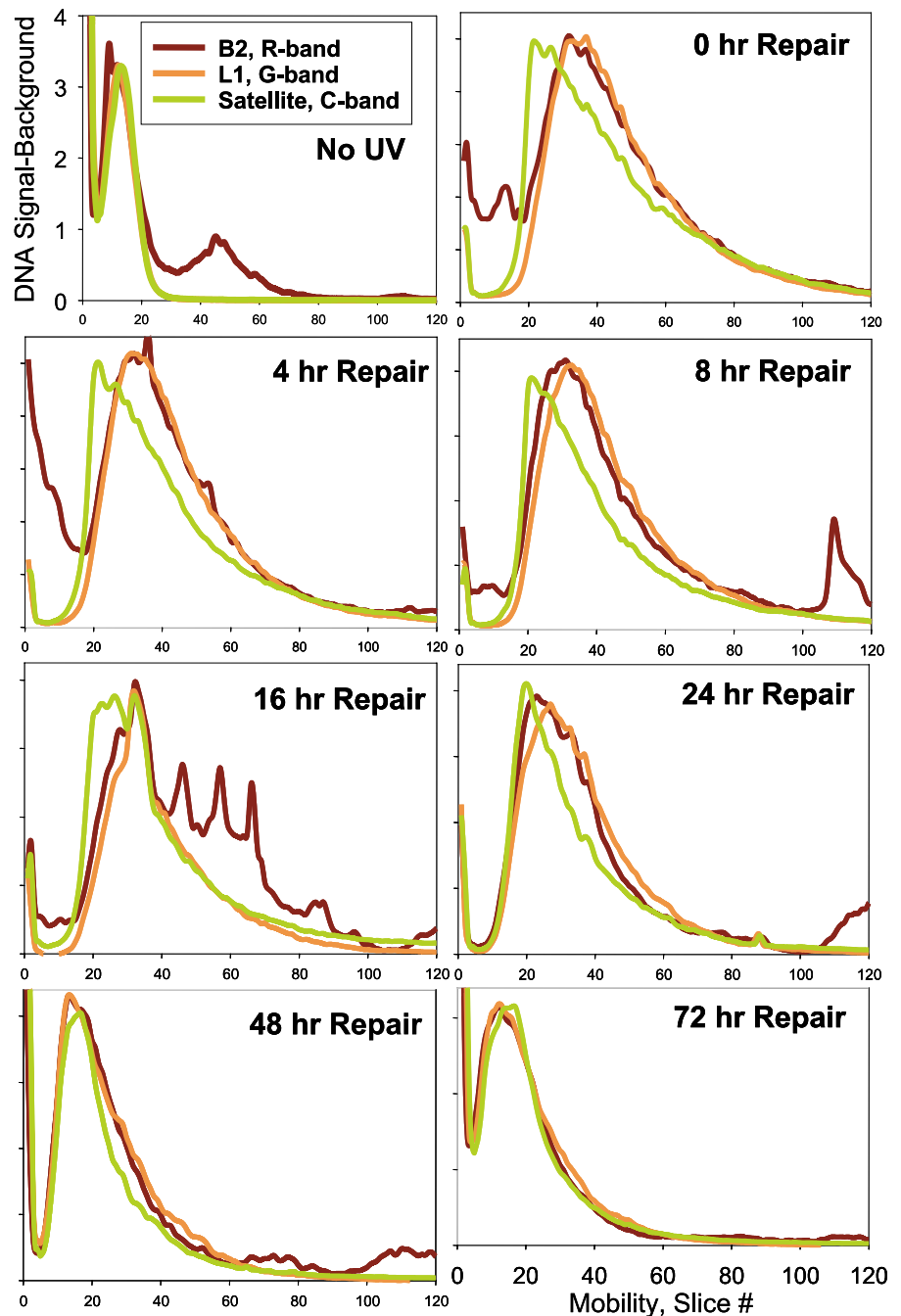


**Fig. 8.** Quantified “lane scans” from the three murine autoradiograms in Fig. 7. Before repair (0 h repair) the satellite probed DNA (filled squares) is less UV damaged than is the B2 or L1-probed DNA due to a low dipyrimidine density in the satellite sequence. After 16 h of repair, a rapidly repaired high  $M_r$  component is apparent as a slow mobility shoulder in the B2 probed DNA relative to the L1 probed DNA.

(R-bands) may be more prone to CPD formation than are AT-rich isochores (G-bands; cf. Kantor and Deiss-Tolbert, 1995). On sampling the entire R- and G-band genome, we find (Fig. 3; 0 h repair) that there is no significant difference between the UVC-induced CPD frequency distributions in Alu- or B1-probed (R-band) DNA vs. L1-probed (G-band) DNA.

Kantor and Deiss-Tolbert (1995) reported that immediately after irradiating human fibroblasts with  $20 \text{ J/m}^2$  of UVC, about 5% of the DNA remains as 50- to 80-kb DNA fragments resistant to T4-pdg (Kantor and Deiss-Tolbert, 1995) that might reflect radiation resistant DNA islands. We also see about 5%

of the DNA from irradiated, 0 h repair, fibroblasts migrating at 50 kb (slice 15 for 0 h repair in Figs. 3 and 4). The proportion of genomic DNA in this low mobility shoulder is the same for all three probed chromosome compartments (Fig. 3) and is not specific to GC-rich isochore DNA (R-band DNA) as previously suggested (Kantor and Deiss-Tolbert, 1995). In previous reports, this shoulder was either absent or apparent as an extremely faint shoulder (Ye et al., 1999; Fig. 2; 0 h repair lanes, +QM and -QM, respectively). The variability of this resistant fraction and its probe independence suggest that this shoulder may be an artifact.

The rapidly repaired R-band component distinguished in Fig. 5 corresponds to about 17% of the Alu-probed signal. The high  $M_r$  signal seen in the 0 h repair panel in Fig. 3 was subtracted from that in Fig. 5 to obtain this number. Since R-band DNA corresponds to about 45% of the genome, this would imply that 7.6% of genomic DNA is in the rapidly repaired R-band fraction. This rapidly repaired fraction is consistent with transcription-coupled repair of transcribed genes and was shown to occur primarily in the subset of R-bands called T-bands (Surralles et al., 2002). In XPC cells, Tolbert and Kantor (1996) showed that repair around the ca. 20-kb p53 gene is limited to the transcribed strand and extends outside the gene to include a domain of about 50 kb. Similar results were obtained for the actin gene cluster (Barsalou et al., 1994; Shanower and Kantor, 1997). Given this evidence that transcription-coupled repair extends to either side of active genes, then 50 kb of transcribed strand per active gene multiplied by 20,000 active genes equals 1/6<sup>th</sup> of the mass of the human genome, or 16%, as showing rapid transcription coupled repair. This is consistent with the magnitude of our rapidly repaired fraction (Fig. 5) as well as the data of Kantor et al. (1990) that 15% of the genome of XPC fibroblasts incorporates 50% of the genome's UVC-dependent unscheduled DNA synthesis after 24 h of repair.

By eliminating the rapidly (TCR) repaired component from the Alu-probed signal, we could measure the global genomic repair (GGR) of the Alu-probed DNA. The Alu-probed distributions fit random distributions quite well throughout the entire repair process. Since there is a great sequence context effect upon CPD repair rate at individual nucleotide positions (Ye et al., 1999), the maintenance of a random CPD distribution throughout repair was not expected. The number average molecular weights  $M_n$ , as estimated from fitting Kuhn's random distributions in Fig. 4, increase with repair time. As determined by Kuhn "P" values, the calculated rate of the disappear-

ance of CPDs fits first order kinetics and has a half-life of 7 h (Fig. 6). After 20 J/m<sup>2</sup> of UVC, the CPD concentration in the cell is lower than the apparent  $K_m$  of nucleotide excision repair so one would expect first order kinetics for CPD disappearance (Ye et al., 1999). The rate constant for global NER of CPD in confluent fibroblasts was determined as  $\ln 2/t_{1/2} = 0.099021 \text{ h}^{-1}$ . This measurement required that  $M_n$  be determined as it varied by ten fold and often with a majority of the DNA molecules in a sample being outside the range of our standard  $M_r$  markers. For example, half of the 24 h repair sample in Fig. 4 migrates less than does the full-length lambda 48.5-kb  $M_r$  marker. Accurate kinetic measurements were accomplished using alkaline elution (Kaufmann and Wilson, 1990) but this was limited to (6-4) photoproduct repair during the first 10 min after irradiation. Previously, phrases such as "74% repair in 18 h" have been used to describe repair rates. Using our analysis method, standard alkaline agarose gel electrophoresis suffices to yield one number which is a rate constant that accurately describes the global CPD repair capacity of R-band DNA in a population of cultured mammalian cells at every instant after acute irradiation.

*Mus spretus* × *M. castaneus* F<sub>1</sub> neonatal skin fibroblasts after crisis in culture show global CPD repair rates which, while only about half that of humans, are not approximately zero as previously reported for other mouse cells. It is possible that the common inbred rodent models that are highly susceptible to mutagen-induced tumors are uncharacteristic of most rodents in that they show compromised global NER.

## Acknowledgements

We thank Steven Lloyd for the T4-pdg glycosylase, Terry Ashley for the murine B2 and L1 plasmids, Walter Tsark for the murine interspecies hybrid, and Ning Ye for her continuous assistance with the experiments.

## References

- Ausubel FM, Brent R, Kingston RE, Moore DD, Seidman JG, Smith JA, Stuart S: Current Protocols in Molecular Biology (John Wiley & Sons, New York 1997).
- Barsalou LS, Kantor GJ, Deiss DM, Hall CE: DNA repair in the genomic region containing the beta-actin gene in xeroderma pigmentosum complementation group C and normal human cells. *Mutat Res* 315:43–54 (1994).
- Bernardi G: Misunderstandings about isochores. Part I. *Gene* 276:3–13 (2001).
- Bohr VA, Okumoto DS, Hanawalt PC: Survival of UV-irradiated mammalian cells correlates with efficient DNA repair in an essential gene. *Proc natl Acad Sci, USA* 83:3830–3833 (1986).
- Boyle AL, Ballard SG, Ward DC: Differential distribution of long and short interspersed element sequences in the mouse genome: Chromosome karyotyping by fluorescence in situ hybridization. *Proc natl Acad Sci, USA* 87:7757–7761 (1990).
- Cremer T, Kreth G, Koester H, Fink RH, Heintzmann R, Cremer M, Solovei I, Zink D, Cremer C: Chromosome territories, interchromatin domain compartment, and nuclear matrix: an integrated view of the functional nuclear architecture 40. *Crit Rev eukaryot Gene Expr* 10:179–212 (2000).
- Deiningner PL, Daniels GR: The recent evolution of mammalian repetitive DNA elements. *Trends Genet* 2:76–80 (1986).
- Drouin R, Gao S, Holmquist GP: Agarose gel electrophoresis for DNA damage analysis, in Pfeifer GP (ed): Technologies for detection of DNA damage and mutations, pp 37–43 (Plenum Press, New York 1996).
- Dutrillaux B: Nouveau systeme de marquage chromosomique: Les bandes T. *Chromosoma* 41:395–402 (1973).
- Goldman MA, Holmquist GP, Gray MC, Caston LA, Nag A: Replication timing of mammalian genes and middle repetitive sequences. *Science* 224:686–692 (1984).
- Hamer DH, Thomas CA Jr: The cleavage of *Drosophila melanogaster* DAN by restriction endonucleases. *Chromosoma* 49:243–267 (1975).
- Hanawalt PC: Selective DNA repair in expressed genes in mammalian cells: Mutation and the Environment, pp 21–222 (Wiley-Liss, New York 1990).
- Holmquist GP: Role of replication time in the control of tissue-specific gene expression. *Am J hum Genet* 40:151–173 (1987).
- Holmquist GP: DNA sequences in G-bands and R-bands, in Adolph KW (ed): Chromosomes and Chromatin, pp 76–121 (CRC Press, Boca Raton 1988).
- Holmquist GP: Evolution of chromosome bands: molecular ecology of noncoding DNA. *J molec Evol* 28:469–486 (1989).
- Holmquist GP: Chromosome bands, their chromatin flavors, and their functional features. *Am J hum Genet* 51:17–37 (1992).
- Holmquist GP, Caston LA: Replication time of interspersed repetitive sequences. *Biochim biophys Acta* 868:164–177 (1986).
- Holmquist GP, Filipiski J: Organization of mutations along the genome: a prime determinant of genome evolution. *Trends Ecol Evol* 9:65–69 (1994).
- Holmquist GP, Gao S: Somatic mutation theory, high resolution DNA repair kinetics, and the molecular epidemiology of p53 mutations. *Mutat Res* 386:69–101 (1997).
- Hsu TC: A possible function of constitutive heterochromatin: the bodyguard hypothesis. *Genetics* 79: 137–150 (1975).

- Kantor GJ, Deiss-Tolbert DM: Identification of a large genomic region in UV-irradiated human cells which has fewer cyclobutane pyrimidine dimers than most genomic regions. *Photochem Photobiol* 62:263–270 (1995).
- Kantor GJ, Barsalou LS, Hanawalt PC: Selective repair of specific chromatin domains in UV-irradiated cells from xeroderma pigmentosum complementation group C. *Mutat Res* 235:171–180 (1990).
- Kaufmann WK, Wilson SJ: DNA repair endonuclease activity during synchronous growth of diploid human fibroblasts. *Mutat Res* 236:107–117 (1990).
- Korenberg JR, Rykowski MC: Human genome organization: Alu, Lines, and the molecular structure of metaphase chromosome bands. *Cell* 53:391–400 (1988).
- Kuhn W: Kinetics of the destruction of high-molecular chains. *Berichte der Deutschen Chemischen Gesellschaft* 63B:1503–1508 (1930).
- Manuelidis L: Repeated DNA sequences and nuclear structure. Dover GA, Flavel R (eds.): *Genome Evolution*, pp 263–285 (Academic Press, New York 1982).
- Manuelidis L, Ward DC: Chromosomal and nuclear distribution of the 1.9-kb human DNA repeat segment. *Chromosoma* 91:28–38 (1984).
- Mellon I, Spivak G, Hanawalt PC: Selective removal of transcription-blocking DNA damage from the transcribed strand of the mammalian DHFR gene. *Cell* 51:241–249 (1987).
- Mitchell DL, Greinert R, de Gruijl FR, Guikers KL, Breitbart EW, Byrom M, Gallmeier MM, Lowery MG, Volkmer B: Effects of chronic low-dose ultraviolet B radiation on DNA damage and repair in mouse skin. *Cancer Res* 59:2875–2884 (1999).
- Mullenders LHF, Vrieling H, Venema J, van Zeeland AA: Hierarchies of DNA repair in mammalian cells: biological consequences. *Mutat Res* 250:223–228 (1991).
- Musio A, Mariani T, Vezzoni P, Frattini A: Heterogeneous gene distribution reflects human genome complexity as detected at the cytogenetic level. *Cancer Genet Cytogenet* 134:168–171 (2002).
- Peleg L, Raz E, Ben-Ishai R: Changing capacity for DNA excision repair in mouse embryonic cells in vitro. *Expl Cell Res* 104:301–307 (1977).
- Peterson RC: Prediction of the frequencies of restriction endonuclease recognition sequences using di- and mononucleotide frequencies. *Biotechniques* 6:34–44 (2000).
- Pfeifer GP, Drouin R, Riggs AD, Holmquist GP: Binding of transcription factors creates hot spots for UV photoproducts in vivo. *Mol cell Biol* 12:1798–1804 (1992).
- Rodriguez H, Valentine MR, Holmquist GP, Akman SA, Termini J: Mapping of peroxy radical induced damage on genomic DNA. *Biochemistry* 38:16578–16588 (1999).
- Ruven HJ, Berg RJ, Seelen CM, Dekkers JA, Lohman PH, Mullenders LH, van Zeeland AA: Ultraviolet-induced cyclobutane pyrimidine dimers are selectively removed from transcriptionally active genes in the epidermis of the hairless mouse. *Cancer Res* 53:1642–1645 (1993).
- Saccone S, Federico C, Solovei I, Croquette MF, Della VG, Bernardi G: Identification of the gene-richest bands in human prometaphase chromosomes. *Chromosome Res* 7:379–386 (1999).
- Shanower GA, Kantor GJ: A difference in the pattern of repair in a large genomic region in UV-irradiated normal human and Cockayne syndrome cells. *Mutat Res* 385:127–137 (1997).
- Singer MF: SINES and LINES: Highly repeated short and long interspersed sequences in mammalian genomes. *Cell* 28:433–434 (1982).
- Smit AF: Interspersed repeats and other mementos of transposable elements in mammalian genomes. *Curr Opin Genet Dev* 9:657–663 (1999).
- Soriano P, Meunier-Rotival M, Bernardi G: The distribution of interspersed repeats is nonuniform and conserved in the mouse and human genomes. *Proc natl Acad Sci, USA* 80:1816–1820 (1983).
- Spivak G, Hanawalt PC: Fine structure mapping of DNA repair within a 100 kb genomic region in Chinese hamster ovary cells. *Mutat Res* 350:207–216 (1996).
- Surrallés J, Ramirez MJ, Marcos R, Natarajan AT, Mullenders LH: Clusters of transcription-coupled repair in the human genome. *Proc natl Acad Sci, USA* 99:10571–10574 (2002).
- Tanford C: *Physical Chemistry of Macromolecules* (John Wiley & Sons, New York 1961).
- Tang JY, Hwang BJ, Ford JM, Hanawalt PC, Chu G: Xeroderma Pigmentosum p48 gene enhances global genomic repair and suppresses UV-induced mutagenesis. *Mol Cell* 5:737–744 (2000).
- Tolbert DM, Kantor GJ: Definition of a DNA repair domain in the genomic region containing the human p53 gene. *Cancer Res* 56:3324–3330 (1996).
- Tornaletti S, Pfeifer GP: Ligation-mediated PCR for analysis of UV damage, in Pfeifer GP (ed): *Technologies for Detection of DNA Damage and Mutations*, pp 199–210 (Plenum Press, New York 1996).
- van Hoffen A, Natarajan AT, Mayne LV, van Zeeland AA, Mullenders LHF, Venema J: Deficient repair of the transcribed strand of active genes in Cockayne's syndrome cells. *Nucleic Acids Res* 21:5890–5895 (1993).
- Venema J, van Hoffen A, Karcagi V, Natarajan AT, van Zeeland AA, Mullenders LHF: Xeroderma pigmentosum complementation group C cells remove pyrimidine dimers selectively from the transcribed strand of active genes. *Mol cell Biol* 11:4128–4134 (1991).
- Willis CE, Willis DG, Holmquist GP: An equation for DNA electrophoretic mobility. *Applied Theoret Electrophoresis* 1:11–18 (1988).
- Wu JC, Manuelidis L: Sequence definition and organization of a human repeated DNA. *J molec Biol* 142:363–386 (1980).
- Ye N, Holmquist GP, O'Connor TR: Heterogeneous repair of N-methylpurines at the nucleotide level in normal human cells. *J molec Biol* 284:269–285 (1998).
- Ye N, Bianchi MS, Bianchi NO, Holmquist GP: Adaptive enhancement and kinetics of nucleotide excision repair in humans. *Mutat Res* 435:43–61 (1999).
- Zhu Q, Wani MA, El-mahdy M, Wani AA: Decreased DNA repair efficiency by loss or disruption of p53 function preferentially affects removal of cyclobutane pyrimidine dimers from non-transcribed strand and slow repair sites in transcribed strand. *J biol Chem* 275:11492–11497 (2000).
- Zolan ME, Cortopassi GA, Smith CA, Hanawalt PC: Deficient repair of chemical adducts in alpha DNA of monkey cells. *Cell* 28:613–619 (1982).

# On the nature of visible chromosomal gaps and breaks

J.R.K. Savage

Reading (UK)

**Abstract.** From the earliest days of chromosomal aberration studies, the distinction, nature and origin of light-microscope observed “gaps” and “breaks” have been topics for debate and controversy. In this paper we survey, briefly, the various ideas that have appeared in the very extensive literature, and attempt

to evaluate them in the light of our current understanding of chromosome structure and aberration formation. Attention is drawn to the problems of interpretation caused by G<sub>2</sub>/S cell imprecision.

Copyright © 2003 S. Karger AG, Basel

It is not an exaggeration to say that the nature of light-microscope-observed achromatic lesions (“gaps”, AL) and of “breaks” (*terminal deletions*), and the distinction between them, form the longest running controversy in the field of aberration cytogenetics.

Although these aberrations were recognised and described from the beginning of work with ionizing radiation effects (Sax, 1938) it was Stanley Revell who first stressed the importance of the distinction between the two types when presenting his “Exchange theory”, (Revell, 1955, 1959), the first serious challenge to the Sax/Lea “Breakage-and-Reunion” theory (B&R) (Sax, 1940, 1941; Lea, 1946) for the origin of chromosomal structural change (reviewed in Evans, 1962; Revell, 1974; Savage, 1989, 1998).

This distinction is now universally applied (perhaps better, attempted) in all critical work, and has had the general effect of making unambiguous breaks much rarer than early workers supposed. However, the reality and nature of the difference is still unclear, in spite of an enormous literature on this topic.

Both AL and breaks are now known to be produced in chromosomes by an extremely wide range of agents in addition to radiation. In the following discussion, attention will be focussed on *chromatid-type* aberrations, since this is predominantly the area covered in most experimental work. AL and true *terminal deletions* are relatively rare for primary *chromosome-type* aberrations.

We will look at some aspects of the problem in the light of our current understanding of aberration formation, and highlight some of the pitfalls that preclude simple answers.

### Working definitions

Before proceeding, it is necessary to define certain terms that will be used in the discussion.

*Primary break* (Lea, 1946. Basis of the Lea/Sax B&R theory)

A complete severance of the chromatid “backbone” or “Chromonema”, leaving open break-ends capable of restituting (re-forming the original sequence), illegitimate rejoining (fusing pairwise with foreign ends to form structural exchanges) or remaining open to appear at metaphase as “breaks” (*terminal deletions*). It is implicit in the B&R theory that “breaks” visible at metaphase are the residue of primary breaks that have neither restituted nor rejoined, i.e. we are viewing the potential progenitors of exchange aberrations.

I would like to dedicate this paper to Prof. Günter Obe upon his retirement, not only because of the enormous contribution he has made to the understanding of chromosomal aberrations, but personally, for his friendship, stimulus and encouragement over many years.

Received 18 August 2003; accepted 20 November 2003.

Request reprints from: Dr. John R.K. Savage  
34 City Road, Tilehurst, Reading RG31 5HB (UK)  
telephone: +44 118 9428159; e-mail: johnsavage@ekpempo.fsnet.co.uk.

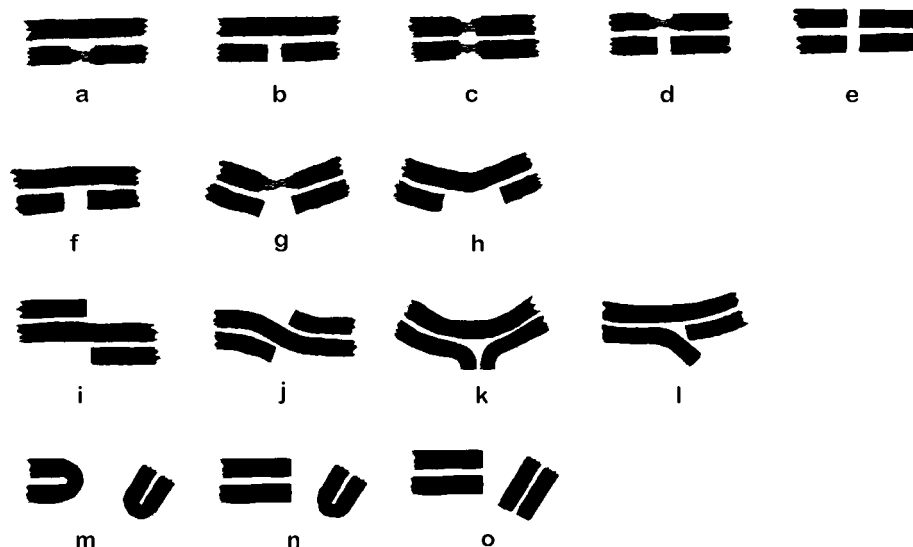


**Fig. 1.** The gap-break continuum. (a) Unilocus constriction; (b) unilocus gap; (c) isolocus constriction; (d) constriction/gap; (e) isolocus gap; (f-h) examples of aligned unilocus breaks; (i-l) examples of dislocated unilocus breaks; (m) isolocus break with complete sister-union (SU); (n) isolocus break with incomplete sister-union (Nup or Nud); (o) isolocus break with no sister-union (Nupd), or a *chromosome-type terminal deletion*. Terminology based on Brøgger (1971) and Savage (1976).

### Discontinuity

Although it is a legitimate term for any break in thread integrity, in the context of our topic, it is strictly a technical term, chosen to distinguish those visible breaks that are the result of structurally incomplete *intra-arm intrachanges*, from those that are simply the result of failed restitution or rejoining of primary breaks (Revell, 1959, 1963). According to Exchange theory, all visible breaks are discontinuities, and therefore, secondary. Unfortunately, the term is seldom used critically in the literature.

### Achromatic Lesion (occasionally, “Achromatic Region”) or “gap”

An unexpected, unstained region, or segment, in the solid-stained chromatid which does not impair its integrity. “Unexpected” since some chromosomes, constitutionally, have quite large secondary constrictions that fulfil the criteria for gaps. With the light microscope (LM), some show various degrees of material linking the gap ends, others are devoid of any visible link.

The term “gap” refers to the visual non-staining nature of the region, and does not imply that chromatin is absent. In retrospect, Revell (1974) regretted introducing this misleading term, but its now universal usage cannot be rescinded.

### Exchange Cycles

Sachs et al. (1999) have introduced a terminology for defining the participation of “break-ends” in the exchange process as cycles of different orders. Thus, the simplest exchange between two chromosomes, a 4-end pairwise interaction, is an exchange cycle of order 2 (or c2, Cornforth, 2001). Complex exchanges from the 6 ends of 3 breaks are c3, 8 ends, c4 and so on. Restitution as defined in the B&R theory becomes c1.

### The gap-break continuum

As mentioned above, both AL and breaks can be produced by a very wide variety of agents in all kinds of cells, plant and animal. They also occur “spontaneously” at a low level.

When scoring, there is found to be a continuous range from a partial attenuation of a chromatid to an apparent complete separation of an acentric fragment. Figure 1 diagrams the principal LM types, the nomenclature used based upon the careful researches of Brøgger (1971a, b) and Revell (1959).

Constrictions (Fig. 1a, c, d, g) vary enormously in size and clarity, and are influenced by preparative methods. They tend to be most frequent in G<sub>2</sub> cells that were close to division at the time of S-independent agent treatments. In older literature, they are often referred to as “sub-chromatid” events. With care, the constriction/gap (Fig. 1d), where both sister chromatids are involved at similar loci, is seen to be quite common, particularly when electron microscopy (EM) is employed (Brinkley and Hittelman, 1975).

Sister chromatid adhesion in G<sub>2</sub> cells, resulting from chromatin inter-strands, is normally very strong, (unless prolonged spindle inhibition has been used) so that the segments each side of a gap tend to remain in alignment (Fig. 1a–e). This means that the transition from gap to break is frequently ambivalent and subjective (Fig. 1f). To overcome this, some resort to a size criterion – non-staining regions larger than the width of a chromatid be counted as breaks. Interestingly, the presence of a unilocus gap seems to have very little influence on the relative lengths of the two sister chromatids (Scheid and Traut, 1973).

Isolocus gaps (Fig. 1e) are generally less frequent than unilocus ones for most treatments, but the relative frequencies may be species dependent, for in *Schistocerca*, this type predominates throughout G<sub>2</sub> (Fox, 1967a).

However, by far the most popular criterion for separating breaks from gaps is that of non-alignment, or dislocation of the two segments. Such dislocation can take many forms (examples, Figure 1i–l).



Figure 1m is a typical *chromatid-type isolocus break*, or *isochromatid deletion* with complete sister union (SU). The union may be incomplete proximal to, or distal to the centromere (Fig. 1n). Figure 1o is a typical *chromosome-type break*, lacking any sister union between ends (although its presence in cells from G<sub>2</sub> at the time of treatment might indicate a doubly incomplete *isochromatid deletion* (Nupd)). In either case, this category is rare in most cell types, recently confirmed for *chromosome-type terminal deletions* by FISH telomeric probing (Boei et al., 2000).

The ultimate test for gap-break distinction, as suggested by Revell is; "Does it lead to an acentric fragment at ana-telophase?". Unfortunately, this can only be investigated in plant cells, where there are few chromosomes, and a spindle inhibitor is not required. Where this has been checked, almost always true breaks are lower at anaphase than metaphase scores predict. Also, unambiguous gaps can readily be seen in anaphase chromatids. However, even this anaphase test is not foolproof, firstly because acentric fragments are not always excluded from the interphase nucleus (Savage, 1988), and secondly, chromosomes are capable of enormous stretching without physical disruption. In plant material, it is not unusual to find bridges between daughter cells, presumed to have ruptured at ana-telophase, reforming at subsequent mitosis.

Whilst on the subject of gap-break distinction, we have also to remember that the slide-making processes normally used are extremely disruptive, designed to achieve maximum spreading and separation of the individual chromosomes, so that mechanical conversion of some gaps to apparent breaks must occur in a proportion of instances.

### The nature of Achromatic Lesions ("gaps")

On the basis of anaphase analysis, most people have accepted that gaps and breaks are distinct aberrations, and should be separated for scoring and analysis. Over the years, there has been much speculation on the nature of gaps versus breaks. The literature is enormous, and I can give here only a few salient references in addition to those already cited: Bender et al., 1974; Brecher, 1977; Brøgger, 1975, 1982; Brinkley and Shaw, 1970; Bucton and Evans, 1973; Chaudhuri, 1972; Comings, 1974; Conger, 1967; Dimitrov, 1981; Evans, 1963, 1967, 1977; Fisher et al., 1974; Harvey and Savage, 1997; Harvey et al., 1997; Heddle and Bodycote, 1970; Heddle et al., 1969a, b; Hittelman and Rao, 1974a, b; IAEA, 1966; Kihlman, 1971; Lazányi, 1968; Lubs and Samuelson, 1967; Migeon and Merz, 1964; Parshad et al., 1985; Savage, 1968; Savage and Harvey, 1991, 1994; Scheid and Traut, 1970, 1971a, b, c; Scott and Evans, 1967; Sturelid, 1971; Wolff and Bodycote, 1975.

Reviewing such work, the principal suggestions that have emerged are as follows:

Primary breaks that have failed to release the acentric fragment. Surviving examples of primary breaks.

Mis-repair of primary breaks or partial failure of restitution.

Sites of restitution.

Sites of unrepaired single-strand DNA breaks (SSB).

Sites of unrepaired double-strand DNA breaks (DSB).

Actual loss of chromatin.

Points of incomplete DNA synthesis.

Sites of very small *intrachanges*.

Errors in the processes of chromosome condensation/packing, "folding defects".

Predominantly technical artefacts.

The first eight suggestions concern the nature of the originating lesions, only the last two refer to the nature of the gap itself.

In making judgement, the following facts are pertinent with respect to *chromatid-type* gaps resulting from treatment with S-independent agents. Although a few are always found spontaneously, their frequency is markedly enhanced in G<sub>2</sub> cells (usually to a level very much higher than that of other structural changes) by all aberration-inducing agents. They are maximal, usually with a very sharp peak, in G<sub>2</sub> cells that were close to mitosis (i.e. in early post-treatment sample times) at the time of treatment.

For low- and intermediate-LET ionizing radiations, the height of the peak is dose dependent, and the fall either side is rapid. Cells in the very earliest sample times have very low levels, as do cells in sample times a few hours after the peak.

Very high-LET radiations like alpha particles produce low gap frequencies, and may lack a clear peak (Griffin et al., 1994), which probably reflects the very small amount of chromatin within the nucleus which actually "sees" any radiation.

Gaps show a typical radiation oxygen effect (Neary and Evans, 1958).

Treatment with S-dependent agents (alkylating agents, UV) also produces gaps, though detailed reports for this kind of aberration in the literature are rather sparse. However, as with other aberrations, gaps are generally absent from G<sub>2</sub> cells, unless the agent also interferes with chromosome condensation or morphology (Hittelman and Rao, 1974b).

Since alkylations and cross-links are formed at all stages of the cell cycle, this suggests that DNA damage per se is not necessarily a causative factor, but, as for other structural changes, damage processing is required. If PCC is used, however, in contrast to metaphase analysis, gaps can be detected immediately in G<sub>2</sub> cells after UV and alkylating agents (Brinkley and Hittelman, 1975; Hittelman and Rao, 1974a, b). Quantitative studies with S-dependent substances are made difficult not only because of the delayed appearance of aberrations, but also because of their longevity of action within the cell, leading to the continuous production of damage.

Restriction endonucleases, which produce defined double-strand breaks (DSB), are very efficient gap producers, and the short-lived ones show frequency peaks in late G<sub>2</sub> cells identical to those found with low-LET radiation (Natarajan and Obe, 1984; Harvey et al., 1997). Long-lived cutters show steady gap frequencies. Likewise, when UV behaves in an S-independent manner, as when *Tradescantia* generative cell nuclei are irradiated, gaps and breaks (together with chromosome shattering at higher doses) are the predominant aberrations in G<sub>2</sub> cells, presumably arising from the pyrimidine dimers, or their repair (Swanson, 1944; Kirby-Smith and Craig, 1957).

Finally, there are a number of agents, not directly damaging to DNA, but which interfere with metabolic processes like DNA and protein synthesis, and these are very efficient in producing gaps and breaks of all kinds, sometimes exclusive of other structural changes, e.g. mercaptoethanol (Brøgger, 1975) deoxyadenosine (Kihlman, 1966) and fluorodeoxyuridine (Bell and Wolff, 1964; Kihlman, 1971).

Gaps do not seem to have a lasting effect, for they do not re-appear nor lead to structural changes at subsequent divisions (Evans, 1966). This has been reported to be true also of breaks (Akif'ev et al., 1990). However, such follow-up studies are, logistically, very difficult, and more work is needed on this point both for gaps and especially for breaks.

All observed *chromatid-type* gaps fall into one of three groups:

(1) The isolated gaps of the sort illustrated in Figure 1.

(2) "Scar gaps": There are many varieties of chromatid *interchanges* (Evans, 1962) and quite often they are complex multi-lesion events (Savage and Harvey, 1994). A fairly substantial proportion are also seen to be structurally incomplete. Because of the strong sister chromatid adhesion, the presumptive regions of rejoining (often termed "break points", though in molecular terms this has no real meaning) can be located, and quite often an obvious gap is present at such rejoin sites, as a sort of "scar". This would suggest that either the torsional stresses introduced by the exchange have led to problems for chromatin packing/condensation, or that the exchange is more complicated than the usually assumed c2. Such "scars" also accompany *intrachanges*, and so will form a component of the isolated gaps of (1) above. Quite frequently, isolated gaps occur in pairs, fairly close but at clearly different loci on one, or both chromatids (illustrated in Revell, 1959). Such exchange-point "scars" are regularly seen in *isochromatid deletions* and one infers that other pairs must also mark *intra-change* sites.

(3) "Associated gaps": It is not unusual to find gaps in different chromosomes (in particular unilocus constrictions, Figure 1a) stuck together in pairs, often with the chromosomes showing torsional bending. These associations give the appearance of a partial, or an abortive exchange. Such figures are more frequent in early sample times after treatment, and were considered by early workers to be evidence for a binemic chromatid. From what we now know of chromosome architecture, they are probably true exchanges that have occurred at a late stage of chromosome condensation, and thus involve only a proportion of the already condensed fibres. They will be the metaphase equivalent of "sub-chromatid" exchanges, normally detected as "side-arm bridges" at anaphase (Kihlman, 1971).

Nevertheless, there are numerous reports from both LM and EM studies for bi-stranded continuity across gaps (Takayama, 1976; Scheid and Traut, 1970, 1971a; Fisher et al., 1974) and treatment of chromosomes with uncoiling agents like hyaluronidase (Iino, 1971) and trypsin (Wolff, 1969, 1970; Trosko and Wolff, 1965; Traut and Scheid, 1973,) often show clear bi-stranded chromatids. Whilst evidence for a uninemic chromatid is now overwhelming, one cannot rule out the possibility that some lateral segregations of chromatin may be involved during packing (Bahr and Larsen, 1974). It is well established

from DNA separation studies that the chromosome has a "near-side" and an "off-side" (Herrosos and Gianelli, 1967).

Because of the heterogeneity of causation, several authors have suggested that gaps be classified into two groups: Those which arise from DNA damage, and those where DNA damage is not required for initiation. Brøgger (1982) has termed these "Clastogenic gaps" and "Turbagenic gaps" respectively.

### The nature of breaks

If the distance between "ends" is large with no visible connection, and/or there is a clear dislocation between the segments, and it is judged that an acentric fragment is likely to be left behind at anaphase, the aberration is scored as a break, or *terminal deletion*. The subjectivity involved inevitably contributes to some of the numerical disagreements found between different laboratories.

Dislocation and chromatid contortion/flexure are fairly common and can take many forms (e.g. Fig. 1g, h, j-l). Very frequently, additional torsional bending is present, and the "broken" ends may not match up on mental re-assembly (Fig. 1h, k, l) and sometimes additional changes are present. Such discrepancies indicate, in most cases, that we are dealing with structurally incomplete *intra-arm intrachanges*, i.e. "discontinuities" and that more than one lesion has been involved in their formation (e.g. Fig. 1h, Revell Type 1a; Fig. 1k or l, Revell Type 1b, Revell, 1959; Savage, 1989). The isolocus forms (Fig. 1m, n, and in some cases Figure 1o) are also *chromatid-type intrachanges* (Revell Type 4 for G<sub>2</sub> cells, although there may be other modes of formation for cells treated in S phase, and for high-LET radiation induction, Savage, 1968; Savage et al., 1968; Revell, 1974).

Whilst some of these *intrachanges* will be simple c2, it is becoming increasingly clear that in many materials, and especially after exposure to high-LET radiations, alkylating agents or restriction endonucleases, complex *intrachanges*, >c3, are rather common. Fox (1967a) made a careful study of these in *Schistocerca* where they are particularly frequent even with low-LET radiation, and has produced diagrams of some types under the term "*insertion intrachanges*" (Savage, 1976).

There are, however, some chromatid breaks which appear quite ordinary, and not associated with any obvious exchange process (e.g. Fig. 1f, l). Are these simple un-rejoined primary breaks the unused residue of initial damage, or are they disguised incomplete *intra-arm intrachanges* (Revell Type-3), because primary breaks, as originally defined, do not exist? This is the heart of the B&R versus the Exchange theory controversy, mentioned above. They are very unlikely to be open-ended DNA DSB. Leaving aside the endonuclease vulnerability of such a situation, the bulk of the DNA in interphase is enwreathed with proteins precluding free flapping ends. Moreover, exposure of porated cells to restriction endonucleases, which introduce very high frequencies of DSB into the chromatin, does not produce the chromosome collapse or shattering that might be expected.

Recent work from irradiation of potentially BrdU-harlequin-stained chromosomes has thrown some interesting light on this controversy. According to original exchange theory, if all breaks are derived from *c2 intrachanges*, 40 % should show a sister-chromatid exchange – a colour-jump (*cj*) – at the site of breakage. Only 9–16 % is the general frequency found in various experiments, and this has led some to the conclusion of mixed origin, some discontinuities, some simple breaks (Wolff and Bodycote, 1975; Heddle and Bodycote, 1970; Comings, 1974).

Unfortunately, these *cj* experiments are not unequivocal. For one thing, it is easy to account for the observed low frequency by making plausible assumptions about the relative frequencies of *inter-* and *intra-chromatid intrachange* types (Savage and Harvey, 1991, 1994). On top of this is the fact that complex *intrachanges* abound, which undermines original numerical predictions.

However, what is of considerable interest is that within a given radiation experiment, the *cj* frequency is invariate with dose; whilst the absolute frequency of breaks increases, the proportion which are *cj* remains constant. This is unexpected, for, according to B&R theory, *intrachanges* have a curvilinear dose-response, whilst simple breaks should be strictly linear, leading to frequency divergence with increasing dose. Slightly higher *cj* frequencies together with constancy are found also for  $\alpha$ -particles (Griffin et al., 1994) and for restriction endonucleases (Harvey and Savage, 1997). Furthermore, and even more surprising, “spontaneous” breaks, from unirradiated control samples, show the same *cj* frequency as the treatment-produced ones!

These observations seem to suggest that, irrespective of initiator, all breaks arise by a common pathway or mechanism, which leads to a fixed proportion of them involving both sister chromatids, thus producing a *cj*.

Some gaps also show a *cj* (Heddle and Bodycote, 1970; Harvey and Savage, unpublished) with frequencies equal to, or less than, that for breaks in the same sample. These gaps could be “scars” from structurally complete Revell type-1 *intrachanges*.

Before leaving the *cj* experiments, one curious observation is worthy of note. BrdU treatment is known to sensitise chromatin to radiation damage in proportion to the amount incorporated in the DNA. Consequently, in a harlequin situation, one would expect more gaps and breaks in the doubly-substituted (BB) chromatid than in its sister (TB). Whilst this is demonstrable for those lesions taking part in *interchanges*, neither Wolff and Bodycote (1975) nor Savage and Harvey (1994) found any TT/BB differences for induced breaks in Chinese hamster cells (contra Jacob, 1979, in *Muntjak*). At present, there is no explanation for these observations, but it cautions against a too simplistic interpretation of “breaks”.

## Resolution

The vast majority of research has been done using the LM, and the categories illustrated in Figure 1 are decided at this level.

One has always to remember that at the height of the gap/break controversy, the assumed structure of the chromosome

was very different from that which we understand today, tending to be regarded essentially as a solid rod, condensed principally by coiling, the broken ends and rejoins of which could readily be seen.

It is obvious, however, from the currently accepted “folded-fibre” model, and its various modifications (Wolfe, 1965; DuPraw, 1966; Belmont and Bruce, 1994) and from the enormous lengths of DNA present in an individual chromosome, that the condensing and condensed chromosome is capable of unravelling and stretching for very long distances without loss of integrity. Even the basic 30-nm fibre, let alone the various lower diameter derivatives from it, is well below the best resolution of the LM so that any continuity maintained at this level would be quite invisible.

Resolution (R) is defined as “the minimum possible distance between two points for them to be seen as two points”.  $R = \lambda/2 \times \text{N.A.}$ , where R is the resolution in  $\mu\text{m}$ ,  $\lambda$  the wavelength of transmitted light in  $\mu\text{m}$ , and N.A. the numerical aperture of the objective. So, for the common set-up using a green filter giving 0.54- $\mu\text{m}$  light, and a N.A. of 1.3,  $R \approx 0.21 \mu\text{m}$ . Note that unless the condenser is also oiled, N.A. cannot exceed 1.0, so most people are working nearer  $R \approx 0.3 \mu\text{m}$ .

Several studies have attempted to overcome this resolution problem by examining gaps and breaks with the EM, using whole mount spreading or scanning methods (Brecher, 1977; Brinkley and Shaw, 1970; Brinkley and Hittelman, 1975; Brøgger, 1971a; Fisher et al., 1974; Scheid and Traut, 1970, 1971a). In some studies, direct comparison with the LM image has been made, using the same aberrations for both techniques. In the majority of cases examined, some degree of continuity has been found at these lower-order fibre levels for both aberrations classified as gaps and for those classified as breaks, even where dislocation was present. However, a few un-joined breaks are seen. One always has to remember, though, that the nature of the EM staining methods does not guarantee that any fibres seen necessarily contain DNA. Several fibrous proteins are associated with chromosome organization and contraction. Some reports also indicate that detection of continuity can be conditioned by the fixation method used (Brøgger, 1971a; Brinkley and Hittelman, 1975).

There is always a much lower density of fibres within the gap area, and those present are often seen to be parallel, or even bundled into two units. Such regions will be more susceptible to mechanical stress, and we need to bear in mind that scoring is normally done in preparations that have been subject to considerable disruption – squashing in plants, or air-drying in animal cells. This will exacerbate stretching and spatial distances prior to observation.

This resolution problem, then, makes it very difficult to be sure we have a real open-ended break, and blurs further the gap/break distinction at LM level.

## Imprecision

There is one factor, seldom taken into account, that has a profound effect on all quantitative work with gaps, breaks and *chromatid-type* aberrations in general, and that is “imprecision” (Savage and Papworth, 1973, 1991, 1994; Fox, 1967b; Gerber and Léonard, 1971).

All  $G_2$  cell systems, without exception, are characterised by sample time fluctuations in the frequency of the various aberration types. This is particularly noticeable for gaps, but to a lesser extent for breaks. The conspicuousness of the fluctuations is dose dependent, especially so for S-independent treatments. Such variations in sensitivity are not unexpected when one considers the chromatin changes that must occur following replication as the cell prepares for mitosis.

In any cycling population, individual  $G_2$  cells have wide differences in transit time (Engelberg, 1968) particularly in complex tissues like root meristems where much aberration work has been done (Miller and Kuehnert, 1972). This can readily be inferred from the ascending limb of FLM or FDM curves, and the fact that they rarely reach 100%. In cases where the actual ratio maximum/minimum  $G_2$  transit times have been measured, factors of 3–6 are quite normal for untreated, unperturbed populations. Once treatment has been given, mitotic delay and perturbation increase this range very significantly.

One immediate consequence of transit time variation is that cells seen together in metaphase will almost certainly have been at quite different developmental positions in  $G_2$  at the time of treatment. The range of positions represented enlarges dramatically as sample time increases, and is exacerbated if spindle inhibition to accumulate metaphases has been used. Given changing sensitivity with development, the observed aberration yield is determined by the mixture of cell positions present in the sample. Since mitotic delay and perturbation are dose dependent, it is obvious that different cell mixtures will be present for different doses at the same fixation time, which negates legitimate yield comparisons (Savage and Papworth, 1991).

I will comment, briefly, on the impact of imprecision in three areas pertinent to our present topic.

(1) Dose-response curves. When the aberration frequency varies with time of sampling, there can be no unique aberration frequency to set against dose, and therefore no fixed shape, or meaningful biophysical interpretation, for any dose-response curve. Faced with this problem, workers tend to use the peak yields, or average yield over the sample time range, or the integrated area under the yield-time curve. None of these are valid measures of sensitivity, for it is not possible to standardise the yield-determining cell mixtures for the sample times after each dose.

Now, much weight has been placed upon the shapes of dose-response curves for gaps and breaks, and linearity versus curvature is an important argument for the origin of these aberrations (Revell, 1966a, b, 1974; Scott and Evans, 1967). However, imprecision means that all  $G_2$  dose-response curves are warped, and the basis for such arguments is seriously undermined. Even Revell came to recognise this (Revell, 1974).

(2) Sensitivity changes with  $G_2$  transit. On the completion of chromosome duplication, the process of sister chromatid segregation and condensation/packing begins and proceeds through the transit of  $G_2$  until anaphase. One can predict that the progressive spatial changes and protein accumulation involved will have considerable influence upon both the types and frequencies of the various *chromatid type* aberrations produced. *Interchanges* should be less frequent at later transit times as the chromatids condense and chromatin extrusions are withdrawn, whereas *intrachanges*, which will include breaks and gaps should come to predominate. Events appearing to involve only parts of a chromatid (“sub-chromatid” aberrations) should also increase as compaction increases. Furthermore, one would also anticipate that the relative frequencies of intra- and inter-chromatid *intrachanges* should change as sister chromatid separation becomes more established.

Multiple fixation time studies have been disappointing, confirming only some general trends, because imprecision is the thwarting factor. The contemporary metaphases in a sample come from wider and wider ranges of  $G_2$  positions as sample time from treatment increases. Time after treatment cannot be equated with cell developmental position within the phase.

(3) The profile of the yield-time curve. Because the observed aberration frequency is determined by the mix of cell stages in a sample, and this mix is not a constant, the position, height and spread of the various peaks and troughs observed with time after treatment are not an exact representation of the changes in sensitivity occurring with phase transit.

Nor are the profiles obtained at different doses strictly comparable for reasons that should be obvious from the foregoing discussions.

Therefore, deductions about sensitivity changes, and about such things as rates of appearance, disappearance or repair have to be made with extreme caution. From theoretical work it seems likely that actual sensitivity changes with  $G_2$  transit are far sharper than appears from observed profiles (Savage and Papworth, 1994).

## The relation of gaps to chromosome bands

We know from EM studies that chromatin packing is not uniform along a chromatid arm, regions of differential density occur (Bahr and Larsen, 1974; Takayama, 1976; Laemmli et al., 1983). This phenomenon is utilised for many organisms in the various “banding” methods that enable visualization of patterns of alternating dark and light bands. Standardised, these patterns facilitate chromosome identification, the location of aberration exchange points, and gene mapping.

The question has therefore arisen as to whether induced gaps are just an enhancement of these already less-dense packed regions. If relaxed packing is an inevitable consequence of damage, will it migrate to the nearest potential pale G-band?

Certainly, spontaneous and induced gaps tend to recur in specific places, and both the within- and between-arm distributions for all species investigated are almost always significantly non-random (Waksvik et al., 1977; Brøgger, 1971a, 1975; Obe,

1972; Obe and Lüers, 1972; Scheid and Traut, 1968, 1969; Vig et al., 1968; Slijepcevic and Natarajan, 1994; Pellicia et al., 1985; Lubs and Samuelson, 1967).

Care, however, needs to be taken in the interpretation of these data in the light of imprecision discussed above. It is clear that gaps are not produced uniformly with time of transit (both as regards position and frequency) because the scattered completion of replication segments will mean scattered start times for the condensation programme along the chromosomes.

This means that the cell mix used (often a single sample time, or bulked times) for analysis is extremely heterogeneous. Not surprisingly, therefore, distribution patterns can change if more than one sample time is used (Van Steenis et al., 1974).

EM studies suggest that a packing reduction, not always obvious at LM level, often occurs in the sister chromatid opposite a unilocus gap, indicating a cross-chromatid influence, and the structural similarities between pale G-bands and gaps have led to the suggestion that some gaps represent expanded bands (Brinkley and Hittelman, 1975). Gaps are predominantly located in pale G-bands and also largely disappear when chromosomes carrying them are G-banded (Waksvik et al., 1977; Bigger and Savage, unpublished). All this, together with frequent recurrence in the larger pale bands (e.g. mid 3p in human cells; Lubs and Samuelson, 1967; Obe and Lüers, 1972) might favour an underlying relationship.

Bearing in mind the very precise nature of the chromosome condensation programme, it would be surprising if the resulting packing reduction did not gravitate to already existing differential low-density regions.

On the other hand, gap induction is frequent in plant chromosomes like *Vicia* and *Tradescantia*, neither of which G-band by the standard methods.

In human and mammalian materials, one has also to think about a small contribution to gaps from the so called "fragile sites". These are specific chromosome locations which, in certain individuals, are prone to display, in vitro, recurrent isolocus gaps (Fig. 1e). They are inherited in a dominant Mendelian manner (Berger et al., 1985; Hecht, 1986). Morphologically, most are identical to gaps induced by regular aberration-inducing agents, showing the same range of variations.

Spontaneous frequencies are very low, and therefore enhancement of expression is required for study, for example by growth of the cells in low-folate conditions. Even so, the sites are not displayed in every cell, and the observed frequency is markedly influenced by culture conditions and pH (Sutherland, 1979; Reidy, 1988).

To be designated as "fragile", a site must also, "under appropriate in vitro conditions", be involved in structural chromosome changes. However, such "conditions" involve treatments with agents known to interfere with DNA metabolism (e.g. excess folate, methotrexate, aphidicolin, etc.). These are aberration-inducing agents in their own right, so the damage is not confined to the particular fragile site alone, but is augmented by a full range of chromatid aberrations throughout the karyotype (Li et al., 1986; Reidy, 1988; Savage and Fitchett, 1988).

The low-folate enhancement of site expression can be eliminated by addition of thymidine, folic acid or bromodeoxyuridine (Reidy, 1988) and for *Fra X*, frequencies fall rapidly, in par-

allel with all other induced aberration types, to control baseline levels, well within the duration of one cell cycle (Savage and Fitchett, 1988).

At least 70 locations have been designated "*Fra*" in the human karyotype (Sutherland, 1979; Berger et al., 1985) but only one (*Fra Xq27*) has been shown, unequivocally, to be associated with any significant clinical effect (mental retardation). The isolocus gap here shows very variable morphology, often with clear displacement of one chromatid element (Savage and Fitchett, 1988). However, many other designated sites correspond to recurrent "breakpoints" in cancer cells.

The predominantly isolocus nature of expression, as well as enhancing conditions, indicate an origin from DNA synthesis/replication problems – an S-dependent gap or aberration production in regions rendered vulnerable by inherited structural or compositional abnormalities. Their overall rarity makes it unlikely that there will be profound effects on either aberration frequencies or distribution.

### Concluding remarks

The chromosome changes we observe at metaphase are the end-product of a chain of events initiated by molecular lesions, particularly DSB in the DNA (Kihlman, 1971; Evans, 1977; Scott, 1980; Natarajan and Obe, 1984; Bryant, 1984). No aberrations are visible until the chromatin has packed/condensed, which inevitably means modification, and in some cases disguise or obliteration.

*Chromatid-type* gaps, therefore, represent an enormous amplification of the initial damage. They are produced by a very wide variety of agents and treatments, and their morphological similarity, regardless of origin, implies that the visible entity is a rather non-specific end-point. This separates "initiator" and "nature", a distinction not often made in literature discussions. With regard to "nature", it seems to me that only some affect on, or interference with, the packing/condensation programme will meet all the observations.

This condensation programme must be very, very precise when one considers the enormous lengths of DNA which a chromosome contains, and the variety of extraneous proteins involved in it (Laemmli et al., 1983; Gasser, 1995; Saitoh et al., 1995). Consequently, it probably does not take very much to disrupt it. This is supported by the fact that infection of the genome with relatively small lengths of foreign viral DNA regularly leads to typical gaps and breaks at the site of insertion (Henderson, 1987; McDougall, 1971).

Is there a real gap/break distinction, or are they actually a real continuum, variant manifestations of a similar basic aberration? We can ask this question from two angles. First, with regard to aberration type, where we must conclude a genuine difference. It is inescapable that many breaks (possibly all) are apparently structurally incomplete *intrachanges* (c2 and above) and as such, irreparable. In contrast, gaps are repairable, and produce no further structural damage on transmission. Regardless of treatment, "simple" breaks are never found without *intrachanges* also being present.

If, however, we ask the question with regard to structural continuity, the answer is much less clear cut, for when EM studies are invoked, even unambiguous LM breaks are often seen to be linked. It is in order, then, to pose an even more fundamental question: Does persistent *chromatid* structural incompleteness ever exist in the absence of mechanical stress?

The mention of repair raises the topic of time of expression. It is clear that for S-independent treatments, G<sub>2</sub> is very non-uniform with regard to gap manifestation, a sharp, high frequency peak occurring in sample times shortly after treatment, which falls off rapidly to very low levels as sample time is increased. Breaks (excluding isolocus types, Figure 1m–o) show a much smaller peak at, or a little later than, the time of that for gaps and show fairly steady levels throughout G<sub>2</sub>. The gap fall is usually interpreted as evidence for time-related lesion repair, removal lessening the chance of packing error expression. Some evidence for this comes from work with the DNA DSB repair inhibitor ara A, which can largely abolish the frequency fall (Bryant and Slijepcevic, 1993). However, there is also a dramatic fall the other side of the peak, in cells that were closer to division, which cannot be related to time-dependent repair. There is, therefore, an additional (probably confounding) expression-related component. Only at a certain critical period of

the condensation programme can a lesion be expressed as a folding defect. This is supported by PCC studies, for if radiation is given at different times after the start of cell fusion, fewer gaps result as chromosomes become more condensed (Hittelman and Rao, 1974a).

Since gaps do not re-appear, or lead to aberrations at the subsequent mitosis, whereas irradiated mitotic chromosomes show abundance of aberrations, we need to ask what is repaired? Have all initiating lesions been removed, or since they are now present before condensation begins will folding troubles be overcome? Cell selection may also play a part.

Unfortunately, imprecision is a very real bar to progress both for qualitative and quantitative studies in this gap/break problem. What is needed is some G<sub>2</sub> cell marker system that will allow us to unscramble scored cells and replace them in the correct developmental sequence. This can be done for S-phase cells utilizing the very precise band replication sequences (Savage and Bhunya, 1980; Savage and Prasad, 1984; Savage et al., 1984; Aghamohammadi and Savage, 1992). Until we have such a system for G<sub>2</sub>, the progressive effects on aberrations of condensation and spatial alterations during transit, and the true shapes of dose-response curves, will remain matters for conjecture.

## References

- Aghamohammadi SZ, Savage JRK: The effect of X-irradiation on cell cycle progression and chromatid aberrations in stimulated human lymphocytes using cohort analysis studies. *Mutat Res* 268:223–230 (1992).
- Akif'ev AP, Belyaev IY, Ivanischeva MY: The general mechanism of chromosomal mutagenesis: Basic and applied aspects. *Acta Biol Hungarica* 41:3–7 (1990).
- Bahr GF, Larsen PM: Structural "bands" in human chromosomes, in DuPrav EJ (ed): *Advances in Cell and Molecular Biology* 3, pp 191–212 (Academic Press, 1974).
- Bell S, Wolff S: Studies on the mechanism of the effect of fluorodeoxyuridine on chromosomes. *Proc natl Acad Sci, USA* 51:195–202 (1964).
- Belmont AS, Bruce K: Visualization of G1 chromosomes: A folded, twisted, supercoiled chromonema model of interphase chromatid structure. *J Cell Biol* 127:287–302 (1994).
- Bender MA, Griggs HG, Bedford JS: Mechanisms of chromosomal aberration production. III. Chemicals and ionizing radiation. *Mutat Res* 23:197–212 (1974).
- Berger R, Bloomfield CD, Sutherland GR: Report of the committee on chromosome rearrangements in neoplasia and on fragile sites. *Cytogenet Cell Genet* 40:490–535 (1985).
- Boei JJWA, Vermeulen S, Natarajan AT: Analysis of radiation-induced chromosomal aberrations using telomeric and centromeric PNA probes. *Int J Radiat Biol* 76:163–167 (2000).
- Brecher S: Ultrastructural observations of X-ray induced chromatid gaps. *Mutat Res* 42:249–268 (1977).
- Brinkley BR, Hittelman WN: Ultrastructure of mammalian chromosome aberrations. *Int Rev Cytol* 42:49–101 (1975).
- Brinkley BR, Shaw MW: Ultrastructural aspects of chromosome damage, in: *Genetic Concepts and Neoplasia*, A collection of papers presented at the 23rd Annual Symposium on Fundamental Cancer Research, 1969, pp 313–345 (Williams and Wilkins, Baltimore 1970).
- Brogger A: Apparently spontaneous chromosome damage in human leukocytes and the nature of chromatid gaps. *Humangenetik* 13:1–14 (1971a).
- Brogger A: Spontaneous chromosome damage and gap morphology. *Humangenetik* 13:15–24 (1971b).
- Brogger A: Is the chromatid gap a folding defect due to protein change? Evidence from mercaptoethanol treatment of human lymphocyte chromosomes. *Hereditas* 80:131–136 (1975).
- Brogger A: The chromatid gap—a useful parameter in genotoxicology? *Cytogenet Cell Genet* 33:14–19 (1982).
- Bryant PE: Enzymatic restriction of mammalian cell DNA using *PvuII* and *BamHI*: Evidence for the double-strand break origin of chromosome aberrations. *Int J Radiat Biol* 46:57–65 (1984).
- Bryant PE, Slijepcevic P: G2 chromatid aberrations: Kinetics and possible mechanisms. *Envir Molec Mutagen* 22:250–256 (1993).
- Bucton KE, Evans HJ: Methods for the analysis of human chromosome aberrations, pp 21–22 (World Health Organization, Geneva 1973).
- Chaudhuri JP: On the origin and nature of achromatic lesions. *Chromosomes Today* 3:147–151 (1972).
- Comings DE: What is a chromosome break? in German, J (ed): *Chromosomes and Cancer*, pp 95–133 (Wiley and Sons, New York 1974).
- Conger AD: Real chromatid deletions versus gaps. *Mutat Res* 4:449–459 (1967).
- Cornforth MN: Analyzing radiation-induced complex chromosome rearrangements by combinatorial painting. *Radiat Res* 155:643–659 (2001).
- Dimitrov B: Nature of chromosome gaps induced by alkylating agents and  $\gamma$ -rays as revealed by caffeine treatment. *Mutat Res* 80:289–295 (1981).
- DuPrav EJ: Evidence for a "folded fibre" organization in human chromosomes. *Nature* 209:577–581 (1966).
- Engelberg J: On deterministic origins of mitotic variability. *J Theoret Biol* 20:249–259 (1968).
- Evans HJ: Chromosome aberrations induced by ionizing radiations. *Int Rev Cytol* 13:221–321 (1962).
- Evans HJ: Chromosome aberrations and target theory, in Wolff S (ed): *Radiation-induced Chromosome Aberrations*, pp 8–40 (Columbia University Press, New York 1963).
- Evans HJ: Repair and recovery from chromosome damage after fractionated X-ray dosage, in: *Genetic Aspects of Radiosensitivity*, pp 31–48 (International Atomic Energy Agency, Vienna, STI/PUB/130, 1966).
- Evans HJ: Repair and recovery from chromosome damage induced by fractionated X-ray exposures, in Silini G (ed): *Radiation Research*, pp 482–501 (North-Holland, Amsterdam 1967).
- Evans HJ: Molecular mechanisms in the induction of chromosome aberrations, in Scott D, Bridges BA, Sobels FH (eds): *Progress in Genetic Toxicology*, pp 57–74 (Elsevier, Amsterdam 1977).
- Fisher KM, Budinger TF, Foin AT, Everhart TE: Spontaneous chromosome gaps in *Marmosa mitis*. *Mutat Res* 22:299–303 (1974).
- Fox DP: The effects of X-rays on the chromosomes of locust embryos. III. The chromatid aberration types. *Chromosoma* 20:386–412 (1967a).
- Fox DP: The effects of X-rays on the chromosomes of locust embryos. IV. Dose-response and variation in sensitivity of the cell cycle for the induction of chromatid aberrations. *Chromosoma* 20:413–441 (1967b).
- Gasser SM: Coiling up chromosomes. *Current Biol* 5:357–360 (1995).

- Gerber GB, Léonard A: Influence of selection, non-uniform cell population and repair on dose-effect curves of genetic effects. *Mutat Res* 12:175–182 (1971).
- Griffin CS, Harvey AN, Savage JRK: Chromatid damage induced by  $^{238}\text{Pu}$   $\alpha$ -particles in G<sub>2</sub> and S phase Chinese hamster V79 cells. *Int J Radiat Biol* 66:85–98 (1994).
- Harvey AN, Savage JRK: Investigating the nature of chromatid breaks produced by restriction endonucleases. *Int J Radiat Biol* 71:21–28 (1997).
- Harvey AN, Costa ND, Savage JRK, Thacker J: Chromosomal aberrations induced by defined DNA double-strand breaks: The origin of achromatic lesions. *Somatic Cell Molec Genet* 23:211–219 (1997).
- Hecht F: Rare, polymorphic, and common fragile sites: A classification. *Hum Genet* 74:207–208 (1986).
- Heddle JA, Bodycote DJ: On the formation of chromosomal aberrations. *Mutat Res* 9:117–126 (1970).
- Heddle JA, Bodycote DJ, Whissell D: Nature of chromatid deletions, in: *Induced Mutations in Plants*, pp 637–643 (IAEA-SM-121/53, International Atomic Energy Agency, Vienna 1969a).
- Heddle JA, Whissell D, Bodycote DJ: Changes in chromosome structure induced by radiations: A test of the two chief hypotheses. *Nature* 221:1158–1160 (1969b).
- Henderson AS: Chromosome accommodation to integration of foreign DNA. *Chromosomes Today* 9:12–21 (1987).
- Herrosos B, Gianelli F: Spatial distribution of old and new chromatid sub-units and frequency of chromatid exchanges in induced human lymphocyte endoreduplications. *Nature* 216:286–288 (1967).
- Hittelman WN, Rao PN: Premature chromosome condensation. I. Visualization of X-ray-induced chromosome damage in interphase cells. *Mutat Res* 23:251–258 (1974a).
- Hittelman WN, Rao PN: Premature chromosome condensation. II. The nature of chromosome gaps produced by alkylating agents and ultraviolet light. *Mutat Res* 23:259–266 (1974b).
- IAEA: What is the nature of radiation-induced achromatic lesions (“gaps”) in chromosomes? in *Genetical Aspects of Radiosensitivity: Mechanisms of Repair*, p 168 (International Atomic Energy Agency, Vienna, STI/PUB/130 1966).
- Iino A: Observations on human somatic chromosomes treated with hyaluronidase. *Cytogenetics* 10:286–294 (1971).
- Jacob M: Differential radiosensitivity of the uni- and bi-filarly BrdUrd-substituted chromatids of muntjac chromosomes. *Mutat Res* 63:211–213 (1979).
- Kihlman BA: Deoxyribonucleotide synthesis and chromosome breakage. *Chromosomes Today* 1:108–117 (1966).
- Kihlman BA: Molecular mechanisms of chromosome breakage and rejoining. *Adv Cell Mol Biol* 1:59–107 (1971).
- Kirby-Smith JS, Craig DL: The induction of chromosome aberrations in *Tradescantia* by ultraviolet radiation. *Genetics* 42:176–187 (1957).
- Laemmler UK, Lewis CD, Earnshaw WC: Long-range order folding of the chromatin fibres in metaphase chromosomes and nuclei, in Rowley JD, Ultmann JE (eds): *Chromosomes and Cancer. From Molecules to Man*, pp 15–27 (Academic Press, New York 1983).
- Lazányi A: The effect of sulphoguanidine in Co-irradiated G<sub>1</sub> and G<sub>2</sub> cells on the incompleteness of exchanges and the question of gaps in *Vicia faba* L. *Mutat Res* 6:67–79 (1968).
- Lea DE: *Actions of Radiations on Living Cells*, 1st ed (Cambridge University Press 1946).
- Li X, Reidy JA, Wheeler VA, Chen, ATL: Folic acid and chromosome breakage. III. Types and frequencies of spontaneous chromosome aberrations in proliferating lymphocytes. *Mutat Res* 173:131–134 (1986).
- Lubs HA, Samuelson J: Chromosome abnormalities in lymphocytes from normal human subjects. A study of 3,720 cells. *Cytogenetics* 6:402–411 (1967).
- McDougall JK: Adenovirus induced chromosome aberrations in human cells. *J gen Virol* 12:43–51 (1971).
- Migeon BR, Merz T: Artefactual chromatid aberrations in untreated and X-ray treated human lymphocytes. *Nature* 203:1395–1396 (1964).
- Miller MW, Kuehnert CC (eds): *The Dynamics of Meristem Populations* (Plenum Press, New York 1972).
- Natarajan AT, Obe G: Molecular mechanisms involved in the production of chromosome aberrations. III. Restriction endonucleases. *Chromosoma* 90:120–127 (1984).
- Neary GJ, Evans HJ: Chromatid breakage by irradiation and the oxygen effect. *Nature* 182:890–891 (1958).
- Obe G: Intrachromosomal distribution of chemically induced achromatic lesions and isochromatid breaks in *Vicia faba*. *Mutat Res* 15:224–226 (1972).
- Obe G, Lüers H: Inter- and intrachromosomal distribution of achromatic lesions and chromatid breaks in human chromosomes. *Mutat Res* 16:337–339 (1972).
- Parshad R, Sanford KK, Jones GM: Chromatid damage induced by fluorescent light during G<sub>2</sub> phase in normal and Gardner syndrome fibroblasts. *Mutat Res* 151:57–63 (1985).
- Pellicia F, Micheli A, Olivieri G: Inter- and intrachromosomal distribution of chromatid breaks induced by X-rays during G<sub>2</sub> in human lymphocytes. *Mutat Res* 150:293–298 (1985).
- Reidy JA: Role of deoxyuridine incorporation and DNA repair in the expression of human chromosomal fragile sites. *Mutat Res* 200:215–220 (1988).
- Revell SH: A new hypothesis for “chromatid” changes, in Bacq ZM, Alexander P (eds): *Proceedings of the Radiobiology Symposium* (1954, Liège), pp 243–253 (Butterworths, London 1955).
- Revell SH: The accurate estimation of chromatid breakage, and its relevance to a new interpretation of chromatid aberrations induced by ionizing radiations. *Proc Roy Soc, Series B* 150:563–589 (1959).
- Revell SH: Chromatid Aberrations – The generalized theory, in Wolff S (ed): *Radiation-induced chromosome Aberrations*, pp 41–72 (Columbia University Press, New York 1963).
- Revell SH: An admonition on chromosome aberration induction, and the question of repair, in *Genetical Aspects of Radiosensitivity: Mechanisms of Repair*, pp 25–29 (International Atomic Energy Agency, Vienna, STI/PUB/130 1966a).
- Revell SH: Evidence for a dose-squared term in the dose-response curve for real chromatid discontinuities induced by X-rays, and some theoretical consequences thereof. *Mutat Res* 3:34–53 (1966b).
- Revell SH: The Breakage-and-Reunion Theory and the Exchange Theory for chromosomal aberrations induced by ionizing radiations: A short history. *Advanc Radiat Biol* 4:367–416 (1974).
- Sachs RK, Chen AM, Simpson PJ, Hlatky LR, Hahnfeldt P, Savage JRK: Clustering of radiation-produced breaks along chromosomes: Modeling the effects on chromosome aberrations. *Int J Radiat Biol* 75:657–672 (1999).
- Saitoh N, Goldberg I, Earnshaw WC: Review: The SMC proteins and the coming of age of the chromosome scaffold hypothesis. *BioEssays* 17:759–766 (1995).
- Savage JRK: Chromatid aberrations induced by 14.1 MeV neutrons in *Vicia faba* root meristem cells, in: *Neutron Irradiation of Seeds*, II, pp 9–28 (International Atomic Energy Agency, Vienna 1968).
- Savage JRK: Annotation: Classification and relationships of induced chromosomal structural changes. *J Med Genet* 13:103–122 (1976).
- Savage JRK: A comment on the quantitative relationship between micronuclei and chromosomal aberrations. *Mutat Res* 207:33–36 (1988).
- Savage JRK: The production of chromosome structural changes by radiation: An update of Lea (1946), Chapter VI. *Brit J Radiol* 62:507–520 (1989).
- Savage JRK: A brief survey of aberration origin theories. *Mutat Res* 404:139–147 (1998).
- Savage JRK, Bhunya SP: Cytological sub-division of S-phase in the Syrian hamster (*Mesocricetus auratus*). *Chromosoma* 77:169–180 (1980).
- Savage JRK, Fitchett M: The behaviour of fragile X and other aberrations during recovery from low folate conditions. *Chromosoma* 96:391–396 (1988).
- Savage JRK, Harvey AN: Revell revisited. *Mutat Res* 250:307–317 (1991).
- Savage JRK, Harvey AN: Investigations of aberration origins using BrdUrd, in Obe G, Natarajan AT (eds): *Chromosomal alterations; origin and significance*, pp 76–91 (Springer-Verlag, Berlin 1994).
- Savage JRK, Papworth DG: The effect of variable G<sub>2</sub> duration upon the interpretation of yield-time curves of radiation-induced chromatid aberrations. *J Theoret Biol* 38:17–38 (1973).
- Savage JRK, Papworth DG: Excogitations about the quantification of structural chromosomal aberrations in Obe G (ed): *Advances in mutagenesis research*, 3, pp 162–189 (Springer-Verlag, Berlin 1991).
- Savage JRK, Papworth DG: Review Article: Mitotic perturbation and G<sub>2</sub> cell chromatid aberrations. *Brazil J Genet* 17:121–125 (1994).
- Savage JRK, Prasad R: Cytological subdivision of S-phase of human cells in asynchronous culture. *J Med Genet* 21:204–212 (1984).
- Savage JRK, Preston RJ, Neary GJ: Chromatid aberrations in *Tradescantia bracteata* and a further test of Revell’s hypothesis. *Mutat Res* 5:47–56 (1968).
- Savage JRK, Prasad R, Papworth DG: Subdivision of S-phase and its use for comparative purposes in cultured human cells. *J Theoret Biol* 111:355–367 (1984).
- Sax K: Chromosome aberrations induced by X-rays. *Genetics* 23:494–516 (1938).
- Sax K: An analysis of X-ray induced chromosomal aberrations in *Tradescantia*. *Genetics* 25:1–68 (1940).
- Sax K: Types and frequencies of chromosomal aberrations induced by X-rays. *Cold Spring Harbor Symp Quant Biol* 9:93–101 (1941).
- Scheid W, Traut H: Non-random distribution of X-ray induced achromatic lesions (“gaps”) in the chromosomes of *Vicia faba*. *Mutat Res* 6:481–483 (1968).
- Scheid W, Traut H: The distribution of X-ray-induced achromatic lesions (“gaps”) within and between the arms of the M-chromosome of *Vicia faba*. *Studia Biophys* 17:125–130 (1969).
- Scheid W, Traut H: Ultraviolet-microscopical studies on achromatic lesions (“gaps”) induced by X-rays in the chromosomes of *Vicia faba*. *Mutat Res* 10:159–161 (1970).
- Scheid W, Traut H: Visualization by scanning electron microscopy of achromatic lesions (“gaps”) induced by X-rays in chromosomes of *Vicia faba*. *Mutat Res* 11:253–255 (1971a).
- Scheid W, Traut H: Visualization of achromatic lesions (gaps) induced by X-rays in chromosomes of *Vicia faba* by staining of chromosomal proteins. *Mutat Res* 12:97–99 (1971b).

- Scheid W, Traut H: On the nature of achromatic lesions ("gaps") induced by X-rays in chromosomes of *Vicia faba*. *Zeitschr Naturforsch* 26b:1384–1385 (1971c).
- Scheid W, Traut H: Comparative length measurements of *Vicia faba* chromatids with X-ray-induced achromatic lesions (gaps). *Mutat Res* 18:25–31 (1973).
- Scott D: Molecular mechanisms of chromosome structural changes, in Alacevic M (ed): *Progress in Environmental Mutagenesis*, pp 101–113 (Elsevier, Amsterdam 1980).
- Scott D, Evans HJ: X-ray-induced chromosomal aberrations in *Vicia faba*: Changes in response during the cell cycle. *Mutat Res* 4:579–599 (1967).
- Slijepcevic P, Natarajan AT: Distribution of X-ray-induced G<sub>2</sub> chromatid damage among Chinese hamster chromosomes: Influence of chromatin conformation. *Mutat Res* 323:113–119 (1994).
- Sturelid S: Chromosome-breaking capacity of tepa and analogues in *Vicia faba* and Chinese hamster cells. *Hereditas* 68:255–276 (1971).
- Sutherland GR: Heritable fragile sites on human chromosomes. I. Factors affecting expression in lymphocyte culture. *Am J Hum Genet* 31:125–135 (1979).
- Swanson CP: X-ray and ultraviolet studies on pollen tube chromosomes. 1. The effect of ultraviolet (2537 Å) on X-ray-induced chromosomal aberrations. *Genetics* 29:61–68 (1944).
- Takayama S: Configurational changes in chromatids from helical to banded structures. *Chromosoma* 56:47–54 (1976).
- Traut H, Scheid W: The structure of chromatid ends and of the ends of experimentally produced chromatid fragments as revealed by trypsin treatment of *Vicia faba* chromosomes. *Mutat Res* 17:335–340 (1973).
- Trosko JE, Wolff S: Strandedness of *Vicia faba* chromosomes as revealed by enzyme digestion studies. *J Cell Biol* 26:125–135 (1965).
- Van Steenis H, Tuscany R, Leigh B: The distribution of X-ray induced chromosomal abnormalities in Rat Kangaroo (*Potorous tridactylis*) cells *in vitro*. *Mutat Res* 22:223–228 (1974).
- Vig BK, Kontras SB, Paddock EF: <sup>3</sup>H-Thymidine-induced chromosome aberrations in cultured human leukocytes. *Cytogenetics* 7:189–195 (1968).
- Waksvik H, Brøgger A, Stene J: Psoralen/UVA treatment and chromosomes. I. Aberrations and sister-chromatid exchange in human lymphocytes *in vitro* and synergism with caffeine. *Hum Genet* 38:195–297 (1977).
- Wolfe SL: The fine structure of isolated metaphase chromosomes. *Exp Cell Res* 37:45–53 (1965).
- Wolff S: Strandedness of chromosomes. *Int Rev Cytol* 25:279–296 (1969).
- Wolff S: On the "tertiary" structure of chromosomes. *Mutat Res* 8:207–214 (1970).
- Wolff S, Bodycote DJ: The induction of chromatid deletions in accordance with the breakage-and-reunion hypothesis. *Mutat Res* 29:85–91 (1975).



# Molecular targets and mechanisms in formation of chromosomal aberrations: contributions of Soviet scientists

I. Belyaev

Department of Genetic and Cellular Toxicology, Stockholm University, Stockholm (Sweden)

**Abstract.** Studies of mechanisms for formation of chromosomal aberrations (CAs) with special emphasis on data from Soviet/Russian investigations are reviewed that argue in favor of a minor fraction of genomic DNA that forms specific molecular targets/contacts for the formation of chromosomal exchanges. This DNA is presumably associated with matrix attachment sites of DNA loops, enriched with AT base pairs and repetitive DNA sequences. It is assumed that there are two main mechanisms in formation of chromosome aberrations: 1) mutually reciprocal recombination, resulting in formation of

all kinds of chromosome exchanges; 2) the process of telomere formation, resulting in the generation of true deletions. A significant part of chromosomal breaks and apparently unrejoined ends in incomplete exchanges as seen with cytogenetic techniques reflect decondensation in the discrete units of chromatin organization such as the megabase-size DNA domains. The possible ways for further analysis of alternative theories with emerging technologies are also discussed.

Copyright © 2003 S. Karger AG, Basel

The “breakage-first” theory was put forward by Levitsky and Araratyan (1931) and Stadler (1931) postulating that breaks of chromatids are needed as primary events in formation of CAs. This theory was opposed by the “contact-first” theory by Serebrovsky (1929). The contact theory considered formation of CAs as an epiphenomenon of hypothetical genetic processes in specific sites of primary contacts, which may occupy just a minor part of the genome. According to the contact theory, formation of CAs must always be “reciprocal” in the sense that the

involved fragments of chromosomes are rejoined completely. In this respect, formation of exchanges was considered as a process similar to crossing over in meiosis. Traditionally, the breakage-first theory or its modification, the Breakage-and Reunion (B&R) theory, has been the principal focus of investigators (for reviews, see Savage, 1998; Natarajan, 2002; Obe et al., 2002). Unfortunately, many studies conducted in Russia are almost unknown in the Western world. In this review, some selected theoretical concepts and results of the Russian authors are presented that argue in favor of the contact theory.

It is now widely believed, that each chromosomal break, including apparently open ends in incomplete exchanges, as visible in an optical microscope, correspond to a DNA double strand break (DSB). This notion is an important basis of the modern B&R theory that has been challenged by the data of electron microscopy and by the analysis of CAs during reduplication as reviewed below.

In addition, the link to other data that can be helpful in further validation of possible mechanisms is discussed.

The Swedish National Board for Laboratory Animals, Swedish Council for Working Life and Social Research, and the Swedish Authority for Radiation Protection supported these studies.

Received 30 September 2003; manuscript accepted 10 December 2003.

Request reprints from Dr. Igor Y. Belyaev, Department of Genetics Microbiology and Toxicology, Stockholm University  
SE-106 91 Stockholm (Sweden)  
telephone: +46-8-16 41 08; fax: +46-8-16 43 15  
e-mail: Igor.Belyaev@genetics.su.se

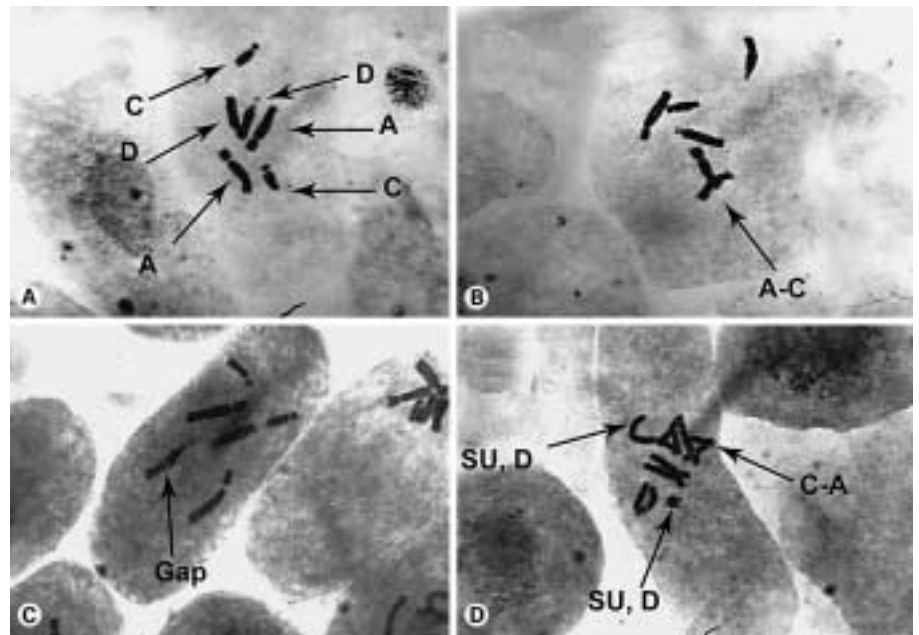


**Fig. 1.** *C. capillaris* cells have three pairs of chromosomes, A, D, and C with distinct individual morphology (A). This morphological individuality allows one to distinguish many kinds of CAs using standard protocols of chromosome staining and optical microscopy. Typical examples of chromatid type CAs are shown: symmetrical complete translocation involving A and C chromosomes (B); gap in the D chromosome (C); isochromatid deletion with sister union (SU), in the D chromosome and asymmetrical complete translocation involving C and A chromosomes (D).

### Reduplication studies in validation of the mechanisms for CAs

Among other cell types, such as human lymphocytes and cultured mammalian cells, *Crepis capillaris* root tip cells became popular in studies of Russian cytogeneticists (Nemtseva, 1970; Dubinina, 1978). *C. capillaris* cells possess only three pairs of chromosomes with distinct individual morphology (Fig. 1). This morphological individuality allows one to distinguish many kinds of CAs using standard protocols of chromosome staining.

*C. capillaris* cells were intensively used in studies of reduplication (reproduction) of CAs. In this technique, the cells are allowed to grow in the presence of colchicine. Colchicine destroys the mitotic spindle and the cells enter the next cycle without division with a reduplicated set of chromosomes. The advantage of this technique is that cells containing CAs are not eliminated by reproductive death. Sidorov and Sokolov (1963) established the reduplication technique to investigate what types of CAs appear in the cell cycles following irradiation. They analyzed CAs in three consecutive mitoses following irradiation in G<sub>2</sub> phase. Their conclusion was that all radiation-induced lesions are transformed to CAs in the first mitosis after irradiation but, in some studies, a significant excess of aberrations was found in later mitosis, which suggests that some lesions can be realized as CAs in later cycles following irradiation (Dubinin et al., 1976; Aptikaeva et al., 1983). This phenomenon was discussed in terms of “replicating instability” implying occurrence of lesions, which are able to pass replication during the cell cycles following treatment with a clastogen (Dubinin et al., 1973, 1976). While this type of instability was only minor in the case of radiation, significant excess of aberrations was usually seen by treatment of cells with chemical clastogens (Dubinina, 1978).

It was shown by the reduplication method that subchromatid aberrations (stickiness) reduplicated to form chromosome-type aberrations (Demin, 1974). These data proved that subchromatid aberrations are actually aberrations of chromatid type.

It was established that gaps do not reduplicate in the cell cycle following irradiation (Protopopova and Shapiro, 1968; Sidorov, 1974; Dubinin et al., 1976). Electron microscopic studies revealed that gaps contain decondensed chromatin (Brinkley and Hittelman, 1975; Brecher, 1977; Mace et al., 1978; Mullinger and Johnson, 1987). Based on these and other mostly indirect evidence, it has been widely accepted that all gaps are sites of chromatin decondensation and do not represent DSBs at the molecular level.

#### Reduplication of radiation-induced exchanges

In metaphase, subchromatid and chromatid-type aberrations often possess gaps at the sites of junctions. A gap resembling a middle sized G-band was detected by scanning electron microscopy in derivative chromosomes of reciprocal translocations (Uehara et al., 1996). Atomic force microscopy has been used to study a translocation involving human chromosomes 11 and 13 and a 0.3- $\mu$ m gap region on the derivative chromosome was found (Ergun et al., 2002). Moreover, decondensed chromatin can be revealed by electron microscopy both in the apparently unrejoined ends of incomplete exchanges and also in some breaks, which are usually scored as deletions by optical microscopy (Brinkley and Hittelman, 1975). We hypothesized that all incomplete chromatid exchanges are, in reality, complete exchanges. According to this hypothesis, incomplete exchanges appear if chromatin structure has not been restored in places of complete DNA exchanges before the onset of mitotic condensation. In this case all chromatid exchanges should reduplicate and form complete chromosome exchanges in the cell

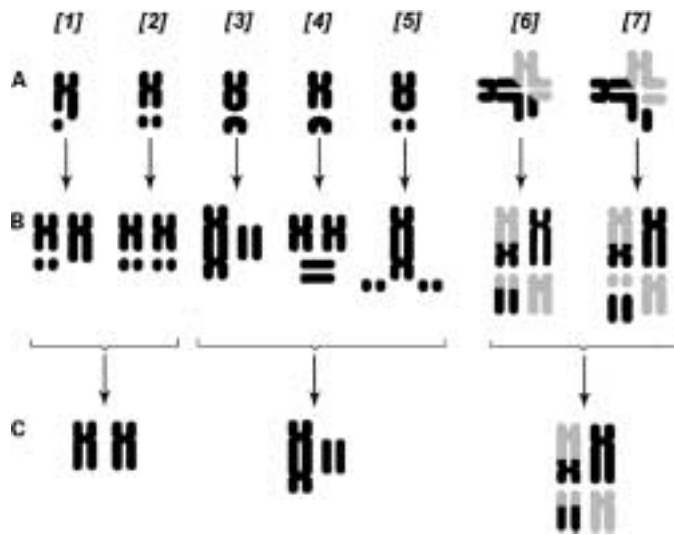


**Fig. 2.** (A) Main kinds of chromatid type aberrations: (1) chromatid deletion; (2) isochromatid deletion without unions, so called non-union (NU); isochromatid deletions with complete (3) and incomplete (4, 5) sister union; (6) complete and (7) incomplete asymmetrical chromatid exchanges. (B) and (C) aberrations after reduplication of CAs in the next cell cycle under the assumption that the formation of CAs is completed and apparent non-rejoins correspond to DSBs (B) and that the breaks and apparent non-rejoins are sites of decondensed chromatin (C).

cycle following irradiation (Fig. 2). To verify this hypothesis, reduplication of different kinds of CAs was analyzed (Belyaev et al., 1985). *C. capillaris* cells were irradiated with  $\gamma$ -rays or X-rays in  $G_2$  phase and treated with colchicine twice in order to collect cells in the first and the second mitosis following irradiation. In the first mitosis, in diploids, all aberrations were of chromatid type. In the second mitosis, in tetraploid cells, only chromosome-type aberrations were observed. The yields of exchanges were equal when compared between mitoses on a per cell basis. Various kinds of chromatid exchanges reduplicated to corresponding chromosome exchanges. However, while approximately 30% of chromatid exchanges were incomplete in the first mitosis (Fig. 2A), all chromosome exchanges were complete after reduplication of chromatid exchanges in the cell cycle following irradiation (Fig. 2C).

#### *Reduplication of CAs induced by 5-fluorodeoxyuridine (FdU)*

A significant amount of breaks of different kinds were observed in metaphases when cells were treated with an inhibitor of DNA synthesis FdU in  $G_2$  phase (Belyaev et al., 1985, 1987b; Ionova, 1994). According to the current B&R theory, FdU-induced chromatid deletions must be assumed to be DSBs, which are formed by nuclease digestion of single-stranded DNA (Bender et al., 1974). Remarkably, all those breaks were restored in the next cell cycle. Neither complete nor incomplete exchanges were formed by the FdU-induced chromatid breaks in the next cell cycle following treatment. We concluded that all chromosomal breaks induced by FdU are not DSBs, but rather represent sites of temporal chromatin decondensation of different sizes (Belyaev et al., 1985).

#### *Combined effects of radiation and 5-fluorodeoxyuridine (FdU)*

FdU abolished formation of the radiation-induced exchanges and increased significantly the amount of breaks if it was applied following irradiation in  $G_2$  phase of *C. capillaris* cells (Belyaev et al., 1985, 1987b; Ionova, 1994). In the next cell cycle, essentially the same spectra of aberrations were observed in cells which were either being treated with radiation plus FdU or just irradiated. All exchanges were complete, the majority of breaks restituted except for a relatively small amount of chromatid breaks which reduplicated to form chromosome-type deletions.

Similar to the chromatid exchanges, formation of subchromatid exchanges was inhibited by FdU (Belyaev et al., 1987a). Subchromatid exchanges reduplicated only as complete chromosome exchanges in the cell cycle following irradiation (Belyaev et al., 1987a). We concluded that radiation-induced subchromatid and incomplete exchanges reflect different stages in formation of complete exchanges that are fixed by the onset of mitotic condensation. In agreement with this conclusion, the proportion of apparently incomplete exchanges increased with decreasing time between fixation of cells and irradiation in  $G_2$  phase (Generalova, 1969, 1975; Belyaev, 1994).

#### *Exchanges are formed by reciprocal recombination regardless of the LET of the radiation, the phase of cell cycle or the type of clastogen*

The same peculiarities in the reduplication of CAs as described above were observed when *C. capillaris* cells were irradiated with neutrons in combination with FdU (Belyaev et al., 1987b). This type of radiation with high linear energy transfer (LET), 66 keV/ $\mu$ m, induced rather dense ionizations. As in case of  $\gamma$ - or X-rays, approximately 30% of chromatid exchanges were incomplete after irradiation with neutrons in  $G_2$  phase. Nevertheless, all exchanges reduplicated to form complete exchanges in the next cell cycle. Formation of almost exclusively complete exchanges was in line with the contact theory. According to the B&R theory, formation of incomplete exchanges should occur especially frequently in the case of high LET radiation which should result in a higher proportion of complex DSBs.

Reduplication of CAs was also studied after their induction by  $\gamma$ -rays and neutrons in S phase (Belyaev, 1994). Both complete and incomplete chromatid exchanges always reduplicated to form complete chromosome type exchanges.

Only a few percent of chromosome type exchanges were usually scored as incomplete by standard cytological techniques after irradiation in  $G_0$ - $G_1$  phases (Dubinina, 1978; Sevan'kaev, 1987). All these data provided strong evidence for the conclusion that radiation-induced exchanges, regardless of LET and the phase of the cell cycle, are always complete and are formed by reciprocal recombination (Belyaev and Akifyev, 1988).

Ionizing radiation is a typical S-independent clastogen (Natarajan, 2002). Approximately 30% of chromatid exchanges were incomplete after treatment of *C. capillaris* cells by the typical S-dependent clastogen N-ethyl-N-nitrosourea (ENU) in  $G_1$  phase (Belyaev, 1994; Ionova, 1994). Both complete and appar-

ently incomplete chromatid exchanges reduplicated to form corresponding complete chromosome exchanges in the cell cycle following treatment. Hence, a recombination mechanism seems to be active following treatment with S-independent and S-dependent clastogens.

#### *Reduplication of deletions*

All chromosome-type deletions induced by radiation in G<sub>1</sub> phase of *C. capillaris* cells reduplicated in the next cell cycle (Sidorov and Sokolov, 1963, 1966; Protopopova and Shapiro, 1968). Contrary to the chromosome deletions, radiation-induced chromatid deletions reduplicated with various efficiencies in different studies. In *C. capillaris* cells, 30–45% of chromatid deletions restituted in the cell cycle following irradiation (Sidorov and Sokolov, 1966; Belyaev et al., 1985, 1987b). An especially high level of the breakage restitution, 60–95%, was observed in case of combined action of radiation and ENU with FdU (Belyaev et al., 1985, 1987b; Belyaev, 1994; Ionova, 1994). No additional exchanges were formed during the restitution. We concluded that most of these breaks are not DSBs but rather reflect sites of temporal chromatin decondensation of different sizes (Belyaev et al., 1985). In some breaks, sister chromatid exchanges or exchanges, which could not be resolved by the standard staining technique, might also be involved.

A proportion of chromatid-type terminal deletions was able to reduplicate in the cell cycle following treatment with clastogens (Sidorov and Sokolov, 1966; Belyaev et al., 1985). Similar to the clastogenic effects of radiation in G<sub>1</sub> and G<sub>0</sub> phases, the amount of those chromatid breaks, which were able to reduplicate, was relatively small as compared to exchanges. We assumed that such breaks should be formed in those specific loci of the chromosome that are able to form telomeres (Belyaev and Akifyev, 1988). In particular, the sites of interstitial telomeric DNA might hypothetically serve as a target for formation of terminal deletions (Belyaev and Akifyev, 1988). Addition of telomeric DNA by telomerases was observed in experiments where DSBs were induced by the *I-SceI* endonuclease (Lo et al., 2002). In ataxia-telangiectasia cells, addition of telomeres has not been detected in breaks by M-FISH analysis (Martin et al., 2003). However, in this and many other studies the breaks were likely just extended gaps but not true deletions.

Isochromatid deletions with non-unions (NUs) never reduplicated to form doubled NUs as shown in Fig. 2B regardless of the type of treatment. The number of NUs was relatively small and whether these aberrations represent extended isochromatid gaps, incomplete chromatid exchanges or sister chromatid exchanges remains to be investigated.

#### **Molecular versions of the contact theory and molecular targets of chromosomal mutagenesis**

The experimental evidence for specific molecular targets in formation of CAs has previously been reviewed (Belyaev and Akifyev, 1988; Belyaev, 1994) and is briefly stated below. First, DNA damage and its repair in the bulk of genomic DNA does

not always correlate with the yield of CAs. Second, ionizing radiation at low LET induces a random distribution of DNA damage in chromosomes. However, the distribution of CAs is frequently non-random. Third, substitution of thymidine by its analogue 5-bromodeoxyuridine (BrdU) in a minor fraction of genomic DNA substantially increases the yield of CAs induced by ultraviolet or ionizing radiation.

Genetically determined dynamic properties of intra- and interchromosomal molecular contacts were postulated in the molecular versions of the contact theory (Luchnik, 1973; Soyfer and Akifyev, 1976; Romanov, 1980). Luchnik (1973) hypothesized that there are two specific checkpoints in the cell cycle where the DNA forms hybrid molecules, P1 immediately before S phase and P2 just before mitosis. Occasional damage of DNA in one of the strands is either repaired in the hybrid molecules or transferred to another strand of DNA. This hypothesis predicts the formation of single-stranded DNA stretches in G<sub>1</sub> and G<sub>2</sub> phases of the cell cycle, which were detected by means of a fluorescent antibody technique (Kon-drashova and Luchnik, 1985).

The molecular model involving homologues recombination (HR) between DNA repeats as a major mechanism for CAs was proposed by Soyfer and Akifyev (1976, 1977). In this model, direct and inverted DNA repeats from the same or different chromosomes were hypothesized to form temporal duplexes. Such duplexes were considered as specific molecular targets for formation of CAs.

#### *Nuclear matrix-associated DNA*

Ganassi and colleagues (1991) hypothesized that only damage localized in DNA associated with the nuclear matrix can result in formation of CAs. The boundaries of DNA domains, which are associated with the nuclear matrix, are hypersensitive to treatment with DNase I (Loc and Stratling, 1988). The same yields of CAs were observed following irradiation or treatment with DNase I under conditions inducing the same amount of DNA breakage (Ganassi et al., 1989). It is interesting to note that DNA involved in tight interaction with matrix proteins is especially sensitive to digestion by restriction endonucleases (REs) (Siakste and Budylin, 1988; Razin et al., 1995). Therefore, data on induction of CAs by REs (Natarajan, 2002) may also point to the role of matrix-associated DNA as a target for chromosomal mutagenesis.

Topoisomerase II (topo II) is a key component of the nuclear matrix that is responsible for attachment of DNA loops (chromatin domains). During regulation of the DNA loop topological structure, topo II cuts DNA at the nuclear matrix attachment sites resulting in DSBs (Razin et al., 1995). Several anti-cancer drugs such as etoposide block the enzyme at the step of resealing of topo II-derived DSBs. Incubation of cells with etoposide results in accumulation of DSBs at the DNA loop attachment points following by formation of CAs (Suzuki and Nakane, 1994; Mosesso et al., 1998).

Various types of DNA repeats are often found at the breakpoints of chromosomal translocations (Echlin-Bell et al., 2003). These involve Alu repeats (Kolomietz et al., 2002), LINE repeats (Taketani et al., 2002), and AT-rich repeats (Kurahashi et al., 2003). Sites of localization of telomeric interstitial

repeats were also shown to be hotspots for CAs (Balajee et al., 1994).

#### *Exchanges between DNA loops; the domain model*

It has been suggested that the chromosomal exchanges are formed between DNA loops (chromatin domains) that have contacts at the attachment sites at the nuclear matrix (Belyaev, 1994). Indirect evidence for this suggestion is that the sequencing of DNA at regions of translocations has shown strong association of breakage/reunion events with the matrix-associated regions (MARs) and topo II sites (Bode et al., 2000). Other types of exchanges, such as rings and inversions, can also have sites for topo II at the exchange region (Wong et al., 1989; Kehrer-Sawatzki et al., 2002). Recent data suggested that topo II may be involved in both RAD51-dependent HR and DNA-PK-dependent non homologous end-joining (NHEJ) (Hansen et al., 2003).

Differences between the total amounts of DSBs and CAs can be explained by assuming that only a minor fraction of DSBs, probably a few percent of the genomic DNA, result in aberrations. DNA associated with nuclear matrix meets this requirement. DNA loop attachment sites and number of DNA loops vary in dependence on cell type, gene activity and cell cycle (Razin et al., 1995). Therefore, different DNA sequences can be localized in the CA breakpoints dependent on the dynamic reattachment of various MARs to the nuclear matrix. Formation of a simple chromosomal exchange occurs with a probability close to one if DSB is induced at the DNA loop attachment sites. The role of single strand breaks (SSBs) is to facilitate recombination by removing topological constraints. The requirement of DSB and SSB can explain the typical dose dependences for radiation-induced CAs. It should be noted that apart from primary DNA damage, the subsequent events in formation of chromosomal aberrations may also be dose dependent (Belyaev, 1994).

Observations of extended prometaphase chromosomes suggested that there are at least 2,000 sub-bands that correspond to the megabase-size chromatin domains in interphase (Kitsberg et al., 1991). If the onset of mitotic condensation starts before restoration of chromatin in one or several such domains they appear in mitotic chromosomes as apparent discontinuities in complete exchanges, gaps, and also extended gaps that are often counted as real chromosomal breaks/deletions. Even stronger interference should be expected in case of premature chromosome condensation (PCC). The time kinetics for radiation-induced changes in chromatin conformation were significantly longer as compared to DSB repair and correlated with kinetics of PCC fragments suggesting that PCC fragments reflect restitution of chromatin rather than repair of DSBs (Belyaev et al., 2001). The majority of PCC fragments along with fragile sites in chromosomes and those deletions, which were not able to reduplicate, were attributed to chromatin decondensation (Belyaev and Akifyev, 1988).

#### **Induction of CAs at the border of the G<sub>1</sub>-S phase**

The hypothetical contacts between chromosomes should disappear before S phase to allow DNA replication (Luchnik, 1973; Soyfer and Akifyev, 1976). In agreement with this prediction,  $\gamma$ -rays and neutrons induced significantly less exchanges at the border of the G<sub>1</sub>-S phases as compared to the middle S phase or G<sub>2</sub> phase (Belyaev et al., 1990). Of these few exchanges, 95% were of chromatid-type and only 5% of chromosome type. Because no more than 10% of DNA was replicated under conditions of synchronization at the G<sub>1</sub>-S phase border, only 10% of the exchanges would be expected to be of chromatid type assuming that CAs are formed by DSBs induced in the bulk of the genomic DNA. In the middle of the S phase, radiations of different qualities induced only chromatid type exchanges. Therefore, the chromosome aberrations were abruptly substituted by the chromatid aberrations at the G<sub>1</sub>-S phase border.

#### **Role of DNA synthesis in the G<sub>1</sub> and G<sub>2</sub> phase in formation of CAs**

According to the hypothesis of duplex formation, DNA synthesis is needed to fill up the DNA gaps during the decay of intra- and interchromosomal contacts, which are formed by homologous pairing of DNA repeats (Soyfer and Akifyev, 1976, 1977). Blockage of this decay should increase the yield of CAs. In agreement with this prediction, pretreatment of cells with inhibitors of DNA synthesis in the G<sub>1</sub> phase of human lymphocytes and *C. capillaris* increased the yield of radiation-induced CAs (Azatian et al., 1976; Tarasov et al., 1976; Korotkov et al., 1980a; Sergievskaya et al., 1985).

It is known, that substitution of thymidine by BrdU increases the yield of CAs induced by ultraviolet or ionizing radiation. Safonova and Tarasov performed experiments, where BrdU was incorporated into DNA of *C. capillaris* cells during different phases of the cell cycle (Safonova and Tarasov, 1973; Tarasov and Safonova, 1973). Incorporation either in G<sub>1</sub> or in G<sub>2</sub> phase resulted in the same sensitization of  $\gamma$ -ray-induced CAs (2.1–2.2 fold) as incorporation in the S phase. Makedonov and Tarasov irradiated cultured Chinese hamster cells with long-wave ultraviolet A (UVA) following incubation with BrdU in G<sub>2</sub> phase (Makedonov and Tarasov, 1982). A significant increase in the yield of CAs was observed. UVA specifically affected BrdU-containing DNA indicating that sites of spontaneous DNA synthesis in the G<sub>2</sub> phase are targets for chromosomal mutagenesis.

In further studies, DNA was pulse-labeled with BrdU in different periods of the S phase in cells synchronized at the G<sub>1</sub>-S phase border (Khakimov et al., 1986, 1989). Wheat root tip cells were pulse-labeled for 2 h in the earliest, middle or late S phase. Despite similar incorporation of BrdU during all three pulses, only labeling in the early S phase resulted in a significant sensitizing effect, an approximately 2-fold increase in the yield of radiation-induced CAs. In later experiments, this 2-hour pulse was split into 30-min pulses. The increase in CAs was 1.5–2 fold following the first 30-min pulse. Only a weak sensi-

tizing effect of BrdU was observed following the subsequent pulses. Similarly, incorporation of BrdU at the very beginning of S phase resulted in maximal radiosensitization in experiments with human lymphocytes (Khakimov et al., 1989).

The radiosensitizing effect of BrdU was approximately 2.4 fold when *C. capillaris* cells were labeled for 1 h in the early S phase immediately after release of the DNA synthesis block (Ionova, 1994). Very similar radiosensitization, namely, 2.9 fold, was observed after labeling for 5 h, i.e., during the whole S phase. In a recent publication (Khakimov et al., 2003), CAs were scored in the metaphase of *C. capillaris* cells following BrdU labeling in early, middle or late S phase and irradiation in the end of the S phase. While sensitization of radiation-induced exchanges was seen in all periods of the S phase, the highest level still occurred at the beginning of S phase. The authors concluded that the DNA sequences responsible for formation of exchanges are replicated at the earliest period of the S phase in synchronized cells and, therefore, should be topologically associated with the nuclear matrix (Ionova, 1994; Khakimov et al., 2003).

Incorporation of BrdU into DNA during the G<sub>1</sub> phase of human lymphocytes, 15–24 h after stimulation with phytohemagglutinin (PHA), resulted in a 1.8-fold increase in radiation-induced exchanges (Akifyev et al., 1995). All exchanges were of the chromosome type indicating that the cells were incubated with BrdU and irradiated in G<sub>1</sub> phase.

Biochemical analysis of DNA which is synthesized in human lymphocytes in G<sub>0</sub> and G<sub>1</sub> phases was performed (Korotkov et al., 1980b; Belyaev et al., 1992). Renaturation kinetics of <sup>3</sup>H-thymidine-labeled DNA was analyzed by elution from a hydroxyapatite column and with digestion of renatured duplexes by S1 nuclease. Preferential localization of the G<sub>1</sub> phase label in DNA repeats was observed. The AT content of G<sub>1</sub> phase-labeled DNA was analyzed either by partial melting followed by S1 digestion or by differential thermal elution from the hydroxyapatite column (Belyaev et al., 1992; Akifyev et al., 1995). In the G<sub>1</sub> phase-labeled DNA, the peak of specific radioactivity was observed in the AT-rich fraction that was denatured by 5% melting of the total extracted DNA. The localization of the G<sub>1</sub> synthesis of DNA in respect to nuclear matrix was analyzed using treatment of nuclear matrix preparations with micrococcal endonuclease. Under most stringent conditions of the treatment, approximately 1% of the label incorporated in S phase remained in the nuclear matrix. Under these conditions, 30–40% of the label incorporated in G<sub>1</sub> phase was still associated with the nuclear matrix. It should be noticed, that peripheral blood lymphocytes usually contain a small fraction, 0.1–1%, of S phase cells. Therefore, the impact of these cells could mask the differences between G<sub>1</sub> and S phase DNA synthesis.

Finally, incorporation of thymidine in DNA of lymphocytes in G<sub>1</sub> phase has been localized to a minor fraction of AT-rich DNA repeats associated with the nuclear matrix. These data are in line with the molecular models predicting local synthesis of DNA at the sites of contacts that are responsible for formation of CAs (Luchnik, 1973; Soyfer and Akifyev, 1976).

### **Modeling of the CA formation in the framework of the contact theory**

In the framework of the contact theory, the mutual position of homologous chromosomes in cells of *D. melanogaster* was analyzed using data from intrachromosomal exchanges (Chubykin and Omel'yanchuk, 1989).

The classification system CPCL (chromosome, position, contacting elements, location) was proposed for theoretical analysis of CAs (Andreev and Eidelman, 2001). In the CPCL system, types and frequencies of CAs were described on the basis of contacts of the damaged chromosome subunits at a given number of initial lesions dependent on dose and LET of ionizing radiation. The exchanges were formed with a probability close to one if the contacts are damaged (Andreev and Eidelman, 2001). The intrachromosomal changes were simulated in the human chromosome 1 using the CPCL system and in assumption of the globular model of the interphase chromosome (Andreev and Eidelman, 1999, 2002). The authors compared the results of simulation with the experimental data and concluded that the proposed model fitted reasonably well to the experimental results for intrachanges in the chromosome 1 as obtained with the FISH technique (Andreev and Eidelman, 2002).

### **Proteins involved in DSB repair as possible markers of CAs**

Several proteins such as the tumor suppressor p53 binding protein 1 (53BP1) and phosphorylated H2AX ( $\gamma$ -H2AX) have been shown to produce discrete foci colocalizing to DSBs and providing a scaffold structure for DSB repair (DiTullio et al., 2002). According to the current model, this scaffold functions by recruiting proteins involved in the repair of DSBs (Fernandez-Capetillo et al., 2002; Iwabuchi et al., 2003; Kao et al., 2003). The scaffold is organized within a megabase-size chromatin domain around an actual DSB regardless of the type of repair that is further involved (Paull et al., 2000).

We have found, that residual 53BP1 foci remained in human lymphocytes, human fibroblasts VH-10, and HeLa cells for a long time after irradiation, 12–24 h, dependent on dose and cell type (Belyaev et al., 2002; Markova et al., 2003). Several studies indicated a correlation between radiosensitivity and residual foci (Belyaev et al., 2002; Iwabuchi et al., 2003; Markova et al., 2003; Rothkamm et al., 2003). We hypothesized that residual foci may colocalize with DSBs occurring in the DNA associated with nuclear matrix and the breakpoints of CAs (Markova et al., 2003). In agreement with this hypothesis, some residual 53BP1 foci remained even upon extraction of proteins with a standard high salt-detergent protocol for nuclear matrix preparation (Markova et al., 2003). The proteins involved in HR may be specific markers for chromosomal exchanges.

Establishment of specific protein markers for breakpoints of CAs would provide a possibility for the analysis of CAs directly in interphase cells. To prove this hypothesis, co-localization of residual foci and CAs should be verified in mitotic cells using

FISH technique. Primary  $\gamma$ -H2AX foci have been observed in anaphases of *M. muntjac* cells and CHO cells, in the prometaphase of HeLa cells and in mitosis of human MCF cells (Rogakou et al., 1999; Jullien et al., 2002; Kao et al., 2003; Rothkamm et al., 2003). We observed few 53BP1 and  $\gamma$ -H2AX residual foci in metaphases of human lymphocytes, VH-10 and HeLa cells following irradiation (Markova et al., 2003).

### CAs and chromatin dynamic rearrangement

It was shown using FISH staining that irradiation of human lymphocytes resulted in the displacement of pericentromeric regions of chromosome 1 from the nuclear periphery to the inner territory of a nucleus (Karpukhin et al., 1994; Spitzkovsky et al., 2002, 2003).

It was also shown that homologous chromosomes 7 and 21 rearranged and became closer together in the interphase nuclei of human skin fibroblasts and lung endothelial cells in response to ionizing radiation (Dolling et al., 1997). A movement of homologous chromosomes 9 in response to treatment of human lymphocytes with mitomycin C or irradiation was recently observed using FISH painting of whole chromosomes and band-specific probes (Abdel-Halim et al., 2004).

These data provided evidence that dose- and time-dependent rearrangement of chromatin and movement of separate

parts and whole chromosomes may occur in response to clastogens resulting in new contacts for formation of CAs. The oscillatory movements of chromosome territories occasionally exceeding a distance of 4  $\mu$ m were observed during interphase in living HeLa cells (Walter et al., 2003). Hence, mutual repositioning of chromosomes and chromatin domains is also possible in intact cells. It is attractive to hypothesize that such repositions are induced in response to clastogenic insults in such mutual configurations of chromosomes, which facilitate repair of DSBs, especially those localized at the nuclear matrix DNA and possibly result in formation of CAs.

### Acknowledgments

I am very thankful to A.P. Akifiev, N.V. Grigorova, D.I. Edneral, M.Yu. Ionova (Ivanishcheva), Kh.A. Khakimov, G.A. Khudoly, E.V. Korotkov, M. Protopopova, G. Selivanova, A.B. Semakin, E. Markova, and N. Schultz for interesting collaborations and discussions. I thank S.G. Andreev, E.E. Ganassi, N.N. Dubinin, O.V. Evgrafov, N.V. Luchnik, G.P. Makedonov, A.V. Sevan'kaev, and D.M. Spitzkovsky for discussions on the nature of CAs. Special thanks to M. Harms-Ringdahl and A.T. Natarajan for encouragement in writing this paper, and J.R.K. Savage for his valuable comments. I would also like to thank O. Terenius for reading and useful corrections to the manuscript, and Y. Belyaev for his help with preparation of figures.

### References

- English translations of titles of articles written in the Russian language are given in square brackets.
- Abdel-Halim HI, Imam SA, Badr FM, Natarajan AT, Mullenders LHF, Boei JJWA: Ionizing radiation induced instant pairing of heterochromatin of homologous chromosomes in human cells. *Cytogenet Genome Res*, this issue pp 193–199 (2004).
- Akifiev AP, Khudoly GA, Iakimenko AV, Krasnopevtsev AV, Khandogina EK: [The G1-process in human lymphocytes cultured with PHA, and formation of radiation-induced chromosome aberrations]. *Genetika* 31:485–491 (1995).
- Andreev SG, Eidelman IA: [Globular model of interphase chromosome and intrachromosomal exchange aberrations]. *Radiats Biol Radioecol* 39:10–20 (1999).
- Andreev SG, Eidelman IA: [Rejoining pathways underlying intrachange formation depend on interphase chromosome structure]. *Radiats Biol Radioecol* 41:469–474 (2001).
- Andreev SG, Eidelman Y: Intrachromosomal exchange aberrations predicted on the basis of the globular interphase chromosome model. *Radiat Prot Dosimetry* 99:193–196 (2002).
- Aptikaeva GF, Zaichkina SI, Ganassi EE: [Modification by caffeine of radiation induced chromosome damage in the first and the second division after irradiation]. *Radiobiologiya* 23:250–253 (1983).
- Azatian RA, Voskanian AZ, Zakarian MS, Akifiev AP: [Modification of radiation-induced injuries of the chromosomes of *Crepis capillaris* L in the G<sub>1</sub> phase by inhibition of additional DNA synthesis in the G<sub>2</sub> phase]. *Radiobiologiya* 16:449–454 (1976).
- Balajee AS, Oh HJ, Natarajan AT: Analysis of restriction enzyme-induced chromosome aberrations in the interstitial telomeric repeat sequences of CHO and CHE cells by FISH. *Mutat Res* 307:307–313 (1994).
- Belyaev IY: [Cytogenetic analysis of radiation- and chemically-induced chromosomal aberrations in *Crepis capillaris* cells], p 41, DSc Thesis (Saint-Petersburg State University, Saint-Petersburg 1994).
- Belyaev IY, Akifiev AP: [Genetic processes and the problem of the target in chromosomal mutagenesis]. *Genetika* 24:1384–1392 (1988).
- Belyaev IY, Semakin AB, Grigorova NV, Akifiev AP: [Reproduction in the second nuclear cycle of chromosome aberrations induced in the G<sub>2</sub> phase of *Crepis capillaris* cells by gamma rays, 5-fluoro-2-deoxyuridine and their combined action]. *Dokl Akad Nauk SSSR* 285:1209–1212 (1985).
- Belyaev IY, Grigorova NV, Ivanishcheva MY, Akifiev AP: [Experimental analysis of radiation-induced stickiness of chromosomes in *Crepis capillaris* cells]. *Radiobiologiya* 27:313–317 (1987a).
- Belyaev IY, Ivanishcheva MY, Akifiev AP: [Reproduction of chromatid aberrations induced in *Crepis capillaris* cells by neutrons and 5-fluoro-2-deoxyuridine in the second nuclear cycle]. *Dokl Akad Nauk SSSR* 295:227–230 (1987b).
- Belyaev IY, Ivanishcheva MY, Yedneral DI, Akifiev AP: [Replicative phase transition in interphase nucleus and its role for formation of radiation-induced exchange aberrations]. *Genetika* 26:971–975 (1990).
- Belyaev IY, Khudoly GA, Korotkov YV, Akifiev AP: Localized recombinational repair in human lymphocytes, in Kyriakidis DA (ed.): 9th Balkan Biochemical and Biophysical Days, pp 206 (Aristotle University of Thessaloniki Press, Thessaloniki 1992).
- Belyaev IY, Czene S, Harms-Ringdahl M: Changes in chromatin conformation during radiation-induced apoptosis in human lymphocytes. *Radiat Res* 156:355–364 (2001).
- Belyaev IY, Torudd J, Protopopova M, Nygren J, Eriksson S, Chovanec M, Selivanova G, Harms-Ringdahl M: Radiation-induced apoptosis in human lymphocytes: possible relationship to unrepaired DNA double strand breaks and DNA-loop organisation, in Boniver J, De Saint-Georges L, Humblet C, Maisin JR (eds): 32nd Annual Meeting of the European Society for Radiation Biology (ESRB), pp 94 (Eurogentec, Liege 2002).
- Bender MA, Griggs HG, Bedford JS: Mechanisms of chromosomal aberration production. 3. Chemicals and ionizing radiation. *Mutat Res* 23:197–212 (1974).
- Bode J, Benham C, Ernst E, Knopp A, Marschalek R, Strick R, Strissel P: Fatal connections: when DNA ends meet on the nuclear matrix. *J Cell Biochem Suppl* 35:3–22 (2000).
- Brecher S: Ultrastructural observations of X-ray induced chromatid gaps. *Mutat Res* 42:249–267 (1977).
- Brinkley BR, Hittelman WN: Ultrastructure of mammalian chromosome aberrations. *Int Rev Cytol* 42:49–101 (1975).
- Chubykin VL, Omel'yanchuk LV: [Mutual positioning of homologous chromosomes based on the data on intrachromosomal exchanges]. *Genetika* 25:292–300 (1989).

- Demin YS: [Cytogenetics of primary radiation injury of chromosomes]. *Uspehi Sovremennoi Biologii* 78: 188–200 (1974).
- DiTullio RA Jr, Mochan TA, Venere M, Bartkova J, Sehested M, Bartek J, Halazonetis TD: 53BP1 functions in an ATM-dependent checkpoint pathway that is constitutively activated in human cancer. *Nature Cell Biol* 4:998–1002 (2002).
- Dolling JA, Boreham DR, Brown DL, Raaphorst GP, Mitchel RE: Rearrangement of human cell homologous chromosome domains in response to ionizing radiation. *Int J Radiat Biol* 72:303–311 (1997).
- Dubinina NP, Akif'ev AP, Vishtynetskaya TA: [Evidence of the transmission of replicating instability to newly synthesized strands in chromosomal DNA molecules]. *Sov Genet* 7:833–837 (1973).
- Dubinina NP, Dubinina LG, Shanazarova AS: [Structural mutations of chromosomes in the 2<sup>nd</sup> cell cycle during radiation and chemical mutagenesis]. *Dokl Akad Nauk SSSR* 228:467–469 (1976).
- Dubinina LG: [Structural mutations in experiments with *Crepis capillaris*]. Nauka, Moscow 1978.
- Echlin-Bell DR, Smith LL, Li L, Strissel PL, Strick R, Gupta V, Banerjee J, Larson R, Relling MV, Raimondi SC, Hayashi Y, Taki T, Zeleznik-Le N, Rowley JD: Polymorphisms in the MLL breakpoint cluster region (BCR). *Hum Genet* 113:80–91 (2003).
- Ergun MA, Karaoguz MY, Ince GD, Tan E, Menevse A: Determination of a translocation chromosome by atomic force microscopy. *Scanning* 24:204–206 (2002).
- Fernandez-Capetillo O, Chen HT, Celeste A, Ward I, Romanienko PJ, Morales JC, Naka K, Xia Z, Camerini-Otero RD, Motoyama N, Carpenter PB, Bonner WM, Chen J, Nussenzweig A: DNA damage-induced G<sub>2</sub>-M checkpoint activation by histone H2AX and 53BP1. *Nature Cell Biol* 4:993–997 (2002).
- Ganassi EE, Zaichkina SI, Rozanova OM: [Modeling, using nucleases, of the effect of radiation on Chinese hamster fibroblasts. On the role of single-stranded DNA breaks, induced by DNAase I, in the initiation of chromosome aberrations]. *Radiobiologiya* 29:742–745 (1989).
- Ganassi EE, Zaichkina SI, Rozanova OM, Aptikaeva GF, Akhmadieva A: [Chromosome mutagenesis and cytogenetic monitoring]. *Radiobiologiya* 31: 882–888 (1991).
- Generalova MV: [Union of chromosome fragments in early stages after X-irradiation]. *Dokl Akad Nauk SSSR* 184:211–213 (1969).
- Generalova MV: [Structure of the interphase nucleus and formation of chromosome aberrations in *Crepis capillaris*]. *Genetika* 11:40–54 (1975).
- Hansen LT, Lundin C, Spang-Thomsen M, Petersen LN, Helleday T: The role of RAD51 in etoposide (VP16) resistance in small cell lung cancer. *Int J Cancer* 105:472–479 (2003).
- Ionova MY: [Cytogenetic evidence for the contact mechanism in the formation of chromosomal aberrations in *Crepis capillaris* cells], p 25, PhD thesis (Institute of General Genetics, Russian Academy of Science, Moscow 1994).
- Iwabuchi K, Basu BP, Kysela B, Kurihara T, Shibata M, Guan D, Cao Y, Hamada T, Imamura K, Jeggo PA, Date T, Doherty AJ: Potential role for 53BP1 in DNA end-joining repair through direct interaction with DNA. *J Biol Chem* 278:36487–36494 (2003).
- Jullien D, Vagnarelli P, Earnshaw WC, Adachi Y: Kinetochores localisation of the DNA damage response component 53BP1 during mitosis. *J Cell Sci* 115:71–79 (2002).
- Kao GD, McKenna WG, Guenther MG, Muschel RJ, Lazar MA, Yen TJ: Histone deacetylase 4 interacts with 53BP1 to mediate the DNA damage response. *J Cell Biol* 160:1017–1027 (2003).
- Karpukhin AV, Gotmar I, Karpukhin SA, Salimov AG, Veiko NN, Bogush AI, Spitkovskii DM: [Disposition of pericentromeric heterochromatin chromosomal segments in human interphase lymphocyte nuclei]. *Dokl Akad Nauk* 336:414–417 (1994).
- Kehrer-Sawatzki H, Schreiner B, Tanzer S, Platzer M, Muller S, Hameister H: Molecular characterization of the pericentric inversion that causes differences between chimpanzee chromosome 19 and human chromosome 17. *Am J Hum Genet* 71:375–388 (2002).
- Khakimov KA, Ergashev A-KE, Makedonov GP, Akif'ev AP: [Peculiarities of the mutagenic effect of gamma-rays and N-nitrosomethylurea in different periods of the DNA synthesis phase]. *Biopolimery i kletka* 2:206–211 (1986).
- Khakimov KA, Chikhladze TA, Khudolii GA, Akif'ev AP: [Cytogenetic effect of the radiosensitizing action of 5-bromo-2'-deoxyuridine on eukaryotic cells at various periods of the DNA synthesis phase]. *Genetika* 25:469–476 (1989).
- Khakimov KA, Latypova EA, Yakubova RA, Akif'ev AP: [Radiosensibilizing effect of 5-bromodeoxyuridine in different periods of S-phase in the root tip cells of *Crepis capillaris*]. *Doklady RUZ* 4:65–68 (2003).
- Kitsberg D, Selig S, Cedar H: Chromosome structure and eukaryotic gene organization. *Curr Opin Genet Dev* 1:534–537 (1991).
- Kolomietz E, Meyn MS, Pandita A, Squire JA: The role of Alu repeat clusters as mediators of recurrent chromosomal aberrations in tumors. *Genes Chrom Cancer* 35:97–112 (2002).
- Kondrashova TV, Luchnik NV: [Appearance of single-stranded regions in DNA molecules in the G<sub>1</sub> stage and the formation of structural mutations]. *Genetika* 21:517–521 (1985).
- Korotkov EV, Akif'ev AP, Ivanov VI: [Effect of 5-fluoro-2-deoxyuridine on gamma-induced chromosome aberration formation in the G<sub>1</sub> phase in human lymphocytes]. *Radiobiologiya* 20:592–595 (1980a).
- Korotkov EV, Bokhon'ko AI, Petrov OE, Akif'ev AP: [Noninduced local DNA synthesis in the G<sub>1</sub> phase and its relationship to chromosomal mutagenesis]. *Dokl Akad Nauk SSSR* 252:475–478 (1980b).
- Kurahashi H, Shaikh T, Takata M, Toda T, Emanuel BS: The constitutional t(17;22): another translocation mediated by palindromic AT-rich repeats. *Am J Hum Genet* 72:733–738 (2003).
- Levitsky GA, Araratyan AG: [Rearrangement of chromosomes by X-rays.] *Trudy po prikladnoi botanike, genetike i selektsii* 27:265–269 (1931).
- Lo AW, Sprung CN, Foualdi B, Pedram M, Sabatier L, Ricoul M, Reynolds GE, Murnane JP: Chromosome instability as a result of double-strand breaks near telomeres in mouse embryonic stem cells. *Mol Cell Biol* 22:4836–4850 (2002).
- Loc PV, Stratling WH: The matrix attachment regions of the chicken lysozyme gene co-map with the boundaries of the chromatin domain. *EMBO J* 7:655–664 (1988).
- Luchnik NV: [Genetic information exchange in the cell cycle]. *Dokl Akad Nauk SSSR* 212:985–988 (1973).
- Mace ML Jr, Daskal Y, Wray W: Scanning-electron microscopy of chromosome aberrations. *Mutat Res* 52:199–206 (1978).
- Makedonov GP, Tarasov VA: [Directed modification of the damaged DNA region in inducing structural chromosomal mutations]. *Genetika* 18:1101–1106 (1982).
- Markova E, Schultz N, Torudd J, Harms-Ringdahl M, Protopopova M, Selivanova G, Khakimov H, Belyaev I: Validation of novel DSB-co-localizing foci assay for radiosensitivity. 12th International Congress of Radiation Research. ICMS, p 235 (Pty Ltd, Brisbane 2003).
- Martin M, Genesca A, Latre L, Ribas M, Miro R, Egozcue J, Tusell L: Radiation-induced chromosome breaks in ataxia-telangiectasia cells remain open. *Int J Radiat Biol* 79:203–210 (2003).
- Mosesso P, Darroudi F, van den Berg M, Vermeulen S, Palitti F, Natarajan AT: Induction of chromosomal aberrations (unstable and stable) by inhibitors of topoisomerase II, m-AMSA and VP16, using conventional Giemsa staining and chromosome painting techniques. *Mutagenesis* 13:39–43 (1998).
- Mullinger AM, Johnson RT: Scanning electron microscope analysis of structural changes and aberrations in human chromosomes associated with the inhibition and reversal of inhibition of ultraviolet light induced DNA repair. *Chromosoma* 96:39–44 (1987).
- Natarajan AT: Chromosome aberrations: past, present and future. *Mutat Res* 504:3–16 (2002).
- Nemtseva LS: [Metaphase technique for chromosome rearrangements] (Nauka, Moscow 1970).
- Obe G, Pfeiffer P, Savage JR, Johannes C, Goedecke W, Jeppesen P, Natarajan AT, Martinez-Lopez W, Folle GA, Drets ME: Chromosomal aberrations: formation, identification and distribution. *Mutat Res* 504:17–36 (2002).
- Paull TT, Rogakou EP, Yamazaki V, Kirchgessner CU, Gellert M, Bonner WM: A critical role for histone H2AX in recruitment of repair factors to nuclear foci after DNA damage. *Curr Biol* 10:886–895 (2000).
- Protopopova EM, Shapiro NI: [On duration of radiation-induced potential lesions in chromosomes]. *Genetika* 4:5–14 (1968).
- Razin SV, Gromova II, Iarovaia OV: Specificity and functional significance of DNA interaction with the nuclear matrix: new approaches to clarify the old questions. *Int Rev Cytol* 162B:405–448 (1995).
- Rogakou EP, Boon C, Redon C, Bonner WM: Megabase chromatin domains involved in DNA double-strand breaks in vivo. *J Cell Biol* 146:905–916 (1999).
- Romanov VP: [DNA molecule interaction in the contact mechanism of chromosome aberration formation]. *Genetika* 16:634–643 (1980).
- Rothkamm K, Kruger I, Thompson LH, Lobrich M: Pathways of DNA double-strand break repair during the mammalian cell cycle. *Mol Cell Biol* 23: 5706–5715 (2003).
- Safonova GM, Tarasov VA: [Sensibilizing effect of 5-bromodeoxyuridine upon gamma-irradiation of *Crepis capillaris* cells in the presynthetic period of mitotic cycle]. *Genetika* 9:41–46 (1973).
- Savage JR: A brief survey of aberration origin theories. *Mutat Res* 404:139–147 (1998).
- Serebrovsky AS: A general scheme for origin of mutations. *Am Naturalist* 63:374–378 (1929).
- Sergievskaia SP, Dubinina LG, Kurashova ZI: [Radiation-induced mutagenesis in presence of the DNA synthesis inhibitor (sensibilization and antimutagenesis)]. *Genetika* 21:69–73 (1985).
- Sevan'kaev AV: [Radiosensitivity of chromosomes of human lymphocytes in mitotic cycle] (Energatomizdat, Moscow 1987).
- Siakste NI, Budylin AV: [Changes in the interaction of DNA with chromatin and nuclear matrix proteins during digestion of nuclei with restrictases and nuclease Bal 31]. *Biokhimiia* 53:54–60 (1988).
- Sidorov VP: [Cytogenetic study of the combined effect of ethyleneimine and gamma rays on cells of *Crepis capillaris* seeds in 2 successive mitotic cycles]. *Genetika* 10:33–41 (1974).
- Sidorov BN, Sokolov NN: [Radiation analysis of chromosome discreteness in process of autoreproduction]. *Radiobiologiya* 3:415–419 (1963).



- Sidorov BN, Sokolov NN: [Experimental investigation of radiosensitivity of different phases of mitosis in *Crepis capillaris*], in Dubinin NP (ed): Effect of Ionizing Radiations on Heredity, pp 220–229 (Nauka, Moscow 1966).
- Soyfer VN, Akifyev AP: [Molecular mechanisms in formation of chromosomal rearrangements]. Zhurnal Obshchej Biologii 37:854–869 (1976).
- Soyfer VN, Akifyev AP: Molecular mechanisms of the origin of chromosomal aberrations and the structural organization of eukaryotic DNA. Theoret Appl Genet 50:63–72 (1977).
- Spitkovsky DM, Kuzmina IV, Makarenkov AS, Terekhov SM, Karpukhin AV: [Interphase chromosome locus displacement induced by low-doses of radiation]. Radiats Biol Radioecol 42:604–607 (2002).
- Spitkovsky DM, Veiko NN, Ermakov AV, Kuz'mina IV, Makarenkov AS, Salimov AG, Terekhov SM, Karpukhin AV: [Structural and functional changing induced by exposure to adaptive doses of X-rays in the human lymphocytes both normal and defective by reparation of DNA double strands breaks]. Radiats Biol Radioecol 43:136–143 (2003).
- Stadler LJ: The experimental modification of heredity in crop plants. J Scient Agric 2:557–572 (1931).
- Suzuki H, Nakane S: Differential induction of chromosomal aberrations by topoisomerase inhibitors in cultured Chinese hamster cells. Biol Pharm Bull 17:222–226 (1994).
- Taketani T, Taki T, Shibuya N, Kikuchi A, Hanada R, Hayashi Y: Novel NUP98-HOXC11 fusion gene resulted from a chromosomal break within exon 1 of HOXC11 in acute myeloid leukemia with t(11;12)(p15;q13). Cancer Res 62:4571–4574 (2002).
- Tarasov VA, Safonova GM: [Sensibilizing effect of 5-bromodeoxyuridine upon gamma-irradiation of *Crepis capillaris* cells in postsynthetic period of mitotic cycle]. Genetika 9:35–42 (1973).
- Tarasov VA, Safonova GM, Sidorov VP, Myasova ZN: [Sensibilizing effect of 5-bromodeoxyuridine on gamma-irradiation in postsynthetic period of cell cycle of *Crepis capillaris*]. Genetika 12:44–49 (1976).
- Uehara S, Sasaki H, Takabayashi T, Yajima A: Structural aberrations of metaphase derivative chromosomes from reciprocal translocations as revealed by scanning electron microscopy. Cytogenet Cell Genet 74:76–79 (1996).
- Walter J, Schermelleh L, Cremer M, Tashiro S, Cremer T: Chromosome order in HeLa cells changes during mitosis and early G<sub>1</sub>, but is stably maintained during subsequent interphase stages. J Cell Biol 160:685–697 (2003).
- Wong C, Kazazian HH Jr, Stetten G, Earnshaw WC, Van Keuren ML, Antonarakis SE: Molecular mechanism in the formation of a human ring chromosome 21. Proc natl Acad Sci, USA 86:1914–1918 (1989).

# Progress towards understanding the nature of chromatid breakage

P.E. Bryant, L.J. Gray and N. Peresse

Cancer Biology Group, Bute Medical School, University of St Andrews, St Andrews (Scotland)

**Abstract.** The wide range of sensitivities of stimulated T-cells from different individuals to radiation-induced chromatid breakage indicates the involvement of several low penetrance genes that appear to link elevated chromatid breakage to cancer susceptibility. The mechanisms of chromatid breakage are not yet fully understood. However, evidence is accumulating that suggests chromatid breaks are not simply expanded DNA double-strand breaks (DSB). Three models of chromatid breakage are considered. The classical breakage-first and the Revell “exchange” models do not accord with current evidence. Therefore a derivative of Revell’s model has been proposed whereby both spontaneous and radiation-induced chromatid breaks result from DSB signaling and rearrangement processes from within large looped chromatin domains. Examples of such rearrangements can be observed by harlequin staining whereby an exchange of strands occurs immediately adjacent to the break site. However, these interchromatid rearrangements comprise less than 20% of the total breaks. The rest are thought to result from intrachromatid rearrangements, including a very small proportion involving complete excision of a looped domain. Work is in progress with the aim of revealing these rearrange-

ments, which may involve the formation of inversions adjacent to the break sites. It is postulated that the disappearance of chromatid breaks with time results from the completion of such rearrangements, rather than from the rejoining of DSB. Elevated frequencies of chromatid breaks occur in irradiated cells with defects in both nonhomologous end-joining (NHEJ) and homologous recombination (HR) pathways, however there is little evidence of a correlation between reduced DSB rejoining and disappearance of chromatid breaks. Moreover, at least one treatment which abrogates the disappearance of chromatid breaks with time leaves DSB rejoining unaffected. The I-SceI DSB system holds considerable promise for the elucidation of these mechanisms, although the break frequency is relatively low in the cell lines so far derived. Techniques to study and improve such systems are under way in different cell lines. Clearly, much remains to be done to clarify the mechanisms involved in chromatid breakage, but the experimental models are becoming available with which we can begin to answer some of the key questions.

Copyright © 2003 S. Karger AG, Basel

Perhaps astonishingly, even after some 70 years of radiation cytogenetic research the precise nature and mechanisms of the origin of chromatid breaks still remain elusive. However, it has become evident that there is little or no similarity between the

mechanism of G<sub>2</sub> phase chromatid breakage and chromosome breakage occurring in G<sub>1</sub> or G<sub>0</sub>. For example, when the frequencies of G<sub>2</sub> chromatid breaks were plotted against micronuclei (following G<sub>0</sub> irradiation) there was a complete lack of correlation between the two end-points (Scott et al., 1999). It has also become clear from radiation studies of both fibroblasts (Sanford et al., 1989) and PHA-stimulated peripheral blood lymphocytes (Scott et al., 1994; Riches et al., 2001) that there is a wide variation in the human response to ionizing radiation when assessed by the frequency of chromatid breaks. It has been known for many years that certain radiosensitive syndromes, e.g. ataxia telangiectasia and Nijmegen breakage syndrome, show elevated frequencies of chromatid breaks (Taylor,

Supported by Cancer Research UK, EPSRC and a SHEFC-Strategic Development Grant.

Received 10 September 2003; manuscript accepted 16 December 2003.

Request reprints from Peter E. Bryant, Cancer Biology Group, Bute Medical School University of St Andrews, St Andrews KY16 9TS (Scotland)  
telephone: 0044 1334 463 510; fax: 0044 1334 463 482  
e-mail: peb@st-and.ac.uk

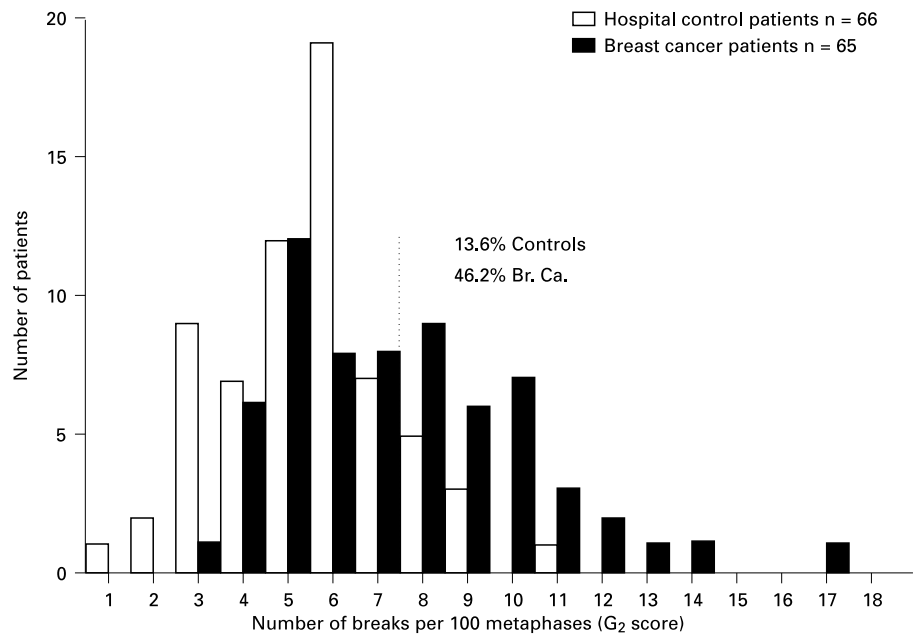


**Fig. 1.** Redrawn from Riches et al. (2001) showing elevated chromatid radiosensitivity of PHA stimulated peripheral blood lymphocytes in a group of breast cancer cases when compared to a matched series of normal non-cancer surgical cases. The dotted line delineates the cut-off point at the 90th percentile. Cases above this line are considered as showing abnormal radiosensitivity.

1978; Taalman et al., 1983). However, interest in the mechanism of chromatid breakage has been reawakened in recent years by the finding that blood from a high proportion of cancer sufferers (particularly breast cancer, but also of other cancer types) shows elevated frequencies of chromatid breaks (Scott et al., 1994, 1999; Terzoudi et al., 2000; Baria et al., 2001; Papworth et al., 2001; Riches et al., 2001). Typically, some 40% of breast cancer cases show this elevated “chromatid radiosensitivity” in contrast to only some 6% in a similar matched group of normal (non-cancer) surgical cases (Fig. 1).

It was postulated that the elevated chromatid radiosensitivity of breast cancer cases is indicative of the presence of low penetrance cancer-predisposing genes (Scott et al., 1994). Furthermore, the radiosensitive phenotype displayed by breast cancer cases is seemingly inherited in a Mendelian fashion (Roberts et al., 1999).

Our current research is therefore aimed at understanding the mechanisms of chromatid breaks, a knowledge of which may help reveal why certain individuals are cancer-prone and eventually lead to identification of the low-penetrance genes involved.

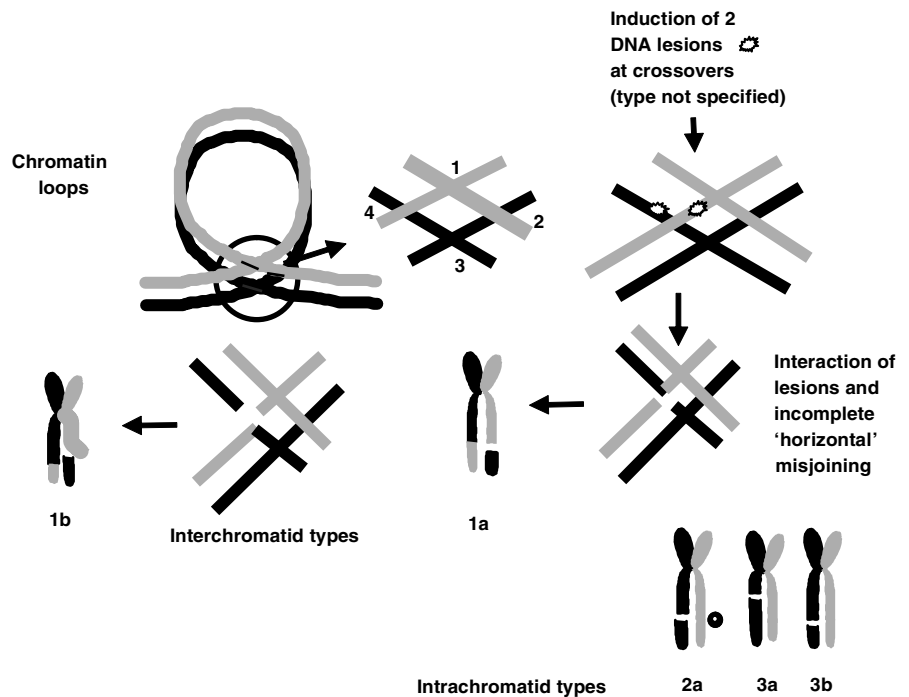
### Models of chromatid breakage

Three models of chromatid breakage have been postulated: the “breakage-first” or “breakage-reunion” hypothesis (Sax, 1940; Bender et al., 1974), Revell’s “exchange” hypothesis (Revell, 1959), and the “signal” model (Bryant, 1998a, b). The breakage-first model assumes the chromatid is broken by the passage of an electron and in the latter version (Bender et al., 1974) a DNA double-strand break (DSB) is assumed to be the lesion, which when expanded leads to a visible chromatid break at metaphase. Evidence does indeed support the DSB as the

initiating lesion (Natarajan et al., 1980; Bryant, 1984; Natarajan and Obe, 1984; Rogers-Bald et al., 2000). However, it is unlikely that a DSB that comprises the loss of only a few base pairs could be expanded into the multi-megabase-pair lesion representing even the smallest visible chromatid break. Indeed, a simple blunt-ended DSB with no nucleotide loss (3′-hydroxyl and 5′-phosphoryl end groups) engendered by treatment of a porated cell with a restriction endonuclease such as *PvuII* (e.g. Bryant, 1984) is capable of efficiently causing chromatid breaks of the same types as those produced by ionizing radiation. Moreover, it is well known that around 16% of radiation, restriction endonuclease or spontaneously induced chromatid breaks are formed by a different mechanism (i.e. different from the breakage-first mechanism) involving sister chromatid interactions and rearrangements (e.g. Harvey and Savage, 1997; Mozdarani et al., 2001). This type of chromatid break can be detected in BrdU-labeled cells by fluorescence-plus-Giemsa (FPG) or harlequin staining.

The Revell exchange model postulated that chromatid breaks arise by interaction of two (undefined) lesions occurring close together at the crossover points of looped chromatin domains (Fig. 2). However, the chance of such a dual event would be exceedingly low in the radiation dose-range used to generate chromatid breaks in G<sub>2</sub> irradiation (typically 0.5 Gy or less) and would be even less probable in the case of spontaneous chromatid breakage. Furthermore, this “two-hit” model predicts a quadratic dose-response since the probability of two events occurring in a small volume (i.e. crossover point of chromatids) would increase with radiation dose. In contrast, evidence demonstrates that chromatid breakage in mammalian cells is a linear function of dose (Bryant, 1998a, b). Evidence from genetically engineered mammalian cells containing a *I-SceI* DSB site shows that a single DSB in a cell’s genome is sufficient to cause a chromatid break (Rogers-Bald et al., 2000).

**Fig. 2.** Revell's "exchange" model for chromatid breaks explained. The two interacting and "exchange-initiating" lesions were not defined (Revell, 1959). Revell classified the various types of single chromatid breaks as shown. Two types (1a and 1b) out of a total of five would according to the model, show color-switches at break points. Hence his prediction that 40% should show color-switches, assuming all types of exchanges (i.e. rearrangements) were equally likely. This prediction was not generally borne out by experimentation, and color-switch breaks are found to comprise only about 16% of total chromatid breaks. Note: As a result of the interchromatid exchange, types 1a and 1b end up with a transferred chromatin loop, lengthening one or the other chromatid.



Also, chromatid breaks, including those known to arise by interchromatid rearrangements are induced by carbon K X-rays, where the generation of DSB in more than one DNA strand is improbable (Bryant et al., 2003). Thus, evidence does not support the Revell model.

The signal model (Bryant, 1998a) was derived from Revell's model (Fig. 2) in the sense that the process of formation of chromatid breaks involved interactions between sister chromatids at the bases of looped domain structures. However, with the significant difference from the Revell model that a single DSB occurring within a large looped domain initiates a chromatin rearrangement either within or between chromatids, by a signaling process. The initiating DSB would itself then be rejoined by the process of NHEJ (Pfeiffer et al., 2004) and would no longer participate in the formation of the rearrangement leading to the chromatid break. Although so far only a model, without supporting evidence, the proposed mechanism allows for the dissociation of DSB rejoining from the chromatin rearrangement process. It has been assumed by some authors (e.g. Parshad et al., 1990) that the disappearance of chromatid breaks with time after irradiation represents DSB rejoining (i.e. based on the breakage-first model outlined above) but there are several examples of experimental data clearly demonstrating a lack of correlation between DSB rejoining and the disappearance of chromatid breaks. For example, Fig. 3a shows that treatment of hamster CHO cells in G<sub>2</sub> with the nucleoside analogue 9-β-D-arabinosyladenine (ara A) at 100 μM leads to a complete inhibition of the normal disappearance of chromatid breaks with time after irradiation, but in this cell line does not affect DSB rejoining at this concentration (Fig. 3b). The action of ara A both in cells and cell extracts has been shown to involve phosphorylation and subsequent competition with dATP lead-

ing to inhibition of both α- and β-polymerase with the greater effect on the β form (Muller et al., 1975).

A second example is afforded by irradiated ataxia telangiectasia (AT) cells that show normal (Lehmann and Stevens, 1977) or faster (Foray et al., 1995) rejoining of DSB than controls over the first few hours (i.e. over the period of the "G<sub>2</sub> assay" of chromatid breaks) although much higher frequencies of chromatid breaks are observed in (AT) G<sub>2</sub> than in normal control irradiated cells (Taylor, 1978; Mozdarani and Bryant, 1989; Antocchia et al., 1994). Similarly, we find that the mutant hamster cell line *irs2* (assigned to the mammalian XRCC8 gene, the function of which is not yet known; Thacker and Zdzienicka, 2003) shows an elevated frequency of "G<sub>2</sub>" chromatid breaks (242 breaks per 100 cells) compared to its parental V79 line (143 breaks per 100 cells) but no defect in DSB induction or rejoining is observed after 30 Gy (Fig. 4a, b) at least over the first few hours after exposure. Taken together these data suggest that the initiating DSB is not itself directly involved in the formation of the chromatid break. Such a dissociation of DSB and chromatid break argues against a breakage-first model of chromatid breaks.

### Mechanisms of chromatid breaks

It was already mentioned above that chromatid breaks can be divided into those showing an interchromatid (i.e. between sister chromatids) rearrangement seen as a color-switch in FPG stained cells, and chromatid breaks of the non-color-switch type. It is proposed that both types result from chromatin rearrangements, initiated by the presence of a DSB within the looped chromatin domain. Examples of these different types of

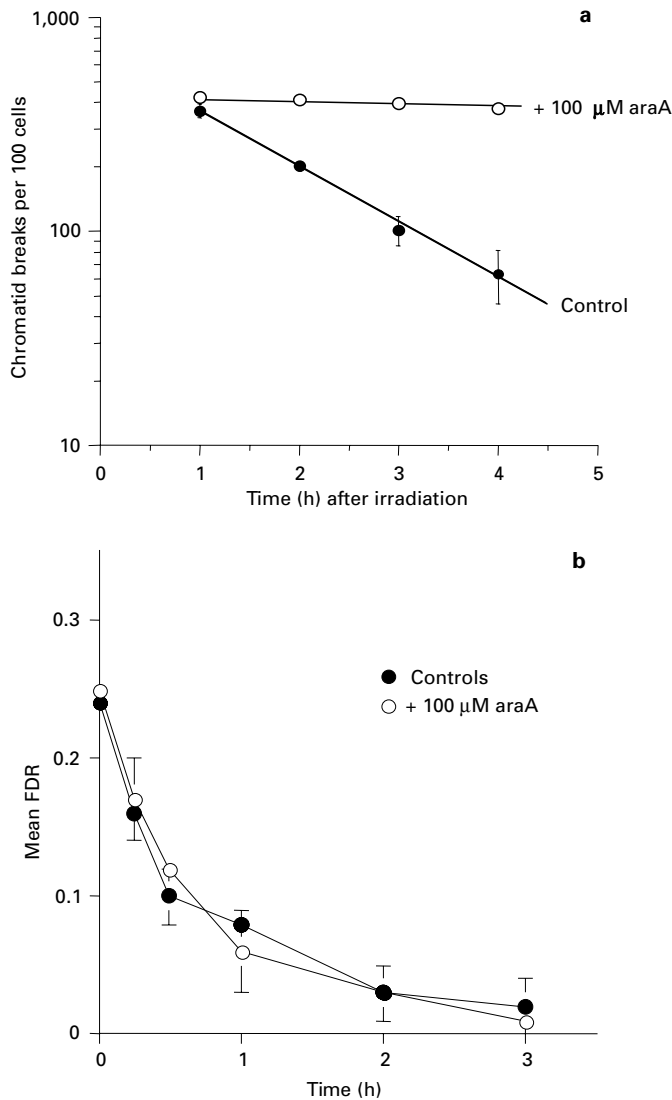


**Fig. 3. (a)** Disappearance of chromatid breaks with time after irradiation in CHO cells is inhibited by ara A at 100 μM. Cells were sampled at 1.5 h after irradiation (0.75 Gy) including a 1-hour colcemid block. **(b)** Rejoining of DSB in irradiated CHO cells after irradiation (30 Gy) is not influenced by the presence of ara A at 100 μM. DSB were measured by constant-field elec-

putative rearrangements are shown in Fig. 5. If the model proposed is correct, then the most frequent type of rearrangement would be of the intrachromatid type. Based on the frequency of the color-switch type (~ 16%) the intrachromatid type should account for around 80% of the remaining (non-color-switch type) breaks. It is also a prediction of the model that these breaks would show a small inversion adjacent to the break site (Fig. 5). Current research is aimed at detecting these inversions at specific DSB sites genetically engineered into cells.

### Use of genetically engineered cell lines with unique I-SceI sites in the study of chromatid breaks

The study of chromosomal rearrangements has been greatly facilitated by the introduction of fluorescence in situ hybridization (FISH) techniques, but also by the use of plasmid vectors containing specific DSB break sites. In such cell lines the intronic 18-bp yeast sequence I-SceI is introduced by transfection, and can then be recognized and cut (DSB with a 3' four-base overlap) either by transient transfection with an expression vector carrying the I-SceI endonuclease gene (e.g. Richardson et al., 1998) or by cell poration in the presence of I-SceI endonuclease, known commercially as Meganuclease (Rogers-Bald et al., 2000). Using a cell line stably transfected with a vector containing the 18-bp I-SceI site we were able to show that single (unique) DSB give rise to chromatid breaks in an enzyme concentration dependent manner (Rogers-Bald et al., 2000). These DSB sites appear to mimic those induced by radiation, since they are recognized and signaled via phosphorylation by ATM protein giving a γH2AX site (see Fig. 6). Also, the types of chromatid breaks induced by the DSB formed at I-SceI sites, and the proportion of color-switch breaks (i.e. those

trophoresis at 0.6 V/cm on 0.7% agarose in 0.5× TBE buffer for 72 h. The Fraction of DNA Remaining (FDR) in the loading wells of the gel was calculated from the ethidium bromide profile using digital capture and analysis by Syngene software.

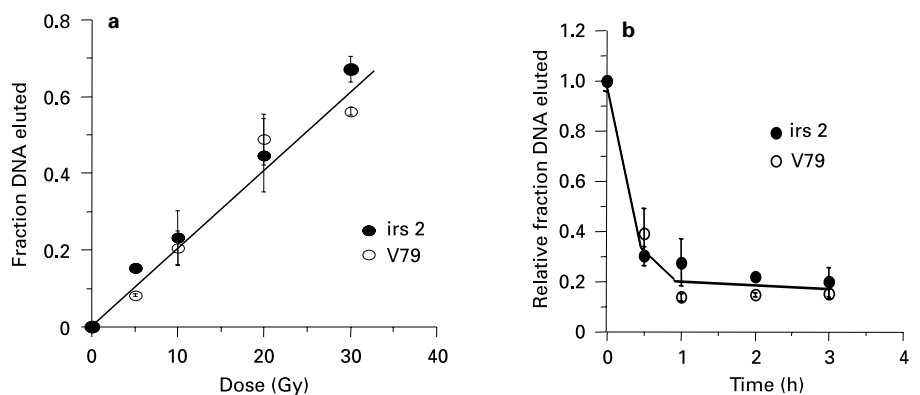


**Fig. 4. Induction (a) and rejoining (b)** (after 30 Gy) of DSB in irs2 and parental V79 Chinese hamster cells. DSB were measured by neutral elution.

involving interchromatid rearrangements) was very similar (18%) to those produced by radiation (Rogers-Bald et al., 2000). In these earlier studies we used streptolysin-O poration (Bryant, 1992) to introduce the Omeganuclease into hamster cells. However, recently we have selected Muntjac and Chinese hamster lines with inducible *I-SceI* endonuclease expression. Expression is under the control of an ecdysone (insect moulting hormone) sensitive element that can be induced by treatment of cells with the hormone analogue ponasterone A.

With ponasterone A treatment rather low frequencies of chromatid breaks are observed at these sites in both Muntjac

and hamster cell systems (e.g. Fig. 6). The reasons for the low yield of chromatid breaks is not fully understood, but may in part be due to the relatively low efficiency of conversion of both 3'- and 5'-cohesive-ended DSB into chromosomal aberrations (Bryant, 1984; Liu and Bryant, 1993) but could also be the result of low endogenous expression of the *I-SceI* endonuclease.

However, using immunocytochemical visualization of  $\gamma$ H2AX sites it became evident that phosphorylated  $\gamma$ H2AX sites occurred at DSB *I-SceI* sites, and that these accumulated over a period of 48 h, reaching a plateau frequency of around

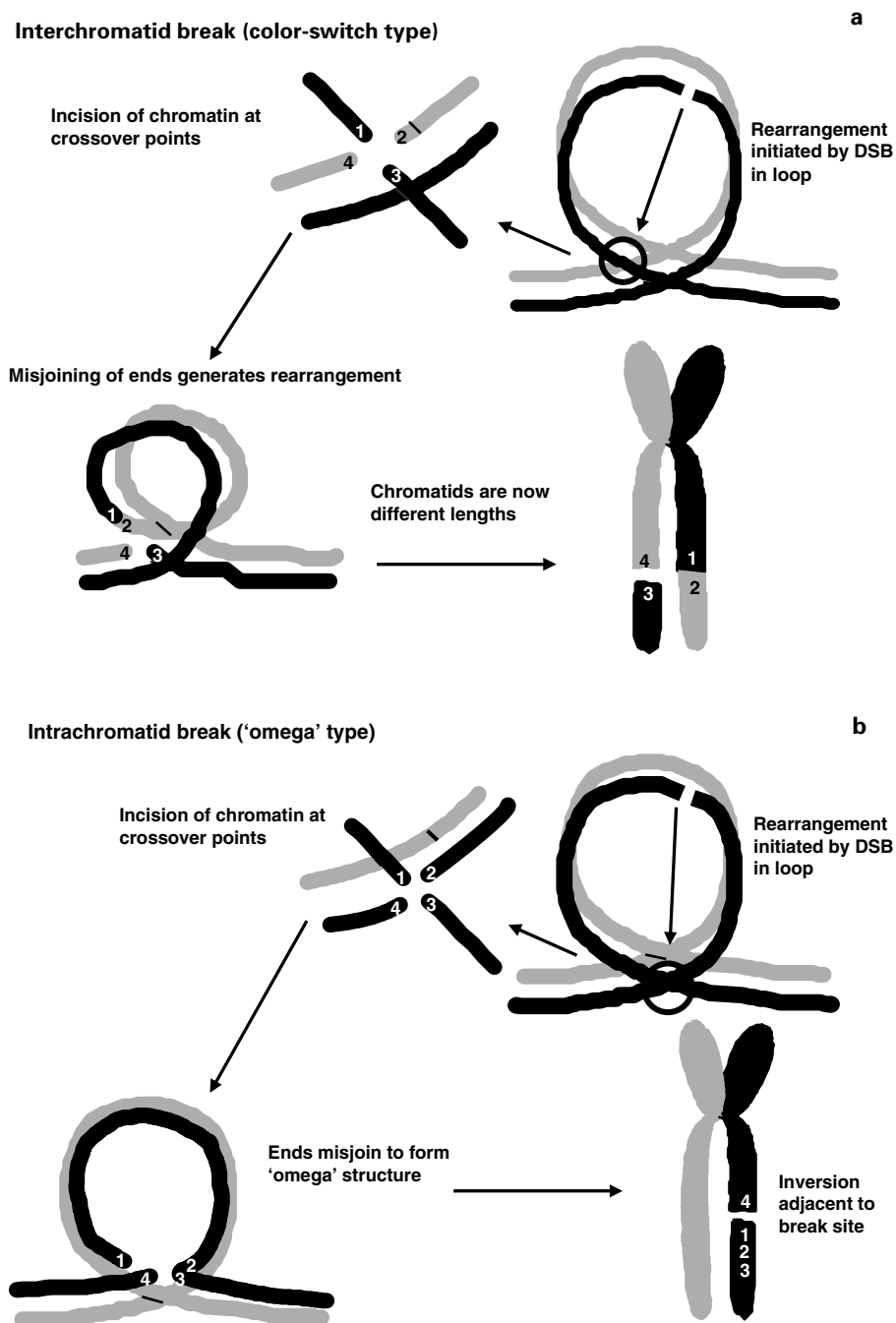


**Fig. 5.** Models of possible rearrangements based on the "signal" model (Bryant, 1998a) leading to (a) a color-switch (interchromatid) break, and (b) a non-color-switch or "omega"-type chromatid break. Note: The initiating DSB would be rejoined by NHEJ and would not itself be involved in the rearrangement leading to the chromatid break.

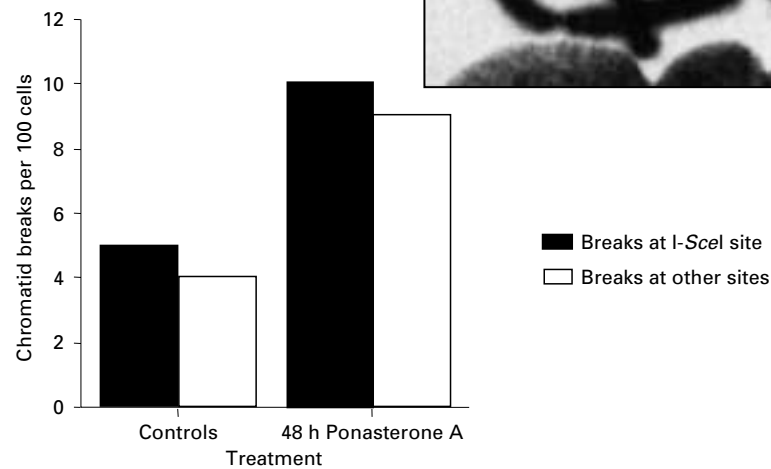


**Fig. 6.** Chromatid break frequency in control and ponasterone A induced Muntjac cell line containing an I-SceI site. The inset shows a break near the insertion site (arrowhead); incomplete metaphase shown.

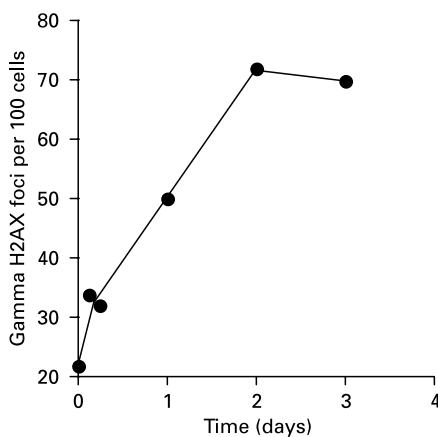


**Fig. 7.** Induction of  $\gamma$ H2AX sites in Muntjac MJR1Z2H2 cells as a function of time after addition of ponasterone A.

70% of cells (Fig. 7). We are therefore currently working on improvements to raise the frequency of chromatid breaks in these lines.

Interestingly, chromatid breaks were also observed at other sites (i.e. other than the I-SceI sites) in cells treated with ponasterone (Fig. 6) indicating a possible intracellular signaling or “bystander” effect. Further work is required to investigate this fully.

Using these systems, chromatid breaks at the known inserted I-SceI sites are being examined for evidence of either misalignment, indicating intrachromatid inversions using nick-translated fluorescent plasmid vector containing the 18-bp I-SceI break site or “split-signal” break sites that would indicate a

breakage-first mechanism. Thus, these cell lines provide a useful system for testing the chromatin rearrangement aspect of the model.

### Summary and conclusions

There is a need to understand the relationship between chromatid break frequency and cancer susceptibility, and to identify the genes of low penetrance that control these processes. Several lines of evidence show that only a single DSB is required to induce a chromatid break, including those involving interchromatid rearrangements. The classical breakage-first and the Revell exchange models do not accord with current evidence. Therefore a model is proposed of chromatid breakage in which a single DSB contained in a large looped chromatin domain is signaled, resulting in the initiation of a chromatin rearrangement at the crossover point of the looped domain. The DSB is then independently rejoined (by NHEJ) and takes no further part in the rearrangement process. Thus, the model predicts a disassociation of the initiating DSB from the actual rearrangement leading to the chromatid break. It is a prediction of the model that around 80% of the chromatid breaks would be the result of an intrachromatid rearrangement leading to an inverted segment of chromatin adjacent to the break. Test systems in hamster and Muntjac cells are being developed whereby single DSB (I-SceI) sites can be inducibly incised by endogenous expression of I-SceI endonuclease, as shown by  $\gamma$ H2AX immunocytochemical staining, enabling future detailed analysis of chromatin inversions adjacent to break sites. Work is in progress to visualize such inversions that could, if they result in a viable cell, lead to downstream genomic instability, mutation or altered gene expression.

## References

- Antoccia A, Palitti F, Raggi T, Catena C, Tanzarella C: Lack of effect of inhibitors of DNA synthesis/repair on the ionizing radiation-induced chromosomal damage in G2 stage of ataxia telangiectasia cells. *Int J Radiat Biol* 66:309–317 (1994).
- Baria K, Warren C, Roberts SA, West CM, Scott D: Chromosomal radiosensitivity as a marker of predisposition to common cancers. *Brit J Cancer* 84:892–896 (2001).
- Bender AM, Griggs HG, Bedford JS: Mechanisms of chromosomal aberrations production, III: Chemicals and ionizing radiation. *Mutat Res* 23:197–212 (1974).
- Bryant PE: Enzymatic restriction of mammalian cell DNA using Pvu II and Bam HI: Evidence for double strand break origin of chromosome aberrations. *Int J Radiat Biol* 46:57–65 (1984).
- Bryant PE: Induction of chromosomal damage by restriction endonuclease in CHO cells porated with streptolysin O. *Mutat Res* 268:27–34 (1992).
- Bryant PE: The signal model: a possible explanation for the conversion of DNA double-strand breaks into chromatid breaks. *Int J Radiat Biol* 73:243–251 (1998a).
- Bryant PE: Mechanisms of radiation-induced chromatid breaks. *Mutat Res* 404:107–111 (1998b).
- Bryant PE, Jones C, Armstrong G, Frankenberg-Schwager M, Frankenberg D: Induction of chromatid breaks by carbon-K ultra-soft X-rays. *Radiat Res* 159:247–250 (2003).
- Foray N, Arlett CF, Malaise EP: Dose-rate effect on induction and repair of radiation-induced DNA double-strand breaks in a normal and an ataxia-telangiectasia human fibroblast cell line. *Biochimie* 77:900–905 (1995).
- Harvey AN, Savage JRK: Investigating the nature of chromatid breaks produced by restriction endonucleases. *Int J Radiat Biol* 71:21–28 (1997).
- Lehmann AR, Stevens S: The production and repair of double-strand breaks in cells from normal humans and from patients with ataxia telangiectasia. *Biochim biophys Acta* 474: 49–60 (1977).
- Liu N, Bryant PE: Response of ataxia-telangiectasia cells to restriction endonuclease induced DNA double strand breaks: I. Cytogenetic characterization. *Mutagenesis* 8:503–510 (1993).
- Mozdarani H, Bryant PE: Induction and rejoining of chromatid breaks in X-irradiated A-T and normal human fibroblasts. *Int J Radiat Biol* 5:645–650 (1989).
- Mozdarani H, Liu N, Jones NJ, Bryant PE: The XRCC2 human repair gene influences recombinational rearrangements leading to chromatid breaks. *Int J Radiat Biol* 77:859–865 (2001).
- Muller WEG, Rohde HJ, Beyer R, Maidhof A, Lachman M, Taschner H, Zahn RK: Mode of action of 9- $\beta$ -D-arabinofuranosyladenine on the synthesis of DNA, RNA, and protein in vivo and in vitro. *Cancer Res* 35:2160–2168 (1975).
- Natarajan AT, Obe G: Molecular mechanism involved in the production of chromosomal aberrations, III. Restriction endonucleases. *Chromosoma* 90:120–127 (1984).
- Natarajan AT, Obe G, van Zeeland AA, Palitti F, Meijers M, Verdegaal-Immerzell EAM: Molecular mechanisms involved in the production of chromosomal aberrations; II. Utilization of Neurospora endonuclease for the study of aberration production by X-rays in G1 and G2 stages of the cell cycle. *Mutat Res* 69:293–305 (1980).
- Papworth R, Slevin N, Roberts SA, Scott D: Sensitivity to radiation-induced chromosome damage may be a marker of genetic predisposition in young head and neck cancer patients. *Brit J Cancer* 84:776–782 (2001).
- Parshad R, Sanford KK, Jones GM: Chromatid damage after G2 phase X-irradiation of cells from cancer prone individuals implicates deficiency in DNA repair. *Proc natl Acad Sci, USA* 80:5612–5616 (1990).
- Pfeiffer P, Goedecke W, Kuhfittig-Kulle S, Obe G: Pathways of DNA double-strand break repair and their impact on the prevention and formation of chromosomal aberrations. *Cytogenet Genome Res* 104:7–13 (2004).
- Revell SH: The accurate estimation of chromatid breakage, and its relevance to a new interpretation of chromatid aberrations by ionizing radiations. *Proc R Soc B* 150:563–589 (1959).
- Richardson C, Moynahan ME, Jasin M: Double-strand break repair by interchromosomal recombination: suppression of chromosomal translocations. *Genes Dev* 12:3831–3842 (1998).
- Riches AC, Bryant PE, Steel CM, Gleig A, Robertson AJ, Preece PE, Thompson AM: Chromosomal radiosensitivity in G2-phase lymphocytes identifies breast cancer patients with distinctive tumour characteristics. *Brit J Cancer* 85:1157–1161 (2001).
- Roberts SA, Spreadborough AR, Bulman B, Barber JBP, Evans DRG, Scott D: Heritability of cellular radiosensitivity: A marker of low penetrance predisposition genes in breast cancer? *Am J hum Genet* 65:784–794 (1999).
- Rogers-Bald M, Sargent RG, Bryant PE: Production of chromatid breaks by single dsb: evidence supporting the signal model. *Int J Radiat Biol* 76:23–29 (2000).
- Sanford KK, Parshad R, Gantt R, Tarone RE, Jones GM, Price FM: Factors affecting the significance of G2 chromatin radiosensitivity in predisposition to cancer. *Int J Radiat Biol* 55:963–981 (1989).
- Sax K: An analysis of X-ray induced chromosomal aberrations in *Tradescantia*. *Genetics* 25:41–68 (1940).
- Scott D, Spreadborough A, Levine E, Roberts SA: Genetic predisposition to breast cancer. *Lancet* 344:1444 (1994).
- Scott D, Barber JBP, Spreadborough AR, Burrill W, Roberts SA: Increased radiosensitivity in breast cancer patients: a comparison of two assays. *Int J Radiat Biol* 75:1–10 (1999).
- Taalman RD, Jaspers NG, Scheres JM, de Wit J, Hustinx TW: Hypersensitivity to ionizing radiation, in vitro, in a new chromosomal breakage disorder, the Nijmegen Breakage Syndrome. *Mutat Res* 112:23–32 (1983).
- Taylor AMR: Unrepaired DNA strand breaks in irradiated ataxia telangiectasia lymphocytes suggested from cytogenetic observations. *Mutat Res* 50:407–418 (1978).
- Terzoudi GI, Jung T, Hain J, Vrouvas J, Margaritis K, Donta-Bakoyiannis C, Makropoulos V, Angelakis PH, Pantelias GE: Increased G2 chromosomal radiosensitivity in cancer patients: the role of cdk/cyclin-B activity level in the mechanisms involved. *Int J Radiat Biol* 76:607–615 (2000).
- Thacker J, Zdzienicka MZ: The mammalian XRCC genes: their roles in DNA repair and genetic stability. *Mutat Res DNA Repair* 2:655–672 (2003).



# Human-hamster hybrid cells used as models to investigate species-specific factors modulating the efficiency of repair of UV-induced DNA damage

F. Marcon, J.J.W.A. Boei, and A.T. Natarajan

Department of Toxicogenetics, Leiden University Medical Centre, Leiden (The Netherlands)

**Abstract.** The human-Chinese hamster hybrid cell line XR-C1#8, containing human chromosome 8, was used as a model system to investigate the relative importance of cellular enzymatic environment and chromosomal structure for modulating the efficiency of repair of UV-induced DNA damage. The hybrid cells were irradiated with UVC light and the extent of cytogenetic damage, detected as frequencies of sister chromatid exchanges (SCEs), was compared between the human and the hamster chromosomes. The combination of immunofluorescent staining for SCEs and chromosome painting with fluorescence in situ hybridization allowed the simultaneous analysis of SCEs in the human and hamster chromosomes. The aim of the present study was to determine if the differences in biological response to comparable UV treatments observed between human and hamster cells were maintained in the hybrid cells in which human and hamster chromosomes are exposed in the same cellular environment. The analysis of replication time of human chromosome 8 indicated the active status of this chro-

mosome in XR-C1#8 hybrid cells. The frequencies of SCEs for human chromosome 8 and a hamster chromosome of comparable size were  $0.35 \pm 0.52$ ,  $0.80 \pm 0.73$ ,  $1.24 \pm 2.24$  and  $0.36 \pm 0.12$ ,  $0.71 \pm 0.2$ ,  $0.97 \pm 0.27$ , respectively, after irradiation with 0, 5, and 10 J/m<sup>2</sup>. The persistence of UV-induced SCEs after three cell cycles was also analyzed, both for the human and hamster chromosomes. The observed frequencies of SCEs were  $0.40 \pm 0.57$ ,  $0.62 \pm 1.05$ ,  $0.58 \pm 0.83$  and  $0.26 \pm 0.08$ ,  $0.67 \pm 0.18$ ,  $0.69 \pm 0.24$ , in human and hamster chromosomes respectively, after treatment with 0, 10, and 20 J/m<sup>2</sup> of UVC light. No significant differences could be observed between the human and hamster chromosomes. These results suggest that the enzymatic environment of human and hamster cells has the main role, in comparison to the structural organization of human and hamster chromosomes, for determining the different level of repair of UV-induced DNA damage observed in these two species.

Copyright © 2003 S. Karger AG, Basel

It has been observed that cells from different species respond differently to the same chemical or physical agents. For example, human and hamster cells treated with comparable doses of benzo(a)pyrene (Tomkins et al., 1982), show different extents of induction of SCEs. Human cells respond with lower frequencies of SCEs than hamster cells. Similar comparative experiments using UV light have not been carried out so

far. This differential response can be related to the efficiency of repair of DNA damage, which can be modulated by the cellular enzymatic machinery or by the organization of the genome. It is known that after treatment with similar doses of UV light, hamster cells remove in about 24 h around 20% of the induced cyclobutane pyrimidine dimers (CPD) while human cells can remove around 80% of the dimers (Van Zeeland et al., 1981). A direct relationship between UV-induced SCEs and CPDs has also been demonstrated, since the disappearance of CPD by photo-reactivation parallels the reduction of the frequency of SCEs (Natarajan et al., 1980; van Zeeland et al., 1980). These observations suggest that the differences in the extent of cytogenetic damage detected after UV irradiation in human and hamster cells could be related to a different activity of the enzymes involved in the repair of the damage.

Supported by a grant from the European Union Radiation Protection Programme to A.T.N.

Received 16 September 2003; manuscript accepted 27 November 2003.

Request reprints from A.T. Natarajan, Burgemeester Warnaarckade 47

2391 AZ Hazerswoude Dorp (The Netherlands)

telephone: 33-172-586757; fax: 33-172-586762; e-mail: Natarajan@LUMC.nl

However, there is evidence indicating a possible role of the physical organization of chromosomes among factors influencing the induction and repair of DNA damage. For example, condensed constitutive heterochromatic regions are known to be susceptible to lower damage followed by poorer repair in comparison to relaxed euchromatic regions (Slijepcevic and Natarajan, 1994b; Surralles et al., 1997). The organization of the telomeric regions also appears to be different in hamster and human cells, when analyzed in the extended DNA loops of chromatin (Balajee et al., 1998). This variation was pointed out as a possible factor responsible for the different amounts of DNA damage detected in the two species in response to the same treatment with restriction enzymes (Balajee et al., 1998).

In this study we used a human-Chinese hamster hybrid cell line, containing human chromosome 8. The frequency of SCEs, as parameter of DNA damage induced by UV irradiation, was estimated specifically in the human chromosome and then compared with the frequencies of SCEs induced in the hamster chromosomes. In order to analyze the SCEs simultaneously in the human and hamster chromosomes, a novel approach, i.e. a combination of a fluorescent staining for SCEs with chromosome painting for the human chromosome was employed.

The rationale for the present investigation was to determine if the human chromosome maintained its higher efficiency of repair compared to the hamster chromosomes in the hybrid cells. If the heterogeneity is maintained, this could be due to distinctive structures of the human chromosome, the enzymatic environment being common for human and hamster chromosomes in a hybrid cell. It is worth noting that in hybrid cells containing human chromosomes in rodent background, human chromosomes exhibit a different staining pattern from the rodent chromosomes, probably related to differences in the structural organization between these chromosomes (Bobrow and Cross, 1974). On the other hand, if the human chromosome had the same extent of damage (SCEs) as the hamster ones, the cellular environment could be considered as the important factor for determining the efficiency of repair.

We also analyzed the persistence of induced SCEs after three cell cycles in the hybrid cells, both in the human and hamster chromosomes. Hamster cells are known to bypass dimers during replication, allowing persistence of increased frequency of SCEs over several generations (Kato, 1977; Natarajan et al., 1980). In the present investigation with human-hamster hybrid cells, persistence of SCEs in the human chromosome was expected, if it was repaired like the hamster chromosomes, confirming in such a case the relevance of the cellular environment for modulating the level of repair of UV-induced damage. The replication time of the human chromosome was also checked to verify whether this chromosome is active or inactive in the human-hamster hybrid cells.

## Materials and methods

### Cell culture

The Chinese hamster cell line XR-C1 and a human-hamster cell line XR-C1#8-3 were isolated and kindly provided by Dr. M. Zdzienicka, in our laboratory. These hybrid cells contain one or two copies of human chromosome 8. The hamster genetic background is defective in DNA-PK activity, but this

defect is complemented in the hybrids by human chromosome 8 (Errami et al., 1998).

Cells were grown in Ham's F-10 medium, supplemented with 10% fetal bovine serum (Gibco), penicillin, streptomycin. Gentamycin (400 µg/ml) was added to the hybrid cell lines in order to force the cells to retain the human chromosomes.

### Treatment and slide preparation

Near-confluent cells were kept for two days in 2% fetal calf serum, to obtain a partial synchronization. Two hours before treatment they were trypsinized, seeded and incubated in fresh complete medium. Irradiation was carried out with UV (Philips TVA lamp) at a dose rate of 0.19 J/m<sup>2</sup>/s of 254-nm light. The plates were rinsed in phosphate-buffered saline (PBS) prior to irradiation. After exposure to the UV light the cells were cultured in fresh medium containing 5-bromo-2-deoxyuridine (BrdU, 5 µM) for one cell cycle, i.e. 15 h, rinsed in PBS and cultured for another cell cycle without BrdU. For the analysis of the persistence of SCEs, cells were grown after treatment for one cell cycle without BrdU, for another cell cycle with added BrdU and a third cell cycle without BrdU. Colcemid (0.1 µg/ml) was added 2 h before harvest. Two fixation times were used (28 h and 36 h) to take into account the mitotic delay associated with the UV treatment. Cells were fixed according to standard procedures (10 min in 0.075 M KCl at 37°C, then fixed three times in methanol:acetic acid 3:1). Slides were prepared and stored at -20°C for in situ hybridization.

Several preliminary experiments were carried out to figure out the optimal protocol. The results presented here come from one experiment.

### Replication time analysis

BrdU (10 µM) was added to the growing cells 6 and 3 h before harvesting, in order to investigate replication events occurring during the early and late S phase respectively. Colcemid (0.1 µg/ml) was added 1 h before harvest. The cells were fixed in methanol:acetic acid 3:1. BrdU incorporation was visualized by indirect immunostaining with mouse anti-BrdU and fluoresceinated (FITC) anti-mouse antibodies (Boehringer). The simultaneous hybridization with a DNA probe specific for the human chromosome, allowed the identification of human chromosome 8 and the analysis of the replication time.

### Simultaneous fluorescence in situ hybridization and sister chromatid differentiation

Total human genomic DNA, was labeled by nick translation (Promega kit) with digoxigenin-dUTP (Boehringer) and used to identify the human chromosome in hamster background.

Before hybridization, the slides were pre-treated with RNase (0.1 µg/ml in 2× SSC, 1 h at 37°C, moist chamber), pepsin (0.005% in 0.01 M HCl, 3 to 5 min at 37°C), fixed in 1% formaldehyde (in 50 mM PBS/MgCl<sub>2</sub> at room temperature for 10 min), dehydrated in ethanol and denatured (2 min at 70°C, in 70% deionized formamide, 2× SSC, 50 mM phosphate buffer, pH 7.0). The digoxigenin-labeled probe (100 ng/slide) was denatured 5 min at 70°C, diluted in 20 µl/slide of hybridization mix (50% deionized formamide, 2× SSC, 50 mM phosphate buffer pH 7.0, 10% dextran sulfate), placed on the slide and then incubated at 37°C in a moist chamber for 16–18 h.

After hybridization, slides were washed in 50% formamide, 2× SSC, 20 min at 42°C, rinsed 3 × 5 min in 0.1× SSC at 60°C and 5 min in 4× SSC/0.05% Tween 20. The cells were then incubated in non-fat dry milk for 20 min at 37°C. The detection of the digoxigenin-labeled probe was performed with sheep anti-digoxigenin conjugated with TRITC (Boehringer). The fluorescent intensity was amplified using mouse anti-digoxigenin antibodies and TRITC conjugate of sheep anti-mouse antibodies (Boehringer) (Boei et al., 1996). Visualization and differentiation of the sister chromatids were achieved using mouse anti-BrdU and FITC goat anti-mouse antibodies (Boehringer). The slides were counterstained with Vectashield mounting medium (Vector Laboratories), containing 0.15 µg/ml of 4',6-diamidino-2-phenylindole (DAPI, Sigma).

### Slide scoring

Slides were observed using a Leitz Orthoplan microscope equipped with a triple band pass filter for the simultaneous detection of TRITC, FITC and DAPI. All the cells were analyzed under the FITC filter to score the frequency of SCEs in the hamster chromosomes and human chromosome 8, previously identified by the triple band pass filter. Only cells containing a single copy of human chromosome 8 were scored for the frequencies of SCEs.

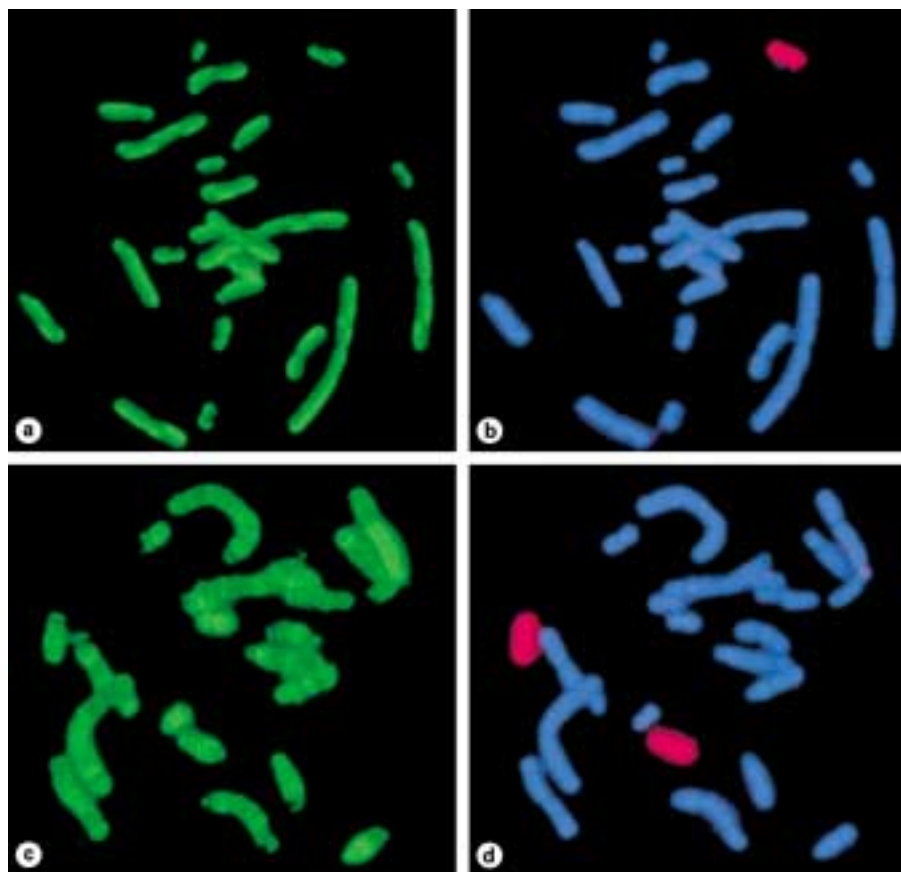


**Fig. 1.** (a) Sister chromatid exchanges in a Chinese hamster-human hybrid cell (XR-C1#8) following UV irradiation. Sister chromatid differentiation obtained with mouse anti-BrdU and FITC goat anti-mouse antibodies. (b) The same cell showing the human chromosome 8 (red color) following FISH with human DNA. (c) Early replicating regions in a hamster-human hybrid cell. (d) The same cell showing the two human chromosomes (red color). Note that these two chromosomes are early replicating (c) indicating that they are not inactivated in the hamster background.

Wherever possible, 50 metaphases were scored per experimental point. The proliferation index (PRI), as a parameter of cell proliferation, was calculated as follows:  $(1 \times M_1 + 2 \times M_2 + 3 \times M_3)/100$ , where  $M_1$ ,  $M_2$  and  $M_3$  are the number of cells in first, second and third division observed in 100 metaphases. Student's *t* test was applied for statistical evaluation.

## Results

The spontaneous and induced frequencies of SCEs observed in the hamster and in the hybrid cell line are presented in Table 1 showing data obtained after 28 and 36 h of culture, respectively. After 28 h, it can be observed that the frequencies of SCEs at 0 and 5 J/m<sup>2</sup> are comparable among the two cell lines, while at the highest dose a lower frequency of SCEs was observed in the hybrid cells than in the hamster cells. At this dose, there are also differences in the PRI among the two cell lines, with the hybrid cells showing a strong delay in the cell cycle progression. As these differences in the frequencies of SCEs could be due to processes of selection in the cell population, the experiment was repeated and the cells were fixed at 36 instead of 28 h.

After 36 h of culture, no significant differences in the frequency of SCEs and in the progression of the cell cycle could be observed between the hamster and hybrid cells.

As shown in Fig. 1a, b, combining the fluorescent staining for the SCEs and the hybridization for the human chromo-

**Table 1.** Frequencies of sister chromatid exchanges (SCEs) per cell in hamster and human-hamster hybrid cells after UV treatment. Mean values standard errors are given.

Harvest time (h)	Dose (J/m <sup>2</sup> )	Chinese hamster cells (XR-C1)			Human-hamster hybrid cells (XR-C1#8)		
		Scored cells	SCEs per cell	PRI <sup>a</sup>	Scored cells	SCEs per cell	PRI <sup>a</sup>
28	0	50	10.74 ± 3.87	1.99	150	12.98 ± 3.90	1.98
28	5	50	24.62 ± 5.78	1.96	150	25.31 ± 6.75	1.72
28	10	50	37.46 ± 9.58	1.69	108	32.37 ± 8.31	1.06
36	0	26	12.62 ± 3.09	2.98	72	14.86 ± 5.29	2.97
36	5	50	28.96 ± 6.67	2.80	94	28.30 ± 7.70	2.21
36	10	36	44.58 ± 11.48	2.15	100	39.04 ± 10.41	2.10

<sup>a</sup> PRI: proliferation index.

some, the frequency of SCEs for each human chromosome 8 and for the hamster chromosomes could be easily analyzed.

The frequency of SCEs observed on the human chromosome was compared with the frequency of SCEs estimated for a fraction of the Chinese hamster genome representing an equal amount of DNA. Human chromosome 8 has a DNA content of 0.151 pg, corresponding to about 5.5% of the hamster genome (Morton, 1991; Slijepcevic and Natarajan, 1994b). The calcu-

**Table 2.** Comparison between human and hamster chromosomes for the induction of sister chromatid exchanges (SCEs) after UV treatment of the human-hamster hybrid cell line XR-C1#8. Mean values  $\pm$  standard errors are given.

Dose (J/m <sup>2</sup> )	Chromosomes analyzed	SCEs per human chromosome	SCEs per hamster chromosome <sup>a</sup>	<i>P</i> (t-test) <sup>b</sup>
0	322	0.35 $\pm$ 0.52	0.36 $\pm$ 0.12	n.s.
5	290	0.80 $\pm$ 0.73	0.71 $\pm$ 0.20	n.s.
10	258	1.24 $\pm$ 2.24	0.97 $\pm$ 0.27	n.s.

<sup>a</sup> Frequencies of SCEs are corrected for length.

<sup>b</sup> n.s. = not significant.

lated frequencies of SCEs for this fraction of the hamster genome are compared with the frequencies obtained in human chromosome 8 (Table 2). An analysis of data indicates no significant differences in the frequencies of SCEs for human and hamster chromosomes before and after UV treatment with 5 and 10 J/m<sup>2</sup>.

#### *Persistence of UV damage*

The data obtained in the hamster and hybrid cells three cell cycles after UV treatment are presented in Table 3. A significant increase of SCEs per cell can be observed at 10 and 20 J/m<sup>2</sup>. A reduction in the frequencies of SCEs after 10 J/m<sup>2</sup> can be observed when compared to the values observed after two cell cycles (Table 1), due to "a dilution effect". The frequency of SCEs per human and hamster chromosomes was still at a comparable level at the third cell cycle following UV treatment.

#### *Replication time*

The replication time of human chromosome 8 in the hybrid cells was analyzed by addition of BrdU during the last 3 and 6 h of culturing. The incorporation pattern of BrdU revealed that the human chromosomes replicate during mid to late S phase and are not heterochromatic in nature (Fig. 1c, d).

## Discussion

In the present study human-hamster hybrid cells were used as a model system to investigate the relative importance of cellular enzymatic environment and chromosome structure for evaluating the efficiency of repair of UV-induced DNA damage. The hybrid cells were treated with UVC light and the extent of cytogenetic damage, detected as frequencies of SCEs, was compared between human and hamster chromosomes. The aim of the experiments was to determine if the generally observed differences between human and hamster cells in response to comparable treatments with genotoxic agents were maintained in the hybrid cells. In the same cellular environment different responses were expected in case strong differences in the structural organization of human and hamster chromosomes would influence the level of repair. A similar extent of damage was considered suggestive of the main role of

**Table 3.** Comparison between human and hamster chromosomes for the persistence of sister chromatid exchanges (SCEs) three cell cycles after UV treatment of the human-hamster hybrid cell line XR-C1#8. Mean values  $\pm$  standard errors are given.

Dose (J/m <sup>2</sup> )	Scored cells	SCEs per cell	SCEs per human chromosome	SCEs per hamster chromosome <sup>a</sup>	<i>P</i> (t-test) <sup>b</sup>
0	72	9.62 $\pm$ 2.87	0.40 $\pm$ 0.57	0.26 $\pm$ 0.08	n.s.
10	73	24.36 $\pm$ 6.57	0.62 $\pm$ 1.05	0.67 $\pm$ 0.18	n.s.
20	73	25.42 $\pm$ 8.76	0.58 $\pm$ 0.83	0.69 $\pm$ 0.24	n.s.

<sup>a</sup> Frequencies of SCEs are corrected for length.

<sup>b</sup> n.s. = not significant.

the enzymatic machinery for determining the level of repair of UV-induced DNA damage.

Previous studies using human-hamster hybrid cells (Phillippe et al., 1993) showed that in the majority of nuclei human chromosomes seemed to remain condensed and in close proximity to the periphery of the nucleus, a characteristic reminiscent of heterochromatic structures. It is generally accepted that replication time of DNA is linked to its chromatin structure, active genes replicating during early S-phase and inactive genes, constitutive and facultative heterochromatin replicating during late S-phase. Furthermore, it has been observed that different chromosomal structures can be repaired with different efficiency, producing a heterogeneity of the repair of induced DNA lesions (Natarajan et al., 1996). Evidences have been obtained indicating that heterochromatin is generally less repaired than euchromatic regions (Slijepcevic and Natarajan, 1994a, b; Surralles et al., 1997a, b; Surralles and Natarajan, 1998). In this work the active or inactive status of human chromosome 8 in the hybrid cells was verified, before and after UV treatment.

The human chromosome 8 showed a replication time comparable to the pattern usually observed in human cells, indicating the absence of any heterochromatic feature. The active status of the human chromosome raised another problem, related to the eventuality that this chromosome could influence the efficiency of repair of the hamster chromosomes, possibly by the expression of human genes involved in the repair of the induced damage. Thus, the spontaneous and induced frequencies of SCEs were compared between the hamster and hybrid cell lines. Only at the highest dose, the hybrid cells showed a lower frequency of SCEs.

It has been suggested that the distribution of SCEs could be non-random along a chromosome, possibly modulated by the presence of heterochromatin, telomeric sequences or other specific chromosome features. In order to avoid bias in the analysis related to these factors, the frequency of SCEs observed in the human chromosome was compared with an average frequency of SCEs estimated for a fraction of the hamster genome with the same DNA content as human chromosome 8, and not to the frequency of SCEs observed in a hamster chromosome of comparable length (i.e. chromosome 7). The comparison between human and hamster chromosomes in the human-ham-

ster hybrid cells showed that similar frequencies of SCEs were induced by the UV treatment. Thus, the different efficiency of repair observed between human and hamster cells was not maintained in the human-hamster hybrid cells, indicating that enzymatic environment could be more relevant than chromosome structure per se, for determining the levels of DNA repair.

The results obtained in our study highlighted a major role of the enzymatic environment for the repair of damage. These data are in agreement with the observation of Vreeswijk et al. (1998) who found that in a human-mouse hybrid cell line, with reduced level of repair of UV-induced photolesions, no repair of either CPD or 6-4PD was observed in mouse genes or in human genes, indicating that human genes, which are very efficiently repaired in human cells (Venema et al., 1990), behave like the mouse genes when introduced in a mouse cell.

Additional observations confirm the main role of the enzymatic environment for modulating the differences in DNA repair observed among species. Recently, it has been suggested that the discrepant sensitivity to DNA methylation damage (induced by *N*-methyl-*N*-nitrosourea) observed between human and rodent cells may be related to a lower level of mismatch repair found in mouse cells compared to human cells (Humbert et al., 1999).

The results obtained in the present investigation evaluating the persistence of SCEs in human and hamster chromosomes

three cell cycles after UV treatment confirm that the human chromosomes behave like hamster chromosomes when maintained in a hamster cell.

In the present study an original experimental system, represented by the human-hamster hybrid cells, was used to evaluate the relative importance of enzymatic or chromosomal factors for influencing the levels of DNA repair. To achieve this aim a method combining fluorescent in situ hybridization with immunofluorescent staining for SCEs (Boei et al., 1996) was applied. The use of fluorescent anti-BrdU antibodies allowed a good analysis of SCE frequencies and the combination with chromosome painting made it possible to analyze specifically human chromosome 8 to make the comparison with the hamster chromosomes within the same hybrid cell.

It is worth noting that this procedure could also be applied in future studies aimed to verify if differences exist among single chromosomes or specific chromosome structures for the induction of SCEs and to obtain more insight into the mechanism(s) of formation and the biological meaning of this cytogenetic end-point.

### Acknowledgements

The authors are grateful to Dr. M. Zdzienicka for kindly providing XR-C1 and XR-C1#8 cell lines.

### References

- Balajee AS, May A, Bohr VA: Fine structural analysis of DNA repair in mammalian cells. *Mutat Res* 404:3–11 (1998).
- Bobrow M, Cross J: Differential staining of mouse chromosomes in interspecific cell hybrids. *Nature* 251:77–79 (1974).
- Boei JJWA, Vermeulen S, Natarajan AT: Determination of chromosomal aberrations by fluorescence in situ hybridization in the three post-irradiation divisions of human lymphocytes. *Mutat Res* 349:127–135 (1996).
- Errami A, Dong Ming HE, Friedl AA, Overkamp WJI, Morolli B, Hendrickson EA, Eckhardt-Schupp F, Oshimura M, Lohman PHM, Jackson SP, Zdzienicka MZ: XR-C 1, a new cell mutant which is defective in DNA-PKcs is impaired in both V(D)J coding and signal joint formation. *Nucl Acids Res* 26:3146–3153 (1998).
- Humbert O, Fiumicino S, Aquilina G, Branch P, Oda S, Zijno A, Karran P, Bignami M: Mismatch repair and differential sensitivity of mouse and human cells to methylating agents. *Carcinogenesis* 20: 205–214 (1999).
- Kato H: Spontaneous and induced sister chromatid exchanges by the BUdR-labeling method. *Int Rev Cytol* 37:55–95 (1977).
- Morton NE: Parameters of human genome. *Proc natl Acad Sci, USA* 88:7474–7476 (1991).
- Natarajan AT, van Zeeland AA, Verdegaal-Immerzeel EAM, Filon AR: Studies on the influence of photoreactivation on the frequencies of UV-induced aberrations and sister chromatid exchanges and pyrimidine dimers in chicken embryonic fibroblasts. *Mutat Res* 180:495–500 (1980).
- Natarajan AT, Balajee AS, Boei JJWA, Darroudi F, Dominguez I, Hande MP, Meijers M, Slijepcevic P, Vermeulen S, Xiao Y: Mechanisms of induction of chromosomal aberrations and their detection by fluorescence in situ hybridization. *Mutat Res* 372:247–258 (1996).
- Philippe C, Nguyen VC, Slim R, Holvoet-Vermaut L, Hors-Cayla MC, Bernheim A: Rearrangements between irradiated chromosomes in three species hybrid cells revealed by two colour in situ hybridization. *Hum Genet* 92:11–17 (1993).
- Slijepcevic P, Natarajan AT: Distribution of radiation-induced G1 exchange and terminal deletion break points in Chinese hamster chromosomes as detected by G banding. *Int J Radiat Biol* 66:747–755 (1994a).
- Slijepcevic P, Natarajan AT: Distribution of X-ray induced G2 chromatid damage among Chinese hamster chromosomes: influence of chromatid configuration. *Mutat Res* 323:113–119 (1994b).
- Surrallés J, Natarajan AT: Radiosensitivity and repair of inactive X-chromosome. Insight from FISH and immunocytogenetics. *Mutat Res* 414:117–124 (1998).
- Surrallés J, Darroudi F, Natarajan AT: Evidence for low level of DNA repair in human chromosome 1 heterochromatin. *Genes Chrom Cancer* 20:173–184 (1997a).
- Surrallés J, Sebastian S, Natarajan AT: Chromosomes with high gene density are preferentially repaired in human cells. *Mutagenesis* 12:437–442 (1997b).
- Tomkins DJ, Kwok SE, Douglas GR, Biggs D: Sister chromatid exchange response in human diploid fibroblasts and Chinese hamster ovary cells to dimethylnitrosamine and benzo(a)pyrene. *Environ Mutagen* 4:203–214 (1982).
- Van Zeeland AA, Natarajan AT, Verdegaal-Immerzeel EAM, Filon RA: Photoreactivation of UV induced cell killing, chromosome aberrations, sister chromatid exchanges, mutations and pyrimidine dimers in *Xenopus laevis* fibroblasts. *Mol gen Genet* 180:495–500 (1980).
- Van Zeeland AA, Smith CA, Hanawalt PC: Sensitive determination of pyrimidine dimers in DNA of UV-irradiated mammalian cells. Introduction of T4 endonuclease V into frozen and thawed cells. *Mutat Res* 82:173–189 (1981).
- Venema J, Mullenders LHF, Natarajan AT, van Zeeland AA, Mayne LV: The genetic defect in Cockayne syndrome is associated with a defect of UV-induced DNA damage in transcriptionally active DNA. *Proc natl Acad Sci, USA* 87:4707–4711 (1990).
- Vreeswijk MPG, Westland BE, Hess MT, Naegeli H, Vrieling H, van Zeeland AA, Mullenders LHF: Impairment of nucleotide excision repair by apoptosis in UV irradiated mouse cells. *Cancer Res* 58:1978–1985 (1998).

# Mechanisms and consequences of methylating agent-induced SCEs and chromosomal aberrations: a long road traveled and still a far way to go

B. Kaina

Division of Applied Toxicology, Institute of Toxicology, University of Mainz, Mainz (Germany)

**Abstract.** Since the milestone work of Evans and Scott, demonstrating the replication dependence of alkylation-induced aberrations, and Obe and Natarajan, pointing to the critical role of DNA double-strand breaks (DSBs) as the ultimate trigger of aberrations, the field has grown extensively. A notable example is the identification of DNA methylation lesions provoking chromosome breakage (clastogenic) effects, which made it possible to model clastogenic pathways evoked by genotoxins. Experiments with repair-deficient mutants and transgenic cell lines revealed both O<sup>6</sup>-methylguanine (O<sup>6</sup>MeG) and N-methylpurines as critical lesions. For S<sub>N</sub>2 agents such as methylmethanesulfonate (MMS), base N-methylation lesions are most critical, likely because of the formation of apurinic sites blocking replication. For S<sub>N</sub>1 agents, such as N-methyl-N'-nitro-N-nitrosoguanidine (MNNG), O<sup>6</sup>-methylguanine (O<sup>6</sup>MeG) plays the major role both in recombination and clastogenicity in the post-treatment cell cycle, provided the lesion is not pre-replicatively repaired by O<sup>6</sup>-methylguanine-DNA methyltransferase (MGMT). The conversion probability of O<sup>6</sup>MeG into SCEs and chromosomal aberrations is estimated to be about 30:1 and >10,000:1 respectively, indicating this mispairing pro-muta-

genic lesion to be highly potent in inducing recombination giving rise to SCEs. O<sup>6</sup>MeG needs replication and mismatch repair to become converted into a critical secondary genotoxic lesion. Here it is proposed that this secondary lesion can be tolerated by a process termed *recombination bypass*. This process is supposed to be important in the tolerance of lesions that can not be processed by translesion synthesis accomplished by low-fidelity DNA polymerases. Recombination bypass results in SCEs and might represent an alternative pathway of tolerance of non-instructive lesions. In the case of O<sup>6</sup>MeG-derived secondary lesions, recombination bypass appears to protect against cell killing since SCEs are already induced with low, non-toxic doses of MNNG. Saturation of lesion tolerance by recombination bypass or translesion synthesis may cause block of DNA replication leading to DSBs at stalled replication forks, which result in chromatid-type aberrations. Along with this model, several putative consequences of methylation-induced aberrations will be discussed such as cell death by apoptosis as well its role in tumor promotion and progression.

Copyright © 2003 S. Karger AG, Basel

This paper is dedicated to Prof. Dr. Günter Obe on the occasion of his 65<sup>th</sup> birthday.

This work was supported by the Deutsche Forschungsgemeinschaft, Grants Ka724/7, Ka724/8, Ka724/11 and Ka724/12.

Received 15 December 2003; manuscript accepted 12 January 2004.

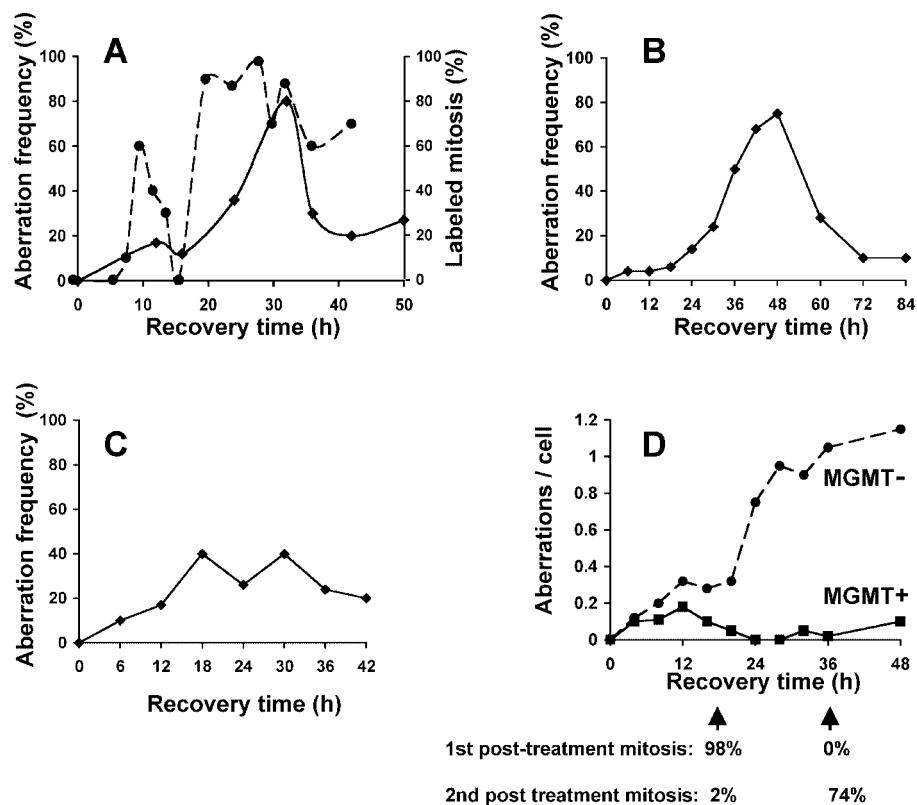
Request reprints from: Dr. Bernd Kaina

Institute of Toxicology, Division of Applied Toxicology  
Obere Zahlbacher Str. 67, DE-55131 Mainz (Germany)  
telephone: +49-6131-393-3246; fax: +49-6131-393-3421  
e-mail: Kaina@uni-mainz.de.

## Introduction

An important discovery concerning chromosomal aberrations was made in 1969 with the demonstration that aberrations induced by nitrogen mustard are strictly bound on the cell's progression through S-phase (Evans and Scott, 1969). This led to the concept of S-phase-dependent and -independent mutagens (for review see Kihlman, 1977). Another milestone in

**Fig. 1.** Aberration frequencies induced by methylating agents. **(A)** Chromatid-type aberrations induced in human non-established fibroblasts by MNU as a function of recovery time. The dashed curve shows the percentage of labelled mitosis. [<sup>3</sup>H]-thymidine was given as a pulse immediately before the treatment with MNU. Data are from Kaina et al. (1977) and unpublished data. **(B), (C)** time-effect curve for cells treated with 1-methyl-1-nitroso-3-phenylurea for V79 cells **(B)** and fetal Chinese hamster cells out of the fourth passage **(C)**. Data are from Thust et al. (1980). **(D)** Time-effect curve for CHO cells treated with MNNG. Cells not expressing MGMT are designated as MGMT<sup>-</sup>. Cells expressing human MGMT upon transfection with an MGMT expression vector are designated as MGMT<sup>+</sup>. The frequency of cells in first and second post-treatment mitosis was determined in parallel labeling experiments and given on the bottom of the figure. Data from Kaina et al. (1993).



this field was reached when it was shown that aberration production is linked to the formation of DNA double-strand breaks (DSBs). Evidence for this was based on the use of T4 endonuclease (Natarajan and Obe, 1978) and restriction enzymes (Natarajan and Obe, 1984) electroporated into cells – an approach that turned out to be very powerful in studying the role of specific DNA lesions in aberration and SCE production. For alkylating agents, notably methylating compounds, which are powerful mutagens, recombinogens and clastogens, the mechanisms involved in aberration production as well as the critical lesions induced were enigmatic for a long time. Approaches to incorporate specific methylated bases, such as O<sup>6</sup>-methylguanine (O<sup>6</sup>MeG) or N<sup>7</sup>-methylguanine (7MeG), in DNA of cultured cells failed. In an alternative approach, the clastogenic and mutagenic potency of different methylating agents was assessed and compared to the spectrum of lesions induced. S<sub>N</sub>2 agents such as methyl methanesulfonate (MMS) induce preferably N-methylpurines and are powerful clastogens, suggesting N-methylpurines to be responsible for aberrations. S<sub>N</sub>1 agents produce relatively high levels of O-alkylations in DNA, including the mispairing lesion O<sup>6</sup>MeG, which correlates with mutagenicity (Vogel and Natarajan, 1979; Morris et al., 1982, 1983; Natarajan et al., 1984). It was therefore paradigmatically believed that N-alkylations are responsible for the clastogenic effect of simple alkylating agents, whereas O-methylated bases, notably O<sup>6</sup>MeG, are the source of point mutations (Loveless, 1969; Natarajan et al., 1984). With the availability of repair-deficient mutants and the advent of gene manipula-

tion technology this concept was reassessed and finally modified.

Some contradictory findings to the paradigm that N-methylpurines are the only source for chromosomal aberrations were obtained from time-response curves of aberrations in different cell systems. If exponentially growing human non-established fibroblasts were pulse treated with N-methyl-N-nitrosourea (MNU), the frequency of chromatid-type aberrations reached a maximum that coincides with cells that were in early S-phase during treatment (as revealed by the curve of [<sup>3</sup>H]-thymidine-labeled mitoses, see Fig. 1A for human fibroblasts). Interestingly, a small peak preceding the main peak can be detected that likely represents cells out of the late S-phase during treatment, as deduced from determination of the percentages of [<sup>3</sup>H]-thymidine-labeled mitoses in a parallel experiment (Fig. 1A). (A similar observation was made by Evans and Scott with root tip meristem cells of *Vicia faba*; Evans and Scott, 1969). In a subsequent study, Thust (Thust et al., 1980) showed that, contrary to human fibroblasts, V79 Chinese hamster cells show the maximum level of chromatid-type aberrations induced by a nitrosourea derivative in the second post-treatment mitoses (Fig. 1B). He also found that primary Chinese hamster fibroblasts surprisingly display two aberration peaks, corresponding to the first (M1) and the second (M2) post-treatment mitoses (Fig. 1C). This indicated that the kinetics of aberration production is dependent on the cell type. What is the reason for these cell-type specific differences?

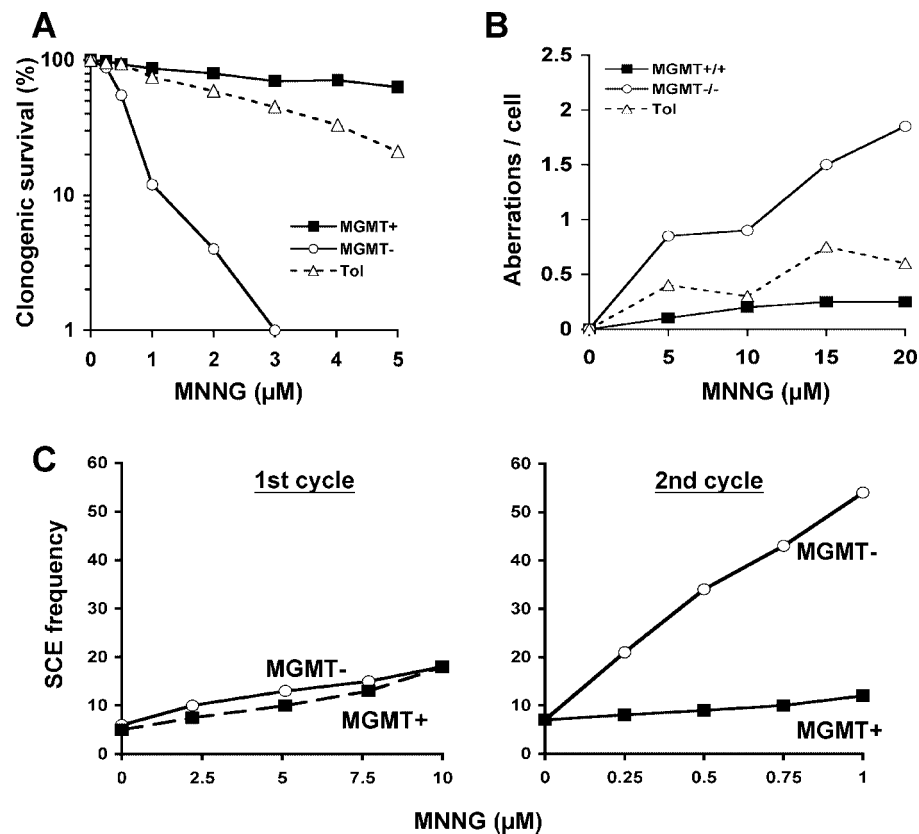


**Fig. 2.** Response of MGMT+, MGMT- and tolerant (Tol) cells to treatment with MNNG. **(A)** clonogenic cell survival; **(B)** Chromosomal aberrations induced as a function of dose of MNNG; **(C)** SCEs induced in the first post-treatment cell cycle (left panel) and the second post-treatment cell cycle (right panel) after MNNG exposure. MNNG treatment occurred for 60 min. Data from Kaina et al. (1993, 1997).

### Critical pre-recombinogenic and pre-clastogenic methylation lesions

An answer to this question was provided by the identification of specific DNA methylation lesions that lead to SCEs and aberrations. This identification was based on molecular dosimetry (Vogel and Natarajan, 1979; van Zeeland et al., 1983) and was further made possible by the availability of DNA repair deficient and genetically engineered cell lines, notably MGMT- (O<sup>6</sup>-methylguanine-DNA methyltransferase deficient), MGMT+ (O<sup>6</sup>-methylguanine-DNA methyltransferase proficient) and the so-called tolerant (MGMT deficient, mismatch repair impaired) cells (for review see Kaina et al., 1993). The main conclusions were: (1) agents inducing predominantly N-methylations (S<sub>N</sub>2 agents) such as MMS and dimethyl sulphate (DMS) exhibit high clastogenic but low point-mutagenic potency. This indicates that N-methylation lesions are responsible for clastogenic effects. (2) Agents inducing a higher level of O-methylations (S<sub>N</sub>1 agents) such as MNU and N-methyl-N'-nitro-N-nitrosoguanidine (MNNG) are still clastogenic but at the same time point-mutagenic, confirming that O-methylations are responsible for the induction of point mutations. (3) Cells deficient in MGMT, which repairs specifically O<sup>6</sup>-methylguanine and O<sup>4</sup>-methylthymine (comprising about 7 and 0.4% of the total DNA methylation products induced by MNU or MNNG, respectively), are highly sensitive to the cytotoxic, clastogenic and SCE-inducing effects of S<sub>N</sub>1 agents compared to the same cells expressing MGMT (Fig. 2). The same holds true for toler-

ant cells, which are impaired in mismatch repair (Fig. 2). From this it has been concluded that O<sup>6</sup>MeG (the minor lesion O<sup>4</sup>MeT is usually neglected because of its rarity) is a critical lesion leading to cell death, SCEs and chromatid-type aberrations. Furthermore, studies with MGMT genetically engineered cell lines further confirmed that O<sup>6</sup>MeG is a major point-mutagenic lesion, which is true for both S<sub>N</sub>1 and S<sub>N</sub>2 agents (Kaina et al., 1991). (4) Treatment of V79 (MGMT-deficient) cells with MNU or MNNG induced only few SCEs in the cell cycle exposed as seen in M1; SCEs were nearly exclusively induced in the second post-treatment cell cycle and therefore detectable in M2 (see Fig. 2C). In contrast, MMS is able to induce SCEs both in the cell cycle exposed and in the post-treatment cell cycle (Kaina and Aurich, 1985). Similar data were obtained for chromosomal aberrations for which the frequency after treatment with MNNG was low in M1 and much higher in M2 (Fig. 1D). Interestingly, if the same cells expressed MGMT upon transfection with an MGMT expression vector, aberrations in M2 cells were reduced to nearly background levels (Fig. 1D). These data indicated that O<sup>6</sup>MeG needs two cell cycles in order to be converted into SCEs and chromatid-type aberrations. It also indicated that the methylation lesion O<sup>6</sup>MeG is converted during the first round of replication into a secondary DNA lesion that acts as the ultimate trigger for either SCEs or aberrations (Kaina and Aurich, 1985; Kaina et al., 1993). Overall, the data support the paradigm that in cells that are deficient for MGMT or express MGMT at very low levels, O<sup>6</sup>MeG is the predominant recombinogenic and clastogenic lesion in M2. On the other hand, if cells are MGMT



proficient (and the dose of the methylating agent is not too high inducing O<sup>6</sup>MeG at levels that do not saturate MGMT repair capacity) N-methylation products (7MeG, 3MeA, 3MeG) appear to be the predominant clastogenic lesions, which provoke the genotoxic effect in M1.

On the basis of these findings the dose-effect curves shown in Fig. 1 can be reinterpreted as follows: human non-established fibroblasts and primary Chinese hamster cells express MGMT. Consequently, they behave like CHO cells transfected with MGMT (MGMT+), showing the highest clastogenic response due to non-repaired N-methylation lesions in M1. In contrast to this, V79 and CHO cells (and many other established cell lines) are MGMT deficient (MGMT-) displaying the highest clastogenic response due to non-repaired O<sup>6</sup>MeG lesions in M2. For S<sub>N</sub>2 agents (MMS, DMS), the aberration maximum is expected to occur in M1 because of the relatively high amount of N-alkylations compared to O<sup>6</sup>MeG induced in DNA.

### Role of mismatch repair

MGMT- cells defective in mismatch repair (MMR) are highly resistant to S<sub>N</sub>2 methylating agents (in the following named as O<sup>6</sup>-methylating agents); they obviously tolerate the pre-toxic lesion O<sup>6</sup>MeG in DNA. Tolerant cells also display lower MNNG-induced aberration frequencies than MGMT- cells not defective in MMR (an example is shown in Fig. 2B; see also Galloway et al., 1995; Armstrong and Galloway, 1996). It has therefore been suggested that MMR is essential for the conversion of O<sup>6</sup>MeG lesions into SCEs and aberrations (Kaina et al., 1997). Several findings strongly suggest that MMR (for review see Christmann et al., 2003) is indeed involved in the processing of O<sup>6</sup>MeG lesions. The heterodimer MutSa, composed of MSH2 and MSH6, binds to O<sup>6</sup>MeG/T mispairs (Duckett et al., 1996; Christmann and Kaina, 2000) which are formed in consequence of the mispairing properties of O<sup>6</sup>MeG during replication. According to an established model (Karran and Stephenson, 1990; Branch et al., 1995), MLH1 and PMS2 assemble the complex and nicks were introduced in the DNA next to the lesion (Sibghat-Ullah et al., 2001) excising the thymine-containing sequence and filling in the resulting gap. However, because of the mispairing properties of O<sup>6</sup>MeG, thymine will again be inserted opposite to O<sup>6</sup>MeG lesions – and the whole process starts again. This faulty MMR cycle at O<sup>6</sup>MeG/T lesions generates a secondary lesion that interferes with the subsequent round of DNA replication and ultimately leads to DSBs (Kaina et al., 1997; Ochs and Kaina, 2000). This model explains why SCEs and aberrations are formed in a replication-dependent manner in M2. Although this model still awaits thorough molecular proof, it provides a firm basis for explaining most of the data obtained in this field.

### Recombinogenic and clastogenic potency of O<sup>6</sup>MeG

The probability for O<sup>6</sup>MeG to be converted, by the mediation of MMR and DNA replication, into SCEs has been determined in two independent studies that compared MGMT+ and

MGMT- cells. For MGMT-deficient CHO-9 (Kaina et al., 1993) and human glioblastoma cells (Rasouli-Nia et al., 1994) it was reported that 1 SCE is produced per 30 and 42 O<sup>6</sup>MeG lesions respectively, that were induced by MNNG or MNU in the G1-phase of the cell cycle. This is quite a high conversion frequency compared, for instance, to cyclobutane dimers for which a relation of 1:600 has been estimated (De Weerd-Kastelein et al., 1977). It should be noted, however, that this calculation might need re-estimation in view of the fact that UV-C-induced BrdU photolysis may contribute to SCE formation (Wojcik et al., 2004). The O<sup>6</sup>MeG conversion probabilities for chromosomal aberrations are much lower, estimated in the range of 1:22,000 and 1:147,000 for aberrations induced in M2 and M1, respectively (Kaina et al., 1993). For lethal events the calculation ranges from 1:360 (Kaina et al., 1993) to 1:6,650 (Rasouli-Nia et al., 1994). The close correlation between induced O<sup>6</sup>MeG lesions and SCEs is striking. Taking into account that O<sup>6</sup>MeG mispairing with thymine occurs in only 1/3 of base pairings (provided equal amounts of deoxynucleotides are present) (Abbott and Saffhill, 1979), the conversion probability of O<sup>6</sup>MeG/T into SCEs would be even higher, i.e. about 1:10. It thus seems that O<sup>6</sup>MeG/T mispairs are exceptionally potent in inducing SCEs. The reason might be found in the particular structure of O<sup>6</sup>MeG/T-derived lesions processed by MMR. Although still hypothetical, it is tempting to speculate that MMR-generated lesions in the DNA cause a severe block of DNA replication, which is efficiently circumvented by a recombination process occurring at the replication fork that finally leads to an SCE. There are many lesions that block DNA replication although they seem to induce SCEs at much lower level, such as CPDs. It might therefore be speculated that most of the presumptive replication-blocking lesions, if they encounter a replication fork, are tolerated by translesion synthesis (*replication bypass*) accomplished by low fidelity SOS polymerases (Lehman, 2002), reading through non-instructive lesions without initiating the recombination process that leads to SCEs. The lesion provoked by O<sup>6</sup>MeG/T with the mediation of MMR can presumably not be processed by SOS polymerases and, therefore, *recombination bypass* will be the preferred mode of circumvention of this replication blockage. It should be noted that the doses of MNNG and MNU inducing SCEs in M2 do not cause any significant inhibition of DNA replication, as measured both by thymidine incorporation and the delay of the entry of BrdU-labelled cells into mitosis (Kaina, 1985; Kaina and Aurich, 1985) suggesting that recombination bypass leading to SCEs is a very efficient and fast process of lesion circumvention. A model of SCE formation triggered by O<sup>6</sup>MeG lesions is shown in Fig. 3.

### Are SCEs toxic events?

The low probability of conversion of O<sup>6</sup>MeG lesions into SCEs as compared to cell killing effects (measured by reduction in colony formation) indicates that SCEs are not necessarily toxic events. Support for this comes from dose-effect curves. SCE frequencies induced in MGMT-deficient V79 cells are a clear linear function of the dose of MNU and MNNG (Kaina

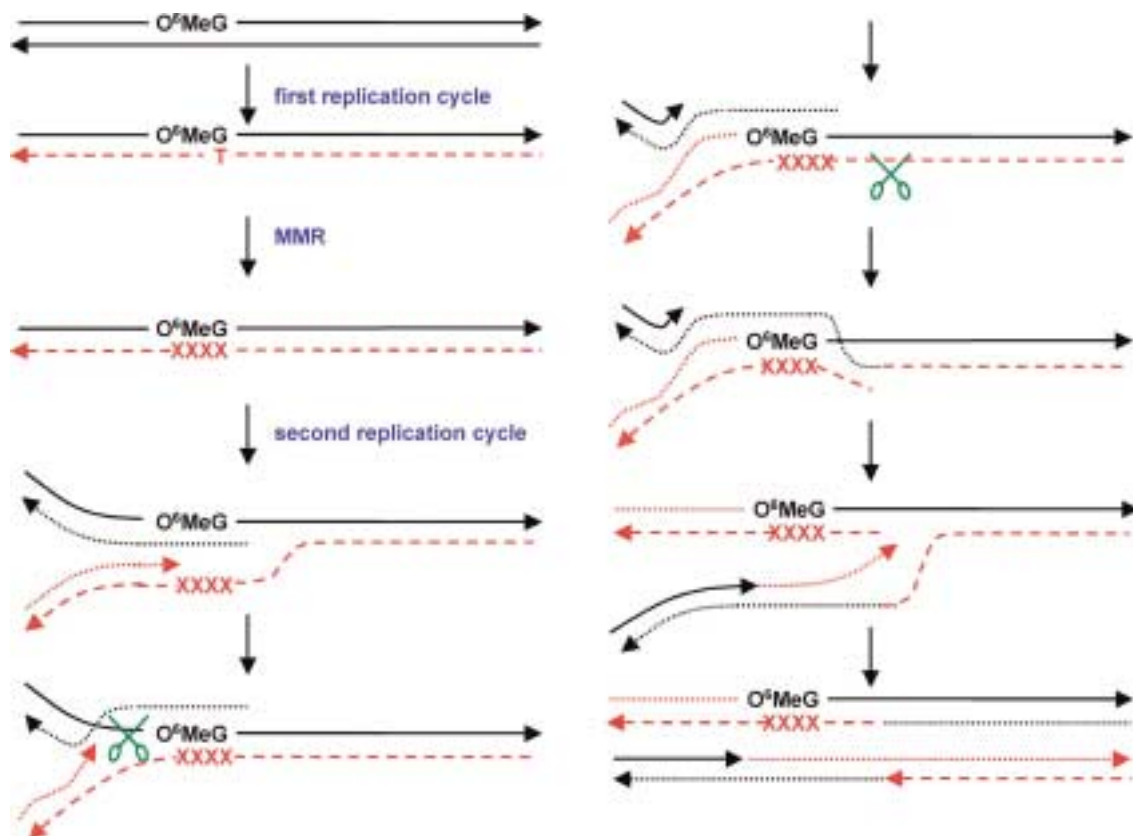


**Fig. 3.** Model of SCE formation by recombination bypass. Mismatch repair (MMR) at  $O^6MeG/T$  lesions is supposed to create a non-instructive lesion (designated by XXXX) that irreversibly blocks replication. Since the lesion cannot be circumvented by translesion synthesis, strand displacement occurs, followed by incision 5' and 3' next to the lesion in either of the parental strands, and rejoining of parental and nascent daughter strand having the same polarity. Thereafter, replication continues.

and Aurich, 1985). They are already induced at very low doses for which side effects were not yet detectable, such as inhibition of DNA synthesis and cell proliferation as well as reduction of the mitotic index. Notably, the dose-response curve for SCEs does not reveal a no-effect threshold (Kaina and Aurich, 1985). In contrast, the dose-response curve for cell kill of V79 cells exhibits a clear threshold (see Fig. 4A). Since SCEs are induced with doses of a methylating agent that are not yet toxic and clastogenic, SCEs appear to be generated by an error-free process. Overall, they seem to represent non-toxic events tolerated by the cell.

In contrast to SCEs, chromosomal aberrations induced by MNU show a threshold (at dose level  $<20 \mu M$ ) that seems to parallel the threshold in the cell survival curve (compare Fig. 4A and B). This may be taken to indicate that chromosomal aberrations rather than SCEs are related to reproductive cell death. This point will be discussed later again.

### Methylation-induced clastogenicity: role of replication fork inhibition

While SCEs are induced at very low dose levels (and are therefore a most sensitive indicator of DNA damage) higher doses of MNNG or MNU are required for the induction of chromosomal aberrations (Kaina, 1985). DNA synthesis is inhibited in the dose-range that induces aberrations in M1 (Kaina, 1985; Kaina, 1998). Based on the overlap in dose-response of replication inhibition and aberrations in M1 (Fig. 4B) it has been proposed that inhibition of replication fork movement due to methylation lesions causes nuclease attack at stalled replication forks that result in DSBs, which cause chromatid-type aberrations (Kaina, 1998). Various N-methylation lesions such as N3-methyladenine (3MeA) are supposed to block DNA replication. Also, apurinic sites resulting from spontaneous hydrolysis of N-methylpurines such as N7-methylguanine and 3MeA are likely critical candidates in blocking replication and thus leading to DSBs. If not repaired, or illegitimately recombined, DSBs will be expressed as chromatid-type aberrations in M1. Likewise, a similar process may give rise to aberrations in M2 with  $O^6MeG/T$ -derived secondary lesions being the trigger (Kaina et al., 1997).

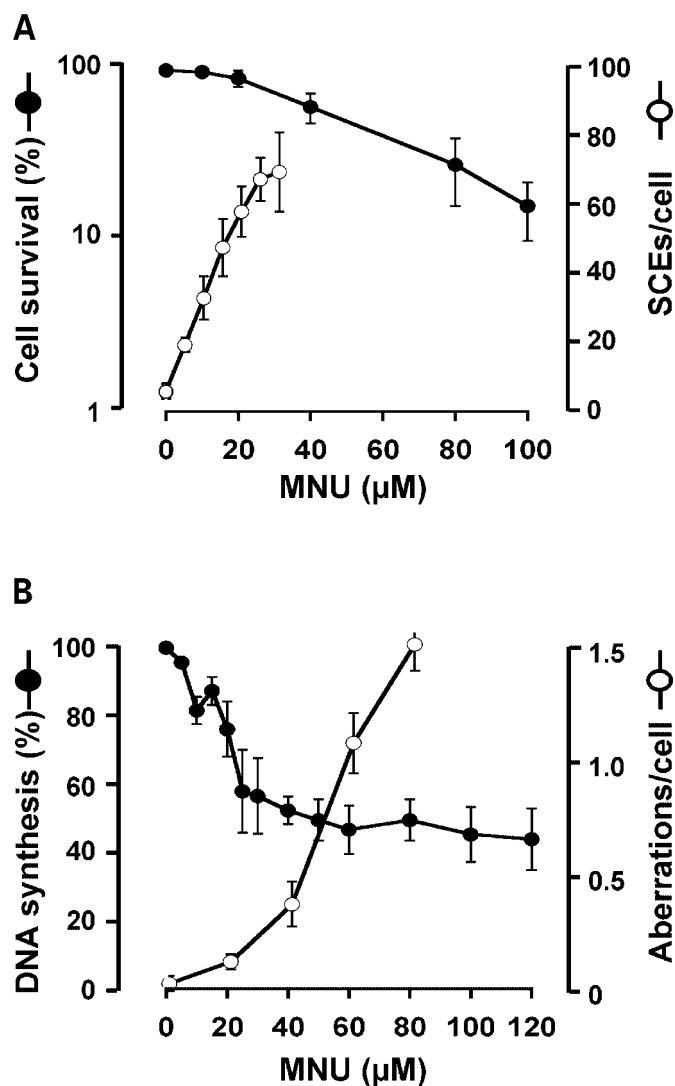


**Fig. 4.** Comparison of various cellular genotoxic responses of V79 cells. (A) clonogenic survival and SCE frequency as a function of dose of MNU. (B) DNA replication measured by thymidine incorporation and aberration frequency in M1 cells as a function of dose of MNU. Data from Kaina (1985) and Kaina and Aurich (1985).

Inhibition of fork movement may be a general mechanism involved in aberration formation. The following arguments are in favor of this: (1) all clastogenic agents inhibit DNA replication (Painter and Howard, 1982); (2) inhibitors of DNA replication that do not directly damage DNA are clastogenic (e.g. hydroxyurea, methotrexate) (Kihlman, 1977); (3) cells which are hypersensitive to DNA damaging agents, such as p53 and c-fos knockout cells, display enhanced S-phase inhibition and enhanced chromosomal breakage, which appear to be related (Haas and Kaina, 1995; Kaina, 1998; Kaina et al., 1998; Lackinger and Kaina, 2000). The molecular cause for the hypersensitivity of p53 and c-fos knockout cells to methylating agents is still unclear. Pathways leading to mutations and genotoxic end points such as SCEs and chromosomal aberrations on the basis of recombination bypass and translesion synthesis are summarized in Fig. 5.

#### DNA repair defects and methylation-induced clastogenicity

While the impact of deficiency in MGMT on chromosomal sensitivity has been studied in detail, the effect of other DNA repair defects, notably of the base excision repair (BER) pathway, has been studied to a lesser degree. It is remarkable that overexpression of N-methylpurine-DNA glycosylase (MPG) in CHO cells provokes sensitivity to methylating agents such as MMS, which has been interpreted to result from imbalance in BER (Ibeanu et al., 1992; Coquerelle et al., 1995). Embryonic knockout stem cells for MPG are hypersensitive to MMS (Engelward et al., 1996) whereas fibroblasts generated from MPG knockout mice do not display chromosomal hypersensitivity upon methylation (Elder et al., 1998). Knockout cells for DNA polymerase  $\beta$  (Pol $\beta$ ) are much more sensitive than the corresponding wild-type cells to the clastogenic effect of MMS and MNNG (Ochs et al., 1999). Knockout cells for apurinic endonuclease (APE) are not viable. However, down-modulation of APE by an antisense approach revealed hypersensitivity of the corresponding cells (Ono et al., 1994) whereas overexpression of yeast APE in CHO cells rendered them more resistant (Tomicic et al., 1997).

As noted above, p53 and c-fos knockout cells are hypersensitive to the clastogenic effect of MMS (Lackinger and Kaina, 2000; Lackinger et al., 2001). This could be due to altered S-phase regulation in response to methylation, impaired DNA repair, or both. Recent data ascribe DNA repair a role in the hypersensitivity to alkylating agents of p53 mutated fibroblasts. Thus, p53 appears to upregulate DNA polymerase  $\beta$  (Pol $\beta$ ) activity (Smith et al., 2001), due to physical interaction and stabilization of the repair protein. The same has been reported for apurinic endonuclease (APE) (Zhou et al., 2001). p53 is also involved in the induction of the MGMT gene by genotoxic stress (Rafferty et al., 1996; Grombacher et al., 1998) and presumably in the upregulation of some BER genes such as FEN1 (Christmann, Tomicic, Origer, Lackinger, and Kaina, manuscript in preparation). Whether this, however, results in protection against methylating agent-induced clastogenicity remains to be seen.

Another repair protein likely to be involved in methylation-induced clastogenicity is ATM (ataxia telangiectasia mutated). ATM is implicated in the repair of radiation-induced DSBs (Shiloh, 2001). Since DSBs are also formed in response to the treatment with DNA methylating agents (Ochs et al., 1999; Ochs and Kaina, 2000), it is conceivable that ATM could play a role in the repair, or processing, of these breaks. Indeed, aberration frequencies are enhanced in ATM null cells treated with MNNG, compared to the corresponding wild-type. This effect could further be enhanced by the MGMT inhibitor O<sup>6</sup>-benzyl-guanine (O<sup>6</sup>BG), which suggests that O<sup>6</sup>MeG-derived secondary lesions, notably DSBs, are processed by ATM. A similar potentiating effect in ATM cells has been observed for SCEs scored in 2<sup>nd</sup> post-treatment mitoses (Debiak et al., 2004), again ascribing a role for ATM in O<sup>6</sup>MeG-induced genotoxicity.

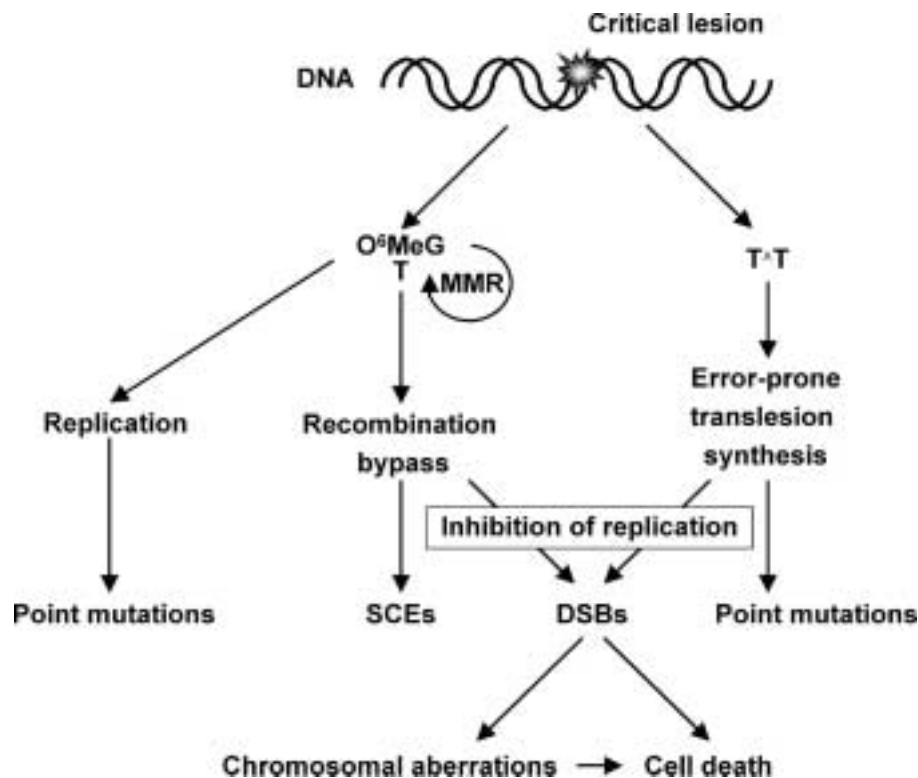


**Fig. 5.** Model for the formation of point mutations, SCEs and chromosomal aberrations involving recombination bypass and translesion synthesis at non-instructive lesions. If either one of the processes is unsuccessful, replication might still be inhibited leading to nuclease attack at arrested replication forks giving rise to DSBs. These may cause chromosomal aberrations and/or reproductive cell death.

### Biological consequences of methylation-induced aberrations

Two aspects will briefly be discussed: cell death by apoptosis and malignant transformation.

#### *DNA methylation lesions in apoptosis*

The apoptotic pathway evoked in CHO cells and other cell types by O<sup>6</sup>MeG has been studied in detail. It is clear that O<sup>6</sup>MeG is a powerful apoptotic lesion triggering the killing response by the mediation of MMR (Kaina et al., 1997; Tomiyama et al., 1997; Meikrantz et al., 1998). DNA replication is essentially involved since replication-arrested CHO-9 cells and non-proliferating human lymphocytes do not undergo apoptosis upon MNNG treatment (Kaina, 2003; Roos et al., 2004, and unpublished data). The pathway proposed on the basis of available data has been discussed recently (Kaina, 2003). In this model, DSBs are considered to be the critical ultimate lesions triggering decline of Bcl-2, which is a hallmark of methylation-induced apoptosis in this cell system (Ochs and Kaina, 2000). Since DSBs give rise to aberrations one might speculate that chromosomal aberrations induce apoptosis, e.g. by loss or inactivation of essential genes (loss of "survival factors"). Cell death by apoptosis could eliminate damaged cells and by this reduce the clastogenic effect. This has indeed been found for p53 wild-type lymphoblastoid cells (Greenwood et al., 1998) which are death receptor sensitive (Dunkern et al., 2003). It is important to note that in CHO cells apoptosis induced by MNNG is a late response occurring >48 h after treatment, whereas aberrations

in M1 and M2 cells clearly appear earlier. This may be taken to indicate that, at least in fibroblasts, apoptosis does not significantly eliminate chromosomally damaged cells. On the other hand, cells exhibiting aberrations could undergo death in the subsequent cell cycle due to apoptosis. Several arguments in favor of the hypothesis that aberrations contribute to apoptosis are: (1) both aberrations and apoptosis upon DNA methylation require DNA replication; (2) aberrations precede cell killing by apoptosis; (3) aberrations and apoptosis induced by methylating agents are provoked by DSBs; (4) for nucleotide analogs a correlation was found between the yield of chromosomal aberrations and apoptosis (Tomicic et al., 2002).

#### *Chromosomal aberrations and tumor formation*

Are chromosomal aberrations, induced by methylating agents, a contributing factor in malignant transformation? It is well established that the carcinogenic potency of methylating agents correlates with their potency to induce point mutations (Margison and O'Conner, 1990; Pegg and Singer, 1984). This is related to the efficiency of the agents to induce O-alkylations, and thus it is believed that the pro-mutagenic lesion O<sup>6</sup>MeG (together with the minor lesion O<sup>4</sup>-methylthymine) is the major driving force in carcinogenesis (Pegg, 1984). This has been confirmed in transgenic mouse models in which MGMT was over-expressed (Dumenco et al., 1993; Nakatsuru et al., 1993) or inactivated (MGMT null mouse) (Kawate et al., 1998). The creation of a mouse strain in which human MGMT was specifically expressed in skin allowed one to study tumorigenesis on the basis of the "classical" tumor initiation-promotion proto-

col. Data obtained showed that MGMT was highly efficient in attenuating the initiating effect of MNU whereas it had no effect on tumor promotion by TPA (Becker et al., 1996). In this study MNU was given as initiator at a single low dose that likely was inefficient to induce aberrations. With this treatment, however, mutations induced in *c-Ha-ras* have been found (Becker et al., 1996). Beside this, MMS applied at dose level inducing aberrations was not effective as an initiator in mouse skin (Fürstenberger et al., 1989b). Thus, the data suggests that point mutations, but not aberrations, are responsible for tumor initiation. MGMT also attenuated the conversion of benign tumors into malignant carcinomas by repeated treatment of papillomas with MNU (Becker et al., 2003). Whether chromosomal changes induced by repeated MNU treatments provoked tumor conversion (tumor progression) is unclear (note that MGMT overexpressed in the benign tumors can suppress theoretically both point mutations and aberrations). It would therefore be interesting to repeat the experiments on tumor conversion in this mouse system using MMS that is ineffective as tumor initiator although it induces chromosomal aberrations.

A study for the involvement of aberrations in carcinogenesis was performed using the so-called two-stage tumor promotion protocol. In this approach, tumor promotion in mouse skin is dissected using the first-stage promoter tetradecanoyl phorbol acetate (TPA) followed by repeated treatment with the second stage (incomplete) promoter retinoyl phorbol acetate (RPA) (Fürstenberger et al., 1981). If initiation occurred by a single dose of dimethyl-benz(a)anthracene (DMBA) followed by treatment with MMS and repeated treatment with RPA, the yield of papillomas was comparable to that obtained in an experiment in which TPA was used instead of MMS (Fürstenberger et al., 1989b). From this it has been concluded that MMS is a potent first-stage tumor promoter. The dose of MMS used induced chromosomal aberrations in skin cells and, therefore, methylation-induced aberrations are likely to be involved (Fürstenberger et al., 1989a, b). It is important to note that TPA is able to induce aberrations as well, presumably because of intracellular radical formation, whereas RPA does not (Marks and Fürstenberger, 1990; Petrussevska et al., 1988). Overall, the data support the concept that chromosomal aberrations are

involved in the early stages of tumor formation (Kaina, 1989) and that methylating agents, which are powerful clastogens, can thus drive the process of carcinogenesis.

## Outlook

Both O<sup>6</sup>MeG and N-methylpurines cause chromosomal aberrations in cells exposed to DNA methylating agents. In this process, DNA replication and, for O<sup>6</sup>MeG driven clastogenesis, MMR is essentially involved. It has been proposed that the arrest of DNA replication is critical for the generation of DSBs, which act as ultimate genotoxic lesions. There are many questions, however, which await resolution. It would be interesting to know to which extent individual DSB repair pathways, namely NHEJ and HR, are involved in methylation-induced clastogenicity. Further, the role of ATM and ATR in the repair or signaling of methylation-induced DNA damage remains to be elucidated. Also the secondary recombinogenic lesion derived from O<sup>6</sup>MeG by the mediation of MMR needs to be identified. Finally, the model of lesion tolerance by recombination bypass and the possible competition of this pathway with translesion synthesis by error-prone DNA polymerases should be substantiated. The proposed model (Fig. 5) suggests that recombination bypass is also important for the tolerance of DNA interstrand crosslinks (ICL) which are strong inducers of SCEs in the treatment cell cycle (Kaina and Aurich, 1985). It would thus be interesting to see whether recombination bypass of ICL is error free. Finally the involvement of many of the newly cloned DNA repair genes encoding e.g. DNA-PK, Rad51, BRCA1 and 2, and XRCC2 in methylation-induced recombination and clastogenicity will be addressed in the future. Overall, it is obvious that our knowledge on methylation-induced aberrations has grown constantly during the last 30 years, but there is still much to do in order to fully resolve the puzzle.

## Acknowledgements

I am grateful to Markus Christmann for his help with the drawings and Wynand Roos for critical reading the manuscript.

## References

- Abbott PJ, Saffhill R: DNA synthesis with methylated poly(dC-dG) templates. Evidence for a competitive nature to miscoding by O<sup>6</sup>-methylguanine. *Biochim biophys Acta* 562:51–61 (1979).
- Armstrong MJ, Galloway SM: Mismatch repair provokes chromosome aberrations in hamster cells treated with methylating agents or 6-thioguanine, but not with ethylating agents. *Mutat Res* 373:167–178 (1996).
- Becker K, Dosch J, Gregel CM, Martin BM, Kaina B: Targeted expression of human O<sup>6</sup>-methylguanine-DNA methyltransferase (MGMT) in transgenic mice protects against tumor initiation in two-stage skin carcinogenesis. *Cancer Res* 56:3244–3249 (1996).
- Becker K, Gregel C, Fricke C, Komitowski D, Dosch J, Kaina B: DNA repair protein MGMT protects against N-methyl-N-nitrosourea-induced conversion of benign into malignant tumors. *Carcinogenesis* 24:541–546 (2003).
- Branch P, Hampson R, Karran P: DNA mismatch binding defects, DNA damage tolerance, and mutator phenotypes in human colorectal carcinoma cell lines. *Cancer Res* 55:2304–2309 (1995).
- Christmann M, Kaina B: Nuclear translocation of mismatch repair proteins MSH2 and MSH6 as a response of cells to alkylating agents. *J Biol Chem* 275:36256–36262 (2000).
- Christmann M, Tomicic MT, Roos WP, Kaina B: Mechanisms of human DNA repair: an update. *Toxicology* 193:3–34 (2003).
- Coquerelle T, Dosch J, Kaina B: Overexpression of N-methylpurine-DNA glycosylase in Chinese hamster ovary cells renders them more sensitive to the production of chromosomal aberrations by methylating agents – a case of imbalanced DNA repair. *Mutat Res* 336:9–17 (1995).
- Debiak G, Nikolova T, Kaina B: Loss of ATM sensitizes against O<sup>6</sup>-methylguanine triggered apoptosis, SCEs and chromosomal aberrations. *DNA Repair* 3:359–368 (2004).
- De Weerd-Kastelein EA, Keijzer W, Rainaldi G, Bootsma D: Induction of sister chromatid exchange in xeroderma pigmentosum cells after exposure to ultraviolet light. *Mutat Res* 45:253–261 (1977).

- Duckett DR, Drummond JT, Hurchie AIH, Reardon JT, Sancar A, Lilley DM, Modrich P: Human Mut-Sa recognizes damaged DNA base pairs containing O<sup>6</sup>-methylguanine, O<sup>4</sup>-methylthymine, or the cisplatin-d(GpG) adduct. *Proc Natl Acad Sci USA* 93:6443–6447 (1996).
- Dumenco LL, Allay E, Norton K, Gerson SL: The prevention of thymic lymphomas in transgenic mice by human O<sup>6</sup>-alkylguanine-DNA alkyltransferase. *Science* 259:219–222 (1993).
- Dunkern TR, Roos WP, Kaina B: Apoptosis induced by MNNG in human TK6 lymphoblastoid cells is p53 and Fas/CD95/Apo-1 related. *Mutat Res* 544:167–172 (2003).
- Elder RH, Jansen JG, Weeks JR, Willington MA, Deans B, Watson AJ, Mynett KJ, Bailey JA, Cooper DP, Rafferty JA, Heeran MC, Wijnhoven SW, van Zeeland AA, Margison GP: Alkylpurine-DNA-N-glycosylase knockout mice show increased susceptibility to induction of mutations by methyl methanesulfonate. *Mol Cell Biol* 18:5828–5837 (1998).
- Engelward BP, Dreslin A, Christensen J, Huszar D, Kurahara C, Samson L: Repair-deficient 3-methyladenine DNA glycosylase homozygous mutant mouse cells have increased sensitivity to alkylation-induced chromosome damage and cell killing. *EMBO J* 15:945–952 (1996).
- Evans HJ, Scott D: The induction of chromosome aberrations by nitrogen mustard and its dependence on DNA synthesis. *Proc R Soc B* 173:491–512 (1969).
- Fürstenberger G, Berry DL, Sorg B, Marks F: Skin tumor promotion by phorbol esters is a two-stage process. *Proc Natl Acad Sci USA* 78:7722–7726 (1981).
- Fürstenberger G, Schurich B, Kaina B, Marks F: Possible involvement of chromosomal damage in tumor induction in initiated mouse skin. *Cancer Res Clin Oncol* 115:57 (1989a).
- Fürstenberger G, Schurich B, Kaina B, Petrusovska RT, Fusenig NE, Marks F: Tumor induction in initiated mouse skin by phorbol esters and methyl methanesulfonate: correlation between chromosomal damage and conversion (stage I of tumor promotion) in vivo. *Carcinogenesis* 10:749–752 (1989b).
- Galloway SM, Greenwood SK, Hill RB, Bradt CI, Bean CL: A role for mismatch repair in production of chromosome aberrations by methylating agents in human cells. *Mutat Res* 346:231–245 (1995).
- Greenwood SK, Armstrong ML, Hill RB, Brandt CI, Johnson TE, Hilliard CA, Galloway SM: Fewer chromosome aberrations and earlier apoptosis induced by DNA synthesis inhibitors, a topoisomerase II inhibitor or alkylating agents in human cells with normal compared with mutant p53. *Mutat Res* 401:39–53 (1998).
- Grombacher T, Eichhorn U, Kaina B: p53 is involved in regulation of the DNA repair gene O<sup>6</sup>-methylguanine-DNA methyltransferase (MGMT) by DNA damaging agents. *Oncogene* 17:845–851 (1998).
- Haas S, Kaina B: c-Fos is involved in the cellular defence against the genotoxic effect of UV radiation. *Carcinogenesis* 16:985–991 (1995).
- Ibeanu G, Hartenstein B, Dunn WC, Chang LY, Hofmann E, Coquerelle T, Mitra S, Kaina B: Overexpression of human DNA repair protein N-methylpurine-DNA glycosylase results in the increased removal of N-methylpurines in DNA without a concomitant increase in resistance to alkylating agents in Chinese hamster ovary cells. *Carcinogenesis* 13:1989–1995 (1992).
- Kaina B: The interrelationship between SCE induction, cell survival, mutagenesis, aberration formation and DNA synthesis inhibition in V79 cells treated with N-methyl-N-nitrosourea or N-methyl-N'-nitro-N-nitrosoguanidine. *Mutat Res* 142:49–54 (1985).
- Kaina B: Chromosomal aberrations as a contributing factor for tumor promotion in the mouse skin. *Teratogen Carcinogen Mutagen* 9:331–348 (1989).
- Kaina B: Critical steps in alkylation-induced aberration formation. *Mutat Res* 404:119–124 (1998).
- Kaina B: DNA damage-triggered apoptosis: critical role of DNA repair, double-strand breaks, cell proliferation and signaling. *Biochem Pharmacol* 66:1547–1554 (2003).
- Kaina B, Aurich O: Dependency of the yield of sister-chromatid exchanges induced by alkylating agents on fixation time. Possible involvement of secondary lesions in sister-chromatid exchange induction. *Mutat Res* 149:451–461 (1985).
- Kaina B, Fritz G, Coquerelle T: Contribution of O<sup>6</sup>-alkylguanine and N-alkylpurines to the formation of sister chromatid exchanges, chromosomal aberrations, and gene mutations: new insights gained from studies of genetically engineered mammalian cell lines. *Environ Mol Mutagen* 22:283–292 (1993).
- Kaina B, Fritz G, Mitra S, Coquerelle T: Transfection and expression of human O<sup>6</sup>-methylguanine-DNA methyltransferase (MGMT) cDNA in Chinese hamster cells: the role of MGMT in protection against the genotoxic effects of alkylating agents. *Carcinogenesis* 12:1857–1867 (1991).
- Kaina B, Fritz G, Ochs K, Haas S, Grombacher T, Dosch J, Christmann M, Lund P, Gregel CM, Becker K: Transgenic systems in studies on genotoxicity of alkylating agents: critical lesions, thresholds and defense mechanisms. *Mutat Res* 405:179–191 (1998).
- Kaina B, Waller H, Waller M, Rieger R: The action of N-methyl-N-nitrosourea on non-established human cell lines in vitro. I. Cell cycle inhibition and aberration induction in diploid and Down's fibroblast. *Mutat Res* 43:387–400 (1977).
- Kaina B, Ziouta A, Ochs K, Coquerelle T: Chromosomal instability, reproductive cell death and apoptosis induced by O<sup>6</sup>-methylguanine in Mex-, Mex+ and methylation-tolerant mismatch repair compromised cells: facts and models. *Mutat Res* 381:227–241 (1997).
- Karran P, Stephenson C: Mismatch binding proteins and tolerance to alkylating agents in human cells. *Mutat Res* 236:269–275 (1990).
- Kawate H, Sakumi K, Tsuzuki T, Nakatsuru Y, Ishikawa T, Takahashi S, Takano H, Noda T, Sekiguchi M: Separation of killing and tumorigenic effects of an alkylating agent in mice defective in two of the DNA repair genes. *Proc Natl Acad Sci USA* 95:5116–5120 (1998).
- Kihlman BA: Caffeine and Chromosomes (Elsevier Scientific, Amsterdam 1977).
- Lackinger D, Eichhorn U, Kaina B: Effect of ultraviolet light, methyl methanesulfonate and ionizing radiation on the genotoxic response and apoptosis of mouse fibroblasts lacking c-Fos, p53 or both. *Mutagenesis* 16:233–241 (2001).
- Lackinger D, Kaina B: Primary mouse fibroblasts deficient for c-Fos, p53 or for both proteins are hypersensitive to UV light and alkylating agent-induced chromosomal breakage and apoptosis. *Mutat Res* 9042:1–11 (2000).
- Lehman AR: Replication of damaged DNA in mammalian cells: new solutions to an old problem. *Mutat Res* 509:23–34 (2002).
- Loveless A: Possible relevance of O<sup>6</sup>-alkylation of deoxyguanosine to the mutagenicity and carcinogenicity of nitrosamines and nitrosamides. *Nature* 223:206–207 (1969).
- Margison GP, O'Conner PJ: Biological consequences of reactions with DNA: Role of specific lesions, in Cooper CS, Grover PL (eds): *Handbook of Experimental Pharmacology*, Vol. 9, p 547 (Springer Verlag, Berlin 1990).
- Marks F, Fürstenberger G: The conversion stage of skin carcinogenesis. *Carcinogenesis* 11:2085–2092 (1990).
- Meikrantz W, Bergom MA, Memisoglu A, Samson L: O<sup>6</sup>-alkylguanine DNA lesions trigger apoptosis. *Carcinogenesis* 19:369–372 (1998).
- Morris SM, Heflich RH, Beranek DT, Kodell RL: Alkylation-induced sister-chromatid exchanges correlate with reduced cell survival, not mutations. *Mutat Res* 105:163–168 (1982).
- Morris SM, Beranek DT, Heflich RH: The relationship between sister-chromatid exchange induction and the formation of specific methylated DNA adducts in Chinese hamster ovary cells. *Mutat Res* 121:261–266 (1983).
- Nakatsuru Y, Matsukuma S, Nemoto N, Sugano H, Sekiguchi M, Ishikawa T: O<sup>6</sup>-methylguanine-DNA methyltransferase protects against nitrosamine-induced hepatocarcinogenesis. *Proc Natl Acad Sci USA* 90:6468–6472 (1993).
- Natarajan AT, Obe G: Molecular mechanisms involved in the production of chromosomal aberrations. I. Utilization of *Neurospora* endonuclease for the study of aberration production in G2 stage of the cell cycle. *Mutat Res* 52:137–149 (1978).
- Natarajan AT, Obe G: Molecular mechanisms involved in the production of chromosomal aberrations. III. Restriction endonucleases. *Chromosoma* 90:120–127 (1984).
- Natarajan AT, Simons JWIM, Vogel EW, van Zeeland AA: Relationship between cell killing, chromosomal aberrations, sister-chromatid exchanges and point mutations induced by monofunctional alkylating agents in Chinese hamster cells. A correlation with different ethylation products in DNA. *Mutat Res* 128:31–40 (1984).
- Ochs K, Kaina B: Apoptosis induced by DNA damage O<sup>6</sup>-methylguanine is Bcl-2 and caspase-9/-3 regulated and Fas/caspase-8 independent. *Cancer Res* 60:5815–5824 (2000).
- Ochs K, Sobol RW, Wilson SH, Kaina B: Cells deficient in DNA polymerase beta are hypersensitive to alkylating agent-induced apoptosis and chromosomal breakage. *Cancer Res* 59:1544–1551 (1999).
- Ono Y, Furuta T, Ohmoto T, Akiyama K, Seki S: Stable expression in rat glioma cells of sense and antisense nucleic acids to a human multifunctional DNA repair enzyme, APEX nuclease. *Mutat Res* 315:55–63 (1994).
- Painter RB, Howard R: The HeLa DNA-synthesis inhibition test as a rapid screen for mutagenic carcinogens. *Mutat Res* 92:427–437 (1982).
- Pegg AE: Methylation of the O<sup>6</sup>-position of guanine in DNA is the most likely initiating event in carcinogenesis by methylating agents. *Cancer Invest* 2:223–231 (1984).
- Pegg AE, Singer B: Is O<sup>6</sup>-alkylguanine necessary for initiation of carcinogenesis by alkylating agents? *Cancer Invest* 2:221–238 (1984).
- Petrusevska RT, Fürstenberger G, Marks F, Fusenig NE: Cytogenetic effects caused by phorbol ester tumor promoters in primary mouse keratinocyte cultures: correlation with the convertogenic activity of TPA in multistage skin carcinogenesis. *Carcinogenesis* 9:1207–1215 (1988).
- Rafferty JA, Clarke AR, Sellappan D, Koref MS, Frayling IM, Margison GP: Induction of murine O<sup>6</sup>-alkylguanine-DNA-alkyltransferase in response to ionizing radiation is p53 gene dose dependent. *Oncogene* 12:693–697 (1996).

- Rasouli-Nia A, Sibghat-Ullah L, Mirzayans R, Paterson MC, Day III RS: On the quantitative relationship between O<sup>6</sup>-methylguanine residues in genomic DNA and production of sister-chromatid exchanges, mutations and lethal events in a Mer-human tumor cell line. *Mutat Res* 314:99–113 (1994).
- Roos WP, Baumgärtner M, Kaina B: Apoptosis triggered by DNA damage O<sup>6</sup>-methylguanine in human lymphocytes required DNA replication and is mediated by p53 and Fas/CD95/Apo-1. *Oncogene* 23:359–367 (2004).
- Shiloh Y: ATM and ATR: networking cellular responses to DNA damage. *Curr Opin Genet Dev* 11:71–77 (2001).
- Sibghat-Ullah L, Day III RS, Dobler KD, Paterson MC: Initiation of strand incision at G:T and O<sup>6</sup>-methylguanine:T base mismatches in DNA by human cell extracts. *Nucleic Acids Res* 29:2409–2417 (2001).
- Smith ML, Ford JM, Hollander C, Bortnick RA, Amundson SA, Seo YR, Deng CX, Hanawalt PC, Fornace AJ: p53-mediated DNA repair responses to UV radiation: studies of mouse cells lacking p53, p21, and/or gadd45 genes. *Mol Cell Biol* 20:3705–3714 (2001).
- Thust R, Mendel J, Schwarz H, Warzok R: Nitrosated urea pesticide metabolites and other nitrosamides. Activity in clastogenicity and SCE assays, and aberration kinetics in Chinese hamster V79E cells. *Mutat Res* 79:239–248 (1980).
- Tomicic M, Eschbach E, Kaina B: Expression of yeast but not human apurinic/apyrimidinic endonuclease renders Chinese hamster cells more resistant to DNA damaging agents. *Mutat Res* 383:155–165 (1997).
- Tomicic MT, Bey E, Wutzler P, Thust R, Kaina B: Comparative analysis of DNA breakage, chromosomal aberrations and apoptosis induced by the anti-herpes purine nucleoside analogues aciclovir, ganciclovir and penciclovir. *Mutat Res* 505:1–11 (2002).
- Tominaga Y, Tsuzuki T, Shiraishi A, Kawate H, Sekiguchi M: Alkylation-induced apoptosis of embryonic stem cells in which the gene for DNA-repair, methyltransferase, had been disrupted by gene targeting. *Carcinogenesis* 18:889–896 (1997).
- van Zeeland AA, Mohn GR, Aaron CS, Glickman BW, Brendel M, de Serres FJ, Hung CY, Brockman HE: Molecular dosimetry of the chemical mutagen ethyl methanesulfonate. Quantitative comparison of the mutagenic potency in *Neurospora crassa* and *Saccharomyces cerevisiae*. *Mutat Res* 119:45–54 (1983).
- Vogel E, Natarajan AT: The relation between reaction kinetics and mutagenic action of mono-functional alkylating agents in higher eukaryotic systems. I. Recessive lethal mutations and translocations in *Drosophila*. *Mutat Res* 62:51–100 (1979).
- Wojcik A, Bruckmann E, Obe G: Insights into the mechanisms of sister chromatid exchange formation. *Cytogenet Genome Res* 104:304–309 (2004).
- Zhou J, Ahn J, Wilson SH, Prives C: A role for p53 in base excision repair. *EMBO J* 15:914–923 (2001).

# Human fibroblasts expressing hTERT show remarkable karyotype stability even after exposure to ionizing radiation

L.M. Pirzio,<sup>a</sup> M.-A. Freulet-Marrière,<sup>a</sup> Y. Bai,<sup>b</sup> B. Fouladi,<sup>b</sup> J.P. Murnane,<sup>b</sup>  
L. Sabatier,<sup>a</sup> and C. Desmaze<sup>a</sup>

<sup>a</sup>CEA-DSV/DRR/LRO, 92265 Fontenay aux roses (France);

<sup>b</sup>Department of Radiation Oncology, University of California, San Francisco, CA (USA)

**Abstract.** Ectopic expression of telomerase results in an immortal phenotype in various types of normal cells, including primary human fibroblasts. In addition to its role in telomere lengthening, telomerase has now been found to have various functions, including the control of DNA repair, chromatin modification, and the control of expression of genes involved in cell cycle regulation. The investigations on the long-term effects of telomerase expression in normal human fibroblast highlighted that these cells show low frequencies of chromosomal aberrations. In this paper, we describe the karyotypic stability of human fibroblasts immortalized by expression of hTERT. The ectopic overexpression of telomerase is associated with

unusual spontaneous as well as radiation-induced chromosome stability. In addition, we found that irradiation did not enhance plasmid integration in cells expressing hTERT, as has been reported for other cell types. Long-term studies illustrated that human fibroblasts immortalized by telomerase show an unusual stability for chromosomes and for plasmid integration sites, both with and without exposure to ionizing radiation. These results confirm a role for telomerase in genome stabilisation by a telomere-independent mechanism and point to the possibility for utilizing hTERT-immortalized normal human cells for the study of gene targeting.

Copyright © 2003 S. Karger AG, Basel

Telomeres are nucleoprotein complexes that protect chromosome ends from nuclease degradation and chromosome fusion (de Lange, 2002). In most human primary cells, telomeres shorten with each round of replication, leading to end-to-end fusions observed in senescent human cells (Counter et al., 1992). The causal factor that drives primary cells to enter replicative senescence is telomere attrition resulting from the lack of telomerase activity. Telomerase is a nuclear ribonucleoprotein that replenishes telomeres in most eukaryotes (Greider and Blackburn, 1985; Collins and Mitchell, 2002). In human cells, the RNA subunit hTR is ubiquitously expressed, whereas hTERT, the catalytic component, would be expressed primarily

in embryonic stem cells and germ cells. Telomerase can protect chromosomes from end-to-end fusion not only by lengthening the telomere but also by providing a cap at the end of the chromosome (Melek and Shippen, 1996; Zhu et al., 1999; Blackburn, 2001; Stewart et al., 2002). Moreover, the presence of hTERT activity in normal human fibroblasts during their transit through S phase (Masutomi et al., 2003) suggests that telomerase and telomere structure are dynamically regulated. Therefore, telomerase might have a role in chromosome end protection that is independent of its ability to elongate telomeres. Furthermore, ectopic expression of telomerase in primary cells may enhance cell survival in the face of proapoptotic cellular stress, although hTERT expression does not protect cells from stress-induced premature senescence (Gorbunova et al., 2002). Telomerase seems to regulate the transcription of a variety of genes implicated in cell growth (Smith et al., 2003), chromatin modification, and in DNA repair, without influencing telomere length. In addition, telomerase expression is associated with a reduction of spontaneous chromosome damage in G1 cells (Sharma et al., 2003), which could be important in the cascade of events leading to chromosome stabilisation. Investi-

This work was supported by EDF and the European Union contract FIGH-CT-2002-00217 (TELOSENS). L.M.P. was a recipient of an EDF fellowship.

Received 26 September 2003; accepted 26 November 2003.

Request reprints from: Dr. Chantal Desmaze, CEA-DSV/DRR/LRO  
18 Route du Panorama, 92265 Fontenay aux roses cedex (France)  
telephone: +33 (1) 46 54 83 27; fax: +33 (1) 46 54 87 58  
e-mail: desmaze@dsvdif.cea.fr.



gation of the long-term effects of forced telomerase expression on normal human fibroblasts highlighted that it does not result in changes typically associated with malignant transformation in these cells, that show low frequencies of chromosomal aberrations (Morales et al., 1999). In sheep fibroblasts, telomerase expression levels correlate with shorter telomere lengths and the extent of karyotypic abnormality. Indeed, highly expressing cell lines showed virtually normal karyotypes, even after extended culture when lower expressing lines exhibited chromosomal abnormalities (Cui et al., 2002). Nevertheless, ectopic hTERT expression in human fibroblasts derived from centenarian individuals also developed chromosomal anomalies (Mondello et al., 2003). Moreover, one of these cell strains acquired the ability to grow in the absence of solid support, a typical feature of transformed cells. Therefore, the outcome of cellular immortalization driven by telomerase reactivation might depend on the frequency of genomic alterations already present in the cell.

In addition to telomere attrition in cycling cells, DNA double strand breaks (DSBs) are also a source of chromosomal instability. DSBs can either be properly repaired, restoring genomic integrity, or misrepaired, resulting in drastic consequences for the cell, including cell death, genomic instability, and cancer. It is well established that exposure to DSB-inducing agents, such as ionizing radiation, is associated with chromosomal abnormalities (Natarajan et al., 1986; Pfeiffer et al., 2000; Obe et al., 2002), and that the progeny of cells exposed to ionizing radiation can exhibit delayed genetic changes, including specific gene mutations (Little et al., 1990) and chromosome aberrations (Kadhim et al., 1992; Sabatier et al., 1992). These delayed mutations and chromosome anomalies are usually regarded as a consequence of the destabilisation of the genome, termed radiation-induced chromosome instability. Moreover, DNA broken ends can be stabilized by the addition of telomeric repeats by recombination or translocations (telomere capture) (Difilippantonio et al., 2002; Lo et al., 2002), or by telomerase (chromosome healing) that can catalyse the synthesis of telomeric repeats on non-telomeric DNA (Slijepcevic and Bryant, 1998; Sprung et al., 1999b). Transgenic integration might constitute a chromosomal DNA repair event in which exogenous DNA is inserted into a chromosomal DSB. In general, the low spontaneous frequency of gene targeting has precluded its widespread experimental use in mammalian somatic cell genetics. A number of studies has shown that transgenes integrate preferentially at sites within chromosomes that are susceptible to DSBs, termed fragile sites (Rassool et al., 1991; Matzner et al., 2003). In addition, it has been reported that the induction of a specific DSB at a chromosomal locus greatly stimulates the integration of a homologous transgene at the site of the induced break (Brenneman et al., 1996; Donoho et al., 1998; Miller et al., 2003; Porteus et al., 2003). Radiation-induced DNA damage has been shown to improve plasmid integration, a phenomenon termed "radiation enhanced integration" (Stevens et al., 1996). As a result, it has been proposed that irradiation of cells prior to transfection can improve stable gene transfer of both plasmid and adenoviral vectors (Zeng et al., 1997) by induction of a hyper-recombination state, possibly related to chromosome instability (Stevens et al., 1999).

In the present paper, we focused on the characterization of the karyotypic stability in human fibroblasts immortalized by telomerase, both spontaneously and after exposure to ionizing irradiation. The effects of telomerase overexpression on karyotypic stability were compared with those of endogenously reactivated telomerase in human tumor cell lines. Chromosome damage after irradiation was determined at the first post-treatment mitosis and a correlation with telomerase activity and telomere length was investigated in these cell lines. The ability to integrate plasmids was assessed and no difference was found between human fibroblasts immortalized by telomerase and a human tumor cell line. We noted that ectopic overexpression of hTERT is associated with peculiar genome stability, even in the case of transgenic integration following ionizing radiation. Furthermore, hTERT overexpression appeared to protect cells from radiation-enhanced integration. Irradiated clones showed both chromosomal and plasmid insertion site stability. These results confirm the role of telomerase in genome stabilisation and suggest the possibility that hTERT immortalized normal human cells may be useful for the study of gene targeting.

## Materials and methods

### *Cells and culture conditions*

HCA-ltrt is a clone of BJ fibroblasts immortalized by the catalytic subunit of human telomerase (hTERT) (Rubio et al., 2002). HCA 17.3 cell line was derived from HCA-ltrt following selection for integration of the pSXpneoD plasmid. The B3 cell line derives from human bladder carcinoma, and has a slightly rearranged karyotype (46;XY,t(11;20),t(15;18), and is telomerase positive (Fouladi et al., 2000). SCC61 and SQ9G are both telomerase-positive cell lines as described elsewhere (Brachman et al., 1992; Cowan et al., 1993). They show rearranged karyotypes: (46;XY),t(2,18),t(3;9),t(9;15),t(7;Y),del4 and (46;XY),t(4;22),t(9;16),t(11;20),del4p respectively. Cells were maintained in DMEM/F12 medium (Life Technologies, Bethesda, USA) supplemented with 10% FCS (Life Technologies, Bethesda, USA) and incubated at 37 °C in a humidified incubator with 5% CO<sub>2</sub>. G418 (200 µg/ml, Life Technologies) was added to medium for HCA17.3 and B3 cell lines.

### *Transfection and irradiation*

Plasmids pCMVGFP and pCMVGFP-Telo (containing 1.6 kb of (TTAGGG)<sub>n</sub> telomere repeats) were extracted from *E. coli* DH5α cells and were purified by standard procedures (Quiagen plasmid giga kit). pCMV and pCMV-Telo plasmids were linearized by *NotI* (Biolabs) digestion before transfection; this endonuclease cuts the plasmid just after T<sub>2</sub>AG<sub>3</sub> repeats in pCMV-Telo. For the pNCT-tel plasmid, transfection and clone analysis were performed as previously described (Sprung et al., 1999a, c; Fouladi et al., 2000). The pSXpneoD plasmid was derived from pNCT-tel and contains the neo and HSV-tk genes, as well as 4 kb of human DNA from the end of chromosome 7q (accession number AF027390) for targeted integration near a telomere.

For electroporation experiments, cells were harvested from subconfluent cultures, washed twice and counted. 5 × 10<sup>6</sup> cells were resuspended in culture medium in a final volume of 800 µl, and 10 µg of plasmid DNA was added. After 1 min incubation at room temperature, cells were transferred into the 4-mm-gap cuvette (Equibio) and electroporated with an EasyjecT (Eurogentec) apparatus: the 1500-µF capacitor was charged to 310 V for HCA17.3 and to 250 V for B3, with Ω<sub>∞</sub>. Cells were transferred into pre-warmed medium immediately after pulse and then dispatched into flasks for irradiation. Cells were irradiated at different doses with a <sup>137</sup>Cs source (0.71 Gy/min). For stable transfections, HCA17.3 cells were plated at low density. After 15 days incubation under hygromycin (30 µg/ml, Life Technologies) selection, clones derived from a single cell were isolated by pipetting under the microscope. Clones were split 1:2, therefore passages correspond to population doublings.

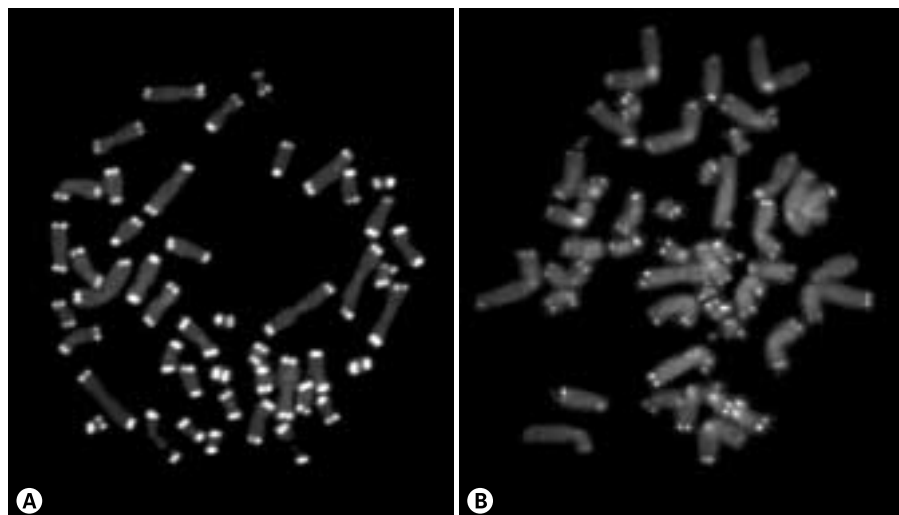


**Fig. 1.** PNA-telomere probe hybridised on metaphase spreads. **(A)** hTERT immortalized human fibroblast HCA17.3; **(B)** human tumor cell line B3. Note the telomere intensity in HCA17.3 and the telomere homogeneity in both cell lines.

#### Plating efficiency

After electroporation with 10 µg of linear pCMV plasmid, a subset of cells were irradiated at 2 Gy. Cells were plated in a 96-well plate, at density of 0.5 cells per well. Controls without electroporation, mock electroporation and irradiation without electroporation were performed simultaneously. After 14 days incubation, colonies were counted.

The enhancement ratio for marker gene transformation was counted as follows (Perez et al., 1985): Enhancement ratio = (transformant per survivor)<sub>irradiated</sub> / (transformant per survivor)<sub>non-irradiated</sub>.

#### Slide preparation

Cells for metaphase preparations were harvested using standard protocols. Briefly, cell cultures were incubated with colcemid (Life Technologies) for 2 h at 37°C, cells were dislodged with trypsin-EDTA solution (Life Technologies), transferred into centrifuge tubes, centrifuged at 1400 rpm for 7 min, and the supernatant was discarded. Pre-warmed hypotonic solution (KCl 0.013 M, human serum in distilled water) was added to cell pellets, gently mixed by pipetting, and incubated for 20 min at 37°C. After 7 min centrifugation at 1400 rpm, cells were re-suspended by vortex and fixed twice in the fixative solution (methanol:acetic acid 3:1). Cell suspension was dropped onto cold, wet slides to make chromosome preparations. The slides were air dried overnight and stored at -20°C until hybridisation. Karyotypes were established on R-banded chromosomes. For each dose of irradiation, the number of breaks was deduced from the number of aberrations (dicentric, rings and acentrics) observed on Giemsa-stained metaphases.

#### Fluorescence in situ hybridization

FISH experiments were performed as previously described (Desmaze and Aurias, 1995). Because of the homology between plasmid sequences, pCMV and pSXPneoD plasmid insertions were simultaneously detected using the pCMV plasmid as probe. The plasmid DNA was labelled with a digoxigenin-11-dUTP nick translation kit (Roche). Telomeres were detected using the (C<sub>3</sub>TA<sub>2</sub>)<sub>3</sub>PNA-Cy3 probe (Perceptive Biosystem). Hybridisation and detection of specific whole chromosome painting probes (Oncor or Bioss), subtelomeres (Cytocell) and multi-FISH probes (MetaSystems, GmbH) were performed according to recommendations of the manufacturers. Hybridized metaphases were captured with a CCD camera (Zeiss) coupled to a Zeiss Axioplan microscope and were processed with ISIS software (MetaSystems, GmbH).

#### Automatic scanning of interphase nuclei

Plasmid integrations were counted on interphase nuclei by an automated scanning procedure coupled to digital processing (MetaCyte software, MetaSystems, GmbH). The system is based on a second generation of the Metafer scanning platform (MetaSystems, GmbH). Individual objects (cell nucleus) within each captured field were automatically detected from the DAPI image

and spots corresponding to plasmid FITC FISH signals within each nucleus were individualized using a set of digital processing parameters (threshold, background subtraction, size, pixel intensity, distance between spots). Once the scan has been completed, the on-screen image gallery comprising objects and their spots measurements data was reviewed to reject unsuitable cells.

## Results

### Characterization of hTERT immortalized cell lines

To investigate the role of the overexpression of the telomerase on the spontaneous and radiation-induced chromosomal instability, we have used a human fibroblast cell line immortalized by the ectopic expression of hTERT, HCA17.3. This overexpression has been confirmed by real time RT-PCR (data not shown). This cell line exhibits a similar morphology as young fibroblasts and maintains a steady growth rate. HCA17.3 was characterized and compared to three human tumor cell lines: B3, SCC61 and SQ9G.

Telomerase activity was measured by the TRAP-ELISA assay (data not shown). HCA17.3 had a high telomerase activity, comparable with that of the human tumor cell line B3. Instead, the other two tumor cell lines showed less telomerase activity than B3, with a very low activity for SCC61. It is noteworthy that with this assay, only the activity of free telomerase in the nuclei is tested, whereas telomerase bound to DNA is not present in protein extract.

We further investigated the telomere length of these cell lines. SCC61 and SQ9G have a mean TRF of about 2.4 kb (Sprung et al., 1999a, c). Telomere length of HCA17.3 and B3 cell lines was measured by Southern blot (data not shown) with a (TTAGGG)<sub>n</sub> probe and the mean TRF was calculated: HCA17.3 has a mean TRF of about 23 kb, whereas it is about 4 kb for B3. Despite their difference in length, HCA17.3 and B3 telomeres are homogeneous among them as expected by ectopic expression of hTERT, and confirmed by a PNA-telomere probe hybridised on metaphase spreads (Fig. 1).

**Table 1.** Frequency of chromosome breaks per cell in non-irradiated cells and in cells irradiated with 2 Gy and 5 Gy

	0 Gy	2 Gy	5 Gy	Slope
HCA	0.02	0.97	2.60	0.52
SCC61	0.29	2.77	7.94	1.54
B3	0.96	2.70	5.00	0.80
SQ-9G	1.90	5.50	8.02	1.19

Slopes correspond to the increase of frequencies of chromosomal breaks as a function of dose.

The effects of hTERT expression on the genome stability of stable transfected human fibroblasts were examined by cytogenetic analysis. The HCA17.3 karyotype was characterized at early passages either by m-FISH or R-banding and it was normal (46; XY). R bands were then made at successive passages and this cell line still showed a normal karyotype, by now suggesting chromosome stability throughout passages. Karyotypes of the other cell lines are (46; XY) with some clonal translocations, which are described in Material and methods. They also remain stable during passages except for SQ9G, which evolved towards polyploidy with newly acquired aberrations.

Spontaneous breaks were also scored on Giemsa-stained metaphases with irrelevant low frequencies either for HCA17.3 (0.02 breaks per cell), SCC61 (0.29 breaks per cell), and B3 cell lines (0.96 breaks per cell), whereas the SQ9G cell line showed a higher spontaneous instability (1.9 breaks per cell). Therefore, HCA17.3 presents a normal karyotype that is stable during passages in culture.

To investigate the chromosomal instability after irradiation, cell lines were irradiated with 2 Gy and 5 Gy. The number of breaks was counted on first generation metaphases after irradiation. As shown in Table 1, the B3 and HCA17.3 cell lines have different rates of breaks both spontaneously and after irradiation, but they are comparable in their increase of radiation-induced chromosome breaks. SCC61 also has a low frequency of spontaneous instability, but it is 9-fold higher at 2 Gy and 27-fold higher at 5 Gy. In contrast, SQ9G shows a rather high rate of spontaneous instability, but after irradiation, the increase ratio was similar to those of B3 cell line: 2.9 at 2 Gy and 4.2 at 5 Gy. In addition, B3 cells exhibit a higher number of chromatid breaks (0.8 breaks per cell at 2 Gy and 2.2 at 5 Gy), suggesting that B3 cells may not be synchronised in the G1 cell cycle phase when irradiated at subconfluence or that the repair of single strand breaks is less efficient in B3 than in HCA17.3 cells, where the frequency of chromatid breaks per cell is only 0.04 at 2 Gy and 0.15 at 5 Gy. Taken together, these results show different frequencies of chromosome and chromatid breaks for HCA17.3 and B3 cell lines but their increase ratio remains the same after irradiation. In addition, HCA17.3 regardless of SCC61, presents low radiation sensitivity, even if both cell lines have a low frequency of spontaneous instability, suggesting an excess of incorrect repair in SCC61 after irradiation.

#### *Ability to integrate plasmids*

The ability to integrate plasmids varies among different cell types. Seeing that HCA17.3 presents fewer rearrangements after irradiation and longer telomeres than B3 but a comparable response to irradiation and telomerase activity, we next

addressed whether these two cell lines present differences in the integration enhancement after irradiation. The ability to integrate a plasmid was tested by electroporation and by electroporation coupled to irradiation.

Integrated plasmids in cellular DNA were detected by FISH to determine the number of integrated plasmids per cell. Preliminary experiments were done to determine when most of the non-integrated plasmids disappear from cells: the number of hybridization signals decreases with time in nuclei prepared between 12 and 96 h after electroporation. In both cell lines, at the first cell division, about 90% of non-integrated plasmids were already withdrawn from the cells. We then performed the analysis on metaphases at the first generation that is 24 h after electroporation and irradiation for B3 and about 48 h for HCA17.3 cells.

Results concerning integrated plasmids on metaphases are shown in Table 2. Non-irradiated HCA17.3 metaphases have a mean of 1.65 plasmids per cell, and about 50% of cells show single integration sites. After irradiation at 2 Gy, the mean number of plasmids per cell is 1.25 and 77% of cells have single plasmid integration. At 5 Gy irradiation, the mean number of plasmid per cell is 1.5 and 73% of cells show single plasmid integration sites. B3 cell line irradiation seems to promote single plasmid integration; actually 83% of 2 Gy irradiated cells present single plasmid integration, with a mean of 1.33 plasmids per cell. Non irradiated B3 have a mean of 1.25 plasmids per cell, and about 78% of cells showing one integration site. Metaphase analysis does not emphasize any correlation between radiation dose and the mean number of integrated plasmids per cell. To confirm these data, we performed the same analysis on interphase nuclei.

The plasmid integrations were counted in interphase nuclei by the use of an automated scanning procedure (MetaCyte software, Metasystem, GmbH). About 350 cells per slide were analyzed in three different FISH experiments. Both the mean number of spots per cell and the percentage of cells with at least one spot were counted. As shown in Table 3, no correlation between radiation dose and the mean number of spots per cell was found at different doses of radiation both in HCA17.3 and B3 cell lines. However, HCA17.3 cells showed a higher percentage of cells with spots. The differences between the mean numbers of integrated plasmids in nuclei and in metaphases are probably due to unspecific hybridisation signals, although the analysis of nuclei was done in such a way that most the unspecific signals were reduced; possibly, not all of these were excluded.

To further investigate the response to irradiation, a plating efficiency test after irradiation was done. As described in Material and methods, HCA17.3 and B3 cells were transfected and

**Table 2.** Analysis of plasmid integration in metaphases at the first post-treatment cells generation

	0 Gy	2 Gy	5 Gy
Mean spot number per metaphase			
HCA17.3	1.65	1.25	1.50
B3	1.25	1.33	nd
Percent cells with single integration			
HCA17.3	53	77	73
B3	78	83	nd

The mean number of integrated plasmids per cell and the percentage of cells with a single integration site are shown for HCA17.3 and B3 cell lines.

**Table 3.** Analysis of plasmid integration in nuclei

	0 Gy	2 Gy	5 Gy
Mean spots number per nucleus			
HCA17.3	2.72	1.91	3.02
B3	1.73	0.83	2.23
Percent cells with spots			
HCA17.3	50.3	43.4	55.0
B3	21.6	23.0	23.2

The mean number of integrated plasmids per cell and the percentage of cells with at least one integration site are shown for HCA17.3 and B3 cell lines.

then irradiated at 2 Gy or not treated with radiation. After treatment, cells were seeded and 14 days later, surviving colonies were counted. Even if the HCA17.3 cell line shows a lower frequency of radiation-induced breaks than the B3 cell line, both cell lines present a similar frequency of survival following irradiation. Indeed, after 2 Gy irradiation, 31% of HCA17.3 and 35% of B3 cells are able to form colonies. Thus, the viability of cells several days after irradiation is the same whatever the frequency of breaks in the first generation, suggesting that the mechanisms of chromosome stability maintenance (or survival) are comparable in the two cell lines. After electroporation, the transfection efficiency in non irradiated samples calculated as percentage of antibiotic resistant colonies was 18.8% for HCA17.3 and 13.8% for B3 cells. The transfection efficiency of these two cell lines is quite similar, even though HCA17.3 shows a small increase in the frequency of integrated plasmid by electroporation than the B3 cell line. The transfection efficiency was tested also after irradiation and the radiation-enhanced integration ratio was measured as the ratio of irradiated transformants per survivor divided by non-irradiated transformants per survivor (Perez et al., 1985). In the HCA17.3 cell line, 2 Gy irradiation does not promote any enhancement of integration, as the enhancement ratio is 0.83. Therefore, less resistant colonies grew after irradiation treatment compared to transfection without irradiation. On the contrary, the B3 cell line enhancement ratio is 1.96, showing that irradiation improves transfection efficiency in this cell line. It is noteworthy that HCA17.3, which presents the higher percentage of cells with spots at the first generation, shows no radiation-enhanced integration at 14 days, suggesting an elimination of a large amount of such cells, while B3 cells which have integrated plasmids are still viable 14

days later. This enhancement, therefore, concerns the number of cells which integrated plasmid but not the number of plasmids integrated per one cell.

For HCA17.3 cells, irradiation does not promote enhancement of plasmid transfection as well as integration of several copies of plasmids into the DNA of a single cell. In B3 cells, the mean number of integrated plasmids does not correlate with irradiation but an enhancement of plasmid transfection is observed 14 days after irradiation. This is a discrepancy in the response to irradiation between the two cell lines.

#### *Chromosome analysis in the progeny of irradiated cells that overexpress hTERT*

We were interested in the role of telomerase to express spontaneous and radiation-induced instability over a long time. We set up two stable transfections with the HCA17.3 cell line, using plasmids with or without telomeric repeats. After electroporation, cells were irradiated at 2 Gy and plated at low density to allow the formation of single cell colonies, which were then isolated and propagated in culture under antibiotic selection. Control transfections without irradiation were also made. Clones were characterized by FISH, with the plasmid sequences as a probe, and by chromosome painting at early passages to assess on which chromosomes the plasmid has integrated and if the chromosomes with the integrated plasmid were rearranged or not. Studying clones derived from a single cell allows the selection of chromosomal aberrations and the ability to follow the evolution of radiation-induced rearrangements during successive passages in culture.

As a result, most irradiated clones show plasmid integrations in normal chromosomes like non-irradiated clones, sug-

gesting that integration has occurred randomly and not at sites of radiation-induced breaks. In a single irradiated clone (E2M), integration is located at the junction of a chromosomal rearrangement, t(7;17). We asked the question whether the insertions of plasmids are unstable. In HCA17.3, another plasmid has previously been inserted in 7p21 region (data not shown) so that this integration site should be detected in all irradiated and non-irradiated clones. FISH experiments have confirmed that both plasmids maintained the same chromosome localization during passages in all clones, supporting that integration sites were also stable when the cells proliferate excluding delayed chromosome instability.

Only 2 out of 20 analyzed clones have shown rearrangements and were further analyzed by m-FISH at successive passages in culture. The clonal rearrangements in E2M has been maintained at late passages after irradiation without new modifications. In the other clone, a second plasmid integration site occurred within one rearranged chromosome in a single metaphase among 100 analyzed. The results obtained from the short and long term studies show that the HCA17.3 cell line is very stable, even at late passages after irradiation. Actually, the rearranged chromosomes found after irradiation were stable during passages, and did not induce any cascades of instability in cell progeny.

Finally, we investigated whether it was possible to seed new telomeres in human fibroblasts immortalized by telomerase. HCA-ltrt, when transfected with the pNCT-tel plasmid, failed to show telomere seeding in more than 350 analyzed clones. This is in contrast with the results obtained from two tumour cell lines in which 2 out of 16 clones and 5 out of 16 clones presented seeding of new telomeres (SCC61; unpublished observation and B3; Fouladi et al., 2000). In addition, the HCA17.3 clone transfected after irradiation with the pCMV-Telo plasmid did not show any stabilized terminal deletion, either at early or late passages in culture. In fact, the same ratio in irradiated and non-irradiated pCMV-Telo clones, i.e.: 33%, showed integration sites at the terminal region of chromosomes. However, as shown by FISH analysis, subtelomeric regions are still present (data not shown), excluding that the plasmid containing telomeric sequences could create a new telomere in this cell line. These results demonstrate that, despite the fact that this cell line has strong telomerase activity, telomeric sequences did not stabilize deletions in the progeny of irradiated cells.

## Discussion

In this study, we have shown that over-expression of hTERT, the catalytic subunit of the telomerase, in a human fibroblast cell line, is strongly associated with chromosome stability. Telomerase expression has already been associated with a reduction of spontaneous chromosome damage in G1 cells (Sharma et al., 2003). Furthermore, our data show that this reduction of chromosome damage is observed both at the first mitosis and long times after irradiation, confirming the accentuated chromosome stability during the cell cycle of hTERT-immortalized cells.

HCA17.3 cells were derived from BJ human primary fibroblasts immortalized by hTERT. The enzyme activity, as tested by a TRAP-ELISA assay, results in very long and homogeneous telomeres, which had a mean TRF of about 23 kb. Cytogenetic analysis revealed a normal (46; XY) karyotype, which is very stable over extended passages in culture. In addition, Giemsa analysis has demonstrated remarkable spontaneous chromosome stability in HCA17.3. This increased stability could not be accounted for by the longer telomere length alone, since SCC61, which has very short telomeres, displays the same low rate of spontaneous breaks. After irradiation at 2 and 5 Gy, the number of chromosome aberrations at the first generation is always lower for HCA17.3 than SCC61. However, if we consider the increase in radiation-induced breaks relative to the dose, SCC61 exhibited an increase of 9-fold at 2 Gy, but only about 2–3 fold for the other cell lines. It is noteworthy that SCC61 showed the lowest levels of telomerase activity, while the B3 cell line showed the highest levels. These results do not support a major role for either telomere length or for telomerase expression in the chromosome response to irradiation, but do not exclude that the level of telomerase activity could interfere with an increase of chromosome damage. We therefore hypothesize that the involvement of telomerase in chromosome stability is a telomere-independent mechanism.

It has been shown that radiation, like other DNA damaging agents (Nakayama et al., 1998; Stevens et al., 1998), promotes plasmid integration in a large subset of cells. Studies by Stevens and colleagues (Stevens et al., 1999) have suggested that this integration enhancement is likely to be due to a hyper-recombination state related to radiation-induced chromosome instability. We questioned whether telomerase overexpression and chromosomal stability could influence the efficiency of plasmid integration after irradiation at similar doses. Analyses at the first post irradiation cell generation were performed in metaphases and interphase nuclei. No relation between radiation dose and the number of integrated plasmids was found in either the HCA17.3 or B3 cell lines, suggesting that, under these experimental conditions, radiation-induced DNA breaks might not be preferential plasmid integration sites. Since radiation-enhanced integration can be enhanced for weeks after irradiation (Stevens et al., 2001), our results do not support the possibility that integration might be due to misrepair at or near the sites of direct radiation-induced breaks. Plating efficiency at 14 days showed that the HCA17.3 cell line is a little more prone to integrate plasmid than B3, although irradiation enhances plasmid integration in B3 and not in HCA17.3. The molecular mechanism(s) by which radiation-enhanced integration occurs is still unknown. However, it was shown that the improvement of integration correlates with the total number of DNA strand breaks induced by damaging agents other than radiation, suggesting that single-strand breaks may play a role in radio-enhanced integration (Stevens et al., 1998). This could explain why HCA17.3, which presents very low levels of chromatid breaks, did not show any significant enhancement of transfection after irradiation at 2 Gy. Moreover, HCA17.3 is quite stable even after irradiation and therefore irradiated cells do not undergo high levels of recombination that might promote plasmid insertion, even long times after irradiation. It is worth not-

ing that the B3 cell line, which shows radiation-enhancement of integration, showed more radiation-induced chromosomal rearrangements than HCA17.3. Thus, telomerase, rather than having a direct involvement in the radiation enhancement of integration, might act as a genome stabilising factor that prevents broken chromosomes to rearrange. All together, these results emphasize the extreme chromosome stability of the hTERT over-expressing cell line, suggesting highly faithful repair mechanisms.

Delayed mutations and chromosome aberrations have been observed in the progeny of cells exposed to heavy ions as well as gamma radiation (Bortoletto et al., 2001; Schwartz et al., 2003). HCA17.3 derived clones were obtained after transfection with a pCMV or pCMV-telo plasmid and the stability of karyotypes and integration sites was followed. We have taken advantage of the presence of other inserted plasmids in these cells as controls for our results regarding plasmid stability. All integrations are located in cytogenetically normal chromosomes without preferential integration sites, demonstrating that no rearrangements have occurred during clonal expansion. Similar integration sites were observed in both unirradiated and irradiated cells, in that no plasmid has integrated at sites of chromosomal rearrangements, with the exception of one clone (E2M). These results suggest that plasmids do not integrate at radiation-induced breaks. Moreover, karyotypes remained extremely stable during passage in culture after irradiation. A few clones have revealed rare chromosome aberrations that did not change during passages. When plasmids containing telomere repeat sequences were transfected, similar frequencies of localizations at subtelomeric sites appeared in irradiated as well as in non irradiated clones, confirming that these plasmids do not integrate at radiation-induced breaks. Moreover, FISH experiments confirmed that subtelomeric regions were stable, favouring integration by homologous recombination rather than the formation of a new telomere or the putative stabilization of a break as a result of the presence of telomerase activity.

Our data demonstrate that telomerase overexpression in HCA-ltrt and HCA17.3 confers a stability to the chromosomes, even after a stress-like ionizing radiation. Actually the low ratio between the irradiated and non irradiated frequency of breaks correlated with a high level of telomerase activity. In addition, even if telomeres are very long in HCA17.3 cells, this does not

explain the observed spontaneous stability, since SCC61 with short telomeres showed a similar level of stability.

A widely recognized function of telomerase concerns the maintaining of telomere length and a capping function (Melek and Shippen, 1996; Zhu et al., 1999; Blackburn, 2001; Stewart et al., 2002). hTERT expression is also associated with non-telomere functions, such as regulation of a set of transcription of DNA repair genes, modification of chromatin (Chang et al., 2003; Sharma et al., 2003; Smith et al., 2003), and resistance to proapoptotic stress (Stewart et al., 2002). Actually, even if B3 and HCA17.3 cell lines present a similar viability of cells after 2 Gy irradiation, HCA17.3 cells show a very low level of apoptosis compared to B3 cells (data not shown). In regard to its activation of cell proliferation, telomerase activity could result in both, very stable karyotypes and unstable ones. Indeed, reactivation of telomerase in tumor or senescent cells after initiation of genetic instability, may accumulate complex karyotypes by perpetuating instability (Chadeneau et al., 1995; Tang et al., 1998; Ducray et al., 1999; DePinho, 2000; Fouladi et al., 2000; Rudolph et al., 2001; Mondello et al., 2003). On the other hand, disruption of genes controlling the cell cycle in telomerase-positive cells, such as immature or hematological cells, is an early event and the resulting karyotype is often quite normal, with few anomalies without excess-involvement of telomeric regions (Lengauer et al., 1998; Gisselsson, 2002). It may therefore be informative to determine whether elimination of telomerase activity in HCA17.3 results in an increase in chromosome aberrations after irradiation as well as delayed chromosome instability. Similarly, an overexpression of telomerase in B3 cells should lead to karyotype stability. Thus, the stability observed in the hTERT immortalized cell lines, HCA-ltrt and HCA17.3, might be due to a specific maintenance of the normal genome, involving a telomere-independent role of telomerase. As a result, opportunities may arise to use hTERT immortalized normal human cells to study gene targeting.

### Acknowledgements

Authors are grateful to Judith Campisi for providing HCA-ltrt cells and to L.M. Martins for helpful technical assistance.

### References

- Blackburn EH: Switching and signaling at the telomere. *Cell* 106:661–673 (2001).
- Bortoletto E, Mognato M, Ferraro P, Canova S, Cherubini R, Celotti L, Russo A: Chromosome instability induced in the cell progeny of human T lymphocytes irradiated in G(0) with gamma-rays. *Mutagenesis* 16:529–537 (2001).
- Brachman DG, Graves D, Vokes E, Beckett M, Haraf D, Montag A, Dunphy E, Mick R, Yandell D, Weichselbaum RR: Occurrence of p53 gene deletions and human papilloma virus infection in human head and neck cancer. *Cancer Res* 52:4832–4836 (1992).
- Brenneman M, Gimble FS, Wilson JH: Stimulation of intrachromosomal homologous recombination in human cells by electroporation with site-specific endonucleases. *Proc natl Acad Sci USA* 93:3608–3612 (1996).
- Chadeneau C, Hay K, Hirte HW, Gallinger S, Bacchetti S: Telomerase activity associated with acquisition of malignancy in human colorectal cancer. *Cancer Res* 55:2533–2536 (1995).
- Chang S, Khoo CM, Naylor ML, Maser RS, DePinho RA: Telomere-based crisis: functional differences between telomerase activation and ALT in tumor progression. *Genes Dev* 17:88–100 (2003).
- Collins K, Mitchell JR: Telomerase in the human organism. *Oncogene* 21:564–579 (2002).
- Counter CM, Avilion AA, LeFeuvre CE, Stewart NG, Greider CW, Harley CB, Bacchetti S: Telomere shortening associated with chromosome instability is arrested in immortal cells which express telomerase activity. *EMBO J* 11:1921–1929 (1992).
- Cowan JM, Beckett MA, Weichselbaum RR: Chromosome changes characterizing in vitro response to radiation in human squamous cell carcinoma lines. *Cancer Res* 53:5542–5547 (1993).
- Cui W, Aslam S, Fletcher J, Wylie D, Clinton M, Clark AJ: Stabilization of telomere length and karyotypic stability are directly correlated with the level of hTERT gene expression in primary fibroblasts. *J Biol Chem* 277:38531–38539 (2002).

- de Lange T: Protection of mammalian telomeres. *Oncogene* 21:532–540 (2002).
- DePinho RA: The age of cancer. *Nature* 408:248–254 (2000).
- Desmazes C, Aurias A: In situ hybridization of fluorescent probes on chromosomes, nuclei or stretched DNA: applications in physical mapping and characterization of genomic rearrangements. *Cell Mol Biol* 41:925–931 (1995).
- Difilippantonio MJ, Petersen S, Chen HT, Johnson R, Jasin M, Kanaar R, Ried T, Nussenzweig A: Evidence for replicative repair of DNA double-strand breaks leading to oncogenic translocation and gene amplification. *J Exp Med* 196:469–480 (2002).
- Donoho G, Jasin M, Berg P: Analysis of gene targeting and intrachromosomal homologous recombination stimulated by genomic double-strand breaks in mouse embryonic stem cells. *Mol Cell Biol* 18:4070–4078 (1998).
- Ducray C, Pommier JP, Martins L, Boussin FD, Sabatier L: Telomere dynamics, end-to-end fusions and telomerase activation during the human fibroblast immortalization process. *Oncogene* 18:4211–4223 (1999).
- Fouladi B, Sabatier L, Miller D, Pottier G, Murnane JP: The relationship between spontaneous telomere loss and chromosome instability in a human tumor cell line. *Neoplasia* 2:540–554 (2000).
- Gisselsson D: Tumour morphology interplay between chromosome aberrations and founder cell differentiation. *Histol Histopathol* 17:1207–1212 (2002).
- Gorbunova V, Seluanov A, Pereira-Smith OM: Expression of human telomerase (hTERT) does not prevent stress-induced senescence in normal human fibroblasts but protects the cells from stress-induced apoptosis and necrosis. *J Biol Chem* 277:38540–38549 (2002).
- Greider CW, Blackburn EH: Identification of a specific telomere terminal transferase activity in *Tetrahymena* extracts. *Cell* 43:405–413 (1985).
- Kadhim MA, Macdonald DA, Goodhead DT, Lormore SA, Marsden SJ, Wright EG: Transmission of chromosomal instability after plutonium alpha-particle irradiation. *Nature* 355:738–740 (1992).
- Lengauer C, Kinzler KW, Vogelstein B: Genetic instabilities in human cancers. *Nature* 396:643–649 (1998).
- Little JB, Gorgojo L, Vetrovs H: Delayed appearance of lethal and specific gene mutations in irradiated mammalian cells. *Int J Radiat Oncol Biol Phys* 19:1425–1429 (1990).
- Lo AW, Sabatier L, Fouladi B, Pottier G, Ricoul M, Murnane JP: DNA amplification by breakage/fusion/bridge cycles initiated by spontaneous telomere loss in a human cancer cell line. *Neoplasia* 4:531–538 (2002).
- Masutomi K, Yu EY, Khurts S, Ben-Porath I, Currier JL, Metz GB, Brooks MW, Kaneko S, Murakami S, DeCaprio JA, Weinberg RA, Stewart SA, Hahn WC: Telomerase maintains telomere structure in normal human cells. *Cell* 114:241–253 (2003).
- Matzner I, Savelyeva L, Schwab M: Preferential integration of a transfected marker gene into spontaneously expressed fragile sites of a breast cancer cell line. *Cancer Lett* 189:207–219 (2003).
- Melek M, Shippen DE: Chromosome healing: spontaneous and programmed de novo telomere formation by telomerase. *Bioessays* 18:301–308 (1996).
- Miller DG, Petek LM, Russell DW: Human gene targeting by adeno-associated virus vectors is enhanced by DNA double-strand breaks. *Mol Cell Biol* 23:3550–3557 (2003).
- Mondello C, Chiesa M, Rebuzzini P, Zongaro S, Verri A, Colombo T, Giulotto E, D'Incalci M, Franceschi C, Nuzzo F: Karyotype instability and anchorage-independent growth in telomerase-immortalized fibroblasts from two centenarian individuals. *Biochem Biophys Res Commun* 308:914–921 (2003).
- Morales CP, Holt SE, Ouellette M, Kaur KJ, Yan Y, Wilson KS, White MA, Wright WE, Shay JW: Absence of cancer-associated changes in human fibroblasts immortalized with telomerase. *Nature Genet* 21:115–118 (1999).
- Nakayama C, Adachi N, Koyama H: Bleomycin enhances random integration of transfected DNA into a human genome. *Mutat Res* 409:1–10 (1998).
- Natarajan AT, Darroudi F, Mullenders LH, Meijers M: The nature and repair of DNA lesions that lead to chromosomal aberrations induced by ionizing radiations. *Mutat Res* 160:231–236 (1986).
- Obe G, Pfeiffer P, Savage JR, Johannes C, Goedecke W, Jeppesen P, Natarajan AT, Martinez-Lopez W, Folle GA, Drets ME: Chromosomal aberrations: formation, identification and distribution. *Mutat Res* 504:17–36 (2002).
- Perez CF, Botchan MR, Tobias CA: DNA-mediated gene transfer efficiency is enhanced by ionizing and ultraviolet irradiation of rodent cells in vitro. I. Kinetics of enhancement. *Radiat Res* 104:200–213 (1985).
- Pfeiffer P, Goedecke W, Obe G: Mechanisms of DNA double-strand break repair and their potential to induce chromosomal aberrations. *Mutagenesis* 15:289–302 (2000).
- Porteus MH, Cathomen T, Weitzman MD, Baltimore D: Efficient gene targeting mediated by adeno-associated virus and DNA double-strand breaks. *Mol Cell Biol* 23:3558–3565 (2003).
- Rassool FV, McKeithan TW, Neilly ME, van Melle E, Espinosa R, 3rd, Le Beau MM: Preferential integration of marker DNA into the chromosomal fragile site at 3p14: an approach to cloning fragile sites. *Proc Natl Acad Sci USA* 88:6657–6661 (1991).
- Rubio MA, Kim SH, Campisi J: Reversible manipulation of telomerase expression and telomere length. Implications for the ionizing radiation response and replicative senescence of human cells. *J Biol Chem* 277:28609–28617 (2002).
- Rudolph KL, Millard M, Bosenberg MW, DePinho RA: Telomere dysfunction and evolution of intestinal carcinoma in mice and humans. *Nature Genet* 28:155–159 (2001).
- Sabatier L, Dutrillaux B, Martin MB: Chromosomal instability. *Nature* 357:548 (1992).
- Schwartz JL, Jordan R, Evans HH, Lenarczyk M, Liber H: The TP53 dependence of radiation-induced chromosome instability in human lymphoblastoid cells. *Radiat Res* 159:730–736 (2003).
- Sharma GG, Gupta A, Wang H, Scherthan H, Dhar S, Gandhi V, Iliakis G, Shay JW, Young CS, Pandita TK: hTERT associates with human telomeres and enhances genomic stability and DNA repair. *Oncogene* 22:131–146 (2003).
- Slijepcevic P, Bryant PE: Chromosome healing, telomere capture and mechanisms of radiation-induced chromosome breakage. *Int J Radiat Biol* 73:1–13 (1998).
- Smith LL, Collier HA, Roberts JM: Telomerase modulates expression of growth-controlling genes and enhances cell proliferation. *Nature Cell Biol* 5:474–479 (2003).
- Sprung CN, Afshar G, Chavez EA, Lansdorp P, Sabatier L, Murnane JP: Telomere instability in a human cancer cell line. *Mutat Res* 429:209–223 (1999a).
- Sprung CN, Reynolds GE, Jasin M, Murnane JP: Chromosome healing in mouse embryonic stem cells. *Proc Natl Acad Sci USA* 96:6781–6786 (1999b).
- Sprung CN, Sabatier L, Murnane JP: Telomere dynamics in a human cancer cell line. *Exp Cell Res* 247:29–37 (1999c).
- Stevens CW, Zeng M, Cerniglia GJ: Ionizing radiation greatly improves gene transfer efficiency in mammalian cells. *Hum Gene Ther* 7:1727–1734 (1996).
- Stevens CW, Cerniglia GJ, Giandomenico AR, Koch CJ: DNA damaging agents improve stable gene transfer efficiency in mammalian cells. *Radiat Oncol Invest* 6:1–9 (1998).
- Stevens CW, Stamato TD, Mauldin SK, Getts RC, Zeng M, Cerniglia GJ: Radiation-induced recombination is dependent on Ku80. *Radiat Res* 151:408–413 (1999).
- Stevens CW, Puppi M, Cerniglia GJ: Time-dose relationships in radiation-enhanced integration. *Int J Radiat Biol* 77:841–846 (2001).
- Stewart SA, Hahn WC, O'Connor BF, Banner EN, Lundberg AS, Modha P, Mizuno H, Brooks MW, Fleming M, Zimonjic DB, Popescu NC, Weinberg RA: Telomerase contributes to tumorigenesis by a telomere length-independent mechanism. *Proc Natl Acad Sci USA* 99:12606–12611 (2002).
- Tang R, Cheng AJ, Wang JY, Wang TC: Close correlation between telomerase expression and adenomatous polyp progression in multistep colorectal carcinogenesis. *Cancer Res* 58:4052–4054 (1998).
- Zeng M, Cerniglia GJ, Eck SL, Stevens CW: High-efficiency stable gene transfer of adenovirus into mammalian cells using ionizing radiation. *Hum Gene Ther* 8:1025–1032 (1997).
- Zhu J, Wang H, Bishop JM, Blackburn EH: Telomerase extends the lifespan of virus-transformed human cells without net telomere lengthening. *Proc Natl Acad Sci USA* 96:3723–3728 (1999).

# Mechanisms of formation of chromosomal aberrations: insights from studies with DNA repair-deficient cells

F. Palitti

Department of Agrobiolology and Agrochemistry, University of Tuscia, Viterbo (Italy)

**Abstract.** In order to understand the mechanisms of formation of chromosomal aberrations, studies performed on human syndromes with genomic instability can be fruitful. In this report, the results from studies in our laboratory on the importance of the transcription-coupled repair (TCR) pathway on the induction of chromosomal damage and apoptosis by ultraviolet light (UV) are discussed. UV61 cells (hamster homologue of human Cockayne's syndrome group B) deficient in TCR showed a dramatic increase in the induction of chromosomal aberrations and apoptosis following UV treatment. At relatively low UV doses, the induction of chromosomal aberrations preceded the apoptotic process. Chromosomal aberrations probably lead to apoptosis and most of the cells had gone through an S phase after the UV treatment before entering

apoptosis. At higher doses of UV, the cells could go into apoptosis already in the G<sub>1</sub> phase of the cell cycle. Abolition of TCR by treatment with  $\alpha$ -amanitin (an inhibitor of RNA polymerase II) in the parental cell line AA8 also resulted in the induction of elevated chromosomal damage and apoptotic response similar to the one observed in UV61 cells treated with UV alone. This suggests that the lack of TCR is responsible for the increased frequencies of chromosomal aberrations and apoptosis in UV61 cells. Hypersensitivity to the induction of chromosomal damage by inhibitors of antitopoisomerases I and II in Werner's syndrome cells is also discussed in relation to the compromised G<sub>2</sub> phase processes involving the Werner protein.

Copyright © 2003 S. Karger AG, Basel

Some of the cancer-prone human disorders are characterized by extreme sensitivity to many clastogenic and mutagenic agents. Increased sensitivity to mutagens has been demonstrated for cells derived from xeroderma pigmentosum (XP), Fanconi anemia (FA), ataxia telangiectasia (AT), Bloom's syndrome (BS) and Werner's syndrome (WS). FA, AT, BS and WS are also characterized by an increased spontaneous frequency of chromosomal aberrations (CA).

It has become increasingly evident that different cellular pathways are involved in response to DNA damage before gross chromosomal aberrations become visible.

In order to dissect the molecular mechanisms involved in the formation of CA various strategies have been employed to

define the types of primary DNA lesions, the different DNA repair pathways involved and additional processes whose roles have not been completely defined, such as signaling pathways and apoptosis.

Studying cells derived from known human genomic instability syndromes have clarified many of these aspects. With the remarkable development of molecular biology and knowledge obtained in the field of molecular genetics (cloning of DNA repair genes) and ultrastructural research it has become plausible that the complex cellular processes that lead to the formation of chromosomal aberrations could be unraveled. One of the first attempts to utilize the tools developed by molecular biologists was made in 1978 by Natarajan and Obe who confirmed that a DNA double strand break (DSB) is the final DNA lesion which leads to the formation of CA. Introducing Neurospora endonuclease (an enzyme which recognizes X-ray induced single stranded DNA regions and converts them into DSB) into X-irradiated Chinese hamster ovary cells, they observed a two- to three-fold increase of the induced frequencies of CA. Later, with a similar molecular approach, Bryant (1984) and Natarajan and Obe (1984) further demonstrated the

This paper is dedicated to Prof. Günter Obe on the occasion of his 65th birthday. Supported by FIRB (RBNED1RNN7).

Received 19 September 2003; revision accepted 8 December 2003.

Request reprints from F. Palitti, Department of Agrobiolology and Agrochemistry  
University of Tuscia, Via San Camillo de Lellis, snc  
I-01100 Viterbo (Italy); telephone: +39 0761 357 206  
fax: +39 0761 357 242; e-mail: palitti@unitus.it



role of DSB in the induction of CA by introducing restriction endonucleases into permeabilized Chinese hamster cells which induce exclusively DSB in the DNA.

Since the penetration of the field of chromosome research by molecular biologists and the results obtained in yeast, the existence of two main pathways of repair of DSB have been suggested in mammalian cells: namely, non-homologous end-joining (NHEJ) and homologous recombination (HR).

NHEJ repair quickly seals the DNA DSB in a manner that need not be error free and this is supposed to be the predominant type of mechanism acting in the pre-replicative phase of the cell cycle ( $G_0$  or  $G_1$ ). HR is a high fidelity repair process based on homologous recombination between sister chromatids or homologous chromosomes or regions of DNA homology and is acting during the S and  $G_2$  phase of the cell cycle.

One could also speculate that NHEJ repair is the most predominant type of repair of DSB induced by S-independent agents, i.e. agents which have the potential to induce chromosome- or chromatid-type aberrations depending on the cell cycle phase in which the cell has been treated. Ionizing radiation is a classical type of S-independent agent, HR is involved in the repair of lesions induced by S-dependent agents, i.e. agents which induce only chromatid type of aberrations and also increases the yield of sister chromatid exchanges (SCEs) and need an S phase to transform the DNA lesions into chromosomal damage. UV light and alkylating agents are typical S-dependent agents.

The types of DNA lesions induced by different clastogens vary and the cell handles these lesions by different ways. The outcome could be just the resumption of the normal cell cycle, cell death or formation of mutated cells that could initiate malignant transformation. In order to identify different pathways that lead to CA, one approach has been to use cells derived from patients prone to high incidence of cancer who are linked to known autosomal recessive disorders due to mutations in genes involved in the maintenance of genomic stability. Some of these disorders show differential sensitivity to many chemicals and physical agents due to defects in specific DNA repair pathways. As the identification of the lesion chiefly responsible for the cytotoxicity is rather difficult since many DNA damaging agents produce a spectrum of lesions, which require the coordinated activities of multiple repair pathways for their removal. The evaluation of the cytotoxicity of cells to different DNA damaging agents allows deducing the biological functions of the genes involved. For example, observation of extreme sensitivity of XP patients to sunlight exposure led to the identification of various XP genes and their concerted role in the nucleotide excision repair pathway.

Among the other cancer prone human diseases, increased sensitivity to mutagens has been demonstrated for cells derived from FA, AT, BS and WS patients. These diseases are also characterized by an increase in spontaneous frequency of chromosomal aberrations in lymphocytes and skin fibroblasts. Some results obtained in our laboratory concerning the relationship of transcription coupled repair (TCR) deficiency, chromosomal aberrations and apoptosis in UV61 cells (analogue of Cockayne's syndrome cells), and the role of WRN protein for maintenance of genomic stability are discussed in this article.

## TCR, chromosomal aberrations and apoptosis

Nucleotide excision repair (NER) is a major DNA repair pathway for the removal of bulky DNA adducts induced by physical and chemical agents. UV irradiation causes two major types of DNA lesions: cyclobutane pyrimidine dimers (CPDs) and pyrimidine-pyrimidone photoproducts (6-4PPs). Two different sub-pathways of NER have been identified: global genome repair (GGR) and transcription-coupled repair (TCR). GGR is responsible for the removal of lesions at any location in the genome and its efficiency depends on the type of lesions induced. GGR rapidly removes 6-4PP after UV irradiation while it is relatively slower in removal of CPDs. TCR is responsible for the fast removal of CPDs from the transcribed strand of active genes. TCR pathway, which is closely linked to transcription, confers cellular resistance to UV irradiation and is critical for transcription recovery after DNA damage (Mellon et al., 1987). Deficiencies in either of the NER sub-pathways result in human hereditary diseases such as XP and CS (Cockayne's syndrome) characterized by extreme photosensitivity.

Two complementation groups (A and B) have been identified among CS patients and the corresponding genes have been cloned (Troelstra et al., 1992; Henning et al., 1995). Both CS gene products are integral components of TCR. Recovery of RNA and DNA synthesis after UV irradiation is deficient in CS cells (Mayne and Lehmann, 1982). Depending on the type and extent of DNA damage, the cell, instead of attempting to repair the damage, can initiate programmed cell death (apoptosis). CS cells are more prone to undergo apoptosis after UV irradiation than cells from normal individuals. CPDs constitute about 65–80% of the total lesions induced by UV (Friedberg et al., 1995) and it seems that their persistence in the transcribing strand of active genes may be the primary trigger for apoptosis (Ljungman and Zhang, 1996; Balajee et al., 2000; Conforti et al., 2000). The transcription blockage resulting from TCR defects is thought to be responsible for the increased apoptotic potential observed in CS cells. This extreme sensitivity of CS cells to UV-induced cell killing has led to the hypothesis that CS cells are proficient in eliminating the heavily damaged cells in a suicidal pathway prior to malignant transformation. As CA are very efficiently induced by UV, CS patients, who have a reduced cancer incidence, would be a case in which increase in CA does not predispose to cancer development. Therefore we addressed the question whether the conversion of UV-induced DNA damage into CA could be required for the apoptotic signal.

Recent studies have shown that in both UV61 cell line (hamster homologue of human Cockayne's syndrome group B cells) and human CS-B cells the apoptotic events induced by UV are initiated at 18 and 30 h after treatment which correlate with the time required for completion of a single cell cycle (Balajee et al., 2000). This raises the possibility that the conversion of DNA damage into CA due to TCR defects may be responsible for apoptotic death. As UV light is an S phase-dependent agent, the cells need to go through an S phase for the manifestation of chromatid-type CA.

As it was not clear whether or not the TCR defect contributes to the formation of CA and apoptosis in CS-B cells, we

evaluated the role of TCR in induction of CA and apoptosis in the TCR-defective hamster homologue (UV61) of human CS-B cells and its parental repair-proficient cell line AA8.

Actively transcribing genes constitute 5–8% of the eukaryotic genome and, hence, the lesions repaired by TCR in those regions might be rare as compared to the remainder of the genome. It is, therefore, logical to expect only a marginal increase in apoptosis and CA in TCR-defective UV61 cells as compared to AA8 cells. Interestingly, significant increase in the induction of both CA and apoptosis was observed in UV61 cells even at very low UV doses (Proietti De Santis et al., 2001). As TCR of CPDs is the only difference between these two cell lines, one can infer that the increased level of CA is mainly due to the lack of CPD removal from the transcribing strand of active genes.

Consistent with this notion, the treatment of AA8 cells with  $\alpha$ -amanitin (RNA polymerase II inhibitor), which abolishes TCR efficiency in both human and hamster cells (Christians and Hanawalt, 1992; Ljungman and Zhang, 1996), also resulted in increased induction of CA and apoptosis similar to that observed in UV61 cells treated with UV alone. Furthermore, cytofluorimetric analysis revealed that the UV61 cells irradiated in G<sub>1</sub> phase synthesized their DNA after a transient delay and reached the G<sub>1</sub> phase of the subsequent division where increased apoptotic cells were observed as a G<sub>1</sub> subpopulation. Our results suggest that the accumulation of CA due to TCR defects might be a trigger for the apoptotic pathway in CS-B cells and that apoptosis occurs after the completion of a single cell cycle following UV irradiation.

In addition to transcription blockage, the impairment of replication process by UV lesions may also cause apoptotic death of UV61 cells. Orren et al. (1997) suggested that a prolonged cell cycle arrest and apoptosis in UV-sensitive hamster mutant cells are due to replication inhibition by the persistence of 6–4PPs, since UV irradiation effectively inhibits both replication and transcription in a dose-dependent manner. In order to address this issue and to determine the relative importance of the two UV induced lesions (CPDs and 6–4PPs) we studied the effects of UV irradiation on cycle progression and apoptosis in G<sub>1</sub> synchronized NER proficient and deficient hamster cell lines. AA8 cells show a proficient removal of 6–4PPs from the overall genome and proficient repair of CPDs only in the transcribed strand of active genes but not from the rest of the genome (Thompson et al., 1989; Lommel and Hanawalt, 1991). The UV5 cell line belonging to rodent complementation group 2 is largely deficient in repair of both major UV-induced photoproducts (Thompson et al., 1989; Orren et al., 1996). The UV61 cell line belongs to rodent complementation group 6 and shows intermediate UV sensitivity and appears to be normal in 6–4PP repair but deficient in the transcription-coupled repair of CPDs in active genes.

Our findings reveal that, at higher UV doses, the majority of cells undergo a prolonged G<sub>1</sub> arrest and apoptosis without entry into S phase. The induction of apoptosis in G<sub>1</sub> phase indicates that the inhibition of DNA replication may not be critical for apoptotic response. Furthermore, UV61 and UV5 cells, which differ in their capacity to repair 6–4PP, displayed identical patterns of cell cycle distribution and apoptosis suggesting that 6–4PP repair does not contribute considerably to the apoptotic

signal. We conclude that the TCR efficiency of CPDs determines the cell cycle progression and apoptosis in hamster cells. In support of this, the treatment of AA8 cells with  $\alpha$ -amanitin, which inhibits both transcription and TCR, also resulted in prolonged G<sub>1</sub> arrest and apoptosis in the first G<sub>1</sub> phase similar to that observed in UV61 and UV5 cells (Proietti De Santis et al., 2002).

### **Sensitivity of Werner's syndrome (WS) cells to DNA-damaging agents**

The importance of RecQ helicases in maintenance of genomic stability is illustrated in humans, where mutations in three different RecQ family members result in autosomal recessive disorder, such as: BS, WS and Rothmund-Thomson syndrome. All three syndromes exhibit spontaneously occurring CA and are also known as "chromosome breakage syndromes". Accelerated aging and high risk of developing neoplasms affect Werner's syndrome patients. At the cellular level WS is characterized by variegated chromosome translocation mosaicism involving the expansion of different structural chromosome rearrangements in different independent clones of the same cell line (Salk et al., 1981; Grigorova et al., 2000). WS cells are not sensitive to common DNA damaging agents such as ionizing radiation, UV light, mono- and polyfunctional alkylating agents. WS cells have been reported to be sensitive to the induction of chromosomal aberrations (Gebhart et al., 1988) and apoptosis by 4-nitroquinoline-1-oxide (4NQO), a chemical which produces bulky adducts by a mechanism similar to UV light (Ogburn et al., 1997). Grigorova et al. (2000) using both Giemsa staining and fluorescent in situ hybridization found only a slight increase in the frequency of radiation-induced chromosomal damage in two WS lymphoblastoid cell lines. WS cells do not show, as opposed to other "cancer prone" syndromes, a higher G<sub>2</sub> radiosensitivity and respond normally to hydroxyurea post-treatment, namely a potentiation of X-ray-induced chromosomal aberrations in G<sub>2</sub> cells similar to wild type cells.

In contrast, caffeine, a drug known to sensitize cells to irradiation by abrogating the G<sub>2</sub> check-point response, did not abrogate the G<sub>2</sub> delay caused by X-ray or mitomycin C of WS cells and did not enhance chromosomal damage (Franchitto et al., 1999). The lack of G<sub>2</sub> arrest abrogation by caffeine indicates the requirement of a functional WRN gene product in the signaling transduction pathway by which caffeine can override the DNA damage-induced G<sub>2</sub> check point. WS cells have also been shown to be sensitive to topoisomerase I (camptothecin) and II (etoposide and amsacrine) inhibitors in S and G<sub>2</sub> phase of the cell cycle (Franchitto et al., 2000; Pichierri et al., 2000 a, b). Although the basis for the enhanced sensitivity of WS cells to antitopoisomerase drugs remains unclear, it can be speculated that the WRN helicase together with topoisomerases may mediate an effective recombinational repair pathway, operating in S and G<sub>2</sub> phases of the cell cycle. Topoisomerase II inhibitors (amsacrine and etoposide) are very potent inducers of CA in WS cells specifically in the G<sub>2</sub> phase of the cell cycle. Furthermore potentiation of X-ray-induced chromosomal damage

by catalytic inhibition of topoisomerase II with IC RF 185 was observed in WS cells only in G<sub>2</sub> (Pichierri et al., 2000a). Instead, the topoisomerase I inhibitor camptothecin induces a much higher yield of chromosomal damage in both the S and G<sub>2</sub> phases of the cell cycle of WS cells compared to normal cells. This chromosomal sensitivity of WS cells to antitopoisomerases during S and G<sub>2</sub> phases points to a potential role of the WRN protein in a recombination pathway of DSB repair in cooperation with topoisomerases I and II in the maintenance of genomic integrity. The involvement of WRN in recombinational repair is also corroborated by the increased apoptosis observed in WS lymphoblastoid cells upon treatment with agents that cause inter-strand cross-links or blockage of replication fork (Yu et al., 1996; Poot et al., 2001). A homologous recombination repair pathway seems to play a critical role in repair of either stalled or collapsed replication forks to permit reinitiation of replication (Haber, 1999; Negritto et al., 2001). WS cells are sensitive to both hydroxyurea and camptothecin, which suggests that WRN may play a vital role either in the repair of stalled replication forks or in reinitiation of replication (Sakamoto et al., 2001). Following hydroxyurea or camptothecin treatment the observed colocalization of WRN protein with the recombination protein Rad51 indicates a functional interaction between the two proteins in the resolution of stalled replication forks. Although the spontaneous level of Rad51 in the absence of damage is high, Rad51 foci formation in response to camptothecin is reduced in WS cells. This could explain the increased apoptosis and chromosomal damage observed in WS cells which resume DNA replication after damage by hydroxyurea or camptothecin treatment as replication recovery may be affected in the absence of WRN protein (Pichierri et al., 2001).

## Conclusions

Studies employing DNA repair deficient cells can elucidate the molecular mechanisms involved in the formation of spontaneous and induced chromosomal aberrations. From the data obtained with UV61 cells (homologue of Cockayne's syndrome) one can speculate that transcription blockage and lack of TCR, can cause a decline in the activity of enzymes involved in the repair of DNA damage, and by this lead to loss of genomic and chromosomal integrity. Alternatively, the transcription blockage induces the cells to activate an alternative repair pathway like the recombinational repair system irrespective of consequences on chromosome stability since a dramatic increase of sister chromatid exchanges is also observed in UV61 due to an intervention of recombination repair accompanied by an increase in Rad 51 foci formation (Lorenti Garcia et al., in preparation).

In Werner's syndrome, it appears that the diverse pathological features of WS patients implicate a role for WRN protein in every aspect of DNA-mediated activities such as repair, transcription and recombination. The involvement of WRN in the regulation of S phase after DNA damage may explain the sensitivity to the induction of CA and apoptosis of WS cells to agents which cause repair of replication-dependent DNA strand breaks suppressing illegitimate recombination between stalled replication fork through the interaction with Rad51.

## References

- Balajee AS, Proietti De Santis L, Brosh RM, Selzer R, Bohr VA: Role of the ATPase domain of the Cockayne syndrome group B protein in UV induced apoptosis. *Oncogene* 19:477-489 (2000).
- Bryant PE: Enzymatic restriction of in situ mammalian cell DNA using *PvuII* and *BamHI*: evidence for the double strand break origin of chromosomal aberrations. *Int J Radiat Biol* 46:56-65 (1984).
- Christians FC, Hanawalt PC: Inhibition of transcription and strand-specific DNA repair by alpha-amanitin in Chinese hamster ovary cells. *Mutat Res* 274:93-101 (1992).
- Conforti G, Nardo T, D'Incalci M, Stefanini M: Prone-ness to UV-induced apoptosis in human fibroblasts defective in transcription coupled repair is associated with the lack of Mdm2 transactivation. *Oncogene* 19:2714-2720 (2000).
- Franchitto A, Proietti De Santis L, Pichierri P, Mosesso P, Palitti F: Lack of effect of caffeine post-treatment on X-ray-induced chromosomal aberrations in Werner's syndrome lymphoblastoid cell lines: a preliminary report. *Int J Radiat Biol* 75:1349-1355 (1999).
- Franchitto A, Pichierri P, Mosesso P, Palitti F: Catalytic inhibition of topoisomerase II in Werner's syndrome cell lines enhances chromosomal damage induced by X-rays in the G<sub>2</sub> phase of the cell cycle. *Int J Radiat Biol* 76:913-922 (2000).
- Friedberg E, Walker G, Siede W: DNA Repair and Mutagenesis. (ASM Press, Washington, DC 1995).
- Gebhart E, Bauer R, Raub U: Spontaneous and induced chromosomal instability in Werner syndrome. *Hum Genet* 80:135-139 (1988).
- Grigorova M, Balajee AS, Natarajan AT: Spontaneous and X-ray induced chromosomal aberrations in Werner syndrome cells detected by FISH using chromosome specific painting probes. *Mutagenesis* 15:303-310 (2000).
- Haber JE: DNA recombination: the replication connection. *Trends Biochem Sci* 24:271-275 (1999).
- Henning KA, Li L, Iyer N, McDaniel LD, Reagan MS, Legerski R, Schultz RA, Stefanini M, Lehmann AR, Mayne LV, Friedberg E: The Cockayne syndrome group A gene encodes a WD repeat protein that interacts with CSB protein and a subunit of RNA polymerase II TFIIH. *Cell* 82:555-564 (1995).
- Ljungman M, Zhang F: Blockage of RNA polymerase as a possible trigger for UV light-induced apoptosis. *Oncogene* 13:823-831 (1996).
- Lommel L, Hanawalt P: The genetic defect in the Chinese hamster ovary cell mutant UV61 permits moderate selective repair of cyclobutane pyrimidine dimers in an expressed gene. *Mutat Res* 255:183-191 (1991).
- Mayne L, Lehmann A: Failure of RNA synthesis to recover after UV irradiation: an early defect in cells from individuals with Cockayne's syndrome and xeroderma pigmentosum. *Cancer Res* 42:1473-1478 (1982).
- Mellon I, Spivak G, Hanawalt PC: Selective removal of transcription-blocking DNA damage from the transcribed strand of the mammalian *DHFR* gene. *Cell* 51:241-249 (1987).
- Natarajan AT, Obe G: Molecular mechanisms involved in the production of chromosomal aberrations. Part I: Utilization of *Neurospora* endonuclease for the study of aberration production in G<sub>2</sub> stage of the cell cycle. *Mutat Res* 52:137-149 (1978).
- Natarajan AT, Obe G: Molecular mechanisms involved in the production of chromosomal aberrations. III. Restriction endonucleases. *Chromosoma* 90:120-127 (1984).
- Negritto MC, Qiu J, Ratay DO, Shen B, Bailis AM: Novel function of Rad27 (FEN-1) in restricting short-sequence recombination. *Mol Cell Biol* 21:2349-2358 (2001).
- Ogburn CE, Oshima J, Poot M, Chen R, Hunt KE, Golahon KA, Rabinovitch PS, Martin GM: An apoptosis-inducing genotoxin differentiates heterozygous carriers for Werner helicase mutation from wild type and homozygous mutants. *Hum Genet* 101:121-125 (1997).

- Orren DK, Dianov GL, Bohr VA: The human CSB (*ERCC6*) gene corrects the transcription-coupled repair defect in the CHO cell mutant UV61. *Nucleic Acids Res* 24:3317–3322 (1996).
- Orren DK, Petersen LN, Bohr VA: Persistent DNA damage inhibits S-phase and G<sub>2</sub> progression and result in apoptosis. *Mol Biol Cell* 8:1129–1142 (1997).
- Pichierri P, Franchitto A, Mosesso P, Proietti de Santis L, Balajee AS, Palitti F: Werner's syndrome lymphoblastoid cells are hypersensitive to topoisomerase II inhibitors in the G<sub>2</sub> phase of the cell cycle. *Mutat Res* 459:123–133 (2000a).
- Pichierri P, Franchitto A, Mosesso P, Palitti F: Werner's syndrome cell lines are hypersensitive to camptothecin-induced chromosomal damage. *Mutat Res* 456:45–57 (2000b).
- Pichierri P, Franchitto A, Mosesso P, Palitti F: Werner's syndrome protein is required for correct recovery after replication arrest and DNA damage induced in S-phase of cell cycle. *Mol Biol Cell* 12:2412–2421 (2001).
- Poot M, Yom JS, Whang SH, Kato JT, Gollahon KA, Rabinovitch PS: Werner syndrome cells are sensitive to DNA cross-linking drugs. *FASEB J* 15:1224–1226 (2001).
- Proietti De Santis L, Lorenti Garcia C, Balajee AS, Brea Calvo GT, Bassi L, Palitti F: Transcription coupled repair deficiency results in increased chromosomal aberrations and apoptotic death in hamster homologue of human Cockayne syndrome group B cells. *Mutat Res* 485:121–132 (2001).
- Proietti De Santis L, Lorenti Garcia C, Balajee AS, Latini P, Pichierri P, Nikaido O, Stefanini M, Palitti F: Transcription coupled repair efficiency determines the cell cycle progression and apoptosis after UV exposure in hamster cells. *DNA Repair* 1:209–223 (2002).
- Sakamoto S, Nishikawa K, Heo SJ, Goto M, Furuichi Y, Shimamoto A: Werner helicase relocates into nuclear foci in response to DNA damaging agents and co-localizes with RPA and Rad51. *Genes Cells* 6:421–430 (2001).
- Salk D, Au K, Hoehn H, Martin GM: Cytogenetics of Werner's syndrome cultured skin fibroblasts: variegated translocation mosaicism. *Cytogenet Cell Genet* 30:92–107 (1981).
- Thompson L, Mitchell D, Regan J, Bouffler S, Stewart S, Carrier W, Nairn R, Johnson R: CHO mutant UV61 removes (6–4) photoproducts but not cyclobutane dimers. *Mutagenesis* 4:140–146 (1989).
- Troelstra C, Van Gool A, de Wit J, Vermeulen W, Bootsma D, Hoeijmakers JH: ERCC6, a member of a subfamily of putative helicases, is involved in Cockayne's syndrome and preferential repair of active genes. *Cell* 71:939–953 (1992).
- Yu Ce, Oshima J, Fu YH: Positional cloning of Werner's syndrome gene. *Science* 272:258–262 (1996).

# In situ DNase I sensitivity assay indicates DNA conformation differences between CHO cells and the radiation-sensitive CHO mutant IRS-20

D.G. Marañon, A.O. Laudicina and M. Muhlmann

National Commission of Atomic Energy (CNEA), Centro Atómico Constituyentes, Buenos Aires (Argentina)

**Abstract.** The radiosensitive mutant cell line IRS-20, its wild type counterpart CHO and a derivative of IRS-20 with a transfected YAC clone (YAC-IRS) that restores radioresistance were tested for DNase I sensitivity. The three cell lines were cultured under the same conditions and had a mitotic index of 2–5%. One drop of fixed cells from the three lines was always spread on the same microscopic slide. After one day of ageing, slides were exposed to DNase I and stained with DAPI. Images from every field were captured and the intensity of blue fluores-

cence was measured with appropriate software. For untreated cells, the fluorescence intensity was similar for all of the cell lines. After DNase I treatment, CHO and YAC-IRS had an intensity of 85% but IRS-20 had an intensity of 60%, when compared with the controls. DNase I sensitivity differences between the cell lines indicate that overall conformation of chromatin might contribute to radiation sensitivity of the IRS-20 cells.

Copyright © 2003 S. Karger AG, Basel

DNA conformation plays an important role in DNA repair by modulating complex enzymatic mechanisms. When DNA is damaged, a modification of chromatin structure might act as a sensor for that injury, leading to a cascade of events to repair the damage (Rouse and Jackson, 2002; Downs and Jackson, 2003). Chromatin structure is also involved in gene expression; e.g. hypermethylation of DNA silences genes by favoring a more compact structure of chromatin (Prantera and Ferraro, 1990). Muhlmann and Bedford (1994) and Surralles and Nata- rajan (1998) found that active and inactive human X chromosomes differ in DNA damage processing after exposure to ionizing radiation.

Chromosome domains with open conformation are more accessible to radiation-induced damage, and this is associated

with hyperacetylation of histones (Folle et al., 1998; Martinez-Lopez et al., 2001).

It has been known for a long time that specific chromatin regions have a particular conformation that renders them more sensitive to DNase I digestion (Weintraub and Groudine, 1976; Sperling et al., 1985). This difference in sensitivity was used to identify active and inactive chromosome regions (Kerem et al., 1983, 1984; Monroe et al., 1992).

The first studies that used in situ nick translation (ISNT) to compare different cell lines were performed by Krystosek and Puck (1990). Detailed analyses using confocal microscopy showed differences in DNA accessibility to DNase I among wild type CHO, transformed CHOK1 and retro-transformed cells (Puck et al., 1991). The fluorescence patterns observed correspond to the structure and conformation of chromatin, which allows enzyme accessibility to the DNA. Fluorescent rims that appeared only in the wild type and reverse transformed cells were much brighter than the interiors of cells and indicate that there are more sites accessible to DNase I. The transformed mutant cells did not have a rim: the interior fluorescence was as bright as in normal cells. Imaging analysis methods were developed to evaluate nuclear structure characteristics and adequate software along with sensors allows one to measure DNA densities in cell nuclei (Yatouji et al., 2000).

This work was supported by grant from the SECYT. PICT 98-0103089.

Received 16 September 2003; accepted 26 January 2004.

Request reprints from: Dr. Maria Muhlmann  
National Commission of Atomic Energy (CNEA)  
Centro Atómico Constituyentes, Av Gral Paz 1499  
(1650) San Martín Buenos Aires (Argentina)  
telephone: +54-1-6772-7819; fax: +54-1-6772-7121  
e-mail: muhlmann@cnea.gov.ar.

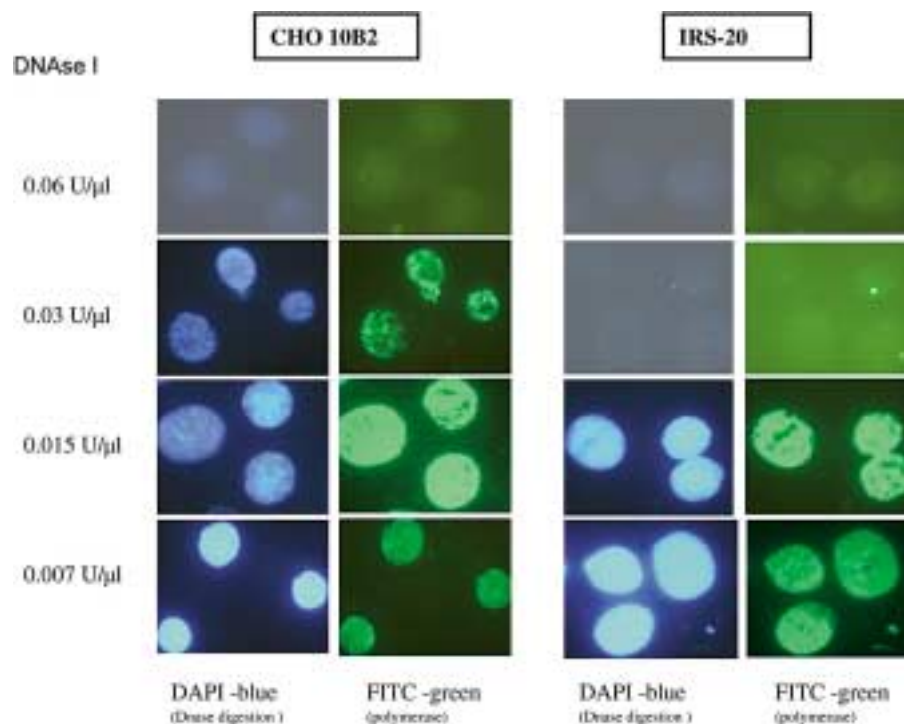


**Fig. 1.** ISNT assay with CHO 10B2 and IRS-20 cells exposed to different concentrations of DNase I.

Downs and Jackson (2003), reviewing the involvement of histone H2AX in DNA repair, suggest that phosphorylation of this particular histone directly affects chromatin structure. Celeste et al. (2002), working with mice lacking the histone H2AX, showed that a structural component of chromatin, such as H2AX protein, may act as tumor suppressor by facilitating the assembly of specific DNA repair complexes on damaged DNA.

Specific mutations are known to cause deficiencies in repair mechanisms. Mutants defective in DNA-PKs such as IRS-20 are sensitive to ionizing radiation and are unable to carry out V(D)J recombination (Lin et al., 1997).

We used the ISNT assay to compare DNA conformation in CHO-10B2 and IRS-20 cell lines. IRS-20 is a radiosensitive mutant of CHO-10B2 (Stackhouse and Bedford, 1993). Normal radiosensitivity was restored by transfecting IRS-20 with a human YAC clone, coding for a gene of the DNA PK family (Priestley et al., 1998). We included such a YAC IRS cell line in the second set of experiments to determine if DNase I sensitivity was restored along with radioresistance.

## Materials and methods

CHO 10B2, IRS-20 and YAC-IRS cells were kindly supplied by Dr. J.S. Bedford, Colorado State University. IRS-20 has a 2- to 3-fold decreased radiation survival compared with CHO 10B2, its wild type counterpart (Stackhouse and Bedford, 1993). A gene in human chromosome 8 restores radioresistance (Lin et al., 1997; Lin and Bedford, 1997). In a regular culture routine, IRS behaves as CHO with the same doubling time and nutrient requirements. IRS-20 belongs to the same complementation group as SCID cells but is less radiosensitive than SCID. Complementation of IRS-20 causes a significant restoration of radioresistance without reaching the wild type level, as shown in experiments with low dose rate continuous irradiation (Priestley et al., 1998).

The cell lines were grown in Alpha MEM 10% FBS with 5% CO<sub>2</sub> at 37°C under the same conditions and fixed when near confluent. Mitotic indices of the three cell lines were 2–5%. Fixation was done at the same time after hypotonic treatment with 3:1 methanol:glacial acetic acid.

Slide preparations were aged one day before processing. Immediate processing of slides resulted in overdigestion with DNase I. Ageing of slides for more than 2 days after spreading resulted in underdigestion. The DNase I concentration was a critical factor in the experiments. ISNT involves two steps: first, DNase I nicks and digests DNA; second, polymerase fills the nicks in the presence of Dig-dUTP, which is detected by an antibody labeled with FITC. Digestion of DNA by DNase I depends on the DNA conformation. The intensity of FITC fluorescence allows one to quantify the gaps filled in by polymerase. Our intention was to detect the extent of digestion and therefore, we firstly determined the concentration of DNase I. This allowed us to see, in a second experiment, possible differences in the ISNT test in the absence of polymerase and nucleotides.

### Determination of DNase I concentration

In these experiments CHO-10B2 and IRS-20 cells were used. Spreads of fixed cells were allowed to age for one day. The ISNT solution was prepared in DNase I buffer as provided by the manufacturer with 1.5 μM of dATP, dGTP, dCTP and digoxigenin-dUTP (1.2 nmol/μl). Polymerase I (0.4 U/μl) and 0.06/0.03/0.015/0.007 U/μl DNase I were used. DNA polymerase was added in excess.

Cell spreads were incubated for 40 min in ISNT solution under a coverslip in a humid chamber at 37°C. Reactions were terminated by removing coverslips and rinsing the slides in 2× SSC, 0.1% Tween for 3 min, 3 times at 40°C.

Digoxigenin was detected with a mouse anti-digoxigenin antibody and an anti-mouse antibody tagged with FITC. This was done in two consecutive incubations of 20 min with 3 rinses in between before mounting slides in a DAPI-antifade solution for image acquisition.

Images were captured using the same exposure times and conditions with a Cool-Snap camera, on the same day of the experiment to avoid changes due to lamp fading. Images were analyzed by using commercial software (Image-Pro plus kindly provided by Bioanalítica Argentina S.A.) which allowed the fluorescence to be quantified in single cells. For each cell line, images in blue (DAPI) and green (FITC) were taken and the fluorescence intensities were measured.

**Table 1.** Results of DNase I digestion and measurements of intensities of DAPI fluorescence

	Cell lines					
	CHO 10B2	Percent of control	IRS-20	Percent of control	YAC- IRS	Percent of control
DNase I treatment 0 (U/ $\mu$ l)	173 $\pm$ 9	100	172 $\pm$ 3	100	175 $\pm$ 4	100
0.03 (U/ $\mu$ l)	144 $\pm$ 23	83	100 $\pm$ 43	58	152 $\pm$ 20	87

Average values and standard deviations of 3 experiments are shown. Approximately 500 cells were scored per cell line. The values of CHO and YAC-IRS are significantly different from IRS-20 ( $p$ : 0.001).

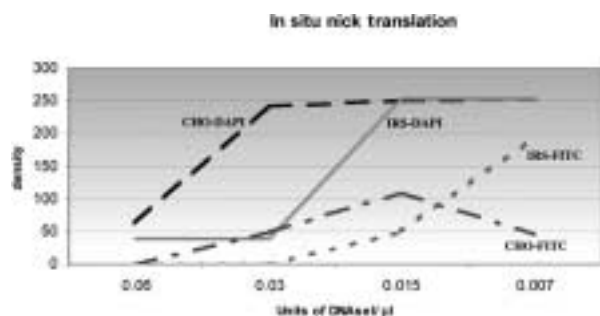


**Fig. 2.** Fluorescence densities of DAPI and FITC following the ISNT assay.

Examples of cells following ISNT are shown in Fig. 1. 0.06 U/ $\mu$ l DNase I completely digested the DNA of both cell lines and nearly no signals were seen. 0.03 U/ $\mu$ l led to overdigestion in IRS but not in CHO cells.

After digestion with 0.015 U/ $\mu$ l DNase I very little difference was seen between both cell lines. 0.007 U/ $\mu$ l DNase I gave similar results as 0.015 U/ $\mu$ l but CHO cells were under-digested. Approximately 50 cells from 10 different fields were analyzed and average intensities were calculated. The graph in Fig. 2 shows the results of this part of our study and led to the decision to use 0.03 U/ $\mu$ l DNase I for the following analysis in which CHO 10B2, IRS-20 and YAC-IRS cells were used.

#### *DNase I treatment*

Cells were grown and prepared as in the first set of experiments. Fixed cells were applied to separate regions of same slides. One day later, slides were incubated under a coverslip with 0.03 U/ $\mu$ l DNase I in buffer for 40 min with ISNT solution in a humid chamber at 37°C. The purpose was to digest DNA but not to fill any gap as in the previous experiment. After rinsing, slides were mounted in DAPI-antifade and images of cells were captured and analyzed. Average DAPI intensities for approximately 500 cells were studied for each sample.

## Results and discussion

The intensity of blue fluorescence of untreated cells was similar for the three cell lines. As expected the three cell lines showed different sensitivities to DNase I: IRS-20 was more sensitive than CHO and YAC-IRS (Table 1).

DNA double strand breaks can be rejoined or left unrejoined. In the first case they can be repaired correctly or can be misrepaired. Cornforth and Bedford (1985) showed that an irradiated AT cell line has a higher fraction of not rejoined fragments than normal human fibroblasts, as detected by PCC. Nevertheless, in many cells classified as double strand repair deficient, an excess of exchanges (chromosomal misrepair) is found in metaphases after irradiation. In order for exchanges to

be formed there must be a joining of the double strand breaks. In repair-proficient cells this joining occurs with less mistakes than in repair-deficient cells. It is possible that apart from the repair process itself chromatin conformation may be another factor that affects repair fidelity. While our results were obtained by an indirect approach and studies at the molecular level need to be done, our data support the hypothesis that chromatin conformation is an important factor for the repair capacities of cells.

Tuschy and Obe (1988) worked with restriction enzymes and high salt concentrations to disrupt the chromatin conformation and induce double strand breaks, while Roos et al. (2002) used radiation to induce damage in different cell lines. In both studies high salt concentrations modified the outcome, demonstrating that chromatin structure is a determinant of radiosensitivity. This also appears to be the case for the radio-sensitive IRS-20.

In conclusion our results suggest that apart from the repair genes, an altered chromatin conformation can influence the fidelity of the entire repair system. IRS-20 cells are more accessible to DNase I in situ than CHO 10B2 and YAC-IRS cells which indicates that they have a relaxed chromatin structure. Our assay could be used with different cells carrying repair deficiencies to study similarities and differences with respect to DNA conformation. It might also be used to determine if toxic chemicals could alter the chromatin conformation of cells rendering them more susceptible to misrepair under damaging conditions.

## Acknowledgements

We would like to thank J. Robinson for proofreading this manuscript.

## References

- Celeste A, Petersen S, Romanienko PJ, Fernandez-Capetillo O, Chen HT, Sedelnikova OA, Reina-San-Martin B, Coppola V, Meffre E, Difilippantonio MJ, Redon C, Pilch DR, Oлару A, Eckhaus M, Camerini-Otter RD, Tessarollo L, Livak F, Manova K, Bonner WM, Nussenzweig MC, Nussenzweig A: Genomic instability in mice lacking histone H2AX. *Science* 296:922–927 (2002).
- Cornforth MN, Bedford JS: On the nature of a defect in cells from individuals with Ataxia Telangiectasia. *Science* 227:1589–1591 (1985).
- Downs J, Jackson S: Cancer: Protective packaging for DNA. *Nature* 424:732–734 (2003).
- Folle GA, Martinez-Lopez W, Boccardo E, Obe G: Localization of chromosome breakpoints: Implication of the chromatin structure and nuclear architecture. *Mutat Res* 404:17–26 (1998).
- Kerem BS, Goitein R, Richler C, Marcus M, Cedar H: In situ nick-translation distinguishes between active and inactive X chromosomes. *Nature* 304:88–90 (1983).
- Kerem BS, Goitein R, Diamond G, Cedar H, Marcus M: Mapping of DNAase I sensitive regions on mitotic chromosomes. *Cell* 38:493–499 (1984).
- Krystosek A, Puck TT: The spatial distribution of exposed nuclear DNA in normal, cancer, and reverse-transformed cells. *Proc natl Acad Sci, USA* 87:6560–6564 (1990).
- Lin J, Muhlmann M, Stackhouse M, Robinson J, Taccioli G, Chen D, Bedford JB: An ionizing radiation sensitive CHO mutant cell line: Irs-20. IV Genetic complementation, V(D)J recombination and the Scid phenotype. *Radiat Res* 147:166–171 (1997).
- Lin J, Bedford JS: Regional gene mapping using mixed radiation hybrids and reverse chromosome painting. *Radiat Res* 148:405–412 (1997).
- Martinez-Lopez W, Folle G, Obe G, Jeppesen P: Chromosome regions enriched in hyperacetylated histone H4 are preferred sites for endonuclease- and radiation-induced breakpoints. *Chromosome Res* 9:69–75 (2001).
- Monroe TJ, Muhlmann-Diaz M, Kovach M, Carlson JO, Bedford JS, Beaty BJ: Stable transformation of a mosquito cell line results in extraordinarily high copy number of the plasmid. *Proc natl Acad Sci, USA* 89:5725–5729 (1992).
- Muhlmann M, Bedford JS: A comparison of radiation-induced aberrations in human cells involving early and late replicating X chromosomes, in Obe G, and Natarajan TA (eds): *Chromosomal Alterations: Origin and Significance* (Springer-Verlag, Berlin 1994).
- Prantera G, Ferraro M: Analysis of methylation and distribution of CpG sequences on human active and inactive X chromosomes by in situ nick translation. *Chromosoma* 99:18–23 (1990).
- Priestley A, Beamish JH, Gell D, Amatucci AG, Muhlmann-Diaz MC, Singleton BK, Smith GC, Blun T, Schalkwyk LC, Bedford JS, Jackson SP, Jeggo PA, Taccioli GE: Molecular and biochemical characterization of DNA-dependent protein kinase-defective rodent mutant irs-20. *Nucleic Acids Res* 26:1965–1973 (1998).
- Puck TT, Bartholdi M, Krystosek A, Johnson R, Haag M: Confocal microscopy of genome exposure in normal, cancer and reverse-transformed cells. *Som Cell molec Genet* 17:489–503 (1991).
- Roos WP, Binder A, Bohm L: The influence of chromatin structure on initial DNA damage and radiosensitivity in CHO-K1 and xrs1 cells at low doses of irradiation 1–10 Gy. *Radiat Environ Biophys* 41:199–206 (2002).
- Rouse J, Jackson SP: Interfaces between the detection, signaling and repair of DNA damage. *Science* 297:547–551 (2002).
- Sperling K, Kerem BS, Goitein R, Kottusch V, Cedar H, Marcus M: DNase I sensitivity in facultative and constitutive heterochromatin. *Chromosoma* 93:38–42 (1985).
- Stackhouse MA, Bedford JS: An ionizing radiation sensitive mutant of CHO cells: irs-20. I. Isolation and initial characterization. *Radiat Res* 136:241–249 (1993).
- Surrallés J, Natarajan AT: Radiosensitivity and repair of the inactive X-chromosome. Insights from FISH and immunocytogenetics. *Mutat Res* 414:117–124 (1998).
- Tuschy S, Obe G: Potentiation of Alu I-induced chromosome aberrations by high salt concentrations in Chinese hamster ovary cells. *Mutat Res* 207:83–87 (1988).
- Weintraub H, Groudine M: Chromosomal subunits in active genes have an altered conformation. *Science* 193:848–856 (1976).
- Yatouji S, Liataud-Roger F, Dufer J: Nuclear chromatin structure and sensitivity to DNaseI in human leukaemic CEM cells incubated with nanomolar okadaic acid. *Cell Prolif* 33:51–62 (2000).



# DNA damage processing and aberration formation in plants

I. Schubert, A. Pecinka, A. Meister, V. Schubert, M. Klatté and G. Jovtchev

Institut für Pflanzengenetik und Kulturpflanzenforschung (IPK), Gatersleben (Germany)

**Abstract.** Various types of DNA damage, induced by endo- and exogenous genotoxic impacts, may become processed into structural chromosome changes such as sister chromatid exchanges (SCEs) and chromosomal aberrations. Chromosomal aberrations occur preferentially within heterochromatic regions composed mainly of repetitive sequences. Most of the preclastogenic damage is correctly repaired by different repair mechanisms. For instance, after N-methyl-N-nitrosourea treatment one SCE is formed per >40,000 and one chromatid-type aberration per ~ 25 million primarily induced O<sup>6</sup>-methylguanine residues in *Vicia faba*. Double-strand breaks (DSBs) apparently represent the critical lesions for the generation of chromosome structural changes by erroneous reciprocal recombination repair. Usually two DSBs have to interact in *cis* or *trans* to form a chromosomal aberration. Indirect evidence is at hand for plants indicating that chromatid-type aberrations mediated by S phase-dependent mutagens are generated by post-replication (mis)repair of DSBs resulting from (rare) interference of repair and replication processes at the sites of lesions, mainly within

repetitive sequences of heterochromatic regions. The proportion of DSBs yielding structural changes via misrepair has still to be established when DSBs, induced at predetermined positions, can be quantified and related to the number of SCEs and chromosomal aberrations that appear at these loci after DSB induction. Recording the degree of association of homologous chromosome territories (by chromosome painting) and of punctual homologous pairing frequency along these territories during and after mutagen treatment of wild-type versus hyper-recombination mutants of *Arabidopsis thaliana*, it will be elucidated as to what extent the interphase arrangement of chromosome territories becomes modified by critical lesions and contributes to homologous reciprocal recombination. This paper reviews the state of the art with respect to DNA damage processing in the course of aberration formation and the interphase arrangement of homologous chromosome territories as a structural prerequisite for homologous rearrangements in plants.

Copyright © 2003 S. Karger AG, Basel

## Spectrum and chromosomal distribution of chromatid-type aberrations

Chromosomal structural aberrations comprise breaks, yielding terminal or intercalary deletions, and rearrangements such as inversions, insertions, symmetric and asymmetric reciprocal exchanges. They represent the consequences of lacking

or incomplete repair or of erroneous recombination repair of various types of DNA lesions caused by exogenous or endogenous genotoxic impacts. When induced before replication, aberrations are manifested as chromosome-type and during or after replication as chromatid-type structural changes.

The spectrum of chromatid-type aberrations observed within the first mitosis after their generation, differs between mammals and plants. In plants, isochromatid breaks are the most frequent aberrations, followed by reciprocal translocations, intercalary deletions, duplication deletions and open chromatid breaks, while in mammals duplication deletions and intercalary deletions are very seldom and open chromatid and isochromatid breaks are much more frequently observed than in plants. However, post-treatment with DNA synthesis inhibitors (e.g., hydroxyurea 10<sup>-2</sup> M, 3 h before fixation) after exposure to S phase-dependent mutagens increases the yield of chro-

Supported by the Deutsche Forschungsgemeinschaft (SCHU 951/10-1).

Received 10 September 2003; manuscript accepted 27 November 2003.

Request reprints from Ingo Schubert

Institut für Pflanzengenetik und Kulturpflanzenforschung (IPK)  
Corrensstrasse 3, DE-06466 Gatersleben (Germany)  
telephone: +49 (0)39482 5239; fax: +49 (0)39482 5137  
e-mail: schubert@ipk-gatersleben.de

Dedicated to Guenter Obe on the occasion of his 65th birthday.

matid-type aberrations 2- to 3-fold and increases the proportion of non-reunion aberrations from 1–5% to 25–35% in plants (Hartley-Asp et al., 1980; Schubert and Rieger, 1987).

The intrachromosomal distribution of aberration breakpoints is not random. Heterochromatic regions, consisting of repetitive DNA sequences, represent “hot spots” of aberration formation (Döbel et al., 1978; Schubert et al., 1986, 1994). Aberration clustering in heterochromatin is more pronounced after exposure to S phase-dependent mutagens causing lesions transformed into breaks via repair or replication and mediating aberrations only when passing through S phase than after exposure to S phase-independent mutagens causing DNA breaks directly (Schubert and Rieger, 1977).

### **Only a minority of potentially clastogenic lesions result in chromosomal aberrations via erroneous recombination repair**

Critical lesions are DNA double-strand breaks (DSB) which are induced either directly or during replication or repair processes at damaged DNA sites and are lethal for proliferating cells if not repaired. Usually, for rearrangements two critical lesions (one per breakpoint) are required (Kihlman et al., 1977; Richardson and Jasin, 2000).

The great majority of potentially clastogenic lesions are repaired correctly. This may occur via reversion of the damage, e.g., photoreactivation of UV-induced pyrimidine dimers or removal of alkyl groups by alkyl-transferase or alkB-like pathways (Begley and Samson, 2003) without generation of discontinuities within the DNA strands. Also excision and mismatch repair pathways, producing DNA discontinuities by an incision step, usually result in a perfect restoration of the pre-damage state. Post-replicative recombination repair that may in part become manifested by mutagen-induced sister chromatid exchange (SCE) represents correct repair (or bypass of lesions) in terms of chromosome structure (Gonzales-Barrera et al., 2003). However, inhibition of complete ligation at sites of recombination may lead to chromosomal aberrations (Lindhahn and Schubert, 1983).

DSBs induced by restriction endonucleases at endogenous or transgenic target sites may induce chromosomal aberrations in non-plant systems (see for instance Bryant, 1984; Natarajan and Obe, 1984; Obe et al., 1987; Winegar and Preston, 1988; Richardson and Jasin, 2000) in an S phase-independent manner (Obe and Winkel, 1985).

Induction of a DSB within one member of two repeats positioned on heterologous chromosomes in mouse ES cells increases homologous recombination between these repeats at least 1000-fold. A similar DSB-mediated increase in homologous recombination between tandem repeats has been reported for plants (Xiao and Peterson, 2000; Orel et al., 2003). However, at recombinationally repaired DSB loci gene conversion, but no crossing over events that would have led to a translocation, has been observed (Richardson et al., 1998). Only when restrictase-mediated DSBs were induced within the repeats of *both* chromosomes, repair by gene conversion was found in one fifth of the cases accompanied by translocation formation (Richardson and Jasin, 2000).

This is in line with more indirect observations on plants.

After treatment of *Vicia faba* meristems with the monofunctional alkylating agent N-methyl-N-nitrosourea (MNU,  $10^{-2}$  M, 1 h), chromatid aberrations were exclusively formed during S phase and appeared in ~30% of metaphases after 12 h recovery (Baranczewski et al., 1997b). More than two thirds of these aberrations occur within heterochromatic regions (~10% of the genome, Baranczewski et al., 1997a). O<sup>6</sup>-methylguanine (O<sup>6</sup>-MeG), the most efficient preclastogenic lesion generated by MNU treatment (Kaina et al., 1991), is induced in a nearly linear dose-dependent manner during all cell cycle stages and later becomes removed in the same proportions in euchromatic and heterochromatic sequences. About one aberration is formed per ~25 million of the originally induced O<sup>6</sup>-MeG residues, as calculated from immuno-slot-blot analyses (Baranczewski et al., 1997a).

Single- but not double-strand breaks (SSB apparently reflect repair intermediates at alkylated sites) were induced by MNU with a linear dose relationship in *Vicia faba* nuclei of all cell cycle stages as measured by the comet assay. Euchromatic and heterochromatic sequences were involved proportionally (Menke et al., 2000).

So-called adaptive conditions (e.g., pre-treatment with a 10-fold lower MNU dose) led to a reduction of the frequency of chromatid aberrations and of O<sup>6</sup>-MeG residues induced by challenge treatment, both by >50%, when protein synthesis was not inhibited (Baranczewski et al., 1997b). About the same reduction was found under adaptive conditions for SSBs and abasic sites, both appearing in the course of repair of alkylated sites (Angelis et al., 2000).

These data show that MNU-induced DNA damages (in particular, O<sup>6</sup>-MeG but also repair-mediated abasic sites and DNA breaks) are evenly distributed and their great majority is correctly repaired along the entire genome during all cell cycle stages.

Only during S phase, recombinational repair of MNU-induced damage may result in (randomly distributed) SCEs (Schubert and Heindorff, 1989) and, at an up to 1000-fold lower frequency (Lindhahn and Schubert, 1983), in chromatid aberrations. Therefore, the majority of randomly distributed preclastogenic lesions, induced for instance by MNU, is correctly repaired or by-passed by a hierarchy of processes (de-alkylation, [base-]excision repair, recombinational repair). Per >40,000 O<sup>6</sup>-MeG residues one SCE and per ~25 million one chromatid aberration is formed. The majority of chromatid aberrations (~70%) are clustered mainly in heterochromatic regions (Baranczewski et al., 1997a). Thus, most of the aberrations induced by S phase-dependent clastogens should be derived from DSBs that may result from (rare) positional coincidence of repair- and replication-mediated DNA discontinuities and are preferentially mis-repaired by reciprocal recombination when broken ends involving homologous repeats interact in *cis* or *trans* (within a chromatid or between sister or non-sister chromatids) (see Fig. 1 and Schubert et al., 1994; Menke et al., 2000).

Using a negatively selectable marker gene combined with a transgenic recognition site for the rare cutting restriction endo-

treatment with:

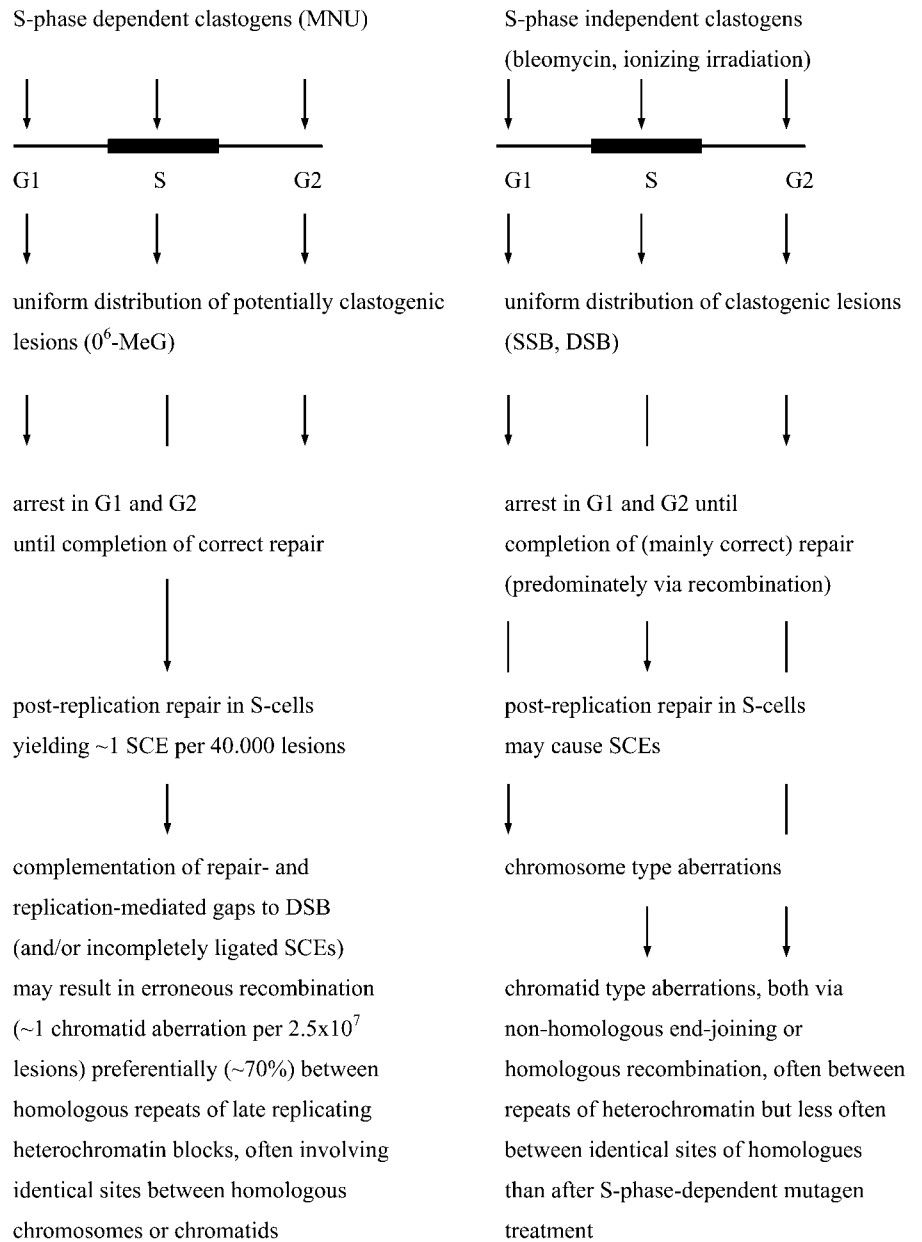


**Fig. 1.** Scheme of DNA damage processing during aberration formation.

nuclease I-*SceI*, various mechanisms of recombinational repair of *SceI*-induced DSBs have been described also for plants (e.g. Puchta, 1999; Kirik et al., 2000; Gisler et al., 2002; Siebert and Puchta, 2002). However, until now these systems did not allow us to quantify the proportions of induced DSBs in relation to those repaired to restore the pre-breakage situation and those potentially resulting in SCEs or different types of chromosomal aberrations. An approach to quantify these proportions is now being established to provide answers as to how DSBs have to be processed to yield SCEs and structural aberrations, respectively, and to compare such data with the calculations derived from experiments with S phase-dependent clastogens and with data obtained from mammalian systems.

**Interphase arrangement of chromosome territories appears to be essential for the origin of chromosomal rearrangements**

The specific side-by-side arrangement of interphase chromosome territories was tested for all possible heterologous pairs of human chromosomes by chromosome painting after ionizing irradiation and measuring their interchange frequencies. Although in these experiments a non-random central clustering was found for the gene-rich chromosomes 1, 16, 17, 19 and 22, a random spatial arrangement was predominant for the majority of chromosomes (Cornforth et al., 2002). Similarly, irradiation of chicken DT40 lymphocytes (with a central clus-

tering of microchromosomes and a peripheral position of macrochromosomes) yielded a low frequency of translocations between micro- and macrochromosomes and most translocations occurred either between microchromosomes or between macrochromosomes (Grandy et al., 2002). Interestingly, mutagen-induced chromatid translocations in a *Vicia faba* karyotype with individually distinguishable chromosome pairs ( $2n = 12$ ) revealed a highly significant (~ 8-fold) excess of translocations between homologous chromosomes and a vast majority (up to >90%) of translocation breakpoints at homologous chromosome positions (Rieger et al., 1973). These effects which were more pronounced for S phase-dependent mutagens than for ionizing irradiation, were interpreted as the result of an at least transient/partial association of homologous chromosomes during interphase.

For the first time painting of chromosome territories of a euploid plant has been established in our lab (Lysak et al., 2001, 2003). Using specific sets of BAC contigs that cover entire chromosome arms as probes for FISH, all five chromosomes of the model plant *Arabidopsis thaliana* can now be traced along various cell cycle and developmental stages. Painting of interphase chromosome territories and FISH with individual chromosome-specific sequences (~ 100 kb) in isolated nuclei, flow-sorted according to their DNA content into different cell cycle and developmental fractions, should reveal the potential dynamics of chromosome territory association and the occurrence of somatic homologous pairing in comparison with model simulations for random chromosome arrangement and punctual homologous pairing.

A "Spherical 1 Mb chromatin domain" (SCD) model (Cremer et al., 2001) and a "Random spatial distribution" (RSD) model simulating a random distribution of all *A. thaliana* chromosomes and of ~ 100 kb chromosome segments, respectively, were computed (in collaboration with Dr. G. Kreth, University of Heidelberg). The frequency of homologous chromosome association was analyzed for chromosome 4 in 2C and 4C nuclei from root and leaf tissues and compared with the punctual homologous pairing of distinct 100-kb segments. The frequency for both phenomena was not identical. Punctual pairing occurred far less frequently than association of homologues but both phenomena occurred with a frequency similar to that predicted by the corresponding computer simulation based on the random models. FISH with individual BAC pairs from different chromosomal positions showed roughly the same frequency of punctual pairing for all tested positions. However, punctual pairing of different loci along a chromosome did not occur simultaneously within the same nucleus indicating that association of homologous territories does not reflect somatic homologous pairing. For chromosomes 1, 3 and 5 we obtained comparable data (Pecinka et al., unpublished results). The at least limited occurrence of homologous pairing might provide a spatial basis for the origin of chromosome rearrangements between homologues. Clustering of aberrations could be reinforced by the tendency of heterochromatic blocks to fuse.

In nearly half of the 4C nuclei, FISH signals for individual BAC pairs (3 or 4 instead of 1 or 2 double signals) indicate that sister chromatids are not permanently cohesed. This supports

the assumption that cohesion along the chromosome arms might be essential only shortly after replication for post-replication repair between sister chromatids (Koshland and Guacci, 2000). Later on, cohesion might be required only around centromeres for their bipolar orientation during nuclear division.

In the future, homologue association and punctual pairing during different cell cycle stages of meristematic cells and after mutagen treatment will be studied. Preliminary data have shown that immediately after bleomycin treatment (5 mg/ml, 1 h) of *Arabidopsis* seedlings chromosome territories are frequently (in ~ 15% of nuclei) disintegrated and dispersed all over the nucleus, while at later recovery times the typical territory structures re-appear. Data obtained with the comet assay showed that bleomycin-induced DSBs increase linearly with dose immediately after treatment and are nearly completely repaired as early as 1 h after treatment (Menke et al., 2001). These data suggest that DSBs may find each other for recombinational repair not only via punctual pairing of homologues, but also randomly due to DSB-mediated dispersion of chromosome territories. The latter may be more typical for treatment with true radiomimetic compounds that lead to less pronounced aberration clustering and fewer translocations between homologous loci than S phase-dependent mutagens (Schubert and Rieger, 1977).

*Arabidopsis* mutants showing a 20- to 50-fold increase in recombination frequency will be characterized as to the proportion of recombination between sister chromatids versus homologues using transgenic recombination substrates in hemi- or homozygous condition (Barbara Hohn and Jean Molinier, personal communication). The frequency of alignment of homologous chromosome territories and of punctual pairing within nuclei of such transgenic mutants will show whether increased homologous recombination is connected with an increased frequency of homologue association or pairing or is rather due to an intensified activity of damaged homologous chromosome segments to find each other, e.g., by a prolongation of the time span during which the DSBs stay "open".

### Acknowledgements

We thank Rigomar Rieger and Holger Puchta for critical reading of the manuscript.

## References

- Angelis KJ, McGuffie M, Menke M, Schubert I: Adaptation to alkylating damage in DNA measured by the comet assay. *Environ Mol Mutagenesis* 36:146–150 (2000).
- Baranczewski P, Nehls P, Rieger R, Pich U, Rajewsky MF, Schubert I: Formation and repair of O<sup>6</sup>-methylguanine in recombination hot spots of plant chromosomes. *Environ Mol Mutagenesis* 29:394–399 (1997a).
- Baranczewski P, Nehls P, Rieger R, Rajewsky MF, Schubert I: Removal of O<sup>6</sup>-methylguanine from plant DNA *in vivo* is accelerated under conditions of clastogenic adaptation. *Environ Mol Mutagenesis* 29:400–405 (1997b).
- Begley TJ, Samson LD: AlkB mystery solved: Oxidative demethylation of N1-methyladenine and N3-methylcytosine adducts by a direct reversal mechanism. *Trends Biochem Sci* 28:2–5 (2003).
- Bryant PE: Enzymatic restriction of mammalian cell DNA using *PvuII* and *BamHI*: evidence for the double-strand break origin of chromosomal aberrations. *Int J Radiat Biol* 46:57–65 (1984).
- Cornforth MN, Greulich-Bode KM, Loucas BD, Arsuaiga J, Vásquez M, Sachs RK, Brückner M, Molls M, Hahnfeldt P, Hlatky L, Brenner DJ: Chromosomes are predominantly located randomly with respect to each other in interphase human cells. *J Cell Biol* 159:237–244 (2002).
- Cremer M, von Hase J, Volm T, Brero A, Kreth G, Walter J, Fischer C, Solovei I, Cremer C, Cremer T: Non-random radial higher-order chromatin arrangements in nuclei of diploid human cells. *Chrom Res* 9:541–567 (2001).
- Döbel P, Schubert I, Rieger R: Distribution of heterochromatin in a reconstructed karyotype of *Vicia faba* as identified by banding- and DNA-late replication patterns. *Chromosoma* 69:193–209 (1978).
- Gisler B, Salomon S, Puchta H: The role of double-strand break-induced allelic homologous recombination in somatic plant cells. *Plant J* 32:177–284 (2002).
- Gonzales-Barrera S, Cortes-Ledesma F, Wellinger RE, Aguilera A: Equal sister chromatid exchange is a major mechanism of double-strand break repair in yeast. *Cell* 11:1661–1671 (2003).
- Grandy I, Hardt T, Schmid M, Haaf T: Effects of higher-order nuclear structure and Rad51 overexpression on radiation-induced chromosome rearrangements. *Cytogenet Genome Res* 98:265–269 (2002).
- Hartley-Asp B, Andersson HC, Sturelid S, Kihlman BA: G2 repair and the formation of chromosomal aberrations. 1. The effect of hydroxyurea and caffeine on maleic hydrazide-induced chromosome damage in *Vicia faba*. *Environ Exp Bot* 20:119–129 (1980).
- Kaina B, Fritz G, Mitra S, Coquerelle T: Transfection and expression of human O<sup>6</sup>-methylguanine-DNA methyltransferase (MGMT) cDNA in Chinese hamster cells: The role of MGMT in protection against the genotoxic effects of alkylating agents. *Carcinogenesis* 12:1857–1867 (1991).
- Kihlman BA, Andersson HC, Natarajan AT: Molecular mechanisms in the production of chromosomal aberrations: studies with the 5-bromo-deoxyuridine-labelling method, in de la Chapelle A, Sorsa M (eds): *Chromosomes Today*, vol 6, p 287 (Elsevier, Amsterdam 1977).
- Kirik A, Salomon S, Puchta H: Species-specific double-strand break repair and genome evolution in plants. *EMBO J* 19:5562–5566 (2000).
- Koshland DE, Guacci V: Sister chromatid cohesion: The beginning of a long and beautiful relationship. *Curr Opin Cell Biol* 12:297–301 (2000).
- Lindenhahn M, Schubert I: On the origin of hydroxyurea-induced chromatid aberrations in G<sub>2</sub> chromosomes with BrdUrd in only one of the sister chromatids. *Mutat Res* 108:301–316 (1983).
- Lysak MA, Fransz PF, Ali HBM, Schubert I: Chromosome painting in *Arabidopsis thaliana*. *Plant J* 28:689–697 (2001).
- Lysak MA, Pecinka A, Schubert I: Recent progress on chromosome painting in *Arabidopsis* and related species. *Chromosome Res* 11:195–204 (2003).
- Menke M, Meister A, Schubert I: N-methyl-N-nitrosourea-induced DNA damage detected by the comet assay in *Vicia faba* nuclei during all interphase stages is not restricted to chromatid aberration hot spots. *Mutagenesis* 15:503–506 (2000).
- Menke M, Chen IP, Angelis KJ, Schubert I: DNA damage and repair in *Arabidopsis thaliana* as measured by the comet assay after treatment with different classes of genotoxins. *Mutat Res* 493:87–93 (2001).
- Natarajan AT, Obe G: Molecular mechanisms involved in the production of chromosomal aberrations. 3. Restriction endonucleases. *Chromosoma* 90:120–127 (1984).
- Obe G, Winkel E-U: The chromosome-breaking activity of the restriction endonuclease *AluI* in CHO cells is independent of the S-phase of the cell cycle. *Mutat Res* 152:25–29 (1985).
- Obe G, Johannes C, Vasudev V, Kasper P, Lamprecht I: Induction of chromosomal aberrations in Chinese hamster ovary cells by the restriction endonuclease *DraI*: dose-effect relationships and effect of substitution of chromosomal DNA with bromodeoxyuridine. *Mutat Res* 192:263–269 (1987).
- Orel N, Kirik A, Puchta H: Different pathways of homologous recombination are used for the repair of double-strand breaks within tandemly arranged sequences in the plant genome. *Plant J* 35:604–612 (2003).
- Puchta H: Doppelstrangbruchreparatur und Genom-evolution bei Pflanzen. *Biospektrum* 5:105–108 (1999).
- Richardson C, Jasin M: Frequent chromosomal translocations induced by DNA double-strand breaks. *Nature* 405:697–700 (2000).
- Richardson C, Moynahan ME, Jasin M: Double-strand break repair by interchromosomal recombinations suppression of chromosomal translocations. *Genes Dev* 12:3831–3842 (1998).
- Rieger R, Michaelis A, Schubert I, Meister A: Somatic interphase pairing of *Vicia* chromosomes as inferred from the hom/het ratio of induced chromatid interchanges. *Mutat Res* 20:295–298 (1973).
- Schubert I, Heindorff K: Are SCE frequencies indicative of adaptive response of plant cells? *Mutat Res* 211:301–306 (1989).
- Schubert I, Rieger R: On the expressivity of aberration hot spots after treatment with mutagens showing delayed or non-delayed effects. *Mutat Res* 44:337–344 (1977).
- Schubert I, Rieger R: Effects of hydroxyurea posttreatment in G<sub>2</sub> on the frequency and distribution of mutagen induced chromatid aberrations in a reconstructed karyotype of *Vicia faba*. *Biol Zentbl* 106:59–66 (1987).
- Schubert I, Heindorff K, Rieger R, Michaelis A: Prinzipien der chromosomalen Verteilung induzierter Chromatidenaberrationen bei *Vicia faba* und deren mögliche biologische Bedeutung. *Kulturpflanze* 34:21–45 (1986).
- Schubert I, Rieger R, Fuchs J, Pich U: Sequence organization and the mechanism of interstitial deletion clustering in a plant genome (*Vicia faba*). *Mutat Res* 325:1–5 (1994).
- Siebert R, Puchta H: Efficient repair of genomic double-strand breaks by homologous recombination between directly repeated sequences in the plant genome. *Plant Cell* 14:1121–1131 (2002).
- Winegar RA, Preston RJ: The induction of chromosome aberrations by restriction endonucleases that produce blunt-end or cohesive-end double strand breaks. *Mutat Res* 197:141–149 (1988).
- Xiao YL, Peterson T: Intrachromosomal homologous recombination in *Arabidopsis* induced by a maize transposon. *Mol Gen Genet* 263:22–29 (2000).

# DNA and telomeres: beginnings and endings

S.M. Bailey<sup>a,b</sup> and E.H. Goodwin<sup>b</sup>

<sup>a</sup>Department of Environmental and Radiological Health Sciences, Colorado State University, Fort Collins, CO;

<sup>b</sup>Bioscience Division, Los Alamos, National Laboratory, Los Alamos NM (USA)

**Abstract.** How a cell deals with its DNA ends is a question that returns us to the very beginnings of modern telomere biology. It is also a question we are still asking today because it is absolutely essential that a cell correctly distinguishes between natural chromosomal DNA ends and broken DNA ends, then processes each appropriately – preserving the one, rejoining the other. Effective end-capping of mammalian telomeres has a seemingly paradoxical requirement for proteins more commonly associated with DNA double strand break (DSB) repair. Ku70, Ku80, DNA-PKcs (the catalytic subunit of DNA-dependent protein kinase), Xrcc4 and Artemis all participate in DSB repair through nonhomologous end-joining (NHEJ). Somewhat surprisingly, mutations in any of these genes cause spontaneous chromosomal end-to-end fusions that maintain large blocks of telomeric sequence at the points of fusion, suggesting loss or

failure of a critical terminal structure, rather than telomere shortening, is at fault. Nascent telomeres produced via leading-strand DNA synthesis are especially susceptible to these end-to-end fusions, suggesting a crucial difference in the postreplicative processing of telomeres that is linked to their mode of replication. Here we will examine the dual roles played by DNA repair proteins. Our review of this rapidly advancing field primarily will focus on mammalian cells, and cannot include even all of this. Despite these limitations, we hope the review will serve as a useful gateway to the literature, and will help to frame the major issues in this exciting and rapidly progressing field. Our apologies to those whose work we are unable to include.

Copyright © 2003 S. Karger AG, Basel

## Background

The year 2003 marks the fiftieth anniversary of an important milestone in genetics, the breakthrough discovery of the hotly pursued structure of DNA (Watson and Crick, 1953; Franklin and Gosling, 1953) – a structure that immediately suggested how this critical molecule (a double helix) could replicate itself and carry life's hereditary information. What was not immediately apparent or appreciated was that DNA could be subject to damage or to unsuccessful attempts at repairing it accurately. Subsequent work has made it clear,

however, that all living organisms are under constant assault by DNA damaging agents, and that their cells possess very effective mechanisms for repairing that damage.

As early as the late 1930's, it was recognized that broken ends of DNA behaved very differently than natural chromosomal termini. Hermann Muller, in his classic studies of the fruit fly *Drosophila melanogaster* (Muller, 1938), first described telomeres, coining the name from the Greek words telos meaning "end" and meros meaning "part" based on their chromosome end protection function. Then in elegant experiments with maize, Barbara McClintock laid the foundation for modern telomere biology by formulating the concept that natural chromosome ends are protected from the sorts of fusion events suffered by broken chromosomes (McClintock, 1941, 1942). Thus telomeres, through their ability to preserve genetic linkage relationships, became one of the earliest cellular mechanisms for maintaining genomic stability to be recognized.

Telomeres are highly specialized nucleoprotein structures that maintain genomic stability by stabilizing and protecting the ends of linear chromosomes, an essential function inferred

Supported by grants from the Department of Energy, Office of Biological and Environmental Research (W-7405-ENG-36, DE-FG03-98ER63239) and the National Institutes of Health (NIH CA-43322).

Received 10 September 2003; manuscript accepted 27 November 2003.

Request reprints from Edwin H. Goodwin, Bioscience Division  
Los Alamos National Laboratory, Los Alamos, NM 87545 (USA)  
telephone: 505-665-2853; fax: 505-665-3024; email: egoodwin@lanl.gov

cytogenetically from the end-to-end fusions that result when telomeric end-capping is compromised. In striking contrast to natural chromosomal termini, broken chromosome ends produced by DSBs are highly recombinogenic, and represent a major threat to the integrity of the cell's genome. Their potential for causing chromosomal rearrangements contributes to genomic instability and tumorigenesis. As can readily be appreciated, it is essential that a cell accurately distinguishes between natural chromosomal ends and broken DNA ends and processes each appropriately. Unexpectedly, recent work demonstrates that these two seemingly opposing processes, i.e., joining of unnatural ends vs. preserving the natural ones, rely on a common subset of proteins, those best known for their role in NHEJ DNA DSB repair. The question now becomes – how does a cell tell which end is which?

### Telomere structure

Telomeric DNA consists of tandem arrays of short, repetitive G-rich sequences that are oriented 5'-to-3' towards the end of the chromosome (Blackburn, 1991; Biessmann and Mason, 1992), forming a 3' single-stranded G-rich overhang (Makarov et al., 1997; Wellinger and Sen, 1997). Because conventional replication machinery cannot synthesize new DNA to the very end of a linear chromosome (Watson, 1972), replication results in progressive erosion of telomeric DNA. Oxidative DNA damage within telomeric DNA may also contribute to this loss (von Zglinicki et al., 1995). Activation of telomerase, which maintains telomere length via de novo addition of RNA-templated repeats (Blackburn et al., 1991) or an alternative-length maintenance (ALT) pathway (Murnane et al., 1994; Bryan and Reddel, 1997) in tumors is required to preserve telomeres' existence and ensure continued cellular proliferation. Critical telomere shortening that occurs prior to activation of these preservation mechanisms has been implicated in contributing to the initial instability required to start a cell down the path of tumorigenesis (Feldser et al., 2003).

It was originally thought that telomeric DNA sequence alone could stabilize chromosome ends. However, it is now recognized that a variety of proteins binding either directly to telomeric DNA, or indirectly to other proteins that are themselves bound to telomeric DNA are also required to form a protective nucleoprotein higher order chromatin structure that serves to "cap" the end of the chromosome and prevent deleterious terminal rearrangements (de Lange, 2002). Direct visualization of mammalian telomeres by electron microscopy revealed the existence of kilobase-sized loops at chromosome ends (Griffith et al., 1999). These "t-loops" are created when a telomere's end loops back on itself and the single-stranded overhang invades an interior segment of duplex telomeric DNA. By sequestering natural chromosome ends, t-loops provide an attractive architectural solution to rendering telomeres nonrecombinogenic.

The human telomere-repeat binding factor 2 (TRF2) protects chromosome ends from fusion (van Steensel et al., 1998) and was the first telomere-associated protein implicated in the maintenance of the correct terminal DNA structure necessary for proper telomere function, as it is required to remodel linear

DNA into t-loops in vitro (Griffith et al., 1999). Because functional telomeres are essential for continuous cellular proliferation and stable genetic inheritance, loss of chromosomal end-capping has consequences in both aging and cancer (Harley et al., 1992; Artandi et al., 2000; DePinho and Wong, 2003).

### Genetic analysis of chromosome end capping

The goal of a genetic analysis of chromosome end capping is to identify the genes and proteins they encode that enable telomeres' protective function. Cytogenetic analysis has proven to be an invaluable tool for assessing the integrity of chromosome end protection. Of several methods available to cytogeneticists, fluorescence in situ hybridization (FISH) with a telomere probe is perhaps the most definitive. Fortunately, the two mammalian species most commonly used in telomere research, mouse and human, do not contain cytogenetically visible blocks of interstitial telomeric sequence within their chromosomes (Meyne et al., 1989). This property allows impaired end capping to be readily inferred from the appearance of internalized telomeric sequence, an unambiguous sign that a telomeric fusion has taken place. We define telomeric fusion operationally as two telomeres fusing into a single FISH signal. This definition is practical and it serves to differentiate telomeric fusion from the chromosomal anomaly referred to as telomeric association, in which two chromosome ends lie within the width of a mitotic chromatid, producing two distinct FISH signals. Table 1 summarizes work from a number of laboratories that is helping to define the role of DNA repair genes at the telomere. In all cases, the studies have had matched wild-type controls displaying normal telomere function. We have not included instances in which chromosomal end fusion appears to be the result of severe loss of telomeric DNA.

The observation of chromosomes oriented end-to-end in a mouse cell line having the severe combined immunodeficiency (*scid*) mutation in DNA-PKcs led to speculation that chromosome fusogenic potential in mammalian cells may not only be determined by telomere length, but also by the status of telomere chromatin structure (Slijepcevic et al., 1997). The participation of DNA repair proteins in telomeric end capping came to light not long after the demonstration that TRF2 is required for telomere protection (van Steensel et al., 1998) when end-to-end fusions between chromosomes were observed in cells from mice having mutations in any of the components of DNA-PK, i.e. Ku70, Ku86 or the catalytic subunit DNA-PKcs (Bailey et al., 1999). Large, bright FISH signals at the point of fusion clearly eliminated shortening of telomeric DNA beyond a critical limit to maintain functionality as a potential cause, and pointed instead towards loss of a protective terminal structure. That mutation in DNA-PKcs was responsible for the telomere dysfunction resulting in inappropriate fusion in *scid* mice, rather than coincidental mutation of another gene, was shown when telomeric fusions were observed in cells from *scid* dogs. In this case the same gene is affected, although the mutation is different. Also, telomeric fusions occur in DNA-PKcs knockout mouse cells demonstrating that telomere deprotection is not confined to specific mutations associated with naturally occurring *scid*. Thus

**Table 1.** DNA repair genes and chromosome end protection. Telomere dysfunction is inferred cytogenetically from the appearance of interstitial telomeric signals in metaphase chromosomes. Thus, end fusions resulting from excessive telomere shortening are excluded.

Genetic defect	Normal gene function	Source	Primary (P), Transformed (T)	Telomere dysfunction (fusion)	Reference
DNA-PKcs (scid)	NHEJ	Mouse	P and T	Yes	Bailey et al., 1999
DNA-PKcs (scid)	NHEJ	Dog	P and T	Yes	Bailey, Goodwin and Meek, unpublished Meek et al., 2001
DNA-PKcs (null)	NHEJ	Human (M059J)	T	Yes	Bailey, Goodwin and Allalunis-Turner, unpublished Leesmiller et al., 1995
DNA-PKcs (KO)	NHEJ	Mouse	P and T	Yes	Bailey et al., 1999 Gilley et al., 2001 Goytisolo et al., 2001
DNA-PKcs (SNPs)	NHEJ	Mouse (Balb/c)	P and T	Yes	Bailey, Goodwin and Ullrich, unpublished Okayasu et al., 2000
DNA-PKcs / mTR (KOs)	NHEJ / telomere length	Mouse	P	Yes	Espejel et al., 2002b
DNA-PKcs <sup>-/-</sup> / Rad54 <sup>+/-</sup>	NHEJ / HR	Mouse	P	Yes	Jaco et al., 2003
DNA-PKcs <sup>-/-</sup> / Rad54 <sup>-/-</sup>				Yes	
DNA-PKcs <sup>+/-</sup> / Rad54 <sup>-/-</sup> (KOs)				Yes	
scid / hRAD54 (mutations)	NHEJ / HR	Mouse	T	Yes	Bailey, Goodwin and Pluth, unpublished Pluth et al., 2001
Ku70 (KO)	NHEJ	Mouse	Virally T and P	Yes	Bailey et al., 1999 d'Adda di Fagagna et al., 2001
Ku86 (KO)	NHEJ	Mouse	Virally T and P	Yes	Bailey et al., 1999 Samper et al., 2000 Espejel et al., 2002a d'Adda di Fagagna et al., 2001
Xrcc4 (KO)	NHEJ	Mouse	P	Yes	d'Adda di Fagagna et al., 2001
Artemis (null mutation)	NHEJ	Mouse	ES cells	Yes	Rooney et al., 2003
Brca2	HR	Mouse	P and T	No	Bailey, Goodwin and Brenneman, unpublished Donoho et al., 2003
NBS1 (deletion)	HR and NHEJ	Human	P and hTERT	No	Bailey, Goodwin and Zdzienicka, unpublished Kraakman-vanderZwet et al., 1999
p53 (KO)	Cell cycle arrest, apoptosis	Mouse	P and T	No	Bailey et al., 1999
p53 (Li Fraumeni)	Cell cycle arrest, apoptosis	Human	T	No	Bailey and Goodwin, unpublished Gollahon et al., 1998
ATM (KO)	Cell cycle arrest	Mouse	P and T	No	Bailey, Goodwin and Turker, unpublished Gage et al., 2001
ATM (AT)	Cell cycle arrest	Human	P	No	Bailey and Goodwin, unpublished
PARP1 (KO)	SSB repair and damage sensing	Mouse	T and P	No	Bailey, Goodwin and Chen, unpublished Samper et al., 2001
WRN	HR	Human	hTert	No	Bailey, Goodwin and Campisi, unpublished Hasty et al., 2003

DNA-PK, best known for its role in the non-homologous pathway of DSB repair, took on a paradoxical new role in preserving the natural ends of chromosomes.

The *scid* mutations in mouse and dog severely depress DNA-PK activity (Blunt et al., 1996; Meek et al., 2001), and the DNA-PKcs knockout abolishes it (Kurimasa et al., 1999b). BALB/c mice possess two naturally occurring single-nucleotide polymorphisms in the DNA-PKcs gene, *Prkdc*, that reduce, but do not eliminate, DNA-PKcs activity and abundance (Yu et al., 2001). Of significance, BALB/c mice are not immunodeficient, so they must retain the capacity for V(D)J recombination. These mice, however, are somewhat radiosensitive suggesting NHEJ has been compromised, and they are more susceptible to induction of cancer by radiation (Yu et al., 2001). Nevertheless, BALB/c mice have an outwardly normal appearance and behavior, and cannot be distinguished by casual observation from other mice on the basis of their genetic deficiency. It is therefore of interest that BALB/c mice experience telomere dysfunction. Apparently even partial loss of DNA-PK activity

is sufficient to impair telomere protection. Whether or not partially inactivating DNA-PKcs polymorphisms occur in humans has yet to be determined.

The two Ku proteins form a heterodimeric ring capable of binding DNA ends and attracting DNA-PKcs (Gottlieb and Jackson, 1993; Gu et al., 1997; Walker et al., 2001) via interaction with the C-terminus of Ku80 (Gell and Jackson, 1999; Singleton et al., 1999). Telomeric fusions have now been observed in several studies of Ku knockouts. The simplest interpretation of these results is that, like its role in DSB repair, the Ku heterodimer exerts its effect on telomeres by recruiting the catalytic subunit to chromosome ends. In support of this, we have recently demonstrated that the kinase activity of DNA-PK is required for telomeric end-protection (Bailey et al., 2004), just as it is for NHEJ (Kurimasa et al., 1999a). How DNA-PKcs phosphorylation can promote the joining of some DNA ends while preserving others remains an open and provocative question.



Studies have also demonstrated that telomeric fusion is itself mediated by the NHEJ component ligase IV (Smogorzewska et al., 2002). However, what mechanism joins unprotected telomeres in NHEJ-deficient cells remains unknown. Possibly, defects in DNA-PK do not completely eliminate NHEJ, or a DNA-PK-independent backup pathway (Wang et al., 2003) may join unprotected chromosome ends. An alternate, error-prone repair pathway is certainly implicated by the end-joining and instability that occurs in NHEJ mutants (Difilippantonio et al., 2000; Ferguson et al., 2000; d'Adda di Fagagna et al., 2001).

A possible role in telomere function has been evaluated for other genes having roles in NHEJ. Telomeric chromosomal end fusions were observed in mouse knockouts of *Xrcc4* (d'Adda di Fagagna et al., 2001). A recently identified member of the NHEJ pathway, Artemis (Moshous et al., 2001), possesses *in vitro* endonuclease and exonuclease activities and complexes with DNA-PKcs (Ma et al., 2002). Artemis appears to function with DNA-PKcs in a subset of end-processing reactions (Rooney et al., 2002). Of the six known NHEJ components, only DNA-PKcs and Artemis are not found in yeast. Inactivating mutations of Artemis result in human radiosensitive severe combined immunodeficiency (RS-scid), and Artemis-deficient mouse ES cells display chromosomal instability, including telomeric fusions (Rooney et al., 2003).

Other genes known to confer severe radiosensitivity when mutated have been examined for a telomere protection role. ATM, the gene that is mutated in Ataxia Telangiectasia (AT), reportedly participates in DNA damage recognition and cell-cycle checkpoints (Szumiel, 1998). In our laboratory, telomeric fusions were not found in cells from either human AT patients or mouse cells in which the ATM gene had been knocked out. Telomere shortening and association have been reported in AT cells (Pandita et al., 1995). Telomeric association appears to be more transient than fusion, but the relationship between the two is not clear at this time. Thus, the impaired telomere phenotype associated with ATM mutations may be less profound than that caused by mutations in DNA-PK. Nijmegen Breakage Syndrome (NBS), a condition that resembles AT in its clinical manifestation, is the result of an intragenic deletion mutation in the NBS1 gene (Carney et al., 1998). Human NBS1 forms a complex with MRE11 and Rad50. This complex has been suggested to function in both HR and NHEJ (Goedecke et al., 1999). Cells from NBS patients do not have telomeric fusions. The ATM and NBS1 results appear to rule out a direct connection between elevated radiosensitivity and the propensity to form telomeric fusions.

BRCA2 and RAD54 participate in homologous recombination (HR) repair (Thompson and Schild, 2001). Deletion of BRCA2's exon 27 elevates sensitivity to mitomycin C-induced crosslinks and increases spontaneous chromosomal instability (Donoho et al., 2003), but does not cause telomeric fusions. In contrast, telomeric fusions were observed in RAD54 knockouts. These seemingly contradictory results for two HR genes might be reconciled in one of two ways. BRCA2 could have a telomere protection function that is not compromised by the rather small truncation mutation. Alternatively, telomere protection may require only a subset of HR proteins. The DNA

configuration at the junction of the t-loop resembles an early step in HR. Thus, t-loop formation may require only those HR proteins that participate in strand invasion and/or stabilization.

Telomeric fusions also occur in double DNA-PKcs/RAD54 knockouts, indicating that end fusion in DNA-PK-deficient cells is not mediated by a RAD54-dependent process (Jaco et al., 2003). Thus, DSB repair by HR is not the mechanism responsible for joining uncapped telomeres. This is perhaps not surprising because resolution of recombination intermediates would not be predicted to join blocks of telomeric DNA in opposite orientations as must occur with end-to-end fusion.

Several additional proteins have been examined for a role in telomere end capping, with mostly negative results. Like ATM, p53 participates in DNA damage-induced cell-cycle arrest and apoptosis, but unlike ATM, p53 mutations do not cause radiosensitivity (Cadwell and Zambetti, 2001). Telomere dysfunction was not found in human cells having the p53 mutation associated with the cancer-prone Li Fraumeni syndrome or in p53 knockout mouse cells. Poly (ADP-ribose) polymerase (PARP) has been reported to have roles in DNA damage sensing and DNA single-strand break repair (Okano et al., 2003), and in telomere length maintenance (diFagagna et al., 1999; Tong et al., 2001), but apparently does not participate in telomere protection. Werner's syndrome is characterized by premature aging (Epstein and Motulsky, 1996). The causative defect lies in the WRN gene, which encodes a protein with helicase and exonuclease activities (Gray et al., 1997; Huang et al., 1998). Given the role played by telomeres in cellular senescence (Campisi et al., 2001), a role for WRN in telomeric end-protection was sought but not found.

In summary, these results strongly implicate genes from the NHEJ pathway of DSB repair in forming protective structures at chromosomal termini. HR repair proteins also may be required, but the extent of participation by genes in this repair pathway requires further study. Other DNA repair genes examined to date appear to have a lesser, if any, role, but many repair genes are yet to be examined.

### Dysfunctional telomeres take the "lead"

FISH identifies telomere dysfunction only indirectly through the appearance of chromosomal end-to-end fusions. In particular, FISH does not reveal which telomeres are capped and which are not. So it remained a possibility that in the studies cited above only a subset of telomeres becomes dysfunctional. The first evidence in support of limited telomere dysfunction came not from what was observed, but from what was not. Because of the proximity of newly replicated sister chromatids, it was expected that sister union telomeric fusions would be common events. However, sister unions were not found among the telomeric fusions occurring in DNA-PK-deficient mouse cells or in HTC75 cells (a telomerase-positive human fibrosarcoma cell line) following the inducible expression of a dominant-negative mutant allele of TRF2, TRF2<sup>ABAM</sup> (Bailey et al., 2001). This implied that of the two sister telomeres replicated from the same parental template, only one became dysfunc-

tional and subject to fusion. Further analysis using the strand-specific CO-FISH technique revealed that dysfunction created by either DNA-PKcs or TRF2 deficiency was limited to telomeres replicated by leading-strand DNA synthesis (Bailey et al., 2001).

Contrasting with these results, sister union telomeric fusions, which necessarily involve one leading- and one lagging-strand telomere, were reported in primary human fibroblasts (IMR90) and hTERT-immortalized human BJ fibroblasts expressing the same dominant-negative TRF2 allele, but introduced by viral transfection (Smogorzewska et al., 2002). The difference between the studies may be attributable to higher expression of the TRF2<sup>ΔBAM</sup> allele in the second study. This interpretation is supported by recent ChIPs analyses using the same TRF2<sup>ΔBAM</sup> system as the first study demonstrating only an ~ 50% reduction of endogenous TRF2 association with telomeric DNA (d'Adda di Fagagna et al., 2003).

Intriguingly, both studies point to an asymmetry in the process (or processes) that transform newly replicated chromosome ends into functional telomeres. Following replication, telomeres created by leading-strand synthesis are either blunt-ended, or possess a small 5' overhang (Cimino-Reale et al., 2003), whereas those created by lagging-strand synthesis have a 3' overhang with a length determined by the position of the most terminal RNA primer (Wright et al., 1997). These different initial DNA structures may dictate different requirements for chromosomal end protection. Processing each type of end may require end-specific sets of proteins, and conceivably could produce end-specific terminal structures. Clearly, these results expand the range of possibilities to be considered when contemplating models of mammalian chromosome end protection.

### Further studies of DNA-PK

The three proteins comprising DNA-PK have each been found at mammalian telomeres (Bianchi and deLange, 1999; Hsu et al., 1999; d'Adda di Fagagna et al., 2001), suggesting that telomeric end-protection requires the holoenzyme. Hypothetically, DNA-PK might act in differentiating natural chromosome ends from unnatural DSB ends, and then direct each type into the correct pathway. A plausible biochemical candidate for this action is DNA-PK's capacity to phosphorylate proteins. Once bound to DSB ends, DNA-PK's kinase activity presumably prompts the rejoining of DSBs. Conversely, the kinase may not be activated by ends composed of telomeric DNA, or activation may be repressed by telomere binding proteins. These ends are then processed to create protective terminal caps. Supporting the first part of this model, a point mutation in DNA-PKcs that eliminates kinase activity also suppresses DSB repair (Kurimasa et al., 1999a). Likewise, the model explains the appearance of both DSB repair deficiency and telomere dysfunction when Ku70, Ku86 or DNA-PKcs have been deleted. In these cells, the DNA-PK holoenzyme is absent, so they lose the ability to effectively direct DNA ends into either pathway, thus compromising both DSB repair and telomere protection.

A critical test of this model was made by exposing cells to a highly specific DNA-PKcs inhibitor designated IC86621 (Kashishian et al., 2003). The kinase inhibitor was expected to impair DSB repair, but not telomere function. However, the inhibitor proved to be an effective inducer of telomeric fusions (Bailey et al., 2003). We conclude that the kinase activity of DNA-PK is required for both of its roles, and does not serve to distinguish natural from unnatural DNA ends.

The same study found only chromatid-type telomeric fusions following exposure to the inhibitor for a single cell cycle. If DNA-PK were required throughout the cell cycle, then some telomeric fusions would occur in G1 and would have been observed as chromosome-type fusions in mitosis. The absence of chromosome-type fusions indicates that DNA-PKcs plays a post-replication role, most likely in reconstructing functional telomeres on newly replicated chromosome ends. Its precise role, however, remains elusive.

### Making ends meet: The dual roles of DSB repair genes

Phosphorylation of the variant histone H2AX occurs in megabase-sized domains about the sites of DSBs (Rogakou et al., 1999). These domains are cytologically visible with immunofluorescence, and allow DSBs to be accurately quantified. By this means, the background level of DSBs in genetically normal cells was found to be quite low, ~ 0.05 DSBs/cell (Rothkamm and Lobrich, 2003), implying NHEJ proteins are rarely called upon to join DSBs in a natural setting. In contrast, with every cell cycle the protective telomeric end-structure must disassemble to allow replication, and then be reconstructed afterwards. In normal human cells, NHEJ proteins participate in capping 92 new leading-strand telomeres. This number of chromosome ends is equivalent to 46 DSBs, far in excess of the naturally occurring number of DSB ends. This prompts us to consider that the primary function of NHEJ proteins may not be to join ends, but to preserve them. Thus, the designation given these genes based on their first-discovered role no longer seems entirely appropriate.

What emerges from the work reviewed here is a sense that two previously separate fields of study, DNA DSB repair and telomere biology, are undergoing a merger driven by a mutual dependence on a subset of genes common to both. One hopes that the secret of how the same cast of actors can simultaneously play such conflicting roles will be revealed as this intriguing story continues to unfold.

### Acknowledgements

The authors thank Mark Brenneman for many thought-provoking discussions, and express their appreciation to the many individuals (Table 1) who graciously donated valuable cell lines for our genetic analysis of telomere dysfunction.

## References

- d'Adda di Fagagna F, Hande MP, Tong WM, Roth D, Lansdorp PM, Wang ZQ, Jackson SP: Effects of DNA nonhomologous end-joining factors on telomere length and chromosomal stability in mammalian cells. *Curr Biol* 11:1192–1196 (2001).
- d'Adda di Fagagna F, Reaper PM, Clay-Farrace L, Fiegler H, Carr P, Von Zglinicki T, Saretzki G, Carter NP, Jackson SP: A DNA damage checkpoint response in telomere-initiated senescence. *Nature* 426:194–198 (2003).
- Artandi SE, Chang S, Lee SL, Alson S, Gottlieb GJ, Chin L, DePinho RA: Telomere dysfunction promotes non-reciprocal translocations and epithelial cancers in mice. *Nature* 406:641–645 (2000).
- Bailey SM, Meyne J, Chen DJ, Kurimasa A, Li GC, Lehnert BE, Goodwin EH: DNA double-strand break repair proteins are required to cap the ends of mammalian chromosomes. *Proc natl Acad Sci, USA* 96:14899–14904 (1999).
- Bailey SM, Cornforth MN, Kurimasa A, Chen DJ, Goodwin EH: Strand-specific postreplicative processing of mammalian telomeres. *Science* 293:2462–2465 (2001).
- Bailey SM, Brenneman MA, Halbrook J, Nickoloff JA, Ullrich RL, Goodwin EH: The kinase activity of DNA-PK is required to protect mammalian telomeres. *DNA Repair (Amst)*, in press (2004).
- Bianchi A, deLange T: Ku binds telomeric DNA in vitro. *J Biol Chem* 274:21223–21227 (1999).
- Biessmann H, Mason JM: Genetics and molecular-biology of telomeres. *Adv Genet* 30:185–249 (1992).
- Blackburn EH: Structure and function of telomeres. *Nature* 350:569–573 (1991).
- Blackburn EH, Bradley J, Greider C, Lee M, Romero D, Shippenlentz D, Yu GL: Synthesis of telomeres by the ribonucleoprotein telomerase. *FASEB J* 5:A1784–A1784 (1991).
- Blunt T, Gell D, Fox M, Taccioli GE, Lehmann AR, Jackson SP, Jeggo PA: Identification of a nonsense mutation in the carboxyl-terminal region of DNA-dependent protein kinase catalytic subunit in the scid mouse. *Proc natl Acad Sci, USA* 93:10285–10290 (1996).
- Bryan TM, Reddel RR: Telomere dynamics and telomerase activity in in vitro immortalised human cells. *Eur J Cancer* 33:767–773 (1997).
- Cadwell C, Zambetti GP: The effects of wild-type p53 tumor suppressor activity and mutant p53 gain-of-function on cell growth. *Gene* 277:15–30 (2001).
- Campisi J, Kim SH, Lim CS, Rubio M: Cellular senescence, cancer and aging: the telomere connection. *Exp Gerontol* 36:1619–1637 (2001).
- Carney JP, Maser RS, Olivares H, Davis EM, LeBeau M, Yates JR, Hays L, Morgan WF, Petrini JHJ: The hMre11/hRad50 protein complex and Nijmegen breakage syndrome: Linkage of double-strand break repair to the cellular DNA damage response. *Cell* 93:477–486 (1998).
- Cimino-Reale G, Pascale E, Alvino E, Starace G, D'Ambrosio E: Long telomeric C-rich 5'-tails in human replicating cells. *J Biol Chem* 278:2136–2140 (2003).
- DePinho RA, Wong KK: The age of cancer: telomeres, checkpoints, and longevity. *J Clin Invest* 111:S9–14 (2003).
- Difilippantonio MJ, Zhu J, Chen HT, Meffre E, Nussenzweig MC, Max EE, Ried T, Nussenzweig A, Max E: DNA repair protein Ku80 suppresses chromosomal aberrations and malignant transformation; Ku80 is essential for maintaining genomic stability. *Nature* 404:510–514 (2000).
- Donoho G, Brenneman MA, Cui TX, Donoviel D, Vogel H, Goodwin EH, Chen DJ, Hasty P: Deletion of *Bra2* exon 27 causes hypersensitivity to DNA crosslinks, chromosomal instability, and reduced life span in mice. *Genes Chrom Cancer* 36:317–331 (2003).
- Epstein CJ, Motulsky AG: Werner syndrome: entering the helicase era. *Bioessays* 18:1025–1027 (1996).
- Espejel S, Franco S, Rodriguez-Perales S, Bouffler SD, Cigudosa JC, Blasco MA: Mammalian Ku86 mediates chromosomal fusions and apoptosis caused by critically short telomeres. *EMBO J* 21:2207–2219 (2002a).
- Espejel S, Franco S, Sgura A, Gae D, Bailey SM, Taccioli GE, Blasco MA: Functional interaction between DNA-PKcs and telomerase in telomere length maintenance. *EMBO J* 21:6275–6287 (2002b).
- di Fagagna FD, Hande MP, Tong WM, Lansdorp PM, Wang ZQ, Jackson SP: Functions of poly(ADP-ribose) polymerase in controlling telomere length and chromosomal stability. *Nature Genet* 23:76–80 (1999).
- Feldser DM, Hackett JA, Greider CW: Telomere dysfunction and the initiation of genome instability. *Nature Rev Cancer* 3:623–627 (2003).
- Ferguson DO, Sekiguchi JM, Chang S, Frank KM, Gao Y, DePinho RA, Alt FW: The nonhomologous end-joining pathway of DNA repair is required for genomic stability and the suppression of translocations. *Proc natl Acad Sci, USA* 97:6630–6633 (2000).
- Franklin R, Gosling R: Molecular configuration in sodium thymonucleate. *Nature* 171:740–741 (1953).
- Gage BM, Alroy D, Shin CY, Ponomareva ON, Dhar S, Sharma GG, Pandita TK, Thayer MJ, Turker MS: Spontaneously immortalized cell lines obtained from adult *Atm* null mice retain sensitivity to ionizing radiation and exhibit a mutational pattern suggestive of oxidative stress. *Oncogene* 20:4291–4297 (2001).
- Gell D, Jackson SP: Mapping of protein-protein interactions within the DNA-dependent protein kinase complex. *Nucl Acids Res* 27:3494–3502 (1999).
- Gilley D, Tanaka H, Hande MP, Kurimasa A, Li GC, Oshimura M, Chen DJ: DNA-PKcs is critical for telomere capping. *Proc natl Acad Sci, USA* 98:15084–15088 (2001).
- Goedecke W, Eijpe M, Offenbergh HH, vanAalderen M, Heyting C: Mre11 and Ku70 interact in somatic cells; but are differentially expressed in early meiosis. *Nature Genetics* 23:194–198 (1999).
- Gollahon LS, Kraus E, Wu TA, Yim SO, Strong LC, Shay JW, Tainsky MA: Telomerase activity during spontaneous immortalization of Li-Fraumeni syndrome skin fibroblasts. *Oncogene* 17:709–717 (1998).
- Gottlieb TM, Jackson SP: The DNA-dependent protein-kinase: requirement for DNA ends and association with Ku antigen. *Cell* 72:131–142 (1993).
- Goytisolo FA, Samper E, Edmonson S, Taccioli GE, Blasco MA: The absence of the DNA-dependent protein kinase catalytic subunit in mice results in anaphase bridges and in increased telomeric fusions with normal telomere length and G-strand overhang. *Mol Cell Biol* 21:3642–3651 (2001).
- Gray MD, Shen JC, Kamath-Loeb AS, Blank A, Sopher BL, Martin GM, Oshima J, Loeb LA: The Werner syndrome protein is a DNA helicase. *Nature Genet* 17:100–103 (1997).
- Griffith JD, Comeau L, Rosenfield S, Stansel RM, Bianchi A, Moss H, deLange T: Mammalian telomeres end in a large duplex loop. *Cell* 97:503–514 (1999).
- Gu YS, Jin SF, Gao YJ, Weaver DT, Alt FW: Ku70-deficient embryonic stem-cells have increased ionizing radiosensitivity; defective-DNA end-binding activity; and inability to support V(D)J recombination. *Proc natl Acad Sci, USA* 94:8076–8081 (1997).
- Harley CB, Vaziri H, Counter CM, Allsopp RC: The telomere hypothesis of cellular aging. *Exp Gerontol* 27:375–382 (1992).
- Hasty P, Campisi J, Hoeijmakers J, van Steeg H, Vijg J: Aging and genome maintenance: lessons from the mouse? *Science* 299:1355–1359 (2003).
- Hsu HL, Gilley D, Blackburn EH, Chen DJ: Ku is associated with the telomere in mammals. *Proc natl Acad Sci, USA* 96:12454–12458 (1999).
- Huang SR, Li BM, Gray MD, Oshima J, Mian SI, Campisi J: The premature ageing syndrome protein; WRN; is a 3'-5' exonuclease. *Nature Genet* 20:114–116 (1998).
- Jaco I, Munoz P, Goytisolo F, Wesoly J, Bailey S, Taccioli G, Blasco MA: Role of mammalian Rad54 in telomere length maintenance. *Mol Cell Biol* 23:5572–5580 (2003).
- Kashishian A, Douangpanya H, Clark D, Schlachter ST, Eary CT, Schiro JG, Huang H, Burgess LE, Kesicki EA, Halbrook J: DNA-dependant protein kinase inhibitors as drug candidates for the treatment of cancer. *Mol Cancer Ther* 2:1257–1264 (2003).
- Kraakman-vanderZwet M, Overkamp WJ, Friedl AA, Klein B, Verhaegh G, Jaspers NG, Midro AT, Eckardt-Schupp F, Lohman PHM, Zdzienicka MZ: Immortalization and characterization of Nijmegen Breakage syndrome fibroblasts. *Mutat Res* 434:17–27 (1999).
- Kurimasa A, Kumano S, Boubnov NV, Story MD, Tung CS, Peterson SR, Chen DJ: Requirement for the kinase activity of human DNA-dependent protein kinase catalytic subunit in DNA strand break rejoining. *Mol Cell Biol* 19:3877–3884 (1999a).
- Kurimasa A, Ouyang H, Dong LJ, Wang S, Li XL, Cordón-Cardo C, Chen DJ, Li GC: Catalytic subunit of DNA-dependent protein kinase: Impact on lymphocyte development and tumorigenesis. *Proc natl Acad Sci, USA* 96:1403–1408 (1999b).
- de Lange T: Protection of mammalian telomeres. *Oncogene* 21:532–540 (2002).
- Leesmiller SP, Godbout R, Chan DW, Weinfeld M, Day RS, Barron GM, Allalunisturner J: Absence of P350 subunit of DNA-activated protein-kinase from a radiosensitive human cell-line. *Science* 267:1183–1185 (1995).
- Ma Y, Pannicke U, Schwarz K, Lieber MR: Hairpin opening and overhang processing by an Artemis/DNA-dependent protein kinase complex in nonhomologous end joining and V(D)J recombination. *Cell* 108:781–794 (2002).
- Makarov VL, Hirose Y, Langmore JP: Long G tails at both ends of human chromosomes suggest a C strand degradation mechanism for telomere shortening. *Cell* 88:657–666 (1997).
- McClintock B: The stability of broken ends of chromosomes in *Zea mays*. *Genetics* 26:234–282 (1941).
- McClintock B: The fusion of broken ends of chromosomes following nuclear fusion. *Proc natl Acad Sci, USA* 28:458–463 (1942).
- Meek K, Kienker L, Dallas C, Wang W, Dark MJ, Venta PJ, Huie ML, Hirschhorn R, Bell T: SCID in Jack Russell terriers: a new animal model of DNA-PKcs deficiency. *J Immunol* 167:2142–2150 (2001).
- Meyne J, Ratliff RL, Moyzis RK: Conservation of the human telomere sequence (TTAGGG)<sub>N</sub> among vertebrates. *Proc natl Acad Sci, USA* 86:7049–7053 (1989).
- Moshous D, Callebaut I, de Chasseval R, Corneo B, Cavazzana-Calvo M, Le Deist F, Tezcan I, Sanal O, Bertrand Y, Philippe N, Fischer A, de Villartay JP: Artemis, a novel DNA double-strand break repair/V(D)J recombination protein, is mutated in human severe combined immune deficiency. *Cell* 105:177–186 (2001).
- Muller H: The remaking of chromosomes. *The Collecting Net Woods Hole* 13:181–198 (1938).

- Murnane JP, Sabatier L, Marder BA, Morgan WF: Telomere dynamics in an immortal human cell-line. *EMBO J* 13:4953–4962 (1994).
- Okano S, Lan L, Caldecott KW, Mori T, Yasui A: Spatial and temporal cellular responses to single-strand breaks in human cells. *Mol Cell Biol* 23:3974–3981 (2003).
- Okayasu R, Suetomi K, Yu Y, Silver A, Bedford JS, Cox R, Ullrich RL: A deficiency in DNA repair and DNA-PKcs expression in the radiosensitive BALB/c mouse. *Cancer Res* 60:4342–4345 (2000).
- Pandita TK, Pathak S, Geard CR: Chromosome end associations; telomeres and telomerase activity in ataxia-telangiectasia cells. *Cytogenet Cell Genet* 71:86–93 (1995).
- Pluth JM, Fried LM, Kirchgessner CU: Severe combined immunodeficient cells expressing mutant hRAD54 exhibit a marked DNA double-strand break repair and error-prone chromosome repair defect. *Cancer Res* 61:2649–2655 (2001).
- Rogakou EP, Boon C, Redon C, Bonner WM: Megabase chromatin domains involved in DNA double-strand breaks in vivo. *J Cell Biol* 146:905–916 (1999).
- Rooney S, Sekiguchi J, Zhu C, Cheng HL, Manis J, Whitlow S, DeVido J, Foy D, Chaudhuri J, Lombard D, Alt FW: Leaky Scid phenotype associated with defective V(D)J coding end processing in Artemis-deficient mice. *Mol Cell* 10:1379–1390 (2002).
- Rooney S, Alt FW, Lombard D, Whitlow S, Eckersdorff M, Fleming J, Fugmann S, Ferguson DO, Schatz DG, Sekiguchi J: Defective DNA repair and increased genomic instability in Artemis-deficient murine cells. *J exp Med* 197:553–565 (2003).
- Rothkamm K, Lobrich M: Evidence for a lack of DNA double-strand break repair in human cells exposed to very low x-ray doses. *Proc natl Acad Sci, USA* 100:5057–5062 (2003).
- Samper E, Goytisolo FA, Slijepcevic P, van Vuul PPW, Blasco MA: Mammalian Ku86 protein prevents telomeric fusions independently of the length of TTAGGG repeats and the G-strand overhang. *EMBO Reports* 1:244–252 (2000).
- Samper E, Goytisolo FA, Menissier-de Murcia J, Gonzalez-Suarez E, Cigudosa JC, de Murcia G, Blasco MA: Normal telomere length and chromosomal end capping in poly(ADP-ribose) polymerase-deficient mice and primary cells despite increased chromosomal instability. *J Cell Biol* 154:49–60 (2001).
- Singleton BK, Torres-Arzayus MI, Rottinghaus ST, Taccioli GE, Jeggo PA: The C terminus of Ku80 activates the DNA-dependent protein kinase catalytic subunit. *Mol Cell Biol* 19:3267–3277 (1999).
- Slijepcevic P, Hande MP, Bouffler SD, Lansdorp P, Bryant PE: Telomere length, chromatin structure and chromosome fusing potential. *Chromosoma* 106:413–421 (1997).
- Smogorzewska A, Karlseder J, Holtgreve-Grez H, Jauch A, de Lange T: DNA ligase IV-dependent NHEJ of deprotected mammalian telomeres in G1 and G2. *Curr Biol* 12:1635 (2002).
- van Steensel B, Smogorzewska A, de Lange T: TRF2 protects human telomeres from end-to-end fusions. *Cell* 92:401–413 (1998).
- Szumiel I: Monitoring and signaling of radiation-induced damage in mammalian cells. *Radiat Res* 150:S92–101 (1998).
- Thompson LH, Schild D: Homologous recombination repair of DNA ensures mammalian chromosome stability. *Mutat Res* 477:131–153 (2001).
- Tong WM, Hande MP, Lansdorp PM, Wang ZQ: DNA strand break-sensing molecule poly(ADP-Ribose) polymerase cooperates with p53 in telomere function, chromosome stability, and tumor suppression. *Mol Cell Biol* 21:4046–4054 (2001).
- Walker JR, Corpina RA, Goldberg J: Structure of the Ku heterodimer bound to DNA and its implications for double-strand break repair. *Nature* 412:607–614 (2001).
- Wang H, Perrault AR, Takeda Y, Qin W, Iliakis G: Biochemical evidence for Ku-independent backup pathways of NHEJ. *Nucl Acids Res* 31:5377–5388 (2003).
- Watson JD: Origin of concatameric T4 DNA. *Nature* 239:197–201 (1972).
- Watson JD, Crick FH: Molecular structure of nucleic acids; a structure for deoxyribose nucleic acid. *Nature* 171:737–738 (1953).
- Wellinger RJ, Sen D: The DNA structures at the ends of eukaryotic chromosomes. *Eur J Cancer* 33:735–749 (1997).
- Wright WE, Tesmer VM, Huffman KE, Levene SD, Shay JW: Normal human chromosomes have long G-rich telomeric overhangs at one end. *Genes Development* 11:2801–2809 (1997).
- Yu Y, Okayasu R, Weil MM, Silver A, McCarthy M, Zabriskie R, Long S, Cox R, Ullrich RL: Elevated breast cancer risk in irradiated BALB/c mice associates with unique functional polymorphism of the *Prkdc* (DNA-dependent protein kinase catalytic subunit) gene. *Cancer Res* 61:1820–1824 (2001).
- von Zglinicki T, Saretzki G, Docke W, Lotze C: Mild hyperoxia shortens telomeres and inhibits proliferation of fibroblasts: a model for senescence? *Exp Cell Res* 220:186–193 (1995).

# DNA repair factors and telomere-chromosome integrity in mammalian cells

M.P. Hande

Department of Physiology, Faculty of Medicine, National University of Singapore, and Oncology Research Institute, National University Medical Institutes, Singapore (Singapore)

**Abstract.** Loss of telomere equilibrium and associated chromosome-genomic instability might effectively promote tumour progression. Telomere function may have contrasting roles: inducing replicative senescence and promoting tumourigenesis and these roles may vary between cell types depending on the expression of the enzyme telomerase, the level of mutations induced, and efficiency/deficiency of related DNA repair pathways. We have identified an alternative telomere maintenance mechanism in mouse embryonic stem cells lacking telomerase RNA unit (mTER) with amplification of non-telomeric sequences adjacent to existing short stretches of telomere repeats. Our quest for identifying telomerase-independent or alternative mechanisms involved in telomere maintenance in mammalian cells has implicated the involvement of potential DNA repair factors in such pathways. We have reported earlier on the telomere equilibrium in *scid* mouse cells which suggested a potential role of DNA repair proteins in telomere maintenance in mammalian cells. Subsequently, studies by us and others have shown the association between the DNA repair factors and telomere function. Mice deficient in a DNA-break sensing

molecule, PARP-1 (poly [ADP]-ribopolymerase), have increased levels of chromosomal instability associated with extensive telomere shortening. Ku80 null cells showed a telomere shortening associated with extensive chromosome end fusions, whereas Ku80<sup>+/-</sup> cells exhibited an intermediate level of telomere shortening. Inactivation of PARP-1 in p53<sup>-/-</sup> cells resulted in dysfunctional telomeres and severe chromosome instability leading to advanced onset and increased tumour incidence in mice. Interestingly, haploinsufficiency of PARP-1 in Ku80 null cells causes more severe telomere shortening and chromosome abnormalities compared to either PARP-1 or Ku80 single null cells and Ku80<sup>+/-</sup>-PARP-1<sup>-/-</sup> mice develop spontaneous tumours. This overview will focus mainly on the role of DNA repair/recombination and DNA damage signalling molecules such as PARP-1, DNA-PKcs, Ku70/80, XRCC4 and ATM which we have been studying for the last few years. Because the maintenance of telomere function is crucial for genomic stability, our results will provide new insights into the mechanisms of chromosome instability and tumour formation.

Copyright © 2003 S. Karger AG, Basel

## Telomeres and telomerase

Telomeres are specialised structures that cap the ends of eukaryotic chromosomes. They consist of (TTAGGG)<sub>n</sub> repeats that are associated with an array of proteins (Blackburn, 1991).

Current research in my laboratory (Genome Stability Laboratory) is supported by grants from Academic Research Fund, National University of Singapore and Oncology Research Institute, Office of Life Sciences, National University Medical Institutes, Singapore.

Received 7 September 2003; manuscript accepted 18 November 2003.

Request reprints from M. Prakash Hande, PhD, Genome Stability Laboratory  
Department of Physiology, Faculty of Medicine  
National University of Singapore, Block MD9, #01-03  
2 Medical Drive, Singapore 117597 (Singapore)  
telephone: +65-6874-3664; fax: +65-6778-8161  
e-mail: phsmph@nus.edu.sg  
(url: [http://www.med.nus.edu.sg/phys/FacultyMembers\\_Hande.htm](http://www.med.nus.edu.sg/phys/FacultyMembers_Hande.htm))

Telomeres have important functions such as: 1) protection of chromosomes from exonuclease attack, illegitimate recombination and degradation; 2) capping the chromosomes with TTAGGG repeats after spontaneous or induced breaks to prevent DNA repair pathways to be triggered; 3) positioning the chromosomes in the nucleus; 4) proper alignment of chromosomes for recombination during meiosis (Blackburn, 1991; Zakian, 1995; Greider, 1996). Vertebrate telomeres end in repeated sequences of (TTAGGG)<sub>n</sub> that are supposed to be folded by telomere-binding proteins into a duplex T loop structure (Moyzis et al., 1988; Griffith et al., 1999). Telomere repeats are synthesized by the reverse transcriptase enzyme telomerase (Greider and Blackburn, 1985; Lingner et al., 1997). Telomerase is required for the stable maintenance of telomere repeats in vivo and in vitro (Blasco et al., 1997). Telomeres are believed to be important in maintaining the chromosome-genomic stability (Greider, 1991).

## Telomeres and ageing

In most somatic cells, telomeric DNA is lost every time a cell divides (Allsopp et al., 1992; Harley et al., 1990). As a result of this progressive shortening of telomeres, somatic cells cease to proliferate and become senescent after finite divisions (~60 population doublings) (Granger et al., 2002). The telomere shortening occurs rapidly in certain cell lines derived from premature aging disorders, i.e. Werner and Ataxia telangiectasia, leading to premature senescence as compared to age-matched control cell lines (Kruk et al., 1995; Metcalfe et al., 1996; Schulz et al., 1996). One characteristic feature of Werner syndrome cells is the "variegated translocation mosaicism" which could be due to shortened telomeres. Thus, telomere shortening is directly related to ageing and senescence in in vitro model systems.

## Telomeres and cancer

The loss of telomere function with age and the resulting genomic instability coupled with onset of telomerase activity are of critical importance in tumorigenesis and in tumour progression (de Lange and DePinho, 1999). Telomere shortening in somatic cells and the subsequent replicative senescence may prevent uncontrolled cell proliferation and thereby malignant transformation. The tumour suppressor function of telomeres has also been suggested (de Lange and DePinho, 1999; Artandi and DePinho, 2000). However, extensive proliferation and the subsequent telomere shortening/lengthening may also result in telomere dysfunction. Chromosome fusions and breaks resulting from telomere dysfunction may facilitate the loss of heterozygosity (LOH) of tumour suppressor genes. Preferential loss of telomere repeats from the ends of a particular chromosome harbouring tumour suppressor genes or oncogenes may result either in their inactivation or activation due to chromosome translocation events and may also facilitate tumour progression. Collectively, telomere dysfunction or loss of telomere equilibrium (see later) and associated chromosome/genetic instability might effectively promote tumour progression. Thus telomere function may have contrasting roles: inducing replicative senescence and promoting tumorigenesis and these roles may vary between cell types depending on the expression of the enzyme telomerase, the level of mutations induced, and efficiency/deficiency of related DNA repair pathways.

## Telomeres and DNA repair factors

The question of whether or not telomere shortening triggers double-stranded DNA break response is still largely unanswered. Telomerase knockout mice showed progressive shortening of telomeres up to the 6<sup>th</sup> generation after which they became infertile (Blasco et al., 1997; Lee et al., 1998). However, embryonic fibroblasts obtained from mTER<sup>-/-</sup> (mouse telomerase RNA; telomerase negative) mice could be immortalized in vitro and displayed telomere maintenance with associated chromosomal defects at later passages in culture (Hande et al.,

1999a). This study has implicated the existence of telomerase-independent mechanisms in the telomere maintenance. Similarly, we have identified an alternative telomere maintenance mechanism in mouse embryonic stem cells lacking telomerase RNA unit (mTER) with amplification of non-telomeric sequences adjacent to existing short stretches of telomere repeats (Niida et al., 2000). Recombination of sub-telomeric sequences has been implicated in the telomere maintenance mechanisms in the telomerase-negative mouse embryonic stem cells (Niida et al., 2000). Our quest for identifying telomerase-independent or alternative mechanisms involved in telomere maintenance has implicated the involvement of potential DNA repair factors in such pathways. Several studies have shown the association between the DNA repair factors and telomere function. Extensive studies in yeast have linked the role of DNA repair/recombination and damage signalling molecules in telomere maintenance mechanisms. However, only recently, such roles for these proteins in mammalian cells have been uncovered. This overview will focus mainly on the role of DNA repair/recombination and DNA damage signalling molecules such as DNA-PKcs, ATM, Ku complex, XRCC4 and PARP in telomere-chromosome integrity in mammalian cells for which we have sufficient knowledge and data.

### *scid (severe combined immuno deficiency) and telomeres*

In one of our earlier studies, probably one of the first in mammalian models, we have shown that mouse *scid* cells possess abnormally longer telomeres compared to their parental cells (Slijepcevic et al., 1997). *scid* cell lines had approximately ten times longer telomeres than their CB17 parental cells. Besides having abnormally long telomeres, the *scid* cell line showed unusual telomeric associations. Several chromosomes in the *scid* cell line were associated with their p-arms to form the so-called multi-branched chromosome configuration. The frequency of such multi-branched chromosomes in the *scid* cell line was about 10% (Slijepcevic et al., 1997). A puzzling observation that longer telomeres and telomere fusions occur in the same cell line has prompted the speculation that probably the telomere-telomerase complex may not be efficient in preventing end-to-end fusions in this particular cell line (Slijepcevic et al., 1997).

To further investigate whether such a difference in telomere length would exist in in vivo conditions, we analysed the telomere length in primary cells for different strains of *scid* mice. In all the strains of *scid* mice with their parental strains we have studied, 1.5 to 2 times longer telomeres could be detected (Hande et al., 1999b). As against the *scid* cell lines, primary bone marrow cells from *scid* mice did not exhibit telomere fusions or chromosome aberrations (Hande, unpublished observation). Therefore, it is possible that evolution of chromosome fusions might have been an in vitro process. It should also be noted that the difference in telomere length is wider in the cell lines (ten times) compared to the primary cells (1.5 to 2 times). Bailey et al. (1999) reported a similar occurrence of telomere fusions in a *scid* cell line though telomere length was not measured in that study. *scid* mice are deficient in the enzyme DNA-PK (DNA-dependent protein kinase) as a result of the mutation in the gene encoding the catalytic subunit (DNA-PKcs) of this enzyme. Our results on *scid* cell lines and primary

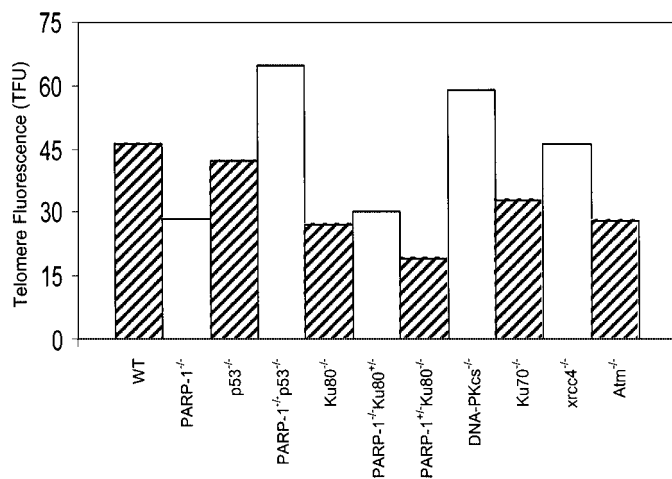


**Fig. 1.** Loss of telomere equilibrium in primary cells from DNA repair-deficient mice.

cells from *scid* mice pointed to the possibility that DNA-PKs either alone or in complex with other proteins in the non-homologous end joining (NHEJ) pathway (see later) may, directly or indirectly, be involved in telomere length regulation in mammalian cells.

#### *Non-Homologous End Joining (NHEJ) complex and telomeres*

Eukaryotic cells use two different pathways for repairing DNA double-strand breaks: homologous recombination (HR) and non-homologous end-joining (NHEJ). A key component of the homologous recombination process is Rad51 (Baumann et al., 1996), a 50-kDa protein whose expression is cell-cycle dependent, peaking at the S/G<sub>2</sub> boundary (Yamamoto et al., 1996). The NHEJ pathway requires the activity of DNA-PK, a multimeric serine-threonine kinase composed of a catalytic subunit (DNA-PKcs) and two regulatory subunits (Ku70 and Ku80). Ku70 and Ku80 are able to recognise and bind DNA DSB and then activate DNA-PKcs (Critchlow and Jackson, 1998). Another protein that plays a key role in NHEJ is XRCC4 (Critchlow et al., 1997) which interacts with, and probably controls the function of ligase IV.

DNA repair by NHEJ relies on the Ku70:Ku80 heterodimer in species ranging from yeast to man. In *Saccharomyces cerevisiae* and *Schizosaccharomyces pombe* Ku also controls telomere functions. Based on our observation in *scid* mouse cells and on the studies in yeast, an analogous role for mammalian Ku complex in telomere maintenance cannot be ruled out. Ku70, Ku80, and DNA-PKcs, with which Ku interacts, are associated in vivo with telomeric DNA in several human cell types and we have shown earlier that these associations are not significantly affected by DNA-damaging agents (d'Adda di Fagagna et al., 2001). It was also demonstrated that inactivation of Ku80 or Ku70 in the mouse yields telomeric shortening in various primary cell types at different developmental stages (Fig. 1) (d'Adda di Fagagna et al., 2001). By contrast, telomere length is not altered in cells impaired in XRCC4 or DNA ligase

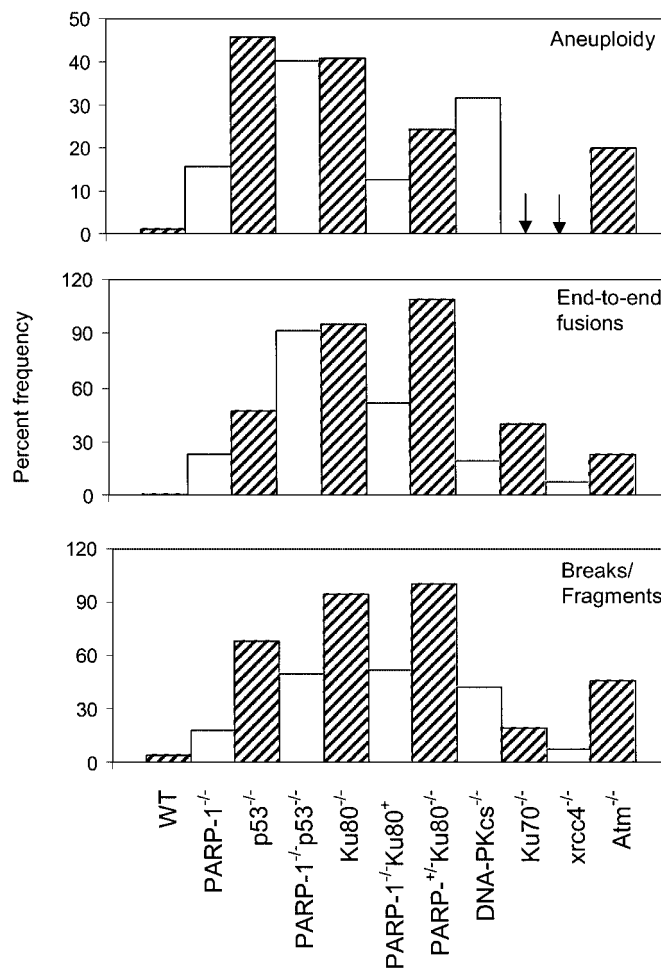


**Fig. 2.** Spontaneous chromosome instability in primary embryonic fibroblasts from DNA repair-deficient mice. Arrows indicate the samples where aneuploidy could not be detected. Mouse embryonic stem cells tend to be intrinsically aneuploid with an average of 41 or 42 chromosomes per metaphase.

IV, two other NHEJ components (Fig. 1). We also observe higher genomic instability in Ku-deficient cells than in XRCC4-null cells (Fig. 2). This study has suggested that chromosomal instability of Ku-deficient cells results from a combination of compromised telomere stability and defective NHEJ (d'Adda di Fagagna et al., 2001).

The telomere repeat binding protein, TRF1 and Ku formed a complex at the telomere (Hsu et al., 2000). The Ku and TRF1 complex was found to have a specific high-affinity interaction, as demonstrated by several in vitro methods, and exists in human cells as determined by co-immunoprecipitation experiments. Ku does not bind telomeric DNA directly but localises to telomeric repeats via its interaction with TRF1. Primary mouse embryonic fibroblasts that are deficient for Ku80 accumulated a large percentage of telomere fusions (Fig. 2), establishing that Ku plays a critical role in telomere capping in mammalian cells (d'Adda di Fagagna et al., 2001; Hsu et al., 2000). It was proposed that Ku localizes to internal regions of the telomere via a high-affinity interaction with TRF1.

The DNA-dependent protein kinase catalytic subunit (DNA-PKcs) is critical for DNA repair via the nonhomologous end joining pathway. As explained above, bone marrow cells and spontaneously transformed fibroblasts from *scid* mice have defects in telomere maintenance (Slijepcevic et al., 1997; Hande et al., 1999b). The genetically defective *scid* mouse arose spontaneously from its parental strain CB17. One known genomic alteration in *scid* mice is a truncation of the extreme carboxyl terminus of DNA-PKcs, but other as yet unidentified alterations may also exist. In another study, we used a defined system, the DNA-PKcs knockout mouse, to investigate specifically the role DNA-PKcs specifically plays in telomere maintenance. Primary mouse embryonic fibroblasts (MEFs) and primary cultured kidney cells from 6–8-month-old DNA-PKcs-deficient mice accumulated a large number of telomere fusions, yet still retain wild-type telomere length (Figs. 1 and 2) (Gilley et al., 2001). Thus, the phenotype of this defect separates the two-telomere-related phenotypes, capping, and length maintenance. DNA-PKcs-deficient MEFs also exhibited elevated levels of chromosome fragments and breaks, which correlate with increased telomere fusions. Based on the high levels of telomere fusions observed in DNA-PKcs-deficient cells, it was concluded that DNA-PKcs plays an important capping role at the mammalian telomere (Gilley et al., 2001).

#### *PARP-1 and telomeres*

In most eukaryotes, poly(ADP-ribose) polymerase (PARP) recognises DNA strand interruptions generated in vivo. DNA binding by PARP triggers primarily its own modification by the sequential addition of ADP-ribose units to form polymers; this modification, in turn, causes the release of PARP from DNA ends (Lindahl, 1995). Studies on the effects of the disruption of the gene encoding PARP-1 (*Adprt1*) in mice have demonstrated roles for PARP in recovery from DNA damage and in suppressing recombination processes involving DNA ends (Lindahl et al., 1995; Morrison et al., 1997; de Murcia et al., 1997; Wang et al., 1997; Jeggo, 1998).

Telomeres are the natural termini of chromosomes and are, therefore, potential targets of PARP. Telomere shortening was seen in different genetic backgrounds and in different tissues, both from embryos and adult mice (Fig. 1) (d'Adda di Fagagna et al., 1999) without any change in the in vitro telomerase activity. Furthermore, cytogenetic analysis of mouse embryonic fibroblasts has revealed that lack of PARP-1 is associated with severe chromosomal instability, characterized by increased frequencies of chromosome fusions and aneuploidy (Fig. 2). The absence of PARP-1 did not affect the presence of single-strand overhangs, naturally present at the ends of telomeres. The above study has therefore revealed an unanticipated role for PARP-1 in telomere length regulation; though a later study using PARP-1 knockout mice with a different genetic background (Samper et al., 2001) did not reveal any significant change in telomere length. However, it cannot be ruled out that different genetic background mice and different mutations of the same gene might yield different results.

#### *Ataxia Telangiectasia Mutated (ATM) and telomeres*

Ataxia-telangiectasia (AT) is an autosomally recessive human genetic disease with pleiotropic defects such as neurological degeneration, immunodeficiency, chromosomal instability, cancer susceptibility and premature aging. Cells derived from AT patients and ataxia-telangiectasia mutated (ATM)-deficient mice show slow growth in culture and premature senescence. ATM, which belongs to the PI3 kinase family along with DNA-PK, plays a major role in signalling the p53 response to DNA strand breaks. Telomere maintenance is perturbed in yeast strains lacking genes homologous to ATM and cells from patients with AT have short telomeres (Metcalf et al., 1996). We examined the length of individual telomeres in cells from *Atm*<sup>-/-</sup> mice by FISH. Telomeres were extensively shortened in multiple tissues of *Atm*<sup>-/-</sup> mice (Hande et al., 2001). More than the expected number of telomere signals was observed in interphase nuclei of *Atm*<sup>-/-</sup> mouse fibroblasts. Signals corresponding to 5–25 kb of telomeric DNA that were not associated with chromosomes were also noticed in *Atm*<sup>-/-</sup> metaphase spreads. Extrachromosomal telomeric DNA was also detected in fibroblasts from AT patients and may represent fragmented telomeres or by-products of defective replication of telomeric DNA. These results suggested a role of ATM in telomere maintenance and replication, which may contribute to the poor growth of *Atm*<sup>-/-</sup> cells and increased tumour incidence in both AT patients and *Atm*<sup>-/-</sup> mice (Hande et al., 2001). Further studies are needed to identify the molecular mechanisms by which ATM interacts with telomerase complex in mammalian cells.

#### *Role of PARP-1 and p53 on telomeres*

Genomic instability is often caused by mutations in genes that are involved in DNA repair and/or cell cycle checkpoints, and it plays an important role in tumourigenesis. To confirm our previous observation of telomere shortening in PARP-1 mice, we took advantage of PARP-1 and p53 double knockout mice to study the telomere-related chromosome instability and tumourigenesis in these mice. PARP was thought to protect genomic stability (Jeggo, 1998) and its functional interaction with p53 was tested using PARP-1<sup>-/-</sup>p53<sup>-/-</sup> mice. Compared to single-mutant cells, PARP-1 and p53 double-mutant cells exhibit many severe chromosome aberrations, including a high degree of aneuploidy, fragmentations, and end-to-end fusions, which may be attributable to telomere dysfunction (Tong et al., 2001). While PARP<sup>-/-</sup> cells showed telomere shortening and p53<sup>-/-</sup> cells showed normal telomere length, inactivation of PARP-1 in p53<sup>-/-</sup> cells surprisingly resulted in very long and heterogeneous telomeres, suggesting a functional interplay between PARP-1 and p53 at the telomeres (Fig. 1). Strikingly, PARP-1 deficiency widens the tumour spectrum in mice deficient in p53, resulting in a high frequency of carcinomas in the mammary gland, lung, prostate, and skin, as well as brain tumours. The enhanced tumourigenesis is likely to be caused by PARP-1 deficiency, which facilitates the loss of function of tumour suppressor genes as demonstrated by a high rate of loss of heterozygosity at the p53 locus in these tumours (Tong et al., 2001). These results indicated that PARP-1 and p53 interact to maintain genome integrity and identify PARP as a cofactor for suppressing tumourigenesis.



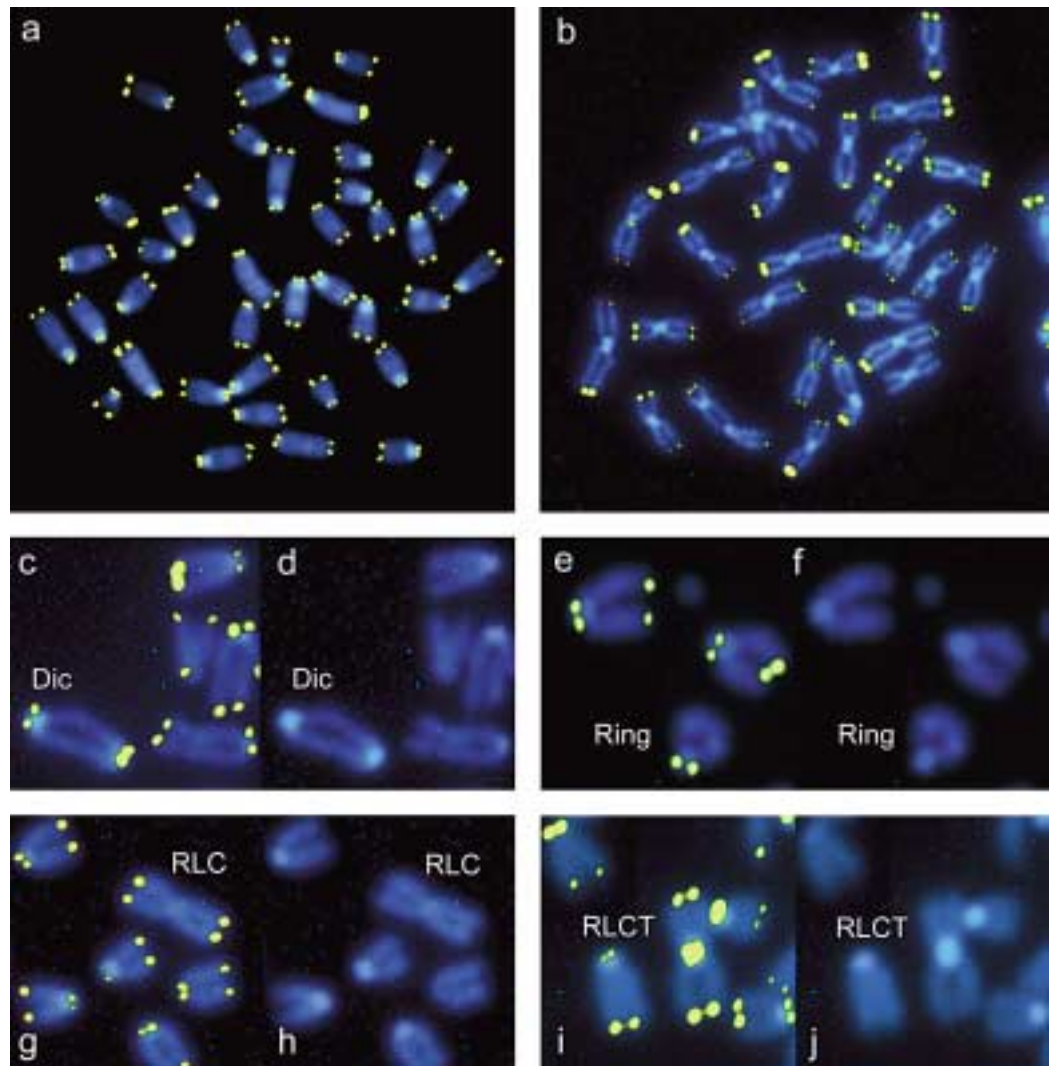


**Fig. 3.** Telomere-mediated chromosome integrity in mouse cells lacking telomerase or DNA repair factors. **(a)** Image of normal mouse chromosomes showing telomere signals on all acro(telo)centric chromosomes after FISH with Cy3-labelled (CCCTAAA)<sub>3</sub> PNA probe. **(b)** Metaphase spread from mouse embryonic stem cells lacking telomerase RNA at post-crisis stage (e.g. population doubling 600). Note that the acrocentric chromosomes fused to each other to generate metacentric Robertsonian like configurations (RLC). These RLCs are generated either by complete loss of telomeres on the p-arm of the chromosomes (telomere erosion) or fusion of a different chromosome with telomeres at fusion point (capping function). Telomeres could also be detected at the fusion point of q-arm fusions leading to the production of long dicentric chromosomes. These cells have acquired recombination-based telomere maintenance mechanisms in the absence of telomerase and chromosome instability is accumulated at population doubling (663 ES cells pro-

vided by Dr. Yoichi Shinkai, Kyoto University, Japan). **(c-j)** Representative images of chromosome fusion events in mouse cells lacking DNA repair factors. **(c)** A dicentric (Dic) chromosome showing telomere signals at the termini with no telomeres at the fusion point of q-arms. **(d)** Image shown in (c) under DAPI. **(e)** A ring like structure possibly due to the telomere loss on q-arm of a chromosome and fusion between the sister chromatids. **(f)** Same image as in (e) under DAPI filter. **(g)** A typical Robertsonian fusion like configuration event due to the loss of telomeres at the p-arm of a mouse chromosome and fusion between the centromeres. No telomeres could be detected at the fusion point. **(h)** DAPI image of the chromosomes shown in (g). **(i)** An example of a Robertsonian fusion-like configuration with telomeres at the fusion point (RLCT) which could have been generated by the loss of telomere equilibrium and the subsequent loss of capping function in these cells. **(j)** DAPI image of the chromosomes shown in (i).

#### *Interplay between PARP and Ku80 on telomere-chromosome integrity*

PARP-1 and Ku80 null cells showed telomere shortening associated with chromosome instability. Interestingly, haplo-insufficiency of PARP-1 in Ku80 null cells caused more severe telomere shortening and accumulation of chromosome abnormalities compared to either PARP-1 or Ku80 single null cells. Cytogenetic analysis of these cells revealed that many chromo-

some ends lack detectable telomeres as well. These results demonstrate that DNA break-sensing molecules, PARP-1 and Ku80, synergistically function at telomeres and play an important role in the maintenance of chromosome integrity. More importantly, haplo-insufficiency of Ku80 in PARP-1<sup>-/-</sup> mice promoted the development of hepatocellular adenoma and hepatocellular carcinoma (HCC) (Tong et al., 2002). These tumours exhibited a multistage tumour progression associated

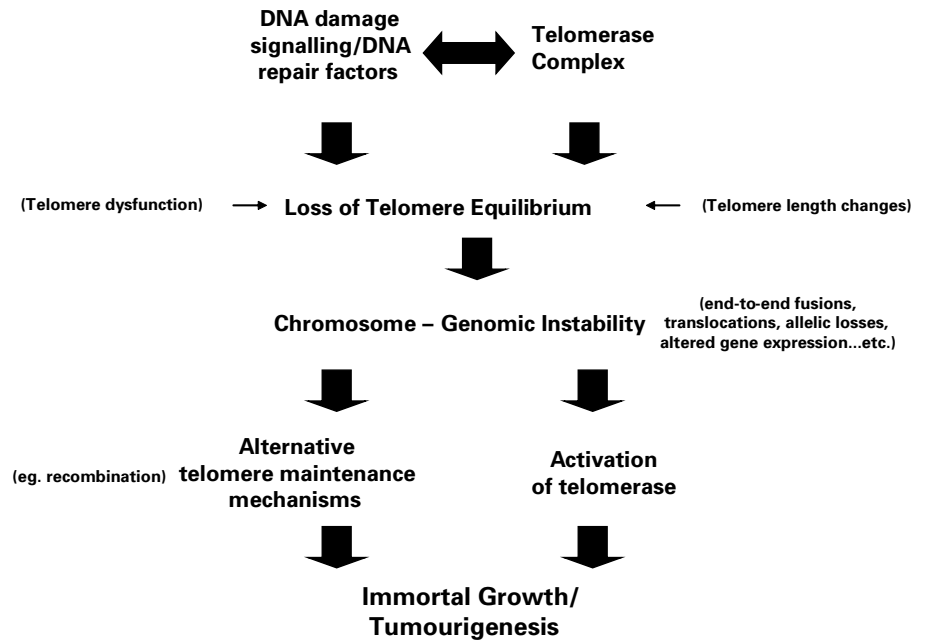


**Fig. 4.** Role(s) of DNA damage-signalling molecules and DNA repair factors in telomere-mediated chromosome-genomic instability and tumourigenesis.

with the loss of E-cadherin expression and the mutation of beta-catenin. Cytogenetic analysis revealed that Ku80 heterozygosity elevated chromosomal instability in PARP-1<sup>-/-</sup> cells and that these liver tumours harboured a high degree of chromosomal aberrations including fragmentations, end-to-end fusions, and recurrent nonreciprocal translocations. These features are reminiscent of human HCC. Taken together, these data implicate a synergistic function of Ku80 and PARP-1 in minimizing chromosome aberrations and cancer development.

### Final thoughts

It is evident from the telomere-chromosome data from DNA repair deficient mouse cells that the DNA damage/repair and signalling molecules play a vital role in the protection of telomeres and chromosomes and thereby maintain the genome integrity. As indicated in Fig. 1, there seems to be a modest loss of telomeres in the cells lacking some of the DNA repair factors. This loss is approximately 30–40% of the original telomeres. Data on telomerase-negative embryonic stem cells and embryonic fibroblasts lacking telomerase RNA indicated that a loss of approximately 60–70% of telomeric repeats was needed for the cells to become fusigenic and to induce the chromosome end-to-end fusion events in these cells (Fig. 3). The telomeres are maintained by telomerase-independent mechanisms in mTER<sup>-/-</sup> mouse cells at later passages. Based on the above observations, it is tempting to speculate that at least in mice, a fraction of telomeres are also maintained by the factors involved in DNA repair/damage response and DNA damage signalling molecules. However, both telomerase-dependent and telomerase-independent mechanisms co-exist to maintain telomeres in the mouse cells. It is plausible that telomere maintenance will be compromised by one pathway in the absence of

another pathway. More interestingly, loss of DNA repair factors will render the cells to lose telomeres and a majority of these cells exhibit premature senescence. On the other hand, telomerase negative mouse cells escape senescence and could be immortalised in vitro with accumulated chromosome instability. These two pathways interact with each other very efficiently and loss of either one of the pathways will lead to severe telomere-mediated chromosome instability leading to tumourigenesis in mice (Fig. 4). Double-knockout mice (e.g. PARP-1<sup>-/-</sup>p53<sup>-/-</sup> and PARP-1<sup>-/-</sup>Ku80<sup>+/-</sup> mice) develop spontaneous tumours and cells from these mice show telomere-related chromosome abnormalities. Loss of telomere equilibrium (either shorter or longer telomeres) might have contributed to the occurrence of severe chromosome instability in these mice which led to the spontaneous development of tumours.

### Acknowledgements

I would like to express my gratitude and thanks to Professor A.T. Natarajan and Dr. Jan Boei, Leiden, The Netherlands, who introduced me to the field of chromosome biology and Dr. Adayabalam S. Balajee for his thoughtful suggestions and criticisms. I acknowledge the support of my collaborators (P. Lansdorp, Vancouver, Canada; P. Slijepcevic, Uxbridge, UK; M.A. Blasco, Madrid, Spain; F.D. Fagagna, Milan, Italy; S.P. Jackson, Cambridge, UK; Z.Q. Wang and W.M. Tong, Lyon, France; Y. Shinkai, Kyoto, Japan; D. Gilley, D.J. Chen, Berkeley, USA; A. Wynshaw-Boris, San Diego, USA) during the course of the studies.

## References

- d'Adda di Fagagna F, Hande MP, Tong WM, Lansdorp PM, Wang ZQ, Jackson SP: Functions of poly(ADP-ribose) polymerase in controlling telomere length and chromosomal stability. *Nature Genet* 23:76–80 (1999).
- d'Adda di Fagagna F, Hande MP, Tong WM, Roth D, Lansdorp PM, Wang ZQ, Jackson SP: Effects of DNA nonhomologous end-joining factors on telomere length and chromosomal stability in mammalian cells. *Curr Biol* 11:1192–1196 (2001).
- Allsopp RC, Vaziri H, Patterson C, Goldstein S, Younglai EV, Futcher AB, Greider CW, Harley CB: Telomere length predicts replicative capacity of human fibroblasts. *Proc natl Acad Sci, USA* 89:10114–10118 (1992).
- Artandi SE, DePinho RA: A critical role for telomeres in suppressing and facilitating carcinogenesis. *Curr Opin Genet Dev* 10:39–46 (2000).
- Bailey SM, Meyne J, Chen DJ, Kurimasa A, Li GC, Lehnert BE, Goodwin EH: DNA double-strand break repair proteins are required to cap the ends of mammalian chromosomes. *Proc natl Acad Sci, USA* 96:14899–4904 (1999).
- Baumann P, Benson FE, West SC: Human Rad51 protein promotes ATP-dependent homologous pairing and strand transfer reactions in vitro. *Cell* 87:757–766 (1996).
- Blackburn EH: Structure and function of telomeres. *Nature* 350:569–573 (1991).
- Blasco MA, Lee HW, Hande MP, Samper E, Lansdorp PM, DePinho RA, Greider CW: Telomere shortening and tumor formation by mouse cells lacking telomerase RNA. *Cell* 91:25–34 (1997).
- Critchlow SE, Jackson SP: DNA end-joining: from yeast to man. *Trends Biochem Sci* 23:394–398 (1998).
- Critchlow SE, Bowater RP, Jackson SP: Mammalian DNA double-strand break repair protein XRCC4 interacts with DNA ligase IV. *Curr Biol* 7:588–598 (1997).
- Gilley D, Tanaka H, Hande MP, Kurimasa A, Li GC, Oshimura M, Chen DJ: DNA-PKcs is critical for telomere capping. *Proc natl Acad Sci, USA* 98:15084–15088 (2001).
- Granger MP, Wright WE, Shay JW: Telomerase in cancer and aging. *Crit Rev Oncol Hematol* 41:29–40 (2002).
- Greider CW: Telomeres. *Curr Opin Cell Biol* 3:444–351 (1991).
- Greider CW: Telomere length regulation. *Annu Rev Biochem* 65:337–365 (1996).
- Greider CW, Blackburn EH: Identification of a specific telomere terminal transferase activity in *Tetrahymena* extracts. *Cell* 43:405–413 (1985).
- Griffith JD, Comeau L, Rosenfield S, Stansel RM, Bianchi A, Moss H, de Lange T: Mammalian telomeres end in a large duplex loop. *Cell* 97:503–514 (1999).
- Hande MP, Samper E, Lansdorp P, Blasco MA: Telomere length dynamics and chromosomal instability in cells derived from telomerase null mice. *J Cell Biol* 144:589–601 (1999a).
- Hande P, Slijepcevic P, Silver A, Bouffler S, van Bui P, Bryant P, Lansdorp P: Elongated telomeres in *scid* mice. *Genomics* 56:221–223 (1999b).
- Hande MP, Balajee AS, Tchirkov A, Wynshaw-Boris A, Lansdorp PM: Extra-chromosomal telomeric DNA in cells from *Atm*<sup>(-/-)</sup> mice and patients with ataxia-telangiectasia. *Hum molec Genet* 10:519–528 (2001).
- Harley CB, Futcher AB, Greider CW: Telomeres shorten during ageing of human fibroblasts. *Nature* 345:458–460 (1990).
- Hsu HL, Gilley D, Galande SA, Hande MP, Allen B, Kim SH, Li GC, Campisi J, Kohwi-Shigematsu T, Chen DJ: Ku acts in a unique way at the mammalian telomere to prevent end joining. *Genes Dev* 14:2807–2812 (2000).
- Jeggo PA: DNA repair: PARP – another guardian angel? *Curr Biol* 8:R49–R51 (1998).
- Kruk PA, Rambino NJ, Bohr VA: DNA damage and repair in telomeres: relation to aging. *Proc natl Acad Sci, USA* 92:258–262 (1995).
- de Lange T, DePinho RA: Unlimited mileage from telomerase? *Science* 283:947–949 (1999).
- Lee HW, Blasco MA, Gottlieb GJ, Horner JW 2<sup>nd</sup>, Greider CW, DePinho RA: Essential role of mouse telomerase in highly proliferative organs. *Nature* 392:569–574 (1998).
- Lindahl T: Recognition and processing of damaged DNA. *J Cell Sci Suppl* 19:73–77 (1995).
- Lindahl T, Satoh MS, Dianov G: Enzymes acting at strand interruptions in DNA. *Phil Trans R Soc London B Biol Sci* 347:57–62 (1995).
- Lingner J, Hughes TR, Shevchenko A, Mann M, Lundblad V, Cech TR: Reverse transcriptase motifs in the catalytic subunit of telomerase. *Science* 276:561–567 (1997).
- Metcalfe JA, Parkhill J, Campbell L, Stacey M, Biggs P, Byrd PJ, Taylor AM: Accelerated telomere shortening in ataxia telangiectasia. *Nature Genet* 13:350–353 (1996).
- Morrison C, Smith GC, Stingl L, Jackson SP, Wagner EF, Wang ZQ: Genetic interaction between PARP and DNA-PK in V(D)J recombination and tumorigenesis. *Nature Genet* 17:479–482 (1997).
- Moyzis RK, Buckingham JM, Cram LS, Dani M, Deaven LL, Jones MD, Meyne J, Ratliff RL, Wu JR: A highly conserved repetitive DNA sequence, (TTAGGG)<sub>n</sub>, present at the telomeres of human chromosomes. *Proc natl Acad Sci, USA* 85:6622–6626 (1988).
- de Murcia JM, Niedergang C, Trucco C, Ricoul M, Dutrillaux B, Mark M, Oliver FJ, Masson M, Die-rich A, LeMour M, Walztinger C, Chambon P, de Murcia G: Requirement of poly(ADP-ribose) polymerase in recovery from DNA damage in mice and in cells. *Proc natl Acad Sci, USA* 94:7303–7307 (1997).
- Niida H, Shinkai Y, Hande MP, Matsumoto T, Takehara S, Tachibana M, Oshimura M, Lansdorp PM, Furuichi Y: Telomere maintenance in telomerase-deficient mouse embryonic stem cells: characterization of an amplified telomeric DNA. *Mol Cell Biol* 20:4115–4127 (2000).
- Samper E, Goytiso FA, Menissier-de Murcia J, Gonzalez-Suarez E, Cigudosa JC, de Murcia G, Blasco MA: Normal telomere length and chromosomal end capping in poly(ADP-ribose) polymerase-deficient mice and primary cells despite increased chromosomal instability. *J Cell Biol* 154:49–60 (2001).
- Schulz VP, Zakian VA, Ogburn CE, McKay J, Jarzebo-wicz AA, Edland SD, Martin GM: Accelerated loss of telomeric repeats may not explain accelerated replicative decline of Werner syndrome cells. *Hum Genet* 97:750–754 (1996).
- Slijepcevic P, Hande MP, Bouffler SD, Lansdorp P, Bryant PE: Telomere length, chromatin structure and chromosome fusing potential. *Chromosoma* 106:413–421 (1997).
- Tong WM, Hande MP, Lansdorp PM, Wang ZQ: DNA strand break-sensing molecule poly(ADP-Ribose) polymerase cooperates with p53 in telomere function, chromosome stability, and tumor suppression. *Mol Cell Biol* 21:4046–4054 (2001).
- Tong WM, Cortes U, Hande MP, Ohgaki H, Cavalli LR, Lansdorp PM, Haddad BR, Wang ZQ: Synergistic role of Ku80 and poly(ADP-ribose) polymerase in suppressing chromosomal aberrations and liver cancer formation. *Cancer Res* 62:6990–6996 (2002).
- Wang ZQ, Stingl L, Morrison C, Jantsch M, Los M, Schulze-Osthoff K, Wagner EF: PARP is important for genomic stability but dispensable in apoptosis. *Genes Dev* 11:2347–2358 (1997).
- Yamamoto A, Taki T, Yagi H, Habu T, Yoshida K, Yoshimura Y, Yamamoto K, Matsushiro A, Nishimune Y, Morita T: Cell cycle-dependent expression of the mouse Rad51 gene in proliferating cells. *Mol Gen Genet* 251:1–12 (1996).
- Zakian VA: Telomeres: beginning to understand the end. *Science* 270:1601–1607 (1995).

# Interstitial telomeric repeats are not preferentially involved in radiation-induced chromosome aberrations in human cells

C. Desmaze,<sup>a</sup> L.M. Pirzio,<sup>a</sup> R. Blaise,<sup>a</sup> C. Mondello,<sup>b</sup> E. Giulotto,<sup>c</sup>  
J.P. Murnane<sup>d</sup> and L. Sabatier<sup>a</sup>

<sup>a</sup>CEA-DSV/DRR/LRO, Fontenay aux roses (France);

<sup>b</sup>Istituto di Genetica Molecolare, CNR, Pavia (Italy);

<sup>c</sup>Dipartimento di Genetica e Microbiologia "A. Buzzati Traverso", University of Pavia, Pavia (Italy);

<sup>d</sup>Radiation Oncology Research Laboratory, UCSF, San Francisco CA (USA)

**Abstract.** Telomeric repeat sequences, located at the end of eukaryotic chromosomes, have been detected at intrachromosomal locations in many species. Large blocks of telomeric sequences are located near the centromeres in hamster cells, and have been reported to break spontaneously or after exposure to ionizing radiation, leading to chromosome aberrations. In human cells, interstitial telomeric sequences (ITS) can be composed of short tracts of telomeric repeats (less than twenty), or of longer stretches of exact and degenerated hexanucleotides, mainly localized at subtelomeres. In this paper, we analyzed the radiation sensitivity of a naturally occurring short ITS localized in 2q31 and we found that this region is not a hot spot of radiation-induced chromosome breaks. We then selected a human

cell line in which approximately 800 bp of telomeric DNA had been introduced by transfection into an internal euchromatic chromosomal region in chromosome 4q. In parallel, a cell line containing the plasmid without telomeric sequences was also analyzed. Both regions containing the transfected plasmids showed a higher frequency of radiation-induced breaks than expected, indicating that the instability of the regions containing the transfected sequences is not due to the presence of telomeric sequences. Taken together, our data show that ITS themselves do not enhance the formation of radiation-induced chromosome rearrangements in these human cell lines.

Copyright © 2003 S. Karger AG, Basel

The ends of eukaryotic chromosomes are characterized by specific nucleoprotein structures called telomeres. These complexes contain repeats of a G-rich oligonucleotide motif that is TTAGGG in all vertebrates. Several proteins have been described that bind specifically to these regions (Bilaud et al., 1997; van Steensel and de Lange, 1997). All together, these components adopt a specific chromatin structure that makes chromosome termini distinguishable from double-strand

breaks (DSB) by DNA repair systems. Telomeres therefore play a major role in the maintenance of chromosome integrity, preventing chromosome fusion and degradation of chromosome ends.

In addition to their location at the ends of the chromosomes, telomeric repeats have also been detected at interstitial locations in many species (Meyne et al., 1990; Wells et al., 1990). For some organisms, there is evidence that interstitial telomeric sequences (ITS) result from chromosome end fusions that occurred during evolution (Ijdo et al., 1991; Lee et al., 1993; Vermeesch et al., 1996). It has been proposed that these ITS may undergo rearrangements such as amplification, deletion or transposition, leading to large ITS within pericentromeric regions in some species (Meyne et al., 1990), to the absence of ITS in one of several branches derived from the same ancestor (Wiley et al., 1992) or, to their transposition into euchromatic locations (Metcalf et al., 1997, 1998). This high degree of rear-

Supported by EDF and the European Union contract FIGH-CT-1999-00009 (TELO-RAD). The work in the J.P.M. laboratory was supported by National Cancer Institute Grant No. RO1 CA69044 from the National Institutes of Health.

Received 16 September 2003; manuscript accepted 20 November 2003.

Request reprints from Laure Sabatier, PhD, CEA-DSV/DRR/LRO  
18 Route du Panorama, 92265 Fontenay aux roses cedex (France)  
telephone: +33 (1) 46 54 83 51; fax: +33 (1) 46 54 87 58  
e-mail: [sabatier@dsvidf.cea.fr](mailto:sabatier@dsvidf.cea.fr)

range of ITS during evolution suggests that they could be unstable. In the human genome, one example of ITS derived from telomeric fusion is the ITS in 2q13 (Ijdo et al., 1991). The majority of human ITS are composed of either short tracts (up to 20 hexamers) of mostly exact telomeric repeats, or stretches of exact and degenerated repeats located at subtelomeric regions (Wells et al., 1990; Ijdo et al., 1991; Weber et al., 1991; Azzalin et al., 1997; Musio and Mariani, 1999; Mondello et al., 2000; Azzalin et al., 2001).

Exposing cells to different kinds of stress, such as chemical mutagens or ionizing radiation, results in DNA damage, including DNA double-strand breaks (DSB). The efficient repair of DSBs is a crucial step for cell survival. Occasional misrepair of DSBs leads to mutations or chromosome rearrangements. Telomeric repeats have been detected at breakpoints of radiation-induced chromosome aberrations in hamster cell lines (Slijepcevic et al., 1998). This could be due either to breakage within ITS or to the addition of telomeric repeats at the site of the break. Indeed, telomerase, a reverse transcriptase specialized for addition or elongation of telomeric repeat sequences, has been detected in these cell lines. Telomerase can act at the ends of chromosomes, with or without the presence of telomeric DNA (Flint et al., 1994; Slijepcevic et al., 1996) and it has also been observed at DSB sites (Gravel et al., 1998; Peterson et al., 2001), as were proteins involved in DSB repair. Thus, telomerase may be involved in stabilization of DSB, which may result in the formation of new telomeres (Farr et al., 1991; Sprung et al., 1999b; Prescott and Blackburn, 2000). In yeast, "healing" of DSB by telomerase in DSB repair-deficient cells occurs in about 1% of the cells (Kramer and Haber, 1993), whereas cryptic translocation or telomere capture occur in about 10% of the cells. Strikingly, deletions are more frequent than exchanges in radiation-induced chromosome rearrangements of telomerase-positive cells (Meltzer et al., 1993). These data suggest an additional role for telomerase in DNA repair and potentially for the origin of ITS.

Numerous studies have reported a high sensitivity of ITS for misrepair after DNA damage, based on the high frequency of chromosome rearrangements at ITS loci (Bertoni et al., 1994; Balajee et al., 1996; Slijepcevic et al., 1996; Day et al., 1998; Mondello et al., 2000; Peitl et al., 2002). Most studies focused on ITS have been performed with Chinese hamster ovary (CHO) cells and described a higher than expected ratio of structural aberrations at these loci (Alvarez et al., 1993; Bertoni et al., 1994; Fernandez et al., 1995; Slijepcevic et al., 1996; Day et al., 1998). In mouse, a correlation was established between the presence of an ITS at a radiation-sensitive site in chromosome 2 and the frequency of breakage in AML cells (Bouffler et al., 1993, 1996; Silver and Cox, 1993; Finnon et al., 2002). These data support the hypothesis that ITS can influence the radiation sensitivity of chromosomes. However, in hamster cells, ITS are often located within the pericentromeric heterochromatin. Compiling literature data, Johnson et al. (1999) have confirmed the radiation sensitivity of heterochromatin in human cells. Thus, whether the ITS or the heterochromatin is responsible for the radiation sensitivity at this location is not clear.

In this paper, we analyzed radiation sensitivity of a naturally occurring short ITS localized in the human 2q31 region (Azzalin et al., 2001), and of 800 bp of telomeric repeats introduced by transfection into human chromosome 4q. Previously, we scored the number of spontaneous chromosome rearrangements involving this artificial ITS, within euchromatin of 4q (Desmaze et al., 1999). The frequency of chromosome breaks in these artificially introduced ITS indicated that human ITS are not prone to spontaneous breakages. To study the involvement of artificially introduced ITS in radiation-induced chromosome rearrangements, the cells mentioned above were irradiated and the number of chromosome aberrations involving ITS was scored. Although more breaks were found at this ITS locus than expected based on a random distribution, the number of rearranged chromosomes containing the ITS was not significantly higher than that observed at integration sites in cells containing only plasmid sequences without telomeric repeats. Moreover, chromosome breakpoints without any plasmid or telomeric repeats are involved to the same extent in radiation-induced chromosome aberrations as ITS loci. Based on these data, we hypothesize that broken regions favour the integration of plasmid sequences and are prone to subsequent breakage regardless of the types of sequences present at these locations.

## Materials and methods

### *Cellular, plasmid and PAC clones*

SCC61 and SQ9G, cell lines established from human squamous cell carcinomas, have been transfected with the pSXneo/gpt-(T2AG3) 0.8-kb and the pSXneo-(T2AG3) 1.6-kb plasmids. Cell cultures were maintained in DMEM/F12 medium (Life Technologies, Bethesda, USA) supplemented with 10% FCS. G418 (200 µg/ml) was added to the transfected clones, SNG28, SNG19 and Q18. A lymphoblastoid cell line, S.A.R.A., established from a normal individual, was grown in suspension in DMEM (Hyclone) supplemented with 10% FBS (Hyclone). All cell lines were incubated at 37 °C in a humidified incubator with 5% CO<sub>2</sub>.

Plasmids used in this study have been described elsewhere (Desmaze et al., 1999; Sprung et al., 1999a). The PAC clone spanning the 2q31 ITS-containing region was isolated by PCR from the RPCI-5 human PAC library (YAC Screening Center, Ospedale San Raffaele, Milano Italy) using unique primers flanking the ITS. The sequence of the primers was 5'-TTCCACC-TACCACATCTTATGC and 5'-ATTTCCCTCTATTCTTGCCCTG. Similarly, a PAC containing a random genomic region from chromosome 2p16 was isolated using the primers: 5'-ATGTTACTGTGGGTGGTCCC and 5'-TTATTTGCATCTGTGCTGGTG. This region is part of the *Homo sapiens* chromosome 2 genomic contig (Accession number gi29791392), which does not contain any ITS.

### *Conditions of irradiation*

Radiation experiments on the tumor cell lines were performed at subconfluence with 2 and 5 Gy (<sup>137</sup>Cs source, 0.71 Gy/min). Flasks were then divided in two and cells of the first post-irradiation generation were harvested using standard protocols. The lymphoblastoid cell line was irradiated with <sup>60</sup>Co γ-ray source at a dose rate of 1.1 Gy/min (2 and 4 Gy). Aliquots of 2 × 10<sup>6</sup> exponentially growing cells were resuspended in 1 ml of complete medium, placed in 7-ml tubes (Bijou, Sterilin) and irradiated. After irradiation, each aliquot was put in a 75-cm<sup>2</sup> flask with 10 ml of fresh medium and incubated for 24 h. During the last 2 or 3 h, colcemid (50 µg/ml) was added to the cultures, and then chromosomes were prepared according to standard procedures.

### *Fluorescence in situ hybridization*

FISH experiments were performed as described (Desmaze and Aurias, 1995). The presence of the plasmid sequences was detected using the pSXN

plasmid as a probe. The DNA was labeled with either biotin-11-dUTP (Sigma) or digoxigenin-11-dUTP (Roche) using a nick translation kit (Roche). Specific whole chromosome painting probes from Oncor or Biosys were used according to manufacturer's recommendations. To verify the presence of the telomeric sequences at the integrated sites of Q18 and SNG28 cell lines, we have hybridized a (C<sub>3</sub>TA<sub>2</sub>)<sub>3</sub> PNA sequence coupled with the Cyanin3 fluorochrome (Perceptive Biosystems).

Hybridized metaphases were captured with a CCD camera (Cohu or Zeiss) coupled to an epifluorescence Leica DMRBE or a Zeiss Axioplan microscope equipped with filters for observation of different fluorochromes. Images were processed with the Cytovision or ISIS softwares (Applied Imaging and Metasystems S.A., respectively).

#### *Analysis of chromosomal instability and chromosome rearrangements*

To assess the general chromosomal instability, the number of breaks was deduced from the number of structural aberrations (dicentric, rings and excess acentrics) observed in 50–150 Giemsa-stained metaphases for each clone, at each dose of irradiation and from two different experiments each. To record structural chromosome aberrations, deletions and translocations, metaphases were captured after hybridisation with specific chromosome painting probes coupled with red or green fluorochromes. The chromosomes were counterstained with DAPI (blue). Chromosome exchanges were illustrated by bicolour chromosomes (red-green, red-blue or green-blue). Each colour junction was recorded as a break. When the painted chromosomes were involved in complex chromosome exchanges the number of breaks was determined according to the FISH pattern. Between 100 and 300 chromosomes 4, 5, 6 or 7 were analyzed per cell line and dose. Intrachromosomal rearrangements that could not be detected by this method were not taken into account.

We considered that a break might have occurred in the transfected sequences when the FISH plasmid signal was at the terminus of a rearranged chromosome or at the breakpoint of an aberration. 50–150 chromosomes 4 in SNG28, chromosomes 7 in SNG19 or marker chromosomes in Q18 were analyzed per dose. The number of breaks is recorded regarding the ploidy level of each chromosome.

#### *Statistics*

$\chi^2$  Tests were performed to compare the radiation sensitivity of different chromosomes and to examine the hypothesis that the induced damage occurs more frequently in an ITS containing locus than expected for non-telomeric loci of the same size. Considering that ionizing radiations cause randomly distributed damages, the expected number of breaks within the integration site was estimated on the basis of the relative length of the studied loci. Integrated sequences are about 7 kb, but the smallest detected chromosome band by cytogenetics techniques is about 5 Mb, corresponding to the minimum size which could be resolved by FISH. The chromosomes 4 and 7 are 186 and 156 Mb long, respectively. Therefore, the size of the investigated locus containing the transfected plasmid is estimated to be 2.7 % of the entire chromosome 4 and 3.2 % of chromosome 5.

## **Results**

### *Chromosome 2 ITS (2q31) is not prone to chromosome breakage*

The radiosensitivity of the 2q31 region containing ITS and of a control region (2p16) lacking ITS was assessed in a lymphoblastoid cell line derived from a normal individual. The 2q31 ITS is polymorphic in the human population, differing by copy number of the telomeric hexanucleotide from 6 to 13 (Mondello et al., 2000). The cell line used in this study is heterozygous with the two alleles containing 6 and 9 repeats (data not shown).

The cells were irradiated with  $\gamma$ -rays (2 and 4 Gy) and metaphases were prepared after 24 h. To identify the regions of interest, two-colour FISH was performed with the PAC containing the 2q31 ITS and with the control PAC localized on

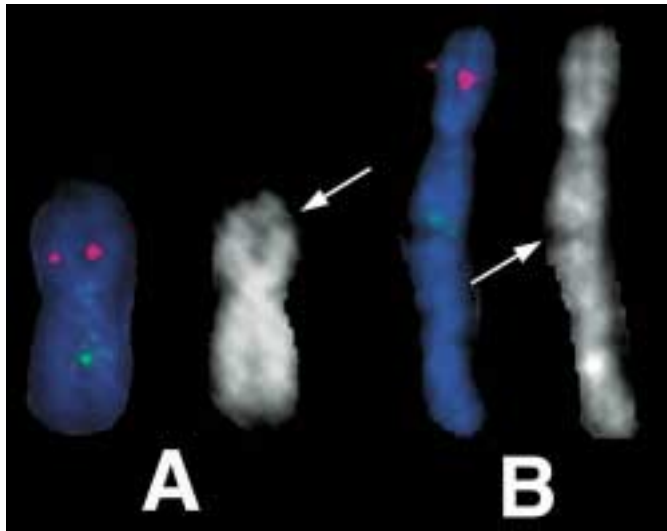
**Table 1.** Chromosome aberrations involving chromosome 2p and 2q in the lymphoblastoid cell line after  $\gamma$ -irradiation

$\gamma$ -ray dose (Gy)	Number of mitoses	Total number of aberrations	Number of aberrations involving		
			chr 2	chr 2q	chr 2p
0	49	2	0	0	0
2	49	35	2	1	1
4	47	80	9	5	4

2p16. The total number of aberrations (breaks and chromosome rearrangements) and the number of aberrations involving chromosome 2q or 2p were determined (Table 1); as shown by the  $\chi^2$  test, these last values are not significantly different from those expected on the basis of the relative length of chromosome 2 (8% of the genome) and on the basis of the ratio between the length of 2q and 2p ( $q/p = 1.6$ ). We identified six rearrangements involving 2q (one after 2 Gy and five after 4 Gy): two dicentric chromosomes, one triradial and three breaks. All the breaks were localized downstream of the hybridization signal and in no case was the signal split, as would be expected if a break had occurred in the ITS containing region (Fig. 1A). A similar number and similar types of rearrangements (Fig. 1B) were found to involve 2p (one after 2 Gy and four after 4 Gy). These results suggest that the ITS containing region is not more prone to breakage upon  $\gamma$ -irradiation than other chromosome regions.

### *Transfection of plasmids does not increase the radiation sensitivity of the studied clones*

To further assess the likelihood of ITS to be involved in structural aberrations after irradiation, we used cell lines transfected with plasmids containing at least 800 bp of telomeric sequences (Murnane et al., 1994). In clone SNG28, the plasmid is stably integrated in one homologue of chromosome 4, which is monosomic, as it is in the parental clone. In SNG19, the plasmid is integrated in chromosome 7. Identification of chromosomes was done by a 24-colour analysis (Xcycling kit, Metasystems) (Fig. 2). Southern blot analysis and rescue of the integrated plasmid sequences showed that plasmid and telomeric repeat sequences are present in a single copy in clone SNG28. In contrast, analysis of the SNG19 clone demonstrated that the integrated plasmid is missing the end containing the telomeric repeats. Thus, clone SNG19 provided a control for an integration site containing only the plasmid sequences. Gamma irradiation (2 and 5 Gy) was applied and the induced structural chromosome aberrations were recorded on Giemsa-stained metaphases. For both transfected clones, SNG28 and SNG19, and the non-transfected cell line SCC61, about fifty Giemsa-stained metaphases were analyzed per dose of irradiation in two independent experiments. The number of induced breaks increased with the dose and was not significantly different between the three clones (Fig. 3). Thus, as were previously described for spontaneous aberrations (Desmaze et al., 1999), the transfection did not enhance chromosome breakage in the clones SNG28 and SNG19 in the first post-irradiation cell division.



### Chromosome-specific radiation sensitivity

Although the general radiation sensitivity of the cells was not increased by transfection, we determined the influence of the artificial ITS on the sensitivity of the chromosome containing the integrated plasmid sequences. Because the number of randomly distributed breaks in a chromosome depends on its size, we compared the number of breaks in chromosome 4 of SNG28 containing the integrated plasmids with the chromosome 4 of the non-transfected parental cell line, SCC61. After FISH with chromosome-specific painting probes, at least 100

**Fig. 1.** Examples of chromosome aberrations involving 2p (**A**) or 2q (**B**) induced by  $\gamma$ -rays. The green hybridization signal is due to the probe for the 2q31 ITS-containing region, the red signal is due to the probe for the control 2p16 region. Chromosomes are counterstained with DAPI. (**A**) Chromatid break on 2p (arrow). (**B**) Dicentric chromosome containing chromosome 2 with a chromatid break downstream to the 2q31 region.

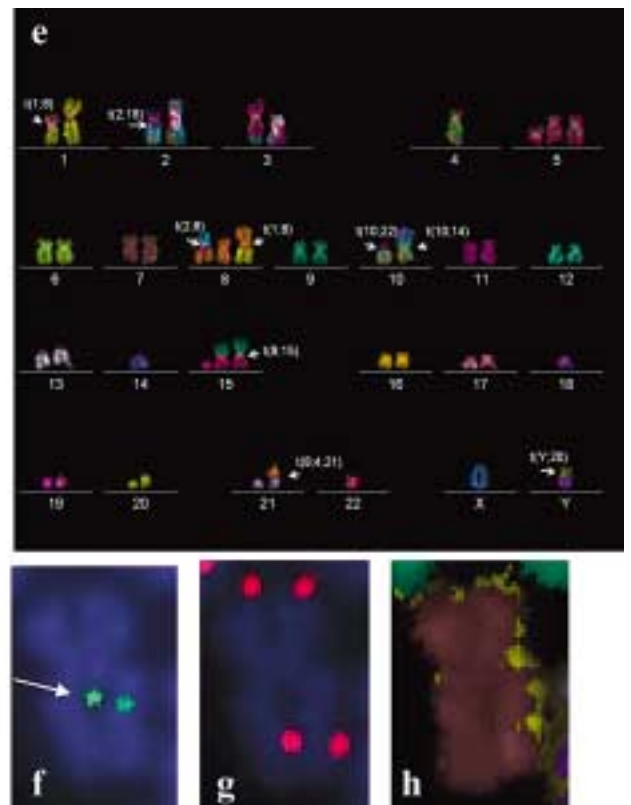
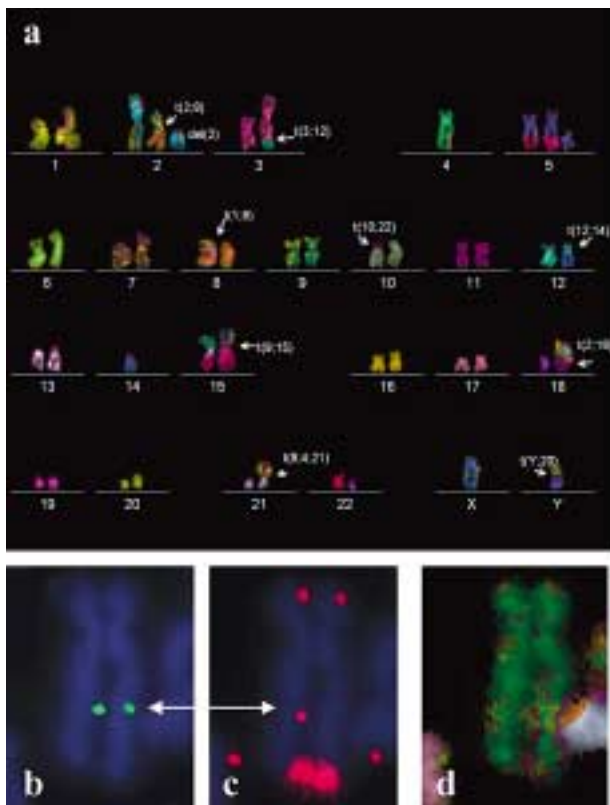


**Fig. 2.** FISH characterization of the SNG28 and SNG19 clones. (**a** and **e**) Multicolour karyotypes of the SNG28 and SNG19 clones. These two clones are pseudo diploid and rather normal. Most rearrangements are present in both clones, supporting a clonal origin. Besides, the parental SCC61 clone also presents these rearrangements (data not shown) and specifically the single chromosome 4. mFISH allows us to determine the chromosomes with the inserted transfected plasmids which are chromosome 4 for SNG28 and chromosome 7 for SNG19. (**b**, **c** and **d**) Chromosomes 4 from the metaphase **a**.

(**f**, **g** and **h**) Chromosomes 7 from metaphase **e**. (**b** and **f**) pSXN plasmid probe, detected in green, is indicated by arrows. (**c** and **g**) Telomeric sequences are hybridized with PNA telomeric probe, coupled with Cy3. All telomeres are fluorescent and interstitial specific red telomeric signal is only seen on the chromosome 4 of SNG28 metaphases at the location of the plasmid insertion region while no signal was ever detected on chromosome 7 of the SNG19 cells.

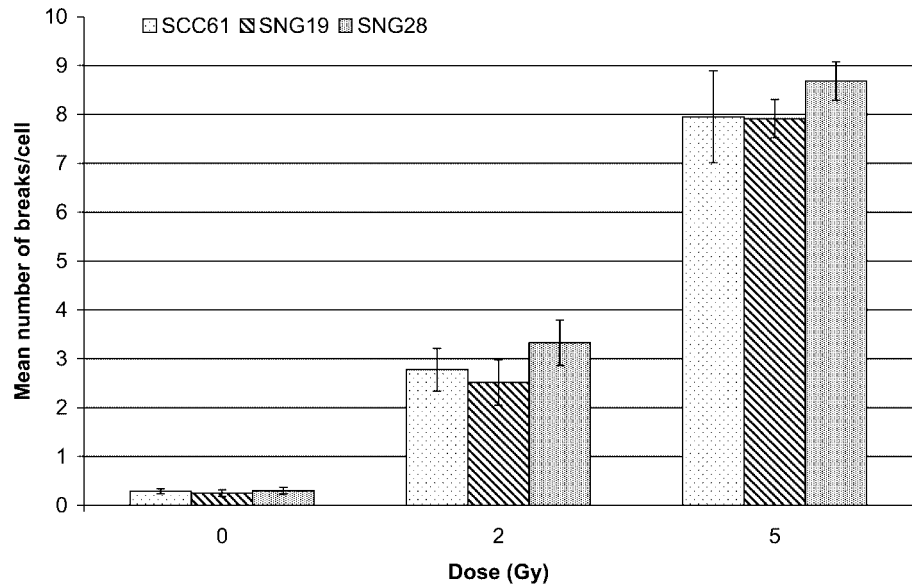


**Fig. 3.** Comparison of the mean number of radiation-induced breaks per cell scored after 2 and 5 Gy irradiation of the SCC61, SNG19 and SNG28 clones.

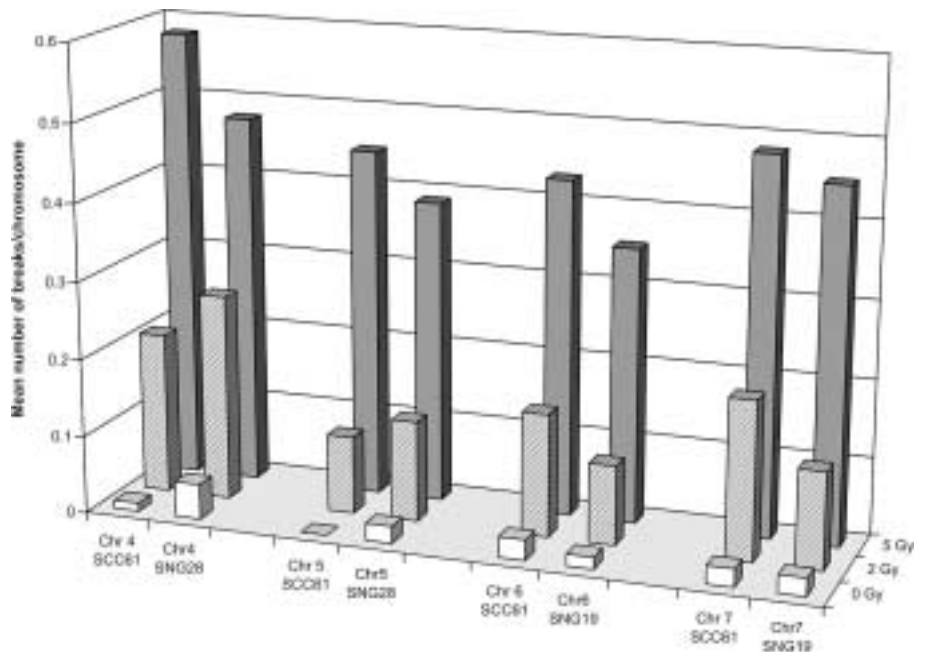


**Fig. 4.** Comparison of the mean number of breaks between chromosomes with or without the transfected plasmids, chromosomes 4 from SNG28 (telomeric and plasmid sequences) and SCC61 clones; chromosomes 5 from SNG28 and SCC61 clones as control; chromosomes 6 and 7 (plasmid sequences only) from SNG19 and from the non-transfected cell line, SCC61.

chromosomes 4 for SNG28 and 100–300 chromosomes 4 from the parental clone were assessed per dose and chromosome. Controls were made with the chromosomes 7 of SNG19 and SCC61 containing or not containing only the plasmid sequences, and also with chromosomes of approximately the same size and morphology without any transfected sequences, in the same genetic background. 200–350 chromosomes 5, 6 or 7 were analyzed per dose and per clone, and the number of breaks was compared according to the number of analyzed chromosomes and to the size of each chromosome. All the data are presented in Fig. 4. After ionizing radiations, no significant difference ( $P > 0.1$ ) was found between chromosomes 4 of SNG28 and SCC61 as well as for chromosomes 7 of SNG19

and SCC61, suggesting that transfected sequences, containing telomeric repeats or not, did not enhance the involvement of chromosomes in rearrangements.

*Increased frequency of rearrangements in chromosomal regions containing plasmid integration sites*

Breaks within the region containing the transfected sequences in chromosome 4 of SNG28 were scored to assess sensitivity of the ITS. The same analysis was performed on the chromosome 7 of the control clone SNG19 for the sensitivity of the plasmid sequences alone. The presence of the plasmid sequences was detected by FISH using the pSXN plasmid as a probe. 50–150 chromosomes were analyzed per dose and chro-



**Fig. 5.** Characterization by FISH and R bands of the chromosome containing the transfected plasmid in the Q18 cell line. Chromosomes are counterstained with DAPI. Green-yellow dots and red dots correspond to the plasmid and telomeric signals, respectively. Hybridizations with specific chromosome painting probes show an alternated green/red/green paint for the t(17;1;7) marker of the Q18 cell line.

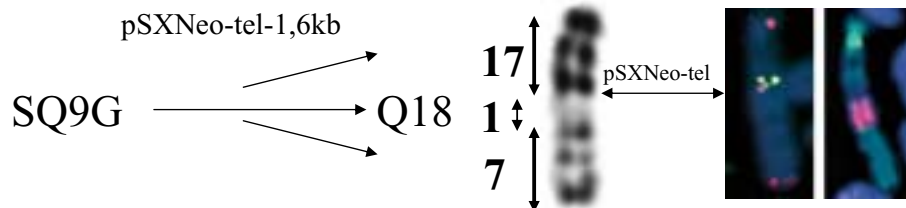


**Table 2.** Specific effect of irradiation on integrated sequences

Dose (Gy)	Number of breaks in the region of the integrated sequences							
	Chromosome 4 in SNG28				Chromosome 7 in SNG19			
	whole chr	expected	observed	ratio <sup>a</sup>	whole chr	expected	observed	ratio <sup>a</sup>
0	5	0.14	0		0	0.00	0	
2	22	0.59	6	10	11	0.35	3	8.5
5	66	1.78	22	12.3	34	1.09	12	11.0

<sup>a</sup> Observed/expected.

**Table 3.** Effect of irradiation on chromosomal breakpoints

Dose (Gy)	Number of breaks at the rearranged junctions of the Q18 cell line marker chromosome						Ratio <sup>b</sup>
	Whole chromosome	Expected	Junction with telomere		Junction without telomere		
			observed	ratio <sup>a</sup>	observed	ratio <sup>a</sup>	
0	3.0	0.12	0.0		3.0		
2	18.0	0.72	2.0	2.8	3.0	4.2	1.5
5	47.0	1.88	4.0	2.1	14.0	7.4	3.5

<sup>a</sup> Observed/expected.

<sup>b</sup> Junction without telomere/junction with telomere.

mosome, as to the position of the plasmid signals and by chromosome painting. As shown in Table 2, the number of breaks occurring in the region containing the integrated plasmid sequences on chromosome 4 in the clone SNG28 is 10- to 12.5-fold higher than expected ( $P < 0.0001$ ). Thus, the region containing the integration site appears to be prone to breakage in this clone. The results for the cell line SNG19 were similar with 8.5- to 11-fold more breaks in the integrated region than expected. Both analyses showed that the regions containing the transfected plasmids are more often rearranged after irradiation than expected, and that telomeric repeat sequences are not the reason for this phenomenon. These results led us to assume that either the plasmid sequences themselves enhance the radiation sensitivity, or that the plasmids are integrated into sites that are already prone to break.

#### *Junctions of chromosome aberrations are sensitive to ionizing radiations*

In order to investigate whether the increase in breakage at the integration sites in clones SNG28 and SNG19 is due to the plasmid sequences themselves or to cellular sequences surrounding the integration site, we used the cell line Q18, which contained the integrated pSXneo-(T<sub>2</sub>AG<sub>3</sub>)1.6-kb plasmid con-

taining telomeric repeat sequences at the junction 17/1 of a rearranged marker chromosome der(17;1;7). In addition to the plasmid integration site, this marker chromosome also contains another junction between a fragment of chromosome 1 and the long arm of the chromosome 7. Unlike the 17/1 junction, the junction between 1 and 7 does not contain any plasmid sequences (Fig. 5). We have scored the number of breaks at these two junctions, before and after irradiation at 2 and 5 Gy, in 183 and 238 marker chromosomes, respectively, as well as in approximately 100 marker chromosomes of non-irradiated cells. Considering the rearrangements of this chromosome, we have estimated the length of the marker chromosome to be around 125 Mb. The investigated region considered to be 5 Mb (see Materials and methods) is then approximately 4% of the chromosome. The number of breaks observed for both sites was higher than expected but only the junction without the transfected sequences was significantly more often involved in radiation-induced rearrangements ( $P < 0.01$ ) (Table 3). We conclude from these results that chromosomal breakpoints of previously rearranged chromosomes are more sensitive to breakage than expected at random, and that the transfected sequences do not further enhance this sensitivity, regardless of whether containing telomeric repeats or not.

## Discussion

Telomeric repeat sequences, present at internal chromosome locations and thought to be "hot spots" of recombination (Hastie and Allshire, 1989), have been shown to be sensitive to ionizing radiation in hamster cells (Alvarez et al., 1993; Slijepcevic et al., 1996; Kilburn et al., 2001). Because in hamster cells ITS are located in heterochromatin, Kilburn et al. (2001) have investigated the spontaneous instability of ITS, constructing a model of hamster cells containing telomeric repeats integrated into the APRT gene located in euchromatin. Their molecular analysis revealed an increase in small deletions and insertions involving the telomeric repeat sequences, demonstrating microrearrangements involving ITS located within euchromatin of hamster cells. In human cells, repeats copy number polymorphism has been reported for four human ITS (Mondello et al., 2000), but the radiation sensitivity of ITS has proven to be elusive.

In this work, using FISH with a probe spanning the short 2q31 ITS, we could not detect a preferential involvement of the region in chromosome aberrations induced by  $\gamma$  irradiation. This result suggests that the short telomeric tract does not confer to this region a hypersensitivity to  $\gamma$ -rays which can be highlighted by cytogenetic analysis. Moreover, we analyzed clones containing integrated plasmid sequences with and without telomeric repeats for their predisposition to form chromosome rearrangements near the integration site, after irradiation with 2 and 5 Gy. First, we found that the stable plasmid integrations did not enhance the total radiation induced number of breaks in one cell. Next, we compared the number of breaks observed for chromosomes containing or not containing plasmid with or without telomeric repeats and found that, even if chromosomes 4 and 7 are more often broken, no significant difference could be observed either in the transfected cell lines or in the parental one. These results indicate a preferential breakage of some chromosomes rather than an effect of transfected sequences, as already described for normal chromosome 4 (Wilt et al., 1994; Boei et al., 1997). More breaks than expected occurred within the regions containing integrated plasmid sequences regardless of whether they contained telomeric repeats or not. However, we could not exclude small rearrangements of a few base pairs in the cloned ITS, as shown for the instability observed in the work of Kilburn et al. (2001). This suggests an intrinsic radiation sensitivity of the plasmid sequences themselves or the possibility of a hypersensitivity to ionizing radiation of the cellular DNA surrounding the inserted plasmids. The increase of breakage we have observed at integration sites did not lead to a higher number of breaks of the entire chromosomes 4 and 7 containing transfected plasmid than those in the non-transfected clone. This indicates that the chromosome regions in the non-transfected cell line should reveal the same level of sensitivity as that observed in the presence of the plasmid sequences. It is likely that such hypersensitive regions would also be preferential sites for plasmid integration. The high fragility at some plasmid integration sites has been shown to result from sequences of surrounding DNA, which act alone or in conjunction with the integrated plasmid sequences forming hotspots for recombination, as might occur when heterochromatin and

euchromatin are brought together due to chromosome rearrangements. Moreover, other integration sites with similar plasmid sequences have shown that rearrangements might be solely confined to the cellular DNA (Murnane, 1990a, b). Consistent with this possibility, we found an increased rate of rearrangement at junctions regardless of whether they contain integrated plasmid sequences. In clone Q18, the regions of junctions of the rearranged marker chromosome revealed an increased fragility in response to ionizing radiation suggesting that a predisposition for breakage might be responsible for the high frequency of structural aberrations observed at some chromosome regions rather than the presence of telomeric repeats or plasmid sequences. Some authors have reported successive breakage-fusion events at ITS of CHO, mediating a positional switch of ITS towards the chromosome termini. As a result, it was assumed that junctions resulting from these rearrangements are prone to break (Bertoni et al., 1994). A higher proportion of breaks was described at the junction of a translocation compared with the remaining genome (Drets and Therman, 1983). Local DNA amplification has been reported for a human cancer cell line with recurrent breakage/fusion/bridge cycles within a specific chromosome region (Lo et al., 2002). Finally, the fragility within the region harbouring transfected ITS in clone SNG28 could also be due to the presence of repetitive sequences that have been found in the short arms of the acrocentric chromosomes (Piccini et al., 2001).

We have shown that ITS do not necessarily increase the sensitivity to ionizing radiation in human cells. Instead, the integration site itself might be prone to breakage, explaining also the integration of the plasmid DNA at such a locus (Lin and Waldman, 2001a, b). These data confirm that instability is not a general property of all DNA in a cell and that sensitivity to ionising radiation is not equally distributed along chromosomes. Possibly, this approach might be used to map radiosensitive chromosomal sites.

## Acknowledgements

Authors are grateful to J.M. Victor and C. Lavelle for the statistic analysis of all the data. We thank S. Coroller, N. Mossadegh, G. Pottier and L.M. Martins for helpful technical assistance. L.M.P. is a recipient of an EDF fellowship.

## References

- Alvarez L, Evans JW, Wilks R, Lucas JN, Brown JM, Giaccia AJ: Chromosomal radiosensitivity at intrachromosomal telomeric sites. *Genes Chrom Cancer* 8:8–14 (1993).
- Azzalin CM, Mucciolo E, Bertoni L, Giulotto E: Fluorescence in situ hybridization with a synthetic (T<sub>2</sub>AG<sub>3</sub>)<sub>n</sub> polynucleotide detects several intrachromosomal telomere-like repeats on human chromosomes. *Cytogenet Cell Genet* 78:112–115 (1997).
- Azzalin CM, Nergadze SG, Giulotto E: Human intrachromosomal telomeric-like repeats: sequence organization and mechanisms of origin. *Chromosoma* 110:75–82 (2001).
- Balajee AS, Dominguez I, Bohr VA, Natarajan AT: Immunofluorescent analysis of the organization of telomeric DNA sequences and their involvement in chromosomal aberrations in hamster cells. *Mutat Res* 372:163–172 (1996).
- Bertoni L, Attolini C, Tessera L, Mucciolo E, Giulotto E: Telomeric and nontelomeric (TTAGGG)<sub>n</sub> sequences in gene amplification and chromosome stability. *Genomics* 24:53–62 (1994).
- Bilaud T, Brun C, Ancelin K, Koering CE, Laroche T, Gilson E: Telomeric localization of TRF2, a novel human telobox protein. *Nature Genet* 17:236–239 (1997).
- Boei JJ, Vermeulen S, Natarajan AT: Differential involvement of chromosomes 1 and 4 in the formation of chromosomal aberrations in human lymphocytes after X-irradiation. *Int J Radiat Biol* 72:139–145 (1997).
- Bouffler S, Silver A, Papworth D, Coates J, Cox R: Murine radiation myeloid leukaemogenesis: relationship between interstitial telomere-like sequences and chromosome 2 fragile sites. *Genes Chrom Cancer* 6:98–106 (1993).
- Bouffler SD, Morgan WF, Pandita TK, Slijepcevic P: The involvement of telomeric sequences in chromosomal aberrations. *Mutat Res* 366:129–135 (1996).
- Day JP, Limoli CL, Morgan WF: Recombination involving interstitial telomere repeat-like sequences promotes chromosomal instability in Chinese hamster cells. *Carcinogenesis* 19:259–265 (1998).
- Desmaze C, Aurias A: In situ hybridization of fluorescent probes on chromosomes, nuclei or stretched DNA: applications in physical mapping and characterization of genomic rearrangements. *Cell molec Biol (Noisy-le-grand)* 41:925–931 (1995).
- Desmaze C, Alberti C, Martins L, Pottier G, Sprung CN, Murnane JP, Sabatier L: The influence of interstitial telomeric sequences on chromosome instability in human cells. *Cytogenet Cell Genet* 86:288–295 (1999).
- Drets ME, Therman E: Human telomeric 6; 19 translocation chromosome with a tendency to break at the fusion point. *Chromosoma* 88:139–144 (1983).
- Farr C, Fantes J, Goodfellow P, Cooke H: Functional reintroduction of human telomeres into mammalian cells. *Proc natl Acad Sci, USA* 88:7006–7010 (1991).
- Fernandez JL, Gosalvez J, Goyanes V: High frequency of mutagen-induced chromatid exchanges at interstitial telomere-like DNA sequence blocks of Chinese hamster cells. *Chrom Res* 3:281–284 (1995).
- Finnon R, Moody J, Mejine E, Haines J, Clark D, Edwards A, Cox R, Silver A: A major breakpoint cluster domain in murine radiation-induced acute myeloid leukemia. *Mol Carcinog* 34:64–71 (2002).
- Flint J, Craddock CF, Villegas A, Bentley DP, Williams HJ, Galanello R, Cao A, Wood WG, Ayyub H, Higgs DR: Healing of broken human chromosomes by the addition of telomeric repeats. *Am J hum Genet* 55:505–512 (1994).
- Gravel S, Larrivée M, Labrecque P, Wellinger RJ: Yeast Ku as a regulator of chromosomal DNA end structure. *Science* 280:741–744 (1998).
- Hastie ND, Allshire RC: Human telomeres: fusion and interstitial sites. *Trends Genet* 5:326–331 (1989).
- Ijdo JW, Baldini A, Ward DC, Reeders ST, Wells RA: Origin of human chromosome 2: an ancestral telomere-telomere fusion. *Proc natl Acad Sci, USA* 88:9051–9055 (1991).
- Johnson KL, Brenner DJ, Geard CR, Nath J, Tucker JD: Chromosome aberrations of clonal origin in irradiated and unexposed individuals: assessment and implications. *Radiat Res* 152:1–5 (1999).
- Kilburn AE, Shea MJ, Sargent RG, Wilson JH: Insertion of a telomere repeat sequence into a mammalian gene causes chromosome instability. *Mol Cell Biol* 21:126–135 (2001).
- Kramer KM, Haber JE: New telomeres in yeast are initiated with a highly selected subset of TGI-3 repeats. *Genes Dev* 7:2345–2356 (1993).
- Lee C, Sasi R, Lin CC: Interstitial localization of telomeric DNA sequences in the Indian muntjac chromosomes: further evidence for tandem chromosome fusions in the karyotypic evolution of the Asian muntjacs. *Cytogenet Cell Genet* 63:156–159 (1993).
- Lin Y, Waldman AS: Capture of DNA sequences at double-strand breaks in mammalian chromosomes. *Genetics* 158:1665–1674 (2001a).
- Lin Y, Waldman AS: Promiscuous patching of broken chromosomes in mammalian cells with extrachromosomal DNA. *Nucl Acids Res* 29:3975–3981 (2001b).
- Lo AW, Sabatier L, Fouladi B, Pottier G, Ricoul M, Murnane JP: DNA amplification by breakage/fusion/bridge cycles initiated by spontaneous telomere loss in a human cancer cell line. *Neoplasia* 4:531–538 (2002).
- Meltzer PS, Guan XY, Trent JM: Telomere capture stabilizes chromosome breakage. *Nature Genet* 4:252–255 (1993).
- Metcalfe CJ, Eldridge MD, McQuade LR, Johnston PG: Mapping the distribution of the telomeric sequence (T<sub>2</sub>AG<sub>3</sub>)<sub>n</sub> in rock-wallabies, *Petrogale* (Marsupialia: Macropodidae), by fluorescence in situ hybridization. I. The penicillata complex. *Cytogenet Cell Genet* 78:74–80 (1997).
- Metcalfe CJ, Eldridge MD, Toder R, Johnston PG: Mapping the distribution of the telomeric sequence (T<sub>2</sub>AG<sub>3</sub>)<sub>n</sub> in the Macropodoidea (Marsupialia), by fluorescence in situ hybridization. I. The swamp wallaby, *Wallabia bicolor*. *Chrom Res* 6:603–610 (1998).
- Meyne J, Baker RJ, Hobart HH, Hsu TC, Ryder OA, Ward OG, Wiley JE, Wurster-Hill DH, Yates TL, Moyzis RK: Distribution of non-telomeric sites of the (TTAGGG)<sub>n</sub> telomeric sequence in vertebrate chromosomes. *Chromosoma* 99:3–10 (1990).
- Mondello C, Pirzio L, Azzalin CM, Giulotto E: Instability of interstitial telomeric sequences in the human genome. *Genomics* 68:111–117 (2000).
- Murnane JP: Influence of cellular sequences on instability of plasmid integration sites in human cells. *Somat Cell molec Genet* 16:195–209 (1990a).
- Murnane JP: The role of recombinational hotspots in genome instability in mammalian cells. *Bioessays* 12:577–581 (1990b).
- Murnane JP, Sabatier L, Marder BA, Morgan WF: Telomere dynamics in an immortal human cell line. *EMBO J* 13:4953–4962 (1994).
- Musio A, Mariani T: Distribution of interstitial telomere-related sequences in the human genome and their relationship with fragile sites. *J Environ Pathol Toxicol Oncol* 18:11–15 (1999).
- Peitl P, Mello SS, Camparoto ML, Passos GA, Hande MP, Cardoso RS, Sakamoto-Hojo ET: Chromosomal rearrangements involving telomeric DNA sequences in Balb/3T3 cells transfected with the Ha-ras oncogene. *Mutagenesis* 17:67–72 (2002).
- Peterson SE, Stellwagen AE, Diede SJ, Singer MS, Haimberger ZW, Johnson CO, Tzoneva M, Gottschling DE: The function of a stem-loop in telomerase RNA is linked to the DNA repair protein Ku. *Nature Genet* 27:64–67 (2001).
- Piccini I, Ballarati L, Bassi C, Rocchi M, Marozzi A, Ginelli E, Meneveri R: The structure of duplications on human acrocentric chromosome short arms derived by the analysis of 15p. *Hum Genet* 108:467–477 (2001).
- Prescott JC, Blackburn EH: Telomerase RNA template mutations reveal sequence-specific requirements for the activation and repression of telomerase action at telomeres. *Mol Cell Biol* 20:2941–2948 (2000).
- Silver A, Cox R: Telomere-like DNA polymorphisms associated with genetic predisposition to acute myeloid leukemia in irradiated CBA mice. *Proc natl Acad Sci, USA* 90:1407–1410 (1993).
- Slijepcevic P, Xiao Y, Dominguez I, Natarajan AT: Spontaneous and radiation-induced chromosomal breakage at interstitial telomeric sites. *Chromosoma* 104:596–604 (1996).
- Slijepcevic P, Natarajan AT, Bryant PE: Telomeres and radiation-induced chromosome breakage. *Mutagenesis* 13:45–49 (1998).
- Sprung CN, Afshar G, Chavez EA, Lansdorp P, Sabatier L, Murnane JP: Telomere instability in a human cancer cell line. *Mutat Res* 429:209–223 (1999a).
- Sprung CN, Reynolds GE, Jasin M, Murnane JP: Chromosome healing in mouse embryonic stem cells. *Proc natl Acad Sci, USA* 96:6781–6786 (1999b).
- van Steensel B, de Lange T: Control of telomere length by the human telomeric protein TRF1. *Nature* 385:740–743 (1997).
- Vermeesch JR, De Meurichy W, Van Den Berghe H, Marynen P, Petit P: Differences in the distribution and nature of the interstitial telomeric (TTAGGG)<sub>n</sub> sequences in the chromosomes of the Giraffidae, okapi (*Okapia johnstoni*), and giraffe (*Giraffa camelopardalis*): evidence for ancestral telomeres at the okapi polymorphic rob(5;26) fusion site. *Cytogenet Cell Genet* 72:310–315 (1996).
- Weber B, Allen L, Magenis RE, Hayden MR: A low-copy repeat located in subtelomeric regions of 14 different human chromosomal termini. *Cytogenet Cell Genet* 57:179–183 (1991).
- Wells RA, Germino GG, Krishna S, Buckle VJ, Reeders ST: Telomere-related sequences at interstitial sites in the human genome. *Genomics* 8:699–704 (1990).
- Wiley JE, Meyne J, Little ML, Stout JC: Interstitial hybridization sites of the (TTAGGG)<sub>n</sub> telomeric sequence on the chromosomes of some North American hybrid frogs. *Cytogenet Cell Genet* 61:55–57 (1992).
- Wilt SR, Burgess AC, Normolle DP, Trent JM, Lawrence TS: Use of fluorescence in situ hybridization (FISH) to study chromosomal damage induced by radiation and bromodeoxyuridine in human colon cancer cells. *Int J Radiat Oncol Biol Phys* 30:861–866 (1994).

# Lack of spontaneous and radiation-induced chromosome breakage at interstitial telomeric sites in murine *scid* cells

H.-P. Wong,<sup>a</sup> H. Mozdarani,<sup>b</sup> C. Finnegan,<sup>b</sup> J. McIlrath,<sup>a</sup> P.E. Bryant<sup>b</sup> and P. Slijepcevic<sup>a</sup>

<sup>a</sup>Brunel Institute of Cancer Genetics and Pharmacogenomics, Brunel University, Uxbridge;

<sup>b</sup>School of Biology, University of St Andrews, St Andrews, Fife (UK)

**Abstract.** Interstitial telomeric sites (ITSs) in chromosomes from DNA repair-proficient mammalian cells are sensitive to both spontaneous and radiation-induced chromosome breakage. Exact mechanisms of this chromosome breakage sensitivity are not known. To investigate factors that predispose ITSs to chromosome breakage we used murine *scid* cells. These cells lack functional DNA-PKcs, an enzyme involved in the repair of DNA double-strand breaks. Interestingly, our results revealed lack of both spontaneous and radiation-induced chromosome breakage at ITSs found in *scid* chromosomes. Therefore, it is possible that increased sensitivity of ITSs to chromosome breakage is associated with the functional DNA double-strand break repair machinery. To investigate if this is the case we used *scid* cells in which DNA-PKcs deficiency was corrected. Our results revealed complete disappearance of ITSs in *scid* cells with functional DNA-PKcs, presumably through chromo-

some breakage at ITSs, but their unchanged frequency in positive and negative control cells. Therefore, our results indicate that the functional DNA double-strand break machinery is required for elevated sensitivity of ITSs to chromosome breakage. Interestingly, we observed significant differences in mitotic chromosome condensation between *scid* cells and their counterparts with restored DNA-PKcs activity suggesting that lack of functional DNA-PKcs may cause a defect in chromatin organization. Increased condensation of mitotic chromosomes in the *scid* background was also confirmed in vivo. Therefore, our results indicate a previously unanticipated role of DNA-PKcs in chromatin organisation, which could contribute to the lack of ITS sensitivity to chromosome breakage in murine *scid* cells.

Copyright © 2003 S. Karger AG, Basel

Molecular mechanisms responsible for spontaneous or induced chromosome breakage in mammalian cells are not yet fully understood in spite of active research interest in this problem. It is clear that the initial molecular lesion responsible for chromosome breakage is the DNA double-strand break (DSB)

(Bryant, 1984; Natarajan and Obe, 1984). However, different regions of mammalian chromosomes show differential sensitivity to DSB-inducing agents suggesting that multiple factors including DNA repair capacity, status of chromatin condensation, gene density and DNA sequence composition may affect conversion of the initial molecular lesions into microscopically visible chromosome breaks (Slijepcevic and Natarajan, 1994a, b; Folle and Obe, 1995, 1996; Suralles et al., 1997). Chromosome regions that show extremely high sensitivity to breakage include interstitial telomeric sites (ITSs). It has been noted that ITSs in Chinese hamster chromosomes are highly sensitive to radiation-induced chromosome breakage (Alvarez et al., 1993). This initial observation was confirmed by several studies, some of which also demonstrated that Chinese hamster ITSs are sensitive to spontaneous chromosome breakage (Bertoni et al., 1994; Balajee et al., 1994; Slijepcevic et al., 1996). For example,

Supported in part by a Euratom grant FIGH-CT 1999-00009 from the European Commission.

Received 2 September 2003; manuscript accepted 25 November 2003.

Request reprints from P. Slijepcevic

Brunel Institute of Cancer Genetics and Pharmacogenomics  
Brunel University, Uxbridge, Middlesex, UB8 3PH (UK)  
telephone: +44 1895 274 000 ext 2109; fax: +44 1895 274 348  
e-mail: predrag.slijepcevic@brunel.ac.uk

Present address of J.M.: Department of Molecular and Cellular Pathology  
Ninewells Hospital and Medical School, Dundee, DD1 9SY (UK).

metacentric chromosomes containing ITSs disappear spontaneously after prolonged in vitro culture of Chinese hamster cells. Molecular cytogenetic analysis revealed that chromosome breakage within ITSs may lead to conversion of a single metacentric chromosome into two telocentric chromosomes (Slijepcevic et al., 1996). A similar process of telomeric fission (TFI) was described in some plant species providing further evidence that ITSs show unusual sensitivity to chromosome breakage (Schubert et al., 1995). In addition, hypersensitivity of ITSs to radiation in mouse chromosome 2 has been implicated in leukaemogenesis (Bouffler et al., 1993). More recently, a molecular study revealed chromosome instability associated with inserted ITSs in Chinese hamster chromosomes (Kilburn et al., 2001).

The exact nature of ITS sensitivity to spontaneous or induced chromosome breakage remains unknown. To investigate possible factors involved in this process we used murine *scid* (severe combined immunodeficiency) cells. These cells show high levels of spontaneous telomeric fusions (TFUs) due to loss of telomere function (Slijepcevic et al., 1997; Bailey et al., 1999). As a result of TFUs telomeric sequences become ITSs (Slijepcevic, 1998). In addition, *scid* cells lack functional DNA-PKcs, an enzyme involved in DSB repair (Smith and Jackson, 1999). Our analysis revealed lack of both spontaneous and radiation-induced chromosome breakage at ITSs in these cells. Our findings therefore suggest that functional DSB repair machinery may be required for the elevated breakage sensitivity at ITSs observed in mammalian cells.

## Materials and methods

### Cell culture and irradiation

All cell lines were obtained from Dr. C. Kirchgesner, Stanford University. CB17 and *scid* cells were grown in Waymouth medium containing 10% fetal calf serum and antibiotics. Cell lines derived from the *scid* cell line, *scid* 50D and *scid* 100E, were grown in the selective Waymouth medium containing puromycin. We performed two types of cytogenetic experiments: a long-term experiment and a  $G_2$  assay. For long-term experiments CB17 and *scid* cells were grown until confluency. Confluent cells were irradiated with 4.0 Gy gamma rays. Following irradiation cells were allowed to recover for 2 h. Following recovery cells were split at the ratio 1:4 and harvested 24 h following irradiation using standard protocols. Between the next harvesting points (7, 14, 21 and 28 days) cells were grown under standard condition. Slides with chromosome spreads were stored in a freezer ( $-20^\circ\text{C}$ ) until required for chromosome painting. For  $G_2$  assay cells were irradiated with 1.0 Gy gamma rays as semi-confluent and harvested 3 h after irradiation. Frequencies of chromatid breaks were counted on Giemsa-stained chromosomes.

### Chromosome painting and telomere visualisation

Two-colour chromosome painting was performed according to manufacturer's instructions (Cambio, UK). Metaphase cells were acquired using a Zeiss Axioskop microscope equipped with a CCD camera and processed using Smart Capture software (Vysis). At least 50 cells per sample were analysed. The following criteria were used for detection of Robertsonian (Rb) chromosomes. Following identification of all Rb chromosomes in a metaphase stained with DAPI, each individual Rb was screened for the presence of painting signals on red and green channels. If an Rb consisted of two painted chromosomes we counted this as a single event. We also counted the total number of chromosomes painted with two colours not involved in Rb formation. Statistical comparison of frequencies of Rb chromosomes in control and irradiated samples was performed in Microsoft Excel using the F test. To visualize telomeres in metaphase chromosomes we used telomeric PNA oligonucleotide  $(\text{CCCAGG})_3$  labeled with Cy3 (Perseptive Biosystems).

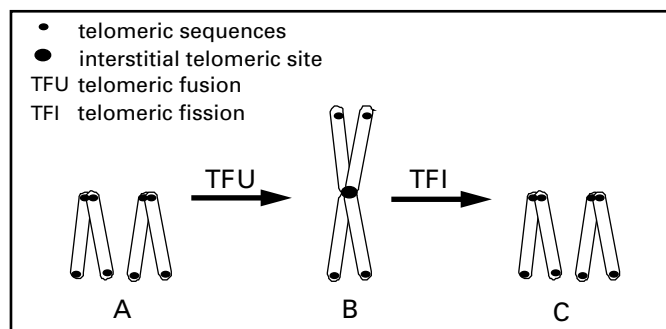


**Fig. 1.** (A) Functional telomeres maintain mouse acrocentric chromosomes as separate entities. (B) Loss of telomere function causes TFU. As a result of TFU telomeric sequences become ITSs. (C) ITSs are sensitive to chromosome breakage leading to TFI. TFU and TFI are reversible both in vitro (Slijepcevic et al., 1997) and in vivo (Schubert et al., 1995).

An event was counted as a TFU only when two chromosomes were joined so that their telomeres formed a single large signal usually twice the size of the normal telomeric signal. It is important to stress that in addition to chromosome-specific TFUs (see Results) *scid* cells also show random TFUs.

### Chromosome length measurement

Chromosome length measurement in cell lines was performed using the following procedure. Cells were grown until semi-confluent. Equal concentrations of colcemid were added to semi-confluent cells after which cells were incubated for 1 h and harvested using standard protocols. Metaphase spreads were painted with the probe for chromosome 1 and digital images of metaphases from cell lines were acquired as above. In the case of animals (purchased from Jackson laboratories), equal concentrations of colcemid were delivered to each animal by intraperitoneal injection. After 1 h animals were sacrificed by cervical dislocation, bone marrow was flushed from both femora and incubated in hypotonic solution for 30 min. Cells were then incubated in the standard fixative solution three times and chromosome spreads were prepared at room temperature. Chromosome painting was performed as above. To obtain mitotic cells without colcemid treatment confluent cells were split at the ratio 4:1 and allowed to grow for 24 h to reach an exponential phase. At this point cells were harvested as above.

To measure chromosome 1 length between 25 and 50 cells per sample were analysed. Chromosome 1 was identified on a colour channel in each metaphase. The same chromosome was then identified on a DAPI image, the image was enlarged to allow a high resolution of pixels and a line was drawn digitally along the chromosome axis and measured using IP Lab software. Length measurement results were compared between samples using t test in Microsoft Excel software.

## Results

### Lack of chromosome breakage at ITSs in *scid* cells

We have identified previously two chromosome-specific TFUs in the murine *scid* cell line (Slijepcevic et al., 1997). These TFUs are similar to Rb (Robertsonian) metacentric chromosomes and we classified them as Rb (3;14) and Rb (12;19) (Slijepcevic et al., 1997). The above two Rb chromosomes were used here to investigate ITS sensitivity to spontaneous and radiation-induced chromosome breakage (see below). Numerous Rb-like chromosomes consisting of randomly fused chromosomes are also present in the *scid* cell line. As a control in this study we used two true Rb metacentrics identified in the wild type (wt) CB17 cell line including Rb (3;3) and

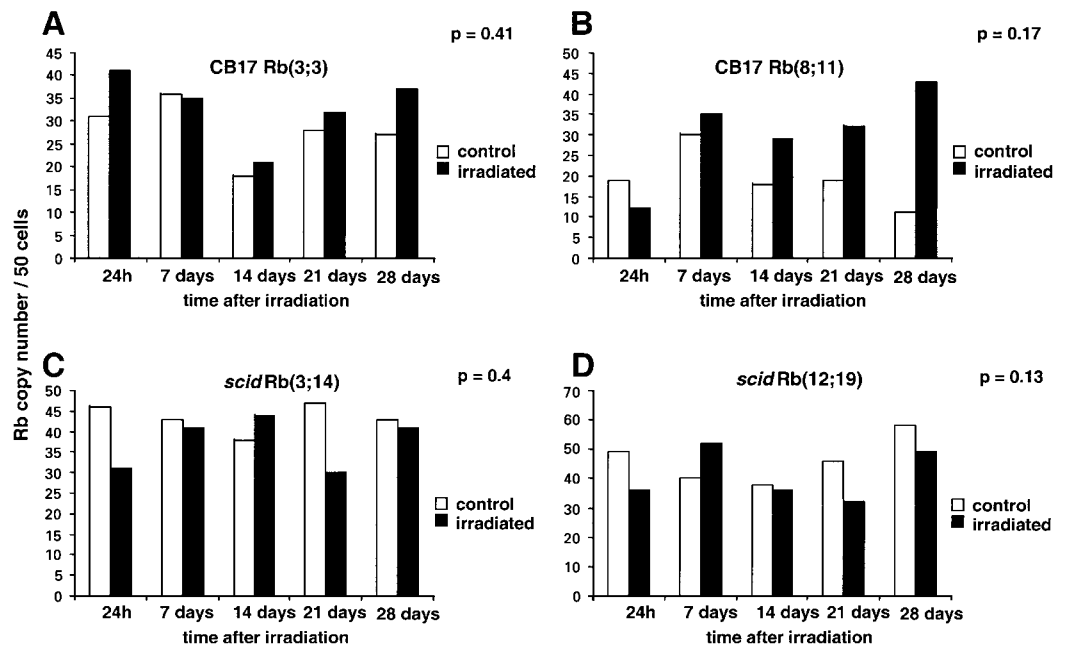


**Fig. 2.** Frequencies of chromosome-specific Rb chromosomes in CB17 cells (**A** and **B**) and *scid* cells (**C** and **D**) following irradiation with 4.0 Gy gamma rays. Statistical analysis (F test) indicated non-significant differences between control and irradiated samples over time (see *P* values in each panel).

Rb (8;11) (Slijepcevic et al., 1997). True Rb metacentric chromosomes lack ITSs at fusion points (Slijepcevic, 1998). We reasoned that if ITSs in *scid* cells are sensitive to chromosome breakage then chromosome-specific TFUs in murine *scid* cells (Rb [3;14] and Rb [12;19]) should be prone to a reverse process termed TFI (see Fig. 1). In this process a single metacentric chromosome splits into two acrocentric chromosomes due to chromosome breakage at ITSs (Fig. 1). To test the existence of TFI we used chromosome painting. We irradiated cells with 4.0 Gy of gamma rays and monitored copy number of Rb-like TFUs 24 h, 7, 14, 21 and 28 days following irradiation. Reduction in copy numbers of TFUs in irradiated *scid* cells in comparison with control counterparts over time, or spontaneous reduction in copy number of TFUs over time were expected to indicate presence of TFI (Fig. 1). Results of this experiment are shown in Fig. 2. When differences in frequencies of Rb-like TFUs between control and irradiated samples were analysed at individual time points it was clear that in many cases these were statistically significant (e.g. 24 h after irradiation in Fig. 2A, 24 h and 28 days in Fig. 2B, and 24 h in Fig. 2C and D). However, when samples were analysed as groups differences in frequencies of Rb-like TFUs over time between irradiated and control samples were not statistically significant neither in *scid* nor in CB17 cells (F test, see Fig. 2). Frequencies of Rb-like TFUs in control *scid* samples were similar at all time points (Fig. 2) suggesting that these TFUs remain stable over time and are not prone to spontaneous chromosome breakage at ITS. Taken together, these results indicate lack of radiation-induced and spontaneous chromosome breakage at ITSs in the murine *scid* cell line.

#### *Disappearance of chromosomes with ITSs following restoration of DNA-PKcs*

Previous studies employing DNA repair-proficient mammalian cells demonstrated preferential spontaneous and radiation-induced chromosome breakage at ITSs (see above). Our results suggest lack of spontaneous and radiation-induced chromosome breakage at ITSs in DSB repair-deficient *scid* cells (Fig. 2). Therefore, it is possible that the functional DSB repair machinery may be required for this breakage sensitivity. To investigate if this is the case we used a *scid* cell line in which DNA-PKcs activity was restored by introduction of a fragment from the human chromosome 8 carrying the DNA-PKcs gene (Kirchgeßner et al., 1995). This cell line, named *scid* 100E, was established from the same *scid* cell line used in the first experiment (Fig. 2) (Kirchgeßner et al., 1995). As a negative control we used the *scid* cell line containing a fragment from human chromosome 8 but without the DNA-PKcs gene. This cell line was named *scid* 50D and was also established from the same *scid* cell line used in the first experiment (Fig. 2) (Kirchgeßner et al., 1995). Cell lines *scid* 100E and *scid* 50D had the same replicative history. To confirm that a normal response to radiation had been restored in *scid* cells containing the human DNA-PKcs gene, we measured frequencies of radiation-induced chromosome breaks in above cell lines (Fig. 3A). As expected, radiation response of *scid* cells containing the normal DNA-PKcs gene was comparable to that of control wt cells. Radiation response of *scid* cells containing the human chromosome 8 fragment without the DNA-PKcs gene was comparable to that of *scid* cells (Fig. 3A).

We reasoned that if ITSs are sensitive to chromosome breakage in DNA repair-proficient cells then a spontaneous

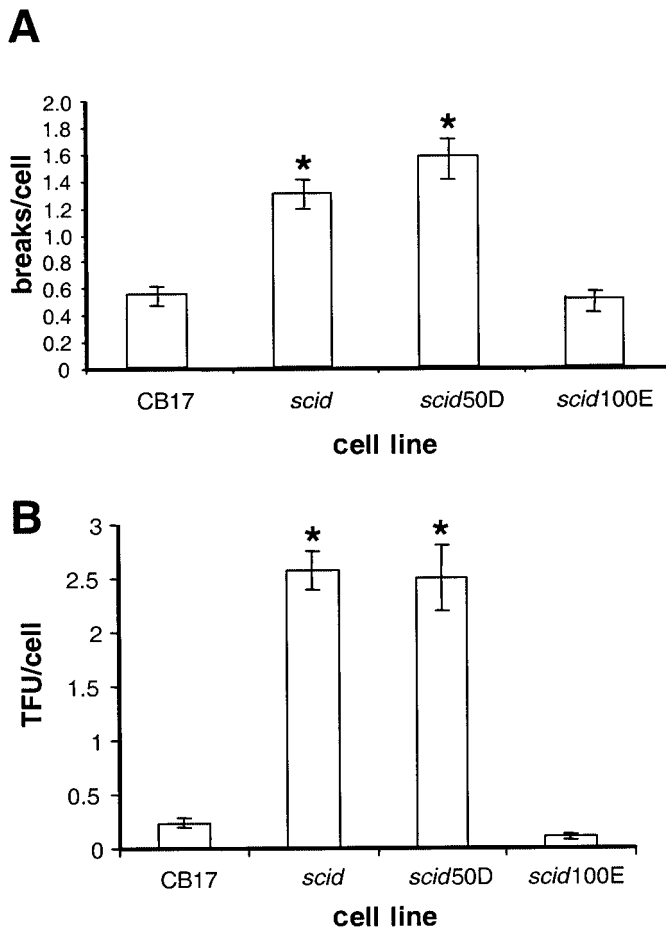


**Fig. 3. (A)** Radiation response of various cell lines assessed by  $G_2$  assay. Cells were irradiated with 1.0 Gy gamma rays and harvested 3 h after irradiation. The difference between *scid* 100E and wt CB17 cells was not statistically significant indicating that DNA-PKcs restored normal radiation response in these cells. \* Significantly different from control ( $P < 0.001$ ; t test) **(B)** Frequencies of TFUs (telomeric fusions) in various cell lines. The difference was statistically significant (\*) between *scid* and *scid* 100E cells ( $P < 0.001$ ; t test), *scid* 50D and *scid* 100E cells ( $P < 0.001$ ) but non-significant between *scid* and *scid* 50D cells.

decrease in the frequency of TFUs (i.e. Rb-like chromosomes) is expected in DNA DSB repair-proficient cells (*scid* 100E) in comparison with their DSB repair-deficient counterparts (*scid*) (see Fig. 1). To investigate this we monitored frequencies of TFUs in the above three cell lines using FISH with the telomeric PNA probe. This analysis revealed almost complete lack of TFUs in *scid* 100E cells and similar frequencies of TFUs in *scid* and *scid* 50D cells (Fig. 3B). Therefore, TFUs originally formed in the parental *scid* background, disappear in cells in which DNA-PKcs activity was restored but remain the same in positive and negative control cells. We could not monitor the rate of disappearance of TFUs because we obtained cells multiple passages after introducing chromosome 8 fragments when this process was essentially over. However, in an independent study it was reported that chromosomes containing ITSs disappeared after only six passages following restoration of DNA-PKcs in *scid* cells (Bailey et al., 1999).

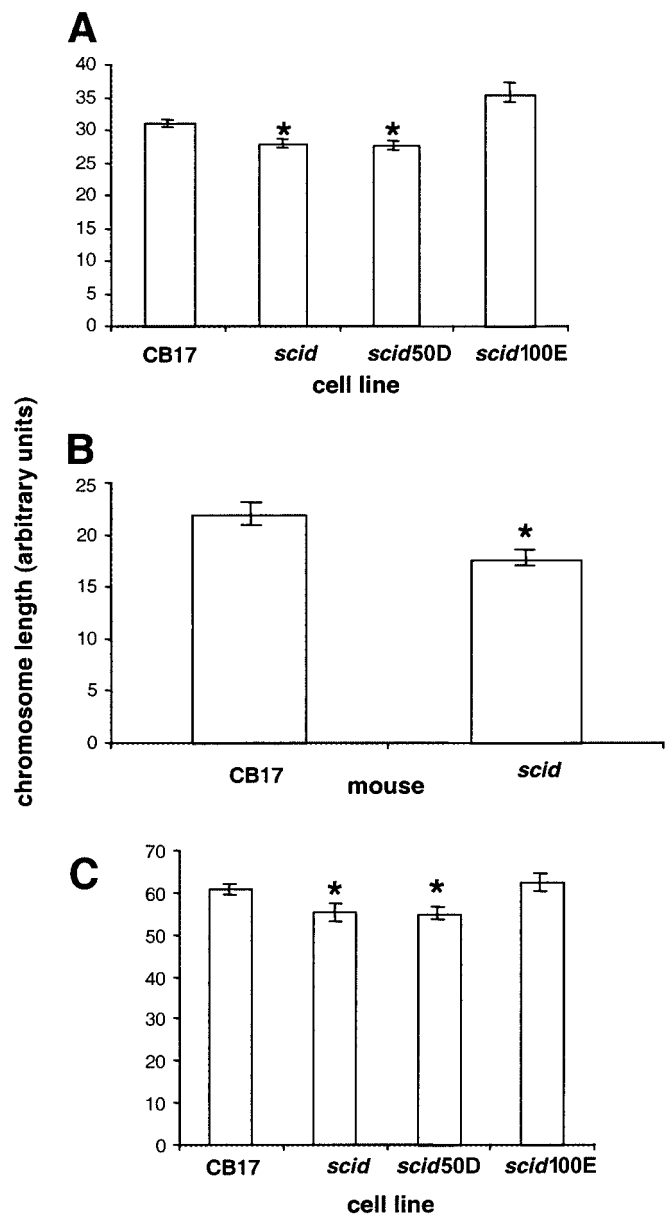


**Fig. 4.** Chromosome 1 length in various cell lines **(A)** and bone marrow cells obtained directly from mice **(B)** following treatment with equal concentrations of colcemid. **(C)** Chromosome 1 length in various cell lines without colcemid treatment. \* Significantly different from control.

#### Chromosome length measurements in cell lines and mice

Potential differences between *scid* cells and their counterparts with restored DNA-PKcs activity may help explain the lack of spontaneous and radiation-induced chromosome breakage at ITSs in *scid* cells. We have noticed that *scid* cells show much more condensed mitotic chromosomes than normal mouse cells following treatment with equal concentrations of colcemid for the same period of time. This may be an indication of a defect in chromatin organization. To investigate if these differences are significant we measured digitally the length of chromosome 1 in wt CB17 cells, *scid* cells, *scid* 100E

and *scid* 50D cells (see Materials and methods). Chromosome 1 was cytogenetically normal in all cell lines and we used chromosome painting to identify it unambiguously. Results of this analysis are presented in Fig. 4A. Interestingly, the differences in chromosome length between CB17 wt cells and *scid* cells were statistically significant ( $P < 0.001$ ; t test). Also, the difference in chromosome 1 length was statistically significant between *scid* cells and *scid* 100E cells with restored DNA-PKcs activity ( $P < 0.001$ ). There was no statistically significant difference between *scid* cells and *scid* 50D cells. Therefore, these results suggest that *scid* cells may have alteration in mitotic chromosome condensation and that this alteration is restored in cells with DNA-PKcs activity. To investigate if the same effect occurs in vivo we monitored chromosome 1 length in a single *scid* female animal and a single wild type CB17 female animal (Fig. 4B). Similarly, this analysis revealed statistically significant differences between two animals ( $P < 0.001$ ) further suggesting that the alteration in chromatin condensation of mitotic chromosomes may be associated with the murine *scid* defect.

To exclude the possibility that the observed hyper-condensation of *scid* chromosomes may result from over-reaction of *scid* cells to colcemid we monitored the length of chromosomes in naturally occurring mitotic cells from the above cell lines without any colcemid treatment. Results of this analysis are shown in Fig. 4C. Again, we observed statistically significant differences in chromosome 1 lengths between CB17 and *scid* cells ( $P < 0.001$ ), as well as between *scid* cells and *scid* 100E cells ( $P < 0.001$ ). There was no statistically significant difference between *scid* and *scid* 50D cells.

## Discussion

Several previous studies demonstrated that ITSs in mammalian chromosomes are sensitive to spontaneous and radiation-induced chromosome breakage (Alvarez et al., 1993; Balajee et al., 1994; Bertoni et al., 1994; Slijepcevic et al., 1996). In all these studies DSB repair-proficient mammalian cells were used. Results presented here, however, indicate that ITSs may not be sensitive to chromosome breakage in DSB repair-deficient mouse *scid* cells which lack functional DNA-PKcs. Restoration of DNA-PKcs activity in *scid* cells resulted in almost complete disappearance of chromosomes containing ITSs (Fig. 3). Since frequencies of chromosomes with ITSs in negative control cells remained the same as in *scid* cells (Fig. 3) this suggests that *scid* cells with restored DNA-PKcs activity may show TFI, a process in which ITSs are eliminated by chromosome breakage (see Fig. 1). Dramatic disappearance of chromosomes containing ITSs following restoration of DNA-PKcs activity in *scid* cells was reported independently by Bailey et al. (1999). Therefore, appearance of TFI, which coincides with the restoration of DNA-PKcs activity, and a complete lack of TFI in *scid* cells suggest that the functional DSB repair machinery may be required to mediate elevated sensitivity of ITSs to chromosome breakage.

Factors that predispose chromosome regions carrying ITSs to spontaneous or induced breakage are not completely under-

stood. It is well documented that the key molecular DNA lesion leading to chromosome breakage is DSB (Bryant, 1984; Nataraajan and Obe, 1984). Since DSB repair proteins, including Ku and DNA-PKcs, play important roles in telomere maintenance (Samper et al., 2000; Goytisolo et al., 2001) it is tempting to speculate that functional interaction between these proteins and telomere-binding proteins or telomerase may affect ITSs breakage sensitivity. It appears that in normal cells these interactions cause increased sensitivity of ITSs to spontaneous or radiation-induced chromosome breakage (Alvarez et al., 1993; Balajee et al., 1994; Bertoni et al., 1994; Slijepcevic et al., 1996). In contrast, lack of functional DNA-PKcs results in the absence of elevated chromosome breakage at ITSs (our results). Exact mechanisms of this process are not known. One possibility would be that the absence of functional DNA-PKcs leads to modification of broken DNA ends in a way that increased ITS breakage sensitivity is prevented. In this scenario, functional DNA-PKcs may not always recognise DSBs within ITSs as internal DSBs but sometimes as telomeres. This will ultimately prevent repair of internal DSBs and cause chromosome breakage as a result of telomere-mediated chromosome healing (Slijepcevic et al., 1996). Lack of functional DNA-PKcs would therefore result in the absence of telomere-mediated chromosome healing and thus absence of chromosome breakage at ITSs. This scenario can be tested experimentally.

An alternative scenario for the lack of ITS breakage sensitivity in murine *scid* cells may be that the lack of functional DNA-PKcs causes non-specific effects which in turn affect processing of DSBs within ITSs. This possibility is in line with the observed increase in chromatin condensation in mitotic *scid* cells in comparison with wt cells (Fig. 4). The apparent hyper-condensation of *scid* mitotic chromosomes may reflect a defect in chromatin condensation caused by the lack of DNA-PKcs. As a result, proteins that participate in DSB repair and telomere maintenance may not be able to function properly on a defectively organized chromatin thus causing differences in the ITS sensitivity profile between wild type and *scid* cells. It is interesting that the role of DNA-PKcs in chromatin organization has not been noted before and future studies are required to elucidate this link.

In conclusion, our results indicate that in contrast to DSB repair-proficient mammalian cells, DSB repair-deficient *scid* cells show lack of spontaneous and induced chromosome breakage at ITSs. This observation suggests that the functional DSB repair machinery may be required for elevated breakage sensitivity of ITSs in comparison with other chromosome regions.



## References

- Alvarez L, Evans JW, Wilks R, Lucas JN, Brown M, Giaccia AJ: Chromosomal radiosensitivity at intrachromosomal telomeric sites. *Genes Chrom Cancer* 8:8–14 (1993).
- Bailey SM, Meyne J, Chen DJ, Kurimasa A, Li GC, Lehnert BE, Goodwin EH: DNA double-strand break repair proteins are required to cap the ends of mammalian chromosomes. *Proc natl Acad Sci, USA* 96:14899–14904 (1999).
- Balajee AS, Oh HJ, Natarajan AT: Analysis of restriction enzyme-induced chromosome aberrations in the interstitial telomeric repeat sequences of CHO and CHE cells by FISH. *Mutat Res* 307:307–313 (1994).
- Bertoni L, Attolini C, Tessera L, Mucciolo E, Giulotto E: Telomeric and nontelomeric (TTAGGG)<sub>n</sub> sequences in gene amplification and chromosome stability. *Genomics* 24:53–62 (1994).
- Bouffler S, Silver A, Papworth D, Coates J, Cox R: Murine radiation myeloid leukaemogenesis: relationship between interstitial telomere-like sequences and chromosome 2 fragile sites. *Genes Chrom Cancer* 6:98–106 (1993).
- Bryant PE: Enzymatic restriction of mammalian cell DNA using *PvuII* and *BamHI*: evidence for the double strand break origin of chromosomal aberrations. *Int J Radiat Biol* 46:57–65 (1984).
- Folle GA, Obe G: Localization of chromosome breakpoints induced by *AluI* and *BamHI* in Chinese hamster ovary cells treated in the G1 phase of the cell cycle. *Int J Radiat Biol* 68:437–445 (1995).
- Folle GA, Obe G: Intrachromosomal localization of breakpoints induced by the restriction endonucleases *AluI* and *BamHI* in Chinese hamster ovary cells treated in S phase of the cell cycle. *Int J Radiat Biol* 69:447–457 (1996).
- Goytisolo FA, Samper E, Edmonson S, Taccioli GE, Blasco MA: The absence of the DNA-dependent protein kinase catalytic subunit in mice results in anaphase bridges and in increased telomeric fusions with normal telomere length and G-strand overhang. *Mol Cell Biol* 21:3642–3651 (2001).
- Kilburn AE, Shea MJ, Sargent RG, Wilson JH: Insertion of a telomere repeat sequence into a mammalian gene causes chromosome instability. *Mol Cell Biol* 21:126–135 (2001).
- Kirchgessner CU, Patil CK, Evans JW, Cuomo CA, Fried LM, Carter T, Oettinger MA, Brown JM: DNA-dependent kinase (p350) as a candidate gene for the murine SCID defect. *Science* 267:1178–1183 (1995).
- Natarajan AT, Obe G: Molecular mechanisms involved in the production of chromosomal aberrations. *Chromosoma* 90:120–127 (1984).
- Samper E, Goytisolo AF, Slijepcevic P, Van Buul PW, Blasco MA: Mammalian Ku86 protein prevents telomeric fusion independently of the length of TTAGGG repeats and the G-strand overhang. *EMBO Rep* 1:244–252 (2000).
- Schubert I, Rieger R, Fuchs J: Alteration of basic chromosome number by fusion fission cycles. *Genome* 38:1289–1292 (1995).
- Slijepcevic P: Telomeres and mechanisms of Robertsonian fusion. *Chromosoma* 107:136–140 (1998).
- Slijepcevic P, Natarajan AT: Distribution of X ray-induced G<sub>2</sub> chromatid damage among Chinese hamster chromosomes: influence of chromatin conformation. *Mutat Res* 323:113–119 (1994a).
- Slijepcevic P, Natarajan AT: Distribution of radiation induced G<sub>1</sub> exchange and terminal deletion breakpoints in Chinese hamster chromosomes as detected by G-banding. *Int J Radiat Biol* 66:747–755 (1994b).
- Slijepcevic P, Xiao Y, Dominguez I, Natarajan AT: Spontaneous and radiation induced chromosomal breakage at interstitial telomeric sites. *Chromosoma* 104:596–604 (1996).
- Slijepcevic P, Hande MP, Bouffler SD, Lansdorp P, Bryant PE: Telomere length, chromatin structure and chromosome fusigenic potential. *Chromosoma* 106:413–421 (1997).
- Smith GC, Jackson SP: The DNA-dependent protein kinase. *Genes Dev* 13:916–934 (1999).
- Surrallés J, Sebastian S, Natarajan AT: Chromosomes with high gene density are preferentially repaired in human cells. *Mutagenesis* 12:437–442 (1997).

# Cytological indications of the complex subtelomeric structure

M.E. Drets

National Service of Cell Sorting and Flow Cytometry; Instituto de Investigaciones Biológicas Clemente Estable, Montevideo (Uruguay)

Dedicated to Prof. Günter Obe for his long and productive research activity and for his permanent and generous cooperation with the development of experimental mutagenesis in Uruguay.

**Abstract.** Research on the subtelomeric region has considerably increased because this chromosome segment (1) keeps the chromosome number constant, (2) intervenes in cancer and cell senescence processes, (3) presents more crossovers than other regions of the genome and, (4) is the site of cryptic chromosome aberrations associated with mental retardation and congenital malformations. Quantitative microphotometrical scanning and computer graphic image analysis enables the detection of differentially distributed Giemsa-stained structures in T-banded subtelomeric segments of human and Chinese hamster ovary (CHO) chromosomes. The presence of high density stain patterns in the subtelomeric region was confirmed using endoreduplicated chromosomes as a model. Besides, prolonging the incubation in the T-buffer, specific holes were induced in subtelomeric segments. Hole specificity was confirmed inducing them in complex CHO chromosome aberrations obtained by

*AluI*. The method was also used to detect minute sister chromatid exchanges in the T-banded subtelomeric area (*t*-SCEs). The presence of *t*-SCEs was suspected to reflect, at the microscope level, the high crossover activity prevailing in the region. Due to the fact that the fluorescent signals obtained with subtelomeric probes seem to be colocalized with subtelomeric high density areas, measurements on the position of both structures with respect to the diffraction and chromosome edges were carried out. Data obtained showed comparable values suggesting that the high density segments were located where telomeric probes usually fluoresce. The possible relationship of the high density patterns, the production of specific holes, the localization of fluorescent areas and the detection of minute SCEs in the subtelomeric segment observed in T-banded CHO and human chromosomes is briefly reviewed.

Copyright © 2003 S. Karger AG, Basel

Mental retardation associated with congenital malformations has been one of the most complex problems in biomedical research. The first indication that a chromosome abnormality was involved in one of these syndromes was the discovery of trisomy 21 followed by the detection of chromosome X fragility. However, many other clinical pictures of retarded and malformed children remained unexplained being named in general

as “idiopathic” syndromes. The present availability of fluorescent probes for the subtelomeric region allowed detection of minute chromosome aberrations located in the subtelomeric region (Fauth et al., 2001; Joyce et al., 2001; Sismani et al., 2001; Popp et al., 2002; Jalal et al., 2003). These aberrations were collectively called “cryptic” because it was not possible to detect them before with the light microscope (de Vries et al., 2001; Fan et al., 2001; Riegel et al., 2001; Anderlid et al., 2002; Baker et al., 2002). Also, an obscure syndrome like autism is apparently related to subtelomeric aberrations (Borg et al., 2002; Wolff et al., 2002; Keller et al., 2003).

These observations, added to the fact that this region not only keeps the number and structure of the chromosomes of each species constant but also intervenes in cancer development and cell senescence, increased the research interest on this multifunctional chromosome segment (Zakian, 1989; Blackburn and Greider, 1995; Greider, 1998).

Supported in part by PEDECIBA (Uruguay).

Received 10 September 2003; manuscript accepted 3 November 2003.

Request reprints from Dr. Máximo E. Drets  
National Service of Cell Sorting and Flow Cytometry  
Instituto de Investigaciones Biológicas Clemente Estable  
Av. Italia 3318, 11.600 Montevideo (Uruguay)  
telephone: (598 2) 487 1616; fax: (598 2) 487 5548  
e-mail: drets@chasque.apc.org

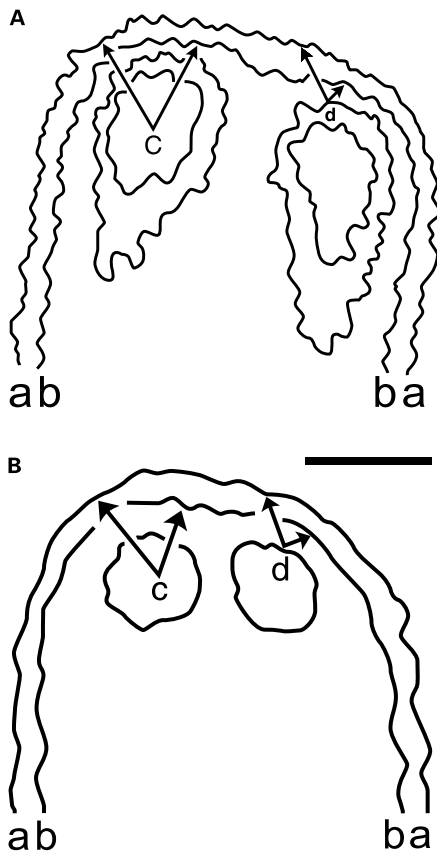


**Fig. 1.** Iso-density outlines of **(A)** T-banded human high density subtelomeric regions and **(B)** fluorescent FITC-labeled and propidium iodide-counterstained subtelomeric segments as detected by microphotometrical scanning. The two differential high density areas appearing in **A** were obtained using density intervals of 3%. The same interval value was used for detecting the diffraction and chromosome edges (see Drets et al., 1992a and 1995a for method details). **a-a** denotes the external border of the diffraction area and **b-b** the chromosome border; **c** indicates approximately the centers of the high density subtelomeric and fluorescent regions; **d** indicates points arbitrarily selected for measuring the distances from the external limit of the chromosome structures to the diffraction and chromosome borders respectively. Bar indicates 1 µm.

### Scanning microphotometry and subtelomeric structures

Scanning microscope photometry, color graphics terminals, software development and appropriate data manipulation have expanded the scope of scanning microphotometry particularly in their applications for cytogenetic studies. The quantitative and visual information given by the interactive graphic method thus contributed to obtain more informative images of the nuclear and chromosome structure (Drets and Monteverde, 1987; Drets et al., 1989, 1994, 1995a).

Microphotometrical scanning of T-banded chromosomes (Dutrillaux, 1973) showed that the high densities of Giemsa-stained subtelomeric regions are distributed in a specific manner at the subtelomeric segment of both human and CHO chromosomes, namely: a) in similar size in both sister chromatids, as would be expected from an orthodox cytogenetic point of

**Table 1.** Chromosome measurements<sup>a</sup>

High density segments (D)				
Vector	c-a	c-b	d-a	d-b
Sample size	25	25	25	25
Mean	26.43	14.25	11.58	6.10
SD	0.40	0.39	0.28	0.19
Fluorescent signals (F)				
Vector	c-a	c-b	d-a	d-b
Sample size	25	25	25	25
Mean	26.23	13.99	11.23	6.12
SD	0.33	0.59	0.37	0.18
$\chi^2$	c-a(D)/c-a(F) 0.26	c-b(D)/c-b(F) 0.90	d-a(D)/d-a(F) 0.58	d-b(D)/d-b(F) 0.25

<sup>a</sup> Distance measurements between chromosome borders and subtelomeric regions of different densities as shown in Fig. 1.

view; b) predominating in one of the chromatids; and c) concentrated in only one chromatid (Drets et al., 1992a). These density patterns were also observed in T-banded endoreduplicated chromosomes in similar subtelomeric sites of sister chromosomes (Drets and Mendizábal, 1998a, b).

Besides, we found that a prolonged incubation time of human and CHO chromosomes in the hot T-banding buffer resulted in the appearance of tiny holes in the subtelomeric regions of sister chromatids. These holes were observed in one or in both sister chromatids. In some chromosomes, the holes were of similar size while, in other cases, they were different in size, their location being comparable to the areas where the high density patterns were found (Drets et al., 1992b). Such holes were also produced in subtelomeric and in the paracentric segments of aberrant CHO chromosomes obtained after *AluI* treatment. Since it is practically impossible to induce holes in specific chromosome areas in complex aberrant chromosomes the method obviously produced a specific removal of chromatin by an unknown mechanism (Drets et al., 1995b).

In some CHO and human chromosomes, areas of high density arranged as minute sister chromatid exchanges were found, that we designated *t*-SCEs (Drets et al., 1992a). We found six cases of such tiny exchanges in 117 CHO chromosomes and eight in 80 human chromosomes. The frequency and size of these structures observed in a higher number of CHO and human chromosomes are under study. These *t*-SCEs were detected without using BrdU and were much smaller than those obtained with BrdU. These observations may represent different active functional stages of this dynamic and variable chromosome area (Mefford and Trask, 2002).

Due to the fact that the fluorescent signals obtained using subtelomeric probes are usually observed in comparable subtelomeric regions particularly those where the density patterns are detected, we made measurements of the position of these structures with respect to the chromosome edge to verify if they were located differently (Fig. 1). Table 1 shows that the distances from the centers or from the edges of both structures were similar and that the differences found were not significant

suggesting that density patterns and fluorescent signals were localized in the same regions. Although we were dealing with distances close to the resolving power of the light microscope, the data obtained by microphotometrical scanning were considered sufficiently accurate and reliable for this analysis.

Complex terminal heterochromatic chromosome substructures were described by Lima-De-Faria (1952) in plant pachytene telomeres at the light microscope level that closely resembled the T-subtelomeric segments as revealed by the banding procedure.

## Subtelomeric/telomeric elements

### I. DNA repeats

Considerable advances have been made in molecular research of telomeres and subtelomeric regions. Blackburn and Gall (1978) demonstrated first that *Tetrahymena* telomeres contain DNA tandem repeats. This finding was confirmed in other organisms from single-celled eukaryotes to mammals and higher plants (Blackburn and Szostak, 1984; Zakian, 1989). In human chromosomes, a telomeric repeated sequence (TTAGGG)<sub>n</sub> was detected using a fluorescent hybridization method (Moyzis et al., 1988). This sequence was subsequently detected in the pericentromeric heterochromatic region and in non-telomeric sites in chromosomes of other mammals (Meyne et al., 1990a). Middle repetitive sequences are found in subtelomeric segments and in the pericentromeric heterochromatic region of many chromosomes (Meyne et al., 1990b).

Telomere DNA has been divided into structural and functional domains. Immediately adjacent to the telomere repeats are telomere sequences constituting a third structural domain formed by very dynamic and numerous telomere-associated sequences which are mainly located in the subtelomeric region (Henderson, 1995).

Research on the distribution of telomeric and internal (TTAGGG)<sub>n</sub> repeats was carried out by Steinmüller et al. (1993) using biotinylated repetitive whole chromosome paint and telomere DNA probes at the electron microscope level. They detected terminal, subterminal and internal repeats in human chromosomes. The subtelomeric repeats were observed close to the terminal ones in sister chromatids and embedded in the chromatin of the chromosome terminus.

In addition, arrays of repetitive nucleotide sequences, believed to be sites for protein and ribonucleoprotein binding, are present not only at the ends of human chromosomes but at numerous interstitial sites and at the paracentromeric areas (Wells et al., 1990).

### II. Proteins

Telomeres are specialized DNA/protein complexes that comprise the ends of eukaryotic chromosomes with proteins that bind sequence-specifically to telomeric DNA, capping the chromosome ends thus preventing nucleolytic degradation and end-to-end ligation. The ribonucleoprotein telomerase is responsible for telomeric maintenance and partly compensates the progressive shortening of the chromosome ends synthesizing DNA back onto chromosome ends by reverse transcriptase

(Greider and Blackburn, 1987). Telomere proteins probably affect the accessibility of telomeric DNA to telomerase and interact with other structural or regulatory proteins (Fang and Cech, 1995).

Chong et al. (1995) identified and cloned a major protein component of human telomeres (TRF factor) showing by means of immunofluorescent labeling that TRF specifically colocalizes with telomeric DNA at chromosome ends. This observation allowed one to prove that the telomeric TTAGGG repeat array forms a specialized nucleoprotein complex. Using FISH analysis, Luderus et al. (1996) showed that TRF is an integral component of the telomeric complex and that the presence of TRF on telomeric DNA correlates with the compact configuration of telomeres.

Using fluorescence in situ hybridization, Moyzis et al. (1988) observed that most of the terminal fluorescent signals are not localized at the chromatid ends, but are surrounded by chromatin material. Smith and de Lange (1997) found that telomeric DNA preserves binding sites for telomeric proteins which form a protective nucleoprotein complex at chromosome ends. Day et al. (1993) claimed that repetitive DNA and proteins could intervene protecting the chromosome end from degradation and break rejoining (reviewed by McEachern et al., 2000).

## Additional evidence of subtelomeric region variability

Bekaert et al. (2002) studied 3D telomere size by means of confocal microscopy using FITC-labeled telomeric peptidic nucleic acid probes, counterstained with propidium iodide, finding that the telomere lengths of two sister chromatids are not of equal size in human lymphocytes and that this variability was not related to a specific chromosome. These findings suggest that a biological phenomenon might be involved in the production of the differences. The finding that subtelomeric segment size may be variable and independent of the chromosome pair corresponds well with our observations on the distribution of the high density patterns. Likewise, Schubert (1992) found signals of variable size, number and position in sister chromatids in plant cells.

These images resembled the distribution of the high density patterns detected by microphotometrical scanning of T-banded chromosomes and comparison of measurements on the localization of fluorescent signals and high density T-segments indicated that they matched topologically. In addition, Fig. 4 in the paper of Chong et al. (1995) shows an immunofluorescent protein labeled HeLa metaphase expressing [HA]<sub>2</sub> epitope-tagged mTRF. In this metaphase the fluorescent signals seem to be of similar or different size in both chromatids or, in other chromosomes, they appear in only one chromatid, all of which resembles the distribution of the subtelomeric density patterns found by us.

## Cytogenetic and molecular perspectives

The relationship between chromosome structure and banding phenomena is still not well understood. Chromosome banding patterns are produced with most of the reported procedures (G-, C-, R-, and T-banding) because of the Giemsa properties to stain specific chromosome structures. Comings and Avelino (1974) investigated the binding of Giemsa dyes to chromatin during the banding treatment showing that thiazins specifically interact with the phosphate groups of DNA and side stack along the molecule. The microphotometrical detection of different density patterns may suggest that they are related not only to the banding procedure but perhaps to the specific staining of T-banded segments by the Giemsa stain. In this connection, Sumner (1990) pointed out that in the banding phenomena dye accessibility may be modified either by proteins or by the variation of DNA base pair composition (or both) along the genome.

Saitoh and Laemmli (1994) claimed that the bands of the metaphase chromosome structure arise from a differential folding path of the highly AT-rich scaffold using the highly AT-specific fluorochrome daunomycin. Although the proposed loop-scaffold model fits well with most of the metaphase chromosome banded structures, the high content of R-banding material found in the T-banded segments composed of compact, fibrous R-structures extremely resistant to heat (Allen et al., 1988; Ludeña et al., 1991), it is difficult to draw a meaningful interpretation of the cytogenetic observations made in this region. Besides, R-bands apparently differ by their combination of *Alu* richness and extreme CG richness (Holmquist, 1992) making it more difficult to get a clear structural picture of the region.

In an interesting review, Pardue and DeBaryshe (1999) stressed the point that several findings suggest that eukaryotic telomeres may play other functions than chromosome end protection and recognition of intact chromosomes. Apparently, many rearrangements occur more frequently in subtelomeric domains than in other regions of the genome. Cornforth and Eberle (2001) claimed that chromosomal regions near the termini of chromosome arms undergo high rates of spontaneous recombination. Mondello et al. (2000) found that stretches of internal repeats can be highly unstable, and Badge et al. (2000)

mapped a subtelomeric recombinational "hotspot". This high crossover regional activity is probably related to the cryptic aberrations found in the subtelomeric region that are associated with congenital abnormalities.

An additional evidence that the subtelomeric region could possess some specific functional activity is the observation of minute sister chromatid exchanges detected by scanning microphotometry in T-banded CHO and human chromosomes (Drets et al., 1992a). The various minute exchanges observed with our system suggested that they could possibly represent, at the microscopic level, structures related to the high number of crossovers occurring in the area (Obe et al., 2002).

The differential distribution of the density patterns observed in normal and endoreduplicated chromosomes strongly suggests that they are real cytological facts probably reflecting the underlying chromatin organization revealed by the T-banding method. In addition, it could represent different functional stages of the region. Moreover, the induction of holes where the highest density chromatin areas are detected by scanning microphotometry may suggest that both phenomena are related (Drets et al., 1995b).

Summarizing, even though the information presently available on the molecular analysis of the telomeric/subtelomeric DNA and associated protein complexes is considerable, a clear picture of the eukaryotic metaphase chromosome at the high level organization is still missing (Drets, 2000). The metaphase subtelomeric segments proved not to be a simple association of DNA and protein molecules linearly aligned but an intricate and compact structure with functional roles not completely understood and awaiting definition. The over-looked structures of the subtelomeric chromosome region found at the microscopic level seem to be much more complex from a structural and functional point of view than formerly believed. A combined molecular and microscopic analysis of large subtelomeric chromosome segments is thus needed to contribute to a better understanding of their regional role.

## Acknowledgements

The author thanks Dr. S. Bekaert for sending an electronic version of Figure 5 from her paper published in *Cytometry*.

## References

- Allen TD, Jack EM, Harrison CJ: The three dimensional structure of human metaphase chromosomes determined by scanning electron microscopy, in Adolph KW (ed): *Chromosomes and Chromatin*, II, pp 51–72 (CRC Press, Boca Raton 1988).
- Anderlid BM, Schoumans J, Anneren G, Sahlen S, Kyllerman M, Vujic M, Hagberg B, Blennow E, Nordenskjöld M: Subtelomeric rearrangements detected in patients with idiopathic mental retardation. *Am J med Genet* 107:275–284 (2002).
- Badge RM, Yardley J, Jeffreys AJ, Armour JA: Crossover breakpoint mapping identifies a subtelomeric hotspot for male meiotic recombination. *Hum molec Genet* 9:1239–1244 (2000).
- Baker E, Hinton L, Callen DF, Altree M, Dobbie A, Eyre HJ, Sutherland GR, Thompson E, Thompson P, Woollatt E, Haan E: Study of 250 children with idiopathic mental retardation reveals nine cryptic and diverse subtelomeric chromosome anomalies. *Am J med Genet* 107:285–293 (2002).
- Bekaert S, Koll S, Thas O, Van Oostveldt P: Comparing telomere length of sister chromatids in human lymphocytes using three-dimensional confocal microscopy. *Cytometry* 48:34–44 (2002).
- Blackburn EH, Gall JG: A tandemly repeated sequence at the termini of the extrachromosomal ribosomal RNA genes in *Tetrahymena*. *J molec Biol* 120:33–53 (1978).
- Blackburn EH, Greider CW: *Telomeres* (Cold Spring Harbor Laboratory Press, 1995).
- Blackburn EH, Szostak JW: The molecular structure of centromeres and telomeres. *Annu Rev Biochem* 53:163–194 (1984).
- Borg I, Squire M, Menzel C, Stout K, Morgan D, Willatt L, O'Brien PC, Ferguson-Smith MA, Ropers HH, Tommerup N, Kalscheuer VM, Sargan DR: A cryptic deletion of 2q35 including part of the PAX3 gene detected by breakpoint mapping in a child with autism and a de novo 2;8 translocation. *J med Genet* 39:391–399 (2002).
- Chong L, van Steensel B, Broccoli D, Erdjument-Bromage H, Hanish J, Tempst P, de Lange T: A human telomeric protein. *Science* 270:1663–1667 (1995).

- Comings DE, Avelino E: Mechanisms of chromosome banding. VII. Interaction of methylene blue with DNA and chromatin. *Chromosoma* 51:365–379 (1974).
- Cornforth MN, Eberle RL: Termini of human chromosomes display elevated rates of mitotic recombination. *Mutagenesis* 16:85–89 (2001).
- Day JP, Marder BA, Morgan WF: Telomeres and their possible role in chromosome stabilization. *Environ molec Mutagen* 22:245–249 (1993).
- de Vries BB, White SM, Knight SJ, Regan R, Homfray T, Young ID, Super M, McKeown C, Splitt M, Quarrell OW, Trainer AH, Niermeijer MF, Malcolm S, Flint J, Hurst JA, Winter RM: Clinical studies on submicroscopic subtelomeric rearrangements: a checklist. *J med Genet* 38:145–150 (2001).
- Drets ME: Insights into the structure of the subtelomeric chromosome segments. *Gen Mol Biol* 23:1087–1093 (2000).
- Drets ME, Mendizábal M: Microphotometrical image analysis of the subtelomeric region of the T-banded endoreduplicated chromosomes of Chinese hamster ovary (CHO) cells. *Gen Mol Biol* 21:219–225 (1998a).
- Drets ME, Mendizábal M: The underlying structure of the subtelomeric segments detected by microphotometrical scanning and graphic image analysis. Fundamental and molecular mechanisms of mutagenesis. *Mutat Res* 404:13–16 (1998b).
- Drets ME, Monteverde FJ: Automated cytogenetics with modern computerized scanning microscope photometer systems, in Obe G, Basler A (eds): *Cytogenetics. Basic and applied aspects*, pp 48–64 (Springer-Verlag, Berlin 1987).
- Drets ME, Folle GA, Monteverde FJ: Quantitative detection of chromosome structures by computerized microphotometric scanning, in Obe G, Natarajan AT (eds): *Chromosomal aberrations. Basic and applied aspects*, pp 1–12 (Springer-Verlag, Berlin 1989).
- Drets ME, Obe G, Monteverde FJ, Folle GA, Medina II, De Galvez MG, Duarte JE, Mechoso BH: Computerized graphic and light microscope analyses of T-banded chromosome segments of Chinese hamster ovary cells and human lymphocytes. *Biol Zentrbl* 111:204–214 (1992a).
- Drets ME, Obe G, Folle GA, Medina II, De Galvez MG, Duarte JE, Mechoso BH: Appearance of “holes” in subtelomeric regions of human and Chinese hamster ovary cell chromosomes due to prolonged incubation in T-banding buffer followed by Giemsa staining. *Brazilian J Genet* 15:927–933 (1992b).
- Drets ME, Folle GA, Martínez W, Bonomi R, Duarte JE, Mechoso BH, Larrañaga J: Quantitative localization of chromatid breaks induced by Alu I in the long arms of chromosome number 1 of Chinese hamster ovary (CHO) cells by microphotometric scanning, in Obe G, Natarajan AT (eds): *International Symposium: Chromosomal Aberrations. Origin and Significance*, pp 169–183 (Springer-Verlag, Berlin 1994).
- Drets ME, Drets GA, Queirolo PJ, Monteverde FJ: Computer graphics as a tool in cytogenetic research and education. *Comp Appl Biosc (CABIOS)* 11: 463–468 (1995a).
- Drets ME, Mendizábal M, Boccardo EM, Bonomi R: Further analyses of subtelomeric and paracentric holes induced in human and Chinese hamster ovary cell chromosomes. *Biol Zentrbl* 114:329–338 (1995b).
- Dutrillaux B: Nouveau système de marquage chromosomique: Les bandes T. *Chromosoma* 41:395–402 (1973).
- Fan YS, Zhang Y, Speevak M, Farrell S, Jung JH, Siu VM: Detection of submicroscopic aberrations in patients with unexplained mental retardation by fluorescence in situ hybridization using multiple subtelomeric probes. *Genet Med* 3:416–421 (2001).
- Fang G, Cech TR: Telomere proteins, in Blackburn EH, Greider CW (eds): *Telomeres*, pp 69–105 (Cold Spring Harbor Laboratory Press, Cold Spring Harbor 1995).
- Fauth C, Zhang H, Harabacz S, Brown J, Saracoglu K, Lederer G, Rittinger O, Rost I, Eils R, Kearney L, Speicher MR: A new strategy for the detection of subtelomeric rearrangements. *Hum Genet* 109: 576–583 (2001).
- Greider CW: Telomerase activity, cell proliferation, and cancer. *Proc natl Acad Sci, USA* 95:90–92 (1998).
- Greider CW, Blackburn EH: The telomere terminal transferase of Tetrahymena is a ribonucleoprotein enzyme with two kinds of primer specificity. *Cell* 51:887–898 (1987).
- Henderson E: Telomere DNA structure, in Blackburn EH, Greider CW (eds): *Telomeres*, pp 11–34 (Cold Spring Harbor Laboratory Press, Cold Spring Harbor 1995).
- Holmquist GP: Chromosome bands, their chromatin flavors and their functional features. *Am J hum Genet* 51:17–37 (1992).
- Jalal SM, Harwood AR, Sekhon GS, Pham Lorentz C, Ketterling RP, Babovic-Vuksanovic D, Meyer RG, Ensenaer R, Anderson MH Jr, Michels VV: Utility of subtelomeric fluorescent DNA probes for detection of chromosome anomalies in 425 patients. *Genet Med* 5:28–34 (2003).
- Joyce CA, Dennis NR, Cooper S, Browne CE: Subtelomeric rearrangements: results from a study of selected and unselected probands with idiopathic mental retardation and control individuals by using high-resolution G-banding and FISH. *Hum Genet* 109:440–451 (2001).
- Keller K, Williams C, Wharton P, Paulk M, Bent-Williams A, Gray B, Ward A, Stalker H, Wallace M, Carter R, Zori R: Routine cytogenetic and FISH studies for 17p11/15q11 duplications and subtelomeric rearrangements studies in children with autism spectrum disorders. *Am J med Genet* 117: 105–111 (2003).
- Lima-De-Faria A: Chromomere analysis of chromosome complement of rye. *Chromosoma* 5:1–68 (1952).
- Ludeña P, Sentis C, De Cabo F, Velazquez M, Fernandez-Piqueras J: Visualization of R-bands in human metaphase chromosomes by the restriction endonuclease MseI. *Cytogenet Cell Genet* 57:82–86 (1991).
- Luderus ME, van Steensel B, Chong L, Sibon OC, Cremers FF, de Lange T: Structure, subnuclear distribution, and nuclear matrix association of the mammalian telomeric complex. *J Cell Biol* 135: 867–881 (1996).
- McEachern MJ, Krauskopf A, Blackburn EH: Telomeres and their control. *A Rev Genet* 34:331–358 (2000).
- Mefford HC, Trask BJ: The complex structure and dynamic evolution of human subtelomeres. *Nature Rev Genet* 3:91–102 (2002).
- Meyne J, Baker RJ, Hobart HH, Hsu TC, Ryder OA, Ward OG, Wiley JE, Wurster-Hill DH, Yates TL, Moyzis RK: Distribution of non-telomeric sites of the (TTAGGG)<sub>n</sub> telomeric sequence in vertebrate chromosomes. *Chromosoma* 99:3–10 (1990a).
- Meyne J, Ratliff RL, Buckingham JM, Jones MD, Wilson JS, Moyzis RK: The Human Telomere, in Fredga K, Kihlman BA, Bennet MD (eds): *Chromosomes Today*, Vol 10, pp 75–80 (Unwin Hyman, London 1990b).
- Mondello C, Pirzio L, Azzalin CM, Giolotto E: Instability of interstitial telomeric sequences in the human genome. *Genomics* 68:111–117 (2000).
- Moyzis R, Buckinham JM, Cram LS, Dani M, Deaven LL, Jones MD, Meyne J, Ratliff RL, Wu JR: A highly conserved repetitive DNA sequence (TTAGGG)<sub>n</sub> present at the telomeres of human chromosomes. *Proc natl Acad Sci, USA* 85:6622–6626 (1988).
- Obe G, Pfeiffer P, Savage JRK, Johannes C, Goedecke W, Jeppesen P, Natarajan AT, Martínez-López W, Folle GA, Drets ME: Chromosomal aberrations: formation, identification and distribution. *Mutat Res* 504:17–36 (2002).
- Pardue ML, DeBaryshe PG: Telomeres and telomerase: more than the end of the line. *Chromosoma* 108:73–82 (1999).
- Popp S, Schulze B, Granzow M, Keller M, Holtgreve-Grez H, Schoell B, Brough M, Hager HD, Tariverdian G, Brown J, Kearney L, Jauch A: Study of 30 patients with unexplained developmental delay and dysmorphic features or congenital abnormalities using conventional cytogenetics and multiplex FISH telomere (M-TEL) integrity assay. *Hum Genet* 111:31–39 (2002).
- Riegel M, Baumer A, Jamar M, Delbecque K, Herens C, Verloes A, Schinzel A: Submicroscopic terminal deletions and duplications in retarded patients with unclassified malformation syndromes. *Hum Genet* 109:286–294 (2001).
- Saitoh Y, Laemmli UK: Metaphase chromosome structure: bands arise from a differential folding path of the highly AT-rich scaffold. *Cell* 76:609–622 (1994).
- Schubert I: Telomeric polymorphism in *Vicia faba*. *Biol Zentrbl* 111:164–168 (1992).
- Sismani C, Armour JA, Flint J, Girgalli C, Regan R, Patsalis PC: Screening for subtelomeric chromosome abnormalities in children with idiopathic mental retardation using multiprobe telomeric FISH and the new MAPH telomeric assay. *Eur J hum Genet* 9:527–532 (2001).
- Smith S, de Lange T: TRF1, a mammalian telomeric protein. *Trends Genet* 13:21–26 (1997).
- Steinmüller J, Schleiermacher E, Scherthan H: Direct detection of repetitive whole chromosome paint and telomere DNA probes by immunogold electron microscopy. *Chrom Res* 1:45–51 (1993).
- Sumner AT: *Chromosome Banding* (Unwin Hyman, London 1990).
- Wells RA, Germino GG, Krishna S, Buckle VI, Reeders ST: Telomere-related sequences at interstitial sites in the human genome. *Genomics* 8:699–704 (1990).
- Wolff DJ, Clifton K, Karr C, Charles J: Pilot assessment of the subtelomeric regions of children with autism: detection of a 2q deletion. *Genet Med* 4: 10–14 (2002).
- Zakian VA: Structure and function of telomeres. *A Rev Genet* 23:579–604 (1989).

# Quantitative analysis of radiation-induced chromosome aberrations

R.K. Sachs,<sup>a</sup> D. Levy,<sup>a</sup> P. Hahnfeldt<sup>b</sup> and L. Hlatky<sup>b</sup><sup>a</sup>Department of Mathematics, University of California at Berkeley, Berkeley CA;<sup>b</sup>Dana Farber Cancer Institute, Harvard Medical School, Boston MA (USA)

**Abstract.** We review chromosome aberration modeling and its applications, especially to biodosimetry and to characterizing chromosome geometry. Standard results on aberration formation pathways, randomness, dose-response, proximity effects, transmissibility, kinetics, and relations to other radiobiological endpoints are summarized. We also outline recent work

on graph-theoretical descriptions of aberrations, Monte-Carlo computer simulations of aberration spectra, software for quantifying aberration complexity, and systematic links of apparently incomplete with complete or truly incomplete aberrations.

Copyright © 2003 S. Karger AG, Basel

Ionizing radiation induces a rich variety of different chromosome aberrations. Simple aberrations, involving only two chromosome breaks (here considered as DNA double strand breaks, DSBs), and complex aberrations, involving three or more DSBs, are readily produced. Frequencies depend systematically on aberration type, chromosome size, dose, dose rate, radiation quality, and cell type. Such a situation, where extensive and diverse data have orderly quantitative interrelations, calls for modeling. In fact, mechanistic aberration models have long been used (reviews: Edwards, 2002; Hlatky et al., 2002; Natarajan, 2002; Savage, 2002). Current goals include analyzing biodosimetric signatures for different radiations, comparing different DNA repair/misrepair pathways, probing interphase chromosome geometry, and extrapolating data to low doses.

This review emphasizes chromosome-type, exchange-type aberrations – the case for which we have the most information. We outline aberration characterizations, proximity effects, classic mathematical approaches applicable primarily to simple

aberrations, computer methods that can also handle the full spectrum of complex aberrations, systematic analysis of exchange complexity and apparent incompleteness using new software, transmissibility, and relations of aberrations to other damage.

## Characterizing aberrations and their formation

An exchange-type aberration, resulting from misrejoining of DSB free ends, can be described either by its observed final pattern at metaphase (e.g. Fig. 1A) or by a possible formation process starting earlier (Fig. 1B). Both description methods have advantages and drawbacks, both have often been used, and both have been clarified by recent quantitative modeling.

Observed final patterns depend on the protocol used, for example mFISH (Greulich et al., 2000; Loucas and Cornforth, 2001; Anderson et al., 2002; Durante et al., 2002) or solid staining. Systematic comparison of results obtained with different protocols is important. Some universal description method will be needed to construct radiation cytogenetic databases. Strong similarities between “detailed” ISCN nomenclature (ISCN, 1995) and mPAINT (Cornforth, 2001) suggest such a method (Sachs et al., 2002). The key idea is that protocols differ mainly in the way they describe chromosome segments; all have some way to identify misrejoinings. Applied to whole-chromosome painting, the unified method is very similar to mPAINT – examples are given in the caption to Fig. 1 and in the subsection on cycle structures below. However, the method is compre-

Supported by NIH GM68423 (R.K.S.), NSF DMS 9971169 (D.L.), DOE DE-FG03-00-ER62909 (L.H.), NIH CA78496 (P.H.).

Received 7 August 2003; manuscript accepted 17 November 2003.

Request reprints from R.K. Sachs, Professor Emeritus  
Departments of Mathematics and of Physics, Main Math office  
9th floor Evans Hall, MC 3840, University of California  
Berkeley, CA 94720 (USA); telephone: 510-642-4384; fax: 510-642-8204  
e-mail: sachs@math.berkeley.edu (URL: <http://math.berkeley.edu/~sachs/>)

hensive, being applicable also to solid staining, G-banding, FISH, armFISH, multicolour banding, synteny based on specifying the order of oriented genes (Pevzner and Tesler, 2003), DNA sequencing, etc. It can be used for apparently incomplete patterns.

Actually, most current modeling concerns aberration formation processes (e.g. Fig. 1B), rather than just final patterns (e.g. Fig. 1A), even though formation processes are harder to observe experimentally, and this approach also has a long history (Savage, 1998). An aberration formation process can be described systematically with a unified “aberration multigraph” that shows DSB locations in the genome, the misjoining process, and the final configuration of rearranged chromosomes (Sachs et al., 2002).

One important biophysical pathway of aberration formation is breakage-and-reunion (Fig. 2A), presumably based on non-homologous end joining. A one-hit pathway based on homologous repair/misrepair also sometimes occurs (Fig. 2B). A third, exchange-first, pathway has been suggested (Fig. 2C). We believe there is strong evidence from aberration spectra, dose-response relations, and analyzing enzyme action that, for irradiation of mammalian cells during G<sub>0</sub>/G<sub>1</sub>, breakage-and-reunion is the dominant pathway (Sachs et al., 2000b). This view is controversial (Goodhead et al., 1993; Cucinotta et al., 2000; Edwards, 2002). Recently, another one-hit pathway has been suggested, involving exchanges localized at transcription factories (Radford, 2002).

### Proximity effects and chromosome geometry

Whatever the pathway, an exchange requires spatial juxtaposition of two or more genomic loci (Fig. 2). Consequently, there are “proximity effects”, i.e. influences of interphase chromosome geometry and motion on aberration frequencies, espe-

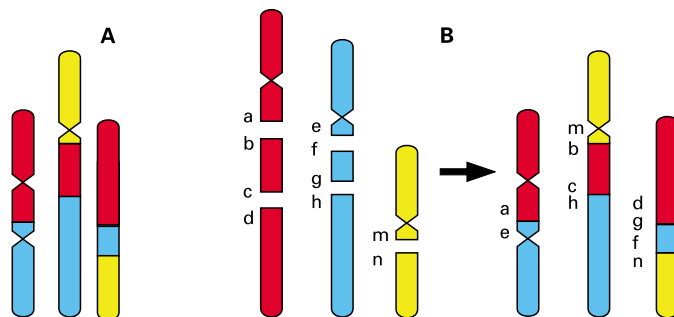


**Fig. 1.** A complex aberration. (A) schematically shows an observed mFISH pattern with at least five misrejoinings. Descriptors are (red'::blue') (yellow'::red::blue) (red::blue::yellow). Here: parentheses indicate rearranged chromosomes; primes denote centromeres; and, as in ISCN (1995), double colons are used for required misrejoinings. Assuming no cryptic DSBs, there are four possible aberration formation processes. One of these four is shown in (B); the other three differ by inversions switching b with c and/or f with g on the right.

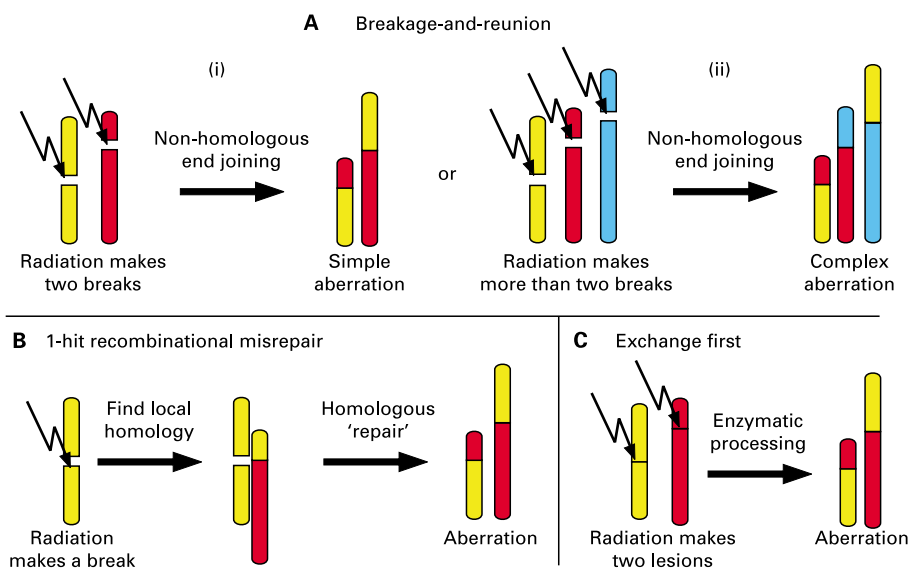


**Fig. 2.** Aberration formation pathways (review: Hlatky et al., 2002). In the breakage-and-reunion pathway (A), radiation makes DSBs, each of which has two free ends. Each free end then rejoins with another free end, either restituting (i.e. restoring the original DNA sequence apart perhaps from some comparatively small scale changes) or misjoining, presumably by non-homologous end joining. In a misjoining, the two free ends of one DSB can either act in concert (Ai), or misjoin independently, at different genomic locations (Aii). Due to the possibility of independent misjoining, complex aberrations can arise readily and very complex aberrations can result. (B) indicates a different pathway. One essential difference is that a

single radiation-induced DSB can initiate an exchange, presumably made by enzymatically-mediated homologous misrepair as shown. In the usual versions of this pathway, DSB free ends are constrained to act in concert during the recombinational event, as shown in panel B. This constraint leads to model predictions of a much smaller proportion of complex aberrations relative to simple ones than in the breakage-and-reunion case. It also limits the type of aberrations that can arise. (C) shows the Revell-type exchange-theory pathway. As in A, a single radiation-induced lesion cannot by itself induce an exchange. As in B, free ends of the same lesion are constrained to act in concert, restricting the type and frequency of complex aberrations.



cially important in conjunction with DSB clustering (reviewed in: Sachs et al., 1997a, 1999; Kretz et al., 1998). Conversely, the surprisingly rich aberration spectra uncovered by current techniques, when combined with biophysically-based computer modeling, help characterize large-scale interphase chromatin architecture.

When analyzing proximity effects chromosomes are often represented by random walk or polymer models (Hahnfeldt et al., 1993; Sachs et al., 1995, 2000a; Münkler et al., 1999; Ostashevsky, 2000; Ottolenghi et al., 2001; Andreev and Eidelman, 2002; Holley et al., 2002) many of which are coarse-grained. However, very detailed models (e.g. Friedland et al., 2003) are also available.

Most proximity results on radiogenic aberrations (review: Hlatky et al., 2002) are consistent with the picture obtained by imaging (review: Parada and Misteli, 2002), wherein chromosomes are mainly confined to territories and interchromosomal interactions involve mainly territory surfaces or perhaps loops protruding far from the home territories. However, observation of highly complex aberrations suggests more intermingling of chromosome territories than does direct imaging. Frequencies of specific mFISH color junctions in irradiated cells (Cornforth et al., 2002b) indicate considerable randomness in chromosome-chromosome juxtapositions, superimposed on more systematic chromosome spatial locations suggested by other methods (e.g. Boyle et al., 2001; Cremer et al., 2001).

### Classic quantitative aberration models

We review three mechanistic approaches which have long been useful, primarily for analyzing simple aberrations detected at the first metaphase after irradiation.

#### *Randomness model (Savage and Papworth, 1982)*

The basic version of this model makes two assumptions: (a) At low LET DSBs occur independently with a probability for any part of the genome proportional to genomic content (averages over regions appropriate for the lower limit of resolution of conventional cytogenetics, having order of magnitude of 5 Mb, are involved); (b) DSB free end misrejoining partners are random. These two randomness assumptions have many testable implications. For the special case of just two DSBs (i.e. pairwise misrejoining of four free DSB ends), the formalism predicts, among other things: (a) equal frequency of asymmetric simple aberrations (dicentrics, centric or acentric rings) and their symmetric counterparts (translocations, peri- or paracentric inversions); (b) the Lucas formula (reviewed in Sachs et al., 2000b) for the fraction of simple translocations that involve a color junction; (c) if proximity effects were negligible the ratio of simple dicentrics to simple centric rings for a human genome would be  $\sim 87$ .

Often, predictions of the Savage-Papworth formalism approximate the data well (reviewed in Johnson et al., 1999; Sachs et al., 2000b). However:

- Painting results (e.g. Knehr et al., 1996; Cigarrán et al., 1998) suggest taking the “effective length” (Savage, 1991) of a chromosome as approximately  $\propto$  (genomic content)<sup>2/3</sup>

rather than  $\propto$  (genomic content) to avoid systematically over-estimating the participation of larger chromosomes (reviewed in: Wu et al., 2001; Cornforth et al., 2002b). It has been suggested that this dependence of effective length on genomic content may be due to interchanges involving primarily chromatin at territory surfaces.

- There is evidence for specific deviations from randomness due to variations in chromatin structure (reviewed in Natarajan, 2002; Obe et al., 2002). It would be of interest to study if these can be related to the putative hot spots recently suggested in comparative genomics (Pevzner and Tesler, 2003).
- Assuming randomness strongly underestimates intrachanges relative to interchanges. Long ago, Savage and Papworth identified proximity effects as the explanation: chromosome localization in territories means a pair of DSBs on one chromosome is much more likely to misrejoin than a pair of DSBs randomly located in the genome (reviewed in Hlatky et al., 1992).
- At high LET, the spectrum of exchange-type aberration is expected to be different due to DSB clustering and proximity effects (Brenner et al., 1994; Chen et al., 1997; Sachs et al., 1997b; Ballarini et al., 2002; Holley et al., 2002). A different spectrum is indeed observed in vitro: there is a higher frequency of complex aberrations compared to simple ones; higher frequencies of aberrations involving several exchange breakpoints within the same chromosome; and perhaps more incompleteness (e.g. Sabatier et al., 1987; Griffin et al., 1995; Knehr et al., 1999; Boei et al., 2001; Fomina et al., 2001; Durante et al., 2002; Anderson et al., 2003; George et al., 2003; Wu et al., 2003a, b). Because of such tell-tale differences, retrospective biodosimetry should eventually be able to identify the type of radiation as well as the dose received. Whether there is a pronounced LET dependence of interchange/intrachange ratios has been quite controversial (e.g. Sachs et al., 1997a; Bauchinger and Schmid, 1998; Savage and Papworth, 1998; Schmid et al., 1999; Deng et al., 2000; Boei et al., 2001; Hande et al., 2003).
- When more than two DSBs are involved, and at high LET, Monte Carlo approaches, discussed below, are considerably more convenient than the randomness formalism.
- We predict that proximity effects should lead to an excess of rings compared to inversions. The reason is that the DSB free ends at the opposite ends of a chromatin segment (e.g. b and c in Fig. 1B) not only have a bias toward being close together when formed (because they are on the same chromosome) but have an additional bias for staying close together. Even if there is considerable motion of chromosome fragments, the two free ends will remain connected by the chromatin between them, and this constraint tends to favor ring formation. Modern protocols should make it possible to check this prediction, especially for the case of centric rings vs. pericentric inversions.

#### *LQ dose-response estimates for simple aberrations*

The theory of dual radiation action, TDRA (Kellerer and Rossi, 1978), gives the following linear-quadratic (LQ) formula

for the dependence of aberration frequency  $Y$  on total dose  $D$  and dose-rate  $R(t)$ :

$$(A) Y = \alpha D + G\beta D^2,$$

where

$$(B) G = \frac{2}{D^2} \int_{-\infty}^{\infty} dt \int_{-\infty}^{\infty} dt' R(t)K(t-t')R(t'), \text{ with (C) } K(s) = \exp(-\lambda s). \quad (1)$$

Here pairwise misrejoining of DSBs and mono-exponential restitution with rate constant  $\lambda \geq 0$  are assumed.  $G$  applies to low dose-rate and/or fractionated irradiation, generalizing the Lea-Catcheside factor (reviewed in Sachs and Brenner, 2003);  $G \leq 1$  and for a single acute dose  $G = 1$ . TDRA also expresses the LQ coefficients  $\alpha$  and  $\beta$  mechanistically, in terms of an energy proximity function, a target proximity function for chromosomes, and a distance dependent interaction probability (Kellerer and Rossi, 1978). When supplied with these characterizations of  $\alpha$  and  $\beta$ , Equation 1 very neatly encapsulates four key factors – radiation track structure, chromatin geometry, repair, and misrepair. Consequently it remains quite useful (e.g. Sachs et al., 1997a; Radivoyevitch et al., 2001) despite having limitations, such as ignoring complex aberrations, that have been uncovered and ameliorated by later formalisms. In biodosimetry (Blakely et al., 2002), LQ approximation is still central (reviewed in: Bauchinger, 1998; Kodama et al., 2001; Tucker, 2001; Edwards, 2002). Equation 1 with  $\lambda \sim 1$  per hour often gives reasonable approximations to observed direct dose rate effects (e.g. Cornforth et al., 2002a; review: Lloyd and Edwards, 1983).

#### *Reaction rate models for simple aberrations*

“Reaction rate” biophysical models track time development, using the formalism (Erdi and Toth, 1989) of deterministic or stochastic chemical mass action kinetics; they are special cases of dynamic equations for genetic regulatory networks and metabolic control (de Jong, 2002). Many reaction rate models for simple aberrations have been investigated over the years (review: Sachs et al., 1997c). Recent examples include saturable repair models quantifying the mechanism shown in Fig. 2B (Cucinotta et al., 2000) and the two-lesions-kinetic (TLK) model, which allows for biphasic repair kinetics corresponding to two different kinds of DSBs (Stewart, 2001). Each deterministic reaction rate model has a corresponding stochastic version (e.g. Albright, 1989; Hahnfeldt et al., 1992; Radivoyevitch et al., 1998) that is computationally more involved, but is actually simpler from a conceptual point of view, is more accurate in many cases (especially at high LET), and can analyze statistical cell-to-cell fluctuations.

Reaction rate models for simple aberrations predict approximately LQ behavior (Equations 1A and 1B) at low and intermediate doses or dose rates (reviewed in: Guerrero et al., 2002), and to date their main application has been interpreting LQ parameters mechanistically. In most aberration studies (unlike many DSB studies) the LQ approximation to a reaction rate model is often adequate. For aberrations formed by high acute doses of low LET radiation (e.g. Sasaki, 2003), neither current reaction rate models nor LQ approximations are accurate, mainly because complex aberrations become so important.

Most radiobiological reaction rate equations ignore proximity effects – they use well-mixed instead of diffusion-limited chemical kinetics. Simple approximations to proximity effects can be incorporated by assuming “interaction sites” – a number of different, non-interacting regions in the nucleus of a cell (e.g. Radivoyevitch et al., 1998).

## **Computer modeling**

### *Monte Carlo models of aberration formation*

More recently, virtual experiments obtained from Monte Carlo simulations have been used to refine the approaches described in the previous section. The simulations are probabilistic, with a computer in effect “rolling dice” to give extremely detailed output. For example, for acute low LET irradiation, CAS (chromosome aberration simulator) software (reviewed in: Sachs et al., 2000a) starts by determining the locations of DSBs on one copy of chromosome 1 in one cell at random, using a random number generator. The other 45 chromosomes are then treated similarly, taking into account their DNA content. Restitution or misrejoining for the DSB free ends according to any of the aberration formation pathways (Fig. 2) is next simulated, as a discrete-time Markov process, taking proximity effects into account. Specifying the relevant scoring protocol (for example mFISH) then determines a simulated karyotype. Iterating, thousands or millions of metaphases are simulated, each with its own aberration pattern. The results can then be compared to experimentally observed aberration spectra and dose-response relationships

This probabilistic approach systematically emphasizes dominant processes and likely outcomes, appropriately discounting, without completely ignoring, minor formation pathways and many possible but unlikely aberration types. Complex aberrations can be simulated in complete detail, as is relevant, for example, to analyzing aberration spectra as biomarkers of radiation quality.

CAS has been applied primarily to low LET aberrations, though alpha particles have also been analyzed (Chen et al., 1997). Other programs for chromosome breakage and misrejoining have been developed (e.g.: Friedland et al., 2001; Ottolenghi et al., 2001; Andreev and Eidelman, 2002; Holley et al., 2002). These incorporate high LET radiation tracks more realistically and thoroughly but give less systematic descriptions of complex aberrations. A Monte Carlo approach by Moiseenko and coworkers (review: Edwards, 2002) has the advantage of tracking actual time dependence, instead of merely a sequence of steps.

### *Cycle structure: quantifying aberration complexity*

A complete exchange-type chromosome aberration formation process has a cycle structure (Bafna and Pevzner, 1996; Sachs et al., 1999) specifying DSB numbers for separate irreducible reactions involved. For example, a simple aberration is formed by a reaction involving two DSBs, i.e. a 2-cycle  $c_2$ ; Fig. 2Aii describes a 3-cycle  $c_3$ ; Fig. 1B involves two separate reactions, one involving two DSBs (namely  $cd$  and  $gh$ ) and the other involving three DSBs, so the cycle structure is  $c_2+c_3$ ; etc.

An observed aberration pattern is often compatible with many different aberration formation processes, having various cycle structures; then the structure with the shortest cycles is designated “obligate” (Cornforth, 2001; Levy et al., 2003). For example, there are four possible five DSB processes for making the final pattern shown in Fig. 1A. The process shown in Fig. 1B has the obligate cycle structure, c2+c3, but each of the other three processes has cycle structure c5, indicating a single more complex exchange in each case.

As the number of misrejoinings required by the observed pattern grows to ~ 10 or more, the number of compatible processes becomes so large that recently developed software (available freely on the internet: Levy and Sachs, 2003) is needed to analyze cycle structures. For example, consider the mFISH pattern (1'::3::2') (4::1) (2::3') (3::1':4') (1::1) (:1:) (:2::1:). Here parentheses enclose different rearranged chromosomes, numbers indicate colours, primes denote centromeres, and double colons denote required misrejoinings; (:1:) and (:2::1:) denote rings. Assuming no cryptic misrejoinings, the software demonstrates 1,152 possible formation processes; 640/1,152 ~ 55.6% have cycle structure c10; only 16/1,152 ~ 1.4% have the obligate cycle structure c2+c4+c4. This example illustrates a general point – assuming obligate cycle structures tends to underestimate aberration complexity. For the more complex pattern (1'::3::2') (2::1) (2'::3') (3::1':2') (1::1) (2::2) (:1:) (:2::1:) there are 20,736 processes with 11 misrejoinings. Only 32/20,736 ~ 0.15% have the obligate cycle structure c2+c3+c3+c3 but 10,368/20,736 = 50% are 11-cycles c11. Such enumeration of cycle statistics can be replaced by Monte Carlo sampling, useful mainly for patterns so complex that > 1,000,000 processes are possible.

#### *Apparently incomplete aberration patterns*

Many observed aberration patterns appear incomplete, either because some DSB free ends have actually failed to rejoin or, more often, because some segments are cryptic, where the difference between these two cases can be analyzed using telomere probes (reviewed in: Boei et al., 2000; Fomina et al., 2001; Loucas and Cornforth, 2001; Holley et al., 2002; Wu et al., 2003b). In complicated situations it may be difficult to relate apparently incomplete patterns to complete or truly incomplete aberrations (Cornforth, 2001). Algorithms have now been developed to handle this problem systematically for any whole-chromosome painting protocol (e.g. mFISH). In brief, first consider colours one at a time, setting T = (apparent telomeres) and C = (centromeres involved), with C > 0. For every colour with T < 2C, add to the observed pattern 2C-T “cryptic terminals” – small acentrics with one telomere and the other end either unrejoined or misrejoined. For every colour with T > 2C, consider T-2C apparent telomeres as actually being DSB free ends instead. Interrelations among complete, apparently incomplete but truly complete, and truly incomplete aberrations can then be methodically worked out as follows. One considers pairwise misrejoinings among the free ends introduced in the steps just described for T < 2C or T > 2C to get a complete pattern, or considers some of these free ends as unrejoined, corresponding to true incompleteness. Free software (Levy and Sachs, 2003) is available for complicated cases. Probabilities, e.g. for cycle structures, can be systematically assigned.

## **Cell proliferation and aberration transmissibility**

It is important to analyze the behavior of aberrations, and of cells that contain them, at mitosis. The main quantitative formalism (Brasemann et al., 1986) extends a model of Carrano and Heddle. The formalism involves parameters defined in terms of behavior at the first post-irradiation cell division in vitro. One parameter is W, the probability that a simple dicentric allows viable daughters; another is the acentric transmissibility parameter T, with 2T specifying the probability that a cell with an acentric transmits at least one copy of the acentric to one or the other daughter cell. For human lymphocytes approximate values W = 0.42 and T = 0.41 were measured (Bauchinger et al., 1986). This approach has been generalized to more complex aberrations, to multiple aberrations, to later metaphases, and to in vivo situations (reviewed in: Lucas, 1999; Gardner and Tucker, 2002; Vázquez et al., 2002). However, chromosomal instability occurring many cell generations after irradiation (reviews: Lorimore and Wright, 2003; Morgan, 2003) needs additional quantitative modeling.

## **Relating aberrations to other endpoints**

Recent results suggest that most total-gene or multi-exon deletions in standard mutation assays may be formed by essentially the same misrepair processes as exchange-type aberrations (reviewed in: Costes et al., 2001; Friedland et al., 2001; Wu and Durante, 2001; Singleton et al., 2002). Also for many cancers there are associations to specific exchange-type chromosome aberrations (Mitelman et al., 2002) which are causative or at least pathognomic in at least one case (CML; reviewed in Radivoyevitch et al., 2001). However, exchange-type aberrations differ significantly from many other radiobiological endpoints in that the aberrations always require more than one DSB (Fig. 2). At low LET for an acute dose of several Gy, most clonogenic lethality may be due to exchange-type aberrations such as dicentrics and rings. But for lower doses and for low dose rates, such aberrations contribute less to lethality than do other, smaller-scale lesions, involving only one track and presumably involving at most one DSB (Sachs et al., 1997c).

## **Discussion: conclusions and challenges**

Studying aberrations with modern computational biology tools helps elucidate the underlying biophysical repair/misrepair mechanisms and interphase chromosome geometry. Mechanistic extrapolations to low doses, modeling aberration transmissibility in vivo, and modeling chromosomal instability are currently drawing considerable attention. Significant future challenges also include:

- Modeling chromosome aberration spectra, including intra-change size spectra, as fingerprints of radiation quality.
- Combining detailed track structure models with more realistic models of chromosome geometry, of cell nucleus architecture, of chromosome motion, and especially of DSB misrejoining.

- More systematic modeling of chromatid aberrations (compare Sipi et al., 2000).
- Extending PCC models (e.g. Wu et al., 1996), important because the process of aberration formation, rather than just the final configuration, is central.
- Quantitative models of other large-scale genome alterations, e.g. duplication and aneuploidy as occur in tumor cytogenetics, telomere fusions as suggested by ZooFISH in comparative genomics, etc. Closer integration of radiation cytogenetics with these other fields is needed.
- Importantly, clarifying the biological significance of aberrations compared to more frequent forms of damage such as

point mutations – does the large-scale nature of the genome alteration entailed in an aberration lead to especially important phenotypic changes, or are aberrations merely easier to observe?

There is still a lot to learn.

## Acknowledgements

We are grateful to Drs. J.R.K. Savage, M.N. Cornforth, B.D. Loucas, D.J. Brenner and R.D. Stewart for wide-ranging discussions.

## References

- Albright N: A Markov formulation of the repair-misrepair model of cell survival. *Radiat Res* 118:1–20 (1989).
- Anderson RM, Stevens DL, Goodhead DT: M-FISH analysis shows that complex chromosome aberrations induced by alpha-particle tracks are cumulative products of localized rearrangements. *Proc Natl Acad Sci, USA* 99:12167–12172 (2002).
- Anderson RM, Marsden SJ, Paice SJ, Bristow AE, Kadhim MA, Griffin CS, Goodhead DT: Transmissible and nontransmissible complex chromosome aberrations characterized by three-color and mFISH define a biomarker of exposure to high-LET alpha particles. *Radiat Res* 159:40–48 (2003).
- Andreev SG, Eidelman Y: Intrachromosomal exchange aberrations predicted on the basis of the globular interphase chromosome model. *Radiat Protect Dosimetry* 99:193–196 (2002).
- Bafna V, Pevzner PA: Genome rearrangements and sorting by reversals. *Siam J Comput* 25:272–289 (1996).
- Ballarini F, Biaggi M, Ottolenghi A: Nuclear architecture and radiation induced chromosome aberrations: models and simulations. *Radiat Protect Dosimetry* 99:175–182 (2002).
- Bauchinger M: Retrospective dose reconstruction of human radiation exposure by FISH/chromosome painting. *Mutat Res* 404:89–96 (1998).
- Bauchinger M, Schmid E: LET dependence of yield ratios of radiation-induced intra- and interchromosomal aberrations in human lymphocytes. *Intl J Radiat Biol* 74:17–25 (1998).
- Bauchinger M, Schmid E, Braselmann H: Experimental findings in human lymphocytes analyzed in first and second post-irradiation metaphases. *Radiat Environ Biophys* 25:253–260 (1986).
- Blakely WF, Brooks AL, Lofts RS, van der Schans GP, Voisin P: Overview of low-level radiation exposure assessment: biodosimetry. *Mil Med* 167:20–24 (2002).
- Boei JJWA, Vermeulen S, Natarajan AT: Analysis of radiation-induced chromosomal aberrations using telomeric and centromeric PNA probes. *Intl J Radiat Biol* 76:163–167 (2000).
- Boei JJWA, Vermeulen S, Mullenders LHF, Natarajan AT: Impact of radiation quality on the spectrum of induced chromosome exchange aberrations. *Intl J Radiat Biol* 77:847–857 (2001).
- Boyle S, Gilchrist S, Bridger JM, Mahy NL, Ellis JA, Bickmore WA: The spatial organization of human chromosomes within the nuclei of normal and emer-in-mutant cells. *Hum molec Genet* 10:211–219 (2001).
- Braselmann H, Bauchinger M, Schmid E: Cell survival and radiation induced chromosome aberrations. I. Derivation of formulae for the determination of transmission and survival parameters of aberrations. *Radiat Environ Biophys* 25:243–251 (1986).
- Brenner D, Ward J, Sachs R: Track structure, chromosome geometry and chromosome aberrations. *Basic Life Sci* 63:93–113 (1994).
- Chen AM, Lucas JN, Simpson PJ, Griffin CS, Savage JR, Brenner DJ, Hlatky LR, Sachs RK: Computer simulation of data on chromosome aberrations produced by X rays or alpha particles and detected by fluorescence in situ hybridization. *Radiat Res* 148:S93–101 (1997).
- Cigarrán S, Barrios L, Barquinero JF, Caballín MR, Ribas M, Egozcue J: Relationship between the DNA content of human chromosomes and their involvement in radiation-induced structural aberrations, analysed by painting. *Intl J Radiat Biol* 74:449–55 (1998).
- Cornforth MN: Analyzing radiation-induced complex chromosome rearrangements by combinatorial painting. *Radiat Res* 155:643–659 (2001).
- Cornforth MN, Bailey SM, Goodwin EH: Dose responses for chromosome aberrations produced in noncycling primary human fibroblasts by alpha particles, and by gamma rays delivered at sublimiting low dose rates. *Radiat Res* 158:43–53 (2002a).
- Cornforth MN, Greulich-KM, Loucas BD, Arsuaiga J, Vazquez M, Sachs RK, Bruckner M, Molls M, Hahnfeldt P, Hlatky L, Brenner DJ: Chromosomes are predominantly located randomly with respect to each other in interphase human cells. *J Cell Biol* 159:237–244 (2002b).
- Costes S, Sachs R, Hlatky L, Vannais D, Waldren C, Fouladi B: Low-LET, large-mutation spectra at hemizygous loci: evidence for intrachromosomal proximity effects. *Radiat Res* 156:545–557 (2001).
- Cremer M, von Hase J, Volm T, Brero A, Kreth G, Walter J, Fischer C, Solovei I, Cremer C, Cremer T: Non-random radial higher-order chromatin arrangements in nuclei of diploid human cells. *Chrom Res* 9:541–567 (2001).
- Cucinotta FA, Nikjoo H, O'Neill P, Goodhead DT: Kinetics of DSB rejoining and formation of simple chromosome exchange aberrations. *Intl J Radiat Biol* 76:1463–1474 (2000).
- de Jong H: Modeling and simulation of genetic regulatory systems: a literature review. *J Comput Biol* 9:67–103 (2002).
- Deng W, Morrison DP, Gale KL, Lucas JN: A comparative study on potential cytogenetic fingerprints for radiation LET in human lymphocytes. *Intl J Radiat Biol* 76:1589–1598 (2000).
- Durante M, George K, Wu H, Cucinotta FA: Karyotypes of human lymphocytes exposed to high-energy iron ions. *Radiat Res* 158:581–590 (2002).
- Edwards AA: Modelling radiation-induced chromosome aberrations. *Intl J Radiat Biol* 78:551–558 (2002).
- Erdi P, Toth J: Mathematical models of chemical reactions: theory and applications of deterministic and stochastic models. (Manchester University Press, Manchester 1989).
- Fomina J, Darroudi F, Natarajan AT: Accurate detection of true incomplete exchanges in human lymphocytes exposed to neutron radiation using chromosome painting in combination with a telomeric PNA probe. *Intl J Radiat Biol* 77:1175–1183 (2001).
- Friedland W, Li WB, Jacob P, Paretzke HG: Simulation of exon deletion mutations induced by low-LET radiation at the HPRT locus. *Radiat Res* 155:703–715 (2001).
- Friedland W, Jacob P, Bernhardt P, Paretzke HG, Dingfelder M: Simulation of DNA damage after proton irradiation. *Radiat Res* 159:401–410 (2003).
- Gardner SN, Tucker JD: The cellular lethality of radiation-induced chromosome translocations in human lymphocytes. *Radiat Res* 157:539–552 (2002).
- George K, Durante M, Willingham V, Wu H, Yang TC, Cucinotta FA: Biological effectiveness of accelerated particles for the induction of chromosome damage measured in metaphase and interphase human lymphocytes. *Radiat Res* 160:425–435 (2003).
- Goodhead DT, Thacker J, Cox R: Weiss Lecture. Effects of radiations of different qualities on cells: molecular mechanisms of damage and repair. *Intl J Radiat Biol* 63:543–556 (1993).
- Greulich KM, Kreja L, Heinze B, Rhein AP, Weier H-UG, Brückner M, Fuchs P, Molls M: Rapid detection of radiation-induced chromosomal aberrations in lymphocytes and hematopoietic progenitor cells by mFISH. *Mutat Res* 452:73–81 (2000).
- Griffin CS, Marsden SJ, Stevens DL, Simpson P, Savage JRK: Frequencies of complex chromosome exchange aberrations induced by 238Pu alpha-particles and detected by fluorescence in situ hybridization using single chromosome-specific probes. *Intl J Radiat Biol* 67:431–439 (1995).
- Guerrero M, Stewart RD, Wang JZ, Li XA: Equivalence of the linear-quadratic and two-lesion kinetic models. *Physic Med Biol* 47:3197–3209 (2002).
- Hahnfeldt P, Sachs RK, Hlatky LR: Evolution of DNA damage in irradiated cells. *J Math Biol* 30:493–511 (1992).
- Hahnfeldt P, Hearst JE, Brenner DJ, Sachs RK, Hlatky LR: Polymer models for interphase chromosomes. *Proc Natl Acad Sci, USA* 90:7854–7858 (1993).

- Hande MP, Azizova TV, Geard CR, Burak LE, Mitchell CR, Khokhryakov VF, Vasilenko EK, Brenner DJ: Past exposure to densely ionizing radiation leaves a unique permanent signature in the genome. *Am J Hum Genet* 72:1162–1170 (2003).
- Hlatky L, Sachs RK, Hahnfeldt P: The ratio of dicentric to centric rings produced in human lymphocytes by acute low-LET radiation. *Radiat Res* 129:304–308 (1992).
- Hlatky L, Sachs R, Vazquez M, Cornforth M: Radiation-induced chromosome aberrations: insights gained from biophysical modeling. *Bioessays* 24:714–723 (2002).
- Holley WR, Mian IS, Park SJ, Rydberg B, Chatterjee A: A model for interphase chromosomes and evaluation of radiation-induced aberrations. *Radiat Res* 158:568–580 (2002).
- ISCN (1995): An International System for Human Cytogenetic Nomenclature, Mitelman F (ed) (S. Karger, Basel 1995).
- Johnson KL, Brenner DJ, Nath J, Tucker JD, Geard CR: Radiation-induced breakpoint misrejoining in human chromosomes: random or non-random? *Intl J Radiat Biol* 75:131–141 (1999).
- Kellerer A, Rossi H: A generalized formulation of dual radiation action. *Radiat Res* 75:471–488 (1978).
- Knehr S, Zitzelsberger H, Braselmann H, Nahrstedt U, Bauchinger M: Chromosome analysis by fluorescence in situ hybridization: further indications for a non-DNA-proportional involvement of single chromosomes in radiation-induced structural aberrations. *Intl J Radiat Biol* 70:385–392 (1996).
- Knehr S, Huber R, Braselmann H, Schraube H, Bauchinger M: Multicolour FISH painting for the analysis of chromosomal aberrations induced by 220 kV X-rays and fission neutrons. *Intl J Radiat Biol* 75:407–418 (1999).
- Kodama Y, Pawel D, Nakamura N, Preston D, Honda T, Itoh M, Nakano M, Ohtaki K, Funamoto S, Awa AA: Stable chromosome aberrations in atomic bomb survivors: results from 25 years of investigation. *Radiat Res* 156:337–346 (2001).
- Kreth G, Munkel C, Langowski J, Cremer T, Cremer C: Chromatin structure and chromosome aberrations: modeling of damage induced by isotropic and localized irradiation. *Mutat Res* 404:77–88 (1998).
- Levy D, Sachs RK: Test applet for analyzing cycle structure and apparent incompleteness (<http://radiobiology.berkeley.edu/CAA/>) (2003).
- Levy D, Vazquez M, Cornforth MN, Loucas BD, Sachs RK, Arsuaga J: Comparing DNA damage-processing pathways by computer analysis of chromosome painting data. *J Comput Biol*, in press (2003).
- Lloyd DC, Edwards AA: Chromosome aberrations in human lymphocytes: effect of radiation quality, dose, and dose rate; in Ishihara T, Sasaki MS (eds): *Radiation-Induced Chromosome Damage in Man*. (Alan R Liss, New York 1983).
- Lorimore SA, Wright EG: Radiation-induced genomic instability and bystander effects: related inflammatory-type responses to radiation-induced stress and injury? A review. *Intl J Radiat Biol* 79:15–25 (2003).
- Loucas BD, Cornforth MN: Complex chromosome exchanges induced by gamma rays in human lymphocytes: an mFISH study. *Radiat Res* 155:660–671 (2001).
- Lucas JN: Translocation frequencies for low to moderate doses remain constant over time. *Intl J Radiat Biol* 75:655–656 (1999).
- Mitelman F, Johansson B, Mertens F: Mitelman Database of Chromosome Aberrations in Cancer (<http://cgap.nci.nih.gov/Chromosomes/Mitelman>) (2002).
- Morgan WF: Non-targeted and delayed effects of exposure to ionizing radiation. II. Radiation-induced genomic instability and bystander effects in vivo, clastogenic factors and transgenerational effects. *Radiat Res* 159:581–596 (2003).
- Munkel C, Eils R, Dietzel S, Zink D, Mehning C, Wedeman G, Cremer T, Langowski J: Compartmentalization of interphase chromosomes observed in simulation and experiment. *J molec Biol* 285:1053–1065 (1999).
- Natarajan AT: Chromosome aberrations: past, present and future. *Mutat Res* 504:3–16 (2002).
- Obe G, Pfeiffer P, Savage JR, Johannes C, Goedecke W, Jeppesen P, Natarajan AT, Martinez-Lopez W, Folle GA, Drets ME: Chromosomal aberrations: formation, identification and distribution. *Mutat Res* 504:17–36 (2002).
- Ostashevsky JY: Higher-order structure of interphase chromosomes and radiation-induced chromosomal exchange aberrations. *Intl J Radiat Biol* 76:1179–1187 (2000).
- Ottolenghi A, Ballarini F, Biaggi M: Modelling chromosomal aberration induction by ionising radiation: the influence of interphase chromosome architecture. *Adv Space Res* 27:369–382 (2001).
- Parada L, Misteli T: Chromosome positioning in the interphase nucleus. *Trends Cell Biol* 12:425–432 (2002).
- Pevzner P, Tesler G: Human and mouse genomic sequences reveal extensive breakpoint reuse in mammalian evolution. *Proc Natl Acad Sci USA* 100:7672–7677 (2003).
- Radford IR: Transcription-based model for the induction of interchromosomal exchange events by ionizing irradiation in mammalian cell lines that undergo necrosis. *Intl J Radiat Biol* 78:1081–1093 (2002).
- Radvoyevitch T, Hoel DG, Chen AM, Sachs RK: Misrejoining of double-strand breaks after X irradiation: relating moderate to very high doses by a Markov model. *Radiat Res* 149:59–67 (1998).
- Radvoyevitch T, Kozubek S, Sachs R: Biologically based risk estimation for radiation-induced CML – inferences from BCR and ABL geometric distributions. *Radiat Environ Biophys* 40:1–9 (2001).
- Sabatier L, Al Achkar W, Hoffschir F, Luccioni C, Dutrillaux B: Qualitative study of chromosomal lesions induced by neutrons and neon ions in human lymphocytes at G<sub>0</sub> phase. *Mutat Res* 178:91–97 (1987).
- Sachs RK, Brenner DJ: “Chromosome Aberrations Produced by Ionizing Radiation: Quantitative Studies”. Beta-test version of part of an NCBI Bookshelf Internet Textbook (2003). PubMed, National Center for Biotechnology Information, NLM, NIH. [http://web.ncbi.nlm.nih.gov/books/bv.fcgi?call=bv.View..ShowSection&rid=mono\\_002](http://web.ncbi.nlm.nih.gov/books/bv.fcgi?call=bv.View..ShowSection&rid=mono_002)
- Sachs RK, van den Engh G, Trask B, Yokota H, Hearst JE: A random-walk/giant-loop model for interphase chromosomes. *Proc natl Acad Sci, USA* 92:2710–2714 (1995).
- Sachs RK, Brenner DJ, Chen AM, Hahnfeldt P, Hlatky LR: Intra-arm and interarm chromosome intrachanges: tools for probing the geometry and dynamics of chromatin. *Radiat Res* 148:330–340 (1997a).
- Sachs RK, Chen AM, Brenner DJ: Review: proximity effects in the production of chromosome aberrations by ionizing radiation. *Intl J Radiat Biol* 71:1–19 (1997b).
- Sachs RK, Hahnfeldt P, Brenner DJ: The link between low-LET dose-response relations and the underlying kinetics of damage production/repair/misrepair. *Intl J Radiat Biol* 72:351–374 (1997c).
- Sachs RK, Chen AM, Simpson PJ, Hlatky LR, Hahnfeldt P, Savage JR: Clustering of radiation-produced breaks along chromosomes: modelling the effects on chromosome aberrations. *Intl J Radiat Biol* 75:657–672 (1999).
- Sachs RK, Levy D, Chen AM, Simpson PJ, Cornforth MN, Ingerman EA, Hahnfeldt P, Hlatky LR: Random breakage and reunion chromosome aberration formation model: an interaction-distance version based on chromatin geometry. *Intl J Radiat Biol* 76:1579–1588 (2000a).
- Sachs RK, Rogoff A, Chen AM, Simpson PJ, Savage JR, Hahnfeldt P, Hlatky LR: Underprediction of visibly complex chromosome aberrations by a re-combinational-repair (“one-hit”) model. *Intl J Radiat Biol* 76:129–148 (2000b).
- Sachs RK, Arsuaga J, Vazquez M, Hlatky L, Hahnfeldt P: Using graph theory to describe and model chromosome aberrations. *Radiat Res* 158:556–567 (2002).
- Sasaki MS: Chromosomal biodosimetry by unfolding a mixed poisson distribution: a generalized model. *Intl J Radiat Biol* 79:83–98 (2003).
- Savage JRK: Testing the participation of chromosomes in structural aberrations; in Sobti RC, Obe G (eds): *Eukaryotic Chromosomes: Structural and Functional Aspects* (Narosa Press, New Delhi 1991).
- Savage JRK: A brief survey of aberration origin theories. *Mutat Res* 404:139–147 (1998).
- Savage JR: Reflections and meditations upon complex chromosomal exchanges. *Mutat Res* 512:93–109 (2002).
- Savage JRK, Papworth DG: Frequency and distribution studies of asymmetrical versus symmetrical chromosome aberrations. *Mutat Res* 95:7–18 (1982).
- Savage JR, Papworth DG: An investigation of LET “finger-prints” in *Tradescantia*. *Mutat Res* 422:313–322 (1998).
- Schmid E, Braselmann H, Bauchinger M: Does the limiting F value at very low doses depend systematically on linear energy transfer? *Radiat Res* 152:563–566 (1999).
- Singleton BK, Griffin CS, Thacker J: Clustered DNA damage leads to complex genetic changes in irradiated human cells. *Cancer Res* 62:6263–6269 (2002).
- Sipi P, Lindholm C, Salomaa S: Kinetics of formation of exchanges and rejoining of breaks in human G<sub>0</sub> and G<sub>2</sub> lymphocytes after low-LET radiation. *Intl J Radiat Biol* 76:823–830 (2000).
- Stewart RD: Two-lesion kinetic model of double-strand break rejoining and cell killing. *Radiat Res* 156:365–378 (2001).
- Tucker JD: Fish cytogenetics and the future of radiation biodosimetry. *Radiat Protect Dosimetry* 97:55–60 (2001).
- Vázquez M, Greulich-Bode K, Arsuaga J, Cornforth M, Brückner M, Sachs R, Hahnfeldt P, Molls M, Hlatky L: Computer analysis of mFISH chromosome aberration data uncovers an excess of very complex metaphases. *Intl J Radiat Biol* 78:1103–1116 (2002).
- Wu H, Durante M: A biophysical model for estimating the frequency of radiation-induced mutations resulting from chromosomal translocations. *Adv Space Res* 27:361–367 (2001).
- Wu H, Durante M, George K, Goodwin EH, Yang TC: Rejoining and misrejoining of radiation-induced chromatin breaks. II. Biophysical model. *Radiat Res* 145:281–288 (1996).
- Wu H, Durante M, Lucas JN: Relationship between radiation-induced aberrations in individual chromosomes and their DNA content: effects of interaction distance. *Intl J Radiat Biol* 77:781–786 (2001).
- Wu H, Durante M, Furusawa Y, George K, Kawata T, Cucinotta FA: M-Fish analysis of chromosome aberrations in human fibroblasts exposed to energetic iron ions in vitro. *Adv Space Res* 31:1537–1542 (2003a).
- Wu H, Durante M, Furusawa Y, George K, Kawata T, Cucinotta FA: Truly incomplete and complex exchanges in prematurely condensed chromosomes of human fibroblasts exposed in vitro to energetic heavy ions. *Radiat Res* 160:418–424 (2003b).

# Models of chromosome aberration induction: an example based on radiation track structure

F. Ballarini and A. Ottolenghi

Università degli Studi di Pavia, Dipartimento di Fisica Nucleare e Teorica, INFN – National Institute of Nuclear Physics, Pavia (Italy)

**Abstract.** A few examples of models of chromosome aberration induction are summarised and discussed on the basis of the three main theories of aberration formation, that is “breakage-and-reunion”, “exchange” and “one-hit”. A model and code developed at the Universities of Milan and Pavia is then presented in detail. The model provides dose-response curves for different aberration types (dicentrics, translocations, rings, complex exchanges and deletions) induced in human lymphocytes by gamma rays, protons and alpha particles of different energies, both as monochromatic fields and as mixed fields. The main assumptions are that only clustered – and thus severe – DNA breaks (“Complex Lesions”, CL) can participate in the production of aberrations, and that only break free ends in neighbouring chromosome territories can interact and form exchanges. The yields of CLs induced by the various radiation types of interest are taken from a previous modelling work. These lesions are distributed within a sphere representing the

cell nucleus according to the radiation track structure, e.g. randomly for gamma rays and along straight lines for light ions. Interphase chromosome territories are explicitly simulated and configurations are obtained in which each chromosome occupies an intranuclear domain with volume proportional to its DNA content. In order to allow direct comparisons with experimental data, small fragments can be neglected since usually they cannot be detected in experiments. The presence of a background level of aberrations is also taken into account. The results of the simulations are in good agreement with experimental dose-response curves available in the literature, that provides a validation of the model both in terms of the adopted assumptions and in terms of the simulation techniques. To address the question of “true” incompleteness, simulations were also run in which all fragments were assumed to be visible.

Copyright © 2003 S. Karger AG, Basel

It is well known that cells exposed to ionising radiation during the  $G_0/G_1$  phase of the cell cycle can show different types of chromosome aberrations including dicentrics, translocations, rings, inversions and complex exchanges, the latter usually defined as rearrangements involving at least three breaks and two chromosomes. An exhaustive classification of the various aberration types has been provided by Savage and Simpson

(1994). In the majority of the experimental studies available in the literature, chromosome aberrations are observed at the first post-irradiation metaphase. However, Premature Chromosome Condensation (PCC) techniques, based either on fusion with mitotic cells or on chemical treatments (Durante et al., 1998), allow observation of aberrations at any time after irradiation. This can help minimising possible biases introduced by phenomena such as cell cycle perturbation and interphase death, which occur with significant probability after exposure to high-dose and/or high-LET radiation. For a long time the experimental observations have been based on Giemsa staining. The introduction of the Fluorescence In Situ Hybridisation (FISH) technique (Pinkel et al., 1986) represented a fundamental turn, allowing selective painting of specific homologue pairs and thus detection of aberration types that are not visible with solid staining, such as translocations and the majority of complex exchanges. The possibility of scoring translocations is of

Supported by the EC (contract no. FIGH-CT1999-00005, “Low Dose Risk Models”) and the Italian Space Agency (contract no. I/R/320/02, “Influence of the shielding on the space radiation biological effectiveness”).

Received 10 September 2003; manuscript accepted 10 November 2003.

Request reprints from Dr. Francesca Ballarini, Università degli Studi di Pavia  
Dipartimento di Fisica Nucleare e Teorica, via Bassi 6  
I-27100 Pavia (Italy); telephone: +39 02 50317399 or +39 0382 507906  
fax: +39 02 50317630; e-mail: francesca.ballarini@mi.infn.it

particular importance, since reciprocal translocations between specific chromosomes have been shown to be correlated with specific tumour types. Typical examples are the BCR-ABL translocation for chronic myeloid leukemia, which involves the ABL gene on chromosome 9 and the BCR gene on chromosome 22 (Mitelman, 2000), and the PML-RAR $\alpha$  translocation for acute promyelocytic leukemia, which involves chromosomes 15 and 17 (de The et al., 1991; Faretta et al., 2001). Causal relationships between aberrations and cancer have also been proposed (Bonassi et al., 2000), and chromosome aberration yields in human lymphocytes have been used to perform estimates of radiation cancer risk (Durante et al., 2001; Radivoyevitch et al., 2001). The recent introduction of the so-called "multi-FISH" technique, which allows painting of each homologue pair with a different colour, has provided further information, especially on the induction of very complex exchanges involving large numbers of chromosomes (Cornforth, 2001; Anderson et al., 2002; Durante et al., 2002). On this subject, it is worthwhile mentioning that complex exchanges have been proposed as possible "biomarkers" of the radiation quality (Anderson et al., 2002), that can have applications in biodosimetry (Durante, 1996, 2002; Edwards 1997; Ballarini and Ottolenghi, 2003).

Despite the significant advances in the experimental techniques and the large amount of available data, some aspects of the mechanisms underlying the induction of chromosome aberrations have not been fully elucidated yet. For example it is still not clear whether any DNA double-strand break (DSB) can participate in the formation of chromosome aberrations, or if more severe (i.e. clustered) breaks are required (Sachs and Brenner, 1993). Furthermore, while it is widely recognised that only breaks sufficiently close in space can interact and form exchanges, the relationship linking the initial distance between two breaks and their interaction probability is still not known: both exponentially decreasing functions (Edwards et al., 1994, 1996; Sachs et al., 2000a) and step functions (Brenner, 1988; Ballarini et al., 2002a; Ballarini and Ottolenghi, 2003) have been applied with equal success. Another object of debate is the possibility of having an exchange starting from a single radiation-induced chromosome break, which may lead to a (simple) exchange-type aberration mediated through subsequent induction of a second break by the enzymatic mechanisms involved in DNA repair (Chadwick and Leenhouts, 1978).

Theoretical models and simulation codes can be of great help both as interpretative tools, for elucidating the underlying mechanisms, and as predictive tools, for performing extrapolations where experimental data are not available, typically at low doses and/or low dose rates. In this paper we will discuss a few examples of available models, generally tested in different specific scenarios, and we will present a model based on radiation track structure, focusing on the main assumptions adopted and on the conclusions that can be drawn by comparing the model predictions to experimental data. Far from being exhaustive, the survey presented in the next section has the main aim of providing at least one example for each of the three "historical" theories of chromosome aberration induction ("breakage-and-reunion" theory, "exchange" theory and "one-hit" theory, see below). More extensive reviews, which are beyond the

scope of this paper, can be found elsewhere (Savage, 1998; Ottolenghi et al., 1999; Edwards, 2002; Hlatky et al., 2002; Natarajan, 2002; Sachs et al., this issue).

### Examples of models of chromosome aberration induction

Before the discovery of the DNA structure, earlier Stadler (1930) and later Sax (1940) introduced the so-called "breakage-and-reunion" theory, which was then formalized by Lea (1946). According to this theory, the induction of exchange-type chromosome aberrations can be described with the production of chromosome breaks by radiation and subsequent pairwise misrejoining of break free ends that are sufficiently close in time and space, provided that each break gives rise to two independent free ends. According to this model, subsequently reformulated by Harder (1988), chromosome breaks are one-hit events and increase linearly with dose, whereas exchange-type aberrations are two-hit events and show a linear-quadratic dose dependence. As an alternative, the "exchange theory" developed by Revell (1963) relies on the hypothesis that all aberrations are exchanges between pairs of radiation-induced "unstable" chromosome lesions, which can either "decay" or become "reactive" and give rise to aberrations by pairwise interaction. Both the breakage-and-reunion theory and the exchange theory require at least two radiation-induced chromosome breaks to form an exchange. However, it has been hypothesised that (simple) chromosome exchanges may also arise from a single radiation-induced break, the second break being produced by enzymatic mechanisms during the DNA repair process ("one-hit" theory, Chadwick and Leenhouts, 1978). This model has received support by the lack of a significant non-linear component in experimental dose-response curves relative to the induction of simple exchanges by Ultrasoft X-rays (Griffin et al., 1998). With the exception of low-energy X-rays, the data obtained following irradiation of mammalian cells in the G<sub>0</sub>/G<sub>1</sub> phase of the cell cycle seem to be more consistent with the breakage-and-reunion model (Sachs et al., 2000b). However, none of these "historical" theories can be rejected on the basis of the currently available knowledge, and all of them have been successfully applied to specific scenarios. Examples were provided by Sachs et al. (2000a), Holley et al. (2002), Ballarini et al. (1999, 2002a) and Ballarini and Ottolenghi (2003) for the breakage-and-reunion model, by Edwards et al. (1994, 1996) for the exchange model and by Cucinotta et al. (2000) for the one-hit model.

#### *Two "breakage-and-reunion" models*

Sachs et al. (2000a) modelled the induction of simple and complex aberrations in human fibroblasts by assuming that chromosome exchanges arise from misrejoining of DSB free ends sufficiently close to each other. Fibroblast nuclei were represented as cylinders and interphase chromosome territories were modelled as intra-nuclear cylinders with radius proportional to the square root of their DNA content. The various territories were allowed to intersect according to a "territory intersection factor" defined as the volume that a pair of territories have in common, summed over all chromosome pairs and

divided by the nucleus volume; this factor was taken as an adjustable parameter. Different configurations for the 46 human chromosomes in the nucleus were obtained with a simulated annealing algorithm. DSBs induced by low-LET radiation were positioned randomly. The misrejoining probability for free ends originated from two DSB with initial distance  $L$  was taken as proportional to  $\exp(-L/L_0)$ , where  $L_0$  is the second adjustable parameter of the model. A third adjustable parameter was introduced to quantify the competition between restitution (i.e. eurejoining, that is rejoining with the original partner) and misrejoining. With an average interaction distance of  $1.5 \mu\text{m}$  and an average territory intersection factor of 1.1, the results showed good agreement with FISH data obtained by irradiation of human fibroblasts with hard X-rays.

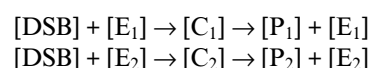
In a model developed by Chatterjee and co-workers for aberration induction in human lymphocytes (Holley et al., 2002), interphase chromatin structure was explicitly taken into account by modelling each of the 46 human chromosomes as a random polymer inside a spherical volume. The chromosome spheres were packed randomly within a spherical nucleus. Overlapping, controlled by an adjustable parameter, was allowed. The induction of DSBs was modelled on the basis of the radiation track structure. As in the work of Sachs et al. (2000a), chromosome exchanges were assumed to arise from pairwise misrejoining of close DSB free ends. Rejoining was modelled on the basis of a Gaussian proximity function controlled by an interaction range parameter. With an overlap parameter of 0.675 and an interaction range of  $0.5 \mu\text{m}$ , the calculated yields of interchromosomal exchanges were found to be in good agreement with various experimental data sets relative to low-LET irradiation of human lymphocytes.

#### *A Revell-type model*

Edwards et al. (1994, 1996) applied the exchange theory of Revell to the prediction of dicentric yields in human lymphocytes following irradiation with different radiation types. Lymphocyte nuclei were modelled as  $3\text{-}\mu\text{m}$  radius spheres in which chromosomal DNA was distributed randomly. The radiation tracks were simulated with an "event-by-event" track structure code. An average yield of  $50 \text{ DSB} \cdot \text{Gy}^{-1} \cdot \text{cell}^{-1}$  was assumed, and the DSBs were located in correspondence with the ionisation positions provided by track structure simulations. Each ionisation was assumed to have an equal chance of inducing a DSB and each DSB was assumed to be able to participate in the production of aberrations, regardless of the break complexity. Exchange-type aberrations were assumed to form following interaction of pairs of DSBs sufficiently close to each other. The ratio of exchange to no-exchange probability between two DSB was expressed as  $bl^{-n}$ , where  $l$  is the initial DSB separation and  $b$  and  $n$  are adjustable parameters. Half the exchanges were scored as dicentrics, the other half as translocations. Comparisons between calculated and experimental values of  $\alpha$  and  $\beta$  (i.e. the linear and quadratic coefficients usually adopted to describe dose-response curves) led to  $n = 1.2$  and  $b = 0.0003$ . With these values, very good agreement was found with low-LET data, whereas dicentric yields following high-LET irradiation were underestimated by a factor of about 1.5–2.0.

#### *A "one-hit" model*

The one-hit hypothesis was applied to the induction of simple chromosome exchanges following (hard) X-ray irradiation by Cucinotta et al. (2000). Simple exchanges by hard X-rays are generally assumed to arise from interaction between two radiation-induced chromosome breaks. However, data exist suggesting that also for hard X-rays, simple exchanges can be produced by a single radiation-induced break (Simpson and Savage, 1996). According to the analytical model of Cucinotta et al. (2000), simple exchanges can be produced following the formation of repair enzyme-DNA complexes, whose processing can result either in DSB restitution, or in simple exchanges such as dicentrics. These processes were formalised as follows:



The letters E, C and P refer to repair enzymes, enzyme-DNA complexes and reaction products (simple exchanges or restituted DSBs), respectively. The square brackets represent the corresponding concentrations, whereas the subscripts refer to the two competing processes (misrepair or restitution). By solving the differential equations for  $[\text{DSB}]$ ,  $[\text{C}_1]$  and  $[\text{C}_2]$  and by describing the formation of an exchange of type  $m$  with the equation  $d[A_m]/dt = k_{2m} \cdot [\text{C}_1]$ , where  $k_2$  is the rate of the reaction  $[\text{C}_1] \rightarrow [\text{P}_1] + [\text{E}_1]$ , the authors calculated dicentric yields as a function of both the repair time and the irradiation dose. The non-linear component in the calculated dose-response curves arose naturally from the introduction of a competition process between two different DNA repair pathways. Good agreement was found with experimental data relative to human lymphocytes irradiated with hard X-rays. It is worthwhile mentioning that the authors themselves stated that both the one-hit mechanism and the pairwise interaction mechanism can contribute to the induction of chromosome exchanges.

#### **A model based on radiation track structure and interphase chromosome organisation**

Development of a mechanistic model and a Monte Carlo code able to simulate chromosome aberration induction began in 1999 at the Universities of Milano and Pavia (Ballarini et al., 1999). The current version of the model (Ballarini and Ottolenghi, 2003) provides dose-response curves for various aberration types (dicentrics, translocations, centric and acentric rings, different categories of complex exchanges and excess acentric fragments) induced by gamma rays, protons and alpha particles of different energies, both as monochromatic fields and as mixed fields. The model is stochastic, because distributions are used rather than average values, and ab initio, because the model predictions can be directly compared with available experimental data without performing any fit of free parameters.

#### *Assumptions*

The following basic assumptions were adopted: I) only clustered DNA damage ("Complex Lesions" or CL, see below) can participate in aberration production; II) CLs are distributed in



the cell nucleus according to the radiation track structure, e.g. randomly for gamma rays and along straight lines for light ions; III) each CL gives rise to two independent chromosome free-ends; IV) only free ends with initial distance smaller than a certain cutoff value  $d$  can interact and form exchanges; V) all free ends finally interact with a partner (“completeness”, see below).

The assumption of a major role of clustered – and thus severe – DNA damage, already adopted by Sachs and Brenner (1993), mainly relies on that while “simple” DSBs do not show significant dependence on radiation quality, clustered breaks increase with the radiation LET and depend on the radiation type (Ottolenghi et al., 1995; Nikjoo et al., 1997). This is consistent with the LET- and particle-type dependence found in experiments on gene mutation and cell killing (Belli et al., 1992). More generally, DNA clustered damage is thought to play an important role in the induction of various endpoints at chromosome and cell level (e.g. Goodhead, 1994). In our model such damage was quantified by introducing the so-called “Complex Lesions”, which in a previous work (Ottolenghi et al., 1995) have been operationally defined as “at least two single-strand breaks on each of the two DNA strands within 30 base pairs” and have been calculated for different radiation types with an “event-by-event” track structure code. The hypothesis of a major role of Complex Lesions is supported by previous works in which CLs have been assumed to lead to clonogenic cell inactivation (Ottolenghi et al., 1997; Biaggi et al., 1999). Systematic, early repair of non-clustered DNA damage is implicitly included in assumption I), since clustered lesions are considered to be long-lived breaks (Sachs and Brenner, 1993).

Assumption IV) reflects the evidence that during interphase the various chromosomes are localized within essentially distinct intra-nuclear territories (e.g. Cremer et al., 1993; Visser and Aten, 1999) and that DNA repair, as well as other functions such as DNA replication and RNA transcription, are likely to occur within a network of channels separating neighbouring domains (Zirbel et al., 1993). The value of the interaction distance  $d$  was fixed at 1.5  $\mu\text{m}$  on the basis of the average distance between the mass centres of two neighbouring chromosome territories (see below). This number is consistent with values adopted by other authors with different modelling approaches (Kellerer, 1985; Savage, 1996; Ostashevsky, 2000; Sachs et al., 2000a).

Concerning assumption V), the question whether incomplete exchanges really occur with significant probability has been the object of debate for a long time. Recently, experiments with telomere probes showed that true incomplete exchanges are rare, and that most incompletes observed experimentally are due to the involvement of small fragments that cannot be detected (Boei et al., 1998; Fomina et al., 2000; Loucas and Cornforth, 2001; Holley et al., 2002).

#### *Simulation of dose-response curves*

In our model, human lymphocyte nuclei are represented as 3- $\mu\text{m}$  radius spheres. The 46 chromosome territories are described as (irregular) compact domains with volume proportional to their DNA content, each domain consisting of the uni-

on of small adjacent cubic elements. Details on the algorithm adopted to simulate interphase chromosome territories can be found elsewhere (Ballarini et al., 2002a; Ballarini and Ottolenghi, 2003). Herein it is sufficient to mention that the various territories are distributed randomly in the nucleus and that repetition of the process allows obtaining a statistically significant number of different configurations. Indeed specific chromosomes have been shown to occupy preferential relative positions in human cells (Nagele et al., 1999); in particular, gene-rich chromosomes tend to be located within the nucleus interior (Kozubek et al., 1999). It has also been found that, while the distances of the various chromosomes from the nucleus centre are not distributed randomly, the angular distributions are random (Kozubek et al., 2002). Since no clear-cut conclusion can be drawn yet due to the existence of conflicting evidence (Cornforth et al., 2002; Obe et al., 2002), the implementation of non-random chromosome distributions in theoretical models is premature and may result in biases. However, this aspect will need to be reconsidered in the future when more soundly-based data become available. It is worthwhile outlining that the approach adopted in our model does *not* reflect a static view of the cell nucleus. In fact each of the configurations obtained as described above refers to the instant of irradiation. The assumption that interaction occurs only between chromosome break free ends with *initial* distance smaller than  $d$  takes into account that during cell cycle progression, small-scale chromatin movement can occur. Large-scale chromosome movement is not included in the model, since it has been shown to be significant during mitosis but not during interphase (Lucas and Cervantes, 2002). The presence of a background level of aberrations is implicitly taken into account. More specifically, the average number of Complex Lesions giving rise to an average of 0.001 dicentric per cell, which is the value usually accepted as a dicentric background in human lymphocytes, was identified for each radiation of interest. These lesions, which were assumed to follow a Poisson distribution, are randomly distributed in the cell nucleus before starting to simulate irradiation. This technique represents a first, pragmatic approach aimed to obtain dicentric dose responses that can be directly compared with dicentric experimental data also at low doses. This approach, which would (incorrectly) predict that the background dicentric yield is the same as the translocation yield, will be modified by explicit implementation of specific background values for each aberration type.

To simulate irradiation with photons, for a given cell and a given dose value an actual number of CL is extracted from a Poisson distribution. These lesions are randomly distributed in the cell nucleus. By contrast, for a given dose of light ions of given LET – and thus a given average number of nucleus traversals – an actual number of (parallel) traversals is extracted from a Poisson distribution. The point where each particle track enters the nucleus is selected randomly and determines the traversal length. The average number of lesions induced by a given track is calculated by multiplying the corresponding traversal length by the yield of Complex Lesions per unit length, which is calculated as follows:  $\text{CL} \cdot \mu\text{m}^{-1} = (\text{CL} \cdot \text{Gy}^{-1} \cdot \text{cell}^{-1}) \cdot 0.16 \cdot \text{LET} \cdot V^{-1}$ . LET is the radiation Linear Energy Transfer in  $\text{keV}/\mu\text{m}$ ,  $V$  is the cell nucleus volume in  $\mu\text{m}^3$  and

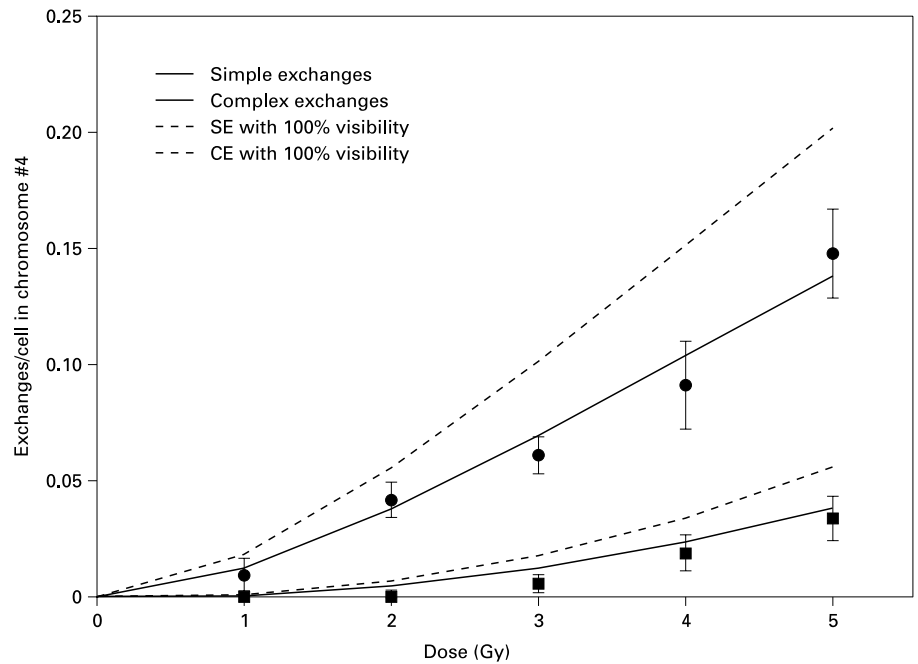


**Fig. 1.** Simple and complex exchanges (upper and lower solid lines, respectively) involving chromosome 4 following gamma-ray irradiation of human lymphocytes. The lines are model predictions, the points are FISH experimental data taken from Wu et al. (1997). Also reported are the corresponding curves obtained by assuming that fragments of any size can be scored (upper dashed line for simple exchanges and lower dashed line for complex exchanges).

0.16 is a factor deriving from the conversion of Joules into eVs. Both for gamma rays and for light ions, if the cell experiences one CL restitution is assumed, whereas if there are two or more CLs the spatial coordinates of the lesions are compared to those of the centres of the cubic elements constituting the various chromosome territories, which allows identification of the hit chromosome(s). Each CL is then assigned to one of the two chromosome arms according to the arm genomic size. On the basis of Lea's breakage-and-reunion theory, chromosome free ends with initial distance smaller than an interaction distance  $d$  are allowed to interact pairwise and randomly, thus giving rise to different types of chromosome exchanges. More specifically, a free end is extracted and its coordinates are compared with those of all other free ends. A partner for rejoining is then extracted among those free ends that are within  $1.5 \mu\text{m}$  with respect to the selected free end (a partner always exists, that is the other free end originated by the same CL). The product of the interaction is recorded, the two interacting free ends are eliminated, a new free end is extracted among the remaining free ends and the process restarts. In order to reproduce as closely as possible the experimental conditions characterising the specific data sets chosen for comparison, fragments smaller than a few Mb (11 Mb for FISH and 15 Mb for the counterstaining according to Kodama et al., 1997) are usually neglected in the simulations. Under these conditions, (false) incomplete exchanges are scored in the simulations even though completeness is assumed. Repetition of the steps described above for a large number of cells (at least 100,000) allows obtaining statistically significant aberration yields, whereas repetition for different dose values provides dose-response curves directly comparable with available experimental data.

## Results and discussion

Simulated dose-response curves for different aberration types were obtained for gamma rays, protons and alpha particles. As expected, gamma rays and low-LET protons showed linear-quadratic dose responses, whereas the response to high-LET alpha particles was essentially linear. Very good agreement was found with various sets of Giemsa data (dicentric and centric rings in human lymphocytes) for all of the considered radiation types, thus providing a validation of the model both in terms of the adopted assumptions and in terms of the simulation techniques. Results relative to the induction of dicentric and centric rings by gamma rays, low-LET (5 keV/ $\mu\text{m}$ ) protons and high-LET (86 keV/ $\mu\text{m}$ ) alpha particles can be found elsewhere (Ballarini and Ottolenghi, 2003). Comparisons could be performed down to low doses, since data were available down to 0.05 Gy. The implementation of background aberrations was a crucial point at low LET. In fact in a previous version of the model (Ballarini et al., 2002a), in which the background was not taken into account, the gamma-ray data below 0.1 Gy were underestimated. By contrast, no significant difference was found with the previous version in the case of high-LET alpha particles. This is due to the observation that for 86 keV/ $\mu\text{m}$  alpha particles, even at doses of a few cGy the number of dicentric per cell induced by radiation (e.g. 0.02 dicentric/cell at 0.06 Gy) is at least one order of magnitude larger than the background.

The possibility of providing reliable predictions even at low doses is of interest in the framework of radiation protection studies, which involve different scenarios including exposure of population and workers to radiation sources on Earth and exposure of astronauts to space radiation, where doses of the order of  $\approx 0.01$  Gy can be reached (Testard et al., 1996; Obe et

al., 1997; George et al., 2001). Much higher doses would be involved in possible missions to Mars (Cucinotta et al., 2001). However, practical applications to low-dose extrapolations need to be considered with caution. In fact the current version of the model applies to acute irradiation that may not be the case of particular scenarios; for example, the equivalent dose rate in space is of the order of 1 mSv/day. The role of dose rate is likely to be less important for high-LET radiation than for low LET. For example, according to our model, a single 86 keV/ $\mu\text{m}$  alpha-particle traversal induces, on average, 2.4 Complex Lesions per cell, which have a significant probability to give rise to a dicentric or a translocation. By contrast, a single 5 keV/ $\mu\text{m}$  proton traversal induces, on average, only 0.07 CLs per cell, indicating that it is extremely unlikely that a single low-LET traversal can induce an aberration. Dose-rate effects need therefore to be incorporated in a future version of the model in view of specific applications.

Our previous publications (Ballarini et al., 1999; Ottolenghi et al., 2001; Ballarini et al., 2002a; Ballarini and Ottolenghi, 2003) are mainly concerned with aberrations visible with Giemsa staining, whereas in this paper we present a test of the model against FISH data. The results are reported in Fig. 1, which shows dose-response curves for simple and complex exchanges involving chromosome 4. The lines are model predictions, whereas the points represent experimental data obtained by gamma-ray irradiation of human lymphocytes in which chromosome 4 was painted with FISH (Wu et al., 1997). The predictions of the model are in good agreement with the data. The data relative to simple exchanges refer to complete patterns (scored as two bicolored chromosomes) and have to be compared with the solid line. As mentioned above, complete exchanges can be underestimated in experiments due to the impossibility of detecting small fragments, which are usually neglected in our simulations to allow direct comparisons with experimental data. In order to quantify the effects of this limitation, simulations were also run in which all fragments were assumed to be visible; the results are represented by the two dashed lines also reported in Fig. 1. As expected, both simple and complex exchanges showed a significant increase (plus  $\approx 45\%$ ).

## Conclusions

The most recent version of a model and code that simulates the induction of different chromosome aberrations by gamma rays, protons and alpha particles was presented and discussed. The model, previously tested against Giemsa data, showed good agreement also with FISH data, providing further support to the underlying assumptions. In particular, the important role of the spatial distribution of the initial energy depositions at the nanometre scale ("small scale clustering", which gives rise to clustered DNA damage) and at the micrometre scale ("large scale clustering", which determines the interaction probability between different chromosome breaks) was confirmed. In view of applications in radiation protection, simulations were run down to low doses (of the order of 0.01 Gy) and the presence of a background level of aberration was taken into account. When

dealing with low doses where only a few cells in the exposed population are hit by radiation, the question may arise whether any form of "bystander effect" can take place. This phenomenon, consisting of damage induction in non-hit cells following communication with irradiated cells via signalling molecules, has been observed for different endpoints including cell killing, oncogenic transformation, gene mutation, altered gene expression and sister chromatid exchanges; reviews can be found elsewhere (Mothersill and Seymour, 2001; Ballarini et al., 2002b; Morgan, 2003). However, up to now no evidence exists of a significant role of bystander effect in the induction of chromosome aberrations. The question has recently been addressed by Little et al. (2003), who irradiated mouse cells (both wild-type and deficient for nonhomologous end-joining DNA repair) with low fluences of alpha particles and scored gross chromosomal aberrations at the first post-irradiation metaphase. At the lowest doses where only 2–3% of the nuclei were traversed by an alpha particle, aberrations were induced in 36–55% of repair deficient cells, but only in 4–9% of wild-type cells. Interestingly, the authors hypothesised that bystander effects in wild-type cells mainly result from oxidative base damage due to increased levels of reactive oxygen species. This would explain why only a small bystander effect was observed in wild-type cells for chromosomal aberrations, which are generally associated with DNA strand breaks rather than base damage. These findings provide support to the choice of not implementing bystander effect when modelling chromosome aberration induction. This choice, which is common to all models discussed above, may need to be reconsidered when new data on bystander-mediated chromosome aberrations will be available. Other questions on chromosome aberration induction that will need further attention in the future are the following: a) the action of Ultrasoft X-rays and the role of the "one-hit" mechanism; b) the transmission of aberrations to the cell progeny, which can give rise to clonal aberrations (George et al., this issue); c) the relationship between aberrations and cancer; d) the role of genomic instability. As stated by R. Sachs, "there is still a lot to learn" (Sachs et al., this issue).

## References

- Anderson RM, Stevens DL, Goodhead DT: M-FISH analysis shows that complex chromosome aberrations induced by  $\alpha$ -particle tracks are cumulative products of localized rearrangements. *Proc natl Acad Sci, USA* 99:12167–12172 (2002).
- Ballarini F, Ottolenghi A: Chromosome aberrations as biomarkers of radiation exposure: modelling basic mechanisms. *Adv Space Res* 31:1557–1568 (2003).
- Ballarini F, Merzagora M, Monforti F, Durante M, Gialanella G, Grossi GF, Pugliese M, Ottolenghi A: Chromosome aberrations induced by light ions: Monte Carlo simulations based on a mechanistic model. *Int J Radiat Biol* 75:35–46 (1999).
- Ballarini F, Biaggi M, Ottolenghi A: Nuclear architecture and radiation-induced chromosome aberrations: models and simulations. *Radiat Protec Dosis* 99:175–182 (2002a).
- Ballarini F, Biaggi M, Ottolenghi A, Sapora O: Cellular communication and bystander effects: a critical review for modelling low-dose radiation action. *Mutat Res* 501:1–12 (2002b).
- Belli M, Goodhead DT, Ianzini F, Simone G, Tabocchini MA: Direct comparison of biological effectiveness of protons and alpha-particles of the same LET II. Mutation induction at the HPRT locus in V79 cells. *Int J Radiat Biol* 61:625–629 (1992).
- Biaggi M, Ballarini F, Burkard W, Egger E, Ferrari A, Ottolenghi A: Physical and biophysical characteristics of a fully modulated 72 MeV therapeutic proton beam: model predictions and experimental data. *Nucl Instr Meth Phys Res B* 159:89–100 (1999).
- Boei JJWA, Vermeulen S, Fomina J, Natarajan AT: Detection of incomplete exchanges and interstitial fragments in X-irradiated human lymphocytes using a telomeric PNA probe. *Int J Radiat Biol* 73:599–603 (1998).
- Bonassi S, Hagmar L, Stromberg U, Huici Montagud A, Tinnerberg H, Forni A, Heikkilä P, Wanders S, Norppa H, for the European Study Group on Cytogenetic Biomarkers and Health (ESCH): Chromosomal aberrations in lymphocytes predict human cancer independently of exposure to carcinogens. *Cancer Res* 60:1619–1625 (2000).
- Brenner DJ: On the probability of interaction between elementary radiation-induced chromosomal injuries. *Radiat Environ Biophys* 27:189–199 (1988).
- Chadwick KH, Leenhouts H: The rejoining of DNA double-strand breaks and a model for the formation of chromosomal aberrations. *Int J Radiat Biol* 33:517–529 (1978).
- Cornforth MN: Analyzing radiation-induced complex chromosome rearrangements by combinatorial painting. *Radiat Res* 155:643–659 (2001).
- Cornforth MN, Greulich-Bode KM, Loucas BD, Arsuaiga J, Vazquez M, Sachs RK, Bruckner M, Molls M, Hahnfeldt P, Hlatky L, Brenner DJ: Chromosomes are predominantly located randomly with respect to each other in interphase human cells. *J Cell Biol* 159:237–244 (2002).
- Cremer T, Kurz A, Zirbel R, Dietzel S, Rinke B, Schroeck E, Speicher MR, Mathieu U, Jauch A, Emmerich P, Scherthan H, Ried T, Cremer C, Lichter P: Role of chromosome territories in the functional compartmentalisation of the cell nucleus. *Cold Spring Harb Symp Quant Biol* 58:777–792 (1993).
- Cucinotta F, Nikjoo H, O'Neill P, Goodhead DT: Kinetics of DSB rejoining and formation of simple chromosome exchange aberrations. *Int J Radiat Biol* 76:1463–1474 (2000).
- Cucinotta FA, Schimmerling W, Wilson JW, Peterson LE, Badhwar GD, Saganti PB, Dicello JF: Space radiation cancer risks and uncertainties for Mars missions. *Radiat Res* 156:682–688 (2001).
- Durante M: Biological dosimetry in astronauts. *La Rivista del Nuovo Cimento* 19:1–44 (1996).
- Durante M: Radiation protection in space. *La Rivista del Nuovo Cimento* 25:1–70 (2002).
- Durante M, Furusawa Y, Gotoh E: A simple method for simultaneous interphase-metaphase chromosome analysis in biodosimetry. *Int J Radiat Biol* 74:457–462 (1998).
- Durante M, Bonassi S, George K, Cucinotta FA: Risk estimation based on chromosomal aberrations induced by radiation. *Radiat Res* 156:662–667 (2001).
- Durante M, George K, Wu H, Cucinotta F: Karyotypes of human lymphocytes exposed to high-energy iron ions. *Radiat Res* 158:581–590 (2002).
- Edwards AA: The use of chromosomal aberrations in human lymphocytes for biological dosimetry. *Radiat Res* 148:S39–S44 (1997).
- Edwards AA: Modelling radiation-induced chromosome aberrations. *Int J Radiat Biol* 78:551–558 (2002).
- Edwards AA, Moiseenko VV, Nikjoo H: Modelling of DNA breaks and the formation of chromosome aberrations. *Int J Radiat Biol* 66:633–637 (1994).
- Edwards AA, Moiseenko VV, Nikjoo H: On the mechanism of the formation of chromosomal aberrations by ionising radiation. *Radiat Environ Biophys* 35:25–30 (1996).
- Faretta M, Di Croce L, Pelicci PG: Effects of the acute myeloid leukemia-associated fusion proteins on nuclear architecture. *Seminars Hematol* 38:42–53 (2001).
- Fomina J, Darroudi F, Boei JJWA, Natarajan AT: Discrimination between complete and incomplete chromosome exchanges in X-irradiated human lymphocytes using FISH with pan-centromeric and chromosome specific DNA probes in combination with telomeric PNA probe. *Int J Radiat Biol* 76:807–813 (2000).
- George K, Durante M, Wu H, Willingham V, Badhwar G, Cucinotta FA: Chromosome aberrations in the blood lymphocytes of astronauts after space flight. *Radiat Res* 156:731–738 (2001).
- George K, Durante M, Willingham V, Cucinotta FA: Chromosome aberrations of clonal origin are present in astronauts' blood lymphocytes. *Cytogenet Genome Res* (this volume pp 245–251).
- Goodhead DT: Initial events in the cellular effects of ionizing radiations: clustered damage in DNA. *Int J Radiat Biol* 65:7–17 (1994).
- Griffin C, Hill M, Papworth D, Townsend K, Savage J, Goodhead DT: Effectiveness of 0.28 keV carbon K ultrasoft X-rays at producing simple and complex chromosome exchanges in human fibroblasts in vitro detected using FISH. *Int J Radiat Biol* 73:591–598 (1988).
- Harder D: The pairwise lesion interaction model, in Kiefer J (ed): *Quantitative Mathematical Models in Radiation Biology*, pp 159–170 (Springer, New York 1998).
- Hlatky L, Sachs R, Vazquez M, Cornforth M: Radiation-induced chromosome aberrations: insights gained from biophysical modeling. *Bioessays* 24:714–723 (2002).
- Holley WR, Mian IS, Park SJ, Rydberg B, Chatterjee A: A model for interphase chromosomes and evaluation of radiation-induced aberrations. *Radiat Res* 158:568–580 (2002).
- Kellerer AM: Fundamentals of microdosimetry, in Kase K, Bjarngard B, Attix F (eds): *The Dosimetry of Ionizing Radiation*, vol 1, pp 77–162 (Academic Press, Orlando 1985).
- Kodama Y, Nakano M, Ohtaki K, Delongchamp R, Awa AA, Nakamura N: Estimation of minimal size of translocated chromosome segments detectable by fluorescence in situ hybridization. *Int J Radiat Biol* 71:35–39 (1997).
- Kozubek S, Lukasova E, Mareckova A, Skalnikova M, Kozubek M, Bartova E, Kroha V, Krahulcova E, Slotova J: The topological organization of chromosomes 9 and 22 in cell nuclei has a determinative role in the induction of t(9;22) translocations and in the pathogenesis of t(9;22) leukemias. *Chromosoma* 108:426–435 (1999).
- Kozubek S, Lukasova E, Jirsova P, Koutna I, Kozubek M, Ganova A, Bartova E, Falk M, Pasekova R: 3D Structure of the human genome: order in randomness. *Chromosoma* 111:321–331 (2002).
- Lea DE: *Actions of radiations on living cells* (Cambridge University Press, Cambridge 1946).
- Little JB, Nagasawa H, Li GC, Chen DJ: Involvement of the nonhomologous end joining DNA repair pathway in the bystander effect for chromosomal aberrations. *Radiat Res* 159:262–267 (2003).
- Loucas BD, Cornforth MN: Complex chromosome exchanges induced by gamma rays in human lymphocytes: an mFISH study. *Radiat Res* 155:660–671 (2001).
- Lucas JN, Cervantes E: Significant large-scale chromosome territory movement occurs as a result of mitosis but not during interphase. *Int J Radiat Biol* 78:449–455 (2002).
- Mitelman F: Recurrent chromosome aberrations in cancer. *Mutat Res* 462:247–253 (2000).
- Morgan WF: Non-targeted and delayed effects of exposure to ionizing radiation: I. Radiation-induced genomic instability and bystander effects in vitro. *Radiat Res* 159:567–580 (2003).
- Mothersill C, Seymour C: Radiation-induced bystander effects: Past history and future directions. *Radiat Res* 155:759–767 (2001).
- Nagele RG, Freeman T, McMorror L, Thomson Z, Kitson-Wind K: Chromosomes exhibit preferential positioning in nuclei of quiescent human cells. *J Cell Sci* 112:525–535 (1999).
- Natarajan AT: Chromosome aberrations: past present and future. *Mutat Res* 504:3–16 (2002).
- Nikjoo H, O'Neill P, Goodhead DT, Terrissol M: Computational modelling of low-energy electron-induced DNA damage by early physical and chemical events. *Int J Radiat Biol* 71:467–483 (1997).
- Obe G, Johannes I, Johannes C, Hallman K, Reiz G, Facius R: Chromosomal aberrations in blood lymphocytes of astronauts after long-term space flights. *Int J Radiat Biol* 72:727–734 (1997).
- Obe G, Pfeiffer P, Savage JR, Johannes C, Goedecke W, Jeppesen P, Natarajan AT, Martinez-Lopez W, Folle GA, Drets ME: Chromosomal aberrations: formation, identification and distribution. *Mutat Res* 504:17–36 (2002).
- Ostashevsky JY: Higher-order structure of interphase chromosomes and the formation of radiation-induced chromosomal exchange aberrations. *Int J Radiat Biol* 76:1179–1187 (2000).
- Ottolenghi A, Merzagora M, Tallone L, Durante M, Paretzke HG, Wilson WE: The quality of DNA double-strand breaks: a Monte Carlo simulation of the end-structure of strand breaks produced by protons and alpha particles. *Radiat Environ Biophys* 34:239–244 (1995).
- Ottolenghi A, Monforti F, Merzagora M: A Monte Carlo calculation of cell inactivation by light ions. *Int J Radiat Biol* 72:505–513 (1997).
- Ottolenghi A, Ballarini F, Merzagora M: Modelling radiation induced biological lesions: from initial energy depositions to chromosome aberrations. *Radiat Environ Biophys* 38:1–13 (1999).
- Ottolenghi A, Ballarini F, Biaggi M: Modelling chromosomal aberration induction by ionising radiation: the influence of interphase chromosome architecture. *Adv Space Res* 27:369–382 (2001).

- Pinkel D, Straume T, Gray JW: Cytogenetic analysis using quantitative high sensitivity fluorescence hybridization. *Proc natl Acad Sci, USA* 83:2934–2938 (1986).
- Radvoyevitch T, Kozubek S, Sachs RK: Biologically based risk estimation for radiation-induced CML – Inferences from BCR and ABL geometrical distributions. *Radiat Environ Biophys* 40:1–9 (2001).
- Revell SH: Chromatid aberrations – the general theory, in Wolff S (ed): *Radiation Induced Chromosome Aberrations*, pp 41–72 (Columbia University Press, New York 1963).
- Sachs RK, Brenner DJ: Effect of LET on chromosomal aberration yields. I. Do long-lived exchange-prone double-strand breaks play a role? *Int J Radiat Biol* 64:677–688 (1993).
- Sachs RK, Levy D, Chen AM, Simpson PJ, Cornforth MN, Ingerman EA, Hahnfeldt P, Hlatky LR: Random breakage and reunion chromosome aberration formation model; an interaction-distance version based on chromatin geometry. *Int J Radiat Biol* 76:1579–1588 (2000a).
- Sachs RK, Rogoff A, Chen AM, Simpson PJ, Savage JRK, Hahnfeldt P, Hlatky LR: Underprediction of visibly complex chromosome aberrations by the recombinational repair (“one-hit”) model. *Int J Radiat Biol* 76:129–148 (2000b).
- Sachs RK, Levy D, Hahnfeldt P, Hlatky L: Quantitative analysis of radiation-induced chromosome aberrations. *Cytogenet Genome Res* (this issue p 142–148, 2004).
- Savage JRK: Insight into sites. *Mutat Res* 366:81–95 (1996).
- Savage JRK: A brief survey of aberration origin theories. *Mutat Res* 404:139–147 (1998).
- Savage JRK, Simpson PJ: FISH-“painting” patterns resulting from complex exchanges. *Mutat Res* 312:51–60 (1994).
- Sax K: An analysis of X-ray induced chromosomal aberrations in *Tradescantia*. *Genetics* 25:41–68 (1940).
- Simpson PJ, Savage JRK: Dose-response curves for simple and complex chromosome aberrations induced by X-rays and detected using fluorescence in situ hybridization. *Int J Radiat Biol* 69:429–436 (1996).
- Stadler LJ: Some genetic effects of X-rays in plants. *J Hered* 21:3 (1930).
- Testard I, Ricoul M, Hoffschir FH, Flury-Herard A, Dutrillaux B, Fedorenko BS, Gerasimenko VN, Sabatier L: Radiation-induced chromosome damage in astronauts’ lymphocytes. *Int J Radiat Biol* 70:403–411 (1996).
- de The H, Lavau C, Marchio A, Chomienne C, Degos L, Dejean A: The PML-RAR fusion mRNA generated by t(15;17) translocation in acute promyelocytic leukemia encodes a functionally altered RAR. *Cell* 66:675–684 (1991).
- Visser AE, Aten JA: Chromosomes as well as chromosomal subdomains constitute distinct units in interphase nuclei. *J Cell Sci* 112:3353–3360 (1999).
- Wu H, Durante M, George K, Yang TC: Induction of chromosome aberrations in human cells by charged particles. *Radiat Res* 148:S102–S107 (1997).
- Zirbel RM, Mathieu UR, Kurz A, Cremer T, Lichter P: Evidence for a nuclear compartment of transcription and splicing located at chromosome domain boundaries. *Chrom Res* 1:93–106 (1993).

# Virtual radiation biophysics: implications of nuclear structure

G. Kreth,<sup>a</sup> J. Finsterle,<sup>a</sup> and C. Cremer<sup>a</sup><sup>a</sup>Kirchhoff Institute for Physics, INF 227 Heidelberg (Germany)

**Abstract.** The non-random positioning of chromosome territories (CTs) in lymphocyte cell nuclei has raised the question whether systematic chromosome-chromosome associations exist which have significant influence on interchange rates. In such a case the spatial proximity of certain CTs or even of clusters of CTs is expected to increase the respective exchange yields significantly, in comparison to a random association of CTs. In the present study we applied computer simulated arrangements of CTs to calculate interchange frequencies between all heterologous CT pairs, assuming a uniform action of

the molecular repair machinery. For the positioning of CTs in the virtual nuclear volume we assumed a) a statistical, and b) a gene density-correlated arrangement. The gene density-correlated arrangement regards the more experimentally observed interior localization of gene-rich and the more peripheral positioning of gene-poor CTs. Regarding one-chromosome yields, remarkable differences for single CTs were observed taking into account the gene density-correlated distribution of CTs.

Copyright © 2003 S. Karger AG, Basel

The formation of interchanges between different chromosome territories (CTs) requires spatial proximity of two or more broken genomic loci which have to be localized mainly at or near CT surfaces (Cremer et al., 1996; Sachs et al., 1997; Cornforth et al., 2002). In this context a non-random positioning of CTs in the nuclear volume and possibly a systematic chromosome-chromosome association will favor the probability by which two CTs undergo an interchange event. To study the influence of such proximity effects on interchange frequencies, Cornforth et al. (2002) determined frequencies between all possible heterologous pairs of CTs with 24-color whole-chromosome painting after damage to interphase lymphocytes by sparsely ionizing radiation *in vitro*. For lymphocyte cells, recently a close relationship between radial positioning of CTs in the nuclear volume and its gene densities was observed. That means that CTs with higher gene densities, e.g. #17, 19 are located more in the interior of the nuclear volume while CTs with lower gene densities, e.g. #18, come closer to the periphery (Boyle et al., 2001; Cremer et al., 2001). In the study of Cornforth et al. (2002), however, only a group of five chromosomes

(#1, 16, 17, 19, 22), previously observed to be preferentially located near to the center of the nucleus (suggested by Boyle et al., 2001), showed a statistically significant deviation of a random CT-CT association. These findings suggest a predominantly random location of CTs with respect to each other in interphase lymphocyte cells.

In the present contribution we applied the “Spherical 1 Mbp Chromatin Domain (SCD)” computer model to calculate interchange frequencies between CTs, assuming a statistical, or a gene density correlated distribution of CTs in a given spherical nuclear volume. Such an approach allows theoretical predictions of the effects of different radial CT arrangements on exchange yields.

## Materials and methods

### *Computer-simulated nuclear structures*

The recent experimental findings about the large-scale interphase chromosome structure (compare Cremer and Cremer, 2001) revealed a compartmentalization of a chromosome territory into 300- to 800-nm sized (diameter) subchromosomal foci (with a mean DNA content of about ~ 1 Mbp). According to the “Spherical 1 Mbp Chromatin Domain (SCD)” model (Kreth et al., 2001; Kreth et al., submitted) each chromosome is built up by a linear chain of 500-nm sized spherical domains with a mean DNA content of ~ 1 Mbp which are linked together by entropic spring potentials. Different domains interact with each other also by a weakly increasing repulsive potential. These domains represent the experimentally observed foci, and the number is given by the respective DNA content of the chromosome. Besides a statistical distribution of the simulated chromosome chains in a spherical

The present study was supported financially by the Deutsche Forschungsgemeinschaft (Grant CR 60/19-1).

Received 10 September 2003; manuscript accepted 18 December 2003.

Request reprints from Gregor Kreth, Kirchhoff Institute for Physics, INF 227 69120 Heidelberg (Germany); telephone: +49-6221-549275  
fax +49-6221-549839; e-mail: gkreth@kip.uni-heidelberg.de

nuclear volume (we choose here a diameter of 10  $\mu\text{m}$ , according to the experimental investigations of Cremer et al. (2001); other diameters, e.g. for small lymphocytes, for the calculation of interchange yields have to be considered in further simulations), we extended the SCD model to take into account the specific positioning of gene rich and gene poor CTs in the nuclear volume. For this purpose the CTs were inserted in the nuclear volume according to the order of their gene densities: #19, 17, 22, 16, 20, 11, 1, 12, 15, 7, 14, 6, 9, 2, 10, 8, 5, 3, 21, X, 18, 4, 13, Y<sup>1</sup>; additionally the distance of CTs to the nuclear center was weighted with a radial probability density function which considers the respective gene density of a CT. In this way the gene-rich CTs are placed closer to the middle of the nucleus and those that are gene poor closer to the periphery (Kreth et al., submitted). The large variation in the position of the CTs is maintained by this procedure. Beginning from a mitotic-like strongly condensed start configuration of the CTs, where the 1-Mbp domains are placed side by side, we used the Importance Sampling Monte Carlo method to create relaxed equilibrium configurations with respect to the potential energy.

#### Virtual irradiation algorithm

On the assumption of a random distribution of double strand breaks (DSBs) within the DNA, the probability of a break occurring within a certain 1-Mbp domain can be modeled using Poisson distribution mathematics. This assumes that, although an ionizing radiation track may produce multiple DSBs, these are distributed randomly throughout the genome. Under the assumption that the number of DSBs induced within a nucleus increases linearly with dose and is proportional to the DNA content of the cell, the probability  $p_n$  of an individual modeled 1-Mbp domain containing  $n$  DSBs is calculated from an adaptation of the equation of Poisson distribution (Johnston et al., 1997):

$$p_n = \frac{n^n e^{-b}}{n!} \quad (1)$$

Here  $n$  is the number of DSBs within an individual domain;  $b$  is the mean number of breaks per domain for the whole nucleus and is given by:

$$b = D \cdot y \cdot q \quad (2)$$

where  $D$  is the dose of radiation (Gy),  $q$  is the size of the domain in bp (here  $1 \cdot 10^6$  bp) and  $y$  is the yield of DSBs which was adapted to  $y = 8.07 \cdot 10^{-9}$  Gy<sup>-1</sup> bp<sup>-1</sup> to ensure a mean number of 50 DSBs per Gy per nucleus according to experimental observations (referred in Cornforth et al., 2002). The DSBs within the 1-Mbp domains were placed randomly. To determine an exchange (inter-/intra-change) between two DSBs, only those 1-Mbp domains containing DSBs were regarded which were directly neighbored. According to Kreth et al. (1998), for an exchange event in dependence of the distance  $d$  of the two DSBs, the normalized probability function  $p_d$  was assumed:

$$p_d = \left(\frac{r}{d}\right)^{1.4} \quad (3)$$

Corresponding to the Monte Carlo process, an exchange event for such a domain pair was counted when a random number of the unit distribution  $[0;1] \leq p_d$ . Here,  $r$  denotes the radius of a 1-Mbp domain which determines the maximal distance by which an exchange takes place in every case. When for a certain DSB an exchange was not counted, other directly neighbored domains containing DSBs were tested. When this procedure failed, the DSB will be considered as repaired. Exchanges between domains of the same chromosome were counted as intrachanges and were separated from interchanges.

#### Experimental comparison

For an experimental comparison of the calculated interchange yields the study of Cornforth et al. (2002) was applied. In this study peripheral blood lymphocytes were exposed during the G<sub>0</sub>/G<sub>1</sub> part of the cell cycle to radiation doses of 2 or 4 Gy, after which the mFISH technique was used to score aberrations at the first subsequent metaphase. A total of nine data sets with 1,587 cells were taken.

## Results

In the simulated case for each of both assumptions about the distribution of CTs in the nuclear volume (statistical or gene density correlated), 50 nuclei were simulated. To get comparable statistics with the experimental data of Cornforth et al. (2002) each simulated nucleus was "irradiated" with 3 Gy (we used a median value between 2 and 4 Gy, because the experimental number of cells irradiated with 2 or 4 Gy was not known) virtually 32 times. That means that in a model nucleus with a given distribution of CTs, a dose of 3 Gy ( $\sim 150$  randomly distributed DSBs) was assumed; the resulting exchanges were determined. Then the same model nucleus was used again, with a new set of randomly distributed DSBs, and the resulting exchanges were calculated. For each simulated nuclear structure, this procedure was repeated 32 times. In the end, an equivalent ensemble of 1,600 cells was obtained, corresponding to the number of cells evaluated experimentally by Cornforth et al. (2002).

The absolute interchange yields in percent for each heterologous autosome pair for the two simulated cases and for the experimental case are given in Fig. 1. While the absolute values of the simulated and the experimental interchange yields were in the same order, in the case of a simulated gene density correlated distribution of CTs, one heterologous pair showed a difference  $\geq 1.5\%$  to the experimental case (marked in black), and 25 heterologous pairs showed a difference  $\geq 0.8\%$  (marked in gray). In the case of a statistical distribution of CTs, three heterologous pairs revealed a difference  $\geq 1.5\%$  and 22 pairs  $\geq 0.8\%$ . On the basis of these absolute interchange yields, an unequivocal conclusion about a better agreement of one of the two simulated yields with the experimental yield cannot be made. In the case of the gene density-correlated distribution however the more interior localization of gene rich CTs like 16, 17 and 19 resulted directly in higher exchange rates between these CTs, which was confirmed partially also in the experimental case.

According to Cornforth et al. (2002), in Fig. 2 we therefore plotted the one-chromosome yields which are derived from Fig. 1 by summing over all interchange yields involving each given chromosome. To visualize differences between the experimental and the simulated gene density-correlated yields to the simulated statistical yields (which describe a random chromosome-chromosome association), all rates were normalized to 1,000 (error bars were determined by Poisson statistics). The one chromosome-yields for CTs #10–22 for the experimental and the simulated gene density-correlated data are in quite good agreement. An exception is the yield for CT #19 which is underrepresented in the experimental case. A possible explanation would be the experimental observation that many cells with a CT #19 (the gene-richest chromosome of the human genome) translocation die. These events are not regarded in the evaluation process (personal communication Karin Greulich-Bode). The largest difference between the experimental and the simulated gene density-correlated yield resulted from chromosome #1: in the case of the simulated gene density-correlated distribution the yield was considerably higher than the experimentally observed yield for this chromosome. It may be noted

<sup>1</sup> Human Genome Resources: <http://www.ncbi.nlm.nih.gov/genome/guide/human/>

## Absolute interchange yields in %

Experiment (Cornforth et al. 2002, 1587 cells)

**A**

	1	2	3	4	5	6	7	8	9	10	11	12	13	14	15	16	17	18	19	20	21
1																					
2	1.26																				
3	1.07	1.5																			
4	1.51	1	0.7																		
5	1.01	1.3	1	0.7																	
6	0.82	1.1	1.2	0.6	0.63																
7	1.01	0.4	0.8	0.8	0.88	0.38															
8	0.69	0.8	0.8	0.6	0.63	0.76	0.5														
9	0.88	0.7	0.9	0.9	0.63	1.01	0.5	0.4													
10	1.01	0.6	0.6	0.8	0.76	0.82	0.44	0.4	0.6												
11	0.63	1.1	0.7	0.4	1.01	0.38	0.82	0.7	1	0.4											
12	0.38	1.1	0.8	0.7	0.88	1.01	0.82	0.3	0.3	0.6	0.8										
13	0.13	0.6	0.8	0.8	0.88	0.57	0.25	0.8	0.8	0.4	0.1	0.38									
14	0.44	0.3	0.6	0.8	0.5	0.69	0.63	0.6	0.9	0.4	0.4	0.5	0.7								
15	0.69	1.1	0.3	0.5	0.82	0.57	0.25	0.5	0.6	0.4	0.6	0.25	0.3	0.63							
16	0.57	0.4	0.6	0.8	0.32	0.44	0.5	0.3	0.6	0.4	0.5	0.32	0.3	0.32	0.69						
17	0.82	0.6	0.5	0.7	0.63	0.13	0.57	0.4	0.6	0.4	0.6	0.38	0.3	0.25	0.5	0.6					
18	0.32	0.2	0.4	0.3	0.25	0.38	0.44	0.4	0.7	0.4	0.3	0.13	0.5	0.57	0.13	0.5	0.3				
19	0.5	0.3	0.6	0.3	0.25	0.44	0.25	0.1	0.2	0.2	0.4	0.44	0.2	0.06	0.25	0.6	0.1	0.1			
20	0.57	0.4	0.4	0.5	0.38	0.25	0.57	0.4	0.2	0.4	0.4	0.38	0.3	0.19	0.32	0.7	0.3	0.4	0.2		
21	0.5	0.4	0.5	0.4	0.32	0.19	0.25	0.1	0.2	0.3	0.2	0.13	0.2	0.5	0.32	0.4	0.3	0.2	0	0.2	
22	0.95	0.7	0.4	0.2	0.13	0.32	0.06	0.2	0.2	0.1	0.4	0.25	0.4	0.38	0.13	0.4	0.4	0	0.2	0.1	0.1

Simulation (gene density correlated, 1600 cells)

**B**

	1	2	3	4	5	6	7	8	9	10	11	12	13	14	15	16	17	18	19	20	21
1																					
2	3.69																				
3	2.56	1.6																			
4	1.69	1.6	0.9																		
5	2.13	0.9	0.8	1																	
6	1.31	1.3	1.2	1.6	1.13																
7	1	1.3	1.5	1.5	0.94	1.06															
8	2.19	1.6	0.5	1.1	0.94	2	0.75														
9	1.44	1.2	1.8	0.6	1.19	0.63	0.88	0.5													
10	2.06	0.5	0.5	0.9	1.06	0.44	1.25	0.9	0.8												
11	1.31	1.3	1.4	1.4	1.06	1	0.63	0.9	0.9	1.6											
12	0.19	1.9	1	1.7	1.06	1.5	0.88	0.7	1.6	0.9	0.4										
13	1.19	1.3	0.5	0.3	0.63	0.75	1	0.4	1.2	0.8	0.8	1.19									
14	0.56	1.3	1.1	1.1	1	0.5	0.69	1.2	0.8	0.7	0.9	0.56	1.1								
15	1.19	1.1	0.7	1.4	0.94	0.94	0.38	1.1	0.9	0.7	0.6	0.25	0.6	0.38							
16	1.38	1.3	0.8	0.4	1	1.19	0.81	0.6	0.5	0.8	0.6	0.44	0.3	0.44	0.56						
17	1.75	1.3	0.3	0.5	0.69	0.63	0.94	0.6	0.3	0.4	1.2	0.63	0.2	0.56	0.19	0.8					
18	1.69	0.5	0.3	0.8	0.69	0.13	1	0.4	0.6	0.6	0.5	0.5	0.8	0.56	0.31	0.3	0.1				
19	1	0.6	0.9	0.3	0.63	0.31	0.44	0.3	0.3	0.4	1	0.31	0.1	0.13	0.31	1.6	1.3	0.3			
20	0.75	0.8	0.7	0.6	0.69	0.94	1	0.6	0.3	0.3	0.6	0.44	0.3	0.31	0.44	0.6	0.8	0.2	0.4		
21	0.56	0.6	0.4	0.4	0.13	0.88	0.31	0.4	0.6	0.4	0.5	0.31	0.4	0.31	0.19	0	0.2	0.2	0	0.3	
22	0.38	0.6	0.4	0.3	0.19	0.38	0.63	0.5	0.9	0.4	0.8	0.63	0.3	0.19	0.31	0.6	0.6	0.1	0.6	0.4	0.3

Simulation (statistical, 1600 cells)

**C**

	1	2	3	4	5	6	7	8	9	10	11	12	13	14	15	16	17	18	19	20	21
1																					
2	2.25																				
3	2.63	1.4																			
4	1.19	1.3	1.5																		
5	1.56	2.2	1.1	1.5																	
6	1.88	1.1	1.3	1.8	0.94																
7	1.75	1.8	1.1	0.6	1.31	1.13															
8	1.25	1.2	1.8	0.6	0.88	1.13	0.81														
9	1.25	1.2	1.3	0.5	0.81	1.06	1.56	0.8													
10	0.88	1.3	1.2	1.8	1.44	1.38	0.94	1.1	1.1												
11	1.38	1	1.1	2.2	0.44	1.06	0.94	0.6	0.9	1.1											
12	1.38	1.6	1.3	0.8	1.25	0.56	0.81	0.5	1.2	0.6	1										
13	1.63	1.1	0.9	0.7	0.88	0.69	1	0.6	0.6	0.8	1.1	0.44									
14	1.5	1.9	1.4	1.1	0.63	0.5	0.63	0.6	0.7	0.3	0.6	0.81	0.5								
15	1.38	1.3	0.4	0.9	0.75	1	0.75	0.6	1.2	0.8	1.1	0.19	0.8	0.56							
16	0.88	0.8	1.1	0.7	0.38	0.69	1	0.3	0.4	1.1	0.4	0.63	0.4	0.38	0.31						
17	0.56	0.8	0.4	0.8	0.56	0.69	0.44	0.3	0.9	0.9	0.6	0.44	0.4	0.31	0.63	0.6					
18	0.56	1.3	0.9	0.6	1.06	0.5	0.19	0.4	0.6	0.6	0.7	0.44	0.4	0.5	0.19	0.4	0.5				
19	0.63	0.4	0.7	0.3	0.5	0.94	0.75	0.3	0.6	0.6	0.5	0.38	0.1	0.63	0.19	0.3	0.3	0.6			
20	0.88	0.4	0.8	0.6	0.63	0.5	0.63	0.8	0.6	0.6	0.2	0.19	0.6	0.44	0.44	0.3	0.3	0.1	0.1		
21	1.06	0.3	0.4	0.3	0.56	0.56	0.63	0.6	0.3	0.9	0.1	0.38	0.2	0.56	0.31	0.5	0.2	0.4	0.4	0.4	
22	0.88	0.9	0.3	1.3	0.63	0.5	0.63	0.5	0.2	0.3	0.3	0.25	0.2	0.06	0.44	0.1	0.2	0.1	0.3	0	0.1

**Fig. 1.** Absolute interchange yields in percent for each heterologous autosome pair for the both simulated (statistical **(C)** and gene density correlated distribution **(B)** of CTs according to the SCD model) and the experimental case **(A)** (irradiated peripheral blood lymphocytes; adapted from Cornforth et al., 2002). For the two simulated cases **(B, C)** an absolute difference of 1.5% or more to the experimental case **(A)** was marked in black and a difference of 0.8% or more in gray.



## individual autosome yields

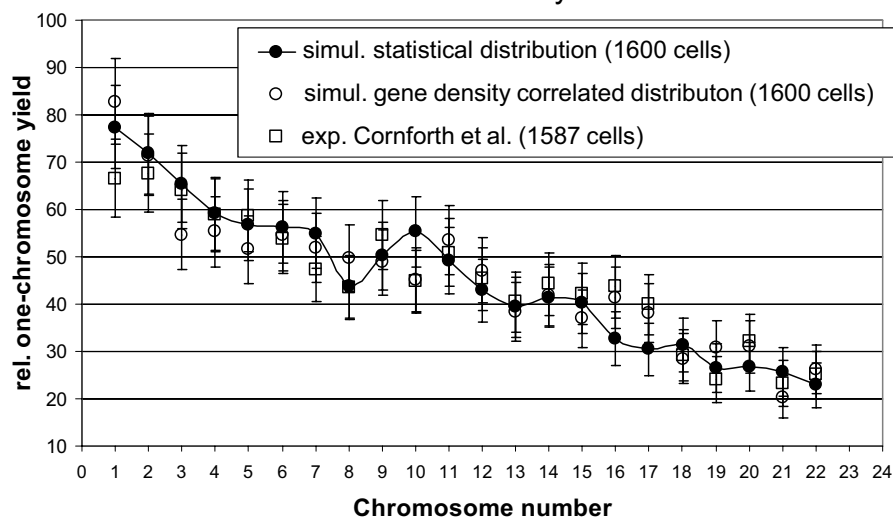


**Fig. 2.** Relative (the plotted yields were normalized to 1,000) one-chromosome yields for the two simulated and the experimental case. The simulated statistical case can be considered as a representation for a random chromosome-chromosome association. Error bars were taken from Poisson statistics.

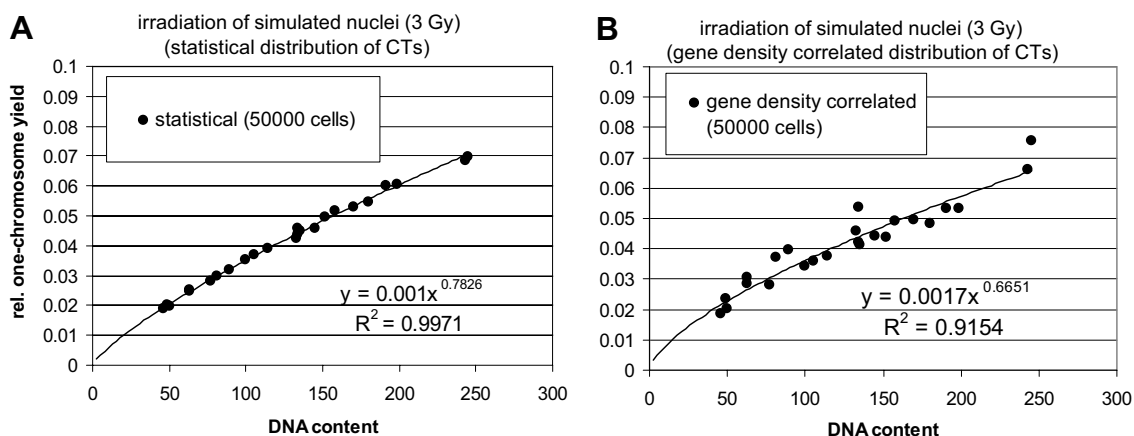


**Fig. 3.** Relative one-chromosome yields for both simulated cases were plotted versus the DNA content (in this graph a simulated ensemble of 50,000 cells was applied for each case). Potential fitting curves revealed the expected dependency of: yield  $\sim$  (DNA content)<sup>2/3</sup>.

that both (experimental and simulated gene density-correlated) yields revealed differences for single chromosomes in comparison to random chromosome-chromosome associations (represented by the simulated statistical distribution). To assure that this behavior is not an effect of insufficient statistics, in Fig. 3 the relative one-chromosome yields were calculated for both simulated CT distribution cases for 50,000 cells (each of the 50 simulated nuclei was irradiated virtually 1,000 times). According to previous studies (Cremer et al., 1996; Kreth et al., 1998), the dependency of one-chromosome yield and DNA content follows the relation: yield  $\sim$  (DNA content)<sup>2/3</sup>. While in the case of the simulated statistical distribution of CTs all data points were close to the potential fitting curve, for the gene density correlated distribution remarkable differences for single CTs were obtained.

## Discussion

In the present contribution we tested the effect of a non-random (gene density-correlated) simulated CT distribution in the nuclear volume on interchange yields. The comparison with an experimentally obtained interchange yield revealed that these one-chromosome yields showed for single CTs remarkable differences to a random chromosome-chromosome association (given by a simulated statistical distribution of CTs in the nuclear volume). For CTs #10–22 the agreement between experimental and simulated gene density-correlated yields was quite good; an exception is CT#19 which is underrepresented in the experimental case. We can conclude that the simulations confirm the influence of proximity effects on interchange yields. To enhance such comparisons a) the ensemble of simulated nuclei has to be increased to be sure that the observed

deviations are not the result of the multiple virtual radiation of single simulated nuclei; this can have a significant influence on the calculated yields. b) The experimental observations were made in the subsequent metaphase. That means that aberrations, e.g. translocations with chromosome #19, or most complex aberrations may lead to cell death and will cause an underestimation of certain CT yields. A direct analysis in interphase nuclei with mFISH techniques after irradiation might be useful in further experimental investigations.

## Acknowledgment

For stimulating discussions we thank T. Cremer (Munich) and K. Greulich-Bode (Heidelberg).

## References

- Boyle S, Gilchrist S, Bridger JM, Mahy NL, Ellis JA, Bickmore WA: The spatial organization of human chromosomes within the nuclei of normal and emerin-mutant cells. *Hum molec Genet* 10:211–219 (2001).
- Cornforth MN, Greulich-Bode KM, Bradford DL, Arsuaga J, Vazquez M, Sachs RK, Brückner M, Molls M, Hahnfeldt P, Hlatky L, Brenner DJ: Chromosomes are predominantly located randomly with respect to each other in interphase human cells. *J Cell Biol* 159:237–244 (2002).
- Cremer C, Muenkel C, Granzow M, Jauch A, Dietzel S, Eils R, Guan XY, Meltzer PS, Trent JM, Langowski J, Cremer T: Nuclear architecture and the induction of chromosomal aberrations. *Mutat Res* 366:97–116 (1996).
- Cremer M, von Hase J, Volm T, Brero A, Kreth G, Walter J, Fischer C, Solovei I, Cremer C, Cremer T: Non-random radial higher-order chromatin arrangements in nuclei of diploid human cells. *Chrom Res* 9:541–567 (2001).
- Cremer T, Cremer C: Chromosome territories, nuclear architecture and gene regulation in mammalian cells. *Nature Rev* 2:292–301 (2001).
- Johnston PJ, Olive PL, Bryant PE: Higher-order chromatin structure-dependent repair of DNA double-strand breaks: modeling the elution of DNA from nucleoids. *Radiat Res* 148:561–567 (1997).
- Kreth G, Muenkel C, Langowski J, Cremer T, Cremer C: Chromatin structure and chromosome aberrations: modeling of damage induced by isotropic and localized irradiation. *Mutat Res* 404:77–88 (1998).
- Kreth G, Edelmann P, Cremer C: Towards a dynamical approach for the simulation of large scale cancer correlated chromatin structures. *Int J Anat Embryol* 106:21–30 (2001).
- Sachs RK, Chen AM, Brenner DJ: Proximity effects in the production of chromosome aberrations by ionizing radiation. *Int J Radiat Biol* 71:1–19 (1997).

# Dose dependency of FISH-detected translocations in stable and unstable cells after $^{137}\text{Cs}$ $\gamma$ irradiation of human lymphocytes in vitro

H. Romm and G. Stephan

Federal Office for Radiation Protection, Department of Radiation Protection and Health, Oberschleissheim (Germany)

**Abstract.** Human peripheral lymphocytes were exposed to  $^{137}\text{Cs}$   $\gamma$ -rays (0–4.3 Gy) in order to check the impact of unstable cells on the dose-response curve for translocations. Chromosomes 2, 4 and 8 were FISH-painted. 17,720 first dividing cells were analysed. For the discrimination between stable and unstable cells the painted and the counter-stained chromosomes were analysed at doses of 1 Gy and higher. The cell distribution of translocations follows a Poisson distribution. The data were fitted to the linear-quadratic function,  $y = c + \alpha D +$

$\beta D^2$ . As expected, the  $\alpha$  coefficients of the dose-response curves for translocations in stable cells or in total cells do not differ. However, at doses  $>1$  Gy, the frequency of all translocations in stable cells seems to be lower than the frequency in total cells. For the establishment of calibration curves for past dose assessment purposes, only complete translocations should be scored, in order to estimate reliable doses.

Copyright © 2003 S. Karger AG, Basel

FISH-detected translocations have been proposed as biomarkers especially for chronic and former radiation exposures, since it was assumed that this exchange aberration will persist for years in peripheral lymphocytes (Lucas et al., 1992). Therefore, for biological dosimetry purposes dose-response curves have been established for this aberration type where only the painted chromosomes were in the focus of the observer. It was argued that this scoring procedure is a fast method, because only three painted chromosome pairs have to be taken into account instead of 46 chromosomes after Giemsa staining, and a reliable method, because lymphocytes containing translocations will be substituted by stem cell-derived lymphocytes containing translocations. For radiation victims it was shown, however, that the translocation frequency in peripheral blood decreases with post-exposure time (Lindholm et al., 2002),

especially when the victims received doses  $>1$  Gy (Natarajan et al., 1998). From these in vivo results the conclusion was drawn that translocations occurring together with aberrations such as dicentric chromosomes, resulting in unstable cells, may be eliminated from peripheral blood. On the other hand, it was shown that the yield of translocations will not be reduced after whole-body exposure if the distributions of translocations and dicentrics are independent (Guerrero-Carbajal et al., 1998).

To investigate the impact of unstable cells on the dose-response curves, we have, therefore, carried out in vitro experiments with  $^{137}\text{Cs}$   $\gamma$ -irradiated lymphocytes and discriminated stable and unstable cells. The results show that for retrospective biological dosimetry purposes the evaluation of complete (reciprocal) translocations in total cells, in stable cells, or exclusively as apparently simple translocations, can be used for the establishment of a calibration curve.

Received 2 October 2003; manuscript accepted 15 December 2003.

Requests reprints from Horst Romm, Federal Office for Radiation Protection  
Department of Radiation Protection and Health  
Ingolstädter Landstrasse 1, D-85764 Oberschleissheim (Germany)  
telephone: +49 188 8333 2214; fax: +49 188 8333 2205  
e-mail: hromm@bfs.de

## Materials and methods

### Radiation exposure

Human peripheral blood was drawn from one healthy male donor (49 years) into heparinized syringes and immediately divided into aliquots of 2 ml and incubated at 37°C. The aliquots were irradiated at the GSF

**Table 1.** Radiation-induced chromosome aberrations in the FISH-painted chromosomes and in the chromosomes of the whole genome (chromosomes 2, 4 and 8 were painted)

Dose (Gy)	Scored cells	Genome equivalent cells	dic in whole genome <sup>a</sup>	Painted aberrations <sup>a</sup>				dic in whole genome/100 cells ± SE	dic/100 cells ± SE (genome equivalent)	tc + ti/100 cells ± SE (genome equivalent)
				dic	tc	ti	tc + ti			
0	3520	1211	–	0	6	1	7	–	0	0.58 ± 0.22
0.11	3362	1157	–	4	9	3	12	–	0.35 ± 0.17	1.04 ± 0.32
0.22	3061	1053	–	12	15	5	20	–	1.14 ± 0.35	1.90 ± 0.44
0.43	3047	1048	–	20	25	5	30	–	1.91 ± 0.43	2.86 ± 0.54
0.65	2431	836	–	23	26	11	37	–	2.75 ± 0.57	4.42 ± 0.74
1.08	1113	383	132	59	27	19	46	11.86 ± 1.06	15.41 ± 1.99	12.01 ± 1.74
2.15	437	150	163	49	35	22	57	37.30 ± 2.90	32.60 ± 4.69	37.92 ± 5.05
3.25	419	144	302	98	79	54	133	72.08 ± 4.10	67.99 ± 6.70	92.27 ± 8.24
4.33	330	114	421	166	95	91	186	127.58 ± 6.08	146.23 ± 11.85	163.85 ± 11.68

<sup>a</sup> dic: dicentric chromosome; tc: complete translocation; ti: incomplete translocation; SE: standard error.

Research Centre for Environment and Health (Neuherberg) with a <sup>137</sup>Cs  $\gamma$ -ray source (0.662 MeV, dose rate 0.4 Gy/min, at 37 °C). The whole blood samples were irradiated with doses of 0.11, 0.22, 0.43, 0.65, 1.08, 2.15, 3.25 and 4.33 Gy. One unexposed sample served as control. After irradiation the samples were incubated for 3 h at 37 °C before culture initiation.

#### Cultivation of human lymphocytes

The culture technique was fully described earlier (Stephan and Pressl, 1997). In brief, cultures were set up with 0.5 ml whole blood in 5 ml RPMI 1640 medium supplemented with 10% fetal calf serum, 2 mM glutamine, 2% PHA, 10 mM 5-bromodeoxyuridine (BrdU) and penicillin/streptomycin (40 U/ml and 40  $\mu$ g/ml, respectively). The cultures were incubated for 46 h at 37 °C. For the last 3 h of culture time, cells were treated with 0.1  $\mu$ g/ml colcemid. The hypotonic treatment of cells was carried out with 75 mM KCl. Cells were then fixed in methanol:acetic acid (3:1) three times and the suspension was stored in the freezer (–18 °C). Chromosome preparations were prepared shortly before the FISH painting.

#### Fluorescence in situ hybridization (FISH)

The freshly prepared slides were treated with bisbenzimidazole and black-light to receive a differential sister chromatid staining (Kulka et al., 1995). After that the FISH method was carried out according to a modification of our standard procedures (Stephan and Pressl, 1997). A cocktail of directly labelled DNA probes (MetaSystems, XCP mix) for chromosome 2 (fluorescein isothiocyanate, FITC), 4 (Texas Red, TR) and 8 (FITC and TR) was used. The target DNA was denatured at 70 °C in 70% formamide, 2 $\times$  SSC (pH = 7.0) and dehydrated in ethanol (70, 90 and 100%) before and after the denaturation. The denatured DNA probes were applied to the slides and hybridised overnight at 37 °C protected by a sealed coverslip. Subsequently, the slides were washed shortly in 2 $\times$  SSC. Coverslips were applied with antifade mountant containing 4,6-diamidino-2-phenylindole (DAPI) for counterstaining.

#### Aberration scoring

Only complete first division metaphases were analysed. All cells with a painted chromosome involved in some rearrangement were digitised using the ISIS software (MetaSystems). The aberrations were described according to the PAINT (Tucker et al., 1995) and S&S (Savage and Simpson, 1994) nomenclature. Translocations were classified as complete (tc) when all painted material was rejoined, resulting in two monocentric bicoloured chromosomes [t(Ab) + t(Ba)], and as incomplete (ti) when only one monocentric bicoloured chromosome was seen. For statistical analysis complete and incomplete translocations were used.

At doses <1 Gy most aberrant cells can be expected to have only one exchange aberration and the number of unstable cells should be very low. Therefore, in these samples the whole genome was analysed only when the painted chromosomes were involved in translocations in order to be able to classify them as stable or unstable. At doses  $\geq$  1 Gy in each cell the whole genome was analysed. The classification of stable cells Cs and unstable cells

Cu was done in accordance with Buckton and Pike (1964). Cells with transmissible monocentric aberrations like symmetrical translocations, insertions or inversions are regarded as stable cells. Cells with acentrics, polycentric aberrations or rings (painted or unpainted chromosomes involved) are counted as unstable cells, even when translocations are included. Complex cells are defined as cells with complex exchanges resulting from  $\geq$  3 breaks in  $\geq$  2 chromosomes. These exchanges were reduced to simple aberration patterns, for example: if there was within one cell a dicentric [dic(AB)] associated with a fragment [ace(a)] and a translocation [t(Ab)], it was recorded as incomplete dicentric and incomplete translocation. All translocations which were not involved in visible complex exchanges were regarded as apparently simple.

The FISH-painted chromosomes 2 (green), 4 (red) and 8 (yellow) cover 19% of the genome (Morton, 1991). The observed aberration frequency ( $F_p$ ) for the applied three colour painting represents 0.344 of the calculated whole genome equivalent ( $F_G$ ) according to the equation:

$$F_p = 2.05 \left[ \sum_i f_i (1 - f_i) - \sum_{i < j} f_i f_j \right] F_G \quad (\text{Lucas, 1997})$$

where  $f_i$  and  $f_j$  are the fractions of the genome covered by the green-, red- or yellow-painting probes. When an exchange aberration appeared between two different colours of the painted chromosomes, it was counted as a single event. An aberration was not counted when it occurred as mono-coloured within one labelled pair of chromosomes.

The distribution of translocations among the cells was tested for Poisson by Papworth's "u" test (Papworth, 1970), which is significant when u exceeds the magnitude of 1.96.

## Results and discussion

In order to investigate the influence of unstable cells on the <sup>137</sup>Cs  $\gamma$ -ray dose-response curves for translocations, a total of 17,720 exclusively first mitoses were analysed (Table 1).

The yield of translocations in the control sample ( $2.0 \pm 0.8/1,000$  cells) was found to be similar to our control group ( $2.8 \pm 0.5/1,000$  cells) for the age group of 40–49 years (Pressl et al., 1999).

At doses of  $\geq$  1 Gy, 1,018 dicentric chromosomes in total were observed, including 372 painted dicentrics. The ratio of painted to whole genome dicentrics is  $0.37 \pm 0.05$  which corresponds to the calculated detection efficiency of  $F_p/F_G = 0.344$  for chromosomes 2, 4 and 8. There is also good agreement with the Lucas formula (Lucas, 1997) when the yield of the observed painted dicentric chromosomes is converted into the genome

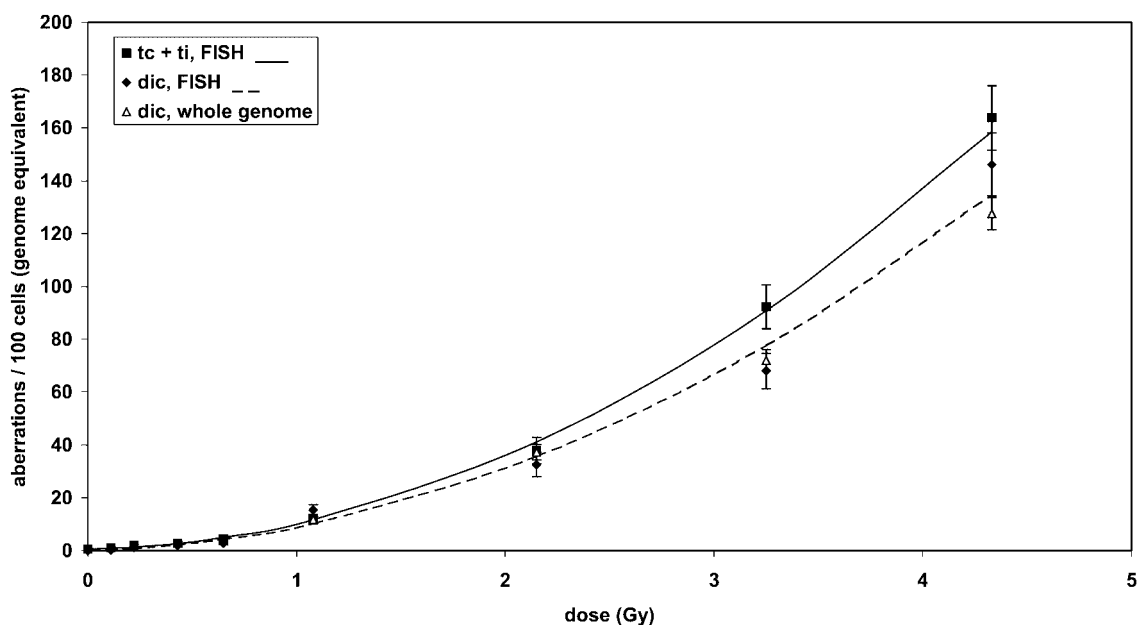


**Fig. 1.** Dose-response curves for translocations (tc + ti) and dicentric chromosomes after  $^{137}\text{Cs}$   $\gamma$ -irradiation (0.66 MeV, 0.4 Gy/min) of human lymphocytes.

equivalent and compared with the observed dicentric frequency in the whole genome (Table 1, Fig. 1).

The ratio of totally observed translocations (tc + ti) to the painted dicentric chromosomes (dic) (Table 1) is  $1.23 \pm 0.07$  (528 tc + ti/431 dic). When the control level of translocations is taken into account, the corrected ratio drops to about  $1.14 \pm 0.07$  (493 tc + ti /431 dic). These values are in agreement with the theoretically expected higher yield of translocations with a ratio of 1.1 to dicentric chromosomes (Lucas et al., 1996).

According to the scoring protocol, the number of unstable cells in the samples exposed to doses <1 Gy must be higher than the observed numbers, since aberrations in the counter-stained chromosomes, which cause unstable cells, were only recorded when painted chromosomes were involved in translocations. For example, the observed proportion of unstable cells is 1.8% at a dose of 0.65 Gy, and on the basis of the labelled fraction of the genome, the estimated proportion of unstable cells in total is about 5%. Since the unstable cells which were not scored contain no translocation, they would have only influenced the total number of cells (2,431 – 125 = 2,306 cells). In consequence the translocation yield will increase only slightly (observed yield: 1.38, corrected yield: 1.43 translocations per 100 cells) which is within the given error bars (Table 3). In the samples with doses <0.65 Gy, the proportion of not recorded unstable cells is <1%. Due to this small influence on translocation frequency, the scoring procedure used seems to be justified.

Within the 142 observed complex cells only three cells are classified as stable cells. The proportion of complex cells is low in comparison with unstable cells. While the percentage of complex cells increased between 1.1 and 4.3 Gy from 1 to 23%, the number of unstable cells increased from 17 to 89% (Table 2).

**Table 2.** Frequency of unstable and complex cells in dependence of dose

Dose (Gy)	Scored cells	Unstable cells (%)	Complex cells (%)
0	3520	2 (0.1)	0 (0)
0.11	3362	11 (0.3)	1 (0)
0.22	3061	22 (0.7)	2 (0.1)
0.43	3047	41 (1.3)	3 (0.1)
0.65	2431	43 (1.8)	2 (0.1)
1.08	1113	192 (17.3)	8 (0.7)
2.15	437	190 (43.5)	11 (2.5)
3.25	419	301 (71.8)	40 (9.5)
4.33	330	292 (88.5)	75 (22.7)

The yields of all translocations (tc + ti) observed in all scored cells and in stable cells and the yield of apparently simple translocations in total cells are given in Table 3. The yields of complete translocations (tc) are shown in Table 4. In addition to the translocation frequencies, the intracellular distribution of translocations was calculated. The distribution of complete translocations (tc) follows a Poisson distribution ( $\sigma^2/y = 1$ ,  $u < \pm 1.96$ ) and for all translocations (tc + ti) this is seen in most samples (Tables 3, 4). At higher doses the yields of all translocations in stable cells tend to be lower in comparison with the yields in total cells. But if the complex exchanges are ignored, the yields of translocations in stable cells become similar to the yields of apparently simple translocations in total cells. Regarding the yield of complete translocations, there is not such an effect of complex cells, and the yield of the complete translocations in stable cells seems to be the same as in total cells (Table 4).

**Table 3.** Yield of complete (tc) and incomplete (ti) translocations in all observed cells and in stable cells

Dose (Gy)	Distribution of tc + ti in total cells				$\sigma^2/y$	u	tc + ti $\pm$ SE per 100 total cells	tc + ti $\pm$ SE (apparently simple) per 100 total cells	Distribution of tc + ti in stable cells			$\sigma^2/y$	u	tc + ti $\pm$ SE per 100 stable cells
	0	1	2	3					0	1	2			
0	3513	7			1.00 $\pm$ 0.02	-0.08	0.20 $\pm$ 0.08	0.20 $\pm$ 0.08	3512	6		1.00 $\pm$ 0.02	-0.07	0.17 $\pm$ 0.07
0.11	3351	10	1		1.16 $\pm$ 0.02	7.00	0.36 $\pm$ 0.11	0.30 $\pm$ 0.09	3342	9		1.00 $\pm$ 0.02	-0.10	0.27 $\pm$ 0.09
0.22	3042	18	1		1.09 $\pm$ 0.02	3.77	0.65 $\pm$ 0.15	0.62 $\pm$ 0.15	3023	15	1	1.11 $\pm$ 0.02	4.52	0.56 $\pm$ 0.14
0.43	3018	28	1		1.06 $\pm$ 0.03	2.27	0.98 $\pm$ 0.18	0.95 $\pm$ 0.18	2982	24		0.99 $\pm$ 0.02	-0.30	0.80 $\pm$ 0.16
0.65	2395	35	1		1.04 $\pm$ 0.03	1.39	1.52 $\pm$ 0.26	1.40 $\pm$ 0.24	2355	33		0.99 $\pm$ 0.03	-0.47	1.38 $\pm$ 0.24
1.08	1067	46			0.96 $\pm$ 0.04	-0.96	4.13 $\pm$ 0.60	3.50 $\pm$ 0.55	886	35		0.96 $\pm$ 0.05	-0.80	3.80 $\pm$ 0.63
2.15	384	49	4		1.01 $\pm$ 0.07	0.18	13.04 $\pm$ 1.74	10.53 $\pm$ 1.51	225	21	1	1.00 $\pm$ 0.09	-0.02	9.31 $\pm$ 1.94
3.25	311	83	25		1.06 $\pm$ 0.07	0.89	31.74 $\pm$ 2.84	23.39 $\pm$ 2.59	92	25	1	0.85 $\pm$ 0.13	-1.15	22.88 $\pm$ 4.07
4.33	186	107	32	5	0.94 $\pm$ 0.08	-0.71	56.36 $\pm$ 4.02	36.36 $\pm$ 3.65	26	9	3	1.03 $\pm$ 0.22	0.14	39.47 $\pm$ 10.36

**Table 4.** Yield of complete (tc) translocations in all observed cells and in stable cells

Dose (Gy)	Distribution of tc in total cells				$\sigma^2/y$	u	tc $\pm$ SE per 100 total cells	tc $\pm$ SE (apparently simple) per 100 total cells	Distribution of tc in stable cells			$\sigma^2/y$	u	tc $\pm$ SE per 100 stable cells
	0	1	2	3					0	1	2			
0	3514	6			1.00 $\pm$ 0.02	-0.07	0.17 $\pm$ 0.07	0.17 $\pm$ 0.07	3512	6		1.00 $\pm$ 0.02	-0.07	0.17 $\pm$ 0.07
0.11	3354	7	1		1.22 $\pm$ 0.02	-0.08	0.27 $\pm$ 0.10	0.21 $\pm$ 0.08	3344	7		1.00 $\pm$ 0.02	-0.08	0.21 $\pm$ 0.08
0.22	3046	15			1.00 $\pm$ 0.02	-0.19	0.49 $\pm$ 0.13	0.49 $\pm$ 0.13	3025	14		1.00 $\pm$ 0.02	-0.17	0.46 $\pm$ 0.12
0.43	3022	25			0.99 $\pm$ 0.03	-0.31	0.82 $\pm$ 0.16	0.82 $\pm$ 0.16	2986	20		0.99 $\pm$ 0.03	-0.25	0.67 $\pm$ 0.15
0.65	2405	26			0.99 $\pm$ 0.03	-0.37	1.07 $\pm$ 0.21	1.07 $\pm$ 0.21	2362	26		0.99 $\pm$ 0.03	-0.37	1.09 $\pm$ 0.21
1.08	1086	27			0.98 $\pm$ 0.04	-0.56	2.43 $\pm$ 0.46	2.43 $\pm$ 0.46	898	23		0.98 $\pm$ 0.05	-0.52	2.50 $\pm$ 0.51
2.15	403	33	1		0.98 $\pm$ 0.07	-0.31	8.01 $\pm$ 1.34	7.55 $\pm$ 1.27	231	15	1	1.05 $\pm$ 0.09	0.61	6.88 $\pm$ 1.71
3.25	346	67	6		0.97 $\pm$ 0.07	-0.50	18.85 $\pm$ 2.08	15.99 $\pm$ 1.86	96	21	1	0.90 $\pm$ 0.13	-0.78	19.49 $\pm$ 3.85
4.33	250	66	13	1	1.05 $\pm$ 0.08	0.67	28.79 $\pm$ 3.03	25.45 $\pm$ 2.98	32	4	2	1.32 $\pm$ 0.22	1.49	21.05 $\pm$ 8.57

**Table 5.** Values of the coefficients  $\alpha$  and  $\beta$  for translocations in the equation  $y = c + \alpha D + \beta D^2$  ( $F_G$  values, genome equivalent)

Translocation type	Cell type	$c \pm SE \times 10^{-2}$	$\alpha \pm SE \text{ Gy}^{-1} \times 10^{-2}$	$\beta \pm SE \text{ Gy}^{-2} \times 10^{-2}$	$\chi^2$	DF
tc+ti	total cells	0.72 $\pm$ 0.21	1.52 $\pm$ 1.08	8.09 $\pm$ 0.61	3.14	6
tc	total cells	0.55 $\pm$ 0.18	2.00 $\pm$ 0.90	4.12 $\pm$ 0.47	2.10	6
tc+ti	stable cells	0.51 $\pm$ 0.18	2.46 $\pm$ 1.10	5.37 $\pm$ 0.92	2.55	6
tc	stable cells	0.49 $\pm$ 0.17	1.84 $\pm$ 1.00	3.90 $\pm$ 0.83	2.51	6
dic	total cells		2.19 $\pm$ 2.16	6.73 $\pm$ 1.56	1.99	6

The data from Tables 3 and 4 have been fitted to the linear-quadratic equation  $Y = c + \alpha D + \beta D^2$  by an iteratively weighted (reciprocal sample mean variance  $n/\sigma^2$ ) least-squares approximation. The parameters of the dose-response relationships are given in Table 5 as whole genomic aberration frequencies.

With respect to the involved uncertainties, the  $\alpha$  coefficients are very similar for all aberrations investigated, because they are barely influenced by heavily damaged cells or cells with complex exchanges. The  $\alpha$  term for translocations (tc + ti) observed here is  $0.015 \pm 0.008$  (corrected for full genome) and is therefore within the range of 0.008–0.030, described in literature for  $\gamma$ -rays (see below). The  $\beta$  coefficient for translocations is 1.2 times higher than that for the dicentric chromosomes.

The dose-response curve for all apparently simple translocations in stable cells is similar to the curve for translocations in

total cells without complex cells or apparently simple translocations in total cells (not shown). Concerning the dose relationship of complete translocations, there is no difference for the coefficients of stable and total cells.

In the literature, several dose-effect curves for translocations after exposure to  $^{60}\text{Co}$ - $\gamma$  or  $^{137}\text{Cs}$ - $\gamma$  rays from different laboratories are available (Bauchinger et al., 1993; Tucker et al., 1993; Lucas et al., 1995, 1997; Lindholm et al., 1998; Matsumoto et al., 1998; Finnon et al., 1999; Hsieh et al., 1999). A direct comparison of the results is not possible due to several differences in irradiation conditions and scoring criteria. Nevertheless, it is obvious that the calculated dose-response curve for all translocations in this study is relatively high concerning the  $\beta$  term, which may be due to the number of complex cells included. It is known that the detection of cells with complex

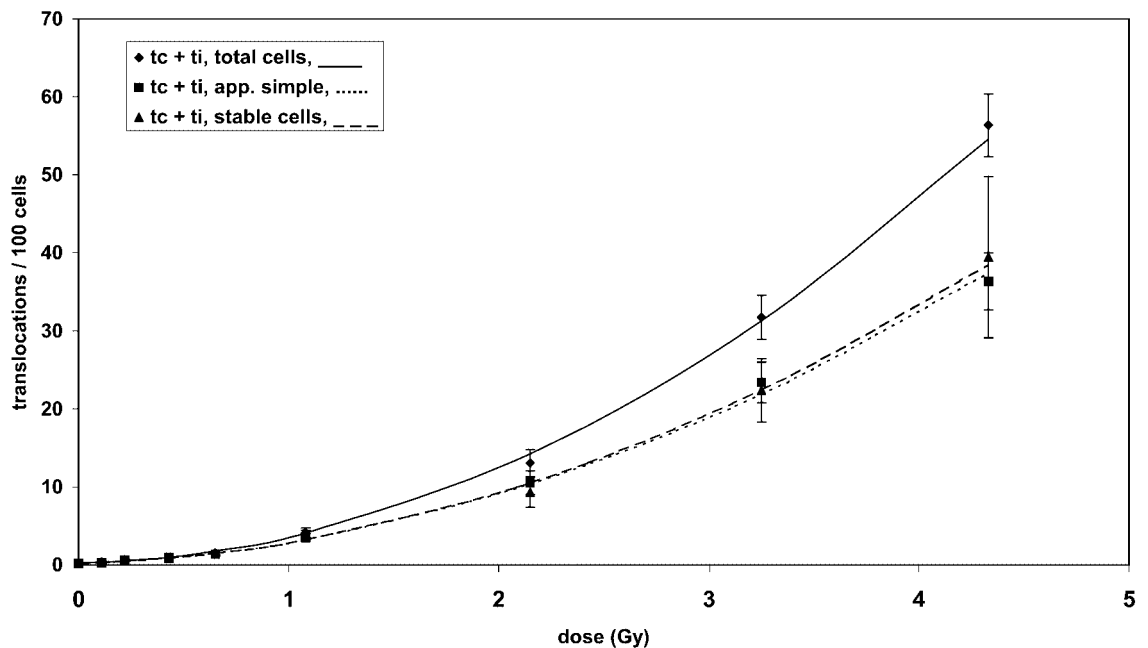


**Fig. 2.** Dose-response curves for translocations (tc + ti) in total or stable cells and for apparently simple translocations in total cells.

aberrations depends on the different patterns of staining (Tucker et al., 1995), and some cells with apparently simple translocations or without any FISH aberrations are not identified as complex cells. With three different colours the involvement of the three labelled chromosomes in complex exchanges is easier to detect than with one colour, and furthermore aberrations between the painted chromosomes can be detected. A possible reason for the higher  $\beta$  coefficient may be the inclusion of complex cells which often contain several apparently simple exchanges in addition to the complex aberration. When the complex cells are excluded from total cells, the  $\beta$  coefficient of dose-response curve declines to  $0.053 \pm 0.003$  which is close to other curves for  $\gamma$ -rays in the literature (mentioned above).

As far as we know, there are, until now, only two publications where the yield of translocations in stable cells after  $\gamma$ -ray exposure is described (Bauchinger et al., 1993; Finnon et al., 1999). In contrast to the results given in this paper for all translocations there was no difference between total or stable cells (Bauchinger et al., 1993) or only a slight but not significant decrease at doses of 3 and 4 Gy (Finnon et al., 1999). In contrast to these results, the observed yield for translocations (tc + ti) in stable cells is lower in comparison with total cells, but becomes identical when apparently simple translocations are regarded or complex cells are excluded (Tables 3 and 4). A possible reason for these diverging results may be due to different selection of scorable cells, pronounced by differences in the number of colours and the use of computerised image enhancement. The yield of complete translocations agrees with the published data (Finnon et al., 1999), and there was no difference between stable cells and total cells.

According to the presented data, the following conclusions on retrospective biological dosimetry can be drawn. Many

years after exposure probably most unstable cells will have been removed from peripheral blood as is well known from dicentric chromosomes. It is assumed that this is also true for complex cells which are damaged to a greater extent. Lymphocytes derived from irradiated stem cells should carry only aberrations of the stable type. The results of Fig. 2 (Table 3) indicate that the translocation yield (tc + ti) obtained after in vitro irradiation is influenced by unstable and complex cells at higher doses. For dose estimations this influence has to be taken into account to receive more reliable estimates about the initial doses. In this in vitro investigation the observed yields do not change only for complete translocations (independently if they were related to total cells or stable cells or if only apparently simple translocations were recorded) (Table 4). The dose-response curves for complete translocations are identical (Table 5). Therefore, for retrospective dose estimations only complete translocations should be used, particularly after exposures to acute doses higher than 1 Gy.

#### Acknowledgement

We are indebted to Dipl.-Phys. Werner Panzer of the GSF for irradiating the blood samples and carrying out the physical dosimetry.

## References

- Bauchinger M, Schmid E, Zitzelsberger H, Braselmann H, Nahrstedt U: Radiation-induced chromosome aberrations analysed by two-colour fluorescence in situ hybridization with composite whole chromosome-specific DNA probes and a pacentromeric DNA probe. *Int J Radiat Biol* 64:179–184 (1993).
- Buckton KE, Pike MC: Time in culture – an important variable in studying in vivo radiation-induced chromosome damage in man. *Int J Radiat Biol* 8:439–452 (1964).
- Finnon P, Moquet JE, Edwards AA, Lloyd DC: The  $^{60}\text{Co}$  gamma ray dose-response for chromosomal aberrations in human lymphocytes analysed by FISH; applicability to biological dosimetry. *Int J Radiat Biol* 75:1215–1222 (1999).
- Guerrero-Carbajal YC, Moquet JE, Edwards AA, Lloyd DC: The persistence of FISH translocations for retrospective biological dosimetry after simulated whole or partial body irradiation. *Radiat Prot Dosim* 76:159–168 (1998).
- Hsieh WA, Deng W, Chang WP, Galvan N, Owens CL, Morrison DP, Gale KL, Lucas JN: Alpha coefficient of dose-response for chromosome translocations measured by FISH in human lymphocytes exposed to chronic  $^{60}\text{Co}$  gamma rays at body temperature. *Int J Radiat Biol* 75:435–439 (1999).
- Kulka U, Huber R, Muller P, Knehr S, Bauchinger M: Combined FISH painting and harlequin staining for cell cycle-controlled chromosome analysis in human lymphocytes. *Int J Radiat Biol* 68:25–27 (1995).
- Lindholm C, Luomahaara S, Koivistoinen A, Ilus T, Edwards AA, Salomaa S: Comparison of dose-response curves for chromosomal aberrations established by chromosome painting and conventional analysis. *Int J Radiat Biol* 74:27–34 (1998).
- Lindholm C, Romm H, Stephan G, Schmid E, Moquet J, Edwards A: Intercomparison of translocation and dicentric frequencies between laboratories in a follow-up of the radiological accident in Estonia. *Int J Radiat Biol* 78:883–890 (2002).
- Lucas JN: Dose reconstruction for individuals exposed to ionizing radiation using chromosome painting. *Radiat Res* 148:S33–38 (1997).
- Lucas JN, Awa A, Straume T, Poggensee M, Kodama Y, Nakamo M, Ohtaki K, Weier HU, Pinkel D, Gray J, Littlefield G: Rapid translocation frequency analysis in humans decades after exposure to ionizing radiation. *Int J Radiat Biol* 62:53–63 (1992).
- Lucas JN, Hill F, Burk C, Fester T, Straume T: Dose-response curve for chromosome translocations measured in human lymphocytes exposed to  $^{60}\text{Co}$  gamma rays. *Health Phys* 68:761–765 (1995).
- Lucas JN, Chen AM, Sachs RK: Theoretical predictions on the equality of radiation-produced dicentrics and translocations detected by chromosome painting. *Int J Radiat Biol* 69:145–153 (1996).
- Lucas JN, Hill FS, Burk CE, Lewis AD, Lucas AK, Chen AM, Sailes FC, Straume T: Dose-response curve for chromosome translocations induced by low dose rate  $^{137}\text{Cs}$  gamma rays. *Radiat Prot Dosim* 71:279–282 (1997).
- Matsumoto K, Ramsey MJ, Nelson DO, Tucker JD: Persistence of radiation-induced translocations in human peripheral blood determined by chromosome painting. *Radiat Res* 149:602–613 (1998).
- Morton NE: Parameters of the human genome. *Proc natl Acad Sci, USA* 88:7474–7476 (1991).
- Natarajan AT, Santos SJ, Darroudi F, Hadjidikova V, Vermeulen S, Chatterjee S, Berg M, Grigorova M, Sakamoto Hojo ET, Granath F, Ramalho AT, Curado MP:  $^{137}\text{Cesium}$ -induced chromosome aberrations analyzed by fluorescence in situ hybridization: eight years follow-up of the Goiania radiation accident victims. *Mutat Res* 400:299–312 (1998).
- Papworth DG: in Appendix to paper by J.R.K. Savage, Sites of radiation-induced chromosome exchanges. *Current Topics Radiat Res* 6:129–194 (1970).
- Pressl S, Edwards A, Stephan G: The influence of age, sex and smoking habits on the background level of FISH-detected translocations. *Mutat Res* 442:89–95 (1999).
- Savage JRK, Simpson PJ: FISH “painting” patterns resulting from complex exchanges. *Mutat Res* 312:51–60 (1994).
- Stephan G, Pressl S: Chromosome aberrations in human lymphocytes analysed by fluorescence in situ hybridization after in vitro irradiation, and in radiation workers, 11 years after an accidental radiation exposure. *Int J Radiat Biol* 71:293–299 (1997).
- Tucker JD, Morgan WF, Awa AA, Bauchinger M, Blakey D, Cornforth MN, Littlefield LG, Natarajan AT, Shasserre C: PAINT: a proposed nomenclature for structural aberrations detected by whole chromosome painting. *Mutat Res* 347:21–24 (1995).
- Tucker JD, Ramsey MJ, Lee DA, Minkler JL: Validation of chromosome painting as a biodosimeter in human peripheral lymphocytes following acute exposure to ionizing radiation in vitro. *Int J Radiat Biol* 64:27–37 (1993).



## Effect of DMSO on radiation-induced chromosome aberrations analysed by FISH

S. Cigarrán,<sup>a</sup> L. Barrios,<sup>b</sup> M.R. Caballín<sup>a</sup> and J.F. Barquinero<sup>a</sup>

<sup>a</sup>Unitat d'Antropologia, Dpt. Biologia Animal, Biologia Vegetal i Ecologia;

<sup>b</sup>Unitat de Biologia Cel.lular, Dpt. Biologia Cel.lular i Fisiologia Universitat Autònoma de Barcelona, Bellaterra (Spain)

**Abstract.** The purpose of the present work was to determine if the described reduction in the frequency of radiation-induced chromosome aberrations by DMSO is homogeneous within different human chromosomes. Blood samples were irradiated with 4 Gy of X-rays in absence and presence of 0.5 M DMSO. FISH painting was carried out independently for human chromosomes 1, 2, 3, 4, 7, 11 and 12. The observed frequencies of apparently simple translocations and dicentrics for all these chromosomes, showed a homogeneous reduction

when the irradiation was done in the presence of DMSO. Moreover, a better fit between the observed and expected frequencies was obtained when (DNA content)<sup>2/3</sup> was used to calculate the expected frequencies, instead of just the DNA content. This result supports the idea that for exchange type aberrations, a better adjustment is obtained when the surface area of spherical chromosome territories is considered.

Copyright © 2003 S. Karger AG, Basel

Ionising radiation induces lesions in DNA, directly and indirectly, through the products of radiolysis of water, especially the OH radical. The direct or indirect effects are related to the degree of binding of water molecules to DNA (Ward, 1991). The effects induced by OH radicals originating from tightly bound water molecules associated with DNA, are considered as direct effects. It has been estimated that about 70% of strand breaks are induced indirectly (Roots and Okada, 1972).

Molecules capable of scavenging water radicals act as radioprotectors, and reduce DNA lesions. Several studies have pointed out the efficiency of dimethylsulfoxide (DMSO) as an

effective radioprotector by its ability to scavenge OH radicals. The protection does not increase at concentrations above 1 M (Chapman et al., 1975). This saturation allows us to define the indirect and direct effects as scavengeable or non-scavengeable, respectively (Ward, 1991).

The conformation of chromosome territories in interphase nuclei could influence the sensitivity of individual chromosomes to ionising radiation. Fluorescence in situ hybridisation allows us to study the involvement of each human chromosome in radiation-induced aberrations. Whereas some studies support a DNA content proportionality (Matsukoa et al., 1994; Gebhart et al., 1996), other studies have pointed out that some other factors like the chromosome gene content could also be relevant (Natarajan et al., 1996; Surralles et al., 1997; Puerto et al., 2001). In a previous study by Cigarrán et al. (1998), the different involvement of human chromosomes in radiation-induced aberrations showed a better correlation when the surface area of spherical territories of each chromosome in the interphase nuclei was considered.

The aim of the present study is to assess if the expected reduction in the radiation-induced chromosome aberrations by the radical scavenger DMSO, depends on DNA content, or on the territories occupied by different human chromosomes in the cell nucleus.

Supported by the Consejo de Seguridad Nuclear SPR/316/99/640 and by the Generalitat de Catalunya 2001SGR 00213.

Received 11 September 2003; manuscript accepted 9 December 2003.

Request reprints from Dr. J.F. Barquinero, Unitat d'Antropologia  
Dpt. Biologia Animal, Biologia Vegetal i Ecologia  
Universitat Autònoma de Barcelona, 08193 Bellaterra (Spain)  
telephone: 34-935812049; fax: 34-935811321  
e-mail: Francesc.Barquinero@uab.es

## Materials and methods

### Irradiation and culture conditions

Peripheral blood samples from a healthy male donor with no history of exposure to clastogenic agents, was obtained by venipuncture and collected in heparinized tubes. DMSO was added to samples five min before irradiation. Samples with or without 0.5 and 1 M of DMSO were irradiated with 4 Gy, using an X-ray source, with a beam quality corresponding to a half-value layer of 1.43 mm Cu (180 kV, 9 mA and 0.5 mm Cu filtration). The dose-rate was 0.27 Gy/min. IAEA recommendations were followed for the irradiation (IAEA, 2001).

A preliminary study to determine the most appropriate concentration of DMSO to be used in the FISH approach was carried out by the analysis of dicentrics in metaphases stained with Giemsa.

After irradiation, lymphocytes were isolated in a Ficoll gradient and cultured for 48 h in RPMI 1640 medium supplemented with 20% fetal calf serum, antibiotics and phytohaemagglutinin. Colcemid was added 2 h before harvest. To determine the proportion of first and second-division metaphases, 12 µg/ml of bromodeoxyuridine (BrdU) was added to the cultures from their start. The frequency of first division metaphases, determined by the FPG technique was always higher than 95%.

### Fluorescence in situ hybridisation

Cy3-labelled DNA whole chromosome probes for chromosomes 1, 2, 3, 4, 7, 11 and 12, and a FITC-labelled pan-centromeric probe (Cambio, UK) were used according to the manufacturer's protocol. Counterstaining was performed with 4',6-diamidino-2-phenylindole (DAPI) with 1 µg/ml antifade solution (Cambio, UK).

### Scoring criteria

Metaphases were examined using a triple-band pass filter, and the painted chromosomes were analysed using the triple-band, Cy3, FITC, and DAPI filters. Only metaphases having all the painted material present were analyzed. Each abnormal metaphase was described using the PAINT modified nomenclature (Knehr et al., 1998) and converted to S&S nomenclature (Savage and Simpson, 1994). Incomplete aberrations were allocated to complete aberrations, using the approach suggested by Simpson and Savage (1996).

### Statistical analyses

For comparisons, genomic equivalent frequencies taking into account the relative DNA content of the painted chromosomes (Morton, 1991; Lucas et al., 1992) or DNA content<sup>2/3</sup> to consider spherical chromosome territories were used (Cremer et al., 1996).

Because the formula described by Lucas et al. (1992) is only applicable for exchanges between painted and unpainted chromosomes involving two breaks, complex aberrations have been reduced to simple ones to include them in the calculations.

## Results

After 4 Gy irradiation without DMSO, the frequency of dicentrics in solid stained metaphases was  $0.92 \pm 0.09$  (Table 1), similar to that described previously in our laboratory,  $0.98 \pm 0.07$  (Barquinero et al., 1997). In the presence of 0.5 and 1 M of DMSO, the frequencies of dicentrics were significantly reduced ( $0.44 \pm 0.05$  and  $0.47 \pm 0.06$  respectively;  $P < 0.01$  in both cases). For the FISH study 0.5 M DMSO was chosen, because although the frequencies of radiation-induced dicentrics at both concentrations of DMSO were very similar, number and quality of metaphases per slide were dramatically reduced at 1 M.

The cytogenetic results obtained with FISH are shown in Table 2. When data from all chromosomes analysed are considered together, after 4 Gy irradiation the genomic frequency of total apparently simple translocations (2Bt) was reduced from

**Table 1.** Chromosome aberrations detected in solid Giemsa-stained metaphases after irradiation with 4 Gy in absence or presence of 0.5 and 1 M DMSO.

DMSO	0	0.5 M	1 M
Cells analysed	118	189	156
% abnormal cells	74.6%	61.9%	54.5%
Dicentrics ( $y \pm SE$ )	108 ( $0.92 \pm 0.09$ )	83 ( $0.44 \pm 0.05$ )	73 ( $0.47 \pm 0.06$ )
Rings	9	10	11
Excess acentrics	42	46	29

$0.799 \pm 0.005$  without DMSO, to  $0.439 \pm 0.003$  with 0.5 M of DMSO. For total apparently simple dicentrics (2At) the frequency shows a similar reduction of about 45% from  $0.630 \pm 0.004$  to  $0.343 \pm 0.003$ . These frequencies are lower than the ones observed after Giemsa stain because dicentrics from complex aberrations are not included. When each chromosome is considered independently, the chi-squared test showed a homogeneous reduction in the frequencies of total apparently simple aberrations (2Bt and 2At).

When complex aberrations observed in all chromosomes were considered together, the frequency falls from  $0.348 \pm 0.026$  to  $0.134 \pm 0.016$ , showing a reduction of about 61%, higher than the ones observed for simple aberrations. Assuming the breakage-first-hypothesis the complex aberrations are grouped considering the minimal number of breaks involved in their production, the reductions were 54, 75 and 86% for aberrations with three, four or more than four breaks, respectively.

In the present study we also checked if the involvement of different chromosomes in radiation-induced aberrations is affected by DMSO. When the relative DNA content for each chromosome was considered to calculate expected frequencies, after 4 Gy irradiation without DMSO significant differences from the observed values were found for both, 2At and 2Bt ( $P < 0.02$  and  $P < 0.05$  respectively) (Fig. 1), indicating a non-random distribution of induced aberrations. The differences were mainly due to chromosomes 2 and 11. When expected values were calculated using the (DNA content)<sup>2/3</sup> the chi-squared test did not show significant differences.

In samples irradiated in the presence of 0.5 M of DMSO, there were no differences between the observed and expected frequencies for 2Bt and 2At, on the basis of the DNA content. When 2Bt and 2At were considered together significant differences on the basis of the DNA content ( $P < 0.01$ ) were found, but not on (DNA content)<sup>2/3</sup>.

## Discussion

In living cells, the direct effect of ionising radiation on DNA would be the damage produced by OH radicals from bound water molecules (Ward, 1991). The ability of DMSO to scavenge induced free radicals was described for high and low LET radiation (deLara et al., 1995). Littlefield et al. (1988), analysed

**Table 2.** Chromosomal aberrations analysed in FISH painted cells after 4 Gy irradiation in absence or presence of 0.5M DMSO

S&S <sup>a</sup>	Chromosome <sup>b</sup> [DMSO]	1		2		3		4		7		11		12		Total	
		0	0.5	0	0.5	0	0.5	0	0.5	0	0.5	0	0.5	0	0.5	0	0.5
	cells analysed (equivalent cells)	667 (104)	647 (101)	552 (84)	544 (82)	398 (51)	402 (52)	788 (97)	709 (87)	576 (60)	582 (61)	945 (84)	913 (81)	583 (51)	484 (43)	4509 (531)	4281 (506)
Apparently simple aberrations																	
2B	t(Ba)t(Ab)	62	28	39	19	26	18	76	27	34	16	63	33	25	16	325	157
I	t(Ba) ace(b)	9	3	0	3	2		8	1	3	1	3				25	8
II	t(Ab)	9	4	6	4	5	3	7	5	6	1	12	12	7	3	52	32
III	t(Ba)	5	6	3	4	3	1	8	4	7	7	10	8	7	4	43	34
	2Bt <sup>p</sup>	78	38	47	28	35	22	93	36	48	24	85	52	38	22	424	222
2A	dic(BA)ace(ab)	44	23	26	14	28	13	48	24	26	16	47	26	34	17	253	133
IV	dic(BA) ace(b)	3	3	5		2	3	1	5	4	3	6	2	2	1	23	17
V	ace(ab)	5	4	4	1	1	2	8	0	1		5	2			24	9
VI	dic(BA)	11	5	5	1	5	2	6	5	10	2	12	7	7	2	56	24
	2At <sup>p</sup>	58	31	36	15	35	18	58	33	40	21	66	35	42	20	335	174
	2Bt±2At	136	69	84	43	70	40	151	70	88	45	150	87	80	42	758	396
CR1	r(B) ace(b)	3	1	1	1			5	5	1		5	1	2		17	8
	r(B)	0	1					0	0			1				1	1
2C	r(b)	4	1					3	2			4	0			11	3
	ace (b)	8	5	13	6	6		5	2	7	3	3	6	10	4	52	26
	TOTAL AS	143	71	85	44	70	40	159	77	89	45	159	88	82	42	786	407
Complex aberrations																	
mnb = 3																	
2F	t(Ba) ace(ab)	14	5	5	1	1	1	12	1	0	1	9	3	3	2	44	14
	2Ft <sup>p</sup>	23	10	8	3	3	2	22	2	2	2	15	5	4	2	77	26
2G	dic(BA) t(Ab)	9	6	6	3	2	3	5	2	2	2	5	2	3	2	32	20
	2Gt <sup>p</sup>	12	8	8	3	3	4	6	3	3	2	7	3	4	2	42	26
	Other mnb =3	9	0	0	0	2	0	2	3	0	2	5	1	4	2	22	8
	subtotal 3	44	18	15	7	7	6	30	7	5	6	27	9	12	7	141	60
	mnb = 4	9	1	3	2	1	0	4	1	2	0	8	1	2	2	29	6
	mnb = 5	5	0	1	0	0	0	2	1	1	0	2	0	0	0	11	1
	mnb = 6	2	0	0	0	0	0	0	1	1	0	0	0	0	0	3	1
	mnb = 7	1	0	0	0	0	0	0	0	0	0	0	0	0	0	1	0
	Total complex	61	19	19	9	8	6	36	10	9	6	37	10	14	9	185	68
	% Complex	29.9	20.8	18.7	16.5	10.6	13.0	18.6	12.0	9.2	12.5	18.7	9.9	14.3	17.4	19.0	14.3
	ace (b)	8	5	13	6	6		5	2	7	3	3	6	10	4	52	26

<sup>a</sup> S&S, Savage and Simpson nomenclature.

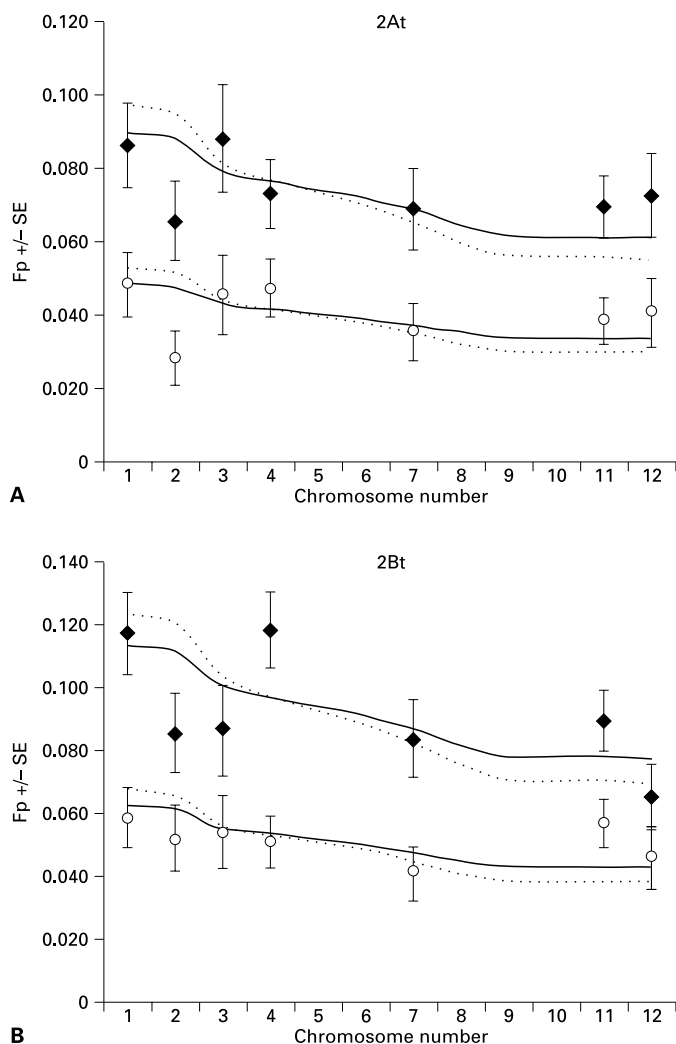
<sup>b</sup> Incomplete "one-way" aberrations have been allocated as 2At, 2Bt, 2Ft and 2Gt following the method proposed by Simpson and Savage (1996). mnb, minimal number of breaks to produce the observed aberration.

the frequency of X-ray-induced dicentrics in the presence of several concentrations of DMSO (from 10<sup>-4</sup> to 2 M), and found an exponential decrease of dicentrics, with a maximum protective level at 1 M DMSO.

With the introduction of FISH techniques to study the radiation-induced chromosome damage, the involvement of different human chromosomes in aberrations was a matter of discussion. When the relative DNA content was considered, deviations from expected values were described for single chromosomes (Pandita et al., 1994; Granath et al., 1996; Knehr et al., 1996; Barquinero et al., 1998; Cigarran et al., 1998). In the present study, the frequencies of induced aberrations in chromosomes 1, 2, 3, 4, 7, 11, and 12 after 4 Gy, were not proportional to the DNA content. The differences were mainly due to chromosomes 2 and 11, which are less or more involved than expected, respectively.

When the surface area of spherical chromosome territories was used to calculate the expected values, the differences between expected and observed frequencies disappeared. This agrees with our previous work (Cigarran et al., 1998), where we discussed that damage induced at the surface of chromosome territories, interacts more easily to form exchange type aberrations. The model also implies that small chromosomes have a higher probability to be involved in exchange type aberrations, because they have a higher surface-to-volume ratio than large chromosomes.

After 4 Gy irradiation the presence of DMSO led to a homogeneous reduction of the frequencies of aberrations in the analysed chromosomes. DMSO permeabilizes and diffuses freely across cell membranes, and it should be present in the interphase nuclei at equal concentrations. Therefore, the proportion of scavengeable damage should be similar for all chromosomes. As can be seen in Fig. 1, for apparently simple dicentrics and



translocations in all chromosomes analyzed, the deviations of the observed in relation to the expected frequencies were very similar after irradiations with and without DMSO.

As a result of the ability of DMSO to scavenge radiation-induced OH radicals, there is a reduction in the number of damaged sites. This is supported by the increased reduction of complex aberrations. Littlefield et al. (1988), showed that DMSO reduces the effective dose by 50%. In the present study the proportion of complex aberrations was 14.3% at a dose of 4 Gy in the presence of DMSO, a value similar to the 18.9% observed after irradiation in the absence of DMSO with 2 Gy of X-rays reported previously (Barquinero et al., 1999).

In conclusion, for the different chromosomes studied DMSO reduces the frequencies of radiation-induced chromosome aberrations homogeneously. The results of the present study also indicate that the surface model, assuming spherical chromosome domains (Cigarran et al., 1998), although it may not reflect all aspects of the organisation of chromosome territories in interphase nuclei (Cremer and Cremer, 2001), seems to be closer to the real situation than the mean amount of DNA and leads to more accurate estimations of chromosome involvement in exchange type aberrations.

**Fig. 1. (A)** Observed frequencies  $\pm$  SE of 2At after 4 Gy irradiation with (empty circles) or without (black diamonds) DMSO. Solid lines indicated expected values taking into account the relative (DNA content)<sup>2/3</sup> and the dotted line expected values taking into account the relative DNA content. **(B)** The same for 2Bt.

## References

- Barquinero JF, Barrios L, Caballin MR, Miro R, Ribas M, Egozcue J: Biological dosimetry in simulated in vitro partial irradiations. *Int J Radiat Biol* 71:435–440 (1997).
- Barquinero JF, Knehr S, Braselmann H, Figel M, Bauchinger M: DNA-proportional distribution of radiation-induced chromosome aberrations analysed by fluorescence in situ hybridization painting of all chromosomes of a human female karyotype. *Int J Radiat Biol* 74:315–323 (1998).
- Barquinero JF, Cigarran S, Caballin MR, Braselmann H, Ribas M, Egozcue J, Barrios L: Comparison of X-ray dose-response curves obtained by chromosome painting using conventional and PAINT nomenclatures. *Int J Radiat Biol* 75:1557–1566 (1999).
- Cigarran S, Barrios L, Barquinero JF, Caballin MR, Ribas M, Egozcue J: Relationship between the DNA content of human chromosomes and their involvement in radiation-induced structural aberrations, analysed by painting. *Int J Radiat Biol* 74:449–455 (1998).
- Cremer C, Munkel CH, Granzow M, Jauch A, Dietzel S, Eils R, Guan XY, Meltzer PS, Trent JM, Langowski J, Cremer T: Nuclear architecture and the induction of chromosomal aberrations. *Mutat Res* 366:97–116 (1996).
- Cremer T, Cremer C: Chromosome territories, nuclear architecture and gene regulation in mammalian cells. *Nature Rev Genet* 2:292–301 (2001).
- Chapman JD, Dugle DL, Reuvers AP, Gillespie CJ, Borsa J: Chemical radiosensitization studies with mammalian cells growing in vitro. *Rad Res* 57:752–760 (1975).
- deLara CM, Jenner TJ, Townsend KM, Marsden SJ, O'Neill P: The effect of dimethyl sulfoxide on the induction of DNA double-strand breaks in V79-4 mammalian cells by alpha particles. *Radiat Res* 144:43–49 (1995).
- Gebhart E, Neubauer S, Schmitt G, Birkenhake S, Dunst J: Use of a three-color chromosome in situ suppression technique for the detection of past radiation exposure. *Radiat Res* 145:47–52 (1996).
- Granath F, Grigorova M, Natarajan AT: DNA content proportionality and persistence of radiation-induced chromosomal aberrations studied by FISH. *Mutat Res* 366:145–152 (1996).
- IAEA: Cytogenetic Analyses for Radiation Dose Assessment. A Manual. Technical Report Series 450. (International Atomic Energy Agency, Vienna 2001).
- Knehr S, Zitzelsberger H, Braselmann H, Nahrstedt U, Bauchinger M: Chromosome analysis by fluorescence in situ hybridization: further indications for a non-DNA-proportional involvement of single chromosomes in radiation-induced structural aberrations. *Int J Radiat Biol* 70:385–392 (1996).
- Knehr S, Zitzelsberger H, Bauchinger M: FISH-based analysis of radiation-induced chromosomal aberrations using different nomenclature systems. *Int J Radiat Biol* 73:135–141 (1998).
- Littlefield LG, Joiner EE, Colyer SP, Sayer AM, Frome EL: Modulation of radiation-induced chromosome aberrations by DMSO, an OH radical scavenger. 1: Dose-response studies in human lymphocytes exposed to 220 kV X-rays. *Int J Radiat Biol* 53:875–890 (1988).
- Lucas JN, Awa A, Straume T, Poggensee M, Kodama Y, Nakano M, Weier HU, Pinkel D, Gray J, Littlefield G: Rapid translocation frequency analysis in man decades after exposure to ionizing radiation. *Int J Radiat Bio* 62:53–63 (1992).

- Matsuoka A, Tucker JD, Hayashi M, Yamazaki N, Sofuni T: Chromosome painting analysis of X-ray-induced aberrations in human lymphocytes in vitro. *Mutagenesis* 9:151–155 (1994).
- Morton NE: Parameters of the human genome. *Proc natl Acad Sci, USA* 88:7474–7476 (1991).
- Natarajan AT, Balajee AS, Boei JJ, Darroudi F, Dominguez I, Hande MP, Meijers M, Slijepcevic P, Vermeulen S, Xiao Y: Mechanisms of induction of chromosomal aberrations and their detection by fluorescence in situ hybridization. *Mutat Res* 372:247–258 (1996).
- Pandita TK, Gregoire V, Dhingra K, Hittelman WN: Effect of chromosome size on aberration levels caused by gamma radiation as detected by fluorescence in situ hybridization. *Cytogenet Cell Genet* 67:94–101 (1994).
- Puerto S, Ramirez MJ, Marcos R, Creus A, Surralles J: Radiation-induced chromosome aberrations in human euchromatic (17cen→p53) and heterochromatic (1cen→1q12) regions. *Mutagenesis* 16:291–296 (2001).
- Roots S, Okada S: Protection of DNA molecules of cultured mammalian cells from radiation-induced single-strand scissions by various alcohols and SH compounds. *Int J Radiat Biol* 21:339–342 (1972).
- Savage JRK, Simpson PJ: On the scoring of FISH-“painted” chromosome exchange aberrations. *Mutat Res* 307:345–353 (1994).
- Simpson PJ, Savage JR: Dose-response curves for simple and complex chromosome aberrations induced by X-rays and detected using fluorescence in situ hybridization. *Int J Radiat Biol* 69:429–436 (1996).
- Surralles J, Sebastian S, Natarajan AT: Chromosomes with high gene density are preferentially repaired in human cells. *Mutagenesis* 12:437–442 (1997).
- Ward JF: Mechanisms of radiation action on DNA in model systems – their relevance to cellular DNA. The early effects of radiation on DNA, in Fielden EM, O'Neill P (eds): NATO ASI series, Serie H, Cell Biology Vol 54, pp 1–16 (Springer, Berlin 1991).

# DNA damage in Chinese hamster cells repeatedly exposed to low doses of X-rays

A.M. Güerci, F.N. Dulout and A.I. Seoane

CIGEBBA (Centro de Investigaciones en Genética Básica y Aplicada) Facultad de Ciencias Veterinarias, Universidad Nacional de La Plata, La Plata (Argentina)

**Abstract.** In a recent paper we reported the results of an experiment carried out by analysing chromosomal damage in Chinese hamster (CHO) cells exposed to low doses of X-rays. The present investigation was undertaken in order to validate those results using a different approach, the single cell gel electrophoresis assay (comet assay) immediately after irradiation. Cells were cultured during 14 cycles, irradiation treatment was performed once per cycle when the cells were at 90–95% of confluence. Doses of 2.5, 5.0 and 10.0 mSv were used. Sequential irradiation of CHO cells induced a decrease of cells without migration and an increase of cells showing DNA damage with the three doses employed. Significant increases of low-level

damaged cells ( $p < 0.001$ ) were found for the 14 exposures when compared to controls except for the first irradiations with 2.5 and 10 mSv, respectively. No significant increase of the frequency of cells with severe damage was observed in any case. These findings could be explained by assuming a complex interactive process of cell recovery, DNA damage and repair together with the induction of genomic instability, the incidence of bystander effects as well as some kind of radioadaptive response of the cells. If these phenomena are limited to the cell line employed deserves further investigation.

Copyright © 2003 S. Karger AG, Basel

Living beings are permanently exposed to ionizing radiation emitted either from natural or from anthropogenic sources. Nevertheless, studies of the biological effects of ionizing radiation were focussed for decades mainly on the consequences of single exposures to relatively high doses. Under these conditions, mechanisms involved in the induction of chromosomal aberrations were interpreted as a direct consequence of unrepaired or misrepaired DNA double-strand breaks. Genetic damage such as point mutations and chromosomal aberrations would thus occur by the incidence of an ionizing particle through or near the DNA molecule.

Estimates of the biological effects of low doses are generally based on extrapolation from data at higher doses. However, experimental results obtained during the last decade seem to indicate that genetic damage induced by low doses and low dose rates is higher than expected. This fact has been attributed to the so called “bystander effect” defined as the induction of damage in cells that were not directly hit by radiation (Ballarini et al., 2002). In addition to the non-targeted effects of radiation exposure, delayed effects observed in cells many generations after the initial injury have been attributed to the induction of genomic instability (Little, 2000; Little et al., 2002; Morgan, 2003a, b; Morgan et al., 1996; Wright, 1998). The term genomic instability describes the increased rate of acquisition of alterations in the genome (Morgan, 2003a) and is evidenced by chromosomal aberrations, aneuploidy, gene mutations and other cytological or molecular alterations. Another consequence of the exposure to low doses of radiation is the radioadaptive response first described by Olivieri et al. (1984) and recently reviewed by Sasaki et al. (2002). Adaptive response is the acquirement of cellular resistance to the genotoxic effects of radiation by prior exposure to low-dose radiation (Sasaki et al., 2002).

In a recent paper we reported the results of an experiment carried out with Chinese hamster (CHO) cells exposed to low doses of X-rays (Güerci et al., 2003). Briefly, cells were cultured

This work is part of the “Proyecto integrado de mutagénesis y carcinogénesis ambiental” of the “Programa de Incentivos para Docentes-Investigadores de Universidades Nacionales”. A.B. Güerci has a fellowship of the National University of La Plata.

Received 13 September 2003; accepted 10 December 2003.

Request reprints from: Prof. Fernando N. Dulout  
CIGEBBA (Centro de Investigaciones en Genética Básica y Aplicada)  
Facultad de Ciencias Veterinarias, Universidad Nacional de La Plata  
Calle 60 y 118, CC 296, B1900AVW La Plata (Argentina)  
telephone: +54 (0)221-421-1799; fax: +54 (0)221-421-1799  
e-mail: dulout@fcv.unlp.edu.ar

during 14 passages. Irradiation was performed once per cycle when the cells were 90–95% confluent with doses of 2.5, 5.0 and 10.0 mSv. Fifteen hours after irradiation cytogenetic analysis was carried out in the first post-irradiation metaphases. Repeated irradiation of CHO cells did not increase the yield of chromatid- or chromosome-type aberrations. Nevertheless, a significant increment of gaps was found after the first or second X-ray hit with the three doses employed.

These results have been interpreted as evidence of the induction of genomic instability by repeated irradiations where the direct effect of each new hit of X-rays was added to the factors secreted by unstable cells affected by previous irradiations. Accordingly, a variation in the frequency of gaps can be the consequence of simultaneous induction of endogenous DNA damage, cell death and cell survival.

The present investigation was undertaken in order to validate previous results using a different approach, the single cell gel electrophoresis assay (comet assay) immediately after irradiation. The comet assay is a sensitive and rapid method used with increasing popularity to determine the level of DNA damage in terms of strand breaks and alkaline labile sites (Wojezdowska et al., 1998; Moller et al., 2000). In addition, while chromosomal aberration techniques only detect the misrepaired DNA lesions persisting in the cell, the comet assay is intended to detect lesions in individual cells at an early stage after exposure, allowing a more efficient evaluation of damage (Singh et al., 1988).

## Material and methods

### Cell culture

Chinese hamster ovary (CHO) cells originally obtained from American Type Culture Collection (ATCC) were used for the experiments. Cells were grown as monolayers in Falcon T-25 flasks with 10 ml of Ham F-10 medium (GIBCO BRL) supplemented with 10% fetal calf serum and antibiotics (penicillin 90 U/ml and streptomycin 90 µg/ml) at 37 °C. Cells were checked for their viability by trypan blue dye exclusion method. In all cases viability was higher than 90%.

### Experimental procedures

Cells were cultured during 14 cycles; irradiation treatment was performed once per cycle when the cells were at 90–95% confluence. An X-ray

apparatus DSJ 65 kV-5 mA was used. To calculate the absorbed dose, a dosimeter Keithley digital 35617 EBS with microchamber PTW N 2336/414 was employed. After treatment, cells were resuspended and divided into two fractions: one was cultured to obtain the repeatedly irradiated population, and the other to carry out the comet assay. Doses of 2.5, 5.0 and 10.0 mSv were employed at a dose rate of 50 mSv/min. All of the experiments were repeated two times. Fifty randomly selected comet images were analyzed per treatment.

### Comet assay

The comet assay was performed according to the method of Singh et al. (1988) with some small modifications (Tice and Strauss, 1995). Briefly, slides were covered with a first layer of 180 µl of 0.5% normal agarose (GIBCO BRL). An amount of 75 µl of 0.5% low melting point agarose (GIBCO BRL) was mixed with approximately 15,000 cells suspended in 15 µl and layered onto the slides, which were then immediately covered with coverslips. After agarose solidification at 4 °C for 10 min, coverslips were removed and slides were immersed overnight at 4 °C in fresh lysis solution (2.5 M NaCl, 100 mM Na<sub>2</sub>EDTA, 10 mM Tris, pH 10) containing 1% Triton X-100 and 10% dimethylsulfoxide, added just before use. The slides were equilibrated in alkaline solution (1 mM Na<sub>2</sub>EDTA, 300 mM NaOH, pH > 13) for 20 min. Electrophoresis was carried out for 30 min at 25 V and 300 mA (1.25 V/cm). Afterwards, slides were neutralized by washing them three times with Tris buffer (pH 7.5) every 5 min and subsequently washed in distilled water. Slides were stained with 1/1000 SYBR Green I (Molecular Probes, Eugene, Oregon) solution (Ward and Marples, 2000).

### Image analysis

Scoring was made at 400× magnification using a fluorescent microscope (Olympus BX40 equipped with a 515–560 nm excitation filter) connected with a Sony 3 CCD-IRIS Color Video Camera. Images for each individual cell were acquired immediately after opening the microscope shutter to the computer monitor. Analyses were made employing the Image Pro Plus® 3.0 Program.

Based on the extent of strand breakage, cells were classified according to their tail length in five categories, ranging from 0 (no visible tail) to 4 (still a detectable head of the comet but most of the DNA in the tail). Additionally a sixth group including apoptotic cells (without a detectable head) were considered (Olive, 1999). The migration length was also analysed (difference between total length-distance between the edge of the comet head and the end of tail and head length).

### Statistical analysis

The effect of radiation treatment on the frequency of damaged cells was analysed using the  $\chi^2$  test. Cells without damage (degree 0) were compared with cells with low damage (degree 1–2) and with high damage (degree 3–4 and apoptosis).

Migration distance analysis was based on median and mean population response using the Kruskal-Wallis and Student t method respectively. The data were analysed using Statgraphics 3.0 Plus® software.

**Table 1.** DNA damage in control CHO cells which were not irradiated

Irradiation number	DNA damage level					
	Degree 0	Degree 1	Degree 2	Degree 3	Degree 4	Apoptosis
1	64	28	8	0	0	0
2	64	34	0	0	0	0
3	98	2	0	0	0	0
4	80	14	6	0	0	0
5	80	20	0	0	0	0
6	38	38	24	0	0	0
7	18	60	18	2	2	0
8	16	70	14	0	0	0
9	16	54	28	0	2	0
10	70	24	4	0	0	2
11	64	36	0	0	0	0
12	84	16	0	0	0	0
13	80	20	0	0	0	0
14	64	36	0	0	0	0

## Results

Tables 1–4 summarize the results obtained. Ionizing radiation did not induce apoptosis in the exposed cell population. Sequential irradiation of CHO cells induced a decrease of cells without migration and an increase of cells showing DNA damage with the three doses employed. For statistical analyses damaged cells were separated into two groups: cells with low-level

damage (degree 1 and 2) and cells with severe damage (degree 3 and 4 and apoptotic cells). Significant increases of low-level-damaged cells ( $p < 0.001$ ) were found for the 14 exposures when compared to controls except for the first irradiations with 2.5 and 10 mSv, respectively. No significant increase of the frequency of cells with severe damage was observed in any case.

The induced genotoxic damage was not or only slightly related with the irradiations during the 14 exposures (2.5 mSv:

**Table 2.** DNA damage in CHO cells exposed during 14 passages to 2.5 mSv X-rays

Irradiation number	DNA damage level					
	Degree 0	Degree 1	Degree 2	Degree 3	Degree 4	Apoptosis
1	82	14	4	0	0	0
2	0	96	4	0	0	0
3	0	84	12	0	2	2
4	0	90	8	0	0	2
5	0	94	4	0	2	0
6	0	96	4	0	0	0
7	0	98	2	0	0	2
8	0	94	6	0	0	0
9	0	70	30	0	0	0
10	18	64	18	0	0	0
11	0	86	8	0	2	4
12	0	60	38	0	2	0
13	4	84	10	0	2	0
14	26	72	0	0	2	0

**Table 3.** DNA damage in CHO cells exposed during 14 passages to 5.0 mSv X-rays

Irradiation number	DNA damage level					
	Degree 0	Degree 1	Degree 2	Degree 3	Degree 4	Apoptosis
1	0	90	8	0	0	2
2	0	64	36	0	0	0
3	0	34	66	0	0	0
4	0	94	6	0	0	0
5	0	92	8	0	0	0
6	0	100	0	0	0	0
7	0	94	6	0	0	0
8	0	98	2	0	0	0
9	0	96	4	0	0	0
10	0	98	0	0	0	2
11	0	98	0	0	0	2
12	0	96	4	0	0	0
13	0	98	0	0	0	2
14	0	80	0	0	0	20

**Table 4.** DNA damage in CHO cells exposed during 14 passages to 10.0 mSv X-rays

Irradiation order	DNA damage level					
	Degree 0	Degree 1	Degree 2	Degree 3	Degree 4	Apoptosis
1	56	36	2	4	0	2
2	0	44	54	0	2	0
3	10	80	8	0	0	2
4	4	94	2	0	0	0
5	14	76	8	2	0	0
6	2	82	14	2	0	0
7	0	98	2	0	0	0
8	0	86	14	0	0	0
9	0	82	18	0	0	0
10	6	76	18	0	0	0
11	0	72	28	0	0	0
12	2	78	20	0	0	0
13	4	66	22	0	6	2
14	0	60	18	0	0	2



**Table 5.** Effects of radiation on the mean migration length in CHO cells exposed during 14 passages

Irradiation order	Control	2.5 mSv	5.0 mSv	10.0 mSv
1	1.75 (0.13)	2.30 (0.15)	6.64 (0.25)	1.67 (0.13)
2	1.45 (0.12)	1.09 (0.10)	2.53 (0.16)	9.64 (0.29)
3	1.80 (0.13)	5.48 (0.23)	1.76 (0.13)	6.29 (0.24)
4	0.87 (0.09)	1.73 (0.13)	0.66 (0.08)	2.98 (0.17)
5	1.05 (0.10)	3.30 (0.18)	1.90 (0.14)	8.84 (0.28)
6	1.44 (0.12)	2.11 (0.14)	0.65 (0.08)	4.66 (0.21)
7	2.99 (0.17)	0.93 (0.09)	1.60 (0.12)	7.32 (0.26)
8	1.56 (0.12)	0.99 (0.10)	1.91 (0.14)	3.73 (0.19)
9	2.78 (0.16)	2.49 (0.15)	3.31 (0.18)	4.49 (0.21)
10	1.54 (0.12)	0.53 (0.07)	1.48 (0.12)	5.25 (0.22)
11	1.72 (0.13)	2.69 (0.16)	2.23 (0.15)	5.95 (0.24)
12	1.64 (0.13)	1.95 (0.14)	2.90 (0.17)	6.31 (0.24)
13	1.62 (0.13)	3.02 (0.17)	0.97 (0.10)	6.68 (0.25)
14	0.92 (0.09)	1.49 (0.12)	2.52 (0.16)	2.10 (0.14)

Standard errors are indicated in parenthesis.

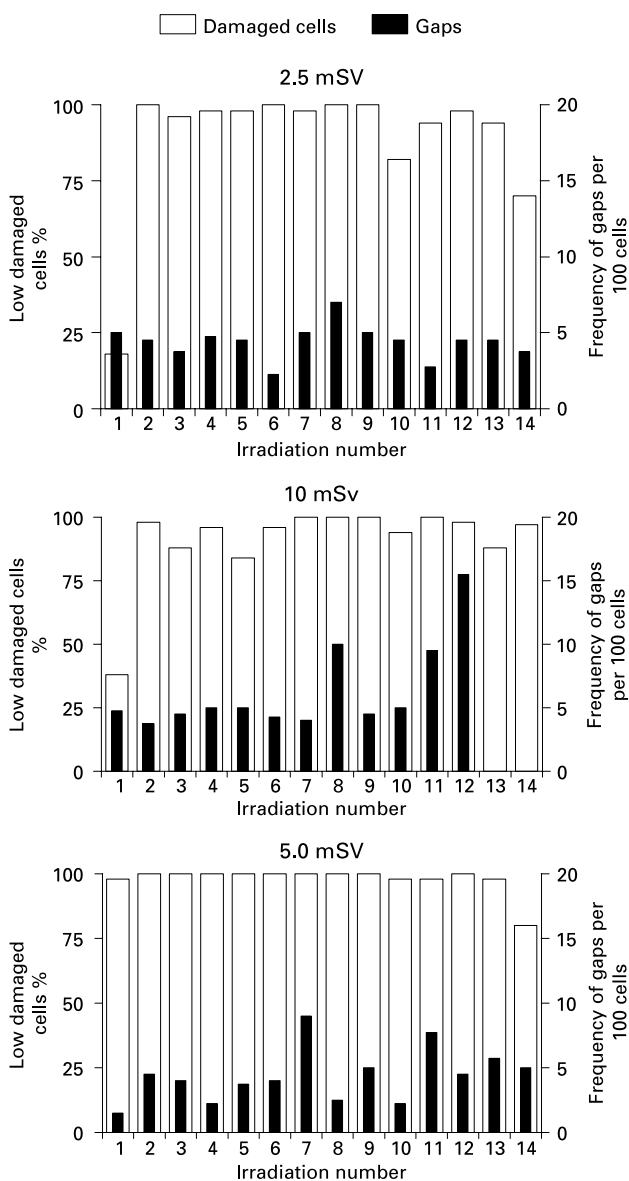


**Fig. 1.** Frequency of gaps per 100 cells (black bars, right abscissa) and percentage of cells with low damage (degrees 1 or 2) (white bars, left abscissa).

$R^2 = 0.23$ ,  $p = 0.43$ ; 5 mSv:  $R^2 = 23.93$ ,  $p = 0.07$ ; 10 mSv:  $R^2 = 10.90$ ,  $p = 0.24$ ).

Table 5 shows the results of the mean migration lengths during the 14 passages analysed. No differences were found for migration length between doses of 2.5 mSv or 5 mSv and the control cells. Significant differences were observed for 10 mSv (KW = 7.10,  $p < 0.001$ , and  $t = 5.6$ ,  $p < 0.001$ ).

## Discussion

Criteria for cytogenetic analysis after in vivo or in vitro exposure to genotoxicants require that the results are reported quantifying chromatid- and chromosome-type aberrations as well as achromatic lesions (gaps). According to the criteria recommended by Archer et al. (1981) and WHO (1985), gaps are nonstaining or very lightly stained chromosome regions in one or both chromatids without displacement of the chromatid fragment(s) distal to the lesion. If there is displacement or the nonstaining region is wider than the width of a chromatid, the aberration is scored as a deletion (break). Achromatic lesions have been a subject of much discussion for years since their significance was not clear. For this reason gaps are in general not included in the total yield of chromosomal damage or, in other words, metaphases carrying only gaps are not considered as abnormal.

The structure of X-ray-induced gaps and breaks was studied several years ago by means of a combination of light microscopy, transmission electron microscopy of whole-mount preparations and sectioned material, and scanning electron microscopy. Results obtained showed that gaps and breaks are not separate phenomena and can be considered as different manifestations of the same events and that gaps may be incomplete breaks (Brecher, 2002). In studies on the clastogenic effects of the Argentinian Hemorrhagic Fever Virus, a significant increase of gaps was found in bone marrow chromosomes of Guinea pigs inoculated with an attenuated strain. Treatment of the animals with very high doses of caffeine 24 h before sacrifice induced a decrease in the frequency of gaps and a correlative increase in the frequency of breaks. These findings were also interpreted as different manifestations of the same phe-

nomenon in the sense that gaps are transformed into breaks by unspecific inhibition of repair mechanisms by caffeine (Dulout et al., 1983, 1985). Studies carried out in peripheral blood lymphocytes of long haul air crew members showed a significant increase of gaps and breaks as well as of translocations (Cavallo et al., 2002). In addition, similar results were found in hospital workers who have high frequencies of stable aberrations as well as chromatid gaps and breaks. The increase of such type of aberrations was attributed to the chronic exposure to low level ionizing radiation (Hagelström et al., 1995). In a study carried out in lymphocytes of hospital workers occupationally exposed to X-rays, the frequency of chromosomal aberrations was compared with the amount of DNA damage measured by the comet assay. Correlation between both methods was higher when gaps were included in the total amount of chromosomal aberrations (Paz-y-Miño et al., 2002).

Figure 1 shows the amounts of DNA damage induced by different doses of X-rays immediately after irradiation. In the same graphs the frequencies of gaps scored 15 h after irradiation (Güerci et al., 2003) are also represented. Immediately after irradiation almost all the cells exhibited some degree of DNA damage. The lapse of 15 h between irradiation and analysis of chromosomal aberrations in the previous experiment can

explain the lower frequency of cells with achromatic lesions in relation to cells with DNA damage observed with the comet assay in this experiment. During the 15 h between irradiation and fixation a great proportion of single- or double-strand breaks should be repaired. However, sequential hits of radiation could progressively increase the level of DNA damage and subsequently the yield of chromosomal aberrations in the next mitoses and this is not the case. After the first irradiation both DNA damage and chromosomal aberrations reached a maximum level that was maintained along the 14 exposures.

These findings could be explained assuming a complex interactive process of cell recovering, DNA damage and repair together with the induction of genomic instability, the incidence of bystander effects as well as some kind of radioadaptive response of the cell line. If these phenomena are limited to the cell line employed, this deserves further investigation.

### Acknowledgements

Authors are grateful to Prof. Juan Andrieu for the calibration of the irradiation equipment and to Prof. Susana J. Barani for the revision of the manuscript.

### References

- Archer PG, Bender M, Bloom AD, Brewen JG, Carrano AV, Preston RJ: Guidelines for cytogenetic studies in mutagen-exposed human populations, in Bloom AD (ed): Guidelines for Studies on Human Populations Exposed to Mutagenic and Reproductive Hazards, pp 1–35 (March of Dimes Birth Defects Foundation, 1981).
- Ballarini F, Biaggi M, Ottolenghi A, Saporita O: Cellular communication and bystander effects: a critical review for modelling low dose radiation action. *Mutat Res* 501:1–12 (2002).
- Brecher S: Ultrastructural observations of X-ray induced chromatid gaps. *Mutat Res* 42:249–267 (2002).
- Cavallo D, Marinaccio A, Perniconi B, Tomao P, Pecorelli V, Moccaldi R, Iavicoli S: Chromosomal aberrations in long-haul air crew members. *Mutat Res* 513:11–15 (2002).
- Dulout FN, Carballal G, Bianchi NO, von Guradze HN: Cytogenetic effect of two strains of Junin virus in the Guinea pig. *Intervirology* 19:44–46 (1983).
- Dulout FN, Carballal G, von Guradze HN, De Luca JC, Oubiña JC, Videla C: Junin virus-induced chromosomal aberrations in the Guinea pig. Synergism between the attenuated strain XJ-clone 3 and caffeine. *Intervirology* 24:193–198 (1985).
- Güerci AM, Dulout FN, Seoane AI: Cytogenetic analysis in Chinese hamster cells chronically exposed to low doses of X-rays. *Int J Radiat Biol* 79:793–799 (2003).
- Hagelström A, Gorla N, Larrripa I: Chromosomal damage in workers occupationally exposed to chronic low level ionizing radiation. *Toxicol Lett* 76:113–117 (1995).
- Little JB: Radiation carcinogenesis. *Carcinogenesis* 21: 397–404 (2000).
- Little JB, Azzam EI, de Toledo SM, Nagasawa H: Bystander effects: intercellular transmission of radiation damage signals. *Radiat Prot Dosim* 99:159–162 (2002).
- Moller P, Knudsen LE, Loft S, Wallin H: The comet assay as a rapid test in biomonitoring occupational exposure to DNA-damaging agents and effect of confounding factors. *Cancer Epidem Biomar* 9: 1005–1015 (2000).
- Morgan WF: Non targeted and delayed effects of exposure to ionizing radiation: I. Radiation-induced genomic instability and bystander effects in vitro. *Radiat Res* 159:567–580 (2003a).
- Morgan WF: Non targeted and delayed effects of exposure to ionizing radiation: II. Radiation-induced genomic instability and bystander effects in vivo, clastogenic factors and transgenerational effects. *Radiat Res* 159:581–596 (2003b).
- Morgan WF, Day JP, Kaplan MI, McGhee EM, Limoli CL: Genomic instability induced by ionizing radiation. *Radiat Res* 146:247–258 (1996).
- Olive PL: DNA damage and repair in individual cells: applications of the comet assay in radiobiology. *Int J Radiat Biol* 75:395–405 (1999).
- Olivieri G, Bodycote J, Wolff S: Adaptive response of human lymphocytes to low concentrations of radioactive thymidine. *Science* 223:594–597 (1984).
- Sasaki MS, Ejima Y, Tachibana A, Yamada T, Ishizaki K, Shimizu T, Nomura T: DNA damage response pathway in radioadaptive response. *Mutat Res* 504:101–118 (2002).
- Singh MP, McCoy MT, Tice RR, Schneider EL: A simple technique for quantitation of low levels of DNA damage in individual cells. *Exp Cell Res* 175:184–191 (1988).
- Tice RR, Strauss GH: The single cell gel electrophoresis/comet assay: a potential tool for detecting radiation-induced DNA damage in humans. *Stem Cells* 1:207–214 (1995).
- Ward TH, Marples B: SYBR Green I and the improved sensitivity of the single-cell electrophoresis assay. *Int J Radiat Biol* 76:61–65 (2000).
- WHO: Guide to short-term tests for detecting mutagenic, carcinogenic chemicals. *Environmental Health Criteria* 51, pp 57–67 (World Health Organization, Geneva 1985).
- Wojewodzka M, Kruszewski M, Iwanenko T, Collins A, Szumiel I: Application of the comet assay for monitoring DNA damage in workers exposed to chronic low-dose irradiation I. Strand breakage. *Mutat Res* 416:21–35 (1998).
- Wright EG: Radiation-induced genomic instability in hemopoietic cells. *Int J Radiat Biol* 74:681–687 (1998).

# Potassium bromate but not X-rays cause unexpectedly elevated levels of DNA breakage similar to those induced by ultraviolet light in Cockayne syndrome (CS-B) fibroblasts

P. Mosesso, S. Penna, G. Pepe, C. Lorenti-Garcia and F. Palitti

Università degli Studi della Tuscia, Dipartimento di Agrobiologia e Agrochimica, Viterbo (Italy)

**Abstract.** It has been previously reported that the elevated accumulation of repair incision intermediates in cells from patients with combined characteristics of xeroderma pigmentosum complementation group D (XP-D) and Cockayne syndrome (CS) XP-D/CS fibroblasts following UV irradiation is caused by an “uncontrolled” incision of undamaged genomic DNA induced by UV-DNA-lesions which apparently are not removed. This could be an explanation for the extreme sensitivity of these cells to UV light. In the present study, we confirm the immediate DNA breakage following UV irradiation also for CS group B (CS-B) fibroblasts by DNA migration in the “comet

assay” and extend these findings to other lesions such as 8-oxodeoxyguanosine (8-oxodG), selectively induced by KBrO<sub>3</sub> treatment. In contrast, X-ray exposure does not induce differential DNA breakage. This indicates that additional lesions other than the UV-induced photoproducts (cyclobutane pyrimidine dimers, CPD, and 6-pyrimidine-4-pyrimidone products, 6-4 PP), such as 8-oxodG, specifically induced by KBrO<sub>3</sub>, are likely to trigger “uncontrolled” DNA breakage in the undamaged genomic DNA in the CS-B fibroblasts, thus accounting for some of the clinical features of these patients.

Copyright © 2003 S. Karger AG, Basel

Cockayne syndrome (CS) is a rare autosomal human genetic disease with features of premature aging and striking somatic and neurological defects. It is caused by mutations in the CS-A or CS-B genes which determine hypersensitivity to a number of DNA damaging agents including UV radiation, ionizing radiation and hydrogen peroxide (Cooper et al., 1997).

The nucleotide excision repair (NER) pathway is involved in a complex process that detects and repairs a wide range of DNA damage including removal of cyclobutane pyrimidine dimers (CPD) and 6-pyrimidine-4-pyrimidone products (6-4

PP) caused by UV irradiation, bulky DNA adducts and DNA cross links caused by chemical agents.

NER is known to operate through two sub-pathways with different kinetics, depending on the function of the damaged DNA: (1) transcription coupled repair (TCR) and (2) global genome repair (GGR) (for review, see Balajee and Bohr, 2000). The TCR sub-pathway repairs only DNA that is actively transcribed by RNA polymerase II (RNAPII). This type of DNA repair is more rapid and complete than GGR.

Both sub-pathways of NER are controlled by all genes involved in xeroderma pigmentosum (XP-A to XP-G) with the exception of XP-C, whose gene product is essential in the recognition and repair of DNA lesions in the overall genome and possibly (XP-E) where its equivalent in TCR-NER is a stalled RNA polymerase II (RNAPII) at a site of a DNA lesion in an actively transcribed gene.

The molecular mechanisms of removal of DNA damage in NER are very similar for the GGR and TCR sub-pathways. After initial recognition of damage and partial unwinding of double stranded DNA, a dual incision of DNA strands at either

The work was partially supported by grants from ASI (Contract No. IR11900) and FIRB (RBNE1RNN7).

Received 7 October 2003; accepted 28 November 2003.

Request reprints from: Prof. Pasquale Mosesso

Università degli Studi della Tuscia

Dipartimento di Agrobiologia e Agrochimica

Via San Camillo de Lellis s.n.c., IT-01100 Viterbo (Italy)

telephone: +39 0761 357205; fax: +39 0761 357242

e-mail: mosesso@unitus.it

sides of the damage is initiated, followed by excision of the damaged DNA strand (approximately 30 nucleotides), filling the gap by de novo DNA synthesis, and DNA ligation. Maintenance of this tight order is highly important to avoid disruption of the rest of the genome while removing DNA lesions at damaged sites.

CS cells are defective in TCR but proficient in GGR to process UV-induced DNA damage (Venema et al., 1990). This feature consistently determines the inability to recover RNA synthesis efficiently after UV damage as has been shown by different cellular studies, in which levels of unscheduled DNA synthesis (UDS) are approximately 30% of the normal value (Mayne and Lehman, 1982).

However, more recently, it has been pointed out that many of the developmental defects of CS arise not only from defective TCR but also from transcriptional defects, particularly in the down-regulation of base excision repair (BER)-related genes and in a decreased efficiency of 8-hydroxyguanine (8-OH-Gua) BER (Dianov et al., 1999; Tuo et al., 2000). This aspect could also explain the progressive neurodegeneration and other clinical features associated with CS since short-wavelength radiation such as UV alone is not sufficient to cause damage to inner tissues and organs.

In the present study we report that CS-B fibroblasts, challenged with potassium bromate (KBrO<sub>3</sub>), which selectively causes oxidative damage in the DNA, essentially the formation of 8-oxodeoxyguanosine (8-oxodG) lesions (Kasai et al., 1987; Sai et al., 1991; Sai et al., 1992; Ballmaier and Epe, 1995; Parson and Chipman, 2000), show unexpectedly, immediate high levels of DNA breakage as measured with the comet assay, similar to those observed following UVB and UVC irradiation in cells from patients with combined features of XP-D and CS (Berneburg et al., 2000). In contrast, X-ray irradiation does not induce differential DNA breakage. The possible implications for these findings are discussed.

## Materials and methods

### Cell culture, cell synchronization, UV and X-ray irradiation and KBrO<sub>3</sub> treatment

Human primary fibroblasts, normal (WT-789), xeroderma pigmentosum group C (XP-C) and Cockayne syndrome group B (CSB-CS8PV) were obtained from Dr. Miria Stefanini (C.N.R. Pavia, Italy). All fibroblasts were grown at 37 °C in Eagle's MEM medium supplemented with 15% foetal bovine serum, L-glutamine and antibiotics.

Synchronization of cells in the G<sub>1</sub> phase of cell cycle was achieved by keeping confluent cultures for 24 h in the presence of low levels of serum (2%). Before UV or X-ray treatments, cultures were washed with PBS and finally exposed to UV or X-rays in the absence of any PBS.

UV irradiation was performed using a germicidal lamp emitting predominantly 254-nm UV light at a dose-rate of 1 J/(m<sup>2</sup>/s). X-irradiation was performed using a Gilardoni X-ray generator (Como, Italy), operating at 250 kV and 6 mA at a dose-rate of 0.75 Gy/min.

Treatment with KBrO<sub>3</sub> for 15 min was performed in PBS after two previous washes. Immediately after irradiation or treatment with KBrO<sub>3</sub>, cells were submitted to a single cell gel electrophoresis "comet" assay in order to evaluate the extent of initial DNA breakage, which essentially results from accumulation of incision repair intermediates, among the different cell lines employed. A time course evaluation of this accumulation was also performed at 0.5, 1, 2 and 24 h after the end of treatment.

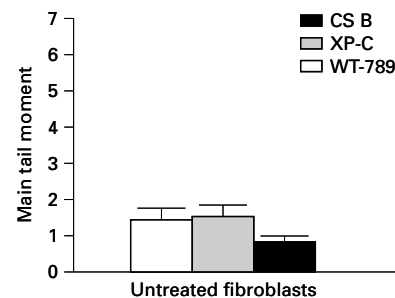


**Fig. 1.** Evaluation of the spontaneous extent of DNA breakage as measured by the comet assay and expressed as mean tail moment in synchronised human primary fibroblasts, normal (WT-789), xeroderma pigmentosum group C (XP-C) and Cockayne syndrome group B (CS B). Results represent the mean ( $\pm$  SD) of four independent experiments performed. Statistical significance was evaluated by Student's t test.

### The alkaline comet assay

Four independently reproduced experiments using the protocol for the alkaline "comet assay" of Singh et al. (1988) were performed. Briefly, 10  $\mu$ l of cell suspension were mixed with 65  $\mu$ l of 0.7% (w/v) low-melting point agarose (Bio-Rad) and sandwiched between a lower layer of 1% (w/v) normal-melting point agarose (Bio-Rad) and an upper layer of 0.7% (w/v) low-melting point agarose on microscope slides (Carlo Erba). Two slides were prepared from each individual treatment. The slides were then immersed in a lysing solution (2.5 M NaCl, 100 mM Na<sub>2</sub>EDTA, 10 mM Tris, pH 10) containing 10% DMSO and 1% Triton X-100 (ICN Biomedicals), overnight at 4 °C. On completion of lysis, the slides were placed in a horizontal gel electrophoresis tank with fresh alkaline electrophoresis buffer (300 mM NaOH, 1 mM Na<sub>2</sub>EDTA, pH  $\geq$ 13) and left in the solution for 25 min at 4 °C to allow the DNA to unwind and to express the alkali-labile sites. Electrophoresis was carried out at 4 °C for 25 min, 30 V (1 V/cm) and 300 mA, using a Bio-Rad power supply. After electrophoresis, the slides were immersed in 0.3 M sodium acetate in ethanol for 30 min. Microgels were then dehydrated in absolute ethanol for 2 h and immersed for 5 min in 70% ethanol. Slides were air-dried at room temperature. Immediately before scoring, slides were stained with 12  $\mu$ g/ml ethidium bromide (Boehringer Mannheim) and examined at 400 $\times$  magnification with an automatic image analyzer (Comet Assay III; Perceptive Instruments, UK) connected to a fluorescence microscope (Eclipse E400; Nikon). To evaluate the amount of DNA damage, computer generated tail moment values and percentage of migrated DNA were used. One hundred cells were scored for each individual treatment from two different slides.

## Results

DNA breakage, which refers to accumulation of incision repair intermediates, is expressed as mean tail moment value in the comet assay. Results represent the mean ( $\pm$  SD) of the four experiments performed. Results obtained for the untreated CS-B, XP-C and WT-789 normal fibroblasts are shown in Fig. 1. The mean tail moment values in the comet assay for the CS-B, XP-C and WT-789 normal fibroblasts following UV irradiation at 20 J/m<sup>2</sup>, X-ray exposure at 1 Gy and KBrO<sub>3</sub> at 2 mM immediately after treatment (0 h) and after 0.5, 1, 2 and 24 h are shown in Figs. 2, 3 and 4 respectively.

Immediately or shortly after treatment, marked significant increases in the mean tail moment were only observed in the CS-B fibroblasts following treatments with UV or KBrO<sub>3</sub> compared to the parallel treatments performed with the WT-789

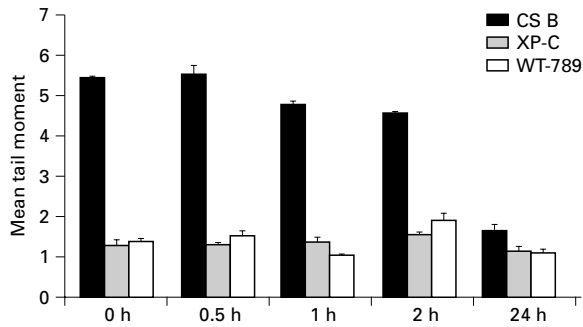


**Fig. 2.** Human primary fibroblasts, normal (WT-789), xeroderma pigmentosum group C (XP-C) and Cockayne syndrome group B (CS B) were irradiated with UVC at 20 J/m<sup>2</sup> and analyzed with the comet assay to evaluate the extent of DNA breakage expressed as mean tail moment after different recovery times (0, 0.5, 1, 2 and 24 h). Results represent the mean ( $\pm$  SD) of four independent experiments performed. Statistical significance was evaluated by Student's t test.

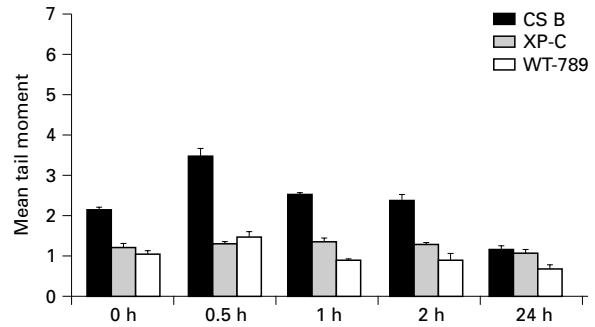


**Fig. 4.** Human primary fibroblasts, normal (WT-789), xeroderma pigmentosum group C (XP-C) and Cockayne syndrome group B (CS B) were treated for 15 min with KBrO<sub>3</sub> (2 mM) and analyzed with the comet assay to evaluate the extent of DNA breakage expressed as mean tail moment after different recovery times (0, 0.5, 1, 2 and 24 h). Results represent the mean ( $\pm$  SD) of four independent experiments performed. Statistical significance was evaluated by Student's t test.

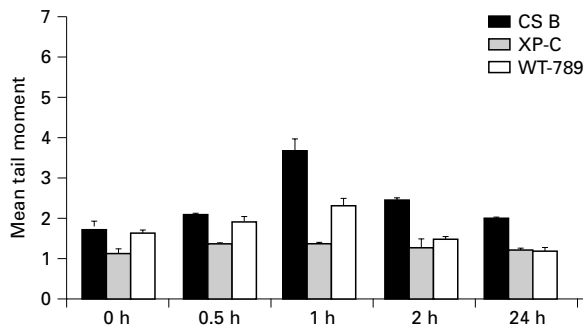


**Fig. 3.** Human primary fibroblasts, normal (WT-789), xeroderma pigmentosum group C (XP-C) and Cockayne syndrome group B (CS B) were irradiated with 1 Gy X-rays and analyzed with the comet assay to evaluate the extent of DNA breakage expressed as mean tail moment after different recovery times (0, 0.5, 1, 2 and 24 h). Results represent the mean ( $\pm$  SD) of four independent experiments performed. Statistical significance was evaluated by Student's t test.

normal fibroblasts (Figs. 2 and 4). In the XP-C fibroblasts this effect was not observed. Increases in the tail moment values observed in CS-B fibroblasts compared to the corresponding values in the WT-789 normal fibroblasts ranged from 2.3 to 4.75 for UV treatment (Fig. 2) and from 2 to 2.8 for the treatment with KBrO<sub>3</sub>. Tail moment values returned to WT-789 normal fibroblast values after 24 hours (Figs. 2 and 4). X-ray treatment did not show any significant differential DNA breakage among the different cell lines used (Fig. 3).

## Discussion

It has been reported by Berneburg et al. (2000) that cells from patients with combined features of XP-D and CS (XP-D/CS), following UV irradiation accumulate DNA repair intermediates even in the absence of the DNA repair synthesis

inhibitors 1- $\beta$ -D-arabinofuranosylcytosine (ara-C) or hydroxyurea (HU), which are required in normal cells in order to accumulate and detect the intermediates with the comet assay. In normal cells, the incision steps of NER are rate limiting and synchronized with the repair synthesis steps so that incised repair intermediates cannot be easily observed following UV irradiation unless DNA repair synthesis inhibitors such ara-C are present during DNA repair. Berneburg et al. (2000) indicate that XP-D/CS cells are able to incise DNA following UV-induced DNA damage and therefore initiate NER but might be unable to complete the process and show that the elevated accumulation of repair incision intermediates in XP-D/CS fibroblasts following UV treatment occurs by a sort of an "uncontrolled" incision of undamaged genomic DNA and that this unique response could account for the extreme sensitivity of these cells to UV light.

We confirmed this unexpected immediate DNA breakage following UV irradiation for CS-B fibroblasts too (2.3 to 4.75 times the corresponding value observed in the WT-789 normal fibroblasts). We extend these findings to different lesions other than CPD and 6-4 PP, such as 8-oxodG selectively induced by KBrO<sub>3</sub>.

The results shown in Fig. 4 clearly indicate marked and significant increases in the extent of DNA breakage in the CS-B fibroblasts (2 to 2.8 times the values observed in the WT-789 normal fibroblasts) following treatment with KBrO<sub>3</sub>. The results with KBrO<sub>3</sub> are similar to those observed following irradiation with UV light.

In conclusion it can be stated that our results extend the findings of Berneburg et al. (2000) about "uncontrolled" DNA breakage induced by UV light in XP-D/CS fibroblasts also to CS-B fibroblasts. Furthermore, additional lesions other than the UV-induced photoproducts CPD and 6-4 PP, such as 8-oxodG, specifically induced by KBrO<sub>3</sub>, are likely to trigger "uncontrolled" DNA breakage in undamaged genomic DNA in CS B fibroblasts and this may account for some of the clinical features of these patients.

## References

- Balajee AS, Bohr VA: Genomic heterogeneity of nucleotide excision repair. *Gene* 250:15–30 (2000).
- Ballmaier D, Epe B: Oxidative damage induced by potassium bromate under cell-free conditions and in mammalian cells. *Carcinogenesis* 16:335–342 (1995).
- Berneburg M, Lowe JE, Nardo T, Arujo S, Foustari MI, Green MHL, Krutmann J, Wood RD, Stefanini M, Lehmann AR: UV damage causes uncontrolled DNA breakage in cells from patients with combined features of XP-D and Cockayne syndrome. *EMBO J* 19:1157–1166 (2000).
- Cooper PK, Nospikel T, Clarkson SG, Leadon SA: Defective transcription-coupled repair of oxidative base damage in Cockayne syndrome patients from XP group G. *Science* 275:990–993 (1997).
- Dianov G, Bischoff C, Sunesen M, Bohr VA: Repair of 8-oxoguanine in DNA is deficient in Cockayne syndrome group B cells. *Nucleic Acid Res* 27:1365–1368 (1999).
- Kasai H, Nishimura S, Kurokawa Y, Hayashi Y: Oral administration of the renal carcinogen, potassium bromate, specifically produces 8-hydroxydeoxyguanosine in rat target organ. *Carcinogenesis* 8:1959–1961 (1987).
- Mayne LV, Lehmann AR: Failure of RNA synthesis to recover after UV irradiation and early defect in cells from individuals with Cockayne's syndrome and xeroderma pigmentosum. *Cancer Res* 42:1473–1478 (1982).
- Parson JL, Chipman JK: The role of glutathione in DNA damage by potassium bromate in vitro. *Mutagenesis* 15:311–316 (2000).
- Sai K, Takagi A, Umemura T, Hasegawa R, Kurokawa Y: Relationship of 8-hydroxydeoxyguanosine formation in rat kidney to lipid peroxidation, glutathione level and relative organ weight after a single administration of potassium bromate. *Jpn J Cancer Res* 82:165–169 (1991).
- Sai K, Uchiyama S, Ohno Y, Hasegawa R, Kurokawa Y: Generation of active oxygen species in vitro by the interaction of potassium bromate with rat kidney cells. *Carcinogenesis* 13:333–339 (1992).
- Singh NP, McCoy MT, Tice RR, Schneider EL: A simple technique for quantitation of low levels of DNA damage in individual cells. *Exp Cell Res* 175:184–191 (1988).
- Tuo J, Chen C, Zeng X, Christiansen M, Bohr VA: Functional crosstalk between hOgg1 and the helicase domain of Cockayne syndrome group B protein. *DNA Repair* 1:913–927 (2000).
- Venema J, Mullenders LH, Natarajan AT, van Zeeland AA, Mayne LV: The genetic defect in Cockayne syndrome is associated with a defect in repair of UV-induced DNA damage in transcriptionally active DNA. *Proc natl Acad Sci USA* 87:4707–4711 (1990).

## Distribution of breakpoints induced by etoposide and X-rays along the CHO X chromosome

W. Martínez-López,<sup>a,b,c,d</sup> G.A. Folle,<sup>b</sup> G. Cassina,<sup>b</sup> L. Méndez-Acuña,<sup>a,b</sup>  
M.V. Di-Tomaso,<sup>b</sup> G. Obe<sup>c</sup> and F. Palitti<sup>d</sup>

<sup>a</sup>Institute of Biology, Faculty of Sciences, Montevideo; <sup>b</sup>Department of Genetic Toxicology and Chromosome Pathology, Instituto de Investigaciones Biológicas Clemente Estable, Montevideo (Uruguay);

<sup>c</sup>Department of Genetics, University of Duisburg-Essen (Germany);

<sup>d</sup>Department of Agrobiological and Agrochemistry, Università degli Studi della Tuscia, Viterbo (Italy)

**Abstract.** SORB (selected observed residual breakpoints) induced by ionizing radiation or endonucleases are often non-randomly distributed in mammalian chromosomes. However, the role played by chromatin structure in the localization of chromosome SORB is not well understood. Anti-topoisomerase drugs such as etoposide are potent clastogens and unlike endonucleases or ionizing radiation, induce DNA double-strand breaks (DSB) by an indirect mechanism. Topoisomerase II (Topo II) is a main component of the nuclear matrix and the chromosome scaffold. Since etoposide leads to DSB by influencing the activity of Topo II, this compound may be a useful tool to study the influence of the chromatin organization on the distribution of induced SORB in mammalian chromosomes. In the present work, we compared the distribution of

SORB induced during S-phase by etoposide or X-rays in the short euchromatic and long heterochromatic arms of the CHO9 X chromosome. The S-phase stage (early, mid or late) at which CHO9 cells were exposed to etoposide or X-rays was marked by incorporation of BrdU during treatments and later determined by immunolabeling of metaphase chromosomes with an anti-BrdU FITC-coupled antibody. The majority of treated cells were in late S-phase during treatment either with etoposide or X-rays. SORB induced by etoposide mapped preferentially to Xq but random localization was observed for SORB produced by X-rays. Possible explanations for the uneven distribution of etoposide-induced breakpoints along Xq are discussed.

Copyright © 2003 S. Karger AG, Basel

Chromosomal aberrations (CA) are induced by ionizing radiation (IR), radiomimetic agents such as restriction endonucleases (RE) and chemicals which react with chromosomal DNA (Obe et al., 1992). Ultimate DNA lesions leading to CA are double-strand breaks (DSB) (Bryant, 1984; Natarajan and Obe, 1984; Obe et al., 1992, 2002; Pfeiffer et al., 2000).

It has been postulated that initial DNA lesions are randomly distributed along mammalian chromosomes but their processed forms, namely breakpoints and exchanges observed at the light microscopic level, may be non-randomly distributed (Savage, 1993). As it is still uncertain that breakpoints represent an unbiased sample with respect to positioning and probably constitute the residue of original lesions fixed in visible aberrations, Savage (1991) coined the term “selected observed residual breakpoints” or SORB for aberration derived breakpoints. Several factors such as DNA repair, intra-nuclear architecture, chromatin structure, and the distribution of transcriptionally active genes may influence the localization of induced SORB (Friedberg et al., 1995; Bassi et al., 1998; Folle et al., 1998; Martínez-López et al., 2001; Proietti De Santis et al., 2001; Pfeiffer et al., 2000).

Clustering of SORB induced by RE and IR in the Giemsa light bands of human and hamster chromosomes has been reported by several authors (Holmberg and Jonasson, 1973;

Supported in part by the Istituto Italo-LatinoAmericano (IILA), the Clemente Estable Fund (Uruguay), the Deutscher Akademischer Austauschdienst (DAAD) and the Sectorial Commission of Scientific Research (CSIC), University of the Republic (Uruguay).

Received 3 September 2003; revision accepted 16 December 2003.

Request reprints from Wilner Martínez-López  
Department of Genetic Toxicology and Chromosome Pathology  
Instituto de Investigaciones Biológicas Clemente Estable  
Ministry of Education and Culture, Avenida Italia 3318  
CP 11.600 Montevideo (Uruguay); telephone: (598 2) 487 16 21/136  
fax: (598 2) 487 55 48; e-mail: wlopez@iibce.edu.uy

W. Martínez-López and G.A. Folle contributed equally to this work.

Barrios et al., 1989; Slijepcevic and Natarajan, 1994a, b; Folle and Obe, 1995, 1996; Folle et al., 1997, 1998; Martínez-López et al., 1998). Giemsa light bands and their subset, the T-bands, are early replicating GC rich transcriptionally active euchromatic regions where constitutional chromosome breakpoints, cancer-associated exchange sites and oncogenes preferentially localize (Holmquist, 1992; Saccone et al., 1992).

Considerable evidence exists that histone H4 hyperacetylation (H4<sup>+</sup>) in metaphase chromosomes defines active chromosome regions (euchromatin) whereas hypoacetylation of histone H4 is associated with facultative or constitutive heterochromatic chromosome segments (Jeppesen, 1997). Thus, H4<sup>+</sup> seems to be a cytogenetic marker for potential transcriptional activity.

To unravel a possible link between transcriptional activity and chromosome damage, Martínez-López et al. (2001) compared the H4<sup>+</sup> pattern along CHO chromosomes with breakpoint patterns induced by endonucleases (*AluI*, *BamHI* and DNase I) and IR (neutrons and  $\gamma$ -rays). The H4<sup>+</sup> pattern revealed by an anti-H4<sup>+</sup> antibody is similar to the pattern of Giemsa light bands. Sites of H4<sup>+</sup> co-localized with endonuclease- and IR-induced breakpoint clusters indicating that CA induced by these agents occur more frequently in active than in inactive chromatin. The long heterochromatic arm of the CHO X chromosome is typically underacetylated (inactive chromatin) while H4<sup>+</sup> concentrates in the short euchromatic arm (Martínez-López et al., 2001).

Anti-topoisomerase drugs are potent inducers of CA (Kihlman, 1971; Degraffi et al., 1989; Palitti et al., 1990; Palitti, 1993; Bassi et al., 1998). DNA topoisomerases play an essential role in maintaining the integrity of DNA molecules since they resolve topological constraints during DNA replication, transcription, recombination and chromatin remodeling by temporarily introducing single-strand breaks (type I and II topoisomerases) or DSB (type II topoisomerases) (Wang, 1985; Liu, 1989).

Type II topoisomerases (Topo II) are major components of the nuclear matrix and the chromosome scaffold. It has been suggested that Topo II molecules form clusters with other proteins, such as Sc2 and histone H1 around the AT-rich scaffold-associated regions (SARs) which attach the chromatin loops to the scaffold (Adachi et al., 1989; Käs et al., 1993; Saitoh and Laemmli, 1994). An association of Topo II with mammalian centromeres as well as its localization at the periphery of heterochromatic regions has also been shown (Petrov et al., 1993; Rattner et al., 1996).

There are two main classes of antitopoisomerases: (1) "cleavable complex" poisons and (2) catalytic inhibitors. The first class acts by trapping the covalent intermediate, the so-called "cleavable complex" of Topo I and II, and thus prevents the resealing of DNA breaks introduced by these enzymes (Hsiang et al., 1985; Ross, 1985; Tewey et al., 1985). Anti-topoisomerase II agents are potent producers of CA in all phases of the cell cycle. Presumably they induce DSB through an indirect mechanism of action. Among Topo II "cleavable complex" poisons are several intercalative drugs such as acridines, anthracyclines, anthracenediones, and ellipticines as well as non-intercalative ones including epipodophyllotoxins (i. e. etoposide) and coumarine (D'Arpa and Liu, 1989).

The second class, catalytic inhibitors such as bis-piperazine-diones and anthracenyl peptides do not trap the "cleavable complex" but prevent the catalytic activity of the enzyme (Tanabe et al., 1991). These drugs are cytotoxic, but do not produce CA.

Anti-topoisomerase II trappers induce chromosome-type aberrations or chromatid-type aberrations depending on the phase of the cell cycle in which treatments are performed (Palitti et al., 1990, 1994). Moreover, these compounds produce sister chromatid exchanges (SCE) if the treatment is performed during the S-phase of the cell cycle (Dillehay et al., 1983; Pomnier et al., 1985; Degraffi et al., 1989; Palitti et al., 1990).

The overall distribution of Topo II in the chromosomes and the possibility of inducing DSB by anti-topoisomerase drugs allow us to analyze the influence of chromatin organization on the distribution of chromosome lesions in the mammalian genome. In the present study, the distribution of SORB induced by etoposide and X-rays in the short (euchromatic) and long (heterochromatic) arms of the X chromosome during S-phase of Chinese hamster ovary (CHO9) cells was studied.

## Materials and methods

### *CHO karyotype*

A subclone of Chinese hamster ovary cells (CHO9 from A.T. Natarajan, Leiden) derived from a Chinese hamster ovary fibroblast culture established by Puck et al. (1958) was used. The modal chromosome number of CHO9 is 21, with 9 seemingly normal Chinese hamster chromosomes (1, 2, 5, 7, 9, 10, the X and pair 8) and 12 rearranged Z-chromosomes (Z1 to Z10, Z12 and Z13) (Deaven and Petersen, 1973; Siciliano et al., 1985). The long arm of the X chromosome is nearly entirely heterochromatic with the exception of a conspicuous intercalary secondary constriction (Ray and Mohandas, 1976).

### *Cell culture and treatments*

Cells were grown as monolayers in Ham F10 medium (Gibco) supplemented with 10% fetal calf serum (Gibco), 200 mM glutamine and antibiotics (100 U/ml penicillin and 125  $\mu$ g/ml dihydrostreptomycin sulfate) at 37 °C in a 5% CO<sub>2</sub> incubator.

Eight hours before harvesting, exponentially growing CHO9 cells (2  $\times$  10<sup>6</sup>) were treated for 30 min with 30  $\mu$ M 5-bromo-2'-deoxyuridine (BrdU) and either etoposide (10 or 20  $\mu$ M) or X-rays (1.5 or 3.0 Gy) using a 250-kV X-ray machine. Controls were processed in the same way excluding etoposide or X-ray treatment.

Following 2 h of exposure to 0.08  $\mu$ g/ml colcemid, mitotic cells were harvested by shake-off, hypotonically treated with 1% sodium citrate for 10 min at 37 °C and fixed twice in methanol-acetic acid (3:1). Cells were dropped onto clean ice-cold slides and air dried. G-banding was carried out as described previously (Folle and Obe, 1995).

### *Immunodetection of incorporated BrdU*

In order to estimate the frequency of treated cells in early, mid, or late S-phase of the cell cycle, slides were immunostained using mouse anti-BrdU antibody conjugated with the fluorochrome FITC. Slides were denatured with 10 mM NaOH in 70% ethanol (1 min), dehydrated in 70, 90 and 100% ethanol and air-dried. Slides were then incubated with 100  $\mu$ l of 1:100 anti-BrdU antibody (Boehringer) in immunological buffer (PBS, 10% BSA, 0.5% Tween 20) for 30 min at 37 °C in a moist chamber. Slides were washed with PBS (3 $\times$ ) and incubated in the dark with 100  $\mu$ l of goat anti-mouse IgG-FITC (Boehringer) for 30 min (37 °C) in a moist chamber. Finally, slides were washed with PBS (3 $\times$ ), dehydrated in 70, 90 and 100% ethanol and incubated for 30 min in the dark with DAPI (2.5% in Mc Ilvaine's buffer; pH 7.0), washed in deionized water, mounted in Mc Ilvaine's buffer (pH 7.0) and covered with a coverslip.



**Table 1.** Frequencies of CA induced by etoposide and X-rays in CHO9 cells; the number of SORB was estimated according to Obe and Winkel (1985)

Treatment	Concentration/ Dose	Damaged metaphases (%)	Aberrations per 100 metaphases <sup>a</sup>								No. of CA <sup>b</sup>	No. of SORB <sup>c</sup>
			DIC	RB'	RB'B''	B'	B''	ID	DD	IC		
Etoposide	0 μM (control)	8	–	–	–	7	1	1	–	–	9	11
	10 μM	43	–	26	1	6	20	–	2	–	55	107
	20 μM	65	3	51	8	17	29	1	7	4	120	238
X-rays	0 Gy (control)	3	–	1	–	–	2	–	–	–	3	6
	1.5 Gy	47	2	8	3	9	34	4	2	–	62	120
	3.0 Gy	76	4	27	14	13	39	13	–	10	120	241

<sup>a</sup> DIC: dicentric = 2; RB': chromatid interchanges = 2; RB'B'': chromatid-isochromatid interchanges = 3; B': chromatid breaks = 1; B'': isochromatid breaks = 2; ID: interstitial deletions = 2; DD: duplication deletions = 3; IC: chromatid rings = 2.

<sup>b</sup> CA: chromosome aberrations.

<sup>c</sup> SORB: selected observed residual breakpoints.

#### Scoring of CA, SORB mapping on the CHO9 X chromosome and classification of BrdU labeled cells

Aberration yields induced by etoposide or X-rays were determined in control and treated metaphases (n = 100) with 18–22 centromeres. The following aberrations were recorded: chromatid interchanges, isochromatid-chromatid interchanges, chromatid and isochromatid breaks, interstitial and duplication deletions, intrachanges, dicentric, translocations and rings (Savage, 1976).

A total of 200 BrdU labeled metaphases were scored per treatment to determine the percentage of damaged or undamaged cells in early, mid or late S-phase.

The distribution of 400 SORB (100 per treatment) in the short euchromatic (Xp) and long heterochromatic (Xq) arms of the X chromosome were analyzed for etoposide or X-ray treatments. A total of 320 SORB (n = 80 per treatment) could be assigned to specific bands on a G-band idiogram of the X chromosome according to Martínez-López et al. (1998).

Chromosome SORB mapping on G-banded metaphases was carried out using an Axioplan microscope (Zeiss) with a 100× Neofluar phase contrast objective. Immunolabeled metaphases were analyzed on a Photo II epifluorescence microscope (Zeiss) with appropriate filter sets for FITC and DAPI.

#### Statistical analysis

Expected SORB frequencies for each X chromosome arm were estimated according to arm length. In order to test for random or non-random occurrence of SORB produced by etoposide or X-rays in the CHO X chromosome arms, a  $\chi^2$  test was used.

## Results

Results obtained by scoring 100 metaphases from CHO9 cells treated with etoposide or X-rays are presented in Table 1. Mainly chromatid type aberrations were found. The percentages of damaged cells were 43 and 65% for etoposide treatments (10 and 20 μM) and 47 and 76% for X-rays (1.5 and 3.0 Gy) with only 8 and 3% in controls, respectively. Comparable frequencies of CA and SORB were observed following exposure to 1.5 Gy X-rays or 10 μM etoposide as well as with 3.0 Gy X-rays or 20 μM etoposide treatment.

In order to ascertain which cells were exposed at early, mid or late S-phase CHO9 cells were pulse labeled with BrdU during etoposide and X-ray treatments. Immunodetection of BrdU incorporation on CHO9 X chromosomes enabled treated cells to be assigned precisely to early, mid or final stages of the S-phase. Early S-phase cells showed BrdU immunolabeling in the short euchromatic arm. Cells were classified as late S-phase when immunostaining was limited to the long heterochromatic

**Table 2.** Frequencies of damaged and undamaged BrdU-labeled CHO9 metaphases in early, mid, late S-phase and unlabeled metaphases from cells treated either with etoposide or X-rays

Treatment	Concentration/ Dose	Number of metaphases <sup>a</sup>							
		ES (%)		MS (%)		LS (%)		UL (%)	
		D	U	D	U	D	U	D	U
Etoposide	10 μM	7 (8)	23	15 (17)	45	54 (63)	45	10 (12)	1
	20 μM	6 (4)	3	23 (16)	20	96 (69)	34	15 (11)	3
X-rays	1.5 Gy	13 (14)	29	32 (36)	49	35 (39)	30	10 (11)	2
	3.0 Gy	8 (5)	10	22 (14)	14	85 (55)	19	40 (26)	2

<sup>a</sup> Percentages of damaged metaphases are denoted in brackets. Recovery time: 8 hours (200 metaphases per treatment).

ES: early S-phase; MS: mid S-phase; LS: late S-phase; UL: unlabeled metaphases; D: damaged; U: undamaged.

**Table 3.** Distribution of 400 SORB induced by etoposide or X-rays in the short (Xp) and long arms (Xq) of the CHO9 X chromosome; expected SORB were calculated according to arm length

Treatment	Concentration	Chromosome arm	Observed	Expected	$\chi^2$
Etoposide	10 μM	Xp	30	41	2.90
Etoposide	10 μM	Xq	70	59	2.00
			100	100	4.90 <sup>a</sup>
Etoposide	20 μM	Xp	21	41	9.70
Etoposide	20 μM	Xq	79	59	6.80
			100	100	16.50 <sup>b</sup>
X-rays	1.5 Gy	Xp	36	41	0.60
X-rays	1.5 Gy	Xq	64	59	0.40
			100	100	1.00
X-rays	3.0 Gy	Xp	48	41	1.20
X-rays	3.0 Gy	Xq	52	59	0.80
			100	100	2.00

<sup>a</sup>  $P < 0.05$ .

<sup>b</sup>  $P < 0.001$ .

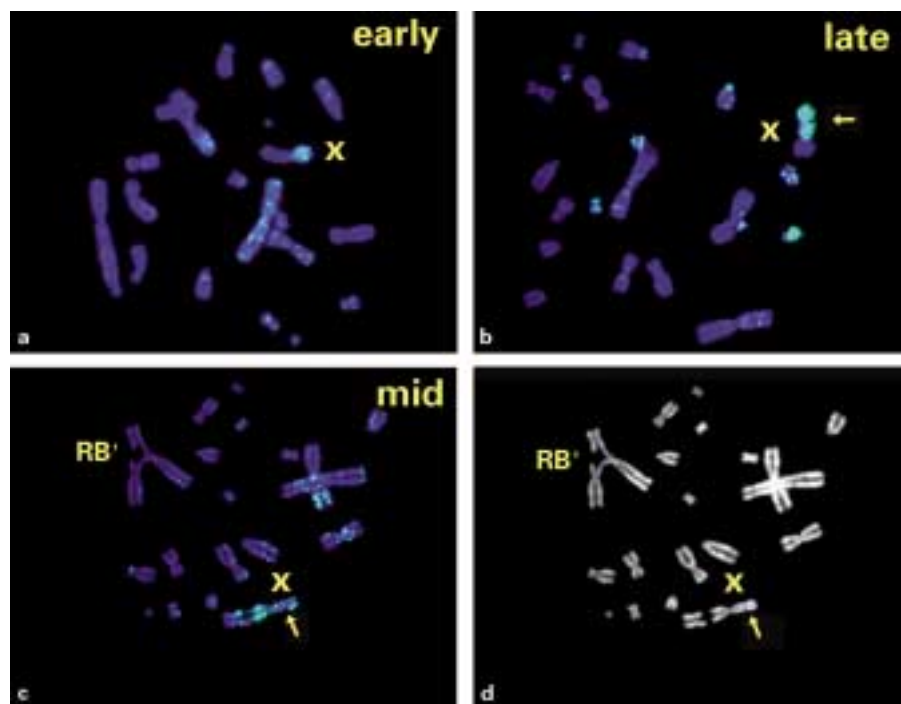


**Fig. 1.** BrdU immunolabeling of CHO9 X chromosomes. Green signals indicate BrdU incorporation. Chromosomes were counterstained with DAPI (blue). (a) Early-S metaphase with the short euchromatic arm labeled; (b) late-S metaphase with the long heterochromatic arm labeled; (c) mid-S metaphase with labeling of both arms; (d) same metaphase as in (c) in DAPI mode. X chromosomes are denoted by X. Arrows indicate the secondary constrictions in the long arms of X chromosomes. RB', chromatid interchange.

arm. The presence of fluorescent labeling along both arms of the X chromosome indicated that the cell was in mid S-phase during treatment with etoposide or X-rays (Fig. 1a–c).

As shown in Table 2, BrdU-labeled damaged metaphases observed at 8 h recovery time mainly corresponded to late S-phase cells for 10 and 20  $\mu$ M etoposide as well as for 3.0 Gy X-rays. However, cells exposed to 1.5 Gy X-rays showed similar frequencies of mid-S and late-S damaged cells (36 and 39%, respectively). Therefore, a clear difference in the cell cycle delay effect with 1.5 Gy X-rays in comparison with 3.0 Gy X-rays and etoposide treatment was observed. Table 2 also shows the distribution of undamaged early-, mid- and late-S cells as well as G2 cells which are unlabeled.

The analysis of the distribution of 400 SORB in G-banded X chromosomes from damaged cells showed that most SORB induced by etoposide mapped preferentially to Xq (10  $\mu$ M,  $P < 0.05$ ; 20  $\mu$ M,  $P < 0.001$ ), those produced by X-rays were randomly distributed (Table 3, Fig. 2). The pericentric region of the X chromosome seems especially sensitive to SORB induction by etoposide (Fig. 2a, b). SORB produced by etoposide localize preferentially in Giemsa light bands with respect to X-rays induced breakpoints (Figs. 2 and 3).

## Discussion

We found a random distribution of SORB produced by X-rays but most of the etoposide-induced SORB mapped to Xq (Tables 1 and 3, Fig. 2). It was demonstrated that a similar cell population was analyzed either with etoposide or X-rays, since most damaged cells were at late S-phase during treatment (Table 2).

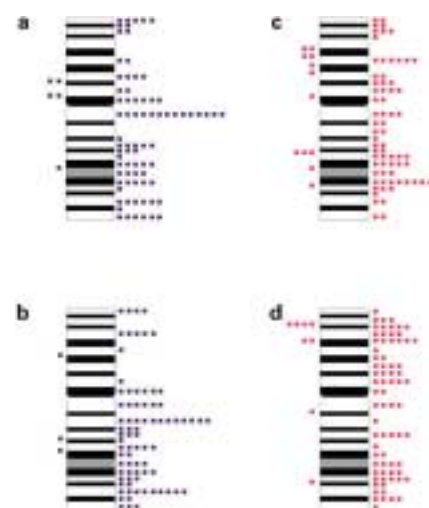


**Fig. 2.** Localization in G-dark and G-light bands of SORB induced in CHO9 X chromosomes during S-phase by 10  $\mu$ M (a) and 20  $\mu$ M (b) etoposide, 1.5 Gy (c) and 3.0 Gy (d) X rays (symbols on the right side of the G-band idiograms). Symbols on the left side represent SORB located at band junctions. Shaded areas in idiograms correspond to the X chromosome long arm secondary constriction.

A non-random distribution of SORB along Chinese hamster chromosomes was found by several authors. Additionally, a preferential induction of SORB in specific chromosome regions was also described (Slijepcevic and Natarajan, 1994a, b; Dominguez et al., 1996; Grigorova et al., 1998; Xiao and Natarajan, 1999a, b, c; Martínez-López et al., 2000).

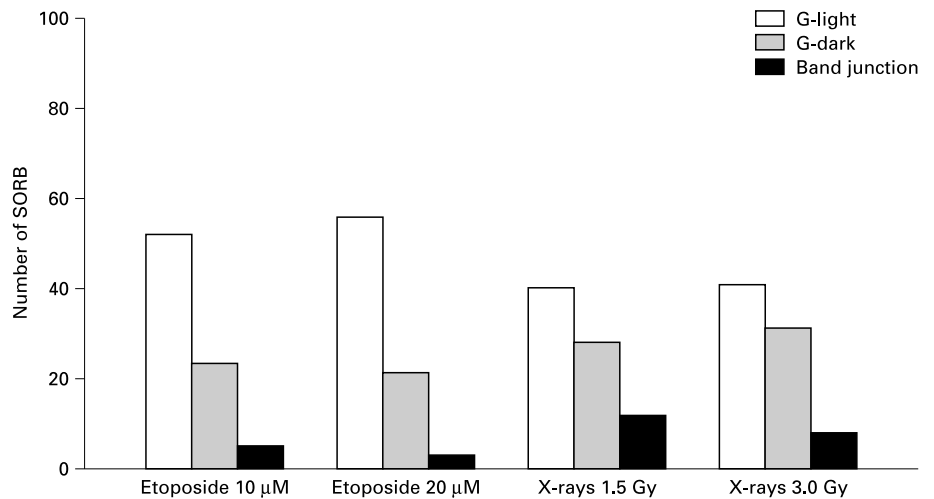


**Fig. 3.** Distribution of 320 SORB induced by etoposide or X-rays in Giemsa light and Giemsa dark bands as well as in band junctions in the CHO9 X chromosome.

Xiao and Natarajan (1999a) studied the frequencies and distribution of X-ray-induced CA in Chinese hamster primary fibroblasts by fluorescence in situ hybridization (FISH) during the G1 phase of the cell cycle. They found that the long arms of the X chromosomes had more breaks than the short arms. However, dicentric and translocations were distributed according to arm length. Slijepcevic and Natarajan (1994b) reported an excess of terminal deletions in the long arms of Chinese hamster X chromosomes after G1 X-irradiation. The presence in heterochromatin of less efficient repair for breakage rejoining rather than damage susceptibility was proposed as an explanation for their results. Interestingly, a significantly higher number of exchanges in the X chromosome long arms of Chinese hamster splenocytes after X-ray and neutron irradiation using FISH was reported by Grigorova et al. (1998).

Notwithstanding, Mühlmann-Diaz and Bedford (1994), using X chromosome-specific DNA probes to study the frequencies of  $\gamma$ -ray-induced aberrations in human cell lines with an increased number of X chromosomes, found a similar frequency of aberrations in the X chromosomes independently of their number, indicating that heterochromatin is less prone to be damaged. Moreover, only few SORB were detected in the long arm of the Chinese hamster X chromosome after treatment with RE, DNase I, neutrons and  $\gamma$ -rays (Folle et al., 1997; Martínez-López et al., 1998).

These apparently contradictory results cannot be explained satisfactorily. Uneven sensitivities of different cell cycle stages, DNA replication, repair efficiency and chromatin conforma-

tion may strongly influence the fate of induced initial lesions in DNA (Obe et al., 2002).

Clustering of SORB in Giemsa light bands has been reported repeatedly (Folle and Obe, 1995, 1996; Folle et al., 1998; Martínez-López et al., 1998). Interestingly, only SORB produced by etoposide mapped preferentially to light Giemsa bands (Figs. 2 and 3). This finding could reflect an increased accessibility of etoposide to its target in these chromosome regions as has been proposed for RE and DNase I (Folle et al., 1997).

The fact that topoisomerase II was found associated with heterochromatin in Chinese hamster fibroblasts (Petrov et al., 1993) could explain the preferential distribution of etoposide-induced breakpoints in Xq. Additionally, clustering of breakpoints induced by etoposide in the centromeric region of the X chromosome could also be the result of topoisomerase association to centromeres (Rattner et al., 1996).

Nevertheless, since in our study damaged cells induced by radiation or etoposide were in late S-phase of the cell cycle at the time of treatment, it can be assumed that Xq heterochromatin was involved in DNA replication during treatment. DNA topoisomerases play a major role in a variety of biological processes such as DNA replication, transcription and repair. Therefore, trapping of active Topo II during Xq replication by etoposide could also account for SORB clustering in the long arm of the X chromosome. However, more experimental evidence is still needed to clarify the mechanism of induction of CA by topoisomerase II trappers in different phases of the cell cycle and especially during DNA replication.

## References

- Adachi Y, Käs E, Laemmli UK: Preferential, cooperative binding of DNA topoisomerase II to scaffold-associated regions. *EMBO J* 8:3997–4006 (1989).
- Barrios L, Miró R, Caballin MR, Fuster C, Guedea F, Subias A, Egozcue J: Cytogenetic effects of radiotherapy breakpoint distribution in induced chromosome aberrations. *Cancer Genet Cytogenet* 41:61–70 (1989).
- Bassi L, Palitti F, Mosesso P, Natarajan AT: Distribution of camptothecin-induced breakpoints in Chinese hamster cells treated in late S and G2 phase of the cell cycle. *Mutagenesis* 13:257–261 (1998).
- Bryant P: Enzymatic restriction of mammalian cell DNA using *PvuII* and *BamHI*: Evidence for the double strand break origin of chromosomal aberrations. *Int J Radiat Biol* 46:57–65 (1984).
- D'Arpa P, Liu LF: Topoisomerase-targeting antitumor drugs. *Biochim biophys Acta* 989:163–177 (1989).
- Deaven LL, Petersen DF: The chromosomes of CHO, an aneuploid Chinese hamster cell line: G-band, C-band, and autoradiographic analyses. *Chromosoma* 41:129–144 (1973).
- Degrassi F, De Salvia R, Tanzarella C, Palitti F: Induction of chromosomal aberrations and SCEs by camptothecin, an inhibitor of mammalian topoisomerase I. *Mutat Res* 211:125–130 (1989).

- Dillehay LE, Thompson LH, Minkler JL, Carrano A: The relationship between sister chromatid exchanges and perturbations in DNA replication in mutant EM9 and normal CHO cells. *Mutat Res* 109:283–296 (1983).
- Dominguez I, Boei JJWA, Balajee AS, Natarajan AT: Analysis of radiation-induced chromosome aberrations in Chinese hamster cells by FISH using chromosome-specific DNA libraries. *Int J Radiat Biol* 70:199–208 (1996).
- Folle GA, Obe G: Localization of chromosome breakpoints induced by *AluI* and *BamHI* in Chinese hamster ovary (CHO) cells treated in the G1 phase of the cell cycle. *Int J Radiat Biol* 68:437–445 (1995).
- Folle GA, Obe G: Intrachromosomal localization of breakpoints induced by the restriction endonucleases *AluI* and *BamHI* in Chinese hamster ovary cells treated in S-phase of the cell cycle. *Int J Radiat Biol* 69:447–457 (1996).
- Folle GA, Boccardo E, Obe G: Localization of chromosome breakpoints induced by DNase I in Chinese hamster ovary (CHO) cells. *Chromosoma* 106:391–399 (1997).
- Folle GA, Martínez-López W, Boccardo E, Obe G: Localization of chromosome breakpoints: implication of the chromatin structure and nuclear architecture. *Mutat Res* 404:17–26 (1998).
- Friedberg E, Walker G, Siede W: DNA Repair and Mutagenesis (ASM Press, Washington DC 1995).
- Grigorova M, Brand R, Xiao Y, Natarajan AT: Frequencies and types of exchange aberrations induced by X-rays and neutrons in Chinese hamster splenocytes detected by FISH using chromosome-specific DNA libraries. *Int J Radiat Biol* 74:297–314 (1998).
- Holmberg M, Jonasson J: Preferential location of X-ray induced chromosome breakage in the R-bands of human chromosomes. *Hereditas* 74:57–67 (1973).
- Holmquist GP: Chromosome bands, their chromatin flavor, and their functional features. *Am J hum Genet* 5:17–37 (1992).
- Hsiang YH, Hertzberg R, Hecht S, Liu LF: Camptothecin induces protein-linked DNA breaks via mammalian DNA topoisomerase. *J Biol Chem* 260:14873–14878 (1985).
- Jeppesen P: Histone acetylation: a possible mechanism for the inheritance of cell memory at mitosis. *Bioessays* 19:67–74 (1997).
- Käs E, Poljak L, Adachi Y, Laemmli UK: A model for chromatin opening: stimulation of topoisomerase II and restriction enzyme cleavage of chromatin by distamycin. *EMBO J* 12:115–126 (1993).
- Kihlman BA: Molecular mechanism of chromosome breakage and rejoining, in DuPraw EJ (ed): *Advances in Cell and Molecular Biology*, pp 59–107 (Academic Press, London 1971).
- Liu LF: DNA topoisomerase poisons as antitumor drugs. *Annu Rev Biochem* 58:351–375 (1989).
- Martínez-López W, Boccardo E, Folle GA, Porro V, Obe G: Intrachromosomal localization of aberration breakpoints induced by neutrons and  $\gamma$ -rays in Chinese hamster ovary (CHO) cells. *Radiat Res* 150:585–592 (1998).
- Martínez-López W, Porro V, Folle GA, Méndez-Acuña L, Savage JRK, Obe G: Interchromosomal distribution of gamma ray-induced chromatid aberrations in Chinese hamster ovary cells. *Genet molec Biol* 23:1071–1076 (2000).
- Martínez-López W, Folle GA, Obe G, Jeppesen P: Chromosome regions enriched in hyperacetylated histone H4 are preferred sites for endonuclease- and radiation-induced breakpoints. *Chrom Res* 9:69–75 (2001).
- Mühlmann-Diaz MC, Bedford JS: A comparison of radiation-induced aberrations in human cells involving early and late replication X-chromosomes, in Obe G, Natarajan AT (eds): *Chromosomal Alterations. Origin and Significance*, pp 125–131 (Springer-Verlag, Berlin 1994).
- Natarajan AT, Obe G: Molecular mechanisms involved in the production of chromosomal aberrations. III. Restriction endonucleases. *Chromosoma* 90:120–127 (1984).
- Obe G, Winkel E-U: The chromosome breaking activity of the restriction endonuclease *AluI* in CHO cells is independent of the S-phase of the cell cycle. *Mutat Res* 152:25–29 (1985).
- Obe G, Johannes C, Schulte-Frohlinde D: DNA double-strand breaks induced by sparsely ionizing radiation and endonucleases as critical lesions for cell death, chromosomal aberrations, mutations and oncogenic transformation. *Mutagenesis* 7:3–12 (1992).
- Obe G, Pfeiffer P, Savage JRK, Johannes C, Goedecke W, Jeppesen P, Natarajan AT, Martínez-López W, Folle GA, Drets ME: Chromosomal aberrations: formation, identification and distribution. *Mutat Res* 504:17–36 (2002).
- Palitti F: Mechanisms of induction of chromosomal aberrations by inhibitors of DNA topoisomerases. *Environ molec Mutagen* 22:275–277 (1993).
- Palitti F, Degrassi F, De Salvia R, Fiore M, Tanzarella C: Inhibitors of DNA topoisomerases and chromosome aberrations, in Obe G, Natarajan AT (eds): *Chromosomal Aberrations: Basic and Applied Aspects*, pp 50–60 (Springer-Verlag, Berlin 1990).
- Palitti F, Mossesso P, Di Chiara D, Schioppi A, Fiore M, Bassi L: Use of anti-topoisomerase drugs to study the mechanism of induction of chromosomal damage, in Obe G, Natarajan AT (eds): *Chromosomal Alterations: Origin and Significance*, pp 103–115 (Springer-Verlag, Berlin 1994).
- Petrov P, Drake FH, Loranger A, Huang W, Hancock R: Localization of DNA topoisomerase II in Chinese hamster fibroblasts by confocal and electron microscopy. *Exp Cell Res* 204:73–81 (1993).
- Pfeiffer P, Goedecke W, Obe G: Mechanism of DNA double-strand break repair and their potential to induce chromosomal aberrations. *Mutagenesis* 15:289–302 (2000).
- Pommier Y, Zwelling LA, Kao-Shan CS, Whang-Peng J, Bradley MO: Correlation between intercalator-induced DNA strand breaks and sister chromatid exchanges, mutations and cytotoxicity in Chinese hamster cells. *Cancer Res* 45:3143–3149 (1985).
- Proietti De Santis L, Garcia CL, Balajee AS, Brea Calvo GT, Bassi L, Palitti F: Transcription coupled repair deficiency results in increased chromosomal aberrations and apoptotic death in the UV61 cell line, the Chinese hamster homologue of Cockayne's syndrome B. *Mutat Res* 485:121–132 (2001).
- Puck TT, Cieciura SJ, Robinson A: Genetics of somatic mammalian cells. III. Long term cultivation of euploid cells from human and animal subjects. *J exp Med* 108:945–956 (1958).
- Rattner JB, Hendzel MJ, Furbee CS, Muller MT, Bazett-Jones DP: Topoisomerase II alpha is associated with the mammalian centromere in a cell cycle- and species-specific manner and is required for proper centromere/kinetochore structure. *J Cell Biol* 134:1097–1107 (1996).
- Ray M, Mohandas T: Proposed nomenclature for the Chinese hamster chromosomes (*Cricetulus griseus*), in Hamerton JL (ed): *Report of the Committee on Chromosome Markers*. *Cytogenet Cell Genet* 16:83–91 (1976).
- Ross WE: DNA topoisomerases as targets for cancer therapy. *Biochem Pharmacol* 34:4191–4195 (1985).
- Saccone S, De Sario A, Della Valle G, Bernardi G: The highest gene concentrations in the human genome are in T bands of metaphase chromosomes. *Proc natl Acad Sci, USA* 89:4913–4917 (1992).
- Saitoh Y, Laemmli UK: Metaphase chromosome structure: bands arise from a differential folding path of the highly AT-rich scaffold. *Cell* 76:609–622 (1994).
- Savage JRK: Annotation: Classification and relationships of induced chromosomal structural changes. *J med Genet* 13:103–122 (1976).
- Savage JRK: Testing the participation of chromosomes in structural aberrations, in Sobti RC, Obe G (eds): *Eukaryotic Chromosomes: Structural and Functional Aspects*, pp 111–125 (Narosa Press, New Delhi 1991).
- Savage JRK: Interchange and intra-nuclear architecture. *Environ molec Mutagen* 22:234–244 (1993).
- Siciliano MJ, Stallings RL, Adair GM: The genetic map of the Chinese hamster and the genetic consequences of chromosomal rearrangements in CHO cells, in Gottesman MM (ed): *Molecular Cell Genetics*, pp 95–135 (John Wiley & Sons, New York 1985).
- Slijepcevic P, Natarajan AT: Distribution of X-ray-induced G2 chromatid damage among Chinese hamster chromosomes: influence of chromatin conformation. *Mutat Res* 323:113–119 (1994a).
- Slijepcevic P, Natarajan AT: Distribution of radiation-induced G1 exchange and terminal deletion breakpoints in Chinese hamster chromosomes as detected by G-banding. *Int J Radiat Biol* 66:747–755 (1994b).
- Tanabe K, Ikegami Y, Ishida R, Andoh T: Inhibition of topoisomerase II by antitumor agents bis(2,6-dioxopiperazine) derivatives. *Cancer Res* 51:4903–4908 (1991).
- Tewey KM, Rowe ZTC, Yang L, Halligan BD, Liu LF: Adriamycin-induced DNA damage mediated by mammalian DNA topoisomerase II. *Science* 226:466–468 (1985).
- Wang JC: DNA topoisomerases. *Annu Rev Biochem* 54:665–697 (1985).
- Xiao Y, Natarajan AT: Heterogeneity of Chinese hamster X chromosomes in X-ray-induced chromosomal aberrations. *Int J Radiat Biol* 75:419–427 (1999a).
- Xiao Y, Natarajan AT: Non proportional involvement of Chinese hamster chromosomes 3, 4, 8, and 9 in X-ray-induced chromosomal aberrations. *Int J Radiat Biol* 75:943–951 (1999b).
- Xiao Y, Natarajan AT: Analysis of bleomycin-induced chromosomal aberrations in Chinese hamster primary embryonic cells by FISH using arm-specific probes. *Mutagenesis* 14:357–364 (1999c).

# The repair of $\gamma$ -ray-induced chromosomal damage in human lymphocytes after exposure to extremely low frequency electromagnetic fields

D. Lloyd,<sup>a</sup> P. Hone,<sup>a</sup> A. Edwards,<sup>a</sup> R. Cox<sup>a</sup> and J. Halls<sup>b</sup>

<sup>a</sup>National Radiological Protection Board, Chilton, Didcot, Oxon;

<sup>b</sup>Brunel Institute for Bioengineering, Brunel University, Uxbridge (UK)

**Abstract.** G<sub>0</sub> human blood lymphocytes were irradiated with 2.0 Gy  $\gamma$ -rays and cultured to metaphase whilst held in a 50-Hz power frequency magnetic field of 0.23, 0.47 or 0.7 mT. No differences were found in the frequencies of  $\gamma$ -induced chromosome aberrations observed in cells held in the EM fields compared with replicates held in a sham coil. Similar field con-

ditions have been reported to increase the frequency of  $\gamma$ -induced HPRT mutations, leading to a suggestion that the EM fields alter the fidelity of repair of genomic lesions. This was not confirmed by the chromosome aberration assay described here.

Copyright © 2003 S. Karger AG, Basel

Electric or magnetic fields at 50/60 Hz at levels of intensity likely to be encountered by members of the public or in most occupational settings are widely accepted as being non-mutagenic (Murphy et al., 1993). However the question remains open as to whether they might nevertheless carry some risk by enhancing the effect of known mutagens. A suggested mode of action is that the field in some way reduces the fidelity of repair of DNA damage caused by the established mutagen (Walleczek et al., 1999). The present paper examines this possibility using the *in vitro* assay of chromosomal aberrations induced in human lymphocytes by gamma radiation (IAEA, 2001).

## Materials and methods

The electromagnetic field (EMF) system was a facility installed in Brunel University and has been fully described by Wolff et al. (1999). It was designed to enable cell biology experiments to be conducted with extraneous variables reduced to an absolute minimum. In essence the apparatus comprises two identical solenoid coils each contained in a mumetal drum so that when in use they only differ by whether the field-producing current is flowing or not. In use, both coils have the earth's magnetic field restored and each is supplied from a common source with a recycled stream of temperature-, humidity- and CO<sub>2</sub>-controlled air. The variations in flux density between replicate specimens within a coil was within 1%. The experimental flux density was produced within one coil whilst the other acted as a sham control. On each occasion the choice of which coil was the positive or sham was made randomly by a control computer and this information remained coded until the study was completed.

Three flux densities (0.23, 0.47 and 0.7 mT at 50 Hz) of 12 h duration were used and each was repeated. Thus there were six runs on the apparatus and these spanned nine weeks. During each run each coil was loaded with six replicate cultures of cells previously irradiated with 2.0 Gy  $\gamma$ -rays and two replicates with unirradiated cells. In addition four replicate cultures of  $\gamma$ -irradiated cells were set up in identical conditions but retained at the NRPB laboratory and incubated in parallel with the material at Brunel.

Heparinized peripheral blood from one healthy, non-smoker, 46-year female donor was used throughout. The objective of the work was to explore whether an effect existed from the combination of the ionising and non-ionising radiations. Thus an extensive series of exposures with matched controls and shams was undertaken with the blood from a single donor. Absolute values of aberration frequencies for any particular exposure regimen would of course have varied had blood from several donors been used. However the

We are grateful to the EMF Biological Research Trust for partial funding of this study.

Received 8 July 2003; manuscript accepted 4 November 2003.

Request reprints from D. Lloyd, N.R.P.B., Chilton, Didcot, Oxon, OX11 0RQ (UK)  
telephone: +44 1235 822700; fax: +44 1235 831600  
e-mail: david.lloyd@nrpb.org

**Table 1.** Aberrations scored in lymphocytes exposed to combinations of 2.0 Gy  $\gamma$ -rays and three EM fields

Run	2 Gy $\gamma$	EM Field	No cells scored	Dicentric	$\chi^2$ on 5DF	Centric rings	Excess acentrics	$\chi^2$ on 5DF	Chromatid		
									Gaps	Breaks	Exchanges
1. 0.23 mT	-	-	400	1		0	0		0	0	0
	+	-	1200	90	1.7	1	71	2.8	3	2	0
	-	+	400	0		0	0		0	0	0
	+	+	1200	123	3.1	2	73	5.0	3	5	0
	NRPB control	+	-	200	16		0	15		3	0
2. 0.23 mT	-	-	400	1		0	0		2	0	0
	+	-	1200	141	7.1	1	98	3.2	3	4	0
	-	+	400	0		0	1		1	1	0
	+	+	1200	146	2.6	4	102	8.7	8	3	1
	NRPB control	+	-	200	19		0	12		1	0
1. 0.47 mT	-	-	400	0		0	4		2	0	0
	+	-	1200	183	17.5	2	107	5.1	3	2	0
	-	+	400	0		0	5		0	0	0
	+	+	1200	160	8.3	6	102	5.2	6	7	0
	NRPB control	+	-	200	34		0	17		1	0
2. 0.47 mT	-	-	400	0		0	1		0	2	0
	+	-	1200	151	5.5	0	97	10.6	6	1	0
	-	+	400	0		0	0		1	0	0
	+	+	1200	184	3.0	3	97	5.8	8	2	2
	NRPB control	+	-	200	29		2	22		2	2
1. 0.7 mT	-	-	400	1		0	4		3	1	0
	+	-	1200	155	10.9	7	92	7.7	7	8	0
	-	+	400	0		0	1		0	1	0
	+	+	1200	153	4.8	2	111	3.2	10	2	0
	NRPB control	+	-	200	17		0	16		1	1
2. 0.7 mT	-	-	400	0		0	1		5	1	0
	+	-	1200	142	3.8	5	109	10.4	6	2	0
	-	+	400	0		0	0		1	0	1
	+	+	1200	138	4.0	5	94	14.5	7	5	0
	NRPB control	+	-	200	25		1	16		0	0

objective was not to explore inter-individual genetic variability, but rather whether an effect occurred per se.

Blood sampling was with informed consent and according to the institutional standing ethical approval. "Vacutainer" tubes of freshly taken blood were cooled over 1 h to 1–5 °C in crushed ice. Some tubes were irradiated at ice temperature to 2.0 Gy with cobalt-60  $\gamma$ -rays at a dose rate of 1.0 Gy/min, while identical tubes remained unirradiated. Reproducibility of the  $\gamma$  dose on the six occasions was within 2%.

After irradiation the subsequent handling of cells continued under cold conditions. Replicate whole blood cultures were set up with 0.3 ml of blood added to 4.5 ml of cooled Eagle's minimum essential culture medium supplemented with 10% foetal calf serum, 1% L-glutamine, 100 IU/ml penicillin, 100  $\mu$ g/ml streptomycin, 1% heparin and 1% 5-bromodeoxyuridine. The same batch numbers for all culture constituents were used throughout the study. The culture vessels were 10-ml capacity plastic screw-top tubes.

The vessels were then transported from the NRPB laboratory on ice to Brunel University; a travelling time of approximately 1.5 h. Two hours after  $\gamma$  irradiation 0.1 ml of phytohaemagglutinin (PHA) was added to each cold culture and they were then installed in the EMF apparatus and exposed to a chosen flux density or sham. Only then did the cell cultures warm to 37 °C. The magnetic field/sham was maintained for only the first 12 h and then the cultures remained in the same apparatus for a further 36 h, making a total culture time of 48 h, which is the standard protocol for obtaining first division metaphases. At 45 h 0.1 ml of colcemid (final conc 0.25  $\mu$ g/ml) was added to each culture.

On removal of the cultures from the apparatus they were transported at ambient temperature back to the NRPB laboratory where metaphases were harvested by the standard procedure of hypotonic treatment in potassium chloride solution and fixation in methanol:acetic acid (IAEA, 2001). Fixed cell suspensions were coded and stored at -20 °C until required for preparing microscope slides.

An aliquot of cells from each coded culture was checked by fluorescence plus Giemsa staining to confirm that >95% of metaphases were in their first in vitro division. With this confirmation further slides were block-stained with Giemsa for aberration scoring. Two hundred cells from each culture were scored by one experienced person recording the presence of dicentric, centric ring and excess acentric chromosome aberrations and chromatid gaps, breaks and exchanges. The criteria for identification and recording the aberrations followed the internationally recommended protocol (IAEA, 2001).

The chi-squared test, based on Poisson assumptions for dicentrics and a Poisson variance increased by a factor 1.1 for acentrics, was used to confirm homogeneity of aberration yields from the replicate samples from each coil. The standard error on difference between the EMF exposed and sham exposed samples in the same run was computed from the sum of the individual variances.

## Results

When all microscope scoring was completed the slide and coil codes were broken. The aberration frequencies in 200 cells scored from each of the six  $\gamma$ -irradiated and two unirradiated replicate blood cultures from each coil (individual data not shown) were compared and found to be homogenous using the  $\chi^2$  test. Only two of the 24 values of  $\chi^2$  were greater than 11.1 which is the  $\chi^2$  value corresponding to a 5% probability on 5 degrees of freedom. Table 1 shows the results from the pooled replicates for each of the six experimental runs and the corre-

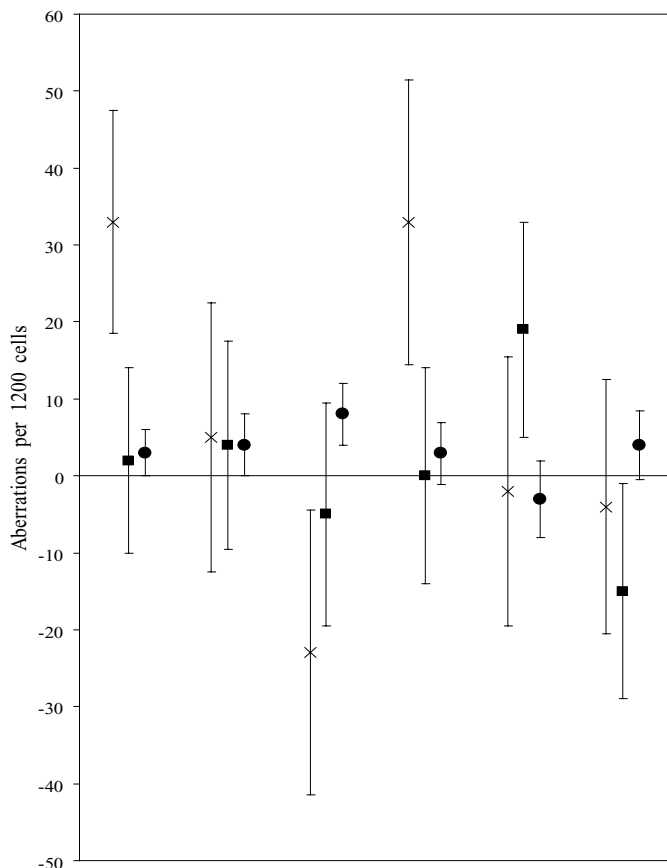


**Fig. 1.** The differences ( $\pm 1$  SE) in aberration frequencies (field minus sham) for lymphocytes exposed to 2.0 Gy  $\gamma$ -rays and held in electromagnetic fields.

sponding  $\chi^2$  values for the 2.0 Gy replicates. The aberration frequencies shown for the NRPB controls, i.e., the  $\gamma$ -irradiated blood that was retained and cultured at NRPB, are combined results from 50 cells scored from each of the four replicates.

## Discussion

This work was prompted by a recent study of Walleczek et al. (1999) which showed that in CHO cells the frequency of gene mutations at the *Hprt* locus induced by  $\gamma$ -rays was modified by subsequent incubation of the cells for 12 h in a power frequency (60 Hz) magnetic field of 0.7 mT. The magnetic field exposure induced an approximate 1.8-fold increase in *Hprt* mutations. Exposures at 0.23 and 0.47 mT also showed an enhancement of the mutation frequency but it was less marked. The field itself did not induce mutations but it was suggested that in some way it reduced the fidelity of repair of the  $\gamma$ -ray induced DNA damage. It was also noted that a similar finding was reported by Miyakoshi et al. (1997, 1999) using, respectively human melanoma and CHO cells but exposed at much higher flux densities of 5 and 400 mT. In view of the positive effect reported by Walleczek et al. (1999), the present study design used the same  $\gamma$  dose, flux densities and exposure duration. It

was considered more important to replicate these EM fields since, whilst also high, they are nevertheless much closer to what might be experienced by humans. The study is not a total replication since a different cell type (primary human lymphocytes) and a different assay endpoint (chromosomal aberrations) have been used. It is believed that the majority of radiation-induced gene mutations and chromosome aberrations have their origins in mis-repair of DNA double strand breaks via non-homologous end joining processes (Chu, 1997; Jeggo, 1998). Therefore the present study was undertaken to test the hypothesis of Walleczek et al. (1999) that EM field exposure can interfere in some way with the repair of a critical form of ionising radiation-induced genomic damage.

The experimental work had to be split between two centres and, to ensure that no DNA repair occurred between  $\gamma$ -irradiation and exposure to the magnetic field, processing and transport was performed with the cells held on ice. The cells were placed into culture and eventually raised to 37°C inside the field or sham coils. The magnetic field apparatus therefore also served as an incubator from which the cells were harvested at 48 h which is the standard time for obtaining first in vitro division metaphases with human blood lymphocytes. To control for possible effects of transporting cells and incubating in an atypical incubator, replicate cultures from aliquots of the  $\gamma$ -irradiated blood were incubated in parallel in the NRPB laboratory. In Table 1 the chromosome aberration yields scored from these "NRPB controls" are not significantly different from either of the two transported  $\gamma$ -irradiated samples. The total number of dicentrics from cultures held in the EMF incubator and the NRPB controls are 1,766 and 140. The ratio is 12.6 compared with the expected 12.0 based on the numbers of cells scored.

The lymphocytes were  $\gamma$  irradiated in the non-cycling  $G_0$  stage when induced damage leads to aberrations of the chromosome type: dicentrics, rings and excess fragments. After mitogenic stimulation with PHA and bringing the cultures to 37°C the cells commenced cycling and were in the  $G_1$  stage during the 12 h of EM field exposure. Damage incurred in  $G_1$  also leads to chromosome-type aberrations. The study was thus designed to measure possible changes caused by the field exposure in the frequencies of these aberrations although, for completeness, chromatid-type aberrations (gaps, breaks and exchanges) were also noted. Table 1 shows the numbers of cells and aberrations scored from each exposure run (two runs per flux density) with data pooled from replicate cultures within each run.

Examination of the data in Table 1 shows, firstly, that few aberrations were scored in cells that had received no  $\gamma$  exposure and for these cells there are no differences between incubating in the field or sham coils. The aberration frequencies are consistent with normal background (IAEA, 2001) and this therefore serves to confirm that the magnetic field alone does not measurably induce chromosomal aberrations.

In considering the results from cells exposed to 2 Gy  $\gamma$ -rays, the differences  $\pm 1$  SE in aberration frequencies, i.e., those observed in the field coil minus those in the sham, are plotted in Fig. 1. Data are shown for dicentrics, acentrics and combined chromatid-type aberrations. Centric rings have been

ignored as few were observed. In Fig. 1 only one data point departs significantly (2 SE) from equal frequencies indicated by the horizontal line. This is the positive value for dicentrics in the first run at 0.23 mT but it was not replicated in the second run at that flux density. It is notable that the  $\gamma$  alone (EMF sham) element of this first run at 0.23 mT gave an unexpectedly low yield of dicentrics and this may explain the positive result obtained. Overall, for dicentrics and acentrics there is a more-or-less even spread of points falling above and below the horizontal. There is no suggestion of a dose response relationship, as was reported for *Hprt* mutations, by Walleczek et al. (1999) where a more marked elevation ( $\times 1.8$ ) was found at 0.7 mT. The distributions of dicentrics and excess acentrics among the cells were tested for conformity with the Poisson distribution. Dicentrics were distributed as the Poisson whilst acentrics were overdispersed with a ratio of variance to mean of 1.1. This agrees with our previous experience (Lloyd et al., 1986). The mean difference in dicentric yields between the  $\gamma$ -ray plus field exposures and  $\gamma$  plus sham is 7 in 1,200 cells with an SE of 9 in 1,200. The distribution of the differences is slightly greater than that expected on the Poisson assumption, mainly caused by the data from run 1 at 0.23 mT, and this has been included in the calculation of SE. For acentrics the mean difference is 1 with an SE of 6 in 1,200 cells. The variation of the differences was less than that expected from the Poisson assumption but the calculation of SE took into account the factor 1.1 above. For dicentrics and acentrics the upper 95% confidence limits were 17% and 13% of their mean respective yields of 147 and 96 in 1,200 cells. Therefore using two standard errors as a criterion for detectability and allowing for inter-experiment variability, a 12% difference between field and sham exposure would have been the borderline of significance for both dicentrics and acentrics.

It is unclear why the gene mutation study of Walleczek et al. (1999) gave a positive result for EMF while the statistically more robust study reported here for dicentric chromosome aberrations did not. One explanation is that the somewhat fluctuating replicates reported by Walleczek et al. provide evidence of the considerable quantitative uncertainty inherent in this gene mutation assay (see Thacker, 1992 for discussion). On this basis we would place more weight on the essentially consistent dicentric data presented here which are inherently more reliable for the quantification of the consequences of genomic damage after ionising radiation.

However it remains possible that biological factors determine the differences seen. For example cell types and cell cycle parameters were different in the two studies and it is also possible that chromosomal exchange processes associated with dicentric formation are subject to less EMF perturbation than those that drive radiation-induced gene mutation (largely DNA/chromosomal deletions) (Thacker, 1992). Although we recognise the above biological factors as being potentially important, on balance we suggest that quantitative reliability is likely to be the most important issue.

Hintenlang (1993) has also reported an interaction (near tetraploidy) when X-irradiated lymphocytes were cultured in the presence of a 60-Hz 1.4-mT magnetic field. Cells exposed only to X-rays or to the field did not exhibit this phenomenon.

It was suggested that the field was able to influence the proper functioning of the mitotic spindle, somehow potentiating damage induced by the X-rays. Such an effect would not have been observed in the present study which was concerned with induced aberrations in M1 metaphases. Hintenlang was observing metaphases in 48-hour cultures that were past their first in vitro division but BrdU/harlequin staining was not used to discern division status. With longer-duration cultures near tetraploidy is a commonly observed effect from X-rays alone, but Hintenlang did not find this at 48 h where predominantly M1 cells would have been present. It is therefore possible that the magnetic field was not influencing mutagenesis or repair but instead increasing the speed of cell cycling and thus permitting ploidy change to be expressed.

Chromatid-type aberrations were also scored in the present study and Fig. 1 shows again that in each run the difference between yields in the field and sham lies close to the horizontal line. However a possible tendency could be construed in that in five of the six points, the yield in the  $\gamma$ -irradiated cells held in an EMF was higher, albeit in no case significantly, than that in its sham. By summing the values in Table 1 it may be inferred that from 7,200 cells the chromatid aberration frequency ( $\pm 1$  SE) in the shams is  $0.0065 \pm 0.0010$  per cell. The corresponding frequency, from 7,200 cells for  $\gamma$ -rays followed by EM field is  $0.0096 \pm 0.0012$ . The difference is  $0.0031 \pm 0.0016$ . By pooling the data in this way there appears to be a trend that 2.0 Gy  $\gamma$  plus EM field has resulted in an elevated chromatid aberration frequency. However as the absolute number of these aberrations scored is small, compared with the chromosome type, this difference is of borderline significance.

It has to be stressed that by giving the  $\gamma$  radiation to freshly taken blood, where lymphocytes are in  $G_0$ , this study was designed to explore the possibility of magnetic field effects on the frequencies of induced chromosome type aberrations. It is axiomatic that aberrations of the chromatid type are induced by ionising radiation only when cycling cells are exposed in S and  $G_2$  (IAEA, 2001). On this basis there is good reason to consider a follow-up study that includes  $\gamma$  irradiation of human lymphocytes in the S/ $G_2$  phases of the cell cycle.

It is interesting to note that in a few surveys of persons occupationally exposed to EM fields (Khalil and Qassem, 1991; Valjus et al., 1993) where aberrations have been reported to be elevated, they have been of the chromatid-type. In vitro, Cho and Chung (2003) reported that frequencies of SCE and micronuclei induced by benzo(a)pyrene were elevated when lymphocytes were exposed concurrently with an ELF-EMF of 0.8 mT. This implies that the field could act as an enhancer of the initiation process of chemical clastogenesis. The present study by contrast concentrated on post  $\gamma$ -ray repair processes which are known (Purrott and Reeder, 1976) to occur over a period of a few hours. Clearly it would be interesting to examine cells exposed concurrently to ELF and ionising radiation.



## Conclusion

Taken overall the results for chromosome type aberrations in the present study indicate no enhancement of aberration yields in cells held in the magnetic fields. Thus, by implication, the presence of these fields does not compromise directly or indirectly the repair of the  $\gamma$ -ray induced lesions, DNA double

strand breaks, that are principally responsible for aberrations. The statistical strength of these data is such that a difference of 12% or more would have been deemed significant. For chromatid type aberrations, for which the study was not primarily designed, no firm conclusion can be drawn. A possible trend in the data requires a more focussed study.

## References

- Chu G: Double strand break repair. *J Biol Chem* 272:24097–24100 (1997).
- Hintenlang DE: Synergistic effects of ionizing radiation and 60 Hz magnetic fields. *Bioelectromagnetics* 14:545–551 (1993).
- IAEA: Cytogenetic Analysis for Radiation Dose Assessment. Tech Rept 405 (International Atomic Energy Agency, Vienna 2001).
- Jeggio PA: Identification of genes involved in repair of DNA double strand breaks in mammalian cells. *Radiat Res* 150:580–591 (1998).
- Khalil AM, Qassem W: Cytogenetic effects of pulsing electromagnetic field on human lymphocytes in vitro: chromosome aberrations, sister-chromatid exchanges and cell kinetics. *Mutat Res* 247:141–146 (1991).
- Lloyd DC, Edwards AA, Prosser JS: Chromosome aberrations induced in human lymphocytes by in vitro acute x and gamma radiation. *Radiat Prot Dosim* 15:83–88 (1986).
- Miyakoshi J, Kitagawa K, Takebe H: Mutation induction by high-density, 50-Hz magnetic fields in human MeWo cells exposed in the DNA synthesis phase. *Int J Radiat Biol* 71:75–79 (1997).
- Miyakoshi J, Koji Y, Wakasa T, Takebe H: Long-term exposure to a magnetic field (5 mT at 60 Hz) increases X-ray-induced mutations. *J Radiat Res* 40:13–21 (1999).
- Murphy JC, Kaden DA, Warren J, Sivak A: Power frequency electric and magnetic fields: A review of genetic toxicology. *Mutat Res* 296:221–240 (1993).
- Purrott RJ, Reeder E: Chromosome aberration yields in human lymphocytes induced by fractionated doses of X-radiation. *Mutat Res* 34:437–446 (1976).
- Thacker J: Radiation-induced mutation in mammalian cells. *Adv Radiat Biol* 16:77–124 (1992).
- Valjus J, Norppa H, Järventaus H, Sorsa M, Nykyri E, Salomma S, Järvinen P, Kajander J: Analysis of chromosomal aberrations, sister chromatid exchanges and micronuclei among power line men with long-term exposure to 50-Hz electromagnetic fields. *Radiat Environ Biophys* 32:325–336 (1993).
- Walleczek J, Shiu EC, Hahn GM: Increase in radiation-induced HPRT gene mutation frequency after non-thermal exposure to nonionising 60 Hz electromagnetic fields. *Radiat Res* 151:489–497 (1999).
- Wolff H, Gamble S, Barkley T, Janaway L, Jowett F, Halls JAT, Arrand JE: The design, construction and calibration of a carefully controlled source for exposure of mammalian cells to extremely low-frequency electromagnetic fields. *J Radiol Prot* 19: 231–242 (1999).

# Ionizing radiation-induced instant pairing of heterochromatin of homologous chromosomes in human cells

H.I. Abdel-Halim,<sup>a,b</sup> S.A. Imam,<sup>b</sup> F.M. Badr,<sup>c</sup> A.T. Natarajan,<sup>a</sup>  
L.H.F. Mullenders,<sup>a</sup> and J.J.W.A. Boei<sup>a</sup>

<sup>a</sup>Department of Toxicogenetics, Leiden University Medical Center, Leiden (The Netherlands);

<sup>b</sup>Department of Zoology, Faculty of Sciences, <sup>c</sup>Department of Anatomy, Faculty of Medicine, Suez Canal University, Ismailia (Egypt)

**Abstract.** Using fluorescence in situ hybridization with human band-specific DNA probes we examined the effect of ionizing radiation on the intra-nuclear localization of the heterochromatic region 9q12→q13 and the euchromatic region 8p11.2 of similar sized chromosomes 9 and 8 respectively in confluent (G<sub>1</sub>) primary human fibroblasts. Microscopic analysis of the interphase nuclei revealed colocalization of the homologous heterochromatic regions from chromosome 9 in a proportion of cells directly after exposure to 4 Gy X-rays. The percentage of cells with paired chromosomes 9 gradually decreased to control levels during a period of one hour. No significant changes in localization were observed for chromosome 8. Using 2-D image analysis, radial and inter-homologue distances were measured for both chromosome bands. In unexposed cells, a random distribution of the chromosomes over the interphase nucleus was found. Directly after irradiation, the average inter-homologue distance decreased for chromosome 9

without alterations in radial distribution. The percentage of cells with inter-homologue distance <3 μm increased from 11% in control cells to 25% in irradiated cells. In contrast, irradiation did not result in significant changes in the inter-homologue distance for chromosome 8. Colocalization of the heterochromatic regions of homologous chromosomes 9 was not observed in cells irradiated on ice. This observation, together with the time dependency of the colocalization, suggests an underlying active cellular process. The biological relevance of the observed homologous pairing remains unclear. It might be related to a homology dependent repair process of ionizing radiation induced DNA damage that is specific for heterochromatin. However, also other more general cellular responses to radiation-induced stress or change in chromatin organization might be responsible for the observed pairing of heterochromatic regions.

Copyright © 2003 S. Karger AG, Basel

With the introduction of fluorescence in situ hybridization (FISH) it became possible to detect specific DNA sequences in single cells. Utilization of chromosome-specific DNA probes on interphase nuclei has unequivocally confirmed circumstantial evidence from earlier studies, that chromosomes occupy

discrete territories in the cell nucleus. Recently, the architecture of the cell nucleus has become a subject of great interest and it is now widely accepted that interphase nuclei possess a high degree of spatial organization (for review see Cremer and Cremer, 2001). Whether reproducible arrangements of chromosome territories (CTs) exist in cells has been the subject of various studies. The conclusions of these studies are conflicting and range from highly ordered arrangements of CTs (Nagele et al., 1995) to barely any order (Allison and Nestor, 1999). The discrepancy in the obtained results might be related to differences in cell type, cell cycle or species concerning the degree of order in the arrangement of CTs. However, the consistent observations that CTs occupy distinct radial nuclear positions depending on their gene density reveal the existence of at least some degree of order (Croft et al., 1999; Boyle et al., 2001).

Supported by the Euratom contract no. FIGH-CT1999-00011.

Received 16 September 2003; manuscript accepted 25 November 2003.

Request reprints from J.J.W.A. Boei, Department of Toxicogenetics  
Leiden University Medical Center, Wassenaarseweg 72  
PO Box 9503, NL-2300 RA Leiden (The Netherlands)  
telephone: +31 71 527 6169; fax: +31 71 527 6173  
e-mail: j.j.w.a.boei@lumc.nl

One way to study the chromatin organization in interphase nuclei is to examine the distances between homologous chromosomes. In general, the large variation in inter-homologue distances suggests a random arrangement of homologous CTs. However, pairing of homologous chromosomes has been clearly documented in several cases such as in yeast (Burgess et al., 1999), *Drosophila* (Fung et al., 1998), and plants (Bender, 1998). Also in human cells, several studies have indicated a transient and/or locus-specific pairing of homologous chromosomes. For example, homologous pairing has been observed for the centromeric region of chromosome 1 in human cerebellar cells (Arnoldus et al., 1989). Brown et al. (1994) studied cells from benign and malignant prostates using centromere specific probes for different chromosomes and found that chromosome 17 showed a significant incidence of apparent monosomy in these cells. Image analysis demonstrated that the monosomic (single) signals contained twice the signal intensity of those in cells not showing monosomy, suggesting that the former represented pairing of the centromeres of the homologous chromosomes 17. Using chromosome 7 and 10 centromeric probes on a follicular lymphoma, Atkin and Jackson (1996) observed a similar phenomenon, i.e. the frequent presence of single hybridization signals in interphase cells despite the presence of both homologues. Moreover, association of homologous centromeres of chromosomes 9 and 17 was evident in cells from prostate cancer (Williams et al., 1995). It has been suggested that the association of homologous chromosomes is of functional significance reflecting specific nuclear organization in relation to gene expression, malignant- or disease-state (Tartof and Henikoff, 1991; Henikoff, 1997; Stout et al., 1999).

Preferred pairing of homologous chromosomes might also be the consequence of the specific properties of the DNA in the centromeric regions. The degree of homology of the highly repetitive DNA sequences abundantly present near the centromeres of some chromosomes might facilitate the pairing of these regions (Haaf et al., 1986). The observed clustering and association of centromeric heterochromatin into so-called chromocenters (Hsu et al., 1971; Schmid et al., 1975) are examples of preferred association of highly repetitive sequences.

In a recent study by Dolling et al. (1997) the rearrangement of homologous territories for chromosomes 7 and 21 was investigated in response to ionizing radiation. In human skin fibroblasts and lung endothelial cells the distance between the homologous chromosome territories was measured in control cells and at several time intervals in cells exposed to 4 Gy gamma rays. At 1–2 h after exposure the inter-homologue distance was significantly reduced when compared with the unexposed control cells. The authors proposed that the observed rearrangement of chromosome territories is an active cellular process to permit repair of induced damage by a homology-dependent recombinational repair process.

In this study we addressed the question as to whether ionizing radiation induces alteration in the positioning of homologous chromosomes within the interphase nucleus. Dual-color fluorescence in situ hybridization (FISH) using the band-specific probes 8p11.2 and 9q12→q13 was applied on confluent ( $G_1$ ) human fibroblasts. The probe 9q12→q13 covers the heterochromatic region flanking the centromere of chromosome 9,

whereas 8p11.2 covers a euchromatic band near the centromere of the similar sized chromosome 8. Using 2-D image analysis, the relative position of homologous chromosome regions was examined. In control cells, both chromosomes 8 and 9 seem to be randomly positioned in the interphase nucleus with a wide range of inter-homologue distances. Directly after exposure to 4 Gy X-rays, we observed a transient pairing between the heterochromatic regions of chromosomes 9 in a proportion of  $G_1$  fibroblasts. The proportion of cells with paired heterochromatin gradually decreased to control levels within one hour after exposure. No rearrangements were observed for the euchromatic regions of chromosomes 8, suggesting a critical role of heterochromatin in the instant pairing of homologous chromosomes after exposure to ionizing radiation.

## Materials and methods

### *Cell culture and irradiation*

Primary human skin fibroblasts derived from a healthy individual (VH25) were grown in Ham's F10 medium, supplemented with 15% fetal bovine serum and antibiotics and incubated at 37°C in 2.5% CO<sub>2</sub> atmosphere. The cells were seeded with a high density ( $\sim 3.0 \times 10^4$  cells/cm<sup>2</sup>) on glass slides and grown to confluency ( $\sim 6.7 \times 10^4$  cells/cm<sup>2</sup>) during seven subsequent days. Confluent cells were X-irradiated with 4 Gy at 37°C (using an Andrex SMART 255 X-ray machine, operating at 200 kV and 4 mA with a dose rate of 2 Gy/min). Cells were fixed either immediately after exposure or after different incubation time intervals at 37°C. Non-irradiated control cultures were processed in parallel. Cycling cells were monitored by incubating parallel slides for 24 h in the presence of 5-bromo-2'-deoxyuridine (BrdU, Sigma) at a final concentration of 5.0  $\mu$ M.

### *Fixation*

Control and irradiated slides with confluent cells were washed twice with ice-cold phosphate buffered saline (PBS) prior to a 5-min fixation step with ice-cold PBS containing 2% paraformaldehyde. In order to permeabilize the nuclear membrane the cells were incubated with methanol (–20°C) for 10 min after which the slides were air-dried prior to in situ hybridization or BrdU detection.

### *Fluorescence in situ hybridization (FISH) and BrdU detection*

Fluorescence in situ hybridization (FISH) was performed using human band-specific DNA probes for the bands 8p11.2 and 9q12→q13 (Research Genetics). The probes were labeled with FITC-12-dUTP (Perkin Elmer) or biotin-16-dUTP (Boehringer Mannheim) during a PCR reaction using a protocol supplied by the manufacturers. The PCR product was purified using a QIAquick kit (Qiagen). The probes were mixed and precipitated together with human Cot1 DNA (Roche) and dissolved in hybridization mixture (50% deionized formamide, 2× SSC, 50 mM phosphate buffer pH 7.0, and 10% dextran sulfate). Denaturation was performed by incubation for 7 min at 80°C followed by probe competition for 1 h at 37°C.

Prior to in situ hybridization, slides were treated with RNase, pepsin, MgCl<sub>2</sub> and formaldehyde as previously described (Boei et al., 1996) followed by denaturation in 60% deionized formamide, 2× SSC and 50 mM phosphate buffer (pH 7.0) for 2.5 min at 80°C. Finally the probes were added to the slides and hybridized overnight at 37°C.

Post-hybridization, slides were washed with 50% formamide in 2× SSC (pH 7.0) at 42°C and treated with 10% blocking protein (Cambio). For immunofluorescent detection of FITC-labeled probes, rabbit anti-FITC and fluorescein-conjugated goat anti-rabbit IgG were used (Cambio), whereas Texas-Red avidin and biotinylated goat anti-avidin (Cambio) were used to detect biotin-labeled probes.

To visualize incorporated BrdU, slides were pretreated and denatured as described above for the FISH procedure. Immunofluorescent detection was performed using a mouse IgG monoclonal anti-bromodeoxyuridine antibody (Boehringer Mannheim) and a secondary goat anti-mouse antibody conjugated with Alexa Fluor 488 (Molecular Probes).

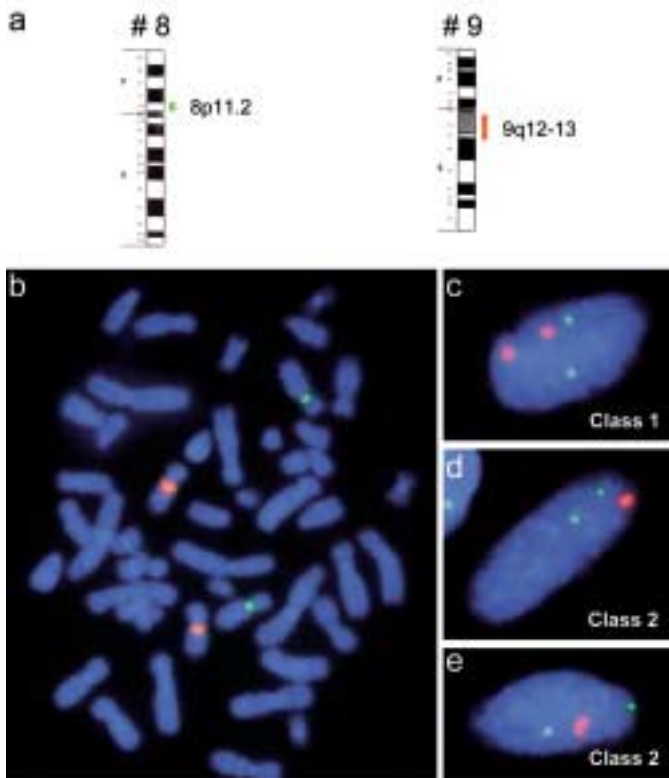


**Fig. 1.** (a) Diagrammatic representation of G-banded human chromosomes 8 and 9. The position and size of the bands covered by band probes 8p11.2 and 9q12→q13 is shown. (b) Metaphase spread of a human lymphocyte hybridized with band probe 8p11.2 (green) and 9q12→q13 (red). (c) Example of a class 1 cell, an interphase human fibroblast with two separated hybridization signals for both band-specific probes. (d) Example of a class 2 cell, the red hybridization signals (of homologous bands 9q12→q13) are overlapping giving one, slightly larger hybridization signal. (e) Example of a cell with two touching red hybridization signals. Also this situation was classified as a class 2 cell during the manual analysis.

After counterstaining with 10 ng/ml DAPI/PBS solution for 10 min, the slides were embedded with Citifluor mounting medium (Agar Scientific).

#### Microscopy and scoring criteria

Fluorescence microscopy was performed with a Zeiss Axioplan microscope equipped with filters for observation of DAPI, FITC and TRITC. Interphase nuclei were analyzed manually or by means of a computerized image analysis system consisting of a Nu200 CCD camera, an Apple Macintosh PowerPC and IPLab software (Scanalytics Inc.).

In the manual scoring, a distinction was made between cells which displayed entirely separated hybridization signals (class 1 cells, Fig. 1c), and cells in which signals were so close together that only a single (usually larger) hybridization signal or two touching signals were observed (class 2 cells, Fig. 1 d, e).

Image analysis was performed on 200 randomly selected images of flat (2-D) fibroblast nuclei both for control and irradiated cells (fixed immediately after exposure). From a single nucleus, the center was determined as a midpoint on the major axis that passes through the longest axis of the ellipsoid nucleus (Fig. 3). The length of both major and minor axis (making a 90° angle with the major axis at the center of the nucleus) was determined and taken as a measure of nuclear size. The position of each chromosome band (8p11.2 and 9q12→q13) was determined by the weighted center of the fluorescent intensity of the hybridization signal. Subsequently the radial distance was measured for each chromosome band. Furthermore, the radial angles with the major axis were calculated and used, along with the radial distances, to plot all hybridization signals in one quadrant of the nucleus (according to

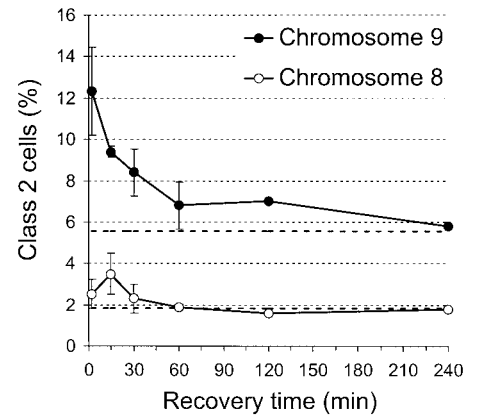


**Fig. 2.** Kinetics of pairing of homologous chromosome bands 8p11.2 and 9q12→q13 in irradiated and control G<sub>1</sub> human fibroblasts. The dashed lines show the percentage of control cells with paired homologous bands 8p11.2 (bottom) and 9q12→q13 (top). The error bars represent the SD of the mean of three different experiments. At 0, 15 and 30 min after exposure to radiation, statistically significant differences ( $P < 0.05$ ) were observed between the colocalization of chromosome 9 in irradiated and control cells.

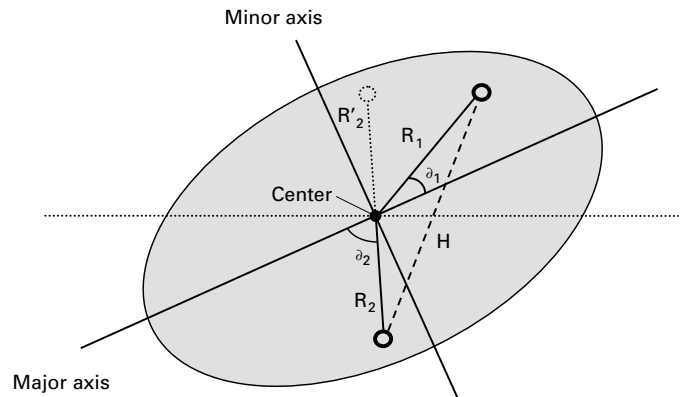


**Fig. 3.** Diagrammatic representation of a fibroblast nucleus with two homologous hybridization sites (round circles).  $R_1$  and  $R_2$  are the radial distances for hybridization sites 1 and 2 respectively. The radial angles  $\delta_1$  and  $\delta_2$  are the angle of  $R_1$  and  $R_2$  respectively with the major axis with values between 0 and 90°. These parameters were used to convert hybridization sites to one quadrant of the nucleus (dotted line and circle  $R'_2$ ).  $H$  represents the distance between the two homologous hybridization sites.

Sun et al., 2000; Fig. 4). Finally, the distance between the homologous chromosome bands was measured, sorted and plotted against ascending nucleus numbers (Fig. 5).

#### Statistical analysis

The Student t test was used to analyze the difference between control and irradiated groups of cells. Chi-square test was used to analyze the difference in the distance spectra and to compare the number of cells displaying different distance ranges in control and irradiated groups.

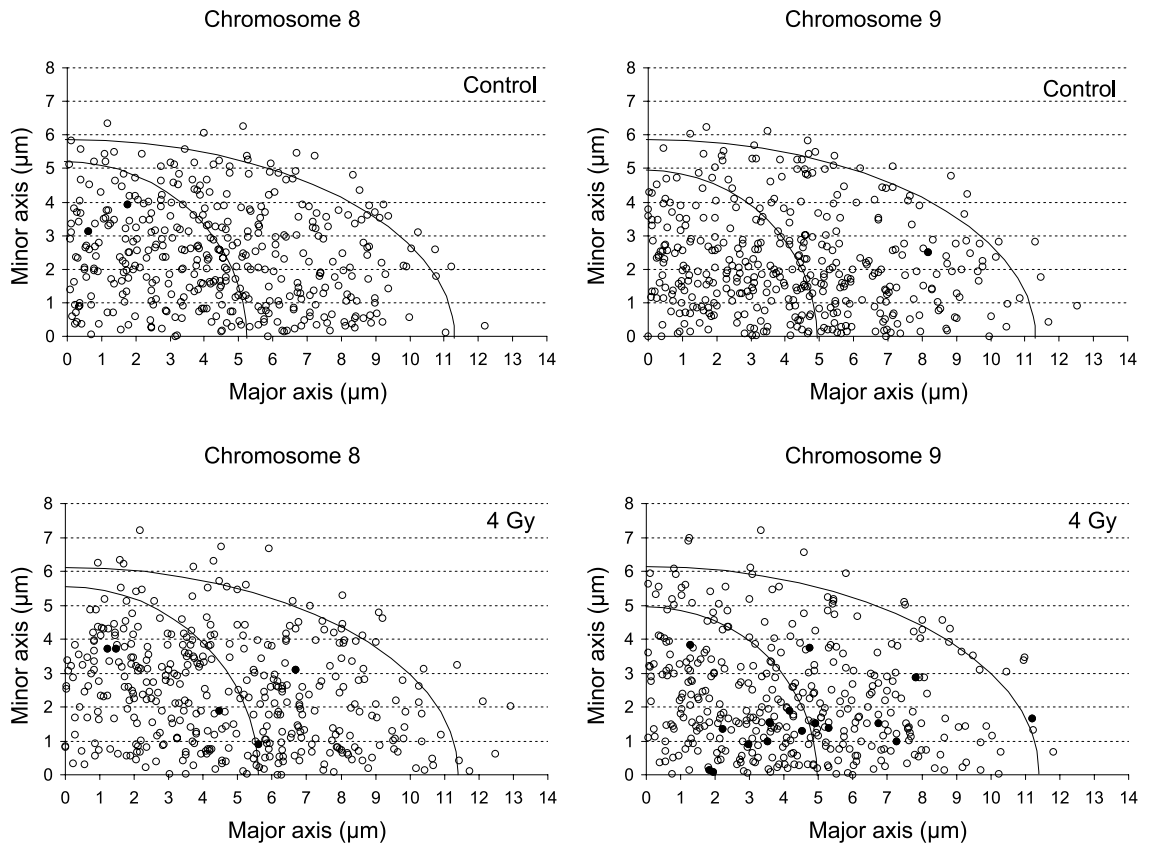


**Fig. 4.** Cumulative plots of hybridization sites for the bands 8p11.2 (left) and 9q12→q13 (right) analyzed in 200 control and 4 Gy X-irradiated  $G_1$  human fibroblasts (fixed directly after exposure). All hybridization sites were plotted in one quadrant of the nucleus, the x- and y-axis representing the major and minor axis respectively. The contour of the average size of the nuclear membrane is represented by the outer curve. The inner curve corresponds to the mean radial distances, thus 50% of hybridization sites are located inside this curve. The black circles represent the position of two fully overlapping hybridization signals.

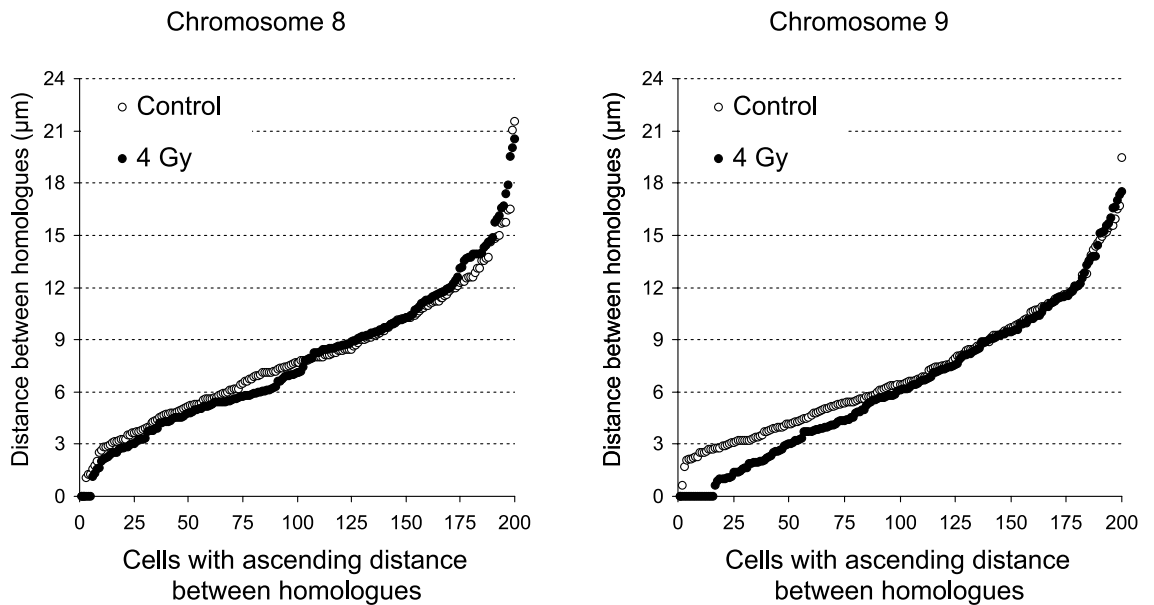


**Fig. 5.** Inter-homologue distance distribution of chromosome bands 8p11.2 (left) and 9q12→q13 (right) in control (white circles) and X-irradiated (4 Gy; black circles) confluent human fibroblasts. Cells with ascending inter-homologue distances are plotted against the inter-homologue distances.

## Results

In order to investigate the positioning of homologous chromosomes in interphase cells, we analyzed G<sub>1</sub> phase primary human fibroblasts by FISH employing the band-specific probe 9q12→q13 (covering the paracentromeric heterochromatic region of chromosome 9), and for comparison, the band-specific probe 8p11.2 (staining a paracentromeric euchromatic band of chromosome 8). The specificity of each probe was established by hybridization to metaphase spreads as shown in Fig. 1b. The hybridization signals using these probes in interphase cells were bright and compact, which allowed reliable analysis (Fig. 1c–e). The advantage of fibroblasts is that these cells are sufficiently flat to allow simple 2-D analysis and that the cells can be synchronized in G<sub>1</sub> by contact inhibition. The applied culture conditions allowed the formation of a true confluent monolayer. Immuno-fluorescent staining of BrdU in parallel cultures revealed that less than 5% of cells in the monolayer had incorporated BrdU during a period of 24 h. Thus the great majority of cells were in the G<sub>1</sub> phase of the cell cycle at the moment of exposure to radiation and fixation.

### Manual analysis

To assess the influence of ionizing radiation on the localization of homologous chromosomes, confluent fibroblasts were exposed to 4 Gy X-rays and fixed immediately or incubated at 37°C for different time intervals before fixation. Per data point 500 cells were scored manually. As shown in Fig. 1c–e, for each chromosome pair the cells were classed among two groups i.e., cells displaying two distinct hybridization signals (class 1) and cells with one or two closely adjacent hybridization signals (class 2). The outcome of three independent experiments is presented in Fig. 2. In control cells we noticed a difference in the percentage of class 2 cells when stained for chromosomes 8 and 9 ( $1.9 \pm 0.6\%$  and  $5.6 \pm 1.2\%$  represented by the lower and upper dashed lines respectively in Fig. 2). This difference can be explained by the different band size covered by the applied probes (Fig. 1). The larger average size of the interphase hybridization signals for probe 9q12→q13 ( $2.15 \mu\text{m}^2$ ) compared to probe 8p11.2 ( $0.90 \mu\text{m}^2$ ) results in an estimated probability of about 5% and 2% respectively to co-localize in case of random positioning in the 2-D area of an average sized ellipsoid interphase nucleus (surface  $\sim 209 \mu\text{m}^2$ ; Fig. 4). The estimates are based on the simplifying assumption of circular hybridization signals, in which the center of colocalizing signals should fall within an area with twice the radius of the hybridization signal.

Exposure of cells to 4 Gy X-rays resulted in an instant increase in the percentage of class 2 cells for chromosome 9. Directly after exposure the percentage of class 2 cells was approximately two-fold ( $12.3 \pm 2.1\%$ ) higher than the control level. At later time intervals, a gradual reduction in the percentage of class 2 cells was observed reaching control levels at about 1 h after exposure. In contrast to chromosome 9, irradiation did not affect the percentage of class 2 cells for chromosome 8, only at 15 min after exposure a non-significant increase of class 2 cells was observed. Irradiation of cells on ice, followed by immediate fixation led to a colocalization frequency for the

homologues of chromosome 9 not different from that of the control cells ( $5.6\% \pm 1.2$ ).

### Image analysis

In the manual analysis we only distinguished between cells with 2 or 1 (or two adjacent) hybridization signals. To gain more detailed insight in the localization of homologous chromosomes we applied interphase image analysis on 200 randomly selected control and irradiated cells fixed directly after exposure.

Firstly, the length of both major and minor axis as well as the nuclear area were measured as parameters for nuclear size. Exposed nuclei were slightly, but not significantly, larger than unexposed nuclei. The average length of the major axis increased from 11.2 to 11.4  $\mu\text{m}$ , the minor axis from 6.0 to 6.1  $\mu\text{m}$  as represented by the outer contour lines of Fig. 4. The average nuclear area increased after exposure about 3% from 206 to 212  $\mu\text{m}^2$ . Since this increase in nuclear size was marginal, no normalization was performed for other parameters measured.

Secondly, the position of hybridization signals was determined relative to the center of the nucleus. This relative distribution was visualized by plotting all hybridization signals in one quadrant of the nuclear area (Fig. 4). The hybridization signals for both chromosome 8 and 9 bands were apparently randomly distributed throughout the unirradiated nucleus. Half of the hybridization signals were found within circles (inner curve of Fig. 4) with radii of 5.3 and 5.0  $\mu\text{m}$  for chromosome 8 and 9 respectively. Thus chromosome 9 occupies a slightly more central position in the interphase nucleus when compared with chromosome 8. After irradiation, the median radial distance increased from 5.3 to 5.6  $\mu\text{m}$  for the position of chromosome 8, but remained the same (5.0  $\mu\text{m}$ ) in case of chromosome 9.

Finally, the effect of 4 Gy X-irradiation on the relative position of homologous chromosomes 8 and 9 was assessed by measurement of the distance between the homologues in each cell. Irradiation did not change the average distance between the homologues of chromosome 8 significantly ( $7.9 \pm 1.1 \mu\text{m}$  in the control cells and  $7.8 \pm 1.1 \mu\text{m}$  in the irradiated cells). For chromosome 9 the reduction in the average distance after irradiation was more pronounced, i.e.,  $7.2 \pm 1.0$  versus  $6.5 \pm 0.9 \mu\text{m}$ , but also not statistically significant. In some cells the position of the hybridization signals of two homologues was so close together (overlapping) that two centers of weighted signal intensities could not be determined. In these cells the distance between the homologues was considered 0  $\mu\text{m}$ . Fully overlapping hybridization signals (the black circles in Fig. 4) were found in 1% of control cells for chromosome 8 and in 0.5% for chromosome 9. Directly after exposure, cells with overlapping signals were found in 2.5% of cells for chromosome 8 and in 8% of cells for chromosome 9.

In Fig. 5, the number of cells with ascending distances between the homologues is plotted against the absolute distances between the homologues. Statistical analysis revealed no significant changes in the spectrum of distances between the homologues of chromosome 8 as a direct response to the exposure to ionizing radiation. In contrast, for chromosome 9 the

distance distribution is significantly different ( $P < 0.001$ ) in irradiated cells compared to the control. In 11% of the unexposed cells the distance between the homologues of chromosome 9 was less than 3  $\mu\text{m}$  while after irradiation a significant increase of cells to 25% in this category was found. The percentage of cells in the category 3–6  $\mu\text{m}$  decreased from 33.5% in control cells to 24% in irradiated cells. No significant changes were observed in cells with inter-homologue distances  $>6 \mu\text{m}$ . These measurements confirm the manual observations and indicate a specific movement of the paracentromeric heterochromatin of chromosome 9 towards each other.

## Discussion

The present study gives information on the effect of ionizing radiation on the organization of interphase nuclei regarding the association of homologous chromosomes 8 and 9. Using band specific DNA probes in combination with fluorescence microscopy and 2-D image analysis, we demonstrated that in confluent ( $G_1$ ) primary human fibroblasts, the homologous bands 8p11.2 and 9q12→q13 are randomly distributed with a large variation in distances between the homologous regions.

Directly after exposure of cells to 4 Gy X-rays we observed a reduction in the average distances between the heterochromatic bands 9q12→q13 of chromosome 9 homologues but not for the euchromatic bands 8p11.2 of chromosome 8 homologues. Irradiation did not alter significantly the shape and size of the cell nucleus, ruling out that the observed changes are due to gross alterations in nuclear structure. In the exponentially growing human leukemia cells the reduced inter-homologue distances observed after ionizing radiation could be explained by a more central position of chromosomes (including chromosomes 8 and 9) in the nucleus (Jirsova et al., 2001). In the present study however, irradiation did not change the average radial distances for chromosomes 9 and pairing of homologous chromosomes seems to occur at random positions throughout the entire nucleus (Fig. 4).

Although the homologous chromosomes 9 seem to move over relatively large distances, induced pairing of 9q12→q13 is observed in only a small proportion (about 7%) of analyzed nuclei. In *Drosophila* the limited pairing was explained by the 3-D nuclear architecture (Marshall et al., 1997; Fung et al., 1998) in which a given chromatin segment undergoes constrained diffusion motion which is confined to a sub-region of the nucleus. It was suggested that the search for homology critically depends on both the initial distance between the loci and the size of the region in which the search takes place (Marshall et al., 1996). Also in human fibroblasts the position of the homologous chromosomes within the highly organized nucleus might be of crucial importance. Perhaps only those cells where homologous chromosomes are located in neighboring territories are able to bring the homologous bands together. Another explanation for the low percentage of cells showing pairing of homologous chromosomes might relate to the transient character of the induced pairing. Pairing is a fast process that is observed with the highest frequency within minutes after exposure to X-rays. If the dissociation of the two homologous chro-

mosomes is also a fast process, the chance to fix (analyze) cells during this short period of association is expected to be low.

The fact that pairing was observed only for the homologous chromosomes 9 and not for the similar sized chromosomes 8, strongly suggests a possible role of heterochromatin in the association process. The heterochromatic block of chromosome 9 (9q12) has been shown to contain a mixture of various tandem repeat sequences such as classical satellite DNA III (Gosden et al., 1975; Tagarro et al., 1994) and DNA sequence repeats which are rich (68%) in GC sequences (Meneveri et al., 1993). In meiosis GC rich sequences were suggested to promote pairing of homologous chromosomes (Chandley, 1989). Perhaps the large size of the GC rich heterochromatic region of chromosome 9 can also promote pairing in somatic cells. Therefore, it would be interesting to compare the response of other chromosomes with large heterochromatic bands such as chromosome 1 and 16 with chromosomes lacking these bands.

The observed transient character of the pairing of homologous chromosomes 9 suggests an underlying active cellular process. Also the absence of pairing in cells X-irradiated on ice implies the involvement of an active process. The similarity in kinetics of homologous pairing and the repair of radiation induced lesions, supports the speculations made by Dolling et al. (1997) about a possible role of a homology dependent repair process. Although recent studies have demonstrated a role for homologous recombination in the repair of DNA double strand breaks (DSBs) in mammalian cells (reviewed by Thompson and Schild, 2001), the activity is generally restricted to the S and  $G_2$  phase of the cell cycle. If the observed instant pairing of homologous chromosomes 9 in  $G_1$  human fibroblasts is related to repair by homologous recombination, this should be a unique feature for the heterochromatic regions of the genome.

In conclusion, the present study has demonstrated that the homologous chromosomes 9 are in closer proximity after exposure to ionizing radiation than they were before. Complete pairing was observed in only a proportion of cells and was most frequently observed directly after irradiation. During a period of about one hour after exposure the pairing frequency decreased to control levels. This transient character and temperature dependency of pairing suggests an underlying active cellular process. Furthermore, since chromosome 8 did not show significant rearrangements it is tempting to subscribe a unique role for heterochromatin (abundantly present in chromosome band 9q12 but not in chromosome band 8p11.2) in the pairing process. At this moment we can only speculate about the possible reasons for the ionizing radiation induced association of homologous chromosomes. Perhaps repair by homologous recombination plays a specific role in the removal of lesions induced by ionizing radiation in heterochromatin. However, other more general cellular responses to radiation induced stress might result in specific changes in the nuclear topology of heterochromatic regions.

## Acknowledgements

We thank Sylvia Vermeulen for her technical assistance to optimize the FISH procedure.

## References

- Allison DC, Nestor AL: Evidence for a relatively random array of human chromosomes on the mitotic ring. *J Cell Biol* 145:1–14 (1999).
- Arnoldus EPJ, Peters ACB, Bots GTAM, Raap AK, van der Ploeg M: Somatic pairing of chromosome 1 centromeres in interphase nuclei of human cerebellum. *Hum Genet* 83:231–234 (1989).
- Atkin NB, Jackson Z: Evidence for somatic pairing of chromosome 7 and 10 homologs in a follicular lymphoma. *Cancer Genet Cytogenet* 89:129–131 (1996).
- Bender J: Cytocine methylation of repeated sequences in eukaryotes: The role of DNA pairing. *Trends Biochem Sci* 23:252–256 (1998).
- Boei JJWA, Vermeulen S, Natarajan AT: Detection of chromosomal aberrations by fluorescence in situ hybridization in the first three postirradiation divisions of human lymphocytes. *Mutat Res* 349:127–135 (1996).
- Boyle S, Gilchrist S, Bridger JM, Mahy NL, Ellis JA, Bickmore WA: The spacial organization of human chromosomes within the nuclei of normal and emerlin-mutant cells. *Hum molec Genet* 10:211–219 (2001).
- Brown JA, Alcaraz A, Takahashi S, Persons DL, Lieber MM, Jenkins RB: Chromosomal aneusomies detected by fluorescent in situ hybridization analysis in clinically localized prostate carcinoma. *J Urol* 152:1157–1162 (1994).
- Burgess SM, Kleckner N, Weiner BM: Somatic pairing of homologs in budding yeast: existence and modulation. *Genes Dev* 13:1627–1641 (1999).
- Chandley AC: Asymmetry in chromosome pairing: a major factor in de novo mutation and the production of genetic disease in man. *J med Genet* 26:546–552 (1989).
- Cremer T, Cremer C: Chromosome territories, nuclear architecture and gene regulation in mammalian cells. *Nature Rev Genet* 2:292–301 (2001).
- Croft JA, Bridger JM, Boyle S, Perry P, Teague P, Bickmore WA: Differences in the localization and morphology of chromosomes in the human nucleus. *J Cell Biol* 145:1119–1131 (1999).
- Dolling JA, Boreham DR, Brown DL Raaphorst GP, Mitchel REJ: Rearrangement of human cell homologous chromosome domains in response to ionizing radiation. *Int J Radiat Biol* 72:303–311 (1997).
- Fung JC, Marshall WF, Dernburg A, Agard DA, Sedat JW: Homologous chromosome pairing in *Drosophila melanogaster* proceeds through multiple independent initiations. *J Cell Biol* 141:5–20 (1998).
- Gosden JR, Mitchell AR, Buckland RA, Clayton RP, Evans HJ: The location of four human satellite DNAs on human chromosomes. *Expl Cell Res* 92:148–158 (1975).
- Haaf T, Steinlein K, Schmid M: Preferential somatic pairing between homologous heterochromatic regions of human chromosomes. *Am J hum Genet* 38:319–329 (1986).
- Henikoff S: Nuclear organization and gene expression: homologous pairing and long-range interactions. *Curr Opin Cell Biol* 9:388–395 (1997).
- Hsu TC, Cooper JEK, Mace ML, Brinkley BR: Arrangement of centromeres in mouse cells. *Chromosoma* 34:73–87 (1971).
- Jirsova P, Kozubek S, Bartova E, Kozubek M, Lukasova E, Cafourkova A, Koutna I, Skalnikova M: Spatial distribution of selected genetic loci in nuclei of human leukemia cell after irradiation. *Radiat Res* 155:311–319 (2001).
- Marshall WF, Dernburg AF, Harmon B, Agard DA, Sedat JW: Specific interactions of chromatin with the nuclear envelope: positional determination within the nucleus in *Drosophila melanogaster*. *Mol Biol Cell* 7:825–842 (1996).
- Marshall WF, Straight A, Marko JF, Swedlow J, Dernburg A, Belmont A, Murray AW, Agard DA, Sedat JW: Interphase chromosomes undergo constrained diffusional motion in living cells. *Curr Biol* 7:930–939 (1997).
- Meneveri R, Agresti A, Marozzi A, Saccone S, Rocchi M, Archidiacono N, Corneo G, Valle GD, Ginelli E: Molecular organization and chromosomal location of human GC-rich heterochromatic blocks. *Gene* 123:227–234 (1993).
- Nagele R, Freeman T, McMorrow L, Lee HY: Precise spatial positioning of chromosomes during prometaphase: evidence for chromosomal order. *Science* 270:1831–1835 (1995).
- Schmid M, Vogel W, Krone W: Association between centric heterochromatin of human chromosomes. *Cytogenet Cell Genet* 15:66–80 (1975).
- Stout K, van der Maarel S, Frants RR, Padberg GW, Ropers HH, Haaf T: Somatic pairing between subtelomeric chromosome regions: implications for human genetic disease? *Chrom Res* 7:323–329 (1999).
- Sun HB, Shen J, Yokota, H: Size-dependent positioning of human chromosomes in interphase nuclei. *Biophys J* 79:184–190 (2000).
- Tagarro I, Fernandez-Peralta AM, Gonzalez-Aguilera JJ: Chromosomal localization of human satellite 2 and 3 by a FISH method using oligonucleotides as probes. *Hum Genet* 93:383–388 (1994).
- Tartof KD, Henikoff S: Trans-sensing effects from *Drosophila* to humans. *Cell* 65:201–203 (1991).
- Thompson LH, Schild D: Homologous recombinational repair of DNA ensures mammalian chromosome stability. *Mutat Res* 477:131–153 (2001).
- Williams BJ, Jones E, Brothman R: Homologous centromere association of chromosomes 9 and 17 in prostate cancer. *Cancer Genet Cytogenet* 58:143–152 (1995).



# Cytogenetic damage in lymphocytes for the purpose of dose reconstruction: a review of three recent radiation accidents

A. Wojcik,<sup>a,b</sup> E. Gregoire,<sup>c</sup> I. Hayata,<sup>d</sup> L. Roy,<sup>c</sup> S. Sommer,<sup>a</sup> G. Stephan<sup>e</sup> and P. Voisin<sup>c</sup>

<sup>a</sup>Department of Radiation Biology and Health Protection, Institute of Nuclear Chemistry and Technology, Warszawa;

<sup>b</sup>Department of Radiation Biology and Immunology, Świętokrzyska Academy, Kielce (Poland);

<sup>c</sup>Institut de Radioprotection et de Sûreté Nucléaire, Département de Protection de la santé de l'Homme et de dosimétrie, BP 17, Fontenay-aux Roses (France);

<sup>d</sup>National Institute of Radiological Sciences, Radiation Safety Research Center, Chiba-shi (Japan);

<sup>e</sup>Institut für Strahlenhygiene, Bundesamt für Strahlenschutz, Neuherberg (Germany)

**Abstract.** The analysis of chromosomal aberrations in peripheral blood of radiation accident victims is an established method of biological dosimetry. The dose estimate on the basis of an *in vitro* calibration curve is straightforward when the radiation exposure is homogeneous and the analysis not delayed. In recent years three radiation accidents occurred, where the irradiation or sampling conditions precluded a simple estimation of the dose. During the Georgian accident soldiers carried in their pockets small sources of <sup>137</sup>Cs leading to partial and protracted body exposures. During the Tokai-mura acci-

dent, three employees involved in the process of <sup>235</sup>U enrichment were exposed to very high doses of gamma rays and neutrons. During the Bialystok accident, five patients with breast cancer undergoing radiotherapy were exposed to a single dose of electrons which reached about 100 Gy. In the present paper the approaches chosen to estimate, by cytogenetic methods, the doses absorbed by the people involved in the accidents are described.

Copyright © 2003 S. Karger AG, Basel

The health consequences of an overexposure to ionising radiation are proportional to the absorbed dose. Therefore, in order to predict the consequences of an accidental overexposure and to choose the right medical treatment, it is necessary to estimate the dose and patient's response (Ricks et al., 2002). When the circumstances of the exposure and the characteristics of the radiation source are well known, it is possible to calculate or measure the dose by physical methods. However, such a possibility often does not exist. In such situations the absorbed dose must be estimated on the basis of the biological effect induced by radiation (Müller and Streffer, 1991). Today, the most specific and most sensitive technique of biological dosim-

etry relies on estimating the frequency of chromosomal aberrations in peripheral blood lymphocytes of the exposed person (IAEA, 2001; Voisin et al., 2002). Numerous studies, performed both on animals and humans, have demonstrated a close correspondence between aberrations induced in peripheral blood lymphocytes under *in vitro* and *in vivo* conditions. This allows a radiation dose absorbed during an accident to be estimated by reference to an *in vitro* calibration curve. Because the aberration frequency varies with the type of radiation and the dose rate, knowledge of exposure conditions improves the precision of dose estimation.

The specificity of dose estimate is given by the low spontaneous dicentric rate which, in a normal population, is around one per 1000 lymphocytes (IAEA, 2001). The precision thus depends on the number of cells scored and allows the assessment of very low dose levels, in the order of 0.01–0.02 Gy. The upper limits substantially exceed the threshold lethal dose to humans.

The highest precision of the dose estimate is achieved in cases of acute, whole body exposures, when the dose does not exceed about 3–4 Gy. Higher doses will inhibit the capacity of

Received 17 September 2003; manuscript accepted 8 December 2003.

Request reprints from Andrzej Wojcik, PhD, DSc  
Department of Radiation Biology and Health Protection  
Institute of Nuclear Chemistry and Technology  
ul. Dorodna 16, 03-195 Warszawa (Poland)  
telephone: +4822 811 07 36; fax: +4822 811 13 32  
e-mail: awojcik@ichtj.waw.pl

**Table 1.** Numbers and, in brackets, frequencies per cell, of unstable chromosomal aberrations in lymphocytes of four Georgian frontier guards. The u test was applied to estimate the homogeneity of exposure (significant overdispersion with  $u > 1.96$  and underdispersion with  $u < 1.96$ ). The names of the hospitals where patients were treated in France are given in brackets.

Patient	Scored cells	Dic <sup>a</sup>	Rc <sup>a</sup>	Ace <sup>a</sup>	Dicentric distribution					u-test
					0	1	2	3	4	
AN (Curie)	502	55 (0.11)	4 (0.008)	24 (0.048)	456	39	5	2	0	4.68
EP (Curie)	518	80 (0.15)	4 (0.008)	25 (0.048)	453	50	15	0	0	3.61
CG (Percy)	500	19 (0.04)	1 (0.002)	15 (0.030)	481	19	0	0	0	-0.59
TK (Percy)	500	14 (0.03)	0 (0.000)	11 (0.022)	486	14	0	0	0	-0.43

<sup>a</sup> Dic: dicentrics, Ace: acentric fragments, Rc: centric rings.

lymphocytes to divide, which may lead to an underestimation of the yield of aberrations and, consequently, of the dose assessment. In cases of partial body exposure a certain fraction of the analysed lymphocytes will have been outside the irradiated field. During cytogenetic analysis these undamaged cells will “dilute” the yield of aberrations, leading to an underestimation of dose. A further factor confounding the precision of dose estimation is a delay between exposure and blood sampling. Due to repopulation processes, the number of exposed peripheral blood lymphocytes will decline with time, resulting in a reduced aberration frequency. Although several methods have been developed which account for the mentioned confounders and allow correction of the aberration frequency (Sasaki, 1983; IAEA, 2001), their application must still be validated.

In recent years three radiation accidents occurred, where the irradiation or sampling conditions precluded an estimation of the dose simply by referring to an in vitro calibration curve. During the Georgian accident, unaware soldiers carried in their pockets small sources of <sup>137</sup>Cs leading to partial and protracted body exposures. During the Tokai-mura accident, three employees involved in the process of <sup>235</sup>U enrichment were exposed to doses of gamma rays and neutrons reaching over 20 GyEq (equivalent to 1.9 MeV X-rays) of average whole body dose. Finally, during the Bialystok accident, five patients with breast cancer undergoing radiotherapy were exposed to a single, localised dose of electrons which reached about 100 Gy.

The aim of the present paper is to summarise the approaches chosen to estimate, by cytogenetic methods of biological dosimetry, the doses absorbed by the people involved in the accidents.

## The Georgian accident

### *Circumstances of the accident*

Eleven young frontier guards were exposed to one or several sources of <sup>137</sup>Cs not exceeding 150 GBq at the Lilo military training center 20 km to the east of Tbilisi. The sources were intended for training and for calibration purposes. They are normally mounted on a source holder and stored in containers. Nine of the eleven sources were found outside the containers. The victims were irradiated for approximately one year, from mid 1996 to April 1997. A recruit showed first symptoms of

fever and reactions on the skin of his abdomen on 2 July 1996. The diagnosis was completed at the end of August, 1997 (IAEA, 2000).

From the eleven victims involved in this accident, seven were sent to the Armed Forces Hospital at Ulm (Germany) and the four most exposed people were sent to France: two were treated at the Burns Treatment Centre at the Percy Hospital and two at the Curie Institute. The circumstances of exposure were reconstructed with some uncertainties. First, a container seemed to have been opened by patient AN, but the source remained in the sourceholder for some time. Then the source was found by another guard and placed in the pocket of EP's coat. The coat was borrowed regularly leading to irradiation of other persons. TK and CG shared the same room with AN and EP and used the coat to cover their beds during the night.

All four patients treated in France suffered from lymphopenia and nausea. AN suffered from contractures affecting the hands and lesions on the abdomen. TK displayed a deep lesion on the right thigh. EP displayed 33 patches on the trunk and the thighs. CG showed lesions on the hands and thighs (IAEA, 2000).

### *Results of dicentric observation*

For the four guards hospitalized in France, blood samples were collected in November, 1997. The results of cytogenetic analysis are shown in Table 1.

For the patients with more damaged cells (AN and EP), there is a strong proportion (13 and 14%) of cells with dicentrics without an accompanying acentric. This percentage is abnormally high for acute irradiation and may be explained by the fact that during cellular division, dicentrics have a 50% chance of passing from the mother cell to one of the two daughter cells. The accompanying acentric fragments, on the other hand, may be lost during the division. This suggests that an exposure of relatively low intensity took place, either continuously or at repeated intervals for several days, weeks, or months, during which partial replenishment occurred.

### *Acute dose estimate*

Dicentrics plus rings were referred to an in vitro calibration curve produced with <sup>60</sup>Co at a dose rate of 0.5 Gy·min<sup>-1</sup>. The first level of dose estimate was based on the assumption that the patients underwent a homogeneous total body irradiation (Ta-

**Table 2.** Comparison of dose estimates assuming an acute, homogeneous exposure (acute dose), a heterogeneous exposure (Dolphin and Qdr) and a protracted, homogeneous exposure (Function G). In cases of the heterogeneous exposures the doses are given for the exposed fraction of lymphocytes. The acute doses and protracted doses are given with 95 % confidence intervals.

Patient	Acute dose (Gy)	Dolphin (Gy)	Percent of lymphocytes irradiated	Qdr (Gy)	Function G (Gy)
AN	1.2 ± 0.2	2.3	0.40	2.8	3.1 ± 0.8
EP	1.6 ± 0.3	2.5	0.50	3.4	4.3 ± 1.0
CG	0.7 ± 0.2	–	–	–	1.0 ± 0.5
TK	0.5 ± 0.2	–	–	–	0.7 ± 0.4

ble 2). When irradiation is homogeneous, the distribution of chromosomal aberrations is Poisson (Edwards, 1994; IAEA, 2001). For CG and TK, the physical dose reconstruction suggested a strongly localized irradiation. Surprisingly, however, the distribution of dicentric per cell did not deviate from Poisson ( $u < 1.96$ , Table 1). It is possible that highly damaged cells were lost and only lymphocytes containing a single aberration remained. Alternatively, the exposure dose rates could have been low, simulating a homogenous whole body exposure due to lymphocyte circulation. Therefore, the doses calculated considering an acute homogeneous exposure are far below the dose estimate of AN and EP (Table 2). In AN and EP the aberration distributions were overdispersed ( $u > 1.96$ ) suggesting a partial-body exposure (Table 1). This is consistent with the circumstances of exposure as reconstructed by physical dosimetry: the source remained in close contact with their bodies leading to high dose-rate exposures.

All four patients probably suffered from lymphopenia before their arrival in France. Consequently, the integrated whole-body dose equivalent may be an underestimation of the received dose.

For these two people, the source remained many minutes/hours in close contact with their body. Therefore dose heterogeneity was detected and is probably the main contribution to the total dose received.

#### *Heterogeneous dose estimate*

For cases of heterogeneous irradiation, two mathematical methods have been developed to better assess the initial dose received by the irradiated body part (IAEA, 2001). Both methods rely on Poisson statistics. The method proposed by Dolphin allows one to calculate not only the dose but also the irradiated fraction of the body. It requires a sufficiently high local dose so that there are enough cells with two or more dicentric chromosomes. The second method was proposed by Sasaki (1983) and is known as Qdr. It is based on the analysis of cells containing dicentric chromosomes, rings and excess acentric fragments. Therefore, the presence of cells with many dicentrics is not necessary. However, it provides no information about the percentage of the body exposed.

Neither method can be used when there are no cells with more than one aberration. Therefore, it was only possible to apply them to patients AN and EP.

*Dose estimate by Dolphin's method.* AN: Based on 55 dicentrics found in 502 cells it was calculated that the absorbed dose for the irradiated fraction of the body was 2.3 Gy. Assuming that 30 % of lymphocytes survive or can reach mitosis at 4 Gy, it was assessed that 40 % of the body was exposed (see IAEA, 2001 for details of calculation).

EP: Based on 80 dicentrics for 518 cells examined, it was determined that the absorbed dose for the irradiated fraction of the body was 2.5 Gy. Again the assumption was made that 30 % of the lymphocytes could reach mitosis after 4 Gy. It was estimated that 50 % of the body was irradiated.

*Dose estimate by the Qdr method.* AN: Considering 55 dicentrics for 65 cells that contained dicentrics, centric rings or acentrics, the absorbed dose for the irradiated part of the body was 2.8 Gy.

EP: Considering 80 dicentrics for 80 cells that contained dicentrics, centric rings or fragments, the absorbed dose for the irradiated part of the body was 3.4 Gy.

The dose estimates using these mathematical methods reflect the doses received by the exposed lymphocytes of the patients. The dose estimate by Qdr is twice the dose estimate assuming an acute exposure, the Dolphin approach being in-between the two others (Table 2). The calculations reveal that a high percentage of lymphocytes were exposed. This is in agreement with the symptoms of AN who had 33 burn patches all over his body suggesting a high percentage of exposed lymphocytes.

#### *Protracted dose estimate*

The exposures probably lasted from mid 1996 to April 1997. In cases of such protracted exposures the dose estimate can be corrected with the help of the G function (IAEA, 2001).

The calibration curve usually used to define the absorbed dose as a function of the frequency of unstable chromosomal aberrations is described by the equation  $Y = \alpha D + \beta D^2$ , where  $Y$  = the frequency of dicentrics,  $D$  the dose, and  $\alpha$  and  $\beta$  the fitted yield coefficients. The  $\alpha$  coefficient represents lesions created by a single hit event of ionizing radiation and the  $\beta$  coefficient is related to lesions from two (or additive) hits. In cases of chronic irradiation the  $\beta$  coefficient is strongly reduced due to DNA repair. This results in a chromosomal aberration number below the expected number for an acute irradiation. To simulate this fact experimentally, a new  $\beta$  coefficient  $G$  is

added to the parameter, reducing it to 0 when the DNA repair time exceeds the irradiation time ( $\geq 6$  h). The dose-effect curve becomes  $Y = \alpha D + (G_x)\beta D^2$ , where  $x = t/t_0$  with  $t$  being the time over which the radiation occurred and  $t_0$  the mean lifetime of breaks (see IAEA, 2001 for the exact definition of  $G$ ).

By applying this approach the dose estimates were calculated and the results are presented in Table 2. The  $G$  function dose estimate is higher than the Qdr dose estimate for AN and EP. For these two patients, the increase between the acute dose estimate and the chronic one is more pronounced than for the two other patients. This could reflect the biological effect of the chronic exposure.

For some of the victims the dose was also estimated by electron paramagnetic resonance (IAEA, 2000). The doses estimated by the  $G$  function were closest to the EPR estimates. This indicates that the protracted effect of exposure in this accident was more pronounced than that of partial-body exposure.

## The Tokai-mura accident

### *Overview of the criticality accident and acute radiation syndrome*

It was in the morning of September 30, 1999, that the criticality accident occurred at the uranium conversion test plant of JCO Co. Ltd. in Tokai-mura located 115 km northeast from the center of Tokyo. Three workers (A, B and C, according to the order of the dose received) were severely exposed to neutrons and gamma rays. The criticality chain reaction started when B was pouring uranyl nitrate solution into a tank through a peep-hole, while A who was standing beside the tank supported the funnel that was inserted into that hole. C, the supervisor, was in the next room. They witnessed a blue flash of light caused by the reaction and in response to an alarm siren for the detection of gamma rays, they immediately left the area. Five to eight minutes later, A developed nausea and vomiting and lost consciousness with cramping for 10 to 20 seconds (Akashi et al., 2001). He had diarrhoea within 10 minutes. His body temperature became high ( $38.5^\circ\text{C}$ ) on the day of accident. B felt a tingling in the neck, chest, arms and hands and numbness in the fingers at the time of accident. He also developed nausea and vomiting within one hour. C became nauseated a few hours after the accident but did not vomit. The three men were first taken to the National Mito Hospital in that region and then transferred by a helicopter and ambulance cars to the National Institute of Radiological Sciences at about 15:30, five hours after the accident.

### *Technical breakthrough in biodosimetry for the unprecedented high-dose exposures*

Blood for dose estimation by chromosome analyses was taken from the three victims three times; 9, 23, and 48 h after the accident. Peripheral lymphocyte numbers in A, B and C were already very low, 1.9, 2.1 and 15% (normal value: 25–48%) when the 9-hour samples were taken. The fall continued and in A and B reached zero on the third and seventh day respectively. In addition, because of the cell cycle arrest caused by high dose radiation exposure, it was difficult to obtain enough mitotic

cells for scoring chromosome aberrations by the ordinary method. Therefore, chromosome preparations were made according to two modified methods developed by the biodosimetry laboratory of NIRS, that is, a high yield chromosome preparation method (Hayata et al., 1992) and a phosphate inhibitor (Okadaic acid) induced prematurely condensed ring chromosome (PCC-ring) scoring method which had been developed one year before the accident (Kanda et al., 1999). The former processing method made it possible to recover enough lymphocytes even from the 48-hour sample of A. The latter scoring method provided more cells for scoring and made it possible to estimate approximate doses for all three victims with just one hour of microscopic work, proving that the method is good for providing a rapid initial dose estimation.

Dose estimation by PCC-ring scoring was done by reference to the observed yields of PCC-rings induced by in vitro 200 kV X-rays in the Kanda et al. (1999) experiment. The estimation based on dicentric and rings in C, who had been least irradiated, was made according to the standard method outlined in IAEA Technical Reports Series No. 405 (2001), based on the equation for calculating  $^{60}\text{Co}$  gamma rays:  $Y = (2.31 \pm 0.88) \times 10^{-2} D + (6.33 \pm 0.25) \times 10^{-2} D^2$ . For cases A and B the doses were higher than can be estimated with this formula, which is applicable in the dose range below 6 Gy. Therefore, estimates were made by a direct comparison of the observed frequencies with those obtained in a study of 1.9 MeV X-rays (Norman and Sasaki, 1966).

The results are summarized in Table 3. In each case there was no statistically significant difference in the frequencies of chromosome aberrations between the samples obtained at the three times after the accident. The precise dose estimation by dicentric and rings was made from the combined data from the three samples in each case. As shown in Table 1, the rapidly obtained dose estimation with the samples obtained at 9 h using PCC-rings were in good agreement with those made using dicentric or dicentric plus rings.

Physically estimated doses for A, B and C were obtained from measurements of  $^{24}\text{Na}$  (sodium) and stable Na and a computer simulation analysis of the ratios between neutrons and gamma rays. They were 17–24, 8.7–13 and 2.5–3.6 GyEq with the assumption that the RBE for the neutron is 1.5–2.0 (Ishigure et al., 2001). Those values agreed reasonably with the biologically estimated doses.

### *Low-dose exposure off the site*

In addition to the three workers mentioned above, chromosomes of 43 people comprising seven nearby residents having unusually low lymphocyte counts, three firemen, seven employees working at a nearby company, and 26 employees of JCO Co. Ltd. were examined. Physically estimated doses were available except for those of the seven local residents. In total 67,879 cells (an average of 1,579 cells per case) were analyzed in a collaboration of five laboratories in Japan (Sasaki et al., 2001). After subtracting the age-dependent background frequencies for the Japanese and that for the patients with aplastic anemia it was possible to detect the increase of chromosomal aberrations in 18 people. In 14 cases among them, physically estimated dose was less than 20 mSv.

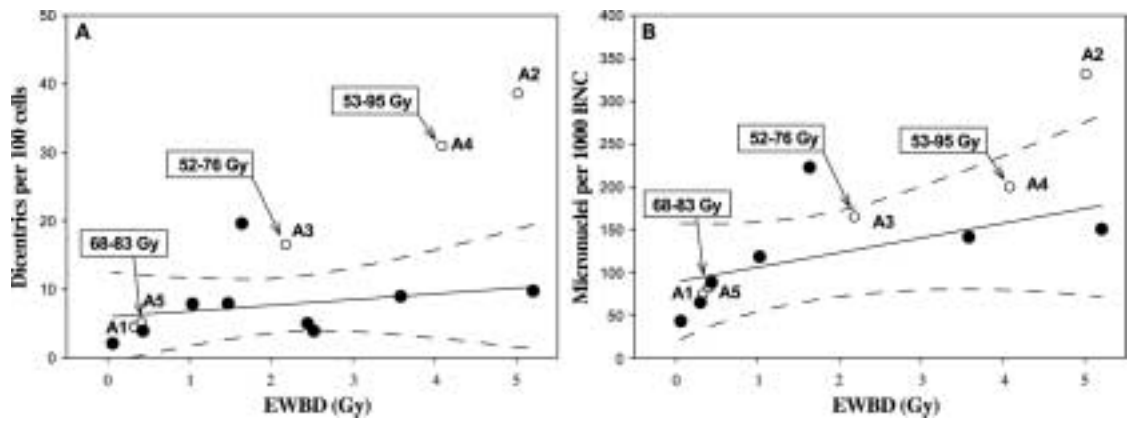


**Fig. 1.** Frequencies of dicentrics (A) and micronuclei (B) plotted against the equivalent whole body doses (EWBD) received by the patients during regular radiotherapy. White symbols represent the accident patients. The values observed in control patients (black symbols) were fitted linearly (solid line). Dashed lines represent the 95% confidence intervals. The doses shown for patients A3, A4 and A5 are the accident doses as estimated by EPR. The accident doses received by patients A1 and A2 are not known but, judged on the basis of late skin reactions, were lower than for the other patients. Data from Wojcik et al. (2003).

**Table 3.** Frequencies of chromosome aberrations in lymphocytes and estimated doses in the three patients after the Tokai-mura accident (data from Hayata et al., 2001)

Worker	Aberrations <sup>a</sup>	9-hour	23-hour	48-hour	Total	Dose in GyEq <sup>b</sup>
A	PCC-ring	150/100	—	—	150/100	>20
	Dic	445/50	197/20	73/8	715/78	22.6 (15.0→30)
	Dic+R	563/50	250/20	90/8	903/78	24.5 (16.0→30)
B	PCC-ring	77/100	—	—	77/100	7.4 (6.5–8.2)
	Dic	199/75	127/50	153/50	479/175	8.3 (6.9–9.8)
	Dic+Rc	224/75	147/50	166/50	537/175	8.3 (6.9–10.0)
C	PCC-ring	24/100	—	—	24/100	2.3 (1.8–2.8)
	Dic+Rc	63/100	64/100	64/100	191/300	3.0 (2.8–3.2)

<sup>a</sup> PCC-ring: prematurely condensed ring chromosome, Dic: dicentrics, R: centric and acentric rings, Rc: centric rings.

<sup>b</sup> GyEq: Dose in Gy equivalent to X or gamma ray dose.

### The Bialystok accident

In February 2001 a radiation accident occurred in a radiotherapy unit of an oncology hospital in Bialystok, Poland. Due to a malfunction of an accelerator, five breast cancer patients received a single, high dose of 8-MeV electrons. The patients were at different stages of therapy and had already received different tumor doses of both electrons and <sup>60</sup>Co gamma radiation. The exact doses received during the accident are not known. However, based on the early and late skin reactions and a measurement performed by a medical physicist immediately after the accident, the exposures were heterogeneous and may have reached 100 Gy. In three patients (A3, A4 and A5; see Fig. 1) the doses received by the rib bones could be assessed by electron paramagnetic resonance (EPR) analysis and the dose estimated by the medical physicist was confirmed (IAEA, 2004).

In order to assess whether such exposure would be detectable in peripheral blood lymphocytes, chromosomal aberrations and micronuclei were analysed in lymphocytes of the accident patients (Wojcik et al., 2003). It was shown previously that the dose-response curve of aberrations in lymphocytes of patients undergoing radiotherapy has different characteristics

than an in vitro calibration curve (Urbanik et al., 2003). Due to this and to the fact that the exposed parts of the patient bodies were very small (between 77 and 221 cm<sup>2</sup>) an estimation of the accident doses on the basis of a standard, in vitro calibration curve was not possible. Therefore, it was decided to compare the aberration and micronucleus frequencies observed in lymphocytes of the accident patients to those in breast cancer patients not involved in the accident, but who had received similar radiotherapy treatments. The frequencies of aberrations and micronuclei were plotted against the equivalent whole body doses (EWBD) received during radiotherapy. The EWBD is the integral dose (total energy in joules) absorbed by the patients divided by their body mass. In the case of the accident patients, the EWBD values reflected the doses received prior to the accident. It could be expected that an excess of aberration and micronucleus frequencies in lymphocytes of the accident patients over the plotted dose-response curve of the control patients would be due to the accident dose.

Although a good agreement between the frequencies of aberrations (dicentrics) and micronuclei was observed, there was a better cut-off between the accident and control patients for dicentrics than for micronuclei (Fig. 1). The dicentric frequen-

cies of patients A2, A3 and A4 are significantly higher than of the control patients (with one exception). In the case of A3 and A4 this result is in accordance with the expectation, since both patients received high accident doses. However, this is not so for A2, who had the highest frequency of dicentric but received a lower accident dose than A3 (as judged by the extent of late skin reactions). Also the frequency of dicentric in lymphocytes of A5 did not match with the accident dose. We have reanalysed the frequencies of micronuclei in lymphocytes of A2 and A5 collected a second time in order to exclude the possibility that the blood specimens had been mixed up. The second analysis revealed that no mistake had occurred during the preparation of slides for the initial analysis.

At present, we have no clear explanation for the lack of correlation between the accident dose and the frequency of dicentric and micronuclei in lymphocytes of A2 and A5. A factor which could be responsible for the low frequency of damage in lymphocytes of A5 could be that she had a relatively large body mass (data not shown). 8-MeV electrons do not penetrate deeply into tissue ( $d_{\max} = 1.9$  cm), hence fat tissue could have acted as an absorber, shielding the blood flowing through the heart and lungs. The high frequency of damage in lymphocytes of A2 is difficult to explain. We have recently compared the in vitro sensitivity of lymphocytes of A2 and A5 to a dose of 2 Gy. Twice as many aberrations were observed in lymphocytes of A2 than A5. It should be mentioned, that A2 was at the end of her therapy and received, among all accident patients, the highest cumulative dose of photons. It is, therefore, possible that the high level of cytogenetic damage is a result of a very high radiosensitivity of her lymphocytes. A higher than expected frequency of dicentric and micronuclei was also observed in lymphocytes of one of the control patients. It has been observed by different authors that the frequencies of aberrations and micronuclei in lymphocytes of patients undergoing radiotherapy are

strongly variable between individuals (Obe et al., 1981; Diener et al., 1988). The reasons for this variability are not well understood. Apart from differences in individual, intrinsic radiosensitivity, they may result from differences in the proportion of lymphoid tissue in the exposed site, the kinetics of lymphocyte repopulation and the speed of blood flow through blood capillaries. Which of the factors might be responsible for the high level of cytogenetic damage in lymphocytes of A2 and the control patient is unclear. This variability precludes the unambiguous identification of the accident patients and may present a major problem in the application of biological dosimetry to accidents during radiotherapy.

## Conclusions

Biological dosimetry based on the analysis of chromosomal aberrations has been used for many years. In cases of whole body exposures, and when the time between exposure and analysis does not exceed several weeks, a precise dose estimation is possible. Frequently however, the exposure conditions are complicated or not exactly defined. As demonstrated by the results of the Georgian accident, protracted and partial body exposures can be accounted for by mathematical methods. In case of the Tokai-mura accident, the assessment of high doses which inhibited cell proliferation required the use of premature chromosome condensation. The Bialystok accident showed that the usefulness of biological dosimetry for assessment of absorbed doses in accidents during radiotherapy must still be validated.

Although the dose estimate is not always exact, biological dosimetry is frequently the only method applicable for dose reconstruction. Therefore, it will remain an extremely important tool in the management of radiation accidents.

## References

- AKASHI M, Hirama T, Tanosaki S, Kuroiwa N, Nakagawa K, Tsuji H, Kato H, Yamada S, Kamata T, Kinugasa T, Ariga H, Maekawa K, Suzuki G, Tsujii H: Initial symptoms of acute radiation syndrome in the JCO criticality accident in Tokai-mura. *J Radiat Res* 42 Suppl:S157–S166 (2001).
- DIENER A, Stephan G, Vogl T, Lissner J: The induction of chromosome aberrations during the course of radiation therapy for Morbus Hodgkin. *Radiat Res* 114:528–536 (1988).
- EDWARDS AA: Dosimetric and statistical aspects of cytogenetics, Reunion Internacional Sobre Dosimetria Biologica, pp 75–85 (Lisse, Madrid 1990).
- HAYATA I, Tabuchi H, Furukawa A, Okabe N, Yamamoto M, Sato K: Robot system for preparing lymphocyte chromosome. *J Radiat Res* 33 Suppl:S231–S241 (1992).
- HAYATA I, Kanda R, Minamihisamatsu M, Furukawa M, Sasaki MS: Cytogenetic dose estimation for 3 severely exposed patients in the JCO criticality accident in Tokai-mura. *J Radiat Res* 42 (Suppl): S149–S155 (2001).
- IAEA: The radiological accident in Lilo (International Atomic Energy Agency, Vienna 2000).
- IAEA: Cytogenetic analysis for radiation dose assessment. A Manual. Technical reports series No. 405 (International Atomic Energy Agency, Vienna 2001).
- IAEA: Accidental overexposure of radiotherapy patients in Bialystok (International Atomic Energy Agency, Vienna 2004).
- ISHIGURE N, Endo A, Yamaguchi Y, Kawachi K: Calculation of the absorbed dose for the overexposed patients at the JCO criticality accident in Tokai-mura. *J Radiat Res* 42 Suppl:S137–S148 (2001).
- KANDA R, Hayata I, Lloyd DC: Easy biodosimetry for high-dose radiation exposures using drug-induced, prematurely condensed chromosomes. *Int J Radiat Biol* 75:441–446 (1999).
- MÜLLER W-U, Streffer C: Biological indicators for radiation damage. *Int J Radiat Biol* 59:863–873 (1991).
- NORMAN A, Sasaki MS: Chromosome-exchange aberrations in human lymphocytes. *Int J Radiat Biol* 11:321–328 (1966).
- OBE G, Matthiessen W, Göbel D: Chromosomal aberrations in peripheral lymphocytes of cancer patients treated with high-energy electrons and bleomycin. *Mutat Res* 81:133–141 (1981).
- RICKS RC, Berger ME, O'Hara M Jr: The medical basis for radiation-accident preparedness (The Parthenon Publishing Group, Boca Raton 2002).
- SASAKI MS: Use of lymphocyte chromosome aberrations in biological dosimetry: possibilities and limitations, in Ishihara T, Sasaki MS (eds): Radiation-induced Chromosome Damage in Man, pp 585–604 (Alan R Liss, New York 1983).
- SASAKI MS, Hayata I, Kamada N, Kodama Y, Kodama S: Chromosome aberration analysis in persons exposed to low-level radiation from the JCO criticality accident in Tokai-mura. *J Radiat Res* 42 Suppl:S105–S116 (2001).
- URBANIK W, Kukolowicz P, Kuszewski T, Gozdz S, Wojcik A: Modelling the frequencies of chromosomal aberrations in peripheral lymphocytes of patients undergoing radiotherapy. *Nukleonika* 48:3–8 (2003).
- VOISIN P, Barquinero JF, Blakely B, Lindholm C, Lloyd D, Luccioni C, Miller S, Palitti F, Prasanna PG, Stephan G, Thierens H, Turai I, Wilkonson D, Wojcik A: Towards a standardization of biological dosimetry by cytogenetics. *Cell molec Biol (Noisy-le-grand)* 48:501–504 (2002).
- WOJCICK A, Stephan G, Sommer S, Buraczewska I, Kuszewski T, Wieczorek A, Gozdz S: Chromosomal aberrations and micronuclei in lymphocytes of breast cancer patients following an accident during radiotherapy with 8 MeV electrons. *Radiat Res* 160:677–683 (2003).

## Complex chromatid-isochromatid exchanges following irradiation with heavy ions?

B.D. Loucas,<sup>a</sup> R.L. Eberle,<sup>a</sup> M. Durante<sup>b</sup> and M.N. Cornforth<sup>a</sup>

<sup>a</sup>Department of Radiation Oncology, University of Texas Medical Branch, Galveston, TX (USA);

<sup>b</sup>Dipartimento di Scienze Fisiche, Università Federico II, Napoli (Italy)

**Abstract.** We describe a peculiar and relatively rare type of chromosomal rearrangement induced in human peripheral lymphocytes that were ostensibly irradiated in G<sub>0</sub> phase of the cell cycle by accelerated heavy ions, and which, to the best of our knowledge, have not been previously described. The novel rearrangements which were detected using mFISH following exposure to 500 MeV/nucleon and 5 GeV/n <sup>56</sup>Fe particles, but

were not induced by either <sup>137</sup>Cs gamma rays or <sup>238</sup>Pu alpha particles, can alternatively be described as either complex chromatid-isochromatid or complex chromatid-chromosome exchanges. Different mechanisms potentially responsible for their formation are discussed.

Copyright © 2003 S. Karger AG, Basel

When normal repair-proficient mammalian cells are exposed to ionizing radiation (IR) in the G<sub>1</sub> or G<sub>0</sub> phases of the cell cycle, aberrations seen at the first postirradiation mitosis are exclusively of the chromosome type. Conversely, IR produces chromatid-type aberrations at the first mitosis following exposure during S or G<sub>2</sub> (Lea, 1946; Savage, 1976). This classic “nondelayed” or “S-independent” action is noteworthy, as it is shared by only a handful of clastogenic agents. The vast majority of clastogens instead operate by “delayed” or “S-dependent” action, producing chromatid-type damage in cells exposed in G<sub>1</sub> (Evans and Scott, 1969; Cornforth and Bedford, 1993). A notable exception to this rule occurs in various repair-deficient, radiosensitive cells, such as those from patients with mutations in the ATM gene, which cause the rare autosomal recessive disorder Ataxia Telangiectasia (AT) (Savitsky et al., 1995). Along with the usual assortment of chromosome-type aberrations, exposure of AT cells to IR during G<sub>1</sub> phase produces some chromatid damage as well (Taylor, 1978). Other examples

include the radiosensitive hamster mutants XRS-5 and XRS-6 (Darroudi and Natarajan, 1987), which harbor defects in the Ku-80 and Ku-70 subunits of the DNA-PK holoenzyme, respectively (Jeggo, 1998).

During DNA synthesis, chromosomes contain both unrepliated and replicated regions, so one might expect to frequently observe cells containing a mixture of chromosome- and chromatid-type aberrations resulting from IR exposure in, for example, mid S. In actuality, the transition from chromosome- to chromatid-type damage is substantially more abrupt than one might predict, and cells with such mixed damage are not common. However, within a duplicated chromosomal region, IR exposure during S or G<sub>2</sub> can also produce breakage across both sister chromatids at approximately the same locus, presumably by the passage of a single charged particle track. In traditional Giemsa-stained preparations, such isochromatid damage is observed as sister unions, involving proximal and/or distal rejoining of breaks between sister chromatids. Less commonly observed in S- or G<sub>2</sub>-irradiated cells are interchromosomal interactions (rejoinings) between chromatid and isochromatid breakage which express themselves as “triradial” exchanges (Savage, 1989).

Prior to the advent of whole chromosome painting by fluorescence in situ hybridization (FISH) (Pinkel et al., 1986, 1988), most of all radiation-induced exchanges were thought to be simple, involving the rejoining of broken chromosome ends produced by a pair of radiogenic lesions. It was subsequently shown that a substantial number of exchanges that appeared to

Supported by the Office of Science (BER), U.S. Department of Energy, Grant No. DE-FG03-02ER63442 and the National Aeronautical and Space Administration Office of Biological and Physical Research (NASA/OBPR).

Received 10 September 2003; manuscript accepted 17 November 2003.

Request reprints from Michael Cornforth, Department of Radiation Oncology  
University of Texas Medical Branch, 301 University Blvd.  
Galveston, Texas 77555-0656 (USA); telephone: 409-772-4244  
fax: 409-772-3387; e-mail: mcornfor@utmb.edu

be simple by standard histological staining, were instead complex, requiring three or more breaks distributed among multiple chromosomes (Brown and Kovacs, 1993). But because such FISH techniques typically involved the painting of only a few homologous chromosome pairs – with the remainder of the genome being counterstained a single contrasting color – they still often produced staining patterns among rearranged chromosomes of a complex exchange that were indistinguishable from that produced by a simple exchange (pseudosimple exchanges) (Savage and Simpson, 1994a, b). Moreover, even when complex aberrations could be unambiguously identified as such, these approaches tended to underestimate the number of exchange breakpoints that had actually occurred. To a large extent such problems are circumvented through the use of newer combinatorial painting techniques such as mFISH (Speicher et al., 1996), which allows each homologous chromosome pair to be rendered a unique color.

Various studies have shown that high LET radiations are far more effective per unit dose in producing complex aberrations than are X- or gamma rays, an observation that has led to their proposed use as a biomarker of past exposure to densely ionizing radiations (Griffin et al., 1995; Grigorova et al., 1998; Anderson et al., 2000). We set out to determine whether marked differences in track structure between two types of high LET radiations – accelerated HZE ions from  $^{56}\text{Fe}$  versus alpha-particles from  $^{238}\text{Pu}$  – would manifest themselves in the spectra of aberrations observed in normal human cells, as analyzed by 24-color mFISH. During these ongoing studies we occasionally observed a peculiar class of chromosomal rearrangement in cells exposed to  $^{56}\text{Fe}$  ions, but which we have never seen following exposure to gamma rays or alpha particles. The purpose of this paper is to characterize these unusual rearrangements, and to discuss possible mechanisms underlying their formation.

## Materials and methods

Peripheral blood was obtained from healthy donors by venous puncture, and the lymphocytes contained therein were cultured in 25-cm<sup>2</sup> tissue culture flasks containing 5 ml RPMI 1640 medium supplemented with 20% fetal bovine serum. Cultures were irradiated with graded doses of 500 MeV/n (200 keV/ $\mu\text{m}$ , Chiba), 1 GeV/n (147 keV/ $\mu\text{m}$ , Brookhaven) or 5 GeV/n (145 keV/ $\mu\text{m}$ , Brookhaven)  $^{56}\text{Fe}$  ions. After irradiation, cultures were stimulated with PHA (2% final concentration) and allowed to grow for 46 h before Colcemid (0.2  $\mu\text{g}/\text{ml}$  final concentration) was added 2 h prior to the harvest of mitotic cells. In some cases Calyculin (50 mM final concentration) was added to colcemid-blocked cultures 45 min before harvest in order to induce prematurely condensed G<sub>2</sub> phase chromosomes (PCC) (Durante et al., 2002). Consequently, chromosome spreads that resulted from such a treatment represent a mixture of G<sub>2</sub> PCC and mitotic chromosomes. At harvest cells were fixed in 3:1 methanol to acetic acid by standard cytogenetic procedures.

Fixed cells were transported to the University of Texas at Galveston where they were spread onto glass slides for subsequent processing and analysis by multiplex fluorescence in situ hybridization (mFISH) following procedures standardized in our laboratory (Loucas and Cornforth, 2001). Briefly, slides were prepared by treatments with acetone, RNase A, proteinase K, before fixation in 3.7% formaldehyde. Following dehydration in ethanol, chromosomes were denatured in 70% formamide in 2 $\times$  SSC at 72°C for 2 min. Following dehydration again in ethanol, 10  $\mu\text{l}$  of denatured Spectra Vision (Vysis) 24-Color mFISH Assay probe mixture was applied to each slide and covered with a 22  $\times$  22-mm glass coverslip which was then sealed in place with rubber cement. The slides were placed in a 37°C incubator where hybridization was allowed to proceed for about 48 h. Following hybridiza-

**Table 1.** Chromosome-type and complex chromatid-isochromatid-type exchanges in human peripheral lymphocytes exposed to  $^{56}\text{Fe}$  ions.

Particle energy	Type of analysis	Donor code	Dose (Gy)	Number of cells	Chromosome exchanges	Chromatid-isochromatid
0.5 GeV/n	Calyculin	A	0.0	98	2	0
	Calyculin	B	0.8	262	231	0
	Calyculin	A	1.0	145	91	1
	Colcemid	B	0.4	210	27	0
	Colcemid	A	0.8	100	36	0
	Colcemid	A	1.0	145	63	4
1 GeV/n	Calyculin	C	0.2	191	32	0
	Calyculin	C	1.0	190	154	0
5 GeV/n	Calyculin	X	1.0	96	119	0
	Colcemid	X	0.75	93	53	1

tion, slides were washed in IGEPAL (0.3%; Rhone-Poulenc Inc.) in 0.4 $\times$  SSC at 72°C for 2 min, followed by a second wash in 0.1% IGEPAL in 2 $\times$  SSC for 30 s at room temperature.

Mitotic spreads were analyzed and mFISH karyotypes were constructed using a Zeiss Axiophot microscope equipped for epifluorescence and fitted with a special slider holding excitor-barrier filters set combinations appropriate for the fluorochromes of the SpectraVision probe cocktail (Vysis). Digital images were collected using a SensSys A2S black and white CCD camera (Photometrics). PowerGene image analysis software (Applied Imaging Inc.) was used to assemble pseudocolored constructs from the black and white images, giving a specific color to each homologous chromosome pair from which karyotypes could then be constructed.

## Results and discussion

Table 1 gives an overview of aberration types found in HPL at the first postirradiation mitosis after being exposed to various energies of accelerated  $^{56}\text{Fe}$  ions. As expected for unstimulated cultures that were exposed to IR during G<sub>0</sub> phase, the vast majority of aberrations were of the chromosome type. These included both simple and complex exchanges which, for the purpose of this report, are not broken down. Also listed are the aforementioned novel rearrangements that are the focus of this paper, and which are provisionally described as complex “chromatid-isochromatid” exchanges. Considered with respect to all donors, particle energies and doses, these aberrations are rather rare, contributing less than one percent to the total aberrations observed. The highest frequency occurred in a particular donor exposed to 1 Gy of 500 MeV/n particles, representing 6% of the exchange aberrations, and about 10% of the damaged cells. Figure 1 shows a particularly vivid example of such an exchange that involves several chromosomes, which can be most easily appreciated in the accompanying schematic. Typical of chromatid-type exchanges in general, there is a relatively high degree of apparent incompleteness. Note that the rearrangement contains elements of chromatid-type breakage and rejoining, as well as “isolocus” breakage and rejoining affecting both sister chromatids. Perhaps the most interesting feature of the rearrangement is that types of damage are seen to interact with one another. As evident from the schematic, this particular exchange involves both homologues of chromosomes 5 and 14. The significance of this observation, if any, is not clear. Since



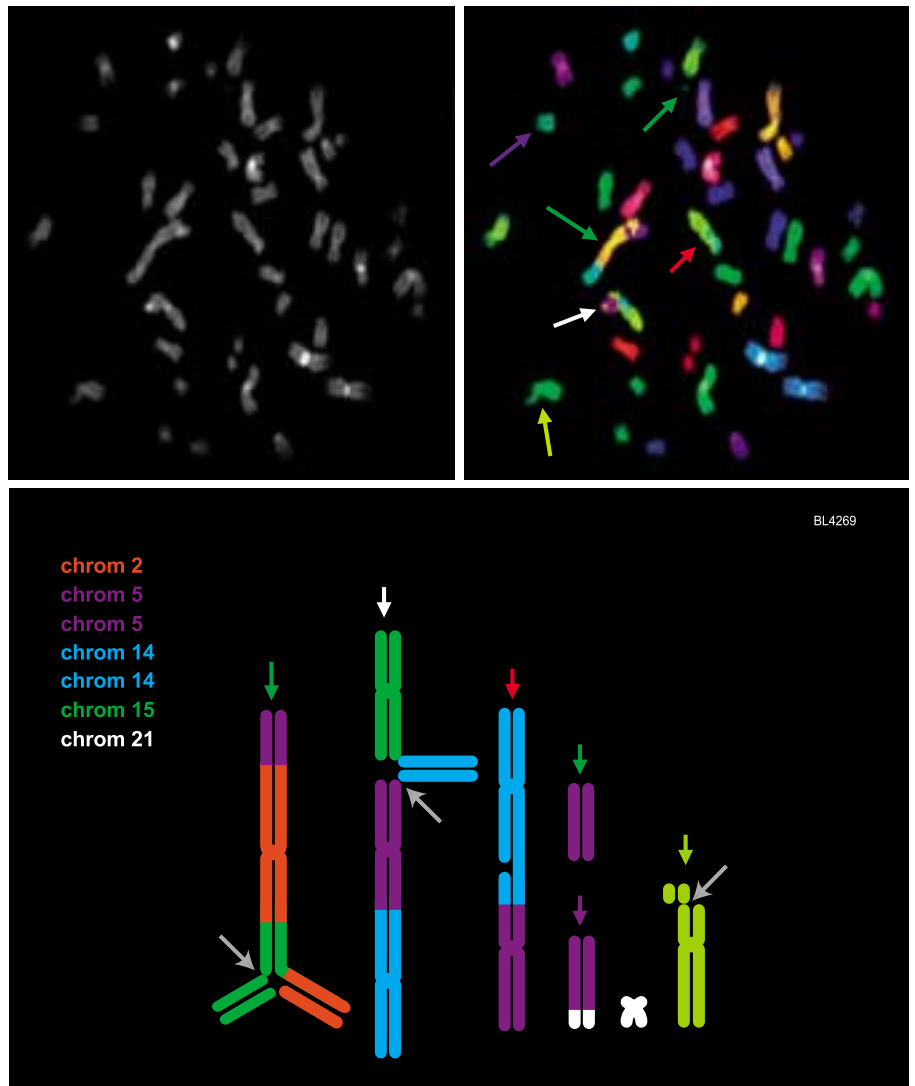


**Fig. 1.** An example of complex chromatid-isochromatid damage in a human lymphocyte following exposure to 1 Gy of 500 MeV/n  $^{56}\text{Fe}$  ions. **(Left panel)** Black and white DAPI image of a metaphase spread. **(Right panel)** 24-color mFISH rendition of the same cell. Elements of the exchange (colored arrows) are not easily discernable largely because the image capture software limits resolution to 72 dpi. **(Bottom panel)** schematic representation of exchange elements found within the cell. Colored arrows correspond to those in the right panel. Because two pairs of homologues are affected in this particular spread, it becomes difficult to determine whether all seven chromosomes are part of one large complex exchange, or whether the rejoinings represent two smaller complex exchanges instead. The rightmost chromosome showing isolocus breakage is apparently not involved. Grey arrows indicate instances where there is uncertainty as to whether complete rejoining has occurred. Diagram is not to scale and chromosome colors do not necessarily correspond to those of the actual mFISH image.

none of the other cells with these types of rearrangements showed any homologue involvement, we are inclined to consider this merely a statistical oddity.

Instances of these novel chromatid-isochromatid complex exchanges were largely limited to a single dose (1 Gy), energy (500 MeV/n) and donor (both Colcemid- and Calyculin-blocked cultures). For that reason we cannot formally rule out the possibility that the effect was somehow peculiar to the donor(s) in question, for example, as regards the aforementioned possibility of some cells being in either S or G<sub>2</sub> at the time of irradiation. It is conceivable that an individual may, for one reason or another, harbor a large cohort of cycling cells in the peripheral blood compartment, although explanations that come easily to mind – lymphocytic preblast crisis or systemic infection? – seem inconsistent with the overall health of the subjects used in this study. As to why 500 MeV/n particles look to be more effective than higher energy ions at inducing this type of exchange, we can only say the track structure of this particular radiation is apparently optimal for producing them. We were somewhat surprised that the aberrations in question

were less frequently found in Calyculin-blocked cultures – as compared to those blocked, more conventionally, with colcemid – especially since Calyculin-induced G<sub>2</sub>/M preparations have been shown to reveal additional chromosome damage from high LET radiations in cells that do not reach mitosis (Durante et al., 1999). A distinct possibility is that unequivocal detection is made more difficult by the compromised morphology that the chromosomes of Calyculin-treated cultures often show.

At issue, as regards the mechanism underlying the formation of such aberrations, is the source of the isolocus breakage and rejoining. When found in a cell also containing chromatid-type damage, it might normally be considered isochromatid in nature, wherein a single charged particle track is assumed to have broken, at approximately the same locus, both sister chromatids of a G<sub>2</sub> chromosome, or of an S-phase chromosome within a region that has already duplicated. True chromatid-isochromatid break interactions such as triradials, while less common than the chromatid-chromatid interchanges that lead to the formation of quadriradials, are nevertheless well documented. This interpretation, if correct, extends chromatid-

isochromatid rejoins to include multiple chromosomes, as exemplified by the ostensible rejoins among the acentric fragment of chromosome 14 and the centric fragments of both chromosomes 15 and 5. Note also the copious isochromatid-isochromatid interchanges that such a mechanism would imply, as for example in Fig. 1: between chromosomes (2'-5), between (5'-14'), and between (5-21) (mPAINT nomenclature; Cornforth, 2001). Classical cytogenetic theory would not necessarily disallow such rejoins. A half century ago Catcheside et al. (1946) reported instances of isochromatid-isochromatid interactions in pollen tube cells of *Tradescantia* that were irradiated in G<sub>2</sub> phase of the cell cycle. Whereas these (rare) exchanges produced dicentric elements, invariably the accompanying acentric fragments – rather than rejoining with one another – each showed sister union, which is certainly not the situation for exchanges reported here. Moreover, the isolocus interactions in question here seem remarkably prevalent within an affected cell, reminiscent of chromosome-type interchanges formed following a G<sub>1</sub> phase exposure. We will return to this point later.

It should be mentioned that we intentionally irradiated lymphocyte cultures with <sup>137</sup>Cs gamma rays during S phase, in an attempt to produce complex chromatid-isochromatid exchanges. While this led to the production of chromatid gaps, breaks and common quadriradials, the novel exchanges were not observed; nor were they observed in either cycling or non-cycling human fibroblasts exposed to gamma rays, or in non-cycling human fibroblasts exposed to <sup>238</sup>Pu alpha particles (data not shown). Thus, irrespective of the issue of cell cycle status at the time of irradiation, it would appear that HZE particles are unique in their ability to produce in mammalian cells complex exchanges of the type under discussion. Let us assume, for example, that the exchanges in question are formed from an S/G<sub>2</sub> exposure, and thus are truly chromatid-isochromatid in nature. It seems intuitively obvious (though perhaps naively so) that individual HZE particle tracks stand a better chance of making isolocus breaks in both sister chromatids than virtually any experimentally relevant dose of low LET radiation.

As stated, cells containing both chromatid- and chromosome-type damage are occasionally found in the same cells when they are irradiated in early S phase (Savage and Bhunya, 1980), a consequence of the genome being composed of both replicated and unreplicated portions of chromosomes. Thus, the potential for chromatid-chromosome interactions exists in cells with such “mixed damage”, a mechanism some have argued is responsible for triradial formation (traditionally considered to be a chromatid-isochromatid exchange). While this would appear to provide an adequate explanation for the formation of aberrations like that of Fig. 1, it would require that a relatively high percentage of circulating lymphocytes be located precisely at that stage of the cell cycle. (Recall that 10% of the damaged cells from Donor A contained complex “chromatid-chromosome” exchanges following 1 Gy.)

In fact, there are reasons to be skeptical of the assumption that cells harboring aberrations of the type shown in Fig. 1 were in S phase at the time of irradiation. Granted, human cells are probably not the best experimental material in which to observe sister union, and this situation is made worse by the

lower resolution and compromised morphology that accompanies FISH, as opposed to routine brightfield microscopy on Giemsa-stained preparations. Still, with the high degree of (presumptive) isochromatid damage observed, it seems odd that no evidence of sister union formation was observed. Nor were any quadriradials found, typically the most common of chromatid interchanges. In addition, chromatid-isochromatid exchanges were essentially the only type of damage observed in the six cells under discussion. With the exception of the small isolocus lesion shown in the rightmost chromosome of Fig. 1, no collateral aberrations of either the chromatid or chromosome type were found. Finally, the experimental approach itself – exposure of unstimulated lymphocytes before addition of PHA – is, of course, specifically designed to insure that cells are in G<sub>0</sub> at the time of irradiation.

It seems at least plausible to us that cells harboring the exchanges in question might well, as experimentally intended, have been in G<sub>0</sub> at the time of irradiation. In this case the term “chromatid-chromosome” exchanges (rather than chromatid-isochromatid exchanges) would also apply. In order to explain the chromatid-type component of the rearrangement we make an analogy to the chromatid-type damage routinely found in IR-sensitive cells, such as AT, following G<sub>1</sub> or G<sub>0</sub> exposure. Whatever the biochemical nature of the initial lesion responsible for such damage, it is clearly not a DNA double strand break (dsb), since such damage would manifest itself as a chromosome-type aberration at mitosis. Instead, the initial lesion must affect one strand of DNA as, for example, an unrepaired single-strand break or, perhaps more likely, some type of base damage. IR produces these lesions in yields that outnumber dsb induction by an order of magnitude, and some investigators have long considered base damage as important in aberration formation (Preston, 1982). Such damage must be repaired with remarkable efficiency in normal cells – otherwise chromatid damage following a G<sub>0</sub>/G<sub>1</sub> exposure would be the norm – whereas some small subset of these persist in AT cells, later being converted to chromatid-type damage following the passage of S phase. We imagine that HZE radiation, owing to its unique type of track structure, is capable of producing some sort of “single-stranded” DNA lesion that the cell has difficulty in repairing, and which occasionally manifests itself as chromatid damage following a pre-replicative exposure, even in normal repair-proficient cells. Within the exchange, the *chromosome-type component* of damage would manifest itself in the usual way, exchanges being formed in G<sub>1</sub>. While most exchanges will be complete, some broken chromosome ends will fail to rejoin, leading to either terminal deletions or incomplete exchanges, a situation that may occur more frequently with HZE radiations than with either gamma rays or alpha particles. The broken ends remain throughout G<sub>1</sub> and into S phase, where they are duplicated as reactive chromosome breaks. These rejoin with the nascent chromatid damage that manifest themselves as breaks upon passage of the replication fork. That we have observed exchange aberrations of the type shown in Fig. 1 in cycling AT cells ostensibly irradiated in G<sub>1</sub> with gamma rays (unpublished data) offers some support for the idea.

Along a line of reasoning similar to the mechanism described above, we also considered the possibility that Donor A

may have previously been inadvertently exposed to any number of chemical clastogens that could later cause chromatid-type breakage in lymphocytes following PHA-induced entry in S phase. The rearrangements in question might then be formed as the result of this chromatid breakage interacting, during S, with unrejoined chromosome-type breaks that were previously induced in G<sub>0</sub> by radiation. However, we think this explanation can be rejected, as no chromatid-type damage was observed in unirradiated controls for Donor A.

In principle, it should be possible to determine whether cells harboring these rearrangements are in S at the time of exposure by pulse-labeling them with DNA deoxyribonucleoside analogues, such as BrdU, shortly before or after irradiation. Alternatively, one might simply irradiate cultures enriched with S phase cells to see whether the frequency of these rearrange-

ments increases. The main obstacle remains the relative rarity of these events in relation to the expenditure of resources required of mFISH analysis and in conducting HZE particle exposures. Obviously from a numerical standpoint, the exchange aberrations discussed in this paper are rather trivial, more of a cytogenetic curiosity. Nevertheless, their study stands to provide additional clues about IR-induced chromosome damage and the recombinogenic machinery that processes it. If, for example, they really are formed through chromatid-isochromatid interactions, we must conclude that isochromatid-isochromatid interchanges are not only possible, but that they can occur with previously unimagined frequency. In either case, it appears that HZE particles are capable of producing in normal cells a qualitatively different type of damage from that produced by either photons or alpha particles.

## References

- Anderson RM, Marsden SJ, Wright EG, Kadhim MA, Goodhead DT, Griffin CS: Complex chromosome aberrations in peripheral blood lymphocytes as a potential biomarker of exposure to high-LET alpha-particles. *Intl J Rad Biol* 76:31–42 (2000).
- Brown JM, Kovacs MS: Visualization of nonreciprocal chromosome exchanges in irradiated human fibroblasts by fluorescence in situ hybridization. *Radiat Res* 136:71–76 (1993).
- Catcheside DG, Lea DE, Thoday JM: Types of chromosome structural change induced by the irradiation of *Tradescantia* microspores. *J Genet* 47:113–136 (1946).
- Cornforth MN: Analyzing radiation-induced complex chromosome rearrangements by combinatorial painting. *Radiat Res* 155:643–659 (2001).
- Cornforth MN, Bedford JS: Ionizing radiation damage and its early development in chromosomes, in Lett JT, Sinclair WK (eds): *Advances in Radiation Biology*, Vol 17, pp 423–496 (Academic Press, San Diego 1993).
- Darroudi F, Natarajan AT: Cytological characterization of Chinese hamster ovary X-ray-sensitive mutant cells xrs 5 and xrs 6. I. Induction of chromosomal aberrations by X-irradiation and its modulation with 3-aminobenzamide and caffeine. *Mutat Res* 177:133–148 (1987).
- Durante M, Furusawa Y, Majima H, Kawata T, Gotoh E: Association between G<sub>2</sub>-phase block and repair of radiation-induced chromosome fragments in human lymphocytes. *Radiat Res* 151:670–676 (1999).
- Durante M, George K, Wu H, Cucinotta FA: Karyotypes of human lymphocytes exposed to high-energy iron ions. *Radiat Res* 158:581–590 (2002).
- Evans HJ, Scott D: The induction of chromosome aberrations by nitrogen mustard and its dependence on DNA synthesis. *Proc R Soc London – Series B: Biol Sci* 173:491–512 (1969).
- Griffin CS, Marsden SJ, Stevens DL, Simpson P, Savage JR: Frequencies of complex chromosome exchange aberrations induced by <sup>238</sup>Pu alpha-particles and detected by fluorescence in situ hybridization using single chromosome-specific probes. *Int J Rad Biol* 67:431–439 (1995).
- Grigorova M, Brand R, Xiao Y, Natarajan AT: Frequencies and types of exchange aberrations induced by X-rays and neutrons in Chinese hamster splenocytes detected by FISH using chromosome-specific DNA libraries. *Intl J Rad Biol* 74:297–314 (1998).
- Jeggo PA: Identification of genes involved in repair of DNA double-strand breaks in mammalian cells. *Radiat Res* 150:S80–91 (1998).
- Lea DE: *Actions of Radiations on Living Cells*, 2<sup>nd</sup> ed (Cambridge University Press, London 1955).
- Loucas BD, Cornforth MN: Complex chromosome exchanges induced by gamma rays in human lymphocytes: an mFISH study. *Radiat Res* 155:660–671 (2001).
- Pinkel D, Straume T, Gray JW: Cytogenetic analysis using quantitative, high-sensitivity, fluorescence hybridization. *Proc natl Acad Sci, USA* 83:2934–2938 (1986).
- Pinkel D, Landegent J, Collins C, Fuscoe J, Segraves R, Lucas J, Gray J: Fluorescence in situ hybridization with human chromosome-specific libraries: detection of trisomy 21 and translocations of chromosome 4. *Proc natl Acad Sci, USA* 85:9138–9142 (1988).
- Preston RJ: The use of inhibitors of DNA-repair in the study of the mechanisms of induction of chromosome aberrations. *Cytogenet Cell Genet* 33:20–26 (1982).
- Savage JR: Classification and relationships of induced chromosomal structural changes. *J med Genet* 13:103–122 (1976).
- Savage JR: The production of chromosome structural changes by radiation. *Experientia* 45:52–59 (1989).
- Savage JR, Bhunya SP: The induction of chromosomal aberrations by X irradiation during S-phase in cultured diploid Syrian hamster fibroblasts. *Mutat Res* 73:291–306 (1980).
- Savage JR, Simpson P: On the scoring of FISH-“painted” chromosome-type exchange aberrations. *Mutat Res* 307:345–353 (1994a).
- Savage JR, Simpson PJ: FISH “painting” patterns resulting from complex exchanges. *Mutat Res* 312:51–60 (1994b).
- Savitsky K, Bar-Shira A, Gilad S, Rotman G, Ziv Y, Vanagaite L, Tagle DA, Smith S, Uziel T, Sfez S, et al: A single ataxia telangiectasia gene with a product similar to PI-3 kinase (comment). *Science* 268:1749–1753 (1995).
- Speicher MR, Gwyn Ballard S, Ward DC: Karyotyping human chromosomes by combinatorial multi-fluor FISH. *Nature Genet* 12:368–375 (1996).
- Taylor AMR: Unrepaired DNA strand breaks in irradiated ataxia telangiectasia lymphocytes suggested from cytogenetic observations. *Mutat Res* 50:407–418 (1978).

# G2 chromatid damage and repair kinetics in normal human fibroblast cells exposed to low- or high-LET radiation

T. Kawata,<sup>a</sup> H. Ito,<sup>a</sup> T. Uno,<sup>a</sup> M. Saito,<sup>a</sup> S. Yamamoto,<sup>a</sup> Y. Furusawa,<sup>b</sup>  
M. Durante,<sup>c</sup> K. George,<sup>d</sup> H. Wu,<sup>d</sup> and F.A. Cucinotta<sup>d</sup>

<sup>a</sup>Department of Radiology, Graduate School of Medicine, Chiba;

<sup>b</sup>Heavy-Ion Research Group, National Institute of Radiological Sciences, Chiba (Japan);

<sup>c</sup>Department of Physics, University Federico II, Naples (Italy);

<sup>d</sup>NASA Lyndon B. Johnson Space Center, Houston, TX (USA)

**Abstract.** Radiation-induced chromosome damage can be measured in interphase using the Premature Chromosome Condensation (PCC) technique. With the introduction of a new PCC technique using the potent phosphatase inhibitor calyculin-A, chromosomes can be condensed within five minutes, and it is now possible to examine the early damage induced by radiation. Using this method, it has been shown that high-LET radiation induces a higher frequency of chromatid breaks and a much higher frequency of isochromatid breaks than low-LET

radiation. The kinetics of chromatid break rejoining consists of two exponential components representing a rapid and a slow time constant, which appears to be similar for low- and high-LET radiations. However, after high-LET radiation exposures, the rejoining process for isochromatid breaks influences the repair kinetics of chromatid-type breaks, and this plays an important role in the assessment of chromatid break rejoining in the G2 phase of the cell cycle.

Copyright © 2003 S. Karger AG, Basel

A number of experiments have been performed to quantify the biological effects of high-LET radiation exposure and results prove that this type of radiation is more lethal to cells than equivalent doses of sparsely ionizing radiation such as  $\gamma$ - or X-rays (Suzuki et al., 1989; Raju et al., 1991; Napolitano et al., 1992). High-LET radiation exposures produce more chromosome breakage and more complex chromosome rearrangements, which usually leads to cell death. However, some types of damage may confer a proliferative advantage on cells leading to oncogenic cell transformation and carcinogenesis. Indeed, the frequencies of transformation and mutations induced by high-LET radiation have been shown to be greater than those

induced by similar doses of low-LET radiation (Thacker et al., 1979; Yang et al., 1985; Suzuki et al., 1989; Tsuboi et al., 1992), suggesting that carcinogenesis is the most important biological effect caused by exposure to high-LET radiation.

Chromosome aberration analysis is one of the most reliable and sensitive methods of measuring radiation-induced damage. Although cytogenetic damage is typically evaluated in the mitotic phase of the cell cycle, this raises problems because many cells experience severe cell cycle delays and interphase cell death (Suzuki et al., 1990; Ritter et al., 1992, 1996; Edwards et al., 1994, 1996; George et al., 2001), especially after high-LET radiation exposure. Assessing damage in interphase chromosomes can reduce some of these problems and produce a more accurate determination of cytogenetic effects following high-LET exposure. The premature chromosome condensation (PCC) technique, first described by Johnson and Rao (Johnson and Rao, 1970), condenses interphase chromosomes by fusion to mitotic inducer cells, and this method contributed greatly to the study of early effects of radiation damage and chromosome break rejoining. However, this fusion PCC method is technically difficult to perform and laborious; the PCC index is low, and

This work was partly supported by NASA Space Radiation Health Program.

Received 16 September 2003; accepted 24 November 2003.

Request reprints from: Dr. Tetsuya Kawata, Department of Radiology (L1)  
Graduate School of Medicine, Chiba University  
1-8-1 Inohana Chuo-ku Chiba-shi, Chiba 260-8670 (Japan)  
telephone: +81-43-226-2100; fax: +81-43-226-2101  
e-mail: tkawata@med.m.chiba-u.ac.jp.



**Fig. 1.** An example of G2 PCC immediately after exposure to 2 Gy of 80 keV/μm carbon particles. Arrows show chromatid-type breaks and arrow heads show isochromatid breaks.

chromosomes are not well condensed. The fusion PCC technique also requires a considerable manipulation time and is therefore not amendable to studying chromosomal breaks induced immediately after irradiation.

With the recent introduction of a technique using the protein phosphatase inhibitor calyculin-A to induce condensation in interphase cells (Gotoh et al., 1995; Durante et al., 1998a), PCC collection is now technically much simpler and a higher index of well-condensed chromosomes can be obtained. Calyculin-A can induce PCC in many types of cells and in different phases of the cell cycle, especially in G2-phase cells and condensation is induced within five minutes of application. Using this technique, Durante and colleagues (Durante et al., 1999) found similar frequencies of aberrations in G2 chromosomes condensed using calyculin-A and in chromosomes condensed in G1 using the fusion PCC technique. However, lower frequencies were observed in chromosomes collected at metaphase, apparently due to the effect of cell cycle delay or cell cycle block. In this report, high-LET radiation-induced chromosome aberrations in G2-phase normal human fibroblast cells are discussed.

#### *Initial chromatid breaks*

Gotoh et al., (1999) studied radiation-induced G2 chromatid breaks using calyculin-A-induced PCC from human fibroblast cells (AG01522) after  $\gamma$ -ray exposure during exponential growth phase, and initial chromatid breaks were found to increase linearly with dose. Using a similar method, Kawata et al. (2000, 2001a, 2001b) studied high-LET radiation-induced G2 chromosome aberrations in AG01522 cells. An example of

chromatid damage observed immediately after exposure to 2 Gy of 80 keV/μm carbon ions is shown in Fig. 1, where more than 20 isochromatid breaks (G2 fragments) and a number of chromatid breaks are observed.

The dose-response curves for chromatid-type breaks, isochromatid breaks, and total break yield (chromatid-type plus isochromatid-type) after exposure to radiation of different LET values are summarized in Fig. 2. The LET values for the radiation used here range from 0.6 to 440 keV/μm. A linear increase in chromatid breaks and total break yield was discovered, which was independent of the radiation type. On the other hand, isochromatid breaks increased linearly after exposure to high-LET radiation, and a linear quadratic increase was observed after  $\gamma$ -ray and 13 keV/μm carbon exposure. Interestingly, as the LET value increased, the initial percentage of chromatid-type breaks decreased and the percentage of isochromatid breaks increased, until finally isochromatid breaks predominated over chromatid-type breaks after the 440 keV/μm iron irradiation. More than 50% of the initial breaks are isochromatid-type after 440 keV/μm iron particle exposure, while more than 90% are chromatid-type breaks after  $\gamma$ -ray exposure.

The differences in break patterns for low- and high-LET radiations may be attributed to the structure of G2 chromosomes and densely ionizing clusters produced by high-LET radiation. In the G2 phase of the cell cycle, sister chromatids are tightly attached to one another (Murray and Hunt, 1993) and the two chromatid breaks that lead to an isochromatid break would be in close proximity. The probability of a single track of low-LET radiation producing two breaks on sister chromatids is low because ionizations are generally spaced farther apart than the distance between sister chromatids, and therefore chromatid-type breaks would predominate after low-LET exposure. However, the probability of an isochromatid break occurring from a single track of high-LET radiation is proportional to the LET of the charged particles because the distance between the ionization clusters decreases with increasing LET. An increased yield of isochromatid breaks after  $\alpha$ -particles or neutron exposure has also been reported (Durante et al., 1994; Griffin et al., 1994; Vral et al., 2000) using mitotic collection and the G2-assay. A high percentage of isochromatid breaks can, therefore, be a signature of high-LET radiation exposure of G2 phase cells.

When the distribution of isochromatid breaks is assessed within the cell, an overdispersion is observed for high-LET exposure when compared with similar doses of low-LET radiation. Kawata et al. (2002) calculated the relative variance ( $s^2/\bar{y}$ ) from the measured value of the mean value ( $\bar{y}$ ) and the variance ( $s^2$ ), which was around 1.3 for 1.2 Gy of  $\gamma$ -rays, 2.0 for 1.5 Gy of 185 keV/μm iron, and around 3.1 for 1.5 Gy of 440 keV/μm iron particles, respectively. Because energy deposition is focused along the high-LET particle tracks, some cells will be very heavily damaged, while cells hit by  $\delta$ -rays alone will suffer modest damage, and other cells with no hits will be normal (Cucinotta et al., 1998). This is in contrast to low-LET radiation exposure, such as  $\gamma$ -rays, where a more even distribution of damage will induce a uniform distribution of isochromatid breaks.

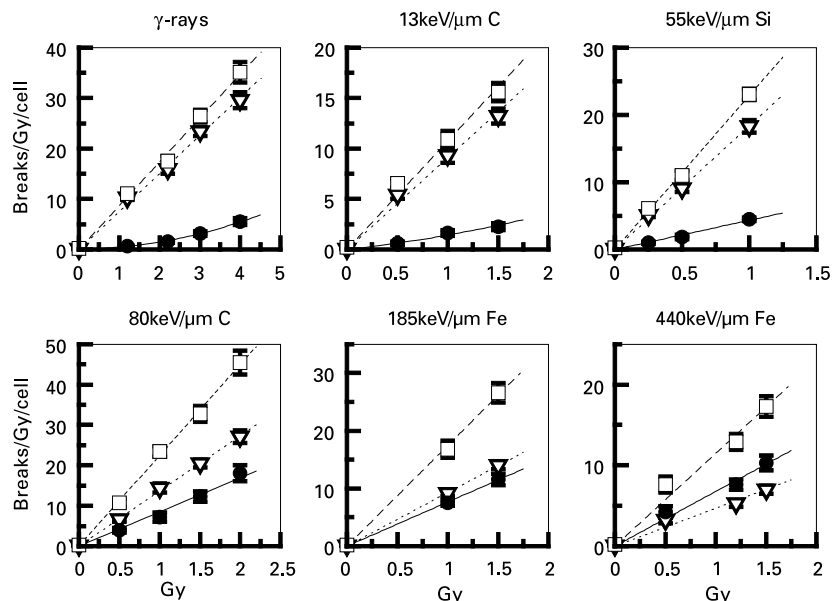


**Fig. 2.** Dose-response curves for the induction of chromatid-type breaks (▽), isochromatid-type breaks (●) and total chromatid breaks (□) after exposure to each type of radiation.

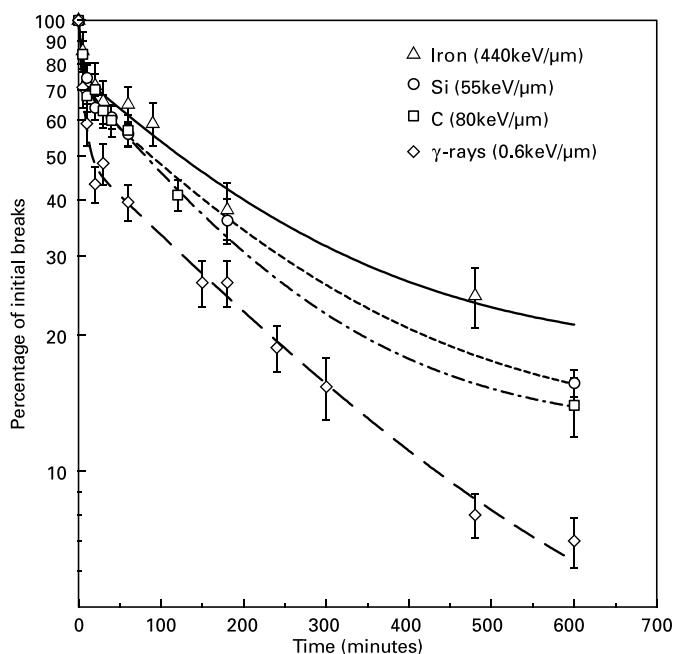


**Fig. 3.** Kinetics of rejoining of chromatid breaks following irradiation as a function of incubation time. Bars represent standard errors of the mean (data from Kawata et al., 2000).

#### Rejoining of chromatid breaks

The kinetics of total break (chromatid-type plus isochromatid-type), isochromatid break, and chromatid break rejoining were investigated after  $\gamma$ -rays, 13 keV/ $\mu$ m carbon, 55 keV/ $\mu$ m silicon, or 440 keV/ $\mu$ m iron particles (Kawata et al., 2000). The repair kinetics for total chromatid breaks showed a similar fast and slow time constant for both high-LET and  $\gamma$ -ray exposure (Fig. 3), and the half time for fast repair was about 4 min,

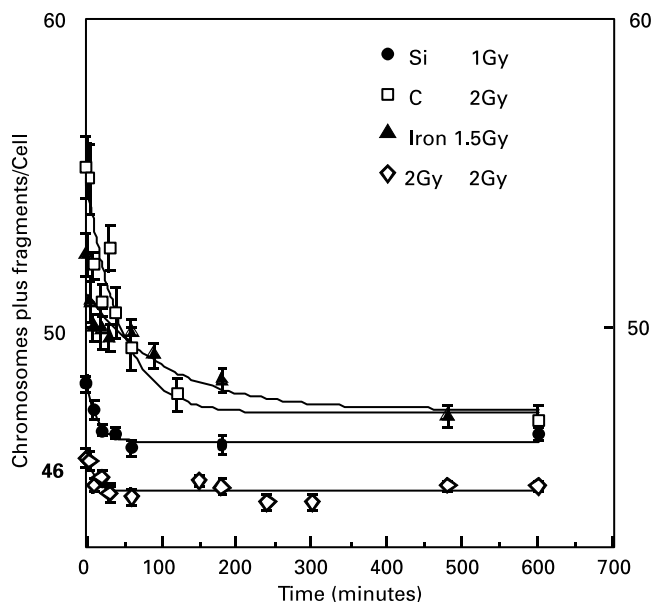


**Fig. 4.** Kinetics of rejoining of isochromatid breaks as a function of incubation times (Data from Kawata et al., 2001b).

regardless of radiation type. Iliakis and colleagues (Iliakis et al., 1993), using a combination of hypertonic treatment and fusion PCC technique, reported a half time of 1.5 min for repair of G1-phase CHO cells after exposure to X-rays. Durante and colleagues (Durante et al., 1998b), using the same technique with fluorescence in situ hybridization (FISH) analysis, also showed that  $\gamma$ -ray-induced chromosome breaks in G0 lymphocytes rejoined very quickly (half time of 5–6 min). Using the G2

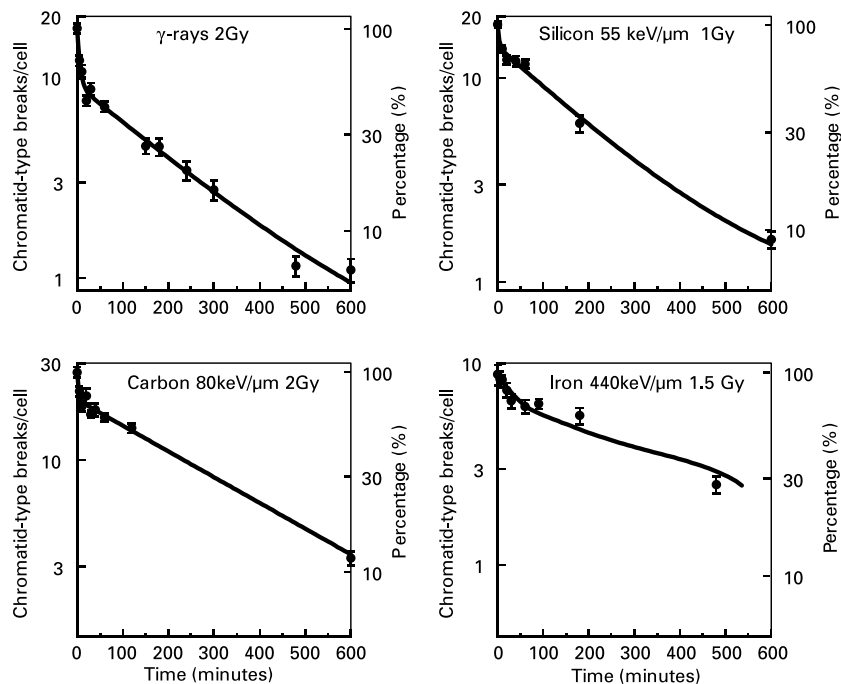


**Fig. 5.** Kinetics of rejoining of chromatid-type breaks as a function of incubation times (Data from Kawata et al., 2001b).

assay, Vral et al. (2002) demonstrated similar kinetics of disappearance of chromatid breaks following  $\gamma$ -rays and high-LET neutrons. These results suggest that the fast component of the repair process may be common throughout the cell cycle and independent of LET.

The percentage of residual breaks induced by high-LET exposure was from 4.2 to 6.2 times higher than  $\gamma$ -rays (Kawata et al., 2000), revealing an LET-dependent trend toward higher levels of residual chromatid breaks. Suzuki et al. (2001) also reported a higher frequency of residual chromatid breaks in human epithelial cells following high-LET iron particle exposure. Goodwin et al. (1994) demonstrated a clear LET-dependent trend in the percentage of excess residual fragments in CHO cells after helium (0.56 keV/ $\mu$ m), carbon (13.7 keV/ $\mu$ m), argon (115 keV/ $\mu$ m), and neon (183 keV/ $\mu$ m) particle exposure, with the reported percentage of residual excess fragments being 49% after 183 keV/ $\mu$ m neon particle exposure, compared to 11% after X-ray exposure. The higher rate of residual breaks induced by high-LET radiation may be due to the more clustered DNA damages induced by this type of exposure.

Kawata et al. (2001b) used calyculin-A-induced PCC method to examine the kinetics of isochromatid break rejoining, and found that high-LET radiation-induced isochromatid breaks rejoin quickly (Fig. 4). Since many more isochromatid breaks are produced by high-LET radiation, chromatid rejoining or exchange formation between isochromatid breaks is more likely to occur in these samples. During the isochromatid break rejoining or exchange formation process, a structural pattern similar to a simple chromatid-type break can be produced, which is therefore classified as residual chromatid-type break, leading to an increase in the number of chromatid-type breaks. This increase in chromatid breaks with repair time is not observed after low-LET radiation, since the initial yield of

isochromatid breaks is much smaller. Therefore, the rejoining process of isochromatid breaks probably leads to the appearance of slower kinetics for chromatid-type break rejoining, especially for 440 keV/ $\mu$ m iron particles (Fig. 5).

## Conclusion

High-LET radiation was found to be more effective at producing isochromatid breaks in the G2 phase of the cell cycle, and the repair process involved in the rejoining of these isochromatid breaks could explain why chromatid break yields remain higher after high-LET irradiation when compared with low-LET irradiation. The PCC technique with calyculin A proved very useful for analysis of the repair kinetics in G2 cells following low- or high-LET irradiation.

## References

- Cucinotta FA, Nikjoo H, Goodhead D: The effects of delta-rays on the number of particle-track traversals per cell in laboratory and space exposures. *Radiat Res* 150:115–119 (1998).
- Durante M, Gialanella G, Grossi GF, Nappo M, Pugliese M, Bettiga D, Calzolari P, Chiorda GN, Ottolenghi A, Tallone-Lombardi L: Radiation-induced chromosomal aberrations in mouse 10T1/2 cells: dependence on the cell-cycle stage at the time of irradiation. *Int J Radiat Biol* 65:437–447 (1994).
- Durante M, Furusawa Y, Gotoh E: A simple method for simultaneous interphase-metaphase chromosome analysis in biodosimetry. *Int J Radiat Biol* 74:457–462 (1998a).
- Durante M, George K, Wu HL, Yang TC: Rejoining and misrejoining of radiation-induced chromatin breaks. III. Hypertonic treatment. *Radiat Res* 149:68–74 (1998b).
- Durante M, Furusawa Y, Majima H, Kawata T, Gotoh E: Association between G2-phase block and repair of radiation-induced chromosome fragments in human lymphocytes. *Radiat Res* 151:670–676 (1999).
- Edwards AA, Finnon P, Moquet JE, Lloyd DC, Darroudi F, Natarajan AT: The effectiveness of high-energy neon ions in producing chromosomal aberrations in human lymphocytes. *Radiat Prot Dosim* 52:299–303 (1994).
- George K, Wu H, Willingham V, Furusawa Y, Kawata T, Cucinotta FA: High- and low-LET induced chromosome damage in human lymphocytes: a time-course of aberrations in metaphase and interphase. *Int J Radiat Biol* 77:175–183 (2001).
- Goodwin EH, Blakely EA, Tobias CA: Chromosomal damage and repair in G1-phase Chinese hamster ovary cells exposed to charged-particle beams. *Radiat Res* 138:343–351 (1994).
- Gotoh E, Asakawa Y, Kosaka H: Inhibition of protein serine/threonine phosphatases directly induces premature chromosome condensation in mammalian somatic cells. *Biomed Res* 16:63–68 (1995).
- Gotoh E, Kawata T, Durante M: Chromatid break rejoining and exchange aberration formation following  $\gamma$ -ray exposure: analysis in G-2 human fibroblasts by chemical-induced premature chromosome condensation. *Int J Radiat Biol* 75:1129–1135 (1999).
- Griffin CS, Harvey AN, Savage JRK: Chromatid damage induced by  $^{238}\text{Pu}$   $\alpha$ -particles in G2 and S phase Chinese hamster V79 cells. *Int J Radiat Biol* 66:85–98 (1994).
- Iliakis G, Okayasu R, Varlotto J, Shernoff C, Wang Y: Hypertonic treatment during premature chromosome condensation allows visualization of interphase chromosome breaks repaired with fast kinetics in irradiated CHO cells. *Radiat Res* 135:160–170 (1993).
- Johnson RT, Rao PN: Mammalian cell fusion: induction of premature chromosome condensation in interphase nuclei. *Nature* 226:717–722 (1970).
- Kawata T, Gotoh E, Durante M, Wu H, George K, Furusawa Y, Cucinotta FA: High-LET radiation-induced aberrations in prematurely condensed G2 chromosomes of human fibroblasts. *Int J Radiat Biol* 76:929–937 (2000).
- Kawata T, Durante M, Furusawa Y, George K, Takai N, Wu H, Cucinotta FA: Dose-response of initial G2-chromatid breaks induced in normal human fibroblasts by heavy ions. *Int J Radiat Biol* 77:165–174 (2001a).
- Kawata T, Durante M, Furusawa Y, George K, Ito H, Wu H, Cucinotta FA: Rejoining of isochromatid breaks induced by heavy ions in G2-phase normal human fibroblasts. *Radiat Res* 156:598–602, (2001b).
- Kawata T, Ito H, Motoori K, Ueda T, Shigematsu N, Furusawa Y, Durante M, George K, Wu H, Cucinotta FA: Induction of chromatin damage and distribution of isochromatid breaks in human fibroblast cells exposed to heavy ions. *J Radiat Res* 43: S169–S173 (2002).
- Murray A, Hunt T: *The cell cycle: an introduction* (Freeman, New York 1993).
- Napolitano M, Durante M, Grossi GF, Pugliese M, Gialanella G: Inactivation of C3H 10T1/2 cells by monoenergetic high LET alpha-particles. *Int J Radiat Biol* 61:813–820 (1992).
- Raju MR, Eisen Y, Carpenter S, Inkret WC: Radiobiology of alpha particles. III. Cell inactivation by alpha-particle traversals of the cell nucleus. *Radiat Res* 128:204–209 (1991).
- Ritter S, Kraft-Weyrather W, Scholz M, Kraft G: Induction of chromosome aberrations in mammalian cells after heavy ion exposure. *Adv Space Res* 12:119–125 (1992).
- Ritter S, Nasonova E, Kraft-Weyrather W, Kraft G: Comparison of chromosomal damage induced by X-rays Ar ions with an LET of 1840 keV/ $\mu\text{m}$  in G1-phase V79 cells. *Int J Radiat Biol* 69:155–166 (1996).
- Suzuki K, Suzuki M, Nakano K, Kaneko I, Watanabe M: Analysis of chromatid damage in G2 phase induced by heavy ions and X-rays. *Int J Radiat Biol* 58:781–789 (1990).
- Suzuki M, Watanabe M, Suzuki K, Nakano K, Kaneko I: Neoplastic cell transformation by heavy ions. *Radiat Res* 120:468–476 (1989).
- Suzuki M, Piao C, Hall EJ, Hei TK: Cell killing and chromatid damage in primary human bronchial epithelial cells irradiated with accelerated 56Fe ions. *Radiat Res* 155:432–439 (2001).
- Thacker J, Stretch A, Stevens MA: Mutation and inactivation of cultured mammalian cells exposed to beams of accelerated heavy ions. II. Chinese hamster V79 cells. *Int J Radiat Biol* 36:137–148 (1979).
- Tsuboi K, Yang TC, Chen DJ: Charged-particle mutagenesis. 1. Cytotoxic and mutagenic effects of high-LET charged iron particles on human skin fibroblasts. *Radiat Res* 129:171–176 (1992).
- Vral A, Thierens H, Baeyens A, De Ridder L: Induction and disappearance of G2 chromatid breaks in lymphocytes after low doses of low-LET gamma-rays and high-LET fast neutrons. *Int J Radiat Biol* 78: 249–257 (2002).
- Yang TC, Graise LM, Mei M, Tobias CA: Neoplastic cell transformation by heavy charged particles. *Radiat Res* 8:S177–S187 (1985).



# Cytogenetic effects of densely ionising radiation in human lymphocytes: impact of cell cycle delays

E. Nasonova,<sup>a,b</sup> and S. Ritter<sup>a</sup>

<sup>a</sup>GSI, Biophysics, Darmstadt (Germany);

<sup>b</sup>JINR, Department of Radiation and Radiobiological Research, Dubna (Russia)

**Abstract.** The classical cytogenetic assay to estimate the dose to which an individual has been exposed relies on the measurement of chromosome aberrations in lymphocytes at the first post-irradiation mitosis 48 h after in vitro stimulation. However, evidence is accumulating that this protocol results in an underestimation of the cytogenetic effects of high LET radiation due to a selective delay of damaged cells. To address this issue, human lymphocytes were irradiated with C-ions (25-mm extended Bragg peak, LET: 60–85 keV/μm) and aberrations were measured in cells reaching the first mitosis after 48, 60, 72 and 84 h and in G<sub>2</sub>-phase cells collected after 48 h by calyculin A induced premature chromosome condensation (PCC). The results were compared with recently published data

on the effects of X-rays and 200 MeV/u Fe-ions (LET: 440 keV/μm) on lymphocytes of the same donor (Ritter et al., 2002a). The experiments show clearly that the aberration yield rises in first-generation metaphase (M1) with culture time and that this effect increases with LET. Obviously, severely damaged cells suffer a prolonged arrest in G<sub>2</sub>. The mitotic delay has a profound effect on the RBE: RBE values estimated from the PCC data were about two times higher than those obtained by conventional metaphase analysis at 48 h. Altogether, these observations argue against the use of single sampling times to quantify high LET induced chromosomal damage in metaphase cells.

Copyright © 2003 S. Karger AG, Basel

The analysis of chromosome aberrations in peripheral blood lymphocytes is regarded as a sensitive method to quantify past radiation exposures and to assess possible health risks (Edwards, 1997; IAEA, 2001). Generally, to estimate the dose to which an individual has been exposed, a venipuncture blood sample is taken and the whole blood or separated lymphocytes are cultured in vitro in the presence of phytohemagglutinin (PHA), a mitogen, which preferentially stimulates T-lymphocytes to traverse the cell cycle. Cells are cultivated for about 48 h, since at that time a high frequency reaches the first mitosis in culture. Then, chromosome spreads are prepared and

aberrations are analysed after solid staining or chromosome painting (for further details see IAEA, 2001).

There is, however, increasing evidence that this standard metaphase assay is not reliable in the case of high LET exposure. High LET radiation produces pronounced cell cycle delays and, as indicated by different experimental approaches, these delays are related to the aberration burden of cells (Ritter et al., 1994, 1996; Durante et al., 1998a; Scholz et al., 1998; George et al., 2003). For example, in recent studies where human lymphocytes were exposed to heavy ions and aberrations were measured in M1 cells collected at several sampling times post-irradiation, a drastic increase in the aberration yield with time was observed (Anderson et al., 2000; George et al., 2001; Ritter et al., 2002a). In contrast, after exposure to γ-rays or X-rays the frequencies of aberrations were the same (Scott and Lyons, 1979; George et al., 2001) or increased slightly with culture time (Boei et al., 1997; Anderson et al., 2000; Ritter et al., 2002a). Thus, the routinely applied protocol to measure chromosomal damage in metaphase cells at only one sampling

This study was partly supported by BMBF, Bonn under contract number 02S8203.

Received 15 September 2003; accepted 20 December 2003.

Request reprints from: Dr. Sylvia Ritter, GSI, Biophysics  
Planckstr. 1, 64291 Darmstadt (Germany)  
telephone: +49 6159-712545; fax: +49 6159 712106  
e-mail: s.ritter@gsi.de.

time can lead to a pronounced underestimation of the cytogenetic effects of high LET particles as discussed in detail elsewhere (Ritter et al., 2002b).

As an alternative to conventional metaphase analysis the application of the PCC technique to biodosimetry was proposed (Pantelias and Maillie, 1984; Durante et al., 1998b; Kanda et al., 1999). Originally, PCC was induced in  $G_0$  lymphocytes by the fusion with mitotic cells (Pantelias and Maillie, 1984). Since this method does not require cell growth, the perturbing influence of radiation-induced cell cycle delays can be bypassed. However, the fusion technique suffers the disadvantage that the number of cells that can be scored is low (Durante et al., 1998b). More recently, a different approach has been developed using inhibitors of type 1 and type 2A serine/threonine protein phosphatases like okadaic acid or calyculin A (Gotoh et al., 1995; Coco-Martin and Begg, 1997). Owing to the fact that these drugs can induce PCC only in cycling cells (Durante et al., 1998b), lymphocytes have to be stimulated as in the conventional metaphase assay. Then, after a culture time of 42 to 47 h, PCCs are chemically induced (Durante et al., 1998b; Kanda et al., 1999) and aberrations are analysed in  $G_2$  cells (Ritter et al., 2002a) or in  $G_2$  and metaphase cells (George et al., 2001, 2003) to account for the selective delay of damaged cells. Since the latter PCC-method is simpler than the fusion technique and results in a much higher frequency of cells that can be scored (Durante et al., 1998b; Kanda et al., 1999), it is preferable for biological dosimetry.

The purpose of this study was to investigate in more detail how particle induced cell cycle progression delays affect the number of aberrations observable in human lymphocytes at mitosis. In particular a better knowledge of the genetic effects of particles is indispensable since they are increasingly used in radiotherapy (Schulz-Ertner et al., 2002; Nishimura et al., 2003) and pose a major risk in manned space explorations (Kiefer, 1999). Lymphocytes were irradiated *in vitro* with C ions and aberrations were measured in M1 cells harvested between 48 and 84 h post-irradiation. Additionally, cytogenetic damage was scored in  $G_2$  phase cells collected at 48 h by means of calyculin A. The results are compared with recently published data on the cytogenetic effects of X-rays and 200 MeV/u Fe ions (LET: 440 keV/ $\mu$ m) on lymphocytes of the same donor (Ritter et al., 2002a).

## Materials and methods

### *In vitro exposure*

For the *in vitro* experiments, peripheral blood from a healthy volunteer (42-year-old female, non-smoker) was drawn into vacutainer cell preparation tubes (Becton Dickinson, NJ, USA) containing sodium heparin (120 USP units) as an anticoagulant. Immediately after collection the samples were centrifuged, lymphocytes were isolated and resuspended in RPMI medium at a concentration of  $4 \times 10^6$  cells/ml as described by Durante et al. (1998b). The cell suspension was loaded into 5-ml plastic centrifuge tubes with an inside diameter of 10 mm, placed in a plastic holder and was irradiated at room temperature with C ions at the SIS (Darmstadt, Germany) with the intensity controlled raster scanning technique as described elsewhere (Haberer et al., 1993).

Irradiation was performed using a 25-mm extended Bragg peak obtained by active energy variation of the beam in the range of 114–158 MeV/u. Samples were placed in the middle of the extended peak, which was designed to

deliver isodose distributions of 0.5, 1 and 2 Gy. Due to the mixture of different beam energies in the extended Bragg peak the dose-average LET increased within the sample from 60 keV/ $\mu$ m at the proximal position to 85 keV/ $\mu$ m at the distal position.

### *Culture conditions*

Immediately after irradiation, the cells were seeded at a density of  $3 \times 10^5$ /ml in RPMI medium containing 20% foetal calf serum, 2 mM L-glutamine, 50 IU/ml penicillin, 50  $\mu$ g/ml streptomycin and 1% PHA. Additionally, to distinguish between cells in the first or later cell generations 5-bromo-2'-deoxyuridine (BrdU) was added for the entire culture period at a concentration of 5  $\mu$ g/ml. Samples were incubated at 37 °C in the dark to avoid photolysis of BrdU.

### *Preparation and cytogenetic analysis of metaphase cells*

For the analysis of chromosomal damage metaphase cells were collected at 48, 60, 72 and 84 h post-irradiation after a 3 h colcemid treatment (400 ng/ml). Metaphase spreads were prepared according to standard techniques and stained with the Fluorescence-plus-Giemsa (FPG) method developed by Perry and Wolff (1974) with minor modifications (Ritter et al., 1996). For each dose and sampling time 100 M1 cells were scored and the yield of terminal deletions, interstitial deletions, dicentric, acentric and centric rings was determined.

### *Preparation and cytogenetic analysis of $G_2$ PCCs*

In parallel to metaphase analysis, aberrations were measured in  $G_2$  cells collected at 48 h by means of the PCC technique as described in detail by Durante et al. (1998b). In brief, 24 h after irradiation and stimulation of the lymphocytes, colcemid was added to the samples (40 ng/ml). Then, after a further incubation for 23 h, the cultures were treated for 1 h with calyculin A (50 nM) to induce PCC. Finally, PCC spreads were prepared and stained with the FPG technique as described above. These samples contained S- and  $G_2$ -phase PCCs as well as metaphases and anaphases as shown in Fig. 1. Aberrations were analysed in first cycle  $G_2$ -phase cells, which were discriminated from metaphase cells by the lack of visible centromeres (see Fig. 1B, C). A PCC spread was identified as damaged when the number of chromosome pieces exceeded 46. Errors on the aberration yield  $A$  were calculated by VA assuming Poisson statistics.

## Results and discussion

### *Analysis of chromosomal damage in metaphases and $G_2$ PCCs 48 h after *in vitro* exposure*

C ion-induced cytogenetic damage was measured in M1 cells collected after an *in vitro* cultivation of 48 h according to the standard protocol (IAEA, 2001) and compared with data obtained for lymphocytes of the same donor after X-ray and Fe ion exposure (Ritter et al., 2002a). As shown in Fig. 2A, C ions were found to be more effective than X-rays. For example, the relative biological effectiveness (RBE) of C ions for the production of 1 aberration per cell is about 2.4. Conversely, high LET Fe ions are less effective than X-rays yielding for the same effect an RBE close to zero consistent with other reports applying the standard cytogenetic protocol (Edwards, 1997 and references therein). The same trend is observed, when the analysis is based on dicentric that are usually used for biological dosimetry (Edwards, 1997; IAEA, 2001).

To gain insights into the effect of cell cycle progression delays on the amount of chromosomal damage observable in mitosis, the aberration yields measured in metaphase cells (Fig. 2A) were compared with the frequencies found in cells that were in  $G_2$  phase at 48 h. Because after solid staining less aberration types can be visualised in PCCs than in metaphase cells, this comparison was restricted to aberrations that result in

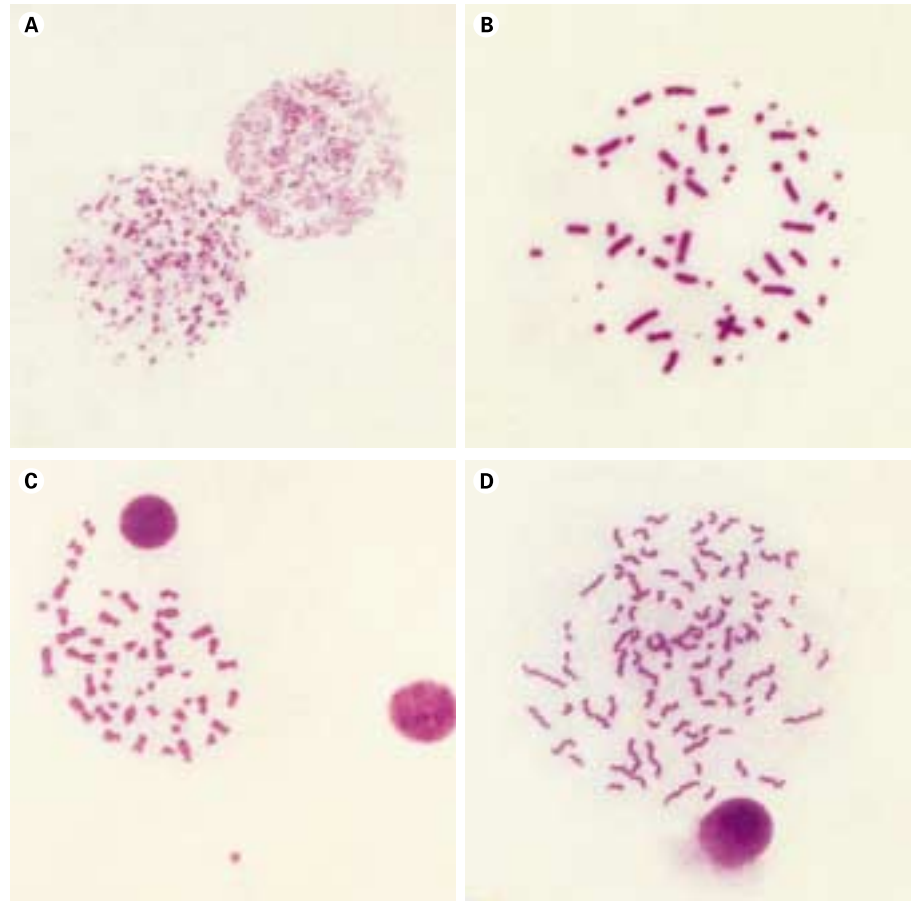


**Fig. 1.** Examples of prematurely condensed chromosomes of human lymphocytes at different stages of the first post-irradiation cell cycle. Lymphocytes were isolated, exposed to C ions and stimulated to grow by the addition of PHA. After an incubation time of 47 h, calyculin A was added to the samples and 1 h later PCC spreads were prepared. **(A)** Two S-phase PCCs. The condensed sections of the chromatin represent replicated DNA. These cells cannot be scored for aberrations. **(B)** G<sub>2</sub>-phase PCC with fully condensed bivalent chromatids; centromeres are not visible. This cell exhibits 14 radiation-induced excess fragments. **(C)** Undamaged anaphase cell with clearly visible centromeres. **(D)** Undamaged anaphase cell with separated chromatids.

an excess of chromosome fragments (terminal and interstitial deletions, acentric and centric rings) which are detectable with both assays.

As shown in Fig. 2B, in M1 cells the number of excess fragments is much lower than the total number of aberrations (Fig. 2A), but the resulting dose-effect curves show the same trend, C ions are more effective than X-rays, while Fe ions are less effective. The RBE of C ions for the production of 1 excess fragment per cell is about 1.7, while the RBE of Fe ions is close to zero. However, when cytogenetic damage was analysed in cells that were in G<sub>2</sub> phase at 48 h a different picture emerged (Fig. 2C). In all experiments higher aberration yields (excess fragments) were detected in G<sub>2</sub> cells than in metaphase cells consistent with data reported by Durante et al. (1999) and George et al. (2003). Obviously, damaged cells suffer a prolonged G<sub>2</sub> arrest. Furthermore, Figs. 2B and C show that the difference in the aberration yield found in G<sub>2</sub> cells and M1 cells is minimal after X irradiation, but becomes more significant after particle exposure. Consequently, when the PCC data are used for RBE calculation, higher values are obtained than with the standard metaphase assay, for C ions and Fe ions RBEs of 4.5 and 2.6 were estimated, respectively. These data are in line with a recent study of George et al. (2003), where metaphases and PCCs were collected at 48–50 h and aberrations were detected by fluorescence in situ hybridisation. The authors report that the RBE values estimated for chemically induced

PCCs are up to three times higher than the RBEs obtained by metaphase analysis. Further studies are in progress using more dose points to allow a more precise estimate of the RBE of particles.

The pronounced difference between the PCC data (Fig. 2C) and the metaphase results (Figs. 2A and B) suggests that cells carrying a higher number of aberrations are unlikely to reach the first post-irradiation mitosis or reach mitosis at a later time. To gain further insight into the relationship between C ion-induced cell cycle delays and the expression of aberrations in metaphase cells, a time-course study was performed.

#### *Time course of chromosomal damage in lymphocytes at the first post-irradiation division following in vitro exposure*

The frequencies of aberrations were measured in lymphocytes reaching the first mitosis at 48, 60, 72 and 84 h after exposure to C ions. Analysis of the full spectrum of aberrations detectable with Giemsa staining showed that cells arriving late at the first mitosis carried twice as many aberrations than those arriving at earlier times (data not shown). The same effect was observed, when the analysis was restricted to aberration types which result in the formation of excess fragments (Fig. 3). Moreover, the data indicate that the major increase in the aberration frequency occurred between 48 and 72 h after C ion exposure. Thereafter, the aberration yield levelled off.

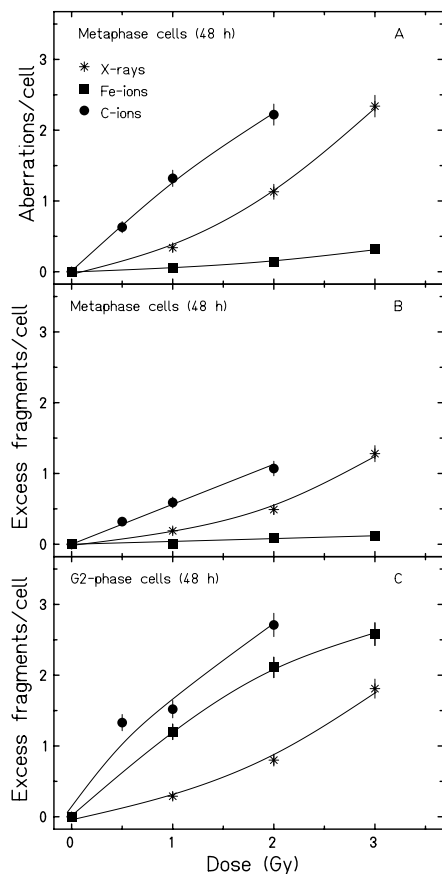


**Fig. 2.** In vitro dose-response curves of the yield of aberrations induced in human lymphocytes by C ions (25 mm extended Bragg peak, LET: 60–85 keV/μm, this study), 200 MeV/u Fe ions (LET: 440 keV/μm) or X-rays (data from Ritter et al., 2002a). Samples were collected 48 h after exposure, stained with the FPG technique and chromosomal damage was analysed in first cycle cells. **(A)** Aberration yield in M1 cells (terminal and interstitial deletions, dicentrics, acentric and centric rings); **(B)** yield of excess fragments in M1 cells (terminal and interstitial deletions, acentric and centric rings); **(C)** yield of excess fragments in G<sub>2</sub>-PCCs (see **B**). Curves are drawn to guide the eye.

Together with recent information on the time course of radiation-induced chromosomal damage in human lymphocytes the following picture emerged. After exposure to γ-rays, X-rays or particles with an LET of up to 30 keV/μm no or only a minimal effect of sampling time can be seen (Scott and Lyons, 1979; Boei et al., 1997; Anderson et al., 2000; George et al., 2001; Ritter et al., 2002a). In contrast, in cultures exposed to particles with higher LET values a profound increase in the aberration frequency occurs. This increase is about twofold after exposure to C-ions with LET of 60–85 keV/μm (Fig. 3), threefold after the exposure to α-particles and Fe ions with LET values of 121 and 140 keV/μm (Anderson et al., 2000; George et al., 2001) and sevenfold when Fe ions with an LET of 440 keV/μm are applied (Ritter et al., 2002a). Similarly, in various Chinese hamster cell lines that represent another model system for radiobiological research, a dramatic effect of LET on the expression of aberrations in metaphase cells was observed (Ritter et al., 1996, 2002b; Nasonova et al., 1998). The most

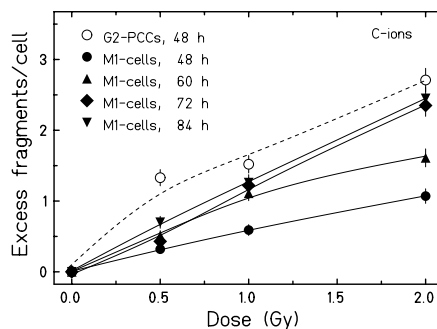


**Fig. 3.** In vitro dose-response curves of the yield of excess fragments induced in human lymphocytes by C ions (25 mm extended Bragg peak, LET: 60–85 keV/μm). G<sub>2</sub> PCCs were harvested at 48 h, while metaphase cells were collected at 48, 60, 72 and 84 h post-irradiation. Aberrations were scored in first cycle cells after FPG staining. Curves are drawn to guide the eye.

pronounced effect was detected in hamster cells exposed to low-energy Ar ions with an LET of 1,840 keV/μm. After this treatment an increase in the aberration yield by a factor of 20 was measured in M1 cells (Ritter et al., 1996). Altogether these data suggest that in several cell systems including human lymphocytes the standard metaphase assay that relies on scoring of aberrations only at an early time point underestimates the cytogenetic effects of particles.

The above described difference in the time-course of high and low LET-induced chromosomal damage can be related to the spatial energy deposition of both radiation types as discussed in more detail elsewhere (Ritter et al., 2002a, b). In brief, when cells are exposed to particles the dose is extremely inhomogeneously deposited both in terms of the energy deposition inside a particle track and the number of particle traversals per cell nucleus (Kraft et al., 1992). As a consequence, cells with quite different numbers of aberrations and cell cycle transition times are produced. In contrast, after exposure to sparsely ionising radiation the ionisations are fairly uniformly deposited between cells leading to a homogeneous distribution of aberrations and delay times within the exposed cell population.

Moreover, comparison of the metaphase values with the PCC values (Fig. 3) shows that the yield of excess fragments is slightly lower in metaphases collected after a culture time of 84 h than in G<sub>2</sub> PCCs collected at 48 h. Probably, this difference results from a reduced stimulation rate or interphase death but not from mitotic delay, since after 84 h more than 93% of all metaphases from unirradiated and irradiated samples belong already to the second, third or fourth post-irradiation cell generation (data not shown). However, at present, detailed information on cell stimulation or apoptosis for human lymphocytes exposed in G<sub>0</sub> and thereafter stimulated to grow is not available. Development of refined experimental approaches which would account for the complexity of the cellular response of human lymphocytes to high LET radiation remains an important challenge for future studies.

In summary, our experiments provide further evidence that after particle exposure the progression of lymphocytes to mito-

sis, which is a prerequisite for classical aberration scoring, is influenced by a selective delay of damaged cells and this effect depends on LET. Similarly, in other cell systems frequently used in radiobiological research like Chinese hamster cells a relationship between radiation-induced cell cycle delays and the number of aberrations carried by a cell was observed (Ritter et al., 1996, 2002b; Nasonova et al., 1998). These observations argue against the use of a single sampling time to quantify heavy ion-induced chromosomal damage in metaphase cells. Instead, for a reliable estimate of the absorbed dose and the genetic risks associated with high LET exposure, modified pro-

ocols should be used which account for the mitotic delay. This can be achieved by means of a time-course study that covers the complete time interval of the first mitosis along with a mathematical analysis as suggested by Scholz et al. (1998). Alternatively, the analysis of chromosomal damage in interphase cells following chemically induced PCC is recommended (Durante et al., 1998b; Kanda et al., 1999). However, apart from the mitotic delay, additional factors such as a reduced stimulation rate or apoptosis might affect the yield of aberrations observable in metaphase cells. Further studies to address this question are in progress.

## References

- Anderson RM, Mardsen SJ, Wright EG, Khadim MA, Goodhead DT, Griffin CS: Complex chromosome aberrations in peripheral blood lymphocytes. *Int J Radiat Biol* 76:31–42 (2000).
- Boei JJ, Vermeulen S, Natarajan AT: Differential involvement of chromosomes 1 and 4 in the formation of chromosomal aberrations in human lymphocytes after X-irradiation. *Int J Radiat Biol* 72: 139–145 (1997).
- Coco-Martin JM, Begg AC: Detection of radiation induced chromosome aberrations using fluorescence in situ hybridisation in drug-induced premature chromosome condensation of tumour cell lines with different radiosensitivities. *Int J Radiat Biol* 71:265–273 (1997).
- Durante M, Furusawa Y, George K, Gialanella G, Greco, O, Grossi, G, Matsufuji N, Pugliese M, Yang TC: Rejoining and misrejoining of radiation-induced chromatin breaks. IV. Charged particles. *Radiat Res* 149:446–454 (1998a).
- Durante M, Furusawa Y, Gotoh E: A simple method for simultaneous interphase-metaphase chromosome analysis in biodosimetry. *Int J Radiat Biol* 74:325–331 (1998b).
- Durante M, Furusawa Y, Majima H, Kawata T, Gotoh E: Association between G<sub>2</sub>-phase block and repair of radiation-induced chromosome fragments in human lymphocytes. *Radiat Res* 151:670–676 (1999).
- Edwards AA: The use of chromosomal aberrations in human lymphocytes for biological dosimetry. *Radiat Res* 148:S39–S44 (1997).
- George K, Durante M, Willingham V, Furusawa Y, Kawata T, Cucinotta FA: High and low LET induced chromosome damage in human lymphocytes: a time-course of aberrations in metaphase and interphase. *Int J Radiat Biol* 77:175–183 (2001).
- George K, Durante M, Willingham V, Wu H, Yang T, Cucinotta FA: Biological effectiveness of accelerated particles for the induction of chromosome damage measured in metaphase and interphase human lymphocytes. *Radiat Res* 160:425–435 (2003).
- Gotoh E, Asakawa Y, Kosaka H: Inhibition of protein serine/threonine phosphatases directly induces premature chromosome condensation in mammalian somatic cells. *Biomed Res* 16:63–68 (1995).
- Haberer T, Becher W, Schardt D, Kraft G: Magnetic scanning system for heavy ion therapy. *Nucl Inst and Meth A* 330:296–305 (1993).
- IAEA: Cytogenetic Analysis for Radiation Dose Assessment: a Manual. Technical Report Series no. 405 (International Atomic Energy Agency, Vienna 2001).
- Kanda R, Hayata I, Lloyd DC: Easy biodosimetry for high-dose radiation exposures using drug-induced, prematurely condensed chromosomes. *Int J Radiat Biol* 75:441–446 (1999).
- Kiefer J: Radiation risk in manned space flights. *Mutat Res* 430:307–313 (1999).
- Kraft G, Krämer M, Scholz M: LET, track structure and models: a review. *Rad Env Biophys* 31:161–180 (1992).
- Nasonova E, Ritter S, Fomenkova T, Kraft G: Induction of chromosomal damage in CHO-K1 and their repair-deficient mutant xrs5 by X-ray and particle irradiation. *Adv Space Res* 22:569–578 (1998).
- Nishimura H, Miyamoto T, Yamamoto N, Koto M, Sugimura K, Tsujii H: Radiographic pulmonary and pleural changes after carbon ion irradiation. *Int J Radiat Oncol Biol Phys* 55:861–866 (2003).
- Pantelias GE, Maillie HD: The use of peripheral blood mononuclear cell prematurely condensed chromosomes for biological dosimetry. *Radiat Res* 99: 140–150 (1984).
- Perry P, Wolff S: New Giemsa method for differential staining of sister chromatids. *Nature* 251:156–158 (1974).
- Ritter S, Nasonova E, Scholz M, Kraft-Weyrather W, Kraft G: Influence of radiation quality on the expression of chromosomal damage. *Int J Radiat Biol* 66:625–628 (1994).
- Ritter S, Nasonova E, Scholz M, Kraft-Weyrather W, Kraft G: Comparison of chromosomal damage induced by X-rays and Ar ions with an LET of 1840 KeV/μm. *Int J Radiat Biol* 69:155–166 (1996).
- Ritter S, Nasonova E, Furusawa Y, Ando K: Relationship between aberration yield and mitotic delay in human lymphocytes exposed to 200 MeV/u Fe-ions and X-rays. *J. Radiat Res* 43:S175–S179 (2002a).
- Ritter S, Nasonova E, Gudowska-Nowak E: Effect of LET on the yield and quality of chromosomal damage in metaphase cells: a time-course study. *Int J Radiat Biol* 78:191–202 (2002b).
- Scholz M, Ritter S, Kraft G: Analysis of chromosome damage based on the time-course of aberrations. *Int J Radiat Biol* 74:457–462 (1998).
- Schulz-Ertner D, Haberer T, Jäckel O, Thilmann C, Krämer M, Enghardt W, Kraft G, Wannemacher M, Debus J: Radiotherapy for chordomas and low-grade chondrosarcomas of the skull base with carbon ions. *Int J Radiat Oncol Biol Phys* 53:36–42 (2002).
- Scott D, Lyons CY: Homogeneous sensitivity of human peripheral blood lymphocytes to radiation-induced chromosome damage. *Nature* 278:756–768 (1979).

# Chromosome aberrations induced by high-LET carbon ions in radiosensitive and radioresistant tumour cells

P. Virsik-Köpp<sup>a</sup> and H. Hofman-Huether<sup>b</sup>

Departments of <sup>a</sup>Clinical Radiobiology and <sup>b</sup>Radiotherapy and Radiation Oncology, Radiology Centre, Medical Faculty, University of Göttingen, Göttingen (Germany)

**Abstract.** Chromosome aberration formation was analysed in two human tumour cell lines displaying different radiosensitivity. Aberrations involving chromosomes 2, 4, and 5 were studied in one radioresistant cell line (WiDr) and in one radiosensitive cell line (MCF-7). Chromosome aberrations were studied by application of single-colour FISH. We studied the effects of monoenergetic 100 MeV/u carbon ions and carbon ions from extended Bragg peak. Chromosome aberrations induced by carbon ions were compared with aberrations induced by standard 200 kV X-rays. In both tumour cell lines, carbon ions induced aberrations more effectively than X-rays. The

radioresistance and radiosensitivity of the corresponding cell lines, as observed for X-rays, were also found after carbon ion irradiation. In both cell lines, the typical effects of ion irradiation were an increased proportion of cells containing complex aberrations, and an increased complexity of these complex exchanges. However, comparable effects were induced in MCF-7 cells by a much lower dose than in WiDr cells. Insertions were also induced more efficiently in MCF-7 cells than in WiDr cells.

Copyright © 2003 S. Karger AG, Basel

High-LET radiation tracks induce in irradiated cells clustered damage, i.e. multiple closely spaced DNA lesions (e.g. Goodhead, 1991; Rydberg, 1996; Stenerlow et al., 2002). Radiation-induced double-strand breaks (DSBs) are then induced in close proximity, clustered to distances that are dependent upon the chromatin geometry (e.g. Hoglund and Stenerlow, 2001). In multiple rejoining studies, DNA damage induced by high-LET radiation has been found to be more difficult and slower to repair (e.g. Rydberg et al., 1994; Stenerlow et al., 1996, 2000; Taucher-Scholz et al., 1996; Pinto et al., 2002).

Complex chromosome aberrations are likely to arise from interactions among the clustered lesions. In studies with normal cells irradiated with high-LET  $\alpha$ -particles (e.g. Griffin et al., 1995; Anderson et al., 2000) or heavy ions (e.g. Testard et al., 1997; Wu et al., 1997; Durante et al., 2000, 2002), the proportion of cells containing complex aberrations was observed to be strongly increased in comparison with cells irradiated with X-rays. Due to their increased biological effectiveness and their physical properties, high-LET ions are of special interest for radiation therapy of radioresistant tumours. The causes of tumour cell radioresistance are not yet clear. An increased DNA repair ability, an increased tolerance to unrepaired damage and to misrepair products and modified chromatin structure are just a few of the possible mechanisms. Studies of cytogenetic effects of high-LET radiations are thus helpful for analysing the mechanisms underlying tumour cell radioresistance, since they reflect the specificity, capacity, and fidelity of repair and misrepair processes taking place in irradiated cells.

Rather few cytogenetic studies with high-energy ion beams and human tumour cells have been accomplished insofar. In these studies, mostly residual chromatin breaks detected by the

Supported by a grant from GSI, Darmstadt, Germany. The work was also generously supported by Prof. F.C. Hess, head of the Department of Radiotherapy and Radiation Oncology, Medical Faculty, University of Göttingen.

Received 10 September 2003; manuscript accepted 30 November 2003.

Request reprints from Dr. P. Virsik-Köpp, Department of Clinical Radiobiology  
University of Göttingen, von Siebold Str. 3, 37075 Göttingen  
Mailing address: Nonnenstieg 42, 37075 Göttingen (Germany)  
telephone: +49-551-392760; fax: +49-551-397966  
e-mail: patricia.virsik@t-online.de

premature chromosome condensation (PCC) technique were measured (e.g. Goodwin et al., 1989; Suzuki et al., 1998, 2001; Ofuchi et al., 1999). Increased ion efficiency, as reported for cell killing, was confirmed for induction of chromatin breaks in normal and tumour cells irradiated with various high-LET ions.

In this paper, we present our study of chromosome aberration induction in one highly radioresistant cell line (WiDr) and in one radiosensitive cell line (MCF-7) irradiated with carbon ions or for comparison, with 200 kV X-rays.

## Methods and materials

### *Cells and culture conditions*

The radioresistant human colon carcinoma cell line WiDr (modal chromosome number = 72) was obtained from the American Type Culture Collection (ATCC), ATCC No. 218. The radiosensitive human breast carcinoma cell line MCF-7 (modal chromosome number = 71) was obtained from the German Cancer Research Center in Heidelberg, Cat. No. 6100030. Radiosensitivity after 200 kV X-ray irradiation with respect to clonogenic survival and chromosome aberration induction has been already reported (e.g. Virsik-Peuckert et al., 1996). The surviving fractions at  $D = 2$  Gy are 0.74 and 0.48 in WiDr and MCF-7 cells, respectively. WiDr cells were grown in minimal essential medium (MEM) supplemented with 10% foetal calf serum, 2% glutamine, penicillin (50 IU/ml) and streptomycin (50 µg/ml). MCF-7 cells were grown in a culture medium containing MEM (50%) and Dulbecco's MEM (50%) supplemented with 10% fetal calf serum, 2% glutamine, penicillin (50 IU/ml), and streptomycin (50 µg/ml). Cells were kept in 5% CO<sub>2</sub> atmosphere at 37°C. Irradiation experiments were performed with plateau-phase cells grown to confluence (90–95%) and kept for 24 h without medium change.

### *In vitro irradiation*

Cell monolayers were irradiated with carbon ions or with 200 kV X-rays (Siemens Stabilipan generator with 0.5-mm Cu filter) in plastic flasks of 25 cm<sup>2</sup> area. Irradiation with carbon ions was performed at the GSI synchrotron SIS (Schwerionensynchrotron; GSI, Darmstadt, Germany) using the raster-scan system as described by Haberer et al. (1993). Monoenergetic 100 MeV/u carbon ions (LET = 28 keV/µm) and ions from a 25-mm extended Bragg peak designed to deliver isodose distributions of 0.5, 1 and 2 Gy were used. Due to the mixture of different beam energies in the extended Bragg peak, the dose-mean LET increased within the irradiated sample from 60 keV/µm at the proximal position to 85 keV/µm at the distal position.

### *Metaphase preparation*

Irradiated cells were seeded at  $2.5 \times 10^5$  cells per T25 flask and cultured for 24–32 h depending upon dose and radiation quality. During the last 2 incubation hours, 0.20 µg/ml colcemide was added. After treatment with hypotonic solution (0.06 M KCl plus 0.6% sodium citrate 1:1) for 20 min at 37°C, the cells were fixed in 3:1 methanol:glacial acetic acid to obtain metaphase chromosomes. Cell suspensions were stored at 4°C.

### *Fluorescence in situ hybridization (FISH)*

Slides with spread cells were pretreated with 2× SSC plus 0.5% octyl-phenoxy polyethoxyethanol solution and then dehydrated through ethanol series. Whole-chromosome probes (APPLIGENE/ONCOR, Heidelberg, Germany) for chromosomes 2, 4 and 5, conjugated with the fluorochrome Texas red, were used for single-colour FISH (sFISH). The probes were denatured for 5 min and preannealed 30 min at 37°C in the dark. Chromosome preparations from WiDr or MCF-7 cells were denatured for 2 min at 72°C or 65°C for WiDr or MCF-7 cells, respectively, and dehydrated through ethanol series. The denatured ONCOR probes were applied to denatured metaphase chromosomes, and incubated about 16 h in a dark humid chamber at 37°C. Slides were washed in 0.5× SSC solution and subsequently in phosphate-buffered saline. The entire chromosomal DNA was counterstained with a 10-µl mix of DAPI and antifade solution (APPLIGENE/ONCOR).

### *Chromosome analysis*

Metaphase chromosomes were analysed with a Zeiss fluorescence microscope with filter sets for DAPI and Texas red, equipped with a CCD camera (Visitron Systems GmbH, Puchheim, Germany). MetaMorph<sup>R</sup> (West Chester, USA) software was used for image analysis. Chromosomes 2, 4, and 5 were chosen for aberration analysis. In both studied cell lines, these chromosomes were present as either intact copies or they contained stable, clearly detectable clonal terminal translocations or deletions. Yields of non-clonal spontaneous translocations involving chromosomes 2, 4, and 5 were low, namely 0.009 per cell in WiDr cells, and 0.02 per cell in MCF-7 cells. The selected chromosomes were also numerically stable, i.e. three copies of chromosome 2 and four copies of chromosomes 4 and 5 were present in about 95% of the evaluated cells. The aberration data are given for these chromosome ploidy classes. Chromosomes 2, 4, and 5 were analysed in unirradiated as well in irradiated cells. When a painted chromosome was involved in an exchange (distinct from the clonal translocation), the painting patterns were classified – as far as possible – according to the Savage and Simpson scheme (Simpson and Savage, 1994). Complete (85–95%) and incomplete (10–15%) apparently simple translocations were scored distinctly, but in the results the pooled frequencies are given. Centromeres were visualised through DAPI filter. They appeared as bright blue dots and thus monocentric and dicentric chromosomes could be distinguished unequivocally. Visible complex exchanges could not always be exactly classified; the most frequent forms comprised a monocentric chromosome participating in a translocation plus a dicentric chromosome (2G form according to Savage and Simpson classification) and exchanges of three chromosomes with four breaks.

## Results

### *Partial yields of apparently simple dicentric chromosomes*

Using sFISH, radiation-induced aberrations were analysed in the selected chromosomes 2, 4, and 5. Sums of partial yields (based on the analysis of chromosomes 2, 4 and 5) of apparently simple dicentrics induced by 100 MeV/u carbon ions or 200 kV X-rays in MCF-7 and WiDr cells are plotted in Fig. 1 in dependence upon dose. No dicentrics involving either chromosome 2, 4 or 5 were detected in unirradiated control samples with sFISH. In the radioresistant WiDr cells, dicentric yields increased nonlinearly with increasing radiation dose of carbon ions or X-rays. In the radiosensitive MCF-7 cells, dicentric yields increased linearly with increasing dose of X-rays, and the yields were lower than in WiDr cells. After irradiation with carbon ions, the dicentric yields increased with increasing dose, reached a maximum, and declined thereafter. Up to 3 Gy, dicentric yields induced by carbon ions in MCF-7 and in WiDr cells were similar. The strong decline in dicentric yield observed in MCF-7 cells irradiated with 4 Gy reflects the parallel strong increase of complex rearrangements involving many dicentrics, as well (Hofman-Huether, 2002).

### *Partial yields of apparently simple reciprocal translocations*

Sums of partial yields of apparently simple reciprocal translocations induced by 100 MeV/u carbon ions or 200 kV X-rays in MCF-7 and WiDr cells are plotted in Fig. 2 in dependence upon dose. Similarly as dicentric yields, translocation yields increased nonlinearly with increasing X-ray or ion dose in WiDr cells. In MCF-7 cells, the yields increased and reached a maximum after ion irradiation, showing a decline thereafter. For X-rays, the possible maximum was not yet achieved for doses up to 4 Gy. For both radiation types, translocation yields in MCF-7 cells were higher than in WiDr cells.

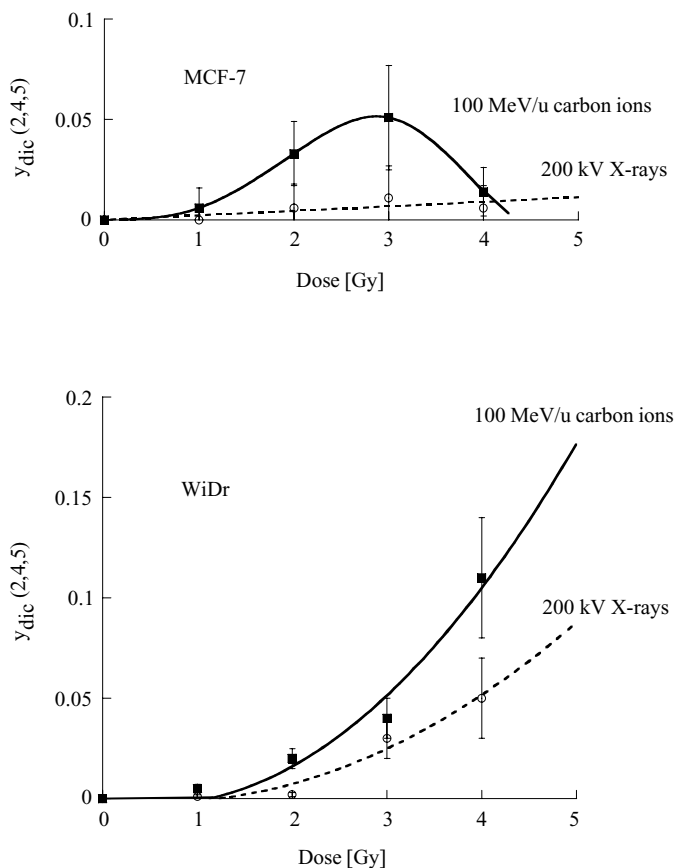


**Fig. 1.** Sums of dose-dependent partial yields of apparently simple dicentric chromosomes as detected by sFISH in chromosomes 2, 4 and 5. Confluent MCF-7 and WiDr cells were irradiated with 100 MeV/u carbon ions and, for comparison, with 200 kV X-rays as reference. For each point, 150–900 cells were analysed. For X-rays, the dose dependence was linear in MCF-7 cells and linear-quadratic in WiDr cells. For carbon ions, the dose dependence was non-linear in MCF-7 cells (fitted by a curve reaching a maximum and declining thereafter) and linear-quadratic in WiDr cells. Vertical bars represent standard errors.

### Complex aberrations

Data on complex aberrations including insertions and other complex exchanges (three or more chromosomes participating) induced in MCF-7 and WiDr cells by 100 MeV/u carbon ions or 200 kV X-rays are summarized in Table 1. Numbers of complex aberrations detected in metaphase cells by sFISH are given separately for each chromosome. Figure 3 shows an example of a cell containing complex exchanges after irradiation with carbon ions. The numbers of complex aberrations increased with dose and were generally higher after ion irradiation. In both cell types, already after irradiation with  $D = 4$  Gy of 200 kV X-rays, up to 20% of cells were found to contain higher-order complexes involving three or four chromosomes. After irradiation with carbon ions, the proportion of higher-order complexes further increased. For example, after irradiation with 100 MeV/u ions and  $D = 4$  Gy, the proportion of complex exchanges involving four chromosomes was 40% in WiDr cells and 50% in MCF-7 cells. Thus, the aberration spectrum in both tumour cell lines irradiated with carbon ions was much more complex

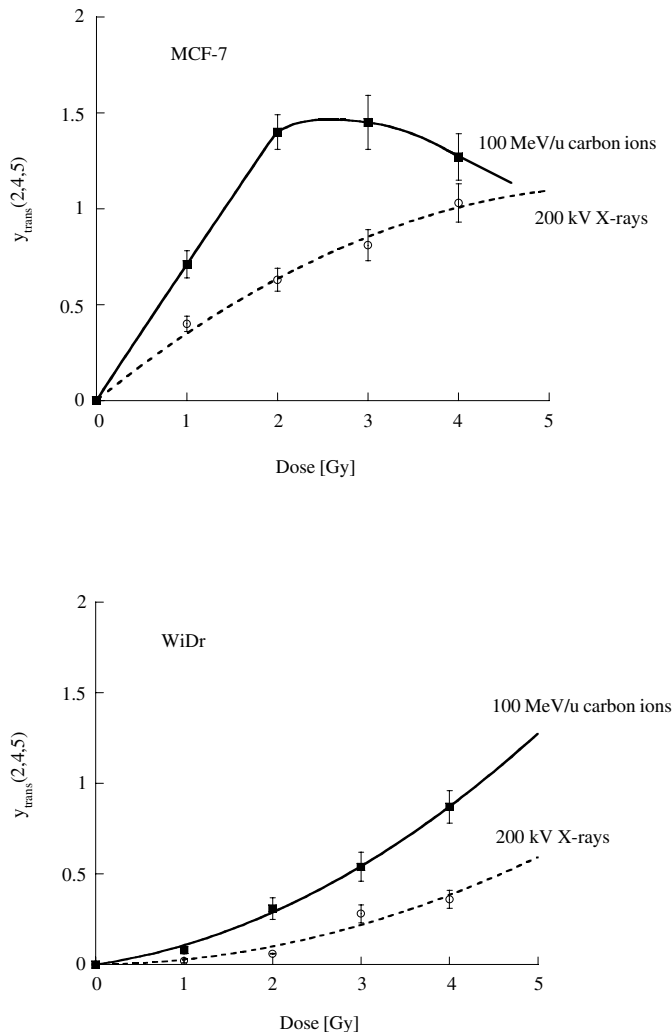


**Fig. 2.** Sums of dose-dependent partial yields of apparently simple reciprocal translocations as detected by sFISH in chromosomes 2, 4 and 5. Yields observed in unirradiated control cells were subtracted. Confluent MCF-7 and WiDr cells were irradiated with 100 MeV/u carbon ions and, for comparison, with 200 kV X-rays as reference. For each point, 150–900 cells were analysed. For X-rays, the dose dependence was supralinear in MCF-7 cells and linear-quadratic in WiDr cells. For carbon ions, the dose dependence was non-linear in MCF-7 cells (fitted by a curve reaching a maximum and declining thereafter) and linear-quadratic in WiDr cells. Vertical bars represent standard errors.

than the spectrum observed after X-ray irradiation. The radio-sensitive MCF-7 cells always contained more complex aberrations than WiDr cells.

### Complex aberrations in cells irradiated with carbon ions from extended Bragg peak

Since the WiDr cells proved to be quite resistant to irradiation by 100 MeV/u carbon ions, we performed further experiments with cells irradiated in extended Bragg peak. These ion tracks have much higher ionisation density than 100 MeV/u ions, i.e. the multiple clustered damage is more frequent and more severe. In Fig. 4, relative numbers of cells containing complex exchanges are compared for irradiation with X-rays



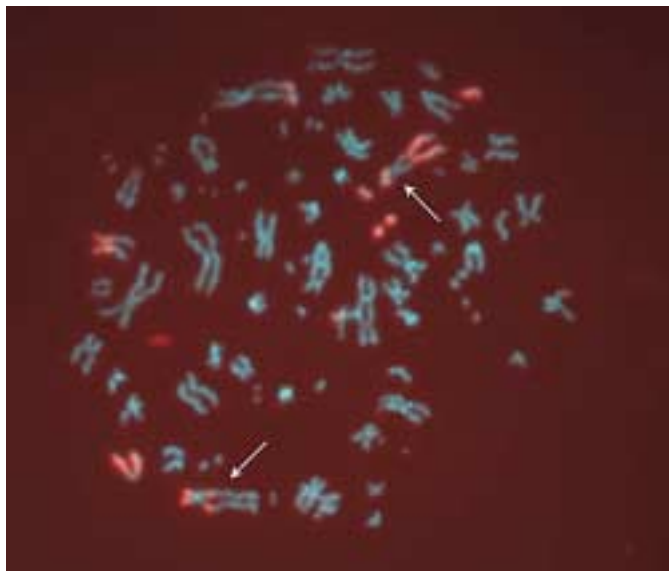


**Fig. 3.** Example of a metaphase WiDr cell containing complex exchange aberrations after irradiation with carbon ions. Chromosome 5 was painted red. Arrows indicate complex aberrations.

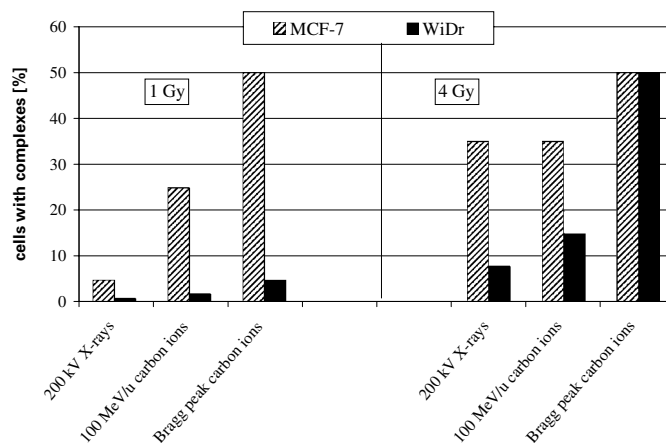


**Fig. 4.** Relative proportions of cells containing complex exchanges after irradiation with 200 kV X-rays and carbon ions (100 MeV/u and extended Bragg peak). Data are shown for MCF-7 and WiDr cells irradiated with  $D = 1$  Gy and  $D = 4$  Gy. For each point, 100–900 cells were analysed.

**Table 1.** Number of complex exchanges involving chromosomes 2, 4 and 5 in MCF-7 and WiDr cells irradiated with graded doses of 200 kV X-rays or 100 MeV/u carbon ions. For each point, different numbers of cells (150–900) were analysed. Therefore, for comparison, numbers of complex exchanges corresponding to 100 cells are given in the Table.

Dose (Gy)	Chromosome 2		Chromosome 4		Chromosome 5	
	X-rays	carbon ions	X-rays	carbon ions	X-rays	carbon ions
<b>MCF-7</b>						
1	10	48	7	16	5	50
2	18	50	16	14	14	140
3	16	48	8	36	6	191
4	86	72	20	58	90	139
<b>WiDr</b>						
1	3	11	0	7	0	3
2	10	19	0	14	4	20
3	14	25	9	40	7	51
4	49	80	19	67	21	87

and carbon ions. In MCF-7 cells, after irradiation with  $D = 1$  Gy, the proportion of these cells increases steeply after irradiation in Bragg peak, reaching a value of about 50%. In contrast, in WiDr cells, very low numbers were observed. In these resistant cells, irradiation with  $D = 4$  Gy in Bragg peak was necessary in order to achieve such a high proportion of cells with complex aberrations. Only then, the relative proportion of cells with complexes reached about 50%, as detected by sFISH. In MCF-7 cells irradiated with  $D = 4$  Gy in Bragg peak, mitotic index was very low and chromosomes and the few metaphases still present were so severely damaged that no aberration analysis was possible. After irradiation with  $D = 1$  Gy in Bragg peak,

using sFISH we also detected complexes involving five chromosomes: 7% of total complexes in WiDr cells and 15% in MCF-7 cells.

#### Insertions

This aberration type is included in our complex aberrations data. The relative proportion of insertions was very different in MCF-7 and WiDr cells. In WiDr cells, insertions were not the predominant complex type aberration. Nevertheless, their relative proportion increased strongly after irradiation with carbon ions as compared with X-rays. In MCF-7 cells, insertions were more frequent than in WiDr cells. The data are summarized in

**Table 2.** Relative proportions of insertions observed in WiDr and MCF-7 cells irradiated with either 200 kV X-rays or carbon ions of different energies, with doses D = 1 Gy or D = 4 Gy. The percentage of insertions was calculated as a relative proportion of cells containing insertions within the class of cells containing any detectable complex exchanges.

Cell line	Dose D = 1 Gy	Proportion of insertions (%)	Dose D = 4 Gy	Proportion of insertions (%)
WiDr	200 kV X-rays	0	200 kV X-rays	3
	100 MeV/u carbon ions	0	100 MeV/u carbon ions	16
	Bragg peak carbon ions	9	Bragg peak carbon ions	17
MCF-7	200 kV X-rays	19	200 kV X-rays	17
	100 MeV/u carbon ions	31	100 MeV/u carbon ions	24
	Bragg peak carbon ions	22	Bragg peak carbon ions	n.d.

Table 2. In MCF-7 cells, similar relative proportions of insertions were observed after irradiation with X-rays and carbon ions. This proportion was practically dose independent. In WiDr cells, after irradiation with D = 1 Gy of X-rays, only a few insertions could be detected. For D = 4 Gy, the proportion increased, but it was similar for carbon ions of either ionisation density.

## Discussion

### *Apparently simple dicentrics and translocations*

The multiple damaged sites induced by carbon ions cannot often be processed by repair enzymes or they are repaired incorrectly (Heilmann et al., 1996; Stenerlow et al., 1996). Consequently, a higher proportion of unrepaired and misrepaired damage can be expected for high-LET particles such as alpha particles, neutrons, or ions. However, as the density of DNA lesions that are possible candidates for complex exchanges increases, yields of simple dicentrics or translocations might decrease due to a simultaneous increase in the proportion of complex exchanges. This effect was observed in MCF-7 cells with respect to dicentrics. The yields of apparently simple dicentrics were lower in MCF-7 cells than in WiDr cells, in spite of many more total dicentrics found after Giemsa staining observed in MCF-7 cells as compared with WiDr cells (Hofman-Huether, 2002). As FISH analysis of dicentrics and complexes has proven, most dicentrics actually belonged to complex exchanges. A similar observation was reported by Durante et al. (2002) for normal lymphocytes. In the dose range studied, this effect was, however, not yet observed in WiDr cells.

### *Clustered damage and complex aberration formation*

A high proportion of complex-type aberrations, including rare forms such as simple and multiple insertions, can be expected to be formed in cells irradiated with high-LET radiations (Bauchinger and Schmid, 1998; Anderson et al., 2000; Ritter et al., 2002). In normal cells, a high proportion of complex aberrations including insertions has been reported (e.g. Wu et al., 1997; Durante et al., 1998; Anderson et al., 2000). For lymphocytes irradiated with  $^{56}\text{Fe}$  ions, Durante et al. (2002) found under application of the sophisticated mFISH method that most aberrations were actually complex. For

tumour cells, we applied sFISH and therefore, the observed yields of complex aberrations are underestimated. Nevertheless, after irradiation with carbon ions in extended Bragg peak, about 50% of the cells could be detected that contained at least one complex exchange. However, in MCF-7 cells this effect was observed after irradiation with D = 1 Gy, whereas in radioresistant WiDr cells a dose D = 4 Gy was needed. After irradiation with X-rays and D = 4 Gy, about 35% of MCF-7 cells and about 10% of WiDr cells contained at least one complex exchange as detected with sFISH. Insertions were reported to predominate after high-LET irradiation in human fibroblasts (Griffin et al., 1995) and Chinese hamster splenocytes (Grigorova et al., 1998). In contrast, insertions did not represent the major complex-type exchange in human lymphocytes (Anderson et al., 2000). Similar to lymphocytes, insertions were not the predominant complex type aberration in WiDr and MCF-7 cells where higher-order complexes were more frequent. Their relative proportion increased strongly after irradiation with carbon ions as compared with X-rays in WiDr cells, but it was quite constant for both radiation types in MCF-7 cells. The residual, i.e. mostly unrepaired proportion of DNA DSBs amounts 20% and 10% in MCF-7 and WiDr cells, respectively (Olive et al., 1994). This moderate difference in DSB rejoining cannot thus explain the large differences in survival radiosensitivity and in radiation-induced aberration spectra observed in these cell lines. Exchanges resulting in misrepair products cannot, however, be detected by a DSB rejoining assay. As our aberration data show, misrepair takes place apparently more frequently in MCF-7 cells than in WiDr cells. Nonhomologous end joining seems to function in both cell lines normally since DNA-PKcs, Ku70, and Ku80 foci could be detected after irradiation (Hofman-Huether, 2002). In MCF-7 cells, complex exchanges were induced by far lower doses than in WiDr cells. The large differences in the yields and spectra of complex exchanges cannot be easily explained. One possible reason for this could be a different chromatin topology present in the studied cells. FISH studies have demonstrated that chromosomes in interphase nuclei form individual territories that are irregularly shaped distinct units containing chromosome subdomains that do not intermingle (e.g. Zink et al., 1998; Visser and Aten, 1999). In this context, our findings would imply an increased density of chromatin and/or larger distances among individual chromosome domains in WiDr cells as compared with MCF-7 cells, as a pos-

sible cause of the observed large differences between the corresponding yields and spectra of complex exchanges. Thus, in agreement with the conclusions of Anderson et al. (2000), nuclear architecture could be an important factor, determining the complexity of aberration spectra observed in a particular cell type.

In summary, increased relative biological effectiveness, i.e. increased RBE values were observed for carbon ions in a resistant tumour cell line for the induction of clonogenic cell death and for chromosome aberrations as well. For both radiation types studied, X-rays and carbon ions, the yields of apparently simple translocations including chromosomes 2, 4, and 5 were much higher than the corresponding yields of apparently simple dicentric chromosomes. Yields of complex exchanges increased largely in both tumour cell lines irradiated with carbon ions. This could be expected due to clustered damage induced

by ions since clustering of damaged sites within proximal chromosomes leads more often to complex-type exchanges arising from interactions among three and more chromosomes. Large differences in aberration yields and spectra as observed in the two studied cell lines point towards an important role of chromatin in the process of the formation of complex exchanges, and thus different chromatin organisation in different tumour cell lines. In this regard, it will be of interest to examine these differences by more powerful microscopic methods.

## Acknowledgements

The authors thank Dr. M. Scholz (GSI, Darmstadt) for his generous help with dosimetry and irradiation with carbon ions, and Dr. S. Ritter for support and discussions.

## References

- Anderson RM, Marsden SJ, Wright EG, Kadhim MA, Goodhead DT, Griffin CS: Complex chromosome aberrations in peripheral blood lymphocytes as a potential biomarker of exposure to high-LET alpha-particles. *Int J Radiat Biol* 76:31–42 (2000).
- Bauchinger M, Schmid E: LET dependence of yield ratios of radiation-induced intra- and interchromosomal aberrations in human lymphocytes. *Int J Radiat Biol* 74:17–25 (1998).
- Durante M, Furusawa Y, George K, Gialanella G, Greco O, Grossi G, Matsufuji N, Pugliese M, Yang TC: Rejoining and misrejoining of radiation-induced chromatin breaks. IV. Charged particles. *Radiat Res* 149:446–454 (1998).
- Durante M, Yamada S, Ando K, Furusawa Y, Kawata T, Majima H, Nakano T, Tsujii H: X-rays vs. carbon-ion tumor therapy: cytogenetic damage in lymphocytes. *Int J Radiat Oncol Biol Phys* 47:793–798 (2000).
- Durante M, George K, Wu H, Cucinotta FA: Karyotypes of human lymphocytes exposed to high-energy iron ions. *Radiat Res* 158:581–590 (2002).
- Goodhead DT: Microscopic features of dose from radionuclides, particularly emitters of alpha-particles and Auger electrons. *Int J Radiat Biol* 60:550–553 (1991).
- Goodwin E, Blakely E, Ivery G, Tobias C: Repair and misrepair of heavy-ion-induced chromosomal damage. *Adv Space Res* 9:83–89 (1989).
- Griffin CS, Marsden SJ, Stevens DL, Simpson P, Savage JR: Frequencies of complex chromosome exchange aberrations induced by <sup>238</sup>Pu alpha-particles and detected by fluorescence in situ hybridization using single chromosome-specific probes. *Int J Radiat Biol* 67:431–439 (1995).
- Grigorova M, Brand R, Xiao Y, Natarajan AT: Frequencies and types of exchange aberrations induced by X-rays and neutrons in Chinese hamster splenocytes detected by FISH using chromosome-specific DNA libraries. *Int J Radiat Biol* 74:297–314 (1998).
- Haberer T, Becher W, Schardt D, Kraft G: Magnetic scanning system for heavy ion therapy. *Nuc Inst and Methods in Phys Res A* 330:296–305 (1993).
- Heilmann J, Taucher-Scholz G, Haberer T, Scholz M, Kraft G: Measurement of intracellular DNA double-strand break induction and rejoining along the track of carbon and neon particle beams in water. *Int J Radiat Oncol, Biol, Phys* 34:599–608 (1996).
- Hofman-Huether H: Wirkung schwerer Ionen auf strahlenresistente und strahlensensitive Tumorzellen. PhD Thesis, University of Göttingen, Göttingen (2002).
- Hoglund E, Stenerlow B: Induction and rejoining of DNA double-strand breaks in normal human skin fibroblasts after exposure to radiation of different linear energy transfer: possible roles of track structure and chromatin organization. *Radiat Res* 155:818–825 (2001).
- Ofuchi T, Suzuki M, Kase Y, Ando K, Isono K, Ochiai T: Chromosome breakage and cell lethality in human hepatoma cells irradiated with X rays and carbon-ion beams. *J Radiat Res (Tokyo)* 40:125–133 (1999).
- Olive PL, Banath JP, MacPhail HS: Lack of a correlation between radiosensitivity and DNA double-strand break induction or rejoining in six human tumor cell lines. *Cancer Res* 54:3939–3946 (1994).
- Pinto M, Prise KM, Michael BD: Double strand break rejoining after irradiation of human fibroblasts with X rays or alpha particles: PFGE studies and numerical models. *Radiat Prot Dosimetry* 99:133–136 (2002).
- Ritter S, Nasonova E, Gudowska-Novak E: Effect of LET on the yield and quality of chromosomal damage in metaphase cells: a time-course study. *Int J Radiat Biol* 78:191–202 (2002).
- Rydberg B: Clusters of DNA damage induced by ionizing radiation: formation of short DNA fragments. II. Experimental detection. *Radiat Res* 145:200–209 (1996).
- Rydberg B, Löbrich M, Cooper PK: DNA double-strand breaks induced by high-energy neon and iron ions in human fibroblasts. I. Pulsed-field gel electrophoresis method. *Radiat Res* 139:133–141 (1994).
- Simpson PJ, Savage JR: Identification of X-ray-induced complex chromosome exchanges using fluorescence in situ hybridization: a comparison at two doses. *Int J Radiat Biol* 66:629–632 (1994).
- Stenerlow B, Blomquist E, Grusell E, Hartman T, Carlsson J: Rejoining of DNA double-strand breaks induced by accelerated nitrogen ions. *Int J Radiat Biol* 70:413–420 (1996).
- Stenerlow B, Hoglund E, Carlsson J, Blomquist E: Rejoining of DNA fragments produced by radiations of different linear energy transfer. *Int J Radiat Biol* 76:549–557 (2000).
- Stenerlow B, Hoglund E, Carlsson J: DNA fragmentation by charged particle tracks. *Adv Space Res* 30:859–863 (2002).
- Suzuki M, Kase Y, Kanai T, Ando K: Correlation between cell death and induction of non-rejoining PCC breaks by carbon-ion beams. *Adv Space Res* 22:561–568 (1998).
- Suzuki M, Piao C, Hall EJ, Hei TK: Cell killing and chromatid damage in primary human bronchial epithelial cells irradiated with accelerated <sup>56</sup>Fe ions. *Radiat Res* 155:432–439 (2001).
- Taucher-Scholz G, Heilmann J, Kraft G: Induction and rejoining of DNA double-strand breaks in CHO cells after heavy ion irradiation. *Adv Space Res* 18:83–92 (1996).
- Testard I, Dutrillaux B, Sabatier L: Chromosomal aberrations induced in human lymphocytes by high-LET irradiation. *Int J Radiat Biol* 72:423–433 (1997).
- Virsik-Peuckert P, Rave-Fränk M, Schmidberger H: Further studies on the possible relationship between radiation-induced reciprocal translocations and intrinsic radiosensitivity of human tumor cells. *Radiother Oncol* 40:111–119 (1996).
- Visser AE, Aten JA: Chromosomes as well as chromosomal subdomains constitute distinct units in interphase nuclei. *J Cell Sci* 112:3353–3360 (1999).
- Wu H, Durante M, George K, Yang TC: Induction of chromosome aberrations in human cells by charged particles. *Radiat Res* 148:102–107 (1997).
- Zink D, Cremer T, Saffrich R, Fischer R, Trendelenburg MF, Ansorge W, Stelzer EH: Structure and dynamics of human interphase chromosome territories in vivo. *Hum Genet* 102:241–251 (1998).

# Induction of homologous recombination in the *hprt* gene of V79 Chinese hamster cells in response to low- and high-LET irradiation

G. Olsson, S. Czene, D. Jenssen and M. Harms-Ringdahl

Department of Genetics, Microbiology and Toxicology, Stockholm University, Stockholm (Sweden)

**Abstract.** Dense ionization tracks from high linear energy transfer (LET) radiations form multiple damaged sites (MDS), which involve several types of DNA lesions in close vicinity. The primary DNA damage triggers sensor proteins that activate repair processes, cell cycle control or eventually apoptosis in subsequent cellular responses. The question how homologous recombination (HR) and non-homologous end joining (NHEJ) interact in the repair of radiation-induced DNA damage of MDS type has been addressed in different model systems but several questions remain to be answered. We have therefore challenged cells with treatments of ionizing radiation of different qualities to investigate whether primary DNA damages of different complexity are reflected in the processes of repair by HR as well as cell survival. We used the V79 derived SPD8 cell line to determine the induction of HR in the *hprt*

exon 7 and clonogenic assay for survival in response to radiation. SPD8 cells were irradiated with  $\gamma$ -rays ( $^{137}\text{Cs}$  0.5 keV/ $\mu\text{m}$ ), boron ions (40 and 80 keV/ $\mu\text{m}$ ) and nitrogen ions (140 keV/ $\mu\text{m}$ ), with doses up to 5 Gy. Analysis of clonogenic survival showed that B-ions (80 keV/ $\mu\text{m}$ ) and N-ions were more toxic than  $\gamma$ -rays, 4.1 and 5.0 times respectively, while B-ions at 40 keV/ $\mu\text{m}$  were 2.0 times as toxic as  $\gamma$ -rays. Homologous recombination in the cells exposed to B-ions (80 keV/ $\mu\text{m}$ ) increased 2.9 times, a significant response as compared to cells exposed to  $\gamma$ -rays, while for B-ions (40 keV/ $\mu\text{m}$ ) and N-ions a nonsignificant increase in HR of 1.2 and 1.4, respectively, was observed. We hypothesize that the high-LET generated formation of MDS is responsible for the enhanced cytotoxicity as well as for the mobilization of the HR machinery.

Copyright © 2003 S. Karger AG, Basel

DNA damage induced by ionizing radiation (IR) may have deleterious genotoxic consequences, such as genomic instability caused by mutations and chromosomal changes, which may lead to cell transformation and cancer development (Little, 2000; Pfeiffer et al., 2000; Van Gent et al., 2001). Ionizing

radiation deposits energy in tracks of moving charged particles within the cell. While low linear energy transfer (low-LET) radiations, such as X-rays or  $\gamma$ -rays, induce a relatively low density of ionizations along the track ( $\sim 0.5$  keV/ $\mu\text{m}$ ), each track of high-LET radiation is more dense in terms of many thousands of ionizations ( $\sim 50$ – $150$  keV/ $\mu\text{m}$ ) (Goodhead, 1992; Singleton et al., 2002). Also, the spatial distribution of energy differs; a dose of 1 Gy of low-LET irradiation corresponds to  $\sim 1000$  sparsely ionizing tracks, while in the case of high-LET, 1 Gy corresponds to  $\sim 4$  densely ionizing tracks (Goodhead, 1994).

The spatial distribution of DNA damage will also be influenced by chromatin structure and organisation, where consequences of DNA damage along the ionization track will depend on the functional and structural properties of the chromatin region exposed (Rydberg, 2001). DNA lesions generated by IR include DNA single- and double-strand breaks and base

This work was supported by grants from the Swedish Radiation Protection Authority and the Swedish Cancer Society.

Received 27 October 2003; accepted 10 November 2003.

Request reprints from: Dr. Mats Harms-Ringdahl, Department of Genetics  
Microbiology and Toxicology, Stockholm University  
S-106 91 Stockholm (Sweden); telephone: +46 8 164109  
fax: +46 8 164315; e-mail: mats.harms-ringdahl@genetics.su.se.

Present address of S.C.: AstraZeneca R&D Södertälje  
Genetic Toxicology, Safety Assessment  
S-151 85 Södertälje, Sweden.

damages, that are repaired by different repair pathways (Hoeijmakers, 2001). DNA double-strand breaks (DSB), are the most lethal DNA damages which might be repaired by two distinct pathways, non-homologous end joining (NHEJ) and homologous recombination (HR) (Kanaar et al., 1998; Jackson, 2002). HR in response to radiation-induced damage is suggested to be an error-free repair pathway preferentially operating in the S-phase of the cell cycle. HR may also process the damage by utilizing the sister chromatid as template, resulting in gene conversion (Johnson and Jasin, 2000, 2001). HR is also required to resolve stalled replication forks encountering chemically induced damage (Haber, 1999; Arnaudeau et al., 2001; Henry-Mowatt et al., 2003). In contrast to HR, NHEJ utilizes little or no homology to join DNA ends (Jeggo, 1998). NHEJ is the primary pathway of DSB repair in G1-/early S-phase of the cell cycle, while both HR and NHEJ contribute to repair DSBs introduced during late S/G2-phase of the cell cycle (Rothkamm et al., 2003).

Previous studies on the kinetics of DSB repair indicate the existence of a fast and a slow phase (Ahnström et al., 2000; Stenerlöv et al., 2000; Wang et al., 2001) suggesting that NHEJ dominates the fast phase (Wang et al., 2001). The nature of repair events during the slow phase is not yet fully understood. It has been postulated that the repair processes of radiation-induced DSBs are dependent upon radiation quality and the structural complexity of DSBs (Pastwa et al., 2003). However, according to Wang and colleagues the contribution to the slow phase of DSB repair was not compatible with the capacity and status of HR (Wang et al., 2001).

A better understanding of the mechanisms leading to mobilization of a specific repair mechanism in response to radiation quality, such as low doses, low dose rates and different LET will also have implications for risk assessment regarding various biological endpoints such as genomic instability, carcinogenesis and aging. Moreover, a better knowledge of the mechanisms may have important implications for a therapeutic use of radiation. Hence, it is of interest to understand the interaction of the repair pathways in the course of radiation-induced DNA damage, in particular those of a more complex type. In this study we focus on the role of HR for repair of DNA damage in Chinese hamster cells induced by low- and high-LET ionizing radiation,  $\gamma$ -rays, nitrogen ions or boron ions. The cell line used exhibits a tandem duplication of exon 7 in its endogenous *hprt* gene, making it useful for determination of intrachromosomal homologous recombination (Helleday et al., 1998).

## Materials and methods

### Cells

The SPD8 cell line derived from V79 Chinese hamster cells (Daré et al., 1996) was used in all experiments. Cells were cultured in Dulbecco's Modified Eagle Medium, 1000 mg/l D-glucose, sodium pyruvate (DMEM), supplemented with 9% fetal bovine serum, penicillin (90 U/ml) and streptomycin (90  $\mu$ g/ml), in a 37°C humidified CO<sub>2</sub> incubator. To prevent spontaneous reversion, 6-thioguanine (5  $\mu$ g/ml) was used during maintenance of the cell line but removed prior to experiments. Cells were seeded in 175-cm<sup>2</sup> flasks two days before each experiment with 3.5–4.0  $\times$  10<sup>6</sup> cells/flask, thus at time of radiation cells were in log-phase, which was verified by cell cycle analysis (Fig. 3).

### Chemicals

DMEM, fetal bovine serum, penicillin-streptomycin, Hanks' balanced salt, and trypsin-EDTA were purchased from Invitrogen AB (Sweden). 6-thioguanine (2-amino-6-purinethiol, 98%), hypoxanthine (6-hydroxypurine, 99%), L-azaserine (o-Diazoacetyl-L-serine), and thymidine (1-[2-Deoxy- $\beta$ -D-ribofuranosyl]-5-methyluracil, 99%) were obtained from Sigma-Aldrich AB (Sweden).

### Exposure conditions

Cells in suspension were exposed to radiation. Adherent cells were washed twice in Hanks' balanced salt without Ca<sup>2+</sup> and Mg<sup>2+</sup>, trypsinized and resuspended as described below. Cells were centrifuged for 10 min at 200 g and resuspended in medium to the final volume of 135–300  $\mu$ l depending on the chamber depth. The cell suspensions were placed into special chambers for exposure to N- or B-ions. Chambers used for N-ion exposure were 22 mm in diameter and had a depth of 1 mm; chambers used for B-ion exposure had the same diameter but the depth was 0.5 mm. For exposure to  $\gamma$ -rays the same chambers were used as for N-ions. A 0.2-mm-thick plastic slip was used to cover the chamber well. Exposures of exponentially growing cells (~60% S- and ~30% G1-phase) were performed at room temperature; the cells were then reseeded into new flasks for 4–5 h of recovery in a 37°C humidified CO<sub>2</sub> incubator.

### Nitrogen ion irradiation

The nitrogen ion irradiations were carried out at the Biomedical Unit at the The Svedberg Laboratory in Uppsala, essentially as previously described (Stenerlöv et al., 1996). In brief, <sup>14</sup>N-ions were accelerated to energies of 45 MeV/u. The particle energy in the middle of the 1-mm-deep chamber was 18.5 MeV/u and the mean unrestricted LET was around 140 keV/ $\mu$ m ( $\pm$  20 keV/ $\mu$ m covering 68% of the cells).

### Boron ion irradiation

The irradiations with boron ions were also carried out at the Biomedical Unit at the The Svedberg Laboratory, Uppsala, mainly as previously described (Persson et al., 2002). Briefly, cells in suspension were irradiated in an 0.5-mm-deep chamber at a mean energy of 36 MeV/u corresponding to a mean LET of 40 keV/ $\mu$ m (max LET variation =  $\pm$  2 keV/ $\mu$ m) or at a mean energy of 16 MeV/u corresponding to a mean LET of 80 keV/ $\mu$ m (max LET variation =  $\pm$  8 keV/ $\mu$ m). Details of beams and dosimetry are described by Höglund and Stenerlöv (manuscript in preparation).

### $\gamma$ Irradiation

Irradiation with  $\gamma$ -rays was carried out at Stockholm University in a <sup>137</sup>Cs source at a dose rate of 0.56 Gy/min.

### Recombination assay and clonogenic survival

To observe early events of homologous recombination in S-phase we used only 4–5 h of expression before selection of revertants. Four to five hours after treatment, cells were rinsed twice with Hanks' balanced salt without Ca<sup>2+</sup> and Mg<sup>2+</sup>, trypsinized and counted using a Coulter Cell Counter. Cloning ability was determined by seeding 3 Petri dishes (100 mm) per dose (500 cells/dish) and the number of clones was scored after 7–8 days incubation. Selection of revertants was performed by seeding 4 Petri dishes (100 mm) per dose (3  $\times$  10<sup>6</sup> cells/dish) in the presence of hypoxanthine-L-azaserine-thymidine, HAsT (50  $\mu$ M hypoxanthine, 10  $\mu$ M L-azaserine, 5  $\mu$ M thymidine). The selection dishes were incubated for 10–12 days. Colonies were fixed and stained with methylene blue/methanol (4 g/l). The reversion frequency (RF) was calculated as the total number of revertants on the selection plates divided by the total number of cells cloned under the same experimental condition. The cloning ability of this cell line is about 80%  $\pm$  7 (SE).

### Cell cycle analysis

Determination of the cell cycle distributions directly before irradiation and 4–5 h post-irradiation were performed with a fluorescence-activated cell sorter FACSCalibur™ System (Becton Dickinson). For FACS analysis, 500,000 cells were collected, fixed with 70% EtOH, washed in PBS, treated with ribonuclease A (100  $\mu$ g/ml) and stained with propidium iodide (5  $\mu$ g/ml). Data on 40,000 cells were then collected on a FACSCalibur according to manufacturer's procedures. The cell cycle analysis was done with WinMdi 2.8 and Cylchred.

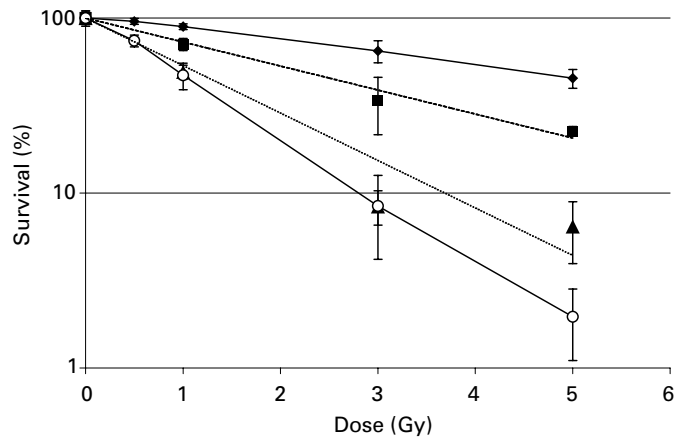


**Fig. 1.** Survival curves of SPD8 cells after treatments with  $\gamma$ -rays (closed diamonds), B-ions (40 keV/ $\mu$ m closed squares, 80 keV/ $\mu$ m closed triangles), N-ions (open circles). Data are the mean of 3–4 experiments. Standard errors ( $\pm$ ) are indicated as error bars.

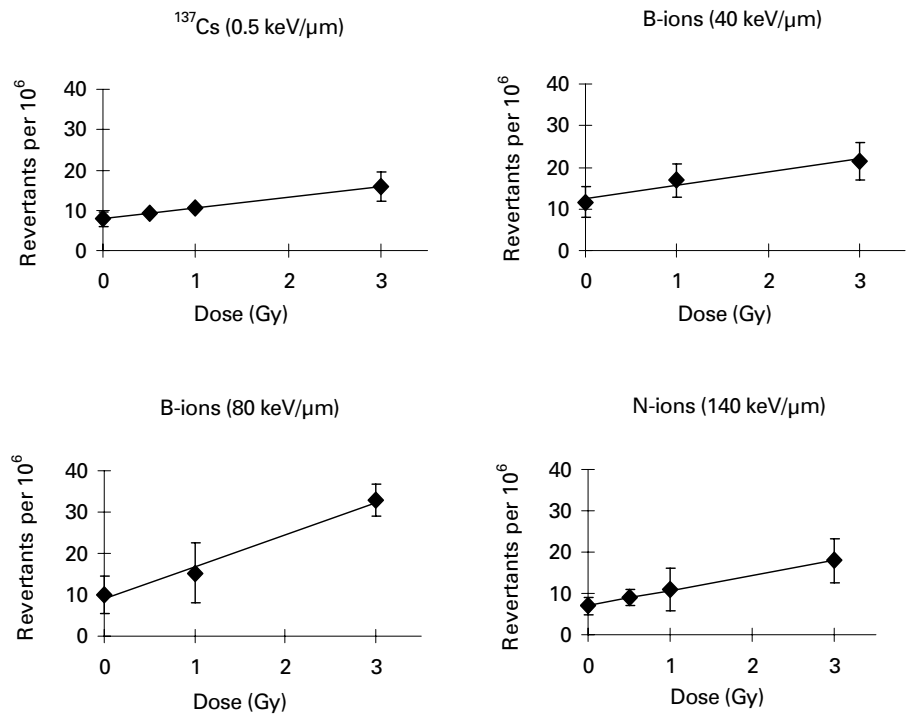


**Fig. 2.** Reversion to a functional *hprt* gene by intrachromosomal homologous recombination as a function of dose after exposure to  $\gamma$ -rays, B-ions and N-ions. Regression lines are indicated. Data are the mean of 3–4 experiments. Standard errors ( $\pm$ ) are indicated as error bars.

## Results

### Cell survival and reversion by homologous recombination

Differences between high- and low-LET irradiated cells with respect to survival (Fig. 1) and HR (Fig. 2) were observed. Radiation with LET in the range of 0.5–140 keV/ $\mu$ m resulted in marked changes in cell survival. The relative biological effectiveness (RBE) for 50% survival for B-ions (80 keV/ $\mu$ m) was 4.1, for N-ions 5.0 and for B-ions (40 keV/ $\mu$ m) 2.0 (Table 1). A linear and statistically significant dose response for HR was found after treatments with all four radiation qualities. The slope of the dose response for HR frequency in cells induced by B-ions (80 keV/ $\mu$ m) was significantly higher as compared to cells exposed to  $\gamma$ -rays. The RBE values for HR are summa-

**Table 1.** The relative biological effectiveness (RBE) of various LET qualities for colony forming ability (survival) and homologous recombination. Estimated from the slope of the dose-response relations. Dose-response curves were analyzed statistically by linear regression. The slopes were tested for significance versus  $b = 0$  by t test.

	RBE at 50 % survival	RBE for HR
$\gamma$ -rays	1.0	1.0
B-ions (40 keV/ $\mu$ m)	2.0	1.2
B-ions (80 keV/ $\mu$ m)	4.1	2.9 <sup>a</sup>
N-ions	5.0	1.4

<sup>a</sup>  $P < 0.001$ .

When comparing B-ions 80 keV/ $\mu$ m and  $\gamma$ -rays, the difference in slopes was tested using t test.

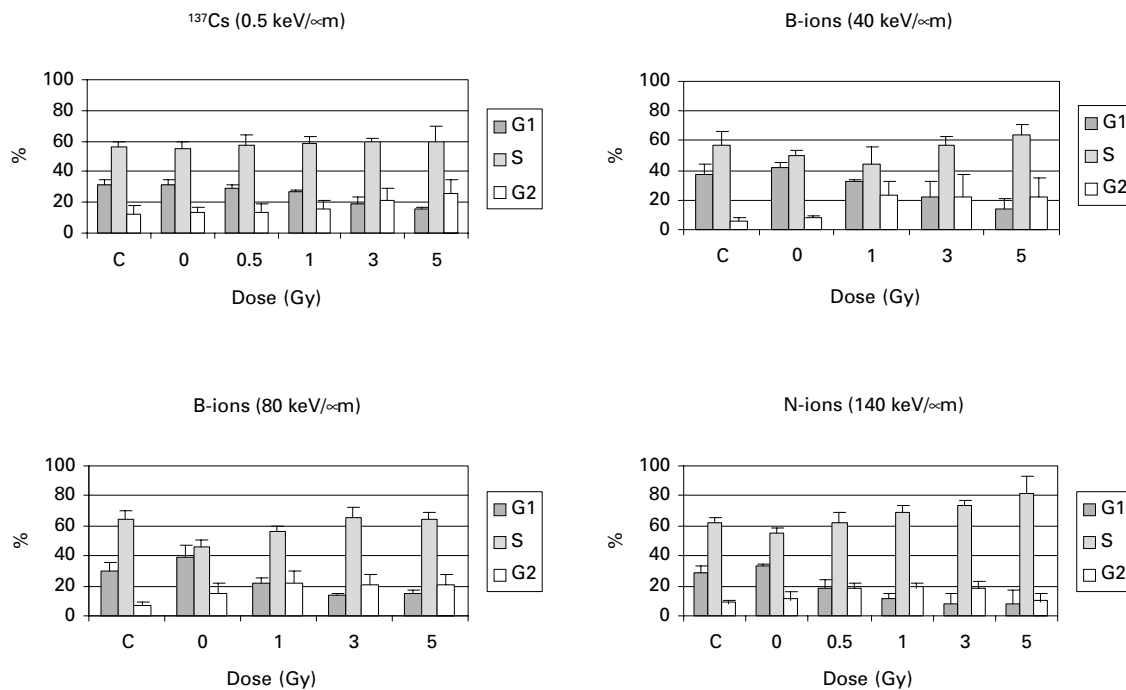


**Fig. 3.** Changes in cell cycle distribution in SPD8 cells. Each column shows the cell cycle distribution 4 h post-irradiation except for the column marked with a C. This column shows the distribution immediately before irradiation.  $\gamma$ -Ray and B-ion data are the mean values of 3 experiments, N-ion data are the mean values of 4 experiments. Standard deviations (+) are indicated as error bars.

ized in Table 1. HR in cells exposed to B-ions (80 keV/ $\mu\text{m}$ ) was enhanced 2.9 times as compared to cells exposed to  $\gamma$ -rays. N-ions enhanced HR 1.4 times and B-ions (40 keV/ $\mu\text{m}$ ) 1.2 times.

#### Cell cycle distribution

Cells exposed to  $\gamma$ -rays responded with a dose-dependent outflow from G1-phase that did not correlate with significant changes in the S- and G2-population except for a weak increase in the G2-population at the highest dose (Fig. 3). On the other hand, cells exposed to high-LET radiations showed an outflow from G1-phase with a simultaneous accumulation of cells in S-phase that was both dose- and LET-dependent (Fig. 3).

#### Discussion

The fidelity of the mechanisms that mobilize appropriate repair pathways in response to DNA damage produced by different radiation qualities may have an impact on various biological endpoints such as genomic instability, carcinogenesis and aging (Little, 2000; Pfeiffer et al., 2000). The IR induced lesions may arise either by direct interaction producing strand breaks and base damages, or indirect, via radiolysis of water forming reactive oxygen species such as  $\text{OH}^{\bullet}$  radicals producing oxidized bases and SSBs. Two or more closely spaced damages on opposing strands within one or a few helical turns, defined as DNA damage clustering (Goodhead, 1994; Ward, 1994, 1995) may compromise the repair machinery

(Goodhead, 1994; Dianov et al., 2001). Nikjoo and co-workers have estimated that almost 30% of the DSBs are of the complex type for low-LET radiation, increasing to about 70% for high-LET. If base damages are considered in addition to strand breaks these figures rise to 60% and 90% for low- and high-LET, respectively (Nikjoo et al., 1999, 2001). Hence it is of interest to understand the interaction of the repair pathways in the course of radiation-induced DNA damage of different complexity.

In the present study we focus on the involvement of HR in DNA damage processing after exposure of cells to low- and high-LET ionizing radiation,  $\gamma$ -rays and N-ions or B-ions, respectively. For all radiation qualities there was an outflow from G1-phase and this is probably caused by a defective G1-phase checkpoint. This may be explained by the fact that the cell line used is derived from V79 Chinese hamster cells which were found to exhibit two base substitutions in the *p53* gene (Arnaudeau et al., 1999) and consequent loss of *p53* function (Chaung et al., 1997). In cells exposed to  $\gamma$ -rays, the G1 outflow was followed by a weak increase in the G2-population at the highest dose (Fig. 3), which might be explained by a transient G2-arrest independent of *p53* function (DeSimone et al., 2003). On the other hand, cells exposed to high-LET radiation showed a simultaneous accumulation of cells in S-phase that was both dose- and LET-dependent (Fig. 3), suggesting an involvement of a *p53*-independent intra S-phase arrest (Bartek and Lukas, 2001).

HR in cells exposed to low-LET radiation increases relative to control by 2.7 events/Gy per  $10^6$  surviving cells (from Fig. 2).

The target size for HR in the SPD8 model system is about 5 kb (Helleday et al., 1998) thus the resolution to detect all HR events, assuming they are randomly distributed over the whole genome ( $3 \times 10^6$  kb), is approximately  $1.7 \times 10^{-6}$ . On the single cell this implies that 1 Gy of low-LET radiation correspond to 5 HR events/Gy. The yield of DSBs per Gy of low-LET radiation has been proposed to be in the range of 25 (Radulescu et al., 2004), a level that led us to the assumption that about 20% of all DSBs in the surviving population is handled by HR, a calculation that is in agreement with the dominating role in DSB repair suggested for NHEJ (Jeggo, 1998).

In response to 1 Gy of high-LET the radiation induced HR will be 13 HR events per Gy, as calculated from data presented in this study, while the yield of DSBs/Gy of high-LET radiation recently has been estimated to be approximately 40 (Radulescu et al., 2004). Thus 33% of these DSBs might be associated with repair by HR.

The quantitative estimates discussed above cannot readily be compared to literature that provide information based on

bulk response since the results presented above reflect the mobilisation of repair pathways in the surviving fraction of cells only. The observed 60% increased levels of HR in high-LET compared to low-LET exposure may suggest that MDS rather than simple DSBs mobilize HR.

The SPD8 recombination assay and other methods now available thus provide unique possibilities to further explore the signalling properties of the primary damage and the mobilization of repair pathways and their fidelity. The present results encourage further studies on the repair of MDS in mammalian cells.

## Acknowledgements

We wish to thank Assoc. Prof. Bo Stenerlöv PhD for experimental support and The Swedberg Laboratory, Uppsala for providing beam time.

## References

- Ahnström G, Nygren J, Eriksson S: The effect of dimethyl sulphoxide on the induction and repair of double-strand breaks in human cells after irradiation with gamma-rays and accelerated ions: rapid or slow repair may depend on accessibility of breaks in chromatin of different compactness. *Int J Radiat Biol* 76:533–538 (2000).
- Arnaudeau C, Helleday T, Jenssen D: The RAD51 protein supports homologous recombination by an exchange mechanism in mammalian cells. *J Mol Biol* 289:1231–1238 (1999).
- Arnaudeau C, Lundin C, Helleday T: DNA double-strand breaks associated with replication forks are predominantly repaired by homologous recombination involving an exchange mechanism in mammalian cells. *J Mol Biol* 307:1235–1245 (2001).
- Bartek J, Lukas J: Mammalian G1- and S-phase checkpoints in response to DNA damage. *Curr Opin Cell Biol* 13:738–747 (2001).
- Chang W, Mi LJ, Boorstein RJ: The p53 status of Chinese hamster V79 cells frequently used for studies on DNA damage and DNA repair. *Nucleic Acids Res* 25:992–994 (1997).
- Daré E, Zhang LH, Jenssen D: Characterization of mutants involving partial exon duplications in the hprt gene of Chinese hamster V79 cells. *Somat Cell Mol Genet* 22:201–210 (1996).
- DeSimone JN, Bengtsson U, Wang X, Lao XY, Redpath JL, Stanbridge EJ: Complexity of the mechanisms of initiation and maintenance of DNA damage-induced G2-phase arrest and subsequent G1-phase arrest: TP53-dependent and TP53-independent roles. *Radiat Res* 159:72–85 (2003).
- Dianov GL, O'Neill P, Goodhead DT: Securing genome stability by orchestrating DNA repair: removal of radiation-induced clustered lesions in DNA. *Bioessays* 23:745–749 (2001).
- Goodhead DT: Track structure considerations in low dose and low dose rate effects of ionizing radiation. *Adv Radiat Biol* 16:7–44 (1992).
- Goodhead DT: Initial events in the cellular effects of ionizing radiations: clustered damage in DNA. *Int J Radiat Biol* 65:7–17 (1994).
- Haber JE: DNA recombination: the replication connection. *Trends Biochem Sci* 24:271–275 (1999).
- Helleday T, Arnaudeau C, Jenssen D: A partial hprt gene duplication generated by non-homologous recombination in V79 Chinese hamster cells is eliminated by homologous recombination. *J Mol Biol* 279:687–694 (1998).
- Henry-Mowatt J, Jackson D, Masson JY, Johnson PA, Clements PM, Benson FE, Thompson LH, Takeda S, West SC, Caldecott KW: XRCC3 and Rad51 modulate replication fork progression on damaged vertebrate chromosomes. *Mol Cell* 11:1109–1117 (2003).
- Hoeijmakers JH: Genome maintenance mechanisms for preventing cancer. *Nature* 411:366–374 (2001).
- Jackson SP: Sensing and repairing DNA double-strand breaks. *Carcinogenesis* 23:687–696 (2002).
- Jeggo PA: Identification of genes involved in repair of DNA double-strand breaks in mammalian cells. *Radiat Res* 150:S80–91 (1998).
- Johnson RD, Jasin M: Sister chromatid gene conversion is a prominent double-strand break repair pathway in mammalian cells. *EMBO J* 19:3398–3407 (2000).
- Johnson RD, Jasin M: Double-strand-break-induced homologous recombination in mammalian cells. *Biochem Soc Trans* 29:196–201 (2001).
- Kanaar R, Hoeijmakers JH, van Gent DC: Molecular mechanisms of DNA double strand break repair. *Trends Cell Biol* 8:483–489 (1998).
- Little JB: Radiation carcinogenesis. *Carcinogenesis* 21:397–404 (2000).
- Nikjoo H, O'Neill P, Terrissol M, Goodhead DT: Quantitative modelling of DNA damage using Monte Carlo track structure method. *Radiat Environ Biophys* 38:31–38 (1999).
- Nikjoo H, O'Neill P, Wilson WE, Goodhead DT: Computational approach for determining the spectrum of DNA damage induced by ionizing radiation. *Radiat Res* 156:577–583 (2001).
- Pastwa E, Neumann RD, Mezhevaya K, Winters TA: Repair of radiation-induced DNA double-strand breaks is dependent upon radiation quality and the structural complexity of double-strand breaks. *Radiat Res* 159:251–261 (2003).
- Persson LM, Edgren MR, Stenerlöv B, Lind BK, Hedlöf I, Jernberg AR, Meijer AE, Brahma A: Relative biological effectiveness of boron ions on human melanoma cells. *Int J Radiat Biol* 78:743–748 (2002).
- Pfeiffer P, Goedecke W, Obe G: Mechanisms of DNA double-strand break repair and their potential to induce chromosomal aberrations. *Mutagenesis* 15:289–302 (2000).
- Radulescu I, Elmroth K, Stenerlöv B: Chromatin organization contributes to non-randomly distributed double-strand breaks after exposure to high-LET radiation. *Radiat Res* 161:1–8 (2004).
- Rothkamm K, Kruger I, Thompson LH, Löbrich M: Pathways of DNA double-strand break repair during the mammalian cell cycle. *Mol Cell Biol* 23:5706–5715 (2003).
- Rydberg B: Radiation-induced DNA damage and chromatin structure. *Acta Oncol* 40:682–685 (2001).
- Singleton BK, Griffin CS, Thacker J: Clustered DNA damage leads to complex genetic changes in irradiated human cells. *Cancer Res* 62:6263–6269 (2002).
- Stenerlöv B, Blomquist E, Grusell E, Hartman T, Carlsson J: Rejoining of DNA double-strand breaks induced by accelerated nitrogen ions. *Int J Radiat Biol* 70:413–420 (1996).
- Stenerlöv B, Höglund E, Carlsson J, Blomquist E: Rejoining of DNA fragments produced by radiations of different linear energy transfer. *Int J Radiat Biol* 76:549–557 (2000).
- van Gent DC, Hoeijmakers JH, Kanaar R: Chromosomal stability and the DNA double-stranded break connection. *Nat Rev Genet* 2:196–206 (2001).
- Wang H, Zeng ZC, Bui TA, Sonoda E, Takata M, Takeda S, Iliakis G: Efficient rejoining of radiation-induced DNA double-strand breaks in vertebrate cells deficient in genes of the RAD52 epistasis group. *Oncogene* 20:2212–2224 (2001).
- Ward JF: The complexity of DNA damage: relevance to biological consequences. *Int J Radiat Biol* 66:427–432 (1994).
- Ward JF: Radiation mutagenesis: the initial DNA lesions responsible. *Radiat Res* 142:362–368 (1995).



# Cytogenetic analyses in peripheral lymphocytes of persons living in houses with increased levels of indoor radon concentrations

U. Oestreicher,<sup>a</sup> H. Braselmann,<sup>b</sup> and G. Stephan<sup>a</sup>

<sup>a</sup>Federal Office for Radiation Protection, Department of Radiation Protection and Health, Oberschleißheim (Germany);

<sup>b</sup>GSF National Research Center for Environment and Health, Institute of Molecular Radiation Biology, Neuherberg (Germany)

**Abstract.** Published data concerning the effects of indoor radon exposure on the frequency of chromosome aberrations in peripheral lymphocytes of residents are contradictory. Possible reasons for this may be the low radon concentration in dwellings and/or the limited number of investigated persons. We therefore studied the relationship of domestic radon exposure and the occurrence of chromosome aberrations in peripheral lymphocytes in 61 persons living in houses with radon concentrations from 80 up to 13,000 Bq/m<sup>3</sup>. We analyzed 60,000 cells from fluorescence plus Giemsa (FPG)-stained slides. It could be clearly demonstrated that in groups of persons living in dwellings with indoor radon concentrations >200 Bq/m<sup>3</sup> the number of cells containing dicentrics and/or centric rings ( $C_{dic+cr}$ ) ( $2.45 \pm 0.50 \times 10^{-3}$ ) was significantly increased ( $p < 0.05$ ) in comparison to the control level ( $1.03 \pm 0.15 \times 10^{-3}$ ). However, there was no difference in the mean frequency of

$C_{dic+cr}$  between the groups living in dwellings with higher radon concentrations. Using the fluorescence in situ hybridization (FISH) technique for the detection of translocations, we analyzed 23,315 cells in 16 persons of the highest exposed group (>5,000 Bq/m<sup>3</sup>). The observed frequency of translocations was  $3.9 \pm 0.64 \times 10^{-3}$ . In comparison to the control group ( $2.02 \pm 0.18 \times 10^{-3}$ ), there was a slight but not statistically significant increase in the exposed group ( $P = 0.055$ ). If, however, the age of the examined persons is taken into account, the values are significantly increased ( $P < 0.05$ ) in the exposed persons older than 40 years in comparison to the age-matched controls. Since most of the translocations were found in stable cells, it is concluded that translocations are also induced in blood-forming tissue and are transmitted to peripheral blood.

Copyright © 2003 S. Karger AG, Basel

Over the last ten years, indoor radon exposure with regard to radiation protection of the general public has become a matter of interest worldwide. Epidemiological studies on indoor radon and lung cancer showed consistently a small increase in lung cancer with increasing radon exposure (Darby and Hill, 2003; Lubin, 2003) that is comparable to the results from the uranium miners studies (BEIR VI, 1999).

To examine the biological effects of radon and its decay products, some cytogenetic studies have been performed on individuals living in houses with elevated radon concentrations. However, the results published so far for chromosome aberrations are contradictory (Albering et al., 1992, 1994; Bauchinger et al., 1994, 1996; Maes et al., 1996; Lindholm et al., 1999). Possible reasons for this may be that the radon concentrations studied are too low, and/or the number of investigated individuals is too small. For this reason we investigated the relationship of domestic radon exposure and the occurrence of chromosome aberrations in peripheral blood lymphocytes of individuals living in houses with elevated radon levels, ranging from 80 to 13,000 Bq/m<sup>3</sup>.

The main target tissue of radon and its decay products is the respiratory tract. Part of the inhaled radon and its decay products is absorbed into the blood and is then transported to other organs. Because radon is easily dissolved in fat, it is also trans-

This work was supported by the Bavarian State Ministry for Regional Development and Environmental Affairs under contract FM 8129.

Received 10 September 2003; accepted 10 December 2003.

Request reprints from: Dipl. Biol. U. Oestreicher  
Federal Office for Radiation Protection  
Department of Radiation Protection and Health  
Ingolstädter Landstrasse 1, D-85764 Oberschleißheim (Germany)  
telephone: +49-(0)1888-333-2213; fax: +49-(0)-1888-333-2205  
e-mail: uoestreicher@bfs.de

**Table 1.** Frequency of cells with dic and/or cr ( $C_{dic+cr}$ )/1,000 cells and frequency of dic + cr/1,000 cells

Exposure group (Bq/m <sup>3</sup> )	Persons	Age range (years)	<sup>a</sup> S/HS	Cells scored	$C_{dic+cr}$ /1000 cells ± SEM	dic + cr/1000 cells ± SEM
I < 200	17	6–69	3/0	16,597	1.33 ± 0.34	1.75 ± 0.46
II 200–1000	13	32–80	2/1	12,436	2.33 ± 0.48	2.65 ± 0.55
without HS	12			11,407	2.45 ± 0.50	2.81 ± 0.58
III 1000–5000	15	10–78	4/2	14,668	1.91 ± 0.46	2.78 ± 0.76
without HS	13			12,620	2.06 ± 0.52	3.01 ± 0.64
IV > 5000	16	17–76	4/0	16,355	2.32 ± 0.38	2.69 ± 0.46
Expo. in total	61	6–80	13/3	60,056	1.95 ± 0.20	2.45 ± 0.28
Expo. in total without HS	58	6–80		56,979	2.00 ± 0.21	2.51 ± 0.21
Control	53	20–73	18/7	54,689	1.19 ± 0.15	1.23 ± 0.15
Control without HS	46	20–73		47,593	1.03 ± 0.15	1.03 ± 0.17

<sup>a</sup> S: smokers; HS: heavy smokers > 20 Cig./day.

ported to the stem cells of the blood-forming tissue (Lindholm et al., 1999). Here the decay products of radon accumulate in the fat tissue and the red bone marrow is chronically exposed to  $\alpha$ -particles (ICRP, 1994). The fluorescence plus Giemsa (FPG) technique was used to study the frequency of chromosome aberrations which are induced in peripheral blood lymphocytes and the fluorescence in situ hybridization (FISH) technique was applied to find out whether chromosome aberrations induced in the blood-forming tissue are transmitted to peripheral blood.

## Material and methods

### Selection of individuals

The Federal Office for Radiation Protection (BfS) carried out measurements of domestic radon concentrations by means of the passive  $\alpha$  track method in the south and southeast of Germany and identified buildings with different levels of radon concentration. Four exposure groups were established in relation to these indoor concentrations (group I: < 200 Bq/m<sup>3</sup>, mean 140 Bq/m<sup>3</sup>; group II: 200–1,000 Bq/m<sup>3</sup>, mean 450 Bq/m<sup>3</sup>; group III: 1,000–5,000 Bq/m<sup>3</sup>, mean 1,900 Bq/m<sup>3</sup>; group IV: > 5,000 Bq/m<sup>3</sup>, mean 8,100 Bq/m<sup>3</sup>). The measurements of the radon concentration for group IV were short-period measurements (3 days to 4 months). Nearly 15 persons per exposure group were recruited. In total, chromosome analyses with the FPG technique were performed on 61 individuals (29 females and 32 males) living in 27 buildings. At the time of blood sampling the persons were aged between 6 and 80 years (8 children and 53 adults). Data of confounding factors such as medical radiation exposure, intake of medical drugs, and smoking habits were recorded in questionnaires.

Additionally, the FISH technique was applied to 16 persons (8 females and 8 males) out of 6 houses of the highest exposure group.

### Cultivation of human lymphocytes

The culture technique has been fully described earlier (Stephan and Pressl, 1999). In brief, cultures were set up with 0.5 ml whole blood in 5 ml RPMI 1640 medium supplemented with 10% fetal calf serum, 2 mM glutamine, 2% PHA, 10 mM BrdU and antibiotics. The cultures were incubated for 48 h at 37 °C. For the last 3 h of culture time, cells were treated with 0.1  $\mu$ g/ml Colcemid. The hypotonic treatment of cells is carried out with 75 mM KCl, and the cells were fixed in methanol:acetic acid (3:1).

### Fluorescence plus Giemsa staining (FPG)

Chromosome preparations were performed according to standard procedures (Stephan and Pressl, 1999). All slides were coded in such a way that no association with the exposure group was possible. Chromosome analyses were carried out exclusively in complete first division metaphases identified

by homogeneously stained chromosomes. From these FPG-stained metaphases, dicentric chromosomes (dic), centric rings (cr), excess acentric fragments (ace) (not accompanying a dicentric or ring), and chromatid breaks (cbr) were analyzed.

### Fluorescence in situ hybridisation (FISH)

The FISH method was carried out according to standard procedures (Stephan and Pressl, 1997). A cocktail of DNA probes for chromosomes 2, 4 and 8 (MetaSystems, XCP mix) labeled directly with fluorescein isothiocyanate (FITC) was used. The target DNA was denatured at 70 °C in 70% formamide/2 $\times$  SSC (pH = 7.0) and dehydrated in ethanol before and after the procedure. The denatured DNA probes were applied to the slides and hybridized overnight at 37 °C. For counterstaining, 4,6-diamidino-2-phenylindole (DAPI) was applied.

All abnormal cells with painted chromosomes involved were digitized and stored computer-aided in ISIS software (MetaSystems). The aberrations were described according to the PAINT nomenclature (Tucker et al., 1995), and classified into complete and incomplete translocations. Chromosome aberrations were considered as being complete when all painted material was rejoined, and as incomplete when one or more parts seemed unjoined which may be due to the resolution of the painting technique. For statistical analysis, complete and incomplete translocations were used together. In cells carrying complete and incomplete translocations unpainted chromosomes were also analyzed, and it was possible to distinguish between stable and unstable cells. Stable cells are defined as cells without any dic, cr and/or ace. Exchanges resulting from  $\geq 3$  breaks in  $\geq 2$  chromosomes were scored as complex.

### Statistical analysis

In FPG analysis, dicentric chromosomes and centric rings (dic + cr) are often not Poisson-distributed between cells, due to the occurrence of cells with two or more of such aberrations. Therefore, statistical analysis was applied to the frequency of cells with dic and/or cr ( $C_{dic+cr}$ ) as quantitative endpoint. Distributions of  $C_{dic+cr}$  or translocation frequencies between persons were examined by the log-likelihood ratio test for binomial or Poisson distribution. Based on the test result, Fisher's exact test and the Wilcoxon rank test was used for  $C_{dic+cr}$  and translocation frequencies, respectively, for the comparison of groups. For the Wilcoxon rank test, translocation frequencies were ranked according to the individual magnitude of translocations per cell.

## Results

### Frequency of dicentric and centric ring chromosomes

From 61 persons in total, 60,056 cells were analyzed, approximately 1,000 cells from each subject. In Table 1 are listed the results for each exposure group (I–IV) and for all

**Table 2.** Cells with  $\geq 2$  dic in the radon-exposed persons and in the control group

Exposure group (Bq/m <sup>3</sup> )	Cells scored	Cells with 2 dic	Cells > 2 dic
I < 200	16,597	3	2
II 200–1000	11,407	2	1
III 1000–5000	12,620	5	2 (1 cell with 6 dic)
IV > 5000	16,355	6	0
in total	56,979	16	5
control	54,689	2	0

**Table 3.** Translocations (complete and incomplete) and dic + cr in persons living in houses with indoor radon concentrations >5,000 Bq/m<sup>3</sup> after FISH painting

Person	Gender	Age (y)	Given living time in the house (y)	Cells scored	dic + cr	Translocations in total (stable)	F <sub>G</sub> trans./1000 <sup>a</sup>	Complex cells, in total (stable)
1	m	17	17	1050	0	2 (2)	5.9	1 (1)
2	w	19	1.5	1016	0	0 (0)	0.0	0 (0)
3	m	20	10	1009	1	1 (1)	3.1	0 (0)
4	w	25	14	1006	0	2 (2)	6.2	1 (0)
5	m	27	27	1015	0	1 (1)	3.1	0 (0)
6	m	48	21	1672	1	11 (10)	20.6	0 (0)
7	w	50	39	2282	1	7 (7)	9.7	1 (1)
8	m	51	18	1536	0	2 (2)	4.1	0 (0)
9	m	55	15	739	0	2 (2)	8.5	0 (0)
10	w	60	28	752	0	1 (0)	4.2	0 (0)
11	m	62	33	991	0	9 (9)	28.4	0 (0)
12	w	66	48	2224	2	7 (5)	9.8	3 (0)
13	m	66	66	2028	2	12 (12)	18.4	4 (3)
14	w	66	45	1726	0	5 (5)	9.1	0 (0)
15	m	69	69	2195	1	14 (13)	19.9	1 (0)
16	w	76	76	2074	1	15 (13)	22.6	0 (0)
Σ	16	48.6		23,315	9	91 (84)	12.19 ± 1.97 <sup>b</sup>	11 (5)
Control								
Σ	53	49.8		136,286	24	275 (270)	6.31 ± 0.56 <sup>b</sup>	5 (1)

<sup>a</sup> F<sub>G</sub>. Frequency of translocations converted to full genome.  
<sup>b</sup> per 1000 cells.

exposed persons together, in comparison to our control group. The control group consists of 53 persons (29 males, 24 females) from which 54,689 cells were scored (Stephan and Pressl, 1999). The mean age of the control group (43.0 years) is nearly the same as in the study group (44.6 years). The members of the control group lived in the Munich area that is in the south of Germany. It can be assumed that radon concentration in their buildings does not exceed the German average of 50 Bq/m<sup>3</sup>. In the control group a significant increase in the frequency of dicentric chromosomes (dic) was found for heavy smokers (>30 cigarettes per day). To avoid smoking as a confounding factor, persons smoking more than 20 cigarettes per day were excluded from the statistical analysis. Only three persons in the exposure groups (one in group I and two in group III) were heavy smokers. For statistical analyses, the number of cells with dic and/or centric rings (cr) (C<sub>dic+cr</sub>) were used as a quantitative endpoint. Compared to the control group, the mean frequency of C<sub>dic+cr</sub> of all exposed persons was significantly different (Fisher's exact test,  $P < 0.005$ ). When subdividing the investigated persons in the corresponding groups, a significant difference in compari-

son to the control group resulted in the groups II, III, and IV (group II: 200–1,000 Bq/m<sup>3</sup>, mean 450 Bq/m<sup>3</sup>; group III: 1,000–5,000 Bq/m<sup>3</sup>, mean 1,900 Bq/m<sup>3</sup>; group IV: >5,000 Bq/m<sup>3</sup>, mean 8,100 Bq/m<sup>3</sup>) ( $P < 0.05$ ). From exposure group I to II, a significant increase in the frequency of C<sub>dic+cr</sub> was shown. In the exposure group II, III, and IV the frequency remained on the same level. In the exposure groups I–IV there were 21 cells with 2 dic, but only 2 in the control group (Table 2).

#### Frequency of translocations

From the 16 persons (mean age 48.6 years) of exposure group IV (>5,000 Bq/m<sup>3</sup>) 23,315 cells were analyzed. The number of translocations (complete + incomplete) in all cells and in stable cells is shown in Table 3. The percentage of translocations in unstable cells was below 10%. For each person is given the observed frequency of translocations and the genome-equivalent frequencies (F<sub>G</sub>) (conversion factor 0.32) calculated by the formula of Lucas et al. (1992), using the length of the target chromosomes given by Morton (1991). The interindividual frequency varied between 0 per 1,000 cells in a 19-year-old

**Table 4.** Frequencies of translocations in relation to age in persons living in houses with indoor radon concentrations >5,000 Bq/m<sup>3</sup>

> 5000 Bq/m <sup>3</sup>	N	Age range	Cells	Translocations	F <sub>G</sub> / 1000 cells
Age group a < 40 years	5	17–27	5,096	6	3.68 ± 1.50
Age group b > 40 years	11	48–76	18,219	78	13.38 ± 2.2
Control	N	Age range	Cells	Translocations	F <sub>G</sub> / 1000 cells
Age group a < 40 years	18	21–37	47,352	57	3.75 ± 0.3
Age group b > 40 years	35	40–85	88,934	213	7.50 ± 0.72

woman living only 1.5 years in a measured house, and 28.4 per 1,000 cells in a 62-year-old man living 33 years in a measured house.

For comparison we used the control group of our laboratory (Pressl et al., 1999). The FISH control group consisted of 53 persons (mean age 49.8 years). In total 136,286 cells were analyzed in this group. The mean frequency of translocations was  $2.02 \pm 0.18$  per 1,000 cells which corresponds to a frequency of  $6.31 \pm 0.56$  per 1,000 cells converted to the full genome.

The mean frequency of translocations in the radon group IV was 1.9 times higher than the control value. The distribution of the translocations in the radon group and the control group were overdispersed, therefore the Wilcoxon rank test was used for statistical analyses. There was no significant difference between the two groups ( $P = 0.055$ ). The frequency of cells with complex aberrations in the radon group is about 12 times higher than in the control group. 84 translocations out of 91 observed translocations occurred in stable cells. 5 out of 11 complex cells were classified as being stable.

It is known that there exists a clear age-dependent effect for translocations (Pressl et al., 1999), therefore we split the groups according to their age: group a (<40 years) and group b (>40 years). Furthermore, it becomes obvious from Table 3 that the mean living time for persons >40 years of age was 41.6 years, whereas persons <40 years of age lived about 13.9 years in their houses. For persons aged <40 years there was no significant difference to the control; however for persons aged >40 years a significantly higher frequency of translocations than in the control group ( $P < 0.05$ ) was observed (Table 4). However, there was no correlation observed between the living time weighted with the measured radon concentration and the frequency of translocations.

## Discussion

In this study we investigated whether an increased level of indoor radon concentrations in dwellings had any effect on the frequency of dic and translocations in peripheral lymphocytes of the persons living in such houses. Since T-lymphocytes have a half-life of about 3 years (Buckton et al., 1967), only a fraction of cells containing dic will be observed in the circulating blood at any time during the period of chronic radon exposure. A replacement from blood-forming tissue should be possible mainly for stable cells, i.e. cells carrying reciprocal translocations. Therefore, translocations should provide a more reliable indicator for a chronic domestic radon exposure than dicentrics. The published data show contradictory results concerning the frequencies of dic in persons living in houses with elevated

radon concentrations (Bauchinger et al., 1994; Maes et al., 1996). When translocations were used as the indicator for radon exposure, no significant effect was observed (Bauchinger et al., 1996; Lindholm et al., 1999). In this study, in 61 persons the dic and centric rings were determined using the conventional FPG technique. The radon concentration in dwellings ranged for these persons from 80 to 13,000 Bq/m<sup>3</sup>. It was found that the mean frequency of cells containing dic and/or cr ( $C_{dic+cr}$ ) was significantly increased in comparison with our control group. When the exposed persons were subdivided into groups (see Table 1), a significant increase in the mean frequency of  $C_{dic+cr}$  in comparison with the control group was observed for persons living in dwellings with radon concentrations >200 Bq/m<sup>3</sup>. In persons living in dwellings with radon concentrations between 230 and 13,000 Bq/m<sup>3</sup>, the mean frequencies of  $C_{dic+cr}$  did not significantly differ between the corresponding exposure groups. Bauchinger et al. (1994) did not find significant differences between two groups of subjects with low and high radon concentrations. The non-linear increase in  $C_{dic+cr}$  frequencies with radon concentration may be influenced by the cell turnover rate. Another reason may be that some of the physical measurements of radon concentrations were short period measurements and are possibly not representative. Due to this uncertainty, persons could change from one exposure group to another.

The observation of cells with multiple chromosomal aberrations (Table 2) can be explained by the inhomogeneous energy deposition of  $\alpha$ -emitting radionuclides.

The mean frequency of translocations analyzed by FISH painting for the persons exposed to radon concentrations >5,000 Bq/m<sup>3</sup> shows a slight but not significant increase in comparison with our control group. If only the persons older than 40 years of age are taken into consideration, the mean frequency of translocations is significantly increased in comparison with the age-matched control. Because the average living time of older persons is longer (41.6 years) in the radon houses than of the persons aged below 40 years (13.9 years), they were exposed to radiation for a longer time and received a higher dose, which may explain our results. The radon level of >5,000 Bq/m<sup>3</sup> in the houses of the investigated persons can also be a reason for the radon effect observed in this study, whereas in other studies no relation between radon concentrations and translocation frequencies was found (Bauchinger et al., 1996; Lindholm et al., 1999). Translocations in stable cells must be considered to answer the question if the observed translocations are induced directly in the peripheral lymphocytes, or if they may be partly induced in the blood-forming tissue and are then transmitted to peripheral blood. It is known from other studies that radon is 16 times more soluble in fat compared to

blood. Therefore the presence of radon in fat in the haemopoetically active marrow provides an enhanced source of  $\alpha$ -radiation from radon and its daughter nuclei (Allen et al., 1995). From in vitro exposure of lymphocytes with  $\alpha$ -particles from an Americium-241 source, we know that in the dose range between 0.02 and 0.1 Gy, the frequency of induced translocations is about 2 times higher than that for dic (Barquinero et al., 2004, in press). If the observed translocation frequency in the study group would be exclusively induced in peripheral blood, the frequency ratio of translocations to dic should also be about 2. In the study group, however, the frequency of translocations in stable cells was about 9 times higher than that of dic (Table 3). If the excess translocations would be induced in the blood-forming tissue and reach the peripheral blood, they should occur in stable cells, since these cells are able to proliferate. As can be seen from Table 3, 84 translocations out of 91 translocations were observed in stable cells.

According to ICRP 65, the dose for the red bone marrow after inhalation of radon without decay products is  $2.00 \times 10^{-10}$  Sv/(Bq·h·m<sup>3</sup>) (ICRP, 1994). The mean living time in the radon houses of the investigated persons is about 42 years, and the mean radon concentration in this group is about 8,000 Bq/m<sup>3</sup>. Assuming for example that subjects stayed in their houses about 12 h a day, they received a calculated bone marrow dose of about 300 mSv, which corresponds to 15 mGy based on an RBE of 20 for  $\alpha$ -radiation. The dose-response curve for  $\alpha$ -particles and translocations only in stable cells was found to be:  $y = (21.52 \pm 2.36) \times 10^{-2} D$  (Barquinero et al., 2004, in press). According to Lloyd et al. (1998), the use of in vitro dose-

response curves allow one to go from a measured frequency of chromosome aberrations in an individual to an absorbed dose in that individual. They found a good agreement of dose reconstruction based on FISH-measured translocations and the dose estimated from initial dic measurements and from measurements of tritium in urine. When the observed translocation frequency in stable cells (Table 3) is used in combination with the dose response curve mentioned above, a mean dose of 17 mGy can be calculated. There is a good correlation between the calculated dose to the bone marrow received by the blood donors and the dose which was obtained from the in vitro calibration curve. This seems to support the assumption that the observed enhanced frequencies of translocations are due to the exposure of the bone marrow to radon.

Since the overwhelming proportion of the translocations occurs in stable cells and there is reasonable agreement considering dose calculations, we conclude that part of the observed translocation frequency in peripheral blood is induced in the blood-forming tissue, and because translocations persist in stable cells they can be observed in peripheral blood

The data of this study demonstrate that chronic exposure of persons to an elevated radon concentration in dwellings causes a significant increase in dic plus cr in peripheral lymphocytes, compared to a control group, when the indoor radon concentration is >200 Bq/m<sup>3</sup>. The distribution of aberrations is overdispersed, as it is expected from inhomogeneous radiation exposure to  $\alpha$ -radiation. The accumulated decay products of radon in the red bone marrow cause a long-term exposure resulting in translocations that are transmitted to peripheral blood.

## References

- Albering HJ, Hageman GJ, Kleinjans JCS, Engelen JJ, Koulischer L, Heres C: Indoor radon exposure and cytogenetic damage. *Lancet* 340:739 (1992).
- Albering HJ, Engelen JJ, Koulischer L, Welle JJ, Kleinjans JCS: Indoor radon, an extrapulmonary genetic risk? *Lancet* 344:750–751 (1994).
- Allen JE, Henshaw DL, Keith PA, Fewes AP, Eatough JP: Fat cells in red bone marrow of human rib: their size and spatial distribution with respect to the radon-derived dose to the haemopoietic tissue. *Int J Radiat Biol* 68:669–678 (1995).
- Barquinero JF, Stephan G, Schmid E: The effect of Americium-241  $\alpha$ -particles on the dose response of chromosome aberrations in human lymphocytes analysed by fluorescence in situ hybridization. *Int J Radiat Biol*, in press (2004).
- Bauchinger M, Schmid E, Braselmann H, Kulka U: Chromosome aberrations in peripheral lymphocytes from occupants of houses with elevated indoor radon concentrations. *Mutat Res* 310:135–142 (1994).
- Bauchinger M, Braselmann H, Kulka U, Huber R, Georgiadou-Schumacher V: Quantification of FISH-painted chromosome aberrations after domestic radon exposure. *Int J Radiat Biol* 70:657–663 (1996).
- BEIR VI, National Research Council. Committee on Health Risk of Exposure to Radon: BEIR VI: Health Effects of Exposure to Radon (National Academy Press Washington DC 1999).
- Buckton KE, Court Brown WM, Smith PG: Lymphocyte survival in men treated with X-rays for ankylosing spondylitis. *Nature* 214:470–473 (1967).
- Darby SC, Hill DC: Health effects of residential radon: a European perspective at the end of 2002. *Radiat Prot Dosim* 104:321–329 (2003).
- ICRP: International Commission on Radiological Protection, Protection against radon-222 at home and at work, Publication No. 65, *Annals of the ICRP* (Pergamon Press, Oxford 1994).
- Lindholm C, Mäkeläinen I, Paile W, Koivistoinen A, Salomaa S: Domestic radon exposure and the frequency of stable or unstable chromosomal aberrations in lymphocytes. *Int J Radiat Biol* 75:921–928 (1999).
- Lubin JH: Studies of radon and lung cancer in North America and China. *Radiat Prot Dosim* 104:315–319 (2003).
- Lucas LN, Awa A, Straume T, Poggensee M, Kodama Y, Nakano M, Ohtaki K, Weier HU, Pinkel D, Gray J, Littlefield G: Rapid translocation frequency analysis in humans decades after exposure to ionizing radiation. *Int J Radiat Biol* 62:53–63 (1992).
- Maes A, Proffijn A, Verschaevae L: Case report: Karyotypic and chromosome aberration analysis of subjects exposed to indoor radon. *Health Phys* 71: 641–643 (1996).
- Morton NE: Parameters of the human genome. *Proc natl Acad Sci, USA* 88:7474–7476 (1991).
- Pressl S, Edward A, Stephan G: The influence of age, sex and smoking habits on the background level of fish-detected translocations. *Mutat Res* 442:89–95 (1999).
- Stephan G, Pressl S: Chromosome aberrations in human lymphocytes analysed by fluorescence in situ hybridization after in vivo irradiation, and in radiation workers, 11 years after an accidental radiation exposure. *Int J Radiat Biol* 71:293–299 (1997).
- Stephan G, Pressl S: Chromosomal aberrations in peripheral lymphocytes from healthy subjects as detected in first cell division. *Mutat Res* 446:231–237 (1999).
- Tucker JD, Morgan WF, Awa AA, Bauchinger M, Blakey D, Cornforth MN, Littlefield LG, Natarajan AT, Shasserre C: A proposed system for scoring structural aberrations detected by chromosome painting. *Cytogenet Cell Genet* 68:211–221 (1995).

# Effect of high-level natural radiation on chromosomes of residents in southern China

I. Hayata,<sup>a</sup> C. Wang,<sup>b</sup> W. Zhang,<sup>b</sup> D. Chen,<sup>b</sup> M. Minamihisamatsu,<sup>a</sup>  
H. Morishima,<sup>c</sup> L. Wei<sup>b</sup> and T. Sugahara<sup>d</sup>

<sup>a</sup>National Institute of Radiological Sciences, Chiba (Japan);

<sup>b</sup>National Institute for Radiological Protection, Chinese Center for Disease Control and Prevention, Beijing (China);

<sup>c</sup>Kinki University, Osaka (Japan);

<sup>d</sup>Health Research Foundation, Kyoto (Japan)

**Abstract.** To study the effect of low-dose (rate) radiation on human health, we analyzed chromosomes of peripheral lymphocytes of residents in a high background radiation area (HBRA) and compared the results with those obtained from residents in a control area (CA) in Guangdong Province, China. Unstable types of chromosome aberrations (dicentrics and rings) were studied in 22 members of eight families in HBRA and 17 members of five families in CA. Each family consists of three generations. On average 2,600 cells per subject were ana-

lyzed. 27 adults and six children in HBRA and 25 adults and eight children in CA were studied with respect to translocations. On average 4,741 cells per subject were examined. We found an increase of the frequency of dicentrics and rings in HBRA, where the natural radiation level is three to five times higher than in the control area. But the increase of translocations in HBRA was within the range of individual variation in the controls.

Copyright © 2003 S. Karger AG, Basel

In the high background radiation area (HBRA) in Guangdong Province of China the level of natural radiation is three to five times higher than it is in other places. The high level of radiation is caused by natural radionuclides such as <sup>238</sup>U, <sup>232</sup>Th and <sup>226</sup>Ra in the soil and in the materials for building houses (Yuan et al., 1997). Most of the residents in the HBRA are farmers and have been living in this area for several generations. The area is rural and far from an air-polluted city.

Chromosome aberrations are extremely sensitive indicators of radiation exposure. Increase of dicentric (Dic) and centric ring (Rc) chromosomes accompanied by fragments can be detected at a dose of 20 mSv in acutely irradiated lymphocytes when chromosomes were analyzed immediately after exposure (Lloyd et al., 1992). Dic and Rc are specific indicators of the effect of radiation, while translocations (Tr) are an indicator of the total effect of all kinds of mutagenic agents such as chemicals and metabolic factors as well as radiation (Hayata et al.,

2000). Dic and Rc are unstable aberration types and are gradually eliminated from the body at a rate of 50% loss per cell division. Fragments are also unstable aberration types and they are 100% eliminated at each cell division. On the other hand, Tr are stable, not lost by cell division, and accumulate in the body.

To determine the effect of low-dose (rate) radiation on human health, we analyzed the chromosomes of peripheral lymphocytes of the residents in the HBRA and compared the results with those obtained from the residents in a control area in Guangdong Province (Hayata, 2000; Hayata et al., 2002; Jiang et al., 2000; Zhang et al., 2003).

In the present paper we review our cytogenetic studies and discuss the effect of low dose (rate) radiation on human health.

## Materials and methods

### Subjects

HBRA and control area (CA) are nearby hamlets and the genetic and cultural backgrounds of the residents in both areas are very similar. For the determination of unstable chromosome aberrations (Dic and Rc), 22 members from eight families in HBRA and 17 members from five families in CA were studied. Each family consists of three generations. For stable chromosome aberrations (Tr), 27 adults and six children in HBRA and 25 adults and eight children in CA were studied.

Received 15 September 2003; manuscript accepted 16 December 2003.

Request reprints from Isamu Hayata, D.Sc.

National Institute of Radiological Sciences

Anagawa 4-9-1, Inage-ku, Chiba-shi, 263-8555 (Japan)

telephone/fax: + 81-43-206-3080; e-mail: hayata@nirs.go.jp

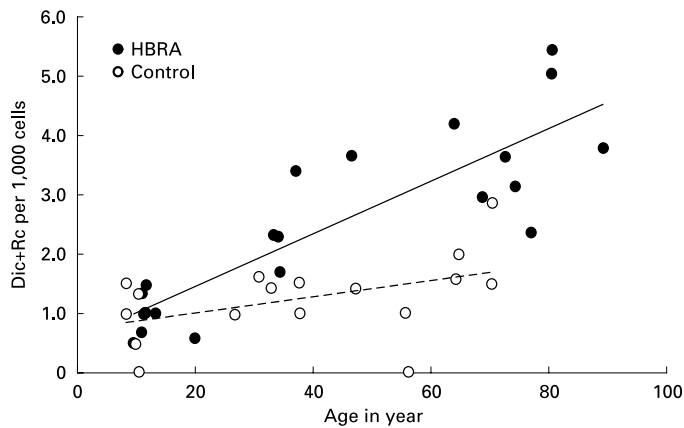


**Fig. 1.** Frequencies of dicentric and ring chromosomes (Dic + Rc) in relation to age of donors. Open circles: control individuals. Filled circles: HBRA individuals. Solid regression line: HBRA; broken regression line: controls.

#### Measuring individual dose

Prior to the cytogenetic study, each individual's exposed dose was measured with electronic pocket dosimeters (Aloka PDM-101) for 24 h and/or thermoluminescence dosimeters (TLD, National UD-200S) for 2 m (Morishima et al., 1997). Average dose rates per year were 3.11 mSv in HBRA and 0.71 mSv in CA. Accumulated doses were calculated by multiplying the measured dose rate with the age of each individual at the time of blood sampling.

#### Cytogenetic preparation

About 3 ml of blood was taken from each subject in HBRA and CA and brought to the Enping Municipal Hospital in CA where we established a laboratory for chromosome preparation. Lymphocyte cultures were set up within 7 h after taking the blood. Colcemid was added to the cultures from the beginning for 48 h. Cultured cells (T cells) were processed for chromosome preparation according to the high-yield chromosome preparation method (Hayata et al., 1992). Fixed cell samples were distributed between two laboratories, one in Beijing, China and the other in Chiba, Japan. Air-dried slides were made at both laboratories and were stained with Giemsa solution for the study of Dic and Rc or with FISH using whole chromosome painting probes for chromosomes 1, 2, and 4 for the analysis of Tr (for details see Zhang et al., 2003).

#### Observation

Observations were performed at both Chinese and Japanese laboratories using microscopes equipped with an automated stage. All the results were reexamined by at least two examiners, one from each laboratory. The average life span (period of observation) of T cells in the body under normal conditions is 22 weeks for CD45RO and 3.5 years for CD45RA cells (IAEA, 2001). In the present subjects, a considerable number of T cells should be in second or later cell division cycles after exposure to radiation and should not have any fragments. Therefore, Dic with or without fragments are pooled in the present results.

Tr included both one-way and reciprocal Tr between two chromosomes, and three-way Tr involving three chromosomes. A three-way Tr involving three chromosomes was counted as two Tr. The frequencies of translocations per 1000 cells were scaled to genome-equivalent frequencies ( $F_G$ ) by the formula reported by Lucas et al. (1992) as follows:  $F_G = F_p / 2.05 (1 - f_p)$ , where  $F_p$  is the frequency of Tr detected by painting and  $f_p$  is the fraction of the genome painted.

#### Statistical analysis

The frequencies of chromosome aberrations in the two areas were compared by using the Mann-Whitney U test. A variance test of the homogeneity of the Poisson distribution was used to test for homogeneity and the Spearman rank correlation test to perform a correlation analysis.

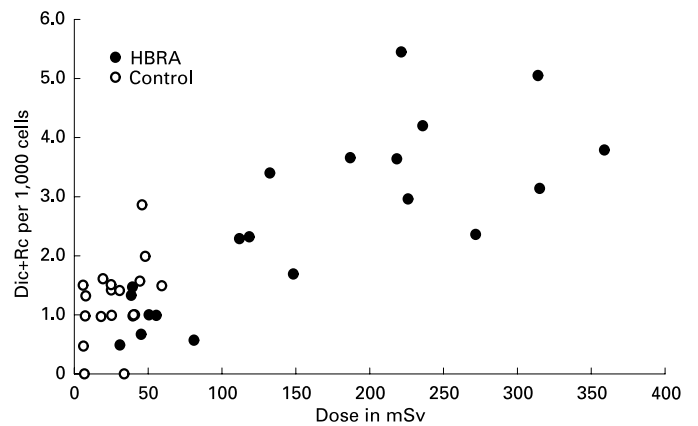


**Fig. 2.** Frequencies of dicentric and ring chromosomes (Dic + Rc) in relation to accumulated dose. Open circles: control, filled circles: HBRA.

## Results and discussion

Regarding unstable aberrations (Dic + Rc), 101,395 cells in total and 2,600 cells average per subject were analyzed. Dic without fragments were found in about equal ratios among total Dic both in HBRA and in CA. The results are summarized in Figs. 1 and 2. As shown in Fig. 1, the frequencies of Dic + Rc seem to increase with age in both groups. However, there is a clear difference in the degree of increase between HBRA and control, with the former being much steeper than the latter (4.44 per 100 years for HBRA and 1.37 per 100 years for control). The contribution ratios due to the regression were much higher in HBRA than in CA ( $r^2 = 0.7544$  for HBRA and  $r^2 = 0.2111$  for control). The frequencies of Dic + Rc per age group among the subjects excluding children are significantly different ( $P < 0.01$ ) between HBRA and CA. The frequencies of Dic + Rc in relation to accumulated doses are shown in Fig. 2, which indicates dose response of the frequencies of Dic + Rc. No factor except radiation was found to explain the difference of the frequencies of Dic + Rc between HBRA and CA. Therefore, the age-related increase of the frequencies of Dic + Rc was considered to be attributable to the high level of background radiation. The dose rate in HBRA is less than 1 cGy per year. This dose rate means that less than one track of radiation passes a cell in more than two months time, which would mean that most of the chromosome aberrations observed are caused by one track of radiation. Therefore, there seems to be no threshold dose for the induction of chromosome aberration. Activation of DNA repair enzymes to reduce subsequent lesions (adaptive response) seems not to be effective at such low dose rates as seen in HBRA.

In the case of stable aberrations (Tr) 312,887 cells in total and 4,741 cells per subject on average were analyzed. The results are summarized in Figs. 3 and 4. In both areas, frequencies of Tr are much higher than those of Dic + Rc and they are lower in children than in adults. Individual variation is small in children but large in the adults. There are two outliers with more than 20 Tr per 1000 cells, one had medical exposure by

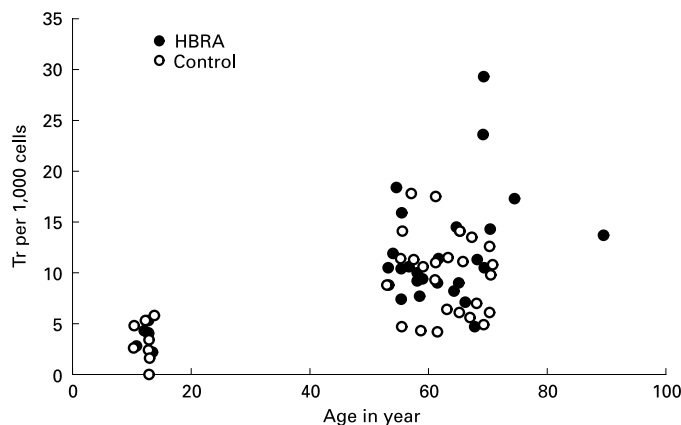


**Fig. 3.** Frequencies of translocations (Tr) in relation to age. Open circles: control, filled circles: HBRA.

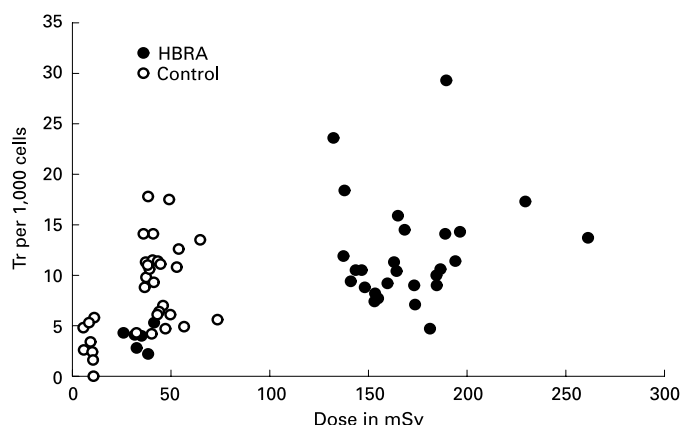


**Fig. 4.** Frequencies of translocations (Tr) in relation to the accumulated dose. Open circles: control, filled circles: HBRA.

fluoroscopy, for the other no reason was found. When those two cases are excluded, there is no significant difference of the frequencies of Tr between HBRA and CA.

Irrespective of the increased frequencies of Dic + Rc in HBRA, the frequencies were within the range of variation in the controls.

The ratio of Dic vs. Rc induced by radiation is about 1:0.1–0.2 (our unpublished data). Dic and Tr are derived from the same types of lesions in two chromosomes caused by radiation. Asymmetric rearrangements lead to a Dic accompanied by fragments and symmetric rearrangements result in Tr. Some types of asymmetric rearrangements are preferentially reduced in their production and therefore, the ratio of Dic vs. Tr is about 0.8–0.9:1 (Zhang and Hayata, 2003). The ratio of Dic + Rc vs. Tr induced by radiation in lymphocytes is about 1:1.

## References

- Hayata I: Insignificant risk at low dose (rate) radiation predicted by cytogenetic studies. Proceedings of the 10<sup>th</sup> International Congress of the International Radiation Protection Association, T-17-3, P2a-90 (in CD), Hiroshima (2000).
- Hayata I, Tabuchi H, Furukawa A, Okabe N, Yamamoto M, Sato K: Robot system for preparing lymphocyte chromosome. *J Radiat Res Suppl* 33:231–241 (1992).
- Hayata I, Wang C, Zhang W, Minamihisamatsu M, Chen D, Morishima H, Yuan Y, Wei L, Sugahara T: Chromosome translocation in residents of high background radiation area in China, in Burkart W, Sohrabi M, Bayer A (eds): *High Levels of Natural Radiation and Radon Areas: Radiation Dose and Health Effects*, International Congress Series 1225 Excerpta Medica, pp 199–205 (Elsevier, Amsterdam 2002).
- IAEA Technical Reports Series No. 405: *Cytogenetic Analysis for Radiation Dose Assessment: A Manual* (International Atomic Energy Agency, Vienna 2001).
- Jiang T, Hayata I, Wang C, Nakai S, Yao S, Yuan Y, Dai L, Liu Q, Chen D, Wei L, Sugahara T: Dose-effect relationship of dicentric and ring chromosomes in lymphocytes of individuals living in the high background radiation areas in China. *J Radiat Res suppl* 41:63–68 (2000).
- Lloyd DC, Edward AA, Leonard GL, Deknudt L, Verschaeve L, Natarajan AT, Darroudi F, Obe G, Palitti F, Tanzarella C, Tawn EJ: Chromosomal aberrations in human lymphocytes induced in vitro by very low doses of X-rays. *Int J Radiat Biol* 61:335–343 (1992).
- Lucas JN, Awa A, Straume T, Poggensee M, Kodama Y, Nakano M, Ohtaki K, Weier HU, Pinkel D, Gray J, Littlefield G: Rapid translocation frequency analysis in humans decades after exposure to ionizing radiation. *Int J Radiat Biol* 62:53–63 (1992).
- Morishima H, Koga T, Tatsumi K, Nakai S, Sugahara T, Yuan Y, Sun Q, Wei L: Study of the indirect method of personal dose assessment for the inhabitants in HBRA of China, in Wei L, Sugahara T, Tao Z (eds): *High Levels of Natural Radiation: Radiation Dose and Health Effects*, International Congress Series 1136 Excerpta Medica, pp 223–233 (Elsevier, Amsterdam 1997).
- Yuan Y, Morishima H, Shen H, Koga T, Sun Q, Tatsumi K, Zha Y, Nakai S, Wei L, Sugahara T: Recent advances in dosimetry investigation in the high background radiation area in Yangjiang, China, in Wei L, Sugahara T, Tao Z (eds): *High Levels of Natural Radiation: Radiation Dose and Health Effects*, International Congress Series 1136 Excerpta Medica, pp 235–240 (Elsevier, Amsterdam 1997).
- Zhang W, Hayata I: Preferential reduction of dicentric in reciprocal exchanges due to the combination of the size of broken chromosome segments by radiation. *J hum Genet* 48:531–534 (2003).
- Zhang W, Wang C, Chen D, Minamihisamatsu M, Morishima H, Yuan Y, Wei L, Sugahara T, Hayata I: Imperceptible effect of radiation based on stable type chromosome aberrations accumulated in the lymphocytes of residents in the high background radiation area in China. *J Radiat Res* 44:69–74 (2003).



## Complex chromosomal rearrangements induced in vivo by heavy ions

M. Durante,<sup>a</sup> K. Ando,<sup>b</sup> Y. Furusawa,<sup>b</sup> G. Obe,<sup>c</sup> K. George<sup>d</sup> and F.A. Cucinotta<sup>d</sup>

<sup>a</sup>Department of Physics, University Federico II, Naples (Italy);

<sup>b</sup>Heavy-Ion Radiobiology Research Group, National Institute of Radiological Sciences, Chiba (Japan);

<sup>c</sup>Department of Genetics, University of Duisburg-Essen, Essen (Germany);

<sup>d</sup>NASA Lyndon B. Johnson Space Center, Houston, TX (USA)

**Abstract.** It has been suggested that the ratio complex/simple exchanges can be used as a biomarker of exposure to high-LET radiation. We tested this hypothesis in vivo, by considering data from several studies that measured complex exchanges in peripheral blood from humans exposed to mixed fields of low- and high-LET radiation. In particular, we studied data from astronauts involved in long-term missions in low-Earth-orbit, and uterus cancer patients treated with accelerated carbon ions. Data from two studies of chromosomal aberrations in astronauts used blood samples obtained before and after space flight, and a third study used blood samples from patients before and after radiotherapy course. Similar methods were used in each study, where lymphocytes were stimulated to

grow in vitro, and collected after incubation in either colcemid or calyculin A. Slides were painted with whole-chromosome DNA fluorescent probes (FISH), and complex and simple chromosome exchanges in the painted genome were classified separately. Complex-type exchanges were observed at low frequencies in control subjects, and in our test subjects before the treatment. No statistically significant increase in the yield of complex-type exchanges was induced by the space flight. Radiation therapy induced a high fraction of complex exchanges, but no significant differences could be detected between patients treated with accelerated carbon ions or X-rays. Complex chromosomal rearrangements do not represent a practical biomarker of radiation quality in our test subjects.

Copyright © 2003 S. Karger AG, Basel

The introduction of the fluorescence in situ hybridization (FISH) method has demonstrated that many chromosomal aberrations are much more complicated than previously predicted based on conventional staining methods (Savage, 2002). Complex-type exchanges were described by Savage (1976) almost three decades ago. With the introduction of the FISH painting technique, Savage and Simpson (1994) defined complexes as those exchange events involving at least three breaks

in two or more chromosomes. It was soon demonstrated that densely ionizing radiation, such as  $\alpha$ -particles (Griffin et al., 1995) or heavy ions (Durante et al., 1998), are much more efficient than sparsely ionizing radiation in the induction of complex-type exchanges. These early results have been recently confirmed using the novel multi-fluor FISH (mFISH), where all 23 chromosome pairs can be painted in different colors. While  $\gamma$ -rays induce very few complexes at doses below 2 Gy (Loucas and Cornforth, 2001), most of the exchanges induced by  $\alpha$ -particles (Anderson et al., 2002), neutrons (Darroudi et al., 2002), or heavy ions (Durante et al., 2002) are indeed complex even at low doses.

Based on those in vitro results, it has been proposed that the ratio complex/simple exchanges (or so called C-ratio) represents a biomarker of exposure to densely ionizing radiation (Anderson et al., 2000, 2003). Measurable “signatures” or “fingerprints” of radiation quality would be highly desirable for improving cancer risk estimates in humans and identifying environmental factors involved in carcinogenesis (Brenner et

Biodosimetry in astronauts was supported by the NASA Space Radiation Health Program and INTAS (EU) contract # 99-00214. Chromosome aberration dosimetry in patients was funded by the NIRS Research Project on Heavy Ions grant. M.D. gratefully acknowledges the support from USRA and STA during his fellowships at NASA and NIRS, respectively.

Received 8 August 2003; manuscript accepted 19 November 2003.

Request reprints from Prof. Marco Durante, Dipartimento di Scienze Fisiche Università Federico II, Monte S. Angelo, Via Cintia, 80126 Napoli (Italy) telephone: +39 081 676 440; fax: +39 081 676 346 e-mail: [durante@na.infn.it](mailto:durante@na.infn.it)

al., 2001). It is of course necessary to test this hypothesis *in vivo*, using a population exposed to densely ionizing radiation or to a mixed high-/low-LET field, and comparing the measured aberration yields with populations unexposed or exposed to sparsely ionizing radiation only. For example, in a recent study of healthy Russian former nuclear weapons workers (Hande et al., 2003), subjects who inhaled large amounts of plutonium ( $\alpha$ -particle doses to bone marrow from 1 to 2 Gy) were compared to workers who were primarily exposed to  $\gamma$ -rays (1.5–3.8 Gy to the bone marrow), and the ratio of chromosomal intra-/inter-changes was evaluated by mBAND. The authors concluded that stable intrachromosomal exchanges represent a biomarker of exposure to densely ionizing radiation.

In the present paper, we analyzed data from several studies of populations exposed to mixed high-/low-LET charged particle fields in the low- and high-dose region. In two of the studies biodosimetry data in astronauts involved in long-term missions in low-Earth-orbit were measured. These subjects were exposed at low-dose rate to a mixed charged particle field, including heavy ions. Doses of up to 9 cGy were accumulated during missions onboard the Mir and the International Space Stations. Data from a third study refer to uterus cancer patients treated with accelerated carbon ions at the HIMAC accelerator in Chiba, Japan (Nakano et al., 1999). The patients received exposures to the pelvic region in daily fractions up to a total dose of about 30 Gy to the target volume. We compare the results from these patients with data from uterus cancer patients treated with high-energy X-rays. Complex- and simple-type chromosomal exchanges were measured by FISH painting of 2–3 chromosomes (approximately 20% of the total genome).

## Materials and methods

### Astronauts

We report here the analysis of 19 astronauts involved in space missions in low-Earth-orbit. Ten astronauts were analyzed at the NASA Lyndon B. Johnson Space Center (George et al., 2001, 2002, 2003a). Nine astronauts were analyzed in the laboratories of the University of Naples or Essen (Greco et al., 2002, 2003; Durante et al., 2003). Space flight missions ranged from 2 to 6 months, and dose measurements by thermoluminescence dosimeters ranged from 30 to 90 mGy. Assuming an average quality factor of 2.34 to 2.5 on Mir (Badhwar et al., 2002; Cucinotta et al., 2000), measured values correspond to equivalent doses ranging from 70 to 200 mSv.

### Patients

A total of 17 Japanese women (age 57–88) treated for squamous cell carcinoma of the uterine cervix were involved in the present study. Nine patients were treated by accelerated carbon ions at the HIMAC synchrotron, while the remainder was treated with 10 MV X-rays produced at a Linac electron accelerator. Treatment planning with 10 MV X-rays consisted of daily fractions of 1.6–2.0 Gy, except in the case of one patient, who was treated with hyperfractionation schedule (1.5 Gy/fraction, two fractions/day). Total dose to the planning target volume (PTV) was around 60 Gy. Patients treated with heavy ions were exposed to 350–400 MeV/nucleon  $^{12}\text{C}$ -ions, 10–15 cm spread-out Bragg-peak (SOBP). Treatment planning was designed to deliver a uniform equivalent dose (in GyE) to the PTV. Dose-average LET was about 10 keV/ $\mu\text{m}$  in the plateau region, and raised on the SOBP from 40 keV/ $\mu\text{m}$  in the proximal edge up to 200 keV/ $\mu\text{m}$  at the distal fall-off. RBE values ranged from 2 to 3 along the SOBP. Daily fractions of 2.7–3.6 GyE/fraction were used, up to a total dose of around 30 Gy C-ions (70 GyE) to the PTV. Planning target area was approximately 200 cm<sup>2</sup> for all patients. Based on *in vitro* dose-response curves for the induction of chromosome-type exchanges in human lymphocytes, the effective whole-body dose

equivalent for these patients at the end of the treatment was around 2 Sv (Durante et al., 1999). Further details concerning patients treated with X-rays (Durante et al., 1999) or C-ions (Durante et al., 2000) have been already reported elsewhere.

### Chromosome analysis

Cytogenetic procedures have been previously provided in detail both for astronauts (George et al., 2001; Greco et al., 2003) and for cancer patients (Durante et al., 1999). Briefly, blood samples were collected before and after space flight (astronauts) or before and after the radiotherapy course (patients) and grown for 48 h at 37°C in RPMI medium supplemented with 20% serum and 1% phytohemagglutinin. Cultures were terminated following either a 2-hour incubation in 0.2  $\mu\text{g}/\text{ml}$  colcemid (astronauts) or 1 h in 50 nM calyculin A (patients). Lymphocytes were spread on humid slides, and hybridized *in situ* with DNA probes specific for human chromosomes of the A-B groups. Cocktails of 2–3 chromosomes, labeled in different colors (green, orange, and yellow, obtained as orange plus green) were used in different experiments, following the procedure recommended by the manufacturer (Vysis Inc., Downers Grove, IL) with a few modifications. Complex-type exchanges were classified as those events involving at least three breaks in at least two chromosomes (Savage and Simpson, 1994), whereas simple-type exchanges were pooled from dicentrics and translocations, including incomplete and one-way types.

### Statistical analyses

The number of cells examined for each subject ranged from 6,000 in controls or low-dose experiments, to a minimum of 150 in patients after the treatment had ended. Uncertainties on measured aberration frequencies were evaluated using Poisson statistics. To compare the aberration frequencies measured with different cocktails of human chromosomes, we used Lucas' formula (Lucas et al., 1992) to calculate whole-genome equivalent (WGE) frequencies from measured frequencies in the painted genome. Although this formula applies to simple-type exchanges, it represents here a simple system to normalize the data obtained with different cocktails. All data provided are expressed as WGE  $\pm$  SE. Significance tests were carried out by pair-wise comparison between specific groups with Fisher's exact test or  $\chi^2$  test for distributions. A threshold of 1% was assumed for statistical significance.

## Results

### Complex exchanges in control subjects

Figure 1 shows the frequency of complex rearrangements in control or pre-treatment subjects. The data is pooled to: nine US or Russian astronauts who had never flown in space before the blood draw; 26 Japanese cancer patients (including 14 uterus cancer patients and 12 esophageal cancer patients) who had not received any treatment before the sampling; ten Italian cancer patients (female, breast carcinoma) who received surgery but had no chemotherapy or radiotherapy before sampling; and four control subjects with no professional or therapeutic exposure to radiation. No significant differences between the different groups were detected ( $\chi^2$  test,  $P > 0.5$ ), and all data for the 49 control subjects are pooled in Fig. 1. Average WGE frequency of complex-type exchanges was  $1.2 \cdot 10^{-3}$ , with a standard deviation of  $1.3 \cdot 10^{-3}$ . Median distribution value was  $1.0 \cdot 10^{-3}$ .

### Astronauts

The yield of total chromosomal aberrations in astronauts' lymphocytes after long-term space flights was higher than the values measured pre-flight. A detailed analysis of the aberrations in these subjects is provided elsewhere (George et al., 2001; Durante et al., 2003). However, the frequency of complex-type exchanges post-flight was very low. Pre-flight distri-

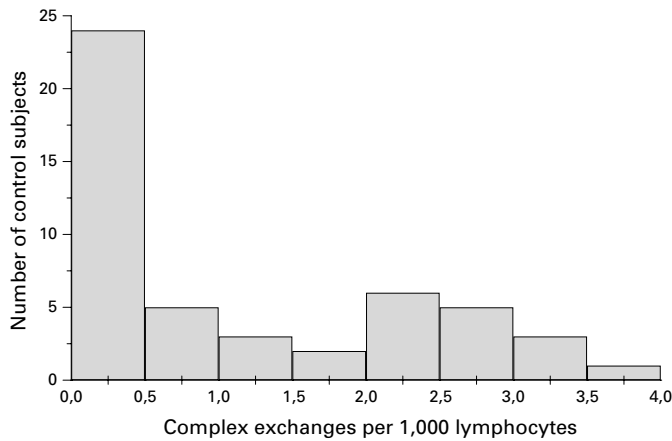


**Fig. 1.** Distribution of complex-type exchanges in lymphocytes from 49 control subjects as measured by FISH painting. WGE frequencies were calculated from measured values as described in Materials and methods and multiplied by 1,000.

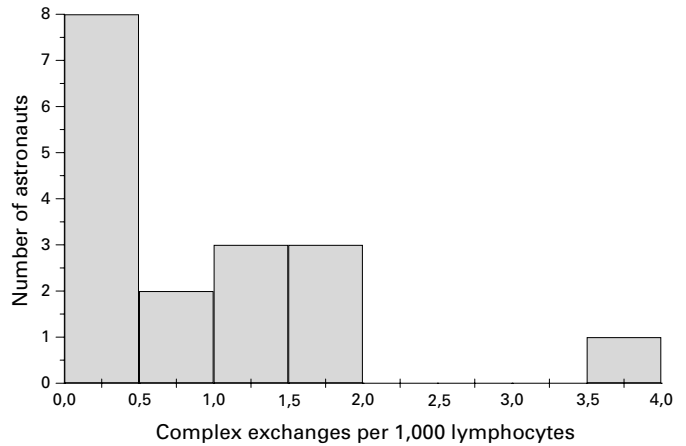


**Fig. 2.** Distribution of complex-type exchanges in lymphocytes from 19 astronauts following long-term space flights on the Mir Space Station. WGE frequencies were calculated from measured values as described in Materials and methods and multiplied by 1,000.

bution in the 19 subjects studied was similar to the control distribution in Fig. 1, and the average WGE frequency  $\pm$  SE was  $(0.97 \pm 0.26) \cdot 10^{-3}$ . The distribution of post-flight values is shown in Fig. 2. The average value is  $(1.01 \pm 0.24) \cdot 10^{-3}$ , which is not statistically different from the average pre-flight value (Fisher's exact test,  $P > 0.5$ ). In Fig. 3 the pre- and post-flight values are directly compared for the 19 astronauts. None of the pre-flight values is significantly different from post-flight yields (Fisher's exact test,  $P > 0.05$ ), with the exception of crewmember #1 ( $P < 0.01$ ). It is noted that statistical uncertainties on individual measurements are between 30 and 100% of the values, reflecting the low frequency of observed complex exchange events.

#### Patients

In patients treated with radiotherapy for uterine cancer, the yield of both simple-type and complex-type exchanges measured at the end of the treatment was significantly higher than the pre-treatment values. Data for total aberrations have been discussed elsewhere (Durante et al., 2000), and here we concentrate on the distribution of complex-type exchanges at the end of the treatment for patients treated with C-ions or X-rays. Data for nine patients treated with C-ions and eight patients treated with X-rays are displayed in Fig. 4. The two distributions are not significantly different ( $\chi^2$  test,  $P > 0.1$ ), and no differences were noted in the average frequency of complex exchanges at the end of the treatment: WGE  $\pm$  SE values were  $0.101 \pm 0.017$  for C-ion patients, and  $0.083 \pm 0.019$  for X-ray patients. We also evaluated the fraction of complex/simple exchanges before and after the treatment. Average values are reported in Fig. 5. Again, no significant differences are observed between patients treated with C-ions or X-rays (Fisher's exact test,  $P > 0.5$ ), while the post-treatment values are significantly higher than pre-treatment ratios (Fisher's exact test,  $P < 0.01$ ).

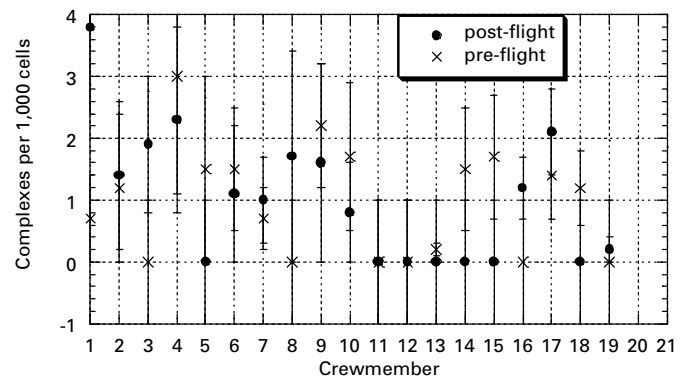


**Fig. 3.** Comparison of pre- and post-flight yields of complex-type exchanges in the same 19 astronauts as in Fig. 2. WGE frequencies  $\pm$  standard errors are plotted.

#### Discussion

We consider data for complex-type chromosomal exchanges found in the peripheral blood lymphocytes of human subjects exposed in vivo to heavy ions. Astronauts received whole-body exposures of low doses of charged particles during space missions, and also received extensive medical diagnostic and aviation exposures from training (Cucinotta et al., 2001). Cancer patients treated at the HIMAC accelerator in Chiba (Japan) received partial-body exposures of high-energy C-ions. Although in vitro data clearly show that heavy ions are much more efficient than sparsely ionizing radiation in the induction of complex-type exchanges, our results show that use of the ratio complex/simple exchanges as a signature of high-LET exposure is problematic for subjects exposed to mixed radiation fields.

Since low doses of sparsely ionizing radiation do not induce complex exchanges, any increase in complex-type cytogenetic

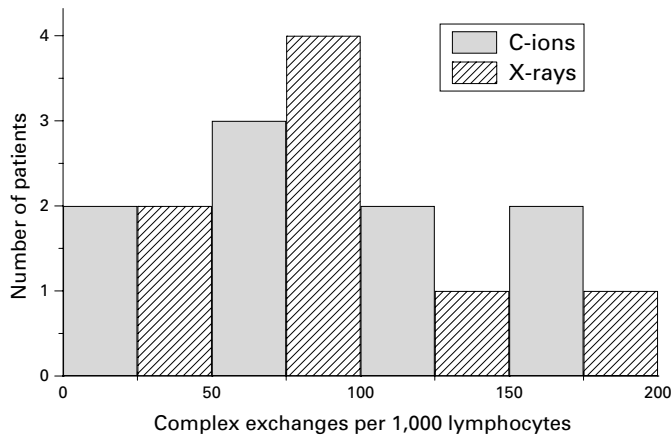


**Fig. 4.** Distribution of complex-type exchanges in lymphocytes from 17 uterus cancer patients at the end of the radiotherapy course with either X-rays or accelerated carbon ions. WGE frequencies were calculated from measured values as described in Materials and methods and multiplied by 1,000.

damage detected in astronauts after space flight would be due entirely to high-LET heavy ions. However, no significant increases after flight were detected here, confirming previous observation in a smaller number of astronauts (George et al., 2002, 2003a). Because the frequency of both complex- and simple-type exchanges is very low in astronauts, actually close to the control background level, it is possible that statistical uncertainties cover any differences. It should be noted that complex exchanges can be detected in the control population, and the interindividual variability is quite large (Fig. 1). Also, although the lifetime of circulating lymphocytes is known, the kinetics of the removal of complex aberrations *in vivo* have not yet been established, which may be a factor in understanding the frequencies of complex aberrations measured after long-term space flights.

Radiotherapy of the uterine cervix induced a high frequency of complex-type exchanges in patients' peripheral blood lymphocytes. However, when patients treated with accelerated C-ions were compared to patients treated with X-rays, no significant differences were observed (Figs. 4 and 5). Although the effective whole-body dose in these patients was about 2 Sv (Durante et al., 1999), lymphocytes can be exposed to much higher doses if they go back to the same pelvic lymph nodes between different fractions (the integral dose to the pelvic region is 60–70 GyE). High yields of complex-type exchanges were also observed in patients treated for esophageal cancer (Yamada et al., 2000) both by X-rays or C-ions, although a direct comparison for those patients is complicated by the different field sizes used. It appears that for localized high-dose exposure in areas rich in lymphatic tissue the frequency of complex-type exchanges will be fairly high with X-rays, and again it is not feasible to use the ratio complex/simple exchanges to elucidate the radiation quality.

The present results do not rule out the possibility that the C-ratio may be a useful indicator of high-LET exposure in specific cases, *i.e.* cases where the dose is not too low (reducing statistical uncertainties) and not too high (avoiding induction

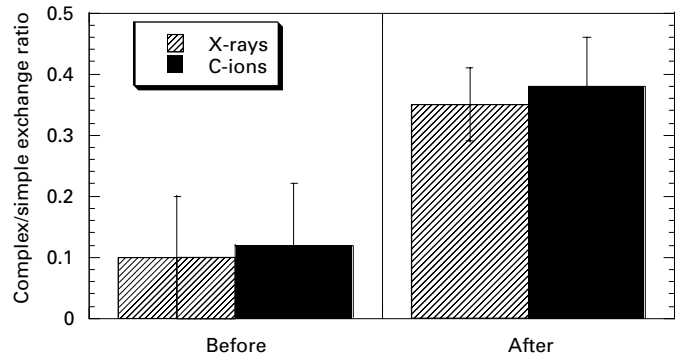


**Fig. 5.** Fraction of complex-type exchanges measured in lymphocytes from uterus cancer patients. Left, complex/simple exchange ratio before the treatment ( $n = 14$ ); right, same ratio measured at the end of the treatment with either X-rays or  $^{12}\text{C}$ -ions ( $n = 17$ ). Bars are SE of the mean values.

of complex rearrangements by low-LET radiation). Perhaps the region 0.5–2 Gy (whole-body) is particularly suitable. In addition, stable complex rearrangements (such as insertions) may be useful in retrospective biodosimetry of high-LET radiation exposure (Anderson et al., 2003; Hande et al., 2003). Estimates of the yield of complex damage from space missions based on a space transport model (Cucinotta et al., 2000), and ground-based accelerator data (George et al., 2003b) are underway to support the understanding of this problem.

#### Acknowledgements

We thank Dr. G. Snigiryova for providing blood samples from Russian cosmonauts, and Drs. S. Yamada and T. Nakano for providing blood samples of the cancer patients.

## References

- Anderson RM, Marsden SJ, Wright EG, Kadhim MA, Goodhead DT, Griffin CS: Complex chromosome aberrations in peripheral blood lymphocytes as a potential biomarker of exposure to high-LET  $\alpha$ -particles. *Int J Radiat Biol* 76:31–42 (2000).
- Anderson RM, Stevens DL, Goodhead DT: M-FISH analysis shows that complex chromosome aberrations induced by  $\alpha$ -particle tracks are cumulative products of localized rearrangements. *Proc natl Acad Sci, USA* 99:12167–12172 (2002).
- Anderson RM, Marsden SJ, Paice SJ, Bristow AE, Kadhim MA, Griffin CS, Goodhead DT: Transmissible and nontransmissible complex chromosome aberrations characterized by three-color and mFISH define a biomarker of exposure to high-LET  $\alpha$ -particles. *Radiat Res* 159:40–48 (2003).
- Badhwar GD, Atwell W, Reitz G, Beaujean R, Heinrich W: Radiation measurements on the Mir Orbital Station. *Radiat Meas* 35:393–422 (2002).
- Brenner DJ, Okladnikova N, Hande P, Burak L, Geard CR, Azizova T: Biomarkers specific to densely-ionising (high-LET) radiations. *Radiat Prot Dosim* 97:69–73 (2001).
- Cucinotta FA, Wilson JW, Williams JR, Dicello JF: Analysis of the Mir-18 results for physical and biological dosimetry: radiation shielding effectiveness in LEO. *Radiat Meas* 132:181–191 (2000).
- Cucinotta FA, Manuel F, Jones J, Izsard G, Murray J, Djojonegoro B, Wear M: Space radiation and cataracts in astronauts. *Radiat Res* 156:460–466 (2001).
- Darroudi F, Bezrookove V, Fomina J, Mesker WE, Wiegant JC, Raap AK, Tanke HJ: Insights into the sites of X-ray and neutron induced chromosomal aberrations in human lymphocytes using COBRAMFISH. *Radiat Prot Dosim* 99:189–192 (2002).
- Durante M, Furusawa Y, George K, Gialanella G, Greco O, Grossi G, Matsufuji N, Pugliese M, Yang TC: Rejoining and misrejoining of radiation-induced chromatin breaks. IV. Charged particles. *Radiat Res* 149:446–454 (1998).
- Durante M, Yamada S, Ando K, Furusawa Y, Majima H, Nakano T, Tsujii H: Measurements of the equivalent whole-body dose during radiation therapy by cytogenetic methods. *Phys Med Biol* 44:1289–1298 (1999).
- Durante M, Yamada S, Ando K, Furusawa Y, Kawata T, Majima H, Nakano T, Tsujii H: X-rays vs. Carbon-ion tumor therapy: cytogenetic damage in lymphocytes. *Int J Radiat Oncol Biol Phys* 47:793–798 (2000).
- Durante M, George K, Wu H, Cucinotta FA: Karyotypes of human lymphocytes exposed to high-energy iron ions. *Radiat Res* 158:581–590 (2002).
- Durante M, Snigiryova G, Akaeva E, Bogomazova A, Druzhinin S, Fedorenko B, Greco O, Novitskaya N, Rubanovich A, Shevchenko V, von Recklinghausen U, Obe G: Chromosome aberration dosimetry in cosmonauts after single or multiple space flights. *Cytogenet Genome Res* 103:40–46 (2003).
- George K, Durante M, Wu H, Willingham V, Badhwar G, Cucinotta FA: Chromosome aberrations in the blood lymphocytes of astronauts after space flight. *Radiat Res* 156:731–738 (2001).
- George K, Wu H, Willingham V, Cucinotta FA: Analysis of complex-type chromosome exchanges in astronauts' lymphocytes after space flight as a biomarker of high-LET exposure. *J Radiat Res* 43: S129–S132 (2002).
- George K, Durante M, Wu H, Willingham V, Cucinotta FA: In vivo and in vitro measurements of complex-type chromosomal exchanges induced by heavy ions. *Adv Space Res* 31:1525–1536 (2003a).
- George K, Durante M, Willingham V, Wu H, Yang T, Cucinotta FA: Biological effectiveness of accelerated particles for the induction of chromosome damage measured in metaphase and interphase human lymphocytes. *Radiat Res* 160:425–435 (2003b).
- Greco O, Obe G, Gialanella G, Grossi G, Horstmann H, Pugliese M, Scampoli P, von Recklinghausen U, Durante M: Chromosome damage in cosmonauts' lymphocytes detected by FISH painting. *Micrograv Space Stat Utiliz* 3:11–18 (2002).
- Greco O, Durante M, Gialanella G, Grossi G, Pugliese M, Scampoli P, Snigiryova G, Obe G: Biological dosimetry in Russian and Italian astronauts. *Adv Space Res* 31:1495–1503 (2003).
- Griffin CS, Marsden SJ, Stevens DL, Simpson P, Savage JRK: Frequencies of complex chromosome exchange aberrations induced by  $^{238}\text{Pu}$   $\alpha$ -particles and detected by fluorescence in situ hybridization using single chromosome-specific probes. *Int J Radiat Biol* 67:431–439 (1995).
- Hande MP, Azizova TV, Geard CR, Burak LE, Mitchell CR, Khokhryakov VF, Vasilenko EK, Brenner DJ: Past exposure to densely ionizing radiation leaves a unique permanent signature in the genome. *Am J hum Genet* 72:1162–1170 (2003).
- Loucas BD, Cornforth MN: Complex chromosome exchanges induced by  $\gamma$ -rays in human lymphocytes: an mFISH study. *Radiat Res* 155:660–671 (2001).
- Lucas JN, Awa A, Straume T, Poggensee M, Kodama Y, Nakano M, Ohtaki K, Weier HU, Pinkel D, Gray J, Littlefield G: Rapid translocation frequency analysis in humans decades after exposure to ionizing radiation. *Int J Radiat Biol* 62:53–63 (1992).
- Nakano T, Suzuki M, Abe A, Suzuki Y, Morita S, Mizoe J, Sato S, Miyamoto T, Kamada T, Kato H, Tsujii H: The phase I/II clinical study of carbon ion therapy for cancer of the uterine cervix. *Cancer J Sci Am* 5:362–369 (1999).
- Savage JRK: Classification and relationships of induced chromosomal structural changes. *J med Genet* 13:103–122 (1976).
- Savage JRK: Reflections and meditations upon complex chromosomal exchanges. *Mutat Res* 512:93–109 (2002).
- Savage JRK, Simpson PJ: FISH "painting" patterns resulting from complex exchanges. *Mutat Res* 312:51–60 (1994).
- Yamada S, Durante M, Ando K, Furusawa Y, Kawata T, Majima H, Tsujii H: Complex-type chromosomal exchanges in blood lymphocytes during radiation therapy correlate with acute toxicity. *Cancer Lett* 150:215–221 (2000).

# Chromosome aberrations of clonal origin are present in astronauts' blood lymphocytes

K. George,<sup>a</sup> M. Durante,<sup>b</sup> V. Willingham,<sup>a</sup> and F.A. Cucinotta<sup>c</sup>

<sup>a</sup>Wyle Laboratories, Houston, TX (USA);

<sup>b</sup>Department of Physics, University Federico II, Naples (Italy);

<sup>c</sup>NASA, Lyndon B. Johnson Space Center, Houston, TX (USA)

**Abstract.** Radiation-induced chromosome translocations remain in peripheral blood cells over many years, and can potentially be used to measure retrospective doses or prolonged low-dose rate exposures. However, several recent studies have indicated that some individuals possess clones of cells with balanced chromosome abnormalities, which can result in an overestimation of damage and, therefore, influence the accuracy of dose calculations. We carefully examined the patterns of chromosome damage found in the blood lymphocytes of twelve astronauts, and also applied statistical methods to screen for the presence of potential clones. Cells with clonal aberrations were identified in three of the twelve individuals. These clonal cells were present in samples collected both before and after

space flight, and yields are higher than previously reported for healthy individuals in this age range (40–52 years of age). The frequency of clonal damage appears to be even greater in chromosomes prematurely condensed in interphase, when compared with equivalent analysis in metaphase cells. The individuals with clonal aberrations were followed-up over several months and the yields of all clones decreased during this period. Since clonal aberrations may be associated with increased risk of tumorigenesis, it is important to accurately identify cells containing clonal rearrangements for risk assessment as well as biodosimetry.

Copyright © 2003 S. Karger AG, Basel

Increased levels of chromosome damage in peripheral blood lymphocytes are a sensitive indicator of radiation exposure, and they are routinely exploited for assessing radiation dose after accidental or occupational exposures (Finnon et al., 1995; Obe et al., 1997; Yang et al., 1997; Lloyd et al., 1998; George et al., 2001; Nakano et al., 2001). Radiation-induced dicentrics, and other unstable chromosome aberrations, decrease in circulating lymphocytes with time after exposure and are generally only used for assessing doses in cases where samples can be obtained fairly soon after the exposure has occurred. Monocentric aberrations (i.e. stable aberrations) can be easily analyzed using the fluorescence in situ hybridization technique (FISH). Stable chromosome aberrations have a high probabili-

ty of survival after cell division compared with multicentric or acentric aberrations (i.e. unstable aberrations), and are therefore likely to remain in peripheral blood cells over many years (Lucas et al., 1992a, b; Lloyd et al., 1998), making them particularly useful for assessing retrospective radiation doses or low-dose rate exposures which occur over many months or years. However, because frequencies of stable aberrations vary considerably in healthy unexposed individuals and have been shown to increase with age (Tucker and Moore, 1996; Pressl et al., 1999), the accuracy of dose reconstruction depends on the assessment of pre-exposure levels.

Another consideration when using stable aberrations for dose assessment is the accurate identification of clonal aberrations. Since monocentric aberrations can survive cell division, analysis of these types of exchanges could potentially include damaged cells that have clonally expanded *in vivo*, resulting in a population of cells with identical rearrangements. Several studies have identified individuals who possess clones of cells with chromosome abnormalities, resulting in artificially high estimates of chromosome damage (Natarajan et al., 1991; Braselmann et al., 1995; Kusunoki et al., 1995; Salassidis et al.,

Supported by NASA.

Received 10 September 2003; manuscript accepted 12 November 2003.

Request reprints from Kerry George, Wyle Laboratories  
1290 Hercules Drive, suite 110, Houston, TX 77058 (USA)  
telephone: 281 483 9593; fax: 281 483 3058  
e-mail: kerry.a.george1@jsc.nasa.gov

1995; Johnson et al., 1998, 1999a, b). Most of these studies describe clonal aberrations in individuals who were exposed to high (greater than 1 Gy) doses of radiation. There is very little data in the literature on the study of clonal expansion in the peripheral blood lymphocytes of healthy unexposed or low-dose-exposed individuals. However, one study did report a higher frequency of clonal aberrations in unexposed individuals of advanced age (>55 years) (Johnson et al., 1999b). In some studies (Kusunoki et al., 1995; Salassidis et al., 1995), subjects possessing clonal aberrations have been followed-up for many years, and it was reported that the yields remained stable with time. However, space radiation is distinct from terrestrial forms of radiation in energy deposition to biomolecules and cells, inducing a higher frequency of chromosome damage with greater complexity (George et al., 2003), and the biological effects of high-energy and charge (HZE) ions in space are poorly understood at this time (National Council on Radiation Protection and Measurement, 2000). Since clonal expansion is involved in the process of cell transformation, clonal aberrations may be associated with increased risk of tumorigenesis, and it is therefore important to accurately identify cells containing clonal rearrangements, for both dose and risk assessments.

In previous studies (Yang et al., 1997; George et al., 2001) we presented data on chromosome damage in the peripheral blood lymphocytes of astronauts that were obtained before and after their respective space flights using a combination of two or three FISH chromosome painting probes. In the present paper the chromosome damage found in twelve astronauts was screened for clonal exchanges by carefully examining chromosome breakpoints, and by using statistical methods. Individuals identified as possessing clonal aberrations were followed-up over several months. The yields of clonal damage were also compared in cells collected in metaphase and in cells prematurely condensed in the G<sub>2</sub> phase of the cell cycle.

## Materials and methods

### Collection of chromosomes

Astronauts' venous blood samples were drawn into vacutainer tubes containing sodium heparin (100 USP units). Whole blood cultures were initiated in RPMI 1640 medium (Gibco BRL) supplemented with 20% calf serum and 1% phytohemagglutinin (Gibco BRL), and were incubated at 37 °C for 48 h. Both metaphase chromosomes and chemically induced prematurely condensed chromosomes (PCC) were collected for analysis, using methods described elsewhere (George et al., 2001). Calyculin-A induced PCC samples contained a population of well-condensed chromosomes in G<sub>2</sub> and metaphase.

A 0.5-ml volume of blood from pre- and post-flight samples was cultured with 10 μM bromodeoxyuridine (BrdU) and differential replication staining procedure was completed on chromosomes from these samples by incubating slides in 0.5 mg/ml of Hoechst during exposure to black light (General Electric 15T8/BL bulb). Spreads were stained with Giemsa to visualize replication rounds. The percentage of cells in first mitosis was greater than 90% for all samples analyzed.

### FISH

Chromosome spreads were hybridized in situ with two or three fluorescence-labeled chromosome-specific DNA probes in different colors: spectrum green, spectrum orange, and yellow (i.e. a 1:1 combination of green and orange probes that fluoresces yellow under a triple band pass filter set). All probes were obtained from Vysis (Woodcreek, IL) and FISH procedure was completed using the manufacturer's recommended procedures. Chromo-

some spreads were counterstained in 4',6-diamidino-2-phenylindole (DAPI) and analyzed using a Zeiss Axioskop fluorescence microscope. All slides were coded and scored blindly to minimize bias.

### Classification of chromosome aberrations

When two bicolor chromosomes each containing one centromere were present, this was classified as an apparent reciprocal translocation, and recorded as a single exchange event. A dicentric was scored when one bicolor exchange contained two centromeres and the other had none. For visibly incomplete translocations and dicentrics, we assumed that in most cases the reciprocal fragments were below the level of detection (Wu et al., 1998) and pooled the data with complete exchanges. Complex exchanges were scored when it was determined that an exchange involved a minimum of three breaks in two or more chromosomes (Savage and Simpson, 1994). Total exchanges were calculated by adding the number of apparently simple translocations, dicentrics, incomplete translocations, incomplete dicentrics and complex exchanges.

### Statistical analysis

The  $\chi^2$  analysis method described by Johnson et al. (1998) was used to determine if a sample contained cells carrying clonal aberrations in the painted chromosomes. The expected number of exchanges for each of the specific chromosomes analyzed was determined by multiplying the observed number of total stable exchanges in the painted genome by the fraction of the genome represented by the specific chromosome pair. The  $\chi^2$  values calculated from the observed number and the expected number of stable exchanges were totaled for all chromosome pairs studied. Individuals with the most skewed non-proportional cytogenetic damage distributions have the highest  $\chi^2$  values. Threshold for the rejection of the null hypothesis (observed interchanges are proportional to the DNA content of the painted chromosomes) was set at  $P = 0.005$ , corresponding to  $\chi^2 = 10.60$  when three chromosomes are painted (2 degrees of freedom) and  $\chi^2 = 7.88$  when two chromosomes are painted (1 degree of freedom). Values exceeding this threshold are suggestive of possible clonal aberrations involving one specific chromosome.

## Results

After examining the exchange patterns and chromosome break points for all aberrations, clonal cells were identified in samples from three of the twelve astronauts. Data are presented in Table 1. The clonal aberration in crewmember A1 was detected in a sample that was collected on the day of return from a 3-month space mission. In this case chromosomes were analyzed using probes for chromosomes 2 and 4, and only metaphase cells were analyzed. Of the 25 aberrant cells detected in this sample, 14 contained a clonal aberration involving an exchange in chromosome 2 (Fig. 1), which appeared to be an incomplete reciprocal translocation. The average frequency of this clone was  $0.34 \pm 0.09$  per 100 cells analyzed.

Lymphocytes collected before flight from crewmember A2 contained two separate clones. In this sample chromosomes were analyzed using probes for chromosomes 1, 2 and 5, and both PCC and metaphase cells were analyzed. The first clone, described as clone 1 (Fig. 2), involved a balanced complex exchange involving both chromosome 1 and 5 and a DAPI-stained chromosome. The second clone involved a translocation between chromosome 2 and a DAPI-stained chromosome. A total of 84 aberrant cells were identified, 62 of which were clonal in nature: 46 copies of clone 1 and 16 copies of clone 2. The average frequencies of clone 1 and 2 were  $0.90 \pm 0.13$  and  $0.31 \pm 0.08$  per 100 cells, respectively. However, both clonal exchanges were present at a much higher frequency in the PCC

**Table 1.** Results of FISH chromosome painting analysis in the blood lymphocytes collected from three astronauts at different times before and after their respective 3-month space flights. Details on the frequencies of clonal and non-clonal aberrations are listed.

ID	Age	Exposure status	Sample number	Days after first analysis	Chromosomes analyzed	Number of cells analyzed	Aberrant cells	Clonal cells	Percentages		
									Aberrant	Clonal	Non-clonal
A1	40	before flight	1		2 and 4	3,995	4	0	0.10 ± 0.05	0	0.10 ± 0.05
		after flight	2	305	2 and 4	4,056	25	14	0.62 ± 0.12	0.34 ± 0.09	0.27 ± 0.08
			3	545	2 and 1	4,745	13	0	0.27 ± 0.08	0	0.27 ± 0.08
			4	723	1, 2 and 5	7,728	14	0	0.18 ± 0.05	0	0.18 ± 0.05
			5	754	1, 2 and 5	13,264	27	0	0.20 ± 0.04	0	0.20 ± 0.04
A2	52	before flight	1		1, 2 and 5	5,132	84	62	1.64 ± 0.18	1.21 ± 0.15	0.43 ± 0.09
			2	73	1, 2 and 5	2,259	16	9	0.71 ± 0.18	0.40 ± 0.13	0.31 ± 0.12
		after flight	3	224	1, 2 and 5	6,360	43	14	0.68 ± 0.10	0.22 ± 0.06	0.46 ± 0.08
			4	735	1, 2 and 5	3,508	16	3	0.45 ± 0.11	0.08 ± 0.05	0.37 ± 0.10
A6	43	before flight	1		1, 2 and 5	5,434	2	0	0.04 ± 0.03	0	0.04 ± 0.03
		after flight	2	239	1, 2 and 5	5,547	26	4	0.47 ± 0.09	0.07 ± 0.04	0.40 ± 0.08
			3	421	1, 2 and 5	2,169	11	0	0.51 ± 0.15	0	0.51 ± 0.15

**Table 2.** Comparison of aberration yields in astronaut A2, measured in metaphase cells and chromosomes prematurely condensed in the G<sub>2</sub> phase of the cell cycle with calyculin-A treatment

Exposure status	Sample number	Sample type	No. of cells analyzed	Aberrant cells	Clonal cells	Percentages		
						Aberrant	Clonal	Non-clonal
Before flight	1	PCC	3,049	68	54	2.23 ± 0.27	1.77 ± 0.24	0.46 ± 0.12
		metaphase	2,083	16	8	0.77 ± 0.19	0.38 ± 0.14	0.38 ± 0.14
	2	PCC	1,070	12	8	1.12 ± 0.32	0.75 ± 0.26	0.34 ± 0.23
		metaphase	1,188	4	1	0.34 ± 0.34	0.08 ± 0.08	0.25 ± 0.14
After flight	3	PCC	3,149	24	6	0.76 ± 0.15	0.19 ± 0.08	0.57 ± 0.13
		metaphase	3,211	19	8	0.59 ± 0.14	0.25 ± 0.09	0.34 ± 0.10
	4	PCC	2,273	11	3	0.48 ± 0.15	0.13 ± 0.08	0.25 ± 0.12
		metaphase	1,235	1	0	0.08 ± 0.08	0.00	0.08 ± 0.08

samples compared with metaphase samples. A comparison of PCC and metaphase analysis on all samples from crewmember A2 is shown in Table 2. For sample 1, the combined frequency of the clones was  $1.77 \pm 0.24$  per 100 PCC cells, compared with  $0.38 \pm 0.14$  per 100 metaphase cells, whereas, the frequencies of non-clonal exchanges in PCC and metaphase samples were not significantly different, with values of  $0.46 \pm 0.12$  and  $0.38 \pm 0.14$  per 100 cells, respectively.

For crewmember A6, four copies of a clone with a balanced translocation in chromosome 5 were identified in a sample collected 15 days after return from a 3-month space mission (Table 1). All four of these clonal cells were detected in the PCC samples. The overall frequency of the clone per 100 cells was  $0.07 \pm 0.04$ , compared with  $0.10 \pm 0.05$  for the PCC analysis alone.

Additional samples were collected from these three astronauts at various times after the clones were identified. Results, shown in Table 1, indicate that in all cases the frequency of the clonal aberrations decreased over the sampling time period. For crewmember A1, the clone was not visible before flight, and appeared in a sample collected 305 days later on the day of return from a 3-month space mission. No evidence of the clonal exchange was detected in a sample collected from this individual another 240 days later. Additional analyses up to 449 days

after flight also indicated no reappearance of the clone. For crewmember A2, the first sample collected before launch contained the two separate clones described above. In a second sample from A2, again collected before launch, clone 1 was still visible but the yield had decreased approximately two-fold, whereas clone 2 was no longer detected. In two additional samples collected from this individual 151 and 662 days later, after return from 3-month space mission, clone 1 was still visible with the yield continuing to decrease. Figure 3 shows the yield of clone 1 plotted against sample collection time. For crewmember A6 the clonal aberration detected 15 days after return from space was no longer visible in a sample collected 182 days later. Both metaphase and PCC were analyzed for crewmembers A2 and A6, and in all except the first post-flight analysis for crewmember A2, the PCC contained much higher frequencies of clones than equivalent analysis of metaphase cells.

Chromosome painting is not the most reliable method for assessing low levels of clonal damage, mostly due to difficulties in accurately identifying chromosome break points and because non-painted chromosomes can not be identified. Chromosome banding is a superior method for assessing clonal exchanges but is not feasible for low dose rate exposures because it is extremely time consuming. Johnson et al. (1999a) have suggested a simple statistical method for identifying indi-



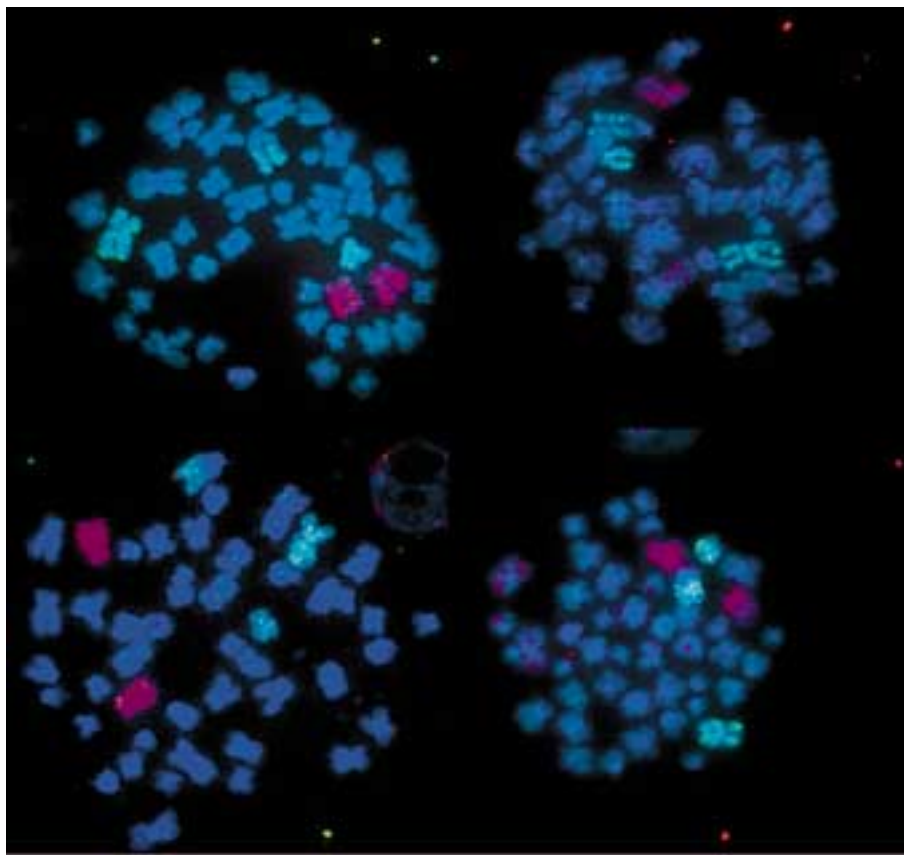


**Fig. 1.** Four metaphases showing the clonal aberration (incomplete translocation in one copy of the green painted chromosome 2) discovered in the blood lymphocytes of astronaut A1 after FISH with chromosome 2 and 4 painting probes.

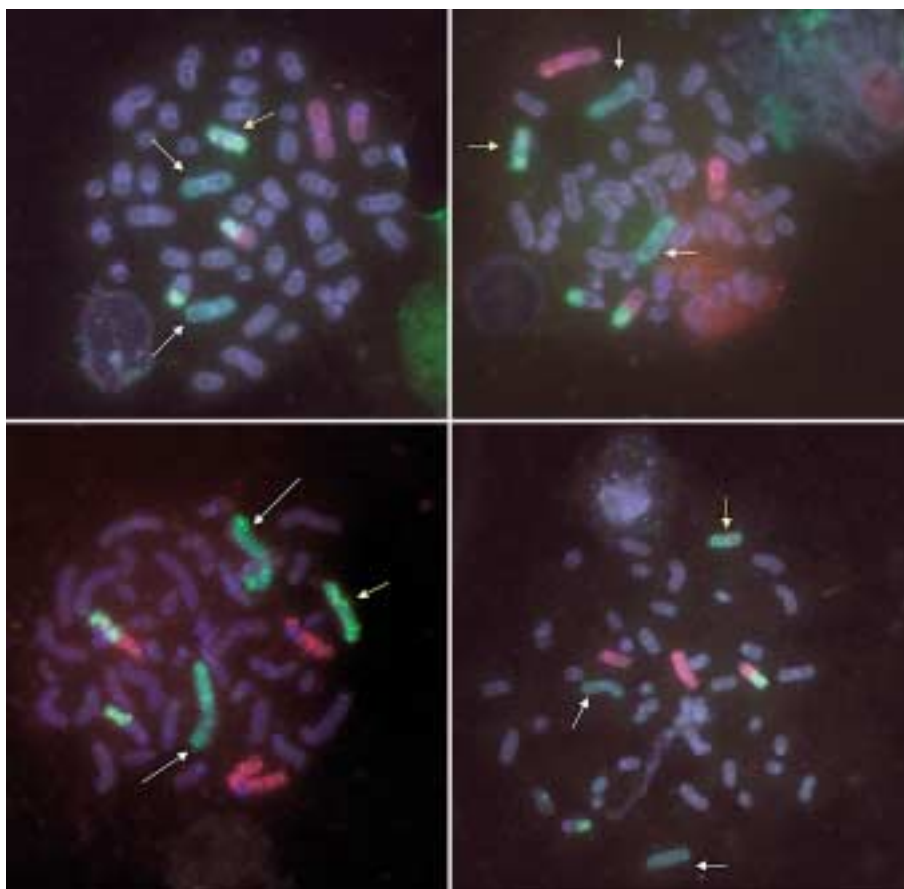


**Fig. 2.** Four metaphases showing the complex clonal aberration discovered in the blood lymphocytes of astronaut A2. The complex exchange involves one copy of chromosome 1 (red-painted chromosome) and chromosome 5 (yellow-painted chromosome). Chromosome 2, painted in green, is identified by the white arrows. The yellow arrows identify the apparently normal copy of chromosome 5.

**Table 3.**  $\chi^2$  Values for all astronauts. Samples with clonal exchanges were recalculated after the clone was subtracted from the data and values are given in the last column.

ID	Age (years)	Exposure status	Chromosomes analyzed	Number of cells analyzed	$\chi^2$ values	$\chi^2$ values after clonal exchanges were subtracted from the analysis	
A1	40	before	2 and 4	3,995	0.04	1.45	
			after	2 and 4	4,056		10.93
		after	2 and 1	4,745	0.34		
			1, 2 and 5	7,728	1.30		
			1, 2 and 5	13,264	1.75		
A2	52	before	1, 2 and 5	5,132	19.86	1.40	
			after	1, 2 and 5	2,259		14.02
		after	1, 2 and 5	6,360	7.35		0.20
			1, 2 and 5	3,508	6.17		3.34
			1 and 2	4,404	0.10		
A3	46	before	1 and 2	6,556	1.08		
A4	42	before	1 and 2	1,892	0.20		
		after	1 and 2	4,677	0.26		
A5	51	before	1, 2 and 5	7,331	0.53		
		after	1, 2 and 5	11,537	1.99		
A6	43	before	1, 2 and 5	5,434	1.33	4.72	
			after	1, 2 and 5	5,547		11.24
		after	1, 2 and 5	2,169	0.50		
A7	52	before	1, 2 and 5	6,239	0.79		
		after	1, 2 and 5	2,621	1.87		
A8	44	before	1, 2 and 5	4,841	0.11		
		after	1, 2 and 5	7,851	0.38		
A9	46	before	1, 2 and 5	5,967	2.61		
		after	1, 2 and 5	4,371	2.31		
A10	41	before	1, 2 and 5	4,997	3.86		
		after	1, 2 and 5	6,696	0.27		
A11	41	before	1, 2 and 5	1,705	3.43		
		after	1, 2 and 5	9,336	0.88		

viduals who might possess clonal aberrations, where  $\chi^2$  values above a pre-determined level may indicate clones are present. We applied this test to our data and results are shown in Table 3. The samples with the clonal aberrations described above had the highest  $\chi^2$  values. The first analysis of crewmember A2, where two separate clones were identified, had the highest  $\chi^2$  value of 19.86, and when corrected for the clones this value decreased to 1.40. The  $\chi^2$  threshold values for deviation from random breakage (at  $P < 0.005$ ) are 10.60 for three chromosome paints and 7.88 for two chromosome paints. Most of the samples containing clonal exchanges have  $\chi^2$  values above these thresholds. However, values for two of the follow-up samples from crewmember A2, containing 14 and 3 clones, fell below the threshold, although the values were still considerably higher than samples without clonal aberrations.

## Discussion

Three of the twelve individuals in the present study were found to possess clonal exchanges, and one of these individuals contained two separate clonal aberrations. Of these four clonal aberrations, two involved an apparently simple reciprocal translocation, one appeared to be an incomplete type translocation, and one was complex in nature involving an insertion. These results suggest that clonal aberrations in human peripheral blood lymphocytes of healthy individuals may be more prevalent than has been reported so far in the literature. Astronauts undergo a rigorous selection process and can be characterized as extremely healthy. Typical ages at selection are

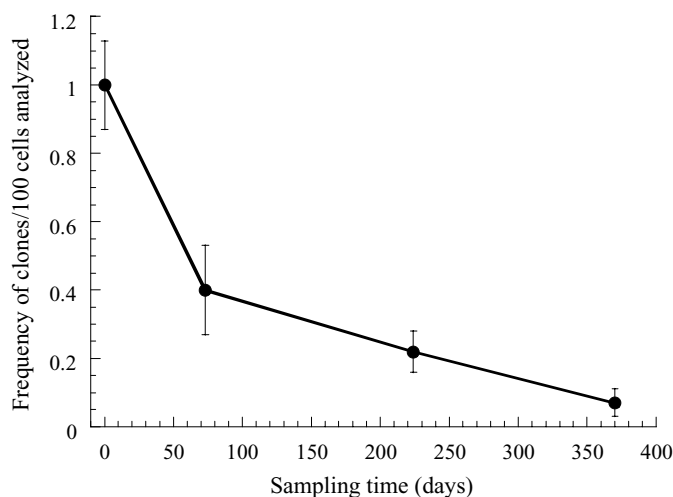


**Fig. 3.** Frequency of clone 1 in blood lymphocytes collected at different times from astronaut A2.

about 35 years, and the average age at first space flight is 39.5 years (Cucinotta et al., 2001). Most clonal aberrations reported in the literature have been observed in individuals who were exposed to high doses of radiation or advanced age (Natarajan et al., 1991; Braselmann et al., 1995; Kusunoki et al., 1995; Salassidis et al., 1995; Johnson et al., 1999b). Salassidis et al. (1995) reported that one of twelve highly irradiated Chernobyl victims (doses 1–6 Gy) possessed a clonal aberration five years after exposure had occurred. Kusunoki et al. (1995) also

showed that atomic bomb survivors with exposures of more than 1 Gy possessed a persistent clonal aberration for many years after exposure. Natarajan et al. (1991) reported a high incidence of specific translocations in chromosome 2 from one individual exposed to over 6 Gy of  $\gamma$ -rays during the Goiania radiation accident. However, there is very little data in the literature on the study of clonal expansion in the peripheral blood lymphocytes of healthy unexposed or low-dose-exposed individuals. Reports from one study of 126 low-dose-exposed Chernobyl liquidators (average exposure of 9 cGy) and 96 control subjects indicate that clonal expansion is present in healthy individuals with low or no exposure, but the over-all frequency of cytogenetically abnormal clones is relatively low (Johnson et al., 1998, 1999a, b). In this study the liquidators with clones ranged in age from 25 to 59 years, whereas all the unexposed individuals with clones were over 55 years of age, and clones were identified in 3% of the total population. In the present study, the three astronauts possessing clones were 40, 43 and 52 years old, and clones were identified in 25% of the study group. However, the astronaut group studied here was much smaller than the Chernobyl group. The clonal aberrations found in astronaut A2 were identified in a pre-flight sample, however this individual had participated in previous space missions, and astronauts also receive other occupational exposures from medical selection and aviation training (Cucinotta et al., 2001).

The reported yields of clonal exchanges in the peripheral blood lymphocytes of individuals exposed to doses over 1 Gy vary between 3 and 9% (Kusunoki et al., 1995; Salassidis et al., 1995). In the present study the yield of clonal aberrations varied from 0.1 to 1.2%, which is consistent with the yields of 0.2–1.1% reported in the literature for unexposed or low-dose-exposed healthy individuals (Johnson et al., 1999b). However, the present study indicates that the yield of clones may be higher if damage is assessed in PCC samples. Analysis in crewmember A2 showed that clonal yields were up to five times higher in PCC compared with metaphase, although the frequency of non-clonal damage was similar in both samples. It is possible that this is due to differences in the *in vitro* growth kinetics of the cells containing clonal exchanges compared to the cell population in general. The only sample from crewmember A2 where the yields of clonal aberrations were similar in PCC and metaphase samples was collected a few days after flight when the growth kinetics of the lymphocytes have been shown to be altered drastically (Yang et al., 1997).

Three of the clonal cells were easily identified through close examination of the exchange patterns and the chromosome break points. However, a low frequency of clonal aberrations was detected in crewmember A6 only after statistical analysis indicated an over-representation of damage in one chromosome pair and subsequent checks revealed four possible clonal exchanges. The  $\chi^2$  analysis indicated that some of the samples containing clonal exchanges were under threshold for  $P = 0.005$ , and this may be due to the low yield of exchanges detected in individual chromosomes. However,  $\chi^2$  values were still considerably higher for samples with clones when compared with samples containing no clones, and this simple statistical method may be useful for corroborating the presence of clonal aberrations.

The yields of all the clonal exchanges identified in the present study decreased within several days to months after they were identified. For crewmembers A1 and A6 the clone was completely eliminated from the circulating lymphocytes sometime within 240 and 182 days respectively. One clonal exchange in crewmember A2 was no longer evident 73 days after it was first identified, and the yield of the second clonal exchange in this individual decreased approximately ten-fold during a 735-day analysis period (Fig. 3). No follow-up results on low-dose rate exposed individuals have been reported in the literature. However, clonal aberrations from high-dose-exposed individuals have been followed-up for many years. Salassidis et al. (1995) and Kusunoki et al. (1995) studied clonal rearrangements in the same individual at various times for three and ten years respectively, and found the frequency remained stable with time, and the latter study concluded that the clones were the progeny of a single stem cell. In the present study the clonal aberrations are likely to involve mature lymphocyte cells that have divided *in vivo* and are being replaced over time with new cells generated from differentiation of stem cells. Ogawa (1993) has proposed a model of stochastic differentiation of stem cells, and the reduction of clonal aberrations observed in our study, where follow-up times are generally less than one year, is not conclusive evidence of the long-term kinetics of the clones observed. Identification of the cell of origin would be extremely useful in this regard.

Clonal aberrations may be more prevalent than previously indicated and because yields may vary at different sampling times, careful screening and multiple sampling may be needed when using balanced translocations for dose reconstruction. Our study provides evidence of clonal aberrations in workers exposed to low doses of radiation, however because of the distinct nature of the HZE ions in space and the small sample size of our study, further research on this issue is needed.

## References

- Brasemann H, Muller P, Peter RU, Bauchinger M: Chromosome painting in highly irradiated Chernobyl victims: a follow-up study to evaluate the stability of symmetrical translocations and the influence of clonal aberrations for retrospective dose estimation. *Int J Radiat Biol* 68:257–262 (1995).
- Cucinotta FA, Manuel F, Jones J, Izsard G, Murray J, Djojonegoro B, Wear M: Space radiation and cataracts in astronauts. *Radiat Res* 156:460–466 (2001).
- Finnon P, Lloyd DC, Edwards AA: Fluorescence in situ hybridization detection of chromosomal aberrations in human lymphocytes: applicability to biological dosimetry. *Int J Radiat Biol* 68:429–435 (1995).
- George K, Durante M, Wu H, Willingham V, Badhwar G, Cucinotta FA: Chromosome aberrations in the blood lymphocytes of astronauts after space flight. *Radiat Res* 156:731–738 (2001).
- George K, Durante M, Willingham V, Wu H, Yang T, Cucinotta FA: Biological effectiveness of accelerated particles for the induction of chromosome damage measured in metaphase and interphase human lymphocytes. *Radiat Res* 160:425–435 (2003).
- Johnson KL, Tucker JD, Nath J: Frequency, distribution and clonality of chromosome damage in human lymphocytes by multi-color FISH. *Mutagenesis* 13:217–227 (1998).
- Johnson KL, Nath J, Pluth JM, Tucker JD: The distribution of chromosome damage, non-reciprocal translocations and clonal aberrations in lymphocytes from Chernobyl clean-up workers. *Mutat Res* 439:77–85 (1999a).
- Johnson KL, Brenner DJ, Geard CR, Nath J, Tucker JD: Chromosome aberrations of clonal origin in irradiated and unexposed individuals: assessment and implications. *Radiat Res* 152:1–5 (1999b).
- Kusunoki Y, Kodama Y, Hirai Y, Kyoizumi S, Nakamura N, Akiyama M: Cytogenetic and immunologic identification of clonal expansion of stem cells into T and B lymphocytes in one atomic-bomb survivor. *Blood* 86:2106–2112 (1995).
- Lloyd DC, Moquet JE, Oram S, Edwards AA, Lucas JN: Accidental intake of tritiated water: a cytogenetic follow-up case on translocation stability and dose reconstruction. *Int J Radiat Biol* 73:543–547 (1998).
- Lucas JN, Poggensee M, Straume T: The persistence of chromosome translocations in a radiation worker accidentally exposed to tritium. *Cytogenet Cell Genet* 60:255–256 (1992a).
- Lucas JN, Awa A, Struame T, Poggensee M, Kodama Y, Nakamo M, Ontaki K, Weier U, Pinkel D, Gray J, Littlefield G: Rapid translocation frequency analysis in humans decades after exposure to ionizing radiation. *Int J Radiat Biol* 62:53–63 (1992b).
- Nakano M, Kodama Y, Ohtaki K, Itoh M, Delongchamp R, Awa AA, Nakamura N: Detection of stable chromosome aberrations by FISH in A-bomb survivors: comparison with previous solid Giemsa staining data on the same 230 individuals. *Int J Radiat Biol* 77:971–977 (2001).
- Natarajan AT, Vyas RC, Wiegand J, Curado MP: Cytogenetic follow-up study of the victims of a radiation accident in Goiania (Brazil). *Mutat Res* 247:103–111 (1991).
- National Council on Radiation Protection and Measurement: Radiation protection guidance for activities in low Earth orbit. NCRP Report 132 (Bethesda MD, 2000).
- Obe G, Johannes I, Johannes C, Hallman K, Reitz G, Facius R: Chromosomal aberrations in blood lymphocytes of astronauts after long-term space flights. *Int J Radiat Biol* 72:727–734 (1997).
- Ogawa M: Differentiation and proliferation of hematopoietic stem cells. *Blood* 81:2844–2850 (1993).
- Pressl S, Edwards A, Stephan G: The influence of age, sex and smoking habits on the background level of fish-detected translocations. *Mutat Res* 442:89–95 (1999).
- Salassidis K, Georgiadou-Schumacher V, Brasemann H, Muller P, Peter RU, Bauchinger M: Chromosome painting in highly irradiated Chernobyl victims: a follow-up study to evaluate the stability of symmetrical translocations and the influence of clonal aberrations for retrospective dose estimation. *Int J Radiat Biol* 68:257–262 (1995).
- Savage JRK, Simpson PJ: On scoring of FISH-“painted” chromosome-type exchange aberrations. *Mutat Res* 307:345–353 (1994).
- Tucker JD, Moore DH: The importance of age and smoking in evaluating adverse cytogenetic effects of exposure to environmental agents. *Environ Health Perspect* 104:489–492 (1996).
- Wu H, George K, Yang TC: Estimate of true incomplete exchanges using fluorescence in situ hybridization with telomere probes. *Int J Radiat Biol* 73:521–527 (1998).
- Yang TC, George K, Johnson AS, Durante M, Federenko BS: Biodosimetry results from space flight Mir-18. *Radiat Res* 148:17–23 (1997).

# Transgenerational transmission of radiation- and chemically induced tumors and congenital anomalies in mice: studies of their possible relationship to induced chromosomal and molecular changes

T. Nomura, H. Nakajima, H. Ryo, L.Y. Li, Y. Fukudome, S. Adachi, H. Gotoh, and H. Tanaka

Graduate School of Medicine, Osaka University, Suita, Osaka (Japan)

**Abstract.** This article provides a broad overview of our earlier studies on the induction of tumors and congenital anomalies in the progeny of X-irradiated or chemically treated mice and our subsequent (published, hitherto unpublished and ongoing) investigations aimed at identifying potential relationships between genetic changes induced in germ cells and the adverse effects manifest as tumors and congenital anomalies using cytogenetic and molecular approaches. The earlier studies document the fact that tumors and congenital anomalies can be induced by irradiation or treatment with certain chemicals such as urethane and that these phenotypes are heritable i.e., transmitted to generations beyond the first generation. These findings support the view that transmissible induced genetic changes are involved. The induced rates of congenital abnormalities and tumors are about two orders of magnitude higher than those recorded in the literature from classical mutation studies with specific locus mutations. The cytogenetic studies addressed the question of whether there were any relationships between induced translocations and induced tumors. The available data permit the inference that gross chromosomal

changes may not be involved but do not exclude smaller induced genetic changes that are beyond the resolution of the techniques used in these studies. Other work on possible relationship between visible chromosomal anomalies (in bone marrow preparations) and tumors were likewise negative. However, there were indications that some induced cytogenetic changes might underlie induced congenital anomalies, i.e., trisomies, deletions and inversions were observed in induced and transmissible congenital anomalies (such as dwarfs, tail anomalies). Studies that explored possible relationships between induction of minisatellite mutations at the *Pc-3* locus and tumors were negative. However, gene expression analysis of tumor (hepatoma)-susceptible offspring of progeny descended from irradiated male mice showed abnormal expression of many genes. Of these, only very few were oncogenes. This lends some support to our hypothesis that cumulative changes in gene expression of many genes, which perform normal cellular functions, may contribute to the occurrence of tumors in the offspring of irradiated or chemically treated mice.

Copyright © 2003 S. Karger AG, Basel

Supported by the Grant-in-Aid for Science of the Japanese Ministry of Education, Science and Culture and Japan Society for the Promotion of Science.

Received 13 September 2003; revision accepted 16 December 2003.

Request reprints from Taisei Nomura

Department of Radiation Biology and Medical Genetics  
Graduate School of Medicine, Osaka University, B4  
2-2, Yamada-oka, Suita, Osaka 565-0871 (Japan)  
telephone: +81-6-6879-3811; fax: +81-6-6879-3819  
e-mail: tnomura@radbio.med.osaka-u.ac.jp

In earlier articles, we presented evidence showing that X irradiation or chemical mutagen treatments of mouse germ cells resulted in congenital anomalies and tumors in the first generation progeny and that these phenotypes (and consequently the induced genetic changes underlying these adverse genetic effects) could be transmitted to generations beyond the first. In this article, we first present a brief overview of these results and using these as a framework, discuss our subsequent cytogenetic and molecular studies aimed at gaining insights into the possible mechanisms underlying transgenerational tumorigenesis and teratogenesis.

**Table 1.** Frequencies of congenital anomalies and respiratory distress syndrome (RDS) in the F<sub>1</sub> fetuses of N5 male mice exposed to 5.04 Gy of X-rays

Treated stage	No. of mice	Living fetuses	RDS <sup>a</sup> (%)	Malformations (%)	Types of malformations <sup>a</sup>
Spermatozoa	9	39	10 <sup>b</sup> (25.6)	3 <sup>c</sup> (7.7)	CP+D+RDS, VSD+RDS, HK+RDS
Spermatogonia	16	155	9 <sup>b</sup> (5.8)	8 <sup>b</sup> (5.2)	2D, Ex+D+RDS, D+RDS, D+VSD, D+VSD+RDS, 2OE
Control	27	275	0 (0.0)	1 (0.4)	D

Estrous females (N5 strain) were mated to X-irradiated or unirradiated males in the evening at 1–21 days or 90–180 days after X-irradiation to sample, respectively, post-meiotic or spermatogonial stages. The pregnant females were euthanized on day 18 of gestation by cervical dislocation, and the fetuses were taken out by Cesarean section. X-ray exposure at post-meiotic stages resulted in a large reduction of live-fetuses because of high incidence of dominant lethals (i.e., preimplantation losses and early deaths). Fetuses were resuscitated just after the operation by patting very gently with tissue paper and wiping amniotic fluid from nose, mouth and body surface, and then classified as apneic or pneic. In the apneic fetuses showing respiratory distress syndrome (RDS), the lung was collapsed and the ductus arteriosus was not closed (Nomura et al., 1990). Morphological anomalies were recorded as described previously (Nomura, 1975a, 1978, 1988). For irradiations, X-ray apparatus (SHT-250 M3, Shimazu, Kyoto, Japan) was used (20 mA and 180 kVp with a filter of 0.5 mm Cu and 1.0 mm Al; dose rate: 0.48–0.50 Gy/min.). Doses were measured using Victoreen Model 570 r-Meter (Victoreen, Cleveland, OH, USA) which was adjusted by Fricke dosimetry and <sup>60</sup>Co standard source.

<sup>a</sup> Abbreviations used: RDS, respiratory distress syndrome; CP, cleft palate; VSD, ventricular septal defect; HK, hypogenesis of kidney; D, dwarf; Ex, exencephaly; OE, open eyelid.

<sup>b</sup>  $P < 0.001$  by  $\chi^2$ -test with Yates' correction.

<sup>c</sup>  $P < 0.01$  by  $\chi^2$ -test with Yates' correction.

### Brief overview of earlier studies on the induction of congenital abnormalities and tumors in mice

In a series of experiments conducted between 1967 and 1981, we obtained convincing evidence for significant increases in the frequencies of tumors and congenital anomalies in the progeny of mice exposed to X irradiation or treated with urethane (ethyl carbamate), a chemical known to be mutagenic, carcinogenic and teratogenic in mice (Nomura, 1975a, b, 1978, 1982, 1983a, b). The rates of induction (as well as spontaneous rates) were at least two orders of magnitude higher than those for specific locus mutations (Nomura, 1975a, 1978, 1982). These studies were later extended to include other chemical mutagens.

For X irradiation, over the range of 0.36 to 2.16 Gy, the dose-response relationships and the overall pattern of response of the post-meiotic and spermatogonial germ cell stages to the induction of both the above adverse genetic effects were similar to those known from studies of radiation-induced specific-locus mutations (Russell et al., 1958, 1982a, b; Lyon et al., 1972; Ehling, 1984). Initially carried out with the ICR strain, the studies were subsequently expanded to include several other strains (such as N5, LT, CBA, B6C3F<sub>1</sub>) which established both the generality of the findings and the existence of some differences between strains in their response to tumor induction (Nomura, 1986, 1990, 2003; reviewed in IARC Monograph, 1999). For instance, most of the radiation-induced tumors (about 90%) in ICR mice were lung tumors (papillary adenomas at eight months of age), the remainder being ovarian tumors, lymphocytic leukemia, stomach tumors, liver haemangiomas, hepatomas, etc. The LT and N5 strains, however, responded with higher induced frequencies of lymphocytic leukemia than the ICR strain but with similar frequencies with respect to lung tumor induction in the F<sub>1</sub> progeny.

As in the case of urethane, treatment with 4-nitroquinoline-1-oxide (4NQO) also induced tumors and congenital anomalies in the offspring (Nomura, 1982). In order to confirm that the induced lung tumors were heritable, the F<sub>1</sub> progeny (of irradiated or chemically treated parental mice) were mated and

their progeny examined. The mice were mated as young adults and the presence or absence of tumors was determined at eight months of age. The F<sub>2</sub> progeny were then classified as to the retrospectively determined type of the F<sub>1</sub> parent (tumor-bearing or not). The results showed that the pattern of inheritance was that of a dominant with about 40% penetrance. Since spontaneously occurring lung tumors do not show such a pattern of inheritance (presumably because most of these tumors owe their origin to somatic mutations), it was inferred that germline genetic changes causing (or predisposing to) lung cancer could be induced by ionizing radiation. Transplantation tests carried out with induced tumors in the N5 strain revealed that most of them were malignant (Nomura, 1986). Many stocks of mice derived from these studies that manifested the tumor phenotype are being maintained in our laboratory (Nomura, 2000, 2003).

The congenital anomalies were scored through in utero analyses of pregnant females euthanized on day 18 of gestation as well as examination of live born progeny seven days after birth (Nomura, 1978). In general, the rate of congenital anomalies detected prenatally was higher than those detected after birth (anomalies such as cleft palate, exencephaly, gastroschisis and buphthalmus are lethal shortly after birth). Dwarfism, i.e., intrauterine-growth-retarded mice with their body weights being less than 75% of the rest of the litter (Nomura, 1978, 1982), open eyelids and tail anomalies were the non-lethal anomalies. Additionally, at least one functional deficit, the respiratory distress syndrome (RDS) was found to be inducible by radiation exposure, and the frequencies were higher after irradiation of post-meiotic germ cells than of spermatogonial stem cells. The results of experiments with 5.04 Gy to male mice and types of anomalies found are summarized in Table 1. Transmission tests of viable anomalies showed that these were inherited as dominants, but with varying degrees of expressivity (Nomura, 1988, 1994).

It is of interest to note that, treatment of males with N-ethyl-N-nitrosourea (ENU), the most potent germ cell chemical mutagen known to date (Russell et al., 1979), resulted in progeny with RDS, in addition to morphological anomalies (Nomura

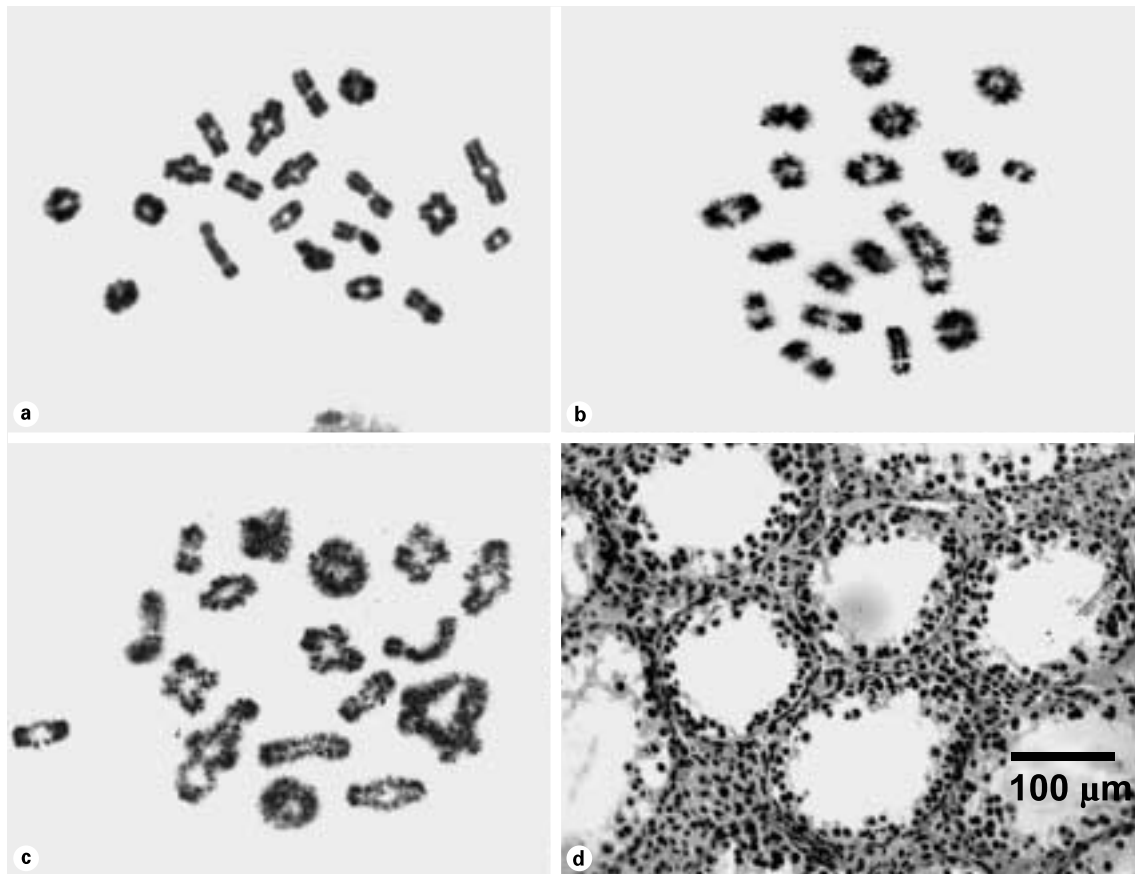


**Fig. 1.** Meiotic configurations of primary spermatocytes in the F<sub>1</sub> offspring of male ICR mice exposed to 5.04 Gy of X-rays at post-meiotic stages. X-rays were given to adult ICR male mice at 1–14 days before conception by Toshiba KC-18-2A, operating at 20 mA and 180 kVp at a rate of 0.72 Gy/min with a filter of 0.5 mm Cu and 0.5 mm Al. Quantitative data are presented in Table 2. The testes were removed from radiation- and chemical-treated male ICR mice and their F<sub>1</sub> offspring and placed in isotonic (2.2%) sodium citrate solution. Meiotic configurations of the primary spermatocytes was prepared by modified air-drying methods (Evans et al., 1964; Leonard and Deknudt, 1969; Nomura, 1978). The tubules were pulled out gently and their contents were teased out by fine straight forceps. The cell suspension was

passed through a tissue screen and centrifuged at 550 rpm for 5 min and the supernatant (mostly containing spermatozoa and spermatids) was discarded. Cell sediments were suspended in 1 ml of hypotonic (1%) sodium citrate solution and incubated at 37 °C for 12 min. Cells were fixed by gently adding 9 ml of methanol-acetic acid (1:1) solution, and centrifuged at 1200 rpm for 10 min. Cells were washed with fixative solution, and then air-dried on the slide. The slides were stained for 8 min in a 4% Giemsa solution (Merck, Darmstadt, Germany) diluted with Sørensen's phosphate buffer solution (1/15 M, pH 6.8). (a) normal bivalent (20II), (b) quadrivalent IV (chain) + 18II, (c) hexavalent VI (ring) + IV (chain) + 15II, (d) histology of the testis. No post-meiotic cells were observed in the seminiferous tubules.

et al., 1990). The incidence of fetuses showing RDS and morphological anomalies was higher after spermatogonial exposure than after post-meiotic germ cell exposure. This finding is reminiscent of those of Russell et al. (1979, 1982c) for ENU-induced specific locus mutations in mouse germ cell stages.

*Is there a relationship between chromosomal changes induced by radiation in germ cells and induced tumors in the offspring?*

There is a considerable amount of literature on the induction of translocations by radiation or chemicals in the germ cells of mice (reviewed in UNSCEAR, 1972). Translocations induced in spermatogonial stem cells have been studied cytogenetically by the analysis of dividing spermatocytes at diakinesis or the first metaphase stages of meiosis and identified through the presence of abnormal chromosomal configurations (such as rings, chains) in the irradiated males themselves.

Translocations induced in pre- as well as post-meiotic germ cells have also been studied genetically through the incidence of semisterility in the offspring of those exposed to radiation or chemicals with subsequent cytological confirmation of translocations in the carriers.

We studied radiation- and urethane-induced translocations cytogenetically in the germ cells of treated adult ICR males as well as in the F<sub>1</sub> male progeny sired by them to examine whether there was any correlation between induced translocations and tumors (Nomura, 1978). Our results confirmed earlier results by other investigators that radiation-induced translocations in spermatogonia (analyzed in the primary spermatocytes of the irradiated males) showed a dose-dependent increase (in the range from 0.36 to 5.04 Gy). Translocations were also studied in the F<sub>1</sub> males descended from post-meiotic germ cells of irradiated (5.04 Gy) parental males (Fig. 1). The data are presented in Table 2 and show that of the total of 81 F<sub>1</sub> males, ten

**Table 2.** Meiotic configurations in primary spermatocytes of F<sub>1</sub> male offspring descended from X-irradiated ICR males (5.04 Gy; post-meiotic stages)

Male F <sub>1</sub> offspring	No. of cells analyzed	Meiotic configurations <sup>a</sup>					Tumors and anomalies <sup>a</sup>
		20II	18II+VI	17II+VI	16II+2IV	Others	
1	39	21	17	0	0	14II+3IV	none
2	19	0	9	7	1	14II+VIII+IV 15II+VI+IV	none
3	44	0	24	3	12	5 (15II+VI+IV)	none
4	71	0	40	24	2	2 (15II+X) 3 (16II+VIII)	none
5	101	0	96	2	2	15II+IV+VI	none
6	68	0	61	1	5	20II+2Fr	none
7	52	0	21	0	27	2 (12II+4IV) 16II+IV+III+I 18II+III+I	none
8	11	5	6	0	0		none
9	18	11	7	0	0		none
10	80	2	78	0	0		none
11–13 <sup>b</sup>	0	no meiotic metaphases	–	–	–		1LT
14–81	20–60	20–60	0	0	0		9LT, 1L, 1D

<sup>a</sup> Abbreviations used: II, bivalent; IV, quadrivalent; VI, hexavalent; VIII, octavalent; X, decavalent; Fr, fragment; I, univalent; LT, lung tumor; L, lymphocytic leukemia; D, dwarf.

<sup>b</sup> Very small testes. Histologically, no postmeiotic cells were found in the tubules, probably due to large and lethal chromosomal changes.

**Table 3.** Analysis of G-banded chromosomes in the F<sub>1</sub> fetuses of N5 male mice exposed to 5.04 Gy of spermatogonial X irradiation

Defects <sup>a</sup>	No. of fetuses	Chromosome abnormality
RDS	8	None
D	2	1 Trisomy 19; 1 trisomy 18
Ex+D+RDS	1	Monosomy 5
D+RDS	1	None
D+VSD	1	None
D+VSD+RDS	1	Trisomy 18
OE	2	None
None	51	1 Trisomy 15

The whole fetal spleen and one third of the fetal liver were used for the preparation of chromosomes (Nomura et al., 1990).

<sup>a</sup> Abbreviations used: RDS, respiratory distress syndrome; D, dwarf; VSD, ventricular septal defect; Ex, exencephaly; OE, open eyelid.

showed characteristic translocation configurations and three a deficit of post-meiotic germ cells in the seminiferous tubules analyzed histologically. In 70 concurrent control F<sub>1</sub> males, there were no translocations. The F<sub>1</sub> males were also screened for the presence of tumors and anomalies. Although these were found in some of the animals, they were not the ones which carried translocations (Table 2), suggesting that there is no correlation between the induction of translocations and the occurrence of tumors.

Then we examined whether any relationship could be discerned between visible chromosomal changes (in bone marrow preparations using G- and CQ-band analyses) in 36 tumor-

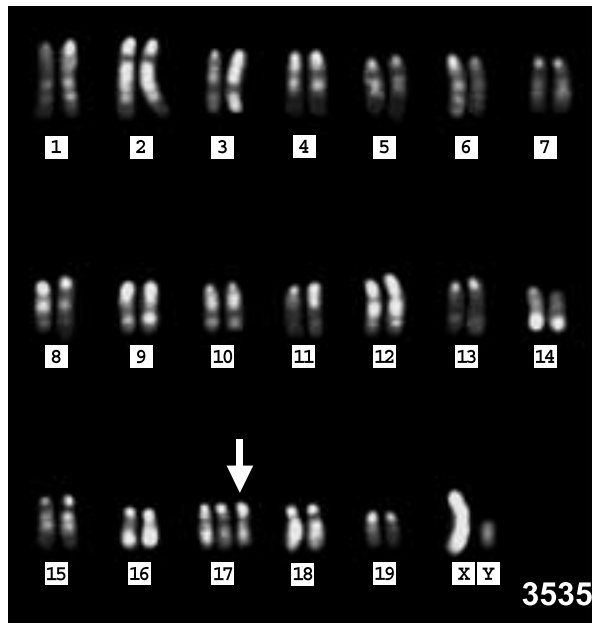
bearing offspring in the N5 strain (from post-radiation generations F<sub>1</sub> to F<sub>5</sub>) and 53 irradiated but non-tumor-bearing controls. The rationale for the choice of the N5 strain is that it is susceptible to several types of induced tumors (such as ovarian tumor, multiple embryonic tumor, myxoma, lymphocytic leukemia) besides lung tumors. The data (not shown) do not provide any evidence for a cytogenetically detectable chromosomal abnormality in these animals with one exception: one leukemic animal was trisomic for chromosome 15 in thymic lymphoma cells. The above sets of data considered together suggest that induced germ cell changes causing tumors are not related to gross chromosomal changes detectable with the cytogenetic techniques employed. However, they do not exclude the possibility that smaller genetic changes may be involved (Nomura, 1978, 1982, 1986).

*Is there a relationship between chromosomal changes induced in the germ cells and induced congenital anomalies in the offspring?*

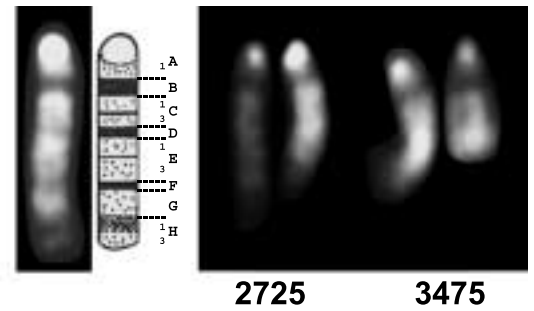
The results of cytogenetic analysis (G-banding) of the abnormal fetuses with morphological and functional defects derived from a radiation experiment (5.04 Gy) are summarized in Table 3. While it is clear that numerical chromosomal abnormalities are present in the abnormal fetuses, it is at present difficult to discern a cause-effect relationship between these and congenital anomalies in view of the fact that numerical chromosomal changes were found in 13–40% of the analyzed cells of each affected fetus in spite of the fact that the fetuses were derived from radiation exposure to spermatogonial cells of the parents. The question of whether germ cell exposure has caused



## Trisomy 17



## Deletion (2, E3) (2, H)



## Inversion (12, A1-C1)

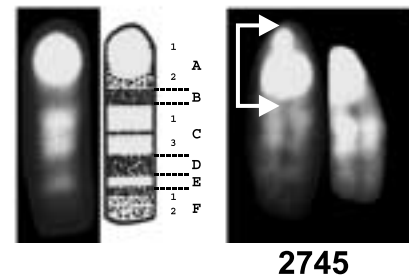


**Fig. 2.** Chromosomal changes found in heritable dwarfs and tail anomalies induced in the offspring of male N5 mice exposed to X-rays. The offspring with inherited malformations were euthanized at 12 months of age, and bone marrow cells were submitted to the examination of chromosomal changes by CQ-banding method. Briefly, mouse bone marrow cells were washed out from femur bone by saline containing 3  $\mu$ g/ml colchicine. Cells were swollen by incubation in 0.075 M KCl hypotonic solution with 3  $\mu$ g/ml colchicine for 25 min at 37°C, and fixed with freshly prepared methanol:acetic acid (1:1) fixative, then spread on a slide and dried overnight at 60°C.

Staining with QM (Quinacrine Mustard, Sigma, St. Louis, MO, USA) and H (Hoechst 33258, Wako Pure Chemical Ind. Ltd., Osaka, Japan) was performed in the dark. Slides were incubated with 0.05 mg/ml of QM and 0.5  $\mu$ g/ml of H in 1/15 M phosphate buffer pH 6.8 for 20 min at 25°C. Q-bands (QM) and C-bands (H) were examined with an Olympus BH2-RFL fluorescence microscope with high-pressure Hg lamp and ultraviolet (334 and 365 nm) excitation unit. The photographs were taken with Kodak Technical pan film 2415-TP 135-36, using Olympus PM-10AD Camera system.

**Table 4.** Chromosomal changes in viable and inherited anomalies in the offspring of N5 male mice exposed to X-rays

Viable anomalies	No. of malformed offspring	Inherited malformed offspring	Expressivity	Chromosomal changes
Dwarfs	8	6	7–40%	Inversion (12, A1-C1), trisomy 17 <sup>a</sup>
Tail anomalies	7	2	7%, 18%	Deletion (2, E3), deletion (2, H)

Eight dwarfs and seven tail anomalies (kinky and/or short) were found in 183 live offspring of male N5 mice exposed to 5.04 Gy of spermatogonial X-irradiation. These F<sub>1</sub> offspring with viable anomalies were mated with normal N5 mice and F<sub>2</sub> were examined for the transmission of congenital anomalies. The examinations continued up to F<sub>3</sub> generation. For X-ray exposure, see the legend to Table 1.

<sup>a</sup> F<sub>2</sub> fetuses were examined on the 18<sup>th</sup> day of gestation. In the un-resuscitated (RDS) dwarf F<sub>2</sub> fetus, trisomy 17 was found.

instability manifest as numerical chromosomal changes in the fetuses remains open. The limited cytogenetic data on viable congenital anomalies induced in the progeny (Table 4) show that most cases of dwarfism and some of tail abnormalities are transmissible to further generations and may be associated with deletions, inversions or trisomies (Fig. 2).

### Intriguing observations

Some intriguing aspects of the observations recorded in our studies are worth noting: (a) radiation exposure of males causes an increase in the frequencies of dominant lethals, congenital anomalies, tumors and translocations in the F<sub>1</sub>, but there does not seem to be any relationship between translocations and congenital anomalies and between translocations and tumors; (b) treatment of males with urethane induces tumors and con-

**Table 5.** Length polymorphism of *Pc-3* PCR products in F<sub>1</sub> fetuses of C.B17 male mice treated with TCDD

TCDD (ng/g)	No. of mice	No. of F <sub>1</sub> fetuses	Mean	SD	No. of F <sub>1</sub> fetuses with abnormal length (%) <sup>a</sup>
100	22	127	585.11	0.72	7 (5.5) <sup>b</sup>
0	19	140	585.13	0.54	1 (0.7)

TCDD (100 ng/g body weight) or solvent of TCDD (corn oil) was administered orally through the esophagus to 3 month-old male C.B17 mice, and then mated with untreated female C.B17 mice to sample spermatogonial cell stages. Respiratory distress syndrome (RDS) and morphological anomalies were recorded as described in the legend to Table 1. The anomalies observed were: 8 dwarfs, 5 short tails, 1 kinky tail, 1 short and kinky tail, 1 syndactyly, 1 giant toe and 1 omphalocele in TCDD group, and 1 dwarf, 1 dwarf + cleft palate, 1 Meckel diverticulum, anterior portal vein and dwarf + open eyelid in control group. DNA was extracted from the fetal liver using QIAamp Tissue kit (Qiagen K.K., Tokyo, Japan) and subjected to amplification of the *Pc-3* locus by PCR. The primers used for PCR were F4: TATCCAAAGCAGGAAATATATAAATCTCAACAAGGC and R: CAGAGGAAACACACAGAAGTAAGTAGAACTCAG. Primers and necessary information were kindly provided by Drs. Y. Takahashi and R. Kominami, Niigata University. PCR products were analyzed by the automated sequencer, Genetic Analyzer ABI PRISM 310 (PE Applied Biosystems, Foster City, CA, USA) with Gene Scan software.

<sup>a</sup> No. of F<sub>1</sub> fetuses with base length over the 99% confidence limit of the corn oil treated concurrent controls.

<sup>b</sup>  $P = 0.06$ . Three of 7 fetuses had congenital anomalies (short tail, short and kinky tail, omphalocele).

genital abnormalities, but not dominant lethals or translocations (Nomura 1978, 1982); (c) the frequencies of tumors and/or congenital anomalies show a significant increase in the F<sub>1</sub> progeny of ICR males treated with different chemical mutagens/carcinogens 4-NQO and 7,12-dimethylbenz(a)anthracene (DMBA), but no translocations were found (Nomura, 1975a, 1978, 1979, 1982, 1988; Nomura and Kurokawa 1997).

### Molecular studies in progress

In order to assess whether genomic instability induced by irradiation of germ cells could show some association with induced congenital anomalies, we studied the induction of minisatellite (expanded simple tandem repeat loci; ESTR) mutations at the *Pc-3* locus in the F<sub>1</sub> progeny of males treated with TCDD (2,3,7,8-tetrachlorodibenzo-*p*-dioxin). Post-meiotic stages were sampled. The choice of TCDD was dictated by earlier work in which TCDD had been found to induce congenital anomalies in man (Cân, 1984) and mice (Nomura et al., 1999). An increase of band shifts, however, was not detected by the usual method, i.e., electrophoresis assay of PCR products (Nomura et al., 1999). In the present work, oral administration of TCDD (100 ng/g body weight) to C.B17 male mice induced congenital anomalies in 18 of 127 F<sub>1</sub> fetuses (14.2%), while in controls five out of 140 fetuses (3.6%) were abnormal. The incidence of RDS in fetuses of the TCDD-treated group was 29.9%, while it was 5.7% in solvent (corn oil) controls ( $P < 0.01$  by  $\chi^2$  test with Yates' correction). As Table 5 shows, there are no differences in the mean base length in the fetuses of the TCDD group relative to the corn-oil-treated groups. However, DNA of abnormal base length (over the 99% confidence limit of controls) was found in the F<sub>1</sub> fetuses in the TCDD group. Furthermore, three of seven of the TCDD group had congenital anomalies (short tail, kinky tail and omphalocele). Similar studies were carried out on the offspring of <sup>60</sup>Co-irradiated (2.16 Gy; 0.57 Gy/min) and unirradiated N5 males (postmeiotic irradiation). Mice were euthanized at twelve months of age and liver and tumor tissues were examined for *Pc-3* mutations. The mean base length of 162 offspring from unirradiated parental males was  $489.00 \pm 1.56$  (99% CI) and there was no increase of outliers either in 65 offspring of irradiated males or

in 13 tumor tissues. These results are at variance with those published in the literature on germ line mutations at the ESTR loci induced by both low and high LET (neutrons from <sup>252</sup>Cf) irradiation (Dubrova et al., 1993, 1998a, b, 2000a, b; Sadamoto et al., 1994; Niwa et al., 1996; reviewed in UNSCEAR, 2001). Further studies are currently underway using mini- and microsatellite probes of the progeny with congenital anomalies and tumors.

The other line of investigation concerns alterations in gene expression that are known to occur in many genes in tumors. These are now being examined using the Gene Chip technology (Affymetrix, Inc., Santa Clara, CA, USA). In these experiments, the affected F<sub>1</sub> offspring (with tumors and malformations) of N5 male mice exposed to 2.16 Gy of X-rays at spermatogonial stage were used as the starting material. These animals were mated to their litter mates as young adults and their offspring were examined for the presence or absence of tumors at twelve months of age and classified as to the retrospectively-determined type of the parent.

Gene Chip expression analysis has been carried out for the hepatoma and normal liver tissue of the affected offspring and compared with the liver tissue of concurrent controls (Fig. 3). There were 4-fold differences in 0.4 and 1.4% of 12,000 genes in the normal liver tissue and hepatomas of irradiated F<sub>1</sub> and F<sub>2</sub> offspring, respectively (Table 6). Abnormal expression of cancer-related genes was observed in only 0.5 and 0.9% of abnormally expressed genes, respectively. The majority of the abnormally expressed genes were those involved in normal physiological, biochemical and immunological functions. Consequently, changes in gene expression seem to occur in various normal functional genes rather than oncogenes per se in irradiated cancer-prone or tumor-susceptible descendants and their progressive accumulation may contribute to cancer; this has been our hypothesis (Nomura, 1978, 1982, 1989). More precise analyses on the genes involved, tumor types, etc. are necessary, before definitive conclusions can be reached.

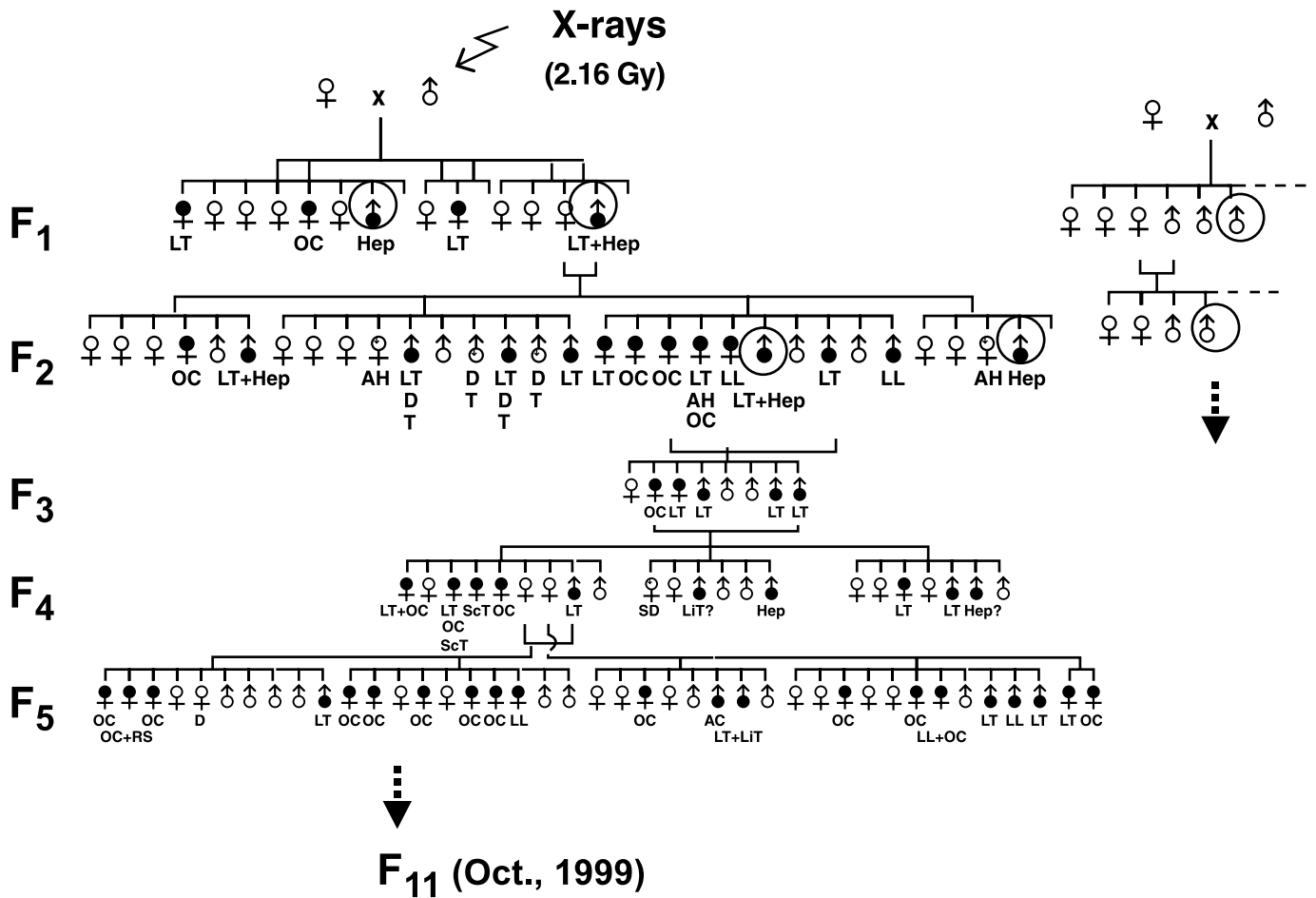


**Fig. 3.** Tumors and congenital anomalies in the offspring of male N5 mice exposed to 2.16 Gy of X-rays at the spermatogonial stages. This is one of the pedigrees of tumor-susceptible offspring of N5 mice exposed to X-rays. A part of the pedigree of concurrent (untreated) controls is shown on the right side. Closed symbols for males and females indicate tumor-bearing offspring, and dotted symbols indicate offspring with congenital anomalies. Open symbols indicate offspring without tumors and anomalies. The abbreviations

used are: Hep, hepatoma; LT, lung tumor; OC, ovarian tumor; LL, lymphocytic leukemia; ScT, subcutaneous tumors (fibrosarcoma, rhabdomyosarcoma); LiT, liver tumor; RS, reticulum cell neoplasia; AH, atresia hymenalis; D, dwarf; T, tail anomalies; SD, diverticulum of stomach; AC, adrenal cyst. Hepatoma lesions and/or normal liver tissues of six circled male offspring in the figure were used for GeneChip analysis (Table 6).

**Table 6.** Changes in gene expression in the descendants of N5 male mice exposed to 2.16 Gy of spermatogonial X irradiation

Liver	Increase $\geq \times 4$ ( $\geq \times 2$ )		Decrease $\leq \times 1/4$ ( $\leq \times 1/2$ )	
	Total	Oncogene	Total	Oncogene
Number of genes	12,000	135	12,000	135
Abnormal expression				
Normal tissue	42 (153)	0.3 <sup>a</sup> (1.3)	10 (52)	0 (0)
Hepatoma	137 (468)	0.8 <sup>b</sup> (5.2)	33 (203)	0.8 <sup>c</sup> (1.3)

Four hepatomas and 4 adjacent normal liver tissues of 4 male offspring of X-irradiated N5 male mice and normal liver tissues of 2 concurrent controls (Fig. 4) were used for Gene Chip analyses (U74Av.2 Array, Affymetrix, Inc., Santa Clara, CA, USA).

Gene expression in the hepatoma and normal liver tissues of the offspring of X-irradiated male N5 mice was compared to those of concurrent controls (offspring of unirradiated N5 mice).

Numbers of genes in 4- (2-)fold increases or decreases were scored and the average of 5 hepatomas and 3 normal liver tissues was shown in the table.

<sup>a</sup> *Myb* proto-oncogene.

<sup>b</sup> Placental and oncofetal gene of the placenta and embryo, myeloblastosis oncogene (2 mice).

<sup>c</sup> Myelocytomatosis oncogene, Kleisler (maf-related) leucine zipper protein, GRO1 (platelet-derived growth factor).

## Discussion

The results presented in this article demonstrate that congenital anomalies and tumors can be induced by exposure of mice to irradiation or certain chemicals and are detectable in the progeny. These effects are trans-generational, i.e., the progeny descended from such treated males transmit these effects to generations beyond the F<sub>1</sub> generation. Further evidence for the X-ray induction of congenital anomalies in mice and for their transmission have been published by Kirk and Lyon (1982, 1984) and Lyon and Renshaw (1988) using the same doses and treated stages as in our studies but with a different strain. Among the malformed fetuses, however, between 30 and 50% were growth retarded. Müller et al. (1999) showed that in the mouse strain "Heiligenberger Stamm" there was an increase in the frequency (4.5 vs 2.3% in control) of one particular malformation, namely gastroschisis in 19-day-old fetuses after <sup>137</sup>Cs  $\gamma$ -irradiation of meiotic stages of parental males. However, in this strain, the above malformation occurs at a comparatively high frequency in controls (around 2% in some up to 4%). Searle and Beechey (1986) showed that the phenotype of growth retardation is transmissible as autosomal dominant albeit with variable penetrance.

Although some deletions and an inversion have been found in our sample of inherited viable congenital anomalies, our data are limited and preclude broad generalizations on the genetic basis of induced congenital anomalies. However, there is good evidence from the work of Cattanaach and colleagues (1993, 1996) that some congenital abnormalities such as growth retardation may be associated with deletions. In their large-scale cytogenetic studies of the progeny of irradiated mice that had known mutant phenotypes (recovered in the specific locus tests) and of those that had only growth retardation as phenotype, these authors found that (a) a significant proportion of these animals carried large deletions and duplications that were compatible with survival of the heterozygotes even if they

reduced viability and caused growth retardation and other developmental abnormalities; (b) the distribution of these structural changes was non-random across the genome and (c) not all growth-retarded animals carried deletions detectable by the cytogenetic techniques used. They also made the point that smaller deletions below the range of cytogenetic detection might occur. Since developmental abnormalities have been postulated to be the predominant type of adverse genetic effects of radiation in humans (Sankaranarayanan, 1999; see also UNSCEAR, 2001), molecular studies of radiation-induced congenital abnormalities are worthwhile.

With respect to radiation-induced tumors, although we demonstrated that they were transmissible, the genetic basis remains elusive. Our data provide limited evidence for the lack of association of induced tumors with induced translocations. The majority of the tumors induced in the offspring were of the same types as those observed spontaneously in each of the mouse strain suggesting that radiation-induced germ line alterations presumably increase/enhance the background incidence (i.e., the inheritance of tumor susceptibility) and that this may come about through changes in gene expression of many normal genes. Although there are some data on the genetic basis for strain differences with respect to their susceptibility to naturally occurring tumors (Dragani, 2003), at present, no firm conclusions can be made on how and which induced germ line alterations contribute to tumors.

## Acknowledgements

The authors are very grateful to Professors Y. Sakamoto, S. Kondo, J. F. Crow, E. Patau, and all the past and/or present members of the former Institute for Cancer Research, Department of Radiation Biology and Medical Genetics, Osaka University, and Medical Genetics, University of Wisconsin for their advice and help over the years and to Professors K. Moriwaki and M. S. Sasaki for their advice in G-band and CQ-band analysis, to Professor K. Sankaranarayanan for his critical reading and editorial help, and to Miss M. Maeda for her help in typing the manuscript.

## References

- Cân N: Effects on offspring of parental exposure to herbicides, in Westing AH (ed): *Herbicides in War – the Long Term Ecological and Human Consequences*, p 137 (Pailor and Francis, Philadelphia 1984).
- Cattanaach BM, Burternshaw MD, Rasberry C, et al: Large deletions and other gross forms of chromosomal imbalance compatible with viability and fertility in the mouse. *Nature Genet* 3:56–61 (1993).
- Cattanaach BM, Evans EP, Rasberry C, et al: Incidence and distribution of radiation-induced large deletions in the mouse, in Hagen U, et al (eds): *Radiation Research 1895–1995, Proceedings of the 10<sup>th</sup> International Congress of Radiation Research*, pp 531–534 (Würzburg 1996).
- Dragani TA: 10 years of mouse cancer modifier loci: human relevance. *Cancer Res* 63:3011–3018 (2003).
- Dubrova YE, Jeffreys AJ, Malashenko AM: Mouse minisatellite mutations induced by ionizing radiation. *Nature Genet* 5:92–94 (1993).
- Dubrova YE, Plumb M, Brown J, Fennelly J, Bois P, Goodhead D, Jeffreys AJ: Stage specificity, dose-response and doubling dose for mouse minisatellite germline mutation induced by acute radiation. *Proc natl Acad Sci, USA* 95:6251–6255 (1998a).
- Dubrova YE, Plumb M, Brown J, Jeffreys AJ: Radiation-induced germline instability at minisatellite loci. *Int J Radiat Biol* 74:689–696 (1998b).
- Dubrova YE, Plumb M, Brown J, Boulton E, Goodhead D, Jeffreys AJ: Induction of minisatellite mutations in the mouse germline by low-dose chronic exposure to  $\gamma$ -radiation and fission neutrons. *Mutat Res* 453:17–24 (2000a).
- Dubrova YE, Plumb M, Gutierrez B, Boulton E, Jeffreys AJ: Transgenerational mutation by radiation. *Nature* 405:37 (2000b).
- Ehling UH: *Methods to estimate the genetic risk*, in Obe G (ed): *Mutations in Man*, pp 292–318 (Springer-Verlag, Berlin 1984).
- Evans EP, Breckon G, Ford CE: An air-drying method for meiotic preparations from mammalian testes. *Cytogenetics* 3:289–294 (1964).
- Evans HJ: Parental mutagenesis and familial cancer. *Nature* 296:488–489 (1982).
- IARC: *IARC Monograph on the Evaluation of Carcinogenic Risks to Humans. Vol. 75: Physical Agents: Ionizing Radiation, Part I, X-Rays,  $\gamma$ -Rays and Neutrons.* (IARC, Lyon 1999).
- Kirk KM, Lyon MF: Induction of congenital anomalies in offspring of female mice exposed to varying doses of X-rays. *Mutat Res* 106:73–83 (1982).
- Kirk KM, Lyon MF: Induction of congenital malformations in the offspring of male mice treated with X-rays at pre-meiotic and post-meiotic stages. *Mutat Res* 125:75–85 (1984).
- Leonard A, Deknuddt GH: Dose-response relationship for translocations induced by X-irradiation in spermatogonia of mice. *Radiat Res* 40:276–284 (1969).
- Lyon MF, Renshaw R: Induction of congenital malformations in mice by parental irradiation: transmission to later generations. *Mutat Res* 198:277–283 (1988).
- Lyon MF, Papworth DG, Phillips RJ: Dose-rate and mutation frequency after irradiation of mouse spermatogonia. *Nature New Biol* 238:101–104 (1972).

- Müller W-U, Streffer C, Wojcik A, Niedereichholz F: Radiation-induced malformations after exposure of murine germ cells in various stages of spermatogenesis. *Mutat Res* 425:99–106 (1999).
- Niwa O, Fan YJ, Numoto M, Kamiya K, Kominami R: Induction of a germline mutation at a hypervariable mouse minisatellite locus by <sup>252</sup>Cf radiation. *J Radiat Res* 37:217–224 (1996).
- Nomura T: Transmission of tumors and malformations to the next generation of mice subsequent to urethan treatment. *Cancer Res* 35:264–266 (1975a).
- Nomura T: Urethan (ethyl carbamate) as a cosolvent of drugs commonly used parenterally in humans. *Cancer Res* 35:2895–2899 (1975b).
- Nomura T: Changed urethan and radiation response of the mouse germ cell to tumor induction, in Severi L (ed): *Tumors of Early Life in Man and Animals*, pp 873–891 (Perugia University Press, Perugia 1978).
- Nomura T: Potent mutagenicity of urethan (ethyl carbamate) gas in *Drosophila melanogaster*. *Cancer Res* 39:4224–4227 (1979).
- Nomura T: Parental exposure to X rays and chemicals induces heritable tumors and anomalies in mice. *Nature* 296:575–577 (1982).
- Nomura T: Comparative inhibiting effects of methylxanthines of urethan-induced tumors, malformations, and presumed somatic mutations in mice. *Cancer Res* 43:1342–1346 (1983a).
- Nomura T: X-ray induced germ-line mutation leading to tumors: its manifestation in mice given urethane post-natally. *Mutat Res* 121:59–65 (1983b).
- Nomura T: Further studies on X-ray and chemically induced germ-line alterations causing tumors and malformations in mice, in Ramel C, Lambert B, Magnusson J (eds): *Genetic Toxicology of Environmental Chemicals – Part B: Genetic Effects and Applied Mutagenesis*, pp 13–20 (Alan R Liss, New York 1986).
- Nomura T: X-ray and chemically induced germ-line mutation causing phenotypical anomalies in mice. *Mutat Res* 198:309–320 (1988).
- Nomura T: Role of radiation-induced mutations in multigeneration carcinogenesis, in Napalkov NP, Rice JM, Tomatis L, Yamasaki H (eds): *Perinatal and Multigeneration Carcinogenesis*, IARC Sci Publ No. 96, pp 375–387 (IARC, Lyon 1989).
- Nomura T: Of mice and men? *Nature* 345:671 (1990).
- Nomura T: Male-mediated teratogenesis: Ionizing radiation/ethylnitrosourea studies, in Mattison DR, Olshan AF (eds): *Male-Mediated Developmental Toxicity*, pp 117–127 (Plenum Press, New York 1994).
- Nomura T: Transplacental and transgenerational late effects of radiation and chemicals. *Cong Anomalies* 40: S54–S67 (2000).
- Nomura T: Transgenerational carcinogenesis: induction and transmission of genetic alterations and mechanisms of carcinogenesis. *Mutat Res* 544: 425–432 (2003).
- Nomura T, Kurokawa N: Comparative study on germ cell mutation induced by urethane (ethyl carbamate) gas and X-rays in *Drosophila melanogaster*. *Jpn J Cancer Res* 88:461–467 (1997).
- Nomura T, Gotoh H, Namba T: An examination of respiratory distress and chromosomal abnormalities in the offspring of male mice treated with ethylnitrosourea. *Mutat Res* 229:115–122 (1990).
- Nomura T, Nakajima H, Li LY, Fukudome Y, Baskar R, Ryo H, Koo JY, Mori K: Concern for the hereditary effects of dioxins. *Environ Mutagen Res* 21:207–211 (1999).
- Russell WL, Kelly EM: Mutation frequencies in male mice and the estimation of genetic hazards of radiation in men. *Proc natl Acad Sci, USA* 79:542–544 (1982a).
- Russell WL, Kelly EM: Specific-locus mutation frequencies in mouse stem-cell spermatogonia at very low radiation dose rates. *Proc natl Acad Sci, USA* 79:539–541 (1982b).
- Russell WL, Russell LB, Kelly EM: Dependence of mutation rate on radiation intensity. *Science* 128:1546–1550 (1958).
- Russell WL, Kelly EM, Hunsicker PR, Bangham JW, Maddux SC, Phipps EL: Specific-locus test shows ethylnitrosourea to be the most potent mutagen in the mouse. *Proc natl Acad Sci, USA* 76:5818–5819 (1979).
- Russell WL, Hunsicker PR, Raymer GD, Steele MH, Stelzner KF, Thompson HM: Dose-response curve for ethylnitrosourea-induced specific-locus mutations in mouse spermatogonia. *Proc natl Acad Sci, USA* 79:3589–3591 (1982c).
- Sadamoto S, Suzuki S, Kamiya K, Kominami R, Dohi K, Niwa O: Radiation induction of germline mutation at a hypervariable mouse minisatellite locus. *Int J Radiat Biol* 65:549–557 (1994).
- Sankaranarayanan K: Ionizing radiation and genetic risks. X. The potential “disease phenotypes” of radiation-induced genetic damage in humans: perspectives from human molecular biology and radiation genetics. *Mutat Res* 429:45–83 (1999).
- Searle AG, Beechey CV: The role of dominant visibles in mutagenicity testing, in Ramel C, et al (eds): *Genetic Toxicology of Environmental Chemicals, Part B, Genetics Effects and Applied Mutagenesis* pp 511–518 (Alan R Liss, New York 1986).
- UNSCEAR: United Nations Scientific Committee on the Effects of Atomic Radiation. *Ionizing Radiation: Levels and Effects. Vol II, Effects, A Report to the General Assembly with annexes.* (United Nations, New York 1972).
- UNSCEAR: United Nations Scientific Committee on the Effects of Atomic Radiation. *Hereditary Effects of Radiation. Report to the General Assembly with Scientific Annex* (United Nations, New York 2001).

# Contribution of chromosomal imbalance to sperm selection and pre-implantation loss in translocation-heterozygous Chinese hamsters

S. Sonta

Department of Genetics, Institute for Developmental Research, Aichi Human Service Center, Kasugai (Japan)

**Abstract.** Chinese hamster stocks with various structurally abnormal chromosomes have been produced by X irradiation. Among these stocks, 18 with various reciprocal translocations were used to investigate the participation of unbalanced gametes in fertilization and the development of unbalanced embryos. Among males as well as females heterozygous for the same translocation, there is no difference in the frequency of each disjunctional class. The participation of chromosomally unbalanced gametes in fertilization was investigated by chromosomal analysis of meiotic cells in heterozygotes for the 18 reciprocal translocations and pronuclei of fertilized ova obtained from crossing these heterozygotes. Compared with the expected frequencies from MII scoring, the frequencies of male pronuclei having a common deficiency of chromosome 1 (1q17→1q42) or chromosome 3 (3p23→3q31) decreased significantly in one-cell embryos. However, the frequencies of male pronuclei with other abnormalities were all consistent with those expected from MII scoring. In contrast, the frequencies of female pronuclei with any karyotype including the same abnormalities as those decreased in male pronuclei from the translocation heterozygotes were all consistent with those estimated from MII scoring. These results revealed clearly that most gametes with nullisomies as well as disomies for any chro-

mosomal segments may participate in fertilization, whereas only male gametes nullisomic for certain segments of chromosomes 1 and 3 failed to participate in fertilization. The zygotic selection of chromosomal imbalance was also investigated by direct chromosomal and morphological analyses of preimplantation embryos from crosses between karyotypically normal females and male heterozygotes from the 18 stocks with various reciprocal translocations. These analyses revealed that some embryos were arrested in development at the two-cell stage. The karyotype of these two-cell embryos had a common deficiency in a segment of chromosome 1 or chromosome 2. Embryos with partial monosomy including chromosomes 1, 3, 4 and 5 showed arrested development at four- to eight-cell stages. Among day 4 embryos, some chromosomally unbalanced embryos, mainly with a deficiency of segments of chromosomes 1p, 1q, 2q, 5q, 7q and 8, had fewer blastomeres than karyotypically normal and balanced embryos. The homology between Chinese hamster and mouse chromosomes relating to abnormal embryogenesis at early stages has been partially confirmed from reported maps of chromosomes. The Chinese hamster is useful for further cytogenetic studies during the stages of meiosis and early embryogenesis.

Copyright © 2003 S. Karger AG, Basel

Supported in part by Grand-in-Aid for Scientific Research (No. 11149229) from the Ministry of Education, Science, Sports and Culture of Japan.

Received 24 September 2003; accepted 20 December 2004.

Request reprints from Dr. Shin-ichi Sonta, Department of Genetics  
Institute for Developmental Research, Aichi Human Service Center  
713-8 Kamiya-cho, Kasugai, Aichi 480-0392 (Japan)  
telephone: +81-568-88-0811 ext 3590; fax: +81-568-88-0829  
e-mail: ssonta@inst-hsc.jp.

## Introduction

Chromosome aberrations are induced by many causes, including radiation and chemical mutagens. Though, for the most part, these aberrations in somatic cells do not confer any damage to the progeny of the individual but can lead to cancer development. Aberrations occurring during the course of ga-

**Table 1.** Various chromosomal abnormalities seen initially in 100 offspring obtained from crosses of non-irradiated females with males irradiated with 450 R of X-rays

Chromosomal abnormality		No. of animals
Reciprocal translocations		83
	A-A <sup>a</sup>	74
	A-X, A-Y	9
Inversions		8
Partial deletions		2
	del(Xq)	1
	del(Yq)	1
Robertsonian translocations		1
Insertions		1
Sex-chromosomal abnormalities		4
	23, XXX	1
	23, XXY	1
	21, X	1
	mosaicism <sup>b</sup>	1
Trisomy 10 <sup>c</sup>		1
Total		100

<sup>a</sup> A-A: Translocations between autosomes.  
<sup>b</sup> 21,X/23,XXY.  
<sup>c</sup> 23,XX,+10.

mete formation may produce serious effects on fertilization, embryogenesis and the development of offspring. To estimate hereditary influences of chromosomal aberrations due to exposure to mutagens, one must investigate the influence of these aberrations on reproductive cells and their participation in fertilization.

It is possible that some reproductive cells having chromosomal damage may cease meiosis; gametes with some chromosomal damage may cease cleavage in the early stages, and some embryos with other chromosome aberrations may die during the period after implantation. Embryos carrying balanced reciprocal translocations may survive and display physical handicaps, such as clump foot or other skeletal defects, and impaired fertility. However, the actual influence of such chromosomal damage on human reproduction is not yet fully understood.

Based on an investigation of human families with translocation carriers, Jacobs et al. (1972) suggested that chromosomal imbalance might be selectively eliminated in the early zygotic stages, shortly after conception. From analyses of sperm in cases of heterozygotes for balanced translocations in humans as well as mice, many researchers have described that unbalanced gametes are usually produced at a high frequency (Daring et al., 1972; Cattanaach et al., 1973; Ford and Evans, 1973; Gropp, 1973). In humans, however, it is almost impossible to investigate the actual role of chromosomally unbalanced gametes in fertilization and the selection of chromosomal imbalance during the early zygotic period.

There is still much to be learned from studies using experimental animals about the phenomena that occur during the gametic and early zygotic development, in addition to those aspects about which speculation can be made from indirect evidence. Research using Chinese hamsters heterozygous for autosomal reciprocal translocations to study segregation from quadrivalents, fertilization of chromosomally unbalanced gametes, and early development of chromosomally unbalanced embryos is reviewed herein.

### Establishment of Chinese hamster stocks with balanced chromosome rearrangements

#### *Usefulness of Chinese hamsters for cytogenetic analyses in meiotic and early zygotic stages*

Cytogenetic in vivo studies in experimental mammals have been performed mainly with mice and rats. However, the chromosomes in rat and mouse are similar. Most chromosomes are acrocentric, and it is very difficult to identify these individually without using banding procedures. After conventional staining, one can distinguish translocation chromosomes only when the translocation product is considerably larger than the largest chromosome, or when it is smaller than the smallest one. As an exception, the mouse *Mus poschiavenus* carries various sets of Robertsonian translocations of each chromosome. By crossing these mice with *Mus musculus* that have only acrocentric chromosomes, various strains carrying a Robertsonian translocation between specific chromosomes have been established (Ford, 1975; Gropp et al., 1975). From these heterozygotes for Robertsonian translocations, disomic and nullisomic gametes and trisomic and nullisomic embryos were obtained, and these animals were used in embryological-cytogenetic studies. However, these animals produce only gametes with disomy or nullisomy, or embryos with trisomy or monosomy, of only whole chromosomes. With these heterozygotes, it is not possible to obtain exact disjunction ratios from trivalents and quadrivalents because of the high and variable non-disjunction rates observed.

In the Chinese hamster, 22 chromosomes are classified into four autosomal groups and the sex chromosomes according to their size and the location of the centromeres. Therefore, each chromosome, except the acrocentric C-group chromosomes, is distinguishable in chromosome preparations from meiotic cells and from early embryos by conventional staining alone. Moreover, due especially to the differences in condensation and staining properties, sex chromosomes are easily detectable in

meiotic cells. In Chinese hamster translocation heterozygotes in which two translocated chromosomes are detectable, addition and loss of translocation chromosomes and translocation-related chromosomes are all detectable in meiotic cells and cells of early embryos. The frequencies of gametes with each karyotype produced by meiotic segregation can be determined. Exact segregation ratios from quadrivalents may be obtained by scoring MII spermatocytes. The success of fertilization may be calculated after analysis of the chromosome constitution of pronuclei in fertilized ova. Therefore, the Chinese hamster is useful for cytogenetic studies during the stages of meiosis and early embryogenesis.

#### *Establishment of animals with chromosomal rearrangements*

In experimental animals such as mice, rats, and Chinese hamsters, the frequency of chromosomal aberrations occurring spontaneously in meiotic cells and fertilized ova (Ford, 1972) is quite low compared with the estimated frequency in humans (Bond and Chandley, 1983). Therefore, it is very difficult to investigate problems such as the role of chromosomally abnormal gametes in fertilization by using only spontaneously occurring chromosomal aberrations.

Methods for systematically obtaining a specific chromosomal aberration at a high frequency are limited. We conducted experiments since 1976 to obtain animals with various structurally abnormal chromosomes produced by X irradiation (Sonta and Oishi, 1982; Sonta and Kitayama, 1991; Sonta et al., 1987). The Chinese hamsters used in our study were in the 17–24<sup>th</sup> generations of inbreeding. Males, 25–30 weeks old, were given 400 R of X irradiation (200 kVp, 15 mA, 27.9 R/min) to the hindquarters (1 R = Roentgen  $\approx$  0.01 Gy). Four weeks after irradiation, they were mated with non-irradiated females. Under these conditions, the sperm involved in fertilization were probably irradiated at the pachytene stage of spermatocytes (Utakoji, 1966). Ear or tail tissue of 5-week-old offspring from these crosses was cultured for chromosome examination. The chromosomes were analyzed with the R-banding technique (Dutrillaux et al., 1973) adopting the nomenclature of Ray and Mohandas (1976). The fertility of hamsters with a chromosomal rearrangement was examined by crossing them with karyotypically normal animals. An attempt was made to establish inbred strains with balanced rearrangements, such as reciprocal translocations in the homozygous state.

Although various structural and numerical chromosome abnormalities are seen in offspring obtained by crossing X-irradiated males (Table 1), balanced abnormalities are generally inherited by the next generation, i.e. inversions and reciprocal translocation. From progeny of irradiated males, we have established many stocks with balanced reciprocal translocations (Sonta and Oishi, 1982; Sonta et al., 1987, 199a, b) (Table 2). Among analyses using Chinese hamsters with various rearrangements, studies using 18 stocks with reciprocal translocations are reviewed.

**Table 2.** Chinese hamster stocks with reciprocal translocations used herein<sup>a</sup>

Stock	Breakpoints <sup>b</sup>
T(4;5)21dr	t(4;5)(q12;q13)
T(2;10)31dr	t(2;10)(q18;q11)
T(1;3)71dr	t(1;3)(q13;q31)
T(1;4)101dr	t(1;4)(q11;p21)
T(1;2)121dr	t(1;2)(q38;p21)
T(7;9)161dr	t(7;9)(q22;q23)
T(1;5)171dr	t(1;5)(q17;q33)
T(4;8)201dr	t(4;8)(p23;p19)
T(3;9)261dr	t(3;9)(p13;p13)
T(2;9)331dr	t(2;9)(p21;p16)
T(1;8)351dr	t(1;8)(p24;p19)
T(1;3)381dr	t(1;3)(p15;p28)
T(2;4)401dr	t(2;4)(q17;p25)
T(2;8)611dr	t(2;8)(q21;q26)
T(5;10)621dr	t(5;10)(q22;q23)
T(3;5)651dr	t(3;5)(p23;q27)
T(1;6)721dr	t(1;6)(q42;q29)
T(1;3)1051dr	t(1;3)(q17;q31)
T(2;3)1081dr	t(2;3)(q21;p29)

<sup>a</sup> Reported by Sonta and Oishi, (1982); Sonta and Kitayama (1987); and Sonta et al. (1991a, b), besides four stocks.

<sup>b</sup> Following Ray and Mohandas (1976).

#### **Chromosomal segregation in translocation heterozygotes**

Using Chinese hamsters heterozygous for reciprocal translocations in which each translocated chromosome can be distinguished, one can determine the exact frequency of each disjunctive class theoretically derived from quadrivalents by cytogenetic analysis of secondary spermatocytes. The classes of meiotic segregation for reciprocal translocations, alternate, adjacent 1, adjacent 2 and 3:1 disjunctions, are shown in Fig. 1 (Ford and Clegg, 1969).

Young (6- to 9-month-old) males and females were used. Males were injected intraperitoneally with 2 mg/kg of colcemid 4 h before sacrifice. Preparations of secondary spermatocytes were made by the method of Evans et al. (1964). From females, preparations of secondary oocytes were made according to the method of Kamiguchi et al. (1976), with slight modifications (Sonta et al., 1984).

Five to ten males and more than 100 females from each translocation stock were examined. As an example of the data obtained, the chromosomal analyses of secondary meiotic (MII) cells from 5 males and 116 females heterozygous for a translocation between chromosomes 2 and 9 [T(2;9)331dr] are summarized in Table 3. The frequency of each disjunctive class was estimated by the MII counts in male and female translocation heterozygotes. The frequency of each disjunctive class was similar among males heterozygous for the same reciprocal translocation (Sonta et al., 1984). Among males and females heterozygous for the same translocation, there is no difference in the frequency of each disjunctive class (Table 3). Similar results have been obtained in previous experiments using other Chinese hamster stocks with reciprocal translocations (Kaseki et al., 1987; data not shown). That is, in males and females heterozygous for the same reciprocal translocation,



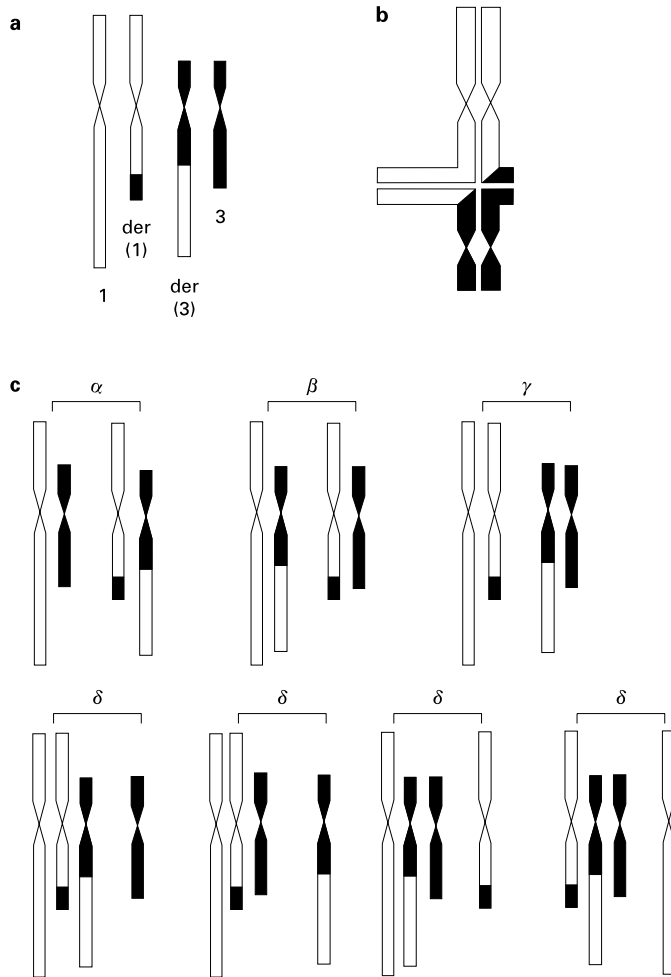


**Fig. 1.** Schematic representation of chromosomal segregation from a quadrivalent in a reciprocal translocation heterozygote. **(a)** An example of a partial karyotype of  $t(1;3)$  translocation heterozygote. **(b)** A quadrivalent seen in  $t(1;3)$  translocation heterozygote. **(c)** Chromosomal constitution of gamete cells derived from various disjunctions; alternate ( $\alpha$ ), adjacent-1 ( $\beta$ ), adjacent-2 ( $\gamma$ ), and 3:1 disjunctions ( $\delta$ ), modified from a figure of Ford and Clegg (1969).

gametes with a specific chromosomal constitution are produced at a constant frequency.

Chromosomal analyses using heterozygotes from 18 stocks revealed that the frequency of each disjunctional class in translocation heterozygotes was different due to the specific reciprocal translocation, i.e., the different chromosomes and locations of breakpoints involved in reciprocal translocations. Among heterozygotes for three different translocations between the same chromosomes,  $T(1;3)7\text{Idr}$ ,  $T(1;3)38\text{Idr}$ , and  $T(1;3)105\text{Idr}$ , however, the frequencies of each class of disjunction were very similar. The frequencies of alternate, adjacent 1, adjacent 2 and 3:1 disjunction were 43.1–43.8%, 28.9–29.4%, 16.8–17.2%, and 10.1–10.4%, respectively. This result, therefore, may suggest that the frequency of every class of disjunction mainly depends on the chromosome but not so much on the location of the breakpoint.

In heterozygotes of 18 stocks, the range of the mean frequencies of alternate and adjacent-1 disjunction were rather similar, i.e. 37.9–48.7% and 23.7–42.1%, respectively. On the other hand, the range of the frequencies of adjacent-2 and 3:1 disjunction for different reciprocal translocations was wider, i.e. 7.6–33.1% and 3.4–24.6%, respectively. Comparison of the frequencies of each disjunctional class of meiotic segregation among heterozygotes for every translocation seems to reveal a slight tendency for lower frequency of 3:1 disjunction in heterozygotes with a high frequency of adjacent 2 disjunction. On the other hand, the reverse relationship between the frequencies of adjacent 2 and 3:1 disjunctions was also seen in other translocation heterozygotes. For example, although the frequency of 3:1 disjunction in heterozygotes for  $T(1;4)10\text{Idr}$ ,  $T(1;2)12\text{Idr}$  and  $T(2;3)108\text{Idr}$  translocation was as high as 22.6, 24.6, and 22.3%, respectively, the frequency of adjacent 2 disjunction was 10.7, 7.6, and 10.5%. In contrast, although the frequency of 3:1 disjunction in heterozygotes for  $T(1;5)17\text{Idr}$  and  $T(1;6)72\text{Idr}$  translocations was as low as 3.4 and 4.2%, the frequency of adjacent 2 disjunction was as high as 32.1 and 29.5%, respectively. Moreover, the range of the frequencies of each disjunctional class in Chinese hamster translocation heterozygotes is almost consistent with that estimated by sperm analysis in human heterozygotes for reciprocal translocations (Table 4).

In addition, other studies of translocation heterozygotes revealed that the presence of reciprocal translocations during meiosis in the Chinese hamster does not induce any interchromosomal effects on non-disjunction, i.e. during first and second meiosis, the presence of rearranged chromosomes exerts no influence on the segregation of chromosomes unrelated to the rearrangement (Sonta and Kitayama, 1991; Sonta et al., 1995). This is a distinct advantage over Robertsonian translocations in mice.

#### Participation of chromosomally unbalanced gametes in fertilization

Data from chromosomal analyses of secondary meiotic cells were used to calculate the expected frequency of gametes with each karyotype in males and females heterozygous for each translocation. By crossing translocation heterozygotes to normal partners, we compared the frequencies of 1-cell embryos with each possible karyotype with the expected frequencies estimated by MII scoring to detect selection against chromosomally abnormal sperm. Young adult (6- to 9-month-old) Chinese hamsters from a karyotypically normal strain,  $\text{CHS/Idr}$ , were mated to young adults from the 18 translocation stocks (Table 2) (Sonta and Oishi, 1982; Sonta et al., 1987, 1991). Chromosomal constitutions of derivatives from the first meiotic quadrivalents in these 18 translocation heterozygotes were identified in MII cells as well as in pronuclei of fertilized ova. Females in proestrus that were karyotypically normal (+/+) or translocation heterozygous (T/+) were caged overnight with T/+ and +/+ males, respectively. From females with confirmed copulation, fertilized ova were collected 2 h before the estimated time of first cleavage division. The ova were subsequently cultured for 3 h in medium containing 15% fetal calf serum,

**Table 3.** Frequency of various classes of MII cells in male and female T(2;9)33Idr heterozygotes

Number of chromosomes	Genotype <sup>a</sup>	Male heterozygotes		Female heterozygotes	
		Spermatocytes counted	Disjunction (%)	Oocytes counted	Disjunction (%)
10	(2,0), (2 <sup>9</sup> ,0), (0,9), etc.	52		41	
	Others	19		12	
11	(2,9), (2 <sup>9</sup> ,9 <sup>2</sup> )	492	47.8 <sup>b</sup>	369	48.3 <sup>b</sup>
	(2 <sup>9</sup> ,9), (2 <sup>9</sup> ,9 <sup>2</sup> )	86		78	
	(2,9 <sup>1</sup> ), (2 <sup>9</sup> ,9 <sup>1</sup> )	15		12	
	(2,9 <sup>2</sup> ), (2 <sup>9</sup> ,9)	306	29.8 <sup>c</sup>	181	30.2 <sup>c</sup>
	(2,2 <sup>9</sup> ), (9,9 <sup>2</sup> ), (2 <sup>9</sup> ,9)	177	15.2 <sup>d</sup>	134	15.1 <sup>d</sup>
	Others	4		3	
12	(2,2 <sup>9</sup> ,9), (2,2 <sup>9</sup> ,9 <sup>2</sup> ), etc.	43	7.2 <sup>e</sup>	33	7.4 <sup>e</sup>
	Others	10		8	
Total		1,204	100.0	921	100.0

<sup>a</sup> 2' and 9' are chromosomes with unequal-length chromatids resulting from crossing-over.

<sup>b-d</sup> Percentage of alternate<sup>b</sup>, adjacent 1<sup>c</sup>, and adjacent 2 disjunctions<sup>d</sup>. Percentage of alternate and adjacent 1 disjunctions were calculated in proportion to the number of cells having chromosomes without unequal-length chromatids.

<sup>e</sup> Frequency of cells due to 3:1 disjunction estimated by doubling the frequency of hyperploidy.

**Table 4.** Frequencies of various classes of disjunctions in males heterozygous for reciprocal translocations in humans and Chinese hamsters

Species	Disjunctions (%)				
	alternate	adjacent 1	adjacent 2	3:1	4:0
Human <sup>a</sup>	39.0–47.7	26.8–51.9	1.9–31.4	0.6–17.0	0
Chinese hamster <sup>b</sup>	37.9–48.7	23.7–42.1	7.6–32.1	3.4–24.6	0

<sup>a</sup> Estimated from 17 reports with more than 100 sperm analyzed (Guttenbach et al., 1997).

<sup>b</sup> Mean frequency of each disjunctional class estimated from data of males heterozygous for reciprocal translocations from 18 strains. More than 500 sperm were analyzed in male heterozygotes in each strain.

0.04 pg/ml colcemid, 0.005 pg/ml vinblastine, and 0.004 pg/ml podophyllotoxin (Sonta et al., 1984). The methods for chromosome preparations of fertilized ova were the same as for MII oocytes, with slight modifications.

As an example of the data obtained from chromosomal analyses of pronuclei in fertilized ova using 18 translocation stocks, the results obtained from crosses of male and female T(1;8)35Idr and T(3;5)65Idr heterozygotes (T35/+ and T65/+) to normal partners are summarized in Table 5. All the karyotypes expected theoretically from T35 and T65 heterozygotes were observed in the pronuclei of ova originating from these crosses. In these ova, the frequencies of male pronuclei with the 11(8, 8<sup>1</sup>) karyotype among embryos of the cross +/+♂ × T35/+♀ and with the 11(5, 5<sup>3</sup>) karyotype among embryos of the cross +/+♂ × T65/+♀ were significantly lower than that estimated from MII scoring. These karyotypes of male pronuclei showing a decreased frequency were nullisomic for a segment of chromosome 1 (1p24 → 1qter) and nullisomic for a segment of chromosome 3 (3p23 → 3qter), respectively. The frequencies of pronuclei with any karyotype other than 11(8, 8<sup>1</sup>) and 11(5, 5<sup>3</sup>) in embryos of these crosses were consistent with expectation. In contrast, in embryos from the respective crosses of female translocation carriers, the frequencies of female pronuclei with any possible karyotypes, including the unbalanced

karyotypes of 11(8, 8<sup>1</sup>) and 11(5, 5<sup>3</sup>), were consistent with those estimated from MII scoring.

Studies using the 18 stocks with different reciprocal translocations revealed clearly that embryos with decreased frequencies compared to theoretical expectation were partially monosomic only for chromosomes 1 and 3. They originated from partially nullisomic sperm of males heterozygous for reciprocal translocations involving chromosomes 1 and 3, such as T(1;3)7Idr, T(1;4)10Idr, T(1;8)35Idr, T(1;3)38Idr, T(3;5)65Idr, and T(1;5)72Idr. The karyotypes of male pronuclei with a decreased frequency among 1-cell embryos have a common nullisomy of a segment of chromosome 1 (1q17 → 1q42). Similarly, some karyotypes with a decreased frequency were commonly characterized by a deficiency of a segment of chromosome 3 (3p23 → 3q31) (Sonta et al., 1991a, b; data not shown). Sperm with other abnormalities from males heterozygous for the 18 translocations had participated in fertilization with the expected frequency. On the other hand, oocytes with partial nullisomies or disomies, including those that decreased the fertilization rate for sperm, had all been fertilized with the expected frequency.

In experimental mammals such as the mouse, rat, and Chinese hamster, the frequencies of chromosomal aberrations occurring spontaneously during the meiotic and early zygotic

**Table 5.** Frequencies of pronuclei with various karyotypes transmitted from each heterozygous parent in one-cell embryos produced by crossing T35 and T65 translocation heterozygotes with karyotypically normal hamsters

Number of chromosomes	Genotypes of pronuclei <sup>a</sup>	Percentage of embryos observed (expected <sup>b</sup> )			
		T35/+ ♀ × +/+ ♂ (n=928)		+/+ ♀ × T35/+ ♂ (n= 1,258)	
10	(1 <sup>8</sup> , 0), etc	5.5	(4.6)	6.3	(4.5)
11	(1, 8)	21.3	(22.1)	23.9	(21.9)
	(1 <sup>8</sup> , 8 <sup>1</sup> )	21.4	(22.1)	23.5	(21.9)
	(1 <sup>8</sup> , 8)	14.6	(14.8)	15.9	(14.8)
	(1, 8 <sup>1</sup> )	14.7	(14.8)	15.8	(14.8)
	(1, 1 <sup>8</sup> )	8.6	(8.7)	8.2	(8.6)
	(8, 8 <sup>1</sup> )	8.8	(8.7)	0.9 <sup>d</sup>	(8.6)
	other	0.3	(-)	0.2	(-)
12	(1, 1 <sup>8</sup> ,8), etc.	4.8	(4.6)	5.3	4.5
Total		100		100	
		T65/+ ♀ × +/+ ♂ (n=987)		+/+ ♀ × T65/+ ♂ (n= 1,352)	
10	(3 <sup>5</sup> , 0), etc.	5.7	(5.1)	6.2	(5.0)
11	(3, 5)	23.3	(23.8)	23.7	(23.3)
	(3 <sup>5</sup> , 5 <sup>3</sup> )	23.4	(23.8)	23.5	(23.3)
	(3 <sup>5</sup> , 5)	12.6	(12.6)	15.9	(13.1)
	(3, 5 <sup>3</sup> )	12.7	(12.6)	15.9	(13.1)
	(3, 3 <sup>5</sup> )	8.6	(8.5)	8.0	(8.6)
	(5, 5 <sup>3</sup> )	8.4	(8.5)	1.3 <sup>c</sup>	(8.6)
	other	0.2	(-)	0.3	(-)
	(3, 3 <sup>3</sup> ,5), etc.	5.1	(5.1)	5.4	
Total		100		100	

<sup>a</sup> The pronucleus genotypes shown are those transmitted from each heterozygous parent.

<sup>b</sup> The expected frequency of pronuclei with each genotype was estimated from MII scoring.

<sup>c</sup> Significantly lower than the expected frequency ( $p < 0.001$ ).

stages (Ford, 1971) are quite low compared with the frequencies estimated for humans (Bond and Chandley, 1983). When one only analyses spontaneous chromosomal abnormalities, it is difficult to investigate detailed problems such as the participation of chromosomal abnormalities in fertilization and early embryogenesis. Therefore, the X-ray-induced translocation heterozygotes of Chinese hamsters provide a tool for efficiently producing gametes and embryos with specific chromosomal abnormalities.

To investigate gametic selection, many researchers have used mainly mouse stocks heterozygous for Robertsonian translocations, which were established from heterozygous *Mus poschiavenus*-F<sub>1</sub> hybrids with some metacentric chromosomes (Ford, 1972; Ford and Evans, 1973; Gropp, 1973; Baranov and Dyban, 1975; Epstein and Travis, 1979; Magnuson et al., 1985; Epstein, 1986; Dyban and Baranov, 1987). These authors concluded that there was no selection against sperm with any chromosomal abnormalities. However, these studies were mostly based on indirect investigations comparing the results of MII scoring and chromosomal data for pre- and post-implantation embryos. Actually, analyses of meiotic and early mitotic cells of mice with conventional staining is limited because of their uniform acrocentric chromosomes.

More useful data regarding sperm selection may be obtained by a direct comparison of chromosomes in MII cells and pronuclei in fertilized ova from 18 Chinese hamster stocks with various reciprocal translocations. These results revealed clearly that only male gametes nullisomic for certain segments of chromosomes 1 and 3 failed to participate in fertilization (Sonta et

al., 1984; Sonta, 2002). Male gametes with other abnormalities and oocytes with any abnormality participated in fertilization at the respective expected frequencies. Thus, the common abnormalities with a disadvantage for fertilization were limited to deficiencies in specific segments of chromosomes 1 and 3. Chinese hamster studies provide the only data to date on the fertilization of chromosomally unbalanced gametes by direct observation of ova in mammals.

#### Development of chromosomally unbalanced embryos at early stages

Embryos with various karyotypes were obtained by crossing karyotypically normal females with males heterozygous for reciprocal translocations. Embryos were collected from these females 2 h before the estimated times of the first, second, third, and fourth cleavages and in the early and late blastocyst stage (Sonta et al., 1984). Chromosome preparations of these embryos were made according to the method of Sonta et al. (1984). The number of blastomeres of embryos with the various karyotypes from each cross was scored and compared with that of embryos from the control matings. Late on day 5 of gestation, the uteri of pregnant females were flushed with Hanks' solution to collect embryos that failed to implant.

In the experiments with all stocks, karyotypes expected from MII scoring in the male heterozygotes were all observed in fertilized ova, and the frequencies of ova with each karyotype, except those partially nullisomic for chromosomes 1 and 3,

**Table 6.** Chromosome analysis of embryos in the cross  $+/+ \text{♀} \times \text{T33}/+\text{♂}$  at different cleavage stages

Number of chromosomes	Genotype	Percentage expected <sup>a</sup>	Number of embryos observed (percentage expected <sup>b</sup> )					
			2 <sup>nd</sup> cleavage		4 <sup>th</sup> cleavage		Blastocyst	
21	(2,9,9),(2,9,9 <sup>2</sup> ),etc.	3.6	10	(3.8)	7	(2.4)	4	(1.6)
22	(2,2,9,9)	23.9	62	(23.9)	72	(23.9)	61	(23.9)
	(2,2 <sup>9</sup> ,9,9 <sup>2</sup> )	23.9	63	(23.9)	70	(23.9)	62	(23.9)
	(2,2 <sup>9</sup> ,9,9)	14.9	39	(14.9)	35	(11.8)	19	(7.4)
	(2,2,9 <sup>2</sup> ,9)	14.9	40	(15.3)	42	(14.1)	35	(13.6)
	(2,2,2 <sup>9</sup> ,9)	7.6	21	(8.0)	21	(7.1)	13	(5.1)
23	(2,9,9,9 <sup>2</sup> )	7.6	0	(0.0)	0	(0.0)	0	(0.0)
	(2,2,2 <sup>9</sup> ,9,9),etc.	3.6	9	(3.4)	10	(3.4)	9	(3.5)
	Total	100	244	(93.2)	257	(86.6)	201	(79.0)

<sup>a</sup> Expected from MII scoring.  
<sup>b</sup> Percentage estimated assuming that the combined frequency of embryos with normal and balanced karyotypes is equal (47.8%), as expected from MII scoring.

were consistent with those expected from MII scoring. The ova in which chromosomes could not be observed at the 1-cell stage were mostly unfertilized.

In these crossings, the percentages of 1-cell embryos successfully karyotyped at the stage of first mitotic division were 96.9–98.2%, compared with 97.2% in the control crosses. That is, there was no evidence for an increase of ova arrested at the first cleavage in any cross using heterozygotes of the 18 stocks with different translocations. At the second cleavage and later the percentages of embryos successfully karyotyped in the experimental crosses decreased slightly compared with the control crosses. The percentage of embryos successfully karyotyped at the second and fourth cleavage stage from the cross of male T(2;9)33Idr heterozygotes ( $+/+ \text{♀} \times \text{T33}/+\text{♂}$ ), for instance, was 78.9 and 70.1%, respectively, whereas the percentage of embryos successfully karyotyped at the same stages in the control cross was 89.6 and 85.3%. The decreased frequencies of embryos successfully karyotyped in the experimental crosses may be due to the developmental arrest and cleavage delay of some chromosomally unbalanced embryos. In Table 6, an example of data for chromosomal analysis of embryos at the different developmental stages from the cross  $+/+ \text{♀} \times \text{T33}/+\text{♂}$  is shown. The differences in numbers of embryos between those collected actually and estimated with the same karyotypes became greater at the later developmental stages. The chromosomal analyses indicated that some karyotypes are no longer seen or reduced in their frequencies in embryos after the second cleavage, although they were observed in first-cleavage metaphases. These karyotypes were 22(2,9,9,9<sup>2</sup>), 21(2,9,9), and 21(2,9,9<sup>2</sup>), and have a deficiency in the segment from the break point of the short arm (p21) to the distal end of the long arm of chromosome 2, except for 21(2,9,9) that is deficient for the entire chromosome 2. Two-cell embryos were observed in 9.5, 9.1 and 8.8% of embryos collected in the cross  $+/+ \text{♀} \times \text{T33}/+\text{♂}$  at the expected times of the third and fourth cleavages and early blastocyst stages, respectively. In the control cross, on the other hand, no 2-cell embryo was seen at any later cleavage stage. The frequency (8.7–9.6%) of 2-cell embryos in the cross  $+/+ \text{♀} \times \text{T33}/+\text{♂}$  was nearly the same as the combined frequency of

22(2,9,9,9<sup>2</sup>), 21(2,9,9), and 21(2,9,9<sup>2</sup>) embryos, which was 9.4% expected from MII scoring. Therefore, the karyotypes of embryos in arrested cleavage at the 2-cell stage were supposed to be the ones no longer seen after the 2-cell stage. Similarly, 2-cell embryos were seen at various cleavage stages in embryos obtained from the crosses of stocks with reciprocal translocations in which chromosome 1 or 2 was involved. The karyotypes of these 2-cell embryos had a common deficiency of a segment of chromosomes 1 or 2.

In other experiments, 4- to 8-cell embryos were seen at the early to late blastocyst stage in embryos obtained from the crosses of the heterozygotes of translocation stocks, in which chromosomes 3 and 4 were involved in the respective translocations. In these crosses, karyotypes with partial monosomy for chromosomes 3 and 4 decreased among the embryos karyotyped after the 8-cell stage. Similarly, the 4- to 8-cell arrest was seen in embryos partially monosomic for chromosomes 1p, 1q and 5.

The numbers of blastomeres found among 201 successfully karyotyped 4-day embryos in the cross  $+/+ \text{♀} \times \text{T33}/+\text{♂}$  are shown in Table 7. The mean numbers of blastomeres of chromosomally balanced embryos was similar to that of embryos from the control cross ( $+/+ \text{♀} \times +/+ \text{♂}$ ). The frequencies of embryos with an unbalanced karyotype, such as 22(2,2<sup>9</sup>,9,9) and 21(2,2<sup>9</sup>,9) in the cross, slightly decreased among embryos successfully karyotyped at the blastocyst stage. The numbers of blastomeres in 21(2,2,9<sup>2</sup>) and 21(2,2,9) embryos was also small but the numbers of embryos observed were insufficient. On the other hand, embryos with other karyotypes such as 22(2,2,9,9<sup>2</sup>) or 23(2,29,9,9,9<sup>2</sup>) had almost the same numbers of blastomeres as that of karyotypically normal embryos. Among embryos obtained from other experiments using heterozygotes for different translocations, the numbers of cells in embryos showing partial monosomy for chromosomes 1p, 1q, 2q, 4, 5q and 8 also decreased. Thus, these chromosomal abnormalities cause disadvantages in early embryogenesis at about the 8-cell stage.

By flushing the uteri on day 5.5 of gestation, a total of 36 embryos were collected in 18  $+/+$  females crossed with T33/+ males: 16 were 2-cell embryos, 2 were 8-cell embryos, 9 were

**Table 7.** The number of blastomeres of embryos in the  $+/+ \text{♀} \times \text{T33}/+ \text{♂}$  cross and the control cross on day 4 of gestation

Cross	Genotype	Number of embryos	Number of blastomeres per embryo (mean $\pm$ SD)
$+/+ \text{♀} \times \text{T33}/+ \text{♂}$	21(2,2,9 <sup>2</sup> )	1	13
	21(2,2,9)	3	16.7 $\pm$ 3.2
	22(2,2,9,9)	61	23.6 $\pm$ 2.0
	22(2,2 <sup>9</sup> ,9,9 <sup>2</sup> )	62	23.5 $\pm$ 1.9
	22(2,2 <sup>9</sup> ,9,9)	17	10.4 $\pm$ 2.1 <sup>a</sup>
	22(2,2,9,9 <sup>2</sup> )	35	22.6 $\pm$ 2.2
	22(2,2,2 <sup>9</sup> ,9)	13	19.3 $\pm$ 2.4
	22(2,9,9,9 <sup>2</sup> )	0	-
	23(2,2,2 <sup>9</sup> ,9,9), etc	9 <sup>b</sup>	20.3 $\pm$ 2.9
	Total	201	21.6 $\pm$ 2.2
	$+/+ \text{♀} \times +/+ \text{♂}$	22(2,2,9,9)	146

<sup>a</sup> Significantly different from normal embryos from the control cross ( $P < 0.001$ ).  
<sup>b</sup> Mean number of blastomeres per embryo in all embryos with 23 chromosomes.

phenotypically abnormal morulae-blastocysts, and 3 were unfertilized ova. Only 7 embryos were collected from 34 females from the control cross: 4 were morulae-blastocysts, and 4 unfertilized ova. Similar results were obtained in experiments using other stocks.

Cytogenetic investigations on the development of chromosomally unbalanced embryos in the early stages have mainly been performed with the mouse (Gropp, 1973; Ford, 1975; Gropp et al., 1975; Oshimura and Takagi, 1975; Epstein and Travis, 1979; Magnuson and Epstein, 1981; Magnuson et al. 1985; Dyban and Baranov, 1987). Analysis of MII spermatoocytes and preimplantation embryos in heterozygous *Mus poschiavenus*-F<sub>1</sub> hybrid and translocation heterozygotes such as T(14;15)6Ca/+ indicated that most monosomic embryos died shortly after implantation, whereas trisomic embryos survived after implantation until early to late organogenesis. The development of embryos monosomic for a few autosomes was arrested during the preimplantation period (Epstein and Travis, 1979; Magnuson and Epstein, 1981), i.e., monosomy 19 generally survive 3.5 days. Our studies in the Chinese hamster, revealed that all embryos with unbalanced chromosomes can develop to at least the 2-cell stage, that embryos with a partial deficiency of chromosomes 1 and 2 cease development at the 2-cell stage, and that partial monosomies for chromosomes 3, 4 and 5 and partial monosomy of another segment of chromosome 1 (1p and 1q) result in arrested development at the 4- to 8-cell stages. Thus, the first evidence for the expression of a specific genome imbalance in early diplophase, such as the 2-cell stage came from studies in Chinese hamster. However, a similar selective elimination at the 2-cell stage has not been found in autosomal monosomies in the mouse.

The discrepancy between the majority of the data on sperm selection and zygotic selection in early stages in mouse and Chinese hamster may be a result of the following phenomena. Firstly, since the proportion of one chromosome to the total genome in the Chinese hamster is larger than that in the mouse, nullisomic gametes and monosomic embryos may have a more conspicuous influence on fertilization and early development, respectively. Secondly, due to the difference in gene order, the different contributions of genes lost in nullisomies and monosomies may be important factors for the lack of participation in

fertilization and for developmental arrest at the 2-cell stage, respectively. Thirdly, there may be differences between the two species in the nature of sperm formation, fertilization and early embryogenesis, which are genetically controlled. In fact, data have been published to show that Chinese hamster embryos develop slower than mouse embryos during early cleavage stages (Pickworth et al., 1968) that may be a reason for loss of gene expression in the early stages. Fourthly, there may be some nullisomic sperm that also fail to participate in fertilization that researchers have not yet detected. Further detailed analyses on the influences of partial nullisomies and monosomies in fertilization and early zygotic development, as well as the development of comparative genome analysis, will help to clarify the causes of this discrepancy in the participation of chromosomally unbalanced sperm in the fertilization and chromosomal unbalance in early zygotic development between the two species.

Chromosomal homology between the Chinese hamster and the mouse has been studied based on comparative gene mapping and FISH analysis (Yang et al., 2000; Mouse Genome Database, 2003). In these studies, the homologous segments are seen sometimes in units of chromosome arms and sometimes in segments of these chromosomes. According to these studies on homologous maps of chromosomes, there is a slight homology between Chinese hamster and mouse chromosomes relating to abnormal embryogenesis at early stages. These facts may therefore suggest that homologous genes relating to early embryogenesis are preserved in homologous segments of chromosomes between the two species. Further molecular and cytological studies may give more useful information to better understand the genes and chromosomes controlling early embryogenesis.

## Conclusion

Damage to DNA caused by various kinds of mutagens may lead to visible chromosome aberrations of different qualities. Chromosomal aberrations are produced in every cell, but to estimate the actual inherited influence of these chromosomal aberrations, one needs to understand the effect of chromosomal aberrations in gamete formation and fertilization, as well as

elimination of chromosomal imbalances during early embryogenesis.

In the transmission of human chromosomal abnormalities from carrier parents, sperm selection has been considered to be one of the possible causes of sex differences (Hamerton, 1968). On the other hand, monosomies for any autosome and the majority of trisomies were not found in human spontaneous abortions in the early period of gestation, which is the earliest developmental stage at which we can analyze chromosomes of embryos and fetuses. It is generally considered that the majority of these chromosomal imbalances, including monosomies, are probably eliminated at an early developmental stage (Boué et al., 1975; Ford, 1975; Hamerton, 1978). However, human specimens available to study fertilization and early development of embryos are limited to newborns and living or aborted fetuses, and it is still difficult to obtain clear evidence of gametic selection and elimination of early embryos. The technique using penetration to Syrian hamster oocytes allows visualization of human sperm chromosomes (Rudak et al., 1978; Brandiff et al., 1986; Martin, 1988). FISH analyses have generated new information on chromosomal constitutions of human sperm (Goldman and Hulten, 1993; Shi and Martin, 2001; Escudero et al., 2003). However, such techniques have also been unable to provide sufficient evidence of sperm selection.

In humans, the frequency of abnormal offspring mainly with a partial duplication of chromosomal segments derived

from paternal carriers of reciprocal and Robertsonian translocations is lower than that from maternal carriers. It has been speculated that the decreased frequency in paternal carriers is a result of sperm selection, as mentioned above. Our findings, however, suggest strongly that the cause of the decreased frequency in paternal carriers is not the selective elimination of chromosomally unbalanced sperm, because sperm with any duplication of chromosomes were at no disadvantage for fertilization, and sperm at a disadvantage for fertilization were limited to those nullisomic for the large segments of the specific chromosomes. In addition, although there is still little information on the early development of chromosomally unbalanced embryos in humans, our data strongly support the assumption that most human monosomic embryos are eliminated during the early stages of embryogenesis, similar to the Chinese hamster and the mouse.

To understand the chromosomes and genes relating to fertilization and early embryogenesis, further studies based on comparative mapping and gene analysis among humans and experimental mammals may give us more useful information.

### Acknowledgements

The author wishes to thank N. Nomura, C. Nakagawa, Y. Kawabata, T. Kawamoto, M. Tsukasaki, M. Nishida, K. Takeshima and M. Yamada for technical assistance.

### References

- Baranov VS, Dyban AP: The prezygotic selection of male gametes in mice. *Tsitologiya* 18:556–561 (1975).
- Boué JG, Boué A, Lazar P: Retrospective and prospective epidemiological studies of 1500 karyotyped spontaneous human abortions. *Teratology* 12:11–26 (1975).
- Brandiff B, Gordon L, Ashworth KK, Littman V, Watchmaker G, Carrano AV: Cytogenetics of human sperm. Meiotic segregation in two translocation carriers. *Am J hum Genet* 38:197–208 (1986).
- Cattanach BM, Moseley H: Nondisjunction and reduced fertility caused by the tobacco mouse metacentric chromosomes. *Cytogenet Cell Genet* 12:264–287 (1973).
- Daring L, Gropp A, Tettenborn U: DNA content and morphological properties of presumably aneuploid spermatozoa of tobacco mouse hybrids. *J Reprod Fert* 30:335–346 (1972).
- Dutrillaux B, Laurent C, Couturier J, Lejeune J: Coloration par l'acridine orange de chromosomes préalablement traités par le 5-bromo-deoxyuridine (BUDR). *C R Acad Sci (Paris)* 276:3179–3181 (1973).
- Dyban AP, Baranov VS: Cytogenetics of Mammalian embryonic Development (Oxford University Press, New York 1987).
- Epstein CJ: The Consequences of Chromosome Imbalance. Principles, mechanisms, and models (Cambridge University Press, London 1986).
- Epstein CJ, Travis B: Preimplantation lethality of monosomy for mouse chromosome 19. *Nature* 280:144–145 (1979).
- Escudero T, Abdelhadi I, Sandalinas M, Munne S: Predictive value of sperm fluorescence in situ hybridization analysis on the outcome of preimplantation genetic diagnosis for translocations. *Fertil Steril* 79:1528–34 (2003).
- Evans EP, Breckon G, Ford CE: An air-drying method for meiotic preparations from mammalian testes. *Cytogenetics* 3:289–294 (1964).
- Ford CE: Gross genome unbalance in mouse spermatozoa: does it influence the capacity to fertilize? in Beatty RA, Gluecksohn-Waelsch S (eds): *The Genetics of the Spermatozoon*, pp 285–304 (Edinburgh/New York 1972).
- Ford CE: The time in development at which gross genome imbalance is expressed, in Balls M, Wild SE (eds): *The Early Development of Mammals* (Cambridge University Press, London 1975).
- Ford CE, Clegg HM: Reciprocal translocations. *Br Med Bull* 25:110–114 (1969).
- Ford CE, Evans EP: Non-expression of genome unbalance in haplophase and early diplophase of the mouse and incidence of karyotypic abnormality in postimplantation embryos, in Boué A, Thibault C (eds): *Chromosomal Errors in Relation to Reproductive Failure*, pp 271–285 (INSERM, Paris 1973).
- Goldman AS, Hulten MA: Meiotic analysis by FISH of a human male 46,XY,t(15;20)(q11.2;q11.2) translocation heterozygote: quadrivalent configuration, orientation and first meiotic segregation. *Chromosoma* 102:102–111 (1993).
- Gropp A: Fetal mortality due to aneuploidy and irregular meiotic segregation in the mouse, in Boué A, Thibault C (eds): *Chromosomal Errors in Relation to Reproductive Failure*, pp 255–269 (INSERM, Paris 1973).
- Gropp A, Kolbus U, Giers D: Systematic approach to the study of trisomy in the mouse. *Cytogenet Cell Genet* 14:42–62 (1975).
- Guttenbach M, Engel W, Schmid M: Analysis of structural and numerical chromosome abnormalities in sperm of normal men and carriers of constitutional chromosome aberrations. A review. *Hum Genet* 100:1–21 (1997).
- Hamerton JL: Robertsonian translocations in man. Evidence for prezygotic selection. *Cytogenetics* 7:260–276 (1968).
- Hamerton JL: *General Cytogenetics, Vol I* (Academic Press, New York 1978).
- Jacobs PA, Frackiewicz A, Law P: Incidence and mutation rates of structural rearrangements of the autosomes in man. *Ann hum Genet* 35:301–319 (1972).
- Kamiguchi Y, Funaki K, Mikamo K: A new technique for chromosome study of murine oocytes. *Proc Japan Acad* 52:316–319 (1976).
- Kaseki H, Tomoda Y, Sonta S: Frequency of chromosomally unbalanced gametes in male and female hamsters heterozygous for reciprocal translocation. *Acta Obstet Gyneec Jpn* 39:675–680 (1987).
- Magnuson T, Epstein CJ: Genetic control of very early mammalian development. *Biol Rev* 56:369–408 (1981).
- Magnuson T, Debot S, Dimpn J, Zweig A, Zamora T, Epstein CJ: The early lethality of autosomal monosomy in the mouse. *J exp Zool* 59:121–129 (1985).
- Martin RH: Abnormal spermatozoa in human translocation and inversion carriers, in A Daniel (ed): *The Cytogenetics of Mammalian Autosomal Rearrangements*, pp 397–417 (Alan R Liss, New York 1988).

- Mouse Genome Database (1999): Mammalian Comparative Mapping Data, Mouse Genome Database, Mouse Genome Informatics Project. The Jackson Laboratory, Bar Harbor, ME.
- Mouse Genome Database (MGD) (2003), Mouse Genome Informatics, The Jackson Laboratory, Bar Harbor, ME (URL: <http://www.informatics.jax.org>).
- Oshimura M, Takagi N: Meiotic disjunction in T(14;15)6Ca heterozygotes and fate of chromosomally unbalanced gametes in embryonic development. *Cytogenet Cell Genet* 15:1–16 (1975).
- Pickworth S, Yerganian G, Chang MC: Fertilization and early development in the Chinese hamster, *Cricetulus griseus*. *Anat Rec* 162:197–208 (1968).
- Ray M, Mohandas T: Proposal banding nomenclature for the Chinese hamster chromosomes (*Cricetulus griseus*). Baltimore Conference (1975): Third International Workshop on Human Gene Mapping. in *Birth Defects: Original Article Series*, Vol. 12, No. 7, pp 83–91 (The National Foundation, New York 1976).
- Rudak E, Jacobs PA, Yanagimachi R: Direct analysis of the chromosome constitution of human spermatozoa. *Nature* 274:911–913 (1978).
- Shi Q, Martin RH: Aneuploidy in human spermatozoa: FISH analysis in men with constitutional chromosomal abnormalities, and in infertile men. *Reproduction* 121:655–666 (2001).
- Sonta S: Transmission of chromosomal abnormalities: participation of chromosomally unbalanced gametes in fertilization and early development of unbalanced embryos in the Chinese hamster. *Mutat Res* 204:193–202 (2002).
- Sonta S, Fukui K, Yamamura H: Selective elimination of chromosomally unbalanced zygotes at the two-cell stage in the Chinese hamster. *Cytogenet Cell Genet* 38:5–13 (1984).
- Sonta S, Kitayama K: No induction of interchromosomal effect in male meiosis of Chinese hamsters with reciprocal translocations. *Cytogenet Cell Genet* 56:9–13 (1991).
- Sonta S, Kitayama K, Narita N: Further Chinese hamster stocks with X-ray-induced chromosome rearrangements and their fertility. *Jpn J Genet* 62:341–348 (1987).
- Sonta S, Oishi H: Chinese hamsters with X-ray-induced reciprocal translocations: their production and fertility. *Congen Anomal* 22:167–171 (1982).
- Sonta S, Tsukasaki M, Kohmura N, Suzumori K: Independent chromosome segregation and absence of interchromosomal effect at first meiotic division in male Chinese hamsters heterozygous for two reciprocal translocations. *Cytogenet Cell Genet* 71:370–384 (1995).
- Sonta S, Yamada M, Iida T, Ohashi M: Developmental arrest at early stages of Chinese hamster embryos homozygous for chromosomal rearrangements. *Dev Biol* 144:30–37 (1991a).
- Sonta S, Yamada M, Tsukasaki M: Failure of chromosomally abnormal sperm to participate in fertilization in the Chinese hamster. *Cytogenet Cell Genet* 57:200–203 (1991b).
- Utakoji T: Chronology of nucleic acid synthesis in meiosis of the male Chinese hamster. *Exp Cell Res* 42:585–596 (1966).
- Yang F, O'Brien PCM, Ferguson-Smith MA: Comparative chromosome map of the laboratory mouse and Chinese hamster defined by reciprocal chromosome painting. *Chromosome Res* 8:219–227 (2000).

# Heritable translocations induced by dermal exposure of male mice to acrylamide

I.-D. Adler,<sup>a</sup> H. Gonda,<sup>a</sup> M. Hrabé de Angelis,<sup>a</sup> I. Jentsch,<sup>b,c</sup> I.S. Otten,<sup>a</sup> and M.R. Speicher<sup>b,c</sup>

Institut für <sup>a</sup>Experimentelle Genetik und <sup>b</sup>Humangenetik, GSF-Forschungszentrum für Umwelt und Gesundheit, Neuherberg; <sup>c</sup>Institut für Humangenetik, Technische Universität München, München (Germany)

**Abstract.** Acrylamide (AA) is an important industrial chemical used mainly in the production of polymers. It can be absorbed through the skin. AA was shown to be a germ cell clastogen that entails a genetic risk for exposed workers. The genetic risk calculation was based on mouse heritable translocation test data obtained after acute intraperitoneal (ip) exposure (Adler et al., 1994). To obtain a correction factor between ip and dermal exposure, dominant lethal and heritable translocation tests were carried out with dermal exposure of male mice to AA. In the dominant lethal test, male (102/El × C3H/El)<sub>F1</sub> mice were exposed by dermal application to the shaved backs of 50 mg/kg AA per day on five consecutive days or to five daily ip injections of 50 mg/kg AA. One day after the end of exposure, the males were mated to untreated females of the same hybrid stock for four days and females were changed every four days for a total of five matings. Dominant lethal effects were found during matings 1–3. For ip exposure, these values were

81.7, 85.7 and 45.4%, respectively; for dermal exposure the corresponding values were 22.1, 30.6 and 16.5%, respectively. In the heritable translocation assay, male C3H/El mice were treated with five dermal exposures of 50 mg/kg AA and mated 1.5–8.5 days after the end of exposure to untreated female 102/El mice. Pregnant females were allowed to come to term and all offspring were raised to maturity. Translocation carriers among the F<sub>1</sub> progeny were selected by a sequential fertility testing and cytogenetic analysis including G-band karyotyping and M-FISH. A total of 475 offspring were screened and 41 translocation carriers were identified. The observed translocation frequency after dermal exposure was 8.6% as compared to 21.9% after similar ip exposure (Adler, 1990). The calculated ratio of ip vs. dermal exposure of 0.39 can be applied to obtain a more realistic calculation of genetic risk for dermally exposed workers.

Copyright © 2003 S. Karger AG, Basel

Acrylamide (AA) is a monomeric chemical widely used in the production of AA polymer flocculants, polyacrylamide gels for electrophoresis, thickening agent, filtration aid and grouting agent. A Swedish group demonstrated that AA is formed during heating of starch-rich foods to high temperatures (Tareke et al., 2000, 2002), which raised a new wave of human health concern.

The neurotoxicity of AA was established quite early and led to the regulation of AA (Tilson, 1981; Miller and Spencer, 1985; O'Donoghue, 1985). Recently, a review on the effects of AA on rodent reproduction was published (Tyl and Friedman,

2003). The evidence that AA was carcinogenic in rodents (Bull et al., 1984; Johnson et al., 1986) increased the concern for AA as a potential human health hazard. Further investigations of AA identified its genotoxicity (Dearfield et al., 1988). Interestingly, AA was not mutagenic in the Ames test (Lijinsky and Andrews, 1980; Bull et al., 1984; Hashimoto and Tanii, 1985). It appeared that the major genotoxicity effect of AA was its clastogenic activity (Shiraishi, 1978; Moore et al., 1987; Adler et al., 1988; Knaap et al., 1988). Using flow cytometer-based analyses, it was demonstrated that the dose-response relationship for AA-induced micronuclei in mouse bone marrow cells was linear down to low single doses of 1–30 mg/kg AA applied by intraperitoneal (ip) injection (Abramsson-Zetterberg, 2003). In rodent germ cells, dominant lethal mutations and heritable translocations were induced by ip injection with AA in late spermatids and sperm (Adler, 1990; Shelby et al., 1986, 1987; Smith et al., 1986). Analysis of structural chromosome aberrations

Received 10 September 2003; manuscript accepted 15 December 2003.

Request reprints from Dr. Ilse-Dore Adler, GSF-Institut für Experimentelle Genetik  
D-85758 Neuherberg (Germany); telephone: +49-89-3187-2302  
fax: +49-89-3187-2210; e-mail: adler@gsf.de



tions in one-cell embryos after paternal AA-treatment was performed using conventional and molecular techniques (Pacchierotti et al., 1994; Marchetti et al., 1997). The data obtained allowed an estimate of the magnitude of AA-induced dominant lethality and heritable translocations showing close correlation of the results obtained by the respective tests. Even though the methodology of one-cell embryo collection and cytogenetic analysis requires great skills and is time-consuming, it may offer an alternative to the animal-consuming dominant lethal and heritable translocation assays. Sperm-chromatin alkylation was measured by accelerator mass spectrometry after ip treatment of male mice with  $^{14}\text{C}$ -acrylamide (Holland et al., 1999). It was correlated to pre-implantation losses of embryos in concurrent analyses of embryonic development in vitro and pre- and postimplantation loss of embryos in a dominant lethal assay with AA. The study confirmed the stage sensitivity of spermatogenesis to AA observed in the earlier dominant lethal studies. While specific locus mutations were observed originally in the same germ cell stages as the dominant lethal mutations (Russell et al., 1991), it was shown later that AA also induced mutations in spermatogonial stem cells of mice (Ehling and Neuhäuser-Klaus, 1992). Originally, alkylation of chromosomal protamines in late spermatids and sperm was assumed to cause the clastogenic effects in male germ cells (Sega et al., 1989). However, it could be demonstrated later that glycidamide was the genotoxic metabolite of AA in somatic and germinal cells of rodents (Adler et al., 2000; Generoso et al., 1996; Paulsson et al., 2003).

The main human exposure at production sites, in biochemical laboratories or during accidents in tunnel construction, where AA was used for gap filling in the rocks, occurred via dermal contact and to a lesser extent by ingestion. In mice, AA is readily absorbed through the skin and binds to DNA in the testes (Carlson and Weaver, 1985). It could be shown that dermal exposure of mice induced a dose-dependent increase of dominant lethal mutations in male mice (Gutierrez-Espeleta et al., 1992).

A dose response for the induction of heritable translocations in mouse spermatids by ip exposure to AA and a calculation of the possible genetic risk from AA-exposure of humans was published earlier (Adler et al., 1994). However, it seemed necessary to determine a conversion factor from ip to dermal exposure to derive a more realistic genetic risk calculation for exposed workers. The present dominant lethal and heritable translocation experiments were performed to compare the clastogenic effects of AA in mouse male germ cells on a quantitative basis between ip and dermal exposure.

## Materials and methods

### *Chemical and dosing*

Acrylamide (AA) was obtained from Sigma, Deisenhofen, Germany. In the dominant lethal assay, male mice were treated with five daily ip injections or five daily dermal applications on the shaved backs with 50 mg/kg of AA dissolved in saline (ip) or corn oil (dermal). The applied volume was 0.1 ml/10 g body weight. Control animals received the same application of the solvents. The heritable translocation assay was performed with dermal exposure only.

### *Animals*

All animals were bred and maintained in the animal facility of the GSF-Research Center in light- and air-conditioned animal rooms (12L/12D, 25 °C, 55 % humidity) and received pellet food and water ad libitum.

For the dominant lethal study, (102/EI  $\times$  C3H/EI) $F_1$  males, age 12–14 weeks, weighing between 24 and 26 g, were treated and mated to untreated virgin females of the same age and stock at a 1:1 ratio, starting one day after the end of treatment. Females were replaced four times every four days for a total of five mating intervals. On days 13–14 post conception (pc), the uterus contents of the females were inspected for live and dead implants. Percent induced dominant lethal was calculated by the formula  $(1 - [\text{live implants per female in the treated group}/\text{live implants per female in the control group}]) \times 100$ .

For the heritable translocation assay, males of the C3H/EI inbred strain, age 10–12 weeks, weighing between 24 and 26 g, were treated by dermal application of 50 mg/kg of AA on five consecutive days and mated 1.5–8.5 days after the end of treatment to untreated virgin 102/EI females of the same age at a mating ratio of 1:2. The experiment was repeated once. Pregnant females were allowed to come to term. Litters were counted and sexed at birth and weaned at the age of 3 weeks.

### *Selection of translocation-suspect $F_1$ animals by litter size reduction*

$F_1$  progeny of both sexes were mated at the age of 10–12 weeks avoiding brother-sister matings. To determine possible translocation heterozygotes by reduced fertility a sequential decision procedure of eliminating pairs with normal litters was employed (Adler, 1990). Up to three litters were observed before  $F_1$  pairs with reduced litter size or pairs without any litter were separated.

### *Confirmation of translocation-suspect $F_1$ males*

Suspect  $F_1$  males were mated to 4–5 (102/EI  $\times$  C3H/EI)  $F_1$  females. Females were sacrificed at mid-pregnancy to determine the frequency of early dead implants. Males that impregnated females with an average of three or more dead implants were subjected to cytogenetic confirmation of the translocation in testis preparations (Evans et al., 1964).  $F_1$  males identified as translocation heterozygotes were subjected to karyotype analysis in Giemsa-banded bone marrow preparations (Gallimore and Richardson, 1973; Evans, 1989; Adler et al., 2002) or by M-FISH (Jentsch et al., 2001).

### *Confirmation of translocation-suspect $F_1$ females*

Suspect  $F_1$  females were mated to (102/EI  $\times$  C3H/EI)  $F_1$  males and were again allowed to have up to four litters. Male  $F_2$  progeny from small litters of suspect  $F_1$  females were weaned and subjected to meiotic chromosome analysis at maturity as described above. Translocation-heterozygous females were confirmed by the presence of at least one translocation carrier among eight  $F_2$  males. The  $F_1$  translocation females or their translocation-carrying offspring were subjected to karyotype analysis of Giemsa-banded bone marrow chromosomes or by M-FISH as stated above.

### *Statistics*

Dominant lethal results were compared between treatment and solvent control groups on a male-to-male basis using the Mann-Whitney U test. Differences in translocation frequencies between the experimental group and the historical control group were analysed using Fisher's exact test (one-sided).

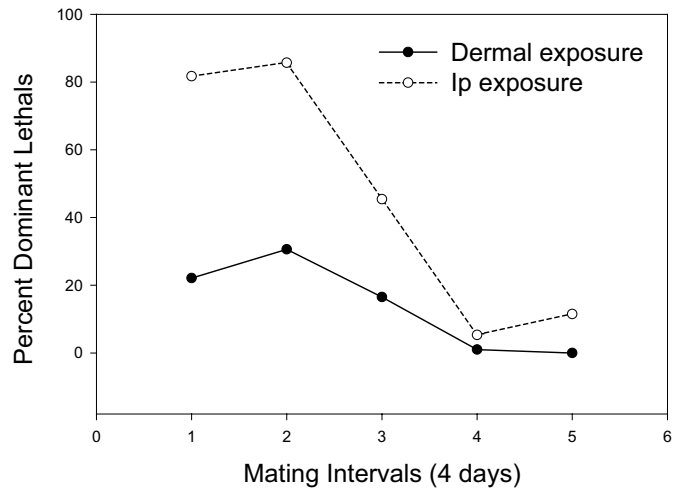
## Results and discussion

Table 1 shows the results of the dominant lethal experiments. The frequencies of dead implants per female are increased with both modes of exposure during the first three mating intervals, which represent sperm and late spermatids. This pattern of sensitivity is in accord with previous publications (Shelby et al., 1986, 1987; Smith et al., 1986, Holland et al., 1999). The dominant lethal effects are illustrated in Fig. 1. The effect was 2–4 times higher after ip exposure compared to dermal exposure. The results after dermal exposure are compa-

table to a previous publication (Gutierrez-Espeleta et al., 1992).

The results of the heritable translocation assay are shown in Table 2. In the first experiment, 242 F<sub>1</sub> progeny (138 males and 104 females) were tested for reduced fertility and 19 (12 males and 7 females) were identified to be translocation carriers. In the second experiment 233 F<sub>1</sub> progeny (120 males and 113 females) were tested for reduced fertility and 22 (16 males and 6 females) were identified to carry translocations. The observed translocation rates of the two experiments (7.85 and 9.44%, respectively) were not significantly different. Therefore, the data were pooled. The observed mean translocation frequency of 8.63% was significantly different from the historical control in our laboratory (Adler et al., 2002).

Table 3 shows the characteristics of the identified male translocation carriers from both experiments. Nine sterile F<sub>1</sub> translocation males were found. One of these carried a reciprocal translocation plus an inversion in chromosome 3 (AAD-229: T[9;13]+Inv.3, mean testis weight 60.9 mg), one carried two independent reciprocal translocations (AAD-240: T[1;12]



**Fig. 1.** Dominant lethal effects in sperm and spermatids of male mice after intraperitoneal (ip) and dermal exposure to 5 × 50 mg/kg of acrylamide. Percent dominant lethals = (1 - [live implants per female in the treated group / live implants per female in the control group]) × 100.

**Table 1.** Results with the dominant lethal test after five daily exposures of male mice to 50 mg/kg of acrylamide

Mating intervals <sup>a</sup> (days)	Application	Pregnant females <sup>b</sup>		Total implants		Live implants (LI)		Dead implants (DI)		% DI	Dominant lethals <sup>c</sup>
		n	%	n	Per female	n	Per female	n	Per female		
1.5–4.5	dermal	45	90	470	10.4	363	8.1	107	2.38 <sup>d</sup>	22.8	22.1
	ip	27	60	159	5.9	52	1.9	107	3.96 <sup>d</sup>	76.3	81.7
	control	50	100	561	11.2	519	10.4	42	0.84	7.5	–
5.4–8.5	dermal	48	96	478	10.0	328	6.8	150	3.13 <sup>d</sup>	31.4	30.6
	ip	35	78	191	5.5	49	1.4	142	4.06 <sup>d</sup>	74.4	85.7
	control	48	96	514	10.7	468	9.8	46	0.96	9.0	–
9.5–12.5	dermal	43	86	454	10.6	350	8.1	104	2.42 <sup>d</sup>	22.9	16.5
	ip	41	91	368	9.0	216	5.3	152	3.71 <sup>d</sup>	41.3	45.4
	control	43	86	465	10.8	419	9.7	46	1.07	10.0	–
13.5–16.5	dermal	44	88	455	10.3	414	9.4	41	0.93	9.0	1.0
	ip	36	80	364	10.1	323	9.0	41	1.14	11.3	5.3
	control	40	80	417	10.4	380	9.5	37	0.93	8.9	–
17.5–20.5	dermal	38	76	434	11.4	397	10.5	37	0.97	8.5	0
	ip	41	91	430	10.5	383	9.3	47	1.15	10.9	11.5
	control	46	92	535	11.6	481	10.5	54	1.17	10.1	–

<sup>a</sup> Mating started in the afternoon of the day after the end of exposure.

<sup>b</sup> Mating ratio 1:1, 50 males treated per group, five males died in the ip group during the course of treatment.

<sup>c</sup> Dominant lethals (%) = (1 - [LI per female<sub>exp</sub> / LI per female<sub>contr.</sub>]) × 100.

<sup>d</sup> P < 0.05.

**Table 2.** Results of the heritable translocation test after five daily dermal exposures of male mice to 50 mg/kg of acrylamide (two repeats)

Experiment	Males treated	Females mated	Litters	F <sub>1</sub> progeny tested	Translocation carriers	Translocation rate
1	50	100	63	242 (138♂ / 104♀)	19 (12♂ / 7♀)	7.85 %
2	50	100	73	233 (120♂ / 113♀)	22 (16♂ / 6♀)	9.44 %
Total	100	200	136	475 (258♂ / 117♀)	41 (28♂ / 13♀)	8.63 % <sup>a</sup>

<sup>a</sup> P < 0.001 compared to the historical control of 0.05%

**Table 3.** Characterization of the male translocation carriers

Animal code	Mean litter size <sup>a</sup>	Translocation multivalents <sup>b</sup> (%)	Chromosomes involved <sup>c</sup>	Presumed break points
<b>First experiment</b>				
AA-5	5.7	9.3	T(14;19)	14E2.2; 19D1
AA-34	2.8	40	T(2;7)	2H3; 7D1
AA-37	st	96	T(5;19)	5EF; 19B
AA-40	3.4	84	T(13;14)	13C3; 14A3
AA-56	3.3	5.2	T(4;9)	4D3; 9A4
AA-58	3.6	39	T(5;19)	5B2; 19B
AA-67	3.2	88	T(9;1)	9B; 11B3
AA-83	2.0	100 (44% 2TM)	nd	nd
AA-86	st	no meioses	T(3;5)	3F1; 5F
AA-89	3.5	28	T(9;16)	9B; 16B5
AA-96	2.3	47	T(4;8)	4C3; 8B3.2
AA-127	st	88	T(7;10)	7F1; 10A4
<b>Second experiment</b>				
AA-155	4.0	13	T(2;15)	2G1; 15C
AA-164	6.3	76	T(11;17)	11D; 17D
AA-165	st	70	T(14;17;19)	14E2; 17E2; 19C2
AA-169	3.8	20	T(9;13)	9E3; 13C2
AA-181	st	6	T(9;Y)	9F1; YD
AA-185	3.5	64	T(1;7)	1D; 7F1
AA-198	5.5	36	T(4;8)	4C6; 8E1
AA-215	st	no meioses	T(3;4)	3E2; 4D3
AA-216	4.7	80	T(4;7)	nd
AA-225	3.5	36	T(10;14)	10C1; 14B
AA-227	st	20 (no sperm)	T(9;Y)	9F1; YC2
AA-229	st	80	T(9;13)+Inv 3	9F1; 13D1; 3E2/G2
AA-233	3.3	76	T(12;17)	12D2; 17B1
AA-236	3.8	56	T(4;8)	4B3; 8D3
AA-240	st	no meioses	T(1;12)+T(5;10)	1F; 12C3; 5A2; 10D2
AA-253	3.3	56	T(3;14)	3H3; 14B

<sup>a</sup> From 3–5 litters, st = sterile.<sup>b</sup> Per animal, 25 spermatocytes at diakinesis were scored for translocation multivalents (chains of four or rings of four chromosomes).<sup>c</sup> nd = not determined.**Table 4.** Characterization of the female translocation carriers

Animal code	Mean litter size <sup>a</sup>	F <sub>1</sub> Translocation carriers / male progeny	Chromosomes involved	Presumed break points <sup>b</sup>
<b>First experiment</b>				
AA-24	4.0	3/6	T(6;11)	6D1; 11A3.2
AA-34	2.6	2/2	T(1;4)	1B; 4D3
AA-45	4.0	2/6	T(5;17)	5F; 17B2
AA-50	4.2	4/8	T(12;17)	12D1; 17D
AA-52	4.7	3/5	T(11;14)	11B3; 14D3
AA-58	3.9	1/3	T(4;8)	4E2; 8C1
AA-101	2.5	3/5	T(1;9)	1F; 9D
<b>Second experiment</b>				
AA-151	3.0	2/5	T(2;11)	2B; 11D
AA-161	2.5	3/3	T(4;10;15)	nd
AA-168	4.0	2/3	T(5;14)	5F; 14D1
AA-189	4.0	1/3	T(12;18)	12E/F; 18C
AA-196	4.0	3/4	T(3;5)	3F2; 5E4
AA-219	3.3	2/6	T(7;17)	7F3; 17B1

<sup>a</sup> From 3–5 litters.<sup>b</sup> nd = not determined.

+ T[5;10], mean testis weight 20.1 mg) and one carried a complex translocation involving three different chromosomes (AAD-165: T[14;17;19], mean testis weight 27.5 mg) which is shown in Fig. 2B. Two sterile males in the second experiment carried a translocation between chromosome 9 and the Y chromosome whereby the presumed breakpoints on the Y chromosome were not identical (AAD-181: YD and AAD-227: YC2). Their mean testes weights were 39.2 and 28.7 mg, respectively, and their spermatocytes at diakinesis were characterized by a high rate of XY univalents (81 and 64%, respectively). The remaining four sterile males carried simple reciprocal translocations, their testes weights ranged between 16.5 and 41 mg, and only one showed a long marker chromosome (AAD-127: T[7;10]). The testes weights of semi-sterile males ranged from 70 to 90 mg and that of normal adult males ranged from 90 to 120 mg. One male that carried two independent reciprocal translocations (testes weight 66.6 mg) sired one litter of two female offspring and died before karyotyping could be performed. It is noteworthy that two of the semi-sterile males carried translocations involving chromosomes 4 and 8, however, with different breakpoints on both chromosomes (AAD-198: 4C6 and 8E1; AAD-236: 4B3 and 8D3), which indicates that they were induced independently.

Table 4 shows the characteristics of the identified female translocation carriers. None of them was sterile even though one carried a complex translocation involving three chromosomes (AAD-161: T[4;10;15], Fig. 2A). The break points for this translocation could not be identified in the M-FISH analysis.

The detailed analysis of the translocation break points allows two conclusions. First, none of the translocations observed was identical to another one, i.e. they were not pre-existing in the mouse stock. Second, there were no hotspots for AA-induced chromosome breakage since the break points were randomly scattered among chromosomes (1–8 breaks per chromosome) and along chromosome axes even though location of breaks in light bands prevailed. Most likely, that is due to the process of karyotyping which is oriented at the displacement of dark bands.

The total translocation frequency after dermal exposure was 8.63% and compared to 21.9% after ip exposures to 5 × 50 mg/kg of AA (Adler, 1990) yields a calculated ratio of ip vs. dermal of 0.39 (8.63:21.9). This ratio pertains only to external exposures and observed biological outcomes (reciprocal translocations). Internal exposures, i.e. plasma or testes levels of AA were not measured. The factor 0.39 should be applied to correct the genetic risk calculation based on ip exposure (Adler et al., 1994) in order to derive a more realistic estimate for human dermal exposures. However, there are two caveats. First, the ip treated males were mated 7–11 days after the end of treatment while the males treated dermally were mated 1.5–8.5 days after the end of treatment, i.e. the exposed germ cell stages were overlapping but not identical, and second, the males exposed dermally were housed individually but were not prevented by collars to lick some of the solutions applied to their backs. Therefore, they may have been exposed dermally as well as orally, the latter to an unknown extent. Yet, AA workers in Chinese family-run factories without any hygienic measures are exposed also through the skin and by ingestion. Even though a

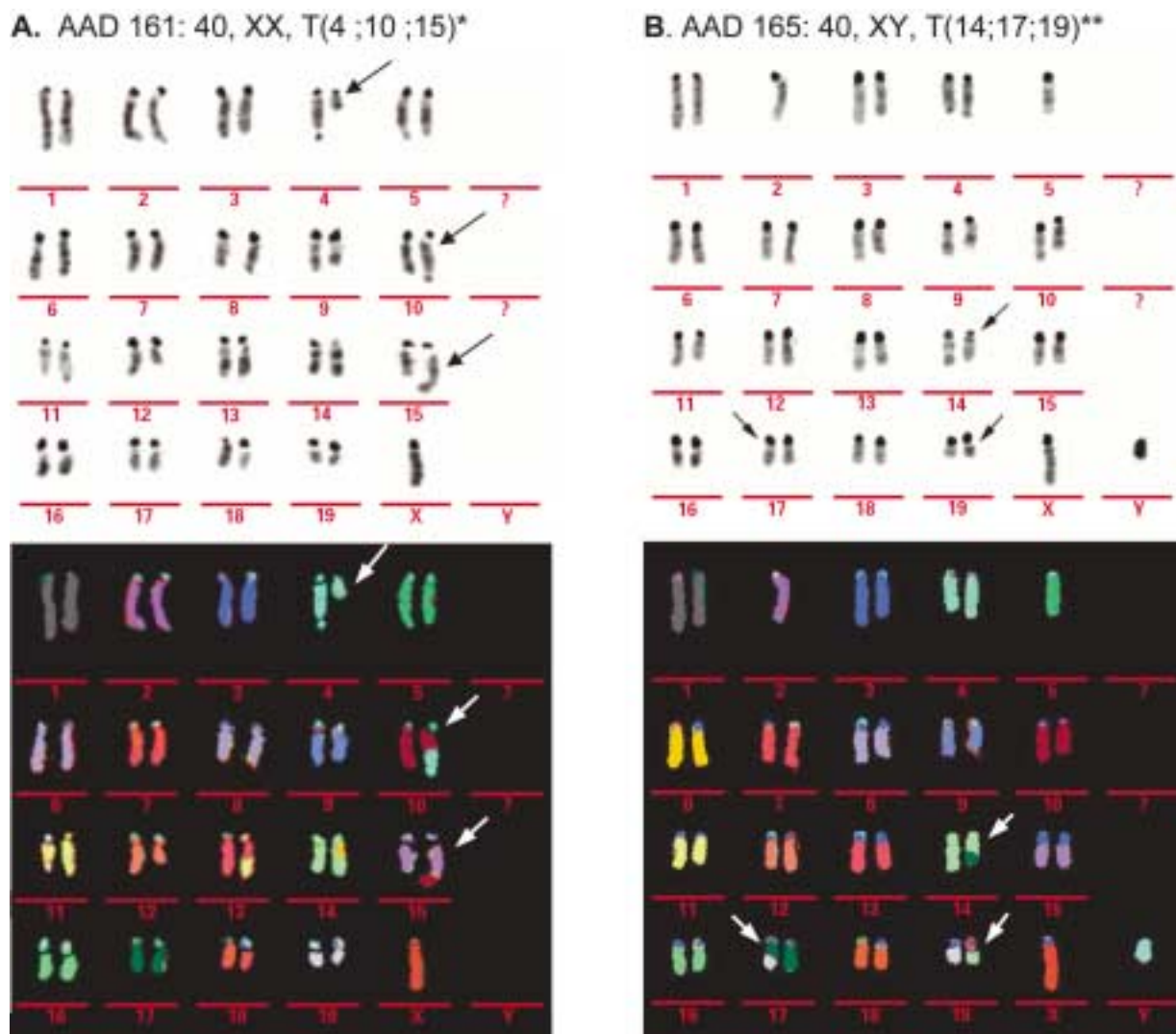


**Fig. 2.** G-banded and M-FISH karyotypes of mice with complex translocations induced by dermal exposure to acrylamide. The notations of the karyotypes refer to the chromosome constitution of the animals not the cells shown. **(A)** AAD 161: 40, XX, T(4;10;15)\*; one X chromosome is missing in this cell. **(B)** AAD 165: 40, XY, T(14;17;19)\*\*; one chromosome 2 and one chromosome 5 are missing in this cell.

linear dose-response could be demonstrated for AA-induced micronuclei in mouse bone marrow cells (Abramsson-Zetterberg, 2003), the extrapolation from linear dose-response at high acute experimental exposure to chronic human exposure with low doses is a matter of debate and ideally should be verified experimentally. Unfortunately, no animal facility is large enough to allow the appropriate heritable translocation experiments. Thus, using the correction factor for ip vs. dermal exposure provides as close a risk estimate as we can presently supply.

By using the linear extrapolation, it was generally assumed that the low-dose effect would be overestimated and an error would be made on the safe side. However, a recent publication alerts to a possible underestimate by this procedure (Witt et al., 2003). For N-hydroxymethylacrylamide (NHMA), these authors demonstrated that high acute ip treatments (MTD  $1 \times$

150 or  $5 \times 50$  mg/kg daily) or subchronic oral treatments (42–168 mg/kg daily for 31 days) did not induce dominant lethal mutations. In contrast, 13 weeks of exposure of male mice to drinking water containing 180–720 ppm NHMA concentration-dependently increased the frequencies of pre- and postimplantation embryonic losses. The concurrent studies of absorption, distribution, metabolism and elimination of  $^{14}\text{C}$ -NHMA suggested that bioaccumulation might be responsible for the dominant lethal effects in the long-term drinking water study. The applied bioaccumulation model also indicated that the total dose rather than the duration or route of exposure determined the genetic responses in male germ cells. Although these studies were performed with relatively high doses, the results point to the necessity of animal experiments with chronic exposures for the detection of germ cell mutagens and for the improvement of genetic risk quantification.

## References

- Abramsson-Zetterberg L: The dose-response relationship at very low doses of acrylamide is linear in the flow cytometer based mouse micronucleus assay. *Mutat Res* 535:215–222 (2003).
- Adler I-D: Clastogenic effects of acrylamide in different germ-cell stages of male mice. *Banbury Report 34: Biology of Mammalian Germ Cell Mutagenesis*, pp 115–131 (Cold Spring Harbor Laboratory Press, Cold Spring Harbor 1990).
- Adler I-D, Ingwersen I, Kliesch U, El Tarras A: Clastogenic effects of acrylamide in mouse bone marrow cells. *Mutat Res* 206:379–385 (1988).
- Adler I-D, Reitmeir P, Schmöller R, Schriever-Schwemmer G: Dose response for heritable translocations induced by acrylamide in spermatids of mice. *Mutat Res* 309:285–291 (1994).
- Adler I-D, Baumgartner A, Gonda H, Friedman MA, Skerhut M: 1-Aminobenzotriazole inhibits acrylamide-induced dominant lethal effects in spermatids of male mice. *Mutagenesis* 15:133–136 (2000).
- Adler I-D, Kliesch U, Jentsch I, Speicher MR: Induction of chromosomal aberrations by dacarbazine in somatic and germinal cells of mice. *Mutagenesis* 17:383–389 (2002).
- Bull RJ, Robinson M, Laurie RD, Stober GD, Geisinger E, Meier JR, Stober J: Carcinogenic effects of acrylamide in Sencar and A/J mice. *Cancer Res* 44:107–111 (1984).
- Carlson GP, Weaver PM: Distribution and binding of [<sup>14</sup>C] acrylamide to macromolecules in SENCAR and BALB/c mice following oral and topical administration. *Toxicol Appl Pharmacol* 79:307–313 (1985).
- Dearfield KL, Abernathy CO, Ottley MS, Brantner JH, Hayes PF: Acrylamide: its metabolism, developmental and reproductive effects, genotoxicity and carcinogenicity. *Mutat Res* 195:45–77 (1988).
- O'Donoghue JL: Acrylamide and related substances, in O'Donoghue JL (ed): *Neurotoxicity of Industrial and Commercial Chemicals*, Vol II, pp 169–177 (CRC Press, Boca Raton 1985).
- Ehling UH, Neuhäuser-Klaus A: Re-evaluation of the induction of specific-locus mutations in spermatogonia of the mouse by acrylamide (AA). *Mutat Res* 283:185–191 (1992).
- Evans EP: Standard normal chromosomes, in Lyon MF, Searle AG (eds): *Genetic Variants and Strains of the Laboratory Mouse*, pp 576–581 (Oxford University Press, Oxford 1989).
- Evans EP, Breckon G, Ford CE: An air-drying method for meiotic preparation from mammalian testis. *Cytogenetics* 3:289–294 (1964).
- Gallimore PH, Richardson CR: An improved banding technique exemplified in the karyotype analysis of two strains of rat. *Chromosoma* 41:259–263 (1973).
- Gutierrez-Espeleta GA, Highes LA, Piegorsch WW, Shelby MD, Generoso WM: Acrylamide: dermal exposure produces genetic damage in male mouse germ cells. *Fundam Appl Toxicol* 18:189–192 (1992).
- Hashimoto K, Tani H: Mutagenicity of acrylamide and its analogues in *Salmonella typhimurium*. *Mutat Res* 158:129–133 (1985).
- Holland N, Ahlborn T, Turteltaub K, Markee C, Moore II D, Wyrobek AJ, Smith MT: Acrylamide causes preimplantation abnormalities in embryos and induces chromatin adducts in male germ cells of mice. *Repro Tox* 13:167–178 (1999).
- Jentsch A, Adler I-D, Carter N, Speicher MR: Karyotyping of mouse chromosomes by multiplex-FISH (M-FISH). *Chrom Res* 9:21–24 (2001).
- Johnson KA, Gorzinski SJ, Bodner KM, Campbell RA, Wolf CH, Friedman MA, Mast RW: Chronic toxicity and oncogenicity study on acrylamide incorporated in the drinking water of Fischer 344 rats. *Toxicol Appl Pharmacol* 85:154–168 (1986).
- Knaap AGAC, Kramers PGN, Voogd CE, Bergkamp WGM, Groot MG, Langebroek PG, Mout HCA, van der Stel J, Verharen HW: Mutagenic activity of acrylamide in eukaryotic systems but not in bacteria. *Mutagenesis* 3:263–268 (1988).
- Lijinsky W, Andrews A: Mutagenicity of vinyl compounds in *Salmonella typhimurium*. *Teratogen Carcinogen Mutagen* 1:259–267 (1980).
- Marchetti F, Lowe X, Bishop J, Wyrobek AJ: Induction of chromosomal aberrations in mouse zygotes by acrylamide treatment of male germ cells and their correlation with dominant lethality and heritable translocations. *Environ Mol Mutagenesis* 30:410–417 (1997).
- Miller MS, Spencer PS: The mechanisms of acrylamide axonopathy. *A Rev Pharmacol Toxicol* 25:643–666 (1985).
- Moore MM, Amtower A, Doerr C, Brock KH, Dearfield KL: Mutagenicity and clastogenicity of acrylamide in L5178Y mouse lymphoma cells. *Environ Mutagen* 9:261–267 (1987).
- Pacchierotti F, Tiveron C, D'Archivio M, Bassani B, Cordelli E, Leter G, Spano M: Acrylamide-induced chromosomal damage in male mouse germ cells detected by cytogenetic analysis of one-cell zygotes. *Mutat Res* 309:273–284 (1994).
- Paulsson B, Kotova N, Grawé J, Henderson A, Granath F, Golding B, Törnqvist M: Induction of micronuclei in mouse and rat by glycidamide, genotoxic metabolite of acrylamide. *Mutat Res* 535:15–24 (2003).
- Russell LB, Hunsicker PR, Cacheiro NLA, Generoso WM: Induction of specific-locus mutations in male germ cells of the mouse by acrylamide monomer. *Mutat Res* 262:101–107 (1991).
- Sega GA, Alcota RPV, Tancongo CP, Brimer PA: Acrylamide binding to DNA and protamine of spermatogenic stages in the mouse and its relationship to genetic damage. *Mutat Res* 216:221–230 (1989).
- Shelby MD, Cain KT, Hughes LA, Braden PW, Generoso WM: Dominant lethal effects of acrylamide in male mice. *Mutat Res* 173:35–40 (1986).
- Shelby MD, Cain KT, Cornett CV, Generoso WM: Acrylamide: induction of heritable translocations in male mice. *Environ Mutagen* 9:363–368 (1987).
- Shiraishi Y: Chromosome aberrations induced by monomeric acrylamide in bone marrow and germ cells of mice. *Mutat Res* 57:313–324 (1978).
- Smith MK, Zenick H, Preston RJ, George EL, Long RE: Dominant lethal effects of subchronic acrylamide administration in the male Long-Evans rat. *Mutat Res* 173:273–277 (1986).
- Tareke E, Rydberg P, Karlsson S, Törnqvist M: Acrylamide: a cooking carcinogen? *Chem Res Toxicol* 13:517–522 (2000).
- Tareke E, Rydberg P, Karlsson S, Eriksson S, Törnqvist M: Analysis of acrylamide, a carcinogen formed in heated foodstuff. *J Agric Food Chem* 50:4998–5006 (2002).
- Tilson HA: The neurotoxicity of acrylamide: an overview. *Neurobehav Toxicol Teratol* 3:445–461 (1981).
- Tyl RW, Friedman MA: Effects of acrylamide on rodent reproductive performance. *Reprod Toxicol* 17:1–13 (2003).
- Witt KL, Hughes LA, Burka LT, McFee AF, Mathews JM, Black SL, Bishop JB: Mouse bone marrow micronucleus test results do not predict the germ cell mutagenicity of N-hydroxymethylacrylamide in the mouse dominant lethal assay. *Environ Mol Mutagenesis* 41:111–120 (2003).

# Chromosome banding in Amphibia

## XXX. Karyotype aberrations in cultured fibroblast cells

M. Schmid,<sup>a</sup> C. Steinlein,<sup>a</sup> and T. Haaf<sup>b</sup>

<sup>a</sup>Department of Human Genetics, Biocenter, University of Würzburg, Würzburg;

<sup>b</sup>Department of Human Genetics, University of Mainz, Mainz (Germany)

**Abstract.** The present study reports for the first time on the numerical and structural chromosome anomalies that spontaneously arise in aging cultured fibroblast cells of Amphibia. The analyses were conducted on kidney fibroblasts of three anuran species with extremely divergent genome sizes (*Bufo rubropunctatus*, *Scaphiopus holbrooki*, *Gastrotheca riobambae*), in the sixth up to the 14th culture passage. The chromosomal rearrangements were identified by means of the 5-bromodeoxyuridine/deoxythymidine (BrdU/dT) replication band-

ing technique. The aberrations can be either confined to a single chromosome, or else involve all chromosomes of the karyotype. The most frequent structural aberrations in the cell cultures of *S. holbrooki* and *G. riobambae* are tandem fusions between two or more chromosomes. These tandem fusions originating in vitro in long-termed cell cultures reflect the chromosome mutations which also took place during amphibian phylogenesis.

Copyright © 2003 S. Karger AG, Basel

The manifold studies on chromosome repatterning that occurred during the phylogeny of the Amphibia have been reviewed repeatedly (Morescalchi, 1973; Schmid, 1980; Schmid and Haaf, 1989; King, 1990). These comparative cytogenetic data permit close insights into the operant laws of karyological evolution in amphibians. Thus, the classical compilation of Morescalchi (1973) impressively demonstrates that in all three amphibian orders (Anura, Urodela, and Apoda) the number of microchromosomes and telocentric chromosomes was reduced in favor of large meta- or submetacentric chromosomes during the evolution from primitive to highly specialized genera. The evolution of karyotypes from the primitive genera, which still possess microchromosomes and telocentric chromosomes alongside a few meta- or submetacentric chromosomes, to the more highly evolved genera with exclusively biarmed chromosomes is explained by assuming a series of tandem fusions, centric (Robertsonian) fusions, and non-reciprocal translocations taking place between the chromosomes.

The wealth of results obtained from these comparative cytogenetic studies has been facilitated mainly by the relatively easy and fast techniques of chromosome preparation. These methods consist in using either short-term cultures of lymphocytes or embryonic cells, or else directly the bone marrow, spleen, gut, cornea, or gonads of animals treated previously in vivo with colchicine. All these techniques reveal the constitutional karyotype of the individuals examined and, with some very few exceptions of occasionally found chromosome mutations, do not offer the possibility to detect systematically all the spontaneously occurring, age-related chromosomal changes.

In contrast, there is no single report in the literature describing the chromosome aberrations arising in long-term amphibian fibroblast cultures. The two major reasons for this are: (1) Amphibian fibroblasts possess only a limited growth efficiency under a variety of different culture conditions, the cells usually giving up mitotic divisions before reaching the fifth culture passage, and (2) the induction of multiple banding patterns with the classical G-, R- and Q-banding procedures for identification of the individual chromosomes is not possible in metaphase chromosomes of amphibians.

The results presented in this article describe the different categories of numerical and structural chromosome aberrations that spontaneously occur in kidney fibroblasts of the anuran species *Bufo rubropunctatus* (Bufonidae), *Scaphiopus holbrooki* (Pelobatidae) and *Gastrotheca riobambae* (Hylidae). The chro-

Received 5 September 2003; manuscript accepted 30 January 2004.

Request reprints from M. Schmid, Department of Human Genetics  
University of Würzburg, Biozentrum, Am Hubland  
D-97074 Würzburg (Germany); telephone: +49-931-888-4077  
fax: +49-931-888-4058; e-mail: m.schmid@biozentrum.uni-wuerzburg.de

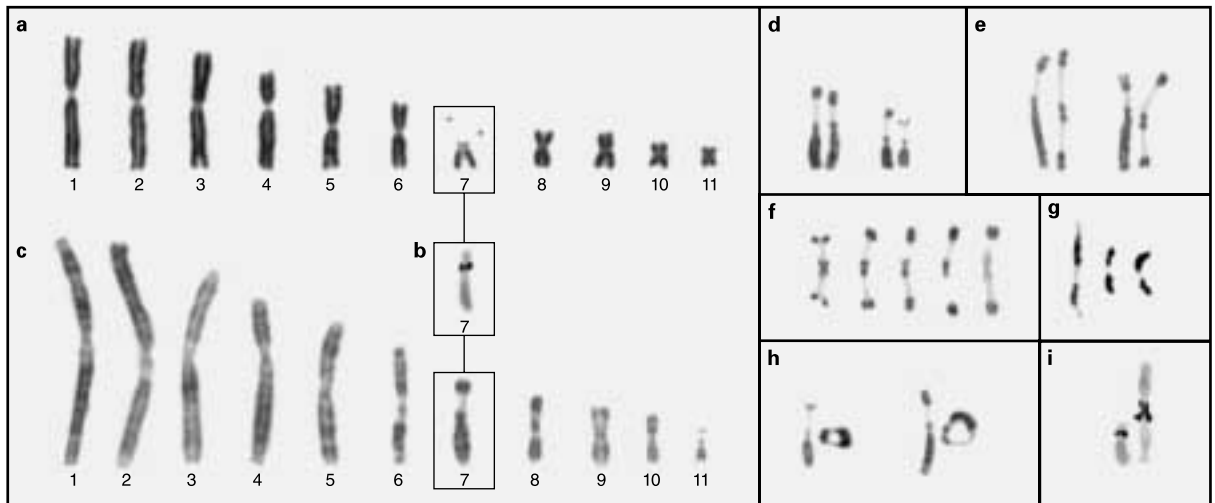


**Fig. 1.** (a) Giemsa-stained haploid karyotype of a male of *Bufo rubropunctatus*. (b) Silver-stained nucleolus organizer region (NOR) in the chromosome 7 short arm. (c) Haploid karyotype showing BrdU/dT replication banding patterns. (d) Two pairs of Giemsa-stained, normal structured chromosomes 7. (e-f) Aberrations of chromosomes 7 found in kidney fibroblasts from the sixth to the tenth culture passage. (e) BrdU/dT-banded chromosomes 7 consisting of one normal (left) and an aberrant isochromosome 7p (right). (f) Selected Giemsa-stained isochromosomes 7p from five different metaphases depicting symmetrical arrangement of nuclear constrictions and terminal satellites on both chromosome arms. (g) Selected silver-stained isochromosomes 7p from three metaphases showing distinct NOR labeling in both chromosome arms. (h) Two pairs of BrdU/dT-banded chromosomes 7 consisting of one normal homolog (left) and one ring chromosome (right). (i) Normal chromosome 7 (left) and two tandemly fused chromosomes 7 (right). Note that both chromosomes 7 are fused at their long arm telomeric regions with their NORs inserted at the fusion site.

mosomes were prepared from cells in the sixth up to the 14th culture passage, and the chromosome aberrations were identified by means of the 5-bromodeoxyuridine/deoxythymidine (BrdU/dT) replication banding technique.

## Materials and methods

### Animals and cell lines

One mature male individual each of *Bufo rubropunctatus*, *Scaphiopus holbrooki*, and *Gastrotheca riobambae* was supplied by a specialized animal dealer. The animals were kept in aquaterraria at 18–20 °C and fed with worms and flies. After sacrificing the animals with diethyl-ether, small kidney pieces were removed to set up cell cultures. All procedures with the animals conformed to the guidelines established by the Animal Care Committees.

### Cell cultures and BrdU treatment

The kidney samples were minced and cultured in MEM (Gibco) supplemented with 13% fetal calf serum (Boehringer) and 0.9% penicillin-streptomycin (stock solution: 10,000 U/ml, Gibco). The cell cultures were maintained for 6 to 14 weeks as monolayer cultures in 25-cm<sup>2</sup> flasks (Nunc), and incubated at 26 °C under ordinary atmospheric conditions. Cells were harvested for chromosome analysis from subcultures using trypsin. Colcemid (Gibco) was added 2 h prior to harvest at a final concentration of 0.15 µg/ml of culture medium. Hypotonic treatment lasted 35 min at 37 °C in 0.027 M sodium citrate. The technique used for fixation of the cells in acetic acid:methanol (1:3) has been described previously (Schmid, 1978).

### Replication banding patterns

All experiments were performed on non-synchronized cells of the sixth to the 14th passage. 24 h before cell harvest, 100 µg/ml BrdU (Sigma) was added to the cultures. After 16 h, the cells were washed twice with conventional culture medium and fed with medium containing 48 µg/ml deoxythymidine (Sigma). Cultures were kept in this medium for the last 8 h. Differential staining of replication bands was achieved with a modified fluorescence-plus-

Giemsa (FPG) technique (Perry and Wolf, 1974). Slides were aged for 3 days, then kept for 30 min in buffered 0.03 µg/ml eosin Y solution (Hazzen et al., 1985). Eosin Y (standard yellow, Fluka) was employed in preference to Hoechst 33258 commonly used for the FPG technique because of the better resolution of the replication bands. After rinsing the slides in distilled water, the cells were UV irradiated for 30 min in buffer at a distance of 10 cm from the UV lamp (254 nm) and 1 cm below the buffer level. The components of the buffer used are: 0.03 M KCl, 0.15 M NaCl, 0.83 mM KH<sub>2</sub>PO<sub>4</sub>, adjusted to pH 5.5. Subsequently, preparations were rinsed in fresh buffer, and incubated in 2× SSC for 90 min (1× SSC = 0.15 M NaCl, 0.015 M sodium citrate). Finally, the slides were stained for 6 min in 5% Giemsa solution (pH 6.8), washed twice in distilled water and air-dried.

### Regional banding of chromosomes

Demonstration of constitutive heterochromatin by C-banding and staining of nucleolus organizer regions with AgNO<sub>3</sub> were performed according to Schmid et al. (1983).

### Photography and analysis of banding patterns

Microscopic analyses were conducted on Zeiss photomicroscopes III. All photographs were taken on Agfaortho 25 ASA film. Each metaphase containing one or more chromosome aberrations was photographed, the chromosomes cut out from the prints, and affixed to double-sided tape in parallel rows. This record system permits an easy identification of all chromosome rearrangements and aneuploidies.

## Results

### *Bufo rubropunctatus*

In accordance with the results obtained by Formas (1978), the South American toad *B. rubropunctatus* has 2n = 22 chromosomes. As in most other *Bufo* species (Bogart, 1972), the karyotype consists of six larger and five distinctly smaller meta- or submetacentric chromosomes (Fig. 1a). A prominent nucleo-

lar constriction is located in the chromosome 7 short arm (Fig. 1a) that proves to be the nucleolus organizer region (NOR) as shown by specific silver staining (Fig. 1b). By application of the BrdU-replication banding technique a large number of dark- and pale-stained replication bands are induced in the chromosomes during the first half of the S-phase, most of them being evenly distributed along the metaphase chromosomes (Fig. 1c).

Among 50 metaphases of the sixth to tenth cell culture passage analyzed, 15 (30%) show a normal diploid karyotype with two unaltered chromosomes 7 (Fig. 1d). In 27 metaphases (54%), one of the chromosomes 7 is missing, and an isochromosome 7p is present instead (Fig. 1e). This metacentric isochromosome 7p exhibits a perfect symmetry, with equal lengths of the nucleolar constrictions and sizes of the terminal satellites (Fig. 1f), as well as equal amounts of silver deposits (Fig. 1g) on both sides of the centromeric region. In six metaphases (12%), one of the chromosomes 7 is replaced by a ring chromosome (Fig. 1h). The ring chromosome 7 shows two nucleolar constrictions located in opposition to each other. It cannot be decided whether the ring chromosome 7 derived from the isochromosome 7p by telomeric fusion, or vice versa, if the isochromosome 7p is the product of a broken ring chromosome 7, although the first alternative seems to be the more likely event. Finally, in two of the cells (4%), a complex isoform of one chromosome 7 is seen in addition to a normal chromosome 7 (Fig. 1i). In this particular rearrangement the two chromosomes 7 are fused in tandem at their long arm telomeric regions with their NORs inserted at the fusion site.

#### *Scaphiopus holbrooki*

The conventional karyotype of the North American spadefoot toad *S. holbrooki* has been reported by Wasserman and Bogart (1968) and Morescalchi et al. (1977), and C-banding, mithramycin fluorescence and BrdU/dT replication banding were studied by Schmid et al. (2003). This species has  $2n = 26$  chromosomes, the pairs 1–6 being distinctly larger than pairs 8–13 (Fig. 2a). Pairs 3–5 have an acrocentric morphology, all the remaining pairs are meta- or submetacentric. The NOR is located in the chromosome 7 short arm. Constitutive heterochromatin is present at the centromeric and telomeric regions of all chromosomes, in the entire short arms of the acrocentric chromosomes 3 and 5, proximally and distally to the NOR in the chromosome 7 short arm, as well as interstitially in the pericentromeric regions of chromosomes 1–5 (Fig. 2a).

Fifty BrdU/dT-banded metaphases from the sixth to eighth cell culture passage were analyzed. Thirty cells (60%) have a normal karyotype, whereas in the remaining 20 metaphases (40%) at least one numerical or structural chromosome aberration can be detected (Fig. 2). The prevalent anomalies are monosomies (34.3%) and trisomies (31.3%). Examples of such monosomic and trisomic cells are depicted in Fig. 2a, b, e–h). Tetrasomies occur at a frequency of 6.5% (Fig. 2e, g). The chromosomes most frequently involved in aneuploidies are 5, 7, 11 and 13. It is remarkable that the only structural aberrations found consist of tandem fusions between two chromosomes, like those shown in Fig. 2c–h). They amount to 27.9% of all aberrations. The chromosome most frequently involved in

these tandem fusions is no. 1 (Fig. 2c–h). It is fused either with a non-homologous chromosome (Fig. 2c, d, f, g), or else with its own homolog (Fig. 2e, h). In most of the tandemly fused chromosomes two centromeric constrictions can be discerned (Fig. 2c–g). Both the long as well as the short arm of the various chromosomes can participate in the tandem fusions. It should be pointed out that in the 50 metaphases analyzed all the 13 chromosomes of *S. holbrooki* are involved in numerical and/or structural aberrations. The lowest number of aberrations per metaphase are simple trisomies (Fig. 2a), the highest number consist of one to three trisomies, one tetrasomy, two to three monosomies, and two tandem fusions (Fig. 2e–h).

#### *Gastrotheca riobambae*

The karyotype of this South American marsupial frog is one of the best studied among the Anura (Schmid et al., 1983, 1986; Schmid and de Almeida, 1988; Schmid and Klett, 1994). It is distinguished by highly heteromorphic XY sex chromosomes. The Y chromosome is considerably larger than the X chromosome and composed almost completely of constitutive heterochromatin. The sole NOR in the karyotype is located in the X chromosome short arm. This causes a sex-specific difference in the number of ribosomal RNA genes of about 2(♀):1(♂). No cytogenetic indications were found for a possible inactivation of one of the two X chromosomes in female cells. The banded karyotype of *G. riobambae* has been described in detail by Schmid et al. (1983), restriction endonuclease banding was reported by Schmid and de Almeida (1988), and the BrdU/dT replication banding patterns in metaphase chromosomes were first presented by Schmid and Klett (1994).

Thirty-six metaphases (72%) out of 50 metaphases from the tenth to the 14th cell culture passage yield a normal karyotype. In each of the remaining 14 cells (28%) at least three chromosome aberrations are present (Fig. 3). As in the cell cultures of *S. holbrooki*, the most frequent anomalies are monosomies (28.3%), trisomies (9.5%), and partial trisomies (9.5%). It should be emphasized that in all 14 aberrant karyotypes the Y chromosome is missing (Fig. 3). Apparently the loss of the complete Y chromosome has no deleterious effects on cell growth and function. This is understandable because the huge Y chromosome mainly consists of constitutive heterochromatin with its non-transcribed repetitive DNA sequences. In all normal and aberrant karyotypes examined, the X chromosome (i.e. chromosome no. 4) shows a normal structure (Fig. 3). Tetrasomies of autosomes occur with a frequency of 2% (Fig. 3e).

Concerning the structural chromosome rearrangements, again tandem fusions between two chromosomes represent the most frequent category (25.7%). They involve autosomes 1, 2, 5, 7 and 8 (Fig. 3a, c–e). In two metaphases (6.7%) two pairs of extremely large chromosomes are present (Fig. 3e) that are interpreted to be the result of multiple tandem fusions between more than two autosomes. However, the BrdU/dT replication banding patterns in these huge chromosomes are too complex to reveal their origin. Two cells (2.7%) contain a non-reciprocal translocation between autosomes 3 and 11 (Fig. 3a). A centric fusion of the acrocentric autosomes 9 and 13 is found in five cells (6.7%) (Fig. 3e). A further centric fusion between the two homologous acrocentric autosomes 11 is counted in another



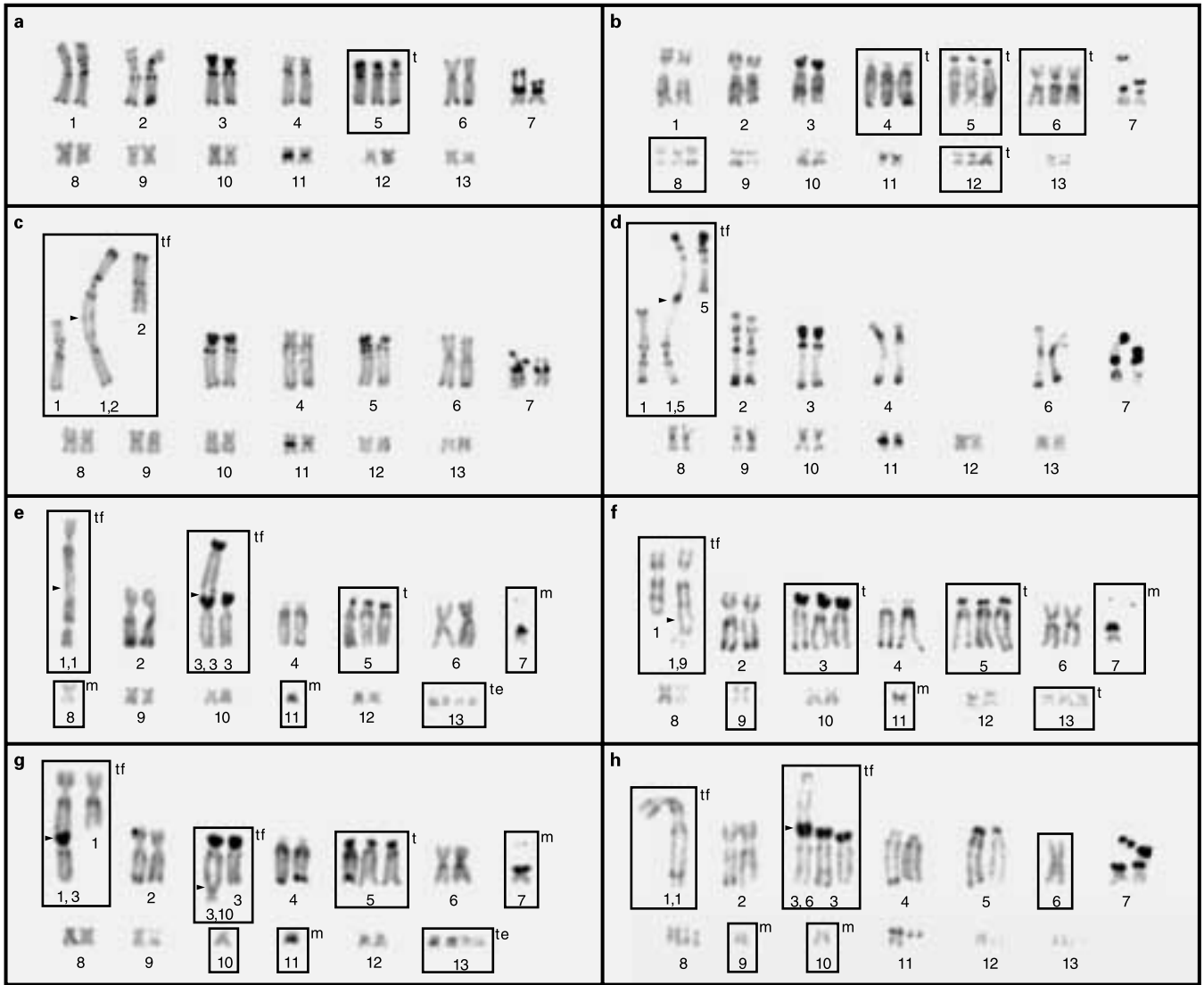


**Fig. 2. (a-h)** BrdU/dT-banded karyotypes of a male of *Scaphiopus holbrooki* prepared from kidney fibroblasts in the sixth to the eighth culture passage. The chromosomes showing numerical and/or structural aberrations are framed. The abbreviations used are as follows: (m) monosomy, (t) trisomy, (te) tetrasomy, (tf) tandem fusion. The black arrowheads beside the tandemly fused chromosomes mark the fusion site.

five cells (6.7%) (Fig. 3d, e). However, this condition can also be explained assuming an isochromosome formation by one homolog 11 plus a simultaneous monosomy of the other homolog, which of course, is a more complex chromosomal mutation event. Finally, in a single metaphase (1.5%), an allocyclic or prematurely condensed chromosome no. 1 is detectable (Fig. 3f).

## Discussion

The only method that induces reliable multiple bands along amphibian metaphase chromosomes, and herewith allows their exact identification, is the 5-bromodeoxyuridine/deoxythymidine (BrdU/dT) technique (Schmid et al., 1990b). BrdU/dT

replication bands were first obtained in bone marrow metaphase chromosomes of *Rana esculenta*, *R. temporaria* and *Pyxicephalus adspersus* (Schempp and Schmid, 1981), and later on in distinctly higher quality in chromosomes from cultured fibroblasts or lymphocytes of 19 anuran species belonging to the genera *Rana*, *Hyla*, *Bufo*, *Xenopus*, *Gastrotheca*, *Litoria*, *Odontophrynus*, and *Scaphiopus* (Schmid and Steinlein, 1991; Schmid and Klett, 1994; Miura, 1995; Miura et al., 1995; Wiley and Little, 2000; Schmid et al., 2002, 2003).

The present work is the very first report focusing on chromosome aberrations spontaneously originating in long-termed, aging amphibian fibroblast cultures. It shows that the rearrangements can be either confined to a single chromosome, like in *B. rubropunctatus*, or else involve all chromosomes of the karyotype, like in *S. holbrooki* and *G. riobambae*.

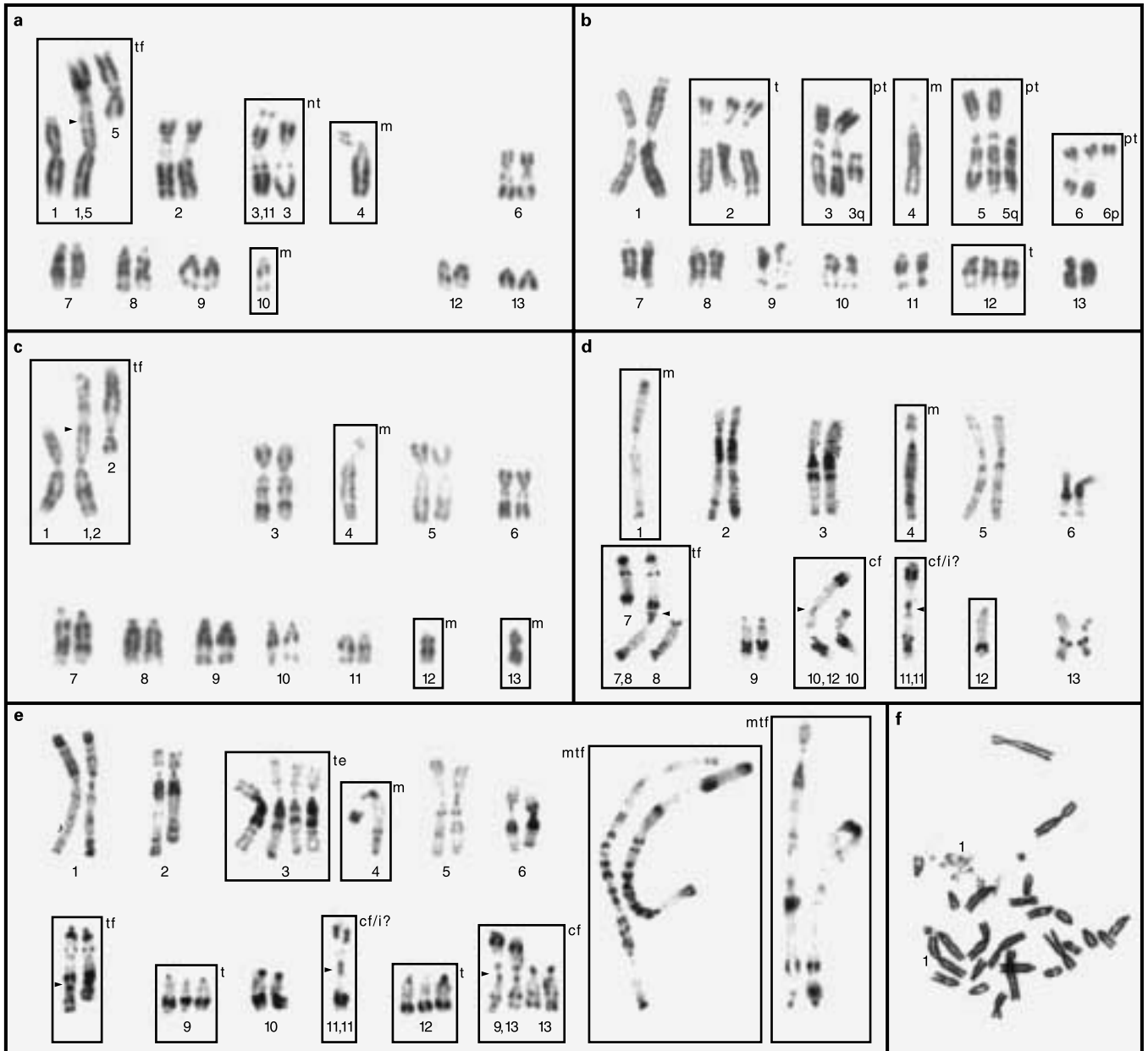


**Fig. 3.** (a-e) BrdU/dT-banded karyotypes of a male *Gastrotheca riobambae* prepared from kidney fibroblasts in the tenth to the 14th culture passage. The chromosomes showing numerical and/or structural aberrations are framed. The abbreviations used are as follows: (cf) centric fusion, (cf/i?) centric fusion or isochromosome, (m) monosomy, (mtf) multiple tandem fusion, (pt) partial trisomy, (t) trisomy, (te) tetrasomy, (tf) tandem fusion, (nt) non-reciprocal translocation. The black arrowheads beside the tandemly fused chromosomes mark the fusion sites. The single chromosome 4 is the X sex chromosome. Note that in all karyotypes the X chromosome is the only chromosome not involved in numerical or structural anomalies. The Y chromosome is missing in all cells. (f) Giemsa-stained metaphase with an alloccyclic or prematurely condensed chromosome 1.

In the *B. rubropunctatus* fibroblasts all aberrations detected are restricted to one of the chromosomes 7. The most frequent anomaly is an isochromosome 7p which most probably originated by a singular event (clonal origin) and has spread throughout the cultures, rather than having arisen independently in different cells. Most probably the ring chromosome 7p was derived from this isochromosome 7p. However, there is no easy parsimonious explanation for the origin of the complex

tandem fusion of two chromosomes 7 with their NORs inserted at their fusion site.

In both *S. holbrooki* and *G. riobambae* a variety of chromosome anomalies appear during senescence of their fibroblast cultures, the most common ones being monosomies and trisomies that apparently are quite well tolerated by the cells. The most frequent structural chromosome aberrations in the cell cultures of both species are tandem fusions between two chro-

mosomes that result in unusually large, mostly dicentric chromosomes. The breaks preceding these tandem fusions are located in the telomeric regions of the chromosomes, which in all chromosomes of both species consist of constitutive heterochromatin (Schmid et al., 1983, 2003). With regard to this high rate of spontaneous in vitro tandem fusions it is important to note the comparative cytogenetic investigation of Morescalchi (1973) which demonstrates that tandem fusions played one of the principal roles during the evolution of amphibian karyotypes (see Introduction). Furthermore, from a detailed comparison between the late replication banding patterns induced in the chromosomes of frogs belonging to the genus *Rana* it was found that a tandem fusion between the two small chromosomes 11 and 13 in an ancestral  $2n = 26$  species has produced the larger chromosome no. 6 in the  $2n = 24$  species (Miura et al., 1995). It is conceivable that the structural chromosome aberrations observed in vitro reflect the chromosome mutations which also preferentially took place during amphibian

phylogenesis. This implies that the telomeric regions of amphibian chromosomes are prone to be involved in tandem fusions and non-reciprocal translocations.

It must be emphasized that the various categories of chromosome anomalies accumulating in aging amphibian fibroblast cells are not related to the genome size of the species examined. Thus, although the various numerical and structural chromosome changes in the fibroblast cultures of *S. holbrooki* and *G. riobambae* are very similar, the genome sizes of the two species are extremely divergent. Whereas *S. holbrooki* has one of the smallest genomes found so far in vertebrates (2.0 pg DNA per nucleus) (Schmid et al., 2003), the nuclear DNA content of *G. riobambae* amounts to 8.5 pg (Schmid et al., 1990a).

### Acknowledgement

We thank Gitta Hesse for her dedicated and expert photographic assistance and Rainer Klett for his efficient help with the amphibian cell cultures.

### References

- Bogart JP: Karyotypes, in Blair WF (ed): Evolution in the Genus *Bufo*, pp 171–195 (University of Texas Press, Austin 1972).
- Formas JR: The chromosomes of *Bufo rubropunctatus* and *Bufo chilensis* (Anura, Bufonidae) and other species of the *spinulosus* group. *Experientia* 34: 452–454 (1978).
- Hazen MJ, Villanueva A, Juarranz A, Canete M, Stockert JC: Photosensitizing dyes and fluorochromes as substitutes for 33258 Hoechst in the fluorescence-plus-Giemsa (FPG) chromosome technique. *Histochemistry* 83:241–244 (1985).
- King M: Amphibia, in John B (ed): Animal Cytogenetics, Vol 4/2 (Gebrüder Borntraeger, Berlin 1990).
- Miura I: The late replication banding patterns of chromosomes are highly conserved in the genera *Rana*, *Hyla*, and *Bufo* (Amphibia: Anura). *Chromosoma* 103:567–574 (1995).
- Miura I, Nishioka M, Borkin LJ, Wu Z: The origin of the brown frogs with  $2n = 24$  chromosomes. *Experientia* 51:179–188 (1995).
- Morescalchi A: Amphibia, in Chiarelli AB, Capanna E (eds): Cytotaxonomy and Vertebrate Evolution, pp 233–348 (Academic Press, London 1973).
- Morescalchi A, Olmo E, Stingo V: Trends of karyological evolution in Pelobatoid frogs. *Experientia* 33:1577–1578 (1977).
- Perry P, Wolff S: New Giemsa method for the differential staining of sister chromatids. *Nature* 251:156–158 (1974).
- Schempp W, Schmid M: Chromosome banding in Amphibia. VI. BrdU-replication patterns in Anura and demonstration of XX/XY sex chromosomes in *Rana esculenta*. *Chromosoma* 83:697–710 (1981).
- Schmid M: Chromosome banding in Amphibia. I. Constitutive heterochromatin and nucleolus organizer regions in *Bufo* and *Hyla*. *Chromosoma* 66:361–388 (1978).
- Schmid M: Chromosome evolution in Amphibia, in Müller HJ (ed): Cytogenetics of Vertebrates, pp 4–27 (Birkhäuser, Basel 1980).
- Schmid M, de Almeida CG: Chromosome banding in Amphibia. XII. Restriction endonuclease banding. *Chromosoma* 96:283–290 (1988).
- Schmid M, Haaf T: Origin and evolution of sex chromosomes in Amphibia: the cytogenetic data, in Wachtel SS (ed): Evolutionary Mechanisms in Sex Determination, pp 37–56 (CRC Press, Boca Raton 1989).
- Schmid M, Klett R: Chromosome banding in Amphibia. XX. DNA replication patterns in *Gastrotheca riobambae* (Anura, Hylidae). *Chromosoma* 65: 122–126 (1994).
- Schmid M, Steinlein C: Chromosome banding in Amphibia. XVI. High-resolution banding patterns in *Xenopus laevis*. *Chromosoma* 101:123–132 (1991).
- Schmid M, Haaf T, Geile B, Sims B: Chromosome banding in Amphibia. VIII. An unusual XY/XX-sex chromosome system in *Gastrotheca riobambae* (Anura, Hylidae). *Chromosoma* 88:69–82 (1983).
- Schmid M, Sims SH, Haaf T, Macgregor HC: Chromosome banding in Amphibia. X. 18S and 28S ribosomal RNA genes, nucleolus organizers and nucleoli in *Gastrotheca riobambae*. *Chromosoma* 94:139–145 (1986).
- Schmid M, Steinlein C, Friedl R, de Almeida CG, Haaf T, Hillis DM, Duellman WE: Chromosome banding in Amphibia. XV. Two types of Y chromosomes and heterochromatin hypervariability in *Gastrotheca pseustes* (Anura, Hylidae). *Chromosoma* 99:413–423 (1990a).
- Schmid M, Steinlein C, Nanda I, Epplen JT: Chromosome banding in Amphibia, in Olmo E (ed): Cytogenetics of Amphibians and Reptiles, pp 21–45 (Birkhäuser, Basel 1990b).
- Schmid M, Ziegler CG, Steinlein C, Nanda I, Haaf T: Chromosome banding in Amphibia. XXIV. The B chromosomes of *Gastrotheca espeletia* (Anura, Hylidae). *Cytogenet Genome Res* 97:205–218 (2002).
- Schmid M, Steinlein C, Haaf T: Chromosome banding in Amphibia. XXVII. DNA replication banding patterns in three anuran species with greatly differing genome sizes. *Cytogenet Genome Res* 101:54–61 (2003).
- Wasserman AO, Bogart JP: Chromosomes of two species of spadefoot toads (genus *Scaphiopus*). *Copeia* 1968:303–306.
- Wiley JE, Little ML: Replication banding patterns of the diploid-tetraploid treefrogs *Hyla chrysocelis* and *H. versicolor*. *Cytogenet Cell Genet* 88:11–14 (2000).

# Investigations into the biological relevance of in vitro clastogenic and aneugenic activity

J.M. Parry, P. Fowler, E. Quick and E.M. Parry

Centre for Molecular Genetics and Toxicology, School of Biological Sciences, University of Wales Swansea, Singleton Park, Swansea (UK)

**Abstract.** In the current study we present a view of events leading to chemically induced DNA damage in vitro from both a cytogenetic and molecular aspect, focusing on threshold mediated responses and the biological relevance of DNA damaging events that occur at low and high cellular toxicity levels. Current regulatory mechanisms do not take into account chemicals that cause significant DNA damage only at high toxicity. Our results demonstrate a defined threshold for micronucleus induction after insult with the alkylating agent MMS. Other results define a significant change in gene expression following treatment with chemicals that give rise to structural DNA damage only at high toxicity. Pairs of chemicals with a similar mode

of action but differing toxicity levels were chosen, the chemicals that demonstrated structural DNA damage only at high levels of toxicity showed an increase in heat shock protein gene expression whereas the chemicals causing DNA damage events at all levels of toxicity did not induce changes in heat shock gene expression at identical toxicity levels. The data presented indicates that there are a number of situations where the linear dose response model is not appropriate for risk estimation. However, deviation from linear risk models should be dependent upon the availability of appropriate experimental data such as that shown here.

Copyright © 2003 S. Karger AG, Basel

Current guidance on the testing of chemicals for their potential genotoxicity requires the determination of their ability to induce structural (clastogenic) and numerical (aneugenic) chromosome change as a critical stage of in vitro assessment (see COM, 2000). A positive result in an in vitro cytogenetic study can lead to the termination of further development of a compound or to the decision to evaluate further using in vivo models. The primary model for the in vivo assessment of cytogenetic activity is the rodent bone marrow micronucleus test which has proved to be an effective test for determining whether cytogenetic activity in vitro is reproduced in whole animals.

However, even when in vitro positive results are not reproduced in the rodent bone marrow test, questions can arise concerning compound distribution and relevant target tissues. In such cases the detection of in vitro cytogenetic activity can raise considerable problems as to the prediction of potential hazards of exposure to the compound. The decision to terminate compound development on the basis of positive in vitro cytogenetic data may also lead to the loss of potentially valuable products.

The frequency of positive results obtained in the in vitro cytogenetic assay in regulatory submissions is illustrated by two data sets from Germany and Japan. Broschinski et al. (1998) reported that of 776 new chemicals introduced in Germany between 1982 and 1997, 25.2% produced positive results when evaluated for potential genotoxicity using in vitro cytogenetic assays. Comparable data sets for Japan published by Sofuni et al. (2000) reported that 38.3% of the 1049 new chemicals evaluated under the 1973 chemical substances control law produced positive results when evaluated using in vitro cytogenetic assays.

These high frequencies of positive results obtained using the in vitro cytogenetic assays inevitably raise questions as to the

Supported in part by grants from the European Commission (PEPFAC) and the UK Food Standards Agency. During the course of the work Emma Quick held a University of Wales Swansea studentship and Paul Fowler a BBSRC studentship in collaboration with Unilever Sharnbrook.

Received 12 September 2003; manuscript accepted 10 December 2003.

Request reprints from James M. Parry, Centre for Molecular Genetics and Toxicology, School of Biological Sciences, University of Wales Swansea Singleton Park, Swansea SA2 8PP (UK); telephone: 01792 295385 fax: 01792 295447; e-mail: jmp@swansea.ac.uk

biological relevance of such data. When positive in vitro cytogenetic data has been obtained, the assessment of potential in vivo activity can involve considerable additional experimental work. In this paper we address the biological relevance of in vitro positive cytogenetic results by examining two situations: i.e. 1) whether thresholds of cytogenetic activity can be demonstrated at low doses for DNA reactive chemicals and 2) whether chemicals which produce positive results only at toxic levels produce patterns of gene expression indicative of a lack of biological relevance to the intact animal.

DNA reactive compounds may produce modifications which potentially lead to the production of chromosome aberrations that can be observed and quantified in metaphase preparations of in vitro cultured cells (Evans, 1984; Scott et al., 1991). For such compounds, it has generally been assumed that the hazard of genotoxic activity is most effectively represented by a linear dose response model in which an increase in exposure to a compound results in the production of genetic change, including those of chromosome structure and number (for review see Parry and Sarrif, 2000) in a dose related way. Such an assessment is in contrast to that undertaken in most other areas of toxicological evaluation where (when supported by appropriate data) the assumption can be drawn that there are exposure doses below which no adverse effects are produced, i.e. there are thresholds of toxicological response. However, there is now increasing information which demonstrates that mammalian cells possess a range of cellular responses which may limit the ability of DNA lesions to be processed into genetic changes including the production of chromosome aberrations. These processes include both error-free and error-prone repair and the destruction of damaged cells by apoptosis and necrosis (Friedberg et al., 1995). In the yeast *Saccharomyces cerevisiae* comparisons between induced mutation frequencies in repair proficient and repair deficient cultures demonstrate that repair activity produces substantial reductions in the proportion of DNA lesions resulting in mutations (reviewed by Moustacchi, 2000). Similarly, Sofuni et al. (2000) demonstrated that strains of *Salmonella typhimurium* defective in the O<sup>6</sup>-methylguanine DNA methyl transferase genes produce mutations at exposure concentrations of the alkylating agent methyl methanesulphonate which did not show an effect in the repair proficient strain.

In this paper we evaluate the dose response relationship for the in vitro induction of micronuclei (as a measure of chromosome damage) by the alkylating agent methyl methane sulphate (MMS) in cultured mammalian cells. MMS preferentially alkylates the N<sup>7</sup> position of guanine (Beranek, 1990) which is subsequently repaired by the DNA glycosylases of the base excision pathway (Friedberg et al., 1995). If a threshold of induction of chromosome aberrations can be demonstrated for MMS this would provide the impetus to determine the mechanisms and gene activities which reduce the biological relevance of DNA reactive chemicals at low doses that may be relevant to potential human exposures.

The concept of the high-toxicity clastogen has been discussed by a number of authors who have questioned the biological relevance of chemicals which induce chromosomal change only at toxic doses (Kirkland, 1992; Müller and Kasper, 2000).

When such activity is observed for a potential pharmaceutical then decision as to the biological relevance can be based upon associated data such as whole animal toxicity and the likelihood of toxic conditions being reproduced under conditions of clinical usage.

A variety of situations have been described where conditions such as extremes of pH and osmolarity can result in the induction of chromosome aberrations. These conditions can be classified as not being relevant to whole animals, including humans (Scott et al., 1991; Kirkland and Müller, 2000). In such cases it can be reasonably simple to demonstrate that the extreme conditions leading to clastogenic activity cannot be achieved in vivo.

However, a number of chemicals can be shown to be capable of inducing chromosome aberrations in vitro only under conditions of high toxicity which cannot be ascribed to extreme cellular conditions (Armstrong et al., 1992; Galloway et al., 1998; Vock et al., 1998). To investigate the potential biological relevance of such high-toxicity effects, we have selected a range of chemicals which induce micronuclei in cultured cells at either low or high levels of toxicity. The determination of the concentration ranges which result in significant induction of micronuclei can then be used to determine the profile of gene expression changes occurring under the relevant exposure conditions.

In this paper we have investigated the relationships between in vitro dose response relationships for the induction of micronuclei and the gene expression profiles of both low and high toxicity clastogens to determine whether there are unique patterns which can be associated with the clastogenic activity under the various conditions.

## Materials and methods

### Chemical selection

Methyl methane sulphate CAS 66-27-3 (MMS) was selected as an agent which primarily produces N<sup>7</sup> alkylations (reviewed by Beranek, 1990).

8-hydroxyquinoline CAS 148-24-3 (8-HQ) was selected as a compound which produces oxidative damage at high levels of toxicity (Leanderson and Tagesson, 1996) and 4-nitroquinoline-N-oxide CAS 56-57-5 (4-NQO) as a compound which produces oxidative damage at low levels of toxicity (Nunoshiba and Demple, 1993).

Etoposide (4'-Desmethylepipodophyllotoxin 9-[4,6-O-ethylidene-β-D-glucopyranoside] Vp-16-213), CAS 33419-42-0 was selected as a topoisomerase II enzyme inhibitor at low toxicity levels (Vock et al., 1998).

Amsacrine (Amsacrine hydrochloride; m-AMSA; 4-[9-Acridinylamino]-N-[methanesulphonyl]-m-anasidine); CAS 54301-15-4 was selected as a topoisomerase II enzyme inhibitor at high toxicity levels (Graziano et al., 1996).

All test substances were freshly prepared as stock solutions in dimethyl sulphoxide (DMSO). All chemicals were purchased as the highest purity supplied by Sigma UK.

### Cell culture and treatment procedure

The cell culture used in this study was a human lymphoblastoid line AHH-1 (Crespi and Thilly, 1984). These cells were cultured in RPMI 1640 (BD Gentest) supplemented with 9% horse serum (BD Gentest) and 1% L-glutamine (Gibco). The use of the AHH-1 cell line in the binucleate micronucleus assay has been described in detail (Parry et al., 2002) and is based upon the protocol developed by Fenech (2000). In this study, AHH-1 cells were seeded at a concentration of  $1.5 \times 10^5$  cells/ml in growth medium, gassed with 5% CO<sub>2</sub> and incubated at 37 °C for a cell cycle (22–24 h). Growing cells

**Table 1.** Genes analysed on Q-series human stress and toxicity membrane array

Proliferation/carcinogenesis	CCNC (cyclin C), CCND1 (cyclin D1), CCNG1 (cyclin G), E2F1, EGR1, PCNA
Growth arrest/senescence	CDKN1A (p2Waf1/p21Cip1), DDIT3, (GADD153/CHOP), GADD45A, GADD45B, IGFBP6, MDM2, PLAB, TP53
Inflammation	CSF2 (GM-CSF), IL1A, IL1B, IL6, IL18, LTA (TNF b/Lt a), MIF, NFKB1, NOS2A (iNOS), SCYA3 (MIP -1a), SCYA4 (MIP-1b), SCYA21 (MIP-2), SCYB10 (IP 10), SERPINE1 (PAI-1)
Necrosis/apoptosis:	
Oxidative and metabolic stress	CAT (catalase), CRYAB (a-Crystallin B), CYP1A1, CYP1B1, CYP2E, CYP7A1, CYP7B1, EPHX2, FMO1, FMO5, GPX1 (glutathione peroxidase) GSR (glutathione reductase), GSTM3 (glutathione S-transferase M3), HMOX1, HMOX2, MT1A, MT2A, MT1H, POR, PTGS2 (cox-2), SOD1, SOD2
Heating stress	DNAJA1, DNAJB4, HSF1 (tcf5), HSP105B (hsp105), HSPA1A (hsp70 1A), HSPA1B (hsp70 1B), HSPA1L (hsp70 1L), HSPA2 (hsp70 2), HSPA4 (hsp 70), HSPA5 (grp78), HSPA6 (hsp70B), HSPA8, HSPA9B (mortalin-2), HSPB1 (hsp27), HSPCA (hsp90), HSPCB (hsp90 b), HSPD1 (chaperonin), HSPE1 (chaperonin 10)
DNA damage and repair	ATM, DDB1, ERCC1, ERCC3, ERCC4, ERCC5, RAD23A, RAD50, CHEK2 (RAD53), UGT1A9, UNG, XRCC1, XRCC2m XRCC4, XRCC5
Apoptosis signalling	ANXA5 (annexin v), BAX, BCL2L1 (bcl-x), BCL2L2 (bcl-w), CASP1 (caspase/ICE), CASP8 (caspase8/FLICE), CASP10 (caspase-10/mch4), NFKBIA (ikBa/mad3), TNF, TNFRSF1A (TNFR1), TNFSF6 (Fas Ligand), TNFSF10 (TRAIL), TRADD

were exposed to test chemicals for one cell cycle. Two modified protocols were used: 1) cells were washed after chemical treatment and then resuspended in fresh growth medium and grown for a further cell cycle in the presence of 3 µg/ml of the actin inhibitor cytochalasin B; or 2) cytochalasin B was added during the period of treatment with the test chemical. In both protocols, the presence of cytochalasin B results in the production of binucleate cells from cells that have undergone nuclear division but not cytokinesis.

Following fixation in 90% methanol, the cells were stained in 12.5 mg/100 ml of acridine orange, slides were viewed using an Olympus BH2-RFCA fluorescent microscope. The frequency of micronuclei in binucleate cells was used as a measure of the induction of clastogenic and/or aneuploid damage and the relative proportions of mononucleate/binucleate cells as a measure of compound toxicity.

#### Gene expression profiles

The GE Assay Q series of membrane arrays contains 96 genes whose expression changes are potential indicators of cellular stress and toxicity. The membrane array monitors physiological processes classified into proliferation/carcinogenesis, growth arrest/senescence, inflammation and necrosis/apoptosis. The genes analysed are listed in Table 1.

The basic principles of the methodology are described in the manufacturer's handbook and include the following steps: analysis of gene expression using GEarray Q series Human Stress and Toxicity Pathway Finder Gene Array.

Preparation of annealing mix: for each RNA sample the following were combined in a sterile PCR tube (0.2 ml): total RNA 1–5 µg/ml, GEprimer mix (buffer A), 3 µl, RNase-free water to a total volume of 10 µl. The sample was mixed gently by pipetting followed by a brief centrifugation. The sample was placed in a heating block at 70 °C for 3 min, cooled to 42 °C and kept for 2 min before adding labelling mix.

Preparation of labelling mix: for each total RNA sample 10 µl of labelling mix was prepared as follows (Table 2): Labelling reagents were combined in a sterile PCR tube, mixed well by gentle pipetting followed by a brief centrifugation and kept on ice until required.

Labelling reaction: 10 µl labelling master mix (pre-warmed to 42 °C for 2 min) was transferred to each annealing reaction and samples were incubated at 42 °C for 90 min. The labelling reaction was stopped by the addition of 2 µl of 10× stop solution (buffer C).

Denaturation: Denaturation of the labelled cDNA probe prior to hybridisation on the array: 2 µl of 10× denaturing solution (buffer D) was added to the labelled cDNA probe (20 µl) and incubated at 68 °C for 20 min. 20 µl of 2× neutralisation solution (buffer E) was added and incubation was continued at 68 °C for 10 min.

Hybridisation reaction: a) 3 ml of GEhyb hybridisation solution was warmed to 60 °C for each sample to dissolve solids. b) Sheared salmon sperm DNA was denatured at 100 °C for 5 min and then chilled on ice before adding to the prewarmed GEhyb hybridisation solution to a final concentra-

**Table 2.** Labelling mix for RNA sampler

	1 sample	2 samples	3 samples
5× GEA BN buffer	4	8	12
Biotin-16-UTP (1 mM)	2	4	6
RNase inhibitor	1	2	3
Reverse transcriptase (50 U/µl)	1	2	3
RNase free water	2	4	6
Final volume	10	20	30

tion of 100 µg DNA/ml and kept at 60 °C until use. c) The array was made wet by the addition of deionised water. d) 2 ml of GEhyb hybridisation solution as prepared in step (b) was added to the hybridisation tube. The remaining 1 ml of solution was kept at 60 °C until step (g). e) The hybridisation tube was gently vortexed and placed into a hybridisation cylinder, pre-hybridised at 60 °C for 1–2 h with continuous agitation at 5–10 rpm. f) The pre-hybridisation solution was drained and discarded. g) The denatured DNA probe was mixed with 0.75 ml of GEhyb hybridisation solution from step (b) and hybridised over night with continuous agitation at 60 °C. h) The membrane was washed twice with 5 ml of pre-warmed wash solution (2× SSC, 1% SDS) for 15 min at 60 °C each time with agitation. i) The membrane was washed twice with 5 ml of pre-warmed wash solution (0.1× SSC, 0.5% SDS) for 15 min at 60 °C each time with agitation.

Chemiluminescent detection was performed at room temperature as follows: The arrays were blocked for 40 min by the addition of 1.5 ml GEblocking solution Q and agitating. Solution Q was discarded and alkaline phosphatase-conjugated streptavidin was diluted 1:7,500. 2 ml diluted AP-streptavidin was added to the tube for 10 min with agitation. The membrane was washed three times with 4 ml of 1× buffer F for 5 min with gentle vortexing. After the final wash the membrane was rinsed twice with 3 ml buffer G. The detection step was performed by adding 1 ml CDP-star substrate onto each array for up to 2 min. The membrane was blotted and placed between plastic sheets for 1 h before being developed and evaluated.

The gene expression studies were performed under concentration conditions which reduced cellular viability (measured by the binucleate cell frequency) by 50%.

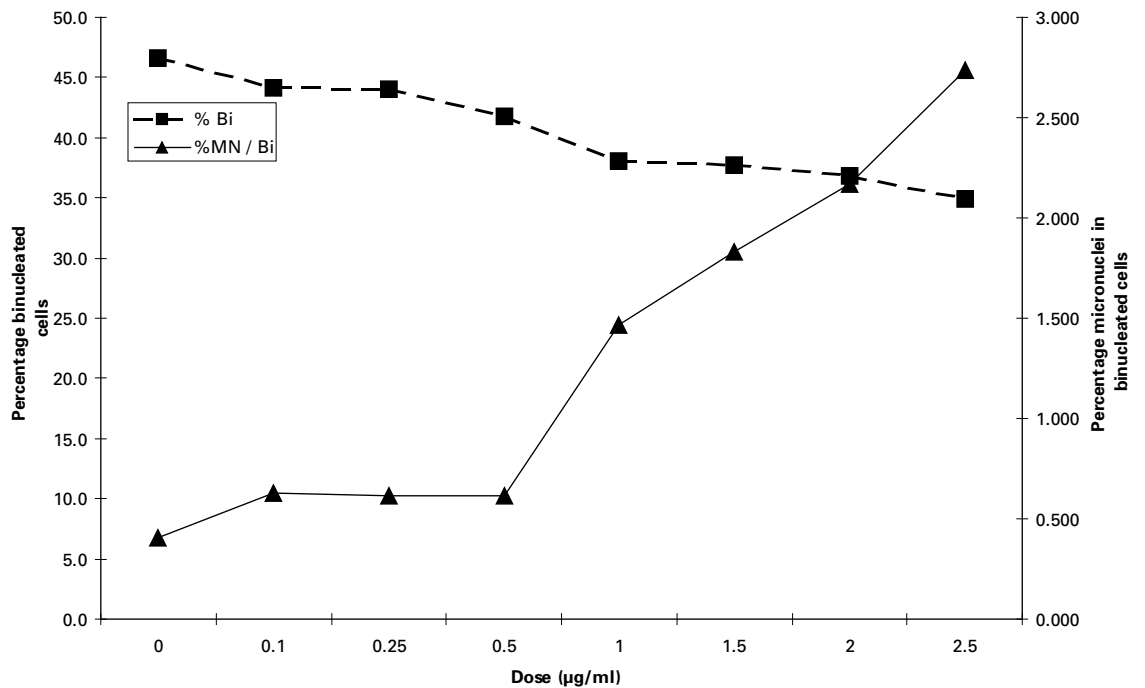


**Fig. 1.** The dose-response relationship for the induction of micronuclei after exposure to low doses of MMS.

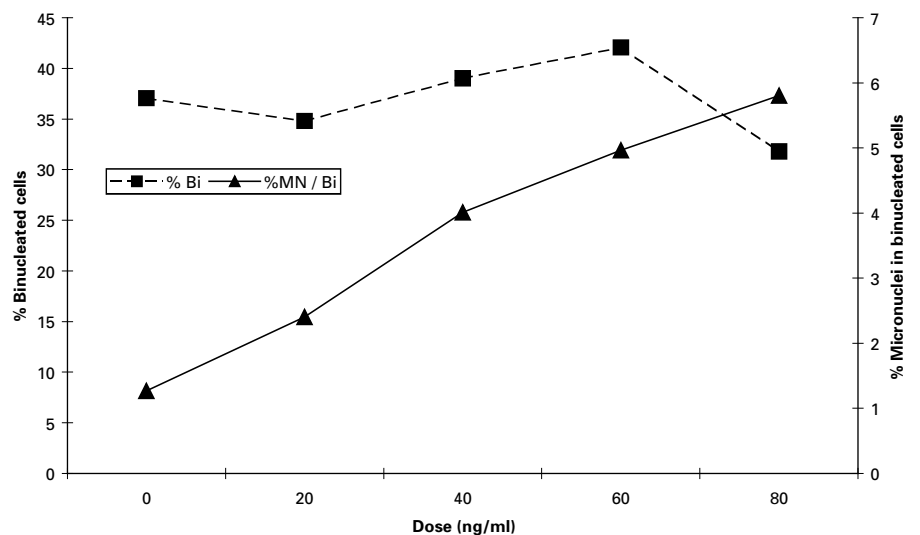


**Fig. 2.** Micronucleus assay data for the low toxicity chemical 4NQO.

## Results and discussion

### *Analysis of the dose-response relationships of methyl methanesulphonate*

The ability of the alkylating agent MMS to induce micronuclei was initially evaluated over a concentration range of 0–10 µg/ml. Following this dose finding study, the relative frequencies of induced micronuclei and reduction in binucleate cells was measured over a concentration range of 0–2.5 µg/ml. To assess the significance of micronucleus induction in the low

dose range, a minimum of 50 micronuclei were counted per dose point. Figure 1 illustrates the dose-response relationships for the induction of micronuclei and the binucleate cell frequencies obtained after exposure to low doses of MMS. The presence of a potential threshold for the induction of micronuclei at MMS exposures below 1 µg/ml can be seen in Fig. 1.

Following the demonstration of a potential threshold for the in vitro clastogenic activity of MMS, we have investigated gene expression changes following exposure to chemicals which we have classified into low-toxicity clastogens and high-toxicity

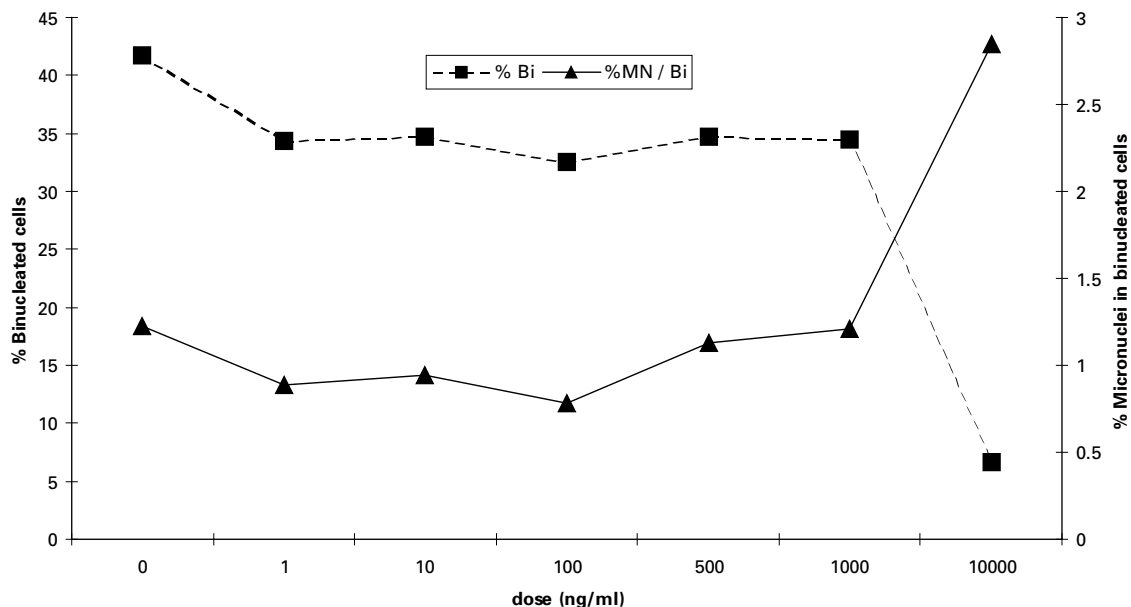


Fig. 3. Micronucleus assay data for the high toxicity chemical 8-HQ.

clastogens. The basis for this classification of 4-NQO and etoposide as clastogens active at low-toxicity and 8-HQ and amsacrine as clastogens active at high-toxicity is described in Materials and methods.

All four test chemicals were evaluated for their ability to induce micronuclei and reduce the binucleate cell frequency over comprehensive dose ranges. Representative results of these studies are shown in Fig. 2 for the low-toxicity chemical 4-NQO and in Fig. 3 for the high-toxicity chemical 8-HQ. These results demonstrate substantial differences in dose-response relationships. In the case of the low-toxicity chemical, 4-NQO, there was an approximately linear relationship between exposure dose and number of micronuclei over the concentration range of 20–80 ng/ml. In contrast, the high-toxicity chemical induced increases in micronuclei only at the highest tested dose of 10,000 ng/ml which produced substantial reductions in the binucleate cell frequency.

The gene expression profiles in the AHH-1 human lymphoblastoid cells for the test chemicals were determined following exposure to concentrations determined by their ability to induce micronuclei in the in vitro binucleate cell micronucleus assay. All the test chemicals were evaluated for their ability to produce gene expression changes measured by the change in intensity of individual gene spots on the array membranes of the genes shown in Table 1 following 24 h exposure to concentrations which reduced the binucleate cell ratio by 50%.

The low-toxicity chemicals 4NQO and etoposide were evaluated for their ability to induce changes in the expression of genes associated with cellular stress and toxicity. In no case were we able to detect gene expression changes under conditions where significant levels of micronuclei were induced (data not shown).

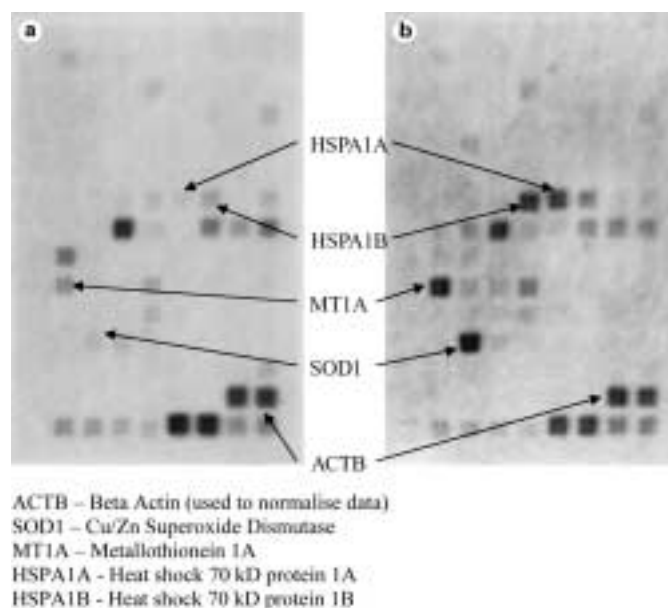


Fig. 4. Comparison of gene expression profiles between (a) untreated AHH-1 cells and (b) AHH-1 cells treated with 10 µg/ml 8-HQ for 24 h.

In contrast, under conditions which result in the induction of micronuclei at high toxicity levels, both 8-HQ and amsacrine produced a similar pattern of gene expression changes. Figure 4 illustrates a comparison of gene expression profiles of untreated AHH-1 cells and cells exposed to 10 µg/ml of 8-HQ. Analysis of the arrays indicates that the test chemical which induces micronuclei only under conditions of high toxicity increases the



expression of two basic classes of genes; i.e. heat shock proteins HSPA2, HSPA1L, HSPA1B, HSPA1A, HSPA6, and metallothioneins MT2A, MT1H and MT1A.

The gene expression changes produced by the high-toxicity chemicals were confirmed by real-time PCR (data not shown). These gene expression changes produced by the high toxicity clastogens 8-HQ and amsacrine were confirmed in studies comparing the alkylating agents MNNG (low-toxicity) and ENU (high-toxicity) (data not shown).

The two groups of genes up-regulated by high-toxicity chemicals are classified as those which indicate exposure to severe

cellular stress. The heat shock proteins are usually expressed under conditions of stress such as elevated temperature and oxidative damage (Slater et al., 1981; Pelham, 1986; Milner and Campbell, 1990). The metallothioneins are normally expressed in cells following heavy metal exposure and some recent studies indicate that they play a protective role during exposure to oxidative damage (You et al., 2002).

Our studies indicate that gene expression arrays provide a valuable tool for the analysis of the biological significance of chemicals which induce chromosome aberrations in vitro.

## References

- Armstrong MJ, Bean CL, Galloway SM: A quantitative assessment of cytotoxicity associated with chromosomal aberration detection in Chinese hamster ovary cells. *Mutat Res* 265:45–60 (1992).
- Beranek DT: Distribution of methyl and ethyl adducts following alkylation with mono-functional alkylating agents. *Mutat Res* 231:11–30 (1990).
- Broschinski LS, Madle S, Hensel C: Genotoxicity tests for new chemicals in Germany: routine in vitro test systems. *Mutat Res* 418:121–129 (1998).
- COM: Guidelines on a Strategy for Testing Chemicals for Mutagenicity (UK Department of Health, London 2000).
- Crespi CL, Thilly G: Assay for gene mutation in a human lymphoblast line, AHH-1, competent for xenobiotic metabolism. *Mutat Res* 128:221–230 (1984).
- Evans HJ: Human peripheral blood lymphocytes for the analysis of chromosome aberrations in mutagen tests, in Kilbey BJ, Legator M, Nicols W, Ramel C (eds): *Handbook of Mutagenicity Test Procedures*, pp 405–428 (Elsevier, Amsterdam 1984).
- Fenech M: The in-vitro micronucleus technique. *Mutat Res* 455:81–95 (2000).
- Friedberg EC, Walker GC, Siede W: *DNA Repair and Mutagenesis* (American Society of Microbiology Press, Washington DC 1995).
- Galloway SM, Miller JE, Armstrong MJ, Bean CL, Skopek TR, Nichols WW: DNA synthesis inhibition as an indirect mechanism of chromosome aberrations: comparison of DNA-reactive and non-DNA-reactive clastogens. *Mutat Res* 400:169–186 (1998).
- Graziano MJ, Courtney CL, Meierhenry EF, Kheoh T, Pegg DG, Gough AW: Carcinogenicity of the anti-cancer topoisomerase inhibitor amsacrine in Wistar rats. *Fund Appl Toxicol* 32:53–65 (1996).
- Heddle JA: The induction of micronuclei as a measure of genotoxicity. *Mutat Res* 123:61–118 (1983).
- Heddle JA: In vivo assays for mutagenicity, in Phillips DH, Venitt S (eds): *Environmental Mutagenesis*, pp 141–154 (Bios Scientific Publishers, Oxford 1995).
- Kirkland DJ: Chromosomal aberration tests in vitro: problems with protocol design and interpretation of results. *Mutagenesis* 7:95–106 (1992).
- Kirkland DJ, Müller L: Interpretation of the biological relevance of genotoxicity test results: the importance of thresholds. *Mutat Res* 464:137–147 (2000).
- Leanderson P, Tagesson C: Iron bound to the lipophilic iron chelator, 8-hydroxyquinoline, causes DNA strand breakage in cultured lung cells. *Carcinogenesis* 17:545–550 (1996).
- Milner CM, Campbell RD: Structure and expression of the three MHC-linked HSP70 genes. *Immunogenetics* 32:242–251 (1990).
- Moustaqchi E: DNA damage and repair: consequences on dose-responses. *Mutat Res* 464:35–40 (2000).
- Müller L, Kasper P: Human biological relevance and the use of threshold-arguments in regulatory genotoxicity assessment; experience with pharmaceuticals. *Mutat Res* 464:19–34 (2000).
- Nunoshiba T, Demple B: Potent intracellular oxidative stress exerted by the carcinogen 4-nitroquinoline-N-oxide. *Cancer Res* 53:3250–3252 (1993).
- Parry EM, Parry JM, Corse C, Doherty A, Haddad F, Hermine TF, Johnson G, Kayani M, Quick E, Warr T, Williamson J: Detection and characterization of mechanisms of action of aneugenic chemicals. *Mutagenesis* 17:509–521 (2002).
- Parry JM, Sarrif AM: Special Issue. Dose Response and Threshold-Mediated Mechanisms in Mutagenesis. Proceedings of an International Symposium held in Salzburg. *Mutat Res* 464:1–159 (2000).
- Pelham HRB: Speculations on the functions of the major heat shock and glucose-regulated proteins. *Cell* 46:959–961 (1986).
- Scott D, Galloway SM, Marshall RR, Ishidate Jr M, Brusick D, Ashby J, Myhr BC: Genotoxicity under extreme conditions. A report from ICPEMC Task Group 9. *Mutat Res* 257:147–204 (1991).
- Slater A, Cato ACB, Sillar GM, Kioussis J, Burdon RH: The pattern of protein synthesis induced by heat shock of HeLa cells. *Eur J Biochem* 117:341–346 (1981).
- Sofuni T, Hayashi M, Nohmi T, Matsuoka A, Yamado M, Kamata E: Semi-quantitative evaluation of genotoxic activity of chemical substances and evidence for a biological threshold of genotoxic activity. *Mutat Res* 464:97–104 (2000).
- Vock EH, Lutz WK, Hormes P, Hoffman HD, Vamvakas S: Discrimination between genotoxicity and cytotoxicity in the induction of DNA double-strand breaks in cells treated with etoposide, melphalan, cisplatin, potassium cyanide, Triton x-100 and gamma-irradiation. *Mutat Res* 413:83–94 (1998).
- You HJ, Lee KJ, Jeong HG: Over-expression of human metallothionein-111 prevents hydrogen peroxide-induced oxidative stress in human fibroblasts. *FEBS Letters* 521:175–179 (2002).

# Region-specific chromatin decondensation and micronucleus formation induced by 5-azacytidine in human TIG-7 cells

T. Satoh,<sup>a</sup> K. Yamamoto,<sup>b</sup> K.F. Miura,<sup>a</sup> and T. Sofuni<sup>c</sup>

<sup>a</sup>Genome Medical Business Division, Olympus Corporation, Hachioji;

<sup>b</sup>Department of Cell Biology, Tokyo Metropolitan Institute of Gerontology, Itabashi;

<sup>c</sup>NovusGene Inc., Hachioji (Japan)

**Abstract.** A human diploid lung fibroblast cell strain, TIG-7, has a heteromorphic chromosome 15 with an extra short arm carrying a homogeneously staining region (15p+hsr). We demonstrated previously that the 15p+hsr consists of an inactive and G+C-rich rDNA cluster characterized by fluorescence in situ hybridization (FISH) and various chromosome banding techniques. Thus, it was suggested that the region could contain highly methylated DNA. To observe methylation status on the target region directly under the microscope, we used a demethylating agent, 5-azacytidine (5-azaC), to induce decondensation of the chromatin containing methylated DNA. At 24 h after

treatment with 0.5  $\mu$ M 5-azaC, marked decondensation of the 15p+hsr was observed in almost all of the metaphases. Furthermore, we observed micronuclei, which were equivalent to the rDNA of the 15p+hsr demonstrated by FISH in the same preparation. In contrast, the DNA cross-linking agent mitomycin C (MMC) preferentially induced 15p+hsr-negative micronuclei. These findings indicated that chromatin decondensation and subsequent DNA strand breakage induced by the demethylating effect of 5-azaC led specifically to 15p+hsr-positive micronuclei.

Copyright © 2003 S. Karger AG, Basel

A human male diploid cell strain, TIG-7, was established at Tokyo Metropolitan Institute of Gerontology (Yamamoto et al., 1991). This fibroblast strain was originally derived from the lung of a fetus from a physically normal Japanese mother. We reported previously that TIG-7 has a heteromorphic chromosome 15 with an extra short arm carrying a homogeneously staining region (15p+hsr) (Satoh et al., 1998). The 15p+hsr consists of an inactive huge rDNA cluster characterized by rDNA-specific FISH and Ag-NOR staining, and seemed to be G+C rich according to the chromomycin A<sub>3</sub> fluorescence pattern. Thus, it was suggested that the region could contain highly methylated DNA. Such heteromorphic variation of the short-

arm in human acrocentric chromosomes is rarely observed (Sofuni et al., 1980; Babu et al., 1986; Velazquez et al., 1991; Friedrich et al., 1996). The results, however, are not always consistent from the cytogenetic viewpoint, because chromosome samples with such alterations would be difficult to obtain from primary cultures, and because it is difficult to perform detailed examinations. The TIG-7 cells could be useful as a model system in vitro for understanding the biological significance of the heteromorphism.

The cytosine analogue 5-azacytidine (5-azaC) induces very distinct decondensation in mammalian constitutive heterochromatin, in particular in human chromosomes 1, 9, 15, 16, and Y, as well as in facultative heterochromatin (inactive X chromosome), when incorporated into late-replicating DNA during the last hours of cell culture (Schmid et al., 1984a; Haaf and Schmid, 2000). In addition, the decondensation results in DNA strand breakage and micronucleus formation (Guttenbach and Schmid, 1994). Such demethylating effects of the genome, which can be directly observed under the microscope, have been restricted to large heterochromatic blocks. On the

Received 15 September 2003; accepted 16 December 2003.

Request reprints from: Takatomo Satoh, Genome Medical Business Division  
Olympus Corporation, 2-3 Kuboyama-cho, Hachioji  
Tokyo 192-8512 (Japan); telephone: +81-426-91-7115  
fax: +81-426-91-7932; e-mail: ta\_sato@ot.olympus.co.jp.

other hand, such chromatin decondensation is induced by other non-demethylating base analogs (Zakharov et al., 1974; Tommerup, 1984; Ott et al., 1998) or AT-specific DNA ligands (Marcus et al., 1979; Rocchi et al., 1979; Schmid et al., 1984b; Haaf et al., 1989). So, if demethylation-specific chromatin decondensation can be detected directly under the microscope, it will be helpful to understand the relationship between gene expression and chromatin condensation from an epigenetic viewpoint.

In the present study, in order to observe demethylating effects on the target 15p+hsr (a huge rDNA cluster) of TIG-7 directly in the microscope, we set up an experiment involving a combined 5-azaC treatment and FISH technique. Not only metaphase but also interphase cytogenetic analyses were performed, focusing especially on micronucleus formation. Cells were also treated with mitomycin C (MMC), a DNA cross-linking agent. Possible applications of micronucleus assay using TIG-7 cells to evaluate demethylating effects of chemicals are discussed.

## Materials and methods

### *Cell culture, chemical treatment and sample preparation*

Human lung fibroblasts, TIG-7 cells (Yamamoto et al., 1991) were maintained as exponentially growing cultures in Eagle's minimum essential medium (MEM) supplemented with 10% fetal bovine serum. The cultures were incubated at 37 °C in 5% CO<sub>2</sub> and 100% humidity. In this experiment, we used cells after 30 passages. The chromosome number was 46 (= 2n), and the cell doubling time was approximately 20–22 h. The cells were seeded into 60-mm plastic plates with 5 ml of culture medium and 1 × 10<sup>4</sup> cells/ml, cultured for 48 h, and then continuously treated with 0.25, 0.5 and 1.0 μM 5-azaC (Sigma) or 0.1 μg/ml MMC (Sigma) for 24 h until cell harvest (24–0 h). The chemicals were dissolved in saline and added to cultures at an appropriate final concentration, in such a way that the final concentration of saline in cultures was 10% (v/v). In another set of experiments cells treated with 0.5 μM 5-azaC or 0.1 μg/ml MMC for 24 h were washed with phosphate-buffered saline (PBS) and cultured with fresh medium for a further 24 h (24–24 h) or 48 h (24–48 h).

The cells were treated with 0.1 μg/ml colcemid for 2 h and harvested by trypsinization (0.25%) at each sampling time, 24–0, 24–24, and 24–48 h. In the 5-azaC-treated 24–0 h group, survivors were counted by trypan blue staining to evaluate the cytotoxic effects of 5-azaC. Metaphase and interphase slide preparations were made by the air drying technique involving hypotonic treatment with 0.075 M KCl for 20 min followed by fixation with cooled methanol-acetic acid (3:1).

### *FISH and cell observation*

To visualize rDNA, two different human rDNA plasmid probes were prepared; pHr21Ab (5' portion) containing a 5.8-kb *EcoRI* fragment consisting of a portion of the 18S gene and the nontranscribed spacer sequence (NTS) region, and pHr14E3 (3' portion) containing a 7.3-kb *EcoRI* fragment, mainly 28S (Health Science Research Resources Bank). The whole plasmid was nick translated with digoxigenin (DIG)-11-dUTP (Roche) according to the manufacturer's instructions.

The DIG-labeled DNA probe (200 ng) was added to SpectrumGreen direct-labeled chromosome 15-specific α-satellite hybridization mixture (Vysis), and applied to each slide. Hybridization was performed according to the manufacturer's instructions. The DIG-labeled probe was visualized by the standard DIG-rhodamine detection system (Roche), which produces a fluorescent signal at the site of hybridization.

After the hybridization, the slides were counterstained with 0.1 μg/ml 4,6-diamidino-2-phenylindole (DAPI) solution. Slide preparations were observed using a 100× objective lens (Olympus BX51), and chromatin decondensation and micronuclei were checked in 100 metaphase and 1000 interphase cells, respectively. The dual-color hybridization signals were captured

by a monochrome cooled CCD camera (Roper Scientific CoolSNAP HQ) and merged by image analysis software (MetaMorph) attached to the fluorescence microscope system.

## Results and discussion

### *Chromatin decondensation of 15p+hsr induced by 5-azaC treatment*

rDNA probes for FISH analysis hybridized with secondary constrictions of the D- and G-group chromosomes, and with the target 15p+hsr (Fig. 1a).

After 5-azaC treatment for 24–0 h at a dose of 0.5 μM, 15p+hsr of TIG-7 cells was specifically decondensed when compared to the solvent-treated group (Fig. 1b, c). This result suggested that 15p+hsr contains highly methylated DNA. Since 15p+hsr is constructed of a G+C-rich and inactive rDNA cluster (Satoh et al., 1998), it is possible that 15p+hsr could be formed by rDNA amplification due to unequal sister chromatid exchange (SCE) as discussed for human cells by Holden et al. (1987) and Friedrich et al. (1996) and by Satoh and Obara (1995) for other mammalian cells. At treatments with 0.25–1.0 μM 5-azaC for 24–0 h, almost all metaphases showed the specific decondensation (> 80%), and surviving cells were not significantly decreased even at the highest dose of 1.0 μM 5-azaC (> 80%) (Fig. 3). In this experiment, demethylation by 5-azaC did not affect rDNA activation of 15p+hsr when checked with Ag-NOR-staining (data not shown). As we have no data regarding successive changes after treatment, it could be important to analyze whether the 15p+hsr will express rDNA activity. For this purpose, 5-azadeoxycytidine treatment or combination with CpG demethylation by 5-azaC analogs and inhibition of histone deacetylation by trypanostatin A may be more effective as previously described (Ferraro and Lavia, 1985; Giaccotti et al., 1995; Malheiro et al., 1995; Glyn et al., 1997; Belyaev et al., 1998).

On the other hand, the chromosome 15 α-satellite region was not susceptible to the demethylating effect of 5-azaC (Fig. 1). This finding is consistent with previous reports that 5-azaC decondenses paracentromeric heterochromatin containing classical satellite DNA sequences, whereas centromeric α-satellite DNAs remain compact (Kokalj-Vokac et al., 1993; Fernandez et al., 1994). In our investigation with 5-azaC treatment for 24–0 h, centromeric heterochromatin decondensation of chromosomes 1, 9, 15, 16, and Y (Schmid et al., 1984a, Haaf and Schmid, 2000) was only rarely observed. Since these heterochromatin decondensations occur when 5-azaC was added during the late S phase, cells with chromosome loss might not survive during cell cycle progression. The decondensation response of the 15p+hsr could be essentially different from that of the constitutive heterochromatin.

### *Micronucleus formation after treatment of 5-azaC and MMC*

In almost all interphase cells of solvent control, the clustered rDNA FISH signal specific to 15p+hsr (Fig. 2a colored in red) was tightly associated with one of the chromosome 15 α-satellite FISH signals (Fig. 2a colored in green). In contrast, after

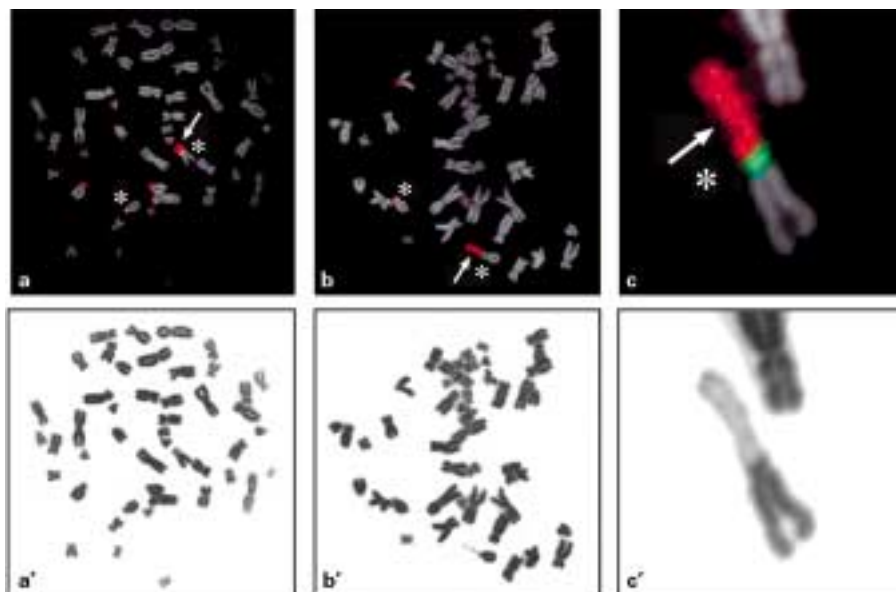


**Fig. 1.** rDNA/chromosome 15  $\alpha$ -satellite FISH (upper panel) and inverted DAPI (lower panel) images of metaphase spreads. **(a, a')** Normal metaphase with the 15p+hsr-not decondensed from the solvent control group. **(b, b')** The 15p+hsr-specific chromatin decondensation after 0.5  $\mu$ M 5-azaC treatment (24–0 h). **(c, c')** Partial metaphase with 15p+hsr decondensation. rDNA signals of 15p+hsr are identified by red (arrows) and chromosome 15  $\alpha$ -satellite signals by green fluorescence (asterisks).

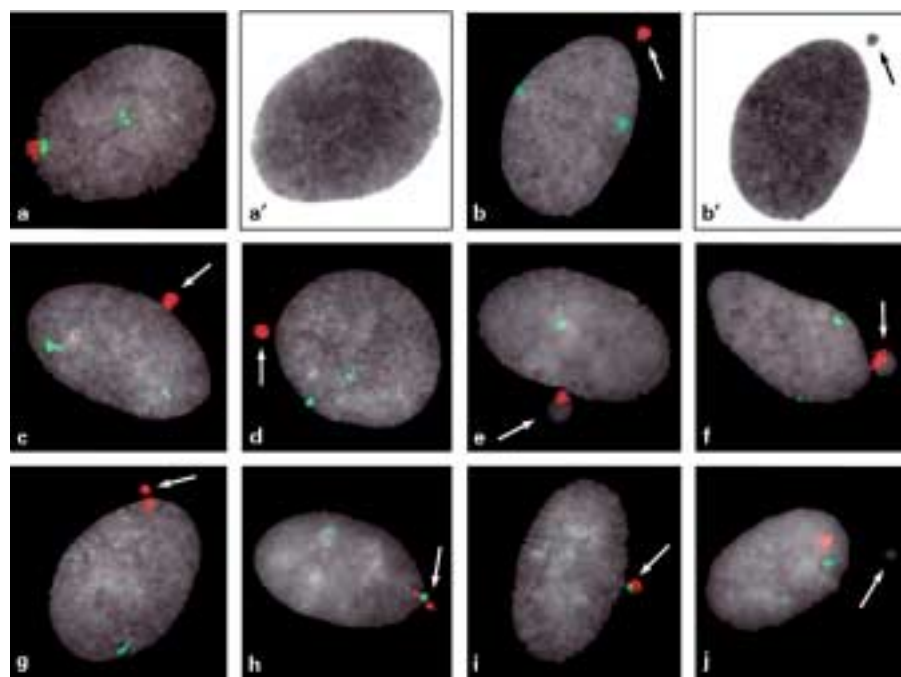


**Fig. 2.** Micronuclei images with rDNA/chromosome 15  $\alpha$ -satellite FISH of interphase cells after 0.5  $\mu$ M 5-azaC treatment (24–0 h). **(a)** Normal interphase without micronucleus formation from the solvent control group. **(a')** Inverted image of **(a)** counterstained with DAPI. **(b–d)** rDNA-positive micronuclei derived from 15p+hsr. **(b')** Inverted DAPI image of **(b)**. **(e, f)** rDNA-positive micronuclei including 15p+hsr and other chromosome materials. **(g, h)** Micronucleus formation derived from chromosome breakage within 15p+hsr. **(i)** Micronucleus including 15p+hsr and chromosome 15  $\alpha$ -satellite. **(j)** rDNA-negative micronucleus formation. rDNA signals of 15p+hsr are colored in red and chromosome 15  $\alpha$ -satellite signals are colored in green. Arrows indicate micronuclei.

treatment with 0.5  $\mu$ M 5-azaC for 24–0 h, the clustered rDNA was separated from the  $\alpha$ -satellite and predominantly excluded into micronuclei (Fig. 2b). The rDNA-positive micronuclei showed several variations depending on the chromatin break-points (Fig. 2c–i). On the other hand, most of 0.1  $\mu$ g/ml MMC-induced micronuclei were rDNA negative (Fig. 2j).

The frequencies of micronuclei following treatment with 5-azaC and/or MMC are shown in Fig. 4. At doses of 0.25–1.0  $\mu$ M and 24–0 h treatment times approximately 20% of

5-azaC-treated cells had micronuclei. MMC at a dose of 0.1  $\mu$ g/ml for the same treatment time induced cells with micronuclei at a lower frequency (< 5%) (Fig. 4, left). After treatment with 5-azaC at a dose of 0.5  $\mu$ M, we recovered the cells for 24–24 and 24–48 h. At both recovery periods, micronucleus formation was maintained, although their frequencies were slightly decreased (approximately 15%). In contrast, MMC-induced micronuclei were observed with a relatively higher frequency (>10%) when compared with that at 24–0 h (Fig. 4, right).

**Fig. 3.** Cell survival (%) and percent of metaphases with 15p+hsr decondensation in cultures treated with 5-azaC at 0 (solvent control), 0.25, 0.5 and 1.0  $\mu\text{M}$  for 24–0 h. One hundred meta-phase spreads were observed at each chemical treatment.

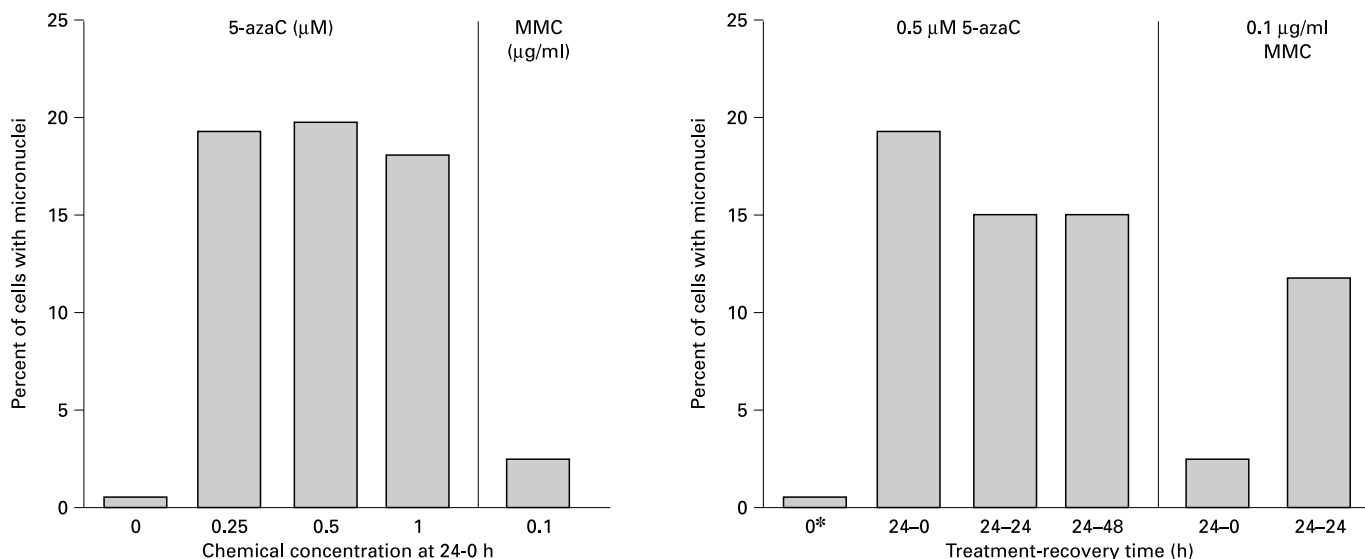
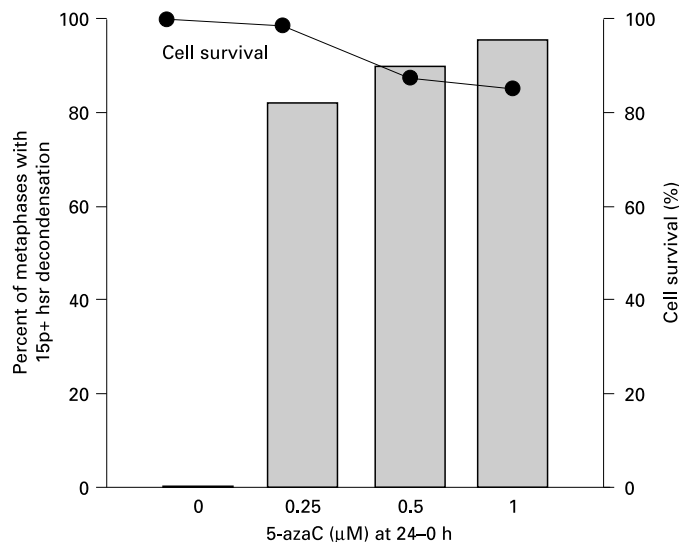


**Fig. 4.** Percent of interphase cells with micronuclei induced by 5-azaC or MMC treatment. One thousand interphase cells were observed at each experimental condition. (right) 0\* indicates the solvent control group at 24–0 h.








**Table 1.** Distribution of 15p+hsr (rDNA)-specific hybridization signals in micronuclei after 5-azaC or MMC treatment in TIG-7 cells for 24–0 h

Treatment							
Saline (solvent)	(100) <sup>a</sup>	-	-	-	-	-	-
5-azaC 0.25 $\mu\text{M}$	8	84	2	2	-	-	2
5-azaC 0.5 $\mu\text{M}$	6	82	4	4	-	-	2
5-azaC 1.0 $\mu\text{M}$	8	78	4	6	-	2	2
MMC 0.1 $\mu\text{g/ml}$	8	12	-	4	-	-	-

Large open circle, cell nucleus; small open circle, rDNA-negative micronucleus; small closed circle, rDNA-positive micronucleus; a small closed circle inside a large open circle; a rDNA-positive FISH signal within a cell nucleus (not micronucleus). Numbers are percentages.

<sup>a</sup> In the case of solvent control only one interphase with an rDNA-negative micronucleus was observed.

**Table 2.** Distribution of 15p+hsr (rDNA)-specific hybridization signals in micronuclei after 5-azaC or MMC treatment in TIG-7 cells for 24–0, 24–24 and 24–48 h

Treatment							
5-azaC 0.5 µM							
24–0	6	82	4	4	2	-	2
24–24	8	68	2	20	-	-	2
24–48	10	72	-	12	2	-	4
MMC 0.1 µg/ml							
24–0	8	12	-	4	-	-	-
24–24	82	8	4	4	-	-	2

Large open circle, cell nucleus; small open circle, rDNA-negative micronucleus; small closed circle, rDNA-positive micronucleus; a small closed circle inside a large open circle; a rDNA-positive FISH signal within a cell nucleus (not micronucleus). Numbers are percentages.

Furthermore, we classified cells with micronuclei according to rDNA FISH patterns as described by Guttenbach and Schmid (1994) (Tables 1 and 2). In total, 50 interphases with micronuclei at each cell preparation were observed. As shown in Table 1, in the 5-azaC-treated groups, more than 90% of micronuclei were rDNA positive at all doses. In contrast to this, MMC-induced micronuclei were predominantly rDNA negative (> 80%). These results suggested that DNA of 15p+hsr was demethylated by 5-azaC treatment and subsequent DNA strand breakage specific to the 15p+hsr induced rDNA-positive micronuclei. MMC treatment induced DNA strand breakage on other chromosome materials and rarely attacked the 15p+hsr. The recovery experiments gave the same results (Table 2).

Micronucleus formation after treatment with the demethylating agent, 5-azaC was reported previously (Guttenbach and Schmid, 1994; Cimini et al., 1996; Fauth et al., 1998). In these reports, the investigators paid special attention to chromosom-

al breakage in constitutive heterochromatin. In our experimental system using TIG-7 cells, the most important point was that only one target 15p+hsr within the genome was detected as a huge rDNA cluster in interphase cells. Since this region was not constitutive heterochromatin but a methylated rRNA gene-coding region, evaluation of the demethylating effect could be performed more clearly in relation to epigenetic significance.

Recently, a validation study of the in vitro micronucleus test to evaluate environmental mutagens has been performed positively (Matsushima et al., 1999). Chromosomal aberration assays require very high technical skill and scientific experience. In contrast, a micronucleus assay is relatively simple and clearer judgement is possible compared to the former. The 15p+hsr-targeted micronucleus formation and rDNA detection assay using TIG-7 might be a useful cytogenetic screening system to evaluate epigenetic influences on the genome, especially the demethylating effect of novel chemicals.

## References

- Babu A, Macera MJ, Verma RS: Intensity heteromorphisms of human chromosome 15p by DA/DAPI technique. *Hum Genet* 73: 298–300 (1986).
- Belyaev ND, Houben A, Baranczewski P, Schubert I: The acetylation patterns of histone H3 and H4 along *Vicia faba* chromosomes are different. *Chromosome Res* 6:59–63 (1998).
- Cimini D, Tanzarella C, Degrossi F: Effects of 5-azacytidine on the centromeric region of human fibroblasts studied by CREST staining and in situ hybridization on cytokinesis-blocked cells. *Cytogenet Cell Genet* 72:219–224 (1996).
- Fauth E, Scherthan H, Zankl H: Frequencies of occurrence of all human chromosomes in micronuclei from normal and 5-azacytidine-treated lymphocytes as revealed by chromosome painting. *Mutagenesis* 13:235–241 (1998).
- Fernandez JL, Goyanes V, Lopez-Fernandez C, Gosalvez J: Human alpha-satellite DNAs are not susceptible to undercondensation after 5-azacytidine treatment. *Cytogenet Cell Genet* 65:92–94 (1994).
- Ferraro M, Lavia P: Differential gene activity visualized on sister chromatids after replication in the presence of 5-azacytidine. *Chromosoma* 91:307–312 (1985).
- Friedrich U, Caprani M, Niebuhr E, Therkelsen AJ, Jorgensen AL: Extreme variant of the short arm of chromosome 15. *Hum Genet* 97:710–713 (1996).
- Giancotti P, Grappelli C, Poggessi I, Abatecola M, de Capoa A, Cozzi R, Perticone P: Persistence of increased levels of ribosomal gene activity in CHO-K1 cells treated in vitro with demethylating agents. *Mutat Res* 348:187–192 (1995).
- Glyn MCP, Egertova M, Gazdova B, Kovarik A, Bezdek M, Leitch AR: The influence of 5-azacytidine on the condensation of the short arm of rye chromosome 1R in *Triticum aestivum* L. root tip meristematic nuclei. *Chromosoma* 106:485–492 (1997).
- Guttenbach M, Schmid M: Exclusion of specific human chromosomes into micronuclei by 5-azacytidine treatment of lymphocyte culture. *Exp Cell Res* 211:127–132 (1994).
- Haaf T, Schmid M: Experimental condensation inhibition in constitutive and facultative heterochromatin of mammalian chromosomes. *Cytogenet Cell Genet* 91:113–123 (2000).
- Haaf T, Feichtinger W, Guttenbach M, Sanchez L, Muller CR, Schmid M: Berenil-induced undercondensation in human heterochromatin. *Cytogenet Cell Genet* 50:27–33 (1989).
- Holden JJ, Hough MR, Reimer DL, White BN: Evidence for unequal crossing-over as the mechanism for amplification of some homogeneously staining regions. *Cancer Genet Cytogenet* 29:139–149 (1987).
- Kokalj-Vokac N, Almeida A, Viegas-Pequignot E, Jeanpierre M, Malfroy B, Dutrillaux B: Specific induction of uncoiling and recombination by azacytidine in classical satellite-containing constitutive heterochromatin. *Cytogenet Cell Genet* 63:11–15 (1993).
- Malheiro I, Porto B, Mello-Sampayo T, Goyanes V: Specific induction of uncoiling in NORs of human acrocentric chromosomes by 5-azacytidine and 5-azadeoxycytidine. *Cytobios* 83:17–23 (1995).

- Marcus M, Goitein R, Gropp A: Condensation of all human chromosomes in G<sub>2</sub> phase and early mitosis can be drastically inhibited by 33258-Hoechst treatment. *Hum Genet* 51:99–105 (1979).
- Matsushima T, Hayashi M, Matsuoka A, Ishidate M Jr, Miura KF, Shimizu H, Suzuki Y, Morimoto K, Oqura H, Mure K, Koshi K, Sofuni T: Validation study of the in vitro micronucleus test in a Chinese hamster lung cell line (CHL/IU). *Mutagenesis* 14:569–580 (1999).
- Ott G, Haaf T, Schmid M: Inhibition of condensation in human chromosomes induced by the thymidine analogue 5-iododeoxyuridine. *Chromosome Res* 6:495–499 (1998).
- Rocchi A, di Castro M, Prantera G: Effects of DAPI on human leukocytes in vivo. *Cytogenet Cell Genet* 23:250–254 (1979).
- Satoh T, Obara Y: Nonrandom distribution of sister chromatid exchanges in the chromosomes of three mammalian species. *Zool Sci* 12:749–756 (1995).
- Satoh T, Yamamoto K, Miura KF, Ishidate M Jr: Cytogenetic analysis of heteromorphic short arm of 15p+ in a human diploid cell strain, TIG-7. *Chromosome Sci* 2:57–62 (1998).
- Schmid M, Haaf T, Grunert D: 5-Azacytidine-induced undercondensations in human chromosomes. *Hum Genet* 67:257–263 (1984a).
- Schmid M, Hungerford DA, Poppen A, Engel W: The effects of distamycin A in human lymphocyte cultures. *Hum Genet* 65:377–384 (1984b).
- Sofuni T, Tanabe K, Awa AA: Chromosome heteromorphisms in the Japanese. Nucleolus organizer regions of variant chromosomes in D and G groups. *Hum Genet* 55:265–270 (1980).
- Tommerup N: Idoxuridine induction of micronuclei containing the long or short arm of human chromosome 9. *Cytogenet Cell Genet* 38:92–98 (1984).
- Velazquez M, Visedo G, Ludena P, de Cabo SF, Sentis C, Fernandez-Piqueras J: Cytogenetic analysis of a human familial 15p+ marker chromosome. *Genome* 34:827–829 (1991).
- Yamamoto K, Kaji K, Kondo H, Matuo M, Shibata Y, Tasaki Y, Utakoji T, Ooka H: A new human male diploid cell strain, TIG-7: Its age-related changes and comparison with a matched female TIG-1 cell strain. *Exp Gerontol* 26:525–540 (1991).
- Zakharov AF, Baranovskaya LI, Ibrahimov AI, Benjusch VA, Demintseva VS, Oblapenko NG: Differential spiralization along mammalian mitotic chromosomes. 5-Bromodeoxyuridine and 5-bromodeoxycytidine-revealed differentiation in human chromosomes. *Chromosoma* 44:343–359 (1974).

# Micronuclei in lymphocytes of uranium miners of the former Wismut SDAG

W.-U. Müller, A. Kryscio and C. Streffer

Institut für Medizinische Strahlenbiologie, Universitätsklinikum Essen, Essen (Germany)

**Abstract.** We studied micronucleus frequencies in former German uranium miners of the Wismut SDAG (Sowjetisch-Deutsche Aktiengesellschaft). Various other groups were analyzed for comparison (individuals with lung tumors or lung fibrosis, controls). We had shown previously that micronucleus frequencies were not different among the various groups. Differences were observed, however, when centromere-positive and -negative micronuclei were distinguished. In the analyses presented here, we looked for the effects of smoking habits, alcohol consumption, vitamin uptake, chronic diseases, allergies, doing sports,  $\gamma$ -GT (gamma-glutamyltranspeptidase), lymphocyte numbers, CEA (carcinoembryonic antigen), X-ray

diagnostics, computer tomographies, and scintigraphies. With the exception of more than one scintigraphy carried out during the last four months before micronucleus analysis, none of the factors mentioned above significantly affected micronucleus numbers. One result deserves specific attention: individuals with low percentages of binucleated lymphocytes after *in vitro* cytochalasin B exposure showed higher micronucleus frequencies than those individuals with high percentages of binucleated cells. The same result was obtained for various other populations that we monitored in the past.

Copyright © 2003 S. Karger AG, Basel

Some years ago, we, together with a couple of other groups, published results of a biomarker study in former German uranium miners (Popp et al., 2000). Our contribution to this study was, among some other endpoints, the evaluation of micronuclei in peripheral lymphocytes. In that study, it was reported that no significant differences in micronucleus numbers were observed, when controls, uranium miners, lung tumor patients, and patients with lung fibrosis were compared. Figure 1 summarizes those results. Marked differences between controls and uranium miners, however, were observed, when centromere-positive and -negative micronuclei were distinguished (Streffer et al., 1998; Kryscio et al., 2001). These differences were attributed to a possible genomic instability in uranium miners.

The publication mentioned above (Popp et al., 2000) was intended as a pilot study comparing various biomarkers and, thus, did not give very detailed information on the micronucleus results. This will be done in the article presented here.

## Materials and methods

Details of the micronucleus analysis in peripheral blood lymphocytes based upon the cytochalasin B technique (Fenech and Morley, 1985) have been published already (Gantenberg et al., 1991). Information on the various groups analyzed in the pilot study of the usefulness of biomarkers in uranium miners have also been published (Popp et al., 2000). The Wismut group comprised 106 individuals; for various reasons, only 85 could be included in the analyses presented in this article.

As a measure of radiation exposure so-called “radon equivalents” (Rn equiv. expressed in WLM = working level months, the unit used to describe radon and radon daughter exposure) were used. These radon equivalents include the exposure to radon and radon daughters, by long-living alpha-emitting radionuclides, and by external  $\gamma$  exposure. The concept was developed by W. Jacobi based upon data ascertained by F. Lehmann and presents an update of the concept outlined previously (Jacobi et al., 1997).

For testing statistical differences, the Mann-Whitney U test or the Kruskal-Wallis test were performed using GraphPad Prism version 4.00 for Windows (GraphPad Software, San Diego California USA). The same software package was used to calculate all regressions.

Supported by a grant from the Hauptverband der gewerblichen Berufsgenossenschaften (HVBG), Sankt Augustin, Germany.

Received 17 September 2003; revision accepted 25 November 2003.

Request reprints from Wolfgang-Ulrich Müller  
Institut für Medizinische Strahlenbiologie  
Universitätsklinikum Essen, DE-45122 Essen (Germany)  
telephone: +49 (0)201 723 4168; fax: +49 (0)201 723 5966  
e-mail: wolfgang-ulrich.mueller@uni-essen.de.



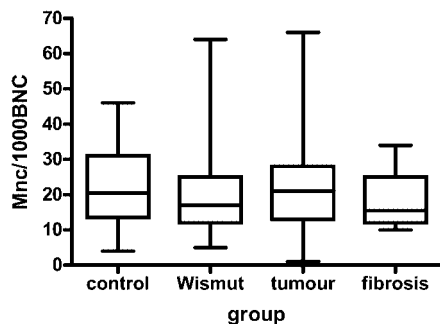


**Fig. 1.** Comparison of micronucleus frequencies in age- and gender-matched controls, uranium miners, lung tumor patients (either with a smoking or asbestos history), and patients with lung fibrosis.

## Results

As mentioned above (Fig. 1) and as published previously (Popp et al., 2000), we did not find statistically significant differences in micronucleus frequencies among the various groups analyzed (controls, uranium miners, lung tumor patients, and patients with lung fibrosis). An interesting question is, of course, whether the amount of radiation exposure is reflected by the number of micronuclei found in the peripheral lymphocytes of the uranium miners. Figure 2 shows that this is definitely not the case. If at all, then one observes a slight decline in micronucleus frequency with the increase of exposure; this decline, however, is statistically not significant.

One has to keep in mind, that most of the workers stopped being exposed many years ago (e.g. 50 out of the 85 analyzed were exposed until 1970 only, and from the remaining 25 who worked after 1970, only 12 worked until the close down of the facility in 1990). In addition, the workers with the highest exposures per year were those who worked before 1955. In order to find out, whether there is a time factor involved, we analyzed separately those miners who were employed before 1955 only, before and after 1955, and after 1955 only. In addition, we looked in those three time intervals for the miners that received an exposure below and above the median of the corresponding group. Figure 3 shows the results of these analyses. Statistically there was no difference among all the groups (Kruskal-Wallis test;  $P > 0.05$ ). Even more surprising was that the micronucleus numbers showed a trend to lower values in the groups with the highest exposures, although none of these differences was significant (Mann-Whitney U test;  $P > 0.05$ ).

A result that might need some intense reflection is shown in Fig. 4. There is a pronounced and statistically significant dependence between micronucleus frequency and the degree of binucleation. Individuals with a high percentage of binucleated cells show less micronuclei than those with low binucleation percentages. When we detected this relationship, we checked all of our bigger data sets analyzed in the past (controls, individuals handling cytostatica, children in the vicinity of Chernobyl, Russian children not affected by the Chernobyl accident). In all cases we found the same relation between micronucleus fre-

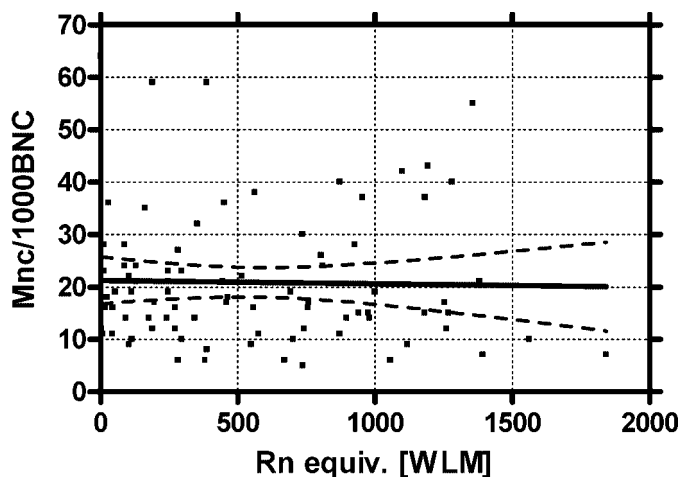


**Fig. 2.** Relation between radiation exposure and micronucleus frequencies in former uranium miners.

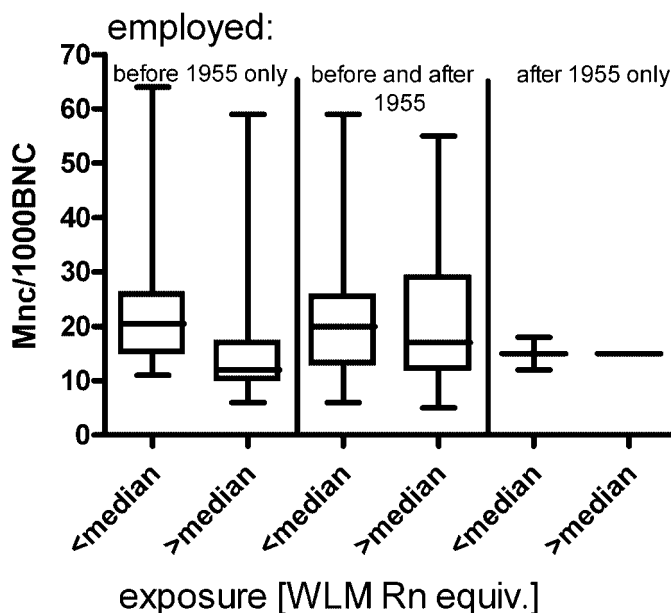


**Fig. 3.** Dependence of micronucleus frequencies on time of employment and on exposure to radionuclides below and above the median.

quency and binucleation as described in Fig. 4 at high statistical significance ( $P < 0.01$ ).

In the course of the study, many individual characteristics were recorded: smoking habits, alcohol consumption, vitamin uptake, chronic diseases, allergies, doing sports,  $\gamma$ -GT (gamma-glutamyltranspeptidase), lymphocyte numbers, CEA (carcinoembryonic antigen), X-ray diagnostics, computer tomographies, and scintigraphies. It is obvious that we were interested, whether any of these parameters affected micronucleus frequencies, being well aware that such an approach can be used as

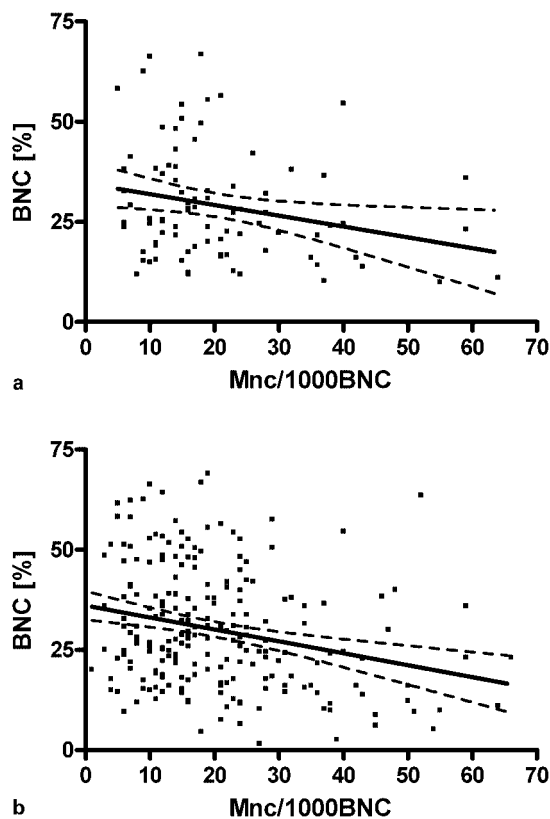


**Fig. 4.** Relation between micronucleus frequencies and binucleation in uranium miners (a) and all individuals in the study (b).

a hypothesis generating procedure only, because of the multiple testing problem. Thus, we looked for the effects of the parameters mentioned above on micronucleus frequencies in the following groups: all individuals in the study ( $n = 320$ ; please note: because of missing data not all could be evaluated in all tests; this also applies to the other groups), uranium miners ( $n = 106$ ), all non-uranium miners ( $n = 214$ ), and controls (23).

Of all the parameters mentioned above, there was only one that was somewhat conspicuous: more than one scintigraphy during the past four months before micronucleus analysis (Fig. 5). The number of individuals receiving more than one scintigraphy was very small (15 with two and 1 with four scintigraphies). This might be the reason why the difference between the medians was not significant ( $P > 0.05$ ; Mann-Whitney U test). It could be interesting, however, to check the effect of scintigraphies on micronucleus frequencies in a study designed specifically for this purpose.

## Discussion

At a first glance, it might be surprising that a population like uranium miners that was exposed to ionizing radiation for many years does not show higher micronucleus frequencies than controls. There are, at least, two aspects, however, that

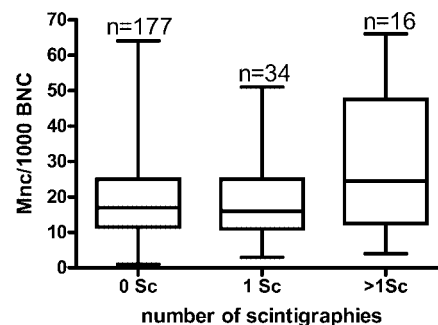


**Fig. 5.** Effect of the number of scintigraphies during the last four months on micronucleus frequencies.

must be kept in mind. Firstly, the exposure was a chronic and not an acute one. Micronuclei are particularly valuable in the latter case and less so, if at all, after chronic exposures (Müller et al., 1995). Secondly, the miners with the highest exposures were working at the Wismut SDAG a long time ago (between 1946 and 1955). Thus, the body had plenty of time to get rid of damaged lymphocytes. As the working conditions improved afterwards (better ventilation, wet drilling), markedly lower exposures were received since about 1955.

The result described in Fig. 4 was unexpected: individuals with a low percentage of binucleated cells showed higher micronucleus frequencies than those with high percentages of binucleated cells. In a first attempt to explain this result, one might suspect a radiation effect on cell proliferation. This, however, can be ruled out for the following reasons. First of all, there was no dependence between radiation dose and binucleation (data not shown;  $P > 0.1$ ), so that cell proliferation was not affected by the radiation doses received by the miners. In addition, the same result was obtained for Wismut employees (Fig. 4a) and for the entire cohort of the study presented here (Fig. 4b), including 237 individuals without a radiation exposure. Further support comes from the observation that identical results were obtained for controls and for various other groups not exposed to ionizing radiation (e.g. Russian children not affected by the Chernobyl accident, smokers with lung tumors, individuals with lung fibrosis, technicians handling cytostatica).

A plausible explanation might be the following one. If a low frequency of binucleated cells is an indication of a comparatively high amount of damage to lymphocytes, this high amount of damage might also be reflected by high micronucleus numbers. Indications for such a mechanism have been found after radiation exposure (e.g. Hoffmann et al., 2002). As outlined above, we observed this inverse relation between binucleation and micronucleation also without radiation exposure.

One must be careful, however, not to be misled by the method itself. We do know, for example, that the optimum time point of the addition of cytochalasin B is crucial and can be different from individual to individual (Gantenberg et al., 1991). In the analyses presented here, cytochalasin B was given at the same time point for all donors. If, in the cases of low

percentages of binucleated cells, the lymphocytes proliferated faster than in those cases with high fractions of binucleated cells, it is most likely those lymphocytes with the least damage, i.e. the lowest micronucleus numbers, that escaped the cytochalasin B block, resulting in high micronucleus frequencies in those samples with low percentages of binucleated cells. This consideration shows that additional analyses are necessary, before one can draw firm conclusions. In any case, the observation seems to be interesting and worth being followed.

One of the major goals of the original study was to look whether employment in a uranium mine resulted in higher micronucleus frequencies in peripheral lymphocytes compared to various other populations (controls, individuals with lung tumors or lung fibrosis). Thus, the study was not designed to evaluate the effects of specific factors on micronucleus frequencies. On the other hand, we had detailed information on various characteristics of the individuals included in the study, so that we could use this information at least for hypothesis generation. That most of the factors did not affect micronucleus frequencies is not very surprising, because, based on the experiences in the past, effects by most of these factors are either absent or small, so that in some studies they do show an effect, in others they do not (Müller and Streffer, 1994). In our analy-

sis, only more than one scintigraphy during the last four months before micronucleus determination showed an enhancing effect on micronucleus frequencies. Unfortunately, we do not have the information on the type of scintigraphy performed, so that we cannot give details with regard to the radiation doses. But it might be interesting to study the role of scintigraphies on micronucleus production in an analysis specifically designed for this purpose.

In the future a second goal of the original study will be touched: is it possible to predict lung tumors in uranium miners using micronucleus results? Some of the miners showed conspicuously high micronucleus frequencies, and there are indications that high frequencies of damaged chromosomes indicate a high tumor risk (Hagmar et al., 1994; Bonassi et al., 1995), although the data obtained for micronuclei so far are not very encouraging and statistically far from being significant (Hagmar et al., 1998).

### Acknowledgements

We would like to thank Marion Czeranski, Sabine Dietl, Ulrike Kaiser and Christel Spaetling for technical assistance.

### References

- Bonassi SA, Abbondandolo A, Camurri L, Dalpra L, DeFerrari M, Degrassi F, Forni A, Lamberti L, Lando C, Padovani P, Sbrana I, Vecchio D, Puntoni R: Are chromosome aberrations in circulating lymphocytes predictive for future cancer onset in humans? *Cancer Genet Cytogenet* 79:133–135 (1995).
- Fenech M, Morley AA: Measurement of micronuclei in lymphocytes. *Mutat Res* 147:29–36 (1985).
- Gantenberg H-W, Wuttke K, Streffer C, Müller W-U: Micronuclei in human lymphocytes irradiated in vitro or in vivo. *Radiat Res* 128:276–281 (1991).
- Hagmar L, Brogger A, Hansteen IL, Heim S, Hogstedt B, Knudsen L, Lambert B, Linnainmaa K, Mittelman F, Nordenson I, Reuterwall L, Salomaa C, Skerfving S, Sorsa M: Cancer risk in humans predicted by increased level of chromosomal aberrations in lymphocytes: Nordic study group on the health risk of chromosome damage. *Cancer Res* 54:2919–2922 (1994).
- Hagmar L, Bonassi S, Stromberg U, Brogger A, Knudsen LE, Norppa H, Reuterwall C: Chromosomal aberrations in lymphocytes predict human cancer: a report from the European Study Group on Cytogenetic Biomarkers and Health (ESCH). *Cancer Res* 58:4117–4121 (1998).
- Hoffmann GR, Sayer AM, Littlefield LG: Higher frequency of chromosome aberrations in late-arising first-division metaphases than in early-arising metaphases after exposure of human lymphocytes to X-rays in G<sub>0</sub>. *Int J Radiat Biol* 78:765–772 (2002).
- Jacobi W, Lehmann F, Renner H-J: Anleitung und Tabellen zur Berechnung der Verursachungswahrscheinlichkeit extrapulmonaler Krebserkrankungen durch die berufliche Strahlenexposition von Beschäftigten der ehemaligen WISMUT AG (BG Feinmechanik und Elektrotechnik, Köln 1997).
- Kryscio A, Ulrich Muller WU, Wojcik A, Kotschy N, Grobelny S, Streffer C: A cytogenetic analysis of the long-term effect of uranium mining on peripheral lymphocytes using the micronucleus-centromere assay. *Int J Radiat Biol* 77:1087–1093 (2001).
- Müller W-U, Streffer C: Micronucleus assays. *Adv Mutag Res* 5:1–133 (1994).
- Müller W-U, Streffer C, Wuttke K: Micronucleus determination as a means to assess radiation exposure. *Stem Cells* 13:199–206 (1995).
- Popp W, Plappert U, Müller WU, Rehn B, Schneider J, Braun A, Bauer PC, Vahrenholz C, Presek P, Brauksiepe A, Enderle G, Wust T, Bruch J, Fliedner TM, Konietzko N, Streffer C, Woitowitz HJ, Norporth K: Biomarkers of genetic damage and inflammation in blood and bronchoalveolar lavage fluid among former German uranium miners: a pilot study. *Radiat Environ Biophys* 39:275–282 (2000).
- Streffer C, Müller W-U, Kryscio A, Böcker W: Micronuclei – biological indicator for retrospective dosimetry after exposure to ionizing radiation. *Mutat Res* 404:101–105 (1998).

# A liver micronucleus assay using young rats exposed to diethylnitrosamine: methodological establishment and evaluation

H. Suzuki,<sup>a</sup> T. Shirotori,<sup>b</sup> and M. Hayashi<sup>c</sup>

<sup>a</sup>Ina Research Inc., Nagano; <sup>b</sup>The Collaborative Study Group of the Micronucleus Test – Mammalian Mutagenicity Study Group/Japanese Environmental Mutagen Society; <sup>c</sup>Division of Genetics and Mutagenesis, National Institute of Health Sciences, Tokyo (Japan)

**Abstract.** We have developed a simple liver micronucleus assay using young rats (up to 4 weeks old) to assess cytogenetic damage of chemicals in liver cells. Diethylnitrosamine (DEN) was used as a model rodent hepatocarcinogen in this study. Compared to the partial hepatectomy method most commonly used for the liver micronucleus assay, the present assay method showed equal or even higher practicability. The young rat liver micronucleus assay was also characterized for rat strain differences, sampling time after treatment, single treatment vs. split treatment, age of animals, administration route, and staining

method. Although based on one model chemical, we propose an acceptable protocol for the micronucleus assay using young rat liver as follows: Up to 4-week-old rats should be used; oral or intraperitoneal administration can be used; single or repeated treatment protocols can be applied; sampling time is 3–5 days after the last treatment; hepatocytes are prepared by the collagenase perfusion method; and cells are stained with the AO-DAPI double staining method.

Copyright © 2003 S. Karger AG, Basel

Micronucleus assays have been widely performed using bone marrow cells to assess the clastogenic potential of chemicals *in vivo*. Since bone marrow (BM) is one of the continuously proliferating tissues in adult animals, it has been used as a common target organ for cytogenetic studies. However, it is well known that some compounds need metabolic activation in the liver, and it has been pointed out that some pro-mutagens elicit a negative response in the BM micronucleus assay (Morita et al., 1997). It may be considered that some active metabolites have a very short lifespan and do not reach the BM at sufficient concentrations to induce micronuclei. In fact, some rodent liver carcinogens, including di-alkyl-nitrosamines, nitro aromatic

compounds, and azo derivatives, gave negative results in a BM assay (Angelosanto, 1995). It is worthwhile, therefore, to consider the selection of other organs for evaluating genotoxicity of test chemicals, especially the liver for detecting liver carcinogens. The use of suitable organs for genotoxicity determination is also recommended in the guidance proposed by the Committee on Mutagenicity of Chemicals in Food, Consumer Products and the Environment (Committee on the Mutagenicity of Chemicals, 2000).

In recent years, various investigators have tried to develop a liver micronucleus assay. Due to extremely low mitotic activity in adult animals, procedures require mitotic stimulation of liver cells together with treatment of animals with test chemicals. Tates et al. (1980) reported a method comprising partial hepatectomy (PH) before or after chemical treatment for the liver micronucleus assay. The division of hepatocytes is stimulated by PH, and positive responses were obtained in induction of micronuclei in liver cells after treatment with liver carcinogens that gave negative results in the BM assay. Other investigators also evaluated the chemical clastogenicity potential in the liver by the PH method (Clivet et al., 1989; Roy and Das, 1990; Mere-

Received 22 August 2003; manuscript accepted 15 December 2003.

Request reprints from Dr. Hiroshi Suzuki, Ina Research Inc.  
2148-188 Nishiminowa, Ina-shi, Nagano 399-4501 (Japan)  
telephone: +81-265-73-8611; fax: +81-265-73-8612  
e-mail: h-suzuki@ina-research.co.jp

to et al., 1994; Zhurkov et al., 1996). There are, however, two shortcomings in the PH method: 1) Technically it is not easy to perform successful hepatectomy on all animals used in the assay, and 2) it has been reported that cytochrome P450, styrene mono-oxygenase, epoxide hydrolase, and glutathione-S-epoxide transferase activities decreased by 50, 35, 50, and 35 %, respectively 12 h after PH (Rossi et al., 1987).

Another method used 4-acetyl aminofluorene (4AAF), a mitogen for liver cells (Braithwaite and Ashby, 1988), to activate cell proliferation. In this method, the possibility of interaction with the test chemical has not been ignored (Parton and Garriott, 1997). An *in vivo/in vitro* assay system has also been reported, i.e., after treatment of animals with test chemicals *in vivo*, hepatocytes were collected and primary cell cultures were established with growth factors before cell harvest for slide preparation (Sawada et al., 1991). However, this *in vivo/in vitro* method is labor-intensive, costly and time consuming; thus it has not been used as a routine method to evaluate chemical clastogenicity in the liver.

The use of proliferating tissue is a prerequisite for the micronucleus assay. In 4-week-old rats, the hepatocytes are still proliferating, and the percentage of S phase cells is more than 40 times higher than in adult rat liver (Parton and Garriott, 1997). Sipes and Gandolfi (1993) reported that P450 levels reach a maximum at 4 weeks of age in the rat. Considering these points, we developed and evaluated the young (4-week-old) rat liver micronucleus assay. We used diethylnitrosamine (DEN), which is a well-known rodent liver carcinogen, as a model compound. DEN was negative in the conventional BM micronucleus assay (Morita et al., 1997), but positive in the liver micronucleus assay using the PH method (Tates et al., 1980). This paper describes the comparison of the PH and young rat methods and investigations of technical points in the young rat liver micronucleus assay.

## Materials and methods

### Animals

Male Fischer 344 (F344) and Sprague Dawley (SD) rats were purchased from Charles River Japan. The animals were housed under a 12-hour light-dark cycle and allowed free access to food and water.

### Chemicals

Diethylnitrosamine (DEN, CAS No. 55-18-5), was purchased from Wako Pure Chemical Industries, Ltd. (Osaka, Japan). DEN was dissolved in physiological saline immediately before treatment and given once or twice by intraperitoneal injection or gavage to rats.

### Comparison of the young rat method with the partial hepatectomy (PH) method

F344 or SD rats were treated orally with 50 mg/kg of DEN at 3 or 4 weeks of age in the young rat method, and at 6 weeks of age in the PH method. In the former method, slide preparations were made 2–5 days after single treatment, and peripheral blood samples were collected and supravitaly stained with acridine orange (AO)-coated slides (Hayashi et al., 1990) before and 1, 2, and 3 days after treatment. In the latter method, PH was performed 7 days after treatment, and the slides were prepared 2–5 days after PH.

### Dose dependency and age effect

DEN at dose levels of 12.5, 25, and 50 mg/kg was administered to 4-week-old rats, and hepatocytes were isolated 5 days after treatment. To investigate the effect of age, F344 rats at 3–9 weeks of age were treated with DEN

(50 mg/kg) once and slide preparations were made on the 5th day after treatment as with the dose-response assay.

### Administration route difference and treatment times

4-week-old F344 rats were treated by gavage or intraperitoneally with DEN once at 40 mg/kg or twice at 20 mg/kg with a 24-hour interval. Hepatocytes were isolated 2–5 days after the last treatment.

### Preparation of hepatocytes

Hepatocytes were isolated from anesthetized rats by the collagenase perfusion method, rinsed with 10% neutral buffered formalin 2 or 3 times and centrifuged at 50 g (500 rpm) for 1 min (Cllet et al., 1989). Hepatocytes were suspended with 10% neutral buffered formalin and stored in a refrigerator until analysis. In the case of PH, two-thirds of the liver was removed according to the published method (Higgins and Anderson, 1931). The hepatocytes were suspended with 10% neutral buffered formalin, and kept in a refrigerator until analysis.

### Microscopy and micronucleus determination

Immediately prior to analysis, 10–20  $\mu$ l of hepatocyte suspensions were mixed with an equal volume of AO-4',6-diamidino-2-phenylindole dihydrochloride (DAPI) stain solution for fluorescent microscopy. The AO-DAPI stain solution contains one part of 500  $\mu$ g/ml of AO aqueous solution and one part of 10  $\mu$ g/ml of DAPI aqueous solution. Approximately 10–20  $\mu$ l of stained hepatocyte suspension was dropped onto a glass slide and covered with a coverslip (24  $\times$  40 mm).

Hepatocytes were analyzed under a fluorescent microscope ( $\times$ 400 or higher) equipped with a UV excitation system. The number of micronucleated hepatocytes (MNHEPs) was recorded based on analysis of 2000 hepatocytes (in two fields) from each animal. In accordance with the methods of Braithwaite and Ashby (1988) and Cllet et al. (1989), the following classification criteria for MNHEPs were used: Round or distinct micronuclei stained with the same color as the nuclei, with diameters of 1/4 or less that of the main nuclei. The number of mitotic cells was also counted in 1000 hepatocytes in each animal to determine the mitotic index (MI) for administration route or treatment time differences. Mitotic cells were defined as cells at any stage from prophase to telophase.

### Peripheral blood micronucleus assay

5–10  $\mu$ l of peripheral blood samples were collected from the tail vein and dropped on AO-coated slides (Hayashi et al., 1990), covered with a coverslip and stored overnight in a refrigerator until analysis. Reticulocytes supravitaly stained with AO were analyzed under a fluorescent microscope ( $\times$ 600 or higher) equipped with a blue light excitation system. The number of micronucleated reticulocytes (MNRETs) was recorded by evaluation of 2000 reticulocytes in two fields per animal.

### Statistical analysis

The incidences of micronucleated hepatocytes or reticulocytes were analyzed statistically by using Kastenbaum's and Bowman's tables (Kastenbaum and Bowman, 1970).

## Results

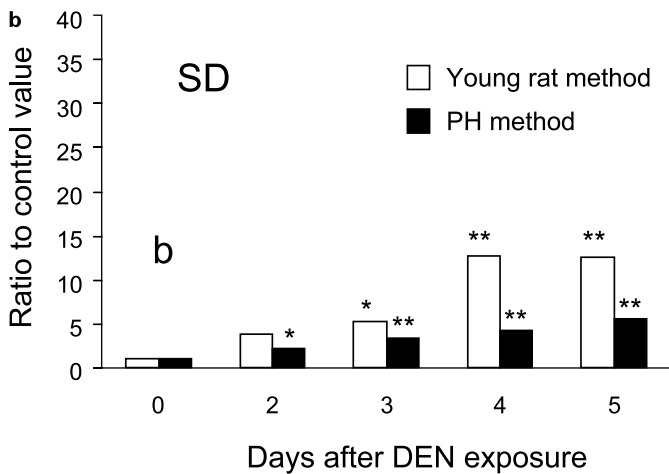
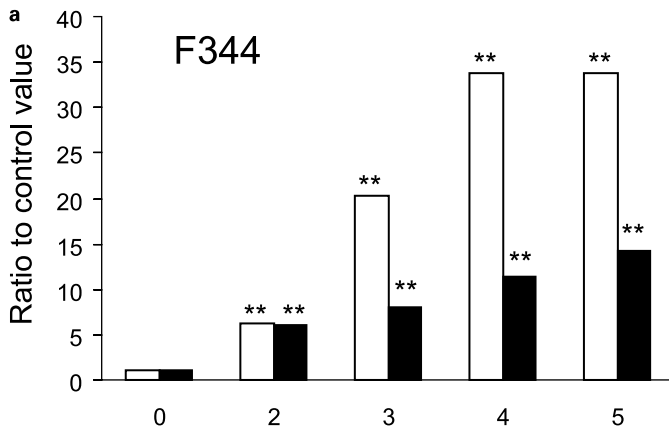
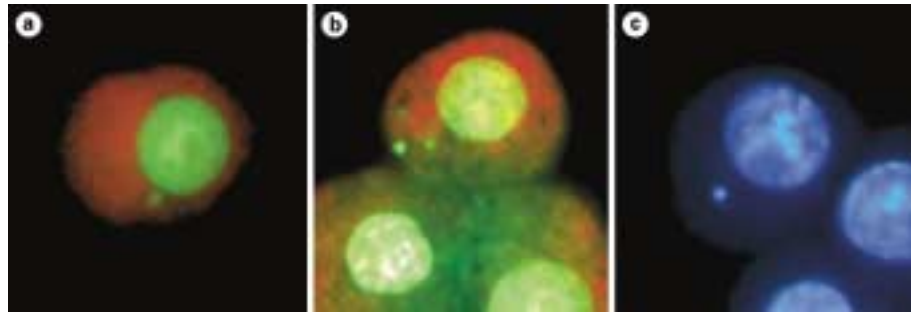
### AO-DAPI double fluorescent staining

Figure 1 shows fluorescent microphotographs of nuclei in young rat hepatocytes stained with AO alone (Fig. 1a), DAPI alone (Fig. 1c), and combination of AO and DAPI (Fig. 1b). Compared to AO or DAPI alone, the double staining allows better distinction of micronuclei and cytoplasm.

### Comparison of the young rat method with the partial hepatectomy method

The results of the assay with DEN at 50 mg/kg are shown in Fig. 2. Both methods revealed significant increases in the numbers of MNHEPs in comparison with concurrent controls. The frequencies of MNHEPs in young rats were generally higher

**Fig. 1.** Fluorescent microphotographs of hepatocyte nuclei from young rats stained with (a) AO alone, (b) a combination of AO and DAPI, and (c) DAPI alone.



**Fig. 2.** Frequencies of MNHEPs (micronuclei/1000 hepatocytes) 2 to 5 days after administration of 50 mg/kg DEN to (a) F344 rats and (b) SD rats in the young rat method and PH method. Mean of 4–5 animals. \*  $P < 0.05$ , \*\*  $P < 0.01$ , significantly different from the concurrent solvent control.

than those of the PH method and it was shown that the MNHEP frequencies of F344 rats (Fig. 2a) were higher than those of SD rats (Fig. 2b) in both methods. There was no statistically significant difference in MNRET induction observed in peripheral blood at any treatment time in either F344 or SD rats (data not shown).

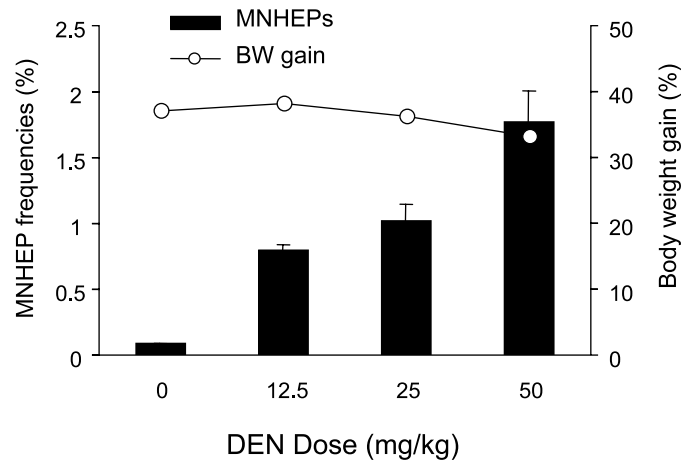


**Fig. 3.** MNHEP frequencies (evaluation of 2000 hepatocytes) 5 days after administration of DEN (12.5, 25 and 50 mg/kg) to F344 rats (column with standard deviation bar). Body weight (BW) gain was only marginally affected at the highest dose.

#### Dose dependency and age effect

The MNHEP frequencies after administration of DEN (12.5, 25, 50 mg/kg) to 4-week-old F344 male rats increased dose dependently and reached approximately 9- to 20-fold the concurrent solvent control (Fig. 3). During this study, the rate of body weight gain was only marginally decreased at the highest DEN dose. The MNHEP frequency after 50 mg/kg DEN administration to F344 rats aged between 3 and 9 weeks decreased age-dependently, with the highest value (2.3%) at 3 weeks of age, and lowest (0.17%) at 9 weeks of age (Fig. 4).

#### Route difference and treatment times

To determine the influence of administration route, DEN was given either orally or intraperitoneally to 4-week-old F344 rats. MNHEP frequency was similar for both routes, 2–5 days after single (40 mg/kg) or the second treatment for a split-dose ( $2 \times 20$  mg/kg) regime (Fig. 5a, b). The MNHEP frequency increased depending on the time after DEN treatment (up to 5 days). On days 2, 3, and 4, split DEN dosing resulted in higher MNHEP frequencies compared to the single dose protocol. Mitotic cells were observed in  $1.2 \pm 0.30\%$  to  $1.5 \pm 0.74\%$  of cells in the solvent control group 5 days after treatment, and in

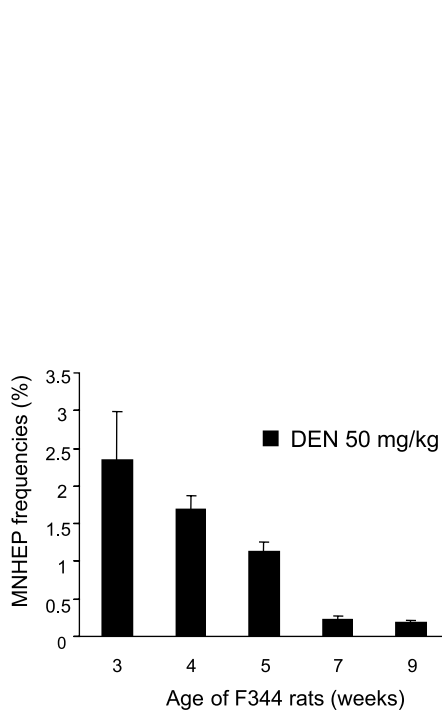


**Fig. 4.** MNHEP frequencies (evaluation of 2000 hepatocytes) after administration of 50 mg/kg DEN to F344 rats aged 3 to 9 weeks. Data are the mean of five animals with standard deviation.

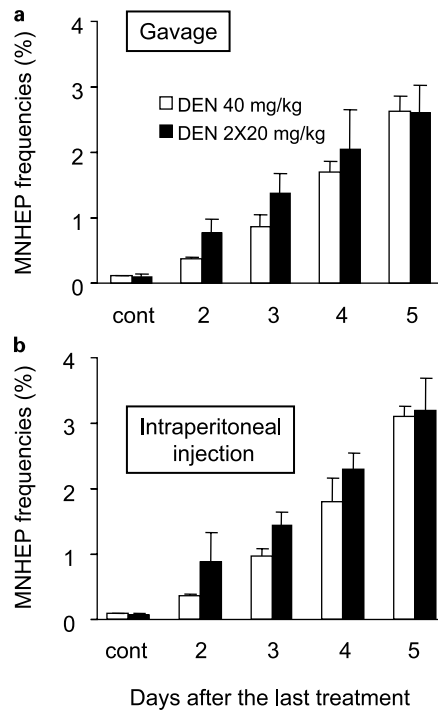


**Fig. 5.** DEN-induced MNHEP frequency (evaluation of 2000 hepatocytes) 2 to 5 days after a single 40 mg/kg dose or two 20 mg/kg doses 24 h apart in 4-week-old F344 rats by (a) gavage or (b) intraperitoneal injection. Results are the mean of five animals with standard deviation.

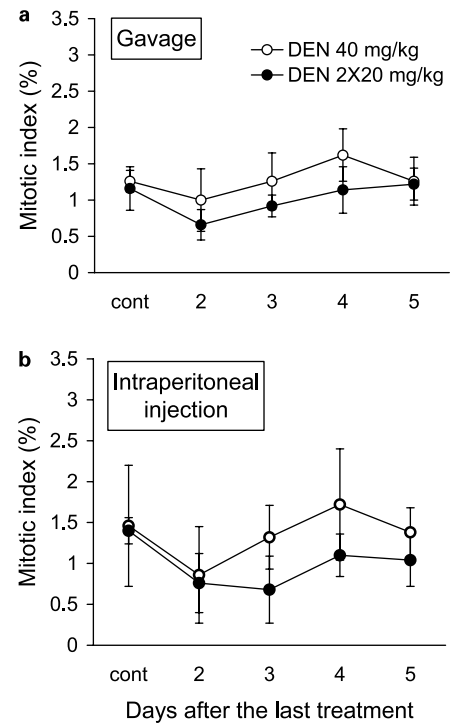


**Fig. 6.** Frequencies of mitotic indexes (evaluation of 1000 hepatocytes) 2 to 5 days after a single 40 mg/kg dose or two 20 mg/kg doses 24 h apart in 4-week-old F344 rats by (a) gavage or (b) intraperitoneal injection. Results are the mean of five animals with standard deviation.

0.7 ± 0.21% to 1.7 ± 0.68% of cells in the DEN group (Fig. 6a, b). The incidence of metaphase cells tended to be lower after the double treatment of DEN.

## Discussion

Since Tates et al. reported a liver micronucleus assay in 1980, a number of variations have been published (Cliet et al., 1989; Roy and Das, 1990; Mereto et al., 1994; Zhurkov et al., 1996). In these studies, the PH method, the chemical mitogens method, and an *in vivo/in vitro* method have been applied to assess micronucleus induction in liver cells. These methods have been used on a case by case basis, but they have not been used routinely for evaluation of genotoxicity of chemicals. Some criticisms of these methods are 1) introduction of abnormal physiological conditions (e.g., PH method), 2) increased unknown factors as a result of interaction between test chemical and mitogen, 3) laborious and time-consuming (e.g., *in vivo/in vitro* method). We have thus paid attention to the method based on proliferating activity of liver cells in young rats up to about 4 weeks of age. Although the method using young rat liver was reported by Parton and Garriott (1997), it has not been well characterized and evaluated.

We consider the young rat liver micronucleus assay method as advantageous because it does not require any physical injury

such as PH, nor pretreatment with mitogens that may interact with a test substance, nor setting up of primary culture that also may cause damage to the target cells. Therefore, we propose to use the present method as a tool for evaluation of chemical genotoxicity that may occur in the liver.

As shown in Fig. 6, we confirmed that there were many mitotic cells in the liver of 4-week-old rats. The mitotic index (MI) observed in the present study was comparable to that reported by Parton and Garriott (1997). As shown in Fig. 4, the incidence of MNHEP decreased with the age of the rats. This can be explained by an age-related decrease in proliferation of hepatocytes and dilution of the cells with micronuclei with undivided normal hepatocytes. This phenomenon was also observed in the PH method. The MI in regenerating hepatocytes is 3.6% and decreases below 1% at 72 h after PH (Grisham, 1962; Parton and Garriott, 1997). To restrict the cell population to one cell division after treatment, co-treatment with cytochalasin B could be considered. It would, however, be important to consider possible interactions between test chemical and cytochalasin B. Therefore we believe that it is acceptable to perform the assay without co-treatment of cytochalasin B as long as rats at 4 weeks of age are used.

The AO-DAPI staining method, which was originally developed for the testis micronucleus assay (Noguchi, 1997), was efficient for analysis of micronuclei in cytoplasm of hepatocytes. This novel staining method gave clearer distinction of

micronucleus, nucleus, and cytoplasm than the single fluorescent staining with either AO or DAPI. To evaluate the practicality of the staining method, 12 laboratories participated in the collaborative trial and obtained similar MNHEP frequencies after treatment with 40 mg/kg DEN. This result indicated that the new staining method is powerful even for novice users of the liver micronucleus assay.

We chose the 4-week-old rat for the liver micronucleus assay based on our present results and also on the knowledge of age-related changes in metabolic enzyme profiles: Cytochrome P-450 content in young rats is similar to that in adult rats (Imaoka et al., 1991); there is no major difference between 30-day-old and 100-day-old rats in the activity of hexobarbital hydroxylation, *N*-demethylation of ethylmorphine, *O*-demethylation of *p*-nitroanisole or hydroxylation of aniline (Furner et al., 1969). P-450-1A2, 2A1, 2B1, 2B2, 2E1, 3A1, and 3A2 activity levels reach a maximum at about 30 days of age, thereafter, the levels of these P-450 species plateau in the liver due to growth hormone action. Conversely, P-450C7, 2C11, 2C12, and 2C22 are expressed rapidly after 30 days of age (Kato and Yamazoe, 1992). Thus, a compound which is principally activated by

P-450C family, may not be easily detected by this assay. Further confirmation of this notion is being pursued.

Based on the present outcomes using DEN, we propose the following standard protocol for the young rat liver micronucleus assay:

Animals: Young rats up to 4 weeks old.

Route: Oral or intraperitoneal administration.

Chemical dosing: Single, or repeatedly if necessary.

Sampling time: 3–5 days after the last treatment.

Hepatocyte preparation: Collagenase perfusion method.

Staining: AO-DAPI double staining.

An extensive collaborative study for validation of the present method is still ongoing organized by The Collaborative Study Group of the Micronucleus Test – Mammalian Mutagenicity Study Group/Japanese Environmental Mutagen Society (CSGMT-MMS/JEMS). This involves evaluating micronucleus induction in young rat liver cells by hepatocarcinogens and some other related chemicals. The degree of validation will determine the extent to which the present method becomes recognized as a useful tool for evaluating genotoxicity of chemicals in the rat liver.

## References

- Angelosanto FA: Tissues other than bone marrow that can be used for cytogenetic analysis. *Environ molec Mutagen* 25:338–343 (1995).
- Braithwaite I, Ashby J: A non-invasive micronucleus assay in the rat liver. *Mutat Res* 203:23–32 (1988).
- Cliet I, Fournier E, Melcion C, Cordier A: In vivo micronucleus test using mouse hepatocytes. *Mutat Res* 216:321–326 (1989).
- Committee on the Mutagenicity of Chemicals: Guidance on a Strategy for Testing Chemicals for Mutagenicity. (London 2000).
- Furner RL, Gram TE, Stitzel RE: The influence of age, sex and drug treatment on microsomal drug metabolism in four rat strains. *Biochem Pharmacol* 18: 1635–1641 (1969).
- Hayashi M, Morita T, Kodama Y, Sofuni T, Ishidate M Jr: The micronucleus assay with mouse peripheral blood reticulocytes using Acridine Orange coated slides. *Mutat Res* 245:245–249 (1990).
- Higgins GM, Anderson RM: Experimental pathology of the liver. I. Restoration of the liver of the white rat following partial surgical removal. *Arch Pathol* 12:186–202 (1931).
- Imaoka S, Fujita S, Funae Y: Age-dependent expression of cytochrome *P*-450s in rat liver. *Biochim biophys Acta* 1097:187–192 (1991).
- Grisham JW: A morphologic study of deoxyribonucleic acid synthesis and cell proliferation in regenerating rat liver; autoradiography with thymidine-<sup>3</sup>H. *Cancer Res* 22:842–849 (1962).
- Kastenbaum MA, Bowman KO: Tables for determining the statistical significance of mutation frequencies. *Mutat Res* 9:527–549 (1970).
- Kato R, Yamazoe Y: Sex-specific cytochrome P450 as a cause of sex- and species-related differences in drug toxicity. *Toxicol Lett* 64/65:661–667 (1992).
- Mereto E, Brambilla-Campart G, Ghia M, Martelli A, Brambilla G: Cinnamaldehyde-induced micronuclei in rodent liver. *Mutat Res* 322:1–8 (1994).
- Morita T, Asano N, Awogi T, Sasaki Y, Sato S, Shimada H, Sutou S, Suzuki T, Wakata A, Sofuni T, Hayashi M: Evaluation of the rodent micronucleus assay in the screening of IARC carcinogens. Groups 1, 2A and 2B. The summary report of the 6th collaborative study by CSGMT/JEMSMMS. *Mutat Res* 389:3–122 (1997).
- Noguchi T: The development of testis micronucleus test (Abstract). 26th JEMS, Hatano, 92 (1997).
- Parton JW, Garriott ML: An evaluation of micronucleus induction in bone marrow and in hepatocytes isolated from collagenase perfused liver or from formalin-fixed liver using four-week-old rats treated with known clastogens. *Environ molec Mutagen* 29:379–385 (1997).
- Rossi AM, Romano M, Zaccaro L, Pulci R, Salmona M: DNA synthesis, mitotic index, drug-metabolizing systems and cytogenetic analysis in regenerating rat liver. *Mutat Res* 182:75–82 (1987).
- Roy B, Das RK: Evaluation of genotoxicity of clofazimine, an antileprosy drug, in mice in vivo. II. Micronucleus test in bone marrow and hepatocytes. *Mutat Res* 241:169–173 (1990).
- Sawada S, Yamanaka T, Yamatsu K, Furihata C, Matsushima T: Chromosome aberrations, micronuclei and sister-chromatid exchanges (SCEs) in rat liver induced in vivo by hepatocarcinogens including heterocyclic amines. *Mutat Res* 251:59–69 (1991).
- Sipes IG, Gandolfi AJ: Biotransformation of toxicants, in Amdur MO, Doull J, Klassen CD (eds): *Casarett and Doull's Toxicology, The Basic Science of Poisons*, pp 88–126 (McGraw-Hill, New York 1993).
- Tates AD, Neuteboom I, Hofker M, Engelse L: A micronucleus technique for detecting clastogenic effects of mutagens/carcinogens (DEN, DMN) in hepatocytes of rat liver in vivo. *Mutat Res* 74:11–20 (1980).
- Zhurkov VS, Sycheva LP, Salamatova O, Vyskubenko IF, Feldt EG, Sherenesheva NI: Selective induction of micronuclei in the rat/mouse colon and liver by 1,2-dimethylhydrazine: a seven-tissue comparative study. *Mutat Res* 368:115–120 (1996).



# Insights into the mechanisms of sister chromatid exchange formation

A. Wojcik,<sup>a,b</sup> E. Bruckmann<sup>c</sup> and G. Obe<sup>c</sup>

<sup>a</sup>Institute of Nuclear Chemistry and Technology, Warszawa;

<sup>b</sup>Institute of Biology, Swietokrzyska Academy, Kielce (Poland);

<sup>c</sup>Institute of Genetics, University of Duisburg-Essen Essen (Germany)

**Abstract.** The DNA lesions responsible for the formation of sister chromatid exchanges (SCEs) have been the object of research for a long time. SCEs can be visualized by growing cells for either two rounds of replication in the presence of 5-bromo-2'-deoxyuridine (BrdU) or for one round with BrdU and the next without. If BrdU is added after cells were treated with a DNA-damaging agent, the effect on SCEs can only be analyzed in the second post-treatment mitosis. If one wishes to analyze the first post-treatment mitosis, cells unifilarly labeled with BrdU must be treated. Due to the highly reactive bromine atom, BrdU interacts with such agents like ionizing and UV

radiation enhancing the frequency of SCEs. However, its precise role in this process was difficult to assess for a long time, because no alternative technique existed that allowed differential staining of chromatids. We have recently developed a method to differentially label sister chromatids with biotin-16-2'-deoxyuridine-5'-triphosphate (biotin-dUTP) circumventing the disadvantage of BrdU. This technique was applied to study the SCEs induced by ionizing and UV radiation as well as by mitomycin C, DNaseI and *AluI*. This article is a review of the results and conclusions of our previous studies.

Copyright © 2003 S. Karger AG, Basel

Sister chromatid exchanges (SCEs) were discovered 65 years ago by Barbara McClintock in ring chromosomes of maize (McClintock, 1938). In linear chromosomes SCEs were first observed by Taylor et al. (1957), via differential labeling of sister chromatids by incorporation of tritiated thymidine and subsequent autoradiography. Disadvantages of the <sup>3</sup>H-thymidine approach are the poor autoradiographic resolution and the fact that <sup>3</sup>H itself induces SCEs. The resolution of differential staining of sister chromatids was drastically improved when it was discovered that 5-bromo-2'-deoxyuridine (BrdU) can be used to substitute thymidine (Huang, 1967). The development of the fluorescence plus Giemsa (FPG) staining technique by Perry and Wolff (1974) simplified the detection of SCEs within differentially BrdU-labeled chromosomes and led to a great number of studies aiming at elucidating the mechanisms of

SCEs as well as at verifying the application of SCEs for testing of mutagens (Latt, 1981).

SCEs can be visualized by growing cells for either two rounds of replication in the presence of BrdU or for one round with BrdU and the next without. If BrdU is added after treatment of cells with a DNA-damaging agent, the effect on SCEs can only be analyzed in the second post-treatment mitosis. If one wishes to analyze the first post-treatment mitosis, cells unifilarly labeled with BrdU must be treated. Similarly to <sup>3</sup>H-thymidine, BrdU itself induces SCEs because the bromine atom in BrdU dissociates easily, generating a highly reactive uracyl radical in the DNA. The influence of BrdU on the SCE frequency was clearly demonstrated when the development of monoclonal antibodies against BrdU allowed a reduction of its concentration (Pinkel et al., 1985). The exact contribution of BrdU to "spontaneous" and "induced" frequencies of SCEs remains a matter of debate (Morris, 1991). In addition, it was realized that not all mutagenic agents lead to SCE formation. These discoveries resulted in a decline of interest in the nature of SCEs and their use to test potential mutagens.

We have for several years carried out experiments to study the nature of SCEs induced by ionizing and UV radia-

Received 17 September 2003; revision accepted 8 December 2003.

Request reprints from G. Obe, Universität Duisburg-Essen, FB-9, Genetik  
D-45117 Essen (Germany); telephone: +49 201 183 3388  
fax: +49 201 183 4397; e-mail: guenter.obe@uni-essen.de

tion. We developed a novel method of differential staining of sister chromatids with biotin-16-2'-deoxyuridine-5'-triphosphate (biotin-dUTP). This DNA analog lacks the reactive halogen atom and can be used to study the role of BrdU in the formation of SCEs. The present article is a review of our studies.

### Are radiation-induced SCEs inversions?

SCEs are assumed to be a consequence of DNA replication on a damaged template and can arise only when a DNA lesion is not removed before the cell enters S-phase (Shafer, 1977; Painter, 1980; Cleaver, 1981; Schubert, 1990). Ionizing radiation is a poor inducer of SCEs and it is only effective when applied to cells in G<sub>1</sub> with chromosomes unifilarly substituted with BrdU (Littlefield et al., 1979; Renault et al., 1982). This fact gave rise to many debates about the nature of radiation-induced lesions responsible for SCEs, because ionizing radiation induces mainly single and double strand breaks which, when induced in G<sub>1</sub>, are expected to be repaired before the cell enters S-phase (Szumiel, 1998). Wolff et al. (1974) were the first to suggest that radiation-induced SCEs could be "false", resulting from chromosomal aberrations. Indeed, when cells are irradiated in G<sub>1</sub> following one round of replication in the presence of BrdU, paracentric inversions are visible as double internal or interstitial SCEs (Fig. 1). The hypothesis of false SCEs was substantiated by the results of Mühlmann-Diaz and Bedford (1995). These authors found similar frequencies of interstitial deletions and interstitial SCEs in fibroblasts pre-labeled with BrdU for one round of replication and irradiated with gamma rays in G<sub>1</sub>. Under the assumption that the ratio of interstitial deletions to paracentric inversions is 1:1, the authors concluded that all interstitial SCEs are paracentric inversions and that exposure of G<sub>1</sub> cells to ionizing radiation does not cause "true" SCEs.

In order to test this hypothesis and to evaluate how many interstitial SCEs are "true" and how many are "false", we have labeled human lymphocytes with BrdU for one round of replication, irradiated in G<sub>1</sub> with X-rays and recovered for a further cell cycle in the absence of BrdU (Wojcik et al., 1999). Chromosome preparations were hybridized with an in situ hybridization probe specific for the p14 band of chromosome 3. Simultaneously, differential staining of chromatids was achieved with an anti-BrdU antibody (Fig. 1). Using this protocol, we analyzed those paracentric, interstitial SCEs which occurred in the p arm of chromosome 3, inside which the probe signal was positioned asymmetrically. SCEs resulting from an inversion event would be accompanied by a shift of the hybridization signal. In case of "true" SCEs the position of the hybridization signal would remain unchanged. The results revealed that the vast majority of SCEs within the p arm of chromosome 3 are not inversions (Fig. 2) clearly showing that X-rays can induce "true" SCEs.

These data do not answer the question about the nature of radiation-induced DNA lesions responsible for SCEs. It is generally agreed that the DNA lesion ultimately responsible for the production of chromosomal aberrations is a DNA double

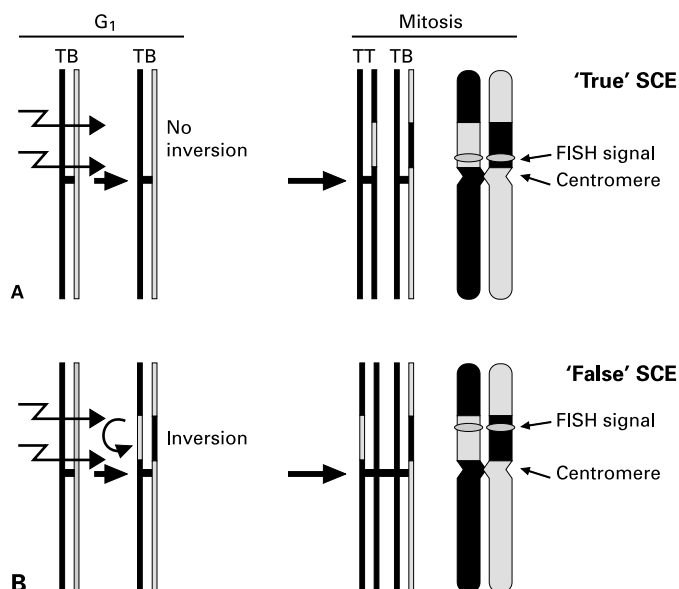


**Fig. 1.** Scheme of the labeling pattern of chromosome 3 with a FISH probe for band p14. (A) A "true" SCE not resulting from an inversion (correct position of the probe), (B) "false" SCE resulting from an inversion (probe displaced). Data from Wojcik et al. (1999).

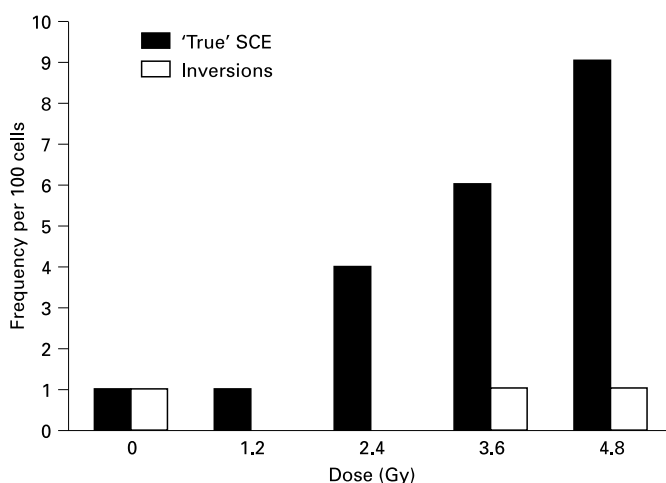


**Fig. 2.** "True" SCE and inversions in the p-arm of chromosome 3. The number of analyzed cells was probably too low for a good dose-response of inversions. From Wojcik et al. (1999).

strand break (DSB) (Pfeiffer et al., 2000). Ionizing radiation is one of the few known agents inducing DSBs in a direct manner. Chemical agents (with the exception of the so called radiomimetic compounds like bleomycin) as well as UV-C radiation induce lesions, which are only transformed into DSBs when the cell passes through S-phase. Consequently, when cells are exposed to ionizing radiation in G<sub>1</sub>, only chromosome type aberrations are visible in the first post-treatment mitoses. However, when cells are exposed to chemical agents or UV-C radiation only chromatid-type aberrations are seen. S-phase depen-

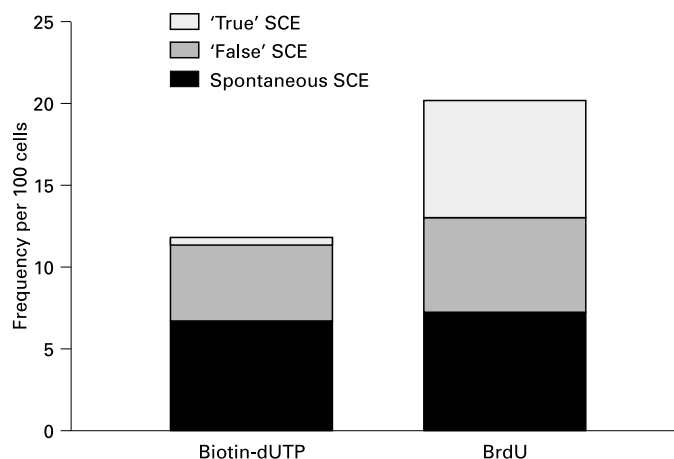


**Fig. 3.** Spontaneous and radiation-induced SCEs in CHO cells pre-labeled with BrdU or biotin-dUTP. The frequencies of “false” SCEs were calculated on the basis of the frequencies of exchange-type aberrations. Data from Bruckmann et al. (1999b).

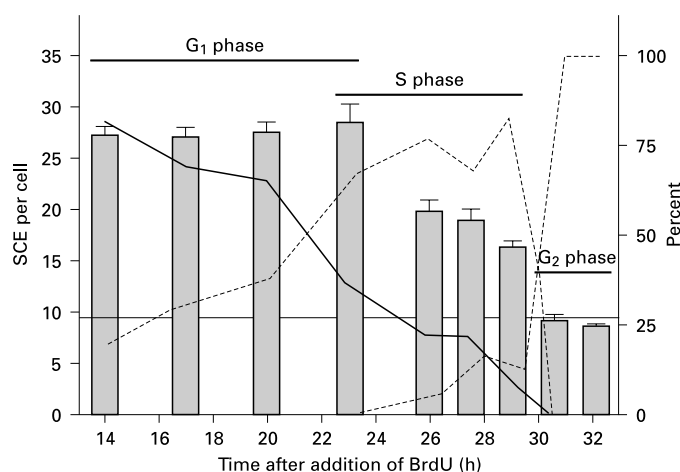


**Fig. 4.** SCE frequencies and types of chromosomal aberrations in cells pre-labeled with BrdU and irradiated with 4.8 Gy X-rays at various phases of the cell cycle. The horizontal line represents the control frequency of SCEs. Columns show the induced SCEs. Curves show the percentages of cells with: chromosome type aberrations (solid curve), mixed types of aberrations (dashed curve) and chromatid type aberrations (dashed-dotted curve). Error bars represent standard deviations from 3 independent experiments. Data from Bruckmann 2000.

dent agents are generally strong inducers of SCEs, whereas ionizing radiation is a poor inducer of SCEs. Interestingly, it has been noticed, that when cells are pre-labeled with BrdU for one round of replication and exposed to X-rays, both chromosome and chromatid-type aberrations appear (Natarajan et al., 1980a; Sayed Aly et al., 2002). This suggests that radiation damage to BrdU gives rise to lesions which last until S-phase when they are transformed into DSBs. These could be the lesions responsible for SCEs.

### The role of BrdU in SCEs induced by X-rays

The role of BrdU in the formation of SCEs could be assessed by an alternative technique for differential staining of chromatids. We found that cells electroporated in the presence of biotin-dUTP incorporated the analogue and remained viable. When cells were harvested after two rounds of replication, biotin could be detected with fluorochrome-labeled avidin yielding high quality differential staining of chromatids (Bruckmann et al., 1999a). Unlike BrdU, biotin-dUTP should not interact with ionizing radiation in damaging DNA, because it lacks the reactive halogen atom which easily dissociates giving rise to uracilyl radicals. This new labeling technique was applied to see how ionizing radiation induces SCEs without BrdU.

CHO cells with DNA unifilarly labeled with either biotin-dUTP or BrdU were exposed to X-rays in G<sub>1</sub>. Both the frequencies of SCEs and chromosomal aberrations were evaluated (Bruckmann et al., 1999b). It is expected, that under such experimental condition, when SCEs are scored in all chromosomes and chromosome fragments, each dicentric chromosome with an accompanying acentric fragment will either give rise to two “false” SCEs or no SCEs (see Sayed Aly et al., 2002 for details). The same is true for symmetrical translocations. If we assume that the frequencies of dicentrics and translocations are 1:1, the frequency of “false” SCEs can be calculated to be twice the frequency of dicentrics. Similar calculations can be made for rings and double minutes. Thus, the frequency of aberrations was used to calculate the expected level of “false” SCEs both in cells pre-labeled with BrdU and biotin-dUTP.

Our results revealed a lower frequency of radiation-induced SCEs in cells pre-labeled with biotin-dUTP than with BrdU (Fig. 3). More than half of the SCEs induced by radiation in cells pre-labeled with BrdU were “true” SCEs. In contrast all SCEs observed in cells pre-labeled with biotin-dUTP were due to chromosomal aberrations. This clearly shows that only damage to BrdU gives rise to lesions which can lead to “true” SCEs. It should be mentioned that we did not observe an enhancing effect of BrdU in cells treated with mitomycin C or the restriction enzyme *AhuI* (Stoilov et al., 2002).

In order to investigate the relationship between the SCE frequency and the phase of the cell cycle in which damage is induced, experiments were performed using cells pre-labeled with BrdU and exposed to 4.8 Gy of X-rays at various times before fixation (Bruckmann 2000). The results are presented in Fig. 4. Scoring was restricted to cells with uniform differential labeling of sister chromatids. In addition to SCEs, percent frequencies of cells showing chromosome-type aberrations, chromatid-type aberrations and both are plotted. The cell cycle phase in which cells were irradiated was determined on the basis of the types of aberrations observed and the time between exposure and harvest. The highest frequency of SCEs was observed in cells treated in G<sub>1</sub>-phase, followed by S-phase. Irradiation during G<sub>2</sub>-phase did not induce SCEs above the control level. A striking observation was that during G<sub>1</sub> the frequency of SCEs remained at a similar level, irrespective of whether cells in early or late G<sub>1</sub>-phase were irradiated. In accordance with the data shown in Fig. 3, a part of the SCEs are due to

aberrations. Nevertheless, it seems that following X-ray irradiation the lesions responsible for SCE formation arise very quickly and their frequency does not decline during the G<sub>1</sub>-phase.

Furthermore we analyzed the relationship between chromosomal aberrations and SCEs following treatment of cells with DNaseI. This endonuclease was shown to be a very efficient inducer of both chromosomal aberrations and SCEs (Obe et al., 1994) when cells were treated in G<sub>1</sub>. CHO cells were labeled with BrdU for one round of DNA replication and treated with DNaseI in G<sub>1</sub>-phase. Using a computer-aided metaphase relocation system, mitoses were first analyzed for SCEs, destained, stained again with orcein and reanalyzed for chromosomal aberrations. Thus, a precise correlation between the frequencies of aberrations and SCEs could be established. For comparison, similar experiments were performed with X-rays. The results showed that the frequencies of SCEs induced by DNaseI were due to chromosomal aberrations. In contrast, X-rays induced more SCEs than expected on the basis of aberrations (Sayed Aly et al., 2002). The fact that radiation does induce "true" SCEs was clearly visible when SCE dose response curves were plotted for cells without any aberrations (Fig. 5). While no clear dose-relationship was visible in cells treated with DNaseI, the frequency of SCEs increased linearly with the X-ray dose.

### The role of BrdU in SCEs induced by UV radiation

UV radiation is known as a strong inducer of SCEs (Latt, 1981). There is no agreement which type of UV-induced DNA damage is responsible for SCEs. Some authors suggested that cyclobutane pyrimidine dimers (CPDs) and (4-6) photoproducts (PDs), located at the same strand, are the ultimate lesions responsible for SCE formation (Kato, 1974; Chao et al., 1985). A further argument for the involvement of CPDs in UV-induced SCEs is based on the fact that cells deficient in excision repair of CPDs display high SCE frequencies (Latt 1981). However, in chicken embryonic fibroblasts no quantitative relationship between CPDs and SCEs was observed after exposure to UV radiation and photoreactivating light: the frequency of SCEs was only reduced by 30–65%, although 75–95% of CPDs were removed (Natarajan et al., 1980b). This suggests that other lesions may also be involved in SCE formation. Similarly as for ionizing radiation, due to the lack of an alternative differential labeling technique, it was difficult to assess the exact role of BrdU in the process.

Applying our biotin-dUTP labeling technique we analyzed the influence of BrdU on the frequency of SCEs induced by UV radiation (Wojcik et al., 2002). CHO cells unifilarly labeled with either BrdU or biotin-dUTP were irradiated in the G<sub>1</sub>-phase of the cell cycle either at 254 or 313 nm. UV radiation at 254 nm is absorbed by all DNA bases including bromouracil (BrU), whereas radiation at 313 nm is predominantly absorbed by BrU. Elevated SCE frequencies were observed in cells irradiated at 254 nm which were pre-labeled with BrdU or biotin-dU. Following irradiation at 313 nm a statistically elevated SCE frequency was observed only in cells pre-labeled with BrdU. Upon irradiation at 254 nm, BrdU had a strong sensitizing effect on SCE induction: the net SCE frequencies (following

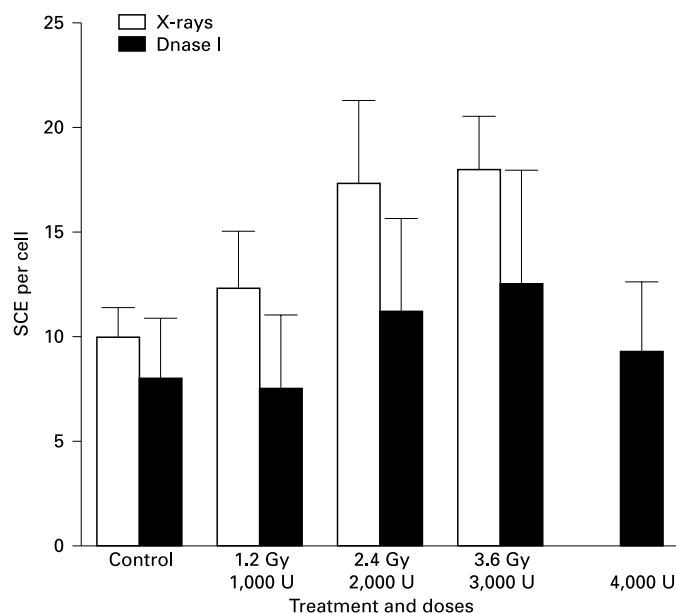


**Fig. 5.** Frequencies of SCEs in cells without chromosomal aberrations following treatment with X-rays or DNase I. Vertical bars represent standard deviations of per cell values. Concentrations of DNaseI are given per 800  $\mu$ l of electroporation buffer. Plots were fitted by linear regression (method of least squares). Data from Sayed Aly et al. (2002).

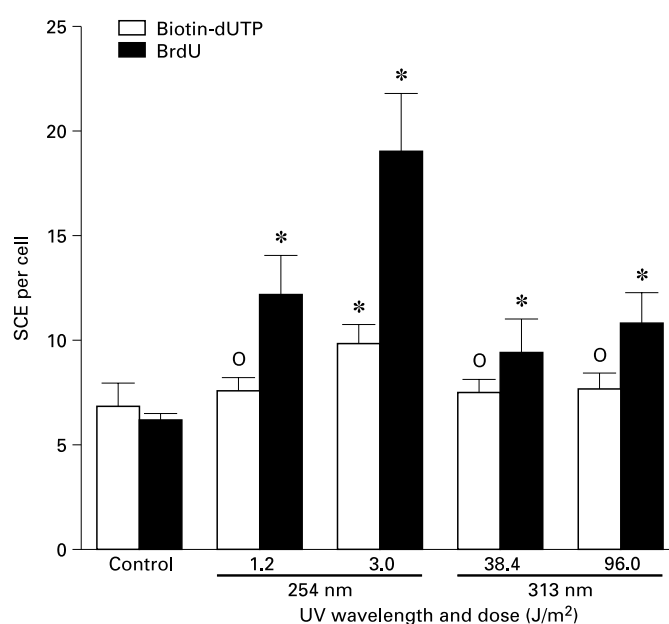


**Fig. 6.** UV-induced SCEs in CHO cells pre-labeled with BrdU or biotin-dUTP. UV radiation was performed at 254 and 313 nm wavelength. Due to the small cross-section for uracil formation at 313 nm UV, higher doses (in comparison to 254 nm UV) had to be applied in order to see a biological effect. \*: difference to control significant with  $P < 0.05$ ; o: difference to control not significant. Data from Wojcik et al. (2002).

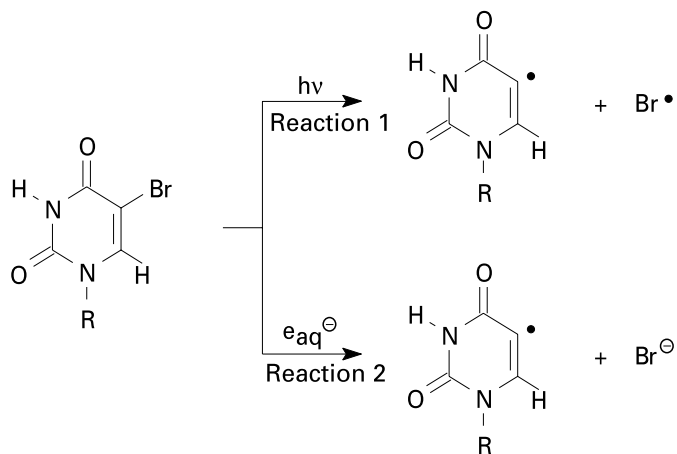


**Fig. 7.** Uracilyl radical formation upon action of UV (reaction 1) and ionizing (reaction 2) radiation on BrdU. Data from Wojcik et al. (2002).

subtraction of spontaneous SCEs) observed in cells pre-labeled with BrdU are ~ 6 times higher than in cells pre-labeled with biotin-dUTP (Fig. 6). Thus BrdU-induced damage is responsible for more than 80% of the SCEs formed in UV-irradiated cells unifilarly labeled with BrdU. The remaining 20% may be due to DNA-lesions induced by UV radiation: pyrimidine dimers and (6-4) photoproducts.

### The possible lesion responsible for SCE formation following exposure to UV and ionizing radiation

The interesting question is what type of DNA damage is responsible for SCE formation in cells pre-labeled with BrdU and irradiated with UV and ionizing radiation. There is convincing evidence that the major photochemical lesion in BrdU-substituted DNA is a single-strand break (SSB) (Hutchinson, 1973). SSBs can also arise during the repair of DNA lesions such as apurinic sites. However, SSBs are repaired quickly: comet assay studies show that no damage is seen after about three hours (Wojcik et al., 1996). In the experiments with UV radiation we allowed 19 h to pass between irradiation and har-

vest, and restricted scoring to cells with differential staining of chromatids indicative of treatment in G<sub>1</sub>-phase of the cell cycle. Since SCEs are formed when DNA replication is stalled at a damaged template (Shafer, 1977; Painter, 1980), it seems unlikely that SSBs induced in G<sub>1</sub> persist until S-phase when becoming transformed into SCEs. The results presented in Fig. 4 indicate that the lesions leading to SCEs are formed shortly after exposure to ionizing radiation. Therefore, it appears unlikely that SSBs are the major lesions responsible for SCE formation.

DNA interstrand crosslinking agents such as mitomycin C are very potent inducers of SCEs (Kaina and Aurich, 1985). It has also been reported that psoralen interstrand cross-links more effectively induce SCEs than monoadducts (Bredberg and Lambert, 1983). These results indicate that interstrand cross-links are a major DNA lesion responsible for SCE formation. Are interstrand DNA crosslinks formed in cells unifilarly labeled with BrdU and exposed to UV or ionizing radiation?

Compared with UV, ionizing radiation is a poor inducer of SCEs. This indicates that it cannot be the reactions of the uracilyl radical alone that lead to SCEs, otherwise they would also be formed by ionizing radiation to a large extent. The main difference between UV and ionizing radiation is the formation of a bromine atom in addition to an uracilyl radical in the case of UV irradiation (Fig. 7, reaction 1). Most probably the bromine atom oxidizes a purine base of the opposing DNA strand (Wojcik et al., 2002). This would yield two radicals at opposing strands in close proximity, i.e. the precondition of an interstrand cross-link. Interestingly, interstrand cross-linking could possibly also be induced by the uracilyl radical without another neighboring radical as a counterpart (Fig. 7, reaction 2). It is, therefore, likely that besides causing SSBs the uracilyl radical itself also induces some interstrand cross-links that may give rise to SCEs (Wojcik et al., 2002). This assumption explains why ionizing radiation is a weaker inducer of SCEs than UV radiation.

Chemical agents which form DNA interstrand cross-links are among the most potent inducers of SCEs. We suggest that DNA interstrand cross-links may also be the major lesions leading to SCE formation in cells unifilarly labeled with BrdU and irradiated with UV or ionizing radiation. Clearly, this hypothesis needs experimental verification.

### References

- Bredberg A, Lambert B: Induction of SCE by DNA cross-links in human fibroblasts exposed to 8-MOP and UVA irradiation. *Mutat Res* 118:191-204 (1983).
- Bruckmann E, Wojcik A, Obe G: Sister chromatid differentiation with biotin-dUTP. *Chrom Res* 7:185-189 (1999a).
- Bruckmann E, Wojcik A, Obe G: X-irradiation of G<sub>1</sub> CHO cells induces SCE which are both true and false in BrdU-substituted cells but only false in biotin-dUTP-substituted cells. *Chrom Res* 7:277-288 (1999b).
- Bruckmann E: Mechanismen der Entstehung strahleninduzierter Schwesterchromatidenaustausche. PhD Thesis, University of Essen (2000).
- Chao CCK, Rosenstein RB, Rosenstein BS: Induction of sister-chromatid exchanges in ICR 2A frog cells exposed to 265-313 nm monochromatic ultraviolet wavelengths and photoreactivating light. *Mutat Res* 149:443-450 (1985).
- Cleaver JE: Correlations between sister chromatid exchange frequencies and replicon sizes. *Expl Cell Res* 136:27-30 (1981).
- Huang CC: Induction of a high incidence of damage to the X chromosome of *Rattus (Mastomys) natalensis* by base analogues, viruses and carcinogens. *Chromosoma* 23:162-179 (1967).
- Hutchinson F: The lesions produced by ultraviolet light in DNA containing 5-bromouracil. *Quart Rev Biophysics* 6:201-246 (1973).
- Kaina B, Aurich O: Dependency of the yield of sister-chromatid exchanges induced by alkylating agents on fixation time. Possible involvement of secondary lesions in sister-chromatid exchange induction. *Mutat Res* 149:451-461 (1985).
- Kato H: Photoreactivation of sister chromatid exchanges induced by ultra violet irradiation. *Nature* 249:552-553 (1974).
- Latt S: Sister chromatid exchange formation. *Ann Rev Genet* 15:11-55 (1981).
- Littlefield LG, Colyer SP, Joiner EJ, DuFrain RJ: Sister chromatid exchanges in human lymphocytes exposed to ionizing radiation during G<sub>0</sub>. *Radiat Res* 78:514-521 (1979).

- McClintock B: The production of homozygous deficient tissues with mutant characteristics by means of aberrant mitotic behaviour of ring-shaped chromosomes. *Genetics* 23:315–376 (1938).
- Morris SM: The genetic toxicology of 5-bromodeoxyuridine in mammalian cells. *Mutat Res* 258:161–188 (1991).
- Mühlmann-Diaz MC, Bedford JS: Comparison of gamma-induced chromosome ring and inversion frequencies. *Radiat Res* 143:175–180 (1995).
- Natarajan AT, Kihlman BA, Obe G: Use of 5-bromodeoxyuridine-labelling technique for exploring mechanisms involved in the formation of chromosomal aberrations. *Mutat Res* 73:307–317 (1980a).
- Natarajan AT, van Zeeland AA, Verdegaal-Immerzeel EAM, Filon AR: Studies on the influence of photoactivation on the frequencies of UV-induced chromosomal aberrations, sister chromatid exchanges and pyrimidine dimers in chicken embryonic fibroblasts. *Mutat Res* 69:307–317 (1980b).
- Obe G, Schunck C, Johannes C: Induction of sister-chromatid exchanges by *AluI*, DNaseI, benzonuclease and bleomycin in Chinese hamster ovary (CHO) cells. *Mutat Res* 307:315–321 (1994).
- Painter RB: A replication model for sister-chromatid exchange. *Mutat Res* 70:337–341 (1980).
- Perry P, Wolff S: New Giemsa method for differential staining of sister chromatids. *Nature* 251:156–157 (1974).
- Pfeiffer P, Goedecke W, Obe G: Review: Mechanisms of DNA double strand break repair and their potential to induce chromosomal aberrations. *Mutagenesis* 15:289–302 (2000).
- Pinkel D, Thompson LH, Gray JW, Vanderlaan M: Measurement of sister chromatid exchanges at very low bromodeoxyuridine substitution levels using a monoclonal antibody in Chinese hamster ovary cells. *Cancer Res* 45:5795–5798 (1985).
- Renault G, Gentil A, Chouroulinkov I: Kinetics of induction of sister-chromatid exchanges by X-rays through two cell cycles. *Mutat Res* 94:359–368 (1982).
- Sayed Aly M, Wojcik A, Schunck C, Obe G: Correlation of chromosomal aberrations and sister chromatid exchanges in individual CHO cells prelabelled with BrdU and treated with DNaseI or X-rays. *Int J Radiat Biol* 78:1037–1044 (2002).
- Schubert I: Sister chromatid exchanges and chromatid aberrations: a comparison. *Biol Zentbl* 109:7–18 (1990).
- Shafer DA: Replication bypass model of sister chromatid exchanges and implications for Bloom's syndrome and Fanconi's anemia. *Hum Genet* 39:177–190 (1977).
- Stoilov L, Wojcik A, Giri A, Obe G: SCE formation after exposure of CHO cells pre-labelled with BrdU or biotin-dUTP to various DNA-damaging agents. *Mutagenesis* 17:399–403 (2002).
- Szumiel I: Monitoring and signaling of radiation-induced damage in mammalian cells. *Radiat Res* 150 (Suppl):S92–S101 (1998).
- Taylor JH, Woods PS, Hughes ML: The organisation and duplication of chromosomes as revealed by autoradiographic studies using tritium-labeled thymidine. *Proc natl Acad Sci, USA* 43:122–128 (1957).
- Wojcik A, Sauer K, Zölzer F, Bauch T, Müller W-U: Analysis of DNA damage recovery processes in the adaptive response to ionizing radiation in human lymphocytes. *Mutagenesis* 11:291–297 (1996).
- Wojcik A, Opalka B, Obe G: Analysis of inversions and sister chromatid exchanges in chromosome 3 of human lymphocytes exposed to X-rays. *Mutagenesis* 14:633–637 (1999).
- Wojcik A, von Sonntag C, Obe G: Application of the biotin-dUTP chromosome labelling technique to study the role of 5-bromo-2'-deoxyuridine in the formation of UV-induced sister chromatid exchanges in CHO cells. *J Photochem Photobiol* 69:139–144 (2002).
- Wolff S, Bodycote J, Painter RB: Sister chromatid exchanges induced in Chinese hamster cells by UV irradiation of different stages of the cell cycle: the necessity for cells to pass through S. *Mutat Res* 25:73–81 (1974).

# Frequent occurrence of UVB-induced sister chromatid exchanges in telomere regions and its implication to telomere maintenance

G. Jin and T. Ikushima

Laboratory of Molecular Genetics, Biology Division, Kyoto University of Education, Fushimi, Kyoto (Japan)

**Abstract.** Sister chromatid exchanges (SCEs) are symmetrical exchanges between newly replicated chromatids and their sisters. While homologous recombination may be one of the principal mechanisms responsible for SCEs, the full details of their molecular basis and biological significance remain to be elucidated. Following exposure to ultraviolet light B (UVB), mitomycin C (MMC) and cisplatin, we analyzed the location of SCEs on metaphase chromosomes in Chinese hamster CHO cells. The frequency of SCEs increased over the spontaneous level in proportion to the agent's dose. UVB-induced SCEs occurred frequently in telomere regions, as cisplatin-induced SCEs did, differing from MMC-induced ones. The remarkable difference of intrachromosomal distribution among the three

mutagens may be attributed to the specificity of induced DNA lesions and structures of different chromosome regions. Telomeric DNA at the end of chromosomes is composed of multiple copies of a repeated motif, 5'-TTAGGG-3' in mammalian cells. Telomeric repeats may be potential targets for UVB and cisplatin, which mainly form pyrimidine dimers and intra-strand d(GpG) cross-links, respectively, resulting in SCE formation. UVB irradiation shortened telomeres and augmented the telomerase activity. The possible implications of the frequent occurrence of SCEs in telomere regions are discussed in connection with the maintenance of telomere integrity.

Copyright © 2003 S. Karger AG, Basel

Sister chromatid exchanges (SCEs) are symmetrical exchanges between sister chromatids, which can be visualized cytologically in higher eukaryotic cells. They occur spontaneously and can be induced by various mutagens. SCE is widely used as an efficient index of the genotoxicity of environmental agents (Tucker et al., 1993). The phenomenon of SCE has long been established (McClintock, 1938; Taylor, 1958) and numerous studies on the induction of SCEs have suggested their tight link with DNA replication, recombination and repair (Kato, 1974; Wolff et al., 1974; Ikushima, 1977; Latt and Loveday,

1978; Ishii and Bender, 1980; Painter, 1980; Cleaver, 1981). It was recently shown that spontaneous and mitomycin C-induced SCE levels were significantly reduced not only in chicken DT40 B cells lacking the key homologous recombination (HR) genes, *RAD51* and *RAD54* (Sonoda et al., 1999), but also in Rad54-deficient murine cells (Dronkert et al., 2000). The involvement of the HR pathway mediated by hMre11/hRad50/Nbs1 complex has also been reported in human cells (Limoli et al., 2000). While these findings suggest that HR between sister chromatids mediates SCE formation, our understanding of their molecular basis and biological significance is not complete.

The distribution pattern of SCEs in mitotic chromosomes has been analyzed for several mutagens, providing insights into the mechanism of SCE induction (Carrano and Johnston, 1977; Ockey, 1980; Ikushima, 1984). Irradiation with ultraviolet light (UV) induces SCEs as well as the formation of chromosomal aberrations, the majority of which are caused by pyrimidine dimers in vertebrate cells (Kato, 1974; Natarajan et al., 1980; Ikushima et al., 1998). As there is no data about intrachromoso-

Supported by the Ministry of Education, Culture, Sports, Science and Technology of Japan.

Received 10 September 2003; revision accepted 5 December 2003.

Request reprints from Takaji Ikushima, Biology Division  
Kyoto University of Education, 1 Fukakusa-Fujinomori  
Fushimi, Kyoto 612-8522 (Japan)  
telephone: +81 75 644 8266; fax: +81 75 645 1734  
e-mail: ikushima@kyokyo-u.ac.jp

mal distribution of SCEs induced by ultraviolet light B (UVB), a major component of solar UV radiation, we decided to examine the SCE levels along metaphase chromosomes from Chinese hamster cells, in comparison with those of spontaneous and mitomycin C (MMC)- or cisplatin-induced SCEs. Distribution of SCEs induced by UVB led to an increased frequency of SCEs in telomere regions. These observations prompted us to study the alteration of telomere length and telomerase activity following UVB irradiation.

## Materials and methods

### Cell culture

Chinese hamster CHO cells and mouse BALB cells were cultured in  $\alpha$ -modified Eagle's minimum essential medium (Sigma) supplemented with 10% fetal bovine serum (Biological Industries), 100  $\mu$ g/ml streptomycin and 100 units/ml penicillin at 37°C in a humidified atmosphere of 5% CO<sub>2</sub> in air.

### SCE analysis

For labeling with 5-bromo-2'-deoxyuridine (BrdU), cells were cultured in the presence of 10  $\mu$ M of BrdU for 32 h (two cell cycle periods) and 0.2  $\mu$ g/ml of Colcemid (Gibco) was added 2 h before harvesting the cells. Cells were irradiated with UVB emitted from two FL20E-S lamps (Toshiba; emission range: 290–400 nm with a peak at 315 nm) in plastic tissue culture flasks (Falcon) before addition of BrdU into the medium. Prior to UVB irradiation, the cells were rinsed with phosphate-buffered saline. Treatments with MMC and cisplatin were done during the last cell cycle. Harvested cells were treated with 75 mM KCl for 10 min and then fixed in methanol-acetic acid (3:1) for 30 min. Cells were dropped onto wet glass slides and air-dried. Dried slides were immersed in 10<sup>-4</sup> M Hoechst 33258 for 10 min, rinsed with distilled water and mounted with 0.174 M Na<sub>2</sub>HPO<sub>4</sub>, 0.013 M Na citrate (pH 7.0). The slides were then exposed to black light for 20 min on a 45°C plate before staining with 2% Giemsa stain (pH 6.8) for 20 min. The slides were serially rinsed in acetone, acetone-toluene (1:1), toluene and air-dried (Perry and Wolff, 1974). The SCE frequency was determined in 100 metaphases and SCEs were separately localized on the images of the largest chromosome in CHO cells.

### Analysis of telomere length

Telomere lengths were analyzed by determining the mean length of the Terminal Restriction Fragments (TRF). Mouse BALB cells were used in this experiment, because the terminal telomere repeats of Chinese hamster cells are hard to be detected by this technique due to the short telomere length and the large amount of interstitial telomere-like sequences (Slijepcevic et al., 1997; Faravelli et al., 2002). Genomic DNA was isolated from UVB-irradiated and non-irradiated control cells by a standard phenol/chloroform extraction method (Sambrook et al., 2001). Cells were lysed in 10 mM Tris-HCl/1 mM EDTA/0.5% SDS/0.1 mg/ml proteinase K (Sigma) at 55°C for 2 h. DNA was isolated by phenol/chloroform extraction, treated with 100  $\mu$ g/ml RNase A, and resuspended in TE buffer. Integrity of the isolated DNA was confirmed by ethidium bromide gel electrophoresis and the concentration was determined spectrophotometrically. DNA (3  $\mu$ g) was completely digested with the restriction enzyme *Hae*III (1 unit/ $\mu$ g of DNA; New England Biolabs) to generate TRF. DNA was electrophoresed on a 0.8% agarose gel and processed for Southern blotting and chemoluminescence detection according to the instruction of the AlkPhos Direct Labeling and Detection System with CDP-Star (Amersham Pharmacia Biotech). Telomere probes were made by direct-labeling of the PCR-amplified telomere sequences. Gel profiles were scanned by NIH Image (ver. 1.6.1).

### Telomerase assay

To detect changes in telomerase levels, UVB-irradiated mouse BALB cells were assayed for telomerase activity using stretch PCR assay (Tatematsu et al., 1996) according to the instructions of TeloChaser (TOYOBO). After PCR reaction, the amount of amplified products was determined by absorbance at 260 nm.

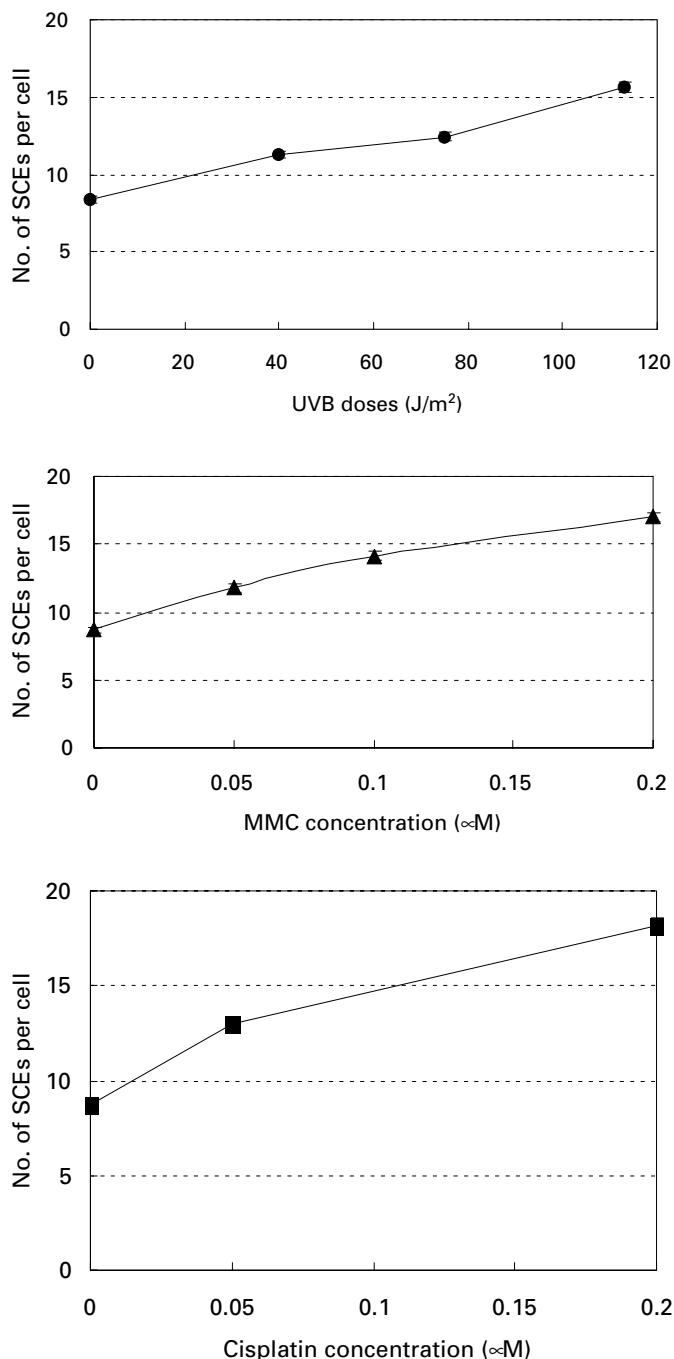


**Fig. 1.** Induction of SCEs by UVB, MMC and cisplatin in Chinese hamster ovary (CHO) cells. Bars at each point show standard errors of the mean.

## Results

### Intrachromosomal distribution of SCEs

The frequency of SCEs increased over the spontaneous level in proportion to the dose of UVB, MMC and cisplatin (Fig. 1). The distribution pattern on the largest chromosome was separately investigated for the SCEs induced by each mutagen. SCEs induced by UVB and cisplatin but not by MMC are high-



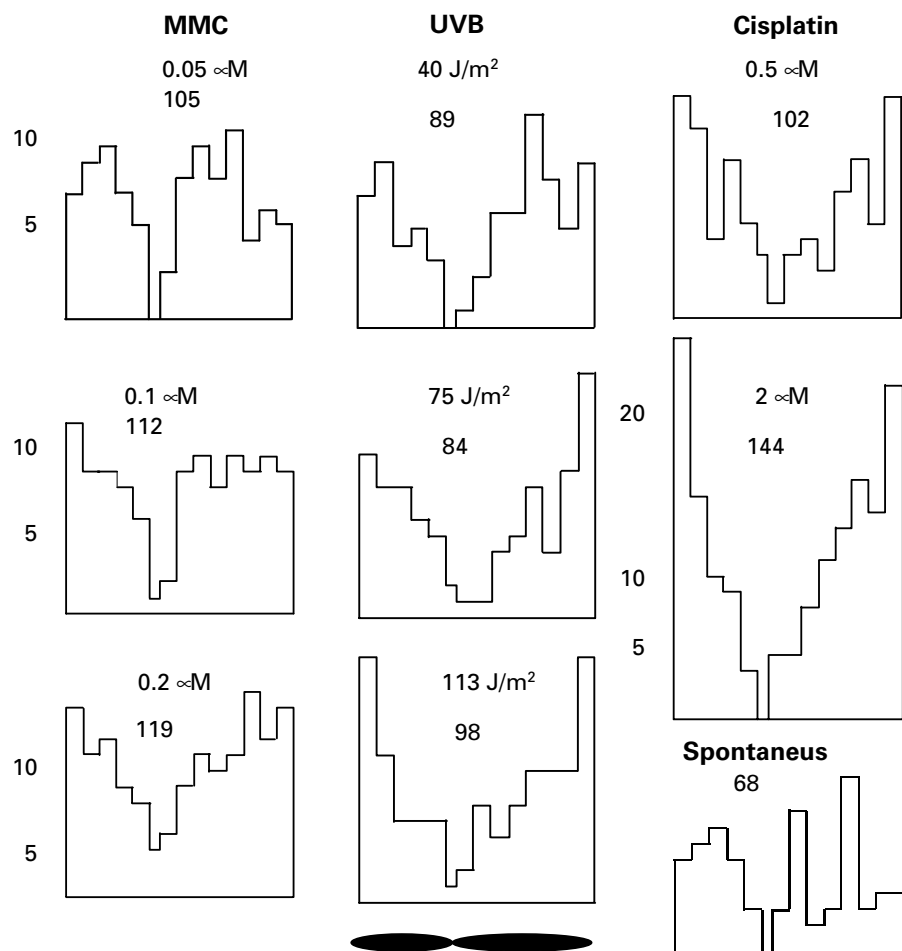


**Fig. 2.** Intrachromosomal distribution of SCEs induced by UVB, MMC and cisplatin in the largest chromosome of CHO cells. The vertical line shows the numbers of SCEs. The figures under the UV doses show the total number of SCEs analyzed. Under the UVB column a scheme of the chromosome analyzed is given.

ly localized (Fig. 2). Interestingly UVB- and cisplatin-induced SCEs occurred at high frequency in telomere regions. This pattern was clearly different from that observed in spontaneous and MMC-induced SCEs, in which they distributed relatively uniformly along the chromosome except centromere regions. In all cases very few SCEs were found in centromere regions, as described previously (Ikushima, 1984). The results of these experiments indicate a mutagen-specific intrachromosomal distribution of SCEs.

#### *Alteration of telomere length and telomerase activity after UVB irradiation*

The observation of frequent occurrence of UVB-induced SCEs in telomere regions prompted us to examine the telomere damage after UVB irradiation. Since Chinese hamster cell lines are unfortunately unsuitable for analyzing the telomere length as described above, we used mouse BALB cells instead. The telomere length of this mouse cell line was estimated to be about 30 kb. Either 1 or 24 h after UVB-irradiation at 40, 75 and 140 J/m<sup>2</sup>, the length of TRF was analyzed by Southern hybridization with a telomere probe. The telomeric signals in UVB-irradiated cells are displayed in Fig. 3. UVB-irradiated cells exhibited a dose-dependent increase in the signals corre-

sponding to shortened telomeres 1 h after UVB-irradiation. The faintest telomere signal was detected at the lowest dose (40 J/m<sup>2</sup>). At 24 h after irradiation, the telomere signals were similar to the ones in non-irradiated cells, a slight decrease in the signal intensity was seen only after the highest dose (140 J/m<sup>2</sup>). Almost all cells irradiated with these doses of UVB radiation completed cell division and survived at 100% (data not shown).

To know whether the telomerase activity changes in response to UVB-irradiation, we examined the telomerase activity 1 or 24 h after exposure to 40, 75 and 140 J/m<sup>2</sup> of UVB radiation. The telomerase activity increased sharply 1 h after irradiation in proportion to the dose (Fig. 4). At 24 h after UVB exposure, the level of activity decreased but was still 2- to 3-fold higher than the control level. These results indicate that UVB irradiation induced telomerase activity.

#### **Discussion**

The present observation of frequent occurrence of UVB- and cisplatin-induced SCEs in telomere regions indicates that long repeats of telomere sequences, which include doublets of

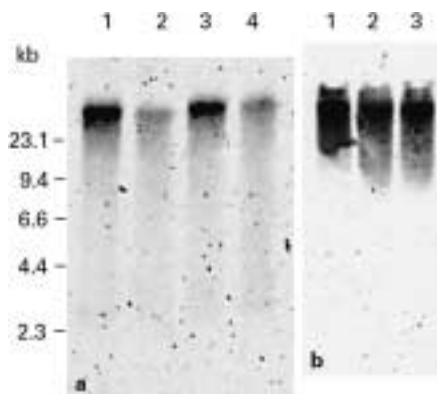


**Fig. 3.** Southern blotting analysis of TRF after UVB irradiation. **(a)** Immediately after irradiation. 1: non-irradiated; 2: 40 J/m<sup>2</sup>; 3: 75 J/m<sup>2</sup>; 4: 140 J/m<sup>2</sup>. **(b)** 24 h after irradiation. 1: non-irradiated; 2: 40 J/m<sup>2</sup>; 3: 140 J/m<sup>2</sup>.

thymine and cytosine residues and triplets of guanine residues, are good targets for UVB and cisplatin (Fig. 2). The clustered pyrimidine dimers and intrastrand d(GpG) cross-links will be formed by UVB and cisplatin in telomere regions, respectively (Friedberg et al., 1995), which may cause SCEs, despite the argument that pyrimidine dimers may not be the major lesion responsible for SCE formation in cells irradiated with UV (Wojcik et al., 2003). Since MMC forms interstrand cross-links at any site and blocks DNA replication, MMC-induced SCEs may distribute relatively uniform along chromosomes. Although SCEs clustered in telomere regions, they are not necessarily within telomere repeats, but they reflect the nature of DNA lesions formed by each mutagen.

With these results, we examined telomere damage after UVB irradiation. Telomeres are essential chromosomal components that stabilize chromosome ends and are required for cell cycle progression (Greider, 1996). While there was a dose-dependent decrease in the telomere signals 1 h after UVB irradiation, they turned back to the control level after 24 h (Fig. 3). Most UVB-induced DNA lesions in the telomere regions will be removed by nucleotide excision repair independently of transcription. Although the precise mechanism is not known, it has been reported that UV-damaged telomeric DNA is less well repaired than a transcriptionally active gene (Kruk et al., 1995). Unrepaired UVB lesions will cause daughter strand gaps during DNA replication. DNA replication across a gap is likely to produce a double-strand break (DSB) in one of the sister chromatids (Wang and Smith, 1986), resulting in substantial loss of terminal telomere repeats or telomere shortening. Telomeres in cisplatin-treated HeLa cells are markedly shortened for a long time and degraded (Ishibashi and Lippard, 1998). The decrease in the telomere signal observed 1 h after UVB irradiation (Fig. 3) can not be attributed to the telomere shortening and degradation alone. It is more likely to be a result of concomitant nucleotide excision repair, clearly seen at the lowest dose that led to the weakest telomere signal. After completion of cell divi-

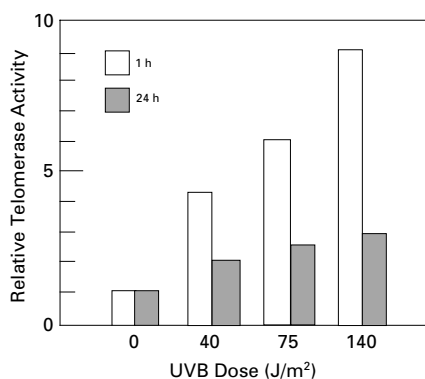


**Fig. 4.** Relative telomerase activity after UVB irradiation.

sion (24 h) after UVB irradiation, telomere lengths shortened only at the highest dose (Fig. 3). We therefore conclude that UVB irradiation at low doses does not cause deleterious telomere shortening and degradation. Usually, UVB-generated strand breaks initiate the HR pathway which is processed by pairing of the two homologous DNA molecules, strand invasion followed by DNA strand exchanges and formation of Holliday structures (Holliday, 1964; Meselson and Radding, 1975). Holliday junctions are normally resolved in a non-recombinogenic way by reverse branch migration to a nick or a gap in DNA (Whitby et al., 1993). Otherwise, Holliday junctions could be resolved to generate either a non-crossover or a crossover product, depending on which of the two strands are cleaved. Since the sister chromatid is used as a substrate for HR rather than the homologous chromosome (non-sister chromatid) (Arbel et al., 1999), the crossover product is visualized by SCEs after another round of DNA replication. In telomere regions, it is likely that HR between telomere repeats of sister chromatids mediates the occurrence of SCEs.

The level of telomerase activity increased sharply 1 h after UVB irradiation in a dose-dependent manner (Fig. 4). The result is consistent with the finding that Chinese hamster cells show an increase in telomerase activity following exposure to UVC radiation (Hande et al., 1997). Telomerase stabilizes the telomere length by extending the telomeric DNA at the 3' G-rich overhang (Greider and Blackburn, 1985). The excision of UVB lesions on 3' G-rich strands will result in the loss of terminal telomere repeats, because 5' strands complementary to 3' overhangs do not exist. Our present result suggests that the loss of terminal telomere repeats in 3' overhangs may be repaired by telomerase whose activity is enhanced by UVB irradiation. Telomeres are maintained by telomere recombination (alternative lengthening of telomere) in addition to telomere DNA synthesis catalyzed by telomerase (Dunham et al., 2000). Telomere recombination may also lead to SCEs in telomere regions, but information of whether UVB or cisplatin induce telomere recombination is missing. In conjunction with this, the frequent occurrence of telomeric SCEs (*t*-SCEs) have been admirably demonstrated in T-banded terminal segments of CHO and

human chromosomes with computer graphic imaging analysis (Drets et al., 1992). Also, it has been reported that the termini of human chromosomes display elevated frequencies of mitotic recombination (Cornforth and Eberle, 2001). SCEs in telomere regions may also be a cytological visualization of telomere recombination. Further studies in telomerase-negative cells should be helpful to prove our speculative hypothesis.

## Acknowledgements

We would like to thank Y. Tanizaki and M. Nakao for their excellent technical assistance.

## References

- Arbel A, Zenvirth D, Simchen G: Sister chromatid-based DNA repair is mediated by *RAD54*, not by *DMC1* or *TID1*. *EMBO J* 18:2648–2658 (1999).
- Carrano AV, Johnston GR: The distribution of mitomycin C-induced sister chromatid exchanges in the euchromatin and heterochromatin of the Indian muntjac. *Chromosoma* 14:97–107 (1977).
- Cleaver JE: Correlations between sister chromatid exchange frequencies and replicon sizes. A model for the mechanism of SCE production. *Expl Cell Res* 136:27–30 (1981).
- Cornforth MN, Eberle RL: Termini of human chromosomes display elevated rates of mitotic recombination. *Mutagenesis* 16:85–89 (2001).
- Drets ME, Obe G, Monteverde FJ, Folle GA, Medina II, DeGalvez MG, Duarte JE, Mechoso BH: Computerized graphic and light microscopic analyses of T-banded chromosome segments of Chinese hamster ovary cells and human lymphocytes. *Biol Zentrbl* 111:204–214 (1992).
- Dronkert ML, Beverloo HB, Johnson RD, Hoeijmakers JH, Jasin M, Kanaar R: Mouse *RAD54* affects DNA double-strand break repair and sister chromatid exchange. *Mol cell Biol* 20:3147–3156 (2000).
- Dunham MA, Neumann AA, Fasching CL, Reddel RR: Telomere maintenance by recombination in human cells. *Nature Genet* 26:447–450 (2000).
- Faravelli M, Azzalin CM, Bertoni L, Chernova O, Attolini C, Mondello C, Giulotto E: Molecular organization of internal telomeric sequences in Chinese hamster chromosomes. *Gene* 283:11–16 (2002).
- Friedberg EC, Walker GC, Siede W: *DNA Repair and Mutagenesis* (ASM Press, Washington DC 1995).
- Greider CW: Telomere length regulation. *Annu Rev Biochem* 65:337–365 (1996).
- Greider CW, Blackburn EH: Identification of a specific telomere terminal transferase activity in *Tetrahymena* extracts. *Cell* 43:405–413 (1985).
- Hande MP, Balajee AS, Natarajan AT: Induction of telomerase activity by UV-irradiation in Chinese hamster cells. *Oncogene* 15:17467–1752 (1997).
- Holliday R: A mechanism for gene conversion in fungi. *Genet Res* 5:282–304 (1964).
- Ikushima T: Role of sister chromatid exchanges in chromatid aberration formation. *Nature* 268:235–236 (1977).
- Ikushima T: SCE and DNA methylation, in Tice RR, Hollaender A (eds): *Sister Chromatid Exchanges, 25 Years of Experimental Research, Part A*, pp 161–172 (Plenum, New York 1984).
- Ikushima T, Shima Y, Ishii Y: Effects of an inhibitor of topoisomerase II, ICRF-193 on the formation of ultraviolet-induced chromosomal aberrations. *Mutat Res* 404:35–38 (1998).
- Ishibashi T, Lippard SJ: Telomere loss in cells treated with cisplatin. *Proc natl Acad Sci, USA* 95:4219–4223 (1998).
- Ishii Y, Bender MA: Effects of inhibitors of DNA synthesis on spontaneous and ultraviolet light-induced sister chromatid exchanges in Chinese hamster cells. *Mutat Res* 79:19–32 (1980).
- Kato H: Possible role of DNA synthesis in formation of sister chromatid exchanges. *Nature* 252:739–741 (1974).
- Kruk PA, Rampino NJ, Bohr VA: DNA damage and repair in telomeres: Relation to aging. *Proc natl Acad Sci, USA* 92:258–262 (1995).
- Latt SA, Loveday KS: Characterization of sister chromatid exchange induced by 8-methoxy-psoralen plus near UV light. *Cytogenet Cell Genet* 21:184–200 (1978).
- Limoli CL, Giedzinski E, Morgan WF, Cleaver JE: Polymerase  $\eta$  deficiency in the xeroderma pigmentosum variant uncovers an overlap between the S phase checkpoint and double-strand break repair. *Proc natl Acad Sci, USA* 97:7939–7946 (2000).
- McClintock B: The production of homozygous deficient tissues with mutant characteristics by means of the aberrant mitotic behavior of ring-shaped chromosomes. *Genetics* 23:315–397 (1938).
- Meselson MS, Radding CM: A general model for genetic recombination. *Proc natl Acad Sci, USA* 72:358–361 (1975).
- Natarajan AT, van Zeeland AA, Verdegaal-Immerzeel AM, Filon AR: Studies on the influence of photoreactivation on the frequencies of UV-induced chromosomal aberrations, sister chromatid exchanges and pyrimidine dimers in chicken embryonic fibroblasts. *Mutat Res* 69:307–317 (1980).
- Ockey CH: Differences between “spontaneous” and induced sister-chromatid exchanges with fixation time and their chromosome localization. *Cytogenet Cell Genet* 26:223–235 (1980).
- Painter RB: A replication model for sister-chromatid exchange. *Mutat Res* 70:337–341 (1980).
- Perry P, Wolff S: New Giemsa method for the differential staining of sister chromatids. *Nature* 252:156–158 (1974).
- Sambrook J, Russell DW: *Molecular Cloning, A Laboratory Manual*, 3rd ed (CSHL Press, New York 2001).
- Slijepcevic P, Hande MP, Bouffler SD, Lansdorp P, Bryant PE: Telomere length, chromatin structure and chromosome fusigenic potential. *Chromosoma* 106:413–421 (1997).
- Sonoda E, Sasaki MS, Morrison C, Yamaguchi-Iwai Y, Takata M, Takeda S: Sister chromatid exchanges are mediated by homologous recombination in vertebrate cells. *Mol cell Biol* 19:5166–5169 (1999).
- Tatematsu K, Nakayama J, Danbara M, Shionoya S, Sato H, Omine M, Ishikawa F: A novel quantitative “stretch PCR assay”, that detects a dramatic increase in telomerase activity during the progression of myeloid leukemias. *Oncogene* 13:2265–2274 (1996).
- Taylor JH: Sister chromatid exchanges in tritium-labeled chromosomes. *Genetics* 43:515–529 (1958).
- Tucker JD, Auletta A, Cimino MC, Dearfield KL, Jacobson-Kram D, Tice RR, Carrano AV: Sister chromatid exchanges: second report of the gene-tox program. *Mutat Res* 297:101–180 (1993).
- Wang T-CV, Smith KC: Postreplicational formation and repair of DNA double-strand breaks in UV-irradiated *Escherichia coli* uvrB cells. *Mutat Res* 165:39–44 (1986).
- Whitby MC, Ryder L, Lloyd RG: Reverse branch migration of Holliday junctions by RecG protein: a new mechanism for resolution of intermediates in recombination and DNA repair. *Cell* 75:341–350 (1993).
- Wojcik A, von Sonntag C, Obe G: Application of the biotin-dUTP chromosome labelling technique to study the role of 5-bromo-2'-deoxyuridine in the formation of UV-induced sister chromatid exchanges in CHO cells. *J Photochem Photobiol B: Biol* 69:139–144 (2003).
- Wolff S, Bodycote J, Painter RB: Sister chromatid exchanges induced in Chinese hamster cells by UV irradiation of different stages of the cell cycle: the necessity for cells to pass through S. *Mutat Res* 25:73–81 (1974).

# SCE analysis in G2 lymphocyte prematurely condensed chromosomes after exposure to atrazine: the non-dose-dependent increase in homologous recombinational events does not support its genotoxic mode of action

S.I. Malik, G.I. Terzoudi and G.E. Pantelias

Health Physics & Environmental Hygiene, National Centre for Scientific Research "Demokritos", Athens (Greece)

**Abstract.** Several studies have been carried out to evaluate the mutagenic and carcinogenic potential of atrazine, the most prevalent of triazine herbicides classified as a "possible human carcinogen". The majority of these studies have been negative but positive responses have been also reported including mammary tumors in female Sprague-Dawley rats. Sister chromatid exchanges (SCEs) caused by the presence of DNA lesions at the moment of DNA replication have been extensively used for genotoxicity testing, but for non-cytotoxic exposures to atrazine controversial results have been reported. Even though exposures to higher concentrations of atrazine could provide clear evidence for its genotoxicity, conventional SCE analysis at metaphase cells cannot be used because affected cells are delayed in G2-phase and do not proceed to mitosis. As a result, the genotoxic potential of atrazine may have been underestimated. Since clear evidence has been recently reported relating SCEs to homologous recombinational events, we are testing here the hypothesis that high concentrations of atrazine will

cause a dose-dependent increase in homologous recombinational events as quantified by the frequency of SCEs analyzed in G2-phase. Towards this goal, a new cytogenetic approach is applied for the analysis of SCEs directly in G2-phase prematurely condensed chromosomes (PCCs). The methodology enables the visualization of SCEs in G2-blocked cells and is based on drug-induced PCCs in cultured lymphocytes. The results obtained for high concentrations of atrazine do not demonstrate a dose-dependent increase in homologous recombinational events. They do not support, therefore, a genotoxic mode of action. However, they suggest that an important part in the variation of SCE frequency reported by different laboratories when conventional SCE analysis is applied after exposure to a certain concentration of atrazine, is due to differences in cell cycle kinetics of cultured lymphocytes, rather than to a true biological variation in the cytogenetic end point used.

Copyright © 2003 S. Karger AG, Basel

Human exposure to agricultural chemicals such as pesticides and herbicides has been linked to undesirable health effects including increased cancer incidence and genetic diseases. The triazine herbicides, which are used both for pre-emergence and post-emergence control of grasses during cultivation of maize, wheat, sorghum, sugar cane, conifers and oth-

ers, have made their way into surface and groundwater supplies due to their widespread use in agriculture (Goldman, 1994). Atrazine is the most prevalent triazine found in rural groundwater and through its occurrence in food such as corn, nuts, fruit, and wheat, is a potential hazard to humans. To evaluate its genotoxic and mutagenic potential, several studies have been carried out in different experimental systems ranging from bacterial to mammalian assays. The majority of these studies have been negative but positive responses have been also reported. Atrazine has been found to induce mammary tumors in female Sprague-Dawley rats and it has been classified by the US Environmental Protection Agency (EPA) as a "possible human carcinogen" (Goldman, 1994).

Received 6 October 2003; accepted 27 November 2003.

Request reprints from: Dr. Georgia Terzoudi  
Laboratory of Health Physics & Environmental Hygiene  
NCSR "Demokritos", Agia Paraskevi, Athens (Greece)  
telephone: +30 210 6503811; fax: +30 210 6534710  
e-mail: georgia@ipta.demokritos.gr.

Sister chromatid exchanges (SCEs) caused by the presence of DNA lesions at the moment of DNA replication have been extensively used for genotoxicity testing. Although SCEs are observed in cells treated with radiation or chemical agents which produce various types of DNA lesions (Latt, 1981; Natarajan, 2002), it has been suggested that DNA interstrand cross-links may be the major lesions leading to SCE formation in cells irradiated with UV or ionizing radiation (Wojcik et al., 2003). Since it was indicated that atrazine induces DNA damage (Ribas et al., 1995; Clements et al., 1997) a number of *in vitro* and *in vivo* studies have been carried out to investigate the mutagenic potential of atrazine using the analysis of SCEs as a cytogenetic end point. Contradictory findings have been reported, however, and the results are not always conclusive. Particularly, when the frequency of SCEs is slightly increased with respect to the controls, the activity of atrazine has been characterized as minimal. Even though the use of higher doses could confirm a more profound effect of this chemical, they cannot be applied since cells will be arrested in G2-phase and not proceed to mitosis, preventing thus their analysis by scoring of SCEs at metaphase. As a result, using exclusively the conventional methodology for the analysis of SCEs, the genotoxic and mutagenic potential of atrazine may have been underestimated. To overcome this shortcoming, a methodology is needed to enable the analysis of SCEs in interphase and particularly in the G2-phase of cultured peripheral blood lymphocytes. The visualization of interphase chromosomes in peripheral blood lymphocytes and their use for biomonitoring purposes following exposure to genotoxic agents became possible using a method for cell fusion and premature chromosome condensation (PCC) induction (Pantelias and Maillie, 1983, 1984). Thus far, researchers have examined interphase chromosomal damage in lymphocytes using the PCC methodology which has been proven to be a powerful cytogenetic tool for the identification of factors involved in the conversion of DNA damage into chromosomal damage (Terzoudi and Pantelias, 1997), affecting thus sensitivity to genotoxic agents (Terzoudi et al., 2000).

In this report, a new cytogenetic approach for the analysis of sister chromatid exchanges directly in the G2-phase of cultured peripheral blood lymphocytes has been applied. The methodology is based on the induction of PCC using Calyculin-A, a potent inhibitor of protein phosphatases type 1 and 2A (Coco-Martin and Begg, 1997; Asakawa and Gotoh, 1997; Durante et al. 1998; Gotoh et al., 1999) and the visualization of SCEs in G2-phase prematurely condensed chromosomes (G2-PCCs) using a modified fluorescent-plus-Giemsa (FPG) technique (Perry and Wolff, 1974; Jan et al., 1982; Terzoudi et al., 2003). This cytogenetic approach enables in a unique way the testing of the hypothesis that high concentrations of atrazine will cause a dose-dependent increase in homologous recombinational events, as quantified by the frequency of SCEs in G2-PCCs. Since clear evidence has been provided relating SCEs to homologous recombinational events (Sonoda et al., 1999), an increase in homologous recombination repair processes is expected to result in an increase in the frequency of SCEs; this finding would favor a genotoxic activity of atrazine.

## Materials and methods

### *Culture conditions and premature chromosome condensation induction in G2-phase*

Peripheral blood was taken with heparinized syringes from healthy individuals. 0.5 ml of whole blood was added to each culture tube containing 5 ml of McCoy's 5A medium supplemented with 10% fetal calf serum, 1% glutamin, 1% antibiotics (penicillin, streptomycin), 1% phytohemagglutinin, and incubated at 37 °C for 72 h in a humidified incubator, in an atmosphere of 5% CO<sub>2</sub> and 95% air. For PCC induction in G2-phase lymphocytes, calyculin-A (Sigma-Aldrich) was used. In order to determine the optimum conditions for PCC induction and scoring, calyculin-A was added to the whole blood cultures at various doses and treatment times. Replicate cultures were also made containing 0.05 µg/ml colcemid throughout the last 3 h culture period, and these were not treated with calyculin-A.

### *Sister chromatid exchanges in G2-and M-phase lymphocytes*

5-Bromodeoxyuridine (Sigma) was added at a final concentration of 20 µM 24 h after culture initiation. Cultures were incubated at 37 °C for 72 h prior to cell harvest. During this culture period, incorporation of BrdU into replicating cells allows for the unequivocal identification of second division metaphase cells. The cultured cells were treated with hypotonic (0.075 M) KCl, fixed with methanol-acetic acid (3:1) and 20 µl of cell suspension were dropped on wet slides. Air dried slides were stored in the dark. For visualization of SCEs, the slides were stained by the Fluorescence-Plus-Giemsa (FPG) technique according to Perry and Wolff (1974) and Jan et al. (1982). A few drops of Hoechst 33258 (5 µg/ml) in Sorensen buffer (pH 6.8) were placed on each slide and covered with coverslips. They were then placed on a slide warmer set at 55 °C and exposed to a black light fluorescent lamp (Radium SupraBlack HBT 125-281) at a distance of 2 cm for 10 min. Coverslips were removed by soaking the slides in Sorensen's buffer and the slides were then stained with 3% Giemsa solution (Gurr R66 in Sorensen's buffer) for 15 min. The slides were finally mounted with cover slips and coded for analysis to avoid bias. For SCE scoring, the criteria suggested by Carrano and Natarajan (1988) were applied. Only second-division metaphases and G2-phase PCCs, identifiable by their uniform differential staining pattern, containing 46 chromosomes were analysed.

For testing whether the mutagenic potential of atrazine may be underestimated when the conventional SCE analysis is applied, and also for the assessment of exposures that arrest cells at G2-phase, whole blood cultures were treated for the last 24 h of the total 72 h culture period. Atrazine (2-chloro-4-ethylamino-6-isopropylamino-1,3,5-triazine), obtained from Sigma-Aldrich, Germany, was used at the concentrations of 5 µg/ml to 220 µg/ml and prepared in dimethyl sulphoxide (DMSO). Mitomycin-C (MMC, Kyowa Hakko Kogyo Co. Ltd., Japan) was prepared in RPMI medium and used as a positive control at a final concentration of 0.1 µg/ml. Calyculin-A was dissolved in absolute ethanol.

For each experiment and chemical concentration within an experimental set, a minimum of 3 lymphocyte cultures was run. Routinely, 30–50 cells were scored for SCEs for each culture. Standard deviations of the mean values from three independent experiments were calculated for each experimental point. Data were evaluated statistically by Student's *t* test.

## Results

Drug-induced PCC in cultured peripheral blood lymphocytes was used to visualize and quantify the frequency of SCEs in G2-phase. Treatment of cultured cells with 50 nM calyculin-A for 1 h was chosen as optimum for PCC induction and analysis of SCEs in G2-phase lymphocytes, considering chromosome morphology as well. SCEs as visualized in G2-PCCs after atrazine exposure are shown in Fig. 1. As a positive control, lymphocyte cultures were treated with 0.1 µg/ml of mitomycin-C, and the SCEs in G2 lymphocyte PCCs are shown in Fig. 2. In contrast to the appearance of chromosomes at metaphase (Fig. 3), the sister chromatids in drug-induced pre-



**Fig. 1.** SCEs as visualized in G2-PCCs of peripheral blood lymphocytes exposed to 20 µg/ml of atrazine. The sister chromatids in drug-induced PCCs are parallel to each other and their centromeres are not clearly visible.



**Fig. 2.** SCEs as visualized in G2-PCCs of peripheral blood lymphocytes treated with 0.1 µg/ml of Mitomycin-C.

turely condensed chromosomes are aligned in close contact, parallel to each other, and their centromeres are not clearly visible.

In order to test whether high concentrations of atrazine will cause a dose-dependent increase in homologous recombinational events, four sets of experiments were carried out. In the first set of experiments it was examined whether the genotoxic potential of atrazine can be evaluated in G2-phase lymphocytes even at exposures exceeding cytotoxic limits that cause accumulation of cells in the G2-phase. The results are shown in Table 1. Even though at concentrations of atrazine of 120 and 220 µg/ml no cells at mitosis were present to be studied by conventional SCE analysis, using prematurely chromosome condensation enough G2-PCCs were present to analyze SCEs.

The second set of experiments was designed to test whether *in vitro* exposure of peripheral blood to atrazine from 5 to 200 µg/ml will cause a dose-dependent increase in homologous recombinational events, as quantified by the frequency of SCEs obtained at each experimental point. As shown in Table 2, the results obtained in particular using high exposures to atrazine, do not demonstrate a dose-dependent increase in the frequencies of SCEs.

In the third set of experiments it was examined whether SCE analysis in metaphase chromosomes is a more sensitive method to estimate the genotoxic potential of atrazine. The results are presented in Table 3. A higher SCE yield per cell was scored in G2-PCCs than in cells at metaphase. In the fourth set of experiments, the involvement of cell cycle kinetics in the variation of SCEs among individuals after exposure to 20 µg/ml of atrazine was examined. The results are also shown in Table 3. A lesser SCE variability, CV = 8.5%, (CV = SD/mean value × 100%) was observed when the analysis was carried out in G2-phase prematurely condensed chromosomes than in metaphase cells (CV = 20%). The range for SCEs per cell among



**Fig. 3.** SCEs as visualized in peripheral blood lymphocytes at metaphase. The clear appearance of the centromeres in metaphase chromosomes differentiates them from the drug-induced G2-PCCs.

healthy individuals after atrazine exposure was 5.5–9.9 when analyzed in cells at metaphase, whereas the range was 8.4–10.4 when SCEs were scored in G2-phase PCCs.

## Discussion

Even though the evidence for the mutagenic and carcinogenic potential of triazines is still equivocal, the extensive human exposure to these herbicides is likely to continue and possibly increase in the near future. For USA alone there are

**Table 1.** Yield of SCEs as scored in G2-PCC cells after exposure to atrazine at high concentrations

[Chemical] in cell culture	SCEs / metaphase cell (Mean ± SD)	SCEs / G2-phase cell (Mean ± SD)
Control	6.10 ± 0.60	6.60 ± 0.52
Atrazine 60 µg/ml	8.50 ± 1.10	9.90 ± 0.71
Atrazine 120 µg/ml	No metaphases <sup>a</sup>	10.30 ± 0.90
Atrazine 220 µg/ml	No metaphases <sup>a</sup>	10.25 ± 0.80
MMC 0.1 µg/ml	15.30 ± 0.91	27.42 ± 1.23

<sup>a</sup> At these chemical concentrations no metaphases were observed. Standard deviations of the mean values from three independent experiments using the same donor were calculated for each experimental point.

**Table 2.** SCEs per G2-PCC cell, in comparison to SCEs per metaphase cell, after exposure to atrazine

[Atrazine] in cell culture	SCEs / metaphase cell Range <sup>a</sup> (Mean ± SD)	Coefficient of variation (%)	SCEs / G2-phase cell Range <sup>a</sup> (Mean ± SD)	Coefficient of variation (%)
Control (w/o atrazine)	4.4 – 8.9 (6.0 ± 1.6)	26.7	6.0 – 7.2 (6.4 ± 0.5)	7.8
5 µg/ml	5.2 – 7.8 (6.5 ± 1.2)	18.5	7.2 – 8.3 (7.7 ± 0.6)	7.8
10 µg/ml	6.0 – 9.2 (8.0 ± 1.4)	17.5	7.9 – 10.0 (8.9 ± 0.9)	10.1
20 µg/ml	5.5 – 9.9 (7.5 ± 1.5)	20.0	8.0 – 10.4 (9.3 ± 0.8)	8.5
50 µg/ml	7.1 – 10.5 (8.1 ± 1.4)	17.3	9.4 – 10.0 (9.6 ± 0.7)	7.3
100 µg/ml	No metaphases	-	9.9 – 12.5 (10.5 ± 0.9)	8.6
150 µg/ml	No metaphases	-	9.9 – 11.9 (10.1 ± 0.9)	8.9
200 µg/ml	No metaphases	-	11.6 – 12.0 (10.4 ± 0.8)	7.7

<sup>a</sup> Range of SCEs / cell from 4-6 donors. Standard deviations of the mean values from six different donors were calculated for each experimental point

**Table 3.** Variation of SCE frequencies among normal individuals as scored in metaphase cells and in G2-phase cells using premature chromosome condensation after exposure to 20 µg/ml of atrazine

Donor No.	SCEs / metaphase cell (Mean <sup>a</sup> ± SD)	SCEs / G2-phase cell (Mean <sup>a</sup> ± SD)	Difference in sample means <sup>b</sup>
1	6.7 ± 0.5	9.2 ± 1.0	2.5
2	6.9 ± 0.7	8.4 ± 0.6	1.5
3	9.9 ± 1.2	10.4 ± 0.9	0.5
4	6.6 ± 0.9	8.4 ± 0.5	1.8
5	5.5 ± 0.8	9.0 ± 0.8	3.5
6	8.2 ± 0.9	9.3 ± 0.9	1.1
7	8.7 ± 1.0	10.2 ± 1.2	1.5
Overall mean ± SD	7.5 ± 1.5	9.3 ± 0.8	1.77 ± 0.98

Coefficient of variation CV = 20 %      Coefficient of variation CV = 8.5 %

<sup>a</sup> Mean from 3 independent experiments.

<sup>b</sup> Significance of the difference in sample means, t-test,  $\alpha = 0.05$  ( $t = 4.78$ ,  $0.01 < p < 0.001$ )

estimates ranging from 90 to 121 million pounds of active ingredient used annually (Goldman, 1994; Kligerman et al., 2000). Most of the studies reported in the literature tend to support the concept that triazines are either not genotoxic or have minimal genotoxic activity (Kligerman et al., 2000; Tennant et al., 2001). Although the precise mechanism of action of atrazine at the cell level has not been clearly defined, the experimental data indicate that atrazine may either cause some form of DNA damage or affect cell cycle kinetics. Two studies have indicated that atrazine can cause DNA damage as measured by the alkaline single cell gel (SCG) assay. Clements et al. (1997) reported that atrazine caused significant DNA damage in bullfrog tadpole erythrocytes. Atrazine was also shown to cause DNA damage with and without S9 activation in human lymphocytes treated in vitro (Ribas et al., 1995). The EPA has pro-

posed to upgrade the classification of atrazine to a “likely human carcinogen”, and re-evaluate of the mutagenic and carcinogenic potential of atrazine (Ribas et al., 1995).

In an attempt to study the genotoxicity of atrazine, in this report a new cytogenetic approach is used for testing the hypothesis that high concentrations of atrazine will cause a dose-dependent increase in homologous recombinational events, as quantified by the frequency of SCEs in G2-PCCs. For this purpose it was examined whether the genotoxic potential of atrazine can be evaluated in G2-phase lymphocytes even at exposures exceeding cytotoxic limits that cause cell accumulation in the G2-phase. Even though it is known that some chemicals are effective inducers of SCEs in the first post treatment mitosis (M1) and not in the second (M2) or vice versa (Kaina and Aurich, 1985), the effect of atrazine was studied

only in M1 since high exposures to atrazine induce G2-block, affecting cell progression to M2. The results shown in Table 1 demonstrate that at high concentrations of atrazine, SCEs could not be scored using conventional analysis since no cells were present at metaphase. However, using premature chromosome condensation the yields of SCEs in G2-phase lymphocytes were easily obtained. With respect to whether in vitro exposure of peripheral blood to atrazine from 5 to 200 µg/ml would cause a dose-dependent increase in homologous recombinational events, as quantified by the frequency of SCEs obtained at each experimental point, the results presented in Table 2 do not support this hypothesis. Particularly, the fact that an increase of chemical concentration from 50 to 200 µg/ml did not increase the frequency of SCEs, as scored in G2 lymphocyte PCCs, does not support a genotoxic activity of atrazine.

The results presented in Table 3 show that a higher SCE yield per cell was scored in G2-PCCs than in cells at metaphase. This suggests that SCE analysis in G2-PCCs is a more sensitive method to estimate the genotoxic potential of atrazine since it includes in the analysis the G2-blocked cells as well. On the average the SCE frequency obtained in the G2-phase is significantly higher ( $0.001 < p < 0.01$ ) than that obtained in metaphase. In Table 3 results are also shown from experiments designed to test whether the variability in the kinetics of cultured peripheral blood lymphocytes among individuals may affect the frequency of SCEs when conventional SCE analysis in metaphase cells is exclusively applied. A lesser SCE variability was observed when the analysis was carried out in G2-PCCs

than in metaphase cells. The range for SCEs per cell among healthy individuals after atrazine in vitro exposure was 5.5–9.9, with a coefficient of variation (CV) value of 20% when analyzed in cells at metaphase, whereas the range was 8.4–10.4, with a CV value of 8.5% when SCEs were scored in G2-phase PCCs. Similar CV values were also obtained for the other atrazine concentrations used as shown in Table 2. These results suggest that an important part in the variation of SCE frequency reported by different laboratories when conventional SCE analysis is applied after exposure to a certain concentration of atrazine, is due to differences in cell cycle kinetics of cultured lymphocytes rather than to a true biological variation in the cytogenetic end point used.

In conclusion, the use of a simple protocol for SCE analysis in G2-phase lymphocyte PCCs enables the evaluation of the genotoxic potential of atrazine even at high concentrations of this pesticide. Even though a minimal genotoxic activity was observed at the low dose range, the fact that an increase of chemical concentration from 50 to 200 µg/ml did not increase the frequency of SCEs, as scored in G2 lymphocyte PCCs, does not support a genotoxic activity of atrazine. Furthermore, since a lesser SCE variability is observed when the analysis is carried out in G2-phase, it is possible that an important part in the variation of the SCE frequencies and the discrepancies between different laboratories reporting on the genotoxic effect of a certain dose of atrazine, is due to differences in cell cycle kinetics of cultured lymphocytes rather than to a true variation in the induction of SCEs.

## References

- Asakawa Y, Gotoh E: A method for detecting sister chromatid exchanges using prematurely condensed chromosomes and immunogold-silver staining. *Mutagenesis* 12:175–177 (1997).
- Carrano AV, Natarajan AT: Consideration for population monitoring using cytogenetic techniques. International Commission for protection against environmental mutagens and carcinogens, ICPEMC Publication No 14, *Mutat Res* 204:397–406 (1988).
- Clements C, Ralph S, Petras M: Genotoxicity of select herbicide in *Rana catesbeiana* tadpoles using alkaline single-cell gel DNA electrophoresis (comet) assay. *Environ Mol Mutagen* 29:277–288 (1997).
- Coco-Martin JM, Begg AC: Detection of radiation-induced chromosome aberrations using fluorescence in situ hybridization in drug-induced premature chromosome condensations of tumour cell lines with different radiosensitivities. *Int J Radiat Biol* 71:265–73 (1997).
- Dorsey L, Portier C: Atrazine: Hazard and Dose-Response Assessment and Characterization. FIFRA SAP Report No. 2000-05, June 27–29 (2000).
- Durante M, Furusawa Y, Gotoh E: A simple method for simultaneous interphase-metaphase chromosome analysis in biodosimetry. *Int J Radiat Biol* 74:457–462 (1998).
- Goldman LR: Atrazine, Simazine and Cyanazine: Notice of Initiation. Special Review Federal Register: 60412–60443 (1994).
- Gotoh E, Kawata T, Durante M: Chromatid break rejoining and exchange aberration formation following  $\gamma$ -ray exposure: analysis in G2 human fibroblasts by chemically induced premature chromosome condensation. *Int J Radiat Biol* 75:1129–1135 (1999).
- Jan KY, Wang-Wuu S, Wen WN: A simplified fluorescence plus Giemsa method for consistent differential staining of sister chromatids. *Stain Technol* 57:45–46 (1982).
- Kaina B, Aurich O: Dependency of the yield of sister-chromatid exchanges induced by alkylating agents on fixation time. Possible involvement of secondary lesions in sister-chromatid exchange induction. *Mutat Res* 149:451–461 (1985).
- Kligerman AD, Doerr CL, Tennant AH, Zucker RM: Cytogenetic studies of three triazine herbicides. I. In vitro studies. *Mutat Res* 465:53–59 (2000).
- Latt S: Sister chromatid exchange formation. *Ann Rev Genet* 15:11–55 (1981).
- Natarajan AT: Chromosome aberrations: past, present and future. *Mutat Res* 504:3–16 (2002).
- Pantelias GE, Maillie HD: A simple method for premature chromosome condensation induction in primary human and rodent cells using polyethylene glycol. *Somat Cell Genet* 9:533–547 (1983).
- Pantelias GE, Maillie HD: The use of peripheral blood mononuclear cell prematurely condensed chromosomes for biological dosimetry. *Radiat Res* 99:140–150 (1984).
- Perry P, Wolff S: New Giemsa method for the differential staining of sister chromatids. *Nature* 251:156–158 (1974).
- Ribas G, Frenzilli G, Barale R, Marcos R: Herbicide-induced DNA damage in human lymphocytes evaluated by single gel electrophoresis (SCGE) assay. *Mut Res* 344: 41–54 (1995).
- Sonoda E, Sasaki MS, Morrison C, Yamaguchi-Iwai Y, Takata M, Taketa S: Sister chromatid exchanges are mediated by homologous recombination in vertebrate cells. *Mol Cell Biol* 19:5166–5169 (1999).
- Tennant AH, Peng B, Kligerman AD: Genotoxicity studies of three triazine herbicides: in vivo studies using the alkaline single cell gel (SCG) assay. *Mutat Res* 493:1–10 (2001).
- Terzoudi GI, Malik SI, Pantelias GE, Margaritis K, Manola K, Makropoulos W: A new cytogenetic approach for the evaluation of mutagenic potential of chemicals that induce cell cycle arrest in the G2 phase. *Mutagenesis* 18:539–543 (2003).
- Terzoudi GI, Pantelias GE: Conversion of DNA damage into chromosome damage in response to cell cycle regulation of chromatin condensation after irradiation. *Mutagenesis* 12:271–276 (1997).
- Terzoudi GI, Jung T, Hain J, Vrouvas J, Margaritis K, Donta-Bakoyianni C, Makropoulos V, Angelakis PH, Pantelias GE: Increased G2 chromosomal radiosensitivity in cancer patients: The role of cdk1/cyclinB activity level in the mechanisms involved. *Int J Radiat Biol* 76:607–616 (2000).
- Wojcik A, von Sonntag C, Obe G: Application of the biotin-dUTP chromosome labelling technique to study the role of 5-bromo-2'-deoxyuridine in the formation of UV-induced sister chromatid exchanges in CHO cells. *J Photochem Photobiol B* 69:139–144 (2003).



# X chromosome inactivation-mediated cellular mosaicism for the study of the monoclonal origin and recurrence of mouse tumors: a review

H. Tanooka

National Institute of Radiological Sciences, Anagawa, Inage-ku, Chiba 263-8555 and Central Research Institute of Electric Power Industry (Japan)

**Abstract.** X chromosome inactivation-mediated cellular mosaicism was applied to study the clonal nature of experimental and human tumors and to judge whether apparently recurrent tumors which appear after therapeutic treatment are truly due to recurrence or due to new induction of a second tumor. Results show that the majority of experimental and human

tumors, including benign tumors, are monoclonal and that the majority of apparently recurrent tumors are due to true recurrence. A series of experimental studies on this topic are reviewed.

Copyright © 2003 S. Karger AG, Basel

We observed a 100% recurrence of mouse tumors of autochthonous origin induced with 3-methylcholanthrene (MCA) after experimental radiation therapy while, in marked contrast 100% of transplanted tumors from the same origin treated in the same manner were cured (Tanooka et al., 1980). It then became necessary to judge whether apparently recurrent tumors can be attributed to true recurrence or are due to induction of new tumors at treated sites. We employed cellular mosaicism produced by random inactivation of the X chromosome first to judge the clonal origin of tumors and then to test the clonal nature of the recurrent tumors after experimental radiation therapy. This review shows that almost all of the tumors, as judged from the mice carrying X chromosome inactivation-mediated mosaicism, were monoclonal, i. e., of a single-cell origin, except for a few cases. Furthermore, the majority of the apparently recurrent tumors were true recurrent tumors.

## Recurrence of autochthonous tumors after radiation therapy

Chemically induced mouse tumors were used as a target of experimental therapy with chemotherapeutic and immunosuppressive agents, and ionizing radiation. As a model, we used solid tumors induced by subcutaneous injection of MCA in the groin of ICR mice. These tumors were induced in a dose-dependent manner (90% yield with 0.5 mg MCA per mouse) and grew to a palpable size 50–200 days after MCA injection (Tanooka et al., 1982). Their growth rates did not depend on the time of their appearance, and the tumors were monoclonal (Tanooka and Tanaka, 1982, 1984). Tumor growth curves are shown in Fig. 1a. Histologically, the majority of tumors were fibrosarcomas and some squamous cell carcinomas were also observed. When they had reached a diameter of 8–10 mm, the tumors were irradiated with an X-ray beam generated from a 6-MeV linear accelerator (NEC/Varian) with a sharp collimation to a 10 × 10 mm irradiation area. With a therapeutic dose of 65 Gy, the tumors stopped growing and started to regress with an average time of six days for regression to half of their volume, and then disappeared as shown in Fig. 1b (Tanooka et al., 1980). However, all the tumors reappeared at the treated sites 60–110 days after treatment and they grew at a volume-doubling time of 2.7 days, the same growth speed as the original tumors.

This paper is dedicated to Professor Guenter Obe for his retirement.

Received 10 September 2003; manuscript accepted 22 November 2003.

Request reprints from Hiroshi Tanooka

National Institute of Radiological Sciences  
Anagawa, Inage-ku, Chiba 263-8555 (Japan)  
telephone: +81-43-206-3090; fax: +81-43-255-6497  
e-mail: tnk@nirs.go.jp

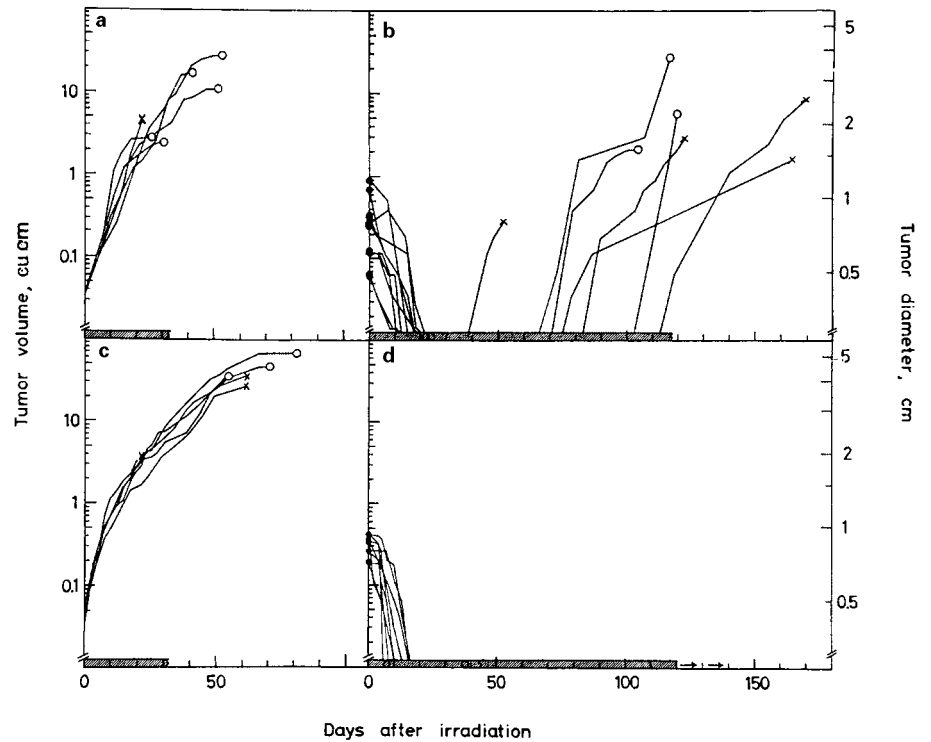


**Fig. 1.** Growth of MCA-induced autochthonous tumors (a) and volume changes after local irradiation with a collimated beam of X-rays (b). Growth of transplanted tumors (c) and volume changes after local irradiation (d). Radiation dose: 65 Gy. (Tanooka et al., 1980; quoted with permission of publisher).

In contrast, tumors transplanted from an MCA-induced primary tumor into recipient mice (Fig. 1c) responded differently. When treated in an identical manner as the primary tumors with linear accelerator-generated X-rays, they disappeared and showed a complete cure, i. e., no reappearance for 120 days after treatment by definition of the cure for experimental tumors (Fig. 1d). The 50% tumor cure dose (TCD<sub>50</sub>) was 42 Gy and a complete cure was achieved with 65–74 Gy (Tanooka et al., 1980) which is in accord with results obtained from other experimental systems with transplanted tumors. Gross radiation sensitivity of tumor cells in the autochthonous tumors was the same as that for the transplanted tumors, as estimated from tumor recurrence time, i. e.,  $D_{37} = 4$  Gy. Some intrinsic factors involved in the radiation response of tumors are different between autochthonous and transplanted tumors. This raises the question of whether the transplanted tumor system is an appropriate test system to determine a treatment regimen for the achievement of a true cure of tumors.

To answer this question, the clonal nature of apparently recurring tumors has to be clarified. The question is: Are they true recurrent tumors or newly induced tumors? If tumors are true recurrent tumors, they will maintain the same clonal nature as the primary tumor. On the other hand, if apparently recurrent tumors are actually newly induced second tumors, a new clonal nature should be seen.

To pursue this problem, application of the mouse system with X chromosome inactivation-mediated cellular mosaicism is a powerful method. The first step is the examination of the clonal nature of experimentally induced tumors.

### Clonal nature of experimental tumors

Studying the clonal nature of tumors themselves is an important task in cancer research as discussed earlier (Tanooka, 1988). X chromosome inactivation-mediated mosaicism of somatic cells is created by random inactivation of one of a pair of X chromosomes (Lyon, 1961) through methylation (Mohandas et al., 1981). Under the assumption that X chromosome inactivation is not disturbed during tumorigenesis, if a tumor is a clone of a single somatic cell, all tumor cells grown from this origin should show the same X inactivation pattern. This system was first applied by Fialkow (1976) to test the clonal nature of human tumors formed in females with a cellular mosaicism for the X chromosome-linked gene of glucose-6-phosphate dehydrogenase (G6PD). The results showed that almost all tested human tumors were monoclonal. New markers for human tumors are now available as described later.

In mice, a variety of X chromosome-linked markers are available. In a series of our experiments, we employed a mutant of the X-linked gene for phosphoglycerate kinase (*pgk-1<sup>a</sup>*). The mutant *pgk-1<sup>a</sup>* mice were supplied by Dr. Chapman (Nielsen and Chapman, 1977). Female mice heterozygous at the *pgk-1* allele on X-chromosome (*pgk-1<sup>a</sup>/pgk-1<sup>b</sup>*) carry somatic cells of two PGK types in a mosaic manner. The mutant and normal PGK phenotypes are distinguishable from electrophoretic patterns. Tumors induced by subcutaneous injection of MCA in the mosaic mice showed a single PGK pattern (A or B) and, with a higher dose of MCA shifted into a polyclonal pattern (AB) (Tanooka et al., 1982). Using PGK mosaic mice, a variety of tumors produced with different carcinogenic agents have

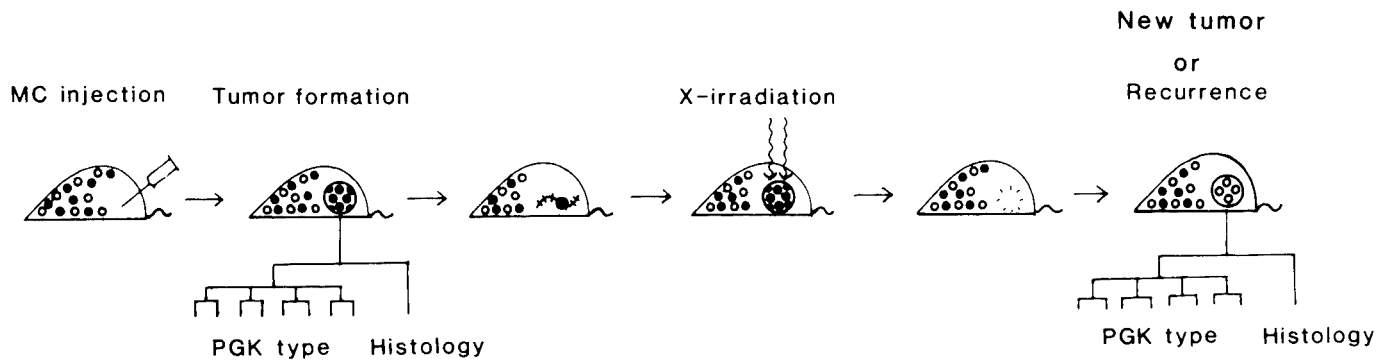


**Fig. 2.** A time schedule of tumor recurrence test. Tumor was induced in a *pgk-1<sup>a</sup>/pgk-1<sup>b</sup>* mosaic cell mouse by subcutaneous injection of MCA into the groin. A part of tumor was resected and examined for PGK and histological types. After tumor regrew to 10 mm diameter, it was irradiated locally with a therapeutic dose. Tumor disappeared once and reappeared after a latent period. PGK and histological types were examined and compared with those of the primary tumor (Tanooka and Tanaka, 1985; quoted with permission of publisher).

**Table 1.** Experimental tumors that were proven to be monoclonal with mice X chromosome inactivation-mediated cellular mosaicism

Organ	Tumor	Carcinogen <sup>a</sup>	Reference
Skin	Fibrosarcoma	MCA	Tanooka and Tanaka 1982, 1984 Woodruff et al. 1982
	Papilloma	DMBA+(TPA)	Deamant and Iannaccone Reddy and Fialkow 1983a Taguchi et al. 1984
	Squamous cell carcinoma	DMBA+(TPA)	Taguchi et al. 1984
	Spindle cell carcinoma	UV	Kim-Burnham et al. 1986
Bladder	Adenocarcinoma	BHBN	Kakizoe et al. 1983
Liver	Preneoplastic nodule	AAF	Rabes et al. 1982
	Hepatocellular carcinoma	PB alone or with NDEA	Williams et al. 1983 Howell et al. 1983
Stomach	Papilloma	DEN	Fukushima et al. 1986
Colon	Adenocarcinoma	DMH	Inoue et al. 1986
Blood forming organ	AKR leukemia	virus	Collins and Fialkow 1982
	Rauscher leukemia	virus	Reddy and Fialkow 1983b
	Thymic lymphoma	X rays	Bessho et al. 1984
	Myeloid leukemia	X rays	Bessho and Hirashima 1987
Mammary gland	Adenocarcinoma	MTV	Tanaka et al. 1984 Ootsuyama et al. 1987

<sup>a</sup> AAF:2-acetylaminofluorene; BHBN: N-butyl-N-(4-hydroxybutyl)nitrosamine; DEN: diethylnitrosamine; DMBA: 7,12-dimethylbenz[a]anthracene; DMH: 1,2-dimethylhydrazine; MCA: 3-methylcholanthrene; MTV: mammary tumor virus; NDEA: N-nitrosodiethanolamine; PB: phenobarbitone; TPA: 12-O-tetradecanoylphorbol-13-acetate.

been shown to possess a monoclonal nature (Table 1). It is noted that benign tumors such as preneoplastic nodules in the liver (Rabes et al., 1982), papillomas in the skin (Taguchi et al., 1984), and preleukemic cells (Bessho and Hirashima, 1987) are already monoclonal before becoming malignant. However, benign tumors are different from hyperplasia of a polyclonal nature, a cell population formed by uniform cell growth.

Mice carrying Cattanach translocation (T[X;7]1CT) between an autosome and the X chromosome which provides a visible pattern of X inactivation mosaicism are useful for such studies (Cattanach, 1961). MCA-induced tumors in these mice showed a monoclonal pattern (Takagi et al., 1986). One case was found where two Cattanach chromosomes were simultaneously replicating in each of the single cells of a tumor, indicating the possibility that a monoclonal tumor might have origi-

inated from a single fused cell. To test this hypothesis, a hybrid of *Mus caroli* with G6PD-mosaic cells carrying the X-linked G6PD mutation was used to look for the presence of the G6PD dimers which are expected to be formed in the fused cells (Tanaka et al., 2000).

Another useful X-linked marker is a restriction fragment length polymorphism (Vogelstein et al., 1985, 1987), by which the monoclonal nature of experimental tumors has been shown. Recently, a new molecular X chromosome-linked marker, a repeat of the trinucleotide sequence GAC in the androgen-receptor gene which is susceptible to methylation in association with X chromosome inactivation (Allen et al., 1992) was used to study the clonal nature of human tumors. The population of females who are heterozygous for this gene locus and carry the cellular mosaicism is very high, i. e., 90%. From restriction pat-

terns of tumor DNA, the monoclonal nature has been shown for seborrheic keratosis in the skin (Nakamura et al., 2001). Interestingly, with this genetic marker it could be shown that diffuse proliferation of interstitial cells of Cajal in patients with familial and multiple gastrointestinal stromal tumors was polyclonal, while gastrointestinal stromal tumors were monoclonal (Chen et al., 2002).

The question to be asked here is why only one clone appears as a tumor in the background of many mutated cells or many tumor origins. A clonal-selection model was proposed by Woodruff et al. (1982). A full answer to this question remains to be obtained by future study.

### Test for clonal nature of recurrent tumors

Our test system is shown in Fig. 2. The tumors were induced by subcutaneous injection with MCA into the groin of *pgk-1<sup>a</sup>/pgk-1<sup>b</sup>* mosaic mice. After they appeared and grew to 1 cm in diameter, parts of the tumors were resected for histology and determination of PGK types. When tumors had regrown to 10 mm in diameter, they were locally irradiated with a collimated X-ray beam from a linear accelerator with a dose of 40 or 60 Gy. The tumors disappeared, but regrew at the treated site after a latent period. These regrown tumors were subjected to histology and determination of PGK types for comparison with those of the original tumors. Only one tumor out of 17 showed a discrepancy of PGK types and histology between the primary tumor and the secondary tumor, indicating the induction of a new tumor after radiation treatment. The majority, 13 cases, showed the same PGK types and histology. The possibility that a newly induced tumor shows the same characteristics as the

primary tumor cannot be ruled out. However, this result indicates that the majority of tumors reappearing after radiation treatment are due to true recurrence.

Such a clonality test is useful to determine the recurrence of human tumors. The recurrence of leukemia after chemotherapy has been examined for G6PD mosaic females (Fialkow, 1976). A new molecular marker in the androgen receptor gene is now available to test for tumor recurrence in human females (Kitamura et al., 2003). The development of a new system with X chromosome-mediated cellular mosaicism will provide a further powerful method for the identification of the true recurrence of cancers.

### Conclusion

X chromosome inactivation-mediated cellular mosaicism is a useful tool to examine the clonal nature of experimental and human tumors, the majority of which have been shown to be monoclonal. Furthermore, this method can be applied to differentiate between true recurrence and new tumor induction in tumors of experimental animals and humans after therapeutic treatment. The question of why only one single cell can develop into a tumor still remains to be answered. The achievement of a true cure is the final goal of cancer therapy.

### Acknowledgements

The author gratefully acknowledges the useful discussions with Dr. Kouichi Tatsumi, the National Institute of Radiological Sciences, Dr. Yukihiko Kitamura, Osaka University Medical School, and Dr. Nobuo Munakata, then at the National Cancer Center.

### References

- Allen RC, Zoghbi HY, Moseley AB, Rosenblatt HM, Belmont JW: Methylation of *HpaII* and *HhaI* sites near the polymorphic CAG repeat in the human androgen-receptor gene correlates with X chromosome inactivation. *Am J hum Genet* 51:1229–1239 (1992).
- Bessho M, Hirashima K: Clonal origin of radiation-induced myeloid leukemia in mice with cellular mosaicism. *Jpn J Cancer Res* 78:670–673 (1987).
- Bessho M, Jinnai I, Hiroshima K, Tanaka K, Tanooka H: Single cell origin of radiation-induced thymic lymphomas in mice with cellular mosaicism. *Jpn J Cancer Res* 75:1002–1005 (1984).
- Cattanach BM: A chemically-induced variegated-type position effect in the mouse. *Z Vererbungsl* 92:165–182 (1961).
- Collins SJ, Fialkow PJ: Clonal nature of spontaneous AKR Leukemia: studies utilizing the X-linked enzyme phosphoglycerate kinase. *Int J Cancer* 29:673–676 (1982).
- Chen H, Hirota S, Isozaki D, Sun H, Ohashi A, Konoshita K, O'Brien P, Kpusta L, Dardick I, Obayashi T, Okazaki T, Shinomura Y, Matuzawa Y, Kitamura Y: Polyclonal nature of diffuse proliferation of interstitial cells of Cajal in patients with familial and multiple gastrointestinal stromal tumors. *Gut* 51:793–796 (2002).
- Deamant FD, Iannaccone PM: Evidence concerning the clonal nature of chemically induced tumors: phosphoglycerate kinase-1 isozyme patterns in chemically induced fibrosarcomas. *J natl Cancer Inst* 74:145–150 (1985).
- Fialkow PJ: Clonal origin of human tumors. *Biochim biophys Acta* 458:283–321 (1976).
- Fukushima Y, Shinozaki H, Mori T, Inoue M, Kitamura Y: Clonal origin of mouse forestomach tumors induced by diethylnitrosamine (DEN). *Proc Jpn Cancer Assoc 45th Annu Meet* (1986).
- Howell S, Wareham KA, Williams ED: Clonal origin mouse liver cell tumors. *Am J Pathol* 121:426–432 (1983).
- Inoue M, Taguchi T, Kitamura Y, Fukushima Y, Mori T: Clonal origin of mouse colon tumors induced by 1,2-dimethylhydrazine. *Proc Jpn Cancer Assoc 45th Annu Meet* (1986).
- Kakizoe T, Tanooka H, Tanaka K, Sugimura T: Single-cell origin of bladder cancer induced by N-butyl-N-(4-hydroxybutyl) nitrosoamine in mice with cellular mosaicism. *Jpn J Cancer Res* 74:462–463 (1983).
- Kim-Burnham D, Gahring IC, Daynes RA: Clonal origin of tumors induced by ultraviolet radiation. *J natl Cancer Inst* 76:151–157 (1986).
- Kitamura Y, Hirota S, Nishida T: Gastrointestinal stromal tumors (GIST): A model for molecule-based diagnosis and treatment of solid tumors. *Cancer Sci* 94:315–320 (2003).
- Lyon MF: Gene action in X-chromosome of the mouse (*Mus musculus* L.). *Nature* 190:372–373 (1961).
- Mohandas T, Sparkes RE, Shapiro JJ: Reactivation of inactive human X-chromosome: evidence for X-inactivation by DNA methylation. *Science* 211:393–396 (1981).
- Nakamura H, Hirota S, Adachi S, Ozaki K, Asada H, Kitamura Y: Clonal nature of seborrheic keratosis demonstrated by using the polymorphism of the human androgen receptor locus as a marker. *J Invest Dermatol* 116:506–510 (2001).
- Nielsen JT, Chapman VM: Electrophoretic variation for X-chromosome-linked phosphoglycerate kinase (P<sub>gk</sub>-1) in the mouse. *Genetics* 87:319–325 (1977).
- Ootsuyama A, Tanaka K, Tanooka H: Evidence by cellular mosaicism for monoclonal metastasis of spontaneous mouse mammary tumors. *J natl Cancer Inst* 78:1223–1227 (1987).
- Rabes HM, Bucher TH, Hartman A, Kinke I, Dunnwald M: Clonal growth of carcinogen-induced enzyme-deficient preneoplastic cell populations in mouse liver. *Cancer Res* 42:3220–3227 (1982).

- Reddy AI, Fialkow PJ: Papillomas induced by initiation-promotion differ from those induced by carcinogen alone. *Nature* 304:69–71 (1983a).
- Reddy AI, Fialkow PJ: Clonal development of lymphomas induced by Rauscher leukemia virus. *Int J Cancer* 31:107–109 (1983b).
- Taguchi T, Yokoyama M, Kitamura Y: Intracлонаl conversion from papilloma to carcinoma in the skin of *Pgk-1<sup>a</sup>/Pgk-1<sup>b</sup>* mice treated by a complete carcinogenesis process by an initiation-promotion regimen. *Cancer Res* 44:3779–3782 (1984).
- Takagi N, Ootuyama A, Tanooka H: Cytological evidence for single-cell origin of tumors induced with 3-methylcholanthrene in female mice carrying Cattanach's translocation. *Jpn J Cancer Res* 77:376–384 (1986).
- Tanaka K, Ootsuyama A, Tanooka H: Clonal origin of spontaneous multiple mammary tumors in mice with cellular mosaicism. *Jpn J Cancer Res* 75:792–797 (1984).
- Tanaka K, Ootsuyama A, Tanooka H: Test for fused-cell origin of tumors with *Mus caroli* carrying glucose-6-phosphate dehydrogenase cellular mosaicism. *Oncol Report* 7:897–898 (2000).
- Tanooka H: Monoclonal growth of cancer cells: Experimental evidence. *Jpn J Cancer Res* 79:657–665 (1988).
- Tanooka H, Tanaka K: Evidence for single-cell origin of 3-methylcholanthrene-induced fibrosarcomas in mice with cellular mosaicism. *Cancer Res* 42:1856–1858 (1982).
- Tanooka H, Tanaka K: Dose response of monoclonal tumor induction with 3-methylcholanthrene in mosaic mice. *Cancer Res* 44:4630–4632 (1984).
- Tanooka H, Tanaka K: Test of recurrence after experimental radiation therapy of chemically induced autochthonous tumors in mosaic mice. *Int J Radiat Oncol Biol Phys* 11:1331–1333 (1985).
- Tanooka H, Hoshino H, Tanaka K, Nagase M: Experimental radiation therapy and apparent radioresistance of autochthonous tumors subcutaneously induced with 3-methylcholanthrene in mice. *Cancer Res* 40:2547–2551 (1980).
- Tanooka H, Tanaka K, Arimoto H: Dose response and growth rates of subcutaneous tumors induced with 3-methylcholanthrene in mice and timing of tumor origin. *Cancer Res* 42:4740–4743 (1982).
- Talmage JE, Wolman SR, Fidler IJ: Evidence for the clonal origin of spontaneous metastasis. *Science* 217:361–363 (1982).
- Vogelstein B, Fearon ER, Hamilton SR, Feinberg AD: Use of restriction fragment length polymorphisms to determine the clonal origin of human tumors. *Science* 227:642–645 (1985).
- Vogelstein B, Fearon ER, Hamilton SR, Preisinger AC, Willard HF, Michelson AM, Riggs AD, Orkin SH: Clonal analysis using recombinant DNA probes from the X-chromosome. *Cancer Res* 47:4806–4813 (1987).
- Williams ED, Wareham KA, Howell S: Direct evidence for the single cell origin of mouse liver cell tumors. *Br J Cancer* 47:723–726 (1983).
- Woodruff MFA, Ansell JD, Forbes GM, Gordon JC, Burton DI, Micklem HS: Clonal interaction in tumors. *Nature* 299:823–825 (1982).

# Chromosomal mutagen sensitivity associated with mutations in BRCA genes

G. Speit and K. Trenz

Universitätsklinikum Ulm, Abteilung Humangenetik, Ulm (Germany)

**Abstract.** Chromosomal mutagen sensitivity is a common feature of cells from patients with different kinds of cancer. A portion of breast cancer patients also shows an elevated sensitivity to the induction of chromosome damage in cells exposed to ionizing radiation or chemical mutagens. Segregation analysis in families of patients with breast cancer indicated heritability of mutagen sensitivity. It has therefore been suggested that mutations in low-penetrance genes which are possibly involved in DNA repair predispose a substantial portion of breast cancer patients. Chromosomal mutagen sensitivity has been determined with the G<sub>2</sub> chromosome aberration test and the G<sub>0</sub> micronucleus test (MNT). However, there seems to be no clear correlation between the results from the two tests, indicating that the inherited defect leading to enhanced G<sub>0</sub> sensitivity is different from that causing G<sub>2</sub> sensitivity. Less than 5% of breast cancer patients have a familial form of the disease due to inherited mutations in the breast cancer susceptibility genes BRCA1 or BRCA2. Heterozygous mutations in BRCA1 or BRCA2 in lymphocytes from women with familial breast cancer are also associated with mutagen sensitivity. Differentiation between mutation carriers and controls seems to be much better with the MNT than with the G<sub>2</sub> assay. Mutagen sensitivity

was detected with the MNT not only after irradiation but also after treatment with chemical mutagens including various cytostatics. The enhanced formation of micronuclei after exposure of lymphocytes to these substances suggests that different DNA repair pathways are affected by a BRCA1 mutation in accordance with the proposed central role of BRCA1 in maintaining genomic integrity. Mutations in BRCA1 and BRCA2 seem to predispose cells to an increased risk of mutagenesis and transformation after exposure to radiation or cytostatics. This raises a question about potentially increased risks by mammography and cancer therapy in women carrying a mutation in one of the BRCA genes. Lymphoblastoid cell lines (LCLs) from breast cancer patients have been used to study the mechanisms and genetic changes associated with tumorigenesis. With respect to mutagen sensitivity, conflicting results have been reported. In particular enhanced induction of micronuclei does not seem to be a general feature of LCLs with a BRCA1 mutation in contrast to lymphocytes with the same mutation. Therefore, LCLs are of limited utility for studying the mechanisms underlying chromosomal mutagen sensitivity.

Copyright © 2003 S. Karger AG, Basel

DNA repair mechanisms constantly monitor the genome and repair DNA damage resulting from exposure to environmental and endogenous mutagens. Cells deficient in DNA repair capacity become hypersensitive towards mutagens, hypermutable and more susceptible to transformation (for review

see Hoeijmakers, 2001). Mutagen sensitivity, i.e. enhanced response of cells to the DNA-damaging action of mutagens/carcinogens has been described repeatedly as a potential marker of susceptibility to cancer in humans. Most studies are based on an approach that compares induced DNA damage to lymphocytes from subjects with cancer with induced DNA damage to lymphocytes from subjects without cancer (for review see Berwick and Vineis, 2000; Berwick et al., 2002). Cytogenetic endpoints such as chromosome aberrations, micronuclei and sister chromatid exchanges (SCEs) have frequently been used for the determination of DNA damage on the chromosome level (Tucker and Preston, 1996). Chromosomal sensitivity to radiation and chemical mutagens has been proposed as a marker for low penetrance predisposition to various common cancers

Supported by the Deutsche Forschungsgemeinschaft (SP 274/8-1).

Received 9 September 2003; manuscript accepted 24 November 2003.

Request reprints from Dr. Günter Speit

Universitätsklinikum Ulm, Abteilung Humangenetik

D-89070 Ulm (Germany)

telephone: +49-731-50023429; fax: +49-731-50023438

e-mail: guenter.speit@medizin.uni-ulm.de

including breast cancer (Baria et al., 2001b). Breast cancer patients have been tested for mutagen sensitivity in various studies (Helzlsouer et al., 1995, 1996; Parshad et al., 1996; Patel et al., 1997; Rao et al., 1998; Scott et al., 1998, 1999; Roberts et al., 1999; Burrill et al., 2000; Rothfuss et al., 2000; Roy et al., 2000; Baria et al., 2001a, b; Baeyens et al., 2002; Buchholz et al., 2002; Trenz et al., 2002, 2003b). Compared with normal healthy controls, a clearly increased portion of breast cancer patients has an enhanced sensitivity to the chromosome-damaging effects of ionizing radiation and other mutagens. The amount of mutagen-sensitive individuals was much higher than the known percentage of individuals with a strong genetic predisposition, caused by highly penetrant genes such as BRCA1 and BRCA2. Therefore, it has been suggested that similar to some other common cancers, a substantial portion of breast cancer patients may carry mutations in low penetrance genes, which may be genes involved in the processing of DNA damage (Parshad et al., 1996; Roberts et al., 1999; Scott et al., 1999; Burrill et al., 2000). Only few studies investigated chromosomal mutagen sensitivity in cells from patients with mutations in BRCA1 or BRCA2 (Rothfuss et al., 2000; Baria et al., 2001a; Baeyens et al., 2002; Buchholz et al., 2002; Trenz et al., 2002, 2003b). Mutagen sensitivity was determined in variable portions of the studied groups depending on the method used to measure mutagen sensitivity. These data will be critically reviewed and the possible mechanisms involved in mutagen sensitivity of cells from breast cancer patients with mutations in BRCA1 or BRCA2 will be discussed.

#### **Detection of chromosomal mutagen sensitivity in cells from breast cancer patients**

Various approaches have been used to determine mutagen sensitivity in cultivated cells from breast cancer patients. The most common test for the detection of mutagen sensitivity is the G<sub>2</sub> chromosome aberration test (Scott et al., 1994, 1999). This assay is based on the induction of chromosome damage in lymphocytes in the G<sub>2</sub> phase of the cell cycle by ionizing radiation and the analysis of metaphase chromosomes in the next mitosis. An increased frequency of induced chromatid breaks is assumed to express enhanced mutagen sensitivity and reduced DNA repair capacity. Alternatively, the G<sub>0</sub> micronucleus test (MNT) has been used (Scott et al., 1998, 1999; Rothfuss et al., 2000; Baria et al., 2001a; Baeyens et al., 2002; Trenz et al., 2002, 2003b). In this assay, cells in G<sub>0</sub> rather than in G<sub>2</sub> are exposed to radiation or chemical mutagens and the frequency of micronuclei is determined after one cell division in the next G<sub>1</sub> phase. Cytochalasin B is usually used in this assay to allow identification of postmitotic cells as binucleates (Fenech, 1997). The MNT simplifies and speeds up the assessment of mutagen sensitivity because it requires less time and cytogenetic expertise than the analysis of metaphase chromosomes. Both, chromosome aberrations and micronuclei mainly reflect the erroneous result from a cell's attempt to handle DNA damage and thus indirectly also indicate repair capacity. With respect to irradiation, high dose rate (HDR) and low dose rate (LDR) were comparatively investigated under the assumption that

LDR allows more repair and thus better discriminates between sensitive and non-sensitive individuals (Scott et al., 1998; Baeyens et al., 2002).

Besides these two endpoints for chromosome mutations, indicator endpoints such as sister chromatid exchanges (SCE test) and DNA strand breaks (comet assay) have been used to study mutagen sensitivity in cells from breast cancer patients (Cianciulli et al., 1995; Jalszynski et al., 1997; Abrahams et al., 1998; Alapetite et al., 1999; Rajeswari et al., 2000; Roy et al., 2000; Nieuwenhuis et al., 2002; Trenz et al., 2002, 2003b; Smith et al., 2003). Effects in indicator tests mainly represent the amount of induced DNA damage after mutagen exposure. The comet assay is also used for measuring repair (e.g. monitoring the time-dependent removal of lesions) but this approach just measures the speed of damage removal and not the fidelity of strand break rejoining (Speit and Hartmann, 1999). Conflicting results have been reported for the SCE test and the comet assay with regard to effects in cells from breast cancer patients. These studies have been discussed previously (Trenz et al., 2002, 2003b) and will not be considered in detail here.

#### **Breast cancer and mutagen sensitivity**

Breast cancer is the most common type of cancer in females but only about 2% of breast cancer cases are related to rare but highly penetrant genes, such as BRCA1 and BRCA2 (Peto et al., 1999). Low-penetrance cancer susceptibility genes, which are more common, might therefore mainly contribute to a large proportion of breast cancer cases (Teare et al., 1994; Roberts et al., 1999). In particular, genetic variability in DNA repair genes might contribute to mutagen sensitivity and cancer susceptibility (Hu et al., 2002; Mohrenweiser, 2002). Like other inherited cancer-prone conditions, a portion of breast cancer patients showed an elevated sensitivity to the induction of chromosome damage in cells exposed to ionizing radiation (Scott et al., 1994, 1999; Parshad et al., 1996; Patel et al., 1997; Terzoudi et al., 2000; Baria et al., 2001b; Riches et al., 2001; Baeyens et al., 2002). In these studies, the G<sub>2</sub> chromosome aberration test was used to evaluate chromosomal radiosensitivity and enhanced chromosome breakage was observed in sporadic breast cancer patients in all of these studies. Using the 90th percentile of the population of healthy donors as a cut off value for radiosensitivity, approximately 40% of breast cancer cases showed elevated chromosomal radiosensitivity (Scott et al., 1994; Parshad et al., 1996; Baeyens et al., 2002).

The MNT has been used in some studies (Scott et al., 1998, 1999; Burrill et al., 2000; Baeyens et al., 2002). It has been shown in all of these studies that the MNT also detects breast cancer patients compared with healthy controls as having elevated radiation sensitivity. Using the 90th percentile of the population of healthy donors as a cut off value for radiosensitivity, between 15 and 60% of breast cancer cases showed elevated chromosomal radiosensitivity in the MNT. Interestingly, LDR irradiation led to a better discrimination between breast cancer patients and controls than HDR irradiation in one study (Baeyens et al., 2002) but not in another study (Scott et al., 1998). Baeyens et al. (2002) also reported a much higher pro-

portion of radiosensitive breast cancer patients (45% with HDR and 61% with LDR) in comparison with Scott et al. (1998) who detected 31% with HDR and 15% with LDR. In both studies, there was only a weak correlation between HDR and LDR responses in patients and controls. This difference may in part be due to experimental variability but may also indicate that the HDR and the LDR assay detect different mechanisms of chromosomal radiosensitivity. Lack of correlation was also observed between the results from the G<sub>2</sub> chromosome aberration test and the (G<sub>0</sub>) MNT (Scott et al., 1999; Baeyens et al., 2002). It has been suggested by Scott et al. (1999) that the inherited defect leading to enhanced G<sub>0</sub> sensitivity is different from that responsible for G<sub>2</sub> sensitivity. Possibly, different DNA repair mechanisms are affected after G<sub>0</sub> or G<sub>2</sub> phase mutagen exposure but both contribute to mutagen sensitivity.

One important aspect in such kind of studies is the potential influence of the presence of a tumor and previous radio- and/or chemotherapy on the determination of mutagen sensitivity. Roberts et al. (1999) did not find significant differences in the G<sub>2</sub> chromosome aberration test between pre- and post-therapy samples. In accordance with these data, Baeyens et al. (2002), using the G<sub>2</sub> assay, did not find significant differences in chromosomal radiosensitivity between groups of patients with and without therapy. In contrast to these observations, the mean spontaneous micronucleus frequency in the group of breast cancer patients was significantly increased compared to the mean spontaneous micronucleus yield in controls in the same study and associated with previous radio- and/or chemotherapy (Baeyens et al., 2002). However, it might also be possible that increased spontaneous micronucleus frequencies reflect genomic instability of cells from cancer patients.

Segregation analysis in families of patients with breast cancer showed evidence of heritability of radiosensitivity (Roberts et al., 1999; Burrill et al., 2000). The proportion of sensitive cases in all of these studies was higher than the expected amount of mutation carriers in BRCA1 or BRCA2. However, since the presence of mutations in BRCA1 and BRCA2 was not determined in these studies, it remained unclear whether mutations in these breast cancer susceptibility genes are related to radiosensitivity.

### **Mutagen sensitivity associated with mutations in BRCA1 and BRCA2**

Besides other cellular functions, BRCA1 and BRCA2 maintain genomic stability through an involvement in DNA repair processes (Venkitaraman, 2001). It was known that deficiency in BRCA1 leads to radiosensitivity in cell lines (Abbott et al., 1999). We therefore evaluated the effect of a heterozygous mutation in BRCA1 or BRCA2 on radiation sensitivity of lymphocytes in the MNT and the utility of the MNT as a screening test for mutations in the breast cancer susceptibility genes BRCA1 and BRCA2 in breast cancer families. Our first results indicated a close relationship between the presence of a heterozygous BRCA1 mutation and sensitivity for the induction of micronuclei by gamma irradiation and H<sub>2</sub>O<sub>2</sub> (Rothfuss et al.,

2000). In this study, ten of eleven women with a BRCA1 mutation showed elevated radiation sensitivity in the MNT when compared to a concurrent control. However, using the +2 standard deviations from the mean micronucleus frequency of the control group as a cut off, 58% (7 out of 12) of BRCA1 mutation carriers were sensitive. In their reply to this study, Baria et al. (2001a) compared healthy BRCA1 mutation carriers (n = 9) with controls (n = 5) from families with BRCA1 mutations who did not themselves carry these mutations with the G<sub>2</sub> chromosome aberration test and did not find a difference between the two groups. The authors concluded that also with respect to the BRCA1 gene, the two assays seem to detect independent kinds of radiosensitivity and suggested that the BRCA1 gene product is involved in the G<sub>0</sub> but not in the G<sub>2</sub> defense mechanism. In their comparative study with the G<sub>2</sub> assay and the MNT, Baeyens et al. (2002) included women (n = 11) carrying either a BRCA1 or a BRCA2 mutation. Among them 27% were sensitive in the G<sub>2</sub> assay, 33% in the MNT with HDR and 78% in the MNT with LDR. The combined investigation of carriers with BRCA1 or BRCA2 mutations seems to be justified in accordance with our results indicating that there is no fundamental difference between BRCA1 and BRCA2 mutation carriers with respect to chromosomal radiosensitivity in the MNT (Trenz et al., 2002). An association between radiation sensitivity and mutations in BRCA1 and BRCA2 was also confirmed in a study with lymphocytes and fibroblasts (Buchholz et al., 2002). With lymphocytes, the G<sub>2</sub> chromosome aberration test was performed while for fibroblasts the surviving fraction of cells after 2 Gy irradiation was determined. Both endpoints clearly indicated increased radiosensitivity of the two cell types carrying a mutation. There was no apparent difference in the radiosensitivity between cells with BRCA1 and BRCA2 mutations. However, the sample size was small and the percentage of sensitive cases was not calculated. In the meantime, we tested 24 cases with a BRCA1 mutation, nine cases with a BRCA2 mutation and 22 controls (Rothfuss et al., 2000; Trenz et al., 2002, 2003b; unpublished results). The results of this ongoing study are summarized in Fig. 1. Using the 90th percentile as a cut off point for sensitivity, 54% of the BRCA1 cases, 78% of the BRCA2 cases and 5% of the controls are sensitive (Fig. 2). A direct comparison of cases with concurrent controls as suggested earlier (Rothfuss et al., 2000) identified 78% of the BRCA1 cases and 79% of the BRCA2 cases as being sensitive in the sample shown in Fig. 1. This difference indicates that methodological factors influence the outcome of the test and reduction of inter-test variability can improve the discrimination between mutation carriers and controls. The source and type of irradiation might be of crucial importance for the detection of mutagen sensitivity in the MNT but it is still unclear which kind of irradiation is optimal. While the results of Baeyens et al. (2002) indicate a better discrimination with LDR we identified a similar percentage of mutation carriers with HDR. However, we did not have the chance to perform comparative experiments with LDR up to now.

Although some data suggest that the presence of a tumor and cancer therapy do not fundamentally modify mutagen sensitivity (Roberts et al., 1999; Baeyens et al., 2002), the available results do not completely exclude a significant influence of the



**Fig. 1.** Box plot of the spontaneous and radiation-induced (2 Gy  $^{137}\text{Cs}$  gamma rays; 4 Gy/min) micronucleus (MN) frequencies in women with BRCA1 (n = 24) or BRCA2 (n = 9) mutations and controls (n = 22). The solid line indicates the median for each group, the box edges mark the 25th and 75th percentile of the observed values and the T-bars indicate the 10th and 90th percentiles.

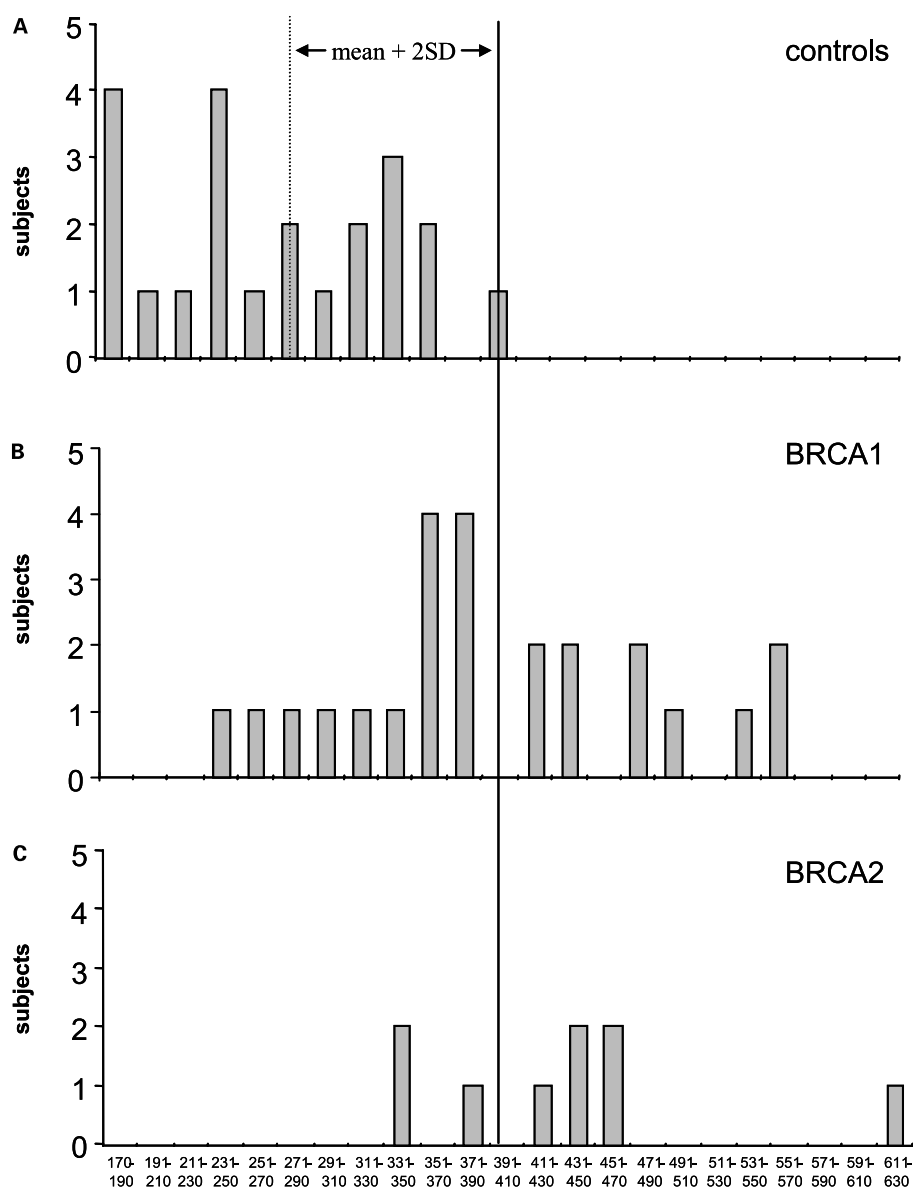
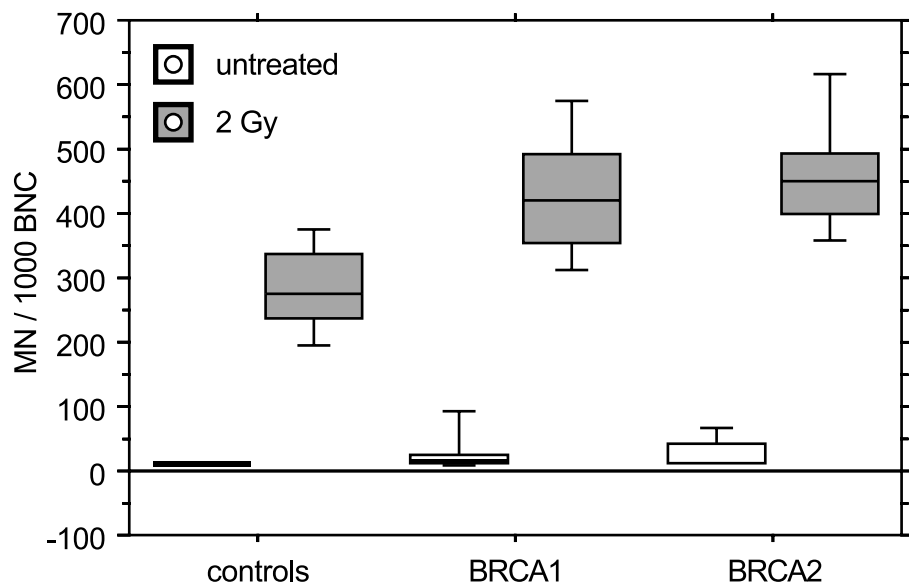


**Fig. 2.** Induced micronucleus frequencies (2 Gy  $^{137}\text{Cs}$  gamma rays; 4 Gy/min) in (A) control subjects (n = 22), (B) women with BRCA1 mutation (n = 24) and (C) in women with BRCA2 mutations (n = 9). Dashed line, mean MN frequency of the control group; solid line, mean + 2 SD.

test outcome. It is interesting to note that Baria et al. (2001a) tested nine healthy mutation carriers with the G<sub>2</sub> assay and did not find mutagen sensitivity in any of the cases. In contrast, Baeyens et al. (2002) used blood samples from women after breast surgery and radio/chemotherapy (range: 9 months to 21 years) and identified three radiosensitive cases out of eleven patients. This might indicate that mutagen sensitivity in the G<sub>2</sub> assay is more closely related to the presence of the tumor than to a mutation in a BRCA gene. However, in our sample three out of four healthy women with a mutation exhibited radiosensitivity in the MNT. These inhomogenous results again indicate differences between the two cytogenetic tests. The high association between the presence of a BRCA1 mutation and radiosensitivity in the MNT suggests a causal relationship, but chromosomal radiosensitivity is obviously not strictly related to specific types or locations of mutations. Our sample included eleven different mutations, the majority being truncating and, therefore, inactivating. The mutations were distributed throughout the coding region of the BRCA1 gene. Therefore, a genotype-phenotype relationship for mutagen sensitivity cannot be established at present. Although there is considerable variability in chromosomal mutagen sensitivity in the MNT among individuals, independently repeated tests (two or three) for 15 of our patients indicated good reproducibility of the first test result (unpublished results). Further studies are needed to prove a causal relationship between heterozygous BRCA mutations and chromosomal mutagen sensitivity and the utility of the MNT as a functional assay of the BRCA mutation status.

#### **Lymphoblastoid cell lines (LCLs) with BRCA 1 mutations as a model for studying mutagen sensitivity**

Chromosomal mutagen sensitivity has mainly been studied with human lymphocytes. However, blood from women with breast cancer is not always repeatedly available for various reasons and the use of blood samples is limited due to the limited lifespan of lymphocytes in culture. Therefore, the utilization of permanent cell cultures is desirable particularly for *in vitro* studies on the mechanisms involved in mutagen sensitivity. Cell lines provide an unlimited source of cells for basic research and can be widely distributed to facilitate comparative studies. However, the use of cell lines can be limited due to problems related to the establishment and long-term cultivation of the cells. Specific features of the primary cells may be changed or lost as a consequence of genetic changes occurring in cell lines. Lymphoblastoid cell lines (LCLs) should be an appropriate *in vitro* model because they can be established easily and transformation with Epstein-Barr virus (EBV) in general does not lead to gross genomic instabilities and loss of genetic characteristics. LCLs from breast cancer patients have been used repeatedly to study radiation sensitivity (Lavin et al., 1994; Ramsey and Birrell, 1995; Foray et al., 1999; Speit et al., 2000; Baldeyron et al., 2002; Trenz et al., 2003a).

Lavin et al. (1994) have demonstrated enhanced radiation sensitivity of LCLs from breast cancer patients when screening for enhanced levels of radiation-induced arrest in the G<sub>2</sub> phase of the cell cycle as is observed in ataxia telangiectasia (AT) het-

erozygotes. Among the LCLs from 108 female patients with breast cancer only 20% exhibited a clear increase in the number of cells in G<sub>2</sub> 18 h after irradiation with 3 Gy, while already 8% of control LCLs showed this effect. Ramsey and Birrell (1995) assessed LCLs from 56 breast cancer patients for *in vitro* radiosensitivity. Surviving fractions after 2 Gy irradiation were generated from survival curves and showed a high degree of variation. Only 16% of the breast cancer LCLs had an equal or greater sensitivity than an LCL derived from an AT heterozygote. Radiosensitivity has also been determined for LCLs with various BRCA1 (n = 5) and BRCA2 (n = 4) genotypes (Foray et al., 1999). In this study, heterozygous BRCA1 and BRCA2 mutations led to impaired proliferative capacity, reduced survival rate and higher yields of micronuclei after irradiation with gamma rays. Increased induction of micronuclei after 6 Gy irradiation was only shown for two cell lines with a BRCA1 mutation and two cell lines with a BRCA2 mutation. In accordance with these findings, our preliminary study (Speit et al., 2000) indicated that LCLs with a BRCA1 mutation have the same mutagen sensitivity in the MNT as found for lymphocytes. Enhanced induction of micronuclei was measured after gamma irradiation or treatment with H<sub>2</sub>O<sub>2</sub> in an LCL with a BRCA1 mutation. However, these results were only based on the comparison of one pair of LCLs with and without BRCA1 mutation and could not be generalized after testing further LCLs (Trenz et al., 2003a). Six LCLs (three with and three without a BRCA1 mutation) were comprehensively characterized with regard to differences in the induction of micronuclei and cytotoxic effects. No systematic difference in radiation sensitivity between LCLs with and without a BRCA1 mutation was found. Spontaneous and gamma radiation-induced micronucleus frequencies were in the same range and the effect of radiation on cell proliferation and viability was similar. The LCLs tested carried BRCA1 mutations (T300G and 5382insC), which were clearly associated with mutagen sensitivity in the MNT with lymphocytes (Rothfuss et al., 2000). Obviously, chromosomal mutagen sensitivity does not seem to be a general feature of LCLs and the utility of LCLs to study the mechanisms underlying mutagen sensitivity requires careful characterization of the cell lines used.

#### **Mutagen sensitivity and the functions of BRCA genes**

It has been reported that a lack of functional BRCA1 protein leads to highly increased radiosensitivity and the accumulation of chromosome aberrations in mouse embryonic fibroblasts and a human tumor cell line deficient in BRCA1 (Shen et al., 1998; Abbott et al., 1999; Foray et al., 1999; Scully et al., 1999). Surprisingly, human lymphocytes and some lymphoblastoid cell lines heterozygous for a BRCA mutation also showed increased chromosomal mutagen sensitivity in the MNT (Foray et al., 1999; Rothfuss et al., 2000; Speit et al., 2000). Both, mutations in BRCA1 and in BRCA2 are associated with mutagen sensitivity and there seems to be no fundamental difference between cells carrying either a mutated BRCA1 or BRCA2 allele (Trenz et al., 2002). These results indicated that heterozygous BRCA mutations may be associated with a haplo-

**Table 1.** Enhanced sensitivity of peripheral blood lymphocytes from women carrying a BRCA1 mutation towards chemical mutagens in the micronucleus test

Subjects (n)	Mutagen	Concentration	MN/1000 BNC <sup>a</sup>
BRCA1 (5)	bleomycin	5 µg/ml	151 ± 18.9 <sup>d</sup>
Controls (5)	bleomycin	5 µg/ml	83 ± 5.0
BRCA1 (6)	H <sub>2</sub> O <sub>2</sub>	2 mM	33 ± 2.6 <sup>d</sup>
Controls (6)	H <sub>2</sub> O <sub>2</sub>	2 mM	13 ± 0.8
BRCA1 (5)	cisplatin	20 µM	105 ± 15.3 <sup>d</sup>
Controls (5)	cisplatin	20 µM	54 ± 6.4
BRCA1 (7)	BCNU <sup>b</sup>	10 µM	38 ± 6.5 <sup>d</sup>
Controls (7)	BCNU <sup>b</sup>	10 µM	17 ± 1.6
BRCA1 (5)	cyclophosphamide <sup>c</sup>	200 µM	114 ± 12.7 <sup>d</sup>
Controls (5)	cyclophosphamide <sup>c</sup>	200 µM	68 ± 7.5

<sup>a</sup> BNC: binucleated cells.

<sup>b</sup> BCNU: bischloroethylnitrosurea.

<sup>c</sup> Treatment in the presence of rat liver S9-mix.

<sup>d</sup> Significantly different from concurrent controls ( $P < 0.05$ ; unpaired t-test).

type insufficiency for DNA repair functions. From the lack of correlation between the G<sub>0</sub> MNT and the G<sub>2</sub> aberration test it has been concluded that the BRCA1 gene product is mainly involved in the G<sub>0</sub> defense mechanism or that it is involved in the processing of chromosome damage both in G<sub>0</sub> and G<sub>2</sub> but requires the presence of both wild type alleles to be fully effective in G<sub>0</sub> cells (Baria et al., 2001a). The obvious differences between the G<sub>0</sub> MNT and the G<sub>2</sub> aberration assay in detecting chromosomal mutagen sensitivity should be further investigated and may lead to a better understanding of the underlying mechanisms.

Chromosomal mutagen sensitivity has mainly been studied with ionizing radiation. Ionizing radiation typically induces DNA double-strand breaks (DSBs) which are the ultimate DNA lesions leading to the formation of chromosome aberrations and micronuclei if not adequately repaired (Obe et al., 2002). Consequently, chromosomal mutagen sensitivity has mainly been discussed in the context of impaired DNA DSB repair and it has been suggested that low penetrance mutations in different genes are responsible for mutagen sensitivity in breast cancer patients in general (Scott et al., 1998, 1999; Baeyens et al., 2002). With respect to mutagen sensitivity associated with mutations in BRCA1 and BRCA2, impaired functions of these genes in DSB repair have been discussed (Trenz et al., 2002, 2003b). There are two major DSB repair pathways in mammalian cells, homologous recombination (HR) and non-homologous end-joining (NHEJ) but NHEJ seems to be the major pathway in adult and differentiated cells (for review see Hoeijmakers, 2001). BRCA2 seems to be mainly involved in HR through its interaction with RAD51, which is the homolog of the bacterial RecA protein and plays a central role in homologous recombination (Venkitaraman, 2002). The BRCA1 gene product also co-localizes with RAD51 in nuclear foci, suggesting that BRCA1 may also be involved in the HR pathway of DSB repair (Scully et al., 1997). However, because of a physical interaction between BRCA1 and RAD50, involvement of BRCA1 in NHEJ has been proposed (Zhong et al.,

1999). Recently, impaired fidelity of NHEJ was demonstrated in LCLs heterozygous for a BRCA1 mutation (Baldeyron et al., 2002). While the overall end-joining efficiency was not substantially affected in cells with a BRCA1 mutation, the error-prone end-joining was significantly enhanced. Based on comparative studies with the MNT and the comet assay, Rothfuss et al. (2000) already concluded that a BRCA1 mutation directly or indirectly leads to a disturbed fidelity of DNA repair in lymphocytes. However, it still has to be established whether the described defect in DSB repair is directly related to the enhanced formation of micronuclei. Possibly, BRCA1 influences both DSB repair pathways because it might act upstream of the DNA repair functions. It has been reported that BRCA1 together with other repair-related proteins forms a complex at sites of DNA damage to protect broken DNA ends from degradation and to favor correct rejoining (Paull et al., 2001). Obviously, BRCA1 is a multifunctional protein but its functions are not yet completely elucidated. Increasing evidence suggests that besides a possible involvement in DNA DSB repair, it plays a role in transcription-coupled repair and in the recognition of abnormal DNA structures such as mismatched DNA and stalled replication forks (for review see Venkitaraman, 2001, 2002). In accordance with these various functions, mutagen sensitivity in BRCA1 heterozygous cells is not limited to ionizing radiation but also occurs after exposure to other mutagens. Experiments with H<sub>2</sub>O<sub>2</sub> indicated that mutagen sensitivity of cells with a BRCA1 mutation is not exclusively related to DSBs because, in contrast to ionizing radiation, H<sub>2</sub>O<sub>2</sub> does not induce DNA DSBs in abundance (Rothfuss et al., 2000; Trenz et al., 2002). The observed hypersensitivity of lymphocytes carrying a BRCA1 mutation towards H<sub>2</sub>O<sub>2</sub> was in agreement with the proposed role of BRCA1 in the transcription-coupled repair of oxidative DNA damage (Gowen et al., 1998; Abbott et al., 1999; Le Page et al., 2000). In the meantime, it has also been shown that lymphocytes heterozygous for a BRCA1 mutation are also hypersensitive towards various DNA-damaging cytostatics such as bleomycin (BLM), cisplatin (CDDP), bischloroethylnitrosurea (BCNU) and cyclophosphamide (CP) (Trenz et al., 2003b). Some of these results demonstrating mutagen sensitivity towards chemical mutagens are summarized in Table 1. BLM acts radiomimetically, i.e. it mainly induces DNA strand breaks and is frequently used to investigate mutagen sensitivity as a substitute for ionizing radiation (Berwick and Vineis, 2000; Berwick et al., 2002). Increased induction of chromosome aberrations by BLM has been reported in breast cancer families (Roy et al., 2000). Therefore, the observed effect in the MNT is not unexpected. However, the other DNA-damaging substances tested (CDDP, BCNU, CP) have a quite different mode of action and cause alkylation and/or crosslinking of DNA. These types of DNA damage are mainly removed by nucleotide excision repair (NER) and mismatch repair (Hoeijmakers, 2001). The enhanced formation of micronuclei after exposure of lymphocytes to these substances which induce different types of DNA damage and activate different repair mechanisms are in accordance with the recently published idea that BRCA1 forms a multi-subunit protein complex (referred to as the BRCA1-associated genome surveillance complex: BASC) which includes

DNA repair proteins involved in double-strand break repair, mismatch repair and recombination (Wang et al., 2000; Futaki and Liu, 2001). The presence of BRCA1 in the BASC might indicate that BRCA1 acts as a coordinator between alternative DNA repair pathways required for the maintenance of genomic integrity. Such a complex model suggests that different genes acting downstream of BRCA1 and BRCA2 influence mutagen sensitivity and thus explain the inhomogeneous results obtained in different studies evaluating different groups of patients with different tests for mutagen sensitivity.

A final aspect of chromosomal mutagen sensitivity associated with BRCA mutations are potential practical implications. Many breast cancer patients with BRCA germ line mutations receive ionizing radiation as a component of their breast cancer care. Some of the chemical mutagens that caused enhanced induction of micronuclei are regularly used in breast cancer chemotherapy and high dose chemotherapy (HDC) with stem cell support. Possibly, women with breast cancer carrying a BRCA1 mutation are at higher risk for the induction of (chromosome) mutations and secondary cancers following standard breast cancer therapies.

## References

- Abbott DW, Thompson ME, Robinson-Benion C, Tomlinson G, Jensen RA, Holt JT: BRCA1 expression restores radiation resistance in BRCA1-defective cancer cells through enhancement of transcription-coupled DNA repair. *J Biol Chem* 274:18808–18812 (1999).
- Abrahams PJ, Houweling A, Cornelissen-Steijger PD, Jaspers NG, Darrroudi F, Meijers CM, Mullenders LH, Filon R, Arwert F, Pinedo HM, Natarajan AP, Terleth C, Van Zeeland AA, van der Eb AJ: Impaired DNA repair capacity in skin fibroblasts from various hereditary cancer-prone syndromes. *Mutat Res* 407:189–201 (1998).
- Alapetite C, Thirion P, de la Rochefordiere A, Cosset JM, Moustacchi E: Analysis by alkaline comet assay of cancer patients with severe reactions to radiotherapy: defective rejoining of radioinduced DNA strand breaks in lymphocytes of breast cancer patients. *Int J Cancer* 83:83–90 (1999).
- Baeyens A, Thierens H, Claes K, Poppe B, Messiaen L, De Ridder L, Vral A: Chromosomal radiosensitivity in breast cancer patients with a known or putative genetic predisposition. *Br J Cancer* 87:1379–1385 (2002).
- Baldeyron C, Jacquemin E, Smith J, Jacquemont C, De Oliveira I, Gad S, Feunteun J, Stoppa-Lyonnet D, Papadopoulo D: A single mutated BRCA1 allele leads to impaired fidelity of double strand break end-joining. *Oncogene* 21:1401–1410 (2002).
- Baria K, Warren C, Roberts SA, West CM, Evans DG, Varley JM, Scott D: Correspondence re: A. Rothfuss et al., Induced micronucleus frequencies in peripheral blood lymphocytes as a screening test for carriers of a BRCA1 mutation in breast cancer families. *Cancer Res* 60:390–394, 2000. *Cancer Res* 61:5948–5949 (2001a).
- Baria K, Warren C, Roberts SA, West CM, Scott D: Chromosomal radiosensitivity as a marker of predisposition to common cancers? *Br J Cancer* 84: 892–896 (2001b).
- Berwick M, Vineis P: Markers of DNA repair and susceptibility to cancer in humans: an epidemiologic review. *J Natl Cancer Inst* 92:874–897 (2000).
- Berwick M, Matullo G, Vineis P: Studies of DNA repair and human cancer: an update, in Wilson SH, Suk WA (eds): *Biomarkers of Environmentally Associated Disease; Technologies, Concepts, and Perspectives*, pp 83–107 (Lewis Publishers, Boca Raton 2002).
- Buchholz TA, Wu X, Hussain A, Tucker SL, Mills GB, Haffty B, Bergh S, Story M, Geara FB, Brock WA: Evidence of haplotype insufficiency in human cells containing a germline mutation in BRCA1 or BRCA2. *Int J Cancer* 97:557–561 (2002).
- Burrill W, Barber JB, Roberts SA, Bulman B, Scott D: Heritability of chromosomal radiosensitivity in breast cancer patients: a pilot study with the lymphocyte micronucleus assay. *Int J Radiat Biol* 76: 1617–1619 (2000).
- Cianciulli AM, Venturo I, Leonardo F, Antonaci S, Greco G, Lopez M, Gandolfo GM: Mutagen sensitivity and cancer susceptibility in patients with multiple primary cancers. *Oncol Rep* 2:1021–1025 (1995).
- Fenech M: The advantages and disadvantages of the cytokinesis-block micronucleus method. *Mutat Res* 392:11–18 (1997).
- Foray N, Randrianarison V, Marot D, Perricaudet M, Lenoir G, Feunteun J: Gamma-rays-induced death of human cells carrying mutations of BRCA1 or BRCA2. *Oncogene* 18:7334–7342 (1999).
- Futaki M, Liu JM: Chromosomal breakage syndromes and the BRCA1 genome surveillance complex. *Trends molec Med* 7:560–565 (2001).
- Gowen LC, Avrutskaya AV, Latour AM, Koller BH, Leoden SA: BRCA1 required for transcription-coupled repair of oxidative DNA damage. *Science* 281:1009–1012 (1998).
- Helzlsouer KJ, Harris EL, Parshad R, Fogel S, Bigbee WL, Sanford KK: Familial clustering of breast cancer: possible interaction between DNA repair proficiency and radiation exposure in the development of breast cancer. *Int J Cancer* 64:14–17 (1995).
- Helzlsouer KJ, Harris EL, Parshad R, Perry HR, Price FM, Sanford KK: DNA repair proficiency: potential susceptibility factor for breast cancer. *J Natl Cancer Inst* 88:754–755 (1996).
- Hoeijmakers JH: Genome maintenance mechanisms for preventing cancer. *Nature* 411:366–374 (2001).
- Hu JJ, Smith TR, Miller MS, Lohman K, Case LD: Genetic regulation of ionizing radiation sensitivity and breast cancer risk. *Environ molec Mutagen* 39: 208–215 (2002).
- Jaloszynski P, Kujawski M, Czub-Swierczek M, Markowska J, Szyfter K: Bleomycin-induced DNA damage and its removal in lymphocytes of breast cancer patients studied by comet assay. *Mutat Res* 385:223–233 (1997).
- Lavin MF, Bennett I, Ramsay J, Gardiner RA, Seymour GJ, Farrell A, Walsh M: Identification of a potentially radiosensitive subgroup among patients with breast cancer. *J Natl Cancer Inst* 86: 1627–1634 (1994).
- Le Page F, Randrianarison V, Marot D, Cabannes J, Perricaudet M, Feunteun J, Sarasin A: BRCA1 and BRCA2 are necessary for the transcription-coupled repair of the oxidative 8-oxoguanine lesion in human cells. *Cancer Res* 60:5548–5552 (2000).
- Mohrenweiser HM: Individual susceptibility to exposures: a role for genetic variation in DNA repair genes. In Wilson SH, Suk WA (eds): *Biomarkers of Environmentally Associated Disease; Technologies, Concepts, and Perspectives*, pp 63–82 (Lewis Publishers, Boca Raton 2002).
- Nieuwenhuis B, Assen-Bolt AJ, Waarde-Verhagen MA, Sijmons RH, Van der Hout AH, Bauch T, Streffer C, Kampering HH: BRCA1 and BRCA2 heterozygosity and repair of X-ray-induced DNA damage. *Int J Radiat Biol* 78:285–295 (2002).
- Obe G, Pfeiffer P, Savage JR, Johannes C, Goedecke W, Jeppesen P, Natarajan AT, Martinez-Lopez W, Folle GA, Drets ME: Chromosomal aberrations: formation, identification and distribution. *Mutat Res* 504:17–36 (2002).
- Parshad R, Price FM, Bohr VA, Cowans KH, Zujewski JA, Sanford KK: Deficient DNA repair capacity, a predisposing factor in breast cancer. *Br J Cancer* 74:1–5 (1996).
- Patel RK, Trivedi AH, Arora DC, Bhatavdekar JM, Patel DD: DNA repair proficiency in breast cancer patients and their first-degree relatives. *Int J Cancer* 73:20–24 (1997).
- Paull TT, Cortez D, Bowers B, Elledge SJ, Gellert M: Direct DNA binding by Brca1. *Proc Natl Acad Sci, USA* 98:6086–6091 (2001).
- Peto J, Collins N, Barfoot R, Seal S, Warren W, Rahman N, Easton DF, Evans C, Deacon J, Stratton MR: Prevalence of BRCA1 and BRCA2 gene mutations in patients with early-onset breast cancer. *J Natl Cancer Inst* 91:943–949 (1999).
- Rajeswari N, Ahuja YR, Malini U, Chandrashekar S, Balakrishna N, Rao KV, Khar A: Risk assessment in first degree female relatives of breast cancer patients using the alkaline Comet assay. *Carcinogenesis* 21:557–561 (2000).
- Ramsay J, Birrell G: Normal tissue radiosensitivity in breast cancer patients. *Int J Radiat Oncol Biol Phys* 31:339–344 (1995).
- Rao NM, Pai SA, Shinde SR, Ghosh SN: Reduced DNA repair capacity in breast cancer patients and unaffected individuals from breast cancer families. *Cancer Genet Cytogenet* 102:65–73 (1998).
- Riches AC, Bryant PE, Steel CM, Gleig A, Robertson AJ, Preece PE, Thompson AM: Chromosomal radiosensitivity in G2-phase lymphocytes identifies breast cancer patients with distinctive tumour characteristics. *Br J Cancer* 85:1157–1161 (2001).
- Roberts SA, Spreadborough AR, Bulman B, Barber JB, Evans DG, Scott D: Heritability of cellular radiosensitivity: a marker of low-penetrance predisposition genes in breast cancer? *Am J Hum Genet* 65: 784–794 (1999).
- Rothfuss A, Schutz P, Bochum S, Volm T, Eberhardt E, Kreienberg R, Vogel W, Speit G: Induced micronucleus frequencies in peripheral lymphocytes as a screening test for carriers of a BRCA1 mutation in breast cancer families. *Cancer Res* 60:390–394 (2000).
- Roy SK, Trivedi AH, Bakshi SR, Patel SJ, Shukla PH, Bhatavdekar JM, Patel DD, Shah PM: Bleomycin-induced chromosome damage in lymphocytes indicates inefficient DNA repair capacity in breast cancer families. *J Expl Clin Cancer Res* 19:169–173 (2000).

- Scott D, Spreadborough A, Levine E, Roberts SA: Genetic predisposition in breast cancer. *Lancet* 344:1444 (1994).
- Scott D, Barber JB, Levine EL, Burrill W, Roberts SA: Radiation-induced micronucleus induction in lymphocytes identifies a high frequency of radiosensitive cases among breast cancer patients: a test for predisposition? *Br J Cancer* 77:614–620 (1998).
- Scott D, Barber JB, Spreadborough AR, Burrill W, Roberts SA: Increased chromosomal radiosensitivity in breast cancer patients: a comparison of two assays. *Int J Radiat Biol* 75:1–10 (1999).
- Scully R, Chen J, Plug A, Xiao Y, Weaver D, Feunteun J, Ashley T, Livingston DM: Association of BRCA1 with Rad51 in mitotic and meiotic cells. *Cell* 88:265–275 (1997).
- Scully R, Ganesan S, Vlasakova K, Chen J, Socolovsky M, Livingston DM: Genetic analysis of BRCA1 function in a defined tumor cell line. *Mol Cell* 4: 1093–1099 (1999).
- Shen SX, Weaver Z, Xu X, Li C, Weinstein M, Chen L, Guan XY, Ried T, Deng CX: A targeted disruption of the murine *Brcal* gene causes gamma-irradiation hypersensitivity and genetic instability. *Oncogene* 17:3115–3124 (1998).
- Smith TR, Miller MS, Lohman KK, Case LD, Hu JJ: DNA damage and breast cancer risk. *Carcinogenesis* 24:883–889 (2003).
- Speit G, Hartmann A: The comet assay (single-cell gel test). A sensitive genotoxicity test for the detection of DNA damage and repair. *Meth molec Biol* 113: 203–212 (1999).
- Speit G, Trenz K, Schutz P, Bendix R, Dork T: Mutagen sensitivity of human lymphoblastoid cells with a BRCA1 mutation in comparison to ataxia telangiectasia heterozygote cells. *Cytogenet Cell Genet* 91:261–266 (2000).
- Teare MD, Wallace SA, Harris M, Howell A, Birch JM: Cancer experience in the relatives of an unselected series of breast cancer patients. *Br J Cancer* 70: 102–111 (1994).
- Terzoudi GI, Jung T, Hain J, Vrouvas J, Margaritis K, Donta-Bakoyianni C, Makropoulos V, Angelakis P, Pantelias GE: Increased G2 chromosomal radiosensitivity in cancer patients: the role of *cdk1/cyclin-B* activity level in the mechanisms involved. *Int J Radiat Biol* 76:607–615 (2000).
- Trenz K, Rothfuss A, Schutz P, Speit G: Mutagen sensitivity of peripheral blood from women carrying a BRCA1 or BRCA2 mutation. *Mutat Res* 500:89–96 (2002).
- Trenz K, Landgraf J, Speit G: Mutagen sensitivity of human lymphoblastoid cells with a BRCA1 mutation. *Breast Cancer Res Treat* 78:69–79 (2003a).
- Trenz K, Lugowski S, Jahrsdörfer U, Jainta S, Vogel W, Speit G: Enhanced sensitivity of peripheral blood from women carrying a BRCA1 mutation towards the mutagenic effects of various cytostatics. *Mutat Res* 544:279–288 (2003b).
- Tucker JD, Preston RJ: Chromosome aberrations, micronuclei, aneuploidy, sister chromatid exchanges, and cancer risk assessment. *Mutat Res* 365:147–159 (1996).
- Venkitaraman AR: Functions of BRCA1 and BRCA2 in the biological response to DNA damage. *J Cell Sci* 114:3591–3598 (2001).
- Venkitaraman AR: Cancer susceptibility and the functions of BRCA1 and BRCA2. *Cell* 108:171–182 (2002).
- Wang Y, Cortez D, Yazdi P, Neff N, Elledge SJ, Qin J: BASC, a super complex of BRCA1-associated proteins involved in the recognition and repair of aberrant DNA structures. *Genes Dev* 14:927–939 (2000).
- Zhong Q, Chen CF, Li S, Chen Y, Wang CC, Xiao J, Chen PL, Sharp ZD, Lee WH: Association of BRCA1 with the Rad50-hMre11-p95 complex and the DNA damage response. *Science* 285:747–750 (1999).

# Possible causes of chromosome instability: comparison of chromosomal abnormalities in cancer cell lines with mutations in BRCA1, BRCA2, CHK2 and BUB1

M. Grigorova, J.M. Staines, H. Ozdag, C. Caldas and P.A.W. Edwards

Cancer Genomics Program, Departments of Pathology and Oncology, University of Cambridge, Hutchison/MRC Research Centre, Cambridge (UK)

**Abstract.** A large proportion of epithelial cancers show the chromosome-instability phenotype, in which they have many chromosome abnormalities. This is thought to be the result of mutations that disrupt chromosome maintenance, but the causative mutations are not known. We identified cell lines known to have mutations that might cause chromosome instability, and examined their karyotypes. Two cell lines, the breast cancer line HCC1937 and the pancreatic cancer line CAPAN-1, that have mutations respectively in BRCA1 and BRCA2, had very abnormal karyotypes, with many structural and numerical chromosome changes and substantial variation between metaphases. However, two colorectal cancer lines with mutations in BUB1, a spindle checkpoint protein involved in chromosome segregation, had rather simple near-tetraploid

karyotypes, with minimal loss or gain of chromosomes other than the endoreduplication event, and minimal structural change. Apart from tetraploidy, these karyotypes were typical of colorectal lines considered to be chromosomally stable. Two lines derived from the same tumour, DLD-1 and HCT-15, with bi-allelic mutation of CHK2, had karyotypes that were typical of near-diploid colorectal lines considered chromosomally stable. The karyotypes observed supported the proposed role for BRCA1 and BRCA2 mutations in chromosomal instability, but showed that the tested mutations in BUB1 and CHK2 did not result in karyotypes that would have been predicted if they were sufficient for chromosomal instability.

Copyright © 2003 S. Karger AG, Basel

The majority of human epithelial cancers have many abnormalities of chromosome number and structure (Dutrillaux, 1995). This has been labelled the chromosomal instability phenotype (Lengauer et al., 1998), and is thought to be the result of defects in DNA repair, mitotic spindle mechanisms or some other aspect of chromosome maintenance. For technical reasons it is difficult to demonstrate that this is an increased rate of change, rather than accumulation of changes over a larger number of divisions, or lack of selection against variants (see for

example Lengauer et al., 1997; Roschke et al., 2002). However, broadly speaking, it is possible to distinguish one group of carcinomas that have near-normal karyotypes (which includes most of those showing microsatellite instability), from the majority, which have highly abnormal karyotypes and therefore seem to have a specific tendency to acquire chromosome abnormalities (Dutrillaux, 1995; Lengauer et al., 1997, 1998; Eshleman et al., 1998; Abdel-Rahman et al., 2001).

The mutations that cause chromosome instability in human cancer have not yet been identified. At issue is not just whether mutating a particular gene can give genetic instability in model systems, but whether the mutations that actually occur in human tumours necessarily contribute to genetic instability.

To see whether mutations found in human tumours are associated with gross chromosomal instability, we looked for human tumour cell lines with relevant mutations and examined their karyotypes and karyotype variability. We identified six such cell lines, with mutations in BRCA1, BRCA2, BUB1, and CHK2 (Table 1).

This work was supported by Cancer Research UK, Biotechnology and Biological Sciences Research Council (BBSRC), European Union.

Received 28 January 2004; accepted 2 February 2004.

Request reprints from: Dr. Paul A.W. Edwards  
Hutchison/MRC Research Centre, Hills Road, Cambridge CB2 2XZ (UK)  
telephone: +44-1223 763338; fax: +44-1223 763241  
e-mail: pawel@cam.ac.uk.

Current Address of J.M.S: Cambridge Cytogenetics Laboratory, Kefford House  
Maris Lane, Cambridge, CB2 2FF (UK)

**Table 1.** Cell lines with candidate chromosome-instability mutations

Gene	Cell line	Cancer type	Mutation				Primer Sequence	Reference	Other mutations <sup>b</sup>
			Base change	Coding change	Somatic? <sup>a</sup>				
BRCA1	HCC1937	Breast	5382insC homozygous	Stop1793	GLHet <sup>a</sup>	5'-TGCTCCACTTCCATTGAAGG-3'	1,2	p53, PTEN (1)	
BRCA2	CAPAN-1	Pancreatic	6174delT homozygous	Stop2002	ND	5'-GAGTGGAAATACAGAGTGGTG-3' 5'-ATAATGATGAATGTAGCACG-3' 5'-CTTGTGAGCTGGTCTGAATG-3'	3	p53, p16 (7,8)	
BUB1	VACO400 (V400)	Colorectal	IVS4+1G→A heterozygous	Deletion of exon 4, followed by frameshift	Yes	5'-GTACAACAGTGACCTCCATC-3' 5'-TGTATTATCCACATTGTCCA-3'	4		
BUB1	VACO429 (V429)	Colorectal	1524C→A heterozygous	S492Y	Yes	5'-GTGTAGCACCTGATGACAAG-3' 5'-TCTGTGATAACCACCTATAA-3'	4		
CHK2	DLD-1 <sup>c</sup>	Colorectal	As HCT-15 (below) <sup>c</sup>	As HCT-15 <sup>c</sup>	ND	As HCT-15 <sup>c</sup>	As HCT-15 <sup>c</sup>	p53 (9); Microsatellite unstable by GTBP mutation (10); p53, p16 (7,8)	
CHK2	HCT-15 <sup>c</sup>	Colorectal	Two heterozygous mutations on separate alleles <sup>c</sup> 463G→T  740C→A	R145W  A247D	ND	GDNAF 5'-GTAAGAGTTTTTAGGACCCA-3' GDNAR 5'-ACAGAATGTGTGAATGACAA-3' CDNAF 5'-ATATCCAGCTCCTCTACCAG-3' CDNAR 5'-TGCCACTGTGATCTTCTATG-3' GDNAF 5'-CCAGGAGTGGTAGGTCTCAT-3' GDNAR 5'-AATTCATCCATCTAAGCAGG-3' CDNAF 5'-TATCCTAAGGCATTAAGAGA-3' CDNAR 5'-CTCTCTTGCTGAACCAATA-3'	5,6	Microsatellite unstable by GTBP mutation (10); p300 (11); p53 (12); Microsatellite unstable by GTBP mutation (10); p300 (13)	

<sup>a</sup> Somatic: whether mutation was somatic or germline. GLHet, heterozygous in germline; Yes, not in germline, but shown present in primary tumour; ND not known.

<sup>b</sup> These 'Other mutations' were not verified in the present study.

<sup>c</sup> The CHK2 mutations were originally reported in cell line HCT-15. DLD-1 and HCT-15 are from the same tumour though cultured separately (Chen et al., 1995). We confirmed the presence of the two mutations in both DLD-1 and HCT-15, though we did not confirm that they were on separate alleles. References: 1, Tomlinson et al., 1998; 2, Chen et al., 1998; 3, Goggins et al., 1996; 4, Cahill et al., 1998; 5, Bell et al., 1999; 6, Lee et al., 2001; 7, Redston et al., 1994; 8, Caldas et al., 1994; 9, Abdel-Rahman et al., 2001; 10, Wheeler et al., 1999; 11, Gayther et al., 2000; 12, O'Connor et al., 1997; 13, Özdag et al., 2002.

There is good evidence that Brca1 and Brca2 proteins are involved in chromosome maintenance. Both are implicated in DNA strand break repair and cell cycle checkpoint control (reviewed in Venkitaraman, 2002). More specifically, mouse cells homozygous mutant for BRCA1 or BRCA2 show structural aberrations in metaphase chromosome spreads, consistent with ongoing structural instability (Patel et al., 1998; Xu et al., 1999; Yu et al., 2000). The breast cancer cell line HCC1937 is homozygous for a frameshift mutation in BRCA1, and is derived from a breast tumour in a patient with a germline mutation (Table 1). It is radiation sensitive and defective for repair of double strand breaks, and wild type BRCA1 alleviates these defects (Scully et al., 1999). The pancreatic cancer cell line CAPAN-1 has a homozygous truncation of BRCA2 (Table 1). The cells are hypersensitive to ionising radiation, and are defective in repair of double strand breaks by homologous recombination, while retaining normal levels of non-homologous end joining (Moynahan et al., 2001; reviewed in Venkitaraman, 2002).

Bub1 functions in the mitotic spindle checkpoint, and defects in spindle assembly might result in numerical, and pos-

sibly also structural, instability. In yeast, *Drosophila* and *C. elegans*, cells mutant for BUB1 show chromosome mis-segregation and sometimes fragmentation (Musacchio and Hardwick, 2002; Warren et al., 2002). The cell lines studied here, VACO400 and VACO429, have somatic, heterozygous mutations of BUB1 (Cahill et al., 1998).

CHK2 mutations might also result in genetic instability. Chk2 is involved in DNA-damage signalling, passing signals from ATM protein to various targets including Brca1 and causing G1-S and S phase arrest (Kastan, 2001; Hirao et al., 2002). Apparent mutations in CHK2 have been reported in some families with Li-Fraumeni syndrome that do not have detectable TP53 mutations (Bell et al., 1999); however the significance of some of these mutations is now uncertain (Schutte et al., 2003; Sodha et al., 2002). The cell line HCT-15 has both alleles of CHK2 mutated, and shows a defective S-phase checkpoint that is restored by wildtype Chk2 (Falck et al., 2001; see also Wu et al., 2001). DLD-1 was derived from the same colorectal cancer (Chen et al., 1995), and we show here that it has the same mutations.

## Materials and methods

Cell lines are detailed in Table 1. HCC1937 was obtained from Dr A. Ashworth; CAPAN-1 and HCT-15 from ATCC; VACO400 and VACO429 from James K.V. Willson (Willson et al., 1987); and DLD-1 from W.F. Bodmer.

### Mutation analysis

Generally, genomic DNA was amplified by PCR (Table 1) using a 55 °C annealing temperature, and the product sequenced directly in both directions using Amersham DyeET Terminators and an ABI3100 genetic analyzer (Applied Biosystems, Foster City, CA USA). All samples were re-amplified and re-sequenced. The CHK2 mutations were confirmed in cDNA as well as gDNA because there are CHK2 pseudogenes (Sodha et al., 2002). For the 463G → T CHK2 mutation in cDNA, touchdown PCR was used with successive annealing temperatures of 70, 68, 65, 62, and 58 °C.

### Cell culture, metaphase preparation and fluorescence in situ hybridization (FISH)

These were as described (Davidson et al., 2000). Spectral Karyotyping (SKY) analysis (Schröck et al., 1996) was as described (Davidson et al., 2000) using the SD-200 and SD-300 spectrometers and SKY chromosome paint kits (Applied Spectral Imaging, Migdal HaEmek, Israel). At least ten metaphases were analysed for each cell line. Where fluorescence colours overlap at the junction between chromosomes, the spectral karyotyping software sometimes misidentifies the overlap as an insertion of a strip of an irrelevant chromosome (Davidson et al., 2000). Although inspection of the spectra identifies most of these errors, we confirmed representative examples of the rearranged chromosomes, by conventional two- or three-colour chromosome painting as described.

### Metaphase heterogeneity

Variability of centromere number was measured, as we (Abdel-Rahman et al., 2001) and others (Roschke et al., 2002) have done previously. We counted the number of centromeres of each chromosome (including those in translocated chromosomes) in each metaphase analysed by SKY. For each chromosome, the percentage of metaphases deviating from the modal number was calculated; this was then averaged over all chromosomes. This approach is similar to that of Lengauer et al. (1997), except that metaphases rather than interphases are used. It gives similar (Roschke et al., 2002) or slightly lower (Abdel-Rahman et al., 2001) figures.

## Results

The reported mutations were confirmed by sequencing (Table 1), and the CHK2 mutations reported in HCT-15 were shown to be present in DLD-1.

The chromosome constitution of the lines was determined by 24-colour fluorescence in situ hybridisation, using the SKY system, and selected chromosomal abnormalities were verified by conventional two- and three-colour FISH. SKY karyotypes are shown in Fig. 1, in order of increasing abnormality, except for DLD-1 which we have reported previously (see Fig. 3 of Abdel-Rahman et al., 2001). The karyotypes are summarised in Table 2.

### BRCA1-mutant cell line HCC1937

As expected, the two cell lines with BRCA1 and BRCA2 mutations had highly abnormal karyotypes, typical of chromosomally unstable lines. As others have briefly reported (Popovici et al., 2002), HCC1937 had an extensively rearranged karyotype, with a modal chromosome number of 86 and many deleted or translocated chromosomes (Fig. 1E, Table 2). About 47% of the chromosomes showed structural alterations and all chromosomes except 17 were affected. The high degree of chro-

mosome rearrangement was confirmed on representative chromosomes using conventional two- and three-colour chromosome painting. Figure 1F shows examples of the more complex rearrangements: the two derivatives of chromosome 6, der(6)t(5;6;1;6;5) (Fig. 1Fa) and der(6)t(5;6;1) (Fig. 1Fb), and the der(4)t(13;4;8;9;12) (Fig. 1F, d and e).

In a few metaphases, variants of these complex translocations were observed, which are an indication of ongoing exchange events. For example two cells analysed by SKY that did not have the der(4)t(13;4;8;9;12) had a der(4) t(13;4;8;9) and one had a der(4)t(13;4;8). In 3 of about 50 metaphases analysed by two-colour FISH, the der(6)t(5;6;1;6;5) was replaced by a der(6)t(5;6;5;6;?;6;5) (Fig. 1Fc), and in 2 metaphases two-colour FISH showed a variant der(6)t(5;6;?;6;?;6;5), the ? in both cases representing segments that did not hybridize with chromosome 5 or 6 paint, presumably from chromosome 1.

Most of the rearrangements were unbalanced translocations and deletions, but one of the translocations, t(8;10), appeared reciprocal (Fig. 1Ff). It was present in two copies, so it might have been an early event that preceded an endoreduplication. We have previously shown that this translocation targets the NRG1 gene (Adelaide et al., 2003). Other translocations, the t(X;3), and t(3;5) could well have been reciprocal translocations that have rearranged further, but the great majority of translocations were non-reciprocal as usual in carcinomas (Dutrillaux, 1995; Abdel-Rahman et al., 2001).

### BRCA2-mutant cell line CAPAN-1

CAPAN-1 had an extremely abnormal karyotype, as summarised previously by others (Ghadimi et al., 1999) (Fig. 1G; Table 2). 70% of the chromosomes were rearranged, and 20% of the chromosomes were multiply translocated, mostly consisting of fragments of three or more chromosomes. The overlap of fluorescence between multiple small fragments of chromosome led to a number of errors in identification of chromosome fragments by the SKY software. However, two- or three-colour FISH was able to confirm the complexity of the rearrangements in representative examples, including the der(1)t(1;15); der(1)t(1;15;10;5) (Fig. 1Ha), der(4)t(16;4;5) (Fig. 1Hb), der(8)t(6;8;17?) (Fig. 1Hc), der(7)t(7;4;7;4) (Fig. 1Hd), and the der(17)t(13;17;8?;17) (Fig. 1Hf). As in HCC1937, there was also evidence of ongoing rearrangement. For example a variant of the der(7)t(7;4;7;4) with a terminal chromosome 1 fragment was observed in 2/20 metaphases by three-colour FISH (Fig. 1Hf). Two of the rearrangements appeared reciprocal: the t(6;15) and t(7;10).

### BUB1-mutant cell line VACO400

The karyotypes of the two cell lines with mutations in BUB1 were surprisingly unlike those expected for chromosomally-unstable lines. VACO400 had a close to tetraploid karyotype (Fig. 1B, Table 2), with a modal chromosome number of 86 (range 80–90). There were three translocated chromosomes: der(4)t(4;11), der(13)t(11;13), and der(14)t(13;14). Since these translocations were present in one copy per cell, the line presumably became tetraploid and later acquired the structural abnormalities. There were few numerical changes: after allowing for the chromosomes replaced by translocations, only three



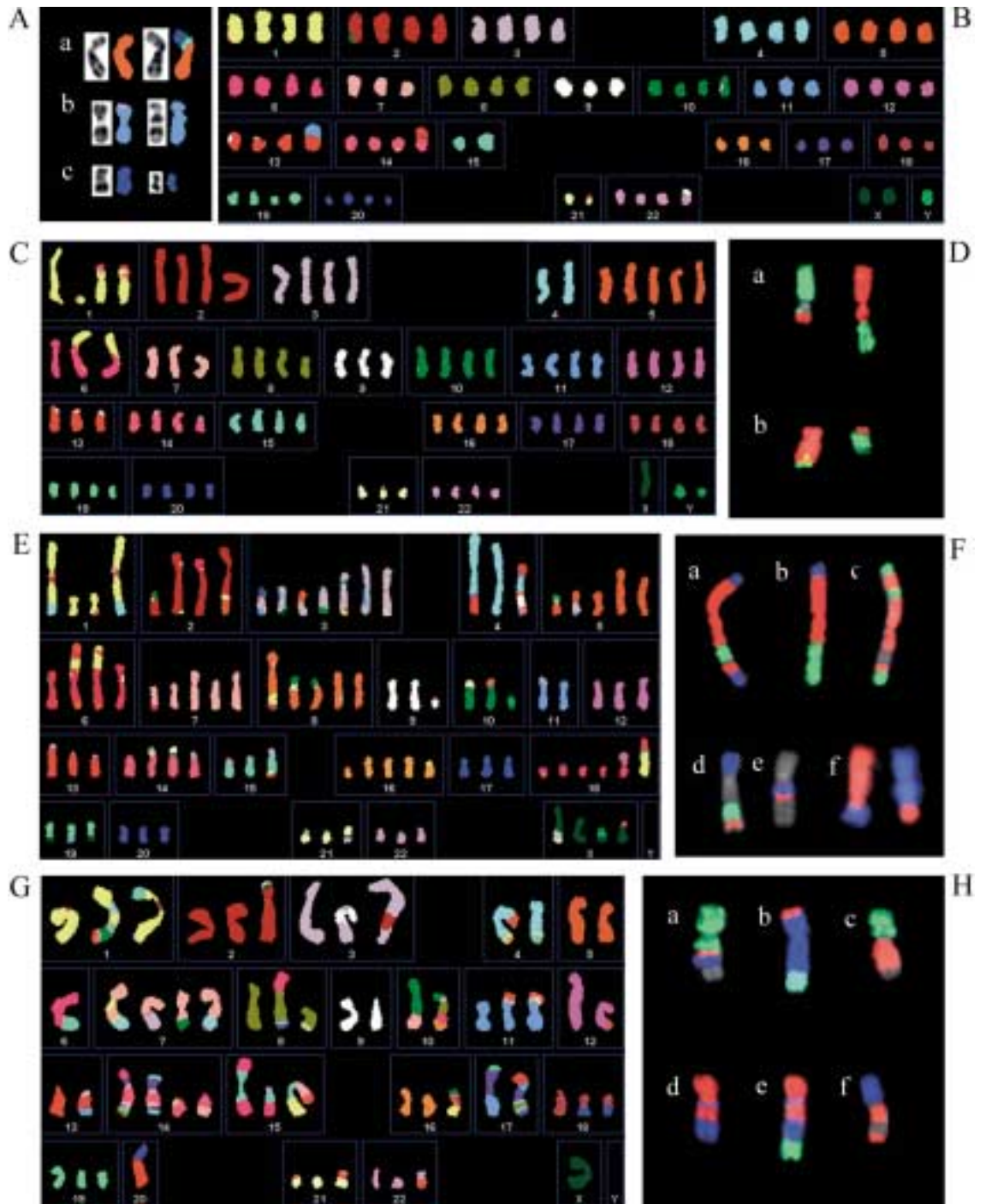


**Fig. 1.** Karyotypes of the cell lines. Typical metaphases analysed by 24-colour FISH (“SKY”) and confirmation of representative abnormalities by conventional two- or three-colour chromosome painting. **(A)** HCT-15. Only abnormal chromosomes are shown. a, normal 8 and translocated 8, der(8)t(8;17); b, normal and inverted 11; c, normal and deleted 17. Inverted DAPI banding and false-coloured image from SKY analysis. **(B)** VACO400, SKY karyotype. This metaphase has an additional nonclonal 21;22 translocation. **(C)** VACO429, SKY karyotype. This metaphase shows the t(1;6) reciprocal translocation that is the only structural abnormality present in all metaphases, and also the chromosome 1 rearrangement that is present only in clone 2. **(D)** Verification of reciprocal translocations by two-colour FISH. a, t(1;6), chromosome 1 green, chromosome 6 red; b, t(12;19) present in clone 3, chromosome 12 red, chromosome 19 green. **(E)** HCC1937, SKY karyotype. **(F)** Examples of verification of representative structural abnormalities

by two- and three-colour FISH. a and b, the two large derivatives of chromosome 6: a, der(6)t(5;6;1;6;5) chromosome 5 blue, chromosome 6 red, chromosome 1 green, b, der(1)t(5;6;1) chromosome 5 blue, chromosome 6 red, chromosome 1 green; c, t(5;6;5;6;?;6;5), an example of a variant of the der(6) shown in a, found in three metaphases, chromosome 5 green, chromosome 6 red (note change of colours). The unlabelled chromosome “?” is presumed to be 1 as in a. d and e, the complex chromosome 4 derivative, der(4)t(13;4;8;9;12). d, chromosome 13 blue, chromosome 9 green, chromosome 12 red. e, chromosome 4 blue, chromosome 8 red. f, reciprocal translocation t(8;10), chromosome 8 red, chromosome 10 blue. **(G)** CAPAN-1, SKY karyotype. **(H)** Examples of verification of representative abnormalities: a, der(1)t(1;15;10;5), chromosome 1 green, chromosome 15 red, chromosome 10 blue (chromosome 5 not labelled in this hybridisation). b, der(4)(16;4;5) chromosome 16 red, chromosome 4 blue, chromosome 5 green. c, der(8)t(6;

**Table 2.** Karyotypes of the cell lines<sup>a</sup>

**CAPAN-1:** 56 (51–60) X, -Y, 1×1, der(1)t(1;15), der(1)t(1;15;10;5), 2×1, der(2)t(2;10), der(2)t(2;X;9?), inv(3)(pq), 3×0, der(3)t(2;3), der(3)t(3;7), 4×0, der(4)t(16;4;5), der(4)t(4;15), 5×1, der(5)del(5)(q3-qter)?, 6×0, der(6)t(6;15)<sup>b</sup>, 7×0, der(7)(7;10)<sup>b</sup>, der(7)t(7;4;7;4)×2, der(7)t(3;7), 8×1, der(8)t(8;15), der(8)t(6;8;17), 9×1, der(9)t(3;9), der(9)del(9), 10×0, der(10)t(7;10)<sup>b</sup>, der(10)t(10;16), 11×1, der(11)t(11;14), der(11)t(5;11), 12×1, der(12) dup(12)(q14-qter), 13×1, der(13)t(11;13), 14×1, der(14)t(7;14), der(14)t(6?;17;14;7?;17;8)×2, 15×0, der(15)t(6;15)<sup>b</sup>×2, der(15)t(1;15;7;5), 16×2, der(16)t(10;16), 17×0, der(17)t(13;17;8;17), der(17)t(11;17;?), 18×1, der(18)t(18;20)×2, 19×2, der(19)t(18;19), 20×1, der(20)t(13;20), 21×2, der(21)t(5;21), 22×2, der(22)t(5;22).

**DLD-1:** 46 (43–46) XY, dup(1)(p?), dup(2)(p13p23), der(6)t(6;11)

**HCC1937:** 86 (74–90) X, X×0/1 der(X)t(X;3), der(X)t(X;5), 1×0, der(1)t(1;4), der(1)del(1)×2, 2×1, der(2)t(2;5), der(2)t(10;2;5), 3×2, der(3)del(3)t(X;3), der(3)del(3)t(3;5), der(3)del(3), 4×0, i(4)(q10), der(4)t(4;13), der(4)t(13;4;8;9;12), 5×2, der(5)del(5)t(3;5), der(5)del(5), 6×2, der(6)t(5;6;1), der(6)t(5;6;1;6;5), 7×2, der(7)del(7)t(7;14), der(7)del(7)×2, 8×2, der(8)t(8;10)<sup>b</sup>×2, der(8)t(8;1;20), 9×2, der(9)del(9), 10×2, der(10)t(8;10)<sup>b</sup>, der(10)t(3;10), der(10)del(10)t(X;10)×2, der(10)del(10), 11×2, der(11)t(11;20), 12×3, 13×3, 14×2, der(14)t(3;14), 15×2, der(15)t(8;15), der(15)dic(15;15), 16×2, der(16)t(1;16), 17×3, 18×0/1, der(18)t(1;18), der(18)t(12;18), der(18)t(18;20)×2, 19×0/1, der(19)t(X;19), der(19)t(11;19), 20×3, 21×1, der(21)t(21;22), 22×3.

**HCT-15:** 46 (45–47) XY, der(8)t(8;17), inv(11), der(17)del(17)

**VACO400:** 86 (80–90) XXYY, der(4)t(4;11), der(13)t(11;13), der(14)t(13;14), -15, -16, -18.

**VACO429:** 85 (85–92) Clone 1: XXYY, t(1;6)<sup>b</sup>×2, -4, +5, -11, [20%]<sup>c</sup>/ Clone 2: idem + dic(1;1), ace(1) [40%]<sup>c</sup>/ Clone 3: 85 (85–92) XXYY, t(1;6)<sup>b</sup>×2, -11, t(12;19)<sup>b</sup>×2 [40%]<sup>c</sup>.

<sup>a</sup> Karyotypes obtained by 24-colour FISH (SKY) analysis, with some additional details judged from the DAPI banding. Chromosomes shown are present in the majority of metaphases unless otherwise noted, and modal numbers of each chromosome are given. The simpler karyotypes DLD-1, HCT-15, VACO400 and VACO429 are given in ISCN nomenclature, i.e. as deviations from diploid or tetraploid. CAPAN-1 and HCC1937 are given more explicitly by listing every chromosome, to show clearly the number of apparently normal chromosomes present. In ISCN notation, t(11;13) means both copies of a reciprocal 11;13 translocation are present, replacing an 11 and a 13. Non-reciprocal translocations are therefore recorded der(11)t(11;13), meaning a derivative of 11 (i.e. the centromere belongs to chromosome 11) which is an 11;13 translocation. The derivative is considered to have replaced one copy of chromosome 11. ace(1), acentric fragment of 1; der(10)del(10), deleted 10; dic(15;15), dicentric formed by fusion of two 15s; dup, duplicated, i.e. the chromosome appears larger than normal and so probably has an internal duplication; queries following chromosome numbers, e.g. t(2;X;9?), indicate that SKY classification was inconsistent and not resolved by conventional FISH.

<sup>b</sup> Apparently reciprocal translocations, both products present.

<sup>c</sup> The proportion of metaphases showing the additional changes was deduced from two-colour FISH experiments, counting >20 metaphases.

of the chromosomes, 15, 16, and 18, showed a modal number of three copies rather than four.

Two of the translocations appeared to be whole-arm translocations. The derivative 13 is a whole-arm translocation of chromosome 13 and 11q. The remaining part of chromosome 11 (p-arm without centromere) has joined to the q-arm of chromosome 4 and could perhaps have been formed in the same pro-

8;17), chromosome 6 green, chromosome 8 red (chromosome 17 not labelled in this hybridisation). d, der(7)t(7;4;7;4), chromosome 7 red, chromosome 4 blue; chromosome 1 also labelled in green but does not hybridise. This is an example of misclassification of small chromosome fragments by SKY software: the region where chromosome 4 and 7 fluorescence overlap is misidentified as chromosome 1 in G. e, variant of this chromosome found in 2/20 metaphases, der(7)t(7;4;7;4;1), colours as in d. f, der(17)t(13;17;8?;17), chromosome 13 blue, chromosome 17 red (chromosome 8 not labelled in this hybridisation).

cess. The der(14) is a Robertsonian translocation, formed by the fusion within the centromeres of chromosomes 13 and 14, but is a separate event.

#### *BUB1-mutant cell line VACO429*

The karyotype of this line (Fig. 1C, Table 2) was even closer to exactly tetraploid. The modal chromosome number was 85 (range 85–92). In around 20% of cells the only structural abnormality was two copies of a reciprocal translocation t(1;6). Verification of this translocation by two-colour FISH is shown in Fig. 1Da. Other metaphases showed in addition either two copies of a reciprocal translocation t(12;19) (Fig. 1Db) or an additional rearrangement between both homologues of chromosome 1 (Fig. 1C). There were only two numerical changes present in the majority of metaphases, loss of one copy of chromosome 4 and gain of one copy each of 5 and 11. The original line appears therefore to have been diploid with a single structural abnormality—a reciprocal translocation t(1;6), after which endoreduplication to tetraploidy occurred, then three numerical changes.

**Table 3.** Metaphase heterogeneity as a measure of numerical instability

Cell line	Variability of centromere number (%)		
	Total variability <sup>a</sup>	Gains only <sup>b</sup>	Gains only, per chromosome <sup>c</sup>
VACO400	14	3	1
VACO429	20	5	1
HCC1937	32	15	4
CAPAN-1	20	8	3
DLD-1 <sup>d</sup>	2	ND	ND
HCT-15	2	0.4	0.2

<sup>a</sup> Variability of centromere number was measured in the metaphases analysed by SKY (see Materials and methods).  
<sup>b</sup> As total variability, but only considering gains from the modal number, not losses, to avoid counting chromosomes lost artefactually during spreading on the slide.  
<sup>c</sup> Dividing gains by average ploidy, to obtain an estimate of gains per copy of each chromosome.  
<sup>d</sup> From Abdel-Rahman et al., 2001.

### CHK2-mutant cell lines DLD-1 and HCT-15

The two cell lines with CHK2 mutations had karyotypes typical of “chromosomally stable” cell lines. We and others have described the karyotype of DLD-1 previously (Ghadimi et al., 2000; Abdel-Rahman et al., 2001) (Table 2). It was diploid with three structural abnormalities: partially duplicated chromosomes 1 and 2, and an unbalanced (6;11) translocation. HCT-15 was diploid with three structural abnormalities—an inversion, a deletion and an unbalanced translocation (Fig. 1A, Table 2), as previously determined (Chen et al., 1995). As pointed out before (Chen et al., 1995), the structural changes in DLD-1 and HCT-15 are entirely different, even though they arose from the same tumour (which is further confirmed by their identical CHK2 and p300 mutations).

### Numerical variability

To attempt to measure ongoing numerical instability, we assessed the variability of chromosome number between metaphases (Table 3). DLD-1 and HCT-15 were typical near-diploid lines, with average percentage deviation of centromere number between metaphases of 2%, while the other lines had deviations of 14–32%. However, some of this heterogeneity would have been due to loss of chromosomes during spreading on slides. To reduce this effect, gains alone were considered (Galloway and Ivett, 1986); the average percentage deviation for VACO400 and VACO429 fell substantially to 8 and 11%, and for the diploid line HCT-15 to 0.5%. To reflect the probability of an individual chromosome being gained, this was converted to an estimate per chromosome. This gave an upper limit estimate of instability of 0.2% gains per metaphase per chromosome for HCT-15; 1% for VACO400 and VACO429; and 3 and 4% respectively for CAPAN-1 and HCC1937.

## Discussion

### BRCA1 and BRCA2 mutation: HCC1937 and CAPAN-1

The karyotypes of the BRCA1- and BRCA2-mutant cell lines were entirely consistent with the idea that such mutations could cause chromosome instability. Both karyotypes were among the most rearranged of breast and pancreatic carcinoma

cell line karyotypes described (Abdel-Rahman et al., 2001; Davidson et al., 2000; Kytola et al., 2000; Sirivatanauksorn et al., 2001), and exhibited substantially more structural changes than any of the colorectal lines considered to be chromosomally unstable (Eshleman et al., 1998; Abdel-Rahman et al., 2001). They also showed a high degree of variability between metaphases, both numerical and structural (Fig. 1 and Table 3), consistent with ongoing instability.

### BUB1 mutations: VACO400 and VACO429

Contrary to prediction, VACO400 and VACO429 did not show the kind of abnormal karyotype that could be described as showing chromosomal instability. They were both close to tetraploid, suggesting endoreduplication, a frequent event in tumours and cell lines. Otherwise, they showed a low level of abnormality typical of colorectal cancer cell lines designated chromosomally stable (and microsatellite-unstable), such as DLD-1, GP2d and HCT-116 (Lengauer et al., 1997; Abdel-Rahman et al., 2001). Apart from endoreduplication, only two microsatellite-unstable colorectal lines among the 12 examined by Eshleman et al. (1998) and Abdel-Rahman et al. (2001) have fewer changes than the most normal clone of VACO429.

Why were these mutations in BUB1 postulated to cause chromosomal instability, particularly numerical instability? The argument (Cahill et al., 1998) was indirect: abnormalities were found in the response of aneuploid colorectal carcinoma cell lines to microtubule-disrupting agents; these were attributed to an abnormal spindle checkpoint; and a panel of non-diploid lines were screened for mutations in human homologues of proteins involved in the spindle checkpoint in yeast, uncovering these two mutations in BUB1. Unfortunately, the two BUB1-mutant lines seem to have been misidentified as chromosomally unstable by two indirect criteria. Firstly, they showed large deviations from diploidy, with modal chromosome numbers reported as 82 and 86 respectively for VACO400 and VACO429 (86 and 85 in our hands). Secondly, their response to microtubule-disrupting agents resembled the typical aneuploid lines tested (Cahill et al., 1998); only a small proportion of the cells arrested in metaphase on prolonged exposure. There is some doubt whether this abnormal response is a spindle checkpoint defect (Tighe et al., 2001) and it does

not seem to correlate precisely to chromosomal instability; indeed HeLa cells, which would be regarded as typically chromosomally unstable, arrest in metaphase efficiently (Tighe et al., 2001).

#### *CHK2 mutation: DLD-1 and HCT-15*

Both CHK2-mutant lines were near-diploid, typical of lines considered chromosomally stable (Eshleman et al., 1998; Abdel-Rahman et al., 2001), indeed, DLD-1 has been used as a model chromosomally stable line (Lengauer et al., 1997). This biallelic mutation of CHK2 is therefore not sufficient to cause gross chromosomal instability. Perhaps more surprising is that both lines have a mutation of p53 as well as Chk2 (Abdel-Rahman et al., 2001; Polyak et al., 1996; O'Connor et al., 1997), showing that even combining these two mutations in the same cell is not enough to give overt chromosomal instability. CHK2 and BUB1 are like TP53—genome-maintenance genes where mutations are present in human cancers but these mutations on their own do not give overt chromosomal instability phenotypes. TP53 mutations are present in several near-diploid cell lines including the perfectly-diploid VACO5 (Eshleman et al., 1998; Abdel-Rahman et al., 2001). DLD1 and HCT-15 have both TP53 and CHK2 mutations. APC may be another such gene, as discussed in Jallepalli and Lengauer (2001); it is also mutant in VACO5 and HCT-15 (Rowan et al., 2000).

#### *Assessment of numerical instability by metaphase heterogeneity*

Attempts have been made to estimate numerical instability of cell lines by examining heterogeneity of chromosome number between metaphases, with or without cloning the line (Lengauer et al., 1997; Abdel-Rahman et al., 2001; Roschke et al., 2002). There are technical difficulties with this. When centromeric probes are used to count chromosomes on interphase nuclei, the number of signals may vary between nuclei for technical reasons, probably the variable access of probes to sequences buried in the flattened nuclei, so that estimates of instability can vary widely between preparations (Roschke et al., 2002). Also, endoreduplicated cells (e.g. tetraploid cells in a diploid population) will contribute disproportionately to estimates of gain. When chromosomes are counted in metaphases, variability may be overestimated, because chromosomes may be lost when they fail to adhere to the slide, or, much more rarely, gained because chromosomes from a neighbouring metaphase may be included in the count. But in this approach tetraploid cells can be excluded, and since chromosomes drifting into metaphases are rare compared to them not adhering,

## References

- Abdel-Rahman WM, Katsura K, Rens W, Gorman PA, Sheer D, Bicknell D, Bodmer WF, Arends MJ, Wyllie AH, Edwards PA: Spectral karyotyping suggests additional subsets of colorectal cancers characterized by pattern of chromosome rearrangement. *Proc natl Acad Sci, USA* 98:2538–2543 (2001).
- Adelaide J, Huang H-E, Murati A, Alsop AE, Orsetti B, Mozziconacci M-J, Popovici C, Ginestier C, Letesier A, Basset C, Courtay-Cahen C, Jacquemier J, Theillet C, Birnbaum D, Edwards PA, Chaffanet M: A recurrent chromosome translocation breakpoint in breast and pancreatic cancer cell lines targets the Neuregulin/NRG1 gene. *Genes Chromosomes Cancer* 37:333–345 (2003).
- Bell DW, Varley JM, Szydlo TE, Kang DH, Wahrer DC, Shannon KE, Lubratovich M, Verselis SJ, Isselbacher KJ, Fraumeni JF, Birch JM, Li FP, Garber JE, Haber DA: Heterozygous germ line hCHK2 mutations in Li-Fraumeni syndrome. *Science* 286:2528–2531 (1999).

the analysis of *gained* chromosomes is considered likely to give a more reliable estimate of numerical instability than losses (Galloway and Ivett, 1986).

Arguably the most reliable measure of variability is the percentage of metaphases showing gain of a given chromosome, and this should be divided by the number of chromosomes to give variability per chromosome (Table 3). Since the lines were not cloned, the estimate of variability is an upper limit. By this criterion (Table 3), DLD-1 and HCT-15 were stable, as expected, at about 0.2% gains per chromosome copy. VACO400 and VACO 429 may be less stable, at about 1% gains per copy, but selection against clones with gains and losses will also be less strong for tetraploid cells than diploid cells. Whether or not there is any instability, it has led to almost no net gain or loss of chromosomes over the evolution of the lines. HCC1937 and CAPAN-1 clearly gave higher figures at around 4% gains per copy, and also had accumulated many numerical changes.

## Conclusions

We set out to test the prediction that carcinomas with candidate chromosome instability mutations would show highly abnormal karyotypes. The surprising finding was that the two cell lines with heterozygous mutations in BUB1 did not have karyotypes expected of chromosomally unstable cancers. CHK2 mutation, for which there was no clear prediction, was also not associated with gross chromosome instability. We cannot exclude that a mutation in BUB1 or CHK2 causes a low level of instability. Or, like TP53 mutation, they may be permissive, but not sufficient, for chromosomal instability—for example, cells with BRCA1 or BRCA2 mutations may be disabled unless they also have mutations in checkpoint components such as p53 and Bub1 (Lee et al., 1999; Xu et al., 2001). Neither have we excluded that the cells with a mutation in BUB1 or CHK2 are unstable but have not undergone enough evolution to show many abnormalities, but this would be incompatible with the current distinction between stable and unstable cancers on the basis of their degree of chromosome abnormality.

## Acknowledgements

We thank Celine Courtay-Cahen, Suet-Feung Chin and Rachel Lyman for metaphases and help with FISH, Sarah Batley for sequencing and Ashok Venkitaraman for advice on the manuscript.

- Cahill DP, Lengauer C, Yu J, Riggins GJ, Willson JK, Markowitz SD, Kinzler KW, Vogelstein B: Mutations in mitotic checkpoint genes in human cancers. *Nature* 392:300–303 (1998).
- Caldas C, Hahn SA, da Costa LT, Redston MS, Schutte M, Seymour AB, Weinstein CL, Hruban RH, Yeo CJ, Kern SE: Frequent somatic mutations and homozygous deletions of the p16 (MTS1) gene in pancreatic adenocarcinoma. *Nature Genet* 8:27–32 (1994).
- Chen J, Silver DP, Walpita D, Cantor SB, Gazdar AF, Tomlinson G, Couch FJ, Weber BL, Ashley T, Livingston DM, Scully R: Stable interaction between the products of the BRCA1 and BRCA2 tumor suppressor genes in mitotic and meiotic cells. *Mol Cell* 2:317–328 (1998).
- Chen TR, Dorotinsky CS, McGuire LJ, Macy ML, Hay RJ: DLD-1 and HCT-15 cell lines derived separately from colorectal carcinomas have totally different chromosome changes but the same genetic origin. *Cancer Genet Cytogenet* 81:103–108 (1995).
- Davidson JM, Gorringe KL, Chin S-F, Orsetti B, Besret C, Courtay-Cahen C, Roberts I, Theillet C, Caldas C, Edwards PA: Molecular cytogenetic analysis of breast cancer cell lines. *Br J Cancer* 83:1309–1317 (2000).
- Dutrillaux B: Pathways of chromosome alteration in human epithelial cancers. *Adv Cancer Res* 67:59–82 (1995).
- Eshleman JR, Casey G, Kochera ME, Sedwick WD, Swinler SE, Veigl ML, Willson JK, Schwartz S, Markowitz SD: Chromosome number and structure both are markedly stable in RER colorectal cancers and are not destabilized by mutation of p53. *Oncogene* 17:719–725 (1998).
- Falck J, Mailand N, Syljuasen RG, Bartek J, Lukas J: The ATM-Chk2-Cdc25A checkpoint pathway guards against radioresistant DNA synthesis. *Nature* 410:842–847 (2001).
- Galloway SM, Ivett JL: Chemically induced aneuploidy in mammalian cells in culture. *Mutat Res* 167:89–105 (1986).
- Gayther SA, Batley SJ, Linger L, Bannister A, Thorpe K, Chin S-F, Daigo Y, Russell P, Wilson A, Sowter HM, Delhanty JD, Ponder BA, Kouzarides T, Caldas C: Mutations truncating the EP300 acetylase in human cancers. *Nature Genet* 24:300–303 (2000).
- Ghadimi BM, Schrock E, Walker RL, Wangsa D, Jauho A, Meltzer PS, Ried T: Specific chromosomal aberrations and amplification of the AIB1 nuclear receptor coactivator gene in pancreatic carcinomas. *Am J Pathol* 154:525–536 (1999).
- Ghadimi BM, Sackett DL, Difilippantonio MJ, Schrock E, Neumann T, Jauho A, Auer G, Ried T: Centrosome amplification and instability occurs exclusively in aneuploid, but not in diploid colorectal cancer cell lines, and correlates with numerical chromosomal aberrations. *Genes Chrom Cancer* 27:183–190 (2000).
- Goggins M, Schutte M, Lu J, Moskaluk CA, Weinstein CL, Petersen GM, Yeo CJ, Jackson CE, Lynch HT, Hruban RH, Kern SE: Germline BRCA2 gene mutations in patients with apparently sporadic pancreatic carcinomas. *Cancer Res* 56:5360–5364 (1996).
- Hirao A, Cheung A, Duncan G, Girard PM, Elia AJ, Wakeham A, Okada H, Sarkissian T, Wong JA, Sakai T, De Stanchina E, Bristow RG, Suda T, Lowe SW, Jeggo PA, Elledge SJ, Mak TW: Chk2 is a tumor suppressor that regulates apoptosis in both an ataxia telangiectasia mutated (ATM)-dependent and an ATM-independent manner. *Mol Cell Biol* 22:6521–6532 (2002).
- Jallepalli PV, Lengauer C: Chromosome segregation and cancer: cutting through the mystery. *Nature Rev* 1:109–117 (2001).
- Kastan MB: Checking two steps. *Nature* 410:766–767 (2001).
- Kytola S, Rummukainen J, Nordgren A, Karhu R, Farnedo F, Isola J, Larsson C: Chromosomal alterations in 15 breast cancer cell lines by comparative genomic hybridization and spectral karyotyping. *Genes Chrom Cancer* 28:308–317 (2000).
- Lee H, Trainer AH, Friedman LS, Thistlethwaite FC, Evans MJ, Ponder BA, Venkitaraman AR: Mitotic checkpoint inactivation fosters transformation in cells lacking the breast cancer susceptibility gene, Brca2. *Mol Cell* 4:1–10 (1999).
- Lee SB, Kim SH, Bell DW, Wahrer DC, Schiripo TA, Jorczak MM, Sgroi DC, Garber JE, Li FP, Nichols KE, Varley JM, Godwin AK, Shannon KM, Harlow E, Haber DA: Destabilization of CHK2 by a missense mutation associated with Li-Fraumeni syndrome. *Cancer Res* 61:8062–8067 (2001).
- Lengauer C, Kinzler KW, Vogelstein B: Genetic instability in colorectal cancers. *Nature* 386:623–627 (1997).
- Lengauer C, Kinzler KW, Vogelstein B: Genetic instabilities in human cancers. *Nature* 396:643–649 (1998).
- Moynahan ME, Pierce AJ, Jasin M: BRCA2 is required for homology-directed repair of chromosomal breaks. *Mol Cell* 7:263–272 (2001).
- Musacchio A, Hardwick KG: The spindle checkpoint: structural insights into dynamic signalling. *Nat Rev Mol Cell Biol* 3:731–741 (2002).
- O'Connor PM, Jackman J, Bae I, Myers TG, Fan S, Mutoh M, Scudiero DA, Monks A, Sausville EA, Weinstein JN, Friend S, Fornace AJ Jr, Kohn KW: Characterization of the p53 tumor suppressor pathway in cell lines of the National Cancer Institute anticancer drug screen and correlations with the growth-inhibitory potency of 123 anticancer agents. *Cancer Res* 57:4285–4300 (1997).
- Özdogan H, Batley SJ, Forst A, Iyer NG, Daigo Y, Boultell J, Arends MJ, Ponder BA, Kouzarides T, Caldas C: Mutation analysis of CBP and PCAF reveals rare inactivating mutations in cancer cell lines but not in primary tumours. *Br J Cancer* 87:1162–1165 (2002).
- Patel KJ, Yu VP, Lee H, Corcoran A, Thistlethwaite FC, Evans MJ, Colledge WH, Friedman LS, Ponder BA, Venkitaraman AR: Involvement of Brca2 in DNA Repair. *Mol Cell* 1:347–357 (1998).
- Polyak K, Waldman T, He T-C, Kinzler KW, Vogelstein B: Genetic determinants of p53-induced apoptosis and growth arrest. *Genes Dev* 10:1945–1952 (1996).
- Popovici C, Basset C, Bertucci F, Orsetti B, Adelaide J, Mozziconacci MJ, Conte N, Murati A, Ginestier C, Charafe-Jauffret E, Ethier SP, Lafage-Pochitaloff M, Theillet C, Birnbaum D, Chaffanet M: Reciprocal translocations in breast tumor cell lines: cloning of a t(3;20) that targets the FHIT gene. *Genes Chrom Cancer* 35:204–218 (2002).
- Redston MS, Caldas C, Seymour AB, Hruban RH, da Costa L, Yeo CJ, Kern SE: p53 mutations in pancreatic carcinoma and evidence of common involvement of homocopolymer tracts in DNA microdeletions. *Cancer Res* 54:3025–3033 (1994).
- Roschke AV, Stover K, Tonon G, Schaffer AA, Kirsch IR: Stable karyotypes in epithelial cancer cell lines despite high rates of ongoing structural and numerical chromosomal instability. *Neoplasia* 4:19–31 (2002).
- Rowan AJ, Lamium H, Ilyas M, Wheeler J, Straub J, Papadopoulou A, Bicknell D, Bodmer WF, Tomlinson IPM: APC mutations in sporadic colorectal tumors: A mutational “hotspot” and interdependence of the “two hits”. *Proc natl Acad Sci, USA* 97:3352–3357 (2000).
- Schröck E, du Manoir S, Veldman T, Schoell B, Wienberg J, Ferguson-Smith MA, Ledbetter DH, Bar-Am I, Soeksen D, Garini Y, Ried T: Multicolor spectral karyotyping of human chromosomes. *Science* 273:494–497 (1996).
- Schutte M, Seal S, Barfoot R, Meijers-Heijboer H, Wasielewski M, Evans DG, Eccles D, Meijers C, Lohman F, Klijn J, Van Den Ouweland A, Futreal PA, Nathanson KL, Weber BL, Easton DF, Stratton MR, Rahman N: Variants in CHEK2 other than 1100delC do not make a major contribution to breast cancer susceptibility. *Am J Hum Genet* 72:1023–1028 (2003).
- Scully R, Ganesan S, Vlasakova K, Chen J, Socolovsky M, Livingston DM: Genetic analysis of BRCA1 function in a defined tumor cell line. *Mol Cell* 4:1093–1099 (1999).
- Sirivatanauskorn V, Sirivatanauskorn Y, Gorman PA, Davidson JM, Sheer D, Moore PS, Scarpa A, Edwards P, Lemoine NR: Non-random chromosomal rearrangements in pancreatic cancer cell lines identified by spectral karyotyping. *Int J Cancer* 91:350–358 (2001).
- Sodha N, Houlston RS, Williams R, Yuille MA, Mangion J, Eccles RA: A robust method for detecting CHK2/RAD53 mutations in genomic DNA. *Hum Mutat* 19:173–177 (2002).
- Tighe A, Johnson VL, Albertella M, Taylor SS: Aneuploid colon cancer cells have a robust spindle checkpoint. *EMBO Rep* 2:609–614 (2001).
- Tomlinson GE, Chen TT, Stastny VA, Virmani AK, Spillman MA, Tonk V, Blum JL, Schneider NR, Wistuba II, Shay JW, Minna JD, Gazdar AF: Characterization of a breast cancer cell line derived from a germ-line BRCA1 mutation carrier. *Cancer Res* 58:3237–3242 (1998).
- Venkitaraman AR: Cancer susceptibility and the functions of BRCA1 and BRCA2. *Cell* 108:171–182 (2002).
- Warren CD, Brady DM, Johnston RC, Hanna JS, Hardwick KG, Spencer FA: Distinct chromosome segregation roles for spindle checkpoint proteins. *Mol Biol Cell* 13:3029–3041 (2002).
- Wheeler JMD, Beck NE, Kim HC, Tomlinson IPM, Mortensen NJMcC, Bodmer WF: Mechanisms of inactivation of mismatch repair genes in human colorectal cancer cell lines: The predominant role of hMLH1. *Proc natl Acad Sci, USA* 96:10296–10301 (1999).
- Willson JK, Bittner GN, Oberley TD, Meisner LF, Weese JL: Cell culture of human colon adenomas and carcinomas. *Cancer Res* 47:2704–2713 (1987).
- Wu X, Webster SR, Chen J: Characterization of tumor-associated Chk2 mutations. *J Biol Chem* 276:2971–2974 (2001).
- Xu X, Weaver Z, Linke SP, Li C, Gotay J, Wang XW, Harris CC, Ried T, Deng CX: Centrosome amplification and a defective G2-M cell cycle checkpoint induce genetic instability in BRCA1 exon 11 isoform-deficient cells. *Mol Cell* 3:389–395 (1999).
- Xu X, Qiao W, Linke SP, Cao L, Li WM, Furth PA, Harris CC, Deng CX: Genetic interactions between tumor suppressors Brca1 and p53 in apoptosis, cell cycle and tumorigenesis. *Nature Genet* 28:266–271 (2001).
- Yu VP, Koehler M, Steinlein C, Schmid M, Hanakahi LA, van Gool AJ, West SC, Venkitaraman AR: Gross chromosomal rearrangements and genetic exchange between nonhomologous chromosomes following BRCA2 inactivation. *Genes Dev* 14:1400–1406 (2000).

# Quantitative PCR analysis reveals a high incidence of large intragenic deletions in the FANCA gene in Spanish Fanconi anemia patients

E. Callén,<sup>a</sup> M.D. Tischkowitz,<sup>b</sup> A. Creus,<sup>a</sup> R. Marcos,<sup>a</sup> J.A. Bueren,<sup>c</sup>  
J.A. Casado,<sup>c</sup> C.G. Mathew<sup>b</sup> and J. Surrallés<sup>a</sup>

<sup>a</sup> Universitat Autònoma de Barcelona, Barcelona (Spain), <sup>b</sup> Division of Genetics and Development, Guy's, King's and St Thomas' School of Medicine, King's College London, London (UK) and <sup>c</sup> CIEMAT/Fundación Marcelino Botín, Madrid (Spain)

**Abstract.** Fanconi anaemia is an autosomal recessive disease characterized by chromosome fragility, multiple congenital abnormalities, progressive bone marrow failure and a high predisposition to develop malignancies. Most of the Fanconi anaemia patients belong to complementation group FA-A due to mutations in the FANCA gene. This gene contains 43 exons along a 4.3-kb coding sequence with a very heterogeneous mutational spectrum that makes the mutation screening of FANCA a difficult task. In addition, as the FANCA gene is rich in Alu sequences, it was reported that Alu-mediated recombination led to large intragenic deletions that cannot be detected in heterozygous state by conventional PCR, SSCP analysis, or DNA sequencing. To overcome this problem, a method based on quantitative fluorescent multiplex PCR was proposed to detect intragenic deletions in FANCA involving the most fre-

quently deleted exons (exons 5, 11, 17, 21 and 31). Here we apply the proposed method to detect intragenic deletions in 25 Spanish FA-A patients previously assigned to complementation group FA-A by FANCA cDNA retroviral transduction. A total of eight heterozygous deletions involving from one to more than 26 exons were detected. Thus, one third of the patients carried a large intragenic deletion that would have not been detected by conventional methods. These results are in agreement with previously published data and indicate that large intragenic deletions are one of the most frequent mutations leading to Fanconi anaemia. Consequently, this technology should be applied in future studies on FANCA to improve the mutation detection rate.

Copyright © 2003 S. Karger AG, Basel

Partially funded by the Universitat Autònoma de Barcelona (UAB), the CIEMAT/ Marcelino Botín Foundation, the Generalitat de Catalunya (project SGR-00197-2002), the Spanish Ministry of Health and Consumption (projects FIS PI020145 and FIS-Red G03/073), the Spanish Ministry of Science and Technology (Projects SAF 2002-03234 and SAF 2003-00328) and the Commission of the European Union (project FIGH-CT-2002-00217). E.C. was supported by a predoctoral fellowship awarded by the UAB. Her visit to CGM laboratory was supported by a short-term travel fellowship by the UAB. M.D.T. is supported by Cancer Research UK. J.S. is supported by a "Ramón y Cajal" project entitled "Genome stability and DNA repair" awarded by the Spanish Ministry of Science and Technology and co-financed by the UAB.

Received 10 September 2003; manuscript accepted 3 December 2003.

Request reprints from Dr. Jordi Surrallés, Group of Mutagenesis  
Department of Genetics and Microbiology, Universitat Autònoma de Barcelona  
08193 Bellaterra, Barcelona (Spain); telephone: +34 93 581 18 30;  
fax: +34 93 581 23 87; e-mail: jordi.surralles@uab.es

Fanconi anaemia (FA) is an autosomal recessive disease characterized by genomic instability, multiple congenital abnormalities, progressive bone marrow failure and a high predisposition to develop malignancies such as acute myeloid leukaemia and squamous cell carcinoma (Auerbach et al., 1993). FA cells are characterized by chromosomal fragility and are hypersensitive to DNA cross-linking agents such as diepoxybutane and mitomycin C. These features are used as a diagnostic tool (Auerbach, 1993).

To date eight different complementation groups have been described (FA-A, -B, -C, -D1, -D2, -E, -F, -G), and the genes corresponding to seven of these complementation groups (FANCA, FANCC, FANCD1/BRCA2, FANCD2, FANCE,

FANCF and FANCG) have been cloned and characterized (Strathdee et al., 1992; Lo Ten Foe et al., 1996; The Fanconi Anemia/Breast Cancer Consortium, 1996; de Winter et al., 1998, 2000a,b; Timmers et al., 2001; Howlett et al., 2002). It is known that although their protein products do not share significant homology to each other or with other genes in the databases, all of them participate in a common pathway (reviewed in Bogliolo et al., 2002). The FANCA, -C, -G, -E and -F proteins assemble in a multisubunit nuclear complex (de Winter et al., 2000c; Medhurst et al., 2001) required for monoubiquitin-mediated activation of FANCD2 after DNA damage or during S-phase and later targeting to nuclear foci containing BRCA1 and Rad51 (Garcia-Higuera et al., 2001; Taniguchi et al., 2002). This suggests a role for the FA pathway in DNA repair by homologous recombination during S-phase (Taniguchi et al., 2002).

The genetic heterogeneity of FA makes the subtyping of FA patients a difficult task, but over 90% of the FA population worldwide is represented by complementation groups FA-A, -C or -G, FA-A being the most prevalent, accounting for ~ 65% of all FA cases (Kutler et al., 2003). There are, however, regional and ethnic differences. It is estimated that about 80% of all FA patients belong to complementation group FA-A in Spain (Casado et al., 2002) or even more in Italy (Savino et al., 1997). Therefore, a proper detection of FANCA mutations is of critical clinical significance.

The FANCA gene contains 43 exons along a 4.3-kb coding sequence (Ianzano et al., 1997) with a very heterogeneous mutational spectrum, with more than 100 different FANCA mutations described to date, including all types of possible point mutations such as frame-shift mutations, small insertions or deletions, splicing defects, and nucleotide substitutions (The Fanconi Anemia/Breast Cancer Consortium, 1996; Lo Ten Foe et al., 1996; Levran et al., 1997; Savino et al., 1997; Morgan et al., 1999; Wijker et al., 1999). This makes the mutation screening of FANCA a very difficult task. As the FANCA gene is rich in Alu sequences, it was suggested and later reported that Alu-mediated recombination is an important mechanism for the generation of FANCA mutations (Centra et al., 1998; Levran et al., 1998), mainly large deletions that cannot be detected by conventional methods such as SSCP analysis or DNA sequencing. To overcome this problem, a method based on quantitative fluorescent multiplex PCR was developed. This method was used to screen 26 cell lines from FA patients belonging to complementation group A (Morgan et al., 1999), and a high frequency of large deletions was found. In some populations with high prevalence of FA such as the South African Afrikaner, this method has also been employed to scan the FANCA gene, and it was found that exon 12–31 deletion is the most common mutation in this population due to a founder effect (Tipping et al., 2001).

Taking advantage of this novel method developed by Morgan and co-workers (Morgan et al., 1999), we applied the proposed strategy to screen a group of 25 FA Spanish patients previously assigned to complementation group FA-A by retroviral transduction (Hanenberg et al., 2002; Casado et al., 2002). The suggested multiplex PCR was performed with some minor modifications and optimisations to amplify the five most com-

monly deleted exons of the FANCA gene and a control exon from an unrelated gene. After analyzing DNA samples from 25 Spanish FA-A patients, a total of eight different large deletions from one to more than 26 exons were detected, all of them in heterozygous state, confirming that this type of mutation is one of the most prevalent amongst FA-A patients.

## Materials and methods

### Patients

Blood samples were obtained from 25 Spanish FA patients with informed consent. All of them were previously diagnosed on the basis of their clinical traits and cellular hypersensitivity to diepoxybutane, and assigned to complementation group FA-A by retroviral transduction (Casado et al., 2002). In some cases, lymphoblastoid cell lines established by Epstein-Barr virus infection were used.

### Quantitative fluorescent multiplex PCR reaction

Genomic DNA was extracted directly from peripheral blood samples or lymphoblastoid cell lines by salt/chloroform or phenol/chloroform standard methods, respectively. DNA concentration was determined spectrophotometrically and a sample was diluted to 25 ng/ $\mu$ l to perform PCR.

Exons 5, 11, 17, 21 and 31 from the FANCA gene were simultaneously amplified together with exon 1 of the myelin protein zero (MPZ1) gene as an external control with respect to the FANCA gene exons in the same reaction. At least four non-FA control samples were included together with the FA sample in every PCR round as normal controls. PCR amplifications were performed in 25- $\mu$ l reactions with 125 ng DNA, 1 $\times$  Taq DNA polymerase buffer, 250  $\mu$ M each dNTP and 1.8 mM MgCl<sub>2</sub>. Primer concentrations and sequences are shown in Table 1. All primers were fluorescently labelled with phosphoramidite 6-FAM dye (PE Biosystems). PCR conditions were an initial denaturation step at 94°C for 5 min, followed by 21 cycles of denaturation at 94°C for 45 s, annealing step at 55°C for 45 s, and extension for 1 min at 72°C. A final extension step at 72°C for 5 min was performed. A 3- $\mu$ l aliquot of the PCR product was then mixed with 15  $\mu$ l of formamide and 0.2  $\mu$ l of Genescan ROX-500 size standard (PE Biosystems). Samples were denatured at 94°C for 5 min and run and analysed on an ABI 310 Gene Analyzer, by means of the GeneScan and Genotyper software, as described in Morgan et al. (1999). Briefly, apart from the FANCA exons (FAAX), another internal control exon from a different gene (exon 1 of the Myelin protein zero; MPZX1) was co-amplified to detect heterozygous deletions. For each of the patients, the peak areas corresponding to the MPZX and each of the five tested FANCA exons were determined in samples from the patient (pt) and from a healthy donor (c). This comparison gave a value called dosage quotient (DQ) that corresponds to the following formula: (ptFAAX peak area/ptMPZX1 peak area)/(cFAAX peak area/cMPZX1 peak area). The DQs range from 0.75 to 1.25 when the DNA copy number of a specific exon is normal, or half/double this value when there is a heterozygous deletion.

## Results and discussion

Mutations in the FANCA gene are the most prevalent cause of FA. More than 70 polymorphisms in this gene and over 100 different mutations have been accumulated in the International Fanconi Anemia Registry Database, most of them being in a heterozygous state. This is a clear indication of the complexity of detecting mutations in this gene. Although several studies have focused in finding pathogenic mutations among these patients, in some cases the successful detection rates were poor (Savino et al., 1997) in part due to the high rate of intragenic deletions (Centra et al., 1998; Levran et al., 1998; Wijker et al., 1999). This high rate of intragenic deletions along the FANCA gene sequence is the consequence of Alu-mediated intragenic

**Fig. 1.** Electrophoretogram showing the peak pattern of the multiplex products from a healthy control (a), compared with an exon 5 deletion carrier (b). Note that the peak area of exon 5 in the patient is half of the same exon in the healthy individual.

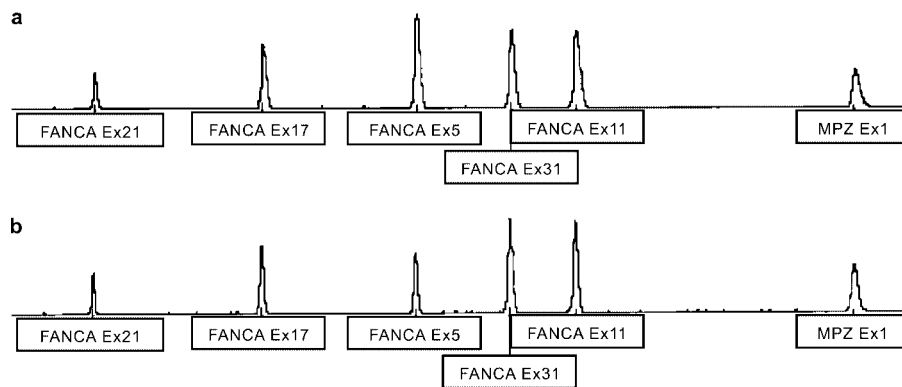


**Table 1.** Sequence, size and concentration of every primer of the set used

Gene: Exon	Primers (5'→3')	Amplicon size (bp)	Concentration ( $\mu$ M)
FANCA:			
Exon 5	Forward: ACC TGC CCG TTG TTA CTT TTA Reverse: AGA ACA TTG CCT GGA ACA CTG	250	0.4 0.2
Exon 11	Forward: GAT GAG CCT GAG CCA CAG TTT GTG Reverse: AGA ATT CCT GGC ATC TCC AGT CAG	301	0.4 0.2
Exon 17	Forward: CCA TGC CCA CTC CTC ACA CC Reverse: GTG AAA AGA AAC TGG ACC TTT GCA	205	0.08 0.2
Exon 21	Forward: TAA GCC ATA GCT GAC TTA ATT Reverse: GCA CAA GTC CCA GAG TGG ACA AG	156	0.6 0.2
Exon 31	Forward: CAC ACT GTC AGA GAA GCA CAG CCA Reverse: CAC CGC GCC TGG CAA TAA ATA TC	285	0.08 0.2
Myelin protein zero:			
Exon 1	Forward: CAG TGG ACA CAA AGC CCT CTG TGT A Reverse: GAC ACC TGA GTC CCA AGA CTC CCA G	389	0.2 0.2

recombination (Centra et al., 1998). Here we have applied an improved fluorescent PCR-based method with conditions similar to those proposed by Morgan et al. (1999), using primers that amplify exons 5, 11, 17, 21 and 31 of the FANCA gene. These exons were chosen based on previous observations showing that at least one of these five exons was absent in all FANCA deletions observed to date (Morgan et al., 1999). Some minor modifications in the sequence and concentration of some primers used by Morgan et al. (1999) were introduced to improve the efficiency of the technique.

We initially established the FA complementation group in all our samples by retroviral complementation to later select those belonging to the complementation group FA-A. Using DNA from these patients (either from blood samples or cell lines), the multiplex PCR reaction was performed. The rationale is that the area of the amplification peak of a given exon should be half the expected size in case of a heterozygous deletion. Figure 1 shows a representative example of an electrophoretogram of an exon 5 deletion carrier and Table 2 shows a numerical example of a typical result of a patient with a heterozygous exon 21 deletion. After analyzing 25 FA-A samples, a total of eight large deletions containing from one to more than 26 exons were detected, all of them in heterozygosis (Fig. 2). Thus, one third of the patients carried a large intragenic deletion, emphasizing the relevance of this type of mutation in FA-A patients.

Because of the very nature of the approach used here, the second pathogenic deletion was not detected. None of the mutations found in this work seem to be novel mutations, although this should be confirmed with a more accurate analysis using RT-PCR and polymorphic marker typing to map the approximate endpoints of the deletions. The percentage of heterozygous deletions described here is similar to that previously reported by Morgan and co-workers (1999). It is important, however, to keep in mind that although we have detected FANCA deletions in 32% of the patients, it is possible that the deletion frequency is even higher. Obviously, the dosage assay would have missed small deletions in the 5' half of the gene between exons that we tested, and also deletions that occur 3' to exon 31.

While detection of point mutations or small insertions/deletions is well established, large genomic deletions constitute a technical problem and it might be difficult to develop a cheap, easy and reliable quantitative method. This is a serious limitation as this type of mutation constitutes an important fraction of the mutations described not only in FA-A patients, but also in several malignancies, although their prevalence is yet underestimated due to the lack of a robust detection method (Armour et al., 2002). Several genes such as MSH21 or BRCA1 might be also affected by large heterozygous deletions and, in both cases, a similar method named quantitative multiplex PCR of short fluorescent fragments or other methods have been developed





**Fig. 2.** Scheme of the large deletions detected in the 25 samples analyzed, along the schematic figure of FANCA gene exons. The amplified exons are shown in grey colour. Continuous lines refer to the exons that are deleted and stippled lines refer to the fact that the exact break points are not detected by this method.

**Table 2.** Results of a dosage multiplex assay of an exon 21 deletion carrier

Exon	Peak area		Dosage quotient					
	Healthy donor	FA patient	MPZX1	FAAX5	FAAX11	FAAX17	FAAX21	FAAX31
MPZX1	62062	17523	–	1.28	1.17	1.05	2.30	1.07
FAAX5	36569	8083	0.78	–	0.91	0.82	1.80	0.84
FAAX11	56996.5	13794	0.86	1.09	–	0.90	1.97	0.92
FAAX17	19361	5218	0.95	1.22	1.11	–	2.19	1.02
FAAX21	23321	2864	0.43	0.56	0.51	0.46	–	0.47
FAAX31	14868	3914	0.93	1.19	1.09	0.98	2.14	–

for this same purpose (Charbonnier et al., 2000; Casilli et al., 2002; Wang et al., 2002, 2003). We proposed that the approach described here could also be applied to the above mentioned genes by just adapting the primers and PCR conditions. Most methods used to date are based on PCR although other techniques should be considered using cytogenetic tools or Southern-blot (Armour et al., 2002). Although PCR is basically a qualitative technique, several modifications can be introduced to get quantitative or semi-quantitative results, for example by using control samples and internal controls to coamplify and compare with the sample under study, in a manner similar to the method described here.

In conclusion, we have found that one third of the Spanish FA-A patients bear large monoallelic deletions in FANCA. This result confirms the suitability of quantitative PCR to find otherwise undetectable pathogenic mutations and hence to increase the mutation detection rate in FA. This would lead to a better molecular tool in pre- and postnatal diagnosis and in carrier detection.

### Acknowledgements

We would like to thank all FA families and haemato-oncologists that have participated in this study.

### References

- Armour JAL, Barton DE, Cockburn DJ, Taylor GR: The detection of large deletions or duplications in genomic DNA. *Hum Mutat* 20:325–337 (2002).
- Auerbach AD: Fanconi anemia diagnosis and the deoxybutane (DEB) test. *Exp Hematol* 21:731–733 (1993).
- Auerbach AD, Buchwald M, Joenje H: Fanconi Anemia, in Volgestein B, Kinzler KW (eds): *The Genetic Basis of Human Cancer*, pp 317–332 (McGraw-Hill, New York 1993).
- Bogliolo M, Cabré O, Callén E, Castillo V, Creus A, Marcos R, Surrallés J: The Fanconi anaemia genome stability and tumour suppressor network. *Mutagenesis* 17:529–538 (2002).
- Casado JA, Callén E, Surrallés J, Segovia JC, Rio P, Lobitz S, Hanenberg H, Bueren JA: Progress in the subtyping analysis of Fanconi anemia patients from Spain using retroviral mediated gene transfer of FA genes and FANCD2 Western blot analysis. Abstract. Twelfth Annual Fanconi Anemia Scientific Symposium, Philadelphia (2002).
- Casilli F, Di Rocco ZC, Gad S, Tournier I, Stoppa-Lyonnet D, Frebourg T, Tosi M: Rapid detection of novel *BRC1A1* rearrangements in high-risk breast-ovarian cancer families using multiplex PCR of short fluorescent fragments. *Hum Mutat* 20:218–226 (2002).
- Centra M, Memeo E, d'Apolito M, Savino M, Ianzano L, Notarangelo A, Liu J, Doggett NA, Zelante L, Savoia A: Fine exon-intron structure of the Fanconi anemia group A (FAA) gene and characterization of two genomic deletions. *Genomics* 51:463–467 (1998).
- Charbonnier F, Raux G, Wang Q, Drouot N, Cordier F, Limacher JM, Saurin J, Puisieux A, Olschwang S, Frebourg T: Detection of exon deletions and duplications of the mismatch repair genes in hereditary nonpolyposis colorectal cancer families using multiplex polymerase chain reaction of short fluorescent fragments. *Cancer Res* 60:2760–2763 (2000).
- Fanconi Anemia/ Breast Cancer Consortium: Positional cloning of the Fanconi anemia group A gene. *Nature Genet* 14:324–328 (1996).
- García-Higuera I, Taniguchi T, Ganesan S, Meyn MS, Timmers C, Hejna J, Grompe M, D'Andrea AD: Interaction of the Fanconi anemia proteins and *BRC1A1* in a common pathway. *Mol Cell* 7:249–262 (2001).

- Hanenberg H, Batish SD, Pollok KE, Vieten L, Verlander PC, Leurs C, Cooper RJ, Gottsche K, Haneline L, Clapp DW, Lobitz S, Williams DA, Auerbach AD: Phenotypic correction of primary Fanconi anemia T cells with retroviral vectors as a diagnostic tool. *Exp Hematol* 30:410–420 (2002).
- Howlett NG, Taniguchi T, Olson S, Cox B, Waisfisz Q, de Die-Smulders C, Persky N, Grompe M, Joenje H, Pals G, Ikeda H, Fox EA, D'Andrea AD: Biallelic inactivation of *BRC1A2* in Fanconi anemia. *Science* 297:606–609 (2002).
- Ianzano L, D'Apolito M, Centra M, Savino M, Levran O, Auerbach AD, Cleton-Jansen AM, Doggett NA, Pronk JC, Tipping AJ, Gibson RA, Mathew CG, Whitmore SA, Apostolou S, Callen DF, Zelante L, Savoia A: The genomic organization of the Fanconi anemia group A (FAA) gene. *Genomics* 41:309–314 (1997).
- Joenje H, Lo Ten Foe JR, Oostra AB, van Berkel CG, Rooimans MA, Schroeder-Kurth T, Wegner RD, Gille JJ, Buchwald M, Arwert F: Classification of Fanconi anemia patients by complementation analysis: evidence for a fifth genetic subtype. *Blood* 86:2156–2160 (1995).
- Kutler DI, Singh B, Satagopan J, Batish SD, Berwick M, Giampietro PF, Hanenberg H, Auerbach AD: A 20-year perspective on the International Fanconi Anemia Registry (IFAR). *Blood* 101:1249–1256 (2003).
- Levran O, Erlich T, Magdalena N, Gregory JJ, Batish SD, Verlander PC, Auerbach AD: Sequence variation in the Fanconi anemia gene FAA. *Proc natl Acad Sci, USA* 94:13051–13056 (1997).
- Levran O, Doggett NA, Auerbach AD: Identification of *Alu*-mediated deletions in the Fanconi anemia gene FAA. *Hum Mutat* 12:145–152 (1998).
- Lo Ten Foe JR, Rooimans MA, Bosnoyan-Collins L, Alon N, Wijker M, Parker L, Lightfoot J, Carreau M, Callen DF, Savoia A, Cheng NC, van Berkel CG, Strunk MH, Gille JJ, Pals G, Kruyt FA, Pronk JC, Arwert F, Buchwald M, Joenje H: Expression cloning of a cDNA for the major Fanconi anemia gene, FAA. *Nature Genet* 14:320–323 (1996).
- Medhurst AL, Huber PA, Waisfisz Q, de Winter JP, Mathew CG: Direct interactions of the five known Fanconi anemia proteins suggest a common functional pathway. *Hum molec Genet* 10:423–429 (2001).
- Morgan NV, Tipping AJ, Joenje H, Mathew CG: High frequency of large intragenic deletions in the Fanconi anemia group A gene. *Am J hum Genet* 65:1330–1341 (1999).
- Savino M, Ianzano L, Strippoli P, Ramenghi U, Arslanian A, Bagnara GP, Joenje H, Zelante L, Savoia A: Mutations of the Fanconi anemia group A gene (FAA) in Italian patients. *Am J hum Genet* 61:1246–1253 (1997).
- Strathdee CA, Duncan AM, Buchwald M: Evidence for at least four Fanconi anaemia genes including FACC on chromosome 9. *Nature Genet* 1:196–198 (1992).
- Taniguchi T, Garcia-Higuera I, Andreassen PR, Gregory RC, Grompe M, D'Andrea AD: S-phase-specific interaction of the Fanconi anemia protein, FANCD2, with BRCA1 and RAD51. *Blood* 100:2414–2420 (2002).
- Timmers C, Taniguchi T, Hejna J, Reifsteck C, Lucas L, Bruun D, Thayer M, Cox B, Olson S, D'Andrea AD, Moses R, Grompe M: Positional cloning of a novel Fanconi anemia gene, *FANCD2*. *Mol Cell* 7:241–248 (2001).
- Tipping AJ, Pearson T, Morgan NV, Gibson RA, Kuyt LP, Havenga C, Gluckman E, Joenje H, de Ravel T, Jansen S, Mathew CG: Molecular and genealogical evidence for a founder effect in Fanconi anemia families of the Afrikaner population of South Africa. *Proc natl Acad Sci, USA* 98:5734–5739 (2001).
- Wang Y, Friedl W, Sengteller M, Jungck M, Filges I, Propping P, Mangold E: A modified multiplex PCR assay for detection of large deletions in *MSH2* and *MSH1*. *Hum Mutat* 19:279–286 (2002).
- Wang Y, Friedl W, Lamberti C, Jungck M, Mathiak M, Pagenstecher C, Propping P, Mangold E: Hereditary nonpolyposis colorectal cancer: Frequent occurrence of large genomic deletions in *MSH2* and *MLH1* genes. *Int J Cancer* 103:636–641 (2003).
- Wijker M, Morgan NV, Herterich S, van Berkel CG, Tipping AJ, Gross HJ, Gille JJ, Pals G, Savino M, Altay C, Mohan S, Dokal I, Cavenagh J, Marsh J, van Weel M, Ortega JJ, Schuler D, Samochatova E, Karwacki M, Bekassy AN, Abecasis M, Ebell W, Kwee ML, de Ravel T, Mathew CG: Heterogenous spectrum of mutations in the Fanconi anaemia group A gene. *Eur J hum Genet* 7:52–59 (1999).
- de Winter JP, Waisfisz Q, Rooimans MA, van Berkel CGM, Bosnoyan-Collins L, Alon N, Bender O, Demuth I, Schindler D, Pronk JC, Arwert F, Hoehn H, Digweed M, Buchwald M, Joenje H: The Fanconi anaemia group G gene FANCG is identical with XRCC9. *Nature Genet* 20:281–283 (1998).
- de Winter JP, Leveille F, Waisfisz Q, van Berkel CG, Rooimans MA, van Der Weel L, Steltenpool J, Demuth I, Morgan NV, Alon N, Bosnoyan-Collins L, Lightfoot J, Leegwater PA, Waisfisz Q, Komatsu K, Arwert F, Pronk JC, Mathew CG, Digweed M, Buchwald M, Joenje H: Isolation of a cDNA representing the Fanconi anemia complementation group E gene. *Am J hum Genet* 67:1306–1308 (2000a).
- de Winter JP, Rooimans MA, van Der Weel L, van Berkel CG, Alon N, Bosnoyan-Collins L, de Groot J, Zhi Y, Waisfisz Q, Pronk JC, Arwert F, Mathew CG, Scheper RJ, Hoatlin ME, Buchwald M, Joenje H: The Fanconi anaemia gene *FANCF* encodes a novel protein with homology to ROM. *Nature Genet* 24:15–16 (2000b).
- de Winter JP, van der Weel L, de Groot J, Stone S, Waisfisz Q, Arwert F, Scheper RJ, Kruyt FA, Hoatlin ME, Joenje H: The Fanconi anemia protein FANCF forms a nuclear complex with FANCA, FANCC and FANCG. *Hum molec Genet* 9:2665–2674 (2000c).

# Analysis of ETV6/RUNX1 fusions for evaluating the late effects of cancer therapy in ALL (acute lymphoblastic leukemia) cured patients

M.S. Brassesco,<sup>a</sup> M.L. Camparoto,<sup>a</sup> L.G. Tone<sup>b</sup> and E.T. Sakamoto-Hojo<sup>a,c</sup>

<sup>a</sup>Departamento de Genética <sup>b</sup>Departamento de Pediatria e Puericultura, Faculdade de Medicina de Ribeirão Preto-USP;  
<sup>c</sup>Departamento de Biologia, Faculdade de Filosofia Ciências e Letras de Ribeirão Preto-USP, Universidade de São Paulo, Ribeirão Preto, SP (Brasil)

**Abstract.** Acute Lymphoblastic Leukemia (ALL) is the most common malignancy in childhood. The improvements of therapies have increased the number of long-term survivors. However, an increased incidence of secondary neoplasias has been observed in this cohort. Our purpose was to evaluate the late effects of cancer therapy in cured patients previously treated for ALL, considering previous reports on the occurrence of gene fusions as putative markers of chromosomal instability. Twelve ALL patients (aged 5 to 16 years) and twelve healthy subjects (aged 18 to 22 years) were studied for the presence of ETV6/RUNX1 (TEL/AML1) translocations, which were detected by FISH (fluorescence in situ hybridization). The blood samples were collected months or years after completion of the therapy, and the frequencies of gene fusions in lymphocytes were compared with those obtained retrospectively for bone marrow samples at the time of diagnosis, and also for the

control group. It was demonstrated that ETV6/RUNX1 gene fusion was a frequent event (0.59–1.84/100 cells) in peripheral blood lymphocytes from normal individuals and the ALL patients who underwent chemotherapy showed significantly ( $P = 0.0043$ ) increased frequencies (0.62–3.96/100 cells) of the rearrangement when compared with the control groups (patients at diagnosis and healthy subjects). However, a significant difference was not found between the groups of patients at diagnosis and healthy subjects, when the two patients who were positive for the rearrangement were excluded. Therefore, increased frequencies of ETV6/RUNX1 fusions in ALL cured patients indicate the influence of previous exposure to anti-cancer drugs, and they may represent an important genetic marker for estimating the risk of relapse, or development of secondary neoplasias.

Copyright © 2003 S. Karger AG, Basel

Current standard treatment of cancer consists of different regimens of combined chemo- and radiotherapy. The improvements of new therapies have been of great importance but imply the exposure of patients to high doses of ionizing radiation and chemotherapeutic drugs, whose mutagenic effects have been well established. Thus, the cured patients provide a model system to evaluate the late effects of antitumor agents (Baker et al., 1995; Byrne, 1999).

ALL is the most common malignancy in childhood and is associated with excellent outcomes (Bacchicet et al., 1997; Blau et al., 1998) resulting in increasing rates of long-term survivors. The treatment of ALL was one of the 20<sup>th</sup> century's successes. Actually, a universally fatal disease in the past has a cure (5-year survival) with a rate of about 75% (Greaves, 1999). Recently, attention is being focused on the potential of therapy-related long-term complications, principally because second malignant neoplasms are reported with increasing frequency in this cohort (Bhatia et al., 2002).

In a large proportion of ALL, recurrent chromosomal aberrations led to the formation of gene fusions and the subsequent expression of chimeric proteins with unique properties (Greaves, 1999). These genetic alterations are relevant for leukemogenesis and are important in prognostic and therapeutic purposes (Coustan-Smith et al., 2000). The most frequent rear-

Supported by FAPESP (Proc. 99/11710-0 and 00/11225-3), CAPES and CNPq.

Received 20 August 2003; manuscript accepted 28 November 2003.

Request reprints from Elza Tiemi Sakamoto-Hojo, Departamento de Biologia  
Faculdade de Filosofia Ciências e Letras de Ribeirão Preto-USP  
Av Bandeirantes 3900, 14040-901 Ribeirão Preto, SP (Brasil)  
telephone: +55-16-602-3827; fax: +55-16-633-0069; e-mail: etshojo@usp.br

rearrangement in childhood ALL (20–25%) is the cryptic translocation t(12;21)(p13;q22), which leads to the juxtaposition of RUNX1(AML1) sequence, from chromosome 21 to the ETV6 (TEL) gene on chromosome 12 (Ford et al., 1998). Both genes code for transcription factors that are essential in normal hematopoiesis (Wang et al., 1998; Asou, 2003) and are also involved in several translocations with multiple partners, which can be found in other types of leukemia and myelodysplastic syndromes (Rowley, 1999).

Recently, chromosomal aberrations exclusively associated with leukemias and lymphomas, such as ETV6/RUNX1 (Eguchi-Ishimae et al., 2001) have been detected in normal individuals with negative history of hematologic disorders. Bäsecke et al. (2002) demonstrated that at least 50% of normal individuals present translocations t(9;22) BCR/ABL, t(14;18) IGH/BCL2, t(2;5) NPM-ALK and MLL duplications, detectable in peripheral blood lymphocytes by PCR (Polymerase Chain Reaction). These and other findings suggested that the measurement of gene fusions in peripheral blood lymphocytes within a study group may be used as a sensitive assay for the detection of genomic instability, and may contribute to risk estimation for the development of lymphoid malignancies (Lipkowitz et al., 1992).

The genotoxicity of anti-cancer drugs has been evaluated by several groups by mutation assays, most of which have been carried out in patients immediately or shortly after the completion of chemotherapy. However, secondary malignancies in children, often related with antineoplastic drugs, usually occur years after therapy (Koishi et al., 1998). Considering that the number of patients with secondary neoplasias has increased among childhood cancer survivors, we aimed to investigate the late effects of cancer therapy in lymphocytes of children treated for ALL, by analyzing ETV6/RUNX1 fusions years after therapy completion, comparing the results retrospectively with those obtained for bone marrow samples collected at the time of diagnosis, and also with the frequencies determined for healthy individuals.

## Materials and methods

### Patients

Twelve patients (aged 5 to 16 years) previously treated for ALL were included in the study. They were diagnosed and treated at the Clinical Hospital (Faculty of Medicine of Ribeirão Preto, University of São Paulo, Brazil) with combined modality treatment according to the Brazilian Group of Pediatric Leukemia Treatment (GBTLL) (Brandalise et al., 1993) including: vincristine, dexamethasone, daunorubicin, L-asparaginase, prednisone, methotrexate, cytosine arabinoside (ARA-C), cyclophosphamide, folic acid, teniposide (VM-26) and 6 mercaptopurine (6 MP). In some cases (two patients: Pa-5 and Pa-10), prophylactic cranial irradiation was also included in the therapy. Twelve healthy subjects aged 18 to 22 years were also studied. 5 ml of peripheral blood were obtained from each individual after informed consent, and the samples were coded to ensure anonymity of the donors.

A retrospective analysis was also carried out with previously fixed bone marrow samples, which were collected from ten of the above patients at the time of diagnosis (between 1992 and 1998).

### Lymphocyte cultures and chromosome preparations

Lymphocyte cultures were prepared by the standard protocol: 0.5 ml of peripheral blood was added to 10 ml RPMI 1640 (Sigma Chemical Co., St. Louis, USA) medium supplemented with 20% fetal calf serum, 2% PHA and

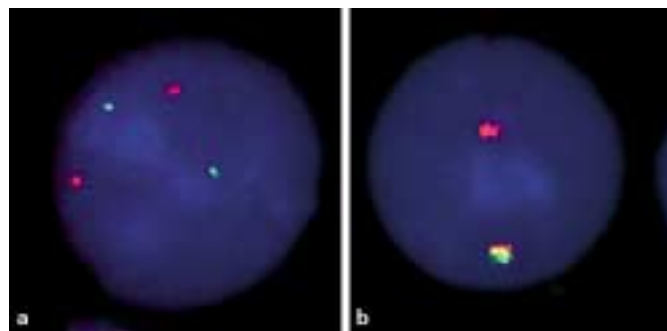


**Fig. 1.** Interphase nuclei of lymphocytes showing hybridization signals with dual-color DNA probe LSI TEL (SpectrumGreen)/AML1 (SpectrumOrange). Normal cell with two signals of each gene, ETV6 and RUNX1 (a); ETV6/RUNX1 fusion with one red-(yellow)-green signal (b).

penicillin/streptomycin (Gibco BRL, Gaithersburg, MD). The cultures were incubated for 72 h at 37 °C and treated with colchicine (0.56%) for the last 30 min. The cells were harvested and slide preparation was performed according to the conventional method. The slides for FISH were kept at -20 °C until processed.

### Fluorescence in situ hybridization

Locus-specific identifier dual-color directly labeled TEL(SpectrumGreen)/AML1(SpectrumOrange) (Vysis, Ill., USA) probes were used for detecting gene fusions. Hybridization and FISH method was applied on the basis of manufacturer's instructions.

For the LSI TEL/AML1 ES dual-color translocation probe, the expected pattern for a normal cell nucleus is two green and two red signals, corresponding to two normal copies of each gene, ETV6 and RUNX1. This probe set contains a 350-kb probe for the 5'-end of ETV6 (exons 1–4) and a 500-kb probe that covers the entire RUNX1 gene. The expected signal pattern for a nucleus with t(12;21) is one green (normal ETV6), two red (normal and residual RUNX1) and one red-(yellow)-green signals. Dual color hybridization with ETV6 (SpectrumGreen) and RUNX1 (SpectrumOrange) probes was applied to interphase nuclei. At least 1000 nuclei were analyzed per slide. The images were captured by using the Axiovision System (Zeiss, Germany).

### Statistical analysis

Kruskal-Wallis ANOVA on ranks was used to evaluate the influence of anti-cancer therapy on the frequency of ETV6/RUNX1 fusions presented by the different groups of individuals, followed by Dunn's method of multiple pair-wise comparison.

## Results

The specific dual-color probe used in this study allowed an accurate detection of ETV6/RUNX1 fusions (Fig. 1). Patients in complete remission presented frequencies of ETV6/RUNX1 fusions varying between 0.62 and 3.96/100 cells, and these values were significantly higher than those obtained for the control group, which varied from 0.59 to 1.84 fusions/100 cells (Table 1). The probes also allowed the detection of extra signals for both genes, with frequencies varying from 0.10 to 2.38/100 cells, and 0.10 to 1.45/100 cells, for patients and controls, respectively (Table 1). For extra signals, the differences between the groups of cured patients and healthy individuals were not statistically significant. The patients (Pa-5 and Pa-10)

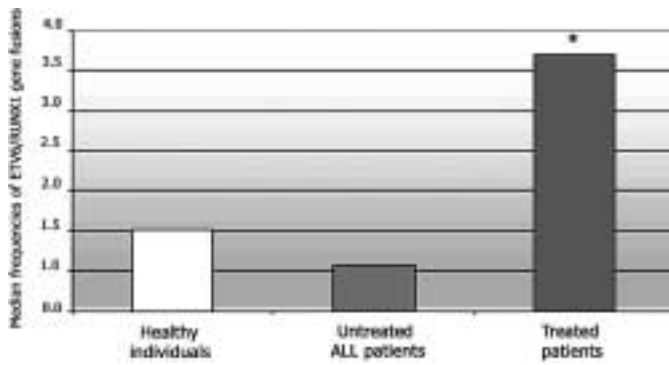


**Fig. 2.** Median frequencies of ETV6/RUNX1 fusions obtained for three groups of subjects: healthy individuals (n = 12), ALL patients at the time of diagnosis (n = 8) and ALL patients analyzed months or year(s) after therapy completion (n = 12). For the statistical analysis, two ALL patients at the time of diagnosis, who were positive for ETV6/RUNX1 fusions, were excluded. \*  $P = 0.0043$ .

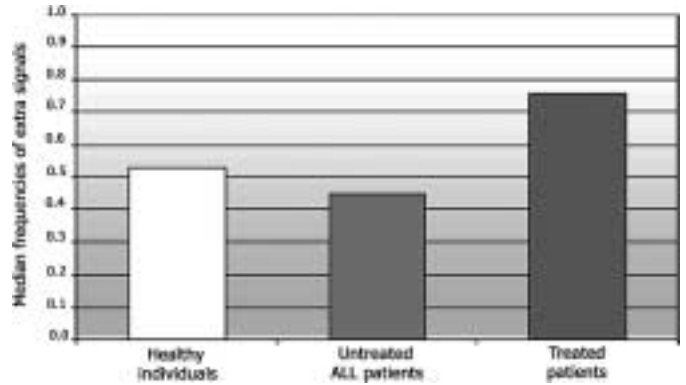


**Fig. 3.** Median frequencies of extra signals of ETV6 and RUNX1 genes determined for the three groups of subjects: control group (n = 12), ALL patients at the time of diagnosis (n = 8) and ALL patients analyzed months or year(s) after therapy completion (n = 12). For the statistical analysis, two ALL patients at the time of diagnosis (positive for ETV6 or RUNX1 extra signals) were excluded.

**Table 1.** Frequencies of ETV6/RUNX1 gene fusions and extra signals for ETV6 and RUNX1 genes in peripheral blood lymphocytes from patients (Pa) treated for ALL during childhood and control (Co) healthy individuals

Individual	Immunophenotype at initial diagnosis	Time after therapy completion (months)	Number of analyzed cells	ETV6/RUNX1 fusions/100 cells	Extra signals/100 cells
Pa-1	Pre-B (cALLA+)	1	1025	3.90	2.38
Pa-2	–	21	1028	3.02	1.07
Pa-3	Pre-B (cALLA+)	82	796	3.52	0.63
Pa-4	Pre-B (cALLA+)	19	1025	3.61	1.99
Pa-5 <sup>a</sup>	T	28	1007	3.38	1.30
Pa-6	Pre-B (cALLA+)	19	1022	1.76	0.60
Pa-7	Pro-B (cALLA–)	34	1065	1.97	0.10
Pa-8	Pre-B (cALLA+)	11	1138	0.62	0.72
Pa-9	–	23	1036	3.96	0.80
Pa-10 <sup>a</sup>	T	11	1005	2.79	1.35
Pa-11	Pre-B (cALLA+)	36	1056	3.41	0.20
Pa-12	Pre-B (cALLA+)	15	1067	0.66	0.49
Co-1	–	–	998	1.40	0.61
Co-2	–	–	1024	0.98	0.20
Co-3	–	–	1048	1.81	1.45
Co-4	–	–	1017	1.18	0.10
Co-5	–	–	1031	1.84	0.49
Co-6	–	–	1016	0.59	0.50
Co-7	–	–	1018	1.18	1.40
Co-8	–	–	1025	0.98	0.20
Co-9	–	–	1021	0.98	0.39
Co-10	–	–	1042	1.06	0.39
Co-11	–	–	1053	0.85	0.40
Co-12	–	–	1024	0.59	0.49

<sup>a</sup> Patients who received cranial irradiation.

who received cranial irradiation presented similar frequencies of ETV6/RUNX1 fusions and extra signals, compared with the other patients.

A retrospective analysis was carried out for fixed bone marrow samples collected from ten untreated ALL patients, in order to verify the presence of the rearrangement at the time of diagnosis. Despite the difficulties of working with this material, 200–500 cells were analyzed per individual. While two patients (Pa-1 and Pa-8) were positive for ETV6/RUNX1 with frequencies of 43.87 and 36.58/100 cells, respectively, eight patients

presented frequencies between 0.24 and 6.69/100 cells (Table 2). For the statistical analysis performed for the frequencies of ETV6/RUNX1 fusions, the patients positive for t(12;21) at diagnosis were excluded, and a significant difference ( $P = 0.0043$ ) was observed between the groups of patients at the time of diagnosis and years after therapy completion (pair-wise comparison). However, a significant difference was not found between the frequencies of ETV6/RUNX1 fusions presented by the patients at diagnosis and the control group (Fig. 2).

**Table 2.** Frequencies of ETV6/RUNX1 fusions and extra signals for ETV6 and RUNX1 genes in bone marrow cells from ALL patients at the time of diagnosis

Individual	Number of analyzed cells	ETV6/RUNX1 fusions/100 cells	Extra signals/100 cells
Pa-1	212	43.87	2.38
Pa-4	538	0.56	0.37
Pa-5	513	0.58	0.58
Pa-6	208	0.48	1.95
Pa-7	515	2.33	0.39
Pa-8	503	36.58	5.17
Pa-9	533	0.38	13.32
Pa-10	538	6.69	0.19
Pa-11	421	0.24	0.48
Pa-12	525	1.71	39.46

Extra signals were also verified for the patients analyzed at diagnosis (Fig. 3). Seven patients showed lower frequencies between 0.19 and 2.38 signals/100 cells, increased levels were presented by Pa-1 (5.17 signals/100 cells), and two other patients (Pa-9 and Pa-12), who showed much higher frequencies, 13.32 and 39.46/100 cells, respectively (Table 2).

## Discussion

Therapy for childhood ALL comprises several doses of anti-tumor drugs given weekly or daily for 2–3 years (Blanco et al., 2001). Since this kind of treatment is systemic, there are several reasons to suspect that anticancer treatment may increase the risk for development of secondary malignancies, mainly because it is well known that antineoplastic drugs and ionizing radiation induce chromosomal translocations.

In the present study, the frequencies of ETV6/RUNX1 gene fusions were significantly increased in patients treated for ALL during childhood when compared to the control groups (patients at diagnosis and healthy subjects). All patients were submitted to chemotherapy regimens; patients (Pa-5 and Pa-10) who also received cranial irradiation presented similar frequencies of ETV6/RUNX1 fusions and extra signals, compared with the other patients. According to Kersey (1997), it is likely that the success for ALL treatment is partially due to the ability of chemical agents to activate the apoptotic pathways in cells that are “poised to die”. Analysis of DNA sequences surrounding the breakpoints of ETV6/RUNX1 fusion exhibited characteristic signs of non-homologous end-joining (Wiemels and Greaves, 1999). These breakpoints reside within the 14-kb intron sequence between the exons 5 and 6 of ETV6 and within RUNX1 intron 1. Double strand breaks within these regions have been demonstrated in short-term cultures of immature B cell lines exposed to serum starvation, and chemical agents, such as H<sub>2</sub>O<sub>2</sub>, salicylic acid and VP-16. ETV6/RUNX1 fusion transcripts were also detected in these systems suggesting a possible relationship between the breakage/fusion of these genes and apoptotic signals (Eguchi-Ishimae et al., 2001).

Translocations involving the RUNX1 gene have been identified in therapy-related secondary leukemias (Rowley, 1999); among them, balanced translocations with ETO (Eight Twenty One) and EVI1 (Ecotropic Viral Integration site 1 oncogene) are characteristic of myeloid leukemia (Loh et al., 1998). This is compatible with reports showing the ability of topoisomerase II inhibitors to induce site-specific double strand breaks within the MLL (Aplan et al., 1996) and RUNX1 (Stanulla et al., 1997) genes. Other translocations of this kind have been identified in neoplasms related to therapy, such as t(3;21) (Hiebert et al., 1996), t(9;22) (Hattori et al., 1995), and patients accidentally exposed to ionizing radiation (Hromas et al., 2000, 2001) demonstrating the susceptibility of specific genes to mutagenic or carcinogenic agents (Seeger et al., 1998).

The significance of ETV6/RUNX1 gene fusions has been subject to some controversy, mainly because the patients positive for this molecular marker have a sustained remission rate after treatment, but a variable relapse rate after the completion of therapy, probably being dependent on the protocol used (Ford et al., 2001). According to Loh et al. (1998) it is possible that the appearance of ETV6/RUNX1 fusions during relapse could represent a therapy-related malignancy, where patients are ETV6/RUNX1 negative at initial leukemia, but positive at relapse; however, in most cases, bone marrow samples from the time of initial diagnosis or their cytogenetic data are not available. Therefore, bone marrow samples from the original leukemia are very important for comparisons during the follow-up of such patients. In the present study, a retrospective analysis was performed for bone marrow samples from ten patients collected at the time of diagnosis, using ETV6/RUNX1-specific probes. Two patients (Pa-1 and Pa-8), who were previously positive for ETV6/RUNX1 fusions at diagnosis, presented decreased frequencies after therapy, which were within the same levels presented by the other eight patients. However, the comparison of the results obtained at diagnosis and after therapy demonstrated that the differences were statistically significant, indicating an increase in the frequencies of ETV6/RUNX1 fusions in cured patients.

In spite of the therapy improvements for childhood ALL, one in four patients relapse (Vora et al., 1998). It has been suggested that relapse is the result of residual leukemic cells that remain after “complete remission”, but are beyond the limits of detection by conventional analysis of bone marrow (Stock and Estrov, 2000). The monitoring of minimal residual disease (MRD) is of great importance for prognosis and follow-up of the patients, and the application of molecular techniques facilitates the detection of these rearrangements at DNA or expression levels (Chomel et al., 1999). However, whether the ETV6/RUNX1 fusions in patients Pa-1 and Pa-8 represent MRD or “de novo” translocations as a result of exposure to anticancer drugs remains to be elucidated by further assays, such as clone-specific antigen receptor gene rearrangements (Konrad et al., 2003).

Another interesting aspect of this study is the high frequency of the ETV6/RUNX1 fusion within the control group. Recent studies have demonstrated the presence of leukemia-related chromosomal translocations in normal individuals, such as t(14;18) (Liu et al., 1994) and t(9;22) (Faderl et al., 1999). These

findings indicate that the presence of these translocations per se does not define an apparent clinical disease.

Another characteristic of ETV6/RUNX1 positive patients is the frequent deletion of the normal ETV6 gene, suggesting that the gene fusion is an initial event conferring predisposition to leukemia followed by the deletion of the gene or genes at 12p as a promoter event (Busson-Le Coniat et al., 1999; Kempfski and Sturt, 2000). Other studies with ETV6/RUNX1 knock-in mice also showed that the expression of this gene fusion is not sufficient for the *in vivo* induction of ALL (Andreasson et al., 2001).

There is evidence indicating that the ETV6/RUNX1 gene fusion originated *in utero*, but in most cases, this event is insufficient for the generation of ALL, secondary events after birth seem to be necessary (Ford et al., 1998, 2001). In twins, the development of ALL was found to occur at different periods and the postnatal latency can be variable and occasionally protracted (Wiemels et al., 1999). Retrospective studies in neonatal blood spots have demonstrated the clonality of the rearrangement. According to Mori et al. (2002) this translocation could, in theory, arise in a high proportion of developing fetuses but would not generate functional chimeric proteins in all of them, or they could arise in an inappropriate cellular context. This context is critical for the impact of chromosomal aberrations, since the biological and clinical implications of ALL are different in infants, children and adults (Greaves, 1999). In order to produce a leukemic phenotype, these rearrangements should fulfill two conditions: (1) the structure of the gene fusion must allow the production of a functional protein and (2) the translocation must occur in early precursors with self-renewal capacity (Bose et al., 1998). Therefore, it is possible that the gene fusions in normal individuals could arise in already differentiated cells or in mature precursors, which might be eliminated by normal mechanisms of cell differentiation, and possibly, they could emerge as a result of exposure to genotoxic agents.

The use of the ETV6/RUNX1 dual color probe also allowed the detection of extra signals for both genes. These extra signals

could be the result of gene amplification or they could represent translocations with other gene partners, since ETV6 and RUNX1 genes are considered to be "promiscuous" (Rowley, 1999). The retrospective analysis of bone marrow samples at the time of diagnosis also revealed two patients, Pa-9 and Pa-12, with high frequencies of extra signals (13.32 and 39.46 fusions/100 cells, respectively); but soon after the therapy, these frequencies decreased to the control levels. For eight patients, the frequencies of extra signals in bone marrow cells were similar to those observed in the control group. Therefore, while extra signals could represent a basal background for some individuals, for some others, they could represent an extent of genomic instability, which deserves to be investigated in more detail.

## Conclusions

The present results demonstrate increased frequencies of ETV6/RUNX1 gene fusions in ALL patients treated during childhood and detected several months or years after therapy, indicating the influence of the previous exposure to anti-cancer drugs. Although the presence of the translocation per se does not seem to be sufficient for leukemogenesis, the ETV6/RUNX1 fusion detected later in cured patients after therapy could represent an important genetic marker for estimating the risk of relapse, or development of secondary neoplasias.

Additionally, considering that the frequencies of extra signals for ETV6 or RUNX1 genes are elevated in some ALL patients, their detection might also be relevant for the evaluation of therapy-related genomic instability in the follow-up of these patients.

## Acknowledgements

We are grateful to all donors and their parents whose cooperative spirit was remarkable. We also thank Sueli A. Neves and Luiz A. da Costa Junior for routine technical assistance.

## References

- Andreasson P, Shwaller J, Anastasiadou E, Aster J, Gilliland DG: The expression of ETV6/CBFA2 (TEL/AML1) is not sufficient for the transformation of hematopoietic cell lines *in vitro* or the induction of hematologic disease *in vivo*. *Cancer Genet Cytogenet* 130:93–104 (2001).
- Aplan PD, Chervinsky DS, Stanulla M, Burhans WC: Site-specific DNA cleavage within the MLL breakpoint cluster region induced by topoisomerase II inhibitors. *Blood* 87:2649–2658 (1996).
- Asou N: The role of a Runt domain transcription factor AML1/RUNX1 in leukemogenesis and its clinical implications. *Crit Rev Oncol Hematol* 45:129–150 (2003).
- Bacchicet A, Qualman S, Sinnott D: Allelic loss in childhood acute lymphoblastic leukemia. *Leuk Res* 21:817–823 (1997).
- Baker A, Cachia P, Ridge S, McGlynn H, Clarke R, Whittaker J, Jacobs A, Padua RA: FMS mutations in patients following cytotoxic therapy for lymphoma. *Leuk Res* 19:309–318 (1995).
- Bäsecke J, Griesinger F, Trümper L, Brittinger G: Leukemia- and lymphoma-associated genetic alterations in healthy individuals. *Ann Hematol* 81:64–75 (2002).
- Bhatia S, Sather HN, Pabustan OB, Trigg ME, Gaynon PS, Robinson LL: Low incidence of second neoplasms among children diagnosed with acute lymphoblastic leukemia after 1983. *Blood* 99:4257–4263 (2002).
- Blanco JG, Dervieux T, Edick MJ, Mehta PK, Rubnitz JE, Shurtleff S, Raimondi SC, Behm FG, Pui C, Relling M: Molecular emergence of acute myeloid leukemia during treatment for acute lymphoblastic leukemia. *Proc natl Acad Sci, USA* 98:10338–10343 (2001).
- Blau O, Avigad S, Frish A, Kilim Y, Stark B, Kodman Y, Luria D, Cohen IJ, Zaizov R: Molecular analysis of childhood acute lymphoblastic leukemia in Israel. *Leuk Res* 22:495–500 (1998).
- Bose S, Deininger M, Gora-Tybor J, Goldman JM, Melo JV: The presence of typical and atypical BCR-ABL fusion genes in leukocytes of normal individuals: biologic significance and implications for the assessment of residual disease. *Blood* 92:3362–3367 (1998).
- Brandalise S, Odone V, Pereira W, Andrea M, Zanichelli M, Aranega V: Treatment results of three consecutive Brazilian cooperative childhood ALL protocols: GBTLI-80, GBTLI-82 and -85. *Leukemia* 7 (suppl 2):S142–145 (1993).
- Busson-Le Coniat M, Poirel H, Leblanc T, Bernard O, Berger R: Loss of the TEL/ETV6 gene by a second translocation in ALL patients with t(12;21). *Leuk Res* 23:895–899 (1999).
- Byrne J: Long-term genetic and reproductive effects of ionizing radiation and chemotherapy agents on cancer patients and their offspring. *Theratology* 59:210–215 (1999).

- Chomel J, Brizard F, Veinstein A, Sadoun A, Guilhot F, Brizard A: Persistence of BCR/ABL genomic rearrangement in chronic myeloid leukemia patients in complete and sustained cytogenetic remission after interferon- $\alpha$  therapy or allogeneic bone marrow transplantation. *Blood* 95:404–409 (1999).
- Coustan-Smith E, Sancho J, Hancock L, Boyett JM, Raimondi S, Sandlund JT, Rivera GK, Rubnitz JE, Ribeiro RC, Pui C, Campana D: Clinical importance of minimal residual disease in childhood acute lymphoblastic leukemia. *Blood* 96:2691–2696 (2000).
- Eguchi-Ishimae M, Eguchi M, Ishii E, Ueda K, Kamada N, Mizutani S: Breakage and fusion of TEL(ETV6) gene in immature B lymphocytes induced by apoptotic signals. *Blood* 97:737–743 (2001).
- Faderl S, Talpaz M, Kantarjian HM, Estrov Z: Should polymerase chain reaction analysis to detect minimal residual disease in patients with chronic myelogenous leukemia be used in clinical decision making? *Blood* 93:2755–2759 (1999).
- Ford AM, Bennet CA, Price CM, Bruim MCA, Van Wering ER, Greaves M: Fetal origins of the TEL/AML1 fusion gene in identical twins with leukemia. *Proc natl Acad Sci, USA* 95:4584–4588 (1998).
- Ford AM, Fasching K, Pranzler-Grümayer R, Koenig M, Haas OA, Greaves MF: Origins of “late” relapse in childhood acute lymphoblastic leukemia with TEL/AML1 fusion genes. *Blood* 98:558–564 (2001).
- Greaves M: Molecular genetics, natural history and demise of childhood leukemia. *Eur J Cancer* 35:173–185 (1999).
- Hattori M, Tanaka M, Yamazaki Y, Nakahara Y, Tsuchita K, Utumi M: Detection of major and minor BCR/ABL fusion gene transcripts in a patient with acute undifferentiated leukemia secondary to treatment with an alkylating agent. *Leuk Res* 19:389–396 (1995).
- Hiebert SW, Sun W, Davis JN, Shurleff S, Bulis A, Downing JR, Grosveld G, Rousell MF, Gilliland DG, Lenny N, Myers S: The t(12;21) translocation converts AML-1B from an activator to a repressor of transcription. *Mol Cell Biol* 16:1349–1355 (1996).
- Hromas R, Shopnick R, Jumean HG, Bowers C, Varella-Garcia M, Richkind K: A novel syndrome of radiation-associated acute myeloid leukemia involving AML1 gene translocations. *Blood* 95:4011–4013 (2000).
- Hromas R, Busse T, Carroll A, Mack D, Shopnick R, Zhang D, Nakshatri H, Richkind K: Fusion AML1 transcript in a radiation-associated leukemia results in truncated inhibitory AML1 protein. *Blood* 97:2168–2170 (2001).
- Kempinski HM, Sturt NT: The TEL/AML1 fusion accompanied by loss of the untranslocated TEL allele in B-precursor acute lymphoblastic leukemia of childhood. *Leuk Lymphoma* 40:39–47 (2000).
- Kersey JH: Fifty years of studies of the biology and therapy of childhood leukemia. *Blood* 90:4243–4251 (1997).
- Koishi S, Kubota M, Sawada M, Hirota H, Hashimoto H, Lin Y, Watanabe K, Usami I, Akiyama Y, Furusho K: Biomarkers in long survivors of pediatric acute lymphoblastic leukemia patients: late effects of cancer chemotherapy. *Mutat Res* 422:213–222 (1998).
- Konrad M, Metzler M, Panzer S, Östreich I, Peham M, Repp R, Haas OA, Gardner H, Panzer-Grümayer R: Late relapses evolve from slow-responding subclones in t(12;21) positive acute lymphoblastic leukemia: evidence for the persistence of a pre-leukemic clone. *Blood* 10:3635–3640 (2003).
- Lipkowitz S, Garry VF, Kirsch IR: Interlocus V-J recombination measures genomic instability in agriculture workers at risk for lymphoid malignancies. *Proc natl Acad Sci, USA* 89:5301–5305 (1992).
- Liu Y, Hernandez AM, Shibata D, Cortopassi GA: BCL2 translocation frequency rises with age in humans. *Proc natl Acad Sci, USA* 91:8910–8914 (1994).
- Loh ML, Silverman LB, Young ML, Neuberger D, Golub TR, Sallan SE, Gilliland DG: Incidence of TEL/AML1 fusion in children with relapsed acute lymphoblastic leukemia. *Blood* 92:4792–4797 (1998).
- Mori H, Colman SM, Xiao Z, Ford A, Healy LE, Donaldson C, Hows JM, Navarrete C, Greaves M: Chromosome translocations and covert leukemic clones are generated during normal fetal development. *Proc natl Acad Sci, USA* 99:8242–8247 (2002).
- Rowley J: The role of chromosome translocations in leukemogenesis. *Semin Hematol* 36:59–72 (1999).
- Seeger H, Dams H, Buchwald D, Beyersmann B, Krems B, Niemeier C, Ritter J, Shwabe D, Harms D, Schappe M, Henze G: TEL/AML1 fusion transcript in relapsed childhood acute lymphoblastic leukemia. *Blood* 91:1716–1722 (1998).
- Stanulla M, Wang J, Chervinsky DS, Aplan PD: Topoisomerase II inhibitors induce double-strand breaks at a specific site within the AML1 locus. *Leukemia* 11:490–496 (1997).
- Stock W, Estrov Z: Studies of minimal residual disease in acute lymphoblastic leukemia. *Hematol Oncol Clin North Am* 14:1289–1305 (2000).
- Vora A, Frost L, Goodeve A, Wilson G, Ireland RM, Lilleyman J, Eden T, Peake I, Richards S: Late relapsing childhood lymphoblastic leukemia. *Blood* 92:2334–2337 (1998).
- Wang LC, Swat W, Fujiwara Y, Davidson L, Visvader J, Kuo F, Alt FW, Gilliland DG, Golub TR, Orkin SH: The TEL/AML1 gene is required specifically for hematopoiesis in the bone marrow. *Genes Dev* 12:2392–2402 (1998).
- Wiemels JL, Greaves M: Structure and possible mechanisms of ETV6/RUNX1 gene fusions in childhood acute lymphoblastic leukemia. *Cancer Res* 59:4075–4082 (1999).
- Wiemels JL, Ford AM, Van Wering ER, Postma A, Greaves M: Protracted and variable latency of acute lymphoblastic leukemia after TEL/AML1 gene fusion in utero. *Blood* 94:1057–1062 (1999).



# Comparative genomic hybridization (CGH): ten years of substantial progress in human solid tumor molecular cytogenetics

E. Gebhart

Institute of Human Genetics, University of Erlangen-Nürnberg, Erlangen (Germany)

**Abstract.** Data from ten years of research using comparative genomic hybridization (CGH) for the detection of chromosomal alterations in human solid tumors are concisely reviewed. By use of a basic methodology with some variations more or less specific patterns of genomic imbalances were found in a large number of tumors of various entities. Specific gains and losses of genomic material have not only opened the

way to the detection of a series of cancer-related genes but also to clinical implications. Not only several areas of basic oncogenetic research, but also differential diagnosis, prognosis of disease progression, and therapeutic decisions have profited by CGH.

Copyright © 2003 S. Karger AG, Basel

Nearly all human malignant tumors are characterized by genomic changes. Classical cytogenetic analyses using chromosome banding techniques, over decades, were the “gold standard” for their detection. A large survey on cytogenetics of 3,185 malignant solid tumors has been presented by Mertens et al. (1997). However, supreme efforts of karyotyping had to be undertaken for their characterization. As a well-known fact, only a limited portion of solid tumors examined by classical cytogenetic techniques yields a sufficient number of evaluable mitoses for establishing the karyotype. Main reasons were low mitotic yield, low number of evaluable metaphases, mostly low quality of chromosome banding, and sometimes very complex karyotypes not allowing definite analysis. All collections of classical tumor cytogenetics data, therefore, had to be based on a rather selected fraction of evaluable tumors.

The advent of comparative genomic hybridization (CGH), a special fluorescence in situ hybridization (FISH) technique (Kallioniemi et al., 1992; Du Manoir et al., 1993) has opened a

reliable way for the detection of all (dissolvable) genomic imbalances (copy number alterations [CNAs] of DNA) in each tumor (including archival material) without selection, by only one single analysis. Not being dependent on mitoses, it overcame most limiting factors of classical cytogenetics. One of its basic disadvantages, however, is its lacking suitability to detect balanced chromosomal rearrangements which, e.g., are most characteristic for neoplasias of the hematopoietic system. Facing the highly complex karyotypes of human solid tumors, which in their great majority are caused by imbalanced alterations of genomic material, this disadvantage is more than outweighed by the substantial insights CGH allows into their genomic changes, and the substantial clinical implications the obtained data have contributed over the ten years of CGH application.

## Methodological aspects

The principle of the CGH technique, as first described by Kallioniemi et al. (1992) and technically improved later on (Kallioniemi et al., 1994) lies in the comparison of total genomic DNA extracted from a tumor with total genomic DNA obtained from normal cells. Briefly, a small aliquot (e.g. 500 ng) of tumor DNA and an identical amount of normal DNA are labeled with biotin and digoxigenin, respectively, by nick trans-

Received 17 July 2003; manuscript accepted 12 November 2003.

Request reprints from Prof. Dr. E. Gebhart  
Institut für Humangenetik der Universität  
Schwabachanlage 10, DE-91054 Erlangen (Germany)  
telephone: +49 9131 8522351; fax: +49 9131 209297  
e-mail: egebhart@humgenet.uni-erlangen.de

lation. A defined quantity of Cot-1 DNA is added for suppression of repetitive DNA sequences and the probe mixture then is denatured in buffered formamide/dextran sulfate for 3 min at 75°C and pre-annealed at 37°C for 20 min. Then the probe mixture is hybridized to a normal lymphocyte metaphase slide denatured in 70% formamide/2× SSC/sodium phosphate buffer, covered with a cover slide, and sealed with rubber cement. Hybridization is carried out for 3 days at 37°C in a humidified chamber. For fluorescence detection, the slides are stained with avidin-fluorescein isothiocyanate and anti-digoxigenin-rhodamine, followed by counter-staining with DAPI (4',6-diamidino-2-phenylindole). The slides then are mounted in antifade solution. Quantities of components and technical details can be found in the numerous CGH publications (Wolff et al., 1998; Jeuken et al., 2002). Evaluation needs a fluorescence microscope of high quality equipped with a CCD camera and an image analysis system. Gains (enh) or losses (dim) of genetic material are calculated as statistically significant by an evaluation software (Du Manoir et al., 1995; Lundsteen et al., 1995), if fluorescence ratio threshold values are exceeded. These thresholds can be defined as "fixed" or "standard reference" intervals (Kirchhoff et al., 1999). A sufficient number of karyotypes obtained from hybridized lymphocyte mitoses are analyzed per experiment. As internal controls contra-sexual DNAs or reverse labels of target and reference DNA may be used for the hybridizations. Further technical details are reviewed by James (1999) and Jeuken et al. (2002).

Two basic limitations of the resolution of the CGH technique, however, must be borne in mind when estimating its power: the minimal size of a chromosomal segment the alteration of which can be reliably shown, and the minimal portion of a cell population carrying the respective change to be detected. Most studies addressing the first limitation agree in that the minimal size of a detectable genomic segment is about 3–5 Mb (Bentz et al., 1998; Kirchhoff et al., 1999; Brecevic et al., 2001). Gebhart et al. (2000) by comparative I-FISH analyses on the same material (leukemic bone marrow) determined the minimal cell population in which a certain change could be found by CGH as 25% of the cells, a value close to the level (32%) shown by experimental cell mixtures (Larsen et al., 1999).

The power of CGH has additionally been increased by further technical improvements, e.g., microdissection of specific areas (e.g. without contamination by normal cells) of archival (e.g. paraffin-embedded) tumor samples using micromanipulator-directed fine needle or laser technology for obtaining small but specific tumor DNA samples and amplifying them by polymerase chain reaction (PCR) for CGH use (Daigo et al., 2001; Hirose et al., 2001). This technique also allows a comparative examination of various areas within the same tumor (and even of single cells) and thus an examination of the intratumoral heterogeneity. More recently, a substantial improvement of the specificity of the obtained data has been attained by the introduction of array techniques (Solinas-Toldo et al., 1997; Wessendorf et al., 2002), i.e. a step from analysis on crude chromosomal segments to the level of specific DNA sequences (e.g. genes). A steadily growing number of studies utilize this new technique now.

## Patterns of genomic imbalances: basic aspects

Thousands of tumors have been analyzed by CGH so far. Characteristic patterns of genomic alterations could be associated with a variety of tumor entities. Most of the obtained data have just been included in large reviews (Zitzelsberger et al., 1997; Knuutila et al., 1998, 1999; Rooney et al., 1999; Gebhart and Liehr, 2000; Koschny et al., 2002; Struski et al., 2002). The average number of CNAs per tumor varies in dependence of the tumor entity (or location) from 23 in oral (Wolff et al., 1998) and 17.7 in head and neck squamous cell carcinomas (HNSCC; Rooney et al., 1999) via 13.6 in colorectal cancer to 2.3 in Wilms tumor (Table 1). These numbers, however, sometimes differ considerably between the various reports on the same tumor entity. As reviewed by Rooney et al. (1999), the most frequent overall gains of genomic sequences (i.e. being present in more than 10% of all 2,210 evaluated tumors) affected the long arms of chromosomes 8, 7, 17, 3, 20, 12, and 11 (in the order of prevalence) and the short arms of chromosomes 7, 5, 12, and 6. In contrast, rare events (present in less than 5% of all tumors) were gains of Xp, 3p, 21q, 11p, 4p, and Y. Most frequent losses were found on 13q, 9p, and 8p, rarest losses (below 3% of the tumors) affected 8q, 7q, 20q, 12p, and 7p.

The non-random involvement of certain chromosomes, chromosome segments and even chromosome bands in imbalances (causing the specific patterns of genomic imbalances presented by Gebhart and Liehr, 2000) led to various speculations on the causative parameters. The clustering of high average CNA numbers in tumors of the ingestion or respiratory ways supports the hypothesis of the latter authors who pointed to the possible role of steady mutagenic influences of environmental factors on the number and the evolving pattern of genomic imbalances in exposed tumors. In fact, clear differences of these patterns, but also of CNA numbers (Table 1) could be found e.g. between tumors directly exposed to ingested mutagens along all their development, and tumors "down-stream" the metabolizing systems (e.g. ependymomas, or tumors with hereditary background). A rough grouping of the tumor entities of Table 1 finds the highest percentage of mutagen-exposed locations among tumors with ten or more CNAs and not one among those with CNA numbers below five. Hormone-dependent cancers are mainly found in the group with six to eight CNAs.

These differences of patterns are just reflected on the level of single exemplary chromosomes (e.g. Fig. 1), but have been confirmed for all chromosomes of the human karyotype by many recent reports (in particular by Gebhart and Liehr, 2000).

## Specific chromosomal changes in single tumor entities

Gains (and amplifications) of genomic material can be associated with an increase of dosage of proliferation enhancing genes (e.g. proto-oncogenes), and losses point to loci of tumor suppressor genes. Therefore, it is of high interest to detect those changes which can be related to the respective tumor type in a more specific way. They seem rather to be tumor immanent than caused by exogenous influences. Most striking examples

**Table 1.** Collection of nearly 8,000 tumors examined by CGH grouped according to their entity and ranked on the average number of copy number alterations (CNAs)<sup>a</sup>

Tumor type/site	No. of cases evaluated	Average no. of CNAs	Most frequent imbalances		References <sup>b</sup>
			genomic losses on	genomic gains on	
HNSCC <sup>c</sup>	351	13.6 <sup>d</sup>	3p, 5q21	3q26q27, 5p15, 11q13	1–12
colorectal carcinomas	223	13.6 <sup>d</sup>	18q, 8p	20q, 8q24	13–20
lung carcinomas	212	11.8 <sup>d</sup>	3p, 5q	3q26q29, 5p	21–29
esophageal carcinoma	285	11.2 <sup>d</sup>	4q21q26, 7p21p22	3q26q27, 8q24	30–40
osteosarcomas	111	11.1 <sup>d</sup>	10q, 13q	8q, 1p, 1q, 17p, 19	250–253
ovarian carcinoma	362	10.9 <sup>d</sup>	16q, 17p, 18q	3q, 8q, 1q, 20q	41–51
pancreatic carcinoma	223	10.8 <sup>d</sup>	9p, 18q	20q, 17q, 7, 8q, 12p	52–61
testicular cancer	100	10.2 <sup>d</sup>	13q, 18q	12p, 7, 8	254–258
myosarcomas	187	9.6		12q13, 2q, 17p, 7q, 1q21	62–70
adrenocortical carcinoma	106	9.3	4, 18q	12q24, 9q34	71–75
malig. fibrous histiocytoma	141	8.2	13q, 12p	12q15q15, 6q, 5p, 1p21	76–80
breast cancer	725	7.9	16q, 9p, 17p, 18q	1q, 8q, 17q, 11q13, 20q	81–102
gastric cancer	584	7.4	Y, 4q, 17p13	17q, 8q34, 20q, 5q15	103–117
liver carcinoma	523	7.4	4q21q26	1q, 8q	118–131
nasopharynx carcinoma	113	7.4	3p14p21, 9p, 11q23	12p12, 12q13q15, 1q21q22	132–134
urinary bladder carcinoma	520	7.2	9, 8p, 11, Y	1q, 5p, 8q, 17q, 3q, 20q	135–146
neuroblastoma	318	7.0	1p36	17q, 2p23p24, 3q24q26, 8q	147–154
uterine carcinomas	292	6.8 <sup>d</sup>	3p, 4q, 13q	8q, 3q, 5p	155–164
prostate carcinoma	262	6.8	8p, 13q	8q, 7q, 17q	165–173
mesothelioma	122	6.5	9p21, 22q	1q, 15q, 8q	174–176
astrocytomas	523	6.3	9p, 10q, 13q, 1q	7, 8q, 20q	177–195
kidney carcinomas	410	5.6	3p, 4q, 9p, Y	1q, 7q, 8q, 17q	196–209
malig. melanoma	118	5.6	9, 10q	8q, 6p, 7	210–215
ependymomas	196	4.4	22q, 6q	1q, 7, 9q, 17q	216–222
pheochromocytoma	100	4.3	1p, 3q, 11	19, 17q	223–226
retinoblastoma	200	4.1	16q	6p, 1q, 2p	227–230
thyroid carcinoma	332	3.1	22q, 11q	19, 9q34	231–240
pituitary adenoma	120	2.9	11	19, X	241–245
Ewing's sarcoma	107	2.3	16q	8, 12, 1q	259–261
Wilms tumor	127	2.3	4q, 9p	1q, 8q, 12q	246–249

<sup>a</sup> Tumors were only included if at least 100 cases could be collected from studies reporting on a minimum of 10 cases.

<sup>b</sup> A complete list of all cited references is available under <http://karger.com/doi/10.1159/000077515>

<sup>c</sup> Head and neck squamous cell carcinomas excluding nasopharynx localization.

<sup>d</sup> Big differences between the cited studies with respect to average numbers of CNAs.

are gain of 12p in seminomas, amplification (amp) of 2p23p24 and loss of 1p36 in neuroblastomas, which by their uniqueness have gained great importance in differential diagnosis. In addition, by number of CNAs and specific patterns of genomic imbalances, tumor sub-entities can often be separated from each other, as has been reported for a great number of cases, e.g. by Rooney et al. (1999). Histologic subtypes, for instance, have been distinguished by CGH in various connective tissue tumors, as have developmental or clinical stages been in colon cancer, tumor classes (pT) in head and neck cancer, and primary vs. recurrent tumor in prostate cancer. Sometimes these separations could be based on single specific imbalances, in other cases clear differences of the frequency of one of the more common alterations delimitate a tumor entity from another (e.g. loss of 9p in cutaneous melanoma vs. colon or gastric cancer). Other differentiations could be made by CGH of benign and malignant phenotype in soft tissue tumors (Levy et al., 2000) and meningioma (Weber et al., 1997), early vs. progressed (metastatic) stages in many tumor entities, or hereditary and non-hereditary forms of breast (Wessels et al., 2002) or ovary tumors and gastrointestinal tumors (Gebhart and Liehr, 2000).

Those alterations sometimes can be and have been used, for instance, for differential diagnosis and for prognostic purposes (see below). Several of them paved the way to the detection of many malignancy-related genes (Monni et al., 2001; Willis et al., 2003) thus rendering CGH one of the most valuable tools of oncogenetic basic research, particularly since the introduction of array-based CGH.

### Tumor progression and metastasis

Karyotypic evolution has been a well-known finding in human neoplasia for decades. Genomic changes accompanying tumor progression and metastasis, of course, are also reflected by changes in the patterns of genomic imbalances. As previously reported by several authors, highly progressed head and neck squamous cell carcinomas (HNSCCs) but also many other tumors are characterized by a large variety of genomic imbalances. Some of those apparently are involved in the process of tumor progression as has been shown by consecutive comparative CGH examinations (Huang et al., 2002; Bastian, 2003). Taking only gain of 8q and loss of 8p as an example,

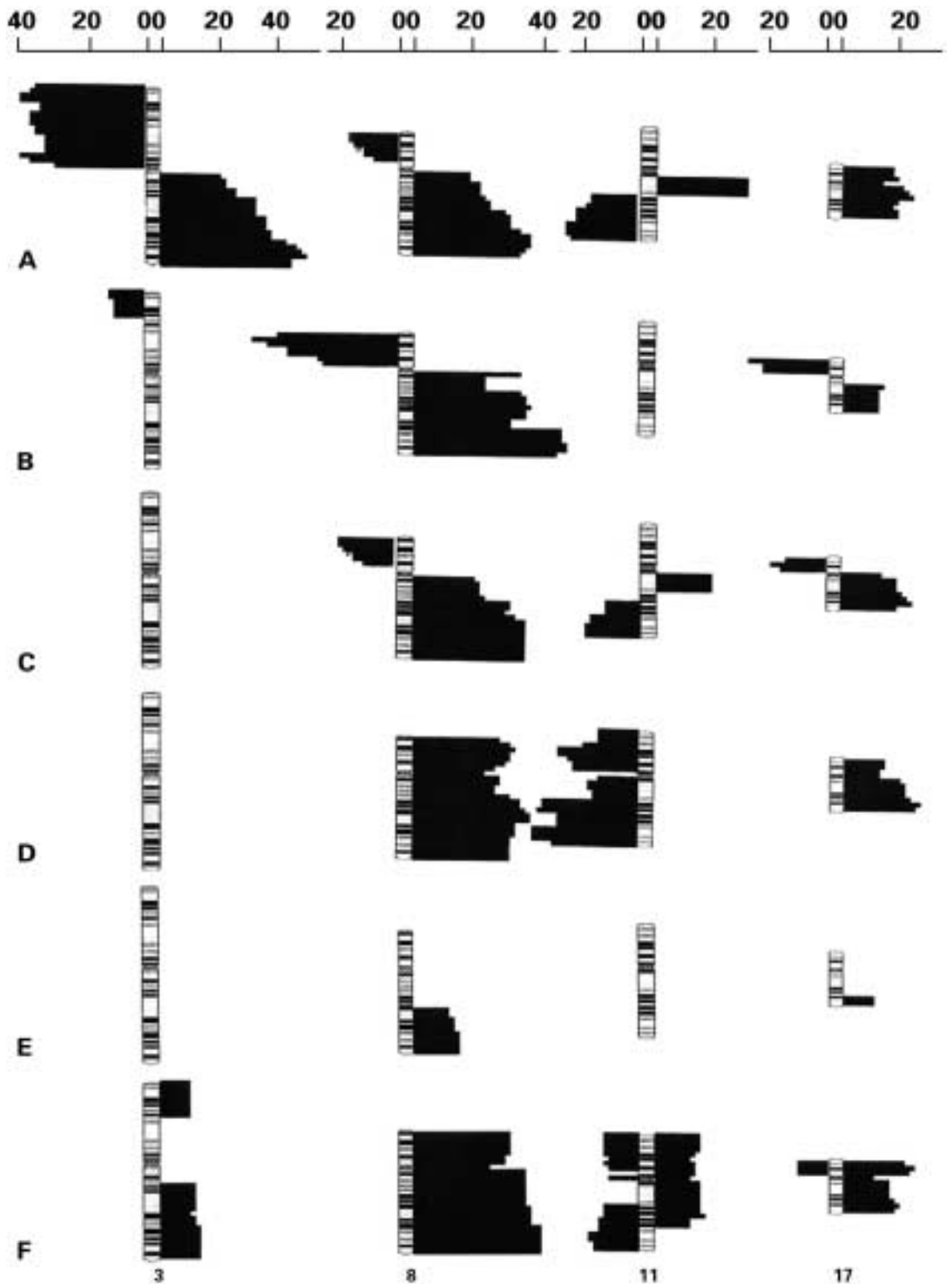


**Fig. 1.** Exemplary CNA patterns on four selected chromosomes (3, 8, 11, 17 presented in this order from left to right) in various tumor entities. **(A)** Head and neck squamous cell carcinoma (from 440 cases). **(B)** Colorectal carcinoma (from 135 cases). **(C)** Breast carcinoma (from 678 cases). **(D)** Glioblastoma/astrocytoma (from 506 cases). **(E)** Myosarcoma (from 251 cases). **(F)** Testicular cancer (from 118 cases). Only reports on more than 10 cases were considered. The columns (left: losses of genomic material, right: gain of genomic material) represent the percentage of tumors carrying the same alteration in the respective chromosomal segment; only values higher than 10% were considered.

Fig. 1 documents that those imbalances may be of general importance in progression of a variety of tumors. Primary tumors and their metastases frequently show similar patterns of CNAs, however, e.g. in HNSCC discordance between primary and paired metastatic specimens may vary from 0 to 100% (Tremmel et al., 2003). The number of CNAs, on average, is usually higher in metastases. A few imbalances also proved to be more clearly associated with metastasis. Frequent gain of 8q in head and neck cancer, uveal melanoma, carcinomas of esophagus, colon and rectum, gastrointestinal, and prostate, and loss of 8p in some of those and in renal and hepatocellular carcinomas may serve as examples for evidence of this statement (Petersen et al., 1997; Qin et al., 1999; Bockmühl et al., 2002; Diep et al., 2003). Another representative imbalance is chromosome 17, the long arm of which has been found amplified in metastases of colorectal, renal cell, pancreatic, and gastrointestinal carcinomas, as has been loss of its short arm in progressed states and in metastases of colorectal, breast, lung, liver, and prostate cancers. Beside a series of further imbalances present in metastases of various tumors (e.g. gains on 17q, losses on 10q), it should be mentioned that there is also a number of specific imbalances restricted to metastases of certain tumor entities only, which as so-called "private" changes may also yield important evidence of genomic regions harboring genes involved in metastasis in an entity-specific way. Those are, e.g., *enh(17q24 q25)* and *dim(21q)* in metastases of colorectal tumors, *dim(18q)* in those of breast carcinomas, and *dim(5p12)*, *dim(10p12)*, *dim(11p13p14)*, or *dim(14q22q24)* in HNSCC metastases. References for all these observations can be found in the reviews and papers cited above and in Knösel et al. (2002).

### Clinical implications

As a consequence of the reported detection of individual genomic changes of high value for differential diagnosis and prognosis by CGH (see above), the clinical impact of this technique is evident: In addition to the examples presented above, practical diagnostic use of CGH in this sense could be adopted for the following neoplasms: lipoma vs. lipoma-like liposarcoma [*amp(12q)*], Ewing's sarcoma [*enh(8, 1q, 12)* and *dim(16q)*], oligodendrogliomas [*dim(1q, 19q)*], neuroblastoma [*enh/amp(2p)*, *enh(17q)* *dim(1p)*], alveolar rhabdomyosarcoma [*enh(2p)*] and mesothelioma [*dim(10, 14)*]. The finding of a general prognostic impact of oncogene amplifications (e.g. *erbB2* etc.) in human solid tumors has also stimulated corresponding CGH examinations in a variety of cancer entities. Others applied CGH as a technique for the detection of CNAs [e.g. *enh(11q13)*, *enh(12q24)*, *enh(17)*, *enh(18p)*] of high prognostic impact (Sallinen et al., 1997; Dellas et al., 1999; Austrup et al., 2000; Aubele et al., 2002; Ueno et al., 2002). CNAs (as e.g. loss of 8p) also proved to be useful markers for distinguishing between organ-confined and locally advanced prostate cancer (Chu et al., 2003). High-level amplification of 18p11.3 differentiated locally recurring from primary soft tissue sarcoma (Popov et al., 2001). Recently, genetic aberrations could be correlated with WHO-defined histology and stage across the spectrum of thymomas (Inoue et al., 2003).

The finding of an involvement of genomic gains and amplifications in therapy resistance in various tumors (Rao et al., 1998; Makhija et al., 2003) or tumor cell lines (Nessling et al., 1999), but also in T-ALL cell lines (Efferth et al., 2002) has opened new perspectives of this technique for choice of the optimal individual therapy. On the other hand, the usually high similarity of CNA patterns between primary tumors and their metastases precludes most CGH-detected genomic imbalances from being markers predictive of metastasis. However, some specific changes, and particularly high numbers of CNAs in a tumor may well signal its grade of progression and its potency of metastasizing (Armengol et al., 2001).

### Is CGH also a suitable technique for mutagenesis research?

As CGH can detect genomic imbalances only if a considerable portion of a cell population is affected by the same alteration, it is not suited for basic screening of random chromosomal aberrations in mutagen-exposed cells. For instance, even a cytostatic treatment with chlorambucil of chronic lymphocytic leukemia for more than one year did not induce CNA patterns in the B-cells of the exposed patients deviating from those usually seen in this disease (Amiel et al., 2003). However, CGH readily detects clonal chromosomal imbalances in tissues (e.g. bone marrow) of patients suffering from chromosomal instability syndromes. Therefore, an increase of those alterations theoretically should also be detectable in individuals exposed to strong mutagens over longer periods as should, in particular, be the clonal amplification of genetic structures as a consequence of those exposures. First attempts of a comparison of patterns of genomic imbalances in renal cell carcinomas of patients who had been occupationally exposed to trichloroethylene with those of sporadic carcinomas did not reveal any significant difference (Schraml et al., 1999). Six PhIP-induced mammary carcinomas in rats, however, showed genomic losses in the same specific regions of chromosomes 2, 3, 11, 18, and X, whereas three carcinomas induced by dimethylbenzanthracene (DMBA) showed no consistent patterns of chromosomal gains or losses as evaluated by CGH (Christian et al., 2002). Future research should be focused on this aspects of mutagen-associated carcinogenesis.

## References

- Amiel A, Biton I, Yukla M, Gaber E, Fejgin MD, Lishner M: The effect of chlorambucil treatment on cytogenetic parameters in chronic lymphocytic leukaemia patients. *Cancer Genet Cytogenet* 143:113–119 (2003).
- Armengol G, Capella G, Farre L, Peinado MA, Miro R, Caballin MR: Genetic evolution in the metastatic progression of human pancreatic cancer studied by CGH. *Lab Invest* 81:1703–1707 (2001).
- Aubele M, Auer G, Braselmann H, Nahrig J, Zitzelsberger H, Quintanilla-Martinez L, Smida J, Walch A, Höfler H, Werner M: Chromosomal imbalances are associated with metastasis-free survival in breast cancer patients. *Anal cell Pathol* 24:77–87 (2002).
- Austrup F, Uciechowski P, Eder C, Böckmann B, Suchy B, Driesel G, Jäckel S, Kusiak I, Grill HJ, Giesing M: Prognostic value of genomic alterations in minimal residual cancer cells purified from the blood of breast cancer patients. *Brit J Cancer* 83:1664–1673 (2000).
- Bastian BC: Understanding the progression of myelocytic neoplasia using genomic analysis: from fields to cancer. *Oncogene* 22:3081–3086 (2003).
- Bentz M, Plesch A, Stilgenbauer S, Döhner H, Lichter P: Minimal size of deletions detected by comparative genomic hybridization. *Genes Chrom Cancer* 21:172–175 (1998).
- Bockmühl U, Schlüns K, Schmidt S, Mathias S, Petersen I: Chromosomal alterations during metastasis formation of head and neck squamous cell carcinoma. *Genes Chrom Cancer* 33:29–35 (2002).
- Breccvic L, Verdorfer I, Saul W, Trautmann U, Gebhart E: The cytogenetic view of standard comparative genomic hybridization (CGH): Deletions of 20q in human leukemia as a measure of the sensitivity of the technique. *Anticancer Res* 21:89–92 (2001).
- Christian AT, Snyderwine EG, Tucker JD: Comparative genomic hybridization analysis of PhIP-induced mammary carcinomas in rats reveals a cytogenetic signature. *Mutat Res* 506–507:113–119 (2002).
- Chu LW, Troncoso P, Johnston DA, Liang JC: Genetic markers useful for distinguishing between organ-confined and locally advanced prostate cancer. *Genes Chrom Cancer* 36:303–312 (2003).
- Daigo Y, Chin SF, Gorrige KL, Bobrow LG, Ponder BA, Pharoah PD, Caldas C: Degenerate oligonucleotide primed-polymerase chain reaction-based array comparative genomic hybridization for extensive amplicon profiling of breast cancers: a new approach for the molecular analysis of paraffin-embedded cancer tissue. *Am J Pathol* 158:1623–1631 (2001).
- Dellas A, Torhorst J, Jiang F, Proffitt J, Schultheiss E, Holzgreve W, Sauter G, Mihatsch MJ, Moch H: Prognostic value of genomic aberrations in invasive cervical squamous cell carcinoma of clinical stage IB detected by comparative genomic hybridization. *Cancer Res* 59:3475–3479 (1999).
- Diep CB, Thorstensen L, Meling GI, Skovlund E, Rognum TO, Lothe RA: Genetic tumor markers with prognostic impact in Dukes' stages B and C colorectal cancer patients. *J Clin Oncol* 21:820–829 (2003).
- Du Manoir S, Speicher MR, Joos S, Schröck E, Popp S, Döhner H, Kovacs G, Robert-Nicoud M, Lichter P, Cremer T: Detection of complete and partial chromosome gains and losses by comparative genomic in situ hybridisation. *Hum Genet* 90:590–610 (1993).
- Du Manoir S, Kallioniemi OP, Lichter P, Piper J, Benedetti BA, Carothers AD, Fantes JA, Garcia-Sagredo JM, Gerdes T, Giollant M, Hemery B, Isola J, Maahr J, Morrison H, Perry P, Stark M, Sudar D, Van Vliet LJ, Verwoerd N, Vrolijk J: Hardware and software requirements for quantitative analysis of comparative genomic hybridization. *Cytometry* 19:4–9 (1995).
- Efferth T, Verdorfer I, Miyachi H, Sauerbrey A, Drexler HG, Chitambar CR, Haber M, Gebhart E: Genomic imbalances in drug-resistant T-cell acute lymphoblastic CEM leukaemia cell lines. *Blood Cells Mol Dis* 29:1–13 (2002).
- Gebhart E, Liehr T: Patterns of genomic imbalances in human solid tumors (Review). *Int J Oncol* 16:383–399 (2000).
- Gebhart E, Verdorfer I, Saul W, Trautmann U, Breccvic L: Delimiting the use of comparative genomic hybridization in human myeloid neoplastic disorders. *Int J Oncol* 16:1099–1105 (2000).
- Hirose Y, Aldape K, Takahashi M, Berger MS, Feuerstein BG: Tissue microdissection and degenerate oligonucleotide primed-polymerase chain reaction (DOP-PCR) is an effective method to analyze genetic aberrations in invasive tumors. *J molec Diagn* 3:62–67 (2001).
- Huang Q, Yu GP, McCormick SA, Mo J, Datta B, Mahimkar M, Lazarus P, Schäffer AA, Desper R, Schantz SP: Genetic differences detected by comparative genomic hybridization in head and neck squamous cell carcinomas from different tumor sites: Construction of oncogenetic trees for tumor progression. *Genes Chrom Cancer* 34:224–233 (2002).
- Inoue M, Starostik P, Zettl A, Ströbel P, Schwarz S, Scaravalli F, Henry K, Wilcox N, Müller-Hermelink HK, Marx A: Correlating genetic aberrations with World Health Organization-defined histology and stage across the spectrum of thymomas. *Cancer Res* 63:3708–3715 (2003).
- James LA: Comparative genomic hybridisation as a tool in tumour cytogenetics. *J Pathol* 187:385–395 (1999).
- Jeuken JWM, Sprenger SHE, Wesseling P: Comparative genomic hybridization: Practical guidelines. *Diagn molec Pathol* 11:193–203 (2002).
- Kallioniemi A, Kallioniemi OP, Sudar D, Rutovitz D, Gray JW, Waldman F, Pinkel D: Comparative genomic hybridization for molecular cytogenetic analysis of solid tumors. *Science* 258:818–821 (1992).
- Kallioniemi OP, Kallioniemi A, Piper J, Isola J, Waldman F, Gray JW, Pinkel D: Optimizing comparative genomic hybridization for analysis of DNA sequence copy number changes in solid tumors. *Genes Chrom Cancer* 10:231–243 (1994).
- Kirchhoff M, Gerdes T, Maahr J, Rose H, Bentz M, Döhner H, Lundsteen C: Deletions below 10 megabase pairs are detected in comparative genomic hybridization by standard reference intervals. *Genes Chrom Cancer* 25:410–413 (1999).
- Knösel T, Petersen S, Schwabe H, Schlüns K, Stein U, Schlag PM, Dietel M, Petersen I: Incidence of chromosomal imbalances in advanced colorectal carcinomas and their metastases. *Virchows Arch* 440:187–194 (2002).
- Knuutila S, Björkqvist AM, Autio K, Tarkkanen M, Wolf M, Monni O, Szymanska J, Larramendy ML, Tapper J, Pere H, El-Rifai W, Hemmer S, Waseinius VM, Vidgren V, Zhu Y: DNA copy number amplifications in human neoplasms: review of comparative genomic hybridization studies. *Am J Pathol* 152:1107–1123 (1998).
- Knuutila S, Aalto Y, Autio K, Björkqvist AM, El-Rifai W, Hemmer S, Huhta T, Kettunen E, Kiuru-Kühlefelt S, Larramendy ML, Lushnikova T, Monni O, Pere H, Tapper J, Tarkkanen M, Varis A, Waseinius VM, Wolf M, Zhu Y: DNA copy number losses in human neoplasms. *Am J Pathol* 155:683–694 (1999).
- Koschny R, Koschny T, Froster UG, Krupp W, Zuber MA: Comparative genomic hybridization in glioma: a meta-analysis of 509 cases. *Cancer Genet Cytogenet* 135:147–159 (2002).
- Larsen J, Kirchhoff M, Rose H, Gerdes T, Lundsteen C, Larsen JK: Improved sensitivity in comparative genomic hybridization analysis of DNA heteroploid cell mixtures after pre-enrichment of subpopulations by fluorescence activated cell sorting. *Anal Cell Pathol* 19:119–124 (1999).
- Levy B, Mukherjee T, Hirschhorn K: Molecular cytogenetic analysis in uterine leiomyoma and leiomyosarcoma by comparative genomic hybridization. *Cancer Genet Cytogenet* 121:1–8 (2000).
- Lundsteen C, Maahr J, Christensen B, Bryndorf T, Bentz M, Lichter P, Gerdes T: Image analysis in comparative genomic hybridization. *Cytometry* 19:42–50 (1995).
- Makhija S, Sit A, Edwards R, Aufman K, Weiss H, Kanbour-Shakir A, Gooding W, D'Angelo GD, Ferrell R, Raja S, Godfrey TE: Identification of genetic alterations related to chemoresistance in epithelial ovarian cancer. *Gynecol Oncol* 90:3–9 (2003).
- Mertens F, Johansson B, Höglund M, Mitelman F: Chromosomal imbalance maps of malignant solid tumors: a cytogenetic survey of 3185 neoplasms. *Cancer Res* 57:2765–2780 (1997).
- Monni O, Hyman E, Mousses S, Barlund M, Kallioniemi A, Kallioniemi OP: From chromosomal alterations to target genes for therapy: integrating cytogenetic and functional genomic views of the breast cancer genome. *Cancer Biol* 11:395–401 (2001).
- Nessling M, Kern M, Schadendorf D, Lichter P: Association of genomic imbalances with resistance to therapeutic drugs in human melanoma cell lines. *Cytogenet Cell Genet* 87:286–290 (1999).
- Petersen I, Petersen S, Bockmühl U, Schwendel A, Wolf G, Dietel M: Comparative genomische Hybridisierung an Bronchialkarzinomen und ihren Metastasen. *Verh Dtsch Ges Path* 81:297–305 (1997).
- Popov P, Virolainen M, Tukiainen E, Asko-Sclyavaara S, Huuhtanen R, Knuutila S, Tarkkanen M: Primary soft tissue sarcoma and its local recurrence: genetic changes studied by comparative genomic hybridization. *Mod Pathol* 14:978–984 (2001).
- Qin LX, Tang ZY, Sham JST, Ma ZC, Ye SL, Zhou XD, Wu ZQ, Trent JM, Guan XY: The association of chromosome 8p deletion and tumor metastasis in human hepatocellular carcinoma. *Cancer Res* 59:5662–5665 (1999).
- Rao PH, Houldsworth J, Palanisamy N, Murty VV, Reuter VF, Motzer RJ, Bosl GJ, Chaganti RS: Chromosomal amplification is associated with cisplatin resistance of human male germ cell tumors. *Cancer Res* 58:4260–4263 (1998).
- Rooney PH, Murray GI, Stevenson DAJ, Haites NE, Cassidy J, McLeod HL: Comparative genomic hybridisation and chromosomal instability in solid tumors. *Brit J Cancer* 80:862–873 (1999).
- Sallinen SL, Sallinen P, Haapasalo H, Kononen J, Karhu R, Helen P, Isola J: Accumulation of genetic changes is associated with poor prognosis in grade II astrocytomas. *Am J Pathol* 151:1799–1807 (1997).

- Schraml P, Zhaou M, Richter J, Bruning T, Pommer M, Sauter G, Mihatsch MJ, Moch H: Analysis of kidney tumors in trichloroethylene exposed workers by comparative genomic hybridization and DNA sequence analysis [German]. *Verh Dtsch Ges Pathol* 83:218–224 (1999).
- Solinas-Toldo S, Lampel S, Stilgenbauer S, Nickolenko J, Benner A, Döhner H, Cremer T, Lichter P: Matrix-based comparative genomic hybridization: Biochips to screen for genomic imbalances. *Genes Chrom Cancer* 20:399–407 (1997).
- Struski S, Doco-Fenzy M, Cornillet-Lefebvre P: Compilation of published comparative genomic hybridization studies. *Cancer Genet Cytogenet* 135:63–90 (2002).
- Tremmel SC, Götte K, Popp S, Weber S, Hörmann K, Bartram CR, Jauch A: Intratumoral genomic heterogeneity in advanced head and neck cancer detected by comparative genomic hybridization. *Cancer Genet Cytogenet* 144:165–174 (2003).
- Ueno T, Tangoku A, Yoshino S, Abe T, Toshimitsu H, Furuya T, Kawauchi S, Oga A, Oka M, Sasaki K: Gain of 5p15 detected by comparative genomic hybridization as an independent marker of poor prognosis in patients with esophageal squamous cell carcinoma. *Clin Cancer Res* 8:526–533 (2002).
- Weber RG, Boström J, Wolters M, Baudis M, Collins VP, Reifenberger G, Lichter P: Analysis of genomic alterations in benign, atypical, and anaplastic meningiomas: Toward a genetic model of meningioma progression. *Proc natl Acad Sci, USA* 94:14719–14724 (1997).
- Wessels LFA, van Welsem T, Hart AAM, van't Veer LJ, Reinders MJT, Nederlof PM: Molecular classification of breast carcinomas by comparative genomic hybridization: A specific somatic genetic profile for BRCA1 tumors. *Cancer Res* 62:7110–7117 (2002).
- Wessendorf S, Fritz B, Wrobel G, Nessling M, Lampel S, Göttel D, Küpper M, Joos S, Hopman T, Kococinski F, Döhner H, Bentz M, Schwänen C, Lichter P: Automated screening for genomic imbalances using matrix-based comparative genomic hybridization. *Lab Invest* 82:47–60 (2002).
- Willis S, Hutchins AM, Hammet F, Ciciulla J, Soo WK, White D, van der Spek P, Henderson MA, Gish K, Venter DJ, Armes JE: Detailed gene copy number and RNA expression analysis of the 17q12-23 region in primary breast cancers. *Genes Chrom Cancer* 36:382–392 (2003).
- Wolff E, Girod S, Liehr T, Vorderwülbecke U, Ries J, Steininger H, Gebhart E: Oral squamous cell carcinomas are characterized by a rather uniform pattern of genomic imbalances detected by comparative genomic hybridization. *Eur J Cancer* 34:186–190 (1998).
- Zitzelsberger H, Lehmann L, Werner M, Bauchinger M: Comparative genomic hybridisation for the analysis of chromosomal imbalances in solid tumours and haematological malignancies. *Histochem Cell Biol* 108:403–417 (1997).

# Chromosomal aberrations in arsenic-exposed human populations: a review with special reference to a comprehensive study in West Bengal, India

J. Mahata,<sup>a</sup> M. Chaki,<sup>a</sup> P. Ghosh,<sup>a</sup> J.K. Das,<sup>b</sup> K. Baidya,<sup>c</sup> K. Ray,<sup>a</sup>  
A.T. Natarajan<sup>d,e</sup> and A.K. Giri<sup>a</sup>

<sup>a</sup>Division of Human Genetics and Genomics, Indian Institute of Chemical Biology, Jadavpur, Kolkata;

<sup>b</sup>Department of Dermatology, West Bank Hospital, Howrah;

<sup>c</sup>Regional Institute of Ophthalmology, Medical College and Hospitals, Kolkata (India);

<sup>d</sup>Department of Toxicogenetics, Leiden University Medical Center (The Netherlands);

<sup>e</sup>University of Tuscia, Viterbo (Italy)

**Abstract.** For centuries arsenic has played an important role in science, technology, and medicine. Arsenic for its environmental pervasiveness has gained unexpected entrance to the human body through food, water and air, thereby posing a great threat to public health due to its toxic effect and carcinogenicity. Thus, in modern scenario arsenic is synonymous with “toxic” and is documented as a paradoxical human carcinogen, although its mechanism of induction of neoplasia remains elusive. To assess the risk from environmental and occupational exposure of arsenic, *in vivo* cytogenetic assays have been conducted in arseniasis-endemic areas of the world using chromosomal aberrations (CA) and sister chromatid exchanges (SCE) as biomarkers in peripheral blood lymphocytes. The primary aim of this report is to critically review and update the existing *in vivo* cytogenetic studies performed on arsenic-exposed popu-

lations around the world and compare the results on CA and SCE from our own study, conducted in arsenic-endemic villages of North 24 Parganas (district) of West Bengal, India from 1999 to 2003. Based on a structured questionnaire, 165 symptomatic (having arsenic induced skin lesions) subjects were selected as the exposed cases consuming water having a mean arsenic content of 214.96 µg/l. For comparison 155 age-sex matched control subjects from an unaffected district (Midnapur) of West Bengal were recruited. Similar to other arsenic exposed populations our population also showed a significant difference ( $P < 0.01$ ) in the frequencies of CA and SCE between the cases and control group. Presence of substantial chromosome damage in lymphocytes in the exposed population predicts an increased future carcinogenic risk by this metalloid.

Copyright © 2003 S. Karger AG, Basel

The earth's crust is the natural reservoir of arsenic. The commonly occurring inorganic forms of this semi-metal are arsenite (As<sup>III</sup>) and arsenate (As<sup>V</sup>), while the methylated metabolites monomethylarsonic acid (MMA), dimethylarsinic acid (DMA) and trimethylarsine oxide (TMAO) are the organic

forms. From a toxicological point of view environmental exposure to trivalent arsenicals including the methylated forms are more toxic than the pentavalent forms (IPCS, 2001). Arsenic is commercially used as medicine, pesticides and in different industrial processes.

Human populations are exposed to this ubiquitous toxicant through inhalation in occupational settings, due to consumption of arsenic-rich seafood and through arsenic-contaminated drinking water. According to the latest report millions of people in 21 countries are consuming water with an arsenic content far above the limit (50 µg/l) recommended by WHO. The worst affected regions include Taiwan, Bangladesh, India, Argentina, Mexico, Chile, Inner Mongolia, Thailand and the USA (Nordstrom, 2002). Epidemiological studies have reported that occu-

Received 14 August 2003; manuscript accepted 28 November 2003.

Request reprints from Dr. Ashok Kumar Giri, Assistant Director  
Division of Human Genetics and Genomics  
Indian Institute of Chemical Biology, 4, Raja S.C. Mullick Road  
Jadavpur, Kolkata- 700 032 (India)  
telephone: +91-33-2473-0492/6793; fax: +91-33-2473-5197  
e-mail: akgiril5@yahoo.com or akgiril@iicb.res.in



**Table 1.** Mean arsenic content in water, nail, hair and urine and the chromosomal aberrations and sister chromatid exchanges in human peripheral lymphocytes after long-term exposure to arsenic through drinking water

Country	Subjects <sup>a</sup>	As in water mean (µg/l) <sup>b</sup>	As in urine mean (µg/l)	As in nails mean (µg/g)	As in hair mean (µg/g)	CA <sup>c</sup>	SCE <sup>c</sup>	References
USA	E: 104, 98 C: 86, 83	109 12	NA	NA	NA	-	-	Vig et al., 1984
Mexico	E: 11 C: 13	390 19	1565 121	NA	NA	-	-	Ostrosky-Wegman et al., 1991
Mexico	E: 31 C: 27	408.17 29.88	739.80 34.0	NA	NA	+	NA	Gonsebatt et al., 1997
Argentina	E: 282 C: 155	130 20	160 70	NA	NA	NA	+	Lerda, 1994
Argentina	E: Women:12 Children:10 C: Women:10 Children:12	200 0.7	Women: 260 Children: 310 Women: 8.4 Children: 13	NA	NA	NA	-	Dulout et al., 1996
Hungary	E: 12 C: not reported	270 10	NA	> 4	0.18	+	NA	Paldy et al., 1991
Finland	E: Current user: 32 Ex-user: 10 C: 8	410 296	180 7 < 1	NA	1.3 3.0 0.05	+	NA	Mäki -Paakkanen et al., 1998
Taiwan	E: 15 C: 34	730 620	NA	NA	NA	NA	+	Hsu et al., 1997
Taiwan	E: 22 C: 22	NA*	NA	NA	NA	+	+	Liou et al., 1999
India	E: 59 C: 36	211.70 6.35	140.52 5.91	9.04 0.44	5.63 0.30	+	+	Mahata et al., 2003

<sup>a</sup> E = exposed; C = control.

<sup>b</sup> As = arsenic; NA = not analyzed; NA\* = population studied from the previously known arsenic area.

<sup>c</sup> CA/SCE in human peripheral lymphocytes; "+" = positive association; "-" = negative association.

pational exposure to arsenic increases the risk of lung cancer while ingestion of arsenic contaminated water causes the manifestation of characteristic skin lesions, keratosis, non-melanocytic skin and other internal organ cancer. Chronic exposure to arsenic also leads to various neurological, vascular and reproductive abnormalities (Bates et al., 1992).

It has been proven that arsenic is not a "classical" mutagen (i.e. does not induce point mutations), but it is clastogenic in both animal and human systems (Basu et al., 2001). Paradoxically the carcinogenic potential in animals is inadequate though in humans arsenic has been found to be a potent inducer of cancer. Based on this evidence, IARC has classified arsenic as a human carcinogen (IARC, 1980). Moreover, arsenic indirectly induces most types of genetic damage suggesting a sub-linear dose response for arsenic induced genetic damage and carcinogenicity which has also been observed repeatedly in different mammalian and human systems (Rudel et al., 1996).

To monitor the carcinogenic effects of different genotoxic agents to which humans are exposed occupationally, accidentally or naturally, cytogenetic techniques have been employed for decades allowing evaluation of the ultimate health outcomes and cancer prediction. Biomarkers such as CA and SCE in peripheral blood lymphocytes are used routinely to analyze the genetic damage as they reflect similar events in the cells undergoing carcinogenesis. Among all the cytogenetic endpoints CAs are considered as the most suitable surrogate biomarker of cancer and frequencies of aberrations are being used for cancer risk assessment (Hagmar et al., 1994). Thus to monitor the genotoxic effects due to chronic exposure to arsenic in

humans, several in vivo cytogenetic studies have been performed. In absence of a suitable animal model the data on frequencies of CA and SCE in lymphocytes may provide additional information about the mechanistic pathway and also give an insight into the susceptible factor as well as help in establishing the sub-linear dose for the induction of neoplasia in human.

Considering the reports of carcinogenic effects of arsenic in human populations, we recognized the need to critically review and update the cytogenetic effects in populations exposed to arsenic either occupationally or through drinking water. Though several studies on micronuclei (MN) have been performed in arsenic exposed populations, the current review concerns mainly the frequencies of CA and SCEs in peripheral lymphocytes. Attempts have also been made to compare the results with our own study, which includes the CA and SCE studies of the exposed population in West Bengal. The equivocal results obtained earlier in SCE assays tempted us to compare its applicability with aberrations in the bio-monitoring study of arsenic-exposed populations.

### Cytogenetic studies

Tables 1 and 2 summarize the results of arsenic-induced CAs and SCEs in peripheral blood lymphocytes in humans from different geographical locations exposed either through drinking water or occupationally.

One of the earliest reports was a two-year survey on humans consuming arsenic-contaminated water (>50 µg/l) for at least

**Table 2.** Mean arsenic content in urine and the chromosomal aberrations in peripheral lymphocytes in humans after occupational exposure to arsenic

Country	Source of exposure	As in urine mean ( $\mu\text{g/l}$ ) <sup>a</sup>	Subject number	End points <sup>b</sup>	Results	References
Sweden	Copper smelter	ND	E = 9	CA	+	Beckman et al., 1977
Sweden	Copper smelter	Low: 167.50 Medium: 386.36 High: 290.55	Low = 4 Medium = 11 High = 18	CA	+	Nordenson et al., 1978
Sweden	Copper smelter	278.12	33	CA	+	Nordenson and Beckman, 1982
China	Copper smelter	ND	ND	CA	+	Hu, 1989
Chile	Copper roasting plant	Low: 120 High: 260	5	CA	-	Harrington-Brock et al., 1999

<sup>a</sup> As = arsenic; ND = no data.  
<sup>b</sup> CA in human peripheral lymphocytes; “+” = positive association; “-” = negative association.

five years from Nevada, USA (Vig et al., 1984). The average arsenic content in the exposed population was about 2.18 times above the maximum level mandated by the US EPA. The frequency of CA per cell was 0.034 and 0.026 for the control and exposed groups, respectively. An average of 8.306 SCEs per cell was observed in the exposed group compared to 8.301 in the controls. The frequency of CAs and SCEs in lymphocytes of the exposed individuals showed no significant increase compared to controls, suggesting that arsenic at this concentration had no cytogenetic effect on the exposed population.

Similarly, from Comarca Lagunera, an arsenic-endemic region of Mexico, two studies conducted at different times by the same groups of investigators revealed different results. The frequency of CA between 11 individuals chronically exposed to arsenic-contaminated drinking water (mean 390  $\mu\text{g/l}$ ) was compared with 13 control individuals having low exposure level of arsenic (19–60  $\mu\text{g/l}$ ) in the first pilot study (Ostrosky-Wegman et al., 1991). No significant increase in CA and SCE frequency in the exposed group was noted. However, complex aberrations and inhibition of cell cycle progression were observed among the highly exposed individuals.

Contrary to the former study, CA in 35 individuals living in Santa Ana, having a mean arsenic content in drinking water of 408.17  $\mu\text{g/l}$  when compared to 27 age-sex matched controls of Nazereno (29.88  $\mu\text{g/l}$ ) showed a significant increase (Gonsebatt et al., 1997). Both groups were from the same Comarca Lagunera area but with different degrees of arsenic exposure through drinking water. Aberration per cell in the exposed group was 0.08 compared to 0.03 in the controls, with chromatid deletion being the most frequent type of aberration followed by isochromatid deletion. The mean frequencies of both chromatid and chromosome type exchanges were higher in the exposed group than in the controls. Interestingly, among the exposed group, males showed more aberrations than females. A strong correlation between CA frequencies in lymphocytes with total arsenic and the percentage of inorganic arsenic in urine was also observed.

Two contradictory results have been reported from Argentina. Lerda (1994) conducted a cytogenetic survey in the Province of Cordoba, one of the arsenic-affected areas of Argentina with reports of arsenic-induced skin and bladder cancers in the

exposed population. Arsenic at a concentration of 130  $\mu\text{g/l}$  induced a significant increase in SCEs in the lymphocytes of the exposed population compared to the controls with a mean arsenic content in water less than 1  $\mu\text{g/l}$ . The exposure period was similar in both groups (>20 years); however, significant differences in age between the exposed and controls were present (56.7 vs 38.9). The mean SCEs per cell in 282 exposed individuals was 10.46 compared to 7.49 in 155 control individuals. A positive correlation between the arsenic content in water and urine with frequency of SCEs was also observed. Frequency of SCEs was not affected by age or sex when older individuals were excluded.

Dulout et al. (1996) observed no such significant increase in the frequency of SCEs in the lymphocytes among the native Indian children and women of northwestern Argentina, exposed to an average of 200  $\mu\text{g/l}$  of arsenic in drinking water in contrast to the controls (0.7  $\mu\text{g/l}$ ). The FISH analysis also revealed that only 3 out of 12 exposed individuals had 0.4% chromosomal translocations, while the mean value was 0.1%, which was not statistically different when compared to controls. However, the frequencies of MN were higher in the exposed population. Cell cycle progression analysis also revealed no significant difference between the exposed and control individuals.

Paldy et al. (1991) observed a highly significant increase in CA in lymphocytes among 12 Hungarian children chronically exposed to high concentrations of arsenic in drinking water (range 100–270  $\mu\text{g/l}$ ) in comparison to control children. On the basis of the arsenic content in hair, the exposed (>4  $\mu\text{g/g}$ ) and control (0.18  $\mu\text{g/g}$ ) subjects were recruited. The percentage of aberrant cells was highly significant in the exposed group with a mean of 4.4% compared to 1.3% in the controls. Interestingly, chromatid type deletions, acentric fragments as well as dicentric and rings were the most predominant forms of aberrations. A large inter-individual variation in the yield of aberrant cells was also noted. The follow-up examination after a one-year interval of 6 out of the 12 exposed children showed no difference in the yield of aberrations induced by arsenic.

Similarly, the Finnish group studied not only the clastogenicity of arsenic as measured by structural CAs in lymphocytes but also its association with other bio-indicators of arsenic

exposure (Mäki-Paakkanen et al., 1998). The mean arsenic content in drinking water in the exposed group was 410 µg/l. However, the exposed group was comprised of 32 current users and 10 ex-users, while 8 subjects were taken as control from the same village consuming water containing less than 1 µg/l of arsenic. Along with different types of aberrations, gaps were also scored. The overall results on CA, both including and excluding gaps, were not statistically significant in the exposed group compared to the control. A significant correlation was observed between CA frequencies (number of breaks and gaps) and concentration of arsenic in urine among the current users, but not in the ex-users, which implies that cessation of exposure probably leads to decrease in the aberration frequencies. A strong association between number of gaps and aberrations including gaps with urinary concentration of MMA in current users indicate that gaps were induced due to arsenic exposure. The predominant forms of aberration were chromatid breaks and gaps.

Two unique studies were performed in Taiwan in the Black-foot hyper-endemic villages where the residents have been exposed to high concentrations of arsenic (700–930 µg/l) through artesian well water for more than 20 years. In both cases cohorts were selected from follow-up study on the basis of development of arsenic-induced skin cancer or other internal cancers. In the first investigation an elevated rate ( $P < 0.05$ ) of SCEs and high frequency cells (HFCs) among 15 arsenic-induced Bowen's diseases patients compared to controls was reported (Hsu et al., 1997). The mean age (years) and duration of drinking contaminated water (years) in the cases were 58.7 and 29.2, respectively, whereas in the controls it was 58.5 and 21.4, respectively. The SCEs per cell in cases and controls were 8.42 and 6.94, respectively. A significantly lower replicative index (RI) was noted in the arsenic-induced Bowen disease patients compared to the matched controls. However, no significant association was observed for spontaneous SCEs, HFCs and RI with age, gender, cigarette smoking and alcohol consumption.

Liou et al. (1999) conducted a nested case-control cytogenetic study on 22 cancer cases and 22 controls exposed to high concentrations of arsenic from an artesian well. The main aim was not only to correlate the frequency of CAs and SCEs in peripheral lymphocytes with arsenic exposure but also to evaluate the association between cytogenetic biomarkers and cancer risk prediction in the exposed population of Taiwan. The mean frequency of total CAs (chromatid and chromosome type) was significantly elevated in the cancer cases compared to that of controls (6.1 vs. 4.4). The frequency of SCEs per cell was higher in the cancer group than in the control group but not statistically significant. The significantly higher number of chromosome type aberrations in cancer cases suggests that chromosome type CAs are better indicators of cancer development than chromatid type CAs or SCEs, but whether this association in other arsenic-exposed populations is valid or not remains to be elucidated.

In southern West Bengal (India) elevated arsenic in ground water was first documented from one district in 1978, and one of the earliest cases showing arsenical dermatomes was recognized in 1983. Within a span of 20 years the arsenic calamity

has extended in 9 out of 18 districts with approximately 300,000 people already manifesting signs of chronic arsenicosis while a large population are at potential health risk. Follow-up studies have also shown development of cancer in individuals suffering from arsenical skin lesions (Rahman et al., 2003). Considering the adverse situation our group first started a cytogenetic survey in the year 1999 in the arsenic exposed population in West Bengal. Initially 59 symptomatic individuals were screened, examined at The School of Tropical Medicine, Kolkata and compared with 36 control subjects for cytogenetic damage induced by arsenic (Mahata et al., 2003). Subsequently for the last three and half years we have been evaluating the genetic damage induced by arsenic through drinking water as measured by CA and SCE in lymphocyte cultures. In contrast to all previous studies, our population is unique in the sense that the degree of exposure level is very wide, ranging from 60 to 800 µg/l, resulting in great variation in the manifestation of chronic arsenicosis. The presence of a stable rural population with heterogeneity in exposure, the individual exposure data along with the frequency of CAs and SCEs may provide critical information for characterizing the exposure-response relationship in our population. Our study area includes the North 24 Parganas (district), one of the affected districts of West Bengal. With a systematic approach through field survey four administrative blocks (Police Station) located in the central part of the district of North 24 Parganas having significantly high arsenic content in drinking water were selected for this study. A group of 165 individuals showing arsenic-related skin lesions of both sexes within the age group of 15–70 years having exposure for more than 5 years were finally recruited for this study. Data on demographic characteristics and other parameters were collected by interview with a structured questionnaire. A physician and dermatologist examined each participant for arsenic-related skin lesions such as raindrop pigmentation, hyperkeratosis, ulcerative lesions and other signs of chronic arsenicism. For a comparative study, 155 age-sex matched individuals from similar socio-economic background having no exposure to arsenic were selected as controls from the unaffected district of East Midnapur, West Bengal. The mean ( $\pm$  SE) arsenic content of water (µg/l) in the exposed group was  $214.96 \pm 8.96$  compared to the controls value of  $9.12 \pm 0.31$ . The arsenic content in nails, hair and urine were used as bio-indicators to measure both chronic and current arsenic exposure via drinking water. Lymphocyte cultures were initiated following a standard protocol for CA and SCE assay. The mean arsenic content in nails (µg/g), hair (µg/g) and urine (µg/l) of the exposed subjects were  $6.72 \pm 0.41$ ,  $4.14 \pm 0.22$  and  $161.98 \pm 9.41$ , respectively, which was found to be significantly high in comparison to the controls ( $0.53 \pm 0.04$ ,  $0.33 \pm 0.02$  and  $11.62 \pm 0.93$ , respectively). Table 3 summarizes the mean frequencies of CA (including and excluding gaps) and SCEs per cell in our arsenic-exposed population. In the exposed population the mean value of CA per cell in lymphocytes was 0.09 which was statistically significant ( $P < 0.01$ ) compared to the corresponding control value of 0.02. Chromatid type breaks, deletions and gaps were the predominant forms of aberrations observed along with dicentrics and rings. The mitotic index (MI) was significantly decreased in the exposed individuals compared to that of

**Table 3.** Mean values (mean  $\pm$  SE) of the frequencies of CA and SCE in lymphocytes of the controls and symptomatic individuals exposed to arsenic through drinking water in West Bengal, India

Number of subjects	Percentage of aberrations		CAs per cell <sup>c</sup>		Percentage of aberrant cells <sup>d</sup>	SCEs per cell	Mitotic index	Replicative index
	+ Gaps <sup>a</sup>	- Gaps <sup>b</sup>	Chromatid type	Chromosome type				
Control (n = 155)	5.44 $\pm$ 0.20	2.59 $\pm$ 0.10	0.024 $\pm$ 0.001	0.002 $\pm$ 0.0003	2.32 $\pm$ 0.09	6.21 $\pm$ 0.06	1.796 $\pm$ 0.04	1.91 $\pm$ 0.02
Symptomatic (n = 165)	16.61 $\pm$ 0.32 <sup>e</sup>	9.25 $\pm$ 0.22 <sup>e</sup>	0.09 $\pm$ 0.002 <sup>e</sup>	0.006 $\pm$ 0.0005 <sup>e</sup>	8.72 $\pm$ 0.21 <sup>e</sup>	7.49 $\pm$ 0.07 <sup>e</sup>	1.44 $\pm$ 0.03 <sup>e</sup>	1.68 $\pm$ 0.01 <sup>e</sup>

<sup>a</sup> Including gaps.

<sup>b</sup> Excluding gaps.

<sup>c</sup> Total number of aberrations (gaps not included) per total number of cells scored.

<sup>d</sup> Gaps not included.

<sup>e</sup>  $P < 0.01$  (Fisher's t Test).

controls. Further, the mean SCEs per cell was also statistically significant ( $P < 0.01$ ) in the exposed group compared to the controls (7.49 vs. 6.21). A slower cell proliferation rate as measured by RI was also noted among the exposed group.

Three studies on smelter workers exposed to arsenic and other compounds have been reported from Sweden. In each study, reported exposure was confirmed by analyzing mean urinary arsenic content. Beckman et al. (1977) studied CA in peripheral blood lymphocytes of nine smelter workers and compared it with non-exposed healthy individuals. Workers were grouped according to arsenic concentration in urine. Gaps, chromatid and chromosome type CAs were taken into consideration. The frequencies of CAs per cell in the exposed and control population were 0.106 and 0.0128, respectively, which was statistically significant ( $P < 0.001$ ). However, a large inter-individual variation in the number of aberrations (0–25/100 cells) was noted. The association between frequency of all aberrations and exposure was not very consistent, only chromatid aberrations showed a good correlation.

Similarly, in another study a statistically significant increase in CA frequency was reported in 39 smelter workers exposed to various doses of arsenic when compared to the non-exposed group (Nordenson et al., 1978). Four years later in the follow-up investigation, frequency of aberrations among 33 smelter workers showed an elevated rate of aberrations compared to the controls (Nordenson and Beckman, 1982). The follow-up study of 8 exposed individuals showed significant increase in the frequency of aberrations per cell including gaps, chromatid and chromosome breaks. Smelter workers in China also showed enhanced rate of CAs in lymphocytes which was considered as the cause of lung cancer in the concerned area (Hu, 1989).

No evidence of CA in the lymphocytes of 5 workers exposed to arsenic in a copper roasting plant in Chile was noted, although the mean urinary arsenic level ( $\mu\text{g/l}$ ) in low- and high-exposed group was 120 and 260, respectively (Harrington-Brock et al., 1999).

## Discussion

Except for a few negative results, the majority of the studies clearly indicate a positive clastogenic effect in populations exposed to arsenic. The negative results obtained by Vig et al. (1984) and Ostrosky-Wegman et al. (1991) may be due to the

absence of a perfect matched control sample, low exposure level and small sample size. An epidemiological study by Vahter et al. (1995) reported that the native Andean population might have developed skin cancer resistance against arsenic. Thus the differences in sensitivity to the clastogenic effects of arsenic in the two studies from Argentina may be attributed to the origin of the concerned population. Additionally the native population studied by Dulout et al. (1996) was comprised of children aged between 8–15 years and that may have been the reason for the negative response of SCEs. Thus the genetic make-up, ethnicity and other environmental factors may have influenced the degree of cytogenetic damage induced by arsenic.

From our study it can be inferred that chronic exposure to arsenic has led to the manifestation of skin pigmentation and keratosis that has subsequently in some cases progressed to cancer. It can be postulated that the increased frequencies of CAs in lymphocytes are due to long-term ingestion of arsenic. Although a significant increase in SCE frequency was observed, however, when compared to the increase in CA, the extent of increase is much less as reported earlier (3.76 times increase in percentage of aberrant cells as compared to only 1.20 times increase in SCEs per cell). Moreover, the higher incidence of genetic damage among the symptomatic individuals predicts an increased possible future carcinogenic risk.

Among all types of aberrations scored gaps, chromatid-type breaks and deletions were dominant. Chromosomal exchanges considered as biological dosimeters for cancer risk assessment were also observed in different studies. Interestingly, in most of the studies in the exposed populations, effects of CAs were more pronounced than of SCEs. Though the frequency of SCE has been found to be elevated, the increase in comparison to CA is less, suggesting that CA may be a better indicator of genetic damage in arsenic-exposed populations than SCE. The positive correlation of CA and other parameters of arsenic exposure clearly indicates that aberrations were induced by arsenic in a dose-dependent manner. As is evident, relatively long-term exposure is a prerequisite for arsenic-induced CA in lymphocytes and that cessation of exposure may sometimes decrease the frequency of aberrations.

## Conclusion

Thus the overall results of CA induced by arsenic indicate that although it is not a point mutagen, it is definitely genotoxic *in vivo* in humans. The more positive result of CA indicates the usefulness of this biomarker. Other bio-indicators of arsenic exposure *viz.* nail and hair should be assessed (which was not done by many investigators) for better understanding of the relationship between cytogenetic damage and individual health effect. Inter-individual variation among the exposed groups has been reported, which points to the fact that both environmental exposure to arsenic and individual susceptibility (either genetic or acquired) may be involved in the manifestation of genetic damage.

## References

- Basu A, Mahata J, Gupta S, Giri AK: Genetic toxicology of a paradoxical human carcinogen, arsenic: a review. *Mutat Res* 488:171–194 (2001).
- Bates MN, Smith AH, Hopenhayn-Rich C: Arsenic ingestion and internal cancers: a review. *Am J Epidemiol* 135:462–476 (1992).
- Beckman G, Beckman L, Nordenson I: Chromosome aberrations in workers exposed to arsenic. *Environ Health Perspect* 19:145–146 (1977).
- Dulout FN, Grillo CA, Seoane AI, Maderna CR, Nilsson R, Vahter M, Darroudi F, Natarajan AT: Chromosomal aberrations in peripheral blood lymphocytes from native Andean women and children from Northwestern Argentina exposed to arsenic in drinking water. *Mutat Res* 370:151–158 (1996).
- Gonsebatt ME, Vega L, Salazar AM, Montero R, Guzman P, Blas J, Del Razo LM, Garcia-Vargas G, Albores A, Cebrian ME, Kelsh M, Ostrosky-Wegman P: Cytogenetic effects in human exposure to arsenic. *Mutat Res* 386:219–228 (1997).
- Hagmar I, Brogger A, Heim IL, Hogstedt B, Knudsen L, Lambert B, Linnainma K, Mitelman F, Nordenson I, Reuterwall C, Salomaa S, Skerfving S, Sorsa M: Cancer risk in humans predicted by increased levels of chromosomal aberrations in lymphocytes: Nordic study group on the health risk of chromosome damage. *Cancer Res* 54:2919–2922 (1994).
- Harrington-Brock K, Cabrera M, Collard DD, Doerr CL, McConnell R, Moore MM, Sandoval H, Fuscoe JC: Effects of arsenic exposure on the frequency of HPRT-mutant lymphocytes in a population of copper roasters in Antofagasta, Chile: a pilot study. *Mutat Res* 431:247–257 (1999).
- Hsu YH, Li SY, Chiou HY, Yeh PM, Liou JC, Hsueh YM, Chang SH, Chen CJ: Spontaneous and induced sister chromatid exchanges and delayed cell proliferation in peripheral lymphocytes of Bowen's disease patients and matched controls of arseniasis-hyperendemic villages in Taiwan. *Mutat Res* 386:241–251 (1997).
- Hu GG: Investigation of protective effect of selenium on genetic materials among workers exposed to arsenic. *Zhonghua Yu Fang Yi Xue Za Zhi* 23:286–288 (1989).
- IARC: Arsenic and arsenic compounds. Some metals and metallic compounds. Monographs on the Evaluation of Carcinogenic Risk to Humans, pp 39–141 (International Agency for Research on Cancer (IARC), Lyon 1980).
- IPGS, International Programme on Chemical Safety; Environmental health criteria No. 224. Arsenic and arsenic compounds, 2<sup>nd</sup> Edition (WHO, Geneva 2001).
- Lerda D: Sister-chromatid exchange (SCE) among individuals chronically exposed to arsenic in drinking water. *Mutat Res* 312:111–120 (1994).
- Liou SH, Lung JC, Chen YH, Yang T, Hsieh LL, Chen CJ, Wu TN: Increased chromosome-type chromosome aberration frequencies as biomarkers of cancer risk in a blackfoot endemic area. *Cancer Res* 59:1481–1484 (1999).
- Mahata J, Basu A, Ghoshal S, Sarkar JN, Roy AK, Poddar G, Nandy AK, Banerjee A, Ray K, Natarajan AT, Nilsson R, Giri AK: Chromosomal aberrations and sister chromatid exchanges in individuals exposed to arsenic through drinking water in West-Bengal, India. *Mutat Res* 534:133–143 (2003).
- Mäki-Paakkanen J, Kurttila P, Paldy A, Pekkanen J: Association between the clastogenic effect in peripheral lymphocytes and human exposure to arsenic through drinking water. *Environ Mol Mutagen* 32:301–313 (1998).
- Nordenson I, Beckman G, Beckman L, Nordstrom S: Occupational and environmental risks in and around a smelter in northern Sweden. II. Chromosomal aberrations in workers exposed to arsenic. *Hereditas* 88:47–50 (1978).
- Nordenson I, Beckman L: Occupational and environmental risks in and around a smelter in northern Sweden. VII. Reanalysis and follow-up chromosomal aberrations in workers exposed to arsenic. *Hereditas* 96:175–181 (1982).
- Nordstrom DK: Worldwide occurrences of arsenic in ground water. *Science* 296:2143–2145 (2002).
- Ostrosky-Wegman P, Gonsebatt ME, Montero R, Vega L, Barba H, Espinosa J: Lymphocyte proliferation kinetics and genotoxic findings in a pilot study on individuals chronically exposed to arsenic in Mexico. *Mutat Res* 250:477–482 (1991).
- Paldy A, Farkas I, Markus V, Gundy S: Chromosomal aberrations in children exposed to high concentration of arsenic in drinking water. *Mutat Res* 271:194 (1991).
- Rahman MM, Mandal BK, Chowdhury TR, Sengupta MK, Chowdhury UK, Lodh D, Chanda CR, Basu GK, Mukherjee SC, Saha KS, Chakraborti D: Arsenic groundwater contamination and sufferings of people in North 24-Parganas, one of the nine arsenic affected districts of West Bengal, India. *J Environ Sci Health* 38:25–59 (2003).
- Rudel R, Slayton TM, Beck BD: Implications of arsenic genotoxicity for dose response of carcinogenic effects. *Regulatory Toxicol Pharmacol* 23:87–105 (1996).
- Vahter M, Concha G, Nermell B, Nilsson R, Dulout F, Natarajan AT: A unique metabolism of inorganic arsenic in native Andean women. *Eur J Pharmacol* 293:455–462 (1995).
- Vig BK, Figueroa ML, Cornforth MN, Jenkins SH: Chromosome studies in human subjects chronically exposed to arsenic in drinking water. *Am J Ind Med* 6:325–338 (1984).

## Acknowledgement

The authors are grateful to the Director, Indian Institute of Chemical Biology for his kind help and cooperation. We are thankful to the Indian Council of Medical Research, Government of India, for providing Senior Research Fellowship to Ms. Julie Mahata.

# Chromosomal radiosensitivity and low penetrance predisposition to cancer

D. Scott

Paterson Institute for Cancer Research, Christie Hospital NHS Trust, Withington, Manchester (UK)

**Abstract.** This mini-review summarises studies in this Institute on the sensitivity of cells of patients with common cancers to the chromosome-damaging effects of ionising radiation, in the context of related studies. Using the 90<sup>th</sup> percentile of healthy controls ( $n > 200$ ) as the cut-off point between a normal and a sensitive response, 40% of patients with breast cancer ( $n = 166$ ) were sensitive when cells were irradiated in the G<sub>2</sub> phase of the cell cycle. Smaller studies showed that patients with colorectal, head and neck (at  $< 45$  years) and childhood cancers also exhibited degrees of enhanced sensitivity, whereas cervical and lung cancer cases did not. Cells from breast and

head and neck cases irradiated in G<sub>0</sub> also showed increased sensitivity. We propose that such elevated sensitivity is a marker of low penetrance predisposition to cancer. The strongest support for this hypothesis was our demonstration of the Mendelian heritability of chromosomal radiosensitivity in 95 family members of breast cancer cases. Challenges for the future include more heritability studies, identification of the underlying genetic determinants, assessment of the associated cancer risk (spontaneous and radiogenic) and population screening for cancer prevention strategies.

Copyright © 2003 S. Karger AG, Basel

## Background

This mini-review summarises investigations of the relationship between human cancer predisposition and the sensitivity of cells to the chromosome-damaging effects of ionising radiation (chromosomal radiosensitivity) undertaken in the Department of Cancer Genetics of this Institute (Table 1). The studies began in the early 1980's but here, the work of the last ten years will be briefly reviewed, when our cytogenetic methods were standardised, facilitating accurate quantification of chromosome damage. Relevant results from other laboratories are also discussed.

The impetus for this work came from early observations of dramatic chromosomal radiosensitivity of patients with the recessively inherited cancer-prone syndrome, ataxia-telangiectasia (A-T) (reviewed by Taylor, 1983). Since then, some degree

of chromosomal radiosensitivity has been reported in about 20 other cancer-prone conditions, many of which have a very high cancer risk mediated through strongly expressed (highly penetrant) genes (reviewed in Scott et al., 1999; see also Baeyens et al., 2002). This suggests some defect in the ability to process DNA damage of the types induced by ionising radiation, although it does not necessarily follow that this is the primary reason for their cancer predisposition.

Amongst these cancer-prone conditions are asymptomatic A-T heterozygotes (references in Scott et al., 1999). Epidemiological data were reviewed by Easton in 1994 who concluded that such individuals comprised approximately 0.5% of the general population and that females had a 4-fold increased risk of breast cancer. This degree of risk, associated with mutation in a single allele of the ATM gene, is regarded as being of low penetrance and would not result in a strong family history of breast cancer of the type seen in families with BRCA mutations (Eeles et al., 1996). Easton (1994) calculated that about 4% of breast cancer patients could be A-T heterozygotes, but the paucity of data allowed estimates from 1 to 13%. We confirmed the radiosensitivity of A-T heterozygotes (Scott et al., 1994) and considered that it might be possible to detect these amongst an unselected series of breast cancer patients if their frequency was at the upper end of Easton's estimate.

Funding was provided by Cancer Research UK, the Christie Hospital Endowment Fund, the National Radiological Protection Board (UK), Westlakes Research Institute (UK) and the UK Coordinating Committee on Cancer Research.

Received 26 August 2003; accepted 18 November 2003.

Request reprints from: Dr. David Scott, Yew Tree Cottage, Bow Green Rd, Bowdon Cheshire, WA14 3LF (UK), telephone: +44-(0)-161-941-2393  
fax: +44-(0)-161-446-3109; e-mail: david.scott2004@btinternet.com

**Table 1.** Summary of results from this institute on the chromosomal radiosensitivity of patients with various cancers

Assay	Diagnosis	No. cases	% sensitive <sup>a</sup>	Significant?	References
G <sub>2</sub>	Adult controls	>200	10	-	Scott et al., 1999; Baria et al., 2001,2002; Papworth et al., 2001
	Breast	166	39	Yes	Scott et al., 1994,1999; Baria et al., 2001
	Colorectal	37	30	Yes	Baria et al., 2001
	Head & neck	42	31	Yes (< 45 yrs)	Papworth et al., 2001
	Young patients	32	44	Yes <sup>b</sup>	Baria et al., 2002
	Young controls	41	15 <sup>c</sup>	No	Baria et al., 2002
	Cervical	27	11	No	Baria et al., 2001
	Lung	35	23	No	Baria et al., 2001
	Chronic illness	34	12	No	Baria et al., 2001
G <sub>0</sub>	Adult controls	99	10	-	Scott et al., 1999; Papworth et al., 2001
	Breast	130	27	Yes	Scott et al., 1999
	Head & neck	49	35	Yes	Papworth et al., 2001

<sup>a</sup> Sensitivity defined as scores above the 90<sup>th</sup> percentile of controls tested in parallel.  
<sup>b</sup> Compared with young controls.  
<sup>c</sup> Compared with adult controls tested in parallel.

### Breast cancer patients

The assay of first choice for this study utilised peripheral blood lymphocytes irradiated in the G<sub>2</sub> phase of the cell cycle with 0.5 Gy X-rays. We first expanded our control database to more than 100 normal donors with repeat assays (up to 11 repeats) on 28 of these (Scott et al., 1994, 1999). This enabled us to demonstrate good reproducibility and true inter-individual differences, recently confirmed by Smart et al. (2003). The distribution of sensitivities was skewed to the right, with about 10% of "outliers" (Fig. 1) and we have used the 90<sup>th</sup> percentile as a cut-off point to distinguish between a normal and a sensitive response. Importantly, there was no significant influence of age or gender on G<sub>2</sub> radiosensitivity.

The control distribution was compared with that for 135 breast cancer patients tested after surgery but before radiotherapy (Fig. 1). The mean aberration score for the patients was greater than that of the controls and 40% gave scores above the cut-off point for defining sensitivity. This value is considerably higher than even the highest estimate of A-T heterozygotes amongst breast cancer patients and suggested that there might be mutant genes, other than ATM in heterozygotes, conferring G<sub>2</sub> radiosensitivity and low penetrance predisposition to breast cancer. The enhanced G<sub>2</sub> sensitivity of breast cancer patients has since been confirmed in five different laboratories (references in Scott et al., 2003).

We also showed that A-T heterozygotes were more chromosomally radiosensitive than controls when lymphocytes were irradiated in the G<sub>0</sub> cell cycle phase (Jones et al., 1995; Scott et al., 1996). With micronucleus induction as the endpoint, in a study of 68 controls, with repeat assays on 14 donors (up to 11 repeats), we were able to demonstrate significant inter-individual differences (Scott et al., 1999). These controls were then compared with 130 breast cancer cases and, using the 90<sup>th</sup> percentile cut-off, 27% of patients were sensitive. Again, this is considerably higher than epidemiological estimates of A-T heterozygotes amongst breast cancer patients.

Eighty patients were tested with both the G<sub>2</sub> and G<sub>0</sub> assays and there was no significant correlation between the results

from the two methods. Patients were either sensitive in one assay or the other, only 4% in both. This suggests that the mechanisms determining chromosomal radiosensitivity are different in these cell cycle phases (references in Scott et al., 1999 and Baeyens et al., 2002) and that sensitive patients usually have a defect in only one of these mechanisms. It also follows that over 60% of all patients are chromosomally radiosensitive via one mechanism or the other. Our hypothesis, that such radiosensitivity could be a marker of low penetrance predisposition to breast cancer, is consistent with epidemiological studies (Teare et al., 1994; Lichtenstein et al., 2000). These show that the overall familial risk of breast cancer cannot be accounted for by the relatively rare mutations in highly penetrant genes such as BRCA1 and BRCA2. A study of breast cancer in twins led to the suggestion that the majority of breast cancers arise in genetically predisposed women (Peto and Mack, 2000). It is perhaps surprising that predisposition to breast cancer could be associated with the ability to cope with DNA damage but support for this concept has come from the observation that the BRCA genes are involved in DNA repair processes and that patients with BRCA mutations exhibit chromosomal radiosensitivity (references in Baeyens et al., 2002).

Confirmation of our two-assay findings on breast cancer cases has recently come from Baeyens et al. (2002), although their study utilised patients with a family history of the disease. Using the 90<sup>th</sup> percentile cut-off point, 20 of 43 (47%) patients without BRCA1 or BRCA2 mutations were G<sub>2</sub> sensitive and 19 of 40 (48%) were sensitive in a G<sub>0</sub> micronucleus assay using high dose rate radiation exposure as we had used. There was no significant correlation between the results of the two assays on the same patients.

### Other cancers

We then considered the possibility that chromosomal radiosensitivity might be a marker of predisposition to cancers other than those of the breast. We therefore selected malignancies for which epidemiological evidence and theoretical considerations

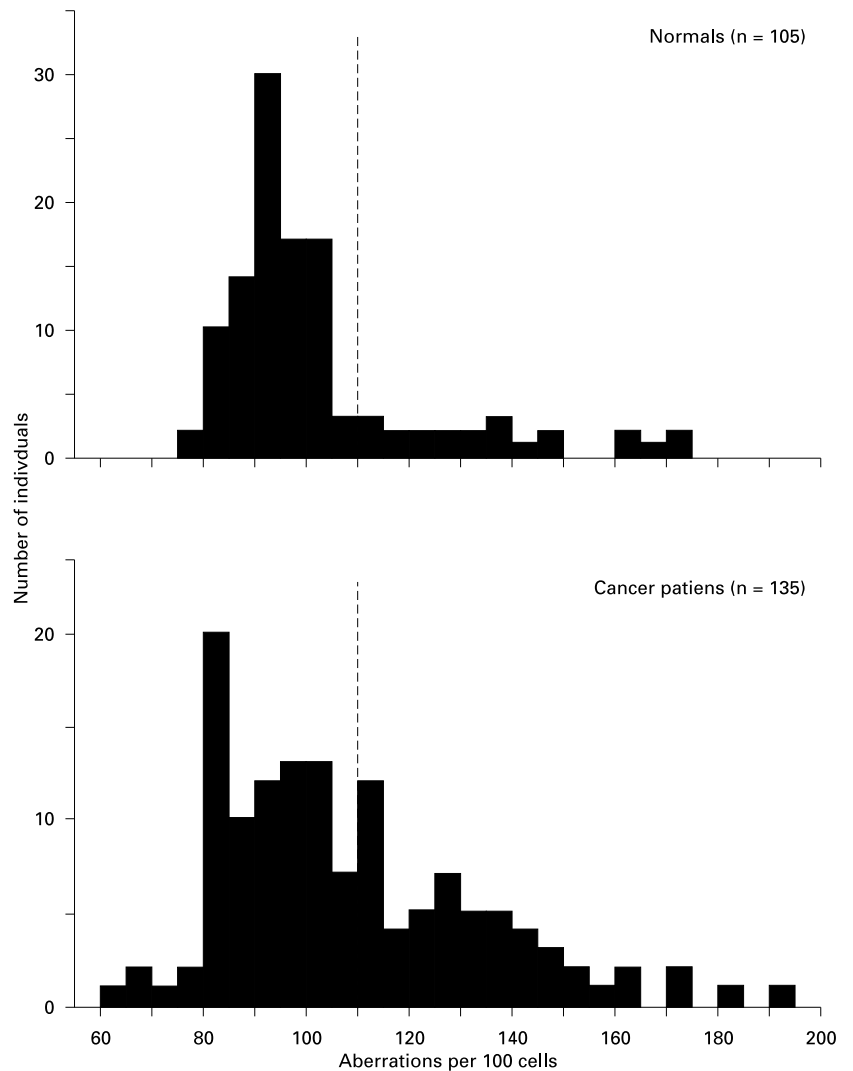


**Fig. 1.** G<sub>2</sub> chromosomal radiosensitivity of (top) normal donors and (bottom) breast cancer patients. The dashed vertical lines indicate the cutoff point between a normal and a sensitive response. Lymphocytes were exposed to 0.5 cGy X-rays. From Scott et al. (1999), with permission from Taylor and Francis Ltd.

suggested various degrees of genetic or environmental aetiology (Table 1). These studies involved smaller numbers of cases than in our breast cancer series and should therefore be considered as preliminary findings.

In our first such study (Baria et al., 2001), using the G<sub>2</sub> assay and 66 controls, we included colorectal cases because of good evidence of low penetrance predisposition in addition to the high cancer risk associated with rare mutations in the APC and mismatch repair genes. We found that 30% (30/37) of patients were sensitive, again using the 90<sup>th</sup> percentile of controls as the cut-off value. We also G<sub>2</sub> tested patients with cervical and lung cancer for which there is evidence of a strong environmental aetiology associated with viral infection and tobacco use, respectively. For neither of these cancers was the proportion of sensitive cases significantly greater than for controls; the values were 11% (3/27) for cervical cases and 23% (8/35,  $p = 0.07$ ) for lung cases. A further group of breast cancer cases was also tested and 39% (12/31) were sensitive. To investigate whether enhanced chromosomal radiosensitivity could simply be a consequence of illness, we assayed 34 patients with chronic dis-

eases other than cancer and found no difference from controls; 12% (4/34) were sensitive.

In a separate study of 42 patients with head and neck cancer (Papworth et al., 2001) compared with 27 controls, 31% (13/42) were sensitive but the difference was not significant ( $p = 0.16$ ). However, unlike the situation with breast and colorectal cancer patients and healthy controls, there was a significant inverse correlation between G<sub>2</sub> scores and age at diagnosis. When patients were stratified into early onset (<45 years) and later onset cases (>45 years) there were significantly more sensitive cases amongst early onset patients than in controls of the same age group whereas this was not the case for late onset patients. A group of 49 head and neck cancer patients was also tested with the G<sub>0</sub> micronucleus assay and compared with 31 controls. Significantly more patients were sensitive (35%, 17/49) and, as in the G<sub>2</sub> assay, there was an inverse correlation between chromosome damage and age and the greatest frequency of sensitive cases was seen in early onset patients. There was no significant correlation between the results in the two assays on 39 patients. For head and neck cancer patients, even



when allowing for known environmental risk factors such as alcohol and tobacco use, there is evidence of a degree of genetic predisposition (Foulkes et al., 1995). Our results suggest that this low penetrance risk may be confined to younger patients and that each of the two assays detects a different subset of these cases.

The results of our head and neck cancer studies suggested that if enhanced sensitivity is indeed associated with low penetrance genes, some genes of this type may predispose to cancer at an early age. Early onset of cancer is a common feature of inherited susceptibility involving highly penetrant genes such as RB1 and TP53, supporting Knudson's two-hit hypothesis (Knudson, 1986), but these account for only a very small proportion of early cases. We therefore conducted a pilot study (Baria et al., 2002) to examine the G<sub>2</sub> sensitivity of an unselected group of young patients (n = 32, 0.5–19 years) with solid tumours, from whom consent could be obtained, over a two-year period. Because our test system involves the use of T-lymphocytes, patients with T-cell lymphomas and all leukaemias were excluded. The cancers included osteosarcomas (n = 9), Hodgkin's disease (n = 6), rhabdomyosarcomas (n = 5), non-Hodgkin's lymphomas (n = 4) and single cases of eight other cancers. The patients were compared with young controls of the same age range (n = 41, 0.25–19 years) and the proportion of sensitive patients (44%, 14/32) was significantly higher than the controls. Stratification of results according to cancer type was considered uninformative because of the small numbers involved. Much larger numbers of cases with specific early onset cancers need to be tested. The results of epidemiological studies relating to the possible existence of low penetrance predisposing genes for early cancers remains controversial (references in Baria et al., 2002).

In general, we feel that our results on other cancers support the hypothesis derived from our breast cancer studies, that chromosomal radiosensitivity is a marker of low penetrance predisposition, but more extensive investigations are required. Terzoudi et al. (2000) reported that the average G<sub>2</sub> radiosensitivity of 185 patients with various cancers was significantly greater than 25 controls but the statistical significance for individual cancers was not given. Bondy et al. (2001) showed greater G<sub>2</sub> sensitivity of 219 patients with gliomas than of 238 healthy age- and sex-matched controls. Early studies by Hsu et al. (1989), using bleomycin as a G<sub>2</sub> clastogen, found that patients with cancers of the colon (n = 83), head and neck (n = 77) and lung (n = 71) had sensitivity profiles that were distinctly higher than those of 335 controls. However, the profile of 82 breast cancer patients was similar to that of the controls. This suggested to us that, although in many respects bleomycin can be considered as being radiomimetic, the spectrum of lesions induced by ionising radiation and bleomycin is not identical and that some G<sub>2</sub>-sensitive individuals (breast cancer patients?) may have a defect in DNA damage processing which is specific for a type of lesion that is induced by ionising radiation and not by bleomycin (e.g. base damage). However, Adema et al. (2003) have recently found a very strong correlation between gamma ray and bleomycin G<sub>2</sub> sensitivity in nine cell lines including those from two breast cancer patients of differing sensitivity. The reason for the apparent discrepancy between

radiation (Scott et al., 1994, 1999) and bleomycin (Hsu et al., 1989) sensitivity of breast cancer patients remains unclear and a larger, parallel study is required.

### Heritability

The strongest support for our hypothesis was the demonstration of heritability of sensitivity in the families of breast cancer patients (Roberts et al., 1999; Scott, 2000). We selected 16 patients with G<sub>2</sub> scores in the sensitive range (above the 90<sup>th</sup> percentile of historic controls) and 8 patients with normal scores; 69 blood relatives of these 24 cases were tested together with 42 parallel controls, many of whom were non-blood relatives such as spouses. Twenty-three of the 37 (62%) first degree relatives of sensitive patients were also sensitive compared with only 1/42 (2.4%) of the controls (Fig. 2). Only 1/24 (4.2%) of first degree relatives of normal-responding patients were sensitive.

A segregation analysis was performed on the pedigree data and showed clear evidence of Mendelian heritability of chromosomal radiosensitivity. For most of the families, a model involving a single gene with two alleles acting co-dominantly, was a good fit to the data. For a few families, a better fit was obtained by including a second, rarer, gene with a similar additive effect. Earlier studies on small numbers of female blood relatives of breast cancer patients had shown evidence of elevated G<sub>2</sub> radiosensitivity compared with normal controls but these studies were not large enough for segregation analysis (references in Roberts et al., 1999). Our results with the G<sub>0</sub> micronucleus assay showed that 22 first degree relatives of 11 breast cancer patients were, on average, more sensitive than 68 controls (Burrill et al., 2000).

The enhanced G<sub>2</sub> sensitivity to bleomycin of head and neck cancer patients (Hsu et al., 1989) has been confirmed in several studies (references in Cloos et al., 1996) and Cloos et al. (1999) have demonstrated a strong inherited component in 135 healthy individuals from 53 pedigrees, including 14 families having a first degree relative with head and neck cancer.

### The future

More, and larger, family studies of chromosomal radiosensitivity, of the type we have undertaken for breast cancer cases, are required for other cancers, to test for heritability.

The relationship between radiation and bleomycin sensitivity also warrants further investigation.

A major task will be the identification of these putative cancer-predisposing genes. At present we only know that they appear to be involved in the processing of DNA damage of the types induced by ionising radiation (and bleomycin?). Where inheritance patterns are fairly simple, as was apparently the case for most of our breast cancer families, genetic linkage studies may be a feasible proposition. However, different genes may be involved in different families so the best approach may be a study on a few large families. An alternative strategy would be to screen chromosomally radiosensitive families for mutations

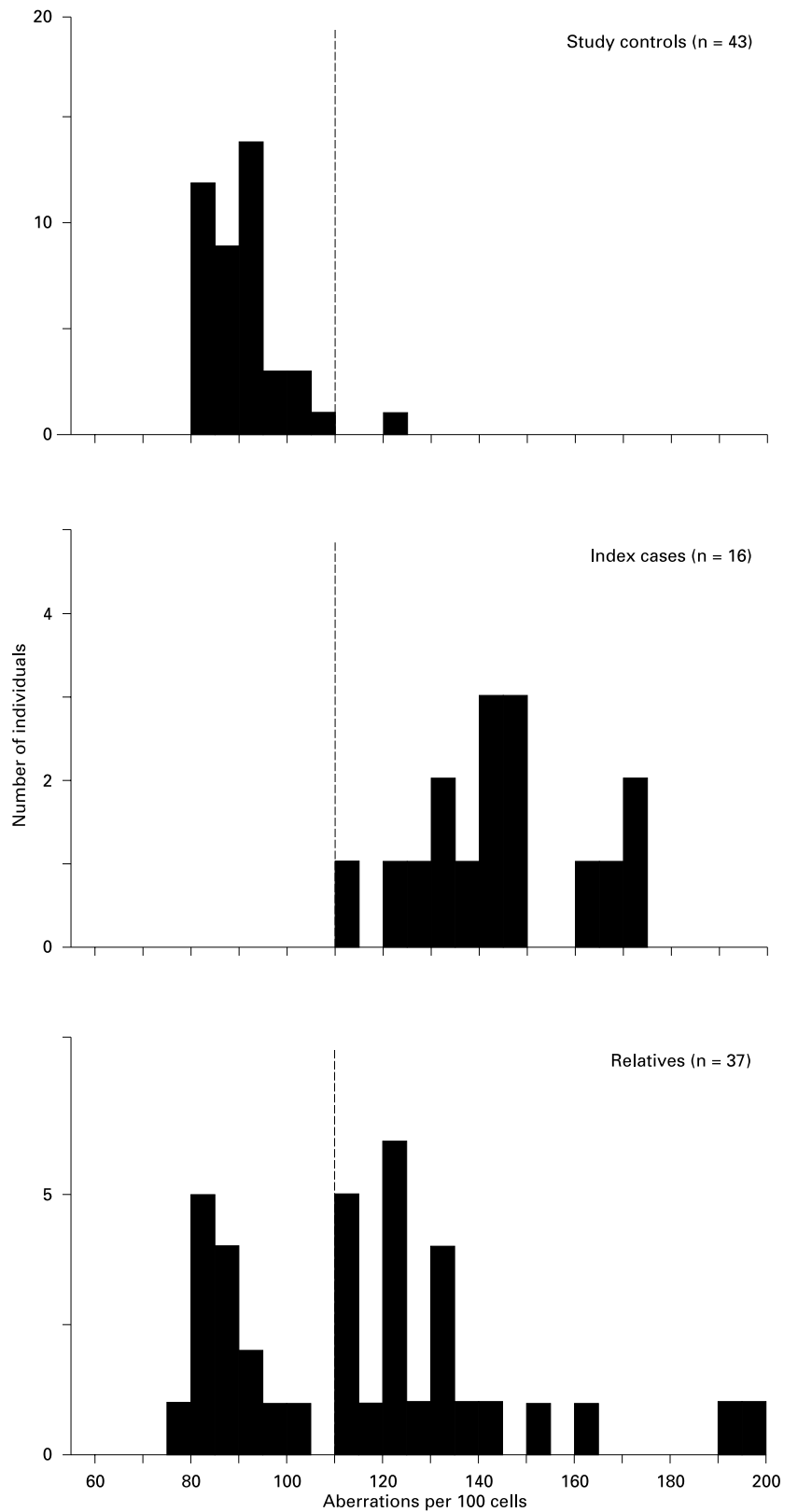


**Fig. 2.** G<sub>2</sub> chromosomal radiosensitivity of (top) healthy controls tested in parallel with samples from families, (middle) patients with breast cancer selected as being sensitive in the assay and (bottom) first degree relatives of the patients shown in the middle panel. The dashed vertical lines indicate the cutoff point between a normal and a sensitive response, from historic control data (see Fig. 1). From Roberts et al. (1999) with permission from the American Society of Human Genetics.

or polymorphisms in candidate genes such as those known to be involved in DNA repair or cell cycle control. A possible contender is the *CHEK2* gene which confers low penetrance susceptibility to breast cancer (Meijers-Heijbour et al., 2002) and is involved in G<sub>2</sub> checkpoint control in response to DNA damage induced by ionising radiation (Matsuoka et al., 1998). We have recently shown that such checkpoint control is less efficient in breast cancer patients than in healthy females (Scott et al., 2003).

When the inherited genetic changes associated with chromosomal radiosensitivity have been identified, epidemiological studies will then be required to estimate the degree of enhanced cancer risk and whether there is also an increased risk of radiogenic cancers (Scott, 2002). Ultimately, population

screening would enable medical resources, such as mammography and preventative chemotherapy in the case of breast cancer, to be concentrated on carriers of such predisposing genetic determinants. Bearing in mind the potentially high frequency of such individuals (Table 1) compared with those carrying high penetrance mutations, which are rare, such screening could have an important impact on cancer incidence.

### Acknowledgements

I would like to thank all my colleagues and collaborators, listed as authors in our publications given below, for their enthusiastic co-operation in these studies.

### References

- Adema AD, Cloos J, Verheijen RHM, Braakhuis BJM, Bryant PE: A comparison of bleomycin and radiation in the G<sub>2</sub> assay of chromatid breaks. *Int J Radiat Biol* 79:655–661 (2003).
- Baeyens A, Thierens H, Claes K, Poppe B, Messiaen L, DeRidder L, Vral A: Chromosomal radiosensitivity in breast cancer patients with a known or putative genetic predisposition. *Br J Cancer* 87:1379–1385 (2002).
- Baria K, Warren C, Roberts SA, West CM, Scott D: Chromosomal radiosensitivity as a marker of predisposition to common cancers? *Br J Cancer* 84:892–896 (2001).
- Baria K, Warren C, Eden OB, Roberts SA, West CM, Scott D: Chromosomal radiosensitivity in young cancer patients: possible evidence of genetic predisposition. *Int J Radiat Biol* 78:341–346 (2002).
- Bondy ML, Wang L-E, El-Zein R, de Andrade M, Selvan MS, Bruner JM, Levin VA, Yung WKA, Adatto P, Wei Q: Gamma-radiation sensitivity and risk of glioma. *J Natl Cancer Inst* 93:1553–1557 (2001).
- Burrill W, Barber JBP, Roberts SA, Bulman B, Scott D: Heritability of chromosomal radiosensitivity in breast cancer patients: a pilot study with the lymphocyte micronucleus assay. *Int J Radiat Biol* 76:1617–1619 (2000).
- Cloos JC, Nieuwenhuis EJC, Boomsma DI, Kuik DJ, van der Sterre MLT, Arwert F, Snow GB, Braakhuis JM: Inherited susceptibility to bleomycin-induced chromatid breaks in cultured peripheral blood lymphocytes. *J Natl Cancer Inst* 91:1125–1130 (1999).
- Cloos J, Spitz MR, Schantz SP, Hsu TC, Zhang Z-F, Tobi H, Braakhuis BJM, Snow JB: Genetic susceptibility to head and neck squamous cell carcinoma. *J Natl Cancer Inst* 88:530–534 (1996).
- Easton DF: Cancer risks in A-T heterozygotes. *Int J Radiat Biol* 66:S177–S182 (1994).
- Eeles R, Ponder B, Easton D, Horwich A: Genetic Predisposition to Cancer (Chapman and Hall, London 1996).
- Foulkes WD, Brunet J-S, Kowalski LP, Narod SA, Franco E: Family history of cancer is a risk factor for squamous cell carcinoma of the head and neck in Brazil: a case-control study. *Int J Cancer* 63:769–773 (1995).
- Hsu TC, Johnston DA, Cherry LM, Ramkissoon D, Schantz SP, Jessup JM, Winn RJ, Shirley L, Furlong C: Sensitivity to genotoxic effects of bleomycin in humans: possible relationship to environmental carcinogenesis. *Int J Cancer* 43:403–409 (1989).
- Jones LA, Scott D, Cowan R, Roberts SA: Abnormal radiosensitivity of lymphocytes from breast cancer patients with excessive normal tissue damage after radiotherapy: chromosome aberrations after low dose-rate irradiation. *Int J Radiat Biol* 67:519–528 (1995).
- Knudson AG: Genetics of human cancer. *Ann Rev Genet* 20:231–251 (1986).
- Lichtenstein P, Holm NV, Verkasalo PK, Iiado A, Kaprio J, Koskenvuo M, Pukkala E, Skytthe A, Hemminki K: Environmental and heritable factors in the causation of cancer. Analysis of cohorts of twins from Sweden, Denmark and Finland. *New Engl J Med* 343:78–85 (2000).
- Matsuoka S, Huang M, Elledge SJ: Linkage of *ATM* to cell cycle regulation by the Chk2 protein kinase. *Science* 282:1893–1897 (1998).
- Meijers-Heijbour H et al.: Low-penetrance susceptibility to breast cancer due to *CHEK2*\*1100delC in noncarriers of *BRC1* or *BRC2* mutations. *Nature Genet* 31:55–59 (2002).
- Papworth R, Slevin N, Roberts SA, Scott D: Sensitivity to radiation-induced chromosome damage may be a marker of genetic predisposition in young head and neck cancer patients. *Br J Cancer* 84:776–782 (2001).
- Peto J, Mack TM: High constant incidence in twins and other relatives of women with breast cancer. *Nature Genet* 26:411–414 (2000).
- Roberts SA, Spreadborough AR, Bulman B, Barber JBP, Evans DJR, Scott D: Heritability of cellular radiosensitivity: A marker of low-penetrance predisposition genes in breast cancer? *Am J Hum Genet* 65:784–794 (1999).
- Scott D: Chromosomal radiosensitivity, cancer predisposition and response to therapy. *Strahlenther Onkol* 176:229–234 (2000).
- Scott D: Individual differences in chromosomal radiosensitivity: implications for radiogenic cancer, in Sugahara T, Nikaïdo O, Niwa O (eds): *Radiation and Homeostasis*, pp 433–437 (Elsevier Science BV, The Netherlands 2002).
- Scott D, Spreadborough A, Levine E, Roberts SA: Genetic predisposition in breast cancer. *Lancet* 344:444 (1994).
- Scott D, Hu Q, Roberts SA: Dose-rate sparing for micronucleus induction in lymphocytes of controls and ataxia-telangiectasia heterozygotes exposed to <sup>60</sup>Co gamma-irradiation in vitro. *Int J Radiat Biol* 70:521–527 (1996).
- Scott D, Barber JBP, Spreadborough AR, Burrill W, Roberts SA: Increased chromosomal radiosensitivity in breast cancer patients: a comparison of two assays. *Int J Radiat Biol* 75:1–10 (1999).
- Scott D, Spreadborough AR, Roberts SA: Less G<sub>2</sub> arrest in irradiated cells of breast cancer patients than in female controls: a contribution to their enhanced chromosomal radiosensitivity? *Int J Radiat Biol* 79:405–411 (2003).
- Smart V, Curwen GB, Whitehouse CA, Edwards A, Tawn EJ: Chromosomal radiosensitivity: a study of the chromosomal G<sub>2</sub> radiosensitivity in human blood lymphocytes indicating significant inter-individual variability. *Mutat Res* 528:105–110 (2003).
- Taylor AMR: The effect of radiation on the chromosomes of patients with an unusual cancer susceptibility, in Ishihara T, Sasaki MS (eds): *Radiation Induced Chromosome Damage in Man*, pp 167–199 (Alan R Liss, New York 1983).
- Teare MD, Wallace SA, Harris M, Howell A, Birch JM: Cancer experience in the relatives of an unselected series of breast cancer patients. *Br J Cancer* 10:102–111 (1994).
- Terzoudi GI, Jung T, Hain J, Vrouvas J, Margaritis K, Donta-Bakoyiannis C, Makropoulos V, Angelakis PH, Pantelias GE: Increased chromosomal radiosensitivity in cancer patients: the role of cdk1/cyclin-B activity levels in the mechanisms involved. *Int J Radiat Biol* 76:605–615 (2000).

## Cytogenetic studies in mice treated with the jet fuels, Jet-A and JP-8

Vijayalaxmi,<sup>a</sup> A.D. Kligerman,<sup>c</sup> T.J. Prihoda<sup>b</sup> and S.E. Ullrich<sup>d</sup>

Departments of <sup>a</sup>Radiation Oncology and <sup>b</sup>Pathology, The University of Texas Health Science Center, San Antonio TX;

<sup>c</sup>Environmental Carcinogenesis Division, U.S. Environmental Protection Agency, Research Triangle Park NC;

<sup>d</sup>Department of Immunology, The University of Texas, M.D. Anderson Cancer Center, Houston TX (USA)

**Abstract.** The genotoxic potential of the jet fuels, Jet-A and JP-8, were examined in mice treated on the skin with a single dose of 240 mg/mouse. Peripheral blood smears were prepared at the start of the experiment ( $t = 0$ ), and at 24, 48 and 72 h following treatment with jet fuels. Femoral bone marrow smears were made when all animals were sacrificed at 72 h. In both tissues, the extent of genotoxicity was determined from the incidence of micronuclei (MN) in polychromatic erythrocytes. The frequency of MN in the peripheral blood of mice

treated with Jet-A and JP-8 increased over time and reached statistical significance at 72 h, as compared with concurrent control animals. The incidence of MN was also higher in bone marrow cells of mice exposed to Jet-A and JP-8 as compared with controls. Thus, at the dose tested, a small but significant genotoxic effect of jet fuels was observed in the blood and bone marrow cells of mice treated on the skin.

Copyright © 2003 S. Karger AG, Basel

The jet-propulsion fuels, Jet-A and JP-8, are kerosene-based middle distillates containing complex mixtures of aliphatic (~ 80%, C<sub>9</sub>–C<sub>16+</sub>), aromatic (~ 18%) and other substituted naphthalene hydrocarbon compounds (Riviere et al., 1999). Jet-A is the common fuel used to power commercial aircraft, and worldwide consumption exceeds 60 billion gallons per year (Armbrust Aviation Group, 1998). JP-8 is widely used by the military, not only for aircraft, but also for ground vehicles and other equipment such as generators, cooking stoves, and tent heaters/air conditioners (NRC, 2003). JP-8 is comprised of Jet-A with additional icing and corrosion inhibitors, and a static dissipater (Cooper and Mattie, 1996). Thus, JP-8 has the

advantage of a lower freezing temperature, which is favorable for high-altitude flights. JP-8 also has a higher flash-point and lower vapor pressure (than previously used jet fuels), which reduces the potential for crash-related explosions and fires and from combustion from natural lightning and static electricity (Mattie et al., 1991). Each year an estimated five billion gallons of JP-8 is used by the U.S. Department of Defense and the North Atlantic Treaty Organization (NRC, 2003).

Measurements of ambient and breath samples collected from several groups of personnel at U.S. Air Force bases contained various concentrations of hydrocarbons present in the jet fuel. These included benzene, butane, decane, dodecane, undecane, hexane, heptane, octane, nonane, pentane, styrene, trichloroethane, toluene, and xylene (Pleil et al., 2000). As such, they represent the most common acute and chronic occupational chemical exposure for thousands of flight and ground crew personnel, aircraft mechanics, workers near flight lines, as well as civilians at air force bases and airports. Routes of human exposure include aerosol, vapor, and liquid through inhalation, dermal and, at times, oral ingestion. Personnel involved in fuel refining, transportation and storage, draining of field and supply tanks, de-fuelling and fuel-maintenance of aircrafts are at greater risk for dermal exposure.

Supported by grants F49620-03-1-0079 (V) and F49620-02-1-0102 (SEU) from the U.S. Air Force Office of Scientific Research.

Received 20 September 2003; manuscript accepted 3 December 2003.

Request reprints from Vijayalaxmi, Department of Radiation Oncology  
The University of Texas Health Science Center  
7703 Floyd Curl Drive, San Antonio, TX 78229 (USA)  
telephone: +1 210 616 5648; fax: +1 210 949 5085  
e-mail: vijay@uthscsa.edu

The health effects of exposures to JP-8 and related jet fuels were reviewed recently (NRC, 2003). The information examined included cardiovascular, immune, liver, kidney, neuronal, respiratory tract, and reproductive and developmental toxicities as well as carcinogenicity. With respect to genotoxicity data, *in vitro* investigations using *Salmonella typhimurium*, *Saccharomyces cerevisiae* and cultured L5178Y mouse lymphoma cells failed to demonstrate any mutagenicity induced by jet fuels, including JP-8 (Brusick and Matheson, 1978a, b; API, 1984; Conaway et al., 1984; NTP, 1986; McKee et al., 1989, 1994; Nessel et al., 1999). Recent studies, however, reported a significant increase in DNA single-strand breaks (SSB) in peripheral blood lymphocytes collected from personnel exposed to petroleum derivatives and engine exhausts, among other exposures, at the Barcelona airport (Pitarque et al., 1999). Also, mammalian cells exposed *in vitro* to JP-8, Jet-A, and related jet fuels exhibited increased SSB and cytotoxicity (Grant et al., 2000, 2001; Jackman et al., 2002). The National Research Council, Committee on Toxicology and Subcommittee on Jet-Propulsion Fuel 8 (JP-8) has considered these reports, and recommended that future studies in animals should include evaluation of *in vivo* genotoxicity (NRC, 2003). The rodent micronucleus (MN) assay, which detects MN arising from both chromosomal fragments and unequal segregation of chromosomes during cell division, has been widely applied as an *in vivo* assay for detecting genotoxic agents. The current study was conducted in mice treated on the skin with a single application of Jet-A or JP-8 to determine the potential of these fuels to induce MN in peripheral blood and bone marrow cells.

## Materials and methods

### Mice

Specific pathogen-free (SPF) female C3H/HeNcr (MTV-) mice, 8 to 10 weeks old, were obtained from the National Cancer Institute Frederick Cancer Research Facility Animal Production Area (Frederick, MD). The animals were maintained in facilities approved by the Association for Assessment and Accreditation of Laboratory Animal Care International, in accordance with current regulations and standards of the U.S. Department of Agriculture, Department of Health and Human Services, and National Institutes of Health and the National Toxicology Program. All animal procedures were reviewed and approved by the University of Texas M.D. Anderson Cancer Center Institutional Animal Care and Use Committee.

### Experimental protocol

The experiment was conducted over a period of 3 days in an animal facility at the M.D. Anderson Cancer Center. A total of 40 age-matched mice were randomized to four groups of 10 each. The mean body weights of the animals in all four groups were not significantly different ( $21.7 \pm 0.59$  g). The treatment groups were: (1) control, (2) Jet-A, (3) JP-8, and (4) cyclophosphamide (CP). Two hours before the start of the experiment, an approximately 8-cm<sup>2</sup> area on the backs of the mice was shaved. The mice in group 1 received no further treatment and served as the negative controls. The mice in groups 2 and 3 were treated with a single total dose of 240 mg of Jet-A and JP-8, respectively. This dose was chosen because, in previous studies, application of 240 mg/mouse of JP-8 or Jet-A was found to be immunotoxic (Ullrich, 1999; Ramos et al., 2002). Jet-A (Lot# 3404) and JP-8 (Lot# 3509) were supplied by The Operational Toxicology Branch, Air Force Research Laboratory, Wright Patterson Air Force Base, Dayton, OH. The fuel was stored and used in a chemical fume hood. The undiluted fuel (300  $\mu$ l or 240 mg/mouse) was applied directly to the shaved dorsal skin with a micropipette. The mice were then caged individually in the chemical fume hood for the next 3 h. This

prevented cage mates from grooming and ingesting the fuel. After 3 h the residual fuel was either absorbed through the skin of the mice or had evaporated. The animals were then returned to standard housing in an SPF-barrier facility. Mice in group 4 were used as positive controls and received CP (Sigma Chemical Co, St. Louis, MO) dissolved in sterile phosphate-buffered saline and injected into the peritoneal cavity to give a final dose of 40 mg/kg body weight (at  $t = 0$ ). Peripheral blood and bone marrow smears were prepared as described below.

### Peripheral blood smears

Small drops of peripheral blood were collected by snipping the tails of all mice at the start of the experiment ( $t = 0$ ), and at 24, 48 and 72 h following treatments. The blood was immediately placed on clean microscope slides and pushed behind another slide held at a 45° angle to form a thin smear covering an area of 3 × 4 cm. The smears were air-dried, fixed in absolute methanol for 30 min, and air-dried again. The slides were then stored at room temperature.

### Bone marrow smears

Both femur bones were collected from all mice when they were sacrificed at 72 h following treatments. The bones were cleaned of the surrounding muscle tissue. A 22 G needle fitted to a syringe filled with 1 ml of newborn calf serum (heat inactivated at 56 °C for 2 h) was inserted at one end of each bone to flush its marrow into a microfuge tube. The marrow in the tube from both bones was pulled gently up and down in the syringe until a fine cell suspension was observed. All tubes were gently centrifuged (1,000 g) for few seconds to pellet the cells at the bottom of the tube. Most of the supernatant in the tube was discarded and the cells in the pellet were resuspended in a very small volume of the remaining serum. Small drops of the resulting viscous cell suspension were placed on clean microscope slides to prepare thin smears, as described above for the blood.

### Evaluation of micronuclei

The study was conducted in a blind manner. Each slide was assigned a random number, without giving the identity of treatment groups. Duplicate sets of slides, each containing both blood and bone marrow smears from each mouse, were sent to the Department of Radiation Oncology, University of Texas Health Science Center (UTHSC), San Antonio, TX. All slides were stained with acridine orange (0.01 mg/ml in 0.2 M sodium phosphate buffer, pH 7.4). One complete set was mailed to the Environmental Carcinogenesis Division, U.S. Environmental Protection Agency (EPA), Research Triangle Park, NC for microscopic examination while the second set was evaluated at UTHSC. Thus, two independent investigators (Inv-1 at UTHSC and Inv-2 at EPA) assessed the incidence of MN in peripheral blood and bone marrow cells. Each investigator used a fluorescence microscope fitted with appropriate filters for acridine orange stain. For each mouse, (a) the percentage of polychromatic erythrocytes (%PCE) was obtained from the examination of 1,000 erythrocytes in peripheral blood and 200 erythrocytes in bone marrow (Inv-1 only), and (b) the incidence of MN was determined from the examination of 2,000 consecutive PCE in both the peripheral blood and bone marrow preparations (Heddle et al., 1984). The results were decoded after complete microscopic evaluation by both investigators.

### Statistical analyses

An SAS User's Guide (1977) was used for statistical analyses. The data were subjected to the analysis of variance (ANOVA) test to assess significant differences between groups, and at each blood collection time. Multiple as well as pair-wise comparisons were also made with Bonferroni adjustments (Cohen, 1988). Treatment means were compared to the concurrent controls using a one-tailed Dunnett's test (Dunnett, 1955). The data were also analyzed for investigator variability. For several pair-wise comparisons, there were significant differences between the Inv-1 and Inv-2 scores, so each set of data was analyzed separately. Pooled data of the two investigators was considered only when there were no significant differences. Square root transformation of the data was used when the conditions for such analyses were valid. Residuals were analyzed for homogeneity of variance and normality of distributions. Statistical significance was taken at a level of  $P < 0.05$ .

## Results

The mean %PCE and the average incidence of MN/2000 PCE for all four groups of animals are presented in Table 1.

### PCE in peripheral blood

There were no significant differences in mean %PCE between control (2.8%), Jet-A- (2.6–2.8%) and JP-8-treated mice (2.6–2.9%) over the 72-hour period. Mice injected with CP (2.3–2.5%) showed a considerable decrease in %PCE at various times, but the overall response was not significantly different from controls.

### PCE in bone marrow

There were no significant differences in %PCE in any of the four groups of mice investigated: controls 70.1%, Jet-A 71.3%, JP-8 71.1%, and CP 67.5%.

### MN in peripheral blood

The incidence of MN at the start of the experiment ( $t = 0$ ) was not significantly different among the four groups of mice, and ranged from 4.1 to 4.5 (Inv-1) and from 4.4 to 5.2 (Inv-2). Both investigators documented an increase in the incidence of MN in Jet-A- and JP-8-exposed mice over the 72-hour period. The differences between control animals and mice treated with the Jet-A (4.4 versus 7.8 [Inv-1] and 4.3 versus 8.6 [Inv-2];  $P < 0.05$ ), and between control animals and mice treated with the JP-8 (4.4 versus 6.9 [Inv-1] and 4.3 versus 9.1 [Inv-2];  $P < 0.05$ ) were statistically significant at 72 h. Both investigators observed statistically significant increases in the frequencies of MN in mice injected with CP at 24, 48 and 72 h. The incidence was maximum at 48 h and then decreased at 72 h to the 24-hour level.

### MN in bone marrow

There was no significant difference between Inv-1 and Inv-2 in the scoring of MN in bone marrow cells. A higher incidence of MN was observed in Jet-A-treated mice (8.3 Inv-1, 8.0 Inv-2) as compared with controls (5.1 [Inv-1] and 5.5 [Inv-2]). The difference from control animals was statistically significant for Inv-1 ( $P = 0.037$ ), while the results obtained by Inv-2 just missed reaching statistical significance ( $P = 0.062$ ). Increases in the frequency of MN were also observed in JP-8-treated mice (6.8 [Inv-1] and 6.0 [Inv-2]), but the difference from control animals was not statistically significant. The incidence of MN in CP-treated mice was clearly statistically significant as compared with control animals ( $P < 0.01$ ).

## Discussion

The great majority of the in vitro studies reported negative results on the genotoxic potential of jet fuels (Brusick and Matheson, 1978a, b; API, 1984; Conaway et al., 1984; NTP, 1986; McKee et al., 1989, 1994; Nessel et al., 1999). Chinese hamster ovary cells exhibited an increase in the incidence of sister chromatid exchanges (SCE) only when the cells were treated with jet fuel in the presence of metabolic activation.

**Table 1.** Incidence of micronuclei in mice treated on the skin with 240 mg of jet fuel, Jet-A or JP-8

Group <sup>a</sup>	Sacrifice hour	% PCE <sup>b</sup>	MN / 2000 PCE <sup>c</sup>	
			Inv-1 (UTHSC)	Inv-2 (EPA)
<b>Peripheral Blood</b>				
Control	0	2.8 ± 0.5	4.5 ± 2.1	4.8 ± 1.4
Jet-A	0	2.7 ± 0.4	4.2 ± 1.7	4.9 ± 2.0
JP-8	0	2.7 ± 0.7	4.1 ± 2.1	4.4 ± 1.8
CP	0	2.5 ± 0.5	4.5 ± 2.5	5.2 ± 2.3
Control	24	2.8 ± 0.5	4.4 ± 2.0	6.4 ± 2.4
Jet-A	24	2.6 ± 0.5	4.4 ± 2.3	5.1 ± 1.5
JP-8	24	2.6 ± 0.5	4.8 ± 1.9	5.5 ± 2.4
CP	24	2.4 ± 0.4	14.4 ± 5.0 <sup>d</sup>	13.5 ± 6.2 <sup>d</sup>
Control	48	2.8 ± 0.4	4.5 ± 2.5	8.3 ± 2.6
Jet-A	48	2.8 ± 0.7	6.4 ± 2.5	9.7 ± 3.1
JP-8	48	2.8 ± 0.7	6.1 ± 2.3	8.4 ± 2.7
CP	48	2.3 ± 0.6	29.6 ± 6.9 <sup>d</sup>	40.1 ± 10.8 <sup>d</sup>
Control	72	2.8 ± 0.6	4.4 ± 2.5	4.3 ± 3.5
Jet-A	72	2.8 ± 0.5	7.8 ± 3.6 <sup>d</sup>	8.6 ± 3.8 <sup>d</sup>
JP-8	72	2.9 ± 0.6	6.9 ± 2.5 <sup>d</sup>	9.1 ± 4.8 <sup>d</sup>
CP	72	2.5 ± 0.4	15.7 ± 3.5 <sup>d</sup>	13.3 ± 3.5 <sup>d</sup>
<b>Bone marrow</b>				
Control	72	70.1 ± 5.6	5.1 ± 2.0	5.5 ± 3.3
Jet-A	72	71.3 ± 5.2	8.3 ± 4.1 <sup>d</sup>	8.0 ± 2.9
JP-8	72	71.1 ± 5.9	6.8 ± 2.9	6.0 ± 2.6
CP	72	67.5 ± 7.9	9.7 ± 4.2 <sup>d</sup>	8.9 ± 2.3 <sup>d</sup>

<sup>a</sup> Number of mice in each group = 10.

<sup>b</sup> For each mouse, 1000 consecutive erythrocytes in peripheral blood and 200 consecutive erythrocytes in bone marrow were examined.

<sup>c</sup> For each mouse, 2000 consecutive PCEs in both peripheral blood and bone marrow were examined. All data are group average ± standard deviation.

<sup>d</sup> Significant difference from control mice at  $P < 0.05$ .

The positive effect observed was inconsistent and was not jet fuel concentration dependent. The authors concluded that the overall effect of jet fuel exposure was negative (API, 1988b). In in vivo investigations, dominant lethal tests were negative in mice and rats administered JP-8 and JP-4 for 5 consecutive days (gavage, 0.01 to 1.3 ml/kg/day) (Brusick and Matheson, 1978a, b). Also, there were no significant increases in incidence of chromosomal aberrations (CA), MN and SCE in bone marrow cells of mice and rats treated with jet fuels (gavage or intraperitoneal injection, acute doses of 0.3–5.0 g/kg) (API, 1984, 1988a; McKee et al., 1994; Nessel et al., 1999). Although increased frequencies of CA were observed in bone marrow cells of rats exposed to the highest dose of middle distillate fuels, the study was concluded as negative since all data were within the historical control values (Conaway et al., 1984). Among human investigations, Lemasters et al. (1997, 1999) determined the incidence of SCE and MN in peripheral blood lymphocytes collected over a 30-week period from personnel occupationally exposed to jet fuels at a U.S. Air Force base. Compared with unexposed controls, lymphocytes from some exposed groups exhibited a small, time-dependent, and statistically significant increase in SCE. The incidence of MN in a number of exposed individuals was increased by 15 weeks and then decreased at 30 weeks. The authors concluded that the changes observed in both SCE and MN remained within the ranges published for the general population. Pitarque et al. (1999) also examined SCE and MN, in addition to SSB, in

peripheral blood lymphocytes collected from 39 male workers at Barcelona airport (exposed to petroleum derivatives and engine exhausts) and 11 healthy controls working at the university campus in Barcelona (without indication of occupational exposure to petroleum derivatives or other suspicious genotoxic agents). SCE analyses failed to detect significant differences between airport workers and controls, and MN frequencies were significantly lower in the exposed group. A small but significant increase in SSB was observed in the exposed group as compared with unexposed controls.

To date, all of the *in vivo* studies conducted in mice and rats have examined the genotoxic potential of various jet fuel(s) that were administered by gavage and intraperitoneal injection. Ours is the first report where the genotoxic potential of Jet-A and JP-8 was examined following application to the skin (dermal exposure). The results indicated that a single dermal treatment of mice with Jet-A and JP-8 (240 mg/mouse) was able to induce a small, but significant increase in the frequency of MN in the peripheral blood. The highest incidence of MN in the blood was recorded at 72 h following treatment with jet fuels. An increase in the frequency of MN was also documented in bone marrow cells collected at 72 h after treatment with Jet-A. As MacGregor et al. (1980) pointed out, in mice treated with CP, the peak level of micronucleated-PCEs in peripheral blood occurs on the day following the maximum incidence observed in bone marrow cells. Thus, it is reasonable to assume that the peak incidence of MN in bone marrow cells of mice treated with Jet-A and JP-8 might have occurred at 48 h and was missed when these cells were collected at 72 h after jet fuel exposure.

In the earlier *in vivo* studies mentioned above, the highest acute dose of jet fuels tested in rodents was 5.0 g/kg (or ~100 mg/mouse; gavage or intraperitoneal injection). This dose was lower than that used in the present investigation (240 mg/mouse; dermal). While the results from earlier studies on CA, MN and SCE analyses were negative, the data obtained in our study indicated an increase in MN in both peripheral blood and bone marrow cells of mice. Perhaps the route of administration of the jet fuels may have a differential effect on the results.

It is estimated that if both hands of humans were constantly wet with JP-8, about 17 mg of various hydrocarbons would penetrate systemically through the skin (Riviere et al., 1999). Benzene, one of the hydrocarbons present in jet fuels, has been shown to induce MN in the peripheral blood, bone marrow and spleen cells of rodents following a single oral administration of 500–2,000 mg/kg (or ~10.0–40.0 mg/mouse) or short-term inhalation (Erexson et al., 1986; Hatakeyama et al., 1992; Chen et al., 1994). It may not be unreasonable to hypothesize the genotoxic effects of benzene may partly be responsible for the observed increase in MN when Jet-A and JP-8 was applied to the skin of mice in our study (see below).

Uncovered skin is an important route for jet fuel exposure in humans. Several studies using animal models and humans have reported percutaneous absorption of various hydrocarbon constituents in Jet-A and JP-8, and significant changes in the barrier function of the skin. Such changes were shown to result in trans-epidermal water loss (TEWL), erythema, irritation,

and local and systemic toxicity in several organs (NRC, 2003). Furthermore, TEWL after exposure to JP-8 might lead to an increased permeation of JP-8 components and/or other chemicals into the skin (Kanikkannan et al., 2001). The mechanistic aspects of such adverse effects have been addressed in some investigations. Rogers et al. (2001) reported a significant increase in the formation of oxidative species and low-molecular-weight DNA in the skin of rats following dermal exposure to JP-8. The percutaneous absorption and perhaps systemic distribution of various hydrocarbon constituents in Jet-A and JP-8 may have led to the formation of toxic oxidative species that could have damaged the DNA resulting in an increase in the incidence of MN in mice treated on the skin with jet fuels. Ullrich (1999) and Ramos et al. (2002) reported that dermal exposure of mice to Jet-A and JP-8 in a large single dose (300 µl) or in small multiple doses (50 µl/day for 4–5 days) resulted in local and systemic effects on the immune system, e.g., suppressed contact- and delayed-hypersensitivity responses. The investigators suggested that the dermal application of the jet fuel damaged the keratinocytes which led to an increase in the production and systemic distribution of interleukin-10, a cytokine that suppresses some immune functions. These observations and the data presented in our study indicating that a single dermal application of 300 µl of Jet-A and JP-8 in mice results in a small but significant increase in genotoxicity in hematopoietic tissues should raise concern about potential health effects of prolonged and repeated dermal exposure of humans to jet fuels.

### Acknowledgements

We are grateful to Jason Lozano, Nasser Kazimi and Polina Khaskina for their technical assistance. We would like to thank Dr. Errol Zeiger, Errol Zeiger Consulting, Chapel Hill, NC, and Dr. R.J. Preston, National Health and Environmental Effects Research Laboratory (NHEERL), U.S. Environmental Protection Agency (EPA) for reviewing the manuscript and for useful comments. The authors also thank Dr. D. Doerfler, NHEERL, U.S. EPA for help with the statistical analyses. This article was reviewed by the NHEERL, U.S. EPA, and approved for publication. Approval does not signify that the contents necessarily reflect the views and policies of the Agency, nor does mention of trade names or commercial products constitute endorsement or recommendation for use.

## References

- API (American Petroleum Institute): Mutagenicity evaluation studies in the rat bone marrow cytogenetic assay, in the mouse lymphoma forward mutation assay: Hydrosulfurized kerosene, API sample 81-07 (API Med Res Publ 32-30240, Washington DC 1984).
- API (American Petroleum Institute): Sister chromatid exchange assay in Chinese hamster ovary (CHO) cells with API 81-07: Hydrosulfurized kerosene (API Med Res Publ 35-32482, Washington DC 1988a).
- API (American Petroleum Institute): In vivo sister chromatid exchange assay with API 81-07: Hydrosulfurized kerosene (API Med Res Publ 36-30043, Washington DC 1988b).
- Armbrust Aviation Group: World jet fuel almanac (The Armbrust Group, Palm Beach Gardens 1998).
- Brusick DJ, Matheson DW: Mutagen and oncogen study on JP-8. Aerospace Medical Research Laboratory Tech Rep 78-20, Wright-Patterson Air Force Base, OH (1978a).
- Brusick DJ, Matheson DW: Mutagen and oncogen study on JP-4. Aerospace Medical Research Laboratory Tech Rep 78-24, Wright-Patterson Air Force Base, OH (1978b).
- Chen H, Rupa DS, Tomar R, Eastmond DA: Chromosomal loss and breakage in mouse bone marrow and spleen cells exposed to benzene in vivo. *Cancer Res* 54:3533-3539 (1994).
- Cohen P: Statistical Power Analysis for the Behavioral Sciences (Lawrence Erlbaum, Hillsdale 1988).
- Conaway CC, Schreiner CA, Cragg ST: Mutagenicity evaluation of petroleum hydrocarbons, in McFarland HN, Holdsworth CE, MacGregor JA, Call RW, Lane ML (eds): *Advances in Modern Environmental Toxicology, Applied Toxicology of Petroleum Hydrocarbons*, vol 6, pp 89-197 (Princeton, NJ 1984).
- Cooper JR, Mattie DR: Developmental toxicity of JP-8 fuel in the rat. *Appl Toxicol* 16:97-200 (1996).
- Dunnnett CW: A multiple comparison procedure for comparing several treatments with a control. *J Am Stat Assoc* 50:1096-1121 (1955).
- Erexson GL, Wilmer JL, Steinhagen WH, Kligerman AD: Induction of cytogenetic damage in rodents after short-term inhalation of benzene. *Env Mutagen* 8:29-40 (1986).
- Grant GM, Schaffer KM, Kao WY, Stenger DA, Pancrazio JJ: Investigation of the in vitro toxicity of jet fuels JP-8 and jet A. *Drug Chem Toxicol* 23:279-291 (2000).
- Grant GM, Jackman SM, Kolanko CJ, Stenger DA: JP-8 jet fuel-induced DNA damage in H4IIE rat hepatoma cells. *Mutat Res* 490:67-75 (2001).
- Hatakeyama Y, Nakajima E, Atai H, Suzuki S: Effects of benzene in a micronucleus test on peripheral blood utilizing acridine orange-coated slides. *Mutat Res* 278:193-195 (1992).
- Heddle JA, Stuart E, Salamone MF: The bone marrow micronucleus test, in Kilbey BJ, Legator M, Nichols W, Ramel CV (eds): *Hand Book of Mutagenicity Test Procedures*, pp 441-457 (Elsevier, Amsterdam 1984).
- Jackman SM, Grant GM, Kolanko CJ, Stenger DA, Nath J: DNA damage assessment by comet assay of human lymphocytes exposed to jet propulsion fuels. *Env Mol Mutagen* 40:18-23 (2002).
- Kanikkannan N, Patel R, Jackson T, Shaik MS, Singh M: Percutaneous absorption and skin irritation of JP-8 (jet fuel). *Toxicol* 161:1-11 (2001).
- Lemasters GK, Livingston GK, Lockey JE, Olsen DM, Shukla R, New GR, Selevan SG, Yiin JR: Genotoxic changes after low-level solvent and fuel exposure on aircraft maintenance personnel. *Mutagenesis* 12:237-243 (1997).
- Lemasters GK, Lockey JE, Olsen DM, Selevan SG, Tabor MW, Livingston GK, New GR: Comparison of internal dose measures of solvents in breath, blood, and urine and genotoxic changes in aircraft maintenance personnel. *Drug Chem Toxicol* 22:181-200 (1999).
- MacGregor JT, Wehr CM, Gould DH: Clastogen-induced micronuclei in peripheral blood erythrocytes: the basis of an improved micronucleus test. *Env Mutagen* 2:509-514 (1980).
- Mattie DR, Alden CL, Newell TK, Gaworski CL, Fleming CD: A 90-day continuous vapor inhalation toxicity study of JP-8 jet fuel followed by 20 or 21 months of recovery in Fisher 344 rats and C57BL/6 mice. *Toxicol Pathol* 19:77-87 (1991).
- McKee RH, Plutnick RT, Przygoda RT: The carcinogenic initiating and promoting properties of a lightly refined paraffinic oil. *Fund Appl Toxicol* 12:748-756 (1989).
- McKee RH, Amoroso MA, Freeman JJ, Przygoda RT: Evaluation of the genetic toxicity of middle distillate fuels. *Env Mol Mutagen* 23: 234-238 (1994).
- Nessel CS, Freeman JJ, Forgash RC, McKee RH: The role of dermal irritation in the skin tumor promoting activity of petroleum middle distillates. *Toxicol Sci* 49:48-55 (1999).
- NRC: National Research Council. *Toxicologic Assessment of Jet-Propulsion Fuel 8* (National Academy Press, Washington DC 2003).
- NTP: National Toxicology Program. *Toxicology and Carcinogenesis Studies of Marine Diesel Fuel and JP-5 Navy Fuel* (CAS No. 8008-20-6) in B6C3F1 Mice (Dermal Studies), NTP 310, NIH 86-2566. Research Triangle Park, NC (1986).
- Pitarque MA, Creus A, Marcos R, Hughes JA, Anderson D: Examination of various biomarkers measuring genotoxic endpoints from Barcelona airport personnel. *Mutat Res* 440:195-204 (1999).
- Pleil JD, Smith LB, Zelnick SD: Personal exposure to JP-8 jet fuel vapors and exhaust at Air Force Bases. *Env Health Persp* 108:183-192 (2000).
- Ramos G, Nghiem DX, Walterscheid JP, Ullrich SE: Dermal application of jet fuel suppresses secondary immune reactions. *Toxicol Appl Pharmacol* 180:136-144 (2002).
- Riviere JE, Brooks JD, Monteiro-Riviere NA, Budsaba K, Smith CE: Dermal absorption and distribution of topically dosed jet fuels Jet-A, JP-8, and JP-8 (100). *Toxicol Appl Pharmacol* 160:60-75 (1999).
- Rogers JV, Gunasekhar PG, Garrett CM, Kabbur MB, McDougal JN: Detection of oxidative species and low-molecular-weight DNA in skin following dermal exposure with JP-8 jet fuel. *J Appl Toxicol* 21:521-525 (2001).
- SAS User's guide: Statistics, SAS vol. 2 (version 6.12, sixth edition, SAS Institute Inc., Cary, NC 1977).
- Ullrich SE: Dermal application of JP-8 jet fuel induces immune suppression. *Toxicol Sci*: 52:61-67 (1999).



# Chromosomal aberrations and risk of cancer in humans: an epidemiologic perspective

S. Bonassi,<sup>a</sup> A. Znaor,<sup>b</sup> H. Norppa,<sup>c</sup> and L. Hagmar<sup>d</sup>

<sup>a</sup>Department of Environmental Epidemiology and Biostatistics, National Cancer Research Institute, Genoa (Italy);

<sup>b</sup>Croatian National Cancer Registry, Croatian National Institute of Public Health, Zagreb (Croatia);

<sup>c</sup>Laboratory of Molecular and Cellular Toxicology, Department of Industrial Hygiene and Toxicology, Finnish Institute of Occupational Health, Helsinki (Finland);

<sup>d</sup>Department of Occupational and Environmental Medicine, University Hospital, Lund (Sweden)

**Abstract.** The pioneering papers published more than one century ago by Theodor Boveri opened the way to extensive research on the mechanism linking chromosomal abnormalities to the pathogenesis of cancer. As a result of this effort, robust theoretical and empirical evidence correlating cytogenetic damage to early stages of cancer in humans was consolidated, and an increased cancer risk was postulated in healthy subjects with high levels of chromosomal aberrations (CA). The first epidemiological investigation aimed at validating CA as predictor of cancer risk was carried out in the early 1990s. In that report the Nordic Study Group described an 80% increased risk of cancer in healthy subjects with high frequencies of CA. The results of this first study were replicated a few years later in a parallel research initiative carried out in Italy, and the subsequent pooled analysis of these two cohorts published in 1998 contributed to refine the quantitative estimate of the CA/cancer association. A small case-control study nested in a cohort of subjects screened for CA in Taiwan found an

increased risk in subjects with high frequency of chromosome-type CA, while in 2001 a significant increase of cancer incidence associated with high levels of CA was described in a new independent cohort of radon exposed workers from the Czech Republic. Despite some common limitations affecting study design, the studies cited above have provided results of great interest both for the understanding of mechanisms of early stages of carcinogenesis, and for their potential implication for cancer prevention. The recent evolution of molecular techniques and the refinement of high throughput techniques have the potential to improve the knowledge about the role of specific sub-types of CA and to provide further insight into the mechanisms. Finally, the most challenging perspective in the field is the passage from research to regulation, with the implementation of preventive policies based on the accumulated knowledge.

Copyright © 2003 S. Karger AG, Basel

The idea that chromosomal rearrangements might be causally involved in early stages of carcinogenesis is not new. The first reports hypothesizing that karyotypic aberrations, that we now know to be typical of tumor cells, may possibly be involved in the transformation of normal cells into malignant ones were

published more than a century ago. Although limited by the poor techniques and the restricted knowledge of cell biology, those early findings allowed Theodor Boveri to formulate what is now known as the somatic mutation theory of cancer, which still holds the central stage of cancer research (Boveri, 1914).

Despite the early intuition of Theodor Boveri, it was not until the early 1960's, with the description of the first specific chromosome abnormality in a human primary tumor, i.e., the Philadelphia chromosome (Nowell and Hungerford, 1960), and especially in the 1970's with the introduction of banding techniques, that the major role of chromosomal rearrangements in carcinogenesis was fully recognized. During the 1980's, a number of new cancer-specific rearrangements (many of them translocations) mostly occurring in hematological tumors were found, and the mechanistic aspects were described

Supported by grants funded by the Associazione Italiana per la Ricerca sul Cancro (AIRC), Finnish Work Environment Fund, and the European Union 5<sup>th</sup> FP (QLK4-CT-2000-00628, QLK4-CT-2002-02831 and QLRT-2001-02198).

Received 10 September 2003; manuscript accepted 11 November 2003.

Request reprints from Dr. Stefano Bonassi

Department of Environmental Epidemiology and Biostatistics  
Istituto Nazionale per la Ricerca sul Cancro, Largo Rosanna Benzi, 10  
IT-16132 Genova (Italy); telephone: +390-10-5600924; fax: +390-10-5600501;  
e-mail: stefano.bonassi@istge.it

in more detail. The observation that many genes affected by chromosomal rearrangements were involved in some critical stages in cell growth, development, or survival has focused the interest on how the rearrangements alter the function of these target genes. This effort has resulted in a better understanding of the mechanisms of formation of chromosomal alterations and their role in cancer development.

An interesting description of the formation and consequences of chromosomal translocations together with some examples of translocations relevant to hematological malignancies can be found in a review paper published by Rowley (1998).

The model linking chromosome breakage to the activation/deactivation of genes relevant to early stages of carcinogenesis was further refined in the 1990's, when the use of the fluorescence in situ hybridization (FISH) technique in irradiated cells contributed to understanding the role of double-strand breaks (DSBs) in the formation of chromosomal aberrations (CA). A further refinement of these models was provided by a number of papers published at the turn of the millennium, which revealed the major role of homology-dependent and homology-independent pathways of DSB repair in the formation of both chromosome-type and chromatid-type aberrations (Pfeiffer et al., 2000; Richardson and Jasin, 2000).

The clastogenic action of many environmental agents has well been documented and their role in turning on the process leading from DSB to altered function of cancer genes is generally recognized. It is also interesting to note that many DSBs are formed endogenously as a consequence of physiologic processes, such as replication, meiosis, V(D)J recombination, DNA repair, etc. (Pfeiffer et al., 2000; Vilenchik and Knudson, 2003). Although endogenous DSBs are repaired with high fidelity, errors in DSB repair are considered to contribute significantly to human cancer rate (Vilenchik and Knudson, 2003).

These brief considerations about the role of chromosome alterations in the early stages of carcinogenesis provide support to observations, from both laboratory and human studies, linking the clastogenic effect of many compounds to their carcinogenic properties (Bonassi, 1999). Furthermore, the availability of a reliable model of causality supports the biological plausibility of studies linking chromosomal damage to the risk of cancer, and is the driving force that justifies the use of the CA assay for cancer prevention policies.

#### **Cohort studies on CA and cancer in human population: literature review**

The first cohort study on healthy subjects screened for CA (and other cytogenetic endpoints) was published in 1990 as a result of a collaborative initiative carried out in Northern Europe (The Nordic Study Group on the Health Risk of Chromosome Damage, 1990a). A group of 1,548 subjects from Finland, Sweden and Norway, free of cancer at the moment of cytogenetic analysis were followed up from 1970 to 1988, accounting for a total of 7,547 person years. Twenty-six cancer cases were found. The result of that early study failed to reach statistical significance, but interestingly subjects in the highest

tertiles of CA frequency experienced a cancer incidence almost double in comparison with the general population (Standardized Incidence Ratio (SIR) = 1.82; 95% Confidence Interval (CI) 0.98–3.01). The follow-up of this cohort was then extended, and in 1994 a new paper, which also included data from one laboratory in Denmark, was published. The size of the cohort was essentially the same, i.e. 1,979 subjects, but the extended follow-up raised the number of person years to 17,666 and the number of incident cancer cases to 66 (Hagmar et al., 1994), enhancing the statistical power of the study. Subjects classified to have high frequency of CA showed incidence rates that were more than doubled with respect to the general population (SIR = 2.1; 95% CI 1.5–2.8), and a highly significant trend of SIRs by frequency of CA was observed ( $P = 0.0009$ ).

The first independent confirmation of these results came from an Italian cohort study published in 1995 (Bonassi et al., 1995a). The cohort constituted 1,455 subjects followed up from 1969 to 1994 for a total of 16,190 person years. A significant increase in mortality rates for all cancers was found in subjects with high and medium frequency of CA (Standardized Mortality Ratio (SMR) = 1.79; 95% CI 1.02–2.90, and SMR = 1.82; 95% CI 1.11–2.81, respectively). In this study the association between CA and some major cancer types was also evaluated, and the results indicated that respiratory tract and hematological cancers, but not digestive tract cancers, were associated with a higher CA frequency.

The launch of the ESCH (European Study Group on Cytogenetic Biomarkers and Health) collaborative project, which involved the Nordic countries and Italy, produced a joint data analysis and a further extension of the follow-up. The results obtained on cancer occurrence strengthened confidence in the previous results, while the survival analysis applied improved understanding of the CA/cancer relationship, showing highly different patterns of survival in the three CA frequency categories (Hagmar et al., 1998). In the discussion of this paper, insufficient control for confounding and the possible role of effect modifiers were considered to be among the major limitations of the study. The effect of smoking habit and occupational exposure to carcinogens was then assessed through a case-control study nested within the cohort. The results showed that CA frequency could predict cancer independently of exposure to major carcinogens, making the point that the predictivity of high rates of CA does not require such exposures (Bonassi et al., 2000). The authors concluded that individual characteristics as yet not identified are probably behind the CA/cancer risk association. Polymorphisms in metabolic, DNA repair, and genetic instability genes as well as nutritional factors were indicated as the most likely candidates.

The first non-European report showing association between CA and cancer risk was published in 1999 by a Taiwanese group (Liou et al., 1999). A case-control study nested in a small cohort of 686 residents in a Blackfoot endemic area showed that a frequency of chromosome-type CA over the median is highly predictive of cancer risk (Odds Ratio (OR) = 12.0; 95% CI 1.56–92.29). Unexpectedly, no association at all was found with chromatid-type CA.

A new independent cohort study was carried out in the Czech Republic, based on a large program of occupational safe-

**Table 1.** Overview of cohort studies evaluating chromosomal aberrations (CA) as cancer risk biomarker

Study	Subjects	Person-years	Follow-up period	Cancer cases (deaths)	SIR (95% CI) <sup>a</sup>	SMR (95% CI) <sup>b</sup>	HR (95% CI) <sup>c</sup>
Nordic Study Group on the Health Risk of Chromosome Damage, 1990a	1,787	7,547	1970–1985	26	0.90 (0.33–1.98) <sup>d</sup> 0.92 (0.34–2.04) <sup>e</sup> 1.80 (0.98–3.01) <sup>f</sup>		
Hagmar et al., 1994	1,979	17,666	1970–1988	66	0.90 (0.50–1.40) <sup>d</sup> 0.70 (0.30–1.20) <sup>e</sup> 2.10 (1.50–2.80) <sup>f</sup>		
Bonassi et al., 1995a	1,455	16,190	1969–1994	44		0.83 (0.36–1.63) <sup>d</sup> 1.79 (1.02–2.90) <sup>e</sup> 1.82 (1.11–2.81) <sup>f</sup>	
Hagmar et al., 1998	3,541	43,827	1970–1995	91 (64)	0.78 (0.50–1.18) <sup>d</sup> 0.81 (0.52–1.25) <sup>e</sup> 1.53 (1.13–2.05) <sup>f</sup>	0.83 (0.46–1.37) <sup>d</sup> 1.16 (0.71–1.80) <sup>e</sup> 2.01 (1.35–2.89) <sup>f</sup>	
Smerhovsky et al., 2001	3,973	37,775	1975–1999	144			1.6 (1.01–2.37) <sup>f</sup>

<sup>a</sup> SIR: Standardized Incidence Ratio; CI: Confidence Interval.  
<sup>b</sup> SMR: Standardized Mortality Ratio.  
<sup>c</sup> HR: Hazard Ratio.  
<sup>d</sup> Low frequency of CA.  
<sup>e</sup> Medium frequency of CA.  
<sup>f</sup> High frequency of CA.

ty surveillance ongoing since 1975. Various groups of workers with heterogeneous exposures had been investigated. An overall number of 3,973 subjects were followed up for cancer incidence and mortality up to 1999, accounting for a total of 37,775 person years (Smerhovsky et al., 2001). Adjusting for gender, age at test, and occupational exposure using a Cox regression model showed a Hazard Ratio (HR) of 1.6 (1.0–2.4) for those with “high” CA scores as compared with those with “low” scores. So far, the results were completely in agreement with the Nordic and Italian cohorts. However, when the analysis of the Czech cohort was stratified for exposure, the increased cancer risk for subjects with a “high” CA score was confined to only the radon-exposed workers. This was in contrast to the earlier studies where no significant effect modification of occupational exposure was observed. Analyzing sub-categories of CA showed a cancer predictive effect for chromatid breaks, but not for chromosome breaks or chromatid exchanges (Smerhovsky et al., 2002). A similar pattern was seen when the analysis was restricted to lung cancer. An update of the Czech study is in progress, and results concerning an extended cohort of more than 11,000 subjects will soon be available. An overview of cohort studies evaluating CA as cancer risk biomarker is reported in Table 1. As a side result of the extensive efforts carried out in many countries to put together study groups large enough for epidemiologic standards, a number of large databases were assembled. The analysis of these data has greatly improved our knowledge of the determinants and characteristics of most cytogenetic biomarkers (Nordic Study Group on the Health Risk of Chromosome Damage, 1990b; Bonassi et al., 1995b; Bolognesi et al., 1997), and methodological improvements in the use of pooling in biomarkers studies have been achieved (Taioli and Bonassi, 2002).

### Chromosomal aberrations and risk of cancer: the epidemiologic approach

The identification of an accurate mechanistic model – based on the consequences of exchange aberrations – is the most important piece of evidence linking the frequency of CA in healthy subjects to the risk of cancer. Other evidence commonly cited for this purpose are the high frequencies of CA in patients affected by cancer, the parallel increase of CA and risk of cancer in subjects affected by genetic diseases interfering with DNA repair, and the already mentioned association between clastogenic and carcinogenic properties.

All these observations give, despite their importance, only circumstantial evidence for a causal relationship and cannot provide any real data about the strength of the association in the general population, which would be required from a public health perspective. The availability of risk estimates based on the frequency of a biomarker in healthy individuals is then a formidable tool for any cancer prevention initiative, and this is the reason that justifies the keen interest of molecular epidemiologists in prospective cohort studies of human populations.

Many methodological papers and textbooks in the field of molecular epidemiology have been published in recent years, and all of them have recognized the validation of candidate biomarkers for long-term prediction of risk as a leading priority. Special concern is given to those biomarkers – as in the case of cytogenetic biomarkers – that are possibly affected by the presence of the disease, i.e., the so called *reverse causality*; in this case cohort studies are preferable for the biomarker validation.

Planning a cohort study of chronic diseases based on biomarker data is a very difficult task. Major problems are the small size of most biomonitoring studies, the differences in methods over years and among laboratories, and the high num-

ber of subjects without demographic data. Therefore, only very popular biomarkers used for many years can be considered for this purpose (although bio-banks of stored samples may provide a possible shortcut).

The considerations described above brought in the late 1980's the Nordic study group to implement the original approach of creating a pooled cohort, assembling cytogenetic biomarker data from a number of genetic toxicology laboratories (The Nordic Study Group on the Health Risk of Chromosome Damage, 1990a). The methodology applied in the first studies was very efficient, and has essentially been maintained since then, including the most recently published cohort studies on cytogenetic biomarkers (Hagmar et al., 1994, 1998; Bonassi et al., 1995a; Smerhovsky et al., 2001).

A number of assumptions were made when the first study was designed and they also applied to the subsequent studies. (1) Because the CA frequency was available only in a surrogate tissue, i.e. peripheral blood lymphocytes (PBL), it was assumed (as supported by literature data) that there was a correlation between CA frequencies in PBL and in target organs (Dave et al., 1995). (2) The type of CA generally measured in biomonitoring studies were unstable CA, whereas chromosome rearrangements important for carcinogenesis are stable. These biological events were assumed to be correlated. (3) Only one CA measurement per lifetime was available for most subjects. It was therefore necessary to assume that a single measurement is a valid parameter for classifying subjects.

Besides these major assumptions there were a few minor issues that in the absence of more detailed information were not considered to seriously affect the association between CA frequency and cancer risk. Among these were the effect of unknown exposures modifying the association studied and the misclassification error for categorizing CA frequency.

A final consideration in the study design was that all of these assumptions imply a *bias towards the null*, i.e. the true association was likely to be stronger than the estimated one.

There are two other aspects concerning the study design that should be mentioned, although they are not assumptions but unavoidable weaknesses. The small number of subjects available for the follow-up did not allow (a) reliable analyses of the associations between CA and specific cancer sites (e.g., hematological malignancies) and (b) a differential evaluation of cancer predictivity in various subclasses of structural CA.

Despite the limitations, the studies cited above provided results of great interest for their implications on both biological mechanisms and public health. The results have in two leading state-of-the-art papers been considered to be among the most important achievements of molecular epidemiology (Perera, 2000; Peto, 2001).

### **Cohort studies on CA and cancer in human population: open issues**

The results accumulated by the cohort studies described above have provided direct evidence of an association between the frequency of CA in healthy subjects and the subsequent risk of cancer. The quantitative estimate of this association largely

varies among studies; this should not be surprising, since both parameters evaluated, i.e. all cancers and overall structural aberrations, are rough indicators of much more specific processes. Further studies of larger size and better quality of cytogenetic data will provide more reliable information.

Some preliminary findings from the Italian cohort indicated that some specific cancer sites, i.e., hematological malignancies, might exhibit a stronger and more specific association with chromosomal damage (Bonassi et al., 1995a). Similar evidence was found for respiratory cancers, although in this case the biological background was not so easy to understand. A more thorough evaluation of whether there is variation in cancer predictivity of the CA biomarker for different types of tumors can be foreseen considering the over-time increasing statistical power in the Nordic, Italian and Czech cohorts.

As regards the sub-classes of CA, the low frequency of some specific types of aberrations did not allow an assessment of their relationship with cancer risk. A good compromise, designed in the framework of the European CancerRiskBiomarkers project and to be adopted in new updates of the Nordic and Italian cohorts, is to separately evaluate chromatid-type and chromosome-type aberrations as well as breaks and exchanges (and their combinations).

Another problem affecting the design of such studies is the uncertainty about the impact of confounding factors and especially the role of effect modifiers. Typical confounders such as sex, age, and calendar year were considered in all studies, and all estimates of relative risk have been adjusted, when necessary, for these factors. Much more complicated was controlling for occupational exposure to mutagens/carcinogens and life style factors. Since the cohorts were assembled from many different biomonitoring studies, the assessment of occupational exposures greatly varied from study to study, making that information unreliable. The heterogeneity among different studies was confirmed by a case-control study nested in the ESCH cohort, where an international panel of occupational hygienists reconstructed past exposures of cases and controls (Bonassi et al., 2000; Tinnerberg et al., 2003). This study emphasized that the risk of cancer due to a high frequency of CA was more attributable to individual predisposition than to exposure to mutagens/carcinogens. The increased risk of cancer associated with the high frequency of CA was the same among subjects with high levels of exposure to carcinogens as in subjects never exposed. These results were partially contradicted afterwards by findings from the Czech cohort, which showed a CA/cancer association only among the radon exposed workers. However, this group was the only sub-cohort within the Czech study to show a number of events comparable to those of the Nordic and Italian cohorts, i.e., 14% of cancer cases and 11.4% of cancer deaths, while the proportion of cancer cases in the other sub-cohorts ranged from 1.0 to 7.4%, and that of cancer deaths from 0.2 to 4.6%, respectively. The extension of the follow-up may change the pattern of risk estimates in different sub-cohorts.

Among the other candidate factors that could have confounded the association under study, diet and exposure to environmental pollution are the most relevant. Unfortunately, the historical nature of these cohort studies makes it difficult to

reconstruct past environmental exposures and diets. It is therefore more promising to get a further insight in the role of polymorphisms of genes involved in xenobiotic metabolism and DNA repair. A study aimed at measuring polymorphisms in old preserved cell samples from subjects in the Italian cohort is ongoing within the CancerRiskBiomarkers framework.

Finally, a major issue to be addressed is an approach that can minimize misclassification of subjects to CA categories. The choice of categorizing individuals as *Low*, *Medium*, and *High* for frequency of CA, based on the percentile distribution of observations, has worked very well in assessing the presence of an association with cancer risk, but more sophisticated approaches may perhaps further reduce the misclassification error. Also in this direction there are studies in progress, mostly based on a database of repeated measures extrapolated from the existing cohorts.

### **Biomarkers of cancer risk in human populations: from research to regulation**

The reliability of CA as a marker of genetic damage has been known since 50 years. Its ability to quantify exposure to genotoxic carcinogens has been known as well, especially in the field of radioprotection, where the frequency of CA is used as a biological dosimeter of ionizing radiation.

Despite the familiarity with the use of CA in occupational settings, little effort has been directed towards transforming the generally accepted assumption that CA frequency reflects exposure to mutagens/carcinogens, and that high CA levels are associated with an increased risk of cancer, into a regulatory tool for improving occupational safety.

An informal survey carried out with major institutions involved in cancer prevention in the occupational environment at the time of preparation of the manuscript revealed that practically nowhere in the world the use of CA in exposed workers has been regulated by law. The only positive reports came from the Czech republic, where CA analysis of peripheral lymphocytes is requested as part of preventive check-ups for selected subjects or groups occupationally exposed to genotoxic agents classified by the International Agency for Research On Cancer (IARC) to classes I (carcinogenic to humans) or 2A (probably carcinogenic to humans) (decree No. 258/2001, §82, article 2f of the Public Health Protection authority, formerly Hygiene Service).

Three main issues have hampered the use of CA for regulatory purposes. The first is the high intra-individual variability of the assay. The reliability of the test is excellent at group level, but individual data are considered too unpredictable to be used for *hard* safety measures such as pension, benefit, displacement, or structural changes in the workplace. The second is the lack of preventive tools for an efficient intervention in subjects at risk. The third, and for many years the most striking, has been the uncertainty about long-term risks in individuals with high frequency of CA.

The restraint to include markers of chromosomal damage in occupational safety laws seems to be mostly determined by the uncertainty of all statistics linked to individual data. Individual

CA estimates could be improved by more extensive analysis and repeated CA determinations (before and during/after occupational exposure). Most cytogenetic studies of human occupational chemical exposure still rely on scoring 100 cells per individual, when the use of metaphase finders would facilitate scoring more cells (as done in radiation dosimetry). From the occupational safety point of view, group level demonstration of a clastogenic effect should, however, be sufficient for actions. As the presence of increased levels of genotoxic damage in exposed populations has a major relevance to public health, new legal tools, more flexible and suitable for preventive purposes, should be developed.

Recent knowledge about the presence of polymorphisms in some major genes involved in crucial processes of carcinogenesis, and the evidence accumulated about gene–environment and gene–gene interactions has set the basis for understanding the reasons of individual differences in the reaction to mutagen exposures (Tuimala et al., 2002).

The problems in dealing with the identification of meaningful intervention strategies for subjects with unexplained high levels of CA are virtually unchanged, since suitable procedures of treatment or prevention are still not available. On the contrary, the strong evidence accumulated from cohort studies has contributed to change the current opinion about long-term risks in subjects with high rates of CA. Although the possible presence of misclassification (one measure of CA in the life may be inadequate to correctly classify an individual) reduces the reliability at an individual level, group data provide evidence supporting law-regulated interventions whenever a group of workers or subjects with hazardous exposures experiences an increased level of CA. Apart from the occupational setting, other examples have been published where CA can efficiently be used in surveying subjects potentially at risk of cancer. The use of CA was proposed in programs for cancer prevention in alcoholics (Maffei et al., 2002) and in cancer screening of small groups where the estimates of relative risks may be impossible, like astronauts during space missions (Durante et al., 2001).

### **Future perspectives**

In the evaluation of results produced by epidemiological studies on CA and cancer it must be taken into account that these data are based on studies performed decades ago, when the Giemsa staining technique and the optical microscope were the standard procedures of cytogenetic analysis.

The use of data from archives has allowed assembling enough person years to perform epidemiologic studies, but the classification of subjects in risk categories was essentially based on chromosomal breaks, the majority of them of the chromatid-type. The rationale has been that, due to similar mechanism of formation, such unstable CA can be used as a surrogate endpoint in a surrogate tissue (lymphocytes) for the more specific rare chromosomal rearrangements directly involved in carcinogenesis in the target tissue (Albertini et al., 2000; Norppa, 2003). Maybe the success of the unstable CA to predict cancer is due to its unspecificity, reflecting the same process that leads to the formation of the multitude of more specific alterations.

However, as the traditional CA analysis is able to reveal only a portion of the chromosomal alterations known to occur in the genome, it is an indirect and incomplete measure of events that are considered relevant for carcinogenesis. Therefore, the use of more specific and complementary endpoints might improve the reliability of risk estimates.

A number of techniques have been developed to give a more comprehensive measure of the whole pattern of chromosomal damage, the most consolidated among these are FISH techniques, chromosome painting and especially multicolor FISH (M-FISH) (Maierhofer et al., 2002). An interesting example of how the new techniques can be used for individual risk assessment comes from a paper published last year where past exposure to plutonium was reconstructed measuring intrachromosomal aberrations in nuclear weapons workers (Hande et al., 2003). This is an endpoint very hard to detect, but probably of great relevance for the carcinogenic process, and only recent chromosome band painting techniques have allowed its analysis. It is presently unclear whether this interesting yet currently laborious approach could be used for detecting the cytogenetic effects of other exposures besides densely ionizing radiation. For the time being, the chromatid-type CA remains the primary cytogenetic lesion induced by most chemical carcinogens.

FISH and polymerase chain reaction (PCR)-based methods exist for the detection of rare cells with certain chromosomal rearrangements typical of specific hematological cancers. Non-cancerous cells containing such rearrangements may be found at a low rate in apparently healthy individuals. Obviously, the rearrangement alone is not enough to induce neoplasia. The presence of such cells could indicate increased risk of (specific) cancer, although this has not been demonstrated.

A second potential perspective for the use of biomarkers to predict the (individual) risk of cancer in healthy subjects comes

from genomics and proteomics. The use of microarrays to identify the expression profile or the quantity of proteins produced by cancer genes could greatly improve the reliability of risk assessment, even at an individual level. This approach seems to be more promising in malignant neoplasms, mostly hematological, where the role of fusion genes has already been described (Rowley, 1998).

## Conclusions

The presence of association between a high level of CA in the PBL of healthy individuals and subsequent risk of cancer is supported by a number of theoretical and experimental findings. Nevertheless, limited knowledge about the role of individual susceptibility and uncertainty about the long-term effects of high rates of CA have made our knowledge about CA practically useless for preventive purposes. Only recently the discussion on the possible applications of CA as a biomarker of cancer risk in healthy individuals has started.

Despite individual factors seeming to play a major role in defining the individual risk of cancer the only validated intervention able to revert chromosomal damage is removing any suspected exposure to chromosome damaging factors. Therefore, from the public health point of view the frequency of CA – often described as the only example of valid marker of cancer risk – should be evaluated in all situations where a group of subjects is potentially exposed to mutagens/carcinogenic agents. In case of an increased level of CA this must be considered as a group at risk of cancer, and prevention measures have to be applied – possibly as a part of a formal policy of occupational safety.

## References

- Albertini RJ, Anderson D, Douglas GR, Hagmar L, Hemminki K, Merlo F, Natarajan AT, Norppa H, Shuker DE, Tice R, Waters MD, Aitio A: IPCS guidelines for the monitoring of genotoxic effects of carcinogens in humans. *Mutat Res* 463:111–172 (2000).
- Bolognesi C, Abbondandolo A, Barale R, Casalone R, Dalpra L, De Ferrari M, Degrassi F, Forni A, Lamberti L, Lando C, Migliore L, Padovani P, Pasquini R, Puntoni R, Sbrana I, Stella M, Bonassi S: Age-related increase of chromosome aberrations, sister-chromatid exchanges and micronuclei in human lymphocytes. *Cancer Epidemiol Biomarkers Prev* 6:249–256 (1997).
- Bonassi S: Combining environmental exposure and genetic effect measurements in health outcome assessment. *Mutat Res* 428:177–185 (1999).
- Bonassi S, Abbondandolo A, Camurri L, Dal Pra L, De Ferrari M, Degrassi F, Forni A, Lamberti L, Lando C, Padovani P, Sbrana I, Vecchio D, Puntoni R: Are chromosome aberrations in circulating lymphocytes predictive of a future cancer onset in humans? Preliminary results of an Italian cohort study. *Cancer Genet Cytogenet* 79:133–135 (1995a).
- Bonassi S, Bolognesi C, Abbondandolo A, Barale R, Bigatti P, Camurri L, Dalpra L, De Ferrari M, Forni A, Lando C, Padovani P, Pasquini R, Stella M, Puntoni R: Influence of sex on cytogenetic endpoints: Evidence from a large human sample and review of the literature. *Cancer Epidemiol Biomarkers Prev* 4:671–679 (1995b).
- Bonassi S, Hagmar L, Strömberg U, Huici Montagud A, Tinnerberg H, Forni A, Heikkilä P, Wanders S, Wilhardt P, Hansteen I-L, Knudsen LE, Norppa H, for the European Study Group on Cytogenetic Biomarkers and Health (ESCH): Chromosomal aberrations in lymphocytes predict human cancer independently of exposure to carcinogens. *Cancer Res* 60:1619–1625 (2000).
- Boveri T: Zur Frage der Entstehung maligner Tumoren (Gustav Fisher, Jena 1914).
- Dave BJ, Hopwood VL, Spitz MR, Pathak S: Shared cytogenetic abnormalities in lung tumours and corresponding peripheral blood lymphocytes. *Int J Oncol* 7:1297–1305 (1995).
- Durante M, Bonassi S, George K, Cucinotta FA: Risk estimation based on chromosomal aberrations induced by radiation. *Radiat Res* 156:662–667 (2001).
- Hagmar L, Brøgger A, Hansteen I-L, Heim S, Högsted B, Knudsen L, Lambert B, Linnainmaa K, Mittelman F, Nordenson I, Reuterwall C, Salomaa S, Skerfving S, Sorsa M: Cancer risk in humans predicted by increased levels of chromosomal aberrations in lymphocytes: Nordic study group on the health risk of chromosomal damage. *Cancer Res* 54:2919–2922 (1994).
- Hagmar L, Bonassi S, Strömberg U, Brøgger A, Knudsen L, Norppa H, Reuterwall C: Chromosomal aberrations in lymphocytes predict human cancer – A report from the European Study Group on Cytogenetic Biomarkers and Health (ESCH). *Cancer Res* 58:4117–4121 (1998).
- Hande MP, Azizova TV, Gerad CR, Burak LE, Mitchell CR, Khokhryakov VF, Vasilenko EK, Brenner DJ: Past exposure to densely ionizing radiation leaves a unique permanent signature in the genome. *Am J Hum Genet* 72:1162–1170 (2003).
- Liou S-H, Lung J-C, Chen Y-H, Yang T, Hsieh L-L, Chen C-J, Wu T-N: Increased chromosome-type chromosome aberration frequencies as biomarkers of cancer risk in a blackfoot endemic area. *Cancer Res* 59:1481–1484 (1999).
- Maffei F, Cantelli Forti G, Castelli E, Stefanini GF, Mattioli S, Hrelia P: Biomarkers to assess the genetic damage induced by alcohol abuse in human lymphocytes. *Mutat Res* 514:49–58 (2002).

- Maierhofer C, Jentsch I, Lederer G, Fauth C, Speicher MR: Multicolor FISH in two and three dimensions for clastogenic analyses. *Mutagenesis* 17:523–527 (2002).
- Nordic Study Group on the Health Risk of Chromosome Damage: An inter-Nordic prospective study on cytogenetic endpoints and cancer risk. *Cancer Genet Cytogenet* 45:85–92 (1990a).
- Nordic Study Group on the Health Risk of Chromosome Damage: A Nordic data base on somatic chromosome damage in humans. *Mutat Res* 241:325–337 (1990b).
- Norppa H: Cytogenetic biomarkers, in Boffeta P, Rice JM, Bird M, Buffler P (eds): *Mechanistic Considerations in the Molecular Epidemiology of Cancer* (IARC Sci Publ 157, Lyon 2004, in press).
- Nowell P, Hungerford D: A minute chromosome in human granulocytic leukemia. *Science* 132:1497 (1960).
- Perera FP: Molecular epidemiology: On the path to prevention? *J natl Cancer Inst* 92:601–612 (2000).
- Peto J: Cancer epidemiology in the last century and the next decade. *Nature* 411:390–395 (2001).
- Pfeiffer P, Goedecke W, Obe G: Mechanisms of DNA double-strand break repair and their potential to induce chromosomal aberrations. *Mutagenesis* 15:289–302 (2000).
- Richardson C, Jasin M: Frequent chromosomal translocations induced by DNA double-strand breaks. *Nature* 405:697 (2000).
- Rowley JD: The critical role of chromosome translocations in human leukemias. *A Rev Genet* 32:495–519 (1998).
- Smerhovsky Z, Landa K, Rössner P, Brabec M, Zudova Z, Hola N, Pokorna Z, Mareckova, Hurychova D: Risk of cancer in an occupationally exposed cohort with increased level of chromosomal aberrations. *Environ Health Perspect* 109:41–45 (2001).
- Smerhovsky Z, Landa K, Rössner P, Juzova D, Brabec M, Zudova Z, Hola N, Zarska H, Nevsimalova E: Increased risk of cancer in radon-exposed miners with elevated frequency of chromosomal aberrations. *Mutat Res* 514:165–176 (2002).
- Taioli E, Bonassi S: Methodological issues in pooled analysis of biomarker studies. *Mutat Res* 512:85–92 (2002).
- Tinnerberg H, Heikkilä P, Huici-Montagud A, Bernal F, Forni A, Wanders S, Welinder H, Wilhardt P, Strömberg U, Norppa H, Knudsen L, Bonassi S, Hagmar L: Retrospective exposure assessment and quality control in an international multicentre case control study. *Ann Occup Hyg* 47:37–47 (2003).
- Tuimala J, Szekely G, Gundy S, Hirvonen A, Norppa H: Genetic polymorphisms of DNA repair and xenobiotic-metabolizing enzymes: role in mutagen sensitivity. *Carcinogenesis* 6:1003–1008 (2002).
- Vilenchik MM, Knudson AG: Endogenous DNA double-strand breaks: Production, fidelity of repair, and induction of cancer. *Proc natl Acad Sci, USA* 100:12871–12876 (2003).

# New developments in automated cytogenetic imaging: unattended scoring of dicentric chromosomes, micronuclei, single cell gel electrophoresis, and fluorescence signals

C. Schunck<sup>a</sup>, T. Johannes<sup>a</sup>, D. Varga<sup>b</sup>, T. Lörch<sup>a</sup> and A. Plesch<sup>a</sup>

<sup>a</sup>MetaSystems GmbH, Altlußheim; <sup>b</sup>University of Ulm, Ulm (Germany)

**Abstract.** The quantification of DNA damage, both in vivo and in vitro, can be very time consuming, since large amounts of samples need to be scored. Additional uncertainties may arise due to the lack of documentation or by scoring biases. Image analysis automation is a possible strategy to cope with these difficulties and to generate a new quality of reproducibility. In this communication we collected some recent results obtained with the automated scanning platform Metafer, cov-

ering applications that are being used in radiation research, biological dosimetry, DNA repair research and environmental mutagenesis studies. We can show that the automated scoring for dicentric chromosomes, for micronuclei, and for Comet assay cells produce reliable and reproducible results, which prove the usability of automated scanning in the above mentioned research fields.

Copyright © 2003 S. Karger AG, Basel

Tests for the estimation of DNA damage, both in vivo and in vitro, can be very time consuming, since due to large inter-individual or inter-experimental variations high numbers of cells and/or donors have to be evaluated to gain statistical coverage. Image analysis automation is a possible strategy to cope with this difficulty and additionally generates a new quality of reproducibility. Already the first automated image analysis systems aimed at the field of biological dosimetry and population monitoring (Weber et al., 1992; Blakely et al., 1995; Böcker et al., 1995; Huber et al., 1995) were used in the 1990's. Today, years of continuous development have passed, and also many new applications and techniques have arisen. Recent studies have been involving techniques like fluorescence in situ hybridization (FISH) in metaphases or interphases (Huber et al., 2001; Plesch and Lörch, 2001), micronucleus detection (Fenech and Morley, 1985; Fenech, 1998; Fenech et al., 1999;

Rothfuss et al., 2000), the single cell gel electrophoresis (Comet) assay (Böcker et al., 1999; Hartmann et al., 2003), the combination of the Comet assay with FISH signal analysis (McKenna et al., 2003), and the detection of fluorescence-labeled protein foci to assess repair processes inside the cell (Rothkamm and Löbrich, 2003). Slide scanning systems also made their way into the clinical environment, where they are routinely used as diagnostic tool for pre- and postnatal diagnoses, cancer diagnosis and therapy monitoring.

In this publication we collected some recent results obtained with the help of the slide scanning system Metafer, covering applications which are being used in radiation research, biological dosimetry, DNA repair research and environmental mutagenesis studies. Since Metafer uses modular software on one hardware platform, various endpoints can be analyzed with the same system. Nevertheless, the principles of automated slide scanning follow basic considerations which are common to all applications.

## *Slide scanning principle*

Automated slide scanning is generally performed by moving the slide with reference to the fixed objective lens of the microscope in a regular meander-like pattern, leaving no gaps

Received 11 September 2003; revision accepted 3 December 2003.

Request reprints from C. Schunck, MetaSystems GmbH  
Robert-Bosch-Str. 6, D-68805 Altlußheim (Germany)  
telephone: +49 6205 39610; fax: +49 6205 32270  
e-mail: cschunck@metasystems.de



between the image fields. Because of speed considerations, image acquisition is done at the lowest possible optical magnification that still allows resolving the features of interest. Each field of view is captured and analyzed for the presence of analyzable objects (i.e., cells or nuclei). If objects of interest are detected within a field, they are further analyzed and stored in an image gallery along with their position and feature measurement data. After the scan the image gallery can be used to review the detected cells, to reject unsuitable cells, and to do corrections if necessary. Since the position data of all objects were stored during the scan, any cell can automatically be relocated under the microscope for direct visual inspection.

### Movement

It is necessary to control all the three axes in space for the scanning of a complete slide or a part of it. Usually a motorized stage is controlling the X- and Y-axis, while various solutions deal with the control of the Z-axis. The most suitable and fastest way to move the specimen in Z-direction is to take advantage of the features provided by modern motorized microscopes. Typically these microscopes have internal software controlling all motorized components, which can be driven either by the microscope controls or by external devices which are connected to the microscopes.

### Focusing

Precision and speed of the auto-focus are of utmost importance for the quality of the object detection and the slide scanning result. With the focusing strategy used by the Metafer system very high speed without sacrificing accuracy is provided. The plane of best focus is determined at a number of grid positions that are regularly distributed across the scan area. This is done by automatically moving the stage into the Z-direction, capturing images in different focus planes, and analyzing the focus quality based on a local contrast criterion. Typically eleven Z-positions are being analyzed within approximately two seconds. During the subsequent scan, the slide is automatically kept within the plane of best focus.

### Image acquisition

In fluorescence imaging signal intensity varies significantly between counterstain and fluorescent labels and even between different positions on the same slide. Automatic exposure control is a must to assure correct image quality and high dynamic range. The software estimates the correct exposure time based on the histogram (the intensity distribution) of an image captured without integration. Depending on the histogram shape a reduced exposure time (using the built-in electronic shutter) or long-time integration is used. This strategy allows exposure times from 1/10,000 s to approximately 30 s. In case of transmitted light imaging the light source of the microscope can be directly controlled by the software to assure optimal image acquisition conditions.

## Materials and methods

### Hardware architecture

The automated slide scanning system Metafer is a multi-purpose scanning platform for the software modules described below. Fig. 1a shows a typical Metafer system for high throughput analyses including the 80-position slide feeder.

**Central unit:** The central unit of any Metafer system is a microcomputer (DELL, Langen, Germany), typically equipped with an Intel® Pentium® 4 Processor (> 2 GHz), 256 MB RAM memory, and an 80-GB hard drive and the operating system Microsoft® Windows® XP Professional. For data archiving purposes the Metafer system is equipped with a magneto-optical disk drive (2.3 GB capacity).

**Image acquisition hardware:** For image acquisition a high-resolution monochrome megapixel charge coupled device (CCD) camera (M1; JAI AS, Glostrup/Copenhagen, Denmark) with a resolution of 1280 × 1024 pixels (2/3" CCD; Pixel size 6.7 μm × 6.7 μm; signal-to-noise ratio 56 dB) is used. It is connected to a gray level digitizer board installed in the central unit, which provides real-time digitization of video signals at a resolution of 1280 × 1024 pixels with 256 gray levels. The system can also be equipped with the peltier-cooled grayscale digital CCD camera Axiocam MRm (Carl Zeiss, Göttingen, Germany), which provides a resolution of 1300 × 1030 pixels with a pixel size of 6.7 μm × 6.7 μm.

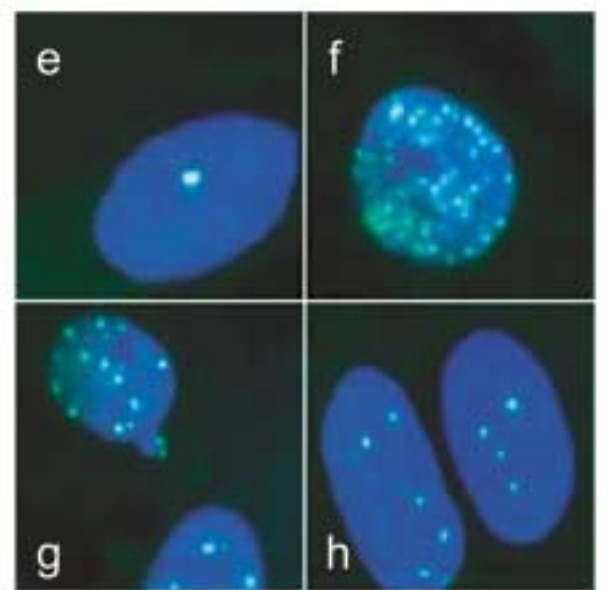
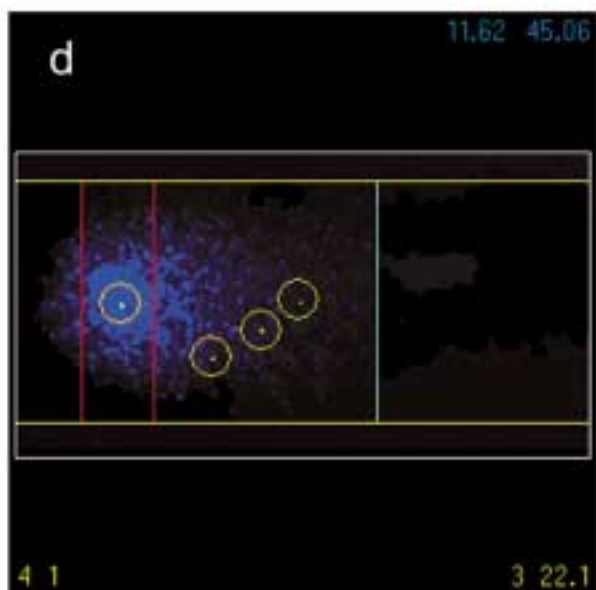
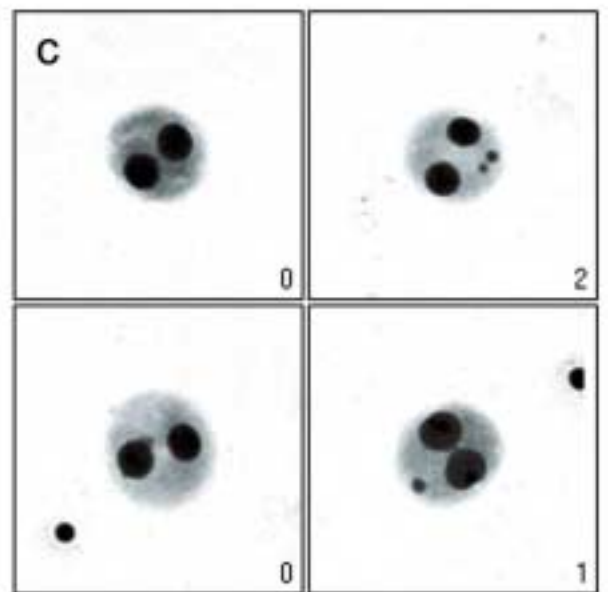
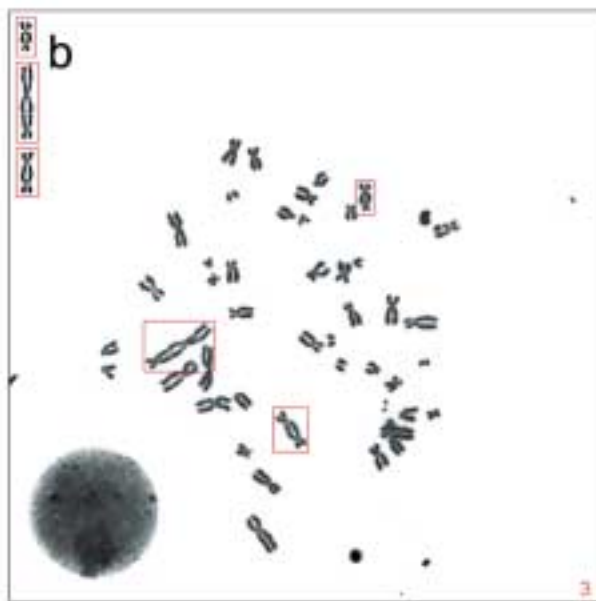
The camera is connected to the microscope via a standard 1.0× TV adapter (C-mount 60 C, 2/3"; Carl Zeiss, Göttingen, Germany).

**Microscope:** Metafer is connected to the motorized microscope Axioplan 2 Imaging E MOT (Carl Zeiss, Göttingen, Germany) and takes full advantage of the microscope components for automated focusing, light source adjustment (for bright-field imaging) and fluorescence filter change. Optionally the microscope may be equipped with an excitation filter wheel (Carl Zeiss/MetaSystems) to decrease the changing time between the color channels, with a motorized fluorescence shutter, and with a motorized objective revolver (the latter is required if Metafer is combined with the external 80-position slide feeder).

**Scanning stage:** 8 slides (3" × 1") per scanning run can be loaded into the motorized scanning stage (Märzhäuser, Wetzlar, Germany) with a range of 225 × 76 mm. The stage is connected to a 2-axis stepping motor controller board inside the central unit (PCSMOC3), providing a step size of 1 μm and a maximum step frequency of 72,000 Hz. For manual movement of the stage a trackball is connected to the system (Microspeed, El Cajon, USA).

Optionally the 8-slide capacity can be extended to 80 slides per scanning session with the external slide feeder, which loads up to ten 8-slide frames to the scanning stage automatically and unattended.

**Fig. 1. (a)** The automated scanning system Metafer (PC not shown) with 80-position slide feeder (left). **(b)** Human lymphocyte metaphase with 3 dicentric chromosomes (DIC), detected by Metafer DCScore. DIC are automatically marked by a rectangle and displayed in the upper left corner of the image. The number of detected DIC per metaphase is displayed in the lower right of the image. **(c)** Gallery of bi-nucleated cells created by Metafer MicroNuclei. The number of detected micronuclei is shown in the lower right corner of the gallery images. **(d)** Gallery image of a Comet FISH cell detected by Metafer CometScan. Parameters of head and tail and of the FISH signals are displayed in the corners of the image: upper right: Olive tail moment (left) and % DNA in tail; lower left: total FISH spot number (left) and number of spots in head; lower right: number of FISH spots in tail (left) and horizontal distance in pixels between closest spot in tail and the center of the head. **(e-f)** Quantification of DNA repair after treatment of primary human fibroblasts with very low doses of ionizing radiation. DNA double strand breaks (DSB) were visualized with γ-H2AX immunofluorescence microscopy, revealing foci on the sites of DNA breakage. While untreated cells show a background level of DSB **(e)**, numbers of foci increase directly after treatment **(f)**, and decrease with time, leaving unrepaired DSB, which are still visible as foci **(g, h)**. Images were captured with MetaSystems Isis FISH imaging system.



#### *Detection of dicentric chromosomes (DIC)*

**Cell treatment and slide preparation:** Venous blood from one healthy donor was irradiated with 0.5, 1, 2 and 3 Gy of X-rays (130 kV/130 mA) at a dose-rate of 1.2 Gy/min. Immediately after irradiation the cells were cultivated (0.5 ml blood, 4 ml McCoy's 5A medium (C.C. Pro), 0.5 ml fetal bovine serum (Gibco), 0.12 ml phytohemagglutinine (Gibco) and antibiotics). Culture time was 48 h including 2 h of exposure to Colcemid (Ciba). Metaphase preparations were made following routine protocols and stained with Giemsa.

**Metaphase finding, high-magnification capturing and automated analysis for DIC:** The analysis of metaphases for the existence of DIC with Metafer involves three subsequent steps, namely a) the automated detection of metaphases with the software module MSearch, b) the automated image acquisition of the metaphases at a higher magnification for DIC analysis (63× or 100×) with the AutoCapt module, and c) the detection of DIC in the captured images with the software module DCscore.

The slides were initially scanned for the presence of metaphases at a microscope magnification of 10× using a Fluor objective. Software setup was performed by selecting a metaphase classifier file for detecting lymphocyte metaphases in transmitted light. After the scan, gallery images of the detected metaphases were revised on screen and unsuitable objects (e.g. false-positives or very compact metaphases) were deleted.

The remaining metaphases were recaptured at a magnification of 63× in the AutoCapt operating mode of Metafer. Metaphases were automatically centered prior to image acquisition. Each metaphase was fine focused, a high resolution image was captured and automatically stored for subsequent analysis.

Automatic detection of dicentric chromosomes was performed using the high-resolution metaphase images created by AutoCapt. Metaphases matching the classification criteria (e.g. number and size of chromosomes) were automatically analyzed for the presence of DIC and labeled as "Evaluated". All other metaphases were rejected, but kept in the dataset. Subsequently after the processing, AutoCapt displays the images for any metaphase which was selected in the image gallery, and DIC are marked with a red rectangle inside the images (Fig. 1b). The number of dicentric chromosomes per metaphase was automatically stored and could be used for generating the evaluation report.

#### *Detection of bi-nucleated cells and counting of micronuclei*

**Cell treatment and slide preparation:** Human venous blood of four healthy donors was irradiated with 0, 1, 2 and 4 Gy of X-rays at a dose-rate of 4 Gy/min. Immediately after irradiation the cells were cultivated (0.3 ml blood, 3 ml Medium 1A (Gibco), 0.06 ml phytohemagglutinine (Gibco) and antibiotics). After 44 h culture time 9 µl Cytochalasin B (1 mg/500 µl DMSO; Sigma) was added and the sample was incubated for another 24 h. Slide preparations were made following routine protocols and stained with DAPI or Giemsa.

**Detection of bi-nucleated cells and counting of micronuclei:** The system for automated micronuclei (MN) detection, Metafer MicroNuclei, automatically identifies bi-nucleated cells that are stained with a single nuclear/cytoplasmic stain (transmitted light or fluorescence).

Scanning for MN was performed using a 10× microscope objective. After automatic image acquisition the object threshold, which is used to separate any object from the background, was set automatically by the system. The threshold algorithm takes into account the presence of discontinuities in the image background. Objects being above this threshold were analyzed for the presence of certain morphometric criteria: a) size (within a size range specified in the classifier setup), b) aspect ratio (the ratio calculated from the longest and the shortest diameter of the object), and c) the sum of concavity areas. With c) single nuclei (with round contour and only small concavity areas) and nucleus clusters (which usually have large concavities) were discriminated. Subsequently the distribution of nuclei inside the image was determined. As the nuclei of a bi-nucleated cell are considered to have approximately the same size, a maximum relative size difference of the two nuclei, as specified in the classifier, was used by the system to reject nuclei of different cells that are close together. Finally the object area of all other objects within a specified region of interest (the central point of the line connecting the centers of the two nuclei is used as center of the region of interest circle) was measured and the cell was rejected if it exceeded a maximum level specified in the classifier. This algorithm was used to reject cells which were situated very closely to other objects.

In a second step the system analyzed the region of interest for the presence of MN. Like nuclei MN were tested for their morphological features, which are principally the same as described above. A micronucleus was counted if it met these criteria and additionally was located within a certain distance from the center of the region of interest. For each bi-nucleated cell a gallery image was generated which indicates the number of micronuclei (Fig. 1c).

#### *Analysis of single cell gel electrophoresis (Comet Assay)*

**Cell treatment and slide preparation:** Human venous blood of two donors was irradiated with 0, 1, 2 and 4 Gy using <sup>60</sup>Co γ-rays. Conventional microscopic slides were prepared with 2 layers of agarose gel, with a bottom layer consisting of 1.0–1.5 % agarose and a second cell-containing layer, generally prepared from low melting point (LMP) agarose at 0.5–1.0 %. After the agarose gel had solidified, the slides were placed in a lysis solution consisting of high salts and detergents for at least 1 h. The recommended lysing solution consists of 100 mM EDTA, 2.5 M sodium chloride and 10 mM Trizma base, adjusted to pH 10.0, with 1 % Triton X-100 added just prior to use.

Prior to electrophoresis, slides were incubated in alkaline electrophoresis buffer (1 mM EDTA and 300 mM sodium hydroxide, pH > 13) for 20 min to produce single-stranded DNA and to express alkali-labile sites as single-strand breaks. The single-stranded DNA in the gels was electrophoresed under alkaline (pH > 13) conditions to produce comets. The voltage used ranged from 0.7 to 1.0 V/cm, with an accompanying amperage of ~ 300 mA (maintaining a constant temperature during electrophoresis of about 5 °C to minimize slide-to-slide variations). After electrophoresis, the gel was neutralized with a suitable buffer (e.g. Trizma base at pH 7.5) and stained with SYBR Green I (using antifade to prevent signal quenching).

**Detection of Comets:** Under lysis conditions during the electrophoresis DNA fragments migrate faster in the electric field than intact DNA. By staining the DNA with an appropriate fluorochrome these fragments are visible as comet tail in the microscope. The level of DNA damage can be derived from the ratio of tail and head (nucleus) intensities and sizes.

The CometScan module of the Metafer scanning platform allows the completely unattended analysis of Comet assay preparations. The scan is performed under fluorescent conditions using the 20× objective.

Cells being initially detected by the system were subsequently rejected if the following criteria were met: a) another object was present in the close neighborhood, that might interfere with the measurements, b) the background around the candidate comet showed significant inhomogeneities, and c) the tail intensity of the comet did not decrease to the background level inside the measurement frame, indicating that the comet is larger than the region of interest.

Once a comet was finally accepted by the system, its intensity profile was automatically analyzed and head and tail of the comet were determined based on the intensity levels. The background level was subtracted from the intensity values obtained. Different comet features (e.g. intensity of head and tail, comet shape, tail moment, Olive tail moment and more) were measured and an image of each cell was stored in a gallery. Overlays within these cell images show thresholds, borderlines between head and tail, and the head and tail regions as they were defined by the analysis algorithms. Depending on the classifier setup, selected cell features (e.g. tail moment and percentage of DNA in the tail) were displayed in the gallery image.

**Comet FISH:** In addition to the detection of comets and the measurement of standard comet features (as described above), CometScan provides the option for automated analysis of fluorescence in situ hybridization signals within up to five color channels (Comet FISH; Fig. 1d). The location of the signals within the comet (i.e. no. of spots in the head, no. of spots in the tail, distance of the tail spots from the head center) can be automatically evaluated. The automated Comet FISH analysis is taking advantage of the imaging algorithms of Metafer MetaCyte described elsewhere in detail (Plesch and Lörch, 2001).

## **Results and discussion**

To demonstrate the usefulness of automated slide scanning for radiation research, biological dosimetry, DNA repair assays and environmental mutagenicity studies, we present the results

**Table 1.** Numbers of dicentric chromosomes (DIC) detected in human peripheral lymphocytes after irradiation with various doses of X-rays. Cells were automatically scored using the Metafer DCSScore module.

Dose (Gy)	Total No. of cells	Automatic detection <sup>a</sup>			Manually rejected cells <sup>b</sup>	Automatic detection with manual rejection <sup>c</sup>			Manual analysis <sup>d</sup> DIC per 100 cells
		Reject. cells	Eval. cells	DIC per 100 cells		Reject. cells	Eval. cells	DIC per 100 cells	
0.5	125	45	80	10	6	51	74	11	4
1	300	133	167	19	49	182	118	21	14
2	112	28	84	26	16	44	68	29	32
3	300	12	288	49	34	46	254	51	50

<sup>a</sup> After the first automatic detection the objects were revised on screen.

<sup>b</sup> Unsuitable metaphases were manually rejected.

<sup>c</sup> A second automatic detection was performed with the remaining cells.

<sup>d</sup> To confirm the automatically obtained data, the same metaphases were analyzed manually.

of various analyses performed with the Metafer slide scanning platform (Fig. 1a). We focused on endpoints which are commonly used in studies of this kind, such as chromosomal aberrations, micronuclei and single cell gel electrophoresis (Comet assay).

Dicentric chromosomes (DIC) are generally accepted as suitable endpoint for the estimation of DNA damage after irradiation of cells. They therefore are commonly used in studies involving biological dosimetry (Voisin et al., 2002).

Table 1 shows automatic DIC scoring results from human peripheral lymphocyte metaphases which were irradiated with various doses of X-rays. For all doses at least 100 cells were scored. The first part of the table gives the results of the initial automated scanning with Metafer DCSScore, showing the numbers of rejected and evaluated cells, and the frequency of DIC calculated for 100 cells (Table 1). The DIC frequency increases with dose in a near-linear manner.

In a second step the image gallery feature of Metafer was used to revise cells which were not suitable for precise DIC scoring, e.g. due to bad spreading or weak staining. The numbers of cells rejected during this step are given in the next column of the table (Table 1). After the manual rejection the remaining cells were analyzed again with the DCSScore module, and the results were calculated to DIC per 100 cells (Table 1). For comparison we also performed a manual DIC scoring with those metaphases that remained after the two rejection steps (Table 1). The results are very similar to the automatically obtained data. However, at doses below 2 Gy the DIC frequency after manual scoring is lower than the automatically obtained data. Though some of these "missing" DIC may be explained with the scoring bias of manual analysis, also the possibility of false-positive DIC analyzed by the system should be taken into consideration. Especially in metaphases with bad chromosome spreading attaching or overlapping chromosomes may be detected as DIC, which possibly would have been identified as two distinct chromosomes by the human researcher.

It is well known that chromosomal aberrations induced by low LET irradiation like X-rays follow a quadratic relationship with dose, including a linear part especially at lower doses. Nevertheless, our results do not reflect the quadratic term. At higher doses complex aberration types (e.g. polycentric chromosomes with more than two centromeres) are found, which

are not distinguished from DIC by the automated system. We followed this criterion also in the manual observation to gain maximum comparability. However, if a calibration with *in vitro* experiments is performed prior to the study, the results produced by the system are reasonable enough to document the usefulness of automated slide scanning for biological dosimetry.

Micronuclei (MN) result from small chromosome fragments that are not incorporated into the nuclei during cell division. They are enveloped by the nuclear membrane and appear as small nuclei outside the main cellular core. MN are mainly induced by aberrant chromosome fragments, which typically arise during exposure to various DNA damaging agents. Therefore they are widely accepted as an endpoint for fast DNA damage estimation (Fenech and Morley, 1985). Today, the *in vitro* MN assay is widely used for the analysis of various cell and DNA damages (Fenech et al., 1999), or for the estimation of genetic predisposition in cancer patients (Rothfuss et al., 2000).

Figure 2 shows the results of an MN experiment performed with irradiated venous human blood from 4 donors. The data was obtained with the Metafer MN analysis software MicroNuclei. Since the system automatically selects bi-nucleated cells, MN are only measured in cells which went through a cell division after the treatment. The MN rate is clearly increasing with dose, revealing a linear-quadratic dose-effect relationship (see figure legend for details).

Although the MN assay superficially leads to fast results, studies have to cope with variations resulting from factors which may heavily vary between donors and experiments (Fenech, 1998). Therefore large cell populations should be involved in any MN study to generate statistically relevant data. However, manual scoring for MN in large cell populations is time consuming and may result in significant scoring biases, probably leading to a lack of reproducibility.

Our results show that the automated scoring of MN in irradiated cells with Metafer leads to useful results. Full documentation of each single bi-nucleated cell in the image gallery after the scan allows the interactive confirmation of the scanning data in a fraction of the time a manual analysis of the same cell number would require.

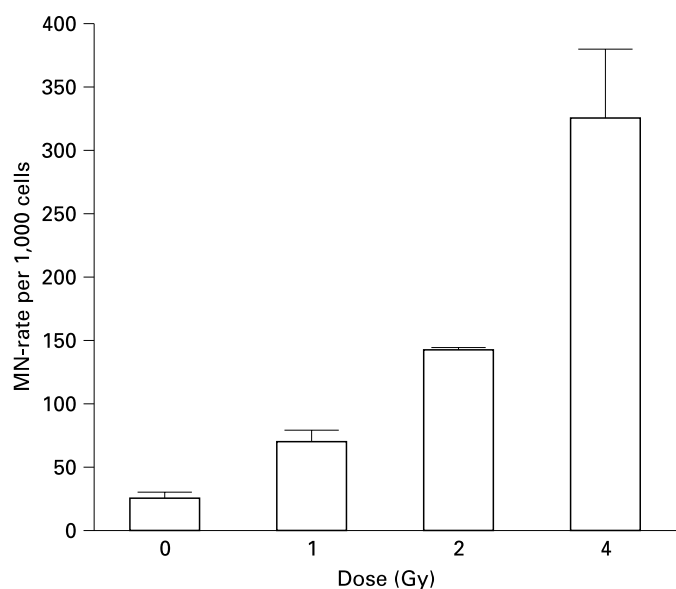


**Fig. 2.** Micronucleus rate per 1,000 cells after irradiation of human lymphocytes with various doses of X-rays. Micronuclei were automatically detected by Metafer MicroNuclei. Pooled data of four donors and standard errors are given (regression:  $y = 8.858x^2 + 40.617x + 22.416$ ;  $r^2 = 0.99$ ).

The single cell gel electrophoresis (Comet) assay is used to investigate DNA damage on the single cell level, based on the principle of the migration of DNA in an agarose gel under electrophoretic conditions (Hartmann et al., 2003). Under the microscope the cell appears like a comet, with the nuclear region revealing the head, and the tail formed by DNA fragments migrating to the anode of the electric field. The ratio between head and tail DNA is calculated and used as a measure for DNA damage inside the cell (see above for details). It is recommended to use image analysis systems for the evaluation of Comet assay results, since it is not possible to precisely determine signal intensities of head and tail by eye. Image analysis systems for Comet assay analysis follow two different approaches: a) interactive systems which require user interaction for capturing images and selecting the cells prior to measurement (like the CometImager system of MetaSystems), and b) systems that are scanning the slides automatically and unattended.

In this communication we present data obtained with Metafer CometScan by analyzing human blood cells which have been irradiated with various doses of  $^{60}\text{Co}$   $\gamma$ -rays (Fig. 3). Olive tail moment values for two independent experiments are given in the figure. The Olive tail moment reflects the ratio of head and tail DNA and is calculated automatically by the system with the following formula:  $[\% \text{ DNA in the tail}] \times ([\text{tail center of gravity}] - [\text{head center of gravity}])$ . Means of both experiments were used to calculate a regression line. The tail moments follow a linear-quadratic dose-effect relationship.

To demonstrate the possibilities for automated scanning of Comet assay preparations in combination with fluorescent sig-

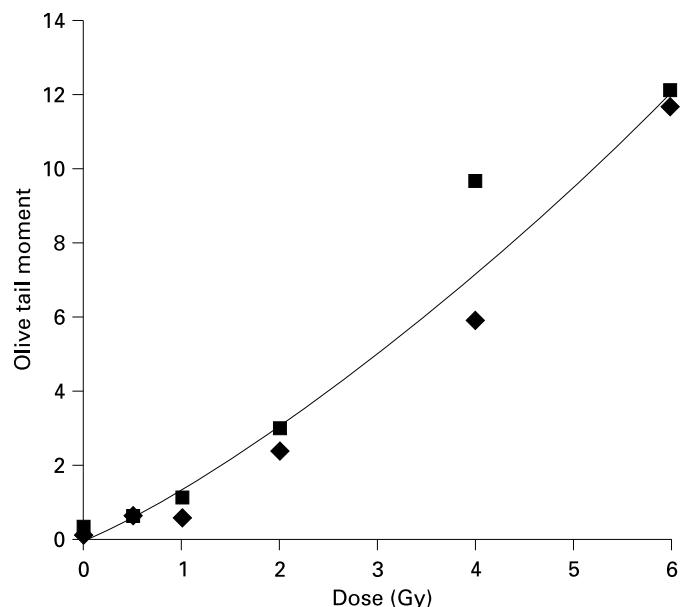


**Fig. 3.** Results of human venous blood irradiated with various doses of  $^{60}\text{Co}$   $\gamma$ -rays and automatically analyzed following the single cell gel electrophoresis (Comet) assay modified from Singh et al. (1988). The analysis was done using the Metafer CometScan slide scanning system. Data from two independent experiments are shown and a regression line was calculated from both experiments ( $y = 0.1137x^2 + 1.3624x - 0.1369$ ;  $r^2 = 0.99$ ).

nal analysis (Comet FISH), Fig. 1d shows a gallery image of a Comet FISH cell together with the parameters which were obtained by the system. Comet FISH can be used as an extension of the standard Comet assay by applying fluorescence-labeled DNA probes that are hybridized to specific gene sequences. The signals can be localized within the comet, and the localization is correlated with the conventional Comet assay data. Results from those experiments bear the potential to analyze whether a certain DNA sequence lies within, or close to, a damaged site (McKenna et al., 2003). The automated analysis of FISH spots inside cells which underwent the Comet assay is possible by combining the capabilities of the Metafer MetaCyte FISH spot analysis system with the CometScan software module. In this configuration, parameters like the Olive tail moment, the number of FISH signals in head and tail of the comet, and the migration distance for the spots can be measured (Fig. 1d).

In conclusion the data presented here summarizes the results of various studies performed with the automated slide scanning system Metafer and its software modules MSearch, DCScore, MicroNuclei, MetaCyte, and CometScan. We could show that the automated scoring for dicentric chromosomes, for micronuclei, and for Comet assay cells produce reliable and reproducible results, which proves the usability of automated scanning in mutagenicity studies, biological dosimetry, and DNA repair research. Metafer's capability to scan for Comet FISH slides increases the benefits gained from Comet assay data, combining FISH spot counting with DNA damage analysis. Anyway, also the automated analysis of FISH signals is probably a useful tool for a wide range of applications in the

field of mutagenicity estimation. As an outlook for future applications in automated FISH image analysis we propose the assay performed by Rothkamm and Löbrich (2003), who labeled DNA breakage sites after low irradiation treatment with the help of  $\gamma$ -H2AX immunofluorescence. Radiation-induced DNA double strand breaks appear as fluorescent, distinct foci (Fig. 1e), whose number increases remarkably after irradiation (Fig. 1f) and decreases with repair time (Fig. 1g and h). The advantage of this technique lies in the possibility to directly visualize radiation induced damage sites without any delay. With Metafer MetaCyte and its capabilities to count fluorescent spots in interphase nuclei, the foci could be analyzed automatically, providing an automated biological dosimetry unit with a resolution down to a single double-strand break per cell.

## References

- Blakely WF, Prasanna PG, Kolanko CJ, Pyle MD, Mosbrook DM, Loats AS, Rippeon TL, Loats H: Application of the premature chromosome condensation assay in simulated partial-body radiation exposures: evaluation of the use of an automated metaphase-finder. *Stem Cells* 13:223–230 (1995).
- Böcker W, Müller WU, Streffer C: Image processing algorithms for the automated micronucleus assay in binucleated human lymphocytes. *Cytometry* 19:283–294 (1995).
- Böcker W, Rolf W, Bauch T, Müller WU, Streffer C: Automated comet assay analysis. *Cytometry* 35: 134–144 (1999).
- Fenech M: Important variables that influence base-line micronucleus frequency in cytokinesis-blocked lymphocytes – a biomarker for DNA damage in human populations. *Mutat Res* 404:155–165 (1998).
- Fenech M, Morley AA: Measurement of micronuclei in lymphocytes. *Mutat Res* 147:29–36 (1985).
- Fenech M, Crott J, Turner J, Brown S: Necrosis, apoptosis, cytostasis and DNA damage in human lymphocytes measured simultaneously within the cytokinesis-block micronucleus assay: description of the method and results for hydrogen peroxide. *Mutagenesis* 14:605–612 (1999).
- Hartmann A, Agurell E, Beevers C, Brendler-Schwaab S, Burlinson B, Clay P, Collins A, Smith A, Speit G, Thyband V, Tice RR: Recommendations for conducting the in vivo alkaline Comet assay. *Mutagenesis* 18:45–51 (2003).
- Huber R, Kulka U, Lörch T, Braselmann H, Bauchinger M: Automated metaphase finding: an assessment of the efficiency of the METAFER2 system in a routine mutagenicity assay. *Mutat Res* 334: 97–102 (1995).
- Huber R, Lörch T, Kulka U, Braselmann H, Bauchinger M: Technical report: automated classification of first and second cycle metaphases. *Mutat Res* 419:27–32 (1998).
- Huber R, Kulka U, Lörch T, Braselmann H, Engert D, Figel M, Bauchinger M: Technical report: application of the Metafer2 fluorescence scanning system for the analysis of radiation-induced chromosome aberrations measured by FISH-chromosome painting. *Mutat Res* 492:51–57 (2001).
- McKenna D, Rajab NF, McKeown SR, McKerr G, McKelvey-Martin VJ: Use of the comet-FISH assay to demonstrate repair of the TP53 gene region in two human bladder carcinoma cell lines. *Radiat Res* 159:49–56 (2003).
- Plesch A, Lörch T: Metafer – a novel ultra high throughput scanning system for rare cell detection and automatic interphase FISH scoring, in Macek M Sr, Bianchi D, Cuckle H (eds.): *Early Prenatal Diagnosis, Fetal Cells and DNA in the Mother, Present State and Perspectives*, pp 329–339 (12th Fetal Cell Workshop, Prague, May 2001; downloadable as PDF-file from [www.metasystems.de](http://www.metasystems.de)).
- Rothfuss A, Schutz P, Bochum S, Volm T, Eberhardt E, Kreienberg R, Vogel W, Speit G: Induced micronucleus frequencies in peripheral lymphocytes as a screening test for carriers of a BRCA1 mutation in breast cancer families. *Cancer Res* 60:390–394 (2000).
- Rothkamm K, Löbrich M: Evidence for the lack of DNA double-strand break repair in human cells exposed to very low x-ray doses. *Proc natl Acad Sci, USA* 100:5057–5062 (2003).
- Singh NP, McCoy MT, Tice RR, Schneider EL: A simple technique for quantitation of low levels of DNA damage in individual cells. *Expl Cell Res* 175:184–191 (1988).
- Voisin P, Barquinero F, Blakely B, Lindholm C, Lloyd D, Luccioni C, Miller S, Palitti F, Prasanna PG, Stephan G, Thierens H, Turai I, Wilkinson D, Wojcik A: Towards a standardization of biological dosimetry by cytogenetics. *Cell mol Biol* 48:501–504 (2002).
- Weber J, Scheid W, Traut, H: Time-saving in biological dosimetry by using the automatic metaphase finder Metafer2. *Mutat Res* 272:31–34 (1992).

## Acknowledgements

The authors thank the following persons for kindly providing us with data from their studies:

C. Johannes and R. Pieper, Universität Duisburg-Essen, Germany (dicentric chromosomes); W. Vogel and B. Patino-Garcia, Universität Ulm, Germany (micronucleus data); U. Rößler, M. Gomolka and S. Hornhardt, Bundesamt für Strahlenschutz, Oberschleißheim, Germany (Comet assay data); C. Volpato and A. De Grandi, Policlinico St. Orsola, Bologna, Italy (Comet FISH image); K. Rothkamm and M. Löbrich, Universität des Saarlandes, Homburg, Germany (immunofluorescence images).

# mBAND: a high resolution multicolor banding technique for the detection of complex intrachromosomal aberrations

I. Chudoba,<sup>a</sup> G. Hickmann,<sup>b</sup> T. Friedrich,<sup>a</sup> A. Jauch,<sup>c</sup> P. Kozlowski<sup>b</sup> and G. Senger<sup>d</sup>

<sup>a</sup>MetaSystems, Altlusheim; <sup>b</sup>Genetics Laboratory, Düsseldorf; <sup>c</sup>Institute of Human Genetics, Heidelberg; <sup>d</sup>Praxis für Medizinische Genetik, Regensburg (Germany)

**Abstract.** Precise breakpoint definition of chromosomal rearrangements using conventional banding techniques often fails, especially when more than two breakpoints are involved. The classic banding procedure results in a pattern of alternating light and dark bands. Hence, in banded chromosomes a specific chromosomal band is rather identified by the surrounding banding pattern than by its own specific morphology. In chromosomal rearrangements the original pattern is altered and therefore the unequivocal determination of breakpoints is not

obvious. The multicolor banding technique (mBAND, see Chudoba et al., 1999) is able to identify breakpoints unambiguously, even in highly complex chromosomal aberrations. The mBAND technique is presented and illustrated in a case of intrachromosomal rearrangement with seven breakpoints all having occurred on one chromosome 16, emphasizing the unique analyzing power of mBAND as compared to conventional banding techniques.

Copyright © 2003 S. Karger AG, Basel

The standard method for cytogenetic investigations is the analysis of banded chromosomes. Its purpose is to distinguish between a normal and an abnormal karyotype. Numerical chromosomal aberrations and simple translocations are reliably defined using these standard techniques. Additionally, sophisticated molecular cytogenetic methods such as mFISH (Speicher et al., 1996) or SKY (Schroeck et al., 1996) can be applied to support the interpretation.

The classic banding procedure results in a pattern of alternating light and dark bands. However, the specific identification of some marker chromosomes and translocations of similar bands is often hard to achieve. Moreover, complex chromosomal rearrangements are often misinterpreted. The multicolor banding (mBAND) technique (Chudoba et al., 1999), else-

where referred to as MCB (Mrasek et al., 2001) is able to identify breakpoints unambiguously, even in highly complex chromosomal aberrations.

## Material and methods

The multicolor banding technique uses region-specific partial chromosome paints (RPCPs) which were generated by microdissection (Lüdecke et al., 1989; Senger et al., 1990). Each region-specific library was generated from eight to ten chromosome fragments. The respective regions were isolated with extended glass needles (Lüdecke et al., 1989) and the DNA was amplified by DOP-PCR (Telenius et al., 1992; Zhang et al., 1993; Chudoba et al., 1996; Senger et al., 1997). As a special feature the chromosome RPCPs are partly overlapping with the neighboring ones. The exact chromosome location of each library was assessed by reverse painting to normal metaphase spreads.

Multicolor banding technique kits were generated for all human chromosomes (Fig. 1A). Depending on the length of the chromosomes, different numbers of libraries were constructed (e.g. from two for chromosome 21, 22 and Y to eight for chromosome 1). Altogether, we generated 109 region-specific partial chromosome paints.

The different libraries were combined for each chromosome and labeled with up to five different fluorochromes (DEAC-dUTP, Applied Biosystems, FITC-dUTP, Roche, SpectrumOrange-dUTP, Abott and Texas Red-dUTP, Molecular Probes; the fifth label was used indirectly via biotin-dUTP,

Supported by the Bundesministerium für Bildung und Forschung, BMBF, grant 0312218/2.

Received 9 October 2003; revision accepted 8 December 2003.

Request reprints from: Ilse Chudoba, MetaSystems

Robert-Bosch-Strasse 6, D-68804 Altlusheim (Germany)

telephone: +49 6205 39 61 0; fax: +49 6205 3 22 70, e-mail: ic@metasystems.de

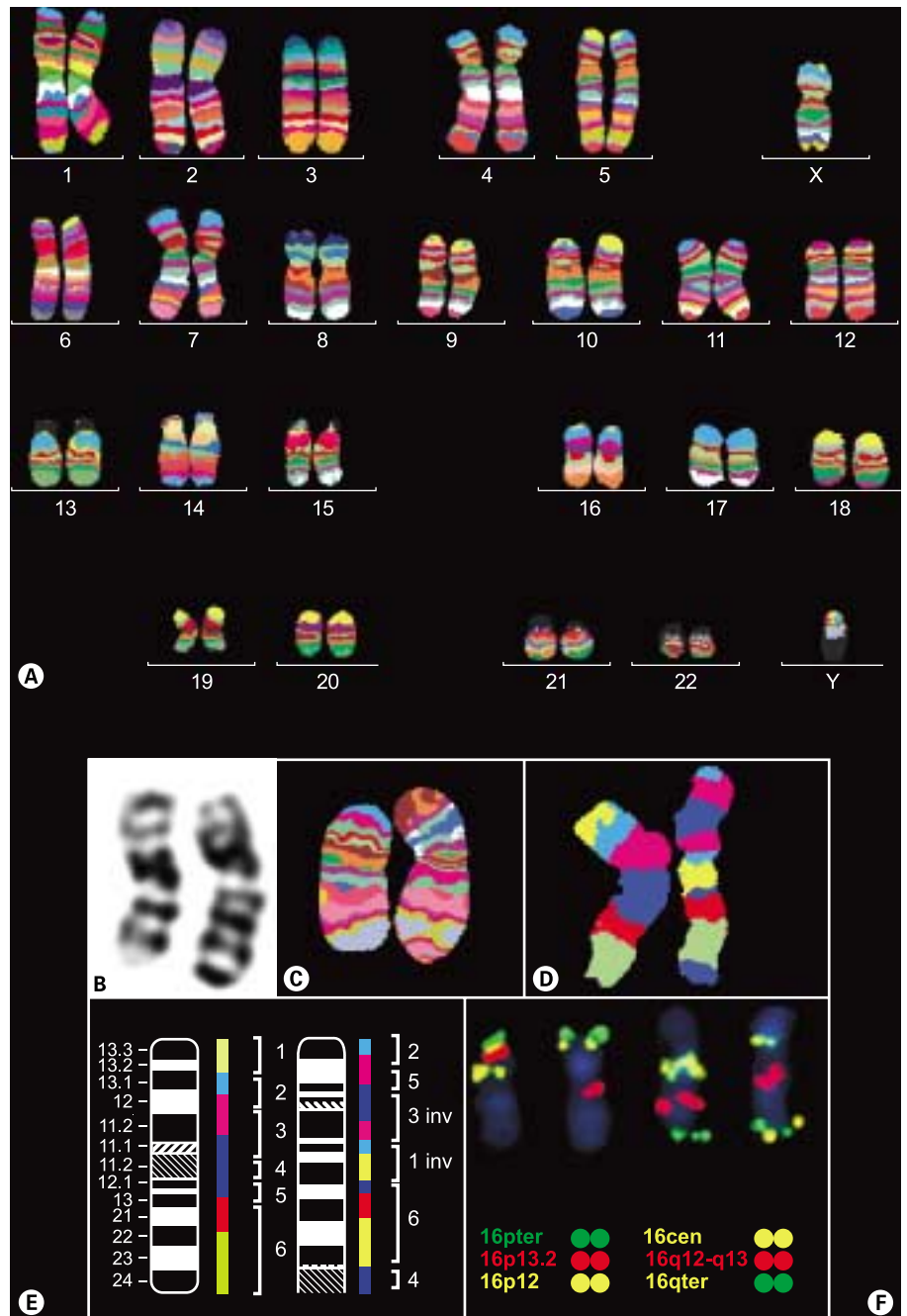


**Fig. 1.** (A) A composite karyotype showing all chromosomes displayed in mBAND. (B-F) Chromosomes 16 of the case described. In all chromosome pairs and in the schemes in E the normal chromosome is shown on the left side, and the aberrant chromosome on the right side. (B) GTG-banded chromosomes 16; (C) mBANDed chromosomes 16 at high resolution level (850 bands); (D) mBANDed chromosomes 16 at reduced resolution (~200 bands); (E) ISCN ideogram and mBAND ideogram. Square brackets indicate breakpoints on the normal chromosome. The resulting fragments are sequentially numbered next to the normal ideogram (left) and rearranged according to the observation made by the mBAND analysis resulting in an aberrant ideogram (right). Inv indicates an inversion of the respective fragment as compared to its original orientation. (F) Signal pattern of the BAC-probes (localization shown below) of the two probe sets hybridized to chromosome 16.

Roche, and detected with StreptavidinCy5, Amersham). All mBAND kits are available from MetaSystems, Altussheim, Germany (XCyte probes).

Hybridization, post-hybridization washes and signal detection of the mBAND kits were carried out following standard protocols (Senger et al., 1993).

For microscopic analyses an Axioplan 2 imaging microscope (Carl Zeiss GmbH, Jena) equipped with an HBO 100 mercury lamp and appropriate filter sets (Chroma Technologies) were used. Images were captured and processed using the Isis/mFISH imaging system (MetaSystems). The software controls the motorized filter revolver, thus automating the capture process completely.

## Results and discussion

Microdissection of eight to ten nearly identical chromosomal fragments are largely sufficient to generate a DNA library which can be used as a DNA probe for forward FISH after labeling with a fluorochrome. Due to the different condensation grades of the chromosomes used for microdissection the excised fragments vary to a certain extent. This results in a distribution of the fluorescence intensity along the chromosome with the highest intensity in the center and a decreasing fluorescence intensity towards the ends of the RPCPs. This feature and the fact that neighboring RPCPs are partly overlapping



result in a variation of fluorescence intensity ratios along the longitudinal axis of the chromosome. The analysis module "mFISH-mBAND" of MetaSystems FISH imaging system Isis divides the chromosome into a definable number of fragments and calculates the fluorescence intensity ratio within these fragments. In this manner an "mBAND-classifier" is generated. It assigns a specific false color to pixels showing a similar intensity ratio of the fluorochromes thus resulting in a color banded chromosome.

It has been shown that this method is highly reliable and reproducible (Chudoba et al., 1999). In addition, the method is flexible as the number of color bands can be pre-selected. This might be of great advantage, when highly complex chromosomal aberrations are analyzed. Figure 1B–F shows an example of an intrachromosomal rearrangement with high complexity. An aberrant chromosome 16 as the only chromosomal rearrangement was found during cytogenetic investigation in a man with azoospermia. The G-band pattern was not compatible with a simple para- or pericentric inversion (Fig. 1B). Detailed clinical data are described elsewhere (Hickmann et al., 2002). After hybridization and mBAND analysis the aberration was interpreted as an intrachromosomal rearrangement involving five breakpoints, all located on one chromosome 16. In Fig. 1C an mBAND image is presented with 20 color bands for chromosome 16 which compares to a resolution level of about 850 bands for the haploid chromosome complement. However, due to the high number of breakpoints in the aberrant chromosome 16 the mBAND image of the aberrant chromosome is difficult to interpret. Therefore, we reduced the number of displayed color bands to six for chromosome 16 and now the rearrangement becomes more obvious (Fig. 1D and E). These results were unexpected, because to the best of our knowledge, an intrachromosomal rearrangement of human chromosomes with such a complexity has not been described in the literature so far. Therefore, we confirmed our results obtained by mBAND with locus specific probes.

A total of six different locus-specific probes, all for chromosome 16, were chosen. Three of them were localized on the p-arm, two on the q-arm, and one was a centromere-specific probe which covered the heterochromatic region as well. The results were in good agreement with the mBAND results. Additional information was gained from the probes specific for subtelomeric regions which indicated that these regions were still localized at the very end of the derivative chromosome. Therefore, two additional breakpoints had to be defined. The final interpretation was a constitutional intrachromosomal aberration with seven breakpoints all on one chromosome 16.

The power of the mBAND technique has been demonstrated in other fields of cytogenetics as well. A systematic reinvestigation of a total of 40 cases with chromosomal aberrations of chromosome 5, formerly analyzed by classical methods, has been performed. This study revealed that in 75 % of these cases at least one breakpoint had to be redefined after mBAND analysis (Lemke et al., 2001).

Johannes et al. (1999) investigated the aberration pattern in lymphocytes irradiated with X-rays *in vitro*. They were able to describe the aberrations observed with a much higher precision compared to earlier applied methods. Hande et al. (2003)

examined the aberration pattern in workers from plutonium plants in the former Soviet Union. The workers were exposed to irradiation due to accidents which occurred in the course of 50 years. Among others Hande et al. detected an unexpected high frequency of nonclonal intrachromosomal aberrations. In both publications the investigators used the chromosome 5-specific mBAND kit (XCyte 5, MetaSystems, Germany) and they both had to observe a high number of metaphases in order to achieve reliable statistic values. The mBAND technique proved to be an optimal tool for these purposes, because the chromosomes hybridized are easily identified due to their fluorescence signals. Furthermore, compared to whole chromosome painting probes which are frequently used for the investigation of irradiation-induced chromosomal aberrations, the mBAND technique provides band-specific information thus enabling descriptions of intrachromosomal aberrations and precise definition of breakpoints precisely even in complex chromosomal rearrangements.

Another field of application for the mBAND technique was demonstrated for cancer cytogenetics by Lestou et al. (2002). They carried out mBAND analyses using the chromosome 1-specific mBAND kit (XCyte 1, MetaSystems, Germany) on a cohort of non-Hodgkin lymphoma. They demonstrated that chromosome 1 was more frequently involved in chromosomal aberrations than previously determined by standard G-banding (especially in the form of complex marker chromosomes). Furthermore, these investigations revealed three "hot spots" for amplifications of different chromosomal regions of chromosome 1.

A further interesting application of the multicolor banding has been shown by Mrasek et al. (2001) by reconstructing the female karyotype of gorilla (*Gorilla gorilla*). They applied the term MCB (multicolor banding) and the investigation was carried out with their own set of probe kits (described in detail in Liehr et al., 2002). The analysis strategy is however identical and they used the same imaging system (Isis-mFISH/mBAND, MetaSystems, Germany) for the generation of the color bands.

Alternative approaches for the realization of multicolor banding have been performed by using locus-specific probes (e.g. YACs or PACs) which are distributed along the chromosome (Lichter, 1991; Lengauer et al., 1993; Speicher et al., 2000) as well as cross-species hybridization using gibbon chromosome-specific paints (Müller et al., 2000) together with "fragmented hybrids" from human/rodent somatic cell hybrids (Müller et al., 1997; Wienberg and Müller, 2002). However, these methods leave gaps because they are not covering a chromosome completely (Lichter et al., 1991; Lengauer et al., 1993; Müller et al., 1997; Speicher et al., 2000) or the banding resolution is limited and ambiguities arise due to the limited number of distinguishable color combinations (Wienberg and Müller, 2002).

The examples presented emphasize that the mBAND technique provides an excellent tool for detailed and specific analysis of chromosomal aberrations and is of unmatched precision when combined with conventional banding analysis and mFISH.

## References

- Chudoba I, Rubtsov N, Senger G, Junker K, Bleck C, Claussen U: Improved detection of chromosome 16 rearrangements in acute myeloid leukemias using 16p and 16q specific microdissection libraries. *Oncol Rep* 3:829–832 (1996).
- Chudoba I, Plesch A, Lorch T, Lemke J, Claussen U, Senger G: High resolution multicolor-banding: a new technique for refined FISH analysis of human chromosomes. *Cytogenet Cell Genet* 84:156–160 (1999).
- Hande MP, Azizova TV, Geard CR, Burak LE, Mitchell CR, Khokhryakov VF, Vasilenko EK, Brenner DJ: Past exposure to densely ionizing radiation leaves a unique permanent signature in the genome. *Am J hum Genet* 72:1162–1170 (2003).
- Hickmann G, Chudoba I, Jauch A, Exeler R, Schubert R, Heinrichs S, Kozlowski P: An unusual intrachromosomal rearrangement in chromosome 16 in an azoospermic man. *Med Genet* 3:293 (2002).
- Johannes C, Chudoba I, Obe G: Analysis of X-ray-induced aberrations in human chromosome 5 using high-resolution multicolour banding FISH (mBAND). *Chrom Res* 7:625–633 (1999).
- Lemke J, Chudoba I, Senger G, Stumm M, Loncarevic IF, Henry C, Zabel B, Claussen U: Improved definition of chromosomal breakpoints using high-resolution multicolour banding. *Hum Genet* 71:478–483 (2001).
- Lengauer C, Speicher MR, Popp S, Jauch A, Taniwaki M, Nagaraja R, Riethman HC, Donis-Keller H, D'Urso M, Schlesinger D, Cremer T: Chromosomal barcode produced by multicolour fluorescence in situ hybridisation with multiple YAC clones and whole chromosome painting probes. *Hum molec Genet* 2:505–512 (1993).
- Lestou VS, Gascoyne RD, Salski C, Connors JM, Horsman DE: Uncovering novel inter- and intrachromosomal chromosome 1 aberrations in follicular lymphomas by using an innovative multicolor banding technique. *Genes Chrom Cancer* 34:201–210 (2002).
- Lichter P, Tang CJ, Call K, Hermanson G, Evans GA, Housman D, Ward DC: High-resolution mapping of human chromosome 11 by in situ hybridisation with cosmid clones. *Science* 247:64–69 (1991).
- Liehr T, Heller A, Starke H, Rubtsov N, Trifonov V, Mrasek K, Weise A, Kuechler A, Claussen U: Microdissection based high resolution multicolor banding for all 24 human chromosomes. *Int J molec Med* 9:335–339 (2002).
- Lüdecke H-J, Senger G, Claussen U, Horsthemke B: Cloning defined regions of the human genome by microdissection of banded chromosomes and enzymatic amplification. *Nature* 338:340–350 (1989).
- Mrasek K, Heller A, Rubtsov N, Trifonov V, Starke H, Rocchi M, Claussen U, Liehr T: Reconstruction of the female *Gorilla gorilla* karyotype using 25-color FISH and multicolor banding (MCB). *Cytogenet Cell Genet* 93:242–248 (2001).
- Müller S, Rocchi M, Ferguson-Smith MA, Wienberg J: Toward a multicolor chromosome bar code for the entire human karyotype by fluorescence in situ hybridisation. *Hum Genet* 100:271–278 (1997).
- Müller S, O'Brien PC, Ferguson-Smith MA, Wienberg J: Cross-species colour segmenting: a novel tool in human karyotype analysis. *Cytometry* 33:445–452 (2000).
- Senger G, Lüdecke H-J, Horsthemke B, Claussen U: Microdissection of banded human chromosomes. *Hum Genet* 84:507–511 (1990).
- Senger G, Ragoussis J, Trowsdale J, Sheer D: Fine mapping of human MHC class II region within chromosome 6p21 and evaluation of probe ordering using fluorescence in situ hybridization. *Cytogenet Cell Genet* 64:49–53 (1993).
- Senger G, Friedrich U, Claussen U, Tommerup N, Brøndum-Nielsen K: Prenatal diagnosis of a half cryptic translocation using chromosome microdissection. *Prenat Diag* 17:369–374 (1997).
- Speicher MR, Gwyn Ballard S, Ward DC: Karyotyping human chromosomes by combinatorial multi-fluor FISH. *Nature Genet* 12:368–375 (1996).
- Speicher MR, Petersen S, Uhrig S, Jentsch I, Fauth C, Eils R, Petersen I: Analysis of chromosomal alterations in non-small cell lung cancer by multiplex-FISH, comparative genomic hybridisation, and multicolor bar coding. *Lab Invest* 80:1031–1041 (2000).
- Schroeck E, du Manoir S, Veldman T, Schoell B, Wienberg J, Ferguson-Smith MA, Ning Y, Ledbetter DH, Bar-Am I, Soenksen D, Garini Y, Ried T: Multicolor spectral karyotyping of human chromosomes. *Science* 273:494–497 (1996).
- Telenius H, Carter NP, Bebb CE, Nordenskjöld M, Ponder BA, Tunnacliffe A: Degenerate oligonucleotide-primed PCR: general amplification of target DNA by a single degenerate primer. *Genomics* 13:718–725 (1992).
- Wienberg J, Müller S: Chromosome bar codes: Defining karyotypes with molecular tags by multi colour FISH. *ECA-Newsletter* 9:3–8 (2002).
- Zhang J, Trent JM, Meltzer P: Rapid isolation and characterization of amplified DNA by chromosome microdissection: identification of IGF1R amplification in malignant melanoma. *Oncogene* 8:2827–2831 (1993).

- Abdel-Halim, H.I. 193  
 Adachi, S. 252  
 Adler, I.-D. 271  
 Ando, K. 240
- Badr, F.M. 193  
 Bai, Y. 87  
 Baidya, K. 359  
 Bailey, S.M. 109  
 Ballarini, F. 149  
 Barquintero, J.F. 168  
 Barrios, L. 168  
 Bates, S.E. 35  
 Belyaev, I. 56  
 Blaise, R. 123  
 Boecker, W. 14  
 Boei, J.J.W.A. 72, 193  
 Bonassi, S. 376  
 Braselmann, H. 232  
 Brassesco, M.S. 346  
 Bruckmann, E. 304  
 Bryant, P.E. 65, 131  
 Bueren, J.A. 341
- Caballín, M.R. 168  
 Caldas, C. 333  
 Callén, E. 341  
 Camparoto, M.L. 346  
 Casado, J.A. 341  
 Cassina, G. 182  
 Chaki, M. 359  
 Chen, D. 237  
 Chudoba, I. 390  
 Cigarrán, S. 168  
 Cornforth, M.N. 206  
 Cox, R. 188  
 Cremer, C. 157  
 Creus, A. 341  
 Cucinotta, F.A. 211, 240, 245  
 Czene, S. 227
- Das, J.K. 359  
 Desmaze, C. 87, 123  
 Di-Tomaso, M.V. 182  
 Drets, M.E. 137  
 Dulout, F.N. 173  
 Durante, M. 206, 211, 240, 245
- Eberle, R.L. 206  
 Edwards, A. 188  
 Edwards, P.A.W. 333
- Finnegan, C. 131  
 Finsterle, J. 157  
 Folle, G.A. 182  
 Fouladi, B. 87  
 Fowler, P. 283  
 Freulet-Marrière, M.-A. 87  
 Friedrich, T. 390  
 Fukudome, Y. 252  
 Furusawa, Y. 211, 240, 245
- Gebhart, E. 352  
 George, K. 211, 240, 245
- Ghosh, P. 359  
 Giri, A.K. 359  
 Giulotto, E. 123  
 Goedecke, W. 7  
 Gonda, H. 271  
 Goodwin, E.H. 109  
 Gotoh, H. 252  
 Gray, L.J. 65  
 Gregoire, E. 200  
 Griffin, C.S. 21  
 Grigороva, M. 333  
 Guan, J. 14  
 Güerci, A.M. 173
- Haaf, T. 277  
 Hagmar, L. 376  
 Hahnfeldt, P. 142  
 Halls, J. 188  
 Hande, M.P. 116  
 Harms-Ringdahl, M. 227  
 Hayashi, M. 299  
 Hayata, I. 200, 237  
 Hickmann, G. 390  
 Hlatky, L. 142  
 Hofman-Huether, H. 221  
 Holmquist, G.P. 35  
 Hone, P. 188  
 Hrabé de Angelis, M. 271
- Ikushima, T. 310  
 Iliakis, G. 14  
 Imam, S.A. 193  
 Ito, H. 211
- Jauch, A. 390  
 Jenssen, D. 227  
 Jentsch, I. 271  
 Jin, G. 310  
 Johannes, T. 383  
 Jovtchev, G. 104
- Kaina, B. 77  
 Kawata, T. 211  
 Klatter, M. 104  
 Kligerman, A.D. 371  
 Kozłowski, P. 390  
 Kreth, G. 157  
 Kryscio, A. 295  
 Kuhfittig-Kulle, S. 7
- Laudicina, A.O. 100  
 Levy, D. 142  
 Li, L.Y. 252  
 Lloyd, D. 188  
 Lörch, T. 383  
 Lorenti-Garcia C 178  
 Loucas, B.D. 206
- Mahata, J. 359  
 Malik, S.I. 315  
 Marañón, D.G. 100  
 Marcon, F. 72  
 Marcos, R. 341  
 Martínez-López, W. 182
- Mathew, C.G. 341  
 McIlrath, J. 131  
 Meister, A. 104  
 Méndez-Acuña, L. 182  
 Minamihisamatsu, M. 237  
 Miura, K.F. 289  
 Mondello, C. 123  
 Morishima, H. 237  
 Mosesso, P. 178  
 Mozdarani, H. 131  
 Muhlmann, M. 100  
 Mullenders, L.H.F. 193  
 Müller, W.-U. 295  
 Murnane, J.P. 87, 123
- Nakajima, H. 252  
 Nasonova, E. 216  
 Natarajan, A.T. 72, 193, 359  
 Nomura, T. 252  
 Norppa, H. 376
- Obe, G. 7, 182, 240, 304  
 Oestreicher, U. 232  
 Olsson, G. 227  
 Otten, I.S. 271  
 Ottolenghi, A. 149  
 Ozdag, H. 333
- Palitti, F. 95, 178, 182  
 Pantelias, G. 14  
 Pantelias, G.E. 315  
 Parry, E.M. 283  
 Parry, J.M. 283  
 Pecinka, A. 104  
 Penna, S. 178  
 Pepe, G. 178  
 Peresse, N. 65  
 Perrault, A.R. 14  
 Pfeiffer, P. 7  
 Pirzio, L.M. 87, 123  
 Plesch, A. 383  
 Prihoda, T.J. 371
- Quick, E. 283
- Ray, K. 359  
 Ritter, S. 216  
 Romm, H. 162  
 Rosidi, B. 14  
 Roy, L. 200  
 Ryo, H. 252
- Sabatier, L. 87, 123  
 Sachs, R.K. 142  
 Saito, M. 211  
 Sakamoto-Hojo, E.T. 346  
 Sanders, M.H. 35  
 Sasaki, M.S. 28  
 Satoh, T. 289  
 Savage, J.R.K. 46  
 Schmid, M. 277  
 Schubert, I. 104  
 Schubert, V. 104  
 Schunck, C. 383
- Scott, D. 365  
 Senger, G. 390  
 Seoane, A.I. 173  
 Shirotori, T. 299  
 Slijepcevic, P. 131  
 Sofuni, T. 289  
 Sommer, S. 200  
 Sonoda, E. 28  
 Sonta, S. 261  
 Speicher, M.R. 271  
 Speit, G. 325  
 Staines, J.M. 333  
 Steinlein, C. 277  
 Stephan, G. 162, 200, 232  
 Streffer, C. 295  
 Sugahara, T. 237  
 Surrallés, J. 341  
 Suzuki, H. 299
- Tachibana, A. 28  
 Takata, M. 28  
 Takeda, S. 28  
 Tanaka, H. 252  
 Tanooka, H. 320  
 Terzoudi, G. 14  
 Terzoudi, G.I. 315  
 Thacker, J. 21  
 Tischkowitz, M.D. 341  
 Tone, L.G. 346  
 Trenz, K. 325
- Ullrich, S.E. 371  
 Uno, T. 211
- Varga, D. 383  
 Vijayalaxmi 371  
 Virsik-Köpp, P. 221  
 Voisin, P. 200
- Wang, C. 237  
 Wang, H. 14  
 Wei, L. 237  
 Wilbur, B.S. 35  
 Willingham, V. 245  
 Windhofer, F. 14  
 Wojcik, A. 200, 304  
 Wong, H.-P. 131  
 Wu, H. 211  
 Wu, W. 14
- Yamamoto, K. 289  
 Yamamoto, S. 211
- Zhang, W. 237  
 Znaor, A. 376

No. 1–4

5 Introduction

Basic Aspects

- 7 **Pathways of DNA double-strand break repair and their impact on the prevention and formation of chromosomal aberrations**  
Pfeiffer P, Goedecke W, Kuhfittig-Kulle S, Obe G
- 14 **Mechanisms of DNA double strand break repair and chromosome aberration formation**  
Iliakis G, Wang H, Perrault AR, Boecker W, Rosidi B, Windhofer F, Wu W, Guan J, Terzoudi G, Pantelias G
- 21 **The role of homologous recombination repair in the formation of chromosome aberrations**  
Griffin CS, Thacker J
- 28 **Recombination repair pathway in the maintenance of chromosomal integrity against DNA interstrand crosslinks**  
Sasaki MS, Takata M, Sonoda E, Tachibana A, Takeda S
- 35 **Repair rates of R-band, G-band and C-band DNA in murine and human cultured cells**  
Sanders MH, Bates SE, Wilbur BS, Holmquist GP
- 46 **On the nature of visible chromosomal gaps and breaks**  
Savage JRK
- 56 **Molecular targets and mechanisms in formation of chromosomal aberrations: contributions of Soviet scientists**  
Belyaev I
- 65 **Progress towards understanding the nature of chromatid breakage**  
Bryant PE, Gray LJ, Peresse N
- 72 **Human-hamster hybrid cells used as models to investigate species-specific factors modulating the efficiency of repair of UV-induced DNA damage**  
Marcon F, Boei JJWA, Natarajan AT
- 77 **Mechanisms and consequences of methylating agent-induced SCEs and chromosomal aberrations: a long road traveled and still a far way to go**  
Kaina B
- 87 **Human fibroblasts expressing hTERT show remarkable karyotype stability even after exposure to ionizing radiation**  
Pirzio LM, Freulet-Marrière M-A, Bai Y, Fouladi B, Murnane JP, Sabatier L, Desmaze C
- 95 **Mechanisms of formation of chromosomal aberrations: insights from studies with DNA repair-deficient cells**  
Palitti F
- 100 **In situ DNase I sensitivity assay indicates DNA conformation differences between CHO cells and the radiation-sensitive CHO mutant IRS-20**  
Marañon DG, Laudicina AO, Muhlmann M
- 104 **DNA damage processing and aberration formation in plants**  
Schubert I, Pecinka A, Meister A, Schubert V, Klatte M, Jovtchev G

Telomeres

- 109 **DNA and telomeres: beginnings and endings**  
Bailey SM, Goodwin EH
- 116 **DNA repair factors and telomere-chromosome integrity in mammalian cells**  
Hande MP
- 123 **Interstitial telomeric repeats are not preferentially involved in radiation-induced chromosome aberrations in human cells**  
Desmaze C, Pirzio LM, Blaise R, Mondello C, Giulotto E, Murnane JP, Sabatier L
- 131 **Lack of spontaneous and radiation-induced chromosome breakage at interstitial telomeric sites in murine *scid* cells**  
Wong H-P, Mozdarani H, Finnegan C, McIlrath J, Bryant PE, Slijepcevic P
- 137 **Cytological indications of the complex subtelomeric structure**  
Drets ME

Modelling

- 142 **Quantitative analysis of radiation-induced chromosome aberrations**  
Sachs RK, Levy D, Hahnfeldt P, Hlatky L
- 149 **Models of chromosome aberration induction: an example based on radiation track structure**  
Ballarini F, Ottolenghi A
- 157 **Virtual radiation biophysics: implications of nuclear structure**  
Kreth G, Finsterle J, Cremer C

Low-LET Radiation

- 162 **Dose dependency of FISH-detected translocations in stable and unstable cells after <sup>137</sup>Cs  $\gamma$  irradiation of human lymphocytes in vitro**  
Romm H, Stephan G
- 168 **Effect of DMSO on radiation-induced chromosome aberrations analysed by FISH**  
Cigarrán S, Barrios L, Caballín MR, Barquinero JF
- 173 **DNA damage in Chinese hamster cells repeatedly exposed to low doses of X-rays**  
Güerci AM, Dulout FN, Seoane AI
- 178 **Potassium bromate but not X-rays cause unexpectedly elevated levels of DNA breakage similar to those induced by ultraviolet light in Cockayne syndrome (CS-B) fibroblasts**  
Mosesso P, Penna S, Pepe G, Lorenti-Garcia C, Palitti F
- 182 **Distribution of breakpoints induced by etoposide and X-rays along the CHO X chromosome**  
Martínez-López W, Folle GA, Cassina G, Méndez-Acuña L, Di-Tomaso MV, Obe G, Palitti F
- 188 **The repair of  $\gamma$ -ray-induced chromosomal damage in human lymphocytes after exposure to extremely low frequency electromagnetic fields**  
Lloyd D, Hone P, Edwards A, Cox R, Halls J
- 193 **Ionizing radiation-induced instant pairing of heterochromatin of homologous chromosomes in human cells**  
Abdel-Halim HI, Imam SA, Badr FM, Natarajan AT, Mullenders LHF, Boei JJWA

- 200 **Cytogenetic damage in lymphocytes for the purpose of dose reconstruction: a review of three recent radiation accidents**  
Wojcik A, Gregoire E, Hayata I, Roy L, Sommer S, Stephan G, Voisin P

High-LET Radiation

- 206 **Complex chromatid-isochromatid exchanges following irradiation with heavy ions?**  
Loucas BD, Eberle RL, Durante M, Cornforth MN
- 211 **G2 chromatid damage and repair kinetics in normal human fibroblast cells exposed to low- or high-LET radiation**  
Kawata T, Ito H, Uno T, Saito M, Yamamoto S, Furusawa Y, Durante M, George K, Wu H, Cucinotta FA
- 216 **Cytogenetic effects of densely ionising radiation in human lymphocytes: impact of cell cycle delays**  
Nasonova E, Ritter S
- 221 **Chromosome aberrations induced by high-LET carbon ions in radiosensitive and radioresistant tumour cells**  
Virsik-Köpp P, Hofman-Huether H
- 227 **Induction of homologous recombination in the *hprt* gene of V79 Chinese hamster cells in response to low- and high-LET irradiation**  
Olsson G, Czene S, Jenssen D, Harms-Ringdahl M
- 232 **Cytogenetic analyses in peripheral lymphocytes of persons living in houses with increased levels of indoor radon concentrations**  
Oestreicher U, Braselmann H, Stephan G
- 237 **Effect of high-level natural radiation on chromosomes of residents in southern China**  
Hayata I, Wang C, Zhang W, Chen D, Minamihisamatsu M, Morishima H, Wei L, Sugahara T
- 240 **Complex chromosomal rearrangements induced in vivo by heavy ions**  
Durante M, Ando K, Furusawa Y, Obe G, George K, Cucinotta FA
- 245 **Chromosome aberrations of clonal origin are present in astronauts' blood lymphocytes**  
George K, Durante M, Willingham V, Cucinotta FA

Heritable Effects

- 252 **Transgenerational transmission of radiation- and chemically induced tumors and congenital anomalies in mice: studies of their possible relationship to induced chromosomal and molecular changes**  
Nomura T, Nakajima H, Ryo H, Li LY, Fukudome Y, Adachi S, Gotoh H, Tanaka H
- 261 **Contribution of chromosomal imbalance to sperm selection and pre-implantation loss in translocation-heterozygous Chinese hamsters**  
Sonta S
- 271 **Heritable translocations induced by dermal exposure of male mice to acrylamide**  
Adler I-D, Gonda H, Hrabé de Angelis M, Jentsch I, Otten IS, Speicher MR
- 277 **Chromosome banding in Amphibia. XXX. Karyotype aberrations in cultured fibroblast cells**  
Schmid M, Steinlein C, Haaf T

Aneuploidy and Micronuclei

- 283 **Investigations into the biological relevance of in vitro clastogenic and aneugenic activity**  
Parry JM, Fowler P, Quick E, Parry EM
- 289 **Region-specific chromatin decondensation and micronucleus formation induced by 5-azacytidine in human TIG-7 cells**  
Sato T, Yamamoto K, Miura KF, Sofuni T
- 295 **Micronuclei in lymphocytes of uranium miners of the former Wismut SDAG**  
Müller W-U, Kryscio A, Streffer C
- 299 **A liver micronucleus assay using young rats exposed to diethylnitrosamine: methodological establishment and evaluation**  
Suzuki H, Shirotori T, Hayashi M

Sister Chromatid Exchanges

- 304 **Insights into the mechanisms of sister chromatid exchange formation**  
Wojcik A, Bruckmann E, Obe G
- 310 **Frequent occurrence of UVB-induced sister chromatid exchanges in telomere regions and its implication to telomere maintenance**  
Jin G, Ikushima T
- 315 **SCE analysis in G2 lymphocyte prematurely condensed chromosomes after exposure to atrazine: the non-dose-dependent increase in homologous recombinational events does not support its genotoxic mode of action**  
Malik SI, Terzoudi GI, Pantelias GE

Applied Aspects/Cancer

- 320 **X chromosome inactivation-mediated cellular mosaicism for the study of the monoclonal origin and recurrence of mouse tumors: a review**  
Tanooka H
- 325 **Chromosomal mutagen sensitivity associated with mutations in BRCA genes**  
Speit G, Trenz K
- 333 **Possible causes of chromosome instability: comparison of chromosomal abnormalities in cancer cell lines with mutations in BRCA1, BRCA2, CHK2 and BUB1**  
Grigorova M, Staines JM, Ozdag H, Caldas C, Edwards PAW
- 341 **Quantitative PCR analysis reveals a high incidence of large intragenic deletions in the FANCA gene in Spanish Fanconi anemia patients**  
Callén E, Tischkowitz MD, Creus A, Marcos R, Bueren JA, Casado JA, Mathew CG, Surrallés J
- 346 **Analysis of ETV6/RUNX1 fusions for evaluating the late effects of cancer therapy in ALL (acute lymphoblastic leukemia) cured patients**  
Brascesco MS, Camparoto ML, Tone LG, Sakamoto-Hojo ET
- 352 **Comparative genomic hybridization (CGH): ten years of substantial progress in human solid tumor molecular cytogenetics**  
Gebhart E
- 359 **Chromosomal aberrations in arsenic-exposed human populations: a review with special reference to a comprehensive study in West Bengal, India**  
Mahata J, Chaki M, Ghosh P, Das JK, Baidya K, Ray K, Natarajan AT, Giri AK
- 365 **Chromosomal radiosensitivity and low penetrance predisposition to cancer**  
Scott D
- 371 **Cytogenetic studies in mice treated with the jet fuels, Jet-A and JP-8**  
Vijayalaxmi, Kligerman AD, Prihoda TJ, Ullrich SE
- 376 **Chromosomal aberrations and risk of cancer in humans: an epidemiologic perspective**  
Bonassi S, Znaor A, Norppa H, Hagmar L
- 383 **New developments in automated cytogenetic imaging: unattended scoring of dicentric chromosomes, micronuclei, single cell gel electrophoresis, and fluorescence signals**  
Schunck C, Johannes T, Varga D, Lörch T, Plesch A
- 390 **mBAND: a high resolution multicolor banding technique for the detection of complex intrachromosomal aberrations**  
Chudoba I, Hickmann G, Friedrich T, Jauch A, Kozłowski P, Senger G
- 394 **Author Index Vol. 104, 2004**